

# Bibliography of Lewis Research Center Technical Publications Announced in 1984

(NASA-TM-87012) BIBLIOGRAPHY OF LEWIS  
RESEARCH CENTER TECHNICAL PUBLICATIONS  
ANNOUNCED IN 1984 (NASA) 322 P  
HC A14/MF A01

N85-28876

CSCI 05B

G3/82

Unclas  
21425



May 1985



## **PREFACE**

In 1984, Lewis Research Center's 1052 research authors published 457 technical publications which were announced to and reached the worldwide scientific community. The 457 papers included 226 symposium/seminar presentations and 52 articles sent directly to journals for publication. The number of reports published per person per year has increased slightly. In 1984, Lewis authors published approximately 61 percent of their research contributions in outside publications and the remainder as NASA research reports. Two-thirds of Lewis-authored society presentations and journal articles were addressed to members of the following technical societies: AIAA, 73 papers; SAE, 42 papers; ASME, 24 papers; IEEE, 23 papers; ASLE, 14 papers.

In 1984, 298 contractor-authored research reports were produced. In addition, 20 patent applications were filed and 23 patents were issued.

Many Lewis authors have received awards for their contributions; among them are the following:

The 1984 Lewis Distinguished Paper Award was presented to Anatole P. Kurkov for his paper entitled "Formulation of the Blade-Flutter Spectral Analyses in Stationary Reference Frame." Stuart H. Loewenthal received an award from the Society of Automotive Engineers for "Best Oral Presentation." The paper was entitled "Advances in Traction Drive Technology" by S. Loewenthal, N.E. Anderson, and D. A. Rohn; it was presented at the International Off-Highway Meeting and Exposition in Milwaukee, Wisconsin in September 1983. In addition, Dr. Henry Brandhorst, Jr. received the William R. Cherry award for sustained outstanding contributions to the advancement of photovoltaic science and technology; Dr. Young-Chung Cho received the 1984 Hugh L. Dryden Memorial Fellowship; Robert L. Fusaro received the Distinguished Member award from the Cleveland Section of the ASLE; and Susan M. Johnson received the 1984 Technical Achievement Award from the Cleveland Technical Societies Council (CTSC).

A few Lewis-authored publications are not included in this compilation due to FEDD (For Early Domestic Dissemination) and ITAR (International Traffic in Arms Regulations) considerations which limit their announcement and distribution.

All the publications in this collection were announced in the 1984 issues of STAR (Scientific and Technical Aerospace Reports) and IAA (International Aerospace Abstracts).

The arrangement of the material is by NASA subject category, as noted in the Contents. The various indexes will help locate specific publications by subject, author, contractor organization, contract number, and report number.

George Mandel  
Chief, Technical Information Services Division

# TABLE OF CONTENTS

## PREFACE

i

## AERONAUTICS

Includes aeronautics (general), aerodynamics; air transportation and safety, aircraft communications and navigation, aircraft design, testing and performance, aircraft instrumentation, aircraft propulsion and power; aircraft stability and control; and research and support facilities (air)

For related information see also *Astronautics*

### 01 AERONAUTICS (GENERAL) 1

### 02 AERODYNAMICS 2

Includes aerodynamics of bodies, combinations, wings, rotors, and control surfaces, and internal flow in ducts and turbomachinery

For related information see also *34 Fluid Mechanics and Heat Transfer*

### 03 AIR TRANSPORTATION AND SAFETY 11

Includes passenger and cargo air transport operations, and aircraft accidents

For related information see also *16 Space Transportation* and *85 Urban Technology and Transportation*

### 04 AIRCRAFT COMMUNICATIONS AND NAVIGATION N.A.

Includes digital and voice communication with aircraft; air navigation systems (satellite and ground based), and air traffic control.

For related information see also *17 Spacecraft Communications, Command and Tracking* and *32 Communications*.

### 05 AIRCRAFT DESIGN, TESTING AND PERFORMANCE 12

Includes aircraft simulation technology.

For related information see also *18 Spacecraft Design, Testing and Performance* and *39 Structural Mechanics*.

### 06 AIRCRAFT INSTRUMENTATION 14

Includes cockpit and cabin display devices; and flight instruments

For related information see also *19 Spacecraft Instrumentation* and *35 Instrumentation and Photography*

### 07 AIRCRAFT PROPULSION AND POWER 15

Includes prime propulsion systems and systems components, e.g., gas turbine engines and compressors, and on-board auxiliary power plants for aircraft.

For related information see also *20 Spacecraft Propulsion and Power*, *28 Propellants and Fuels*, and *44 Energy Production and Conversion*

### 08 AIRCRAFT STABILITY AND CONTROL 36

Includes aircraft handling qualities; piloting; flight controls; and autopilots.

### 09 RESEARCH AND SUPPORT FACILITIES (AIR) 36

Includes airports, hangars and runways; aircraft repair and overhaul facilities; wind tunnels; shock tube facilities; and engine test blocks.

For related information see also *14 Ground Support Systems and Facilities (Space)*.

## ASTRONAUTICS

Includes astronautics (general); astrodynamics, ground support systems and facilities (space); launch vehicles and space vehicles, space transportation, spacecraft communications, command and tracking, spacecraft design, testing and performance; spacecraft instrumentation; and spacecraft propulsion and power

For related information see also *Aeronautics*

### 12 ASTRONAUTICS (GENERAL) 37

For extraterrestrial exploration see *91 Lunar and Planetary Exploration*

### 13 ASTRODYNAMICS N.A.

Includes powered and free-flight trajectories, and orbit and launching dynamics.

### 14 GROUND SUPPORT SYSTEMS AND FACILITIES (SPACE) 37

Includes launch complexes, research and production facilities; ground support equipment, e.g., mobile transporters; and simulators.

For related information see also *09 Research and Support Facilities (Air)*

### 15 LAUNCH VEHICLES AND SPACE VEHICLES 38

Includes boosters, manned orbital laboratories; reusable vehicles; and space stations.

### 16 SPACE TRANSPORTATION 39

Includes passenger and cargo space transportation, e.g., shuttle operations; and rescue techniques.

For related information see also *03 Air Transportation and Safety* and *85 Urban Technology and Transportation*.

### 17 SPACECRAFT COMMUNICATION, COMMAND AND TRACKING 39

Includes telemetry; space communications networks; astronavigation; and radio blackout.

For related information see also *04 Aircraft Communications and Navigation* and *32 Communications*

### 18 SPACECRAFT DESIGN, TESTING AND PERFORMANCE 40

Includes spacecraft thermal and environmental control; and attitude control.

For life support systems see *54 Man/System Technology and Life Support* For related information see also *05 Aircraft Design, Testing and Performance* and *39 Structural Mechanics*

### 19 SPACECRAFT INSTRUMENTATION N.A.

For related information see also *06 Aircraft Instrumentation* and *35 Instrumentation and Photography*.

### 20 SPACECRAFT PROPULSION AND POWER 42

Includes main propulsion systems and components, e.g., rocket engines; and spacecraft auxiliary power sources

For related information see also *07 Aircraft Propulsion and Power*, *28 Propellants and Fuels*, and *44 Energy Production and Conversion*

## CHEMISTRY AND MATERIALS

Includes chemistry and materials (general); composite materials; inorganic and physical chemistry; metallic materials; nonmetallic materials; and propellants and fuels.

### 23 CHEMISTRY AND MATERIALS (GENERAL) 50

Includes biochemistry and organic chemistry.

### 24 COMPOSITE MATERIALS 51

Includes laminates.

### 25 INORGANIC AND PHYSICAL CHEMISTRY 58

Includes chemical analysis, e.g., chromatography, combustion theory; electrochemistry; and photochemistry.

For related information see also 77 *Thermodynamics and Statistical Physics*

### 26 METALLIC MATERIALS 63

Includes physical, chemical, and mechanical properties of metals, e.g., corrosion; and metallurgy.

### 27 NONMETALLIC MATERIALS 77

Includes physical, chemical, and mechanical properties of plastics, elastomers, lubricants, polymers, textiles, adhesives, and ceramic materials.

### 28 PROPELLANTS AND FUELS 88

Includes rocket propellants, igniters, and oxidizers; storage and handling; and aircraft fuels.

For related information see also 07 *Aircraft Propulsion and Power*, 20 *Spacecraft Propulsion and Power*, and 44 *Energy Production and Conversion*.

## ENGINEERING

Includes engineering (general); communications; electronics and electrical engineering; fluid mechanics and heat transfer; instrumentation and photography; lasers and masers; mechanical engineering; quality assurance and reliability; and structural mechanics

For related information see also *Physics*.

### 31 ENGINEERING (GENERAL) 92

Includes vacuum technology; control engineering; display engineering; and cryogenics.

### 32 COMMUNICATIONS 93

Includes land and global communications; communications theory; and optical communications.

For related information see also 04 *Aircraft Communications and Navigation* and 17 *Spacecraft Communications, Command and Tracking*

### 33 ELECTRONICS AND ELECTRICAL ENGINEERING 101

Includes test equipment and maintainability; components, e.g., tunnel diodes and transistors; micro-miniaturization; and integrated circuitry.

For related information see also 60 *Computer Operations and Hardware* and 76 *Solid-State Physics*

### 34 FLUID MECHANICS AND HEAT TRANSFER 112

Includes boundary layers; hydrodynamics; fluidics; mass transfer; and ablation cooling.

For related information see also 02 *Aerodynamics* and 77 *Thermodynamics and Statistical Physics*.

### 35 INSTRUMENTATION AND PHOTOGRAPHY 129

Includes remote sensors; measuring instruments and gages; detectors; cameras and photographic supplies; and holography.

For aerial photography see 43 *Earth Resources*. For related information see also 06 *Aircraft Instrumentation* and 19 *Spacecraft Instrumentation*.

### 36 LASERS AND MASERS 134

Includes parametric amplifiers.

### 37 MECHANICAL ENGINEERING 135

Includes auxiliary systems (non-power); machine elements and processes; and mechanical equipment.

### 38 QUALITY ASSURANCE AND RELIABILITY 148

Includes product sampling procedures and techniques; and quality control.

### 39 STRUCTURAL MECHANICS 149

Includes structural element design and weight analysis; fatigue; and thermal stress.

For applications see 05 *Aircraft Design, Testing and Performance* and 18 *Spacecraft Design, Testing and Performance*.

## GEOSCIENCES

Includes geosciences (general); earth resources; energy production and conversion; environment pollution; geophysics; meteorology and climatology; and oceanography.

For related information see also *Space Sciences*

### 42 GEOSCIENCES (GENERAL) N.A.

### 43 EARTH RESOURCES 159

Includes remote sensing of earth resources by aircraft and spacecraft; photogrammetry; and aerial photography.

For instrumentation see 35 *Instrumentation and Photography*.

### 44 ENERGY PRODUCTION AND CONVERSION 159

Includes specific energy conversion systems, e.g., fuel cells and batteries; global sources of energy; fossil fuels; geophysical conversion; hydroelectric power; and wind power.

For related information see also 07 *Aircraft Propulsion and Power*, 20 *Spacecraft Propulsion and Power*, 28 *Propellants and Fuels*, and 85 *Urban Technology and Transportation*.

### 45 ENVIRONMENT POLLUTION 173

Includes air, noise, thermal and water pollution; environment monitoring; and contamination control.

### 46 GEOPHYSICS 173

Includes aeronomy; upper and lower atmosphere studies; ionospheric and magnetospheric physics; and geomagnetism.

For space radiation see 93 *Space Radiation*

### 47 METEOROLOGY AND CLIMATOLOGY 174

Includes weather forecasting and modification.

### 48 OCEANOGRAPHY N.A.

Includes biological, dynamic and physical oceanography; and marine resources.



## LIFE SCIENCES

Includes sciences (general); aerospace medicine; behavioral sciences; man/system technology and life support; and planetary biology.

**51 LIFE SCIENCES (GENERAL)** N.A.  
Includes genetics.

**52 AEROSPACE MEDICINE** 174  
Includes physiological factors; biological effects of radiation, and weightlessness.

**53 BEHAVIORAL SCIENCES** N.A.  
Includes psychological factors; individual and group behavior, crew training and evaluation; and psychiatric research.

**54 MAN/SYSTEM TECHNOLOGY AND LIFE SUPPORT** 175  
Includes human engineering, biotechnology; and space suits and protective clothing.

**55 PLANETARY BIOLOGY** N.A.  
Includes exobiology; and extraterrestrial life.

## MATHEMATICAL AND COMPUTER SCIENCES

Includes mathematical and computer sciences (general); computer operations and hardware; computer programming and software; computer systems; cybernetics; numerical analysis; statistics and probability; systems analysis; and theoretical mathematics.

**59 MATHEMATICAL AND COMPUTER SCIENCES (GENERAL)** N.A.

**60 COMPUTER OPERATIONS AND HARDWARE** 175  
Includes computer graphics and data processing  
For components see 33 *Electronics and Electrical Engineering*

**61 COMPUTER PROGRAMMING AND SOFTWARE** 176  
Includes computer programs, routines, and algorithms.

**62 COMPUTER SYSTEMS** 177  
Includes computer networks

**63 CYBERNETICS** 178  
Includes feedback and control theory  
For related information see also 54 *Man/System Technology and Life Support*.

**64 NUMERICAL ANALYSIS** 178  
Includes iteration, difference equations, and numerical approximation.

**65 STATISTICS AND PROBABILITY** 179  
Includes data sampling and smoothing; Monte Carlo method; and stochastic processes.

**66 SYSTEMS ANALYSIS** N.A.  
Includes mathematical modeling; network analysis; and operations research.

**67 THEORETICAL MATHEMATICS** N.A.  
Includes topology and number theory

## PHYSICS

Includes physics (general); acoustics; atomic and molecular physics; nuclear and high-energy physics; optics; plasma physics; solid-state physics; and thermodynamics and statistical physics.

For related information see also *Engineering*

**70 PHYSICS (GENERAL)** 179  
For geophysics see 46 *Geophysics*. For astrophysics see 90 *Astrophysics* For solar physics see 92 *Solar Physics*.

**71 ACOUSTICS** 179  
Includes sound generation, transmission, and attenuation;  
For noise pollution see 45 *Environment Pollution*.

**72 ATOMIC AND MOLECULAR PHYSICS** 187  
Includes atomic structure and molecular spectra.

**73 NUCLEAR AND HIGH-ENERGY PHYSICS** N.A.  
Includes elementary and nuclear particles; and reactor theory.  
For space radiation see 93 *Space Radiation*.

**74 OPTICS** 187  
Includes light phenomena

**75 PLASMA PHYSICS** 189  
Includes magnetohydrodynamics and plasma fusion.  
For ionospheric plasmas see 46 *Geophysics* For space plasmas see 90 *Astrophysics*

**76 SOLID-STATE PHYSICS** 190  
Includes superconductivity  
For related information see also 33 *Electronics and Electrical Engineering* and 36 *Lasers and Masers*.

**77 THERMODYNAMICS AND STATISTICAL PHYSICS** 192  
Includes quantum mechanics; and Bose and Fermi statistics  
For related information see also 25 *Inorganic and Physical Chemistry* and 34 *Fluid Mechanics and Heat Transfer*.

## SOCIAL SCIENCES

Includes social sciences (general); administration and management, documentation and information science, economics and cost analysis; law and political science; and urban technology and transportation.

**80 SOCIAL SCIENCES (GENERAL)** 192  
Includes educational matters.

**81 ADMINISTRATION AND MANAGEMENT** 193  
Includes management planning and research.

**82 DOCUMENTATION AND INFORMATION SCIENCE N.A.**

Includes information storage and retrieval technology; micrography; and library science.

For computer documentation see *61 Computer Programming and Software*.

**83 ECONOMICS AND COST ANALYSIS - - - 193**

Includes cost effectiveness studies.

**84 LAW AND POLITICAL SCIENCE N.A.**

Includes space law; international law; international cooperation; and patent policy.

**85 URBAN TECHNOLOGY AND TRANSPORTATION 193**

Includes applications of space technology to urban problems; technology transfer; technology assessment, and surface and mass transportation

For related information see *03 Air Transportation and Safety*, *16 Space Transportation*, and *44 Energy Production and Conversion*.

**SPACE SCIENCES**

Includes space sciences (general); astronomy; astrophysics; lunar and planetary exploration, solar physics; and space radiation.

For related information see also *Geosciences*.

**88 SPACE SCIENCES (GENERAL) N.A.**

**89 ASTRONOMY N.A.**

Includes radio and gamma-ray astronomy; celestial mechanics; and astrometry

**90 ASTROPHYSICS N.A.**

Includes cosmology; and interstellar and interplanetary gases and dust.

**91 LUNAR AND PLANETARY EXPLORATION N.A.**

Includes planetology; and manned and unmanned flights.

For spacecraft design see *18 Spacecraft Design, Testing and Performance*. For space stations see *15 Launch Vehicles and Space Vehicles*.

**92 SOLAR PHYSICS N.A.**

Includes solar activity, solar flares, solar radiation and sunspots.

**93 SPACE RADIATION N.A.**

Includes cosmic radiation; and inner and outer earth's radiation belts

For biological effects of radiation see *52 Aerospace Medicine*. For theory see *73 Nuclear and High-Energy Physics*

**GENERAL**

**99 GENERAL N.A.**

Note: N.A. means that no abstracts were assigned to this category for this issue.

<b>SUBJECT INDEX .....</b>	<b>A-1</b>
<b>PERSONAL AUTHOR INDEX .....</b>	<b>B-1</b>
<b>CORPORATE SOURCE INDEX .....</b>	<b>C-1</b>
<b>CONTRACT NUMBER INDEX .....</b>	<b>D-1</b>
<b>REPORT/ACCESSION NUMBER INDEX .....</b>	<b>E-1</b>

---

# Bibliography of Lewis Research Center Technical Publications Announced in 1984

---

01

## AERONAUTICS (GENERAL)

**N84-13140\*#** National Aeronautics and Space Administration.  
Lewis Research Center, Cleveland, Ohio.

### **A REAL-TIME IMPLEMENTATION OF AN ADVANCED SENSOR FAILURE DETECTION, ISOLATION, AND ACCOMMODATION ALGORITHM**

J. C. DELAAT and W. C. MERRILL Dec. 1983 12 p refs  
Presented at the 21st Aerospace Sci. Meeting, Reno, Nev., 9-12  
Jan. 1984

(NASA-TM-83553; E-1928; NAS 1.15:83553) Avail: NTIS HC  
A02/MF A01 CSCL 01B

A sensor failure detection, isolation, and accommodation algorithm was developed which incorporates analytic sensor redundancy through software. This algorithm was implemented in a high level language on a microprocessor based controls computer. Parallel processing and state-of-the-art 16-bit microprocessors are used along with efficient programming practices to achieve real-time operation. Author

**N84-16119\*#** National Aeronautics and Space Administration.  
Lewis Research Center, Cleveland, Ohio.

### **AERONAUTICAL PROPULSION: PRESENT STATUS AND FUTURE DIRECTIONS**

M. J. HARTMANN 1984 23 p Presented at the 29th Intern.  
Gas Turbine Conf., Amsterdam, 3-7 Jun. 1984

(NASA-TM-83589; E-1987; NAS 1.15:83589) Avail: NTIS HC  
A02/MF A01 CSCL 01B

The advancement of aeropropulsion systems continues to provide technology to various portions of the gas turbine field. It is recognized that this area is undergoing considerable change, which will result in substantially improved gas turbine components and systems. These changes are occurring in a number of technical areas including advanced analytical and physical measurement methods, the application of large scientific computers, the dynamic modeling of components and systems, the application of integrated control systems that optimize and improve performance and system condition monitoring, and the development of new and unique materials and structures. As these areas evolve, the ways in which technology will advance, and factors affecting the design and development of new systems, will probably be considerably different than those of today. It is also anticipated that the necessary skilled work force will be different. Certainly there will be changes, but the nature, extent, and rate of those changes can only be surmised at this time. Author

**N84-14111\*#** National Aeronautics and Space Administration.  
Lewis Research Center, Cleveland, Ohio.

### **FIBEROPTICS FOR PROPULSION CONTROL SYSTEM**

R. J. BAUMBICK 1984 15 p refs Proposed for presentation  
at the 29th Ann. Intern. Gas Turbine Conf., Amsterdam, 4-7 Jun.  
1984; sponsored by ASME

(NASA-TM-83542; E-1913; NAS 1.15:83542) Avail: NTIS HC  
A02/MF A01 CSCL 20F

In aircraft systems with digital controls, fiber optics has advantages over wire systems because of its inherent immunity to electromagnetic noise (EMI) and electromagnetic pulses (EMP). It also offers a weight benefit when metallic conductors are replaced by optical fibers. To take full advantage of the benefits of optical waveguides, passive optical sensors are also being developed to eliminate the need for electrical power to the sensor. Fiber optics may also be used for controlling actuators on engine and airframe. In this application, the optical fibers, connectors, etc. will be subjected to high temperature and vibrations. This paper discussed the use of fiber optics in aircraft propulsion systems together with the optical sensors and optically controlled actuators being developed to take full advantage of the benefits which fiber optics offers. The requirements for sensors and actuators in advanced propulsion systems are identified. The benefits of using fiber optics in place of conventional wire systems are discussed as well as the environmental conditions under which the optical components must operate. B.W.

**N84-22527\*#** National Aeronautics and Space Administration.  
Lewis Research Center, Cleveland, Ohio.

### **ANALYSIS OF INVISCID AND VISCOUS FLOWS IN CASCADES WITH AN EXPLICIT MULTIPLE-GRID ALGORITHM**

R. V. CHIMA 1984 14 p refs Proposed for presentation at  
the 17th Fluid Dyn., Plasma Dyn., and Lasers Conf., Snowmass,  
Colo., 25-27 Jun. 1984; sponsored by AIAA

(NASA-TM-83636; E-2078; NAS 1.15:83636) Avail: NTIS HC  
A02/MF A01 CSCL 20D

A rapid technique is used for calculating inviscid and viscous flows in turbomachinery cascades. The Euler and thin-layer Navier-Stokes equations are solved using the original explicit MacCormack algorithm. The Baldwin-Lomax eddy viscosity model is used for turbulent flows. Convergence to a steady state is accelerated by use of a variable time-step and a multiple-grid scheme. Computer time is reduced through vectorization. Details of the numerical method are presented along with computed results for two low-speed wind tunnel turning vanes, a space shuttle fuel pump turbine rotor, and a supersonic inflow compressor rotor. The method can predict subtle viscous flow phenomena in cascades and is fast enough to be used as a design tool. M.A.C.

## 01 AERONAUTICS (GENERAL)

**N84-25605\*#** National Aeronautics and Space Administration. Lewis Research Center, Cleveland, Ohio.

### **AN ADVANCED PITCH CHANGE MECHANISM INCORPORATING A HYBRID TRACTION DRIVE**

B. M. STEINETZ, D. F. SARGISSON (GE, Evendale, Ohio), G. WHITE (Transmission Research Inc.), and S. H. LOEWENTHAL 1984 18 p refs Presented at the 20th Joint Propulsion Conf., Cincinnati, 11-13 Jun. 1984

(Contract NAS3-23044)

(NASA-TM-83709; E-2137; NAS 1.15:83709; AIAA-84-1383)

Avail: NTIS HC A02/MF A01 CSCL 01A

A design of a propeller pitch control mechanism is described that meets the demanding requirements of a high-power, advanced turboprop. In this application, blade twisting moment torque can be comparable to that of the main reduction gearbox output; precise pitch control, reliability and compactness are all at a premium. A key element in the design is a compact, high-ratio hybrid traction drive which offers low torque ripple and high torsional stiffness. The traction drive couples a high speed electric motor/alternator unit to a ball screw that actuates the blade control links. The technical merits of this arrangement and the performance characteristics of the traction drive are discussed. Comparisons are made to the more conventional pitch control mechanisms.

Author

**N84-25606\*#** National Aeronautics and Space Administration. Lewis Research Center, Cleveland, Ohio.

### **AN ANALYTICAL METHOD TO PREDICT EFFICIENCY OF AIRCRAFT GEARBOXES**

N. E. ANDERSON, S. H. LOEWENTHAL, and J. D. BLACK (Allison Gas Turbine Operations) 1984 23 p refs Presented at the 20th Joint Propulsion Conf., Cincinnati, 11-13 Jun. 1984

(NASA-TM-83716; E-2169; NAS 1.15:83716;

USAAVSCOM-TR-84-C-8; AIAA-84-1500) Avail: NTIS HC

A02/MF A01 CSCL 01A

A spur gear efficiency prediction method previously developed by the authors was extended to include power loss of planetary gearsets. A friction coefficient model was developed for MIL-L-7808 oil based on disc machine data. This combined with the recent capability of predicting losses in spur gears of nonstandard proportions allows the calculation of power loss for complete aircraft gearboxes that utilize spur gears. The method was applied to the T56/501 turboprop gearbox and compared with measured test data. Bearing losses were calculated with large scale computer programs. Breakdowns of the gearbox losses point out areas for possible improvement.

Author

**N84-25607\*#** National Aeronautics and Space Administration. Lewis Research Center, Cleveland, Ohio.

### **APPLICATION OF AN OPTIMIZATION METHOD TO HIGH PERFORMANCE PROPELLER DESIGNS**

K. C. LI (Purdue Univ.) and G. L. STEFKO 1984 11 p refs Presented at the 20th Joint Propulsion Conf., Cincinnati, 11-13 Jun. 1984

(NASA-TM-83710; E-2086; NAS 1.15:83710; AIAA-84-1203)

Avail: NTIS HC A02/MF A01 CSCL 01A

The application of an optimization method to determine the propeller blade twist distribution which maximizes propeller efficiency is presented. The optimization employs a previously developed method which has been improved to include the effects of blade drag, camber and thickness. Before the optimization portion of the computer code is used, comparisons of calculated propeller efficiencies and power coefficients are made with experimental data for one NACA propeller at Mach numbers in the range of 0.24 to 0.50 and another NACA propeller at a Mach number of 0.71 to validate the propeller aerodynamic analysis portion of the computer code. Then comparisons of calculated propeller efficiencies for the optimized and the original propellers show the benefits of the optimization method in improving propeller performance. This method can be applied to the aerodynamic design of propellers having straight, swept, or nonplanar propeller blades.

Author

**N84-32344\*#** National Aeronautics and Space Administration. Lewis Research Center, Cleveland, Ohio.

### **SUMMARY OF RECENT NASA PROPELLER RESEARCH**

D. C. MIKKELSON, G. A. MITCHELL, and L. J. BOBER 1984 38 p refs Proposed for presentation at the AGARD Fluid Dyn. Panel Meeting on Aerodyn. and Acoustics of Propellers, Toronto, 1-4 Oct. 1984

(NASA-TM-83733; E-2216; NAS 1.15:83733) Avail: NTIS HC

A03/MF A01 CSCL 01B.

Advanced high-speed propellers offer large performance improvements for aircraft that cruise in the Mach 0.7 to 0.8 speed regime. At these speeds, studies indicate that there is a 15 to near 40 percent block fuel savings and associated operating cost benefits for advanced turboprops compared to equivalent technology turboprop powered aircraft. Recent wind tunnel results for five eight to ten blade advanced models are compared with analytical predictions. Test results show that blade sweep was important in achieving net efficiencies near 80 percent at Mach 0.8 and reducing nearfield cruise noise by about 6 dB. Lifting line and lifting surface aerodynamic analysis codes are under development and some results are compared with propeller force and probe data. Also, analytical predictions are compared with some initial laser velocimeter measurements of the flow field velocities of an eightbladed 45 swept propeller. Experimental aeroelastic results indicate that cascade effects and blade sweep strongly affect propeller aeroelastic characteristics. Comparisons of propeller near-field noise data with linear acoustic theory indicate that the theory adequately predicts near-field noise for subsonic tip speeds but overpredicts the noise for supersonic tip speeds.

B.W.

## 02

### **AERODYNAMICS**

Includes aerodynamics of bodies, combinations, wings, rotors, and control surfaces; and internal flow in ducts and turbomachinery.

**A84-10078\*#** Cincinnati Univ., Ohio.

### **A DIRECT METHOD FOR THE SOLUTION OF UNSTEADY TWO-DIMENSIONAL INCOMPRESSIBLE NAVIER-STOKES EQUATIONS**

K. N. GHIA, G. A. OSSWALD, and U. GHIA (Cincinnati, University, Cincinnati, OH) IN: Symposium on Numerical and Physical Aspects of Aerodynamic Flows, 2nd, Long Beach, CA, January 17-20, 1983, Proceedings. Long Beach, CA, California State University, 1983, 16 p. refs

(Contract AF-AFOSR-80-0160; NSG-3267)

The unsteady incompressible Navier-Stokes equations are formulated in terms of vorticity and stream function in generalized curvilinear orthogonal coordinates to facilitate analysis of flow configurations with general geometries. The numerical method developed solves the conservative form of the transport equation using the alternating-direction implicit method, whereas the stream-function equation is solved by direct block Gaussian elimination. The method is applied to a model problem of flow over a back-step in a doubly infinite channel, using clustered conformal coordinates. One-dimensional stretching functions, dependent on the Reynolds number and the asymptotic behavior of the flow, are used to provide suitable grid distribution in the separation and reattachment regions, as well as in the inflow and outflow regions. The optimum grid distribution selected attempts to honor the multiple length scales of the separated-flow model problem. The asymptotic behavior of the finite-differenced transport equation near infinity is examined and the numerical method is carefully developed so as to lead to spatially second-order accurate wiggle-free solutions, i.e., with minimum dispersive error. Results have been obtained in the entire laminar range for the backstep channel and are in good agreement with the available experimental data for this flow problem.

Author

**A84-10133\*#** Purdue Univ. School of Science at Indianapolis, Ind

**APPLICATION OF A FINITE ELEMENT ALGORITHM TO THE SOLUTION OF STEADY TRANSONIC EULER EQUATIONS**

H. U. AKAY and A. ECER (Purdue University, Indianapolis, IN) AIAA Journal (ISSN 0001-1452), vol. 21, Nov. 1983, p. 1518-1524. refs  
(Contract NSG-3294)

Previously cited in issue 15, p. 2344, Accession no. A82-31939

**A84-11042\*#** National Aeronautics and Space Administration. Lewis Research Center, Cleveland, Ohio.

**INVESTIGATION OF TANGENTIAL BLOWING APPLIED TO A SUBSONIC V/STOL INLET**

R. R. BURLEY and D. P. HWANG (NASA, Lewis Research Center, Aerodynamics and Engine Systems Div., Cleveland, OH) Journal of Aircraft (ISSN 0021-8669), vol. 20, Nov. 1983, p. 926-934. refs

Previously cited in issue 17, p. 2675, Accession no. A82-35195

**A84-11591\*#** Cincinnati Univ., Ohio.

**HYBRID C-H GRIDS FOR TURBOMACHINERY CASCADES**

U. GHIA, K. N. GHIA, and R. RAMAMURTI (Cincinnati, University, Cincinnati, OH) IN: Advances in grid generation; Proceedings of the Applied Mechanics, Bioengineering, and Fluids Engineering Conference, Houston, TX, June 20-22, 1983. New York, American Society of Mechanical Engineers, 1983, p. 143-149. refs  
(Contract NAG3-194)

The three basic types of grids available for two-dimensional cascade configurations are examined with respect to their relative advantages and disadvantages. Subsequently, a hybrid coordinate system is proposed such that it combines the major advantages of the C-type and the H-type meshes. The development of the hybrid grid system employs the patching of appropriate regions of these two basic mesh systems such that the transformed domain has a multi-block structure. Viewing the transformed domain as a three-dimensional surface enables the coordinates to be continuous across the boundaries of the patches in a natural manner.

Author

**A84-13574\*#** Pennsylvania State Univ., University Park.

**THREE-DIMENSIONAL FLOWFIELD INSIDE A LOW-SPEED AXIAL FLOW COMPRESSOR ROTOR**

M. POUAGARE, K. N. S. MURTHY, and B. LAKSHMINARAYANA (Pennsylvania State University, University Park, PA) AIAA Journal (ISSN 0001-1452), vol. 21, Dec. 1983, p. 1679, 1680.  
(Contract NSG-3266)

Previously cited in issue 15, p. 2347, Accession no. A82-31964

**A84-13592\*#** Delaware Univ., Newark.

**INLET FLOW DISTORTION IN TURBOMACHINERY - COMPARISON OF THEORY AND EXPERIMENT IN A TRANSONIC FAN STAGE**

B. S. SEIDEL (Delaware, University, Newark, DE) and M. D. MATWEY AIAA Journal (ISSN 0001-1452), vol. 21, Dec. 1983, p. 1769, 1770. refs  
(Contract NSG-3189)

Consideration is given to both velocity and temperature circumferential inlet distortions at upstream infinity (Seidel et al., 1980). The blade rows here are modeled as semiactuator disks, and losses and quasi-steady deviation angle correlations are included in the analysis. The governing equations are linearized, and the perturbations in stagnation pressure and stagnation temperature at upstream infinity are represented as Fourier series. The flow in the rotor is modeled as inviscid, one-dimensional, unsteady, and compressible. The flow is steady elsewhere. The deviation angles for the rotor and stator are taken to be functions of the relative inlet angle and Mach number, and use is made of the correlations contained in Johnson and Bullock (1965). It is assumed that the losses in relative stagnation pressure in the

rotor and stator occur across the trailing edge. Boundary conditions applied at the various stations furnish the equations that make it possible to solve for the several quantities introduced in the linearization of the governing equations. C.R.

**A84-17437\*#** Pennsylvania State Univ., University Park.

**THREE-DIMENSIONAL TURBULENT \* BOUNDARY-LAYER DEVELOPMENT ON A FAN ROTOR BLADE**

B. LAKSHMINARAYANA, C. HAH, and T. R. GOVINDAN (Pennsylvania State University, University Park, PA) AIAA Journal (ISSN 0001-1452), vol. 22, Jan. 1984, p. 83-89. refs  
(Contract NSG-3266)

Previously cited in issue 15, p. 2347, Accession no. A82-31965

**A84-17841\*#** Pennsylvania State Univ., University Park.

**THE APPLICATION OF VORTEX THEORY TO THE OPTIMUM SWEEP PROPELLER**

B. W. MCCORMICK (Pennsylvania State University, University Park, PA) American Institute of Aeronautics and Astronautics, Aerospace Sciences Meeting, 22nd, Reno, NV, Jan. 9-12, 1984. 8 p · refs  
(Contract NAS3-22251)  
(AIAA PAPER 84-0036)

It is shown that an optimum propeller generating a swept wake must satisfy the Betz condition, at least to a first order. A numerical solution for swept propellers generating a rigid helicoidal wake is formulated and some results are presented. These results indicate that sweep has a significant effect on Goldstein's kappa factor, particularly at high advance ratios typical of those at which advanced turboprops operate.

Author

**A84-17881\*#** Case Western Reserve Univ., Cleveland, Ohio.

**EXPERIMENTAL STUDIES ON TWO DIMENSIONAL SHOCK BOUNDARY LAYER INTERACTIONS**

S. A. SKEBE, I. GREBER (Case Western Reserve University, Cleveland, OH), and W. R. HINGST (NASA, Lewis Research Center, Cleveland, OH) American Institute of Aeronautics and Astronautics, Aerospace Sciences Meeting, 22nd, Reno, NV, Jan. 9-12, 1984. 13 p. refs  
(Contract NAG3-61; NAG3-102)  
(AIAA PAPER 84-0099)

Experiments have been performed on the interaction of oblique shock waves with flat plate boundary layers in the 30.48 cm x 30.48 cm (1 ft x 1 ft.) supersonic wind tunnel at NASA Lewis Research Center. High accuracy measurements of the plate surface static pressure and shear stress distributions as well as boundary layer velocity profiles were obtained through the interaction region. Documentation was also performed of the tunnel test section flow field and of the two-dimensionality of the interaction regions. The findings provide detailed description of two-dimensional interaction with initially laminar boundary layers over the Mach number range 2.0 to 4.0. Additional information with regard to interactions involving initially transitional boundary layers is presented over the Mach number range 2.0 to 3.0 and those for initially turbulent boundary layers at Mach 2.0. These experiments were directed toward providing well documented information of high accuracy useful as test cases for analytic and numerical calculations. Flow conditions encompassed a Reynolds number range of 4.72E6 to 2.95E7 per meter. The shock boundary layer interaction results were found to be generally in good agreement with the experimental work of previous authors both in terms of direct numerical comparison and in support of correlations establishing laminar separation characteristics.

Author

**A84-17925\*#** Cornell Univ., Ithaca, N.Y.

**AN IMPLICIT LU SCHEME FOR THE EULER EQUATIONS APPLIED TO ARBITRARY CASCADES**

E. K. BURATYNSKI and D. A. CAUGHEY (Cornell University, Ithaca, NY) American Institute of Aeronautics and Astronautics, Aerospace Sciences Meeting, 22nd, Reno, NV, Jan. 9-12, 1984. 11 p. refs

(Contract NAG3-19)

(AIAA PAPER 84-0167)

An implicit scheme for solving the Euler equations is derived and demonstrated. The alternating-direction implicit (ADI) technique is modified, using two implicit-operator factors corresponding to lower-block-diagonal (L) or upper-block-diagonal (U) algebraic systems which can be easily inverted. The resulting LU scheme is implemented in finite-volume mode and applied to 2D subsonic and transonic cascade flows with differing degrees of geometric complexity. The results are presented graphically and found to be in good agreement with those of other numerical and analytical approaches. The LU method is also 2.0-3.4 times faster than ADI, suggesting its value in calculating 3D problems. T.K.

**A84-18090\*#** New Mexico Univ., Albuquerque.

**BOUNDARY LAYER TRANSITION EFFECTS ON FLOW SEPARATION AROUND V/STOL ENGINE INLETS AT HIGH INCIDENCE**

D. C. CHOU (New Mexico University, Albuquerque, NM), D. P. HWANG (NASA, Lewis Research Center, Wind Tunnel and Flight Div., Cleveland, OH), K. SALARI, and C. P. WONG American Institute of Aeronautics and Astronautics, Aerospace Sciences Meeting, 22nd, Reno, NV, Jan. 9-12, 1984. 9 p. refs (AIAA PAPER 84-0432)

Numerical methods for calculating laminar and turbulent boundary layer development around vertical-short take off and landing engine inlets at high incidence angles are investigated. Various transition models were compared and evaluated in calculations off flow separation bound inside the inlet. Results of the transition effects on the boundary layer characteristics at onset of separation for two types of engine inlet geometries are presented. Some of the numerical results are compared with existing wind-tunnel test data for scaled inlet models to demonstrate the effects of transition models in the numerical scheme. The effects of transition modeling on the boundary layer development are illustrated for typical engine operating conditions. Author

**A84-18094\*#** Sverdrup Technology, Inc., Arnold Air Force Station, Tenn.

**ONE-DIMENSIONAL UNSTEADY MODELING OF SUPERSONIC INLET UNSTART/RESTART**

J. C. ADAMS, JR., W. R. MARTINDALE, and M. O. VARNER (Sverdrup Technology Computer Service Center, Tullahoma, TN) American Institute of Aeronautics and Astronautics, Aerospace Sciences Meeting, 22nd, Reno, NV, Jan. 9-12, 1984. 34 p. refs (Contract NAS3-23682) (AIAA PAPER 84-0439)

A quasi-one-dimensional unsteady inviscid analysis of mixed-compression supersonic inlet flow is presented with emphasis on modeling of inlet unstart/restart phenomena. Numerical solution of the governing equations of motion is performed using a computationally efficient shock-capturing split-characteristics algorithm. Inlet unstart is modeled using a mass balance method which relates the expelled normal shock position ahead of the inlet cowl to the amount of spilled mass flow over the inlet housing. Comparison of computed results with experimental data for an axisymmetric inlet at a free-stream Mach number of 2.50 shows quite reasonable agreement over an entire unstart/restart transient which includes centerbody translation and retraction as well as bypass mass flow variations. Author

**A84-19228\*#** Tennessee Univ., Tullahoma.

**COMPARISON OF EXPERIMENTAL AND COMPUTATIONAL COMPRESSIBLE FLOW IN A S-DUCT**

A. VAKILI, J. M. WU (Tennessee University, Tullahoma, TN), W. R. HINGST, and C. E. TOWNE (NASA, Lewis Research Center, Cleveland, OH) American Institute of Aeronautics and Astronautics, Aerospace Sciences Meeting, 22nd, Reno, NV, Jan. 9-12, 1984. 9 p. refs

(Contract NAG3-233)

(AIAA PAPER 84-0033)

This paper describes experimental measurements of secondary flow in a constant area, circular cross-section 30-30 deg S-duct, and compares the results obtained with the computations performed using the PEPSIG code, a parabolized Navier-Stokes code. The flow entering the duct was turbulent, with entrance Mach number of 0.6, and the boundary layer thickness at the duct entrance was 10 percent of the duct diameter. The duct mean radius of curvature to the duct diameter was 5.077. Flow parameters were measured at six stations along the length of the duct. These measurements were made using a five-port cone probe. At least ten radial traverses were made at each station on both sides of the symmetry plane. Wall static pressures along three azimuth angles of zero, 90, and 180 deg along the duct were measured. Plots presenting the secondary velocity field as well as contour plots of the total and static-pressure fields have been obtained. Strong secondary flows were observed in the first bend, and these continued into the second bend with the formation of new vorticity in the opposite sense in the second bend. The flow exiting the duct contained two pairs of counter-rotating vortices. The computational results are in general agreement with the experiments. However, it appears that the computations underestimate the extent of the pressure distortion, due to simplifications made in the pressure field calculations. Author

**A84-21290\*#** National Aeronautics and Space Administration, Lewis Research Center, Cleveland, Ohio.

**THREE-DIMENSIONAL VISCOUS DESIGN METHODOLOGY FOR ADVANCED TECHNOLOGY AIRCRAFT SUPERSONIC INLET SYSTEMS**

B. H. ANDERSON (NASA, Lewis Research Center, Cleveland, OH) American Institute of Aeronautics and Astronautics, Aerospace Sciences Meeting, 22nd, Reno, NV, Jan. 9-12, 1984. 63 p. refs (AIAA PAPER 84-0194)

A broad program to develop advanced, reliable, and user oriented three-dimensional viscous design techniques for supersonic inlet systems, and encourage their transfer into the general user community is discussed. Features of the program include: (1) develop effective methods of computing three-dimensional flows within a zonal modeling methodology; (2) ensure reasonable agreement between said analysis and selective sets of benchmark validation data; (3) develop user orientation into said analysis; and (4) explore and develop advanced numerical methodology. Previously announced in STAR as N84-13190

Author

**A84-31289\*** National Aeronautics and Space Administration, Lewis Research Center, Cleveland, Ohio.

**A RAPID BLADE-TO-BLADE SOLUTION FOR USE IN TURBOMACHINERY DESIGN**

E. R. MCFARLAND (NASA, Lewis Research Center, Cleveland, OH) ASME, Transactions, Journal of Engineering for Gas Turbines and Power (ISSN 0022-0825), vol 106, April 1984, p. 376-382. refs (ASME PAPER 83-GT-67)

A rapid technique for solving the blade-to-blade turbomachinery flow problem was developed. Approximate governing flow equations, which include the effects of compressibility, radius change, rotation, and variable stream sheet thickness are solved using a panel method. The development and solution of these equations are described. Sample calculations are presented to illustrate the method's capabilities and accuracy. Previously announced in STAR as N83-13077

Author

**A84-36960\*#** National Aeronautics and Space Administration. Lewis Research Center, Cleveland, Ohio.

**REDESIGN AND CASCADE TESTS OF A SUPERCRITICAL CONTROLLED DIFFUSION STATOR BLADE-SECTION**

J. F. SCHMIDT, T. F. GELDER, and L. F. DONOVAN (NASA, Lewis Research Center, Cleveland, OH) AIAA, SAE, and ASME, Joint Propulsion Conference, 20th, Cincinnati, OH, June 11-13, 1984. 8 p. refs

(AIAA PAPER 84-1207)

A supercritical stator blade section, previously tested in cascade, and characterized by a flat-roof-top suction surface Mach number distribution, has been redesigned and retested. At near design conditions, the losses and air turning were improved over the original blade by 50 percent and 7 percent, respectively. The key element in the improved performance was a small blade reshaping. This produced a continuous flow acceleration over the first one-third chord of the suction surface which successfully prevented a premature laminar separation bubble. Several recently available inviscid analysis codes and one fully viscous (Navier-Stokes) analysis code were used in the redesign process. The validity of these codes was enhanced by the test results. Previously announced in STAR as N84-22533

Author

**A84-36971\*#** Pennsylvania State Univ., University Park.

**COMPUTATION OF THREE-DIMENSIONAL VISCOUS FLOWS USING A SPACE-MARCHING METHOD**

K. N. S. MURTHY and B. LAKSHMINARAYANA (Pennsylvania State University, University Park, PA) AIAA, SAE, and ASME, Joint Propulsion Conference, 20th, Cincinnati, OH, June 11-13, 1984. 9 p. refs

(Contract NSG-3266)

(AIAA PAPER 84-1298)

A space-marching method, developed to compute three-dimensional flows for internal geometries, has been utilized to predict viscous flows through a curved duct and over a swept wing. The Navier-Stokes equations have been posed as an initial value problem by neglecting the streamwise viscous diffusion terms and by treating the pressure gradient as a known source term. The resulting equations have been solved by a non-iterative (single pass) algorithm at each streamwise step. The results are compared with earlier computations (based on iterative methods) and the experimental data. The agreement between the present predictions, the experimental data, and the earlier predictions is good for the cases computed. The computation time is only a fraction of the iterative methods.

Author

**A84-38004\*#** Scientific Research Associates, Inc., Glastonbury, Conn.

**DYNAMIC RESPONSE OF SHOCK WAVES IN TRANSONIC DIFFUSER AND SUPERSONIC INLET - AN ANALYSIS WITH THE NAVIER-STOKES EQUATIONS AND ADAPTIVE GRID**

N.-S. LIU, S. J. SHAMROTH, and H. MCDONALD (Scientific Research Associates, Inc., Glastonbury, CT) American Institute of Aeronautics and Astronautics, Fluid Dynamics, Plasma Dynamics, and Lasers Conference, 17th, Snowmass, CO, June 25-27, 1984. 13 p. refs

(Contract NAS3-23053)

(AIAA PAPER 84-1609)

An existing method which solves the multi-dimensional ensemble-averaged compressible time-dependent Navier-Stokes equations in conjunction with mixing length turbulence model and shock capturing technique has been extended to include the shock-tracking adaptive grid systems. The numerical scheme for solving the governing equations is based on a linearized block implicit approach. The effects of grid-motion and grid-distribution on the calculated flow solutions have been studied in relative detail and this is carried out in the context of physically steady, shocked flows computed with non-stationary grids. Subsequently, the unsteady dynamics of the flows occurring in a supercritically operated transonic diffuser and a mixed compression supersonic inlet have been investigated with the adaptive grid systems by solving the Navier-Stokes equations.

Author

**A84-38043\*#** National Aeronautics and Space Administration. Lewis Research Center, Cleveland, Ohio.

**ANALYSIS OF INVISCID AND VISCOUS FLOWS IN CASCADES WITH AN EXPLICIT MULTIPLE-GRID ALGORITHM**

R. V. CHIMA (NASA, Lewis Research Center, Cleveland, OH) American Institute of Aeronautics and Astronautics, Fluid Dynamics, Plasma Dynamics, and Lasers Conference, 17th, Snowmass, CO, June 25-27, 1984. 13 p. refs

(AIAA PAPER 84-1663)

A rapid technique is used for calculating inviscid and viscous flows in turbomachinery cascades. The Euler and thin-layer Navier-Stokes equations are solved using the original explicit McCormack algorithm. The Baldwin-Lomax eddy viscosity model is used for turbulent flows. Convergence to a steady state is accelerated by use of a variable time-step and a multiple-grid scheme. Computer time is reduced through vectorization. Details of the numerical method are presented along with computed results for two low-speed wind tunnel turning vanes, a space shuttle fuel pump turbine rotor, and a supersonic inflow compressor rotor. The method can predict subtle viscous flow phenomena in cascades and is fast enough to be used as a design tool. Previously announced in STAR as N84-22527

M.A.C.

**A84-38828\*#** Purdue Univ., Lafayette, Ind.

**THREE-DIMENSIONAL FLOW SIMULATIONS FOR SUPERSONIC MIXED-COMPRESSION INLETS AT INCIDENCE**

J. D. HOFFMAN (Purdue University, West Lafayette, IN), A. R. BISHOP (NASA, Lewis Research Center, Propulsion Aerodynamics Div., Cleveland, OH), and J. VADYAK (AIAA Journal (ISSN 0001-1452), vol. 22, July 1984, p. 873-881. refs

(Contract NSG-3311)

Previously cited in issue 07, p. 965, Accession no. A82-19778

**A84-38839\*#** National Aeronautics and Space Administration. Lewis Research Center, Cleveland, Ohio.

**IMPROVED DESIGN OF SUBCRITICAL AND SUPERCRITICAL CASCADES USING COMPLEX CHARACTERISTICS AND BOUNDARY-LAYER CORRECTION**

J. M. SANZ (NASA, Lewis Research Center, Fluid Mechanics and Acoustics Div., Cleveland, OH; Universities Space Research Association, Columbia, MD) (International Symposium on Air Breathing Engines, 6th, Paris, France, June 6-11, 1983) AIAA Journal (ISSN 0001-1452), vol. 22, July 1984, p. 950-956.

The method of complex characteristics and hodograph transformation for the design of shockless airfoils was extended to design supercritical cascades with high solidities and large inlet angles. This capability was achieved by introducing a conformal mapping of the hodograph domain onto an ellipse and expanding the solution in terms of Tchebycheff polynomials. A computer code was developed based on this idea. A number of airfoils designed with the code are presented. Various supercritical and subcritical compressor, turbine and propeller sections are shown. The lag-entrainment method for the calculation of a turbulent boundary layer was incorporated to the inviscid design code. The results of this calculation are shown for the airfoils described. The elliptic conformal transformation developed to map the hodograph domain onto an ellipse can be used to generate a conformal grid in the physical domain of a cascade of airfoils with open trailing edges with a single transformation. A grid generated with this transformation is shown for the Korn airfoil. Previously announced in STAR as N83-24474

S.L.

**A84-39304\*#** Pennsylvania State Univ., University Park.  
**LASER DOPPLER VELOCIMETER MEASUREMENT IN THE TIP REGION OF A COMPRESSOR ROTOR**  
 K. N. S. MURTHY and B. LAKSHMINARAYANA (Pennsylvania State University, University Park, PA) American Institute of Aeronautics and Astronautics, Fluid Dynamics, Plasma Dynamics, and Lasers Conference, 17th, Snowmass, CO, June 25-27, 1984. 15 p. refs  
 (Contract NSG-3212)  
 (AIAA PAPER 84-1602)

The axial and tangential velocity components near the tip region of a compressor rotor were measured by a laser Doppler velocimeter. The measurements were taken at 25 radial locations in the outer twenty percent of the blade span and at 10 axial locations upstream, inside and at the exit of the rotor. The results are interpreted to derive the behavior of the leakage flow, annulus wall boundary layer growth, inviscid effects and the rotor wake decay characteristics in the tip region. The inviscid and annulus wall boundary layer effects dominate up to quarter chord, beyond which the leakage phenomena has a major influence in altering the flow characteristics in the outer ten percent of the blade span. The annulus wall boundary layer undergoes drastic change through the passage. The velocity field measured near the leading edge reveals the effects of rapid acceleration near the suction surface and the stagnation point on the pressure surface. Author

**A84-40241\*#** National Aeronautics and Space Administration. Lewis Research Center, Cleveland, Ohio.  
**CALCULATION OF TRANSONIC FLOW IN A LINEAR CASCADE**  
 L. F. DONOVAN (NASA, Lewis Research Center, Cleveland, OH) AIAA, SAE, and ASME, Joint Propulsion Conference, 20th, Cincinnati, OH, June 11-13, 1984. 13 p. refs  
 (AIAA PAPER 84-1301)

Turbomachinery blade designs are becoming more aggressive in order to achieve higher loading and greater range. New analysis tools are required to cope with these heavily loaded blades that may operate with a thin separated region near the trailing edge on the suction surface. An existing, viscous airfoil code was adapted to cascade conditions in an attempt to provide this capability. Comparisons with recently obtained data show that calculated and experimental surface Mach numbers were in good agreement but loss coefficients and outlet air angles were not. Previously announced in STAR as N84-24539 Author

**A84-44177\*#** Army Propulsion Lab, Cleveland, Ohio.  
**APPLICATION OF A QUASI-3D INVISCID FLOW AND BOUNDARY LAYER ANALYSIS TO THE HUB-SHROUD CONTOURING OF A RADIAL TURBINE**  
 K. CIVINSKAS (U.S. Army, Propulsion Laboratory, Cleveland, OH) and L. A. POVINELLI (NASA, Lewis Research Center, Cleveland, OH) AIAA, SAE, and ASME, Joint Propulsion Conference, 20th, Cincinnati, OH, June 11-13, 1984. 20 p. Previously announced in STAR as N84-25647. refs  
 (AIAA PAPER 84-1297)

Application of a quasi-3D approach to the aerodynamic analysis of several radial turbine configurations is described. The objective was to improve the rotor aerodynamic characteristics by hub-shroud contouring. The approach relies on available 2D inviscid methods coupled with boundary layer analysis to calculate profile, mixing, and endwall losses. Windage, tip clearance, incidence, and secondary flow losses are estimated from correlations. To eliminate separation along the hub and blade suction surfaces of a baseline rotor, the analysis was also applied to three alternate hub-shroud geometries. Emphasis was on elimination of an inducer velocity overshoot as well as increasing hub velocities. While separation was never eliminated, the extent of the separated area was progressively reduced. Results are presented in terms of mid-channel and blade surface velocities; kinetic energy loss coefficients; and efficiency. The calculation demonstrates a first step for a systematic approach to radial turbine design that can be used to identify and control aerodynamic characteristics that ultimately determine heat transfer and component life.

Experimentation will be required to assess the extent to which flow and boundary layer behavior were predicted correctly. M.G.

**A84-44187\*#** North Carolina State Univ., Raleigh  
**ANALYTICAL STUDY OF SUCTION BOUNDARY LAYER CONTROL FOR SUBSONIC V/STOL INLETS**  
 M. A. BOLES, K. RAMESH (North Carolina State University, Raleigh, NC), and D. P. HWANG (NASA, Lewis Research Center, Cleveland, OH) AIAA, SAE, and ASME, Joint Propulsion Conference, 20th, Cincinnati, OH, June 11-13, 1984. 11 p. refs  
 (Contract NSG-389)  
 (AIAA PAPER 84-1399)

Analytical procedures used to evaluate the application of suction boundary-layer control (BLC) to subsonic V/STOL inlets are presented. These procedures have been used to analytically predict the optimum (minimum suction power required) location and extent for a suction slot of two different surface resistances within a subsonic V/STOL inlet. Results of this analytical study are presented Author

**A84-44639\*#** Georgia Inst. of Tech., Atlanta.  
**VISCOUS-INVISCID INTERACTIVE PROCEDURE FOR ROTATIONAL FLOW IN CASCADES OF AIRFOILS**  
 W. JOHNSTON (Georgia Institute of Technology, Atlanta, GA) and P. SOCKOL (NASA, Lewis Research Center, Cleveland, OH) AIAA Journal (ISSN 0001-1452), vol. 22, Sept. 1984, p. 1281, 1282. Abridged. Previously cited in issue 5, p. 583, Accession no. A83-16614. refs

**A84-46103\*#** Texas Univ., Austin.  
**TRANSONIC CASCADE FLOW ANALYSIS USING VISCOUS/INVISCID COUPLING CONCEPTS**  
 C. R. OLLING and G. S. DULIKRAVICH (Texas, University, Austin, TX) American Institute of Aeronautics and Astronautics, Applied Aerodynamics Conference, 2nd, Seattle, WA, Aug. 21-23, 1984. 9 p. refs  
 (Contract NAG3-317)  
 (AIAA PAPER 84-2159)

Transonic two-dimensional cascade flows have been analyzed using viscous/inviscid coupling concepts. A full potential cascade code is coupled with an inverse integral boundary layer/wake method that permits calculation of separated laminar or turbulent flow. The semi-inverse coupling method of Wight converges slowly in the case of a strong shock in the region between the shock and the trailing edge. The location of a strong shock is not well predicted by the coupling method, which indicates the need for an entropy correction in the potential code or the inclusion of a shock-boundary layer interaction module. Author

**A84-46926\*#** United Technologies Research Center, East Hartford, Conn.  
**INLET BOUNDARY LAYER EFFECTS IN AN AXIAL COMPRESSOR ROTOR. I BLADE-TO-BLADE EFFECTS**  
 J. H. WAGNER, R. P. DRING, and H. D. JOSLYN (United Technologies Research Center, East Hartford, CT) American Society of Mechanical Engineers, International Gas Turbine Conference and Exhibit, 29th, Amsterdam, Netherlands, June 4-7, 1984. 7 p. refs  
 (Contract F33615-77-C-2083; NAS3-23157)  
 (ASME PAPER 84-GT-84)

This paper discusses experimental data measured on the blading and downstream of an isolated compressor rotor with thick inlet endwall boundary layers. The objective of the study was to compare these results with data acquired previously with thin inlet boundary layers and to assess the impact of inlet boundary layer thickness on the secondary flow. Flow visualization results showed the powerful impact of the hub corner stall and how at the same near stall flow coefficient where with thin inlet boundary layers the blade was separated at midspan, with thick inlet boundary layers it was attached. It was also shown that while secondary flow was very weak, it did produce sufficient radial redistribution to cause an apparent negative loss at the blade root. Author



**A84-46927\*#** United Technologies Research Center, East Hartford, Conn.

**INLET BOUNDARY LAYER EFFECTS IN AN AXIAL COMPRESSOR ROTOR. II - THROUGHFLOW EFFECTS**

J. H. WAGNER, R. P. DRING, and H. D. JOSLYN (United Technologies Research Center, East Hartford, CT) American Society of Mechanical Engineers, International Gas Turbine Conference and Exhibit, 29th, Amsterdam, Netherlands, June 4-7, 1984. 6 p. refs

(Contract F33615-77-C-2083; NAS3-23157)  
(ASME PAPER 84-GT-85)

This paper presents results of an experimental aerodynamic study conducted in the rotating frame of reference downstream of an isolated compressor rotor with both thick and thin inlet endwall boundary layers. The paper focuses on those aspects of the data having particular significance to the assumptions and application of throughflow theory. These aspects include the spanwise distributions of static pressure and blockage, and the radial redistribution of fluid as it passes through the blade row. It is demonstrated that the main contributions to total pressure loss, blockage, and the distortion of the static pressure field were due to the hub corner stall and tip leakage. This is a significant departure from previous conclusions which looked to the endwall boundary layer and to secondary flow as major loss and blockage producing mechanisms.

Author

**A84-46985\*#** General Electric Co., Cincinnati, Ohio.

**LOSS REDUCTION IN AXIAL-FLOW COMPRESSORS THROUGH LOW-SPEED MODEL TESTING**

D. C. WISLER (General Electric Co., Aircraft Engine Group, Cincinnati, OH) American Society of Mechanical Engineers, International Gas Turbine Conference and Exhibit, 29th, Amsterdam, Netherlands, June 4-7, 1984. 10 p. refs

(Contract NAS3-20070)  
(ASME PAPER 84-GT-184)

A systematic procedure for reducing losses in axial-flow compressors is presented. In this procedure, a large, low-speed, aerodynamic model of a high-speed core compressor is designed and fabricated based on aerodynamic similarity principles. This model is then tested at low speed where high-loss regions associated with three-dimensional endwall boundary layers flow separation, leakage, and secondary flows can be located, detailed measurements made, and loss mechanisms determined with much greater accuracy and much lower cost and risk than is possible in small, high-speed compressors. Design modifications are made by using custom-tailored airfoils and vector diagrams, airfoil endbends, and modified wall geometries in the high-loss regions. The design improvements resulting in reduced loss or increased stall margin are then scaled to high speed. This paper describes the procedure and presents experimental results to show that in some cases endwall loss has been reduced by as much as 10 percent, flow separation has been reduced or eliminated, and stall margin has been substantially improved by using these techniques.

Author

**A84-46991\*#** Pennsylvania State Univ., University Park.

**AN EXPERIMENTAL STUDY OF THE COMPRESSOR ROTOR BLADE BOUNDARY LAYER**

M. POUAGARE, B. LAKSHMINARAYANA (Pennsylvania State University, University Park, PA), and J. M. GALMES (Pennsylvania State University, University Park, PA; Societe Europeenne de Propulsion, Vernon, Eure, France) American Society of Mechanical Engineers, International Gas Turbine Conference and Exhibit, 29th, Amsterdam, Netherlands, June 4-7, 1984. 9 p. refs

(Contract NSG-3268)  
(ASME PAPER 84-GT-193)

The three-dimensional turbulent boundary layer developing on a rotor blade of an axial flow compressor was measured using a miniature 'x' configuration hot-wire probe. The measurements were carried out at nine radial locations on both surfaces of the blade at various chordwise locations. The data derived includes streamwise and radial mean velocities and turbulence intensities. The validity of conventional velocity profiles such as the 'power

law profile' for the streamwise profile, and Mager and Eichelbrenner's for the radial profile, is examined. A modification to Mager's crossflow profile is proposed. Away from the blade tip, the streamwise component of the blade boundary layer seems to be mainly influenced by the streamwise pressure gradient. Near the tip of the blade, the behavior of the blade boundary layer is affected by the tip leakage flow and the annulus wall boundary layer. The 'tangential blockage' due to the blade boundary layer is derived from the data. The profile losses are found to be less than that of an equivalent cascade, except in the tip region of the blade.

Author

**A84-46995\*#** Army Propulsion Lab., Cleveland, Ohio.

**INVESTIGATION OF THE THREE-DIMENSIONAL FLOW FIELD WITHIN A TRANSONIC FAN ROTOR - EXPERIMENT AND ANALYSIS**

M. J. PIERZGA (U.S. Army, Propulsion Laboratory, Cleveland, OH) and J. R. WOOD (NASA, Lewis Research Center, Cleveland, OH) American Society of Mechanical Engineers, International Gas Turbine Conference and Exhibit, 29th, Amsterdam, Netherlands, June 4-7, 1984. 13 p. refs

(ASME PAPER 84-GT-200)

An experimental investigation of the three-dimensional flow field through a low aspect ratio, transonic, axial flow fan rotor has been conducted, using an advanced laser anemometer (LA) system. Laser velocimeter measurements of the rotor flow field at the design operating speed and over a range of throughflow conditions are compared to analytical solutions. The numerical technique used herein yields the solution to the full, three-dimensional, unsteady Euler equations using an explicit time-marching, finite volume approach. The numerical analysis, when coupled with a simplified boundary layer calculation, generally yields good agreement with the experimental data. The test rotor has an aspect ratio of 1.56, a design total pressure ratio of 1.629 and a tip relative Mach number of 1.38. The high spatial resolution of the LA data matrix (9 radial x 30 axial x 50 blade-to-blade) permits details of the transonic flow field such as shock location, turning distribution, and blade loading levels to be investigated and compared to analytical results.

Author

**N84-10022\*#** Massachusetts Inst. of Tech., Cambridge.

**EIGENMODE ANALYSIS OF UNSTEADY ONE-DIMENSIONAL EULER EQUATIONS Final Report**

M. GILES Aug. 1983 19 p. refs

(Contract NAS1-17130; NAG3-9)

(NASA-CR-172217; NAS 1.26:172217; REPT-83-47) Avail: NTIS HC A02/MF A01 CSCL 01A

The initial boundary value problem describing the evolution of unsteady linearized perturbations of a steady, uniform subsonic flow is analyzed. The eigenmodes and eigenfrequencies of the system are derived and several examples are presented to illustrate the effect of different boundary conditions on the exponential decay rate of the eigenmodes. The resultant implications for the stability and convergence rates of finite difference computations are discussed.

Author

**N84-13149\*#** Georgia Inst. of Tech., Atlanta.

**A VISCOUS-INVISCID INTERACTIVE PROCEDURE FOR ROTATIONAL FLOW IN CASCADES OF TWO DIMENSIONAL AIRFOILS OF ARBITRARY SHAPE Final Report, 15 Mar. 1979 - 13 Aug. 1982**

W. A. JOHNSTON 1983 65 p. refs

(Contract NSG-3260)

(NASA-CR-174609, NAS 1.26:174609) Avail: NTIS HC A04/MF A01

A viscous-inviscid interactive calculation procedure is developed for application to flow in cascades of two-dimensional airfoils. This procedure has essentially three components. First, a numerical solution of the Euler equations which can accommodate an arbitrarily specified cascade geometry is carried out on a nonorthogonal curvilinear grid mesh that is fitted to the geometry of the cascade. A method of grid generation has been used which relies in part on a succession of conformal mappings. Second, a viscous solution

## 02 AERODYNAMICS

for use in boundary layers and wake regions was programmed. Finally, an interactive scheme which takes the form of a source-sink distribution along the blade surface and wake centerline is employed. Results were obtained with this procedure for several cascade flow situations, and some comparisons with experiment are presented. Author

**N84-14120\*#** National Aeronautics and Space Administration. Lewis Research Center, Cleveland, Ohio.

### **DESIGN AND PERFORMANCE OF A FIXED, NONACCELERATING, GUIDE VANE CASCADE THAT OPERATES OVER AN INLET FLOW ANGLE RANGE OF 60 DEG**

J. M. SANZ, E. R. MCFARLAND, N. L. SANGER, T. F. GELDER, and R. H. CAVICCHI 1984 18 p refs Proposed for presentation at the 29th Ann. Intern. Gas Turbine Conf., Amsterdam, 3-7 Jun. 1984; sponsored by ASME (NASA-TM-83519; E-1868; NAS 1.15:83519) Avail. NTIS HC A02/MF A01 CSCL 01A

A unique set of wind tunnel guide vanes are designed with an inverse design code and analyzed with a panel method and an integral boundary layer code developed at the NASA Lewis Research Center. The fixed guide vanes, 80 feet long with 6-foot chord length, were designed for the NASA Ames 40 x 80/80 x 120 ft Wind Tunnel. Low subsonic flow is accepted over a 60 deg range of inlet angle from either the 40 x 80 leg or the 80 x 120 leg of the wind tunnel, and directed axially into the main leg of the tunnel where drive fans are located. Experimental tests of 1/10-scale models were conducted to verify design calculations. Author

**N84-14121\*#** National Aeronautics and Space Administration. Lewis Research Center, Cleveland, Ohio

### **MULTICOMPONENT VELOCITY MEASUREMENT IN A PISTON-CYLINDER CONFIGURATION USING LASER VELOCIMETRY**

H. J. SCHOCK, C. A. REGAN, W. J. RICE, and R. A. CHLEBECEK (TSI, Inc., St. Paul) Dec. 1983 19 p refs (NASA-TM-83534; E-1835; NAS 1.15:83534) Avail. NTIS HC A02/MF A01 CSCL 01A

Because of its nonintrusive nature, Laser Doppler Velocimetry (LDV) has become a popular tool for velocity measurements in internal combustion engines. This work shows how one can use an on-axis measurement technique, in conjunction with the standard two-channel LDV technique, to make simultaneous three-component measurements using a single focusing lens. Simultaneous measurement of two of these three components in a piston-cylinder configuration is demonstrated. Author

**N84-16141\*#** National Aeronautics and Space Administration. Lewis Research Center, Cleveland, Ohio.

### **ANALYTICAL STUDY OF BLOWING BOUNDARY-LAYER CONTROL FOR SUBSONIC V/STOL INLETS**

D. P. HWANG 1984 15 p refs Presented at the 7th Ann. Energy-Sources Technol. Conf. and Exhibition, New Orleans, 12-16 Feb. 1984

(NASA-TM-83576; E-1963; NAS 1.15:83576) Avail. NTIS HC A02/MF A01 CSCL 01A

The analytical methods used to study blowing boundary-layer control (BLC) for subsonic V/STOL inlets are described. The methods are then shown to give good agreement with experimental results, both with and without blowing BLC. Finally, because of this good agreement, the methods were used to determine analytically the optimum (minimum blowing power required) location and height for a blowing slot within a subsonic V/STOL inlet. S.L.

**N84-16142\*#** National Aeronautics and Space Administration. Lewis Research Center, Cleveland, Ohio.

### **ASSESSMENT OF THREE-DIMENSIONAL INVISCID CODES AND LOSS CALCULATIONS FOR TURBINE AERODYNAMIC COMPUTATIONS**

L. A. POVINELLI 1984 27 p refs To be presented at the 29th Ann. Intern. Gas Turbine Conf., Amsterdam, 3-7 Jun. 1984 (NASA-TM-83571; E-1951; NAS 1.15:83571) Avail. NTIS HC A03/MF A01 CSCL 01A

An assessment of several three dimensional inviscid turbine aerodynamic computer codes and loss models used at the NASA Lewis Research Center is presented. Five flow situations are examined, for which both experimental data and computational results are available. The five flows form a basis for the evaluation of the computational procedures. It was concluded that stator flows may be calculated with a high degree of accuracy, whereas, rotor flow fields are less accurately determined. Exploitation of contouring, learning, bowing, and sweeping will require a three dimensional viscous analysis technique. Author

**N84-16145\*#** Ohio State Univ., Columbus. Dept. of Aeronautical and Astronautical Engineering.

### **RESULTS OF AN EXPERIMENTAL PROGRAM INVESTIGATING THE EFFECTS OF SIMULATED ICE ON THE PERFORMANCE OF THE NACA 63A415 AIRFOIL WITH FLAP Final Report**

R. J. ZAGULI, M. B. BRAGG, and G. M. GREGOREK Jan. 1984 183 p refs

(Contract NAG3-28)

(NASA-CR-168288; NAS 1.26:168288; AARL-TR-83-2) Avail. NTIS HC A09/MF A01 CSCL 01A

Aerodynamic data from a test program in the Icing Research Tunnel are reported for a NACA 63A415 airfoil, with fowler flap, clean and with simulated ice shapes. The effect of three ice shapes on airfoil performance are presented, two of the simulated ice shapes are from earlier Icing Tunnel tests. Lift, drag, and moment coefficients are reported for the airfoil, clean and with ice, for angles of attack from approximately zero lift to maximum lift and for flap deflections of 0, 10, 20, and 30 degrees. Surface pressure distribution plots for the airfoil and flap are presented for all runs. Some preliminary oil flow visualization data are also discussed. Large drag penalties were measured in all instances. Maximum lift penalties were in general serious, and depend upon the ice shape and flap deflection S.L.

**N84-16146\*#** Ohio State Univ., Columbus. Dept. of Aeronautical and Astronautical Engineering.

### **POTENTIAL FLOW ANALYSIS OF GLAZE ICE ACCRETIONS ON AN AIRFOIL Final Report**

R. J. ZAGULI Jan. 1984 87 p refs

(Contract NAG3-28)

(NASA-CR-168282; NAS 1.26:168282) Avail. NTIS HC A05/MF A01 CSCL 01A

The results of an analytical/experimental study of the flow fields about an airfoil with leading edge glaze ice accretion shapes are presented. Tests were conducted in the Icing Research Tunnel to measure surface pressure distributions and boundary layer separation reattachment characteristics on a general aviation wing section to which was affixed wooden ice shapes which approximated typical glaze ice accretions. Comparisons were made with predicted pressure distributions using current airfoil analysis codes as well as the Brstow mixed analysis/design airfoil panel code. The Brstow code was also used to predict the separation reattachment dividing streamline by inputting the appropriate experimental surface pressure distribution. S.L.

**N84-17138\*#** National Aeronautics and Space Administration. Lewis Research Center, Cleveland, Ohio.  
**PROGRAMS FOR CALCULATING QUASI-THREE-DIMENSIONAL FLOW IN A TURBOMACHINE BLADE ROW**  
 T. KATSANIS 1984 22 p refs Presented at the Computational Fluid Dyn User's Workshop, Tullahoma, Tenn. 12-16 Mar. 1984 (NASA-TM-83588; E-1983; NAS 1.15:83588) Avail: NTIS HC A02/MF A01 CSCL 01A

MERIDL is a program that calculates a meridional plane stream function solution, and TSONIC is a program that calculates a blade to blade stream function solution for turbomachine blade passages. Both programs are discussed, including input required and assumptions and limitations. Examples of use and references are included. Author

**N84-17139\*#** Ohio State Univ., Columbus. Lab. for Aeronautical and Astronautical Research.  
**DOCUMENTATION OF ICE SHAPES ON THE MAIN ROTOR OF A UH-1H HELICOPTER IN HOVER** Final Report  
 J. D. LEE, R. HARDING (Hovey and Assoc., Ltd.), and R. L. PALKO (Calspan Field Services, Inc.) Jan. 1984 30 p refs (Contract NAG3-273) (NASA-CR-168332; NAS 1.26:168332) Avail: NTIS HC A03/MF A01 CSCL 01C

A helicopter icing flight test program in the hover mode was conducted with a UH-1H aircraft. The ice formations were documented after landing by means of silicone rubber molds, stereo photography and outline tracings for later use in aerodynamic analyses. The documentation techniques are described and the results presented for a typical flight S.L.

**N84-17142\*#** National Aeronautics and Space Administration. Lewis Research Center, Cleveland, Ohio.  
**COMPARISON OF SECONDARY FLOWS PREDICTED BY A VISCOUS CODE AND AN INVISCID CODE WITH EXPERIMENTAL DATA FOR A TURNING DUCT**  
 J. R. SCHWAB and L. A. POVINELLI 1984 21 p refs Presented at the Symp on Computation of Internal Flows: Methods and Appl, New Orleans, 13-15 Feb. 1984; sponsored by ASME (NASA-TM-83575; E-1958; NAS 1.15:83575) Avail: NTIS HC A02/MF A01 CSCL 01A

A comparison of the secondary flows computed by the viscous Kreskovsky-Briley-McDonald code and the inviscid Denton code with benchmark experimental data for turning duct is presented. The viscous code is a fully parabolized space-marching Navier-Stokes solver while the inviscid code is a time-marching Euler solver. The experimental data were collected by Taylor, Whitelaw, and Yianneskis with a laser Doppler velocimeter system in a 90 deg turning duct of square cross-section. The agreement between the viscous and inviscid computations was generally very good for the streamwise primary velocity and the radial secondary velocity, except at the walls, where slip conditions were specified for the inviscid code. The agreement between both the computations and the experimental data was not as close, especially at the 60.0 deg and 77.5 deg angular positions within the duct. This disagreement was attributed to incomplete modelling of the vortex development near the suction surface. Author

**N84-17143\*#** National Aeronautics and Space Administration. Lewis Research Center, Cleveland, Ohio.  
**INVESTIGATION OF FLOW PHENOMENA IN A TRANSONIC FAN ROTOR USING LASER ANEMOMETRY**  
 A. J. STRAZISAR 1984 23 p refs Proposed for presentation at the 29th Ann Intern. Gas Turbine Conf., Amsterdam, 3-7 Jun. 1984; sponsored by ASME (NASA-TM-83555; E-1934; NAS 1.15:83555) Avail: NTIS HC A02/MF A01 CSCL 01A

Several flow phenomena including flowfield periodicity, rotor shock oscillation, and rotor shock system geometry were investigated in a transonic low aspect ratio fan rotor using laser anemometry. Flow periodicity is found to increase with increasing rotor pressure rise, and to correlate with blade geometry variations. Analysis of time-accurate laser anemometer data indicates that

the rotor shock oscillates about its mean location with an amplitude of 3 to 4 percent of rotor chord. The shock surface is nearly two-dimensional or levels of rotor pressure rise at and above the peak efficiency level but becomes more complex for lower levels of pressure rise. Spanwise shock lean generates radial flows due to streamline deflection in the hub-to-shroud streamsurface.

Author

**N84-20488\*#** Southern Methodist Univ., Dallas, Tex.  
**AN EXPERIMENTAL STUDY OF THE PROPERTIES OF SURFACE PRESSURE FLUCTUATIONS IN STRONG ADVERSE PRESSURE GRADIENT TURBULENT BOUNDARY LAYERS** Final Report, 1 Dec. 1982 - 31 Jan. 1984  
 R. L. SIMPSON 25 Mar. 1984 8 p refs (Contract NAG3-17) (NASA-CR-175410; NAS 1.26:175410) Avail: NTIS HC A02/MF A01 CSCL 01A

Experimental data were obtained on blade self-noise generation by strong adverse-pressure-gradient attached boundary layers and by separated turbulent boundary layers that accompany stall. Two microphones were calibrated, placed in plastic housing, and installed in a wind tunnel where observations of acoustic and turbulent signals permitted decomposition of the surface pressure fluctuation signals into the propagated acoustic part and the turbulent-flow generated portion. To determine the convective wave speed of the turbulent contributions, the microphones were spaced a small distance apart in the streamwise direction and correlations were obtained. The turbulent surface pressure spectra upstream of detachment and downstream of the beginning of separation are discussed as well as measurements of turbulent velocity spectra and wavespeeds. A.R.H.

**N84-20490\*#** National Aeronautics and Space Administration. Lewis Research Center, Cleveland, Ohio.  
**PROGRESS TOWARD THE DEVELOPMENT OF AN AIRCRAFT ICING ANALYSIS CAPABILITY**  
 R. J. SHAW 1984 37 p refs Presented at the 22nd Aerospace Sci. Meeting, Reno, Nev., 9-12 Jan. 1984; sponsored by AIAA (NASA-TM-83562; E-1941; NAS 1.15:83562) Avail: NTIS HC A03/MF A01 CSCL 01A

An overview of the NASA efforts to develop an aircraft icing analysis capability is presented. Discussions are included of the overall and long term objectives of the program as well as current capabilities and limitations of the various computer codes being developed. Descriptions are given of codes being developed to analyze two and three dimensional trajectories of water droplets, airfoil ice accretion, aerodynamic performance degradation of components and complete aircraft configurations, electrothermal deicer, and fluid freezing point depressant deicer. The need for bench mark and verification data to support the code development is also discussed. Author

**N84-20493\*#** National Aeronautics and Space Administration. Lewis Research Center, Cleveland, Ohio.  
**EXPERIMENTAL INVESTIGATION OF TANGENTIAL BLOWING APPLIED TO A SUBSONIC V/STOL INLET**  
 R. R. BURLEY Apr. 1984 20 p refs (NASA-TP-2297; E-1907; NAS 1.60:2297) Avail: NTIS HC A02/MF A01 CSCL 01A

Engine inlets for subsonic V/STOL aircraft must operate over a wide range of conditions without the severe internal flow separation that can cause sudden changes in engine thrust, excessively high fan blade stresses, and possibly core-compressor stall. An experimental investigation was conducted to evaluate the effectiveness of tangential blowing to maintain attached flow at high inlet angles of attack. The inlet had a relatively thin lip (lip contraction ratio of 1.46). Two blowing slot locations were investigated: one on the lip and the other in the diffuser. The effect of two slot heights (0.0508 and 0.152 cm) and three slot circumferential extents, the largest being 120 deg, also was investigated. The results showed that both lip and diffuser blowing were effective in maintaining attached flow at high angles of attack.

## 02 AERODYNAMICS

However, higher angle-of-attack capability was achieved with lip blowing than with diffuser blowing. This capability was achieved with the largest slot circumferential extent and either of the two slot heights. The tests were conducted in a low-speed wind tunnel at free-stream velocities between 18 and 62 m/sec and inlet angles of attack to 110 deg. B.W.

**N84-22533\*#** National Aeronautics and Space Administration. Lewis Research Center, Cleveland, Ohio.

### REDESIGN AND CASCADE TESTS OF A SUPERCRITICAL CONTROLLED DIFFUSION STATOR BLADE-SECTION

J. F. SCHMIDT, T. F. GELDER, and L. F. DONOVAN 1984 13 p refs Proposed for presentation at the 20th Joint Propulsion Conf., Cincinnati, 11-13 Jun. 1984; sponsored by AIAA, SAE and ASME

(NASA-TM-83635; E-2077; NAS 1.15:83635) Avail: NTIS HC A02/MF A01 CSCL 01A

A supercritical stator blade section, previously tested in cascade, and characterized by a flat-roof-top suction surface Mach number distribution, has been redesigned and retested. At near design conditions, the losses and air turning were improved over the original blade by 50 percent and 7 percent respectively. The key element in the improved performance was a small blade reshaping. This produced a continuous flow acceleration over the first one-third chord of the suction surface which successfully prevented a premature laminar separation bubble. Several recently available inviscid analysis and one fully viscous (Navier-Stokes) analysis code were used in the redesign process. The validity of these codes was enhanced by the test results. Author

**N84-24539\*#** National Aeronautics and Space Administration. Lewis Research Center, Cleveland, Ohio.

### CALCULATION OF TRANSONIC FLOW IN A LINEAR CASCADE

L. F. DONOVAN 1984 13 p refs Presented at the 20th Joint Propulsion Conf., Cincinnati, 11-13 Jun. 1984; sponsored by AIAA, SAE and ASME

(NASA-TM-83697; E-2155; NAS 1.15:83697) Avail: NTIS HC A02/MF A01 CSCL 01A

Turbomachinery blade designs are becoming more aggressive in order to achieve higher loading and greater range. New analysis tools are required to cope with these heavily loaded blades that may operate with a thin separated region near the trailing edge on the suction surface. An existing, viscous airfoil code was adapted to cascade conditions in an attempt to provide this capability. Comparisons with recently obtained data show that calculated and experimental surface Mach numbers were in good agreement but loss coefficients and outlet air angles were not. Author

**N84-25646\*#** Tennessee Univ., Knoxville. Dept. of Mechanical and Aerospace Engineering.

### MEASUREMENT OF LOCAL CONNECTIVE HEAT TRANSFER COEFFICIENTS OF FOUR ICE ACCRETION SHAPES Final Report

M. E. SMITH, R. V. ARMILLI, and E. G. KESHOCK May 1984 97 p refs

(Contract NAG3-83)

(NASA-CR-174680; NAS 1.26:174680) Avail: NTIS HC A05/MF A01 CSCL 20D

In the analytical study of ice accretions that form on aerodynamic surfaces (airfoils, engine inlets, etc.) it is often necessary to be able to calculate convective heat transfer rates. In order to do this, local convective heat transfer coefficients for the ice accretion shapes must be known. In the past, coefficients obtained for circular cylinders were used as an approximation to the actual coefficients since no better information existed. The purpose of this experimental study was to provide local convective heat transfer coefficients for four shapes that represent ice accretions. The shapes were tested with smooth and rough surfaces. The experimental method chosen was the thin-skin heat rate technique. Using this method local Nusselt numbers were determined for the ice shapes. In general it was found that the convective heat transfer was higher in regions where the model's

surfaces were convex and lower in regions where the model's surfaces were concave. The effect of roughness was to increase the heat transfer in the high heat transfer regions by approximately 100% while little change was apparent in the low heat transfer regions. Author

**N84-25647\*#** National Aeronautics and Space Administration. Lewis Research Center, Cleveland, Ohio.

### APPLICATION OF A QUASI-3D INVISCID FLOW AND BOUNDARY LAYER ANALYSIS TO THE HUB-SHOULD CONTOURING OF A RADIAL TURBINE

K. C. CIVINSKAS and L. A. POVINELLI 1984 21 p refs Presented at the 20th Joint Propulsion Conf., Cincinnati, 11-13 Jun. 1984; sponsored by the AIAA, SAE and ASME

(Contract DA PROJ. 1L1-61102-AH-45)

(NASA-TM-83669; E-2112; NAS 1.15:83669;

USAAVSCOM-TR-84-C-1; AIAA-84-1297) Avail: NTIS HC

A02/MF A01 CSCL 21E

Application of a quasi-3D approach to the aerodynamic analysis of several radial turbine configurations is described. The objective was to improve the rotor aerodynamic characteristics by hub-shroud contouring. The approach relies on available 2D inviscid methods coupled with boundary layer analysis to calculate profile, mixing, and endwall losses. Windage, tip clearance, incidence, and secondary flow losses are estimated from correlations. To eliminate separation along the hub and blade suction surfaces of a baseline rotor, the analysis was also applied to three alternate hub-shroud geometries. Emphasis was on elimination an inducer velocity overshoot as well as increasing hub velocities. While separation was never eliminated, the extent of the separated area was progressively reduced. Results are presented in terms of mid-channel and blade surface velocities; kinetic energy loss coefficients; and efficiency. The calculation demonstrates a first step for a systematic approach to radial turbine design that can be used to identify and control aerodynamic characteristics that ultimately determine heat transfer and component life. Experimentation will be required to assess the extent to which flow and boundary layer behavior were predicted correctly. M.G.

**N84-31091\*#** National Aeronautics and Space Administration. Lewis Research Center, Cleveland, Ohio.

### FEEDBACK IN SEPARATED FLOWS OVER SYMMETRIC AIRFOILS

H. M. ATASSI 1984 15 p refs Proposed for presentation at the 9th Aeroacoustics Conf., Williamsburg, Va., 15-17 Oct. 1984;

sponsored by the American Inst. of Aeronautics and Astronautics (NASA-TM-83758; E-2246; NAS 1.15:83758) Avail: NTIS HC

A02/MF A01 CSCL 01A

For a flow over an airfoil with laminar separation, a feedback cycle may exist whereby a Kelvin-Helmholtz instability wave emanating from the separation point on the airfoil surface grows along the shear layer and is diffracted as it interacts with the sharp trailing edge of the airfoil, causing acoustic radiation which, in turn, propagates upstream and regenerates the initial instability wave. The analysis is restricted to the high frequency limit. Solutions to the boundary-value problem are obtained using the slowly varying approximation and the method of matched asymptotic expansions. Resonant solutions exist for certain discrete values of the Reynolds and Strouhal numbers. The results are discussed and compared with available data. Author

**N84-31096\*#** National Aeronautics and Space Administration. Lewis Research Center, Cleveland, Ohio.

### ACOUSTIC EXCITATION: A PROMISING NEW MEANS OF CONTROLLING SHEAR LAYERS

J. R. STONE and D. J. MCKINZIE, JR. 1984 33 p refs Presented at the ASME Appl. Mech. Div. Summer Meeting, San Antonio, 17-21 Jun. 1984

(NASA-TM-83772; E-2263; NAS 1.15:83772) Avail: NTIS HC

A03/MF A01 CSCL 01A

Techniques have long been sought for the controlled modification of turbulent shear layers, such as in jets, wakes, boundary layers, and separated flows. Relatively recently published

results of laboratory experiments have established that coherent structures exist within turbulent flows. These results indicate that even apparently chaotic flow fields can contain deterministic, nonrandom elements. Even more recently published results show that deliberate acoustic excitation of these coherent structures has a significant effect on the mixing characteristics of shear layers. Therefore, we have initiated a research effort to develop both an understanding of the interaction mechanisms and the ability to use it to favorably modify various shear layers. Acoustic excitation circumvents the need for pumping significant flow rates, as required by suction or blowing. Control of flows by intentional excitation of natural flow instabilities involves new and largely unexplored phenomena and offers considerable potential for improving component performance. Nonintrusive techniques for flow field control may permit much more efficient, flexible propulsion systems and aircraft designs, including means of stall avoidance and recovery. The techniques developed may also find application in many other areas where mixing is important, such as reactors, continuous lasers, rocket engines, and fluidic devices. It is the objective of this paper to examine some potential applications of the acoustic excitation technique to various shear layer flows of practical aerospace systems. Author

**N84-32351\*#** National Aeronautics and Space Administration. Lewis Research Center, Cleveland, Ohio.

#### UNSTEADY TRANSONIC FLOW IN CASCADES

S. P. SURAMPUDI (Cleveland State Univ.) and J. J. ADAMCZYK 1984 8 p refs Presented at the Unsteady Aerodyn. of Turbomachines and propellers, Cambridge, England, 24-27 Sep. 1983; sponsored by IUTAM (NASA-TM-83780; E-2272; NAS 1.15:83780) Avail: NTIS HC A02/MF A01 CSDL 01A

There is a need for methods to predict the unsteady air loads associated with flutter of turbomachinery blading at transonic speeds. The results of such an analysis in which the steady relative flow approaching a cascade of thin airfoils is assumed to be transonic, irrotational, and isentropic is presented. The blades in the cascade are allowed to undergo a small amplitude harmonic oscillation which generates a small unsteady flow superimposed on the existing steady flow. The blades are assumed to oscillate with a prescribed motion of constant amplitude and interblade phase angle. The equations of motion are obtained by linearizing about a uniform flow the inviscid nonheat conducting continuity and momentum equations. The resulting equations are solved by employing the Weiner Hopf technique. The solution yields the unsteady aerodynamic forces acting on the cascade at Mach number equal to 1. Making use of an unsteady transonic similarity law, these results are compared with the results obtained from linear unsteady subsonic and supersonic cascade theories. A parametric study is conducted to find the effects of reduced frequency, solidity, stagger angle, and position of pitching axis on the flutter. Author

**N84-32355\*#** United Technologies Research Center, East Hartford, Conn.

#### A LINEAR AERODYNAMIC ANALYSIS FOR UNSTEADY TRANSONIC CASCADES Final Report

J. M. VERDON and J. R. CASPAR Washington NASA Sep. 1984 80 p refs (Contract NAS3-23696) (NASA-CR-3833; E-2202; NAS 1.26:3833; R34-956393-8) Avail: NTIS HC A05/MF A01 CSDL 01A

A potential flow analysis to predict unsteady airloads produced by the vibrations of turbomachinery blades operating at transonic Mach numbers is presented. The unsteady aerodynamic model includes the effects of blade geometry, finite mean pressure variation across the blade row, high frequency blade motion, and shock motion within the framework of a linearized, frequency domain formulation. The unsteady equations are solved implicit, least squares, finite difference approximation which is applicable on arbitrary grids. A numerical solution for the entire unsteady field is determined by matching a solution determined on a rectilinear type cascade mesh, which covers an extended blade

passage region, to a solution determined on a detailed polar type local mesh, which covers and extends well beyond the supersonic region(s) adjacent to a blade surface. Cascades of double circular arc and flat plate blades demonstrate the unsteady analysis, and partially illustrate the effects of blade geometry, inlet Mach number, blade vibration frequency and shock motion on unsteady response. E.A.K.

**N84-32357\*#** National Aeronautics and Space Administration. Lewis Research Center, Cleveland, Ohio.

#### INVESTIGATION OF THE THREE-DIMENSIONAL FLOW FIELD WITHIN A TRANSONIC FAN ROTOR: EXPERIMENT AND ANALYSIS

M. J. PIERZGA and J. R. WOOD 1984 26 p refs Presented at the 29th Ann. Intern. Gas Turbine Conf., Amsterdam, 3-7 Jun 1984; sponsored by ASME Prepared in cooperation with Army Research and Technology Labs., Cleveland (NASA-TM-83739; E-2150; NAS 1.15:83739; USAAVSCOM-TR-83-C-16) Avail: NTIS HC A03/MF A01 CSDL 01A

An experimental investigation of the three dimensional flow field through a low aspect ratio, transonic, axial flow fan rotor has been conducted using an advanced laser anemometer (LA) system. Laser velocimeter measurements of the rotor flow field at the design operating speed and over a range of through flow conditions are compared to analytical solutions. The numerical technique used herein yields the solution to the full, three dimensional, unsteady Euler equations using an explicit time marching, finite volume approach. The numerical analysis, when coupled with a simplified boundary layer calculation, generally yields good agreement with the experimental data. The test rotor has an aspect ratio of 1.56, a design total pressure ratio of 1.629 and a tip relative Mach number of 1.38. The high spatial resolution of the LA data matrix (9 radial by 30 axial by 50 blade to blade) permits details of the transonic flow field such as shock location, turning distribution and blade loading levels to be investigated and compared to analytical results. Author

## 03

### AIR TRANSPORTATION AND SAFETY

Includes passenger and cargo air transport operations; and aircraft accidents.

**A84-26580\*#** Minnesota Univ., Minneapolis  
**STEADY STATE STRESSES IN RIBBON PARACHUTE CANOPIES**

W. L. GARRARD, K. Y. WU (Minnesota, University, Minneapolis, MN), and K. K. MURAMOTO (NASA, Lewis Research Center, Cleveland, OH; Minnesota, University, Minneapolis, MN) IN: Aerodynamic Decelerator and Balloon Technology Conference, 8th, Hyannis, MA, April 2-4, 1984, Technical Papers. New York, American Institute of Aeronautics and Astronautics, 1984, p. 191-199. Research supported by Sandia National Laboratory. refs (AIAA PAPER 84-0816)

An experimental study of the steady state stresses in model ribbon parachute canopies is presented. The distribution of circumferential stress was measured in the horizontal ribbons of two parachutes using Omega sensors. Canopy pressure distributions and overall drag were also measured. Testing was conducted in the University of Minnesota Low-Speed Wind Tunnel at dynamic pressures ranging from 1.0 to 1.5 inches of water. The stresses in the parachute canopies were calculated using the parachute structural analysis code, CANO. It was found that the general shape of the measured and calculated stress distributions was fairly similar; however, the measured stresses were somewhat less than the calculated stresses. Author

**A84-37935\*#** Ohio State Univ., Columbus.

**EFFECT OF GEOMETRY ON AIRFOIL ICING CHARACTERISTICS**

M. B. BRAGG (Ohio State University, Columbus, OH) Journal of Aircraft (ISSN 0021-8669), vol. 21, July 1984, p. 505-511. refs (Contract NAG3-28)

A droplet trajectory computer code is used to predict the water droplet impingement characteristics of several low- and medium-speed airfoils. The maximum impingement efficiency, total collection efficiency, and limits of impingement are analyzed as functions of the airfoil geometry and freestream conditions. The airfoil geometry is represented by leading edge radius, maximum thickness, maximum camber, and angle of attack. The analysis shows that the primary effects are an increase in maximum impingement efficiency with a decrease in leading edge radius, a reduction in total collection efficiency for thicker airfoils, and a change in the limits of impingement for airfoils of different maximum camber. Author

**A84-39280\*#** Wichita State Univ., Kans.

**FLIGHT AND WIND TUNNEL TESTS OF AN ELECTRO-IMPULSE DE-ICING SYSTEM**

G. W. ZUMWALT (Wichita State University, Wichita, KS) and A. A. MUELLER (Cessna Aircraft Co., Wichita, KS) IN: General Aviation Technology Conference, Hampton, VA, July 10-12, 1984, Technical Papers. New York, American Institute of Aeronautics and Astronautics, 1984, p. 26-36. Research supported by the Kansas State Advance Technology Commission. refs (Contract NAG3-284) (AIAA PAPER 84-2234)

A joint University-Industry project has been sponsored by NASA Lewis Research Center to develop the Electro-Impulse method for de-icing aircraft. The program has consisted of basic analyses, laboratory testing, icing tunnel tests, and flight tests. During the past two years, the EIDI system has been tested and refined, and has been shown to be a low-energy, highly reliable de-icing system for a wide range of conditions. This paper gives a brief review of conditions. This paper gives a brief review of the basic principles, the development history, and results of recent flight tests by NASA and by Cessna Aircraft Company. Author

**A84-45054\*#** Ohio State Univ., Columbus.

**EXPERIMENTAL AND ANALYTICAL INVESTIGATIONS INTO AIRFOIL ICING**

M. B. BRAGG, G. M. GREGOREK, and J. D. LEE (Ohio State University, Columbus, OH) IN: International Council of the Aeronautical Sciences, Congress, 14th, Toulouse, France, September 9-14, 1984, Proceedings. Volume 2. New York, American Institute of Aeronautics and Astronautics, 1984, p. 1127-1138. refs (Contract NAG3-28)

Methods of analyzing and measuring experimentally the accretion of ice and its effect on airfoil aerodynamic performance are presented. An analytical method for predicting water droplet impingement has been developed and shows the influence of airfoil leading edge radius and thickness on droplet impingement to be significant. Rime ice accretions are predicted including time dependent effects and these shapes compare well to experiment. Scaling water droplet impingement and rime ice accretion is discussed. Predictions of the effect of rime ice on airfoil performance are developed based on empirical and analytical methods. Techniques for measuring and simulating ice accretions for wind tunnel tests compare well to actual iced airfoil aerodynamic data. Data showing the effect of ice on measured airfoil performance using real and simulated ice are presented. Author

**N84-11152\*#** Control Data Corp., Minneapolis, Minn.

**TEMPERATURE HISTORIES OF COMMERCIAL FLIGHTS AT SEVERE CONDITIONS FROM GASP DATA Final Report**

W. H. JASPERSON and G. D. NASTROM Oct. 1983 64 p refs

(Contract NAS3-21249)

(NASA-CR-168247; NAS 1.26:168247) Avail NTIS HC A04/MF A01 CSCL 01C

The thermal environment of commercial aircraft from a data set gathered during the Global Atmospheric Sampling Program (GASP) is studied. The data set covers a four-year period of measurements. The report presents plots of airplane location and speed and atmospheric temperature as functions of elapsed time for 35 extreme-condition flights, selected by minimum values of several temperature parameters. One of these parameters, the severity factor, is an approximation of the in-flight wing-tank temperature. Representative low-severity-factor flight histories may be useful for actual temperature-profile inputs to design and research studies. Comparison of the GASP atmospheric temperatures to interpolated temperatures from National Meteorological Center and Global Weather Central analysis fields shows that the analysis temperatures are slightly biased toward warmer than actual temperatures, particularly over oceans and at extreme conditions. Author

## 05

### AIRCRAFT DESIGN, TESTING AND PERFORMANCE

Includes aircraft simulation technology.

**A84-17406\*#** Texas A&M Univ., College Station.

**PERFORMANCE DEGRADATION OF PROPELLER SYSTEMS DUE TO RIME ICE ACCRETION**

K. D. KORKAN (Texas A & M University, College Station, TX), L. DADONE (Boeing Vertol Co., Philadelphia, PA), and R. J. SHAW (NASA, Lewis Research Center, Icing Research Section, Cleveland, OH) Journal of Aircraft (ISSN 0021-8669), vol. 21, Jan. 1984, p. 44-49. refs (Contract NAG3-109; NAG3-242) (AIAA PAPER 82-0286)

A theoretical ice accretion model has been established applicable to both aircraft propellers and helicopter rotors to determine the effect of rime ice on the thrust, power, and efficiency as a function of exposure time in a natural icing condition. Comparisons have been made of theoretical performance levels with previously published experimentally determined propeller thrust and efficiency for five natural icing conditions. Agreement between test and theory was acceptable. Author

**A84-17412\*#** Texas A&M Univ., College Station.

**HELICOPTER ROTOR PERFORMANCE DEGRADATION IN NATURAL ICING ENCOUNTER**

K. D. KORKAN (Texas A & M University, College Station, TX), L. DADONE (Boeing Vertol Co., Philadelphia, PA), and R. J. SHAW (NASA, Lewis Research Center, Cleveland, OH) Journal of Aircraft (ISSN 0021-8669), vol. 21, Jan. 1984, p. 84, 85. (Contract NAG3-109; NAG3-242)

The analytical model described by Korkan et al. (1982) for predicting the performance degradation of propellers in a natural icing encounter is used to determine the feasibility of predicting helicopter performance degradation in hover during natural icing. The flight condition selected for analysis involves an altitude of 3000 ft and a free-air temperature of 1 F. The values of degradation yielded by the model for rime ice accretion are representative of those experienced in actual flight. C.R.



**A84-17937\*# Texas A&M Univ., College Station.**  
**EXPERIMENTAL STUDY OF PERFORMANCE DEGRADATION**  
**OF A MODEL HELICOPTER MAIN ROTOR WITH SIMULATED**  
**ICE SHAPES**

K. D. KORKAN, E. J. CROSS, JR. (Texas A & M University, College Station, TX), and C. C. CORNELL American Institute of Aeronautics and Astronautics, Aerospace Sciences Meeting, 22nd, Reno, NV, Jan. 9-12, 1984. 14 p refs  
 (Contract NAG3-242)  
 (AIAA PAPER 84-0184)

An experimental study utilizing a remote controlled model helicopter has been conducted to measure the performance degradation due to simulated ice accretion on the leading edge of the main rotor for hover and forward flight. The 53.375 inch diameter main rotor incorporates a NACA 0012 airfoil with a generic ice shape corresponding to a specified natural ice condition. Thrust coefficients and torque coefficients about the main rotor were measured as a function of velocity, main rotor RPM, angle-of-incidence of the fuselage, collective pitch angle, and extent of spanwise ice accretion. An experimental airfoil data bank has been determined using a two-dimensional twenty-one inch NACA 0012 airfoil with scaled ice accretion shapes identical to that used on the model helicopter main rotor. The corresponding experimental data are discussed with emphasis on Reynolds number effects and ice accretion scale model testing. Author

**A84-21289\*# National Aeronautics and Space Administration.**  
 Lewis Research Center, Cleveland, Ohio.

**PERFORMANCE DEGRADATION OF A TYPICAL TWIN ENGINE**  
**COMMUTER TYPE AIRCRAFT IN MEASURED NATURAL ICING**  
**CONDITIONS**

R. J. RANAUDO, K. L. MIKKELSEN, R. C. MCKNIGHT (NASA, Lewis Research Center, Cleveland, OH), and P. J. PERKINS, JR. (Analex Corp., Dayton, OH) American Institute of Aeronautics and Astronautics, Aerospace Sciences Meeting, 22nd, Reno, NV, Jan. 9-12, 1984. 31 p. refs  
 (AIAA PAPER 84-0179)

The performance of an aircraft in various measured icing conditions was investigated. Icing parameters such as liquid water content, temperature, cloud droplet sizes and distributions were measured continuously while in icing. Flight data were reduced to provide plots of the aircraft drag polars and lift curves (CL vs. alpha) for the measured 'iced' condition as referenced to the uniced aircraft. These data were also reduced to provide plots of thrust horsepower required vs. single engine power available to show how icing affects engine out capability. It is found that performance degradation is primarily influenced by the amount and shape of the accumulated ice. Glaze icing caused the greatest aerodynamic performance penalties in terms of increased drag and reduction in lift while aerodynamic penalties due to rime icing were significantly lower. Previously announced in STAR as N84-13173. Author

**A84-24195\*# Texas A&M Univ., College Station.**  
**PERFORMANCE DEGRADATION OF A MODEL HELICOPTER**  
**MAIN ROTOR IN HOVER AND FORWARD FLIGHT WITH A**  
**GENERIC ICE SHAPE**

K. D. KORKAN, E. J. CROSS, JR. (Texas A & M University, College Station, TX), and T. L. MILLER IN: Aerodynamic Testing Conference, 13th, San Diego, CA, March 5-7, 1984, Technical Papers. New York, American Institute of Aeronautics and Astronautics, 1984, p. 187-200. refs  
 (Contract NAG3-242)  
 (AIAA PAPER 84-0609)

A model helicopter has been used to collect test data and provide an experimental means of studying helicopter performance in a subsonic wind tunnel. A simulated generic ice shape was attached to the rotor blades and performance data were obtained for both hover and forward flights. Significant degradation in helicopter performance with respect to torque and thrust coefficient was observed; the rotor tip region was especially sensitive. Two-dimensional wind tunnel tests were conducted over a Reynolds number range  $0.7-3 \times 10^6$  to the 6th in order to investigate the

effect of Reynolds number on the aerodynamic performance of the airfoil in both clean and iced configurations. Only minimal dependence of the aerodynamic data on Reynolds number was observed. C.D.

**A84-29452\* Air Force Systems Command, Wright-Patterson AFB, Ohio.**

**UNCERTAINTY METHODOLOGY FOR IN-FLIGHT THRUST**  
**DETERMINATION**

G. R. ADAMS (USAF, Wright-Patterson AFB, OH), J. W. THOMPSON, JR. (Sverdrup Technology, Inc., Tullahoma, TN), R. B. ABERNETHY (United Technologies Corp., Pratt and Whitney Group, East Hartford, CT), T. BIESIADNY (NASA, Lewis Research Center, Cleveland, OH), C. T. HAVEY (Boeing Military Airplane Co., Wichita, KS), J. W. STEURER (McDonnell Aircraft Co., St. Louis, MO), J. C. ASCOUGH (Royal Aircraft Establishment, Farnborough, Hants., England), and D. D. WILLIAMS (Rolls-Royce, Ltd., London, England) IN: Advances in aerospace propulsion; Proceedings of the Aerospace Congress and Exposition, Long Beach, CA, October 3-6, 1983. Warrendale, PA, Society of Automotive Engineers, Inc., 1983, p. 1-8.  
 (SAE PAPER 831438)

A methodology is proposed for the evaluation of uncertainty in the in-flight determination of aircraft thrust, which provides error traceability to a national standards laboratory, and is independent of the procedure used to calculate or measure thrust in flight, thereby yielding a consistent means for the evaluation of measurement capabilities. Attention is given to the factors of measurement error, precision, bias, uncertainty, error estimation and classification, error propagation, ground testing, and the related problems of model bias error, model precision error, and the uncertainty limit. O.C.

**A84-29453\* Air Force Systems Command, Wright-Patterson AFB, Ohio.**

**APPLICATION OF IN-FLIGHT THRUST DETERMINATION**  
**UNCERTAINTY**

G. R. ADAMS (USAF, Wright-Patterson AFB, OH), J. W. THOMPSON, JR. (Sverdrup Technology, Inc., Tullahoma, TN), R. B. ABERNETHY (United Technologies Corp., Pratt and Whitney Group, East Hartford, CT), T. BIESIADNY (NASA, Lewis Research Center, Cleveland, OH), C. T. HAVEY (Boeing Military Airplane Co., Wichita, KS), J. W. STEURER (McDonnell Aircraft Co., St. Louis, MO), J. C. ASCOUGH (Royal Aircraft Establishment, Farnborough, Hants., England), and D. D. WILLIAMS (Rolls-Royce, Ltd., London, England) IN: Advances in aerospace propulsion; Proceedings of the Aerospace Congress and Exposition, Long Beach, CA, October 3-6, 1983. Warrendale, PA, Society of Automotive Engineers, Inc., 1983, p. 9-22  
 (SAE PAPER 831439)

A numerical example is given of a previously proposed methodology for the evaluation of in-flight thrust measurement uncertainty, using data extracted from a performance report comparing two different missile prototypes under a variety of flight conditions. Attention is given to the data for the AGM-68B Air Launched Cruise Missile, which is powered by the F107 dual-spool, mixed flow turbofan engine. Assessments are made of the definition of the measurement process, instrumentation error estimation, the propagation of errors to thrust calculation, mathematical model errors, the in-flight thrust error component, and correction to standard conditions. It is concluded that in-flight thrust measurement uncertainty limits can be evaluated from measurement system error analysis results and test data for the missile evaluation process presently described. O.C.

## 05 AIRCRAFT DESIGN, TESTING AND PERFORMANCE

**A84-49096\*#** Texas A&M Univ., College Station.  
**PERFORMANCE DEGRADATION OF A MODEL HELICOPTER ROTOR WITH A GENERIC ICE SHAPE**  
K. D. KORKAN, E. J. CROSS, JR., and T. L. MILLER (Texas A&M University, College Station, TX) *Journal of Aircraft* (ISSN 0021-8669), vol. 21, Oct. 1984, p. 823-830. refs (Contract NAG3-242)

An experimental program using a commercially available remotely controlled model helicopter in the Texas A&M University (TAMU) subsonic wind tunnel has been conducted to investigate the performance degradation resulting from the simulated formation of ice on the leading edge of the main rotor blades in both hover and forward flight. The rotor blades utilized a NACA 0012 airfoil with a 2.5-in constant chord. A generic ice shape derived from a predetermined natural ice condition was applied to the 53.375-in.-diameter main rotor, and thrust and torque coefficients were measured for the main rotor as functions of velocity, main rotor rpm, fuselage angle of incidence, collective pitch angle, and spanwise extent of icing. The model helicopter test exhibited significant performance degradation of the main rotor when generic ice was added. An increase of approximately 150 percent in torque coefficient to maintain a constant thrust coefficient was noted when generic ice had been applied to the 85 percent rotor radial location. Also, considerable additional degradation occurred when generic ice was applied to the 100 percent rotor radial location, as compared with the 85 percent simulated ice performance values, indicating the sensitivity of the rotor tip region. Author

**N84-13173\*#** National Aeronautics and Space Administration. Lewis Research Center, Cleveland, Ohio.  
**PERFORMANCE DEGRADATION OF A TYPICAL TWIN ENGINE COMMUTER TYPE AIRCRAFT IN MEASURED NATURAL ICING CONDITIONS**  
R. J. RANAUDO, K. L. MIKKELSEN, R. C. MCKNIGHT, and P. J. PERKINS, JR. (Analex Corp.) 1984 31 p refs Presented at the 22nd Aerospace Sci. Meeting, Reno, Nev., 9-12 Jan. 1984; sponsored by AIAA (NASA-TM-83564; E-1943; NAS 1.15-83564) Avail: NTIS HC A03/MF A01 CSCL 01C

The performance of an aircraft in various measured icing conditions was investigated. Icing parameters such as liquid water content, temperature, cloud droplet sizes and distributions were measured continuously while in icing. Flight data were reduced to provide plots of the aircraft drag polars and lift curves (CL vs. alpha) for the measured "iced" condition as referenced to the uniced aircraft. These data were also reduced to provide plots of thrust horsepower required vs. single engine power available to show how icing affects engine out capability. It is found that performance degradation is primarily influenced by the amount and shape of the accumulated ice. Glaze icing caused the greatest aerodynamic performance penalties in terms of increased drag and reduction in lift while aerodynamic penalties due to rime icing were significantly lower. E.A.K.

**N84-23641\*#** National Aeronautics and Space Administration. Lewis Research Center, Cleveland, Ohio.  
**FUEL SYSTEM RESEARCH AND TECHNOLOGY: AN OVERVIEW OF THE NASA PROGRAM**  
B. R. PHILLIPS *In its* Assessment of Alternative Aircraft Fuels p 111-120 Apr. 1984  
Avail: NTIS HC A09/MF A01 CSCL 01C

The interactions between the design and operation of aircraft fuel systems and the properties of alternative aircraft fuels are discussed. An overview of fuels system research and technology in terms of its rationale, its progress, and future plans is given. The measurement of ambient air temperatures for a wide range of seasonal and geographic variations, design studies on the use of fuels with increased as well as conventional freezing temperatures, the evaluation of fuel heating systems, and the low temperature behavior of fuels are among the topics discussed. R.J.F.

**N84-23646\*#** Simmonds Precision Products, Inc., Vergennes, Vermont.  
**ECONOMIC IMPACT OF FUEL PROPERTIES ON TURBINE POWERED BUSINESS AIRCRAFT**  
F. D. POWELL *In* NASA. Lewis Research Center Assessment of Alternative Aircraft Fuels p 171-184 Apr. 1984 refs (Contract NAS3-22827)  
Avail: NTIS HC A09/MF A01 CSCL 01C

The principal objective was to estimate the economic impact on the turbine-powered business aviation fleet of potential changes in the composition and properties of aviation fuel. Secondary objectives include estimation of the sensitivity of costs to specific fuel properties, and an assessment of the directions in which further research should be directed. The study was based on the published characteristics of typical and specific modern aircraft in three classes; heavy jet, light jet, and turboprop. Missions of these aircraft were simulated by computer methods for each aircraft for several range and payload combinations, and assumed atmospheric temperatures ranging from nominal to extremely cold. Five fuels were selected for comparison with the reference fuel, nominal Jet A. An overview of the data, the mathematic models, the data reduction and analysis procedure, and the results of the study are given. The direct operating costs of the study fuels are compared with that of the reference fuel in the 1990 time-frame, and the anticipated fleet costs and fuel break-even costs are estimated. R.J.F.

## 06

### AIRCRAFT INSTRUMENTATION

Includes cockpit and cabin display devices; and flight instruments.

**N84-29870\*#** National Aeronautics and Space Administration. Lewis Research Center, Cleveland, Ohio.  
**COMPARISON OF ICING CLOUD INSTRUMENTS FOR 1982-1983 ICING SEASON FLIGHT PROGRAM**  
R. F. IDE and G. P. RICHTER 1984 26 p refs Presented at the 22nd Aerospace Sci. Meeting, Reno, Nev., 9-12 Jan. 1984; sponsored by the American Inst. of Aeronautics and Astronautics Prepared in cooperation with Army Research and Technology Labs. (NASA-TM-83569; E-1950; NAS 1.15:83569; USAAVSCOM-TR-84-C-1) Avail: NTIS HC A03/MF A01 CSCL 01D

A number of modern and old style liquid water content (LWC) and droplet sizing instruments were mounted on a DeHavilland DHC-6 Twin Otter and operated in natural icing clouds in order to determine their comparative operating characteristics and their limitations over a broad range of conditions. The evaluation period occurred during the 1982-1983 icing season from January to March 1983. Time histories of all instrument outputs were plotted and analyzed to assess instrument repeatability and reliability. Scatter plots were also generated for comparison of instruments. The measured LWC from four instruments differed by as much as 20 percent. The measured droplet size from two instruments differed by an average of three microns. The overall effort demonstrated the need for additional data, and for some means of calibrating these instruments to known standards. Author



## AIRCRAFT PROPULSION AND POWER

Includes prime propulsion systems and systems components, e.g., gas turbine engines and compressors; and on-board auxiliary power plants for aircraft.

**A84-15204\*#** National Aeronautics and Space Administration. Lewis Research Center, Cleveland, Ohio.

**EFFECTS OF WIND ON TURBOFAN ENGINES IN OUTDOOR STATIC TEST STANDS**

J. G. MCARDLE and A. S. MOORE (NASA, Lewis Research Center, Cleveland, OH) AIAA, AHS, IES, SETP, SFTE, and DGLR, Flight Testing Conference, 2nd, Las Vegas, NV, Nov. 16-18, 1983. 8 p. refs

(AIAA PAPER 83-2766)

Wind can affect measured thrust and can cause turbofan engine speed to fluctuate during outdoor testing. Techniques used at an outdoor test stand at NASA Lewis Research Center to make testing easier and faster and to improve data repeatability include using an inflow control device (ICD) to make fan speed steadier, taking many raw data samples for better averaging, and correcting thrust for wind direction and speed. Data from engine tests are presented to show that the techniques improve repeatability of thrust and airflow measurements under various wind conditions. Previously announced in STAR as N83-34945

Author

**A84-15205\*#** National Aeronautics and Space Administration. Lewis Research Center, Cleveland, Ohio.

**USE OF COOLING AIR HEAT EXCHANGERS AS REPLACEMENTS FOR HOT SECTION STRATEGIC MATERIALS**

J. W. GAUNTNER (NASA, Lewis Research Center, Cleveland, OH) American Institute of Aeronautics and Astronautics, Aircraft Design, Systems and Technology Meeting, Fort Worth, TX, Oct. 17-19, 1983. 9 p. refs

(AIAA PAPER 83-2540)

Because of financial and political constraints, strategic aerospace materials required for the hot section of future engines might be in short supply. As an alternative to these strategic materials, this study examines the use of a cooling air heat exchanger in combination with less advanced hot section materials. Cycle calculations are presented for future turbofan systems with overall pressure ratios to 65, bypass ratios near 13, and combustor exit temperatures to 3260 R. These calculations quantify the effect on TSFC of using a decreased materials technology in a turbofan system. The calculations show that the cooling air heat exchanger enables the feasibility of these engines. Previously announced in STAR as N83-34946

Author

**A84-15206\*#** National Aeronautics and Space Administration. Lewis Research Center, Cleveland, Ohio.

**SUPERSONIC FAN ENGINES FOR MILITARY AIRCRAFT**

L. C. FRANCISCUS (NASA, Lewis Research Center, Cleveland, OH) American Institute of Aeronautics and Astronautics, Aircraft Design, Systems and Technology Meeting, Fort Worth, TX, Oct. 17-19, 1983. 10 p. refs

(AIAA PAPER 83-2541)

Engine performance and mission studies were performed for turbofan engines with supersonic through-flow fans. A Mach 2.4 CTOL aircraft was used in the study. Two missions were considered: a long range penetrator mission and a long range intercept mission. The supersonic fan engine is compared with an augmented mixed flow turbofan in terms of mission radius for a fixed takeoff gross weight of 75,000 lbm. The mission radius of aircraft powered by supersonic fan engines could be 15 percent longer than aircraft powered with conventional turbofan engines at moderate thrust to gross weight ratios. The climb and acceleration performance of the supersonic fan engines is better than that of the conventional

turbofan engines. Previously announced in STAR as N83-34947

Author

**A84-15207\*#** National Aeronautics and Space Administration. Lewis Research Center, Cleveland, Ohio.

**STUDY OF A LH<sub>2</sub>-FUELED TOPPING CYCLE ENGINE FOR AIRCRAFT PROPULSION**

G. E. TURNEY and L. H. FISHBACH (NASA, Lewis Research Center, Cleveland, OH) American Institute of Aeronautics and Astronautics, Aircraft Design, Systems and Technology Meeting, Fort Worth, TX, Oct. 17-19, 1983. 19 p. refs

(AIAA PAPER 83-2543)

An analytical investigation was made of a topping cycle aircraft engine system which uses a cryogenic fuel. This system consists of a main turboshaft engine which is mechanically coupled (by cross-shafting) to a topping loop which augments the shaft power output of the system. The thermodynamic performance of the topping cycle engine was analyzed and compared with that of a reference (conventional-type) turboshaft engine. For the cycle operating conditions selected, the performance of the topping cycle engine in terms of brake specific fuel consumption (bsfc) was determined to be about 12 percent better than that of the reference turboshaft engine. Engine weights were estimated for both the topping cycle engine and the reference turboshaft engine. These estimates were based on a common shaft power output for each engine. Results indicate that the weight of the topping cycle engine is comparable to that of the reference turboshaft engine. Previously announced in STAR as N83-34942

Author

**A84-16528\*** National Aeronautics and Space Administration. Lewis Research Center, Cleveland, Ohio.

**ADVANCED ELECTRICAL POWER SYSTEM TECHNOLOGY FOR THE ALL ELECTRIC AIRCRAFT**

R. C. FINKE and G. R. SUNDBERG (NASA, Lewis Research Center, Cleveland, OH) IN: NAECON 1983; Proceedings of the National Aerospace and Electronics Conference, Dayton, OH, May 17-19, 1983. Volume 1. New York, Institute of Electrical and Electronics Engineers, 1983, p. 53-55.

The application of advanced electric power system technology to an all electric airplane results in an estimated reduction of the total takeoff gross weight of over 23,000 pounds for a large airplane. This will result in a 5 to 10 percent reduction in direct operating costs (DOC). Critical to this savings is the basic electrical power system component technology. These advanced electrical power components will provide a solid foundation for the materials, devices, circuits, and subsystems needed to satisfy the unique requirements of advanced all electric aircraft power systems. The program for the development of advanced electrical power component technology is described. The program is divided into five generic areas: semiconductor devices (transistors, thyristors, and diodes); conductors (materials and transmission lines); dielectrics; magnetic devices; and load management devices. Examples of progress in each of the five areas are discussed. Bipolar power transistors up to 1000 V at 100 A with a gain of 10 and a 0.5 microsec rise and fall time are presented. A class of semiconductor devices with a possibility of switching up to 100 kV is described. Solid state power controllers for load management at 120 to 1000 V and power levels to 25 kW were developed along with a 25 kW, 20 kHz transformer weighing only 3.2 kg. Previously announced in STAR as N83-24764

Author

**A84-17362\*#** National Aeronautics and Space Administration. Lewis Research Center, Cleveland, Ohio.

**REAL-TIME PEGASUS PROPULSION SYSTEM MODEL V/STOL-PILOTTED SIMULATION EVALUATION**

J. R. MIHALOEWSKI (NASA, Lewis Research Center, Cleveland, OH), S. P. ROTH, and R. CREEKMORE (United Technologies Corp., Pratt and Whitney Aircraft Group, West Palm Beach, FL) Journal of Guidance, Control, and Dynamics (ISSN 0731-5090), vol. 7, Jan.-Feb. 1984, p. 77-84. refs

Previously cited in issue 07, p. 982, Accession no. A82-19221

**A84-17997\*#** General Electric Co., Cincinnati, Ohio.  
**COMPARISON OF FULL-SCALE ENGINE AND SUBSCALE MODEL PERFORMANCE OF A MIXED FLOW EXHAUST SYSTEM FOR AN ENERGY EFFICIENT ENGINE (E3) PROPULSION SYSTEM**

A. P. KUCHAR (General Electric Co., Cincinnati, OH) and R. CHAMBERLIN (NASA, Lewis Research Center, Cleveland, OH) American Institute of Aeronautics and Astronautics, Aerospace Sciences Meeting, 22nd, Reno, NV, Jan. 9-12, 1984. 10 p. refs (AIAA PAPER 84-0283)

A full scale engine test of the NASA/General Electric Company (GE) Energy Efficient Engine (E3) was conducted to demonstrate the E3 engine concept and evaluate its performance. The test program, performed at the GE outdoor engine test facilities in Peebles, OH, included a detailed evaluation of the total pressure and temperature profiles at the exit of the mixed flow exhaust system to determine its mixing effectiveness. Subscale model tests of the same mixed flow exhaust system had been previously conducted at Fluidyne Engineering Corporation in Minneapolis, Minnesota as part of the GE E3 mixer aerodynamic technology development program. The scale model and full scale engine nozzle exit survey data and the calculated mixing effectiveness are compared and discussed. Results indicate the full scale engine mixing effectiveness to be five percent higher than the scale model as a result of a geometric difference and higher turbulence levels in the engine exhaust flowfield

Author

**A84-18582\*** National Aeronautics and Space Administration. Lewis Research Center, Cleveland, Ohio.

**IDENTIFICATION OF MULTIVARIABLE HIGH PERFORMANCE TURBOFAN ENGINE DYNAMICS FROM CLOSED LOOP DATA**  
 W. MERRILL (NASA, Lewis Research Center, Cleveland, OH) IN: Identification and system parameter estimation 1982; Proceedings of the Sixth Symposium, Washington, DC, June 7-11, 1982. Volume 1. Oxford and New York, Pergamon Press, 1983, p. 427-434. refs

The multivariable instrumental variable/approximate maximum likelihood (IV/AML) method of recursive time-series analysis is used to identify the multivariable (four inputs-three outputs) dynamics of the Pratt and Whitney F100 engine. A detailed nonlinear engine simulation is used to determine linear engine model structures and parameters at an operating point using open loop data. Also, the IV/AML method is used in a direct identification made to identify models from actual closed loop engine test data. Models identified from simulated and test data are compared to determine a final model structure and parameterization that can predict engine response for a wide class of inputs. The ability of the IV/AML algorithm to identify useful dynamic models from engine test data is assessed. Previously announced in STAR as N82-20339

Author

**A84-21300\*#** National Aeronautics and Space Administration. Lewis Research Center, Cleveland, Ohio.

**FLAME RADIATION AND LINEAR HEAT TRANSFER IN A TUBULAR CAN COMBUSTOR**

R. W. CLAUS, G. M. NEELY, and F. M. HUMENIK (NASA, Lewis Research Center, Cleveland, OH) American Institute of Aeronautics and Astronautics, Aerospace Sciences Meeting, 22nd, Reno, NV, Jan. 9-12, 1984. 14 p. refs (AIAA PAPER 84-0443)

Heat transfer within a combustor were examined. Total and spectral flame radiation in a tubular can combustor at a series of parametric operating conditions was measured. Radiation measurements were taken for a range of inlet air pressures from 0.34 to 2.0 MPa, inlet air temperatures from 533 to 700 K, with two different fuels, Jet-A and ERBS. Measurements of linear temperatures combined with the parametric radiation results allowed a calculation of the combustor linear heat loads. Flame emissivity was determined from the spectral measurements. Previously announced in STAR as N84-13188

Author

**A84-21852\*#** National Aeronautics and Space Administration. Lewis Research Center, Cleveland, Ohio.

**FLOW VISUALIZATION AND INTERPRETATION OF VISUALIZATION DATA FOR DEFLECTED THRUST V/STOL NOZZLES**

H. C. KAO, P. L. BURSTADT, and A. L. JOHNS (NASA, Lewis Research Center, Cleveland, OH) American Institute of Aeronautics and Astronautics, Aerospace Sciences Meeting, 22nd, Reno, NV, Jan. 9-12, 1984. 50 p. refs (AIAA PAPER 84-0102)

Flow visualization studies were made for four deflected thrust nozzle models at subsonic speeds. Based on topological rules and the assumption that observed streaks constitute continuous vector fields, available visualization pictures are interpreted and flow patterns on interior surfaces of the nozzles are synthesized. In particular, three dimensional flow structure and separations are discussed. From the synthesized patterns, the overall features of the flow field in a given nozzle can be approximately perceived. Previously announced in STAR as N84-14147

Author

**A84-22174\*#** National Aeronautics and Space Administration. Lewis Research Center, Cleveland, Ohio.

**TONE GENERATION BY ROTOR-DOWNSTREAM STRUT INTERACTION**

R. P. WOODWARD and J. R. BALOMBIN (NASA, Lewis Research Center, Cleveland, OH) Journal of Aircraft (ISSN 0021-8669), vol. 21, Feb. 1984, p. 135-142. refs

Previously cited in issue 10, p. 1378, Accession no. A83-25957

**A84-22877\*#** Pratt and Whitney Aircraft Group, East Hartford, Conn.

**SIMPLIFIED ANALYTICAL PROCEDURES FOR REPRESENTING MATERIAL CYCLIC RESPONSE**

V. MORENO (United Technologies Corp., Pratt and Whitney Group, East Hartford, CT) and A. KAUFMAN (NASA, Lewis Research Center, Cleveland, OH) Auburn University, Southeastern Conference on Theoretical and Applied Mechanics, 12th, Callaway Gardens, GA, May 10, 11, 1984, Paper. 5 p. refs

Requirements for increased durability of gas turbine hot section structural components have made it necessary to place greater emphasis on accurate structural analysis and life prediction. Linear finite-element analysis is generally sufficient for structural analysis applications. However, for structures in the hot part of the engine, nonlinear structural analysis may be required under certain conditions for the accurate prediction of the local stress-strain response. Nonlinear finite element analysis represents a costly effort which is generally incompatible with the iterative nature of the design process. The present investigation is, therefore, concerned with two simplified procedures for estimating the local hysteretic response produced by cyclic thermal loading. These procedures reduce the need for nonlinear finite-element analysis.

G.R.

**A84-24033\*#** General Electric Co., Cincinnati, Ohio.  
**NASA/GENERAL ELECTRIC BROAD-SPECIFICATION FUELS COMBUSTION TECHNOLOGY PROGRAM - PHASE I.**

W. J. DODDS, E. E. EKSTEDT, D. W. BAHR (General Electric Co., Aircraft Engine Business Group, Cincinnati, OH), and J. S. FEAR (NASA, Lewis Research Center, Cleveland, OH) Journal of Energy (ISSN 0146-0412), vol. 7, Nov.-Dec. 1983, p. 508-517. refs

Previously cited in issue 17, p. 2687, Accession no. A82-35000

**A84-26959\*#** National Aeronautics and Space Administration. Lewis Research Center, Cleveland, Ohio.

**THE COUPLED RESPONSE OF TURBOMACHINERY BLADING TO AERODYNAMIC EXCITATIONS**

D. HOYNIK (NASA, Lewis Research Center, Cleveland, OH; Purdue University, West Lafayette, IN) and S. FLEETER (Purdue University, West Lafayette, IN) (Structures, Structural Dynamics and Materials Conference, 24th, Lake Tahoe, NV, May 2-4, 1983, Collection of Technical Papers. Part 2, p. 137-148) Journal of Aircraft (ISSN 0021-8669), vol. 21, April 1984, p. 278-286. USAF-supported research refs

Previously cited in issue 12, p. 1742, Accession no. A83-29822

**A84-27140\*#** National Aeronautics and Space Administration. Lewis Research Center, Cleveland, Ohio.

**INVESTIGATION OF MIXING IN A TURBOFAN EXHAUST DUCT. II COMPUTER CODE APPLICATION AND VERIFICATION**

L. A. POVINELLI and B. H. ANDERSON (NASA, Lewis Research Center, Cleveland, OH) AIAA Journal (ISSN 0001-1452), vol. 22, April 1984, p. 518-525. refs

A three-dimensional analysis of turbofan forced mixer nozzle aerodynamics demonstrates that the complex flow structure is dominated by geometrically induced secondary flow rather than by turbulence. The test apparatus consisted of a fixed upstream model section and a rotating shroud. The Mach number of the fan and core streams at the mixing plane (lobe exit) was 0.45, the bypass ratio was about 4, and the Reynolds number based on the shroud radius was 1,100,000. The three velocity components near the exit plane of the lobes were measured using flow angularity probes to provide information about the mixer inflow conditions for turbulent computations. The validity of a previous computer code was demonstrated in a comparison of the nozzle exit temperature data with the computed temperature distributions. The mechanism most responsible for the generation of secondary flow within the lobes is due to the turning of the fan and core streams in opposite radial directions. J.N.

**A84-28982\*#** General Electric Co., Cincinnati, Ohio.

**NASA ADVANCED LOW EMISSIONS COMBUSTOR PROGRAM**  
A. GOYAL, E. E. EKSTEDT (General Electric Co., Aircraft Engine Business Group, Cincinnati, OH), and A. J. SZANISZLO (NASA, Lewis Research Center, Cleveland, OH) American Society of Mechanical Engineers and Institute of Electrical and Electronics Engineers, Joint Power Generation Conference, Indianapolis, IN, Sept. 25-29, 1983. 9 p. refs  
(ASME PAPER 83-JPGC-GT-10)

The purpose of this program is to conduct combustion tests on lean, premixed, and prevaporized (LPP) combustor concepts designed for use in commercial aircraft engines to attain improved performance, durability, and lower pollutant emissions levels relative to current technology combustor designs. Four full annular combustors were designed for the CF6-50 engine. These concepts utilize premixing of the fuel and air, variable geometry, and fuel staging to control the equivalence ratios of the burning zone. The testing is being conducted on these four full annular combustors over a wide range of operating conditions at pressures up to actual subsonic cruise (1.16 MPa). The test results for the most promising of these combustor concepts are reported in this paper. Author

**A84-29460\*** Teledyne CAE, Toledo, Ohio.

**AERODYNAMIC EFFECTS OF MOVEABLE SIDEWALL NOZZLE GEOMETRY AND ROTOR EXIT RESTRICTION ON THE PERFORMANCE OF A RADIAL TURBINE**

C. ROGO, T. HAJEK (Teledyne CAE, Toledo, OH), and R. ROELKE (NASA, Lewis Research Center, Cleveland, OH) IN. Advances in aerospace propulsion; Proceedings of the Aerospace Congress and Exposition, Long Beach, CA, October 3-6, 1983. Warrendale, PA, Society of Automotive Engineers, Inc., 1983, p. 71-81. NASA-Army-sponsored research. refs  
(SAE PAPER 831517)

Attention is given to the experimental results obtained with a high work capacity radial inflow turbine of known performance, whose baseline configuration was modified to accept a variety of movable nozzle sidewall, diffusing or accelerating rotor inlet ramp, and rotor exit restriction ring combinations. The performance of this variable geometry turbine was measured at constant speed and pressure ratio for 31 different test configurations, yielding test data over a nozzle area range from 50 to 100 percent of maximum depending on the movement of the nozzle assembly's forward and rearward sidewalls. Performance comparisons with data for a variable stagger angle vane concept indicate the present system's viability. O.C.

**A84-31905\*#** Carnegie-Mellon Univ., Pittsburgh, Pa.

**MODEL DEVELOPMENT AND STATISTICAL INVESTIGATION OF TURBINE BLADE MISTUNING**

J. H. GRIFFIN (Carnegie-Mellon University, Pittsburgh, PA) and T. M. HOOSAC ASME, Transactions, Journal of Vibration, Acoustics, Stress and Reliability in Design (ISSN 0739-3717), vol. 106, April 1984, p. 204-210. refs  
(Contract NAG3-231)

This paper discusses the development of an efficient algorithm which calculates the individual blade response of a bladed turbine disk, the subsequent statistical investigation to establish mistuning dependencies, and procedures which reduce the increase in blade amplitudes caused by mistuning. Author

**A84-35204\*#**

**DESIGN OF A HIGH-PERFORMANCE ROTARY STRATIFIED-CHARGE RESEARCH AIRCRAFT ENGINE**

C. JONES and R. E. MOUNT (John Deere Technologies International, Inc., Rotary Engine Div., Wood-Ridge, NJ) AIAA, SAE, and ASME, Joint Propulsion Conference, 20th, Cincinnati, OH, June 11-13, 1984. 11 p. refs  
(Contract NAS3-23056)  
(AIAA PAPER 84-1395)

The power section for an advanced rotary stratified-charge general aviation engine has been designed under contract to NASA. The single-rotor research engine of 40 cubic-inches displacement (RCI-40), now being procured for test initiation this summer, is targeted for 320 T.O. horse-power in a two-rotor production engine. The research engine is designed for operating on jet-fuel, gasoline or diesel fuel and will be used to explore applicable advanced technologies and to optimize high output performance variables. Design of major components of the engine is described in this paper. Author

**A84-36951\*#** National Aeronautics and Space Administration. Lewis Research Center, Cleveland, Ohio.

**PRELIMINARY INVESTIGATION OF A TWO-ZONE SWIRL FLOW COMBUSTOR**

J. A. BIAGLOW, S. M. JOHNSON, and J. M. SMITH (NASA, Lewis Research Center, Cleveland, OH) AIAA, SAE, and ASME, Joint Propulsion Conference, 20th, Cincinnati, OH, June 11-13, 1984. 13 p. refs  
(AIAA PAPER 84-1169)

The effect of full-annular swirling-flow on a flow-zone combustor design is investigated. Swirl flow angles of 25, 35, and 45 degrees were investigated in a combustor design envelope typical of those used in modern engines. The two-zone combustor had 24 pilot-zone fuel injectors and 24 main-fuel injectors located in the centerbody between the pilot and swirl passage. Combustor performance was

determined at idle, and two parametric 589 K inlet temperature conditions. Combustor performance was highest with the 45 degree swirl vane design; at the idle condition, combustion efficiency was 99.5 percent. The 45 degree swirl vane also produced the lowest pattern factor of the three angles and showed a combustor lean blowout limit below a 0.001 fuel-air ratio. Combustor total pressure drop varied from a low of 4.6 percent for the 25 degree swirl to a high of 4.9 percent for the 45 degree swirl. Previously announced in STAR as N84-22565 M.A.C.

**A84-36952\*#** National Aeronautics and Space Administration. Lewis Research Center, Cleveland, Ohio.

### EXPERIMENTAL INVESTIGATION OF THE LOW NOX VORTEX AIRBLAST ANNULAR COMBUSTOR

S. M. JOHNSON, J. A. BIAGLOW, and J. M. SMITH (NASA, Lewis Research Center, Cleveland, OH) AIAA, SAE, and ASME, Joint Propulsion Conference, 20th, Cincinnati, OH, June 11-13, 1984. 7 p. refs (AIAA PAPER 84-1170)

A low oxides of nitrogen vortex airblast annular combustor was evaluated which has attained the goal of 1 gm NO<sub>2</sub>/kg fuel or less during operation. The experimental combustor test conditions were a nominal inlet-air temperature of 703 K, inlet total pressures between 0.52 to 0.83 MPa, and a constant inlet Mach number of 0.26. Exit temperature pattern factors for all test points were between 0.16 and 0.20 and exit swirl flow angles were 47 degrees at isothermal conditions and 23 degrees during combustion. Oxides of nitrogen did not exceed 1.05 gm NO<sub>2</sub>/kg fuel at the highest inlet pressure and exhaust temperature tested. Previous correlations have related NO<sub>x</sub> proportionally to the combustor inlet pressure raised to some exponent. In this experiment, a band of exponents between 0.5 and 1.0 resulted for fuel-air ratios from 0.023 to 0.027 and inlet pressures from 0.52 to 0.83 MPa. Previously announced in STAR as N84-22567 S.L.

**A84-36957\*#** General Motors Corp., Indianapolis, Ind. **ADVANCED PROPPAN DRIVE SYSTEM CHARACTERISTICS AND TECHNOLOGY NEEDS**

R. D. ANDERSON, D. A. WAGNER, R. E. DEVLIN, and A. S. NOVICK (General Motors Corp., Allison Gas Turbine Div., Indianapolis, IN) AIAA, SAE, and ASME, Joint Propulsion Conference, 20th, Cincinnati, OH, June 11-13, 1984. 9 p. refs (Contract NAS3-23046) (AIAA PAPER 84-1194)

Characteristics of a single-rotation drive system for an advanced turboprop engine are described. The gearbox is designed for a 10,000 shp three-spool, free-turbine engine and is installed in a wing-mounted nacelle. An offset gearbox from an earlier APET study provided the background for the preliminary design and benefit analysis for a 1990s advanced technology versus 1980s state-of-the-art gearbox. High efficiencies were achieved for both designs with inherently high life goals. Increases in design allowables for gears, bearings, and lubricants resulted in improvements for the 1990s design. Author

**A84-36959\*#** National Aeronautics and Space Administration. Lewis Research Center, Cleveland, Ohio.

### DETERMINATION OF COMPRESSOR IN-STALL CHARACTERISTICS FROM ENGINE SURGE TRANSIENTS

C. F. LORENZO, F. P. CHIARAMONTE, and C. M. MEHALIC (NASA, Lewis Research Center, Cleveland, OH) AIAA, SAE, and ASME, Joint Propulsion Conference, 20th, Cincinnati, OH, June 11-13, 1984. 19 p. refs (AIAA PAPER 84-1206)

A technique for extracting the in-kill pumping characteristics for an axial flow compressor operating in an engine system environment is developed. The technique utilizes a Hybrid computer simulation of the compressor momentum equation in which actual transient data are used to provide all terms but the desired compressor characteristic. The compressor force characteristic as a function of corrected flow and speed results from the computation. The critical problem of data filtering is addressed.

Results for a compressor operating in a turbofan engine are presented and comparison is made with the conventional compressor map. The relationship of the compressor surge characteristic with its rotating stall characteristic is explored. Initial interpretation of the measured results is presented. Previously announced in STAR as N84-22566 Author

**A84-36972\*#** National Aeronautics and Space Administration. Lewis Research Center, Cleveland, Ohio.

### COMPARISON BETWEEN MEASURED TURBINE STAGE PERFORMANCE AND THE PREDICTED PERFORMANCE USING QUASI-3D FLOW AND BOUNDARY LAYER ANALYSES

R. J. BOYLE, T. KATSANIS (NASA, Lewis Research Center, Cleveland, OH), and J. E. HAAS (U.S. Army, Propulsion Laboratory, Cleveland, OH) AIAA, SAE, and ASME, Joint Propulsion Conference, 20th, Cincinnati, OH, June 11-13, 1984. 18 p. refs (AIAA PAPER 84-1299)

A method for calculating turbine stage performance is described. The usefulness of the method is demonstrated by comparing measured and predicted efficiencies for nine different stages. Comparisons are made over a range of turbine pressure ratios and rotor speeds. A quasi-3D flow analysis is used to account for complex passage geometries. Boundary layer analyses are done to account for losses due to friction. Empirical loss models are used to account for incidence, secondary flow, disc windage, and clearance losses. Previously announced in STAR as N84-22564 Author

**A84-37639\*#** ISTAR, Inc., Santa Monica, Calif.

### DETONATION WAVE AUGMENTATION OF GAS TURBINES

A. WORTMAN (ISTAR, Inc., Santa Monica; California State University, Fullerton, CA) AIAA, SAE, and ASME, Joint Propulsion Conference, 20th, Cincinnati, OH, June 11-13, 1984. 10 p. refs (Contract NAS3-24098) (AIAA PAPER 84-1266)

The results of a feasibility study that examined the effects of using detonation waves to augment the performance of gas turbines are reported. The central ideas were to reduce compressor requirements and to maintain high performance in jet engines. Gasdynamic equations were used to model the flows associated with shock waves generated by the detonation of fuel in detonator tubes. Shock wave attenuation to the level of Mach waves was found possible, thus eliminating interference with the compressor and the necessity of valves and seals. A preliminary parametric study of the performance of a compressor working at a 4:1 ratio in a conceptual design of a detonation wave augmented jet engine in subsonic flight indicated a clear superiority over conventional designs in terms of fuel efficiency and thrust. M.S.K.

**A84-37640\*#** Beltran Associates, Inc., Syosset, N.Y.

### HEAT PIPE APPLICATIONS IN AIRCRAFT PROPULSION

M. R. BELTRAN, D. L. ANDERSON, and P. J. MARTO (Beltran Associates, Inc., Syosset, NY) AIAA, SAE, and ASME, Joint Propulsion Conference, 20th, Cincinnati, OH, June 11-13, 1984. 24 p. refs (Contract NAS3-24095) (AIAA PAPER 84-1269)

Heat pipes for improving the cycle efficiency and/or thrust-to-weight ratio of aircraft gas turbines are examined. A heat pipe employs a capillary structure, a wick, and an evacuated chamber to transfer heat between condenser and evaporator ends. Heat absorbed at the evaporator is transported to the condenser. In an aircraft, the heat pipe can be stationary or rotating, can be used for cooling stators and rotors, and is amenable to shapes such as cylinders, cones, and flat plates. Heat pipes in aircraft gas turbines can be applied for intercooling between stages, regeneration, reheat, and blade cooling. Improvements are projected in the cycle efficiency, thrust and thrust specific fuel consumption in the fanjet by using heat pipes. Consideration is also given to heat pipe heat exchangers with high axial heat transfer for stationary heat pipes and high heat transport for rotating heat pipes. M.S.K.

**A84-40239\*#** National Aeronautics and Space Administration. Lewis Research Center, Cleveland, Ohio.

**PERFORMANCE OF A HIGH-WORK LOW ASPECT RATIO TURBINE TESTED WITH A REALISTIC INLET RADIAL TEMPERATURE PROFILE**

R. G. STABE, W. J. WHITNEY, and T. P. MOFFITT (NASA, Lewis Research Center, Cleveland, OH) AIAA, SAE, and ASME, Joint Propulsion Conference, 20th, Cincinnati, OH, June 11-13, 1984. 25 p. refs

(AIAA PAPER 84-1161)

Experimental results are presented for a 0.767 scale model of the first stage of a two-stage turbine designed for a high by-pass ratio engine. The turbine was tested with both uniform inlet conditions and with an inlet radial temperature profile simulating engine conditions. The inlet temperature profile was essentially mixed-out in the rotor. There was also substantial underturning of the exit flow at the mean diameter. Both of these effects were attributed to strong secondary flows in the rotor blading. There were no significant differences in the stage performance with either inlet condition when differences in tip clearance were considered. Performance was very close to design intent in both cases. Previously announced in STAR as N84-24589

Author

**A84-40244\*#** National Aeronautics and Space Administration. Lewis Research Center, Cleveland, Ohio.

**AN OVERVIEW OF NASA INTERMITTENT COMBUSTION ENGINE RESEARCH**

E. A. WILLIS and W. T. WINTUCKY (NASA, Lewis Research Center, Cleveland, OH) AIAA, SAE, and ASME, Joint Propulsion Conference, 20th, Cincinnati, OH, June 11-13, 1984. 34 p. refs (AIAA PAPER 84-1393)

This paper overviews the current program, whose objective is to establish the generic technology base for advanced aircraft I.C. engines of the early 1990's and beyond. The major emphasis of this paper is on development of the past two years. Past studies and ongoing confirmatory experimental efforts are reviewed, which show unexpectedly high potential when modern aerospace technologies are applied to inherently compact and balanced I.C. engine configurations. Currently, the program is focussed on two engine concepts, the stratified-charge, multi-fuel rotary and the lightweight two-stroke diesel. A review is given of contracted and planned high performance one-rotor and one-cylinder test engine work addressing several levels of technology. Also reviewed are basic supporting efforts, e.g., the development and experimental validation of computerized airflow and combustion process models, being performed in-house at Lewis Research Center and by university grants. Previously announced in STAR as N84-24583

Author

**A84-40245\*#** National Aeronautics and Space Administration. Lewis Research Center, Cleveland, Ohio.

**TANDEM FAN APPLICATIONS IN ADVANCED STOVL FIGHTER CONFIGURATIONS**

C. L. ZOLA (NASA, Lewis Research Center, Cleveland, OH), S. B. WILSON, III, and M. A. ESKEY (NASA, Ames Research Center, Moffett Field, CA) AIAA, SAE, and ASME, Joint Propulsion Conference, 20th, Cincinnati, OH, June 11-13, 1984. 20 p. refs (AIAA PAPER 84-1402)

The series/parallel tandem fan engine is evaluated for application in advanced STOVL supersonic fighter aircraft. Options in engine cycle parameters and design of the front fan flow diverter are examined for their effects on engine weight, dimensions, and other factors in integration of the engine with the aircraft. Operation of the engine in high-bypass flow mode during cruise and loiter flight is considered as a means of minimizing fuel consumption. Engine thrust augmentation by burning in the front fan exhaust is discussed. Achievement of very short takeoff with vectored thrust is briefly reviewed for tandem fan engine configurations with vectorable front fan nozzles. Examples are given of two aircraft configuration platforms, a delta-canard, and a forward-swept wing, to illustrate the major features, design considerations, and potential performance of the tandem fan installation in each. Full realization of the advantages of tandem fan propulsion are found to depend

on careful selection of the aircraft configuration, since integration requirements can strongly influence the engine performance. Previously announced in STAR as N84-24579

- Author

**A84-40246\*#** National Aeronautics and Space Administration. Lewis Research Center, Cleveland, Ohio.

**SUPERSONIC STOVL EJECTOR AIRCRAFT FROM A PROPULSION POINT OF VIEW**

R. LUIDENS, R. PLENCNER, W. HALLER, and A. GLASSMAN (NASA, Lewis Research Center, Cleveland, OH) AIAA, SAE, and ASME, Joint Propulsion Conference, 20th, Cincinnati, OH, June 11-13, 1984. 18 p. refs (AIAA PAPER 84-1401)

A baseline supersonic STOVL ejector aircraft, its propulsion and typical operating modes is described, and important propulsion parameters are identified. Then a number of propulsion system changes are evaluated for improvement of the lift-off performance: aft deflection of the ejector jet and heating of the ejector primary air either by burning or using the hot engine core flow. The possibility for cooling the footprint is illustrated for mixing or interchanging the fan and core flows, and in use of a core flow ejector. The application of a new engine concept: the turbine bypass engine plus a turbocompressor to supply the ejector primary air and thrust during takeoff combat are presented. Previously announced in STAR as N84-24581

E.A.K.

**A84-40247\*#** National Aeronautics and Space Administration. Lewis Research Center, Cleveland, Ohio.

**SUPERSONIC STOVL AIRCRAFT WITH TURBINE BYPASS/TURBO-COMPRESSOR ENGINES**

L. C. FRANCISCUS and R. W. LUIDENS (NASA, Lewis Research Center, Cleveland, OH) AIAA, SAE, and ASME, Joint Propulsion Conference, 20th, Cincinnati, OH, June 11-13, 1984. 15 p. refs (AIAA PAPER 84-1403)

Three propulsion systems for a Mach 2 STOVL fighter were compared. The three propulsion systems are: (1) turbine bypass engine with a turbocompressor used for STOVL only; (2) turbine bypass engine with a turbocompressor for both STOVL and thrust during forward flight; and (3) mixed flow afterburning turbofan with a remote burner lift system. In the first system, the main engines have afterburners and the turbocompressors use afterburning during STOVL. In the second system, the turbine bypass engines are dry and the turbocompressors have afterburners. The mission used in the study is a deck launched intercept mission. It is indicated that large improvements in combat time are possible when the turbocompressors are used for both lift and thrust for forward flight. Previously announced in STAR as N84-24582

E.A.K.

**A84-40787\*** General Electric Co., Lynn, Mass.

**POWERPLANT DESIGN FOR ONE-ENGINE-INOPERATIVE OPERATION**

R. HIRSCHKRON, E. MARTIN (General Electric Co., Lynn, MA), and N. SAMANICH (NASA, Lewis Research Center, Cleveland, OH) Vertiflite (ISSN 0042-4455), vol. 30, July-Aug. 1984, p. 34-38.

Regulatory changes are proposed for new engine certification for multi-engine helicopters to account for contingency operations when one engine goes out at take-off. The new rules are needed because current regulations define category A and B conditions as one-engine out, land immediately, or continue take-off, respectively. Category A is seldom feasible while Category B requires oversize engines, implying lowered fuel efficiencies. However, NASA studies have shown that engines with large contingency power can operate more efficiently in normal conditions due to decreased coolant flow. Techniques for realizing up to a 50 percent power augmentation with minor modifications of existing engines are described.

M S K.

**A84-42378\*** National Aeronautics and Space Administration. Lewis Research Center, Cleveland, Ohio.

### **A PIECEWISE LINEAR STATE VARIABLE TECHNIQUE FOR REAL TIME PROPULSION SYSTEM SIMULATION**

J. R. MIHALOEWSKI (NASA, Lewis Research Center, Cleveland, OH) and S. P. ROTH (United Technologies Corp., Government Products Div., West Palm Beach, FL) IN: Annual Pittsburgh Conference, 13th, Pittsburgh, PA, April 22, 23, 1982, Proceedings. Part 1. Research Triangle Park, NC, Instrument Society of America, 1982, p. 1-12. Previously announced in STAR as N82-24201.

The emphasis on increased aircraft and propulsion control system integration and piloted simulation has created a need for higher fidelity real time dynamic propulsion models. A real time propulsion system modeling technique which satisfies this need and which provides the capabilities needed to evaluate propulsion system performance and aircraft system interaction on manned flight simulators was developed and demonstrated using flight simulator facilities at NASA Ames. A piecewise linear state variable technique is used. This technique provides the system accuracy, stability and transient response required for integrated aircraft and propulsion control system studies. The real time dynamic model includes the detail and flexibility required for the evaluation of critical control parameters and propulsion component limits over a limited flight envelope. The model contains approximately 7.0 K bytes of in-line computational code and 14.7 K of block data. It has an 8.9 ms cycle time on a Xerox Sigma 9 computer. A Pegasus-Harrier propulsion system was used as a baseline for developing the mathematical modeling and simulation technique. A hydromechanical and water injection control system was also simulated. The model was programmed for interfacing with a Harrier aircraft simulation at NASA Ames. Descriptions of the real time methodology and model capabilities are presented. Author

**A84-42382\*** Notre Dame Univ., Ind.

### **AN APPLICATION OF TENSOR IDEAS TO NONLINEAR MODELING OF A TURBOFAN JET ENGINE**

T. A. KLINGLER, S. YURKOVICH, and M. K. SAIN (Notre Dame, University, Notre Dame, IN) IN: Annual Pittsburgh Conference, 13th, Pittsburgh, PA, April 22, 23, 1982, Proceedings. Part 1. Research Triangle Park, NC, Instrument Society of America, 1982, p. 45-54. refs (Contract NSG-3048)

An application of tensor modelling to a digital simulation of NASA's Quiet, Clean, Shorthaul Experimental (QCSE) gas turbine engine is presented. The results show that the tensor algebra offers a universal parametrization which is helpful in conceptualization and identification for plant modelling prior to feedback or for representing scheduled controllers over an operating line. C.D.

**A84-44178\*** National Aeronautics and Space Administration. Lewis Research Center, Cleveland, Ohio.

### **DEVELOPMENT OF DYNAMIC SIMULATION OF TF34-GE-100 TURBOFAN ENGINE WITH POST-STALL CAPABILITY**

S. M. KROSEL (NASA, Lewis Research Center, Cleveland, OH) AIAA, SAE, and ASME, Joint Propulsion Conference, 20th, Cincinnati, OH, June 11-13, 1984. 11 p. Previously announced in STAR as N84-25712. refs (AIAA PAPER 84-1184)

This paper describes the development of a hybrid computer simulation of a TF34-GE-100 turbofan engine with post-stall capability. The simulation operates in real-time and will be used to test and evaluate stall recovery control modes for this engine. The simulation calculations are performed by an analog computer with a peripheral multivariable function generation unit used for computing bivariate functions. Tabular listings of simulation variables are obtained by interfacing to a digital computer and using a custom software package for data collection and display. Author

**A84-44180\*** Army Propulsion Lab., Cleveland, Ohio

### **AN ANALYTICAL METHOD TO PREDICT EFFICIENCY OF AIRCRAFT GEARBOXES**

N. E. ANDERSON (U.S. Army, Propulsion Laboratory, Cleveland, OH), S. H. LOEWENTHAL (NASA, Lewis Research Center, Cleveland, OH), and J. D. BLACK (General Motors Corp., Detroit Diesel Allison Div., Indianapolis, IN) AIAA, SAE, and ASME, Joint Propulsion Conference, 20th, Cincinnati, OH, June 11-13, 1984. 15 p. Previously announced in STAR as N84-25606. refs (AIAA PAPER 84-1500)

A spur gear efficiency prediction method previously developed by the authors was extended to include power loss of planetary gearsets. A friction coefficient model was developed for MIL-L-7808 oil based on disc machine data. This combined with the recent capability of predicting losses in spur gears of nonstandard proportions allows the calculation of power loss for complete aircraft gearboxes that utilize spur gears. The method was applied to the T56/501 turboprop gearbox and compared with measured test data. Bearing losses were calculated with large scale computer programs. Breakdowns of the gearbox losses point out areas for possible improvement. Author

**A84-44181\*** Purdue Univ., Lafayette, Ind.

### **APPLICATION OF AN OPTIMIZATION METHOD TO HIGH PERFORMANCE PROPELLER DESIGNS**

K. C. LI (Purdue University, West Lafayette, IN) and G. L. STEFKO (NASA, Lewis Research Center, Cleveland, OH) AIAA, SAE, and ASME, Joint Propulsion Conference, 20th, Cincinnati, OH, June 11-13, 1984. 7 p. Previously announced in STAR as N84-25607. refs (AIAA PAPER 84-1203)

The application of an optimization method to determine the propeller blade twist distribution which maximizes propeller efficiency is presented. The optimization employs a previously developed method which has been improved to include the effects of blade drag, camber and thickness. Before the optimization portion of the computer code is used, comparisons of calculated propeller efficiencies and power coefficients are made with experimental data for one NACA propeller at Mach numbers in the range of 0.24 to 0.50 and another NACA propeller at a Mach number of 0.71 to validate the propeller aerodynamic analysis portion of the computer code. Then comparisons of calculated propeller efficiencies for the optimized and the original propellers show the benefits of the optimization method in improving propeller performance. This method can be applied to the aerodynamic design of propellers having straight, swept, or nonplanar propeller blades. Author

**A84-44182\*** National Aeronautics and Space Administration. Lewis Research Center, Cleveland, Ohio.

### **AN ADVANCED PITCH CHANGE MECHANISM INCORPORATING A HYBRID TRACTION DRIVE**

B. M. STEINETZ, S. H. LOEWENTHAL (NASA, Lewis Research Center, Cleveland, OH), D. F. SARGISSON (General Electric Co., Evendale, OH), and G. WHITE (Transmission Research, Inc., Cleveland, OH) AIAA, SAE, and ASME, Joint Propulsion Conference, 20th, Cincinnati, OH, June 11-13, 1984. 12 p. Previously announced in STAR as N84-25605. refs (Contract NAS3-23044) (AIAA PAPER 84-1383)

A design of a propeller pitch control mechanism is described that meets the demanding requirements of a high-power, advanced turboprop. In this application, blade twisting moment torque can be comparable to that of the main reduction gearbox output: precise pitch control, reliability and compactness are all at a premium. A key element in the design is a compact, high-ratio hybrid traction drive which offers low torque ripple and high torsional stiffness. The traction drive couples a high speed electric motor/alternator unit to a ball screw that actuates the blade control links. The technical merits of this arrangement and the performance characteristics of the traction drive are discussed. Author



**A84-44185\*#** General Electric Co., Lynn, Mass.  
**THE APPLICATION OF LQR SYNTHESIS TECHNIQUES TO THE TURBO-SHAFT ENGINE CONTROL PROBLEM**

W. H. PFEIL, G. DE LOS REYES (General Electric Co., Aircraft Engine Business Group, Lynn, MA), and G. A. BOBULA (U.S. Army, Propulsion Laboratory, Cleveland, OH) AIAA, SAE, and ASME, Joint Propulsion Conference, 20th, Cincinnati, OH, June 11-13, 1984. 8 p. refs  
 (Contract NAS3-22763)  
 (AIAA PAPER 84-1455)

A power turbine governor was designed for a recent-technology turboshaft engine coupled to a modern, articulated rotor system using Linear Quadratic Regulator (LQR) and Kalman Filter (KF) techniques. A linear, state-space model of the engine and rotor system was derived for six engine power settings from flight idle to maximum continuous. An integrator was appended to the fuel flow input to reduce the steady-state governor error to zero. Feedback gains were calculated for the system states at each power setting using the LQR technique. The main rotor tip speed state is not measurable, so a Kalman Filter of the rotor was used to estimate this state. The crossover of the system was increased to 10 rad/s compared to 2 rad/sec for a current governor. Initial computer simulations with a nonlinear engine model indicate a significant decrease in power turbine speed variation with the LQR governor compared to a conventional governor. Author

**A84-44186\*#** General Electric Co., Cincinnati, Ohio.  
**THE AERODYNAMIC DESIGN AND PERFORMANCE OF THE NASA/GE E3 LOW PRESSURE TURBINE**

D. G. CHERRY (General Electric Co., Cincinnati, OH) and R. P. DENGLER (NASA, Lewis Research Center, Cleveland, OH) AIAA, SAE, and ASME, Joint Propulsion Conference, 20th, Cincinnati, OH, June 11-13, 1984. 8 p.  
 (AIAA PAPER 84-1162)

The aerodynamic design and scaled rig test results of the low pressure turbine (LPT) component for the NASA/General Electric Energy Efficient Engine (E3) are presented. The low pressure turbine is a highly loaded five-stage design featuring high outer wall slope, controlled vortex aerodynamics, low stage flow coefficient, and reduced clearances. An assessment of its performance has been made based on a series of scaled air turbine tests which were divided into two phases: Block I (March through August, 1979) and Block II (June through September, 1981). Results from the Block II five-stage test, summarized in the paper, indicate that the E3 LPT will attain an efficiency level of 91.5 percent at the Mach 0.8/35,000 ft. max. climb altitude design point. This is relative to program goals of 91.1 percent for the E3 demonstrator engine and 91.7 percent for a fully developed flight propulsion system LPT. Author

**A84-44645\*#** Rensselaer Polytechnic Inst., Troy, N. Y.  
**STRUCTURAL DYNAMICS OF ROTATING BLADED-DISK ASSEMBLIES COUPLED WITH FLEXIBLE SHAFT MOTIONS**

R. G. LOEWY (Rensselaer Polytechnic Institute, Troy, NY) and N. KHADER AIAA Journal (ISSN 0001-1452), vol. 22, Sept. 1984, p. 1319-1327. Previously cited in issue 14, p. 1976, Accession no. A83-32787. refs  
 (Contract NAG3-37)

**A84-46106\*#** National Aeronautics and Space Administration. Lewis Research Center, Cleveland, Ohio  
**VELOCITY AND TEMPERATURE CHARACTERISTICS OF TWO-STREAM, COPLANAR JET EXHAUST PLUMES**

U. VON GLAHN, J. GOODYKOONTZ, and C. WASSERBAUER (NASA, Lewis Research Center, Cleveland, OH) American Institute of Aeronautics and Astronautics, Applied Aerodynamics Conference, 2nd, Seattle, WA, Aug. 21-23, 1984. 38 p. Previously announced in STAR as N84-28790. refs  
 (AIAA PAPER 84-2205)

The subsonic jet exhaust velocity and temperature characteristics of model scale, two stream coplanar nozzles were obtained experimentally. The data obtained included the effects of fan to primary stream velocity and temperature ratios on the

jet axial and radial flow characteristics. Empirical parameters were developed to correlate the measured data. The resultant equations were shown to be extensions of a previously published single stream jet velocity and temperature correlation. Author

**A84-46354\*#** National Aeronautics and Space Administration. Lewis Research Center, Cleveland, Ohio.

**DEVELOPMENT OF LARGE ROTORCRAFT TRANSMISSIONS**  
 N. E. SAMANICH (NASA, Lewis Research Center, Cleveland, OH), R. J. DRAGO, and J. C. MACK (Boeing Vertol Co., Philadelphia, PA) IN: American Helicopter Society, Annual Forum, 39th, St. Louis, MO, May 9-11, 1983, Proceedings. Alexandria, VA, American Helicopter Society, 1984, p. 293-302. refs  
 (Contract NAS3-22143)

The U.S. Army Heavy Lift Helicopter (HLH) represents a large rotorcraft which was developed by an American aerospace company. In the early 1970's with the HLH Advanced Technology Components (ATC) program, the development of large rotorcraft transmission and drive systems was started. Failures in the spiral bevel gearing were experienced in tests because the employed method of analysis had not considered the effect of rim bending. Consequently, new gears with strengthened rims were designed and fabricated. For a more accurate prediction of the load capacity of the gears, an extensive Finite Element Method (FEM) system was developed. The U.S. Army's XCH-62 HLH aft rotor transmission was finally successfully tested at full design torque and speed. A description of the test program is provided, and the analytical program is discussed. The analytical phase includes the development of a preprocessing program which aids in the review of calculated FEM stresses. G.R.

**A84-46993\*#** Massachusetts Inst. of Tech., Cambridge.  
**OPTIMIZATION AND MECHANISMS OF MISTUNING IN CASCADES**

E. F. CRAWLEY and K. C. HALL (MIT, Cambridge, MA) American Society of Mechanical Engineers, International Gas Turbine Conference and Exhibit, 29th, Amsterdam, Netherlands, June 4-7, 1984. 9 p. Research supported by the Fannie and John Hertz Foundation. refs  
 (Contract NSG-3079)  
 (ASME PAPER 84-GT-196)

In the present inverse design procedure for the optimum mistuning of a high bypass ratio shroudless fan that is modeled as a cascade of blades (each with a single torsional degree-of-freedom), linearized supersonic aerodynamic theory is used to compute the unsteady aerodynamic forces in the 'influence coefficient' form at a typical blade section. The mistuning pattern is then numerically optimized in order to achieve a specified increase in the aeroelastic stability margin with a minimum amount of mistuning. If the blades are self-damped, an optimized mistuning pattern can be found that achieves a given stability margin for a much lower level of mistuning than required for the alternate mistuning pattern, which requires only two blade frequencies and is relatively insensitive to implementation errors. O.C.

**N84-10054\*#** California Univ., Berkeley.  
**EXPERIMENTAL AND THEORETICAL STUDY OF COMBUSTION JET IGNITION Final Report**

D. Y. CHEN, A. F. GHONIEM, and A. K. OPPENHEIM Mar. 1983 138 p refs  
 (Contract NAG3-131; W-7405-ENG-48; NSF CPE-81-15163)  
 (NASA-CR-168139; DOE/NASA/0131-1; NAS 1.26:168139)  
 Avail: NTIS HC A07/MF A01 CSCL 21E

A combustion jet ignition system was developed to generate turbulent jets of combustion products containing free radicals and to discharge them as ignition sources into a combustible medium. In order to understand the ignition and the inflammation processes caused by combustion jets, the studies of the fluid mechanical properties of turbulent jets with and without combustion were conducted theoretically and experimentally. Experiments using a specially designed igniter, with a prechamber to build up and control the stagnation pressure upstream of the orifice, were conducted to investigate the formation processes of turbulent jets of

## 07 AIRCRAFT PROPULSION AND POWER

combustion products. The penetration speed of combustion jets has been found to be constant initially and then decreases monotonically as turbulent jets of combustion products travel closer to the wall. This initial penetration speed to combustion jets is proportional to the initial stagnation pressure upstream of the orifice for the same stoichiometric mixture. Computer simulations by Chorin's Random Vortex Method implemented with the flame propagation algorithm for the theoretical model of turbulent jets with and without combustion were performed to study the turbulent jet flow field. In the formation processes of the turbulent jets, the large-scale eddy structure of turbulence, the so-called coherent structure, dominates the entrainment and mixing processes. The large-scale eddy structure of turbulent jets in this study is constructed by a series of vortex pairs, which are organized in the form of a staggered array of vortex clouds generating local recirculation flow patterns. Author

**N84-10055\*#** National Aeronautics and Space Administration. Lewis Research Center, Cleveland, Ohio.

### **AIRCRAFT ELECTRIC SECONDARY POWER**

Washington Jun. 1983 199 p refs Workshop held in Cleveland, 14-15 Sep. 1982

(NASA-CP-2282; E-1632; NAS 1.55:2282) Avail: NTIS HC A09/MF A01 CSCL 01C

Technologies resulted to aircraft power systems and aircraft in which all secondary power is supplied electrically are discussed. A high-voltage dc power generating system for fighter aircraft, permanent magnet motors and generators for aircraft, lightweight transformers, and the installation of electric generators on turbine engines are among the topics discussed. R.J.F.

**N84-10063\*#** National Aeronautics and Space Administration. Lewis Research Center, Cleveland, Ohio.

### **APPLICATION OF ADVANCED MATERIALS TO ROTATING MACHINES**

J. E. TRINER *In its Aircraft Elect. Secondary Power* p 93-101 Jun. 1983

Avail: NTIS HC A09/MF A01 CSCL 21E

In discussing the application of advanced materials to rotating machinery, the following topics are covered: the torque speed characteristics of ac and dc machines, motor and transformer losses, the factors affecting core loss in motors, advanced magnetic materials and conductors, and design tradeoffs for samarium cobalt motors. B.W.

**N84-10070\*#** National Aeronautics and Space Administration. Lewis Research Center, Cleveland, Ohio.

### **ALL-PURPOSE BIDIRECTIONAL FOUR-QUADRANT CONTROLLER**

I. G. HANSEN *In its Aircraft Elect. Secondary Power* p 189-196 Jun. 1983 refs

Avail: NTIS HC A09/MF A01 CSCL 21E

The basic purpose of this paper is to provide some information regarding bidirectional four quadrant resonant power conversion and describe possible applications to aircraft electrical systems. As this technology has been developed sufficiently to demonstrate its feasibility, this is an appropriate time to evaluate the benefits of its application to aircraft electrical systems. Author

**N84-11170\*#** General Electric Co., Evendale, Ohio. Aircraft Engine Business Group.

### **ENERGY EFFICIENT ENGINE: FLIGHT PROPULSION SYSTEM, PRELIMINARY ANALYSIS AND DESIGN UPDATE Topical Report, Nov. 1978 - Jul. 1982**

E. M. STEARNS Nov. 1982 61 p refs

(Contract NAS3-20643)

(NASA-CR-167980; NAS 1.26:167980; R82AEB532) Avail: NTIS HC A04/MF A01 CSCL 21E

The preliminary design of General Electric's Energy Efficient Engine (E3) was reported in detail in 1980. Since then, the design has been refined and the components have been rig-tested. The changes which have occurred in the engine and a reassessment of the economic payoff are presented in this report. All goals for

efficiency, environmental considerations, and economic payoff are being met. The E3 Flight Propulsion System has 14.9% lower *sfc* than a CF6-50C. It provides a 7.1% reduction in direct operating cost for a short haul domestic transport and 14.5% reduction for an international long distance transport. Author

**N84-11171\*#** National Aeronautics and Space Administration. Lewis Research Center, Cleveland, Ohio.

### **F100. MULTIVARIABLE CONTROL SYNTHESIS PROGRAM. COMPUTER IMPLEMENTATION OF THE F100 MULTIVARIABLE CONTROL ALGORITHM**

J. F. SOEDER Oct. 1983 46 p

(NASA-TP-2231; E-1496; NAS 1.60:2231) Avail: NTIS HC

A03/MF A01 CSCL 21E

As turbofan engines become more complex, the development of controls necessitate the use of multivariable control techniques. A control developed for the F100-PW-100(3) turbofan engine by using linear quadratic regulator theory and other modern multivariable control synthesis techniques is described. The assembly language implementation of this control on an SEL 810B minicomputer is described. This implementation was then evaluated by using a real-time hybrid simulation of the engine. The control software was modified to run with a real engine. These modifications, in the form of sensor and actuator failure checks and control executive sequencing, are discussed. Finally recommendations for control software implementations are presented. S.L.

**N84-12166\*#** National Aeronautics and Space Administration. Lewis Research Center, Cleveland, Ohio.

### **A GENERALIZED COMPUTER CODE FOR DEVELOPING DYNAMIC GAS TURBINE ENGINE MODELS (DIGTEM)**

C. J. DANIELE Nov. 1983 18 p refs To be presented at the Aerospace Conf., San Diego, Calif., 2-3 Feb. 1984

(NASA-TM-83508; NAS 1.15:83508; E-1853) Avail: NTIS HC

A02/MF A01 CSCL 21E

This paper describes DIGTEM (digital turbofan engine model), a computer program that simulates two spool, two stream (turbofan) engines. DIGTEM was developed to support the development of a real time multiprocessor based engine simulator being designed at the Lewis Research Center. The turbofan engine model in DIGTEM contains steady state performance maps for all the components and has control volumes where continuity and energy balances are maintained. Rotor dynamics and duct momentum dynamics are also included. DIGTEM features an implicit integration scheme for integrating stiff systems and trims the model equations to match a prescribed design point by calculating correction coefficients that balance out the dynamic equations. It uses the same coefficients at off design points and iterates to a balanced engine condition. Transients are generated by defining the engine inputs as functions of time in a user written subroutine (TMRSP). Closed loop controls can also be simulated. DIGTEM is generalized in the aerothermodynamic treatment of components. This feature, along with DIGTEM's trimming at a design point, make it a very useful tool for developing a model of a specific turbofan engine. B.W.

**N84-13186\*** Hamilton Standard, Windsor Locks, Conn.

### **TECHNOLOGY AND BENEFITS OF AIRCRAFT COUNTER ROTATION PROPELLERS**

A. L. WEISBRICH, J. GODSTON (Pratt & Whitney Aircraft, East Hartford, Conn.), and E. BRADLEY (Lockheed-Georgia Co., Marietta) Dec. 1982 330 p

(Contract NAS3-23043)

(NASA-CR-168258; NAS 1.26:168258; HSER-8856) Avail:

Technical Monitor, NASA. Lewis Research Center, Cleveland CSCL 01A

Results are reported of a NASA sponsored analytical investigation into the merits of advanced counter rotation propellers for Mach 0.80 commercial transport application. Propeller and gearbox performance, acoustics, vibration characteristics, weight, cost and maintenance requirements for a variety of design parameters and special features were considered. Fuel savings in



the neighborhood of 9 percent relative to single rotation configurations are feasible through swirl recovery and lighter gearboxes. This is the net gain which includes a 5 percent acoustic treatment weight penalty to offset the broader frequency spectrum of the noise produced by counter rotation propellers. Author

**N84-13187\*#** Pennsylvania State Univ., University Park.  
**A THEORETICAL AND EXPERIMENTAL STUDY OF TURBULENT PARTICLE-LADEN JETS** Annual Report  
 J. S. SHUEN, A. S. P. SOLOMON, Q. F. ZHANG, and G. M. FAETH Nov. 1983 106 p refs  
 (Contract NAG3-190)  
 (NASA-CR-168293; NAS 1.26:168293) Avail: NTIS HC A06/MF A01 CSCL 21E

Mean and fluctuating velocities of both phases, particle mass fluxes, particle size distributions in turbulent particle-laden jets were measured. The following models are considered: (1) a locally homogeneous flow (LHF) model, where slip between the phases was neglected; (2) a deterministic separated flow (DSF) model, where slip was considered but effects of particle dispersion by turbulence were ignored; and (3) a stochastic separated flow (SSF) model. The SSF model performed reasonably well with no modifications in the prescriptions for eddy properties from its original calibration. A modified k- model, incorporating direct contributions of interphase transport on turbulence properties (turbulence modulation), was developed within the framework of the SSF model. E.A.K.

**N84-13188\*#** National Aeronautics and Space Administration. Lewis Research Center, Cleveland, Ohio.  
**FLAME RADIATION AND LINER HEAT TRANSFER IN A TUBULAR-CAN COMBUSTOR**  
 R. W. CLAUS, G. M. NEELY, and F. M. HUMENIK 1983 23 p refs Proposed for presentation at the 22nd Aerospace Sci. Meeting, Reno, 9-12 Jan. 1984; sponsored by AIAA  
 (NASA-TM-83538; E-1909; NAS 1.15:83538) Avail: NTIS HC A02/MF A01 CSCL 21E

Heat transfer within a combustor were examined. Total and spectral flame radiation in a tubular can combustor at a series of parametric operating conditions was measured. Radiation measurements were taken for a range of inlet air pressures from 0.34 to 2.0 MPa, inlet air temperatures from 533 to 700 K, with two different fuels, Jet-A and ERBS. Measurements of liner temperatures combined with the parametric radiation results allowed a calculation of the combustor liner heat loads. Flame emissivity was determined from the spectral measurements. E.A.K.

**N84-13189\*#** California Univ., Berkeley.  
**NUMERICAL MODELING OF TURBULENT FLOW IN A CHANNEL** Final Report  
 Y. W. DAI, A. F. GHONIEM, F. S. SHERMAN, and A. K. OPPENHEIM Mar. 1983 68 p refs  
 (Contract NAG3-131; W-7405-ENG-48; NSF CPE-81-15163)  
 (NASA-CR-168278; DOE/NASA/0131-2, NAS 1.26:168278)  
 Avail: NTIS HC A04/MF A01 CSCL 21E

Two-dimensional incompressible turbulent flow in a channel with a backward-facing step was studied numerically by Chorin's Random Vortex Method (RVM), an algorithm capable of tracing the action of elementary turbulent eddies and their cumulative effects without imposing any restrictions upon their motions. The step occurs in one side of a channel with otherwise flat, parallel walls; its height equals 1/3, 1/4 or 1/5 the width of the channel downstream. The main objective was to investigate the behavior of the large-scale turbulent eddies in a flow and the flow characteristics in the separated shear layer, the reattached zone, and the rebuilding boundary layer after reattachment. The unsteady vorticity field and the distribution of time-averaged turbulent statistics were obtained. The effects of expansion step height and initial boundary layer state were also studied. Comparisons were made with the available experimental results. The agreement is satisfactory in the velocity profiles and in the reattachment length, and fairly good in the turbulence profiles. Also a mechanism of

the development of the reattaching turbulent flow was suggested by the numerical results. Author

**N84-13190\*#** National Aeronautics and Space Administration. Lewis Research Center, Cleveland, Ohio.  
**THREE-DIMENSIONAL VISCOUS DESIGN METHODOLOGY FOR ADVANCED TECHNOLOGY AIRCRAFT SUPERSONIC INLET SYSTEMS**  
 B. H. ANDERSON Dec. 1983 64 p refs Presented at the 21st Aerospace Sci. Meeting, Reno, Nev., 9-12 Jan. 1984  
 (NASA-TM-83558; E-1936; NAS 1.15:83558; AIAA-84-0192)  
 Avail: NTIS HC A04/MF A01 CSCL 21E

A broad program to develop advanced, reliable, and user oriented three-dimensional viscous design techniques for supersonic inlet systems, and encourage their transfer into the general user community is discussed. Features of the program include: (1) develop effective methods of computing three-dimensional flows within a zonal modeling methodology; (2) ensure reasonable agreement between said analysis and selective sets of benchmark validation data; (3) develop user orientation into said analysis; and (4) explore and develop advanced numerical methodology. Author

**N84-13193\*#** General Electric Co., Cincinnati, Ohio. Aircraft Engine Business Group.  
**BLADE LOSS TRANSIENT DYNAMICS ANALYSIS WITH FLEXIBLE BLADED DISK** Final Report  
 V. C. GALLARDO, G. BLACK, L. BACH, S. CLINE, and A. STORACE Apr. 1983 269 p refs  
 (Contract NAS3-23281)  
 (NASA-CR-168176; NAS 1.26:168176) Avail: NTIS HC A12/MF A01 CSCL 21E

The transient dynamic response of a flexible bladed disk on a flexible rotor in a two rotor system is formulated by modal synthesis and a Lagrangian approach. Only the nonequibrated one diameter flexible mode is considered for the flexible bladed disk, while the two flexible rotors are represented by their normal modes. The flexible bladed disk motion is modeled as a combination of two one diameter standing waves, and is coupled inertially and gyroscopically to the flexible rotors. Application to a two rotor model shows that a flexible bladed disk on one rotor can be driven into resonance by an unbalance in the other rotor, and at a frequency equal to the difference in the rotor speeds. Author

**N84-14143\*#** Solar Turbines International, San Diego, Calif.  
**EXPERIMENTAL STUDY OF THE OPERATING CHARACTERISTICS OF PREMIXING-PREVAPORIZING FUEL/AIR MIXING PASSAGES** Final Report  
 D. A. ROHY and J. G. MEIER Nov. 1983 60 p  
 (Contract NAS3-20662)  
 (NASA-CR-168279; NAS 1.26:168279; SR83-R-4663-30) Avail: NTIS HC A04/MF A01 CSCL 21E

Fuel spray and air flow characteristics were determined using nonintrusive (optical) measurement techniques in a fuel preparation duct. A very detailed data set was obtained at high pressures (to 10 atm) and temperatures (to 750 K). The data will be used to calibrate an analytical model which will facilitate the design of a lean premixed prevaporized combustor. This combustor has potential for achieving low pollutant emissions and low levels of flame radiation and pattern factors conducive to improved durability and performance for a variety of fuels. Author

**N84-14145\*#** National Aeronautics and Space Administration. Lewis Research Center, Cleveland, Ohio.

**CERAMIC COMPOSITE LINER MATERIAL FOR GAS TURBINE COMBUSTORS**

D. B. ERCEGOVIC, C. L. WALKER, and C. T. NORNGREN 1984 19 p refs Presented at the 22nd Aerospace Sci. Meeting, Reno, Nev., 9-12 Jan. 1984; sponsored by AIAA Prepared in cooperation with Army Aviation Research and Development Command, Cleveland

(NASA-TM-83490; E-1819; NAS 1.15:83490; AVRADCOM-TR-83-C-11) Avail: NTIS HC A02/MF A01 CSCL 21E

Advanced commercial and military gas turbine engines may operate at combustor outlet temperatures in excess of 1920 K (3000 F). At these temperatures combustors liners experience extreme convective and radiative heat fluxes. The ability of a plasma sprayed ceramic coating to reduce liner metal temperature has been recognized. However, the brittleness of the ceramic layer and the difference in thermal expansion with the metal substrate has caused cracking, spalling and some separation of the ceramic coating. Research directed at turbine tip seals (or shrouds) has shown the advantage of applying the ceramic to a compliant metal pad. This paper discusses recent studies of applying ceramics to combustor liners in which yttria stabilized zirconia plasma sprayed on compliant metal substrates which were exposed to near stoichiometric combustion, presents performance and durability results, and describes a conceptual design for an advanced, small gas turbine combustor. Test specimens were convectively cooled or convective-transpiration cooled and were evaluated in a 10 cm square flame tube combustor at inlet air temperatures of 533 K (500 F) and at a pressure of 0.5 MPa (75 psia). The ceramics were exposed to flame temperatures in excess of 2000 K (3320 F). Results appear very promising with all 30 specimens surviving a screening test and one of two specimens surviving a cyclic durability test.

Author

**N84-14146\*#** National Aeronautics and Space Administration. Lewis Research Center, Cleveland, Ohio.

**A REVIEW OF NASA COMBUSTOR AND TURBINE HEAT TRANSFER RESEARCH**

R. A. RUDEY and R. W. GRAHAM 1984 26 p refs Proposed for presentation at the 29th Ann. Intern. Gas Turbine Conf., Amsterdam, 3-7 Jun. 1984; sponsored by ASME

(NASA-TM-83541; E-1912; NAS 1.15:83541) Avail: NTIS HC A03/MF A01 CSCL 21E

The thermal design of the combustor and turbine of a gas turbine engine poses a number of difficult heat transfer problems. The importance of improved prediction techniques becomes more critical in anticipation of future generations of gas turbine engines which will operate at higher cycle pressure and temperatures. Research which addresses many of the complex heat transfer processes holds promise for yielding significant improvements in prediction of metal temperatures. Such research involves several kinds of program including: (1) basic experiments which delineate the fundamental flow and heat transfer phenomena that occur in the hot sections of the gas turbine but at low enthalpy conditions; (2) analytical modeling of these flow and heat transfer phenomena which results from the physical insights gained in experimental research; and (3) verification of advanced prediction techniques in facilities which operate near the real engine thermodynamic conditions. In this paper, key elements of the NASA program which involves turbine and combustor heat transfer research will be described and discussed.

B.W.

**N84-14147\*#** National Aeronautics and Space Administration. Lewis Research Center, Cleveland, Ohio.

**FLOW VISUALIZATION AND INTERPRETATION OF VISUALIZATION DATA FOR DEFLECTED THRUST V/STOL NOZZLES**

H. C. KAO, P. L. BURSTADT, and A. L. JOHNS 1984 51 p refs Presented at the 22nd Aerospace Sci. Meeting, Reno, Nev., 9-12 Jan. 1984; sponsored by AIAA

(NASA-TM-83554; E-1933; NAS 1.15:83554) Avail: NTIS HC A04/MF A01 CSCL 21E

Flow visualization studies were made for four deflected thrust nozzle models at subsonic speeds. Based on topological rules and the assumption that observed streaks constitute continuous vector fields, available visualization pictures are interpreted and flow patterns on interior surfaces of the nozzles are synthesized. In particular, three dimensional flow structure and separations are discussed. From the synthesized patterns, the overall features of the flow field in a given nozzle can be approximately perceived.

Author

**N84-14148\*#** Textron Bell Aerospace Co., Buffalo, N. Y. **NASTRAN FLUTTER ANALYSIS OF ADVANCED TURBOPROPELLERS Final Report**

V. ELCHURI and G. C. C. SMITH Apr. 1982 121 p refs (Contract NAS3-22533)

(NASA-CR-167926; NAS 1.26:167926; D2536-941009) Avail: NTIS HC A06/MF A01 CSCL 02A

An existing capability developed to conduct modal flutter analysis of tuned bladed-shrouded discs in NASTRAN was modified and applied to investigate the subsonic unstalled flutter characteristics of advanced turbopropellers. The modifications pertain to the inclusion of oscillatory modal aerodynamic loads of blades with large (backward and forward) variable sweep. The two dimensional subsonic cascade unsteady aerodynamic theory was applied in a strip theory manner with appropriate modifications for the sweep effects. Each strip is associated with a chord selected normal to any spanwise reference curve such as the blade leading edge. The stability of three operating conditions of a 10-bladed propeller is analyzed. Each of these operating conditions is iterated once to determine the flutter boundary. A 5-bladed propeller is also analyzed at one operating condition to investigate stability. Analytical results obtained are in very good agreement with those from wind tunnel tests.

Author

**N84-15151\*#** General Electric Co., Cincinnati, Ohio. Aircraft Engine Business Group.

**CLEAN CATALYTIC COMBUSTOR PROGRAM Final Report, Oct. 1979 - Jul. 1982**

E. E. EKSTEDT, T. F. LYON, P. E. SABLA, and W. J. DODDS Nov. 1983 152 p refs

(Contract NAS3-22003)

(NASA-CR-168323; NAS 1.26:168323) Avail: NTIS HC A08/MF A01 CSCL 21E

A combustor program was conducted to evolve and to identify the technology needed for, and to establish the credibility of, using combustors with catalytic reactors in modern high-pressure-ratio aircraft turbine engines. Two selected catalytic combustor concepts were designed, fabricated, and evaluated. The combustors were sized for use in the NASA/General Electric Energy Efficient Engine (E3). One of the combustor designs was a basic parallel-staged double-annular combustor. The second design was also a parallel-staged combustor but employed reverse flow annular catalytic reactors. Subcomponent tests of fuel injection systems and of catalytic reactors for use in the combustion system were also conducted. Very low-level pollutant emissions and excellent combustor performance were achieved. However, it was obvious from these tests that extensive development of fuel/air preparation systems and considerable advancement in the steady-state operating temperature capability of catalytic reactor materials will be required prior to the consideration of catalytic combustion systems for use in high-pressure-ratio aircraft turbine engines.

Author

**N84-15152\*#** General Electric Co., Cincinnati, Ohio. Aircraft Engine Business Group.

**AEROTHERMAL MODELING. EXECUTIVE SUMMARY Final Report**

M. K. KENWORTHY, S. M. CORREA, and D. L. BURRUS Dec. 1983 55 p refs

(Contract NAS3-23525)

(NASA-CR-168330; NAS 1.26:168330) Avail: NTIS HC A04/MF A01 CSCL 21E

One of the significant ways in which the performance level of aircraft turbine engines has been improved is by the use of advanced materials and cooling concepts that allow a significant increase in turbine inlet temperature level, with attendant thermodynamic cycle benefits. Further cycle improvements have been achieved with higher pressure ratio compressors. The higher turbine inlet temperatures and compressor pressure ratios with corresponding higher temperature cooling air has created a very hostile environment for the hot section components. To provide the technology needed to reduce the hot section maintenance costs, NASA has initiated the Hot Section Technology (HOST) program. One key element of this overall program is the Aerothermal Modeling Program. The overall objective of his program is to evolve and validate improved analysis methods for use in the design of aircraft turbine engine combustors. The use of such combustor analysis capabilities can be expected to provide significant improvement in the life and durability characteristics of both combustor and turbine components B.W.

**N84-15153\*#** Textron Bell Aerospace Co., Buffalo, N. Y. **NASTRAN DOCUMENTATION FOR FLUTTER ANALYSIS OF ADVANCED TURBOPROPELLERS Final Report**

V. ELCHURI, A. M. GALLO, and S. C. SKALSKI Apr. 1982 216 p refs

(Contract NAS3-22533)

(NASA-CR-167927; NAS 1.26:167927; D2536-941010) Avail: NTIS HC A10/MF A01 CSCL 20K

An existing capability developed to conduct modal flutter analysis of tuned bladed-shrouded discs was modified to facilitate investigation of the subsonic unstalled flutter characteristics of advanced turbopropellers. The modifications pertain to the inclusion of oscillatory modal aerodynamic loads of blades with large (backward and forward) varying sweep. Author

**N84-15154\*#** Textron Bell Aerospace Co., Buffalo, N. Y. **BLADED-SHROUDED-DISC AEROELASTIC ANALYSES: COMPUTER PROGRAM UPDATES IN NASTRAN LEVEL 17.7 Final Report**

A. M. GALLO, V. ELCHURI, and S. C. SKALSKI Dec. 1981 348 p

(Contract NAS3-22533)

(NASA-CR-165428; NAS 1.26:165428; D2536-941006) Avail: NTIS HC A15/MF A01 CSCL 21E

In October 1979, a computer program based on the state-of-the-art compressor and structural technologies applied to bladed-shrouded-disc was developed. The program was more operational in NASTRAN Level 16. The bladed disc computer program was updated for operation in NASTRAN Level 17.7. The supersonic cascade unsteady aerodynamics routine UCAS, delivered as part of the NASTRAN Level 16 program was recorded to improve its execution time. These improvements are presented. Author

**N84-15155\*#** General Electric Co., Cincinnati, Ohio. Advanced Technology Operation.

**AEROTHERMAL MODELING, PHASE 1. VOLUME 1: MODEL ASSESSMENT Final Report**

M. J. KENWORTHY, S. M. CORREA, and D. L. BURRUS Nov. 1983 386 p refs 2 Vol.

(Contract NAS3-23525)

(NASA-CR-168296-VOL-1; NAS 1.26:168296-VOL-1) Avail: NTIS HC A17/MF A01 CSCL 21E

Phase 1 was conducted as part of the overall NASA Hot Section Technology (HOST) Program. The purpose of this effort was to

determine the predictive accuracy of and the deficiencies within the various analytical modules comprising the overall combustor aerothermal model used at General Electric, as well as to formulate recommendations for improvement where needed. This effort involved the assembly of a benchmark quality data base from selected available literature, and from General Electric engine and combustor component test data. This data base was supplemented with additional definitive data obtained from an experimental test program conducted as part of the Phase 1 effort. Using selections from this data base, assessment studies were conducted to evaluate the various modules. Assessment of the internal flow module was conducted using 2-D parabolic and elliptic, as well as 3-D elliptic internal flow calculations of definitive test data selected from the assembled data base. The 2-D assessment provided methodical examination of the mathematical techniques and the physical submodules, while the 3-D assessment focused on usefulness as a design tool. Calculations of combustor linear metal temperatures, pressure loss performance, and airflow distribution were performed using aerothermal modules which were in general use for many years at General Electric. The results of these assessment provided for the identification of deficiencies within the modules. The deficiencies were addressed in some detail providing a foundation on which to formulate a prioritized list of recommendations for improvement. Author

**N84-15156\*#** General Electric Co., Cincinnati, Ohio. Advanced Technology Operation.

**AEROTHERMAL MODELING, PHASE 1. VOLUME 2: EXPERIMENTAL DATA Final Report**

M. J. KENWORTHY, S. M. CORREA, and D. L. BURRUS Nov. 1983 161 p 2 Vol.

(Contract NAS3-23525)

(NASA-CR-168296-VOL-2; NAS 1.26:168296-VOL-2) Avail: NTIS HC A08/MF A01 CSCL 21E

The experimental test effort is discussed. The test data are presented. The compilation is divided into sets representing each of the 18 experimental configurations tested. A detailed description of each configuration, and plots of the temperature difference ratio parameter or pattern factor parameter calculated from the test data are also provided. Author

**N84-16181\*#** National Aeronautics and Space Administration. Lewis Research Center, Cleveland, Ohio.

**DYNAMIC BEHAVIOR OF SPIRAL-GROOVE AND RAYLEIGH-STEP SELF-ACTING FACE SEALS**

E. DIRUSSO Jan. 1984 19 p refs

(NASA-TP-2266; NAS 1.60:2266; E-1754) Avail: NTIS HC A02/MF A01 CSCL 21E

Tests were performed to determine the dynamic behavior and establish baseline dynamic data for five self-acting face seals employing Rayleigh-step lift-pads and inward pumping as well as outward-pumping spiral grooves for the lift-generating mechanism. The primary parameters measured in the tests were film thickness, seal seat axial motion, and seal frictional torque. The data show the dynamic response of the film thickness to the motion of the seal seat. The inward-pumping spiral-groove seals exhibited a high-amplitude film thickness vibratory mode with a frequency of four times the shaft speed. This mode was not observed in the other seals tested. The tests also revealed that high film thickness vibration amplitude produces considerably higher average film thickness than do low amplitude film thickness vibrations. The seals were tested at a constant face load of 73 N (16.4 lb) with ambient air at room temperature and atmospheric pressure as the fluid medium. The test speed range was from 7000 to 17000 rpm. Seal tangential speed range was 34.5 to 83.7 m/sec (113 to 274 ft/sec). Author

**N84-16184\*#** National Aeronautics and Space Administration. Lewis Research Center, Cleveland, Ohio.

## **HYTESS: A HYPOTHETICAL TURBOFAN ENGINE SIMPLIFIED SIMULATION**

W. C. MERRILL, E. C. BEATTIE (United Technologies Corp., East Hartford, Conn.), R. F. LAPRAD (United Technologies Corp., East Hartford, Conn.), S. M. ROCK (Systems Control Technologies, Inc., Palo Alto, Calif.), and M. M. AKHTER (Systems Control Technologies, Inc., Palo Alto, Calif.) Jan. 1984 23 p refs (NASA-TM-83561; E-1940; NAS 1.15:83561) Avail: NTIS-HC A02/MF A01 CSCL 21E

A users manual for a hypothetical turbofan engine simplified simulation is presented. This digital simulation exists as FORTRAN source code. The program is self-contained and was developed to offer those interested in engine dynamics and controls research an efficient, realistic, and easily used engine simulation. The engine is modeled using a state space formulation. Matrix elements within the linear state space structure are nonlinear functions of various engine variables. S.L.

**N84-16185\*#** National Aeronautics and Space Administration. Lewis Research Center, Cleveland, Ohio.

## **DIGITAL COMPUTER PROGRAM FOR GENERATING DYNAMIC TURBOFAN ENGINE MODELS (DIGTEM)**

C. J. DANIELE, S. M. KROSEL, J. R. SZUCH, and E. J. WESTERKAMP Sep. 1983 109 p refs (NASA-TM-83446; E-1748; NAS 1.15:83446) Avail: NTIS HC A06/MF A01 CSCL 21E

This report describes DIGTEM, a digital computer program that simulates two spool, two-stream turbofan engines. The turbofan engine model in DIGTEM contains steady-state performance maps for all of the components and has control volumes where continuity and energy balances are maintained. Rotor dynamics and duct momentum dynamics are also included. Altogether there are 16 state variables and state equations. DIGTEM features a backward-difference integration scheme for integrating stiff systems. It trims the model equations to match a prescribed design point by calculating correction coefficients that balance out the dynamic equations. It uses the same coefficients at off-design points and iterates to a balanced engine condition. Transients can also be run. They are generated by defining controls as a function of time (open-loop control) in a user-written subroutine (TMRSP). DIGTEM has run on the IBM 370/3033 computer using implicit integration with time steps ranging from 1.0 msec to 1.0 sec. DIGTEM is generalized in the aerothermodynamic treatment of components. B.W.

**N84-16186\*#** National Aeronautics and Space Administration. Lewis Research Center, Cleveland, Ohio.

## **DESIGN CONCEPTS FOR LOW-COST COMPOSITE ENGINE FRAMES**

C. C. CHAMIS 1983 28 p refs Presented at Aircraft Design Systems and Operations Meeting, Fort Worth, Tex., 17-19 Oct. 1983; sponsored by AIAA and AHS Previously announced in IAA as A83-48331 (NASA-TM-83544; E-1916; NAS 1.15:83544) Avail: NTIS HC A03/MF A01 CSCL 21E

Design concepts for low-cost, lightweight composite engine frames were applied to the design requirements for the frame of commercial, high-bypass turbine engines. The concepts consist of generic-type components and subcomponents that could be adapted for use in different locations in the engine and to different engine sizes. A variety of materials and manufacturing methods were assessed with a goal of having the lowest number of parts possible at the lowest possible cost. The evaluation of the design concepts resulted in the identification of a hybrid composite frame which would weigh about 70 percent of the state-of-the-art metal frame and cost would be about 60 percent. Author (IAA)

**N84-16207\*#** Pennsylvania State Univ., University Park. Dept. of Aerospace Engineering.

## **ANNULUS WALL BOUNDARY LAYER DEVELOPMENT IN A COMPRESSOR STAGE, INCLUDING THE EFFECTS OF TIP CLEARANCE**

B. LAKSHMINARAYANA, K. N. S. MURTHY, M. POUGARE, and T. R. GOVINDAN In AGARD Viscous Effects in Turbomachines 17 p Sep. 1983 refs (Contract NSG-3212) Avail: NTIS HC A17/MF A01

The end-wall boundary layer development in a compressor stage, including the inlet guide vane (IGV) passage and the rotor passage, was measured. The measurement upstream of the rotor and inside the IGV passage were carried out with a five-hole probe. The data (blade-to-blade) inside the IGV passage were carried out with a five-hole probe. The data (blade-to-blade) inside the rotor passage were measured using a three-sensor rotating hot-wire below the tip clearance region and "V" configuration probe inside the clearance region. The rotor exit measurements (blade-to-blade) were acquired with a laser Doppler velocimeter. The velocity profiles and the integral properties are presented and interpreted. The boundary layer is comparatively well behaved up to the leading edge of the rotor, beyond which complex interactions result in very unconventional profiles. The momentum thicknesses decrease in the leakage flow region of the rotor. The momentum thicknesses and the limiting streamline angles predicted from a momentum integral technique agree well with the data up to the leading edge of the rotor. M.G.

**N84-16208\*#** National Aeronautics and Space Administration. Lewis Research Center, Cleveland, Ohio.

## **END-WALL BOUNDARY LAYER MEASUREMENTS IN A TWO-STAGE FAN**

C. L. BALL, L. REID, and J. F. SCHMIDT In AGARD Viscous Effects in Turbomachines 23 p Sep. 1983 refs Avail: NTIS HC A17/MF A01 CSCL 21E

Detailed flow measurements made in the casing boundary layer of a two-stage transonic fan are summarized. These measurements were taken at stations upstream of the fan, between all blade rows, and downstream of the last blade row. At the design tip speed of 429 m/sec the fan achieved a peak efficiency of 0.846 at a pressure ratio of 2.471. The boundary layer data were obtained at three weight flows at the design speed: one near choke flow, one near peak efficiency, and one near stall. Conventional boundary layer parameters were calculated from the data measured at each measuring station for each of the three flows. A classical two dimensional casing boundary layer was measured at the fan inlet and extended inward to approximately 15 percent of span. A highly three dimensional boundary layer was measured at the exit of each blade row and extended inward to approximately 10 percent of span. The steep radial gradient of axial velocity noted at the exit of the rotors was reduced substantially as the flow passed through the stators. This reduced gradient is attributed to flow mixing. The amount of flow mixing was reflected in the radial redistribution of total temperature as the flow passed through the stators. The data also show overturning of the tip flow at the stator exits that is consistent with the expected effect of the secondary flow field. The blockage factors calculated from the measured data show an increase in blockage across the rotors and a decrease across the stators. M.G.

**N84-16210#** United Technologies Research Center, East Hartford, Conn. Gas Turbine Technology Div.

## **COMPRESSOR ROTOR AERODYNAMICS**

R. P. DRING, H. D. JOSLYN, and J. H. WAGNER In AGARD Viscous Effects in Turbomachines 16 p Sep. 1983 refs (Contract NAS3-23157; F33615-77-C-2083) Avail: NTIS HC A17/MF A01 CSCL 20E

Although the numerical sophistication of multi-stage turbomachinery through-flow calculations has evolved to a very high level, the aerodynamic inputs of total pressure loss, deviation and blockage are subject to a high degree of empiricism. There is a need for detailed flow field data in a multi-stage environment in

order to bring some discipline to this important aspect of turbomachinery design. A survey of some of the initial results of an in-depth investigation of the aerodynamics of the second stage of a large scale two stage axial compressor is presented. The second stage rotor data are compared with data obtained on an isolated rotor with very thin and then very thick inlet hub and tip boundary layers. The single and multi-stage rotor data presented include surface flow visualization and rotating frame radial/circumferential traverse measurements presented in the form of fullspan contour plots of rotary total pressure. Also presented are the spanwise distributions of loss, deviation and blockage. Some implications of these results for through-flow analyses are discussed. M.G.

**N84-18202\*#** Santa Clara Univ., Calif. School of Engineering.  
**SECONDARY FLOW SPANWISE DEVIATION MODEL FOR THE STATORS OF NASA MIDDLE COMPRESSOR STAGES**  
W. B. ROBERTS and D. M. SANDERCOCK Feb. 1984 40 p refs  
(Contract NAG3-212)  
(NASA-CR-173360; NAS 1.26:173360) Avail: NTIS HC A03/MF A01 CSCL 21E

A model of the spanwise variation of deviation for stator blades is presented. Deviation is defined as the difference between the passage mean flow angle and the metal angle at the outlet of a blade element of an axial compressor stage. The variation of deviation is taken as the difference above or below that predicted by blade element, (i.e., two-dimensional) theory at any spanwise location. The variation of deviation is dependent upon the blade camber, solidity and inlet boundary layer thickness at the hub or tip end-wall, and the blade channel aspect ratio. If these parameters are known or can be calculated, the model provides a reasonable approximation of the spanwise variation of deviation for most compressor middle stage stators operating at subsonic inlet Mach numbers. A.R.H.

**N84-19353\*#** Pratt and Whitney Aircraft Group, East Hartford, Conn.  
**PARALLEL PROCESSOR ENGINE MODEL PROGRAM Final Report**  
P. MCLAUGHLIN Jan. 1984 70 p refs  
(Contract NAS3-23283)  
(NASA-CR-174641; NAS 1.26:174641; PWA-5896-21) Avail: NTIS HC A04/MF A01 CSCL 21E

The Parallel Processor Engine Model Program is a generalized engineering tool intended to aid in the design of parallel processing real-time simulations of turbofan engines. It is written in the FORTRAN programming language and executes as a subset of the SOAPP simulation system. Input/output and execution control are provided by SOAPP; however, the analysis, emulation and simulation functions are completely self-contained. A framework in which a wide variety of parallel processing architectures could be evaluated and tools with which the parallel implementation of a real-time simulation technique could be assessed are provided. Author

**N84-20524\*#** Stevens Inst. of Tech., Hoboken, N. J. Dept. of Mechanical Engineering.  
**THE INFLUENCE OF GYROSCOPIC FORCES ON THE DYNAMIC BEHAVIOR AND FLUTTER OF ROTATING BLADES Final Technical Report, 1 Jun. 1980 - 31 Aug. 1983**  
F. SISTO and A. T. CHANG Dec. 1983 118 p refs  
(Contract NAG3-47)  
(NASA-CR-175444; NAS 1.26:175444; ME-RT-82006) Avail: NTIS HC A06/MF A01 CSCL 21E

The structural dynamics of a cantilever turbomachine blade mounted on a spinning and precessing rotor are investigated. Both stability and forced vibration are considered with a blade model that increases in complexity (and verisimilitude) from a spring-restrained point mass, to a uniform cantilever, to a twisted uniform cantilever turbomachine blade mounted on a spinning and precessing rotor are investigated. Both stability and forced vibration are considered with a blade model that increases in complexity

(and verisimilitude) from a spring-restrained point mass, to a uniform cantilever, to a twisted uniform cantilever, to a tapered twisted cantilever of arbitrary cross-section. In every instance the formulation is from first principles using a finite element based on beam theory. Both ramp-type and periodic-type precessional angular displacements are considered. In concluding, forced vibrating and flutter are studied using the final and most sophisticated structural model. The analysis of stability is presented and a number of numerical examples are worked out. S.L.

**N84-20525\*#** National Aeronautics and Space Administration. Lewis Research Center, Cleveland, Ohio.  
**COMBUSTION FUNDAMENTALS RESEARCH**  
Washington Apr. 1984 303 p refs Conf. held in Cleveland, 16-18 Apr. 1984  
(NASA-CP-2309, E-2062; NAS 1.55:2309) Avail: NTIS HC A14/MF A01 CSCL 21E

The various physical processes that occur in the gas turbine combustor and the development of analytical models that accurately describe these processes are discussed. Aspects covered include fuel sprays; fluid mixing; combustion dynamics; radiation and chemistry and numeric techniques which can be applied to highly turbulent, recirculating, reacting flow fields.

**N84-20536\*#** Pratt and Whitney Aircraft, West Palm Beach, Fla. Engineering Div.  
**ERROR REDUCTION PROGRAM: A PROGRESS REPORT**  
S. A. SYED In NASA. Lewis Research Center Combustion Fundamentals Res. p 83-95 Apr. 1984 refs  
(Contract NAS3-23686)  
Avail: NTIS HC A14/MF A01 CSCL 21E

Five finite differences schemes were evaluated for minimum numerical diffusion in an effort to identify and incorporate the best error reduction scheme into a 3D combustor performance code. Based on this evaluation, two finite volume method schemes were selected for further study. Both the quadratic upstream differencing scheme (QUDS) and the bounded skew upstream differencing scheme two (BSUDS2) were coded into a two dimensional computer code and their accuracy and stability determined by running several test cases. It was found that BSUDS2 was more stable than QUDS. It was also found that the accuracy of both schemes is dependent on the angle that the streamline make with the mesh with QUDS being more accurate at smaller angles and BSUDS2 more accurate at larger angles. The BSUDS2 scheme was selected for extension into three dimensions. A.R.H.

**N84-20562\*#** National Aeronautics and Space Administration. Lewis Research Center, Cleveland, Ohio.  
**FORMULATION OF BLADE-FLUTTER SPECTRAL ANALYSES IN STATIONARY REFERENCE FRAME**  
A. P. KURKOV Mar. 1984 32 p refs  
(NASA-TP-2296; E-1888; NAS 1.60:2296) Avail: NTIS HC A03/MF A01 CSCL 21E

Analytic representations are developed for the discrete blade deflection and the continuous tip static pressure fields in a stationary reference frame. Considered are the sampling rates equal to the rotational frequency, equal to blade passing frequency, and for the pressure, equal to a multiple of the blade passing frequency. For the last two rates the expressions for determining the nodal diameters from the spectra are included. A procedure is presented for transforming the complete unsteady pressure field into a rotating frame of reference. The determination of the true flutter frequency by using two sensors is described. To illustrate their use, the developed procedures are used to interpret selected experimental results. Author

**N84-20580\*#** National Aeronautics and Space Administration. Lewis Research Center, Cleveland, Ohio.  
**IDENTIFICATION OF MULTIVARIABLE HIGH-PERFORMANCE TURBOFAN ENGINE DYNAMICS FROM CLOSED LOOP DATA**  
 W. C. MERRILL /in NASA Langley Research Center NASA Aircraft Controls Research, 1983 p 221-238 Mar. 1984 refs  
 Avail: NTIS HC A25/MF A01 CSCL 21E

A typical engine control design cycle consists of developing a dynamic engine simulation from steady-state component performance data, designing a control based upon this simulation, and then testing and modifying the control in an engine test cell to meet performance requirements. This design cycle was successful for state-of-the-art engines. However, for more advanced multivariable engines that exhibit strong variable interactions, this procedure will result in substantial trial and error modification of the control during the testing phase. One method to automate the design process and reduce control modification testing and development cost would be to identify accurate dynamic models directly from the closed-loop test data. These identified models would then be used in conjunction with a synthesis procedure to systematically refine the control. Recent advances in closed-loop identifiability present a methodology for this direct identification of engine model dynamics from closed-loop test data. The application of an identification method to simulated and actual closed-loop F100 engine data is described. This study was undertaken to determine if useful dynamic engine models could be identified directly from closed-loop engine test data. Author

**N84-20590\*#** National Aeronautics and Space Administration. Lewis Research Center, Cleveland, Ohio.  
**APPLICATION OF ADVANCED CONTROL TECHNIQUES TO AIRCRAFT PROPULSION SYSTEMS**  
 B. LEHTINEN /in NASA Langley Research Center NASA Aircraft Controls Research, 1983 p 429-442 Mar. 1984 refs  
 Avail: NTIS HC A25/MF A01 CSCL 21E

Two programs are described which involve the application of advanced control techniques to the design of engine control algorithms. Multivariable control theory is used in the F100 MVCS (multivariable control synthesis) program to design controls which coordinate the control inputs for improved engine performance. A systematic method for handling a complex control design task is given. Methods of analytical redundancy are aimed at increasing the control system reliability. The F100 DIA (detection, isolation, and accommodation) program, which investigates the uses of software to replace or augment hardware redundancy for certain critical engine sensor, is described. R.J.F.

**N84-21548\*#** National Aeronautics and Space Administration. Lewis Research Center, Cleveland, Ohio.  
**REAL-TIME HYBRID COMPUTER SIMULATION OF A SMALL TURBOSHAFT ENGINE AND CONTROL SYSTEM**  
 C. E. HART and L. M. WENZEL Feb. 1984 39 p refs  
 (NASA-TM-83579; E-1968; NAS 1.15:83579) Avail: NTIS HC A03/MF A01 CSCL 21E

The development of an analytical model of a small turboshaft engine designed for helicopter propulsion systems is described. The model equations were implemented on a hybrid computer system to provide a real time nonlinear simulation of the engine performance over a wide operating range. The real time hybrid simulation of the engine was used to evaluate a microprocessor based digital control module. This digital control module was developed as part of an advanced rotorcraft control program. After tests with the hybrid engine simulation the digital control module was used to control a real engine in an experimental program. A hybrid simulation of the engine's electrical hydromechanical control system was developed. This allowed to vary the fuel flow and torque load inputs to the hybrid engine simulation for simulating transient operation. A steady-state data and the experimental tests are compared. Analytical model equations, analog computer diagrams, and a digital computer flow chart are included. E.A.K.

**N84-21549\*#** National Aeronautics and Space Administration. Lewis Research Center, Cleveland, Ohio.  
**ANALYSIS OF A TOPPING-CYCLE, AIRCRAFT, GAS-TURBINE-ENGINE SYSTEM WHICH USES CRYOGENIC FUEL**  
 G. E. TURNEY and L. H. FISHBACH Apr. 1984 23 p refs  
 Presented at the AIAA Aircraft Systems and Operational Meeting, Fort Worth, Tex., 17-19 Oct. 1983  
 (NASA-TP-2294; E-1735; NAS 1.60:2294) Avail: NTIS HC A02/MF A01 CSCL 21E

A topping-cycle aircraft engine system which uses a cryogenic fuel was investigated. This system consists of a main turboshaft engine that is mechanically coupled (by cross-shafting) to a topping loop, which augments the shaft power output of the system. The thermodynamic performance of the topping-cycle engine was analyzed and compared with that of a reference (conventional) turboshaft engine. For the cycle operating conditions selected, the performance of the topping-cycle engine in terms of brake specific fuel consumption (bsfc) was determined to be about 12 percent better than that of the reference turboshaft engine. Engine weights were estimated for both the topping-cycle engine and the reference turboshaft engine. These estimates were based on a common shaft power output for each engine. Results indicate that the weight of the topping-cycle engine is comparable with that of the reference turboshaft engine. Author

**N84-22559\*** National Aeronautics and Space Administration. Lewis Research Center, Cleveland, Ohio.  
**REAL TIME PRESSURE SIGNAL SYSTEM FOR A ROTARY ENGINE Patent**  
 W. J. RICE, inventor (to NASA) 31 Jan. 1984 11 p Filed 19 Feb. 1982  
 (NASA-CASE-LEW-13622-1; US-PATENT-4,428,226;  
 US-PATENT-APPL-SN-350473; US-PATENT-CLASS-73-115;  
 US-PATENT-CLASS-364-558) Avail: US Patent and Trademark Office CSCL 21A

A real-time IMEP signal which is a composite of those produced in any one chamber of a three-lobed rotary engine is developed by processing the signals of four transducers positioned in a Wankel engine housing such that the rotor overlaps two of the transducers for a brief period during each cycle. During the overlap period of any two transducers, their output is compared and sampled for 10 microseconds per 0.18 degree of rotation by a sampling switch and capacitive circuit. When the switch is closed, the instantaneous difference between the value of the transducer signals is provided while with the switch open the average difference is produced. This combined signal, along with the original signal of the second transducer, is fed through a multiplexer to a pressure output terminal. Timing circuits, controlled by a crank angle encoder on the engine, determine which compared transducer signals are applied to the output terminal and when, as well as the open and closed periods of the switches.

Official Gazette of the U.S. Patent and Trademark Office

**N84-22560\*** National Aeronautics and Space Administration. Lewis Research Center, Cleveland, Ohio.  
**TIP CAP FOR A ROTOR BLADE**  
 W. K. KOFEL (GE, Cincinnati), E. N. TULEY (GE, Cincinnati), C. H. GAY, JR. (GE, Cincinnati), R. E. TROEGER (GE, Cincinnati), and A. P. STERMAN, inventors (to NASA) (GE, Cincinnati) 25 Oct. 1983 7 p Filed 20 Mar. 1981 Sponsored by NASA  
 (NASA-CASE-LEW-13654-1; US-PATENT-4,411,597;  
 US-PATENT-APPL-SN-245571; US-PATENT-CLASS-416-92;  
 US-PATENT-CLASS-416-97R; US-PATENT-CLASS-416-224;  
 US-PATENT-CLASS-416-233) Avail: US Patent and Trademark Office CSCL 21E

A replaceable tip cap for attachment to the end of a rotor blade is described. The tip cap includes a plurality of walls defining a compartment which, if desired, can be divided into a plurality of subcompartments. The tip cap can include inlet and outlet holes in walls thereof to permit fluid communication of a cooling fluid there through. Abrasive material can be attached with the radially



outer wall of the tip cap.

Official Gazette of the U.S. Patent and Trademark Office

**N84-22562\*#** National Aeronautics and Space Administration. Lewis Research Center, Cleveland, Ohio.

**DUAL CLEARANCE SQUEEZE FILM DAMPER Patent Application**

D. P. FLEMING, inventor (to NASA) 5 Apr. 1984 13 p (NASA-CASE-LEW-13506-1; US-PATENT-APPL-SN-596960)

Avail: NTIS HC A02/MF A01 CSCL 21E

A dual clearance hydrodynamic liquid squeeze film damper for a gas turbine engine is presented. Under normal operating conditions the device functions as a conventional squeeze film damper, using only one of its oil films. When an unbalance reaches abusive levels, as may occur with a blade loss or foreign object damage, a second, larger clearance film becomes active, controlling vibration amplitudes in a near optimum manner until the engine can be safely shut down and repaired. NASA

**N84-22563\*#** National Aeronautics and Space Administration. Lewis Research Center, Cleveland, Ohio.

**OXIDIZING SEAL FOR A TURBINE TIP GAS PATH Patent Application**

J. D. CAWLEY, inventor (to NASA) 19 Apr. 1984 12 p (NASA-CASE-LEW-14053-1; US-PATENT-APPL-SN-602050)

Avail: NTIS HC A02/MF A01 CSCL 21E

The sealing of the gas path in a gas turbine engine at the blade tips is improved by maintaining a minimum clearance between the rotor blade tips and the gas path seal. This is accomplished by taking advantage of an increase in volume during controlled oxidation of certain intermetallic compounds which have high melting points. The increase in volume closes the clearance subsequent to a rub between the blades and the seal. Thus, these compounds re-form the tip seal surface to assure continued engine efficiency. NASA

**N84-22564\*#** National Aeronautics and Space Administration. Lewis Research Center, Cleveland, Ohio

**COMPARISON BETWEEN MEASURED TURBINE STAGE PERFORMANCE AND THE PREDICTED PERFORMANCE USING QUASI-3D FLOW AND BOUNDARY LAYER ANALYSES**

R. J. BOYLE, J. E. HAAS, and T. KATSANIS 1984 27 p refs Proposed for presentation at the 20th Joint Propulsion Conf., Cincinnati, 11-13 Jun. 1984; sponsored by AIAA, SAE and ASME (NASA-TM-83640; E-2065; NAS 1.15:83640; AVRADCOM-TR-84-C-6) Avail: NTIS HC A03/MF A01 CSCL 21E

A method for calculating turbine stage performance is described. The usefulness of the method is demonstrated by comparing measured and predicted efficiencies for nine different stages. Comparisons are made over a range of turbine pressure ratios and rotor speeds. A quasi-3D flow analysis is used to account for complex passage geometries. Boundary layer analyses are done to account for losses due to friction. Empirical loss models are used to account for incidence, secondary flow, disc windage, and clearance losses. Author

**N84-22565\*#** National Aeronautics and Space Administration. Lewis Research Center, Cleveland, Ohio.

**PRELIMINARY INVESTIGATION OF A TWO-ZONE SWIRL FLOW COMBUSTOR**

J. A. BIAGLOW, S. M. JOHNSON, and J. M. SMITH 1984 20 p refs Proposed for presentation at the 20th Joint Propulsion Conf., Cincinnati, 11-13 Jun. 1984; sponsored by AIAA, SAE, and ASME

(NASA-TM-83637; E-2029, NAS 1.15:83637) Avail: NTIS HC A02/MF A01 CSCL 21E

The effect of full-annular swirling-flow on a flow-zone combustor design is investigated. Swirl flow angles of 25, 35, and 45 degrees were investigated in a combustor design envelope typical of those used in modern engines. The two-zone combustor had 24 pilot-zone fuel injectors and 24 main-fuel injectors located in the centerbody between the pilot and swirl passage. Combustor performance was

determined at idle, and two parametric 589 K inlet temperature conditions. Combustor performance was highest with the 45 degree swirl vane design; at the idle condition, combustion efficiency was 99.5 percent. The 45 degree swirl vane also produced the lowest pattern factor of the three angles and showed a combustor lean blowout limit below a 0.001 fuel-air ratio. Combustor total pressure drop varied from a low of 4.6 percent for the 25 degree swirl to a high of 4.9 percent for the 45 degree swirl. M.A.C.

**N84-22566\*#** National Aeronautics and Space Administration. Lewis Research Center, Cleveland, Ohio.

**DETERMINATION OF COMPRESSOR IN-STALL CHARACTERISTICS FROM ENGINE SURGE TRANSIENTS**

C. F. LORENZO, F. P. CHIARAMONTE, and C. M. MEHALIC 1984 27 p refs Proposed for presentation at the 20th Joint Propulsion Conf., 11-13 Jun. 1983; sponsored by the AIAA, SAE and ASME

(NASA-TM-83639; E-2082; NAS 1.15:83639) Avail: NTIS HC A03/MF A01 CSCL 21E

A technique for extracting the in-stand pumping characteristics for an axial flow compressor operating in an engine system environment is developed. The technique utilizes a Hybrid computer simulation of the compressor momentum equation into which actual transient data are used to provide all terms but the desired compressor characteristic. The compressor force characteristic as a function of corrected flow and speed result from the computation. The critical problem of data filtering is addressed. Results for a compressor operating in a turbofan engine are presented and comparison is made with the conventional compressor map. The relationship of the compressor surge characteristic with its rotating stall characteristic is explored. Initial interpretation of the measured results is presented. Author

**N84-22568\*#** Teledyne CAE, Toledo, Ohio.

**VARIABLE STATOR RADIAL TURBINE Final Report**

C. ROGO, T. HAJEK, and A. G. CHEN May 1984 302 p refs (Contract NAS3-23163; DA PROJ. 1L1-61102-AH-45)

(NASA-CR-174663; NAS 1.26:174663; TELEDYNE-CAE-1987)

Avail: NTIS HC A14/MF A01 CSCL 21E

A radial turbine stage with a variable area nozzle was investigated. A high work capacity turbine design with a known high performance base was modified to accept a fixed vane stagger angle moveable sidewall nozzle. The nozzle area was varied by moving the forward and rearward sidewalls. Diffusing and accelerating rotor inlet ramps were evaluated in combinations with hub and shroud rotor exit rings. Performance of contoured sidewalls and the location of the sidewall split line with respect to the rotor inlet was compared to the baseline. Performance and rotor exit survey data are presented for 31 different geometries. Detail survey data at the nozzle exit are given in contour plot format for five configurations. A data base is provided for a variable geometry concept that is a viable alternative to the more common pivoted vane variable geometry radial turbine. E.A.K.

**N84-23629\*#** Pratt and Whitney Aircraft, West Palm Beach, Fla. Government Products Div.

**V/STOL MODEL FAN STAGE RIG DESIGN REPORT**

J. G. CHEATHAM and T. L. CREASON Aug. 1983 280 p refs

(Contract NAS3-22779)

(NASA-CR-174688; NAS 1.26:174688; PWA/GPD-FR-17826)

Avail: NTIS HC A13/MF A01 CSCL 21E

A model single-stage fan with variable inlet guide vanes (VIGV) was designed to demonstrate efficient point operation while providing flow and pressure ratio modulation capability required for a V/STOL propulsion system. The fan stage incorporates a split-flap VIGV with an independently actuated ID flap to permit independent modulation of fan and core engine airstreams, a flow splitter integrally designed into the blade and vanes to completely segregate fan and core airstreams in order to maximize core stream supercharging for V/STOL operation, and an EGV with a variable leading edge fan flap for rig performance optimization. The stage was designed for a maximum flow size of 37.4 kg/s (82.3 lb/s)

## 07 AIRCRAFT PROPULSION AND POWER

for compatibility with LeRC test facility requirements. Design values at maximum flow for blade tip velocity and stage pressure ratio are 472 m/s (1550 ft/s) and 1.68, respectively. Author

**N84-23630\*#** National Aeronautics and Space Administration. Lewis Research Center, Cleveland, Ohio.  
**ASSESSMENT OF ALTERNATIVE AIRCRAFT FUELS**  
Washington Apr. 1984 188 p refs Conf. held in Cleveland, 2-3 Nov. 1983  
(NASA-CP-2307; E-1878; NAS 1.55:2307) Avail: NTIS HC A09/MF A01 CSCL 21D

The purpose of this symposium is to provide representatives from industry, government, and academia concerned with the availability and quality of future aviation turbine fuels with recent technical results and a status review of DOD and NASA sponsored fuels research projects. The symposium has included presentations on the potential crude sources, refining methods, and characteristics of future fuels; the effects of changing fuel characteristics on the performance and durability of jet aircraft components and systems; and the prospects for evolving suitable technology to produce and use future fuels.

**N84-23648\*#** National Aeronautics and Space Administration. Lewis Research Center, Cleveland, Ohio.  
**CONTINGENCY POWER CONCEPTS FOR HELICOPTER TURBOSHAFT ENGINE**  
R. HIRSCHKRON (General Electric Co., Lynn, Mass.), R. H. DAVIS (General Electric Co., Lynn, Mass.), D. N. GOLDSTEIN (General Electric Co., Lynn, Mass.), J. F. HAYNES (General Electric Co., Lynn, Mass.), and J. W. GAUNTNER 1984 14 p refs Presented at the 40th Ann. Forum of the American Helicopter Society, Arlington, Va., 16-18 May 1984  
(NASA-TM-83679; E-2128; NAS 1.15:83679; A-83-40-66-7000) Avail: NTIS HC A02/MF A01 CSCL 21E

Twin helicopter engines are often sized by power requirement of safe mission completion after the failure of one of the two engines. This study was undertaken for NASA Lewis by General Electric Co. to evaluate the merits of special design features to provide a 2-1/2 minute Contingency Power rating, permitting an engine size reduction. The merits of water injection, cooling flow modulation, throttle push and an auxiliary power plant were evaluated using military life cycle cost (LCC) and commercial helicopter direct operating cost (DOC) merit factors in a rubber engine/rubber aircraft scenario. Author

**N84-23649\*#** Rensselaer Polytechnic Inst., Troy, N. Y. Gas Dynamics Lab.  
**INVESTIGATION OF THE EFFECTS OF PRESSURE GRADIENT, TEMPERATURE AND WALL TEMPERATURE RATIO ON THE STAGNATION POINT HEAT TRANSFER FOR CIRCULAR CYLINDERS AND GAS TURBINE VANES Final Report**  
H. T. NAGAMATSU and R. E. DUFFY Apr. 1984 43 p refs Sponsored in part by National Science Foundation (Contract NAG3-292)  
(NASA-CR-174667; NAS 1.26:174667) Avail: NTIS HC A03/MF A01 CSCL 21E

Low and high pressure shock tubes were designed and constructed for the purpose of obtaining heat transfer data over a temperature range of 390 to 2500 K, pressures of 0.3 to 42 atm, and Mach numbers of 0.15 to 1.5 with and without pressure gradient. A square test section with adjustable top and bottom walls was constructed to produce the favorable and adverse pressure gradient over the flat plate with heat gages. A water cooled gas turbine nozzle cascade which is attached to the high pressure shock tube was obtained to measure the heat flux over pressure and suction surfaces. Thin-film platinum heat gages with a response time of a few microseconds were developed and used to measure the heat flux for laminar, transition, and turbulent boundary layers. The laminar boundary heat flux on the shock tube wall agreed with Mirel's flat plate theory. Stagnation point heat transfer for circular cylinders at low temperature compared with the theoretical prediction, but for a gas temperature of 922 K the heat fluxes were higher than the predicted values. Preliminary

flat plate heat transfer data were measured for laminar, transition, and turbulent boundary layers with and without pressure gradients for free-stream temperatures of 350 to 2575 K and flow Mach numbers of 0.11 to 1.9. The experimental heat flux data were correlated with the laminar and turbulent theories and the agreement was good at low temperatures which was not the case for higher temperatures. Author

**N84-24577\*** National Aeronautics and Space Administration. Lewis Research Center, Cleveland, Ohio.  
**COMBUSTOR LINER CONSTRUCTION Patent**  
H. M. CRAIG (United Technologies Corp., East Hartford, Conn.), W. B. WAGNER (United Technologies Corp., East Hartford, Conn.), and W. J. STROCK, inventors (to NASA) (United Technologies Corp., East Hartford, Conn.) 15 Nov. 1983 6 p Filed 2 Apr. 1980 Sponsored by NASA  
(NASA-CASE-LEW-14035-1; US-PATENT-4,414,816; US-PATENT-APPL-SN-136652; US-PATENT-CLASS-60-757) Avail: US Patent and Trademark Office CSCL 21E

A combustor liner is fabricated from a plurality of individual segments each containing counter/parallel Finwall material and are arranged circumferentially and axially to define the combustion zone. Each segment is supported by a hook and ring construction to an opened lattice frame with sufficient tolerance between the hook and ring to permit thermal expansion with a minimum of induced stresses.

Official Gazette of the U.S. Patent and Trademark Office

**N84-24578\*#** National Aeronautics and Space Administration. Lewis Research Center, Cleveland, Ohio.  
**LEWIS RESEARCH CENTER SPIN RIG AND ITS USE IN VIBRATION ANALYSIS OF ROTATING SYSTEMS**  
G. V. BROWN, R. E. KIELB, E. H. MEYN, R. E. MORRIS, and S. J. POSTA May 1984 19 p refs  
(NASA-TP-2304; E-1829; NAS 1.60:2304) Avail: NTIS HC A02/MF A01 CSCL 21E

The Lewis Research Center spin rig was constructed to provide experimental evaluation of analysis methods developed under the NASA Engine Structural Dynamics Program. Rotors up to 51 cm (20 in.) in diameter can be spun to 16,000 rpm in vacuum by an air motor. Vibration forcing functions are provided by shakers that apply oscillatory axial forces or transverse moments to the shaft, by a natural whirling of the shaft, and by an air jet. Blade vibration is detected by strain gages and optical blade-tip motion sensors. A variety of analogy and digital processing equipment is used to display and analyze the signals. Results obtained from two rotors are discussed. A 56-blade compressor disk was used to check proper operation of the entire spin rig system. A special two-blade rotor was designed and used to hold flat and twisted plates at various setting and sweep angles. Accurate Southwell coefficients have been obtained for several modes of a flat plate oriented parallel to the plane of rotation. Author

**N84-24579\*#** National Aeronautics and Space Administration. Lewis Research Center, Cleveland, Ohio.  
**TANDEM FAN APPLICATIONS IN ADVANCED STOVL FIGHTER CONFIGURATIONS**  
C. L. ZOLA, S. B. WILSON, III, and M. A. ESKEY 1984 20 p refs Presented at the 20th Joint Propulsion Conf., Cincinnati, 11-13 Jun. 1984  
(NASA-TM-83689; E-2140; NAS 1.15:83689) Avail: NTIS HC A02/MF A01 CSCL 21E

The series/parallel tandem fan engine is evaluated for application in advanced STOVL supersonic fighter aircraft. Options in engine cycle parameters and design of the front fan flow diverter are examined for their effects on engine weight, dimensions, and other factors in integration of the engine with the aircraft. Operation of the engine in high-bypass flow mode during cruise and loiter flight is considered as a means of minimizing fuel consumption. Engine thrust augmentation by burning in the front fan exhaust is discussed. Achievement of very short takeoff with vectored thrust is briefly reviewed for tandem fan engine configurations with vectorable front fan nozzles. Examples are given of two aircraft



configuration planforms, a delta-canard, and a forward-swept wing, to illustrate the major features, design considerations, and potential performance of the tandem fan installation in each. Full realization of the advantages of tandem fan propulsion are found to depend on careful selection of the aircraft configuration, since integration requirements can strongly influence the engine performance.

Author

**N84-24580\*#** General Electric Co., Lynn, Mass. Aircraft Business Group.

**ROTORCRAFT CONTINGENCY POWER STUDY Final Report**

R. HIRSCHKRON, J. F. HAYNES, D. N. GOLDSTEIN, and R. H. DAVIS May 1984 157 p refs

(Contract NAS3-23705)

(NASA-CR-174675; NAS 1.26:174675; R84AEB012) Avail: NTIS HC A08/MF A01 CSCL 21E

Twin helicopter engines are often sized by the power requirement of a safe mission completion after the failure of one of the two engines. This study was undertaken for NASA Lewis by General Electric Co. to evaluate the merits of special design features to provide a 2-1/2 Contingency Power rating, permitting an engine size reduction. The merits of water injection, turbine cooling airflow modulation, throttle push, and a propellant auxiliary power plant were evaluated using military Life Cycle Cost (LCC) and commercial helicopter Direct Operating Cost (DOC) merit factors in a rubber engine and a rubber aircraft scenario. Author

**N84-24581\*#** National Aeronautics and Space Administration. Lewis Research Center, Cleveland, Ohio.

**SUPERSONIC STOVL EJECTOR AIRCRAFT FROM A PROPULSION POINT OF VIEW**

R. W. LUIDENS, R. PLENCNER, W. HALLER, and A. GLASSMAN 1984 18 p refs Presented at the 20th Joint Propulsion Conf., Cincinnati, 11-13 Jun. 1984; sponsored by AIAA, SAE and ASME

(NASA-TM-83641; E-2084; NAS 1.15:83641) Avail: NTIS HC A02/MF A01 CSCL 21E

A baseline supersonic STOVL ejector aircraft, its propulsion and typical operating modes is described, and important propulsion parameters are identified. Then a number of propulsion system changes are evaluated for improvement of the lift-off performance aft deflection of the ejector jet and heating of the ejector primary air either by burning or using the hot engine core flow. The possibility for cooling the footprint is illustrated for mixing or interchanging the fan and core flows, and in use of a core flow ejector. The application of a new engine concept the turbine bypass engine plus a turbocompressor to supply the ejector primary air, and thrust during takeoff combat are presented. E.A.K.

**N84-24582\*#** National Aeronautics and Space Administration. Lewis Research Center, Cleveland, Ohio.

**SUPERSONIC STOVL AIRCRAFT WITH TURBINE BYPASS/TURBO-COMPRESSOR ENGINES**

L. C. FRANCISCUS and R. W. LUIDENS 1984 15 p refs Presented at the 20th Joint Propulsion Conf., Cincinnati, 11-13 Jun. 1984; sponsored by AIAA, SAE and ASME

(NASA-TM-83686; E-2138; NAS 1.15:83686) Avail: NTIS HC A02/MF A01 CSCL 21E

Three propulsion systems for a Mach 2 STOVL fighter were compared. The three propulsion systems are: (1) turbine bypass engine with a turbocompressor used for STOVL only; (2) turbine bypass engine with a turbocompressor for both STOVL and thrust during forward flight; and (3) mixed flow afterburning turbofan with a remote burner lift system. In the first system, the main engines have afterburners and the turbocompressors use after burning during STOVL. In the second system, the turbine bypass engines are dry and the turbocompressors have afterburners. The mission used in the study is a deck launched intercept mission. It is indicated that large improvements in combat time are possible when the turbocompressors are used for both left and thrust for forward flight. E.A.K.

**N84-24583\*#** National Aeronautics and Space Administration. Lewis Research Center, Cleveland, Ohio.

**AN OVERVIEW OF NASA INTERMITTENT COMBUSTION ENGINE RESEARCH**

E. A. WILLIS and W. T. WINTUCKY 1984 33 p refs Presented at the 20th Joint Propulsion Conf., Cincinnati, 11-13 Jun. 1984; sponsored by AIAA, SAE and ASME

(NASA-TM-83668; E-2111; NAS 1.15:83668) Avail: NTIS HC A03/MF A01 CSCL 21E

This paper overviews the current program, whose objective is to establish the generic technology base for advanced aircraft I.C. engines of the early 1990's and beyond. The major emphasis of this paper is on development of the past two years. Past studies and ongoing confirmatory experimental efforts are reviewed, which show unexpectedly high potential when modern aerospace technologies are applied to inherently compact and balanced I.C. engine configurations. Currently, the program is focussed on two engine concepts the stratified-charge, multi-fuel rotary, and the lightweight two-stroke diesel. A review is given of contracted and planned high performance one-rotor and one-cylinder test engine work addressing several levels of technology. Also reviewed are basic supporting efforts, e.g., the development and experimental validation of computerized airflow and combustion process models, being performed in-house at Lewis Research Center and by university grants. Author

**N84-24584\*#** National Aeronautics and Space Administration. Lewis Research Center, Cleveland, Ohio

**COMBUSTION GAS PROPERTIES OF VARIOUS FUELS OF INTEREST TO GAS TURBINE ENGINEERS**

R. E. JONES, A. M. TROUT, and J. D. WEAR 1984 11 p refs Presented at the Joint Power Generation Conf., Toronto, 1-4 Oct. 1984; sponsored by ASME

(NASA-TM-83682; E-2133; NAS 1.15:83682) Avail: NTIS HC A02/MF A01 CSCL 21E

A series of computations were made using the gas property computational schemes of Gordon and McBride to compute the gas properties and species concentration of ASTM-Jet A and dry air. The computed gas thermodynamic properties in a revised graphical format which gives information which is useful to combustion engineers is presented. A series of reports covering the properties of many fuel and air combinations will be published. The graphical presentation displays on one chart of the output of hundreds of computer sheets. The reports will contain microfiche cards, from which complete tables and graphs can be obtained. The extent of the planned effort and is documented samples of the many tables and charts that will be available on the microfiche cards are presented. E.A.K.

**N84-24585\*#** National Aeronautics and Space Administration. Lewis Research Center, Cleveland, Ohio.

**SENSOR FAILURE DETECTION FOR JET ENGINES USING ANALYTICAL REDUNDANCE**

W. C. MERRILL 1984 24 p refs Presented at the 20th Joint Propulsion Conf., Cincinnati, 11-13 Jun. 1984; sponsored by AIAA, SAE and ASME

(NASA-TM-83695; E-2123; NAS 1.15:83695; AIAA-84-1452) Avail: NTIS HC A02/MF A01 CSCL 21E

Analytical redundant sensor failure detection, isolation and accommodation techniques for gas turbine engines are surveyed. Both the theoretical technology base and demonstrated concepts are discussed. Also included is a discussion of current technology needs and ongoing Government sponsored programs to meet those needs. Author

**N84-24586\*#** Massachusetts Inst. of Tech., Cambridge. Gas Turbine and Plasma Dynamics Lab.  
**FLUTTER AND FORCED RESPONSE OF MISTUNED ROTORS USING STANDING WAVE ANALYSIS**  
 D. J. BUNDAS and J. DUNGUNDJI Mar. 1983 155 p refs  
 Previously announced as A83-29823  
 (Contract NAG3-214)  
 (NASA-CR-173555; NAS 1.26:173555; GT/PDL-170) Avail: NTIS HC A08/MF A01 CSCL 21E

A standing wave approach is applied to the analysis of the flutter and forced response of tuned and mistuned rotors. The traditional traveling wave cascade airforces are recast into standing wave arbitrary motion form using Pade approximants, and the resulting equations of motion are written in the matrix form. Applications for vibration modes, flutter, and forced response are discussed. It is noted that the standing wave methods may prove to be more versatile for dealing with certain applications, such as coupling flutter with forced response and dynamic shaft problems, transient impulses on the rotor, low-order engine excitation, bearing motion, and mistuning effects in rotors. V.L. (IAA)

**N84-24589\*#** National Aeronautics and Space Administration. Lewis Research Center, Cleveland, Ohio.  
**PERFORMANCE OF A HIGH-WORK LOW ASPECT RATION TURBINE TESTED WITH A REALISTIC INLET RADIAL TEMPERATURE PROFILE**  
 R. G. STABE, W. J. WHITNEY, and T. P. MOFFITT 1984 24 p refs  
 Presented at the 20th Joint Propulsion Conf., Cincinnati, 11-13 Jun. 1984  
 (NASA-TM-83655; E-2098; NAS 1.15:83655; AIAA-84-1161)  
 Avail: NTIS HC A02/MF A01 CSCL 21E

Experimental results are presented for a 0.767 scale model of the first stage of a two-stage turbine designed for a high by-pass ratio engine. The turbine was tested with both uniform inlet conditions and with an inlet radial temperature profile simulating engine conditions. The inlet temperature profile was essentially mixed-out in the rotor. There was also substantial underturning of the exit flow at the mean diameter. Both of these effects were attributed to strong secondary flows in the rotor blading. There were no significant differences in the stage performance with either inlet condition when differences in tip clearance were considered. Performance was very close to design intent in both cases. Author

**N84-25710\*#** Flow Research, Inc., Kent, Wash.  
**DIRECT SIMULATIONS OF CHEMICALLY REACTING TURBULENT MIXING LAYERS Final Report**  
 J. J. RILEY and R. W. METCALFE Mar. 1984 149 p refs  
 (Contract NAS3-23531)  
 (NASA-CR-174640; NAS 1.26:174640; REPT-274) Avail: NTIS HC A07/MF A01 CSCL 20D

The report presents the results of direct numerical simulations of chemically reacting turbulent mixing layers. The work consists of two parts: (1) the development and testing of a spectral numerical computer code that treats the diffusion reaction equations; and (2) the simulation of a series of cases of chemical reactions occurring on mixing layers. The reaction considered is a binary, irreversible reaction with no heat release. The reacting species are nonpremixed. The results of the numerical tests indicate that the high accuracy of the spectral methods observed for rigid body rotation are also obtained when diffusion, reaction, and more complex flows are considered. In the simulations, the effects of vortex rollup and smaller scale turbulence on the overall reaction rates are investigated. The simulation results are found to be in approximate agreement with similarity theory. Comparisons of simulation results with certain modeling hypotheses indicate limitations in these hypotheses. The nondimensional product thickness computed from the simulations is compared with laboratory values and is found to be in reasonable agreement, especially since there are no adjustable constants in the method. Author

**N84-25711\*#** TRW, Inc., Cleveland, Ohio. Materials and Manufacturing Technology Center.  
**FABRICATION DEVELOPMENT FOR ODS-SUPERALLOY, AIR-COOLED TURBINE BLADES**  
 D. J. MORACZ Jan. 1984 105 p refs  
 (Contract NAS3-22507)  
 (NASA-CR-174650; NAS 1.26:174650; ER-8162-F) Avail: NTIS HC A06/MF A01 CSCL 21E

MA-600 is a gamma prime and oxide dispersion strengthened superalloy made by mechanical alloying. At the initiation of this program, MA-6000 was available as an experimental alloy only and did not go into production until late in the program. The objective of this program was to develop a thermal-mechanical-processing approach which would yield the necessary elongated grain structure and desirable mechanical properties after conventional press forging. Forging evaluations were performed to select optimum thermal-mechanical-processing conditions. These forging evaluations indicated that MA-6000 was extremely sensitive to die chilling. In order to conventionally hot forge the alloy, an adherent cladding, either the original extrusion can or a thick plating, was required to prevent cracking of the workpiece. Die design must reflect the requirement of cladding. MA-6000 was found to be sensitive to the forging temperature. The correct temperature required to obtain the proper grain structure after recrystallization was found to be between 1010-1065 C (1850-1950 F). The deformation level did not affect subsequent crystallization; however, sharp transition areas in tooling designs should be avoided in forming a blade shape because of the potential for grain structure discontinuities. Starting material to be used for forging should be processed so that it is capable of being zone annealed to a coarse elongated grain structure as bar stock. This conclusion means that standard processed bar materials can be used. Author

**N84-25712\*#** National Aeronautics and Space Administration. Lewis Research Center, Cleveland, Ohio.  
**DEVELOPMENT OF DYNAMIC SIMULATION OF TF34-GE-100 TURBOFAN ENGINE WITH POST-STALL CAPABILITY**  
 S. M. KROSEL 1984 11 p refs  
 Presented at the 20th Joint Propulsion Conf., Cincinnati, 11-13 Jun. 1984  
 (NASA-TM-83660; E-2104; NAS 1.15:83660; AIAA-84-1184)  
 Avail: NTIS HC A02/MF A01 CSCL 21E

This paper describes the development of a hybrid computer simulation of a TF34-GE-100 turbofan engine with post-stall capability. The simulation operates in real-time and will be used to test and evaluate stall recovery control modes for this engine. The simulation calculations are performed by an analog computer with a peripheral multivariable function generation unit used for computing bivariate functions. Tabular listings of a simulation variables are obtained by interfacing to a digital computer and using a custom software package for data collection and display. Author

**N84-25713\*#** National Aeronautics and Space Administration. Lewis Research Center, Cleveland, Ohio.  
**ON MODELING DILUTION JET FLOWFIELDS**  
 J. D. HOLDEMAN and R. SRINIVASAN (Garrett Turbine Engine Co.) 1984 19 p refs  
 Presented at the 20th Joint Propulsion Conf., Cincinnati, 11-13 Jun. 1984  
 (NASA-TM-83708; E-2168; NAS 1.15:83708; AIAA-84-1379)  
 Avail: NTIS HC A02/MF A01 CSCL 21E

This paper compares temperature field measurements from selected experiments on a single row, and opposed rows, of jets injected into a ducted crossflow with profiles calculated using an empirical model based on assumed vertical profile similarity and superposition, and distributions calculated with a 3-D elliptic code using a standard K-E turbulence model. The empirical model predictions are very good within the range of the generating experiments, and the numerical model results, although exhibiting too little mixing, correctly describe the effects of the principal flow and geometric variables. Author

**N84-26702\*#** Garrett Turbine Engine Co., Phoenix, Ariz.  
**DILUTION JET MIXING PROGRAM**  
 R. SRINIVASAN, E. COLEMAN, and K. JOHNSON Jun. 1984  
 354 p refs  
 (Contract NAS3-22110)  
 (NASA-CR-174624; NAS 1.26:174624; GARRETT-21-4804)  
 Avail: NTIS HC A16/MF A01 CSCL 21E

Parametric tests were conducted to quantify the mixing of opposed rows of jets (two-sided injection) in a confined cross flow. Results show that jet penetrations for two sided injections are less than that for single-sided injections, but the jet spreading rates are faster for a given momentum ratio and orifice plate. Flow area convergence generally enhances mixing. Mixing characteristics with asymmetric and symmetric convergence are similar. For constant momentum ratio, the optimum S/H(0) with in-line injections is one half the optimum value for single sided injections. For staggered injections, the optimum S/H(0) is twice the optimum value for single-sided injection. The correlations developed predicted the temperature distributions within first order accuracy and provide a useful tool for predicting jet trajectory and temperature profiles in the dilution zone with two-sided injections.

A.R.H.

**N84-27737\*#** Pratt and Whitney Aircraft Group, East Hartford, Conn.  
**ENERGY EFFICIENT ENGINE FAN COMPONENT DETAILED DESIGN REPORT**  
 J. E. HALLE and C. J. MICHAEL Sep. 1981 141 p refs  
 (Contract NAS3-20646)  
 (NASA-CR-165466; NAS 1.26:165466; PWA-5594-165) Avail:  
 NTIS HC A07/MF A01 CSCL 21E

The fan component which was designed for the energy efficient engine is an advanced high performance, single stage system and is based on technology advancements in aerodynamics and structure mechanics. Two fan components were designed, both meeting the integrated core/low spool engine efficiency goal of 84.5%. The primary configuration, envisioned for a future flight propulsion system, features a shroudless, hollow blade and offers a predicted efficiency of 87.3%. A more conventional blade was designed, as a back up, for the integrated core/low spool demonstrator engine. The alternate blade configuration has a predicted efficiency of 86.3% for the future flight propulsion system. Both fan configurations meet goals established for efficiency surge margin, structural integrity and durability.

E.A.K.

**N84-27738\*#** Pratt and Whitney Aircraft Group, East Hartford, Conn. Commercial Products Div.  
**ENERGY EFFICIENT ENGINE: LOW-PRESSURE TURBINE SUBSONIC CASCADE COMPONENT DEVELOPMENT AND INTEGRATION PROGRAM**  
 O. P. SHARMA, F. C. KOPPER, L. K. KNUDSEN, and J. B. YUSTINICH Jan. 1982 98 p refs  
 (Contract NAS3-20646)  
 (NASA-CR-165592; NAS 1.26:165592; PWA-5594-167) Avail:  
 NTIS HC A05/MF A01 CSCL 21E

A subsonic cascade test program was conducted to provide technical data for optimizing the blade and vane airfoil designs for the Energy Efficient Engine Low-Pressure Turbine component. The program consisted of three parts. The first involved an evaluation of the low-chamber inlet guide vane. The second, was an evaluation of two candidate aerodynamic loading philosophies for the fourth blade-root section. The third part consisted of an evaluation of three candidate airfoil geometries for the fourth blade mean section. The performance of each candidate airfoil was evaluated in a linear cascade configuration. The overall results of this study indicate that the aft-loaded airfoil designs resulted in lower losses which substantiated Pratt & Whitney Aircraft's design philosophy for the Energy Efficient Engine low-pressure turbine component.

Author

**N84-27739\*#** United Technologies Corp., East Hartford, Conn. Aircraft Group.  
**ENERGY EFFICIENT ENGINE HIGH-PRESSURE TURBINE SUPERSONIC CASCADE TECHNOLOGY REPORT**  
 F. C. KOPPER, R. MILANO, R. L. DAVIS, R. P. DRING, and R. C. STOEFFLER Nov. 1981 155 p refs  
 (Contract NAS3-20646)  
 (NASA-CR-165567; NAS 1.26:165567; PWA-5594-152) Avail:  
 NTIS HC A08/MF A01 CSCL 21E

The performance of two vane endwall geometries and three blade sections for the high-pressure turbine was evaluated in terms of the efficiency requirements of the Energy Efficient Engine high-pressure turbine component. The vane endwall designs featured a straight wall and S-wall configuration. The blade designs included a base blade, straightback blade, and overcambered blade. Test results indicated that the S-wall vane configuration and the base blade configuration offered the most promising performance characteristics for the Energy Efficient Engine high-pressure turbine component.

Author

**N84-28788\*#** Pratt and Whitney Aircraft Group, East Hartford, Conn.  
**ENERGY EFFICIENT ENGINE HIGH-PRESSURE TURBINE DETAILED DESIGN REPORT**  
 R. D. THULIN, D. C. HOWE, and I. D. SINGER Jan. 1982 164 p refs  
 (Contract NAS3-20646)  
 (NASA-CR-165608; NAS 1.26:165608; PWA-5594-171) Avail:  
 NTIS HC A08/MF A01 CSCL 21E

The energy efficient engine high-pressure turbine is a single stage system based on technology advancements in the areas of aerodynamics, structures and materials to achieve high performance, low operating economics and durability commensurate with commercial service requirements. Low loss performance features combined with a low through-flow velocity approach results in a predicted efficiency of 88.8 for a flight propulsion system. Turbine airfoil durability goals are achieved through the use of advanced high-strength and high-temperature capability single crystal materials and effective cooling management. Overall, this design reflects a considerable extension in turbine technology that is applicable to future, energy efficient gas-turbine engines.

Author

**N84-28789\*#** Pratt and Whitney Aircraft Group, East Hartford, Conn. Commercial Products Div.  
**ENERGY EFFICIENT ENGINE: TURBINE INTERMEDIATE CASE AND LOW-PRESSURE TURBINE COMPONENT TEST HARDWARE DETAILED DESIGN REPORT**  
 K. LEACH, R. D. THULIN, and D. C. HOWE Jan. 1982 288 p refs  
 (Contract NAS3-20646)  
 (NASA-CR-167973; NAS 1.26:167973; PWA-5594-191) Avail:  
 NTIS HC A13/MF A01 CSCL 21E

A four stage, low pressure turbine component has been designed to power the fan and low pressure compressor system in the Energy Efficient Engine. Designs for a turbine intermediate case and an exit guide vane assembly also have been established. The components incorporate numerous technology features to enhance efficiency, durability, and performance retention. These designs reflect a positive step towards improving engine fuel efficiency on a component level. The aerodynamic and thermal/mechanical designs of the intermediate case and low pressure turbine components are presented and described. An overview of the predicted performance of the various component designs is given.

R.S.F.

## 07 AIRCRAFT PROPULSION AND POWER

**N84-28790\*#** National Aeronautics and Space Administration. Lewis Research Center, Cleveland, Ohio.

### **VELOCITY AND TEMPERATURE CHARACTERISTICS OF TWO-STREAM, COPLANAR JET EXHAUST PLUMES**

U. H. VONGLAHN, J. H. GOODYKOONTZ, and C. WASSERBAUER 1984 39 p refs Presented at the 2nd Appl. Aerodyn. Conf., Seattle, 21-23 Aug. 1984; sponsored by AIAA

(NASA-TM-83730; E-2205; NAS 1.15:83730; AIAA-84-2205)

Avail: NTIS HC A03/MF A01 CSCL 21E

The subsonic jet exhaust velocity and temperature characteristics of model scale, two stream coplanar nozzles were obtained experimentally. The data obtained included the effects of fan to primary stream velocity and temperature ratios on the jet axial and radial flow characteristics. Empirical parameters were developed to correlate the measured data. The resultant equations were shown to be extensions of a previously published single stream jet velocity and temperature correlation Author

**N84-28791\*#** National Aeronautics and Space Administration. Lewis Research Center, Cleveland, Ohio.

### **AN OVERVIEW OF THE NASA ROTARY ENGINE RESEARCH PROGRAM**

P. R. MENG and W. F. HADY 1984 26 p refs Presented at the West Coast Intern. Meeting, San Diego, Calif., 6-9 Aug. 1984; sponsored by SAE

(NASA-TM-83699; E-2157; NAS 1.15:83699) Avail: NTIS HC

A03/MF A01 CSCL 21E

A brief overview and technical highlights of the research efforts and studies on rotary engines over the last several years at the NASA Lewis Research Center are presented. The test results obtained from turbocharged rotary engines and preliminary results from a high performance single rotor engine were discussed. Combustion modeling studies of the rotary engine and the use of a Laser Doppler Velocimeter to confirm the studies were examined. An in-house program in which a turbocharged rotary engine was installed in a Cessna Skymaster for ground test studies was reviewed. Details are presented on single rotor stratified charge rotary engine research efforts, both in-house and on contract.

Author

**N84-28794\*#** Case Western Reserve Univ., Cleveland, Ohio. Dept. of Mechanical and Aerospace Engineering.

### **DILUTION JETS IN ACCELERATED CROSS FLOWS Ph.D. Thesis Final Report**

A. LIPSHITZ and I. GREBER Jun. 1984 315 p refs

(Contract NSG-3206)

(NASA-CR-174717; NAS 1.26:174717) Avail: NTIS HC A14/MF A01 CSCL 21E

Results of flow visualization experiments and measurements of the temperature field produced by a single jet and a row of dilution jets issued into a reverse flow combustor are presented. The flow in such combustors is typified by transverse and longitudinal acceleration during the passage through its bending section. The flow visualization experiments are designed to examine the separate effects of longitudinal and transverse acceleration on the jet trajectory and spreading rate. A model describing a dense single jet in a lighter accelerating cross flow is developed. The model is based on integral conservation equations, including the pressure terms appropriate to accelerating flows. It uses a modified entrainment correlation obtained from previous experiments of a jet in a cross stream. The flow visualization results are compared with the model calculations in terms of trajectories and spreading rates. Each experiment is typified by a set of three parameters: momentum ratio, density ratio and the densimetric Froude number. M.A.C.

**N84-28795\*#** National Aeronautics and Space Administration. Lewis Research Center, Cleveland, Ohio.

### **DETAILED FLOW MEASUREMENTS IN CASING BOUNDARY LAYER OF 429-METER-PER-SECOND-TIP-SPEED TWO-STAGE FAN**

W. T. GORRELL Jan. 1984 33 p refs Prepared in cooperation with Army Aviation Research and Development Command, Cleveland

(NASA-TP-2052; E-219; NAS 1.60:2052,

AVRADCOM-TR-81-C-28) Avail: NTIS HC A03/MF A01 CSCL 21E

Detailed flow measurements between all blade rows were taken in the outer 30 percent of passage height of a two stage fan. Tabulations of the detailed flow measurements are included. Results of these measurements revealed the steep axial velocity profiles near the casing. The axial velocity profile near the casing at the rotor exists was much steeper than at the stator exits. The data also show overturning of the flow at the tip at the stator exits. The effect of mixing is shown by the redistribution of the first stage rotor exit total temperature profile as it passes through the following stator. Author

**N84-29875\*#** Purdue Univ., Lafayette, Ind. School of Mechanical Engineering.

### **PURDU-WINCOF: A COMPUTER CODE FOR ESTABLISHING THE PERFORMANCE OF A FAN-COMPRESSOR UNIT WITH WATER INGESTION Final Report**

M. LEONARDO, T. TSUCHIYA, and S. N. B. MURTHY Jan. 1982 292 p refs

(Contract NAG3-204)

(NASA-CR-168005; NAS 1.26:168005) Avail: NTIS HC A13/MF A01 CSCL 21E

A model for predicting the performance of a multi-spool axial-flow compressor with a fan during operation with water ingestion was developed incorporating several two-phase fluid flow effects as follows: (1) ingestion of water, (2) droplet interaction with blades and resulting changes in blade characteristics, (3) redistribution of water and water vapor due to centrifugal action, (4) heat and mass transfer processes, and (5) droplet size adjustment due to mass transfer and mechanical stability considerations. A computer program, called the PURDU-WINCOF code, was generated based on the model utilizing a one-dimensional formulation. An illustrative case serves to show the manner in which the code can be utilized and the nature of the results obtained. Author

**N84-29876\*#** National Aeronautics and Space Administration. Lewis Research Center, Cleveland, Ohio.

### **ENERGY EFFICIENT ENGINE PROGRAM CONTRIBUTIONS TO AIRCRAFT FUEL CONSERVATION**

P. G. BATTERTON 1984 28 p refs Proposed for presentation at the Aviation Fuel Conservation Symp., Washington, D.C., 10-11 Sep. 1984; sponsored by FAA

(NASA-TM-83741; E-2226; NAS 1.15:83741) Avail: NTIS HC A03/MF A01 CSCL 21E

Significant advances in high bypass turbofan technologies that enhance fuel efficiency have been demonstrated in the NASA Energy Efficient Engine Program. This highly successful second propulsion element of the NASA Aircraft Energy Efficiency Program included major contract efforts with both General Electric and Pratt & Whitney. Major results of these efforts will be presented including highlights from the NASA/General Electric E3 research turbofan engine test. Direct application of all the E3 technologies could result in fuel savings of over 18% compared to the CF6-50 and JT9D-7. Application of the E3 technologies to new and derivative engines such as the CF6-80C and PW 2037, as well as others, will be discussed. Significant portions of the fuel savings benefit for these new products can be directly related to the E3 technology program. Finally, results of a study looking at far term advanced turbofan engines will be briefly described. The study shows that substantial additional fuel savings over E3 are possible with additional turbofan technology programs. Author

**N84-29877\*** Pennsylvania State Univ., University Park. Mechanical Engineering Building.  
**A THEORETICAL AND EXPERIMENTAL STUDY OF TURBULENT NONEVAPORATING SPRAYS** Final Report  
 A. S. P. SOLOMON, J. S. SHUEN, Q. F. ZHANG, and G. M. FAETH Jun. 1984 138 p refs  
 (Contract NAG3-190)  
 (NASA-CR-174668; NAS 1.26:174668) Avail: NTIS HC A07/MF A01 CSCL 21E

Measurements and analysis limited to the dilute portions of turbulent nonevaporating sprays injected into a still air environment were completed. Mean and fluctuating velocities and Reynolds stress were measured in the continuous phase. Liquid phase measurements included liquid mass fluxes, drop sizes and drop size and velocity correlation. Initial conditions needed for model evaluation were measured at a location as close to the injector exit as possible. The test sprays showed significant effects of slip and turbulent dispersion of the discrete phase. The measurements were used to evaluate three typical models of these processes: (1) a locally homogenous flow (LHF) model, where slip between the phases were neglected; (2) a deterministic separated flow (DSF) model, where slip was considered but effects of drop dispersion by turbulence were ignored; and (3) a stochastic separated flow (SSF) model, where effects of interphase slip and turbulent dispersion were considered using random-walk computations for drop motion. The LHF and DSF models did not provide very satisfactory predictions for the present measurements. In contrast, the SSF model performed reasonably well with no modifications in the prescription of eddy properties from its original calibration. Some effects of drops on turbulence properties were observed near the dense regions of the sprays. B.W.

**N84-29878\*** National Aeronautics and Space Administration. Lewis Research Center, Cleveland, Ohio.  
**FUEL SAVINGS POTENTIAL OF THE NASA ADVANCED TURBOPROP PROGRAM**  
 J. B. WHITLOW, JR. and G. K. SIEVERS 1984 56 p Presented at the Aviation Fuel Conservation Symp., Washington, D.C., 10-11 Sep. 1984; sponsored by FAA  
 (NASA-TM-83736; E-2218; NAS 1.15 83736) Avail: NTIS HC A04/MF A01 CSCL 21E

The NASA Advanced Turboprop (ATP) Program is directed at developing new technology for highly loaded, multibladed propellers for use at Mach 0.65 to 0.85 and at altitudes compatible with the air transport system requirements. Advanced turboprop engines offer the potential of 15 to 30 percent savings in aircraft block fuel relative to advanced turbofan engines (50 to 60 percent savings over today's turbofan fleet). The concept, propulsive efficiency gains, block fuel savings and other benefits, and the program objectives through a systems approach are described. Current program status and major accomplishments in both single rotation and counter rotation propeller technology are addressed. The overall program from scale model wind tunnel tests to large scale flight tests on testbed aircraft is discussed. Author

**N84-32388\*** National Aeronautics and Space Administration. Lewis Research Center, Cleveland, Ohio.  
**ANALYTICAL AND EXPERIMENTAL INVESTIGATION OF STATOR ENDWALL COUTOURING IN A SMALL AXIAL-FLOW TURBINE**  
 J. E. HAAS and R. J. BOYLE Sep. 1984 23 p refs Prepared in cooperation with Army Research and Technology Labs., Cleveland  
 (NASA-TP-2309; E-2050; NAS 1.60:2309, AVSCOM-TR-84-C-5) Avail: NTIS HC A02/MF A01 CSCL 21E

An experimental and analytical investigation was conducted to determine the effect of stator endwall contouring on turbine stage performance. In this investigation three stator configurations were evaluated using a common rotor. The three stator configurations were a cylindrical endwall design and two contoured endwall designs, one having a S-shaped outer wall profile and the other having a conical-shaped outer wall profile. Experimental data were obtained over a range of equivalent speeds, total pressure ratios,

and rotor tip clearances for each stator-rotor combination. Detailed analytical loss assessments were conducted to aid in the determination of the contouring effect on turbine performance. Author

**N84-32389\*** Pratt and Whitney Aircraft Group, East Hartford, Conn. Commercial Products Div.  
**ENERGY EFFICIENT ENGINE COMPONENT DEVELOPMENT AND INTEGRATION PROGRAM** Semiannual Status Report, 1 Apr. - 30 Sep. 1980  
 19 Dec. 1980 392 p  
 (Contract NAS3-20646)  
 (NASA-CR-173884; NAS 1.26:173884; SASR-5; PWA-5594-142) Avail: NTIS HC A17/MF A01 CSCL 21E

The design of an energy efficient commercial turbofan engine is examined with emphasis on lower fuel consumption and operating costs. Propulsion system performance, emission standards, and noise reduction are also investigated. A detailed design analysis of the engine/aircraft configuration, engine components, and core engine is presented along with an evaluation of the technology and testing involved. M.A.C.

**N84-32390\*** Pennsylvania State Univ., University Park.  
**A THEORETICAL AND EXPERIMENTAL STUDY OF TURBULENT EVAPORATING SPRAYS** Final Report  
 A. S. P. SOLOMON, J. S. SHUEN, Q. F. ZHANG, and G. M. FAETH Sep. 1984 138 p refs  
 (Contract NAG3-190)  
 (NASA-CR-174760; NAS 1.26:174760) Avail: NTIS HC A07/MF A01 CSCL 21E

Measurements and analysis limited to the dilute portions of turbulent evaporating sprays, injected into a still air environment were completed. Mean and fluctuating velocities and Reynolds stress were measured in the continuous phase. Liquid phase measurements included liquid mass fluxes, drop sizes and drop size and velocity correlation. Initial conditions needed for model evaluation were measured at a location as close to the injector exit as possible. The test sprays showed significant effects of slip and turbulent dispersion of the discrete phase. The measurements were used to evaluate three typical models of these processes: (1) a locally homogeneous flow (LHF) model, where slip between the phases were neglected; (2) a deterministic separated flow (DSF) model, where slip was considered but effects of drop dispersion by turbulence were ignored; and (3) a stochastic separated flow (SSF) model, where effects of interphase slip and turbulent dispersion were considered using random-walk computations for drop motion. For all three models, a k-epsilon model as used to find the properties of the continuous phase. The LHF and DSF models did not provide very satisfactory predictions for the present measurements. In contrast, the SSF model performed reasonably well—with no modifications in the prescription of eddy properties from its original calibration B.W.

**N84-33410\*** National Aeronautics and Space Administration. Lewis Research Center, Cleveland, Ohio.  
**AIR MODULATION APPARATUS** Patent  
 D. T. LENAHER (GE, Cincinnati), R. J. CORSMEIER (GE, Cincinnati), and A. P. STERMAN, inventors (to NASA) (GE, Cincinnati) 22 Nov. 1983 8 p Filed 25 Feb. 1981 Supersedes N83-30957 (21 - 19, p 3136) Sponsored by NASA  
 (NASA-CASE-LEW-13524-1; NAS 1.71:LEW-13524-1; US-PATENT-4,416,111; US-PATENT-APPL-SN-238257; US-PATENT-CLASS-60-39.29; US-PATENT-CLASS-60-39.83, US-PATENT-CLASS-415-115) Avail: US Patent and Trademark Office CSCL 20E

An air modulation apparatus, such as for use in modulating cooling air to the turbine section of a gas turbine engine is described. The apparatus includes valve means disposed around an annular conduit, such as a nozzle, in the engine cooling air circuit. The valve means, when in a closed position, blocks a portion of the conduit, and thus reduces the amount and increases the velocity of cooling air flowing through the nozzle. The apparatus also includes actuation means, which can operate in response to

predetermined engine conditions, for enabling opening and closing of the valve means.

Official Gazette of the U.S. Patent and Trademark Office

**N84-33412\*#** Arizona State Univ., Tempe. Dept. of Mechanical and Aerospace Engineering.

## **AN EXPERIMENTAL INVESTIGATION OF GAS JETS IN CONFINED SWIRLING AIR FLOW Final Report**

H. MONGIA, S. A. AHMED, and H. C. MONGIA Washington  
NASA Sep. 1984 159 p refs

(Contract NAG3-260)

(NASA-CR-3832, L-2178; NAS 1.26:3832) Avail: NTIS HC

A08/MF A01 CSCL 21E

The fluid dynamics of jets in confined swirling flows which is of importance to designers of turbine combustors and solid fuel ramjets used to power missiles fired from cannons were examined. The fluid dynamics of gas jets of different densities in confined swirling flows were investigated. Mean velocity and turbulence measurements are made with a one color, one component laser velocimeter operating in the forward scatter mode. It is shown that jets in confined flow with large area ratio are highly dissipative which results in both air and helium/air jet centerline velocity decays. For air jets, the jet like behavior in the tube center disappears at about 20 diameters downstream of the jet exit. This phenomenon is independent of the initial jet velocity. The turbulence field at this point also decays to that of the background swirling flow. A jet like behavior in the tube center is noticed even at 40 diameters for the helium/air jets. The subsequent flow and turbulence field depend highly on the initial jet velocity. The jets are fully turbulent, and the cause of this difference in behavior is attributed to the combined action swirl and density difference. This observation can have significant impact on the design of turbine combustors and solid fuel ramjets subject to spin. E.A.K.

**N84-33414\*#** National Aeronautics and Space Administration. Lewis Research Center, Cleveland, Ohio.

## **RESPONSE OF A SMALL-TURBOSHAFT-ENGINE COMPRESSION SYSTEM TO INLET TEMPERATURE DISTORTION**

T. J. BIESIADNY, G. A. KLANN, and J. K. LITTLE Sep 1983  
28 p refs

(NASA-TM-83765; E-2198; NAS 1.15:83765;

USAAVSCOM-TR-84-C-13) Avail: NTIS HC A03/MF A01

CSCL 21E

An experimental investigation was conducted into the response of a small-turboshaft-engine compression system to steady-state and transient inlet temperature distortions. Transient temperature ramps ranged from less than 100 deg K/sec to above 610 deg K/sec and generated instantaneous temperatures to 420 K above ambient. Steady-state temperature distortion levels were limited by the engine hardware temperature limit. Simple analysis of the steady-state distortion data indicated that a particle separator at the engine inlet permitted higher levels of temperature distortion before onset of compressor surge than would be expected without the separator. Author

**N84-34444\*#** National Aeronautics and Space Administration. Lewis Research Center, Cleveland, Ohio.

## **IDENTIFICATION OF QUASI-STEADY COMPRESSOR CHARACTERISTICS FROM TRANSIENT DATA Final Report**

K. B. NUNES and S. M. ROCK Sep. 1984 290 p

(Contract NAS3-23537)

(NASA-CR-174685; NAS 1.26:174685) Avail: NTIS HC A13/MF A01 CSCL 20E

The principal goal was to demonstrate that nonlinear compressor map parameters, which govern an in-stall response, can be identified from test data using parameter identification techniques. The tasks included developing and then applying an identification procedure to data generated by NASA LeRC on a hybrid computer. Two levels of model detail were employed. First was a lumped compressor rig model; second was a simplified turbofan model. The main outputs are the tools and procedures generated to accomplish the identification. Author

## AIRCRAFT STABILITY AND CONTROL

Includes aircraft handling qualities; piloting; flight controls; and autopilots.

**A84-46524\*** National Aeronautics and Space Administration. Lewis Research Center, Cleveland, Ohio.

## **ROTORCRAFT FLIGHT-PROPULSION CONTROL INTEGRATION**

J. R. MIHALOEWS (NASA, Lewis Research Center, Cleveland, OH) and R. T. N. CHEN (NASA, Ames Research Center, Moffett Field, CA) Vertiflite (ISSN 0042-4455), vol. 30, Sept.-Oct. 1984, p. 45-47.

The parallel development of digital engine and flight controls for U.S. Army helicopters has made possible the future derivation of a fully integrated digital flight/propulsion control system. A NASA/Army research program has been undertaken to exploit these possibilities, ultimately yielding a generation of helicopters with exceptional agility and maneuverability in military roles and low pilot workloads in all-weather civil aviation missions. The program's three phases respectively address system modeling and analysis, flight hardware and software development, and flight evaluations aboard a research vehicle. O.C.

**N84-33417\*#** General Electric Co., Cincinnati, Ohio. Aircraft Engine Business Group.

## **SUBSONIC/TRANSONIC STALL FLUTTER INVESTIGATION OF A ROTATING RIG Final Report**

R. R. JUTRAS, R. B. FOST, R. M. CHI, and B. F. BEACHER Feb. 1981 319 p refs

(Contract NAS3-20605)

(NASA-CR-174625; NAS 1.26:174625; R81AEG282) Avail:

NTIS HC A14/MF A01 CSCL 01C

Stall flutter is investigated by obtaining detailed quantitative steady and aerodynamic and aeromechanical measurements in a typical fan rotor. The experimental investigation is made with a 31.3 percent scale model of the Quiet Engine Program Fan C rotor system. Both subsonic/transonic (torsional mode) flutter and supersonic (flexural) flutter are investigated. Extensive steady and unsteady data on the blade deformations and aerodynamic properties surrounding the rotor are acquired while operating in both the steady and flutter modes. Analysis of this data shows that while there may be more than one traveling wave present during flutter, they are all forward traveling waves. M.A.C.

## RESEARCH AND SUPPORT FACILITIES (AIR)

Includes airports, hangars and runways; aircraft repair and overhaul facilities; wind tunnels; shock tube facilities; and engine test blocks.

**N84-19360\*#** Virginia Univ., Charlottesville. Dept. of Electrical Engineering.

## **CARRIER RECOVERY METHODS FOR A DUAL-MODE MODEM: A DESIGN APPROACH**

C. W. RICHARDS and S. G. WILSON Mar. 1984 104 p refs

(Contract NAG3-3161)

(NASA-CR-173355; NAS 1.26:173355; UVA/528219/EE84/102)

Avail: NTIS HC A06/MF A01 CSCL 01E

A dual mode model with selectable QPSK or 16-QASK modulation schemes is discussed. The theoretical reasoning as well as the practical trade-offs made during the development of a modem are presented, with attention given to the carrier recovery method used for coherent demodulation. Particular attention is

given to carrier recovery methods that can provide little degradation due to phase error for both QPSK and 16-QASK, while being insensitive to the amplitude characteristic of a 16-QASK modulation scheme. A computer analysis of the degradation is symbol error rate (SER) for QPSK and 16-QASK due to phase error is presented. Results find that an energy increase of roughly 4 dB is needed to maintain a SER of  $1 \times 10^{-5}$  for QPSK with 20 deg of phase error and 16-QASK with 7 deg. phase error. Author

## 12

## ASTRONAUTICS (GENERAL)

**A84-11793\*#** National Aeronautics and Space Administration, Washington, D. C.

**NASA PRIORITY TECHNOLOGIES**

S. R. SADIN (NASA, Office of Aeronautics and Space Technology, Washington, DC) and H. O. SLONE (NASA, Lewis Research Center, Cleveland, OH) International Astronautical Federation, International Astronautical Congress, 34th, Budapest, Hungary, Oct. 10-15, 1983. 10 p.  
(IAF PAPER 83-345)

Significant research areas deserving of attention within the NASA Space Research and Technology program are discussed, noting that the program is pursued to strengthen the U.S. technology base, improve low-cost access to space, and to aid in the expanded use of space, including a space station. Study areas being pursued include new Orbiter thermal protection system materials, developing longer-life reusable engines, and providing the technology for orbital transfer vehicle propulsion and aeroassisted braking. Attention is also being given to CFD techniques for entry body and rocket engine design, verifying the feasibility of advanced sensor concepts, defining the technology for large deployable RF antennas, and improving on-board data management systems. Of particular concern is to establish technologies which will enhance and extend a permanent, manned presence in space. M.S.K.

**N84-10109\*#** TRW, Inc., Redondo Beach, Calif.

**APPARATUS ANALYSIS AND PRELIMINARY DESIGN OF LOW GRAVITY POROUS SOLIDS EXPERIMENT FOR STS ORBITER MID-DECK Final Report, Dec. 1981 - Oct. 1983**

R. D. FLEETER and J. L. KROPP Oct. 1983 258 p refs  
(Contract NAS3-23254)

(NASA-CR-168248; NAS 1.26:168248; TRW-38884-6001-UT-00)  
Avail: NTIS HC A12/MF A01 CSCL 22A

The apparatus analysis laboratory equipment design and fabrication and the preliminary design of the Combustion of Porous Solids Experiment for operation in the mid-deck area of the Shuttle are described. The apparatus analysis indicated that the mid-deck region of the STS was a feasible region of the Shuttle for operation. A sixteen tube concept was developed with tubes of 75 cm length and up to 5.6 cm accommodated. The experiment is viewed by IR sensors and a 16 mm camera. Laboratory equipment was designed and fabricated to test the particle injection, mixing and venting concepts. This equipment was delivered to NASA/LeRC. A preliminary design was made for the experiment based upon the apparatus analysis. The design incorporated results from the Phase "O" Safety Review. This design utilizes a closed tube concept in which the particles are stored, injected and burned with no coupling to the Shuttle environment. Drawings of the major components and an assembly are given. The electronics are described for the experiment. An equipment list is presented and an experiment weight estimate is determined. The mission operation requirements are outlined. Author

**N84-15164\*#** National Aeronautics and Space Administration, Lewis Research Center, Cleveland, Ohio.

**DETROIT SPACE ODESSEY Final Report**

H. ALLEN, JR. 1983 119 p Presented at the Aerospace Educational Symp. for the City of Detroit, 3-8 May 1982; sponsored in part by Detroit Public Schools and Wayne State Univ., Detroit (NASA-TM-85487; NAS 1.15:85487) Avail: NTIS HC A06/MF A01 CSCL 22A

The symposium included personal appearances by NASA astronauts, NASA exhibits, aerospace science lecture demonstrations (Spacemobile Lectures), and talks on job opportunities in aerospace and on the benefits of the Space Program. The program was directed mainly at (public, parochial and private) student groups, each of which spent three hours at the symposium site, Wayne State University campus, to participate in the symposium activities. The symposium was open to the general public and consisted of the NASA exhibits, aerospace science lecture demonstrations, films, talks on the benefits of the space program, and a special tasting demonstration of "space food" meal systems. Author

## 14

## GROUND SUPPORT SYSTEMS AND FACILITIES (SPACE)

Includes launch complexes, research and production facilities; ground support equipment, e.g., mobile transporters; and simulators.

**A84-22346\*#** Rensselaer Polytechnic Inst., Troy, N. Y.

**GRAVITATIONAL EFFECTS IN DENDRITIC GROWTH**

M. E. GLICKSMAN, N. B. SINGH, and M. CHOPRA (Rensselaer Polytechnic Institute, Troy, NY) IN: Manufacturing in space; Proceedings of the Winter Annual Meeting, Boston, MA, November 13-18, 1983. New York, American Society of Mechanical Engineers, 1983, p. 207-218. refs  
(Contract NAG3-333)

The theories of diffusion-controlled dendritic crystallization will be reviewed briefly, along with recently published critical experiments on the kinetics and morphology of dendritic growth in pure substances. The influence of the gravitational body force on dendritic growth kinetics will be shown to be highly dependent on the growth orientation with respect to the gravity vector and on the level of the thermal supercooling. In fact, an abrupt transition occurs at a critical supercooling, above which diffusional transport dominates the growth process and below which convective transport dominates. Our most recent work on binary mixtures shows that dilute solute additions influence the crystallization process indirectly, by altering the interfacial stability, rather than by directly affecting the transport mode. Directions for future studies in this field will also be discussed. Author

**N84-16229\*#** National Aeronautics and Space Administration, Lewis Research Center, Cleveland, Ohio.

**ELECTROMAGNETIC PROPULSION TEST FACILITY**

S. T. GOODER Jan. 1984 17 p  
(NASA-TM-83568; E-1948; NAS 1.15:83568) Avail: NTIS HC A02/MF A01 CSCL 14B

A test facility for the exploration of electromagnetic propulsion concept is described. The facility is designed to accommodate electromagnetic rail accelerators of various lengths (1 to 10 meters) and to provide accelerating energies of up to 240 kilojoules. This accelerating energy is supplied as a current pulse of hundreds of kiloamps lasting as long as 1 millisecond. The design, installation,



## 15 LAUNCH VEHICLES AND SPACE VEHICLES

and operating characteristics of the pulsed energy system are discussed. The test chamber and its operation at pressures down to 1300 Pascals (10 mm of mercury) are described. Some aspects of safety (interlocking, personnel protection, and operating procedures) are included. Author

### 15

#### LAUNCH VEHICLES AND SPACE VEHICLES

Includes boosters; manned orbital laboratories; reusable vehicles; and space stations.

**A84-11718\*#** National Aeronautics and Space Administration. Lewis Research Center, Cleveland, Ohio.

##### SHUTTLE/CENTAUR - MORE CAPABILITY FOR THE 1980'S

O. F. SPURLOCK (NASA, Lewis Research Center, Cleveland, OH) International Astronautical Federation, International Astronautical Congress, 34th, Budapest, Hungary, Oct. 10-15, 1983. 7 p. (IAF PAPER 83-18)

Design features of the Centaur upper stage for the Shuttle are described, noting interfaces with the Orbiter and intended missions. The Shuttle will carry the Centaur stage into a 241 km eastward orbit, open the payload doors, and by the fourth orbit rotate the Centaur 45 deg so it points out of the bay. An integrated support system will limit the actual equipment added to the Orbiter to 122 kg. Separation from the Orbiter will be effected by a spring-loaded mechanism that will impart a 1/3 m/sec velocity to the Centaur, which carries its own LOX/LH2 fuel supply for two RL 10A-3-3A engines. The fuel is moved to the bottom of the tanks by auxiliary thrusters which propel the Centaur forward. Planned missions for the Shuttle-Centaur are boosting the ESA Solar Polar Mission and launching the Galileo probe in 1986, possibly followed by a Venus radar mapper mission in 1988. M.S.K.

**N84-16234\*#** National Aeronautics and Space Administration. Lewis Research Center, Cleveland, Ohio.

##### CENTAUR D-1A GUIDANCE/SOFTWARE SYSTEM

A. L. GORDAN Nov. 1983 17 p refs Presented at the Ann. Rocky Mountain Guidance and Control Conf., Keystone, Colo., 4-8 Feb. 1984; sponsored by the Am. Astronautical Soc. (NASA-TM-83552; E-1927; NAS 1.15:83552) Avail: NTIS HC A02/MF A01 CSCL 22B

The main body of this paper describes the evolution of the Centaur D-1A Guidance and Software System. Specifically, the performance of the explicit guidance equations, using a linear tangent steering law. Inherent flexibility exists in the equations in that they have multimission capability. They can accommodate both Earth-orbital and Earth-escape missions with either one or two Centaur burns. They can also guide for multi-burn orbital missions. The Centaur performance is indicated in terms of optimality (propellant usage), accuracy, flexibility and computer requirements. In the course of the Centaur Guidance development substantial changes and improvements have been made and more improvements are on the way for the Shuttle/Centaur Guidance. It is the intent of this paper to describe, provide insight into, and identify certain unique aspects of the individual Centaur flight profiles. Mission profile(s) are described narratively with some numerical data given in cases where it may be useful. Author

**N84-20611\*#** Future Systems, Inc., Gaithersburg, Md. **ADVANCED TECHNOLOGY SATELLITES IN THE COMMERCIAL ENVIRONMENT. VOLUME 1: EXECUTIVE SUMMARY**

Mar. 1984 25 p refs 2 Vol. (Contract NAS3-23783) (NASA-CR-174635-VOL-1; NAS 1.26:174635-VOL-1) Avail: NTIS HC A02/MF A01 CSCL 22B

A set of scenarios, based on a set of traffic demand forecasts is postulated. The scenarios use a demand-driven model to launch

satellites, with other limits on the available (and economical) technology. The results using a low traffic forecast show a continuing oversupply of transponders. However, the scenarios using a high traffic forecast show that considerable advanced technology including the use of 30/20 GHz is needed to satisfy demand S.L.

**N84-20612\*#** Future Systems, Inc., Gaithersburg, Md. **ADVANCE TECHNOLOGY SATELLITES IN THE COMMERCIAL ENVIRONMENT, VOLUME 2 Final Report**

Mar. 1984 294 p refs 2 Vol. (Contract NAS3-23783) (NASA-CR-174635-VOL-2; NAS 1.26:174635-VOL-2) Avail: NTIS HC A13/MF A01 CSCL 22B

A forecast of transponder requirements was obtained. Certain assumptions about system configurations are implicit in this process. The factors included are interpolation of baseline year values to produce yearly figures, estimation of satellite capture, effects of peak-hours and the time-zone staggering of peak hours, circuit requirements for acceptable grade of service capacity of satellite transponders, including various compression methods where applicable, and requirements for spare transponders in orbit. The graphical distribution of traffic requirements was estimated. S.L.

**N84-23662\*#** Ohio State Univ., Columbus. ElectroScience Lab **ENGINEERING CALCULATIONS FOR COMMUNICATIONS SATELLITE SYSTEMS PLANNING** Interim Report, 15 Jan. - 15 Jul. 1983

C. H. MARTIN, D. J. GONSALVEZ, C. A. LEVIS, and C. W. WANG Dec. 1983 36 p (Contract NAG3-159) (NASA-CR-173532; NAS 1.26:173532; ESL-713533-4) Avail: NTIS HC A03/MF A01 CSCL 22B

Progress is reported on a computer code to improve the efficiency of spectrum and orbit utilization for the Broadcasting Satellite Service in the 12 GHz band for Region 2. It implements a constrained gradient search procedure using an exponential objective function based on aggregate signal to noise ratio and an extended line search in the gradient direction. The procedure is tested against a manually generated initial scenario and appears to work satisfactorily. In this test it was assumed that alternate channels use orthogonal polarizations at any one satellite location. M.A.C.

**N84-32411\*#** National Aeronautics and Space Administration. Lewis Research Center, Cleveland, Ohio.

##### A. HIGH ENERGY STAGE FOR THE NATIONAL SPACE TRANSPORTATION SYSTEM

A. J. STOFAN Washington 1984 13 p refs Presented at the 35th Congr. of the Intern. Astronautical Federation, Lausanne, Switzerland, 7-13 Oct. 1984 (NASA-TM-83795; E-2292; NAS 1.15:83795; IAF-84-15) Avail: NTIS HC A02/MF A01 CSCL 22B

The Shuttle/Centaur is an expendable hydrogen/oxygen cryogenic upper stage for use with the National Space Transportation System. It is a modification of the existing Atlas/Centaur which was used by NASA since 1966 to launch interplanetary and Earth orbital payloads for numerous organizations. Two configurations of the Shuttle/Centaur are being developed. Vehicle capability includes placing approximately 4500 kg (10,000 lb) in geostationary orbit, and initial applications will be for the interplanetary Galileo and Ulysses Missions in 1986. The Shuttle/Centaur development program is discussed, the configurations and performance are described, and the unique integration and operations requirements related to the Shuttle are indicated. Design changes to the current Atlas/Centaur required for Shuttle operation are described here, and include those related to Orbiter cargo bay dimensions, environment, and safety considerations. Author

## SPACE TRANSPORTATION

Includes passenger and cargo space transportation, e.g., shuttle operations; and rescue techniques.

**N84-23667\*#** TRW Space Technology Labs., Redondo Beach, Calif.

**PRELIMINARY DESIGN OF TWO SPACE SHUTTLE FLUID PHYSICS EXPERIMENTS Final Report**

N. GAT and J. L. KROPP May 1984 225 p

(Contract NAS3-23774)

(NASA-CR-174649; NAS 1.26:174649; REPT-41763-6001-UT-00)

Avail: NTIS HC A10/MF A01 CSCL 22A

The mid-deck lockers of the STS and the requirements for operating an experiment in this region are described. The design of the surface tension induced convection and the free surface phenomenon experiments use a two locker volume with an experiment unique structure as a housing. A manual mode is developed for the Surface Tension Induced Convection experiment. The fluid is maintained in an accumulator pre-flight. To begin the experiment, a pressurized gas drives the fluid into the experiment container. The fluid is an inert silicone oil and the container material is selected to be comparable. A wound wire heater, located axisymmetrically above the fluid can deliver three wattages to a spot on the fluid surface. These wattages vary from 1-15 watts. Fluid flow is observed through the motion of particles in the fluid. A 5 mw He/Ne laser illuminates the container. Scattered light is recorded by a 35mm camera. The free surface phenomena experiment consists of a trapezoidal cell which is filled from the bottom. The fluid is photographed at high speed using a 35mm camera which incorporated the entire cell length in the field of view. The assembly can incorporate four cells in one flight. For each experiment, an electronics block diagram is provided. A control panel concept is given for the surface induced convection. Both experiments are within the mid-deck locker weight and c-g limits

A.R.H.

**N84-25753\*#** National Aeronautics and Space Administration, Lewis Research Center, Cleveland, Ohio

**ON-ORBIT CRYOGENIC FLUID TRANSFER**

J. C. AYDELOTT, J. P. GILLE (Martin Marietta Aerospace, Denver), and R. N. EBERHARDT (Martin Marietta Aerospace, Denver), 1984 11 p refs Presented at the 20th Joint Propulsion Conf., Cincinnati, 11-13 Jun. 1984; sponsored by the AIAA, SAE and ASME

(NASA-TM-83688; E-2139; NAS 1.15:83688; AIAA-84-1343)

Avail: NTIS HC A02/MMF A01 CSCL 20D

A number of future NASA and DOD missions have been identified that will require, or could benefit from resupply of cryogenic liquids in orbit. The most promising approach for accomplishing cryogenic fluid transfer in the weightlessness environment of space is to use the thermodynamic filling technique. This approach involves initially reducing the receiver tank temperature by using several charge hold vent cycles followed by filling the tank without venting. Martin Marietta Denver Aerospace, under contract to the NASA Lewis Research Center, is currently developing analytical models to describe the on orbit cryogenic fluid transfer process. A detailed design of a shuttle attached experimental facility, which will provide the data necessary to verify the analytical models, is also being performed.

Author

## SPACECRAFT COMMUNICATION, COMMAND AND TRACKING

Includes telemetry; space communications networks; astronavigation; and radio blackout.

**A84-21397\*** National Aeronautics and Space Administration, Washington, D. C.

**NASA'S MULTIBEAM COMMUNICATIONS TECHNOLOGY PROGRAM**

D. SANTARPIA (NASA, Washington, DC) and J. BAGWELL (NASA, Lewis Research Center, Cleveland, OH) Microwave Journal (ISSN 0026-2897), vol. 27, Jan. 1984, p. 97, 98, 100 (5 ff). refs

It is noted that the multiyear contracts described here were designed to advance the state of the art in frequency reuse antennas, baseband processors, high-speed, wide bandwidth IF matrix switches and various RF components. Although the 30/20 GHz frequency band was selected for the RF components, the technology has applications at several other frequency bands of interest, both military and civilian. Test results thus far have demonstrated that significant progress has been made toward meeting the contract objectives. Whereas original projections of performance at the solid-state device level have been optimistic, conservative projections of performance at the circuit/component/system level in general have been met or exceeded.

C.R.

**A84-46620\*** LNR Communications, Inc., Hauppauge, N. Y.

**RECENT DEVELOPMENTS IN EHF SATCOM TECHNOLOGY**

H. C. OKEAN (LNR Communications, Inc., Hauppauge, NY) IN: ITC/USA/ '83; Proceedings of the International Telemetry Conference, San Diego, CA, October 24-27, 1983 Research Triangle Park, NC, Instrument Society of America, 1983, p. 225-238.

(Contract F33575-80-C-1182, N00123-79-C-1529, NAS3-22491; NAS3-22494)

The state-of-the-art in EHF Satcom technology is assessed and hardware samples are described. Travelling wave tube amplifiers provide up to 30 percent efficiency for 20 GHz spaceborne operations and up to 20 percent efficiency at 30/44 GHz in ground operations. Solid-state power amplifiers incorporate FET and IMPATT diode technologies for 20-44 GHz transmissions using GaAs FETs and Si or GaAs diodes. Noise is reduced with loss image-enhanced mixers coupled to an IF FET amplifier, resulting ultimately in 6-7 dB noise levels compared to 19 dB gain. Finally, high power varactor upconverters have been developed to provide up to 50 mW RF output at at least 10 percent efficiency at frequencies up to 50 GHz.

M.S.K.

**A84-49176\*** National Aeronautics and Space Administration, Lewis Research Center, Cleveland, Ohio.

**CENTAUR D-1A GUIDANCE/SOFTWARE SYSTEM**

A. L. GORDAN (NASA, Lewis Research Center, Cleveland, OH) IN: Guidance and control 1984; Proceedings of the Seventh Annual Rocky Mountain Conference, Keystone, CO, February 4-8, 1984 San Diego, CA, Univelt, Inc., 1984, p. 311-326. Previously announced in STAR as N84-16234 refs

(AAS PAPER 84-043)

The main body of this paper describes the evolution of the Centaur D-1A Guidance and Software System. Specifically, the performance of the explicit guidance equations, using a linear tangent steering law. Inherent flexibility exists in the equations in that they have multimission capability. They can accommodate both earth-orbital and earth-escape missions with either one or two Centaur burns. They can also guide for multi-burn orbital missions. The Centaur performance is indicated in terms of optimality (propellant usage), accuracy, flexibility and computer requirements. In the course of the Centaur Guidance development substantial changes and improvements have been made and more

improvements are on the way for the Shuttle/Centaur Guidance. It is the intent of this paper to describe, provide insight into, and identify certain unique aspects of the individual Centaur flight profiles. Mission profile(s) are described narratively with some numerical data given in cases where it may be useful. Author

**A84-49250\*** National Aeronautics and Space Administration. Lewis Research Center, Cleveland, Ohio.

## ADVANCED 30/20 GHZ MULTIPLE-BEAM ANTENNAS FOR COMMUNICATIONS SATELLITES

R. W. MYHRE (NASA, Lewis Research Center, Cleveland, OH) IN: ICC '83 - Integrating communication for world progress; International Conference on Communications, Boston, MA, June 19-22, 1983, Conference Record. Volume 1. New York, Institute of Electrical and Electronics Engineers, 1983, p. 338-343. Previously announced in STAR as N83-13154.

Design concepts under development utilize two separate spacecraft antenna systems, one uplink at 30 GHz and the other a downlink at 20 GHz, where each antenna provides multiple fixed and scanning beams. Two contractors completed configuration trade-off studies and breadboarding of critical technology components, and are fabricating and testing proof-of-concept (POC) models to demonstrate the technology feasibility. Technology developments required for the proposed systems are presented, along with each contractor's progress to date. The technology development areas discussed include: (1) offset Cassegrain and shaped reflector systems for narrow beams with low sidelobes and wideangle off-axis scan; (2) diplexed beam-forming networks for dual polarization, low sidelobes, and fixed and scan-beam operation; (3) fast switching networks for scanning beams; and (4) fabrication of precision feed components and large offset reflectors. A R.H.

**A84-49288\*#** National Aeronautics and Space Administration. Lewis Research Center, Cleveland, Ohio.

## A STUDY OF 60 GHZ INTERSATELLITE LINK APPLICATIONS

G. ANZIC, D. J. CONNOLLY, E. J. HAUGLAND, H. G. KOSMAHL (NASA, Lewis Research Center, Cleveland, OH), and J. S. CHITWOOD (NASA, Goddard Space Flight Center, Greenbelt, MD) IN: ICC '83 - Integrating communication for world progress; International Conference on Communications, Boston, MA, June 19-22, 1983, Conference Record. Volume 3. New York, Institute of Electrical and Electronics Engineers, 1983, p. 1181-1188. Previously announced in STAR as N83-20994. refs

Applications of intersatellite links operating at 60 GHz are reviewed. Likely scenarios, ranging from transmission of moderate and high data rates over long distances to low data rates over short distances are examined. A limited parametric tradeoff is performed with system variables such as radiofrequency power, receiver noise temperature, link distance, data rate, and antenna size. Present status is discussed and projections are given for both electron tube and solid state transmitter technologies. Monolithic transmit and receive module technology, already under development at 20 to 30 GHz, is reviewed and its extension to 60 GHz, and possible applicability is discussed. Author

**N84-16243\*#** Analox Corp., Cleveland, Ohio.

## APPROACHES TO OPTIMIZATION OF SS/TDMA TIME SLOT ASSIGNMENT

T. O. WADE Jan. 1984 13 p refs Presented at 10th Commun. Satellite Systems Conf., Orlando, Fla., 18-22 Mar. 1984; sponsored by AIAA (Contract NAS3-23293) (NASA-CR-168328; NAS 1.26:168328) Avail: NTIS HC A02/MF A01 CSCL 12A

Reduction techniques for traffic matrices are explored in some detail. These matrices arise in satellite switched time-division multiple access (SS/TDMA) techniques whereby switching of uplink and downlink beams is required to facilitate interconnectivity of beam zones. A traffic matrix is given to represent that traffic to be transmitted from  $n$  uplink beams to  $n$  downlink beams within a TDMA frame typically of 1 ms duration. The frame is divided into segments of time and during each segment a portion of the traffic

is represented by a switching mode. This time slot assignment is characterized by a mode matrix in which there is not more than a single non-zero entry on each line (row or column) of the matrix. Investigation is confined to decomposition of an  $n \times n$  traffic matrix by mode matrices with a requirement that the decomposition be 100 percent efficient or, equivalently, that the line(s) in the original traffic matrix whose sum is maximal (called critical line(s)) remain maximal as mode matrices are subtracted throughout the decomposition process. A method of decomposition of an  $n \times n$  traffic matrix by mode matrices results in a number of steps that is bounded by  $n(2) - 2n + 2$ . It is shown that this upper bound exists for an  $n \times n$  matrix wherein all the lines are maximal (called a quasi doubly stochastic (QDS) matrix) or for an  $n \times n$  matrix that is completely arbitrary. That is, the fact that no method can exist with a lower upper bound is shown for both QDS and arbitrary matrices, in an elementary and straightforward manner. Author

# 18

## SPACECRAFT DESIGN, TESTING AND PERFORMANCE

Includes spacecraft thermal and environmental control; and attitude control.

**A84-18025\*#** Systems Science and Software, La Jolla, Calif.

## PLASMA SHEATH STRUCTURE SURROUNDING A LARGE POWERED SPACECRAFT

M. J. MANDELL, G. A. JONGEWARD, and I. KATZ (System, Science and Software, La Jolla, CA) American Institute of Aeronautics and Astronautics, Aerospace Sciences Meeting, 22nd, Reno, NV, Jan. 9-12, 1984. 5 p. refs (Contract NAS3-23058) (AIAA PAPER 84-0329)

Various factors determining the floating potential of a highly biased (about 4-kV) spacecraft in low earth orbit are discussed. While the common rule of thumb (90 percent negative; 10 percent positive) is usually a good guide, different biasing and grounding patterns can lead to high positive potentials. The NASCAP/LEO code can be used to predict spacecraft floating potential for complex three-dimensional spacecraft. Author

**N84-16247\*#** National Aeronautics and Space Administration. Lewis Research Center, Cleveland, Ohio.

## RADIATING DIPOLE MODEL OF INTERFERENCE INDUCED IN SPACECRAFT CIRCUITRY BY SURFACE DISCHARGES

R. N. METZ (Colby College) Jan. 1984 7 p refs (NASA-TP-2240; E-1775; NAS 1.60:2240) Avail: NTIS HC A02/MF A01 CSCL 22B

Spacecraft in geosynchronous orbit can be charged electrically to high voltages by interaction with the space plasma. Differential charging of spacecraft surfaces leads to arc and blowoff discharging. The discharges are thought to upset interior, computer-level circuitry. In addition to capacitive or electrostatic effects, significant inductive and less significant radiative effects of these discharges exist and can be modeled in a dipole approximation. Flight measurements suggest source frequencies of 5 to 50 MHz. Laboratory tests indicate source current strengths of several amperes. Electrical and magnetic fields at distances of many centimeters from such sources can be as large as tens of volts per meter and meter squared, respectively. Estimates of field attenuation by spacecraft walls and structures suggest that interior fields may be appreciable if electromagnetic shielding is much thinner than about 0.025 mm (1 mil). Pickup of such fields by wires and cables interconnecting circuit components could be a source of interference signals of several volts amplitude. Author

**N84-17252\*#** California Univ., San Diego, La Jolla. Center for Astrophysics and Space Sciences  
**ANOMALOUSLY HIGH POTENTIALS OBSERVED ON ISEE Final Technical Report, 15 Sep. 1982 - 30 Sep. 1983**  
 E. C. WHIPPLE, I. S. KRINSKY, R. B. TORBERT, and R. C. OLSEN (Alabama Univ.) Feb. 1984 11 p refs  
 (Contract NAG3-320)  
 (NASA-CR-172791; NAS 1.26:172791). Avail: NTIS HC A02/MF A01 CSCL 22B

Data from the two electric field experiments and from the plasma composition experiment on ISEE-1 show that the spacecraft charged to close to -70 V in sunlight at about 0700 UT on March 17, 1978. Data from the electron spectrometer experiment show that there was a potential barrier of some -10 to -20 V about the spacecraft during this event. The potential barrier was effective in turning back emitted photoelectrons to the spacecraft. Potential barriers can be formed because of differential charging on the spacecraft or because of the presence of space charge. The stringent electrostatic cleanliness specifications imposed on ISEE make the presence of differential charging unlikely, if these precautions were effective. Modeling of this event is required to determine if the barrier was produced by the presence of space charge. Author

**N84-17258\*#** California Univ., La Jolla. Center for Astrophysics and Space Sciences.  
**ANOMALOUSLY HIGH POTENTIALS OBSERVED ON ISEE**  
 E. C. WHIPPLE, I. S. KRINSKY, R. B. TORBERT, and R. C. OLSEN (Alabama Univ., Huntsville) In ESA Spacecraft/Plasma Interactions and their Influence on Field and Particle Meas. p 35-40 Nov. 1983 refs  
 (Contract NAG3-20)  
 Avail: NTIS HC A10/MF A01 CSCL 22B

Data from two electric field experiments and from the plasma composition experiment on ISEE-1 are used to show that the spacecraft charged to close to -70 V in sunlight at 0700 UT on March 17, 1978. Data from the electron spectrometer experiment show that there was a potential barrier of -10 to -20 V about the spacecraft during this event. The potential barrier was effective in turning back emitted photoelectrons to the spacecraft. The stringent electrostatic cleanliness specifications imposed on ISEE make the presence of differential charging unlikely. Modeling of this event is required to determine if the barrier was produced by the presence of space charge. Author (ESA)

**N84-17262\*#** Alabama Univ., Huntsville.  
**COMPARISON OF THERMAL PLASMA OBSERVATIONS ON SCATHA AND GEOS**  
 R. C. OLSEN, J. F. E. JOHNSON (Southampton Univ., England), P. DECREAU (CNRS, Orleans, France), G. WRENN (Univ. Coll., London), A. PEDERSEN (ESTEC, Noordwijk, Netherlands), and K. KNOTT In ESA Spacecraft/Plasma Interactions and their Influence on Field and Particle Meas. p 57-61 Nov. 1983 refs  
 (Contract NAS8-35339; NAS8-33982; NSG-3150, F04701-77-C-0062)  
 Avail: NTIS HC A10/MF A01 CSCL 22B

The SCATHA and GEOS 2 observations are compared in order to determine the relationship between the hidden ion population measured by SCATHA, and the missing density component of the GEOS particles detectors. Analysis shows that the wave instruments on GEOS measure the cold plasma population which is only visible to the SCATHA/UCSD detector in eclipse. Given a -28 V bias, the GEOS suprathermal plasma analyzers can also measure this plasma, at the cost of little or no energy resolution on the cold plasma. It is not clear if the missing component of the plasma found at apogee on GEOS-1 is identified. Author (ESA)

**N84-17268\*#** National Aeronautics and Space Administration. Lewis Research Center, Cleveland, Ohio.  
**NASCAP SIMULATIONS OF SPACECRAFT CHARGING OF THE SCATHA SATELLITE**  
 I. KATZ (Systems, Science and Software), P. R. STANNARD (Systems, Science and Software), L. GEDEON, J. C. ROCHE, A. G. RUBIN (AFGL), and M. F. TAUZ (AFGL) In ESA Spacecraft/Plasma Interactions and their Influence on Field and Particle Meas p 109-114 Nov. 1983 refs  
 (Contract NAS3-22536)  
 Avail: NTIS HC A10/MF A01 CSCL 22B

Data collected by the SCATHA spacecraft were used with NASCAP to simulate the charging response of the spacecraft ground conductor and dielectric surfaces. Spacecraft charging in eclipse, during moderate and severe substorms, and in sunlight was reproduced using the code. Close agreement between measured currents and potentials and the NASCAP simulated response is obtained for differential charging. Results reveal a strong correlation between the collection of particles with energies below 50 keV and the degree of charging. Author (ESA)

**N84-17269\*#** National Aeronautics and Space Administration. Lewis Research Center, Cleveland, Ohio.  
**THE ROLE OF POTENTIAL BARRIER FORMATION IN SPACECRAFT CHARGING**  
 C. K. PURVIS In ESA Spacecraft/Plasma Interactions and their Influence on Field and Particle Meas. p 115-124 Nov. 1983 refs  
 Previously announced as N83-35005  
 Avail: NTIS HC A10/MF A01 CSCL 22B

The role of potential barrier formation in spacecraft charging at geosynchronous orbit is discussed. Sudden dramatic shifts in structure potential at eclipse entry and exit, and in response to injections of hot plasma during eclipse do not indicate the magnitude of differential charging. All daylight charging and some long-term eclipse charging is barrier dominated. Shaded or low yield surfaces charge negatively, forming vacuum potential barriers which suppress emission of photoelectrons and secondary electrons, causing the spacecraft to charge negatively. This process, which is configuration and material dependent, limits the magnitude of insulator-negative differential charging to values substantially lower than supposed, and allows the possibility of insulator-positive differential charging. Discharges are less energetic and more localized than supposed. If the spacecraft changes its potential when electrons are emitted in a discharge, then when the structure is driven positive, electron emission should cease. Author (ESA)

**N84-18310\*#** National Aeronautics and Space Administration. Lewis Research Center, Cleveland, Ohio.  
**LABORATORY DEGRADATION OF KAPTON IN A LOW ENERGY OXYGEN ION BEAM**  
 D. C. FERGUSON 1984 15 p refs Presented at the AIAA Shuttle Environment and Operations Meeting, Washington, 31 Oct. - 2 Nov. 1983  
 (NASA-TM-83530; E-1841; NAS 1.15:83530) Avail: NTIS HC A02/MF A01 CSCL 14B

An atomic oxygen ion beam, accelerated from a tunable microwave resonant cavity, was used at Lewis Research Center to bombard samples of the widely used polyimide Kapton. The Kapton experienced degradation and mass loss at high rates, which may be comparable to those found in Space Shuttle operations if the activation energy supplied by the beam enabled surface reactions with the ambient oxygen. The simulation reproduced the directionality (ram-wake dependence) of the degradation, the change in optical properties of the degraded materials, and the structure seen in scanning electron micrographs of samples returned on the Shuttle Trails with a substituted argon ion beam produced no rapid degradation. Energy Dispersive X-ray Analysis (EDAX) showed significant surface composition changes in all bombarded samples. Mass loss rates and surface composition changes are discussed in terms of the possible oxidation chemistry of the interaction. Finally, the question of how the harmful

degradation of materials in low Earth orbit can be minimized is addressed. Author

**N84-22615\*#** National Aeronautics and Space Administration. Lewis Research Center, Cleveland, Ohio.  
**HIGH VOLTAGE-HIGH POWER COMPONENTS FOR LARGE SPACE POWER DISTRIBUTION SYSTEMS**

D. D. RENZ 1984 16 p refs To be presented at the 19th Intersoc. Energy Conversion Eng. Conf., San Francisco, 19-24 Aug. 1984

(NASA-TM-83648; E-2093; NAS 1.15:83648) Avail: NTIS HC A02/MF A01 CSCL 22B

Space power components including a family of bipolar power switching transistors, fast switching power diodes, heat pipe cooled high frequency transformers and inductors, high frequency conduction cooled transformers, high power-high frequency capacitors, remote power controllers and rotary power transfer devices were developed. Many of these components such as the power switching transistors, power diodes and the high frequency capacitor are commercially available. All the other components were developed to the prototype level. The dc/dc series resonant converters were built to the 25 kW level. S.L.

**N84-33452\*#** National Aeronautics and Space Administration. Lewis Research Center, Cleveland, Ohio.

**DESIGN GUIDELINES FOR ASSESSING AND CONTROLLING SPACECRAFT CHARGING EFFECTS**

C. K. PURVIS, H. B. GARRETT (JPL), A. C. WHITTLESEY (JPL), and N. J. STEVENS (Hughes Aircraft Co., El Segundo, Calif.) Sep. 1984 48 p refs

(NASA-TP-2361; E-2073; NAS 1.60:2361) Avail: NTIS HC A03/MF A01 CSCL 22B

The need for uniform criteria, or guidelines, to be used in all phases of spacecraft design is discussed. Guidelines were developed for the control of absolute and differential charging of spacecraft surfaces by the lower energy space charged particle environment. Interior charging due to higher energy particles is not considered. A guide to good design practices for assessing and controlling charging effects is presented. Uniform design practices for all space vehicles are outlined. E.A.K.

## 20

### SPACECRAFT PROPULSION AND POWER

Includes main propulsion systems and components, e.g., rocket engines; and spacecraft auxiliary power sources.

**A84-11819\*#** Washington Univ., Seattle.

**HIGH EFFECTIVENESS LIQUID DROPLET/GAS HEAT EXCHANGER FOR SPACE POWER APPLICATIONS**

A. P. BRUCKNER and A. T. MATTICK (Washington, University, Seattle, WA) International Astronautical Federation, International Astronautical Congress, 34th, Budapest, Hungary, Oct. 10-15, 1983. 9 p. refs

(Contract NAG3-16)  
 (IAF PAPER 83-433)

A high-effectiveness liquid droplet/gas heat exchanger (LDHX) concept for thermal management in space is described. Heat is transferred by direct contact between fine droplets (approximately 100-300 microns in diameter) of a suitable low vapor pressure liquid and an inert working gas. Complete separation of the droplet and gas media in the zero-g environment is accomplished by configuring the LDHX as a vortex chamber. The large heat transfer area presented by the small droplets permits heat exchanger effectiveness of 0.9-0.95 in a compact, lightweight geometry which avoids many of the limitations of conventional plate and fin or tube and shell heat exchangers, such as their tendency toward single point failure. The application of the LDHX in a high temperature Brayton cycle is discussed to illustrate the performance

and operational characteristics of this new heat exchanger concept. Author

**A84-22134\*#** Aerojet Liquid Rocket Co., Sacramento, Calif.

**TEST VERIFICATION OF LOX/RP-1 HIGH-PRESSURE FUEL/OXIDIZER-RICH PREBURNER DESIGNS**

B. R. LAWVER (Aerojet Liquid Rocket Co., Sacramento, CA) Journal of Spacecraft and Rockets (ISSN 0022-4650), vol. 20, Nov.-Dec. 1983, p. 567-573.

(Contract NAS3-22647)

Previously cited in issue 17, p. 2706, Accession no. A82-35032

**A84-22980\*** Spire Corp., Bedford, Mass.

**LARGE AREA SPACE SOLAR CELL ASSEMBLIES**

M. J. NOWLAN and M. B. SPITZER (Spire Corp., Bedford, MA) IN: Photovoltaic Specialists Conference, 16th, San Diego, CA, September 27-30, 1982, Conference Record. New York, Institute of Electrical and Electronics Engineers, 1982, p. 150-155. refs  
 (Contract NAS3-22236)

Results of the development of a 34.3 sq cm space solar cell and integral glass cover are presented. Average AM(0) cell efficiency is 14 percent. The cell design includes a high performance back surface reflector yielding a thermal alpha of approximately 0.66. A novel process is described which integrates cell fabrication and encapsulation thereby achieving a reduction of encapsulation cost. Test results indicate the potential of this new technology. Author

**A84-30143\*** Spire Corp., Bedford, Mass.

**ION IMPLANTED JUNCTIONS FOR SILICON SPACE SOLAR CELLS**

M. B. SPITZER, M. M. SANFACON, and R. G. WOLFSON (Spire Corp., Bedford, MA) IN: IECEC '83; Proceedings of the Eighteenth Intersociety Energy Conversion Engineering Conference, Orlando, FL, August 21-26, 1983. Volume 3. New York, American Institute of Chemical Engineers, 1983, p. 1213-1218. refs  
 (Contract NAS3-22236)

This paper reviews the application of ion implantation to emitter and back surface field formation in silicon space solar cells. Experiments based on 2 ohm-cm boron-doped silicon are presented. It is shown that the implantation process is particularly compatible with formation of a high-quality back surface reflector. Large area solar cells with AM0 efficiency greater than 14 percent are reported. Author

**A84-32031\*** National Aeronautics and Space Administration. Lewis Research Center, Cleveland, Ohio.

**LERC RAIL ACCELERATORS - TEST DESIGNS AND DIAGNOSTIC TECHNIQUES**

L. M. ZANA, W. R. KERSLAKE, J. C. STURMAN, S. Y. WANG, and F. F. TERDAN (NASA, Lewis Research Center, Cleveland, OH) (Institute of Electrical and Electronics Engineers, Symposium on Electromagnetic Launch Technology, 2nd, Boston, MA, Oct. 10-13, 1983) IEEE Transactions on Magnetics (ISSN 0018-9464), vol. MAG-20, March 1984, p. 324-327. refs

The feasibility of using rail accelerators for various in-space and to-space propulsion applications was investigated. A 1 meter, 24 sq mm bore accelerator was designed with the goal of demonstrating projectile velocities of 15 km/sec using a peak current of 200 kA. A second rail accelerator, 1 meter long with a 156.25 sq mm bore, was designed with clear polycarbonate sidewalls to permit visual observation of the plasma arc. A study of available diagnostic techniques and their application to the rail accelerator is presented. Specific topics of discussion include the use of interferometry and spectroscopy to examine the plasma armature as well as the use of optical sensors to measure rail displacement during acceleration. Standard diagnostics such as current and voltage measurements are also discussed. Previously announced in STAR as N83-35053 S.L.

**A84-34013\*** National Aeronautics and Space Administration. Lewis Research Center, Cleveland, Ohio.

**SPACE POWER TECHNOLOGY INTO THE 21ST CENTURY**

K. A. FAYMON and J. S. FORDYCE (NASA, Lewis Research Center, Space Power Technology Div., Cleveland, OH) IN: Space Systems Technology Conference, Costa Mesa, CA, June 5-7, 1984, Technical Papers. New York, American Institute of Aeronautics and Astronautics, 1984, p. 80-88. refs (AIAA PAPER 84-1136)

This paper discusses the space power systems of the early 21st century. The focus is on those capabilities which are anticipated to evolve from today's state-of-the-art and the technology development programs presently in place or planned for the remainder of the century. The power system technologies considered include solar thermal, nuclear, radioisotope, photovoltaic, thermionic, thermoelectric, and dynamic conversion systems such as the Brayton and Stirling cycles. Energy storage technologies considered include nickel hydrogen bipolar batteries, advanced high energy rechargeable batteries, regenerative fuel cells, and advanced primary batteries. The present state-of-the-art of these space power and energy technologies is discussed along with their projections, trends and goals. A speculative future mission model is postulated which includes manned orbiting space stations, manned lunar bases, unmanned earth orbital and interplanetary spacecraft, manned interplanetary missions, military applications, and earth to space and space to space transportation systems. The various space power/energy system technologies anticipated to be operational by the early 21st century are matched to these missions.

Author

**A84-34037\*** Michigan State Univ., East Lansing  
**DEMONSTRATION OF A NEW ELECTROTHERMAL THRUSTER CONCEPT**

S. WHITEHAIR, J. ASMUSSEN (Michigan State University, East Lansing, MI), and S. NAKANISHI (NASA, Lewis Research Center, Cleveland, OH) Applied Physics Letters (ISSN 0003-6951), vol. 44, May 15, 1984, p. 1014-1016. refs (Contract NSG-3305)

The design and test of a microwave electrothermal thruster are described. The device, which employs a coaxial microwave discharge, was tested in nitrogen gas with 200-600 W of 2.45-GHz input power. Experimental measurements of thrust, specific impulse, and energy efficiency are presented for different flow and discharge pressures. Measured energy efficiencies varied between 30-60 percent and the performance compared favorably with other electrothermal thrusters operating in nitrogen gas. The experimental performance demonstrated the feasibility of the concept. Author

**A84-35157\*** Aerojet Techsystems Co., Sacramento, Calif.  
**SELECTION OF BURN-RESISTANT MATERIALS FOR OXYGEN-DRIVEN TURBOPUMPS**

L. SCHOENMAN (Aerojet TechSystems Co., Sacramento, CA) AIAA, SAE, and ASME, Joint Propulsion Conference, 20th, Cincinnati, OH, June 11-13, 1984. 13 p. refs (Contract NAS3-23772) (AIAA PAPER 84-1287)

NASA goals for reusable space-based, high-performance orbit transfer vehicle propulsion systems have resulted in a need for oxygen/hydrogen engines which include lightweight, highly reliable, liquid oxygen pumps. The selection of ignition- and burn-resistant materials is a major factor in the design of a compact 75,000-rpm turbopump which can deliver 6 lbM/sec of liquid oxygen at 5,000 psia. The potential operational hazards of rubbing friction and impact of foreign particles at high velocity were investigated experimentally for a wide range of candidate materials, i.e., nickel, copper, monel, 316 Stainless Steel, Hastelloy-X, Invar-36, and silicon carbide. Test parameters included oxygen pressure and temperature up to 5,000 psia and 800 F, respectively. The effect of increasing the O<sub>2</sub> pressure from 1000 to 5000 psi is discussed. The applicability of the candidate materials to oxygen pump design was ranked by comparing the experimental results among themselves and with an analytically determined parameter, i.e., the burn factor. Nickel and copper demonstrated superior

resistance to ignition and burn in the friction rubbing and particle impact tests relative to monel, stainless steel, and nickel-iron base superalloys.

Author

**A84-35201\*** GT-Devices, Alexandria, Va.  
**EXPERIMENTAL INVESTIGATION OF THE PULSED ELECTROTHERMAL (PET) THRUSTER**

R. L. BURTON, S. A. GOLDSTEIN, B. K. HIKO, D. A. TIDMAN, and N. K. WINSOR (GT-Devices, Inc., Alexandria, VA) AIAA, SAE, and ASME, Joint Propulsion Conference, 20th, Cincinnati, OH, June 11-13, 1984. 10 p. refs (Contract NAS3-23779; NAS3-23866) (AIAA PAPER 84-1386)

Burton et al. (1982) have discussed the theory of the Pulsed Electrothermal (PET) thruster, a device which in principle can operate with 70 percent efficiency at a specific impulse of 1000 seconds and higher. It is pointed out that this level of performance would be particularly attractive for orbit raising of large satellites and other near-earth missions, which cannot be easily accomplished by chemical propulsion. The present investigation is concerned with two PET thruster operating modes. A PET thruster was built and tested on a thrust stand. Exhaust velocities for polyethylene propellant vary from 20 to 27 km/sec. Single pulse specific impulse and efficiency measurements based on ablated mass show a thruster efficiency of 37-56 percent in the time range from 1000 to 1750 seconds. It is believed that an improved design with a thruster efficiency in the range from 70 to 80 percent might be possible.

G.R.

**A84-35202\*** GT-Devices, Alexandria, Va.  
**PROPOSED SYSTEM DESIGN FOR A 20 KW PULSED ELECTROTHERMAL THRUSTER**

R. L. BURTON, S. A. GOLDSTEIN, B. K. HILKO, D. A. TIDMAN, and N. K. WINSOR (GT-Devices, Inc., Alexandria, VA) AIAA, SAE, and ASME, Joint Propulsion Conference, 20th, Cincinnati, OH, June 11-13, 1984. 6 p. refs (Contract NAS3-23866) (AIAA PAPER 84-1387)

A conceptual design is presented for a Pulsed Electrothermal (PET) propulsion system for the Air Force Space Based Radar satellite, which has a mass of 7000 kg. The proposed system boosts the SBR satellite from 150 n.m. to 600 n.m. with a 4 deg plane change, for a total mission Delta v of 1 km/sec. Satellite power available is 50 kW, and 45 kW are used to drive two water-injected 20 kW PET thrusters, delivering 5.6 N thrust to the SBR at 1000 seconds specific impulse. The predicted mission trip time is 15 days. The proposed system consumes 850 kg of water propellant, stored in a central tank and injected with pressurized helium. Component mass estimates based on space-qualified hardware are presented for the propellant handling, power conditioning and thruster subsystems. The estimated total mass is 400 kg and the propulsion system specific mass is  $\alpha = 10$  kg/kW. The proposed system efficiency of 0.62 at 1000 seconds specific impulse is supported by experimental performance measurements.

Author

**A84-36559\*** Southwest Research Inst., San Antonio, Tex.  
**VAPOR FLOW INTO A CAPILLARY PROPELLANT-ACQUISITION DEVICE**

F. T. DODGE and E. B. BOWLES (Southwest Research Institute, San Antonio, TX) Journal of Spacecraft and Rockets (ISSN 0022-4650), vol. 21, May-June 1984, p. 267-273. refs (Contract NAS3-22664)

Previously cited in issue 16, p. 2321, Accession no. A83-36371

**A84-44045\*#** National Aeronautics and Space Administration. Lewis Research Center, Cleveland, Ohio

# **INTEGRATION BECOMES THE NAME OF THE OTV GAME**

S. GARLAND (NASA, Lewis Research Center, Space Propulsion Technology Div., Cleveland, OH) Aerospace America (ISSN 0740-722X), vol. 22, Aug. 1984, p. 70-73.

Since 1981, NASA has been supporting an Orbit Transfer Vehicle (OTV) propulsion technology development program which encompasses the efforts of three major engine manufacturers. A thrust variability ratio of 30:1 has been stipulated for the baseline 520 lbf-sec/lbm engines, in order to yield the versatility needed for low acceleration missions, orbit-transfer missions, and aeromaneuvering tasks. These goals may not be reachable either individually or collectively; the program supports generic technology benefitting all three engine concepts, as well as concept-specific technology. Engine/vehicle integration will determine the final configuration. The three engines under study differ as to turbomachinery types and operating speeds. O.C.

**A84-44176\*#** National Aeronautics and Space Administration. Lewis Research Center, Cleveland, Ohio.

# **ON-ORBIT CRYOGENIC FLUID TRANSFER**

J. C. AYDELOTT (NASA, Lewis Research Center, Cleveland, OH), J. P. GILLE, and R. N. EBERHARDT (Martin Marietta Aerospace, Denver, CO) AIAA, SAE, and ASME, Joint Propulsion Conference, 20th, Cincinnati, OH, June 11-13, 1984. 10 p. Previously announced in STAR as N84-25753. refs (AIAA PAPER 84-1343)

A number of future NASA and DOD missions have been identified that will require, or could benefit from resupply of cryogenic liquids in orbit. The most promising approach for accomplishing cryogenic fluid transfer in the weightlessness environment of space is to use the thermodynamic filling technique. This approach involves initially reducing the receiver tank temperature by using several charge hold vent cycles followed by filling the tank without venting. Martin Marietta Denver Aerospace, under contract to the NASA Lewis Research Center, is currently developing analytical models to describe the on orbit cryogenic fluid transfer process. A detailed design of a Shuttle attached experimental facility, which will provide the data necessary to verify the analytical models, is also being performed. Author

**A84-44179\*#** National Aeronautics and Space Administration. Lewis Research Center, Cleveland, Ohio.

# **SPACE STATION PROPULSION ANALYSIS STUDY**

R. M. DONOVAN, J. S. SOVEY, and N. B. HANNUM (NASA, Lewis Research Center, Cleveland, OH) AIAA, SAE, and ASME, Joint Propulsion Conference, 20th, Cincinnati, OH, June 11-13, 1984. 22 p. Previously announced in STAR as N84-25764. (AIAA PAPER 84-1326)

This paper summarizes the impacts on the weight, volume and power usage of a manned space station and its 90-day resupply for three integrated, auxiliary propulsion subsystems. The study was performed in coordination with activities of the Space Station Concept Development Group (CDG). The study focused on three space station propulsion high-low thrust options that make use of fluids that will be available on the manned space station. Specific uses of carbon dioxide, water and cryogen boiloff were considered. For each of the options the increase in station hardware mass and volume to accommodate the dual thrust option is offset by the resupply savings, relative to the reference hydrazine system, after one to several resupplies. Over the life of the station the savings in cost of logistics could be substantial. The three options are examples of alternative technology paths that, because of the opportunity they provide for integration with the environmental control life support system (ECLSS) and OTV propellant storage systems, may reduce the scarring which is required on the early station to meet the increasing propulsion requirements of the growth station. Author

**A84-44184\*#** Martin Marietta Aerospace, Denver, Colo.

# **CRYOGENIC FLUID MANAGEMENT FACILITY**

R. N. EBERHARDT, W. J. BAILEY (Martin Marietta Aerospace, Denver, CO), E. P. SYMONS, and E. W. KROEGER (NASA, Lewis Research Center, Cleveland, OH) AIAA, SAE, and ASME, Joint Propulsion Conference, 20th, Cincinnati, OH, June 11-13, 1984. 17 p. refs

(Contract NAS3-23355)

(AIAA PAPER 84-1340)

The Cryogenic Fluid Management Facility (CFMF) is a reusable test bed which is designed to be carried into space in the Shuttle cargo bay to investigate systems and technologies required to efficiently and effectively manage cryogenics in space. The facility hardware is configured to provide low-g verification of fluid and thermal models of cryogenic storage, transfer concepts and processes. Significant design data and criteria for future subcritical cryogenic storage and transfer systems will be obtained. Future applications include space-based and ground-based orbit transfer vehicles (OTV), space station life support, attitude control, power and fuel depot supply, resupply tankers, external tank (ET) propellant scavenging, space-based weapon systems and space-based orbit maneuvering vehicles (OMV). This paper describes the facility and discusses the cryogenic fluid management technology to be investigated. A brief discussion of the integration issues involved in loading and transporting liquid hydrogen within the Shuttle cargo bay is also included. Author

**A84-49509\*#** National Aeronautics and Space Administration. Lewis Research Center, Cleveland, Ohio.

# **SIMPLIFICATION OF POWER ELECTRONICS FOR ION THRUSTER NEUTRALIZERS**

R. P. GRUBER (NASA, Lewis Research Center, Cleveland, OH) Journal of Spacecraft and Rockets (ISSN 0002-4650), vol. 21, Sept.-Oct. 1984, p. 473-480. Previously cited in issue 07, p. 873, Accession no A83-21099. refs

**A84-49511\*#** National Aeronautics and Space Administration. Lewis Research Center, Cleveland, Ohio.

# **IMPROVED ION CONTAINMENT USING A RING-CUSP ION THRUSTER**

J. S. SOVEY (NASA, Lewis Research Center, Electric Propulsion Technology Section, Cleveland, OH) Journal of Spacecraft and Rockets (ISSN 0002-4650), vol. 21, Sept.-Oct. 1984, p. 488-495. Previously cited in issue 07, p. 873, Accession no. A83-21100. refs

**N84-10180\*#** Hughes Research Labs., Malibu, Calif.

# **DEVELOPMENT OF ADVANCED INERT-GAS ION THRUSTERS Final Report**

R. L. POESCHEL Jul. 1983 89 p refs

(Contract NAS3-22474)

(NASA-CR-168206; NAS 1.26:168206) Avail: NTIS HC A05/MF A01 CSCL 21C

Inert gas ion thruster technology offers the greatest potential for providing high specific impulse, low thrust, electric propulsion on large, Earth orbital spacecraft. The development of a thruster module that can be operated on xenon or argon propellant to produce 0.2 N of thrust at a specific impulse of 3000 sec with xenon propellant and at 6000 sec with argon propellant is described. The 30 cm diameter, laboratory model thruster is considered to be scalable to produce 0.5 N thrust. A high efficiency ring cusp discharge chamber was used to achieve an overall thruster efficiency of 77% with xenon propellant and 66% with argon propellant. Measurements were performed to identify ion production and loss processes and to define critical design criteria (at least on a preliminary basis). S.L.



**N84-11206\*#** National Aeronautics and Space Administration. Lewis Research Center, Cleveland, Ohio.

**RESISTOJET PROPULSION FOR LARGE SPACECRAFT SYSTEMS**

M. J. MIRTICH 1982 32 p refs Presented at the 16th Intern. Elec. Propulsion Conf., New Orleans, 17-19 Nov. 1982; sponsored by AIAA, the Japan Soc. for Aeron. and Space Sci., and Deutsche Gesellschaft für Luft- und Raumfahrt (NASA-TM-83489, E-1813; NAS 1.15:83489) Avail. NTIS HC A03/MF A01 CSCL 21H

Resistojet propulsion systems have characteristics that are ideally suited for the on-orbit and primary propulsion requirements of large spacecraft systems. These characteristics which offer advantages over other forms of propulsion are reviewed and presented. The feasibility of resistojets were demonstrated in space whereas only a limited number of ground life tests were performed. The major technology issues associated with these ground tests are evaluated. The past performance of resistojets is summarized and, looks into the present day technology status is reviewed. The material criteria, along with possible concepts, needed to attain high performance resistojets are presented. S.L.

**N84-12225\*#** United Technologies Corp., East Hartford, Conn  
**DEPOSIT FORMATION AND HEAT TRANSFER IN HYDROCARBON ROCKET FUELS** Final Progress Report, Jul. 1982 - May 1983

A. J. GIOVANETTI, L. J. SPADACCINI, and E. J. SZETELA Oct. 1983 170 p refs

(Contract NAS3-23344)

(NASA-CR-168277; NAS 1.26:168277; R83-956152-10) Avail. NTIS HC A08/MF A01 CSCL 21H

An experimental research program was undertaken to investigate the thermal stability and heat transfer characteristics of several hydrocarbon fuels under conditions that simulate high-pressure, rocket engine cooling systems. The rates of carbon deposition in heated copper and nickel-plated copper tubes were determined for RP-1, propane, and natural gas using a continuous flow test apparatus which permitted independent variation and evaluation of the effect on deposit formation of wall temperature, fuel pressure, and fuel velocity. In addition, the effects of fuel additives and contaminants, cryogenic fuel temperatures, and extended duration testing with intermittent operation were examined. Parametric tests to map the thermal stability characteristics of RP-1, commercial-grade propane, and natural gas were conducted at pressures of 6.9 to 13.8 MPa, bulk fuel velocities of 30 to 90 m/s, and tube wall temperatures in the range of 230 to 810 K. Also, tests were run in which propane and natural gas fuels were chilled to 230 and 160 K, respectively. Corrosion of the copper tube surface was detected for all fuels tested. Plating the inside of the copper tubes with nickel reduced deposit formation and eliminated tube corrosion in most cases. The lowest rates of carbon deposition were obtained for natural gas, and the highest rates were obtained for propane. For all fuels tested, the forced-convection heat transfer film coefficients were satisfactorily correlated using a Nusselt-Reynolds-Prandtl number equation. Author

**N84-12226\*#** Boeing Aerospace Co., Seattle, Wash.  
**STUDY OF AUXILIARY PROPULSION REQUIREMENTS FOR LARGE SPACE SYSTEMS. VOLUME 1: EXECUTIVE SUMMARY**

W. W. SMITH and G. W. MACHLES Sep. 1983 22 p (Contract NAS3-23248)

(NASA-CR-168193-VOL-1; NAS 1.26:168193-VOL-1;

D180-27728-1) Avail. NTIS HC A02/MF A01 CSCL 21H

An insight into auxiliary propulsion systems (APS) requirements for large space systems (LSS) launchable by a single shuttle is presented. In an effort to scope the APS requirements for LSS, a set of generic LSSs were defined. For each generic LSS class a specific structural configuration, representative of that most likely to serve the needs of the 1980's and 1990's was defined. The environmental disturbance forces and torques which would be acting on each specific structural configuration in LEO and GEO

orbits were then determined. Auxiliary propulsion requirements were determined as a function of: generic class specific configuration, size and openness of structure, orbit, angle of orientation, correction frequency, duty cycle, number and location of thrusters and direction of thrusters and APS/LSS interactions. The results of this analysis were used to define the APS characteristics of: (1) number and distribution of thrusters, (2) thruster modulation, (3) thrust level, (4) mission energy requirements, (5) total APS mass component breakdown, and (6) state of the art adequacy/deficiency. S.L.

**N84-12227\*#** GT-Devices, Alexandria, Va  
**INVESTIGATION OF A PULSED ELECTROTHERMAL THRUSTER**

R. L. BURTON, S. A. GOLDSTEIN, B. K. HILKO, D. A. TIDMAN, and N. K. WINSOR 1 Oct. 1983 45 p refs

(Contract NAS3-23779)

(NASA-CR-168266; NAS 1.26:168266; GTD-83-10) Avail. NTIS HC A03/MF A01 CSCL 21C

Exhaust velocity and thrust measurements are performed on a pulsed electrothermal thruster using polyethylene and Teflon propellants. The results verify theoretical predictions of equilibrium flow in the nozzle, resulting in substantial recovery of the energy of dissociation and ionization. The thruster is tested in an unsteady mode (15 micro sec current pulse and 15 cm discharge length) and in a quasi-steady mode (48 micro sec current pulse and 5 cm discharge length). All tests are run at 2 kJ. The exhaust velocity of the propellant mass exiting during the current pulse is measured with two types of time of flight probes, and the impulse bit is measured on a thrust stand. It is inferred from both theory and experiment that an additional amount of mass is exhausted after the pulse. The measured thrust to power ratio for polyethylene is  $T/P = 0.10$  N/kW at 21 km/sec in the unsteady mode, and  $T/P = .053$  N/kW at 27 km/sec in the quasi-steady mode, where the velocities are measured by the time-of-flight probes. For Teflon propellant,  $T/P = .20$  N/kW at 15 km/sec (unsteady mode) and 0.090 N/kW at 20 km/sec (quasi-steady mode). The discharge pressure and temperature predicted by a computational model for polyethylene are consistent with the measured thrust and discharge resistance. S.L.

**N84-12247\*#** National Aeronautics and Space Administration. Lewis Research Center, Cleveland, Ohio.

**SOME COMMENTS ON LONGEVITY BY A TECHNOLOGIST**

L. H. THALLER /in NASA. Langley Research Center Integrated Flywheel Technol., 1983 p 175-185 Dec. 1983

Avail. NTIS HC A10/MF A01 CSCL 12B

The durability of flywheels was investigated. Since only composite flywheels possess the potential for system energy densities in the range of 20 to 40 W hr/kg, and they are not yet at a level of maturity where a comfortable data base exists, the longevity aspects of the yet to be developed devices is still a speculation. The general methodologies that have been used in some of the more established technology areas to establish some degree of credibility in the ability to predict the upper limits of expected useful life based on the current limiting decay mechanism are outlined. E.A.K.

**N84-13218\*#** Boeing Aerospace Co., Seattle, Wash.  
**STUDY OF AUXILIARY PROPULSION REQUIREMENTS FOR LARGE SPACE SYSTEMS, VOLUME 2 Final Report**

W. W. SMITH and G. W. MACHLES Sep. 1983 305 p refs (Contract NAS3-23248)

(NASA-CR-168193-VOL-2; NAS 1.26:168193-VOL-2;

D180-27728-2) Avail. NTIS HC A14/MF A01 CSCL 21H

A range of single shuttle launched large space systems were identified and characterized including a NASTRAN and loading dynamics analysis. The disturbance environment, characterization of thrust level and APS mass requirements, and a study of APS/LSS interactions were analyzed. State-of-the-art capabilities for chemical and ion propulsion were compared with the generated propulsion requirements to assess the state-of-the-art limitations and benefits of enhancing current technology. Author

**N84-18321\*#** Colorado State Univ., Fort Collins. Dept. of Mechanical Engineering.  
**EXPERIMENTAL INVESTIGATION OF A HALL-CURRENT THRUSTER M.S. Thesis**  
 G. M. PLANK Jan. 1983 49 p refs  
 (Contract NSG-3011)  
 (NASA-CR-168133; NAS 1.26:168133) Avail: NTIS HC A03/MF A01 CSCL 21C

The Hall-current accelerator is being investigated for use in the 1000-2000 sec. range of specific impulse. Three models of this thruster were tested. The first two models had three permanent magnets to supply the magnetic field and the third model had six magnets to supply the field. The third model thus had approximately twice the magnetic field of the first two. The first and second models differ only in the shape of the magnetic field. All other factors remained the same for the three models except for the anode-cathode distance, which was changed to allow for the three thrusters to have the same magnetic field integral between the anode and the cathode. These Hall thrusters were tested to determine the plasma properties, the beam characteristics, and the thruster characteristics. The thruster operated in three modes: (1) main cathode only, (2) main cathode with neutralizer cathode, and (3) neutralizer cathode only. The plasma properties were measured along an axial line, 1 mm inside the cathode radius, at a distance of 0.2 to 6.2 cm from the anode. Results show that the current used to heat the cathode produced nonuniformities in the magnetic field, hence also in the plasma properties. In a Hall thruster this general design appears to provide the most thrust when operated at a magnetic field less than the maximum value studied. Author

**N84-18322\*#** Colorado State Univ., Fort Collins. Dept. of Physics.  
**SPUTTERING PHENOMENA IN ION THRUSTERS Final Report**  
 R. S. ROBINSON and S. M. ROSSNAGEL Feb. 1983 32 p refs  
 (Contract NAG3-209)  
 (NASA-CR-168172; NAS 1.26:168172) Avail: NTIS HC A03/MF A01 CSCL 21C

Sputtering effects in discharge chambers of ion thrusters are lifetime limiting in basically two ways: (1) ion bombardment of critical thruster components at energies sufficient to cause sputtering removes significant quantities of material; enough to degrade operation through adverse dimensional changes or possibly lead to complete component failure, and (2) metals sputtered from these intensely bombarded components are deposited in other locations as thin films and subsequently flake or peel off; the flakes then lodge elsewhere in the discharge chamber with the possibility of providing conductive paths for short circuiting of thruster components such as the ion optics. This experimental work has concentrated in two areas. The first has been to operate thrusters for multi-hour periods and to observe and measure the films found inside the thruster. The second was to simulate the environment inside the discharge chamber of the thruster by means of a dual ion beam system. Here, films were sputter deposited in the presence of a second low energy bombarding beam to simulate film deposition on thruster interior surfaces that undergo simultaneous sputtering and deposition. No presents serious problems for use in a thruster as far as film deposition is concerned. No films were found to be in high stress, making them more likely to peel and flake. Author

**N84-19472\*#** O'Donnell and Associates, Inc., Pittsburgh, Pa.  
**DEVELOPMENT OF A SIMPLIFIED PROCEDURE FOR ROCKET ENGINE THRUST CHAMBER LIFE PREDICTION WITH CREEP Final Report**  
 M. L. BADLANI, J. S. POROWSKI, W. J. O'DONNELL, and D. B. PETERSON Oct. 1983 87 p  
 (Contract NAS3-23343)  
 (NASA-CR-168261; NAS 1.26:168261; OAI-1512-11-83) Avail: NTIS HC A05/MF A01 CSCL 21H

An analytical method for predicting engine thrust chamber life is developed. The method accounts for high pressure differentials

and time-dependent creep effects both of which are significant in limiting the useful life of the shuttle main engine thrust chamber. The hot-gas-wall ligaments connecting adjacent cooling channels ribs and separating the coolant flow from the combustion gas are subjected to a high pressure induced primary stress superimposed on an alternating cyclic thermal strain field. The pressure load combined with strain-controlled cycling produces creep ratcheting and consequent bulging and thinning of these ligaments. This mechanism of creep-enhanced ratcheting is analyzed for determining the hot-gas-wall deformation and accumulated strain. Results are confirmed by inelastic finite element analysis. Fatigue and creep rupture damage as well as plastic tensile instability are evaluated as potential failure modes. It is demonstrated for the NARLOY Z cases analyzed that when pressure differentials across the ligament are high, creep rupture damage is often the primary failure mode for the cycle times considered. Author

**N84-20634\*#** Boeing Aerospace Co., Seattle, Wash.  
**EVALUATION OF PROPELLANT TANK INSULATION CONCEPTS FOR LOW-THRUST CHEMICAL PROPULSION SYSTEMS Final Report**  
 T. KRAMER, E. BROGREN, and B. SEIGEL Mar. 1984 257 p refs  
 (Contract NAS3-22824)  
 (NASA-CR-168320; NAS 1.26:168320; BAC-D180-28273-1) Avail: NTIS HC A12/MF A01 CSCL 21H

An analytical evaluation of cryogenic propellant tank insulations for liquid oxygen/liquid hydrogen low-thrust 2224N (500 lbf) propulsion systems (LTPS) was conducted. The insulation studied consisted of combinations of N<sub>2</sub>-purged foam and multilayer insulation (MLI) as well as He-purged MLI-only. Heat leak and payload performance predictions were made for three Shuttle-launched LTPS designed for Shuttle bay packaged payload densities of 56 kg/cu m, 40 kg/cu m and 24 kg/cu m. Foam/MLI insulations were found to increase LTPS payload delivery capability when compared with He-purged MLI-only. An additional benefit of foam/MLI was reduced operational complexity because Orbiter cargo bay N<sub>2</sub> purge gas could be used for MLI purging. Maximum payload mass benefit occurred when an enhanced convection, rather than natural convection, heat transfer was specified for the insulation purge enclosure. The enhanced convection environment allowed minimum insulation thickness to be used for the foam/MLI interface temperature selected to correspond to the moisture dew point in the N<sub>2</sub> purge gas. Experimental verification of foam/MLI benefits was recommended. A conservative program cost estimate for testing a MLI-foam insulated tank was 2.1 million dollars. It was noted this cost could be reduced significantly without increasing program risk. Author

**N84-20639\*#** National Aeronautics and Space Administration. Lewis Research Center, Cleveland, Ohio.  
**PARAMETRIC ANALYSIS OF HOLLOW CONDUCTOR PARALLEL AND COAXIAL TRANSMISSION LINES FOR HIGH FREQUENCY SPACE POWER DISTRIBUTION**  
 K. S. JEFFRIES and D. D. RENZ Mar. 1984 43 p refs  
 (NASA-TM-83601; E-2013; NAS 1.15:83601) Avail: NTIS HC A03/MF A01 CSCL 09C

A parametric analysis was performed of transmission cables for transmitting electrical power at high voltage (up to 1000 V) and high frequency (10 to 30 kHz) for high power (100 kW or more) space missions. Large diameter (5 to 30 mm) hollow conductors were considered in closely spaced coaxial configurations and in parallel lines. Formulas were derived to calculate inductance and resistance for these conductors. Curves of cable conductance, mass, inductance, capacitance, resistance, power loss, and temperature were plotted for various conductor diameters, conductor thickness, and alternating current frequencies. An example 5 mm diameter coaxial cable with 0.5 mm conductor thickness was calculated to transmit 100 kW at 1000 Vac, 50 m with a power loss of 1900 W, an inductance of 1.45 micron and a capacitance of 0.07 micron-F. The computer programs written for this analysis are listed in the appendix. Author

**N84-22631\*#** National Aeronautics and Space Administration. Lewis Research Center, Cleveland, Ohio.

**CATHODE DEGRADATION AND EROSION IN HIGH PRESSURE ARC DISCHARGES**

T. L. HARDY and S. NAKANISHI 1983 22 p refs Proposed for presentation at the 17th Ann. Intern. Elec. Propulsion Conf., Tokyo, 28-31 May 1984; sponsored by AIAA (NASA-TM-83638; E-2000; NAS 1.15:83638) Avail: NTIS HC A02/MF A01 CSCL 21C

The various processes which control cathode erosion and degradation were identified and evaluated. A direct current arc discharge was established between electrodes in a pressure-controlled gas flow environment. The cathode holder was designed for easy testing of various cathode materials. The anode was a water cooled copper collector electrode. The arc was powered by a dc power supply with current and voltage regulated cross-over control. Nitrogen and argon were used as propellants and the materials used were two percent thoriated tungsten, barium oxide impregnated porous tungsten, pure tungsten and lanthanum hexaboride. The configurations used were cylindrical solid rods, wire bundles supported by hollow molybdenum tubes, cylindrical hollow tubes, and hollow cathodes of the type used in ion thrusters. The results of the mass loss tests in nitrogen indicated that pure tungsten eroded at a rate more than 10 times faster than the rates of the impregnated tungsten materials. It was found that oxygen impurities of less than 0.5 percent in the nitrogen increased the mass loss rate by a factor of 4 over high purity nitrogen. At power levels less than 1 kW, cathode size and current level did not significantly affect the mass loss rate. The hollow cathode was found to be operable in argon and in nitrogen only at pressures below 400 and 200 torr, respectively. M.A.C.

**N84-23690\*#** National Aeronautics and Space Administration. Lewis Research Center, Cleveland, Ohio.

**DISCHARGES ON A NEGATIVELY BIASED SOLAR ARRAY IN A CHARGED PARTICLE ENVIRONMENT**

D. B. SNYDER 1983 15 p refs Presented at the Environ. Interactions Conf., Colorado Springs, 4-6 Oct. 1983; sponsored by the Air Force and NASA (NASA-TM-83644; E-2090; NAS 1.15:83644) Avail: NTIS HC A02/MF A01 CSCL 21H

The charging behavior of a negatively biased solar cell array when subjected to a charged particle environment is studied in the ion density range from 200 to 12 000 ions/sq cm with the applied bias range of -500 to -1400 V. The profile of the surface potentials across the array is related to the presence of discharges. At the low end of the ion density range the solar cell cover slides charge to from 0 to +5 volts independent of the applied voltage. No discharges are seen at bias voltages as large as -1400 V. At the higher ion densities the cover slide potential begins to fluctuate, and becomes significantly negative. Under these conditions discharges can occur. The threshold bias voltage for discharges decreases with increasing ion density. A condition for discharges emerging from the experimental observations is that the average coverslide potential must be more negative than -4 V. The observations presented suggest that the plasma potential near the array becomes negative before a discharge occurs. This suggests that discharges are driven by an instability in the plasma. Author

**N84-23691\*#** National Aeronautics and Space Administration. Lewis Research Center, Cleveland, Ohio.

**GROUND CORRELATION INVESTIGATION OF THRUSTER SPACECRAFT INTERACTIONS TO BE MEASURED ON THE IAPS FLIGHT TEST**

J. L. POWER 1984 36 p refs Proposed for presentation at the 17th Intern. Elec. Propulsion Conf., Tokyo, 28-31 May 1984; sponsored by AIAA, Japan Society for Aeronautical and Space Sciences and Deutsche Gesellschaft fuer Luft- und Raumfahrt (NASA-TM-83598; E-2007; NAS 1.15:83598) Avail: NTIS HC A03/MF A01 CSCL 20H

Preliminary ground correlation testing has been conducted with an 8 cm mercury ion thruster and diagnostic instrumentation

replicating to a large extent the IAPS flight test hardware, configuration, and electrical grounding/isolation. Thruster efflux deposition retained at 25 C was measured and characterized. Thruster ion efflux was characterized with retarding potential analyzers. Thruster-generated plasma currents, the spacecraft common (SCC) potential, and ambient plasma properties were evaluated with a spacecraft potential probe (SPP). All the measured thruster/spacecraft interactions or their IAPS measurements depend critically on the SCC potential, which can be controlled by a neutralizer ground switch and by the SPP operation. Author

**N84-24708#** National Aeronautics and Space Administration. Lewis Research Center, Cleveland, Ohio.

**DILUTE PLASMA COUPLING CURRENTS TO A HIGH VOLTAGE SOLAR ARRAY IN WEAK MAGNETIC FIELDS**

N. T. GRIER 1984 13 p refs Presented at the 19th Intersoc. Energy Conversion Enge. Conf., San Francisco, 19-24 Aug. 1984

(NASA-TM-83687; E-2054; NAS 1.15:83687) Avail: NTIS HC A02/MF A01 CSCL 21C

The plasma coupling current to an approximately 2000 sq cm array was measured for externally biased positive and negative voltages on the array to 1000 V in applied magnetic field strengths from 0 to 0.93 G. The plasma density varied from 2,000 to 1.3 million electrons/cu cm. It was found that the magnetic field primarily increased the plasma coupling current for negative biases. For positive bias, the current could increase or decrease depending on the voltage, field strength, and plasma density. It was also found that the plasma coupling current was not very sensitive to how the plane of the array was oriented relative to the magnetic field. Author

**N84-25762\*#** National Aeronautics and Space Administration. Lewis Research Center, Cleveland, Ohio.

**PROPULSION ISSUES FOR ADVANCED ORBIT TRANSFER VEHICLES**

L. P. COOPER 1984 21 p refs Presented at the JANNAF Propulsion Meeting, New Orleans, 6-9 Feb. 1984

(NASA-TM-83624; E-2058; NAS 1.15:83624) Avail: NTIS HC A02/MF A01 CSCL 21H

Studies of the United States Space Transportation System show that in the mid to late 1990s expanded capabilities for orbital transfer vehicles (OTV) will be needed to meet increased payload requirements for transporting materials and possibly men to geosynchronous orbit. Discussion and observations relative to the propulsion system issues of space basing, aerassist compatibility, man reliability and enhanced payload delivery capability are presented. These issues will require resolution prior to the development of a propulsion system for the advanced OTV. The NASA program in support of advanced propulsion for an OTV is briefly described along with conceptual engine design characteristics. Author

**N84-25764\*#** National Aeronautics and Space Administration. Lewis Research Center, Cleveland, Ohio.

**SPACE STATION PROPULSION ANALYSIS STUDY**

R. M. DONOVAN, J. S. SOVEY, and N. B. HANNUM 1984 15 p refs Presented at the 20th Joint Propulsion Conf., Cincinnati, 11-13 Jun. 1984

(NASA-TM-83715; E-2180; NAS 1.15:83715; AIAA-84-1326) Avail: NTIS HC A02/MF A01 CSCL 21H

This paper summarizes the impacts on the weight, volume and power usage of a manned space station and its 90-day resupply for three integrated, auxiliary propulsion subsystems. The study was performed in coordination with activities of the Space Station Concept Development Group (CDG). The study focused on three space station propulsion high-low thrust options that make use of fluids that will be available on the manned space station. Specific uses of carbon dioxide, water and cryogen boiloff were considered. For each of the options the increase in station hardware mass and volume to accommodate the dual thrust option is offset by the resupply savings, relative to the reference hydrazine system, after one to several resupplies. Over the life of the station the

savings in cost of logistics could be substantial. The three options are examples of alternative technology paths that, because of the opportunity they provide for integration with the environmental control life support system (ECLSS) and OTV propellant storage systems, may reduce the scarring which is required on the early station to meet the increasing propulsion requirements of the growth station  
Author

**N84-26746\*#** National Aeronautics and Space Administration. Lewis Research Center, Cleveland, Ohio.

### SPACE POWER TECHNOLOGY INTO THE 21ST CENTURY

K. A. FAYMON and J. S. FORDYCE 1983 18 p refs Presented at the Space Power Systems Technol. Conf., Costa Mesa, Calif., 5-7 Jun. 1984; sponsored by AIAA (NASA-TM-83690; E-2144; NAS 1.15 83690) Avail: NTIS HC A02/MF A01 CSCL 21H

The space power systems of the early 21st century are discussed. The capabilities which are anticipated to evolve from today's state of the art and the technology development programs presently in place or planned for the remainder of the century are emphasized. The power system technologies considered include: solar thermal, nuclear, radioisotope, photovoltaic, thermionic, thermoelectric, and dynamic conversion systems such as the Brayton and Stirling cycles. Energy storage technologies considered include: nickel hydrogen biopolar batteries, advanced high energy rechargeable batteries, regenerative fuel cells, and advanced primary batteries. The present state of the art of these space power and energy technologies is discussed along with their projections, trends and goals. A speculative future mission model is postulated which includes manned orbiting space stations, manned lunar bases, unmanned Earth orbital and interplanetary spacecraft, manned interplanetary missions, military applications, and Earth to space and space to space transportation systems. The various space power/energy system technologies which are anticipated to be operational by the early 21st century are matched to these missions.  
E.A.K.

**N84-27824\*#** National Aeronautics and Space Administration. Lewis Research Center, Cleveland, Ohio.

### CHARACTERISTICS OF ARC CURRENTS ON A NEGATIVELY BIASED SOLAR CELL ARRAY IN A PLASMA

D. B. SNYDER 1984 12 p refs Presented at the Nucl. and Space Radiation Effects Conf., Colorado Springs, 22-25 Jul. 1984 (NASA-TM-83728; E-2170; NAS 1.15:83728) Avail: NTIS HC A02/MF A01 CSCL 21H

The time dependence of the emitted currents during arcing on solar cell arrays is being studied. The arcs are characterized using three parameters: the voltage change of the array during the arc (i.e., the charge lost), the peak current during the arc, and the time constant describing the arc current. This paper reports the dependence of these characteristics on two array parameters, the interconnect bias voltage and the array capacitance to ground. It was found that the voltage change of the array during an arc is nearly equal to the bias voltage. The array capacitance, on the other hand, influences both the peak current and the decay time constant of the arc. Both of these characteristics increase with increasing capacitance.  
Author

**N84-27825\*#** National Aeronautics and Space Administration. Lewis Research Center, Cleveland, Ohio.

### PERFORMANCE CAPABILITIES OF THE 12-CENTIMETER XENON ION THRUSTER

M. MANTENIEKS and M. SCHATZ 1984 18 p refs Presented at the 17th Intern. Elec. Propulsion Conf., Tokyo, 28-31 May 1984 (NASA-TM-83674; E-2022; NAS 1.15:83674) Avail: NTIS HC A02/MF A01 CSCL 21H

The 8- and 12-cm mercury ion thruster systems were developed primarily to provide N-S station keeping of satellites with masses up to about 1800 to 3600 kg respectively. The on-orbit propulsion requirements of recently proposed Large Space Systems (LSS) are beyond the thrust capabilities of the baseline 8- and 12-cm thruster systems. This paper presents a characterization of the performance capabilities of the 12-cm Xenon ion thruster to enable

an evaluation of its application to LSS auxiliary propulsion requirements. With minor thruster modifications and simplifications the thrust was increased to 64 mN, a factor of six over the baseline 12-cm mercury thruster performance. The thruster was operated over a range of specific impulse of about 2000 to 4000 seconds and at total efficiencies up to 68.0 percent. The operating levels reached in this study were found to be close to the operating limits of the thruster design in terms of permeance, grid breakdown voltage and thruster component temperatures such as those of the magnets and cathode baffle.  
Author

**N84-28901\*#** Pratt and Whitney Aircraft, West Palm Beach, Fla. Government Products Div.

### NASA ORBIT TRANSFER ROCKET ENGINE TECHNOLOGY PROGRAM Final Report

23 Apr. 1984 104 p refs (Contract NAS3-23171) (NASA-CR-168156; N1.26:168156) Avail: NTIS HC A06/MF A01 CSCL 21H

The advanced expander cycle engine with a 15,000 lb thrust level and a 6:1 mixture ratio and optimized performance was used as the baseline for a design study of the hydrogen/oxygen propulsion system for the orbit transfer vehicle. The critical components of this engine are the thrust chamber, the turbomachinery, the extendible nozzle system, and the engine throttling system. Turbomachinery technology is examined for gears, bearing, seals, and rapid solidification rate turbopump shafts. Continuous throttling concepts are discussed. Components of the OTV engine described include the thrust chamber/nozzle assembly design, nozzles, the hydrogen regenerator, the gaseous oxygen heat exchanger, turbopumps, and the engine control valves.  
A.R.H.

**N84-29931\*#** National Aeronautics and Space Administration. Lewis Research Center, Cleveland, Ohio.

### FACTORS THAT INFLUENCE SPACE STATION PROPULSION REQUIREMENTS

W. W. SMITH (Rocket Research Co., Redmond, Wash.), C. L. WILKINSON (Boeing Aerospace Co., Kent, Wash.), and M. E. VALGORA /in APL The 1984 JANNAF Propulsion Meeting, Vol. 1 p 303-318 Feb. 1984 refs (Contract NAS3-23353)

Avail: NTIS HC A17/MF A01 CSCL 21H

The manned space station major propulsion system requirements were outlined and the important influencing factors were defined. To accomplish these objectives, a range of configuration designs were defined and subjected to an environmental perturbation analysis over a range of altitudes. Sensitivities to design and operation were identified and top level propulsion system requirements defined. Conclusions and recommendations regarding operational altitude, configuration design, and ways to minimize the propellant requirements for the space station mission were discussed. A principal finding is that station modules and, more importantly, solar array configuration design, must be limited to strictly balanced or gravity gradient stable designs, otherwise propulsion and momentum system requirements will be unacceptably large.  
Author

**N84-29937\*#** National Aeronautics and Space Administration. Lewis Research Center, Cleveland, Ohio.

### PROPULSION ISSUES FOR ADVANCED ORBIT TRANSFER VEHICLES

L. P. COOPER /in APL The 1984 JANNAF Propulsion Meeting, Vol. 1 p 365-378 Feb. 1984 refs Previously announced as N84-25762

Avail: NTIS HC A17/MF A01 CSCL 21H

Studies of the United States Space Transportation System show that in the mid to late 1990s expanded capabilities for orbital transfer vehicles (OTV) are needed to meet increased payload requirements for transporting materials and possibly men to geosynchronous orbit. Discussion and observations relative to the propulsion system issues of space basing, aeroassist compatibility, man ratibility, and enhanced payload delivery capability are

presented. These issues require resolution prior to the development of a propulsion system for the advanced OTV. The NASA program in support of advanced propulsion for an OTV is briefly described along with conceptual engine design characteristics. Author

**N84-31272\*#** National Aeronautics and Space Administration. Lewis Research Center, Cleveland, Ohio.

**THE POTENTIAL IMPACT OF NEW POWER SYSTEM TECHNOLOGY ON THE DESIGN OF A MANNED SPACE STATION**

J. S. FORDYCE and H. J. SCHWARTZ 1984 12 p refs Presented at the 14th Intern. Symp. on Space Technol. and Sci., Tokyo, 28 May - 1 Jun. 1984; sponsored by Inst. of Space and Astronautical Science (NASA-TM-83770; E-2261; NAS 1.15:83770) Avail: NTIS HC A02/MF A01 CSCL 21H

Larger, more complex spacecraft of the future such as a manned Space Station will require electric power systems of 100 kW and more, orders of magnitude greater than the present state of the art. Power systems at this level will have a significant impact on the spacecraft design. Historically, long-lived spacecraft have relied on silicon solar cell arrays, a nickel-cadmium storage battery and operation at 28 V dc. These technologies lead to large array areas and heavy batteries for a Space Station application. This, in turn, presents orbit altitude maintenance, attitude control, energy management and launch weight and volume constraints. Size (area) and weight of such a power system can be reduced if new higher efficiency conversion and lighter weight storage technologies are used. Several promising technology options including concentrator solar photovoltaic arrays, solar thermal dynamic and ultimately nuclear dynamic systems to reduce area are discussed. Also, higher energy storage systems such as nickel-hydrogen and the regenerative fuel cell (RFC) and higher voltage power distribution which add system flexibility, simplicity and reduce weight are examined. Emphasis is placed on the attributes and development status of emerging technologies that are sufficiently developed so that they could be available for flight use in the early to mid 1990's. Author

**N84-31280\*#** National Aeronautics and Space Administration. Lewis Research Center, Cleveland, Ohio.

**A COMPARISON OF THE EFFICIENCY OF NUMERICAL METHODS FOR INTEGRATING CHEMICAL KINETIC RATE EQUATIONS**

K. RADHAKRISHNAN In APL Computational Methods. 1984 JPM Spec. Session p 69-82 Feb. 1984 refs (Contract NAG3-147)

Avail: NTIS HC A05/MF A01 CSCL 21H

The efficiency of several algorithms used for numerical integration of stiff ordinary differential equations was compared. The methods examined included two general purpose codes EPISODE and LSODE and three codes (CHEMEQ, CREK1D and GCKP84) developed specifically to integrate chemical kinetic rate equations. The codes were applied to two test problems drawn from combustion kinetics. The comparisons show that LSODE is the fastest code available for the integration of combustion kinetic rate equations. It is shown that an iterative solution of the algebraic energy conservation equation to compute the temperature can be more efficient than evaluating the temperature by integrating its time-derivative. Author

**N84-32425\*#** National Aeronautics and Space Administration. Lewis Research Center, Cleveland, Ohio.

**IMPROVED HEAT EXCHANGER FOR ELECTROTHERMAL DEVICES Patent Application**

R. J. ZAVESKY, J. S. SOVEY, M. J. MIRTICH, C. MARINOS, and P. F. PENKO, inventors (to NASA) 31 Jul. 1984 10 p (NASA-CASE-LEW-14037-1; NAS 1.71:LEW-14037-1; US-PATENT-APPL-SN-636463) Avail: NTIS HC A02/MF A01 CSCL 21C

This research is concerned with improving electrothermal devices. An electrothermal thruster utilizes a generally cylindrical heat exchanger chamber to convert electricity to heat which raises

the propellant temperature. A textured, high emissivity heat element radiatively transfers heat to the inner wall of this chamber that is ion beam morphologically controlled for high absorptivity. This, in turn, raises the temperature of a porous heat exchanger material in an annular chamber surrounding the cylindrical chamber. Propellant gas flows through the annular chamber and is heated by the heat exchanger material. B.W.

**N84-32427\*#** National Aeronautics and Space Administration. Lewis Research Center, Cleveland, Ohio.

**PRELIMINARY DESIGN OF A 10-KW THERMOPHOTOVOLTAIC SYSTEM FOR SPACE APPLICATIONS**

M. F. PISZCZOR, JR. and M. GHALLA-GORADIA (Cleveland State Univ.) 1984 15 p refs Presented at the 19th Ann. Intersoc. Energy Conversion Eng. Conf. (IECEC), San Francisco, 19-24 Aug. 1984; sponsored by the AIAA, IEEE, ACS, AIChE, ANS, ASME and SAE

(NASA-TM-83768; E-2259; NAS 1.15:83768) Avail: NTIS HC A02/MF A01 CSCL 21C

A very high degree of reflection of sub-bandgap energy photons from the cell back to the emitter was found to be crucial in achieving high efficiencies for a TPV system. Results show that small increases in reflectance above 0.85 lead to progressively larger increases in cell efficiency. In general, for a required power output, the radiator area, emitter temperature, emitter material and cell temperature may be chosen to satisfy various external constraints. The results can then be used to determine the optimum cell material and its operating temperature. Author

**N84-32428\*#** CHAM of North America, Inc., Huntsville, Ala. **ROCKET INJECTOR ANOMALIES STUDY. VOLUME 1: DESCRIPTION OF THE MATHEMATICAL MODEL AND SOLUTION PROCEDURE Final Report**

A. J. PRZEKOWAS, A. K. SINGHAL, and L. T. TAM Aug. 1984 95 p refs 2 Vol.

(Contract NAS3-23352)

(NASA-CR-174702; NAS 1.26:174702; CHAM-H3605/15-VOL-1)

Avail: NTIS HC A05/MF A01 CSCL 21H

The capability of simulating three dimensional two phase reactive flows with combustion in the liquid fuelled rocket engines is demonstrated. This was accomplished by modifying an existing three dimensional computer program (REFLAN3D) with Eulerian Lagrangian approach to simulate two phase spray flow, evaporation and combustion. The modified code is referred as REFLAN3D-SPRAY. The mathematical formulation of the fluid flow, heat transfer, combustion and two phase flow interaction of the numerical solution procedure, boundary conditions and their treatment are described. E.A.K.

**N84-32429\*#** CHAM of North America, Inc., Huntsville, Ala. **ROCKET INJECTOR ANOMALIES STUDY. VOLUME 2: RESULTS OF PARAMETRIC STUDIES Final Report**

A. J. PRZEKOWAS, A. K. SINGHAL, and L. T. TAM Jul. 1984 71 p refs 2 Vol.

(Contract NAS3-23352)

(NASA-CR-174703; NAS 1.26:174703; CHAM-H3605/16-VOL-2)

Avail: NTIS HC A04/MF A01 CSCL 21H

The employment of a existing computer program to simulate three dimensional two phase gas spray flows in liquid propellant rocket engines. This was accomplished by modification of an existing three dimensional computer program (REFLAN3D) with Euler/Lagrange approach for simulating two phase spray flow, evaporation and combustion. The modified code is referred to as REFLAN3D-SPRAY. Computational studies of the model rocket engine combustion chamber are presented. The parametric studies of the two phase flow and combustion shows qualitatively correct response for variations in geometrical and physical parameters. The injection nonuniformity test with blocked central fuel injector holes shows significant changes in the central flame core and minor influence on the wall heat transfer fluxes. E.A.K.

**N84-33462\*#** Rocket Research Corp., Redmond, Wash.  
**RADIATIVE RESISTOJET PERFORMANCE CHARACTERIZATION TESTS Final Report**  
 C. I. MIYAKE Sep. 1984 55 p refs  
 (Contract NAS3-23868)  
 (NASA-CR-174763; NAS 1.26:174763; REPT-84-R-958) Avail:  
 NTIS HC A04/MF A01 CSCL 21H

The test article, test approach, data analysis and results of a study undertaken to characterize performance of the augmentation section of the Rocket Research Company Augmented Catalytic Thruster as a gas resistojets using hydrogen, nitrogen and ammonia as propellants are described. This renewed interest in resistojets is a result of propulsion systems definition studies which indicate potential application to space station auxiliary propulsion. Author

## 23

## CHEMISTRY AND MATERIALS (GENERAL)

Includes biochemistry and organic chemistry.

**A84-10680\*** National Aeronautics and Space Administration. Lewis Research Center, Cleveland, Ohio.  
**SURFACES**  
 D. H. BUCKLEY (NASA, Lewis Research Center, Cleveland, OH) IN: Adhesives in manufacturing. New York, Marcel Dekker, Inc., 1983, p. 13-49. refs

Techniques for the characterization of surface cleanliness and roughness for predicting the quality of an adhesive bond are outlined. Generally, smooth surfaces are only available from cleavage of crystalline materials along a natural cleavage plane. Films must be deposited on metal surfaces to achieve the same smoothness. Once the surfaces are clean, however, reaction with the ambient atmosphere becomes likely through diffusive and absorption processes, producing asperities. Electron diffraction, Auger electron, and X ray emission spectroscopy are used to characterize surface condition. Once the surface is observed to be clean, the application of an adhesive will usually prohibit separation along the adhesive; separation is then confined to the weaker of the two materials. Finally, the use of polytetrafluoroethylene adhesive to test the adhesion between polymers and metal surfaces is described. M.S.K.

**A84-20465\*** National Aeronautics and Space Administration. Lewis Research Center, Cleveland, Ohio.  
**THE X-RAY PHOTOELECTRON SPECTROSCOPY DEPTH PROFILING AND TRIBOLOGICAL CHARACTERIZATION OF ION-PLATED GOLD ON VARIOUS METALS**  
 K. MIYOSHI, T. SPALVINS, and D. H. BUCKLEY (NASA, Lewis Research Center, Cleveland, OH) (International Conference on Metallurgical Coatings, San Diego, CA, Apr. 18-22, 1983) Thin Solid Films (ISSN 0040-6090), vol. 108, 1983, p. 199-207. refs

For the case of ion-plated gold, the graded interface between gold and a nickel substrate and a nickel substrate, such tribological properties as friction and microhardness are examined by means of X-ray photoelectron spectroscopy analysis and depth profiling. Sliding was conducted against SiC pins in both the adhesive process, where friction arises from adhesion between sliding surfaces, and abrasion, in which friction is due to pin indentation and groove-plowing. Both types of friction are influenced by coating depth, but with opposite trends: the graded interface exhibited the highest adhesion, but the lowest abrasion. The coefficient of friction due to abrasion is inversely related to hardness. Graded interface microhardness values are found to be the highest, due to an alloying effect. There is almost no interface gradation between the vapor-deposited gold film and the substrate. O.C.

**A84-32646\*** National Aeronautics and Space Administration. Lewis Research Center, Cleveland, Ohio.  
**PREDICTIVE CAPABILITY OF LONG-TERM CAVITATION AND LIQUID IMPINGEMENT EROSION MODELS**  
 P. V. RAO and D. H. BUCKLEY (NASA, Lewis Research Center, Cleveland, OH) Wear (ISSN 0043-1648), vol. 94, March 15, 1984, p. 259-274. refs  
 (Contract NCC3-21)

A brief overview of long-term cavitation and liquid impingement erosion and modeling methods proposed by different investigators, including the curve-fit approach is presented. A table was prepared to highlight the number of variables necessary for each model in order to compute the erosion-versus-time curves. A power law relation based on the average erosion rate is suggested which may solve several modeling problems. Previously announced in STAR as N83-22386 M.G.

**N84-20643\*#** National Aeronautics and Space Administration. Lewis Research Center, Cleveland, Ohio.  
**HOMOGENEOUS REACTIONS OF HYDROCARBONS, SILANE, AND CHLOROSILANES IN RADIOFREQUENCY PLASMAS AT LOW PRESSURES**  
 R. AVNI, U. CARMELI (Nuclear Research Center Negev, Beer Sheva, Israel), A. INSPEKTOR (Nuclear Research Center Negev, Beer Sheva, Israel), and I. ROSENTHAL (Nuclear Research Center Negev, Beer Sheva, Israel) Apr. 1984 13 p refs Presented at the 6th Intern. Symp. on Plasma Chem., Montreal, 24-28 Jul. 1983; sponsored by International Union of Pure and Applied Chemistry (NASA-TP-2301; E-1919; NAS 1.60:2301) Avail: NTIS HC A02/MF A01 CSCL 07A

The ion-molecule and radical-molecule mechanisms are responsible for the dissociation of hydrocarbon, silane, and chlorosilane monomers and the formation of polymerized species, respectively, in an RF plasma discharge. In a plasma containing a mixture of monomer and argon the rate-determining step for both dissociation and polymerization is governed by an ion-molecule type of interaction. Adding hydrogen or ammonia to the monomer-argon mixture transforms the rate-determining step from an ion-molecule interaction to a radical-molecule interaction for both monomer dissociation and polymerization. Author

**N84-23693\*#** National Aeronautics and Space Administration. Lewis Research Center, Cleveland, Ohio.  
**KINETICS OF CHROMIUM ION ABSORPTION BY CROSS-LINKED POLYACRYLATE FILMS**  
 C. E. MAY May 1984 17 p refs  
 (NASA-TM-83661; E-2105; NAS 1.15:83661) Avail: NTIS HC A02/MF A01 CSCL 11G

Three cross-linked ion exchange membranes were studied as to their ability to absorb chromium ion from aqueous chromium III nitrate solutions. Attention was given to the mechanism of absorption, composition of the absorbed product, and the chemical bonding. The membranes were: calcium polyacrylate, polyacrylic acid, and a copolymer of acrylic acid and vinyl alcohol. For the calcium polyacrylate and the copolymer, parabolic kinetics were observed, indicating the formation of a chromium polyacrylate phase as a coating on the membrane. The rate of absorption is controlled by the diffusion of the chromium ion through this coating. The product formed in the copolymer involves the formation of a coordination complex of a chromium ion with 6 carboxylic acid groups from the same molecule. The absorption of the chromium ion by the polyacrylic acid membranes appears to be more complicated, involving cross-linking. This is due to the coordination of the chromium ion with carboxylic acid groups from more than one polymer molecule. The absorption rate of the chromium ion by the calcium salt membrane was found to be more rapid than that by the free polyacrylic acid membrane. Author



## COMPOSITE MATERIALS

**N84-25766\*#** National Aeronautics and Space Administration. Lewis Research Center, Cleveland, Ohio.

**TRIBOLOGICAL APPLICATIONS OF SURFACE ANALYSIS**

D. R. WHEELER 1984 16 p refs Presented at TSEM, Philadelphia, 15-20 Apr. 1984  
(NASA-TM-83707; E-2166; NAS 1.15:83707) Avail: NTIS HC A02/MF A01 CSCL 07D

For some years, surface analysis was used in fundamental studies of solid-solid contacts existing in tribological systems. Analysis was used to detect material transfer in sliding contacts. The effects of surface films on the adhesion of contacts was monitored. Finally electron spectroscopic analysis of interfaces has shed some light on the fundamental electronic nature of the interfacial bond. More recently, surface analysis was applied to many tribological engineering problems. In particular, identification of chemical films formed during the sliding contact of lubricated systems and study of the surface chemistry of lubricant additives were active areas of research. One or more of four properties of the analytical technique will be important in determining its utility. The four are: lateral resolution, specimen damage, depth resolution and the availability of chemical information. In each of the applications discussed here, the important factors are brought out.

Author

**N84-26749\*#** National Aeronautics and Space Administration. Lewis Research Center, Cleveland, Ohio.

**MICROSTRUCTURE AND ORIENTATION EFFECTS ON PROPERTIES OF DISCONTINUOUS SILICON CARBIDE/ALUMINUM COMPOSITES**

D. L. MCDANIELS and C. A. HOFFMAN Jul. 1984 32 p refs (NASA-TP-2302; E-1977; NAS 1.60:2302) Avail: NTIS HC A03/MF A01 CSCL 11D

Composite panels containing up to 40 vol % discontinuous silicon carbide SiC whisker, nodule, or particulate reinforcement in several aluminum matrices are commercially fabricated and the mechanical properties and microstructural characteristics are evaluated. The yield and tensile strengths and the ductility are controlled primarily by the matrix alloy, the temper condition, and the reinforcement content. Particulate and nodule reinforcements are as effective as whisker reinforcement. Increased ductility is attributed to purer, more uniform starting materials and to more mechanical working during fabrication. Comparing mechanical properties with those of other aluminum alloys shows that these low cost, lightweight composites demonstrate very good potential for application to aerospace structures.

M.A.C.

**N84-31283\*#** National Aeronautics and Space Administration. Lewis Research Center, Cleveland, Ohio.

**CALCULATION OF VAPORIZATION RATES ASSUMING VARIOUS RATE DETERMINING STEPS: APPLICATION TO THE RESISTOJET**

C. E. MAY Aug. 1984 58 p refs  
(NASA-TM-83757; E-2244; NAS 1.15:83757) Avail: NTIS HC A04/MF A01 CSCL 07D

The various steps that could control the vaporization rate of a material are discussed. These steps include the actual vaporization, flow rate of matrix gas, chemical reaction, gas diffusion, and solid state diffusion. The applicable equations have been collected from diverse appropriate sources, and their use is explained. Rate equations are derived for conditions where more than one step is rate controlling. Calculations are made for two model materials: rhenium which vaporizes congruently, and tantalum carbide which vaporizes incongruently. The case of vaporization under thermal gradient conditions is also treated. The existence of a thermal gradient in the resistojets means that the vaporization rate of a material may be only one thousandth of that predicted under isothermal conditions. Calculations show that rhenium might have a 100,000 hr lifetime at temperature in a 2500 C resistojets. Tantalum carbide would have a life of only 660 sec under similar conditions.

Author

Includes laminates.

**A84-10430\*** Virginia Polytechnic Inst. and State Univ., Blacksburg.

**CHARACTERIZATION OF COMPOSITE MATERIALS BY MEANS OF THE ULTRASONIC STRESS WAVE FACTOR**

J. C. DUKE, JR., E. G. HENNEKE, W. W. STINCHCOMB, and K. L. REIFSNIDER (Virginia Polytechnic Institute and State University, Blacksburg, VA) IN: Composite structures 2; Proceedings of the Second International Conference, Paisley, Scotland, September 14-16, 1983. London, Applied Science Publishers, 1983, p. 53-60.

(Contract NAG3-172; NAG3-323)

The usual approach to nondestructively evaluating a composite structure involves inspection and mechanical analysis of the inspection results. Such an approach has met with only limited success. On the other hand, the ultrasonic stress wave factor technique directly evaluates the material. Despite requiring access to only one surface of the material, the technique interrogates the material in the directions of applied load. Using the stress wave factor technique it is possible to determine the failure location in the material. The correlation of the stress wave factor with stiffness is shown. In addition, the use of the technique for determining the strength or life of composite material structures is discussed.

Author

**A84-14285\*** National Aeronautics and Space Administration. Lewis Research Center, Cleveland, Ohio.

**PREDICTION OF COMPOSITE HYGRAL BEHAVIOR MADE SIMPLE**

C. C. CHAMIS and J. H. SINCLAIR (NASA, Lewis Research Center, Cleveland, OH) (Society of Plastics Industry, Annual Conference, 37th, Washington, DC, Jan. 1982) SAMPE Quarterly (ISSN 0036-0821), vol. 14, Oct. 1982, p. 30-39. refs

A convenient procedure is described to determine the hygral behavior (moisture expansion coefficients and moisture stresses) of angleplyed fiber composites using a pocket calculator. The procedure consists of equations and appropriate graphs for various (+ or - theta) ply combinations. These graphs present reduced stiffness and moisture expansion coefficients as functions of (+ or - theta) in order to simplify and expedite the use of the equations. The procedure is applicable to all types of balanced, symmetric fiber composites including interply and intraply hybrids. The versatility and generality of the procedure is illustrated using several step-by-step numerical examples. Previously announced in STAR as N82-16181

Author

**A84-17444\*#** National Aeronautics and Space Administration. Lewis Research Center, Cleveland, Ohio.

**ENVIRONMENTAL AND HIGH STRAIN RATE EFFECTS ON COMPOSITES FOR ENGINE APPLICATIONS**

C. C. CHAMIS and G. T. SMITH (NASA, Lewis Research Center, Cleveland, OH) (Structures, Structural Dynamics and Materials Conference, 23rd, New Orleans, LA, May 10-12, 1982, Collection of Technical Papers, Part 1, p. 405-419) AIAA Journal (ISSN 0001-1452), vol. 22, Jan. 1984, p. 128-134. refs

Previously cited in issue 13, p. 2034, Accession no. A82-30118

**A84-19780\*** National Aeronautics and Space Administration. Lewis Research Center, Cleveland, Ohio.

**PROCESSING OF FUSED SILICIDE COATINGS FOR CARBON-BASED MATERIALS**

J. L. SMIALEK (NASA, Lewis Research Center, Cleveland, OH) Ceramic Engineering and Science Proceedings (ISSN 0196-6219), vol. 4, Sept.-Oct. 1983, p. 757-783. refs

The processing and oxidation resistance of fused Al-Si and Ni-Si slurry coatings on ATJ graphite was studied. Ni-Si coatings



in the 70 to 90 percent Si range were successfully processed to melt, wet, and bond to the graphite. The molten coatings also infiltrated the porosity in graphite and reacted with it to form SiC in the coating. Cyclic oxidation at 1200 C showed that these coatings were not totally protective because of local attack of the substrate, due to the extreme thinness of the coatings in combination with coating cracks. Previously announced in STAR as N83-27019 S.L.

**A84-21515\*# Illinois Univ., Urbana.  
EDGE DELAMINATION IN ANGLE-PLY COMPOSITE LAMINATES**

S. S. WANG (Illinois, University, Urbana, IL) (Structures, Structural Dynamics and Materials Conference, 22nd, Atlanta, GA, Apr. 6-8, 1981, Technical Papers, Part 1, p. 473-484) AIAA Journal (ISSN 0001-1452), vol. 22, Feb. 1984, p. 256-264. refs (Contract NSG-3044)

Previously cited in issue 12, p. 1966, Accession no. A81-29426

**A84-21844\* National Aeronautics and Space Administration. Lewis Research Center, Cleveland, Ohio  
THE EFFECT OF A COATING ON THE THERMO-OXIDATIVE STABILITY OF CELION 6000 GRAPHITE FIBER/PMR 15 POLYIMIDE COMPOSITES**

F. I. HURWITZ and J. D. WHITTENBERGER (NASA, Lewis Research Center, Cleveland, OH) Composites Technology Review, vol. 5, Winter 1983, p. 109-114. refs

The thermooxidative stability in air at 316 C of unidirectional, uncoated and aluminum-coated Celion 6000 graphite fiber/PMR 15 polyimide composites has been determined for exposure times up to nominally 2000 h. Comparison of the weight loss data and microstructural integrity reveals that a thin aluminum-foil coating can provide significant protection from oxidation. A quantitative description of the average depth of the reaction zone and the maximum length of cracks produced during oxidation as a function of time in uncoated Celion 6000/PMR 15 are given. Author

**A84-21847\* California Univ., Livermore.  
AGING RESULTS FOR PRD 49 III/EPOXY AND KEVLAR 49/EPOXY COMPOSITE PRESSURE VESSELS**

M. A. HAMSTAD (California, University, Livermore, CA) Composites Technology Review, vol. 5, Winter 1983, p. 120-122. (Contract NASA ORDER C-13980-C; W-7405-ENG-48)

Kevlar 49/epoxy composite is growing in use as a structural material because of its high strength-to-weight ratio. Currently, it is used for the Trident rocket motor case and for various pressure vessels on the Space Shuttle. In 1979, the initial results for aging of filament-wound cylindrical pressure vessels which were manufactured with preproduction Kevlar 49 (Hamstad, 1979) were published. This preproduction fiber was called PRD 49 III. This report updates the continuing study to 10-year data and also presents 7.5-year data for spherical pressure vessels wound with production Kevlar 49. For completeness, this report will again describe the specimens of the original study with PRD 49 as well as specimens for the new study with Kevlar 49. Author

**A84-27356\* Purdue Univ., Lafayette, Ind.  
INDENTATION LAW FOR COMPOSITE LAMINATES**

S. H. YANG and C. T. SUN (Purdue University, West Lafayette, IN) IN: Composite materials: Testing and design (Sixth Conference). Philadelphia, PA, American Society for Testing and Materials, 1982, p. 425-449. (Contract NSG-3185)

Static indentation tests are described for glass/epoxy and graphite/epoxy composite laminates with steel balls as the indenter. Beam specimens clamped at various spans were used for the tests. Loading, unloading, and reloading data were obtained and fitted into power laws. Results show that: (1) contact behavior is not appreciably affected by the span; (2) loading and reloading curves seem to follow the 1.5 power law; and (3) unloading curves are described quite well by a 2.5 power law. In addition, values were determined for the critical indentation,  $\alpha$  sub cr which

can be used to predict permanent indentations in unloading. Since  $\alpha$  sub cr only depends on composite material properties, only the loading and an unloading curve are needed to establish the complete loading-unloading-reloading behavior. Previously announced in STAR as N82-15123 Author

**A84-27359\* National Aeronautics and Space Administration. Lewis Research Center, Cleveland, Ohio.  
DURABILITY/LIFE OF FIBER COMPOSITES IN HYGROTHERMOMECHANICAL ENVIRONMENTS**

C. C. CHAMIS and J. H. SINCLAIR (NASA, Lewis Research Center, Cleveland, OH) IN: Composite materials: Testing and design (Sixth Conference). Philadelphia, PA, American Society for Testing and Materials, 1982, p. 498-512. refs

Statistical analysis and multiple regression were used to determine and quantify the significant hygrothermomechanical variables which influence the tensile durability/life (cycle loading, fatigue) of boron-fiber/epoxy-matrix (B/E) and high-modulus-fiber/epoxy-matrix (HMS/E) composites. The use of the multiple regression analysis reduced the variables from fifteen, assumed initially, to six or less with a probability of greater than 0.999. The reduced variables were used to derive predictive models for compression and intralaminar shear durability/life of B/E and HMS/E composites assuming isoparametric fatigue behavior. The predictive models were subsequently generalized to predict the durability/life of graphite/fiber-r generalized model is of simple form, predicts conservative values compared with measured data and should be adequate for use in preliminary designs. Previously announced in STAR as N82-14287 B.W.

**A84-28227\* National Aeronautics and Space Administration. Lewis Research Center, Cleveland, Ohio.  
FACTORS INFLUENCING THE THERMALLY-INDUCED STRENGTH DEGRADATION OF B/AL COMPOSITES**

J. A. DICARLO (NASA, Lewis Research Center, Cleveland, OH) IN: Mechanical behavior of metal-matrix composites; Proceedings of the Symposium, Dallas, TX, February 16-18, 1982. Warrendale, PA, The Metallurgical Society of AIME, 1983, p. 1-14. refs

Literature data related to the thermally-induced strength degradation of B/Al composites were examined in the light of fracture theories based on reaction-controlled fiber weakening. Under the assumption of a parabolic time-dependent growth for the interfacial reaction product, a Griffith-type fracture model was found to yield simple equations whose predictions were in good agreement with data for boron fiber average strength and for B/Al axial fracture strain. The only variables in these equations were the time and temperature of the thermal exposure and an empirical factor related to fiber surface smoothness prior to composite consolidation. Such variables as fiber diameter and aluminum alloy composition were found to have little influence. The basic and practical implications of the fracture model equations are discussed. Previously announced in STAR as N82-24297 Author

**A84-28229\* National Aeronautics and Space Administration. Lewis Research Center, Cleveland, Ohio.  
THERMAL DEGRADATION OF THE TENSILE PROPERTIES OF UNIDIRECTIONALLY REINFORCED FP-AL203/EZ 33 MAGNESIUM COMPOSITES**

R. T. BHATT (U.S. Army, Propulsion Laboratory, Cleveland, OH) and H. H. GRIMES (NASA, Lewis Research Center, Cleveland, OH) IN: Mechanical behavior of metal-matrix composites; Proceedings of the Symposium, Dallas, TX, February 16-18, 1982. Warrendale, PA, The Metallurgical Society of AIME, 1983, p. 51-64. refs

The effects of isothermal and cyclic exposure on the room temperature axial and transverse tensile strength and dynamic flexural modulus of 35 volume percent and 55 volume percent FP-AL203/EZ 33 magnesium composites were studied. The composite specimens were continuously heated in a sand bath maintained at 350 C for up to 150 hours or thermally cycled between 50 and 250 C or 50 and 350 C for up to 3000 cycles. Each thermal cycle lasted for a total of six minutes with a hold time of two minutes at the maximum temperature. Results indicate

no significant loss in the room temperature axial tensile strength and dynamic flexural modulus of composites thermally cycled between 50 and 250 C or of composites isothermally heated at 350 C for up to 150 hours from the strength and modulus data for the untreated, as-fabricated composites. In contrast, thermal cycling between 50 and 350 C caused considerable loss in both room temperature strength and modulus. Fractographic analysis and measurement of composite transverse strength and matrix hardness of thermally cycled and isothermally heated composites indicated matrix softening and fiber/matrix debonding due to void growth at the interface and matrix cracking as the likely causes of the strength and modulus loss behavior. Previously announced in STAR as N82-21260 Author

**A84-28241\*** National Aeronautics and Space Administration. Lewis Research Center, Cleveland, Ohio.

**TUNGSTEN-FIBER-REINFORCED SUPERALLOY COMPOSITE, HIGH-TEMPERATURE COMPONENT DESIGN CONSIDERATIONS**

E. A. WINSA (NASA, Lewis Research Center, Cleveland, OH) IN: Mechanical behavior of metal-matrix composites; Proceedings of the Symposium, Dallas, TX, February 16-18, 1982. Warrendale, PA, The Metallurgical Society of AIME, 1983, p. 283-299. refs

Tungsten fiber reinforced superalloy composites (TFRS) are intended for use in high temperature turbine components. Current turbine component design methodology is based on applying the experience, sometimes semiempirical, gained from over 30 years of superalloy component design. Current composite component design capability is generally limited to the methodology for low temperature resin matrix composites. Often the tendency is to treat TFRS as just another superalloy or low temperature composite. However, TFRS behavior is significantly different than that of superalloys, and the high environment adds consideration not common in low temperature composite component design. The methodology used for preliminary design of TFRS components are described. Considerations unique to TFRS are emphasized. Previously announced in STAR as N82-21259 Author

**A84-29894\*** National Aeronautics and Space Administration. Lewis Research Center, Cleveland, Ohio.

**COMPRESSIVE BEHAVIOR OF UNIDIRECTIONAL FIBROUS COMPOSITES**

J. H. SINCLAIR and C. C. CHAMIS (NASA, Lewis Research Center, Cleveland, OH) IN: Compression testing of homogeneous materials and composites; Proceedings of the Symposium, Williamsburg, VA, March 10, 11, 1982. Philadelphia, PA, American Society for Testing and Materials, 1983, p. 155-174. refs

The longitudinal compressive behavior of unidirectional fiber composites was investigated by using the Illinois Institute of Technology Research Institute (IITRI) test method with thick and thin test specimens. The test data obtained are interpreted by means of stress/strain curves from back-to-back strain gages, examination of fracture surfaces by scanning electron microscope, and predictive equations for distinct failure modes including fiber compression failure, Euler buckling, delamination, and flexure. The results show that longitudinal compressive fracture is induced by a combination of delamination, flexure, and fiber fiber breaks. No distinct fracture surface characteristics can be associated with unique failure modes. An equation is described that can be used to extract the longitudinal compressive strength from the longitudinal tensile and flexural strengths of the same composite system. Author

**A84-33389\*** Illinois Univ., Urbana.

**ELASTICITY SOLUTIONS FOR A CLASS OF COMPOSITE LAMINATE PROBLEMS WITH STRESS SINGULARITIES**

S. S. WANG (Illinois, University, Urbana, IL) IN: Mechanics of composite materials: Recent advances; Proceedings of the Symposium, Blacksburg, VA, August 16-19, 1982. New York and Oxford, Pergamon Press, 1983, p. 259-281. refs (Contract NSG-3044; N00014-79-C-0579)

A study on the fundamental mechanics of fiber-reinforced composite laminates with stress singularities is presented. Based

on the theory of anisotropic elasticity and Lekhnitskii's complex-variable stress potentials, a system of coupled governing partial differential equations are established. An eigenfunction expansion method is introduced to determine the orders of stress singularities in composite laminates with various geometric configurations and material systems. Complete elasticity solutions are obtained for this class of singular composite laminate mechanics problems. Homogeneous solutions in eigenfunction series and particular solutions in polynomials are presented for several cases of interest. Three examples are given to illustrate the method of approach and the basic nature of the singular laminate elasticity solutions. The first problem is the well-known laminate free-edge stress problem, which has a rather weak stress singularity. The second problem is the important composite delamination problem, which has a strong crack-tip stress singularity. The third problem is the commonly encountered bonded composite joints, which has a complex solution structure with moderate orders of stress singularities. Author

**A84-41858\*** National Aeronautics and Space Administration. Lewis Research Center, Cleveland, Ohio.

**SIMPLIFIED COMPOSITE MICROMECHANICS EQUATIONS FOR STRENGTH, FRACTURE TOUGHNESS AND ENVIRONMENTAL EFFECTS**

C. C. CHAMIS (NASA, Lewis Research Center, Cleveland, OH) SAMPE Quarterly (ISSN 0036-0821), vol. 15, July 1984, p. 41-55. refs

A unified set of composite micromechanics equations of simple form is summarized and described. This unified set includes composite micromechanics equations for predicting: (1) ply in-plane uniaxial strengths; (2) through-the-thickness strength (interlaminar and flexural); (3) in-plane fracture toughness; (4) in-plane impact resistance; and (5) through-the-thickness (interlaminar and flexural) impact resistance. Equations are also included for predicting the hygrothermal effects on strength, fracture toughness and impact resistance. Several numerical examples are worked out to illustrate the ease of use of the various composite micromechanics equations. Author

**A84-43553\*** National Aeronautics and Space Administration. Lewis Research Center, Cleveland, Ohio.

**OFF-AXIS TENSILE PROPERTIES AND FRACTURE IN A UNIDIRECTIONAL GRAPHITE/POLYIMIDE COMPOSITE (CELION 6000/PMR 15)**

J. HARPER, J. D. WHITTENBERGER, and F. I. HURWITZ (NASA, Lewis Research Center, Cleveland, OH) Polymer Composites (ISSN 0272-8397), vol. 5, July 1984, p. 179-185. refs

Tensile properties of unidirectional Celion 6000 graphite/PMR 15 polyimide composites prepared by hot molding and cold molding processes were measured at room temperature and 316 C, the upper use temperature of the polyimide resin, at both 45 and 90 deg to the fiber axis. The resulting fractures were characterized by scanning electron microscopy and materialographic techniques. Variation in tensile properties with processing history occurred in the elastic modulus and strain to failure for specimens loaded at 90 deg at 316 C, and in the fracture stress, and hence the in-plane shear stress, for those loaded at 45 deg at room temperature. Significant plastic deformation was observed in the 45 deg orientation at 316 C for material produced by both processing methods. In general, fracture occurred by both failure within the matrix and at the fiber-matrix interface; the degree of interfacial failure increased with temperature. Secondary cracking below the primary fracture surface was also observed. Author

**A84-49377\*** National Aeronautics and Space Administration. Lewis Research Center, Cleveland, Ohio.

**SIMPLIFIED COMPOSITE MICROMECHANICS EQUATIONS OF HYGRAL, THERMAL, AND MECHANICAL PROPERTIES**

C. C. CHAMIS (NASA, Lewis Research Center, Cleveland, OH) SAMPE Quarterly (ISSN 0036-0821), vol. 15, April 1984, p. 14-23. Previously announced in STAR as N83-19817. refs

A unified set of composite micromechanics equations of simple form is summarized and described. This unified set can be used

to predict unidirectional composite (ply) geometric, mechanical, thermal and hygral properties using constituent material (fiber/matrix) properties. This unified set also includes approximate equations for predicting (1) moisture absorption; (2) glass transition temperature of wet resins; and (3) hygrothermal degradation effects. Several numerical examples are worked-out to illustrate ease of use and versatility of these equations. These numerical examples also demonstrate the interrelationship of the various factors (geometric to environmental) and help provide insight into composite behavior at the micromechanistic level. Author

**N84-13224\*#** National Aeronautics and Space Administration. Lewis Research Center, Cleveland, Ohio.  
**INHYD: COMPUTER CODE FOR INTRAPLY HYBRID COMPOSITE DESIGN. A USERS MANUAL**  
 C. G. CHAMIS and J. H. SINCLAIR Dec. 1983 41 p refs  
 (NASA-TP-2239; E-1755; NAS 1.60:2239) Avail: NTIS HC A03/MF A01 CSCL 11D

A computer program (INHYD) was developed for intraply hybrid composite design. A users manual for INHYD is presented. In INHYD embodies several composite micromechanics theories, intraply hybrid composite theories, and an integrated hygrothermomechanical theory. The INHYD can be run in both interactive and batch modes. It has considerable flexibility and capability, which the user can exercise through several options. These options are demonstrated through appropriate INHYD runs in the manual S.C.L.

**N84-15203\*#** National Aeronautics and Space Administration. Lewis Research Center, Cleveland, Ohio.  
**ARC SPRAY FABRICATION OF METAL MATRIX COMPOSITE MONOTAPE Patent Application**  
 L. J. WESTFALL, inventor (to NASA) 9 Dec 1983 12 p  
 (NASA-CASE-LEW-13828-1; US-PATENT-APPL-SN-560035)  
 Avail: NTIS HC A02/MF A01 CSCL 11D

Arc metal spraying is used to spray liquid metal onto an array of high strength fibers that have been previously wound onto a large drum contained inside a controlled atmosphere chamber. This chamber is first evacuated to remove gaseous contaminants and then backfilled with a neutral gas up to atmospheric pressure. This process is used to produce a large size metal matrix composite monotapec. NASA

**N84-16266\*#** National Aeronautics and Space Administration. Lewis Research Center, Cleveland, Ohio.  
**OXIDATION RESISTANT SLURRY COATING FOR CARBON-BASED MATERIALS Patent Application**  
 J. L. SMIALEK and G. RYBICKI, inventors (to NASA) 17 Jan. 1984 10 p  
 (NASA-CASE-LEW-13923-1; US-PATENT-APPL-SN-571617)  
 Avail: NTIS HC A02/MF A01 CSCL 11D

An oxidation resistant coating is produced on carbon-based materials, and the same processing step effects an infiltration of the substrate with silicon containing material. A slurry of nickel and silicon powders in a nitrocellulose lacquer is made, is sprayed onto the graphite or carbon-carbon substrate, and is sintered in vacuum to form a fused coating that wets and covers the surface as well as penetrates into the pores of the substrate. Optimum wetting and infiltration occurs in the range of Ni-60 w/o Si to Ni-90 w/o Si with deposited thicknesses of 25 to 100 mg/sq cm. Sintering temperatures of about 1200 C to about 1400 C are used, depending, on the melting point of the specific coating composition. The sintered coating results in Ni-Si intermetallic phases and SiC, both of which are highly oxidation resistant. The final coating composition can be further controlled by the length of the sintering time. NASA

**N84-21666\*#** National Aeronautics and Space Administration. Lewis Research Center, Cleveland, Ohio.  
**ANALYSIS OF STRESS-STRAIN, FRACTURE AND DUCTILITY BEHAVIOR OF ALUMINUM MATRIX COMPOSITES CONTAINING DISCONTINUOUS SILICON CARBIDE REINFORCEMENT**  
 D. L. MCDANIELS 2 Mar. 1984 25 p refs Prepared for presentation at 113th Ann. Meeting of the Am. Inst. of Mining, Met. and Petrol. Engr., Los Angeles, 26 Feb. - 2 Mar. 1984 (NASA-TM-83610; E-2032; NAS 1.15:83610) Avail: NTIS HC A02/MF A01 CSCL 11D

Mechanical properties and stress-strain behavior for several types of commercially fabricated aluminum matrix composites, containing up to 40 vol % discontinuous SiC whisker, nodule, or particulate reinforcement were evaluated. It was found that the elastic modulus of the composites was isotropic, to be independent of type of reinforcement, and to be controlled solely by the volume percentage of SiC reinforcement present. The yield/tensile strengths and ductility were controlled primarily by the matrix alloy and temper condition. Ductility decreased with increasing reinforcement content, however, the fracture strains observed were higher than those reported in the literature for this type of composite. This increase in fracture strain is attributed to cleaner matrix powder and increased mechanical working during fabrication. Conventional aluminum and titanium structural alloys were compared and have shown that the properties of these low cost, lightweight composites have good potential for application to aerospace structures. E.A.K.

**N84-22695\*#** National Aeronautics and Space Administration. Lewis Research Center, Cleveland, Ohio.  
**DIAMONDLIKE FLAKE COMPOSITES Patent**  
 B. A. BANKS, inventor (to NASA) 20 Mar. 1984 6 p Filed 17 May 1983  
 (NASA-CASE-LEW-13837-1; US-PATENT-4,437,962; US-PATENT-APPL-SN-495381; US-PATENT-CLASS-204-192C; US-PATENT-CLASS-204-192R; US-PATENT-CLASS-204-192SP; US-PATENT-CLASS-423-414; US-PATENT-CLASS-423-445; US-PATENT-CLASS-423-446; US-PATENT-CLASS-423-449; US-PATENT-CLASS-423-DIG.10) Avail: US Patent and Trademark Office CSCL 11D

A carbon coating is vacuum arc deposited on a smooth surface of a target which is simultaneously ion beam sputtered. The bombarding ions have sufficient energy to create diamond bonds. Spalling occurs as the carbon deposit thickens. The resulting diamond-like carbon flakes are mixed with a binder or matrix material to form a composite material having improved thermal, electrical, mechanical, and tribological properties when used in aerospace structures and components.

Official Gazette of the U.S. Patent and Trademark Office

**N84-22696\*#** National Aeronautics and Space Administration. Lewis Research Center, Cleveland, Ohio.  
**DIAMONDLIKE FLAKES Patent Application**  
 B. A. BANKS, inventor (to NASA) 19 Mar. 1984 10 p  
 (NASA-CASE-LEW-13837-2; US-PATENT-APPL-SN-591089)  
 Avail: NTIS HC A02/MF A01 CSCL 11D

A carbon coating which is vacuum arc deposited on a smooth surface of a target which is simultaneously ion beam sputtered is discussed. The bombarding ions have sufficient energy to create diamond bonds. Spalling occurs as the carbon deposit thickens. The resulting diamondlike carbon flakes have improved thermal, electrical, mechanical, and tribological properties when used in aerospace structures and components. NASA

**N84-22698\*#** National Aeronautics and Space Administration. Lewis Research Center, Cleveland, Ohio.

**CHEMICAL APPROACH FOR CONTROLLING NADIMIDE CURE TEMPERATURE AND RATE Patent Application**

R. W. LAUVER, inventor (to NASA) 14 Dec. 1983 18 p (NASA-CASE-LEW-13770-3; US-PATENT-APPL-SN-561431)  
 Avail: NTIS HC A02/MF A01 CSCL 11D

Polyimide resins suitable for use as composite matrix materials are formed by copolymerization of maleic and norbornenyl end capped monomers and oligomers. The copolymers can be cured at temperatures under about 300 C by controlling the available concentration of the maleic end-capped reactant. This control can be achieved by adding sufficient amounts of said maleic reactant, or by chemical modification of either copolymer, so as to either increase Diels-Alder retrogression of the norbornenyl capped reactant and/or holding initiation and polymerization to a rate compatible with the availability of the maleic-capped reactant.

NASA

**N84-22699\*#** National Aeronautics and Space Administration. Lewis Research Center, Cleveland, Ohio.

**CHEMICAL APPROACH FOR CONTROLLING NADIMIDE CURE TEMPERATURE AND RATE Patent Application**

R. W. LAUVER, inventor (to NASA) 14 Dec. 1983 18 p (NASA-CASE-LEW-13770-4; US-PATENT-APPL-SN-561429)  
 Avail: NTIS HC A02/MF A01 CSCL 11D

Polyimide resins suitable for use as composite matrix materials are formed by copolymerization of maleic and norbornenyl endcapped monomers and oligomers. The copolymers can be cured at temperatures under about 300 C by controlling the available concentration of the maleic-capped reactant. This control can be achieved by adding sufficient amounts of said maleic reactant, or by chemical modification of either copolymer, so as to either increase Diels-Alder retrogression of the norbornenyl capped reactant and/or holding initiation and polymerization to a rate compatible with the availability of the maleic-capped reactant.

NASA

**N84-22700\*#** National Aeronautics and Space Administration. Lewis Research Center, Cleveland, Ohio.

**CHEMICAL APPROACH FOR CONTROLLING NADIMIDE CURE TEMPERATURE AND RATE Patent Application**

R. W. LAUVER, inventor (to NASA) 14 Dec. 1983 18 p (NASA-CASE-LEW-13770-5; US-PATENT-APPL-SN-561435)  
 Avail: NTIS HC A02/MF A01 CSCL 11D

Polyimide resins suitable for use as composite matrix materials are formed by copolymerization of maleic and norbornenyl endcapped monomers and oligomers. The copolymers can be cured at temperatures under about 300 C by controlling the available concentration of the maleic end-capped reactant. This control can be achieved by adding sufficient amounts of said maleic reactant, or by chemical modification of either copolymer, so as to either increase Diels-Alder retrogression of the norbornenyl capped reactant and/or holding initiation and polymerization to a rate compatible with the availability of the maleic-capped reactant.

NASA

**N84-22701\*#** National Aeronautics and Space Administration. Lewis Research Center, Cleveland, Ohio.

**CHEMICAL APPROACH FOR CONTROLLING NADIMIDE CURE TEMPERATURE AND RATE Patent Application**

R. W. LAUVER, inventor (to NASA) 14 Dec. 1983 18 p (NASA-CASE-LEW-13770-6; US-PATENT-APPL-SN-561434)  
 Avail: NTIS HC A02/MF A01 CSCL 11D

Polyimide resins suitable for use as composite matrix materials are formed by copolymerization of maleic and norbornenyl endcapped monomers and oligomers. The copolymers can be cured at temperatures under about 300 C by controlling the available concentration of the maleic end-capped reactant. This control can be achieved by adding sufficient amounts of said maleic reactant, or by chemical modification of either copolymer, so as to either increase Diels-Alder retrogression of the norbornenyl capped reactant and/or holding initiation and polymerization to a

rate compatible with the availability of the maleic-capped reactant.

NASA

**N84-22702\*#** National Aeronautics and Space Administration. Lewis Research Center, Cleveland, Ohio.

**SELECT FIBER COMPOSITES FOR SPACE APPLICATIONS: A MECHANISTIC ASSESSMENT**

C. A. GINTY and C. C. CHAMIS 1984 26 p refs Presented at the 29th SAMPE Symp and Exhibition, Reno, Nev., 3-5 Apr. 1984

(NASA-TM-83631; E-2069; NAS 1.15 83631) Avail: NTIS HC A03/MF A01 CSCL 11D

Three fiber composites (graphite-fiber epoxy, graphite-fiber aluminum, and graphite-fiber magnesium) are evaluated for their possible use in space applications. Using the composite mechanics theories for thermomechanical behavior embodied in the ICAN (Integrated Composites Analyzer) computer code, select composite thermal and mechanical properties are predicted and also their response to cryogenic temperatures, resembling those which occur in space applications. The predicted results are presented in graphical form as a function of the composite's laminate configuration, fiber volume ratio and the selected use temperature. These results are suitable for preliminary design purposes only and should serve as an aid in selecting controlled experiments for obtaining corresponding measured data.

Author

**N84-24711\*#** National Aeronautics and Space Administration. Lewis Research Center, Cleveland, Ohio.

**METHOD FOR STRENGTHENING BORON FIBERS Patent Application**

J. A. DICARLO, inventor (to NASA) 10 May 1984 12 p (NASA-CASE-LEW-13826-2; US-PATENT-APPL-SN-608742)  
 Avail: NTIS HC A02/MF A01 CSCL 11D

Commercially available boron fibers, produced by the chemical vapor deposition of boron onto tungsten wire substrates, are strengthened by treating them in an oxygen plus inert gas (argon) containing atmosphere for a few minutes at about 880 C. High temperature oxidation increases the residual compression on the tungsten core because the fiber contracts axially during formation of a thin boron oxide coating on the fiber surface. This increases the intrinsic strength of the fiber by raising the tensile strength level required for core initiated fracture. After cooling to room temperature, the fibers are chemically polished to reduce their diameters by 0.2 mils to 0.5 mils. The chemical polish removes both original and oxidation induced surface flaws. The strengthened fibers are intended to be utilized as reinforcement in composite materials. Such materials may be boron/aluminum or boron/epoxy.

NASA

**N84-24712\*#** National Aeronautics and Space Administration. Lewis Research Center, Cleveland, Ohio.

**IMPACT RESISTANCE OF FIBER COMPOSITES: ENERGY ABSORBING MECHANISMS AND ENVIRONMENTAL EFFECTS**

C. C. CHAMIS and J. H. SINCLAIR 1983 25 p refs Presented at the 2nd US/Japan Conf. on Composite Mater.: Mech. Properties, Processing Sci. and Technol. and Appl., Hampton, Va., 6-8 Jun. 1983

(NASA-TM-83594; E-1996; NAS 1.15:83594) Avail: NTIS HC A02/MF A01 CSCL 11D

Energy absorbing mechanisms were identified by several approaches. The energy absorbing mechanisms considered are those in unidirectional composite beams subjected to impact. The approaches used include: mechanic models, statistical models, transient finite element analysis, and simple beam theory. Predicted results are correlated with experimental data from Charpy impact tests. The environmental effects on impact resistance are evaluated. Working definitions for energy absorbing and energy releasing mechanisms are proposed and a dynamic fracture progression is outlined. Possible generalizations to angle-ply laminates are described.

E A.K.

## 24 COMPOSITE MATERIALS

**N84-25770\*#** National Aeronautics and Space Administration. Lewis Research Center, Cleveland, Ohio.

### **DYNAMIC STRESS ANALYSIS OF SMOOTH AND NOTCHED FIBER COMPOSITE FLEXURAL SPECIMENS**

P. L. N. MURTHY and C. C. CHAMIS 1984 27 p refs Presented at the 7th Conf. on Composite Mater.: Testing and Design, Philadelphia, 2-5 Apr. 1984; sponsored by the American Society for Testing and Materials (NASA-TM-83694; E-2152; NAS 1.15:83694) Avail: NTIS HC A03/MF A01 CSCL 11D

A detailed analysis of the dynamic stress field in smooth and notched fiber composite (Charpy-type) specimens is reported in this paper. The analysis is performed with the aid of the direct transient response analysis solution sequence of MSC/NASTRAN. Three unidirectional composites were chosen for the study. They are S-Glass/Epoxy, Kevlar/Epoxy and T-300/Epoxy composite systems. The specimens are subjected to an impact load which is modeled as a triangular impulse with a maximum of 2000 lb and a duration of 1 ms. The results are compared with those of static analysis of the specimens subjected to a peak load of 2000 lb. For the geometry and type of materials studied, the static analysis results gave close conservative estimates for the dynamic stresses. Another interesting inference from the study is that the impact induced effects are felt by S-Glass/Epoxy specimens sooner than Kevlar/Epoxy or T-300/Epoxy specimens. Author

**N84-26755\*#** National Aeronautics and Space Administration. Lewis Research Center, Cleveland, Ohio.

### **ICAN: INTEGRATED COMPOSITES ANALYZER**

P. L. N. MURTHY and C. C. CHAMIS 1984 25 p refs Presented at the 25th Struct., Struct. Dyn. and Mater. Conf., Palm Springs, Calif., 14-16 May 1984; sponsored by the AIAA, ASME, ASCE and AHS (NASA-TM-83700; E-2158; NAS 1.15:83700) Avail: NTIS HC A02/MF A01 CSCL 11D

The ICAN computer program performs all the essential aspects of mechanics/analysis/design of multilayered fiber composites. Modular, open-ended and user friendly, the program can handle a variety of composite systems having one type of fiber and one matrix as constituents as well as intraply and interply hybrid composite systems. It can also simulate isotropic layers by considering a primary composite system with negligible fiber volume content. This feature is specifically useful in modeling thin interply matrix layers. Hygrothermal conditions and various combinations of in-plane and bending loads can also be considered. Usage of this code is illustrated with a sample input and the generated output. Some key features of output are stress concentration factors around a circular hole, locations of probable delamination, a summary of the laminate failure stress analysis, free edge stresses, microstresses and ply stress/strain influence coefficients. These features make ICAN a powerful, cost-effective tool to analyze/design fiber composite structures and components. A.R.H.

**N84-26756\*#** National Aeronautics and Space Administration. Lewis Research Center, Cleveland, Ohio.

### **INTERPLY LAYER DEGRADATION EFFECTS ON COMPOSITE STRUCTURAL RESPONSE**

C. C. CHAMIS and G. C. WILLIAMS 1983 30 p Presented at the 25th Struct., Struct. Dyn. and Mater. Conf., Palm Springs, Calif., 14-16 May 1984; cosponsored by AIAA, ASME, ASCE, and AHS (NASA-TM-83702; E-2160; NAS 1.15:83702) Avail: NTIS HC A03/MF A01 CSCL 11D

Recent research activities at NASA Lewis Research Center to computationally evaluate the effects of interply layer progressive weakening (degradation) on the structural response of a composite beam are summarized. The structural responses of interest include: (1) bending, (2) buckling, (3) free vibrations, (4) periodic excitation, and (5) impact. Finite element analysis was used for the computational evaluations. The interply layer degradation effects on the various structural responses were determined and assessed as a function of the interply layer modulus varying from 1 million

psi down to 1000 psi and even lower for some limiting cases. The results obtained show that the interply layer degradation has generally negligible effects on composite structural response and, therefore, structural integrity, unless the interply layer modulus degrades to about 10,000 psi or less. Author

**N84-27829\*** National Aeronautics and Space Administration. Lewis Research Center, Cleveland, Ohio.

### **METHOD AND APPARATUS FOR GRIPPING UNIAXIAL FIBROUS COMPOSITE MATERIALS Patent**

J. D. WHITTENBERGER and F. I. HURWITZ, inventors (to NASA) 5 Jun. 1984 5 p Filed 15 Sep. 1982 Supersedes N83-12176 (21 - 03, p 0339) (NASA-CASE-LEW-13758-1; US-PATENT-4,452,088; US-PATENT-APPL-SN-418139; US-PATENT-CLASS-73-856; US-PATENT-CLASS-73-833) Avail: US Patent and Trademark Office CSCL 11D

A strip specimen is cut from a unidirectional strong, brittle fiber composite material, and the surfaces of both ends of the specimen are grit blasted. The specimen is then placed between metal load transfer members having grit blasted surfaces. Sufficient compressive stress is applied to the load transfer members to prevent slippage during testing at both elevated temperatures and room temperatures. The need for adhesives, load pads, and other secondary composite processing is eliminated. This gripping system was successful in tensile testing, creep rupture testing, and fatigue testing uniaxial composite materials at 316 C.

Official Gazette of the U.S. Patent and Trademark Office

**N84-27831\*#** National Aeronautics and Space Administration. Lewis Research Center, Cleveland, Ohio.

### **PROGRESSIVE FRACTURE OF FIBER COMPOSITES**

T. B. IRVIN and C. A. GINTY 1983 24 p refs Presented at the 9th Ann. Mech. of Composites Rev., Dayton, 24-26 Oct. 1983 (NASA-TM-83701; E-2159; NAS 1.15:83701) Avail: NTIS HC A02/MF A01 CSCL 11F

Refined models and procedures are described for determining progressive composite fracture in graphite/epoxy angleplied laminates. Lewis Research Center capabilities are utilized including the Real Time Ultrasonic C Scan (RUSCAN) experimental facility and the Composite Durability Structural Analysis (CODSTRAN) computer code. The CODSTRAN computer code is used to predict the fracture progression based on composite mechanics, finite element stress analysis, and fracture criteria modules. The RUSCAN facility, CODSTRAN computer code, and scanning electron microscope are used to determine durability and identify failure mechanisms in graphite/epoxy composites. M.A.C.

**N84-27832\*#** National Aeronautics and Space Administration. Lewis Research Center, Cleveland, Ohio.

### **SIMPLIFIED COMPOSITE MICROMECHANICS EQUATIONS FOR STRENGTH, FRACTURE TOUGHNESS AND ENVIRONMENTAL EFFECTS**

C. C. CHAMIS 1984 27 p refs Presented at the 39th Ann. Conf. of the Soc. of the Plastics Ind. (SPI) Reinforced Plastics/Composites Inst., Houston, 16-20 Jan. 1984 (NASA-TM-83696; E-2154; NAS 1.15:83696) Avail: NTIS HC A03/MF A01 CSCL 11D

A unified set of composite micromechanics equations of simple form is summarized and described. This unified set includes composite micromechanics equations for predicting: (1) ply in plane uniaxial strengths, (2) through the thickness strength, (3) in plane fracture toughness, (4) in plane impact resistance, and (5) through the thickness impact resistance. Equations are also included for predicting the hygrothermal effects on strength, fracture toughness and impact resistance. Several numerical examples are worked out. The numerical examples are selected to demonstrate the interrelationships of the various constituent properties in composite strength and strength related behavior, to make comparisons with available experimental data and to provide insight into composite strength behavior. M.A.C.

**N84-28917\*#** National Aeronautics and Space Administration. Lewis Research Center, Cleveland, Ohio.  
**EFFECTS OF LONG-TIME ELEVATED TEMPERATURE EXPOSURES ON HOT-ISOSTATICALLY-PRESSED POWER-METALLURGY UDIMET 700 ALLOYS WITH REDUCED COBALT CONTENTS**

F. H. HART 1984 18 p refs Presented at 113th Ann. Meeting of the Am. Inst. of Mining and Metallurgical and Petroleum Engr., Los Angeles, 26 Feb. - 2 Mar. 1984 (NASA-TM-83632, E-2071; NAS 1.15:83632) Avail: NTIS HC A02/MF A01 CSCL 11D

Because almost the entire U.S. consumption of cobalt depends on imports, this metal has been designated 'strategic'. The role and effectiveness of cobalt is being evaluated in commercial nickel-base superalloys. Udimet 700 type alloys in which the cobalt content was reduced from the normal 17% down to 12.7%, 8.5%, 4.3%, and 0% were prepared by standard powder metallurgy techniques and hot isostatically pressed into billets. Mechanical testing and microstructural investigations were performed. The mechanical properties of alloys with reduced cobalt contents which were heat-treated identically were equal or better than those of the standard alloy, except that creep rates tended to increase as cobalt was reduced. The effects of long time exposures at 760 C on mechanical properties and at 760 C and 845 C on microstructures were determined. Decreased tensile properties and shorter rupture lives with increased creep rates were observed in alloy modifications. The exposures caused gamma prime particle coarsening and formation of sigma phase in the alloys with higher cobalt contents. Exposure at 845 C also reduced the amount of MC carbides.

Author

**N84-28918\*#** National Aeronautics and Space Administration. Lewis Research Center, Cleveland, Ohio.

**HYGROTHERMOMECHANICAL FRACTURE STRESS CRITERIA FOR FIBER COMPOSITES WITH SENSE-PARITY**

C. C. CHAMIS and C. A. GINTY 1983 15 p refs Presented at the 7th Conf. on Composite Mater.: Testing and Design, Philadelphia, 2-5 Apr. 1984; sponsored by Am. Soc. for Testing and Mater.

(NASA-TM-83691; E-2146; NAS 1.15:83691) Avail: NTIS HC A02/MF A01 CSCL 11D

Hygrothermomechanical fracture stress criteria are developed and evaluated for unidirectional composites (plies) with sense-parity. These criteria explicitly quantify the individual contributions of applied, hygral and thermal stresses as well as couplings among these stresses. The criteria are for maximum stress, maximum strain, internal friction, work-to-fracture and combined-stress fracture. Predicted results obtained indicate that first ply failure will occur at stress levels lower than those predicted using criteria currently available in the literature. Also, the contribution of the various stress couplings (predictable only by fracture criteria with sense-parity) is significant to first ply failure and attendant fracture modes

Author

**N84-31288\*#** National Aeronautics and Space Administration. Lewis Research Center, Cleveland, Ohio.

**APPLICATION OF FINITE ELEMENT SUBSTRUCTURING TO COMPOSITE MICROMECHANICS M.S. Thesis - Akron Univ., May 1984**

J. J. CARUSO Aug. 1984 70 p refs (Contract NSG-350)

(NASA-TM-83729; E-2203; NAS 1.15:83729) Avail: NTIS HC A04/MF A01 CSCL 11D

Finite element substructuring is used to predict unidirectional fiber composite hygral (moisture), thermal, and mechanical properties. COSMIC NASTRAN and MSC/NASTRAN are used to perform the finite element analysis. The results obtained from the finite element model are compared with those obtained from the simplified composite micromechanics equations. A unidirectional composite structure made of boron/HM-epoxy, S-glass/IMHS-epoxy and AS/IMHS-epoxy are studied. The finite element analysis is performed using three dimensional isoparametric brick elements and two distinct models. The first

model consists of a single cell (one fiber surrounded by matrix) to form a square. The second model uses the single cell and substructuring to form a nine cell square array. To compare computer time and results with the nine cell superelement model, another nine cell model is constructed using conventional mesh generation techniques. An independent computer program consisting of the simplified micromechanics equation is developed to predict the hygral, thermal, and mechanical properties for this comparison. The results indicate that advanced techniques can be used advantageously for fiber composite micromechanics.

Author

**N84-33522\*#** National Aeronautics and Space Administration. Lewis Research Center, Cleveland, Ohio.

**FRACTURE SURFACE CHARACTERISTICS OF NOTCHED ANGLEPLY GRAPHITE/EPOXY COMPOSITES**

C. A. GINTY and T. B. IRVINE 1984 25 p refs Presented at the Intern. Symp. on Composites: Mater. and Eng., Newark, Del., 24-28 Sep. 1984; sponsored by the Center for Composite Materials

(NASA-TM-83786; E-2284; NAS 1.15:83786) Avail: NTIS HC A02/MF A01 CSCL 11D

Composite fracture surface characteristics and related fracture modes have been investigated through extensive microscopic inspections of the fracture surfaces of notched angleply graphite/epoxy laminates. The investigation involved 4 ply laminates of the configuration  $\pm$  or  $\theta$  (s) where  $\theta = 0$  deg, 3 deg, 5 deg, 10 deg, 15 deg, 30 deg, 45 deg, 60 deg, 75 deg, and 90 deg. Two-inch wide tensile specimens with 0.25 in. by 0.05 in. through-slits centered across the width were tested to fracture. The fractured surfaces were then removed and examined using a scanning electron microscope. Evaluation of the photomicrographs combined with analytical results obtained using the CODSTRAN computer code culminated in a unified set of fracture criteria for determining the mode of fracture in notched angleply graphite/epoxy laminates.

Author

**N84-34575\*#** Case Western Reserve Univ., Cleveland, Ohio.

**MECHANICAL BEHAVIOR OF CARBON-CARBON COMPOSITES Final Report**

G. A. ROZAK Sep. 1984 31 p refs (Contract NAG3-464)

(NASA-CR-174767; NAS 1.26:174767) Avail: NTIS HC A03/MF A01 CSCL 11D

A general background, test plan, and some results of preliminary examinations of a carbon-carbon composite material are presented with emphasis on mechanical testing and inspection techniques. Experience with testing and evaluation was gained through tests of a low modulus carbon-carbon material, K-Karb C. The properties examined are the density - 1.55 g/cc; four point flexure strength in the warp - 137 MPa (19,800 psi) and the fill - 95.1 MPa (13,800 psi) directions; and the warp interlaminar shear strength - 14.5 MPa (2100 psi). Radiographic evaluation revealed thickness variations and the thinner areas of the composite were scrapped. The ultrasonic C-scan showed attenuation variations, but these did not correspond to any of the physical and mechanical properties measured. Based on these initial tests and a survey of the literature, a plan has been devised to examine the effect of stress on the oxidation behavior, and the strength degradation of coated carbon-carbon composites. This plan will focus on static fatigue tests in the four point flexure mode in an elevated temperature, oxidizing environment.

Author



**N84-34576\*#** National Aeronautics and Space Administration. Lewis Research Center, Cleveland, Ohio.

**FRACTURE MODES IN NOTCHED ANGLEPLY COMPOSITE LAMINATES**

T. B. IRVINE and C. A. GINTY 1984 27 p refs Presented at Symp. on Composite Fatigue and Fracture, Dallas, 24-25 Oct. 1984; sponsored by American Society for Testing and Materials (NASA-TM-83802; E-2307; NAS 1.15:83802) Avail: NTIS HC A03/MF A01 CSCL 11D

The Composite Durability Structural Analysis (CODSTRAN) computer code is used to determine composite fracture. Fracture modes in solid and notched, unidirectional and angleplyed graphite/epoxy composites were determined by using CODSTRAN. Experimental verification included both nondestructive (ultrasonic C-Scanning) and destructive (scanning electron microscopy) techniques. The fracture modes were found to be a function of ply orientations and whether the composite is notched or unnotched. Delaminations caused by stress concentrations around notch tips were also determined. Results indicate that the composite mechanics, structural analysis, laminate analysis, and fracture criteria modules embedded in CODSTRAN are valid for determining composite fracture modes. R.J.F.

## 25

## INORGANIC AND PHYSICAL CHEMISTRY

Includes chemical analysis, e.g., chromatography; combustion theory; electrochemistry; and photochemistry.

**A84-10140\*#** California Univ., Berkeley.

**COMBUSTION IN A TURBULENT MIXING LAYER FORMED AT A REARWARD-FACING STEP**

R. W. PITZ and J. W. DAILY (California, University, Berkeley, CA) AIAA Journal (ISSN 0001-1452), vol. 21, Nov. 1983, p. 1565-1570. refs

(Contract NSF-ENG-77-02019; NSG-3227)

A premixed propane/air flame was stabilized in a turbulent mixing layer formed at a rearward-facing step. The mean and rms averages of the turbulent velocity flowfield were determined by laser velocimetry for both reacting ( $\phi = 0.57$ ) and nonreacting flows ( $Re = 15,000-37,000$  based on step height). The reacting-flow was visualized by high-speed schlieren photography. Large-scale structures dominate the reacting mixing layer. The growth of the large-scale structures was tied to the propagation of the flame. The linear growth rate of the reacting mixing layer defined by the mean velocity profiles was unchanged by combustion but the virtual origin moves downstream. The reacting mixing layer boundaries based on the mean velocity profiles were shifted toward the recirculation zone and reattachment lengths were shortened by 30 percent. The edge of the flame controlled by the large-scale structure development propagated faster into the incoming reactants than the boundary of the mixing layer given by the mean velocity flowfield. Thus, the region of high velocity gradient did not coincide with the region of high reaction and heat transfer.

Author

**A84-11636\*** Pennsylvania State Univ., University Park.

**EVAPORATION AND COMBUSTION OF SPRAYS**

G. M. FAETH (Pennsylvania State University, University Park, PA) Progress in Energy and Combustion Science (ISSN 0360-1285), vol. 7, no. 1-2, 1983, p. 1-76. refs

(Contract NGR-39-009-077; NSG-3306; NAG3-190)

A description is provided of recent spray evaporation and combustion models, taking into account turbulent two- and three-dimensional spray processes found in furnaces, gas turbine combustors, and internal combustion engines. Within the class of spray models of interest, two major categories are distinguished, including locally homogeneous flow (LHF) models and separated flow (SF) models. SF models are of the greatest practical

importance, but LHF models have distinct advantages in some cases. Attention is also given to recent progress on modeling interactions between drops and the flow in both dilute and dense sprays, involving sprays having low and high liquid volume fractions, respectively. G.R.

**A84-12644\*** Giner, Inc., Waltham, Mass.

**IMPORTANCE OF INTERATOMIC SPACING IN CATALYTIC REDUCTION OF OXYGEN IN PHOSPHORIC ACID**

V. JALAN and E. J. TAYLOR (Giner, Inc., Waltham, MA) Electrochemical Society, Journal (ISSN 0013-4651), vol. 130, Nov. 1983, p. 2299-2302. refs

(Contract DEN3-294)

A correlation between the nearest-neighbor distance and the oxygen reduction activity of various platinum alloys is reported. It is proposed that the distance between nearest-neighbor Pt atoms on the surface of a supported catalyst is not ideal for dual site absorption of O<sub>2</sub> or 'HO<sub>2</sub>' and that the introduction of foreign atoms which reduce the Pt nearest-neighbor spacing would result in higher oxygen reduction activity. This may allow the critical O-O bond interatomic distance and hence the optimum Pt-Pt separation for bond rupture to be determined from quantum chemical calculations. A composite analysis shows that the data on supported Pt alloys are consistent with Appleby's (1970) data on bulk metals with respect to specific activity, activation energy, preexponential factor, and percent d-band character. C.D.

**A84-17436\*#** California Univ., Berkeley.

**SECONDARY EFFECTS IN COMBUSTION INSTABILITIES LEADING TO FLASHBACK**

L. VANEVELD, K. HOM, and A. K. OPPENHEIM (California, University, Berkeley, CA) AIAA Journal (ISSN 0001-1452), vol. 22, Jan. 1984, p. 81, 82.

(Contract NSG-3227; W-7405-ENG-48)

Previously cited in issue 06, p. 829, Accession no. A82-17746

**A84-18925\*** Northwestern Univ., Evanston, Ill.

**AN INVARIANT DERIVATION OF FLAME STRETCH**

S. H. CHUNG and C. K. LAW (Northwestern University, Evanston, IL) Combustion and Flame (ISSN 0010-2180), vol. 55, Jan. 1984, p. 123-125. refs

(Contract NAG3-361)

The flame stretch factor is derived using an invariant formulation in a consistent manner. The derived generalized expression has two terms and completely describes the flame area evolution with its movement. One term represents the stretch due to the nonuniform tangential velocity field and the other represents the effect of the curvature of the propagating flame. The effect of curvature for stationary flames is implicitly included in the former term through variations of the tangential velocity. The flame sheet assumption, and thereby the stretch factor, are uniquely defined. Another expression is derived under the assumption that the tangential velocity of the flame equals the tangential component of the fluid velocity. C.D.

**A84-23593\*** Northwestern Univ., Evanston, Ill.

**EXTINCTION OF PREMIXED FLAMES BY STRETCH AND RADIATIVE LOSS**

S. H. SOHRAB and C. K. LAW (Northwestern University, Evanston, IL) International Journal of Heat and Mass Transfer (ISSN 0017-9310), vol. 27, Feb. 1984, p. 291-300. refs

(Contract NAG3-53; NAG3-361)

The extinction of laminar premixed flames by stretch and radiative loss is studied for the model problem of counterflow opposed-jet combustion by using the matched asymptotic expansion technique for the highly temperature sensitive processes of radiative heat loss and large-activation-energy reaction kinetics. Explicit expressions for the critical Damkoehler number at extinction are derived and the influence of upstream vs downstream heat losses assessed. Results show that stretch exerts a much stronger influence than radiative loss on flame extinction. Author



**A84-27724\*** California Univ., Santa Barbara.

**THE CHEMICAL KINETICS AND THERMODYNAMICS OF SODIUM SPECIES IN OXYGEN-RICH HYDROGEN FLAMES**

A. J. HYNES, M. STEINBERG, and K. SCHOFIELD (California, University, Santa Barbara, CA) *Journal of Chemical Physics* (ISSN 0021-9606), vol. 80, March 15, 1984, p. 2585-2597. refs (Contract NSG-3256; DE-AM03-76SF-00034-PA-372)

Results are presented which, it is claimed, lead to a correction of previous misconceptions over the relative importance and kinetics of NaO<sub>2</sub>. It is shown that its rapid conversion to NaO and NaOH is such that it can severely perturb the NaOH/Na ratio and produce significant concentration overshoots over that predicted from the balance of the reaction of Na with H<sub>2</sub>O. This becomes increasingly the case in flames of large O<sub>2</sub> concentrations and temperatures below 2500 K; and the corresponding large rate constants for the termolecular formation of the other alkali peroxides imply that similar considerations will be necessary for them. Depending on the rate constants for the exothermic conversions of MO<sub>2</sub> to MO or MOH, the steady-state concentrations of MO<sub>2</sub> could be more or less significant than for sodium. Owing to numerous reactions that produce these conversions, the MOH species will probably be the dominant species in all cases in oxygen-rich hydrogen or hydrocarbon flames, with MO concentrations at not greater than 1 percent of the bound metal. B.J.

**A84-29128\*** California Univ., Berkeley.

**DYNAMIC EFFECTS OF COMBUSTION**

A. K. OPPENHEIM (California, University, Berkeley, CA) IN: U.S. National Congress of Applied Mechanics, 9th, Ithaca, NY, June 21-25, 1982, Proceedings. New York, American Society of Mechanical Engineers, 1982, p. 29-40. refs (Contract W-7405-ENG-48; NSF CPE-81-15163; NAG3-131; NAG3-137)

The dynamic effects of combustion are due to the evolution of exothermic energy and its deposition in the compressible medium where the process takes place. The paper examines the dynamics of combustion phenomena, including ignition, turbulent flame propagation (inflammation), explosion, and detonation, with emphasis on their exothermic characteristics. Ignition and explosion are treated as problems of nonlinear mechanics, and their dynamic behavior is described in terms of phase space models and cinematographic laser shear interferograms. The results of a numerical random vortex model of turbulent flame propagation are confirmed in a combustion tunnel experiment, where it was observed that a fresh mixture of burnt and unburnt gases can sustain combustion with a relatively small expenditure of overall mass flow, due to the increasing specific volume of burnt gases inside the flame front. An isentropic pressure wave is found to precede the accelerating flame in the process of detonation, and components of this pressure wave are shown to propagate at local sonic velocities. I.H.

**A84-29999\*** Clarkson Coll. of Technology, Potsdam, N.Y.

**ELECTRODE KINETICS OF OXYGEN REDUCTION - A THEORETICAL AND EXPERIMENTAL ANALYSIS OF THE ROTATING RING-DISC ELECTRODE METHOD**

K.-L. HSUEH, D.-T. CHIN (Clarkson College of Technology, Potsdam, NY), and S. SRINIVASAN (Los Alamos National Laboratory, Los Alamos, NM) *Journal of Electroanalytical Chemistry and Interfacial Electrochemistry* (ISSN 0022-0728), vol. 153, 1983, p. 79-95. Research sponsored by the U.S. Department of Energy. refs (Contract NAG3-238)

In order to calculate most of the rate constants for the intermediate formation of H<sub>2</sub>O<sub>2</sub> in the electroreduction of O<sub>2</sub> to H<sub>2</sub>O, the theoretical treatments of the rotating ring-disc electrode method by Damjanovic et al. (1966, 1967), Bagotskii et al. (1968, 1969), and Wroblowa et al. (1976) are modified. Rotating ring-disc electrode experimental data obtained for O<sub>2</sub> reduction in Pt in 0.55 M H<sub>2</sub>SO<sub>4</sub> are used to illustrate the calculations of rate constants according to the above theoretical treatments. A simple reaction model as proposed by the first author is consistent with

the experimental data. The results indicate that O<sub>2</sub> (97 percent) reduces to H<sub>2</sub>O in a direct four-electron transfer reaction. The adsorption of O<sub>2</sub> is probably the rate-determining step in the potential region more negative than 0.5 V vs. reversible hydrogen electrode. J.N.

**A84-32612\*** Cornell Univ., Ithaca, N.Y.

**TIME-RESOLVED DENSITY MEASUREMENTS IN PREMIXED TURBULENT FLAMES**

F. C. GOULDIN (Cornell University, Ithaca, NY) and K. V. DANDEKAR (Illinois, University, Chicago, IL) *AIAA Journal* (ISSN 0001-1452), vol. 22, May 1984, p. 655-663. Research supported by the General Motors Corp. and U.S. Navy. refs (Contract NSG-3019)

Previously cited in issue 08, p 1196, Accession no. A83-22033

**A84-35401\***

**SYMPOSIUM (INTERNATIONAL) ON COMBUSTION, 19TH, TECHNION ISRAEL INSTITUTE OF TECHNOLOGY, HAIFA, ISRAEL, AUGUST 8-13, 1982, PROCEEDINGS**

Symposium sponsored by the Ministry of Energy and Infrastructure, Ministry of Industry and Trade, National Council for Research and Development, U.S. Army, U.S. Department of Energy, NASA, NBS, NSF, et al.; Pittsburgh, PA, Combustion Institute, 1982, 1598 p. (Contract DE-FG22-82PC-50259; NAS3-23370; NSF CPE-81-2019; NSF CPE-81-20506)

Topics discussed are related to elementary reactions, reaction mechanisms and modeling, laminar flames, flame chemistry, turbulent reacting shear flows, turbulent premixed flames, turbulent combustion measurements, continuous combustors, detonation, detonation and explosion, heterogeneous detonation, propellant combustion, fire-ignition and thermal degradation, fire-flame spread and burning, fire-modeling, spray combustion, and droplet combustion. Coal combustion kinetics and mechanisms are considered along with coal combustion mechanisms and pyrolysis, coal combustion techniques, NO<sub>x</sub> in coal combustion, gaseous pollutants, soot and PAH, soot and inorganic pollutants, I.C. engine combustion, and ignition and extinction. Attention is given to intricate paths and simple steps in chemical kinetics and combustion, the formation of polycyclic aromatic hydrocarbons by combustion, turbulent flame structure and speed in spark ignition engines, and unresolved problems in SO<sub>x</sub>, NO<sub>x</sub>, and soot control in combustion. G.R.

**A84-35425\*** Northwestern Univ., Evanston, Ill.

**AN EXPERIMENTAL STUDY ON EXTINCTION AND STABILITY OF STRETCHED PREMIXED FLAMES**

S. ISHIZUKA (Saitama Institute of Technology, Okabe, Japan) and C. K. LAW (Northwestern University, Evanston, IL) IN: Symposium (International) on Combustion, 19th, Haifa, Israel, August 8-13, 1982, Proceedings. Pittsburgh, PA, Combustion Institute, 1982, p. 327-334; Comments and Author's Reply, p. 334, 335. refs (Contract N00014-80-C-0568; NAG3-53)

Law et al. (1981) and Ishizuka et al. (1982) have experimentally investigated the effects of flame stretch, preferential diffusion, and downstream heat loss on the extinction and stability of propane/air flames. The obtained results suggest that in the case of rich propane/air mixtures downstream heat loss, in addition to flame stretch, is needed for flame extinction. In the case of lean mixtures, flames can be extinguished by flame stretch alone. The data obtained in connection with the present study provide convincing evidence regarding the correctness of the previous results on the nature of flame extinction due to stretch. It is found that, in accordance with theoretical predictions, extinction by stretch alone is possible only when there is a deficiency regarding the less mobile reactant. G.R.

**A84-45917\*** National Aeronautics and Space Administration. Lewis Research Center, Cleveland, Ohio.

**CORRELATION OF ELECTRON EMISSION WITH CHANGES IN THE SURFACE CONCENTRATION OF BARIUM AND OXYGEN ON A TUNGSTEN SURFACE**

R. FORMAN (NASA, Lewis Research Center, Cleveland, OH) Applications of Surface Science (ISSN 0378-5963), vol. 17, 1984, p. 429-462. refs

**A84-48139\*#** Massachusetts Inst. of Tech., Cambridge. **NUMERICAL SOLUTION FOR THE PROBLEM OF FLAME PROPAGATION BY THE RANDOM ELEMENT METHOD** A. F. GHONIEM (MIT, Cambridge, MA) and A. K. OPPENHEIM (California, University, Berkeley, CA) AIAA Journal (ISSN 0001-1452), vol. 22, Oct. 1984, p. 1429-1435. Previously cited in issue 16, p. 2326, Accession no. A83-36062. refs (Contract W-7405-ENG-48; NSF CPE-81-15163; NAG3-131)

**N84-11228\*#** Ultrasystems, Inc., Irvine, Calif. **SYNTHESIS OF PERFLUOROALKYLENE DIANILINES** Final Contractor Report, 5 Sep. 1980 - 5 Nov. 1981 K. L. PACIOREK, T. I. ITO, D. H. HARRIS, C. M. BEECHAN, J. H. NAKAHAM, and R. H. KRATZER Nov. 1981 43 p refs (Contract NAS3-22519) (NASA-CR-168004; NAS 1.26:168004; SN-1021-F) Avail: NTIS HC A03/MF A01 CSCL 07D

The objective of this contract was to optimize and scale-up the synthesis of 2,2-bis(4-aminophenyl)-hexafluoropropane and 1,3-bis(4-aminophenyl)hexafluoropropane, as well as to explore avenues to other perfluoroalkyl-bridged dianilines. Routes other than Friedel-Crafts reaction leading to 2,2-bis(4-aminophenyl)hexafluoropropane were investigated. The processes utilizing bisphenol-AF were all unsuccessful; reactions aimed at the production of 4-(hexafluoro-2-halo-isopropyl)aniline from the hydroxyl intermediate failed to yield the desired products. Tailoring the conditions of the Friedel-Crafts reaction of 4-(hexafluoro-2-hydroxyisopropyl)aniline, aniline, and aluminum chloride by using hydrochloride salts and selecting optimum reagent ratios, reaction times, and temperature resulted in approx. 20% yield of pure crystallized 2,2-bis(4-aminophenyl)hexafluoropropane in 0.2 mole reaction batches. Yields up to approx. 40% were realized in small, approx. 0.01 mole, batches. The synthesis of 1,3-bis(4-aminophenyl)hexafluoropropane starting with perfluoroglutanidine was reinvestigated. The yield of the 4-step reaction sequence giving 1,3-bis(4-acetamidophenyl)hexafluoropropane was raised to 44%. The yield of the subsequent hydrolysis process was improved by a factor of approx. 2. Approaches to prepare other perfluoroalkyl-bridged dianilines were unsuccessful. Reactions reported to proceed readily with trifluoromethyl substituents failed when longer chain perfluoroalkyl groups were employed. Author

**N84-11229\*#** Ultrasystems, Inc., Irvine, Calif. **THERMAL OXIDATIVE DEGRADATION REACTIONS OF PERFLUOROALKYLETHERS** Contractor Report, 6 Nov. 1981 - 30 Jun. 1983 K. L. PACIOREK, D. H. HARRIS, M. E. SMYTHE, and R. H. KRATZER Jul. 1983 39 p refs (Contract NAS3-22517) (NASA-CR-168224; NAS 1.26:168224; SN-1020-A2-F) Avail: NTIS HC A03/MF A01 CSCL 07D

The objective of this contract was to investigate the mechanisms operative in thermal and thermal oxidative degradation of Fomblin Z and hexafluoropropene oxide derived fluids and the effect of alloys and additives upon these processes. The nature of arrangements responsible for the inherent thermal oxidative instability of the Fomblin Z fluids has not been established. It was determined that this behavior was not associated with hydrogen end-groups or peroxy linkages. The degradation rate of these fluids at elevated temperatures in oxidizing atmospheres was found to be dependent on the surface/volume ratio. Once a limiting ratio was reached, a steady rate appeared to be attained. Based on elemental analysis and oxygen consumption data,

-CF<sub>2</sub>OCF<sub>2</sub>CF<sub>2</sub>O-, not -CF<sub>2</sub>CF<sub>2</sub>O-, is one of the major arrangements present. The action of the M-50 and Ti(4 Al, 4 Mn) alloys was found to be much more drastic in the case of Fomblin Z fluids than that observed for the hexafluoropropane oxide derived materials. The effectiveness of antioxidation/anticorrosion additives, P-3 and phospho-s-triazine, in the presence of metal alloys was very limited at 316 C; at 288 C the additives-arrested almost completely the fluid degradation. The phospho-s-triazine appeared to be at least twice as effective as the P-3 compound; it also protected the coupon better. The Ti(4 Al, 4 Mn) alloy degraded the fluid mainly by chain scission processes; this took place to a much lesser degree with M-50. B.W.

**N84-12263\*#** Garrett Turbine Engine Co., Phoenix, Ariz. **EXECUTIVE SUMMARY, AEROTHERMAL MODELING PROGRAM, PHASE 1** R. SRINIVASAN, R. REYNOLDS, I. BAIL, R. BERRY, K. JOHNSON, and H. MONGIA Aug 1983 54 p (Contract NAS3-23523) (NASA-CR-174602; NAS 1.26:174602; GARRETT-21-4766) Avail: NTIS HC A04/MF A01 CSCL 21B

Submodels used in the combustor analytical models that were successfully used in designing advanced technology combustors were assessed. Specific recommendations for further improvement of model accuracy for combustor design purposes were made. Based upon an exhaustive literature survey, a number of test cases were selected to assess accuracy of submodels of turbulence, turbulence/chemistry interaction, spray combustion, and dilution jet mixing processes within a confined cross-stream. These test cases included simple flows and complex flows with and without swirl Nonrecirculating and recirculating, and nonreactive and reactive flows were investigated. It was concluded that the current models give qualitative trends for the recirculating secondary flows (as encountered in a gas turbine combustor primary zone), but the predictions are good for the dilution zone. S.L.

**N84-12265\*#** Garrett Turbine Engine Co., Phoenix, Ariz. **AEROTHERMAL MODELING PROGRAM, PHASE 1** R. SRINIVASAN, R. REYNOLDS, I. BALL, R. BERRY, K. JOHNSON, and H. MONGIA Aug. 1983 351 p refs (Contract NAS3-23523) (NASA-CR-168243-VOL-2; NAS 1.26:168243-VOL-2; GARRETT-21-4742-2) Avail: NTIS HC A16/MF A01 CSCL 21B

The combustor performance submodels for complex flows are evaluated. The benchmark test cases for complex nonswirling flows are identified and analyzed. The introduction of swirl into the flow creates much faster mixing, caused by radial pressure gradients and increase in turbulence generation. These phenomena are more difficult to predict than the effects due to geometrical streamline curvatures, like the curved duct, and sudden expansion. Flow fields with swirl, both confined and unconfined are studied. The role of the dilution zone to achieve the turbine inlet radial profile plays an important part, therefore temperature field measurements were made in several idealized dilution zone configurations. S.L.

**N84-16276\*** National Aeronautics and Space Administration. Lewis Research Center, Cleveland, Ohio. **MICRONIZED COAL BURNER FACILITY Patent** F. D. CALFO and M. W. LUPTON, inventors. (to NASA) 17 Jan. 1984 6 p Filed 30 Jun. 1982 Supersedes N82-31769 (20 - 22, p 3149) (NASA-CASE-LEW-13426-1; US-PATENT-4,425,854; US-PATENT-APPL-SN-393588; US-PATENT-CLASS-110-262; US-PATENT-CLASS-110-186; US-PATENT-CLASS-110-263; US-PATENT-CLASS-110-265; US-PATENT-CLASS-431-1) Avail: US Patent and Trademark Office CSCL 21B

A combustor or burner system in which the ash resulting from burning a coal in oil mixture is of submicron particle size is described. The burner system comprises a burner section, a flame exit nozzle, a fuel nozzle section, and an air tube by which preheated air is directed into the burner section. Regulated air

pressure is delivered to a fuel nozzle. Means are provided for directing a mixture of coal particles and oil from a drum to a nozzle at a desired rate and pressure while means returns excess fuel to the fuel drum. Means provide for stable fuel pressure supply from the fuel pump to the fuel nozzle.

Official Gazette of the U.S. Patent and Trademark Office

**N84-19495\*#** Drexel Univ., Philadelphia, Pa Dept. of Mechanical Engineering and Mechanics.

**COMBUSTION CHARACTERISTICS IN THE TRANSITION REGION OF LIQUID FUEL SPRAYS** Annual Progress Report, Jan. 1983 - Jan. 1984

N. P. CERNANSKY, I. NAMER, and R. J. TIDONA Jan. 1984 28 p refs

(Contract NAG3-382)

(NASA-CR-175396; NAS 1.26:175396) Avail: NTIS HC A03/MF A01 CSCL 21B

A number of important effects were observed in the droplet size transition region in spray combustion systems. In this region, where the mechanism of flame propagation is transformed from diffusive to premixed dominated combustion, the following effects have been observed (1) maxima in burning velocity; (2) extension of flammability limits; (3) minima in ignition energy; and (4) minima in NO(x) formation. Unfortunately, because of differences in experimental facilities and limitations in the ranges of experimental data, a unified description of these transition region effects is not available at this time. Consequently, a fundamental experimental investigation was initiated to study the effect of droplet size, size distribution, and operating parameters on these transition region phenomena in a single well controlled spray combustion facility.

Author

**N84-20530\*#** Tennessee Univ. Space Inst., Tullahoma. Applied Physics Research Group.

**MEASUREMENT OF SPRAY COMBUSTION PROCESSES**

C. E. PETERS, E. F. ARMAN, J. O. HORNKOHL, and W. M. FARMER In NASA. Lewis Research Center Combust. Fundamentals Res. p 47-50 Apr. 1984 refs

(Contract NAG3-370)

Avail: NTIS HC A14/MF A01 CSCL 21B

A free jet configuration was chosen for measuring noncombusting spray fields and hydrocarbon-air spray flames in an effort to develop computational models of the dynamic interaction between droplets and the gas phase and to verify and refine numerical models of the entire spray combustion process. The development of a spray combustion facility is described including techniques for laser measurements in spray combustion environments and methods for data acquisition, processing, displaying, and interpretation.

A.R.H.

**N84-20532\*#** Pennsylvania State Univ., University Park.

**PREDICTIONS OF SPRAY COMBUSTION INTERACTIONS**

J. S. SHUEN, A. S. P. SOLOMON, and G. M. FAETH In NASA. Lewis Research Center Combust. Fundamentals Res. p 55-66 Apr. 1984 refs

(Contract NAG3-190)

Avail: NTIS HC A14/MF A01 CSCL 21B

Mean and fluctuating phase velocities; mean particle mass flux; particle size, and mean gas-phase Reynolds stress, composition and temperature were measured in stationary, turbulent, axisymmetric, and flows which conform to the boundary layer approximations while having well-defined initial and boundary conditions in dilute particle-laden jets, nonevaporating sprays, and evaporating sprays injected into a still air environment. Three models of the processes, typical of current practice, were evaluated. The local homogeneous flow and deterministic separated flow models did not provide very satisfactory predictions over the present data base. In contrast, the stochastic separated flow model generally provided good predictions and appears to be an attractive approach for treating nonlinear interphase transport processes in turbulent flows containing particles (drops).

A.R.H.

**N84-20535\*#** Carnegie-Mellon Univ., Pittsburgh, Pa. Dept. of Mechanical Engineering.

**TURBULENT SWIRLING COMBUSTION**

H. T. SOMMER, R. J. MOSULA, and E. SEIDEN In NASA. Lewis Research Center Combust. Fundamentals Res. p 81-82 Apr. 1984 refs

(Contract NAG3-401)

Avail: NTIS HC A14/MF A01 CSCL 21B

The non-reacting flow produced by two confined, co- and/or counter-swirling jets were measured by means of a two-color laser Doppler velocimeter. These results are compared with earlier experiments and with numerical predictions. It is shown that under both swirl conditions, a closed recirculation zone is created at the combustor center line. This zone is characterized by the presence of a one-cell toroidal vortex, low tangential velocities, high turbulent intensity, and large dissipation rates of the kinetic energy of turbulence.

A.R.H.

**N84-20554\*#** National Aeronautics and Space Administration. Lewis Research Center, Cleveland, Ohio.

**FAST ALGORITHMS FOR COMBUSTION KINETICS CALCULATIONS: A COMPARISON**

K. RADHAKRISHNAN (Michigan Univ.) In NASA. Lewis Research Center Combust. Fundamentals Res. p 257-267 Apr. 1984 refs

(Contract NAG3-147; NAG3-294)

Avail: NTIS HC A14/MF A01 CSCL 21B

To identify the fastest algorithm currently available for the numerical integration of chemical kinetic rate equations, several algorithms were examined. Findings to date are summarized. The algorithms examined include two general-purpose codes EPISODE and LSODE and three special-purpose (for chemical kinetic calculations) codes CHEMEQ, CRK1D, and GCKP84. In addition, an explicit Runge-Kutta-Merson differential equation solver (MSL Routine DASCURU) is used to illustrate the problems associated with integrating chemical kinetic rate equations by a classical method. Algorithms were applied to two test problems drawn from combustion kinetics. These problems included all three combustion regimes: induction, heat release and equilibration. Variations of the temperature and species mole fraction are given with time for test problems 1 and 2, respectively. Both test problems were integrated over a time interval of 1 ms in order to obtain near-equilibration of all species and temperature. Of the codes examined in this study, only CREK1D and GCDP84 were written explicitly for integrating exothermic, non-isothermal combustion rate equations. These therefore have built-in procedures for calculating the temperature.

R.J.F.

**N84-20555\*#** Princeton Univ., N. J.

**THE ROLE OF SURFACE GENERATED RADICALS IN CATALYTIC COMBUSTION**

D. A. SANTAVICCA, Y. STEIN, and B. S. H. ROYCE In NASA. Lewis Research Center Combust. Fundamentals Res. p 269-274 Apr. 1984 refs

(Contract NAG3-353; AF-AFOSR-6475)

Avail: NTIS HC A14/MF A01 CSCL 21B

The role of surface generated OH radicals in determining the catalytic ignition characteristics for propane oxidation on platinum were studied. The experiments were conducted in a stacked-plate, catalyst bed. Transient measurements, during catalytic ignition, of the catalyst's axial temperature profile were made and the effect of equivalence ratio, inlet temperature and inlet velocity was investigated. These measurements will provide insights which will be useful in planning and interpreting to OH measurements. Attempts to measure OH concentration in the catalyst bed using resonance absorption spectroscopy were unsuccessful, indicating that OH concentrations are below 10 to the 16th power/cc but still possibly above equilibrium values. Measurements are currently underway using forward scatter laser induced fluorescence which should extend the OH detection limits several orders of magnitude below the equilibrium concentrations.

R.J.F.

**N84-20558\*#** National Aeronautics and Space Administration. Lewis Research Center, Cleveland, Ohio.

**RANDOM VORTEX METHOD FOR COMBUSTING FLOWS**

C. J. MAREK *In its* Combust. Fundamentals Res. p 297-300 Apr. 1984 refs

Avail: NTIS HC A14/MF A01 CSCL 21B

The random vortex method (RVM) of Chorin was developed by the recirculating flows. The RVM method models turbulence from first principles, tracking the vorticity and obtaining the interaction of vorticity with the bulk flow field. A computer program was produced called MIMOC, Modeling the Interface Motion of Combustion, which can be used to calculate the reacting flow field behind a rearward facing step. Several comparisons between experimental data and calculations were made. The RVM method computes qualitatively good results, but the quantitative agreement as yet is not completely satisfactory. Much of the difficulty may be caused by the treatment of boundary conditions and the techniques used for obtaining statistical averages of velocities and turbulence quantities. For the rearward facing step the computed reattachment length equals the experimental value. However, the reverse velocity in the recirculation zone is over predicted by 300 percent. In the calculations, a uniform entrance velocity was assumed with no boundary layer at the step lip. This high velocity may be overdriving the reverse flow region. R.J.F.

**N84-20560\*#** National Aeronautics and Space Administration. Lewis Research Center, Cleveland, Ohio.

**TRANSIENT FLOW COMBUSTION**

R. R. TACINA *In its* Combust. Fundamentals Res. p 309-310 Apr. 1984

Avail: NTIS HC A14/MF A01 CSCL 21B

Non-steady combustion problems can result from engine sources such as accelerations, decelerations, nozzle adjustments, augmentor ignition, and air perturbations into and out of the compressor. Also non-steady combustion can be generated internally from combustion instability or self-induced oscillations. A premixed-prevaporized combustor would be particularly sensitive to flow transients because of its susceptibility to flashback-autoignition and blowout. An experimental program, the Transient Flow Combustion Study is in progress to study the effects of air and fuel flow transients on a premixed-prevaporized combustor. Preliminary tests performed at an inlet air temperature of 600 K, a reference velocity of 30 m/s, and a pressure of 700 kPa. The airflow was reduced to 1/3 of its original value in a 40 ms ramp before flashback occurred. Ramping the airflow up has shown that blowout is more sensitive than flashback to flow transients. Blowout occurred with a 25 percent increase in airflow (at a constant fuel-air ratio) in a 20 ms ramp. Combustion resonance was found at some conditions and may be important in determining the effects of flow transients. R.J.F.

**N84-20561\*#** National Aeronautics and Space Administration. Lewis Research Center, Cleveland, Ohio.

**COMBUSTOR FLAME FLASHBACK**

M. P. PROCTOR (Case Western Reserve Univ.), D. N. ANDERSON, and J. S. TIEN (Case Western Reserve Univ.) *In its* Combust. Fundamentals Res. p 311-312 Apr. 1984

Avail: NTIS HC A14/MF A01 CSCL 21B

Flashback, a problem that occurs in premixed-prevaporized combustors, is the upstream propagation of the flame from the combustor into the premixing tubes. Not only does flashback change the combustion process from premixed burning to diffusion burning, thus creating more pollutants, but it also inflicts considerable damage to the fuel injector, premixing tube and other equipment upstream. The conditions at which flashback occurs in steady burning and the mechanism that causes flashback in both steady and transient flow are studied. The equivalence ratio at which flashback occurs is being measured for inlet temperatures of 600-950 K, pre-mixer wall temperatures of 450-1050 K and pre-mixer velocities of 40-80 ft/s. These data are presented. R.J.F.

**N84-21677\*#** Louisiana State Univ., Baton Rouge. Dept. of Chemical Engineering.

**SHOCK TUBE STUDY OF THE FUEL STRUCTURE EFFECTS ON THE CHEMICAL KINETIC MECHANISMS RESPONSIBLE FOR SOOT FORMATION**

M. FRENKLACH Nov. 1983 100 p refs

(Contract NAS3-23542)

(NASA-CR-174661; NAS 1.26:174661) Avail: NTIS HC A05/MF A01 CSCL 21B

Soot formation in toluene-, benzene-, and acetylene-oxygen-argon mixtures was investigated to study soot formation in a combustion environment. High concentrations of oxygen completely suppress soot formation. The addition of oxygen at relatively low concentrations uniformly suppresses soot formation at high pressures, while at relatively lower pressures it suppresses soot formation at higher temperatures while promoting soot production at lower temperatures. The observed behavior indicates that oxidation reactions compete with ring fragmentation. The main conclusion to be drawn from the results is that the soot formation mechanism is probably the same for the pyrolysis and oxidation of hydrocarbons. That is, the addition of oxygen does not alter the soot route but rather promotes or inhibits this route by means of competitive reactions. An approach to empirical modeling of soot formation during pyrolysis of aromatic hydrocarbons is also presented. Author

**N84-22712\*#** National Aeronautics and Space Administration. Lewis Research Center, Cleveland, Ohio.

**SEPARATOR DEVELOPMENT AND TESTING OF NICKEL-HYDROGEN CELLS**

O. D. GONZALEZ-SANABRIA and M. A. MANZO 1984 15 p refs To be presented at the 19th Intersoc. Energy Conversion Eng. Conf., San Francisco, 19-24 Aug. 1984

(NASA-TM-83653; E-2017; NAS 1.15:83653) Avail: NTIS HC A02/MF A01 CSCL 10C

The components, design, and operating characteristics of Ni-H<sub>2</sub> cells batteries were improved. A separator development program was designed to develop a separator that is resistant to penetration by oxygen and loose active material from the nickel electrode, while retaining the required chemical and thermal stability, reservoir capability, and high ionic conductivity. The performance of the separators in terms of cell operating voltage was to at least match that of state-of-the-art separators while eliminating the separator problems. The separators were submitted to initial screening tests and those which successfully completed the tests were built into Ni-H<sub>2</sub> cells for short term testing. The separators with the best performance are tested for long term performance and life. S.L.

**N84-23637\*#** National Aeronautics and Space Administration. Lewis Research Center, Cleveland, Ohio.

**NASA BROAD-SPECIFICATION FUELS COMBUSTION TECHNOLOGY PROGRAM**

J. S. FEAR *In its* Assessment of Alternative Aircraft Fuels p 75-78 Apr. 1984

Avail: NTIS HC A09/MF A01 CSCL 21B

The NASA Broad-Specification Fuels Combustion Technology Program was initiated in response to concerns that the supply of high-quality petroleum middle distillates for jet fuel, abundant in the past, would diminish in availability toward the end of the century. The specific program objective is to evolve the combustion system technology required to use fuels with moderate ranges of broadened properties in the engines used on commercial jet aircraft. The first phase of the program, in which effects of the use of broadened-properties fuels were identified and technology with the potential to offset these effects was also identified, has been completed. The second phase, in which the technology identified in Phase 1 is being refined, will be completed within the next three months. B.W.

**N84-32446\*#** National Aeronautics and Space Administration. Lewis Research Center, Cleveland, Ohio.

**GCKP84-GENERAL CHEMICAL KINETICS CODE FOR GAS-PHASE FLOW AND BATCH PROCESSES INCLUDING HEAT TRANSFER EFFECTS**

D. A. BITTKER and V. J. SCULLIN Sep. 1984 101 p refs (NASA-TP-2320; E-1885; NAS 1.60:2320) Avail: NTIS HC A06/MF A01 CSCL 07D

A general chemical kinetics code is described for complex, homogeneous ideal gas reactions in any chemical system. The main features of the GCKP84 code are flexibility, convenience, and speed of computation for many different reaction conditions. The code, which replaces the GCKP code published previously, solves numerically the differential equations for complex reaction in a batch system or one dimensional inviscid flow. It also solves numerically the nonlinear algebraic equations describing the well stirred reactor. A new state of the art numerical integration method is used for greatly increased speed in handling systems of stiff differential equations. The theory and the computer program, including details of input preparation and a guide to using the code are given R.J.F.

**N84-33536\*#** National Aeronautics and Space Administration. Lewis Research Center, Cleveland, Ohio.

**EFFECT OF GRAVITY ON HALOGENATED HYDROCARBON FLAME RETARDANT EFFECTIVENESS**

P. D. RONNEY 1984 14 p refs Presented at the 35th Congr. of the International Astronautical Federation, Lausanne, Switzerland, 7-13 Oct. 1984 (NASA-TM-83761; E-2251; NAS 1.15:83761) Avail: NTIS HC A02/MF A01 CSCL 21B

Flammability limits, burning velocities, and minimum ignition energies under initially quiescent conditions were measured for stoichiometric and fuel-lean methane-, ethane-, and propane-air mixtures containing varying concentrations of Halon 1301. The characteristics of near-limit flames were strongly affected by fuel type but not Halon concentration. The conclusions were that the mechanism of the flammability limits was affected by fuel type but not Halon concentration, that the zero-g flammability limit is probably related to a stability criterion which is affected mostly by the molecular diffusion characteristics of the reactant gases and is mostly independent of chemical kinetics, and that the one-g upward flammability and ignition limits provide adequate criteria for safety at one-g and zero-g for both uninhibited and inhibited mixtures. Author

## 26

## METALLIC MATERIALS

Includes physical, chemical, and mechanical properties of metals, e.g., corrosion; and metallurgy.

**A84-10597\*** National Aeronautics and Space Administration. Lewis Research Center, Cleveland, Ohio.

**THE DEVELOPMENT OF DIRECTIONAL COARSENING OF THE GAMMA-PRIME PRECIPITATE IN SUPERALLOY SINGLE CRYSTALS**

R. A. MACKAY (NASA, Lewis Research Center, Cleveland, OH) and L. J. EBERT (Case Western Reserve University, Cleveland, OH) Scripta Metallurgica (ISSN 0036-9748), vol. 17, Oct. 1983, p. 1217-1222. refs (Contract NSG-3246)

A study has been made of the kinetics of the directional coarsening of the gamma-prime precipitates in Ni-5.8Al-14.6Mo-6.2Ta single crystals during creep at 982 C. In this alloy, which is characterized by a large negative lattice misfit between the gamma-prime precipitate and the gamma matrix, the formation of gamma-prime rafts begins during primary creep, and the rafts grow in length as the deformation proceeds into

steady-state creep. After that, the length of the rafts stabilizes. The thickness of the rafts remains constant from primary up to tertiary creep. The directional coarsening behavior of the alloy studied is similar to that of a more conventional single-crystal superalloy having a substantially smaller negative misfit. V.L.

**A84-11194\*#** Louisiana State Univ., Baton Rouge. **BENCHMARK CYCLIC PLASTIC NOTCH STRAIN MEASUREMENTS**

W. N. SHARPE, JR and M. WARD (Louisiana State University, Baton Rouge, LA) ASME, Transactions, Journal of Engineering Materials and Technology (ISSN 0094-4289), vol. 105, Oct. 1983, p. 235-241. Research supported by the General Electric Co., and Louisiana State University. refs (Contract NAS3-22522)

Plastic strains at the roots of notched specimens of Inconel 718 subjected to tension-compression cycling at 650 C are reported. These strains were measured with a laser-based technique over a gage length of 0.1 mm and are intended to serve as 'benchmark' data for further development of experimental, analytical, and computational approaches. The specimens were 250 mm by 2.5 mm in the test section with double notches of 4.9 mm radius subjected to axial loading sufficient to cause yielding at the notch root on the tensile portion of the first cycle. The tests were run for 1000 cycles at 10 cpm or until cracks initiated at the notch root. The experimental techniques are described, and then representative data for the various load spectra are presented. All the data for each cycle of every test are available on floppy disks from NASA. Author

**A84-12385\*#** National Aeronautics and Space Administration. Lewis Research Center, Cleveland, Ohio.

**STRUCTURE OF TRANSIENT OXIDES FORMED ON NICRAL ALLOYS**

J. L. SMIALEK (NASA, Lewis Research Center, Cleveland, OH) and R. GIBALA (Case Western Reserve University, Cleveland, OH) Metallurgical Transactions A - Physical Metallurgy and Materials Science (ISSN 0360-2133), vol. 14A, Oct. 1983, p. 2143-2161. refs

It is one of the three objectives of the present study to document the fine internal structure of the transient scales in order to clarify the development of the stable alpha-Al<sub>2</sub>O<sub>3</sub> from a structural point of view. Another objective is concerned with the origin of features found in the mature alpha-Al<sub>2</sub>O<sub>3</sub> scales, such as voids, taking into account an examination in the early stages of oxidation. The third objective is to relate any difference in scale structure caused by oxide adherence additives (Y or Zr) to the current oxide adherence theories. The primary effect of short-time oxidation on the NiCrAl substrate structure is found to be production of dislocations and aluminum-depleted phases. The random alpha-Al<sub>2</sub>O<sub>3</sub> scale is the primary oxide phase observed in contact with the metal. G.R.

**A84-12395\*#** National Aeronautics and Space Administration. Lewis Research Center, Cleveland, Ohio.

**THE EFFECT OF MICROSTRUCTURE ON 650 C FATIGUE CRACK GROWTH IN P/M ASTROLOY**

J. GAYDA and R. V. MINER (NASA, Lewis Research Center, Cleveland, OH) Metallurgical Transactions A - Physical Metallurgy and Materials Science (ISSN 0360-2133), vol. 14A, Nov. 1983, p. 2301-2308. refs

The effect of microstructure on fatigue crack propagation at 650 C has been studied in a P/M nickel-base superalloy, Astroloy. Crack propagation data were obtained in air and vacuum at 20 cpm with a modified compact tension specimen. The rate of crack growth, da/dN, was correlated with the stress intensity range. Key microstructural variables examined were grain size and the distribution and size of the strengthening gamma prime phase. A fine grain size less than 20 microns always promoted rapid, intergranular failure, while a large grain size promoted slower, transgranular failure which decreased as the size and volume fraction of aging gamma prime was manipulated so as to increase

alloy strength. The rapid, intergranular mode of failure of the fine grain microstructures was suppressed in vacuum. Author

**A84-14286\*** National Aeronautics and Space Administration. Lewis Research Center, Cleveland, Ohio.  
**HIGH-TEMPERATURE FATIGUE IN METALS - A BRIEF REVIEW OF LIFE PREDICTION METHODS DEVELOPED AT THE LEWIS RESEARCH CENTER OF NASA**

G. R. HALFORD (NASA, Lewis Research Center, Cleveland, OH). SAMPE Quarterly. (ISSN-0036-0821), vol. 14, April 1983, p. 17-25. refs

The presentation focuses primarily on the progress we at NASA Lewis Research Center have made. The understanding of the phenomenological processes of high temperature fatigue of metals for the purpose of calculating lives of turbine engine hot section components is discussed. Improved understanding resulted in the development of accurate and physically correct life prediction methods such as Strain-Range partitioning for calculating creep fatigue interactions and the Double Linear Damage Rule for predicting potentially severe interactions between high and low cycle fatigue. Examples of other life prediction methods are also discussed. Previously announced in STAR as A83-12159 Author

**A84-18244\*** National Aeronautics and Space Administration. Lewis Research Center, Cleveland, Ohio.

**MORPHOLOGY OF AN ALUMINUM ALLOY ERODED BY A NORMALLY INCIDENT JET OF ANGULAR ERODENT PARTICLES**

P. V. RAO, S. G. YOUNG, and D. H. BUCKLEY (NASA, Lewis Research Center, Cleveland, OH) Wear (ISSN 0043-1648), vol. 92, Dec. 1, 1983, p. 31-49. refs

The erosion morphologies resulting from the normal impact of crushed glass particles upon 6061-T6 aluminum alloy are examined by scanning electron microscopy and energy-dispersive X-ray spectroscopy. Four distinct erosion regions are identified. It is shown that the transition to cutting wear occurs simultaneously with the transition from the incubation stage of erosion to the acceleration stage. It is also shown that the erosion rate depends exponentially on the velocity of the particles, with an exponent of 3.68, which is in good agreement with other investigations at normal incidence. V.L.

**A84-18733\*** Rensselaer Polytechnic Inst., Troy, N. Y.  
**THE EFFECTS OF FREQUENCY AND HOLD TIMES ON FATIGUE CRACK PROPAGATION RATES IN A NICKEL BASE SUPERALLOY**

S. GOLWALKAR, N. S. STOLOFF, and D. J. DUQUETTE (Rensselaer Polytechnic Institute, Troy, NY) IN: Strength of metals and alloys (ICSMA 6); Proceedings of the Sixth International Conference, Melbourne, Australia, August 16-20, 1982. Volume 2. Oxford, Pergamon Press, 1983, p. 879-885. (Contract NAG3-22)

The elevated temperature cyclic crack propagation behavior of a nickel base superalloy, Astroloy, produced by a hot isostatic pressing technique has been evaluated. Environment, frequency and peak load hold times have been controlled to evaluate the effects of creep and environment of fatigue crack propagation rates at several temperatures. Author

**A84-19225\*** National Aeronautics and Space Administration. Lewis Research Center, Cleveland, Ohio.

**TRIBOLOGICAL AND MICROSTRUCTURAL CHARACTERISTICS OF ION-NITRIDED STEELS**

T. SPALVINS (NASA, Lewis Research Center, Cleveland, OH). (International Conference on Metallurgical Coatings, San Diego, CA, Apr. 18-22, 1983) Thin Solid Films (ISSN 0040-6090), vol. 108, 1983, p. 157-163. refs

Three steels AISI 4140, AISI 4340 and AISI 304 stainless steel were ion nitrided in a plasma consisting of a 75:25 mixture of H<sub>2</sub>:N<sub>2</sub>, sometimes with a trace of CH<sub>4</sub>. Their surface topography was characterized by SEM and two distinct compound phases were identified: the gamma and the epsilon. The core-case hardness profiles were also established. The low Cr alloy steels

have an extended diffusion zone in contrast to the 3034 stainless steels which have a sharp interface. The depth of ion-nitriding is increased as the Cr content is decreased. Friction tests reveal that the gamma surface phase has a lower coefficient of friction than the epsilon phase. The lowest coefficient of friction is achieved when both the rider and the specimen surface are ion nitrided. Previously announced in STAR as N83-24635 S.L.

**A84-22012\*** National Aeronautics and Space Administration. Lewis Research Center, Cleveland, Ohio.

**A SIMPLE APPLICATION OF THE BAILEY-OROWAN CREEP MODEL TO FE-39.8 AT. PCT AL AND GAMMA/GAMMA PRIME - ALPHA**

J. D. WHITTENBERGER (NASA, Lewis Research Center, Cleveland, OH) and R. V. KRISHNAN (National Aeronautical Laboratory, Bangalore, India) Journal of Materials Science (ISSN 0022-2461), vol. 19, Feb. 1984, p. 509-517. refs

The results of a study to determine the recovery rates and work-hardening coefficients for creep from constant cross-head speed compressive tests are presented. Stressing and straining rates are computed from measured time-load curves obtained from compression testing between 1200 and 1400 K of several B2 crystal structure Fe-39.8 Al intermetallic materials and the directionally solidified eutectic alloy gamma/gamma prime alpha. These quantities are then fitted to the universal form of the Bailey-Orowan equation for creep. The recovery rates were found to be functions of nominal strain rate, stress, and temperature, while the hardening coefficients were dependent only on temperature. While the work-hardening coefficient for gamma/gamma prime - alpha was about 0.05 of the elastic modulus, the work-hardening coefficients for Fe-39.8 at. pct Al were less than 0.002 of the modulus J.N.

**A84-22879\*#** United Stirling A.B. Malmö (Sweden).  
**COMPARISON OF SEAL MATERIALS FOR USE IN STIRLING ENGINES**

G. LUNDHOLM (United Stirling AB, Malmö, Sweden) American Society of Mechanical Engineers, International Conference on Wear Materials, Reston, VA, Apr. 11-14, 1983, Paper. 7 p. Research sponsored by the U.S. Department of Energy. refs (Contract DEN3-32)

In a dry, reciprocating sliding test, rods of 12 different surface materials rubbed against a glass filled PTFE gas seal. To simulate operation in a Stirling engine a gas (N<sub>2</sub>) pressure of 1 MPa differential pressure was applied across the seal. Gas leakage rates, rods surface temperatures, changes in the surface finish of the rod, surface hardness of the rod and wear rate of the seals were measured. The rod surface materials that produced the least seal wear were: plasma sprayed molybdenum (75 Mo 18 Ni 4 Cr), gas nitrided steel, and plasma sprayed aluminum oxide (94 Al<sub>2</sub>O<sub>3</sub> 6 TiO<sub>2</sub>). In contrast to almost all other mating surfaces, the surface roughness of the rods coated with Mo did not decrease during wear. This property is very important for the formation of a PTFE transfer film on the mating surface. The presence of a stable transfer film gives a low PTFE wear rate. Author

**A84-26815\*** United Technologies Research Center, East Hartford, Conn.

**CARBIDES IN IRON-RICH FE-MN-CR-MO-AL-SI-C SYSTEMS**

F. D. LEMKEY (United Technologies Research Center, East Hartford, CT), H. GUPTA, H. NOWOTNY, and S. F. WAYNE (Connecticut, University, Storrs, CT) Journal of Materials Science (ISSN 0022-2461), vol. 19, March 1984, p. 965-973. refs (Contract NAG3-271)

The optimization of high carbon iron-base superalloy properties with duplex microstructure gamma + M<sub>7</sub>C<sub>3</sub> carbide requires analysis in the context of a seven-component system. Data are first provided here for the Fe-Mn-Cr-Mo-C quinary system, at 30 at. pct carbon. A characterization of competing carbides, according to a pseudoternary phase diagram at 35 wt pct iron, is made from isothermal sections. It is noted that while M<sub>7</sub>C<sub>3</sub> and M<sub>3</sub>C carbides' occurrences are respectively favored at the Cr and Mn corners, the M<sub>2</sub>C carbide and molybdenum cementite are



predominant with increasing amounts of Mo. Lattice parameters are reported for the various carbides. O.C.

**A84-27485\*** National Aeronautics and Space Administration. Lewis Research Center, Cleveland, Ohio.

**THE EFFECTS OF CR, AL, TI, MO, W, TA, AND CB ON THE CYCLIC OXIDATION BEHAVIOR OF CAST NI-BASE SUPERALLOYS AT 1100 AND 1150 C**

C. A. BARRETT, R. V. MINER, and D. R. HULL (NASA, Lewis Research Center, Cleveland, OH) *Oxidation of Metals* (ISSN 0030-770X), vol. 20, Dec. 1983, p. 255-278. refs

Fifty Ni-base superalloys with concentrations of Cr, Al, Ti, Mo, W, Ta, and Cb systematically varied between two nonzero levels, were tested for cyclic oxidation resistance at 1100 and 1150 C. Oxidation resistance was interpreted in terms of the rate of specific weight change and the types of oxides formed. It is found that the resistance of the alloys to cyclic oxidation is largely determined by Al content, with a sharp increase in the oxidation resistance observed in the Al concentration range 5-8 at. pct. The effects of the other elements studied were small compared with that of aluminum. Best oxidation resistance characteristics were predicted for high Al (13 at. pct), low Cr (10 at. pct), low Ti (2 at. pct), low Cb (1 at. pct), and high Mo, W, and Ta (3 at. pct each). The effects of the refractory metals, however, are somewhat ambiguous and should be investigated further. Higher boron contents, which were unintentionally varied, were clearly detrimental even for the most resistant compositions. V.L.

**A84-31915\*** National Aeronautics and Space Administration. Lewis Research Center, Cleveland, Ohio.

**RAPID SOLIDIFICATION VIA MELT SPINNING - EQUIPMENT AND TECHNIQUES**

R. W. JECH, T. J. MOORE, T. K. GLASGOW, and N. W. ORTH (NASA, Lewis Research Center, Processing Science Section, Cleveland, OH) *Journal of Metals* (ISSN 0148-6608), vol. 36, April 1984, p. 41-45. refs

One of the simpler methods available to accomplish rapid solidification processing is free jet melt spinning. With only a modest expenditure of time, effort, and capital, an apparatus suitable for preliminary experimentation can be assembled. Wheel and crucible materials, process atmospheres, crucible design, heating methods, and process parameters and their relationship to melt composition are described. Practical solutions to processing problems, based on 'hands-on' experience, are offered. Alloys with melting points up to 3000 F have been rapidly solidified using the techniques described. Author

**A84-33440\*** National Aeronautics and Space Administration. Lewis Research Center, Cleveland, Ohio.

**REACTION OF COBALT IN SO<sub>2</sub> ATMOSPHERES AT ELEVATED TEMPERATURES**

N. S. JACOBSON (NASA, Lewis Research Center, Cleveland, OH) and W. L. WORRELL (Pennsylvania, University, Philadelphia, PA) (Electrochemical Society, Meeting, Washington, DC, Oct. 9-14, 1983) *Electrochemical Society, Journal* (ISSN 0013-4651), vol. 131, May 1984, p. 1182-1188. refs

(Contract NSF DMR-79-23647)

The reaction rate of cobalt in SO<sub>2</sub> argon environments was measured at 650 C, 700 C, 750 C and 800 C. Product scales consist primarily of an interconnected sulfide phase in an oxide matrix. At 700 C to 800 C, a thin sulfide layer adjacent to the metal is also observed. At all temperatures, the rapid diffusion of cobalt outward through the interconnected sulfide appears to be important. At 650 C, the reaction rate slows dramatically after five minutes due to a change in the distribution of these sulfides. At 700 C and 750 C, the reaction is primarily diffusion controlled; values of diffusivity of cobalt (CoS) calculated from this work show favorable agreement with values of diffusivity of cobalt (CoS) calculated from previous sulfidation work. At 800 C, a surface step becomes rate limiting. Previously announced in STAR as N83-35104 Author

**A84-36047\*** Dartmouth Coll., Hanover, N.H.

**THE STRUCTURE OF EXTRUDED NIAl**

I. BAKER and E. M. SCHULSON (Dartmouth College, Hanover, NH) *Metallurgical Transactions A - Physical Metallurgy and Materials Science* (ISSN 0360-2133), vol. 15A, June 1984, p. 1129-1136. refs

(Contract NAG3-13)

The deformation structure of Ni-rich NiAl extruded at 550 C has been characterized by transmission electron microscopy and by optical microscopy. Dislocations having a(100) Burgers vectors were found as complex networks, tangles, and prismatic loops. a(110) dislocations, which were rare, were concluded to arise from reactions of a(100) dislocations. Evidence of recovery and recrystallization was obtained. Extrusion was deemed to have been possible by the operation of (hko)(001) slip systems (often in plane strain flow) plus diffusion-assisted processes. Author

**A84-36173\*#** Illinois Inst. of Tech., Chicago.

**CREEP-RUPTURE BEHAVIOR OF SIX CANDIDATE STIRLING ENGINE SUPERALLOYS TESTED IN AIR**

S. BHATTACHARYYA (Illinois Institute of Technology, Chicago, IL) *ASME, Transactions, Journal of Engineering Materials and Technology* (ISSN 0094-4289), vol. 106, Jan. 1984, p. 50-58. refs

(Contract DEN3-217)

The creep-rupture behavior of six candidate Stirling engine iron-base superalloys was determined in air. The alloys included four wrought alloys (A-286, Alloy 800H, N-155, and 19-9DL) and two cast alloys (CRM-6D and XF-818). The specimens were tested to rupture for times up to 3000 h at 650 to 925 C. Rupture life,  $t(r)$  minimum creep rate, and time to 1-percent creep strain  $t(0.01)$  were statistically analyzed as a function of stress and temperature. Estimated stress levels at different temperatures to obtain 3500 h  $t(r)$  and  $t(0.01)$  lives were determined. These data will be compared with similar data being obtained under 15 MPa hydrogen. Author

**A84-42658\*** Michigan Technological Univ., Houghton.

**SOLUTE TRANSPORT AND THE PREDICTION OF BREAKAWAY OXIDATION IN GAMMA + BETA NI-CR-AL ALLOYS**

J. A. NESBITT and R. W. HECKEL (Michigan Technological University, Houghton, MI) IN: *High-temperature protective coatings; Proceedings of the Symposium, Atlanta, GA, March 7, 8, 1983*. Warrendale, PA, Metallurgical Society of AIME, 1984, p. 75-91. refs

(Contract NSG-3215)

The Al transport and the condition leading to breakaway oxidation during the cyclic oxidation of gamma + beta NiCrAl alloys have been studied. The Al concentration/distance profiles were measured after various cyclic oxidation exposures at 1200 C. It was observed that cyclic oxidation results in a decreasing Al concentration at the oxide/metal interface, maintaining a constant flux of Al to the Al<sub>2</sub>O<sub>3</sub> scale. It was also observed that breakaway oxidation occurs when the Al concentration at the oxide/metal interface approaches zero. A numerical model was developed to simulate the diffusional transport of Al and to predict breakaway oxidation in gamma + beta NiCrAl alloys undergoing cyclic oxidation. In a comparison of two alloys with similar oxide spalling characteristics, the numerical model was shown to predict correctly the onset of breakaway oxidation in the higher Al-content alloy. Author

**A84-42667\*** National Aeronautics and Space Administration. Lewis Research Center, Cleveland, Ohio.

**OXIDATION BEHAVIOR OF A THERMAL BARRIER COATING**

R. A. MILLER (NASA, Lewis Research Center, Cleveland, OH) IN: *High-temperature protective coatings; Proceedings of the Symposium, Atlanta, GA, March 7, 8, 1983*. Warrendale, PA, Metallurgical Society of AIME, 1984, p. 293-303. refs

Thermal barrier coatings, consisting of a plasma sprayed calcium silicate ceramic layer and a CoCrAlY or NiCrAlY bond coat, were applied on B-1900 coupons and cycled hourly in air in a rapid-response furnace to maximum temperatures of 1030, 1100, or 1160 C. Eight specimens were tested for each of the six



conditions of bond-coat composition and temperature. Specimens were removed from test at the onset of failure, which was taken to be the formation of a fine surface crack visible at 10X magnification. Specimens were weighed periodically, and plots of weight gain vs time indicate that weight is gained at a parabolic rate after an initial period where weight was gained at a much greater rate. The high initial oxidation rate is thought to arise from the initially high surface area in the porous bond coat. Specimen life (time to first crack) was found to be a strong function of temperature. However, while test lives varied greatly with time, the weight gain at the time of specimen failure was quite insensitive to temperature. This indicates that there is a critical weight gain at which the coating fails when subjected to this test. Author

**A84-43872\*** Northwestern Univ., Evanston, Ill.  
**FINITE ELASTIC-PLASTIC DEFORMATION OF POLYCRYSTALLINE METALS**  
 T. IWAKUMA and S. NEMAT-NASSER (Northwestern University, Evanston, IL) Royal Society (London), Proceedings, Series A - Mathematical and Physical Sciences (ISSN 0080-4630), vol. 394, no. 1806, July 9, 1984, p. 87-119. refs  
 (Contract NAG3-134)

Applying Hill's self-consistent method to finite elastic-plastic deformations, the overall moduli of polycrystalline solids are estimated. The model predicts a Bauschinger effect, hardening, and formation of vertex or corner on the yield surface for both microscopically non-hardening and hardening crystals. The changes in the instantaneous moduli with deformation are examined, and their asymptotic behavior, especially in relation to possible localization of deformations, is discussed. An interesting conclusion is that small second-order quantities, such as shape changes of grains and residual stresses (measured relative to the crystal elastic moduli), have a first-order effect on the overall response, as they lead to a loss of the overall stability by localized deformation. The predicted incipience of localization for a uniaxial deformation in two dimensions depends on the initial yield strain, but the orientation of localization is slightly less than 45 deg with respect to the tensile direction, although the numerical instability makes it very difficult to estimate this direction accurately. Author

**A84-45570\*** National Aeronautics and Space Administration. Lewis Research Center, Cleveland, Ohio.  
**A STUDY OF THE EFFECT OF SOLID PARTICLE IMPACT AND PARTICLE SHAPE ON THE EROSION MORPHOLOGY OF DUCTILE METALS**  
 P. V. RAO, S. G. YOUNG, and D. H. BUCKLEY (NASA, Lewis Research Center, Cleveland, OH) Journal of Microscopy (ISSN 0022-2720), vol. 135, July 1984, p. 49-59. Previously announced in STAR as N82-33493. refs

Impulsive versus steady jet impingement of spherical glass bead particles on metal surfaces was studied using a gas gun facility and a commercial sand blasting apparatus. Crushed glass particles were also used in the sand blasting apparatus as well as glass beads. Comparisons of the different types of erosion patterns were made. Scanning electron microscopy, surface profilometry and energy dispersive X-ray spectroscopy analysis were used to characterize erosion patterns. The nature of the wear can be divided into cutting and deformation, each with its own characteristic features. Surface chemistry analysis indicates the possibility of complex chemical and/or mechanical interactions between erodants and target materials. S.L.

**A84-46785\*#** National Aeronautics and Space Administration. Lewis Research Center, Cleveland, Ohio.  
**ELEVATED TEMPERATURE COMPRESSIVE STEADY STATE DEFORMATION AND FAILURE IN THE OXIDE DISPERSION STRENGTHENED ALLOY MA 6000E**  
 J. D. WHITTENBERGER (NASA, Lewis Research Center, Cleveland, OH) Metallurgical Transactions A - Physical Metallurgy and Materials Science (ISSN 0360-2133), vol. 15A, Sept. 1984, p. 1753-1762. refs

The compressive flow strength-strain rate behavior of the oxide-dispersion-strengthened alloy MA 6000E has been studied

in the temperature range 1144-1366 K, with strain rates ranging from  $2.1 \times 10^{-5}$  to the  $-5$ th to  $2.1 \times 10^{-2}$  to the  $-7$ th per s. It is found that the inherent strength of the alloy is essentially the same in all test directions and that the low strength observed in tensile tests results from the inability of grain boundaries to support high tensile stresses. The failure of MA 6000E under high-temperature, slow plastic flow conditions is shown to be the result of concentrated slip. Slow plastic deformation in MA 6000E can be described by a threshold stress model of creep where threshold stresses are calculated from relatively fast testing procedures and the effective stress exponent for creep is assumed to be 3.5.

V.L.

**A84-48715\*** National Aeronautics and Space Administration. Lewis Research Center, Cleveland, Ohio.  
**EFFECTS OF PROCESSING AND MICROSTRUCTURE ON THE FATIGUE BEHAVIOUR OF THE NICKEL-BASE SUPERALLOY RENE95**

R. V. MINER and J. GAYDA (NASA, Lewis Research Center, Processing Science Section, Cleveland, OH) International Journal of Fatigue (ISSN 0142-1123), vol. 6, July 1984, p. 189-193. refs

Forms of the nickel-base superalloy Rene95 produced by three processing methods were evaluated in tensile, low cycle fatigue and fatigue crack propagation tests at 540 and 650 C. Two powder-metallurgy (PM) forms, hot-isostatically-pressed and extruded-and-forged, and a conventionally cast-and-wrought form were all given the same heat treatment. The extruded-and-forged form showed superior fatigue life in low strain range tests though the two PM forms exhibited nearly identical mechanical behavior in all other respects. Further, this life difference could not be explained by significant differences in the types, sizes or shapes of the defects initiating failure. The cast-and-wrought Rene95, however, had lower strength, ductility and fatigue life, but higher fatigue crack propagation resistance because of a larger grain size. It did not exhibit the environmentally-assisted intergranular mode of propagation which occurs in PM Rene95 and other fine-grained superalloys at these test temperatures. and frequencies. Author

**N84-10267\*#** Rensselaer Polytechnic Inst., Troy, N. Y. Dept. of Materials Engineering.

**FATIGUE CRACK GROWTH AND LOW CYCLE FATIGUE OF TWO NICKEL BASE SUPERALLOYS Final Report**

N. S. STOLOFF, D. J. DUQUETTE, S. J. CHOE, and S. GOLWALKAR 16 Sep. 1983 51 p refs

(Contract NAG3-22)

(NASA-CR-174534; NAS 1.26:174534) Avail: NTIS HC A04/MF A01 CSCL 11F

The fatigue crack growth and low cycle fatigue behavior of two P/M superalloys, Rene 95 and Astrology, in the hot isostatically pressed (HIP) condition, was determined. Test variables included frequency, temperature, environment, and hold times at peak tensile loads (or strains). Crack initiation sites were identified in both alloys. Crack growth rates were shown to increase in argon with decreasing frequency or with the imposition of hold times. This behavior was attributed to the effect of oxygen in the argon. Auger analyses were performed on oxide films formed in argon. Low cycle fatigue lives also were degraded by tensile hold, contrary to previous reports in the literature. The role of environment in low cycle fatigue behavior is discussed. M.G.

**N84-10268\*#** Pratt and Whitney Aircraft Group, West Palm Beach, Fla. Government Products Div.

**LOW STRAIN, LONG LIFE CREEP FATIGUE OF AF2-1DA AND INCO 718**

A. B. THAKKER and B. A. COWLES Apr. 1983 152 p refs  
 (Contract NAS3-22387)

(NASA-CR-167989; NAS 1.26:167989; FR-15652) Avail: NTIS HC A08/MF A01 CSCL 11F

Two aircraft turbine disk alloys, GATORIZED AF2-DA and INCO 718 were evaluated for their low strain long life creep-fatigue behavior. Static (tensile and creep rupture) and cyclic properties of both alloys were characterized. The controlled strain LCF tests

were conducted at 760 C (1400 F) and 649 C (1200 F) for AF2-1DA and INCO 718, respectively. Hold times were varied for tensile, compressive and tensile/compressive strain dwell (relaxation) tests. Stress (creep) hold behavior of AF2-1DA was also evaluated. Generally, INCO 718 exhibited more pronounced reduction in cyclic life due to hold than AF2-1DA. The percent reduction in life for both alloys for strain dwell tests was greater at low strain ranges (longer life regime). Changing hold time from 0 to 0.5, 2.0 and 15.0 min. resulted in corresponding reductions in life. The continuous cycle and cyclic/dwell initiation failure mechanism was predominantly transgranular for AF2-1DA and intergranular for INCO 718.

Author

**N84-11254\*#** National Aeronautics and Space Administration. Lewis Research Center, Cleveland, Ohio.

**SIZE SCALE EFFECT IN CAVITATION EROSION**

P. V. RAO, B. C. RAO, and D. H. BUCKLEY 1982 11 p refs (NASA-TM-83533; E-1538-1; NAS 1.15 83533) Avail: NTIS HC A02/MF A01 CSCL 11F

An overview and data analyses pertaining to cavitation erosion size scale effects are presented. The exponents  $n$  in the power law relationship are found to vary from 1.7 to 4.9 for venturi and rotating disk devices supporting the values reported in the literature. Suggestions for future studies were made to arrive at further true scale effects.

Author

**N84-12287\*#** National Aeronautics and Space Administration. Lewis Research Center, Cleveland, Ohio.

**SOLID IMPINGEMENT EROSION MECHANISMS AND CHARACTERIZATION OF EROSION RESISTANCE OF DUCTILE METALS**

V. P. RAO (Cleveland State Univ., Ohio) and D. H. BUCKLEY 1982 21 p refs To be presented at the Fluids, Eng. Conf., New Orleans, 11-17 Feb. 1984; sponsored by ASME (NASA-TM-83492; E-1823; NAS 1.15:83492) Avail: NTIS HC A02/MF A01 CSCL 11F

Experimental results pertaining to spherical glass bead and angular crushed glass particle impingement are presented. A concept of energy adsorption to explain the failure of material is proposed. The erosion characteristics of several pure metals were correlated with the proposed energy parameters and with other properties. Correlations of erosion and material properties were also carried out with these materials to study the effect of the angle of impingement. Analyses of extensive erosion data indicate that surface energy, strain energy, melting point, bulk modulus, hardness, ultimate resilience, atomic volume and product of linear coefficient of thermal expansion, bulk modulus, and temperature rise required for melting, and ultimate resilience, and hardness exhibit the best correlations. It appears that both energy and thermal properties contribute to the total erosion.

Author

**N84-13264\*#** National Aeronautics and Space Administration. Lewis Research Center, Cleveland, Ohio.

**REPLACING CRITICAL AND STRATEGIC REFRACTORY METAL ELEMENTS IN NICKEL-BASE SUPERALLOYS**

J. R. STEPHENS, R. L. DRESHFIELD, and M. V. NATHAL Dec. 1983 21 p refs Presented at the 1st USA-Brazil Superalloy Conf., Araxa (Brazil), 6-13 Apr. 1984 (NASA-TM-83528; E-1894; NAS 1.15:83528) Avail: NTIS HC A02/MF A01 CSCL 11F

Because of the import status and essential nature of their use, cobalt, chromium, tantalum, and niobium were identified as strategic and critical in the aerospace industry. NASA's Conservation of Strategic Aerospace Materials (COSAM) program aims to reduce the need for strategic materials used in gas turbine engines. Technological thrusts in two major areas are under way to meet the primary objective of conserving the use of strategic materials in nickelbase superalloys. These thrusts consist of strategic element substitution and alternative material identification. The program emphasizes cooperative research teams involving NASA Lewis Research Center, universities, and industry. The adoption of refractory metals in nickel-base superalloys is summarized including their roles in mechanical strengthening and environmental

resistance; current research activities under way in the COSAM Program are presented as well as research findings to date.

A.R.H.

**N84-13265\*#** Battelle Columbus Labs., Ohio.

**CREEP FATIGUE OF LOW-COBALT SUPERALLOYS:**

**WASPALLOY, PM U 700 AND WROUGHT U 700 Final Report** B. N. LEIS, R. RUNGTA, and A. T. HOPPER 1 Sep. 1983 61 p refs

(Contract NAS3-23289)

(NASA-CR-168260; NAS 1.26:168260) Avail: NTIS HC A04/MF A01 CSCL 11F

The influence of cobalt content on the high temperature creep fatigue crack initiation resistance of three primary alloys was evaluated. These were Waspalloy, Powder U 700, and Cast U 700, with cobalt contents ranging from 0 up to 17 percent. Waspalloy was studied at 538 C whereas the U 700 was studied at 760 C. Constraints of the program required investigation at a single strain range using diametral strain control. The approach was phenomenological, using standard low cycle fatigue tests involving continuous cycling tension hold cycling, compression hold cycling, and symmetric hold cycling. Cycling in the absence of or between holds was done at 0.5 Hz, whereas holds when introduced lasted 1 minute. The plan was to allocate two specimens to the continuous cycling, and one specimen to each of the hold time conditions. Data was taken to document the nature of the cracking process, the deformation response, and the resistance to cyclic loading to the formation of small cracks and to specimen separation. The influence of cobalt content on creep fatigue resistance was not judged to be very significant based on the results generated. Specific conclusions were that the hold time history dependence of the resistance is as significant as the influence of cobalt content and increased cobalt content does not produce increased creep fatigue resistance on a one to one basis.

S.L.

**N84-14287\*#** Columbia Univ., New York. Center for Strategic Materials.

**EFFECTS OF COBALT IN NICKEL-BASE SUPERALLOYS Final Report**

J. K. TIEN and R. N. JARRETT Dec. 1983 26 p refs Presented at High Temp. Alloys for Gas Turbines Conf., Liege, 4-6 Oct. 1982

(Contract NAG3-57)

(NASA-CR-168308; NAS 1.26:168308) Avail: NTIS HC A03/MF A01 CSCL 11F

The role of cobalt in a representative wrought nickel-base superalloy was determined. The results show cobalt affecting the solubility of elements in the gamma matrix, resulting in enhanced gamma' volume fraction, in the stabilization of MC-type carbides, and in the stabilization of sigma phase. In the particular alloy studied, these microstructural and microchemistry changes are insufficient in extent to impact on tensile strength, yield strength, and in the ductilities. Depending on the heat treatment, creep and stress rupture resistance can be cobalt sensitive. In the coarse grain, fully solutioned and aged condition, all of the alloy's 17% cobalt can be replaced by nickel without deleteriously affecting this resistance. In the fine grain, partially solutioned and aged condition, this resistance is deleteriously affected only when one-half or more of the initial cobalt content is removed. The structure and property results are discussed with respect to existing theories and with respect to other recent and earlier findings on the impact of cobalt, if any, on the performance of nickel-base superalloys.

Author

## 26. METALLIC MATERIALS

**N84-14288\*#** National Aeronautics and Space Administration. Lewis Research Center, Cleveland, Ohio.

### TOPOLOGICAL REACTION RATE MEASUREMENTS RELATED TO SCOFFING

J. L. LAUER (Rensselaer Polytechnic Inst.), S. S. FUNG (Rensselaer Polytechnic Inst.), and W. R. JONES, JR. 1983 19 p refs Presented at the Joint Lubrication Conf., Hartford, Conn., 18-20 Oct. 1983

(NASA-TM-83486; NAS 1.15:83486; E-1810) Avail: NTIS HC A02/MF A01 CSCL 11F

A ball-on-plate (both consisting of hardened M-50 steel) sliding elastohydrodynamic contact was run with trimethylolpropane triheptanoate (TMPTH) with and without tricresyl phosphate (TCP). The contact area of the plate was optically profiled with a phase-locked interference microscope (PLIM) both before and after exposure to alcoholic hydrochloric acid. As scuffing was approached, the profile within the contact region changed more rapidly after the acid treatment; after scuffing, it assumed a constant high value. A metallurgical phase found in the scuff mark was apparently responsible for the high reactivity. The microscopic profile changes (sensitivity,  $\pm$  or  $-$  3 nm ( $\pm$  or  $-$  A) in depth) involved primarily the small asperities (radius, 3 microns); the larger ones were unaffected. Soaking the steel in TCP smoothed the fine structure of the surface profile but increased its reactivity toward alcoholic hydrochloric acid before sliding was started. Thus it would appear that PLIM examination could be used for screening potentially scuff-resistant materials. Author

**N84-14289\*#** National Aeronautics and Space Administration. Lewis Research Center, Cleveland, Ohio.

### PARTICULATE EROSION MECHANISMS

P. VEERABHADRARAO (Cleveland State Univ.) and D. H. BUCKLEY 1983 12 p refs To be presented at the Cavitation and Multiphase Flow Forum, New Orleans, 11-17 Feb. 1984 (NASA-TM-83551; NAS 1.15:83551; E-1914) Avail: NTIS HC A02/MF A01 CSCL 11F

Particulate damage and erosion of ductile metals are today plaguing design and field engineers in diverse fields of engineering and technology. It was found that too many models and theories were proposed leading to much speculation from debris analysis and failure mechanism postulations. Most theories of solid particle erosion are based on material removal models which do not fully represent the actual physical processes of material removal. The various mechanisms proposed thus far are: melting, low-cycle fatigue, extrusion, delamination, shear localization, adhesive material transfer, etc. The experimental data on different materials highlighting the observed failure modes of the deformation and cutting wear processes using optical and scanning electron microscopy are presented. The most important mechanisms proved from the experimental observations of the specimens exposed to both spherical and angular particles are addressed, and the validity of the earlier theories discussed. Both the initial stages of damage and advanced stages of erosion were studied to gain a fundamental understanding of the process. Author

**N84-15246\*#** National Aeronautics and Space Administration. Lewis Research Center, Cleveland, Ohio.

### EVALUATION OF CO<sub>2</sub> AND CO DOPANTS IN HYDROGEN TO REDUCE HYDROGEN PERMEATION IN THE STIRLING ENGINE HEATER HEAD TUBE ALLOY CG-27 Final Report

J. A. MISENICK Jul. 1983 34 p refs

(Contract DE-A101-77CS-51040)

(NASA-TM-83535; E-1901; DOE/NASA/51040-50; NAS 1.15:83535) Avail: NTIS HC A03/MF A01 CSCL 11F

Tubes of CG-27 alloy, filled with hydrogen doped with various amounts of carbon dioxide and carbon monoxide, were heated in a diesel fuel fired Stirling engine simulator materials test rig for 100 hours at 820 C and at a gas pressure of 15 MPa to determine the effectiveness of the dopants in reducing hydrogen permeation through the hot tube wall. This was done for clean as-heat treated tubes and also for tubes that had previously been exposed for 100 hours to hydrogen doped with 1.0 volume percent carbon dioxide to determine if the lower levels of dopant could maintain

a low hydrogen permeation through the hot tube wall. Carbon dioxide, as a dopant in hydrogen, was most effective in reducing hydrogen permeation through clean tubes and in maintaining low hydrogen permeation after prior exposure to 1.0 volume percent carbon dioxide. Only the lowest level of carbon dioxide (0.05 volume percent) was not as effective in the clean or prior exposed tubes. Carbon monoxide as a dopant in hydrogen was less effective than carbon dioxide at a given concentration level. Of the four dopant levels studied, 1.0, 0.5, 0.2, and 0.05 volume percent carbon monoxide, only the 1.0 and 0.5 volume percent were effective in reducing and maintaining low hydrogen permeation through the CG-27. Author

**N84-15247\*#** Garrett Turbine Engine Co., Phoenix, Ariz.

### LOW-COST SINGLE-CRYSTAL TURBINE BLADES, VOLUME 1 Final Report

T. E. STRANGMAN, B. HEATH, and M. FUJII Nov. 1983 218 p refs

(Contract NAS3-20073)

(NASA-CR-168218; GARRETT-21-4314-1; NAS 1.26:168218)

Avail: NTIS HC A10/MF A01 CSCL 11F

The exothermic casting process was successfully developed into a low cost nonproprietary method for producing single crystal (SC) castings. Casting yields were lower than expected, on the order of 20 percent, but it is felt that the casting yield could be significantly improved with minor modifications to the process. Single crystal Mar-M 247 and two derivative SC alloys were developed. NASAIR 100 and SC Alloy 3 were fully characterized through mechanical property testing. SC Mar-M 247 shows no significant improvement in strength over directionally solidified (DS) Mar-M 247, but the derivative alloys, NASAIR 100 and Alloy 3, show significant tensile and fatigue improvements. The 1000 hr/238 MPa (20 ksi) stress rupture capability compared to DS Mar-M 247 was improved over 28 C. Firtree testing; holography, and strain gauge rig testing were used to evaluate the effects of the anisotropic characteristics of single crystal materials. In general, the single crystal material behaved similarly to DS Mar-M 247. Two complete engine sets of SC HP turbine blades were cast using the exothermic casting process and fully machined. Author

**N84-15249\*#** National Aeronautics and Space Administration. Lewis Research Center, Cleveland, Ohio.

### TENSILE AND COMPRESSIVE CONSTITUTIVE RESPONSE OF 316 STAINLESS STEEL AT ELEVATED TEMPERATURES

S. S. MANSON (Case Western Reserve Univ.), U. MURALIDHARAN, and G. R. HALFORD (Case Western Reserve Univ.) 1982 26 p refs Presented at the Symp. on Nonlinear Constitutive Relations for High Temp. Appl., Akron, Ohio, 19-20 May 1982; sponsored by Akron Univ. and NASA Previously announced as N83-34353

(NASA-TM-83506; NAS 1.15:83506) Avail: NTIS HC A03/MF A01 CSCL 11F

It is demonstrated that creep rate of 316 SS is lower by factors of 2 to 10 in compression than in tension if the microstructure is the same and tests are conducted at identical temperatures and equal but opposite stresses. Such behavior was observed for both monotonic creep and conditions involving cyclic creep. In the latter case creep rate in both tension and compression progressively increases from cycle to cycle, rendering questionable the possibility of expressing a time-stabilized constitutive relationship. The difference in creep rates in tension and compression is considerably reduced if the tension specimen is first subjected to cycles of tensile creep (reversed by compressive plasticity), while the compression specimen is first subjected to cycles of compressive creep (reversed by tensile plasticity). In both cases, the test temperature is the same and the stresses are equal and opposite. Such reduction is a reflection of differences in microstructure of the specimens resulting from different prior mechanical history. B.W.

**N84-16311\*#** National Aeronautics and Space Administration. Lewis Research Center, Cleveland, Ohio.

**APPLICATION OF INDUCTION COIL MEASUREMENTS TO THE STUDY OF SUPERALLOY HOT CORROSION AND OXIDATION**

D. L. DEADMORE Jan. 1984 15 p refs  
(NASA-TM-83560, E-1937; NAS 1.15:83560) Avail: NTIS HC A02/MF A01 CSCL 11F

The assessment of the degree of hot corrosion attack on nickel based alloys is a difficult task, especially when the definition specifies that it must be in terms of metal consumed and even more difficult if the measurement must be nondestructive. The inductance of a solenoid coil responds to changes in volume of fill and composition of metal cores, therefore, it may be used for nondestructive measurement of hot corrosion. The hot corrosion of U700 was studied at 900 C in a Mach 0.3 flame doped with 0.85 wppm of sodium. The change of inductance was found to define the known corrosion behavior and to suggest its use as a tool with predictive capabilities. Sufficient sensitivity exists to detect oxidation of this alloy at 900 C. Author

**N84-17350\*#** National Aeronautics and Space Administration. Lewis Research Center, Cleveland, Ohio.

**PRELIMINARY STUDY OF THERMOMECHANICAL FATIGUE OF POLYCRYSTALLINE MAR-M 200**

R. C. BILL (USAAVSCOM Research and Technology Labs.), M. J. VERRILLI (Northwestern Univ.), M. A. MCGAW, and G. R. HALFORD Feb. 1984 17 p refs  
(NASA-TP-2280; E-1795; NAS 1.60:2280, AVSCOM-TR-83-C-6) Avail: NTIS HC A02/MF A01 CSCL 11F

Thermomechanical fatigue (TMF) experiments were conducted on polycrystalline MAR-M 200 over a cyclic temperature range of 500 to 1000 C. Inelastic strain ranges of 0.03 to 0.2 percent were imposed on the specimens. The TMF lives were found to be significantly shorter than isothermal low-cycle-fatigue (LCF) life at the maximum cycle temperature, and in-phase cycling was more damaging than out-of-phase cycling. Extensive crack tip oxidation appeared to play a role in promoting the severity of in-phase cycling. Carbide particle - matrix interface cracking was also observed after in-phase TMF cycling. The applicability of various life prediction models to the TMF results obtained was assessed. It was concluded that current life prediction models based on isothermal data as input must be modified to be applicable to the TMF results. M.G.

**N84-17351\*#** National Aeronautics and Space Administration. Lewis Research Center, Cleveland, Ohio.

**METALLIC GLASS AS A TEMPERATURE SENSOR DURING ION PLATING**

K. MIYOSHI, T. SPALVINS, and D. H. BUCKLEY 1984 12 p refs Presented at the 11th Intern. Conf. on Metallurgical Coatings, San Diego, Calif., 9-13 Apr. 1984  
(NASA-TM-83566; E-1938; NAS 1.15:83566) Avail: NTIS HC A02/MF A01 CSCL 11F

The temperature of the interface and/or a superficial layer of a substrate during ion plating was investigated using a metallic glass of the composition Fe<sub>67</sub>Co<sub>18</sub>B<sub>14</sub>Si<sub>1</sub> as the substrate and as the temperature sensor. Transmission electron microscopy and diffraction studies determined the microstructure of the ion-plated gold film and the substrate. Results indicate that crystallization occurs not only in the film, but also in the substrate. The grain size of crystals formed during ion plating was 6 to 60 nm in the gold film and 8 to 100 nm in the substrate at a depth of 10 to 15 micrometers from the ion-plated interface. The temperature rise of the substrate during ion plating was approximately 500 C. Discontinuous changes in metallurgical microstructure, and physical, chemical, and mechanical properties during the amorphous to crystalline transition in metallic glasses make metallic glasses extremely useful materials for temperature sensor applications in coating processes. A.R.H.

**N84-17352\*#** National Aeronautics and Space Administration. Lewis Research Center, Cleveland, Ohio.

**TRIBOLOGICAL CHARACTERISTICS OF GOLD FILMS DEPOSITED ON METALS BY ION PLATING AND VAPOR DEPOSITION**

K. MIYOSHI, T. SPALVINS, and D. H. BUCKLEY 1984 20 p refs Presented at the 3rd Intern. Conf. on Solid Lubrication, Denver, 5-9 Aug 1984  
(NASA-TM-83572, E-1877; NAS 1.15:83572) Avail: NTIS HC A02/MF A01 CSCL 11F

The graded interface between an ion-plated film and a substrate is discussed as well as the friction and wear properties of ion-plated gold. X-ray photoelectron spectroscopy (XPS) depth profiling and microhardness depth profiling were used to investigate the interface. The friction and wear properties of ion-plated and vapor-deposited gold films were studied both in an ultra high vacuum system to maximize adhesion and in oil to minimize adhesion. The results indicate that the solubility of gold on the substrate material controls the depth of the graded interface. Thermal diffusion and chemical diffusion mechanisms are thought to be involved in the formation of the gold-nickel interface. In iron-gold graded interfaces the gold was primarily dispersed in the iron and thus formed a physically bonded interface. The hardness of the gold film was influenced by its depth and was also related to the composition gradient between the gold and the substrate. The graded nickel-gold interface exhibited the highest hardness because of an alloy hardening effect. The effects of film thickness on adhesion and friction were established. S.L.

**N84-17353\*#** National Aeronautics and Space Administration. Lewis Research Center, Cleveland, Ohio.

**FACTORS WHICH INFLUENCE DIRECTIONAL COARSENING OF GAMMA PRIME DURING CREEP IN NICKEL-BASE SUPERALLOY SINGLE CRYSTALS**

R. A. MACKAY and L. J. EBERT (Case Western Reserve Univ.) 1984 12 p refs Proposed for presentation at the 5th Intern. Symp. on Superalloys, Seven Springs, Pa., 7-11 Oct. 1984; sponsored by American Inst. of Mining, Metallurgical and Petroleum Engineers  
(Contract NSG-3246)  
(NASA-TM-83595; E-1997; NAS 1.15:83595) Avail: NTIS HC A02/MF A01 CSCL 11F

Changes in the morphology of the gamma prime precipitate were examined as a function of time during creep at 982 C in 001 oriented single crystals of a Ni-Al-Mo-Ta superalloy. In this alloy, which has a large negative misfit of -0.80 pct., the gamma prime particles link together during creep to form platelets, or rafts, which are aligned with their broad faces perpendicular to the applied tensile axis. The effects of initial microstructure and alloy composition on raft development and creep properties were investigated. Directional coarsening of gamma prime begins during primary creep and continues well after the onset of second state creep. The thickness of the rafts remains constant up through the onset of tertiary creep a clear indication of the stability of the finely-spaced gamma/gamma prime lamellar structure. The thickness of the rafts which formed was equal to the initial gamma prime size which was present prior to testing. The single crystals with the finest gamma prime size exhibited the longest creep lives, because the resultant rafted structure had a larger number of gamma/gamma prime interfaces per unit volume of material. Reducing the Mo content by only 0.73 wt. pct. increased the creep life by a factor of three, because the precipitation of a third phase was eliminated. Author

**N84-17354\*#** National Aeronautics and Space Administration. Lewis Research Center, Cleveland, Ohio.

**INFLUENCE OF COMPOSITION ON THE MICROSTRUCTURE AND MECHANICAL PROPERTIES OF A NICKEL-BASE SUPERALLOY SINGLE CRYSTAL**

M. V. NATHAL and L. J. EBERT (Case Western Reserve Univ.) 1984 11 p refs Proposed for presentation at the 5th Intern. Symp. on Superalloys, Seven Springs, Pa., 7-11 Oct. 1984; sponsored by American Inst. of Mining, Metallurgical and Petroleum Engineers

(NASA-TM-83563; E-1942; NAS 1.15:83563) Avail: NTIS HC

A02/MF A01 CSCL 11F

The effects of cobalt, tantalum, and tungsten contents on the microstructure and mechanical properties of single crystal Mar-M247 were investigated. Elevated temperature tensile and creep-rupture properties of 001 oriented single crystals were related to microstructural features of the alloys. Substitution of Ni for Co in the high refractory metal alloys increased the lattice mismatch, which was considered to be the cause of the increases in tensile and creep strength. Substitution of Ni for Ta caused large decreases in tensile strength and creep life, consistent with decreases in gamma prime volume fraction, lattice mismatch, and solid solution hardening. Substitution of W for Ta resulted in decreased life at high stresses, which was related to small decreases in mismatch and volume fraction. However, the W substitution resulted in improved life at low stresses, which was related to solid solution strengthening by W. Author

**N84-17355\*#** National Aeronautics and Space Administration. Lewis Research Center, Cleveland, Ohio.

**INFLUENCE OF COBALT, TANTALUM AND TUNGSTEN ON THE HIGH TEMPERATURE MECHANICAL PROPERTIES OF SINGLE CRYSTAL NICKEL-BASE SUPERALLOYS Ph.D. Thesis - Case Western Reserve Univ.**

M. V. NATHAL Jan 1984 219 p refs

(NASA-TM-83479; E-1796; NAS 1.15:83479) Avail: NTIS HC

A10/MF A01 CSCL 11F

For alloys with the baseline refractory metal level of 3 percent Ta and 10 percent W, decreases in Co level from 10 to 0 percent resulted in increased tensile strength and creep resistance. Substitution of W for Ta resulted in decreased creep life at high stresses but improved life at low stresses. Substitution of Ni for Ta caused large reductions in tensile strength and creep resistance, and corresponding increases in ductility. For these alloys with low Ta plus W totals, strength was independent of Co level. The increases in tensile strength with increases in refractory metal content were related to the increases in gamma volume fraction and solid solution hardening. Increases in strength as Co level decreased were considered to be the result of coherency strain hardening from the increased lattice mismatch. Dislocation shear through the gamma-gamma interface is considered to be the rate limiting step in the deformation process. A.R.H.

**N84-18370\*#** National Aeronautics and Space Administration. Lewis Research Center, Cleveland, Ohio.

**ANALYSIS OF THERMOELECTRIC PROPERTIES OF HIGH-TEMPERATURE COMPLEX ALLOYS OF NICKEL-BASE, IRON-BASE AND COBALT-BASE GROUPS**

R. HOLANDA Jan 1984 23 p refs

(NASA-TP-2278; E-1854; NAS 1.60:2278) Avail: NTIS HC

A02/MF A01 CSCL 11F

The thermoelectric properties alloys of the nickel-base, iron-base, and cobalt-base groups containing from 1% to 25% 106 chromium were compared and correlated with the following material characteristics: atomic percent of the principle alloy constituent; ratio of concentration of two constituents; alloy physical property (electrical resistivity); alloy phase structure (percent precipitate or percent hardener content); alloy electronic structure (electron concentration). For solid-solution-type alloys the most consistent correlation was obtained with electron concentration, for precipitation-hardenable alloys of the nickel-base superalloy group, the thermoelectric potential correlated with hardener content in the alloy structure. For solid-solution-type alloys, no problems

were found with thermoelectric stability to 1000; for precipitation-hardenable alloys, thermoelectric stability was dependent on phase stability. The effects of the compositional range of alloy constituents on temperature measurement uncertainty are discussed. A.R.H.

**N84-19523\*#** Columbia Univ., New York. Center for Strategic Materials.

**THE ROLE OF COBALT ON THE CREEP OF WASPALOY Final Report**

R. N. JARRETT, L. CHIN, and J. K. TIEN Feb. 1984 35 p refs

(Contract NAG3-57)

(NASA-CR-174628; NAS 1.26:174628) Avail: NTIS HC A03/MF

A01 CSCL 11F

Cobalt was systematically replaced with nickel in Waspaloy (which normally contains 13% Co) to determine the effects of cobalt on the creep behavior of this alloy. Effects of cobalt were found to be minimal on tensile strengths and microstructure. The creep resistance and the stress rupture resistance determined in the range from 704 to 760 C (1300 to 1400 C) were found to decrease as cobalt was removed from the standard alloy at all stresses and temperatures. Roughly a ten-fold drop in rupture life and a corresponding increase in minimum creep rate were found under all test conditions. Both the apparent creep activation energy and the matrix contribution to creep resistance were found to increase with cobalt. These creep effects are attributed to cobalt lowering the stacking fault energy of the alloy matrix. The creep resistance loss due to the removal of cobalt is shown to be restored by slightly increasing the gamma' volume fraction. Results are compared to a previous study on Udimet 700, a higher strength, higher gamma' volume fraction alloy with similar phase chemistry, in which cobalt did not affect creep resistance. An explanation for this difference in behavior based on interparticle spacing and cross-slip is presented. Author

**N84-20672\*#** National Aeronautics and Space Administration. Lewis Research Center, Cleveland, Ohio.

**MECHANISM OF CORROSION OF NI BASE SUPERALLOYS BY MOLTEN Na<sub>2</sub>MoO<sub>4</sub> AT ELEVATED TEMPERATURES**

A. K. MISRA (NAS-NRC, Washington, D.C.) and C. A. STEARNS 1983 41 p Presented at the Fall Meeting of the Electrochem. Soc., Washington, D.C., 9-14 Oct. 1983

(NASA-TM-83580; E-1970; NAS 1.15:83580) Avail: NTIS HC

A03/MF A01 CSCL 11F

The corrosion of nickel base superalloy, U-700, by molten Na<sub>2</sub>MoO<sub>4</sub> was studied in the temperature range of 750 deg to 950 deg C. After an induction period, the rate of corrosion is linear and catastrophic corrosion is observed. It is shown that the induction period is associated with the attainment of a minimum MoO<sub>3</sub> activity in the melt, which corresponds to the equilibrium MoO<sub>3</sub> activity for the reaction, 2MoO<sub>3</sub>(l) + Mo = 3MoO<sub>2</sub>(s). A mechanism is proposed to describe the catastrophic nature of corrosion, which involves transport of Ni++ through the melt resulting in formulation of NiO at the melt gas interface and basic fluxing of Cr<sub>2</sub>O<sub>3</sub>. The effect of the amount of Na<sub>2</sub>MoO<sub>4</sub> on the corrosion kinetics was also studied. It is found that evaporation and the thermodynamic calculations for the Na<sub>2</sub>MoO<sub>4</sub> - MoO<sub>3</sub> system the activity of MoO<sub>3</sub> is reduced considerably when dissolved in Na<sub>2</sub>MoO<sub>4</sub>, which causes a sharp decrease in the rate of evaporation of MoO<sub>3</sub> from a Na<sub>2</sub>MoO<sub>4</sub> - MoO<sub>3</sub> melt. E.A.K.

**N84-20673\*#** National Aeronautics and Space Administration. Lewis Research Center, Cleveland, Ohio.

**MECHANICAL CONTACT INDUCED TRANSFORMATION FROM THE AMORPHOUS TO THE CRYSTALLINE STATE IN METALLIC GLASS**

K. MIYOSHI and D. H. BUCKLEY 13 Apr. 1984 22 p refs Presented at 11th Conf. on Metallurg. Coatings, San Diego, Calif., 9-13 Apr. 1984; sponsored by American Vacuum Society and American Society for Metals and Indian Vacuum Society (NASA-TM-83583; E-1947; NAS 1.15:83583) Avail: NTIS HC A02/MF A01 CSCL 11F

Friction and wear tests were conducted with 3.2- and 6.4-millimeter-diameter aluminum oxide spheres sliding, in reciprocating motion, on a Fe67Co18B14Si1 metallic foil. Crystallites with a size range of 10 to 150 nanometers were produced on the wear surface of the amorphous alloy. A strong interaction between transition metals and metalloids such as silicon and boron results in strong segregation during repeated sliding, provides preferential transition metal-metalloid clustering in the amorphous alloy, and subsequently produces the diffused honeycomb structure formed by dark grey bands and primary crystals, that is, alpha-Fe in the matrix. Large plastic flow occurs on an amorphous alloy surface with sliding and the flow film of the alloy transfers to the aluminum oxide pin surface. Multiple slip bands due to shear deformation are observed on the side of the wear track. Two distinct types of wear debris were observed as a result of sliding: an alloy wear debris, and/or powdery-whiskery oxide debris. A.R.H.

**N84-20674\*#** Syracuse Univ., N. Y. Dept. of Chemical Engineering and Materials Science.

**LITERATURE SURVEY ON OXIDATIONS AND FATIGUE LIVES AT ELEVATED TEMPERATURES Final Report**

H. W. LIU and Y. OSHIDA Apr. 1984 52 p refs (Contract NAG3-348)

(NASA-CR-174639; NAS 1.26:174639) Avail: NTIS HC A04/MF A01 CSCL 11F

Nickel-base superalloys are the most complex and the most widely used for high temperature applications such as aircraft engine components. The desirable properties of nickel-base superalloys at high temperatures are tensile strength, thermomechanical fatigue resistance, low thermal expansion, as well as oxidation resistance. At elevated temperature, fatigue cracks are often initiated by grain boundary oxidation, and fatigue cracks often propagate along grain boundaries, where the oxidation rate is higher. Oxidation takes place at the interface between metal and gas. Properties of the metal substrate, the gaseous environment, as well as the oxides formed all interact to make the oxidation behavior of nickel-base superalloys extremely complicated. The important topics include general oxidation, selective oxidation, internal oxidation, grain boundary oxidation, multilayer oxide structure, accelerated oxidation under stress, stress-generation during oxidation, composition and substrate microstructural changes due to prolonged oxidation, fatigue crack initiation at oxidized grain boundaries and the oxidation accelerated fatigue crack propagation along grain boundaries. S.L.

**N84-20676\*#** Pittsburgh Univ., Pa. Dept. of Metallurgical and Materials Engineering.

**INVESTIGATION INTO THE ROLE OF SODIUM CHLORIDE DEPOSITED ON OXIDE AND METAL SUBSTRATES IN THE INITIATION OF HOT CORROSION Final Report, Apr. 1980 - Aug. 1983**

N. BIRKS 1983 108 p refs

(Contract NAG3-44)

(NASA-CR-173377; NAS 1.26:173377; FR-6) Avail: NTIS HC A06/MF A01 CSCL 11F

Sodium chloride is deposited on the surface of alumina substrates and exposed to air containing 1% SO<sub>2</sub> at temperatures between 500 C and 700 C. In all cases the sodium chloride was converted to sodium sulfate. The volatilization of sodium chloride from the original salt particles was responsible for the development of a uniform coating of sodium sulfate on the alumina substrate.

At temperatures above 625 C, a liquid NaCl-Na<sub>2</sub>SO<sub>4</sub> autectic was formed on the substrate. The mechanisms for these reactions are given. One of the main roles of NaCl in low temperature hot corrosion lies in enabling a corrosive liquid to form. Author

**N84-21716\*#** National Aeronautics and Space Administration. Lewis Research Center, Cleveland, Ohio.

**FRICITION AND WEAR OF IRON IN SULFURIC ACID**

G. W. P. RENGSTORFF (Toledo Univ.), K. MIYOSHI, and D. H. BUCKLEY Apr. 1983 22 p refs

(Contract NAG3-276)

(NASA-TP-2289; E-1635; NAS 1.60:2289) Avail: NTIS HC A02/MF A01 CSCL 11F

Elemental iron sliding on aluminum oxide in aerated sulfuric acid concentrations ranging from very dilute (0.00007 N; i.e., 4 ppm) to very concentrated (96 percent acid) was studied. Load and reciprocating sliding speeds were kept constant. With the most dilute acid of 0.7 to 0.0002 N, a complex corrosion product formed that was friable and often increased friction and wear. At concentrations of 0.001 N, metal losses were essentially by wear alone. Because no buildup of corrosion products occurred, this acid concentration became the standard from which to separate metal loss from direct corrosion and mechanical wear losses. When the acid concentration was increased to 5 percent, the high corrosion rate of iron in sulfuric acid strongly dominated the total wear loss. This strong corrosion increased to 30 percent acid, and decreased somewhat at 50 percent in accordance with expectations. However, the low corrosion of iron expected at acid concentrations of 65 to 96 percent was not observed in the wear area. It is apparent that the normal passivating film was being worn away and a galvanic cell established which rapidly attached to the wear area. A.R.H.

**N84-21719\*#** National Aeronautics and Space Administration. Lewis Research Center, Cleveland, Ohio.

**ION-BEAM NITRIDING OF STEELS**

J. SALIK 13 Apr. 1984 15 p refs Presented at 11th Intern. Conf. on Met. Coatings, San Diego, Calif., 9-13 Apr. 1984; sponsored by American Vacuum Society

(NASA-TM-83599; E-1992; NAS 1.15:83599) Avail: NTIS HC A02/MF A01 CSCL 11F

The application of the ion beam technique to the nitriding of steels is described. It is indicated that the technique can be successfully applied to nitriding. Some of the structural changes obtained by this technique are similar to those obtained by ion nitriding. The main difference is the absence of the iron nitride diffraction lines. It is found that the dependence of the resultant microhardness on beam voltage for super nitralloy is different from that of 304 stainless steel. E.A.K.

**N84-21720\*#** Research Inst. of Colorado, Fort Collins.

**PHOTODEPOSITION OF NITRIDE INSULATORS ON 3-5 SUBSTRATES Annual Report, 1 Apr. 1983 - 31 Mar. 1984**

G. J. COLLINS 31 Mar. 1984 17 p

(Contract NCC3-28)

(NASA-CR-173393; NAS 1.26:173393) Avail: NTIS HC A02/MF A01 CSCL 11F

Laser assisted chemical vapor deposition (LCVD) of nitride insulators, using an excimer laser operating on either KrF or ArF transitions (248 nm or 193 nm respectively) was explored. The properties of silicon nitride films Deposited with 193 nm photons on quartz and silicon substrates in a SiH<sub>4</sub>, NH<sub>3</sub>, N<sub>2</sub> and He mixture are discussed. Aluminum films were deposited at substrate temperatures from room temperature to 200 C using 248 nm or 193 nm photons to dissociate trimethylaluminum (TMA). Deposition of Al films were investigated to isolate problems associated with TMA such as C and O contamination during AlN depositions. The Al film properties were evaluated on SiO<sub>2</sub> and Si substrates. Preliminary results were obtained for aluminum nitride films using TMA and NH<sub>3</sub> as the gas phase Al and N donors. The properties of Cr films deposited over areas 5 square cm using 193 nm or 248 nm photons to dissociate Cr(CO) were investigated. Author



**N84-21721\*#** National Aeronautics and Space Administration. Lewis Research Center, Cleveland, Ohio.

**FRICION AND WEAR OF NICKEL IN SULFURIC ACID**

G. W. P. RENGSTORFF (Toledo Univ., Ohio), K. MIYOSHI, and D. H. BUCKLEY Apr. 1984 17 p refs  
(Contract NAG3-276)  
(NASA-TP-2290; E-1817; NAS 1.60.2290) Avail: NTIS HC A02/MF A01 CSCL 11F

Experiments were conducted with elemental nickel sliding on aluminum oxide in aerated sulfuric acid in concentrations ranging from very dilute (10<sup>-4</sup> N, i.e., 5 ppm) to very concentrated (96 percent) acid. Load and reciprocating sliding speeds were kept constant. With the most dilute concentration (10<sup>-4</sup> N) no observable corrosion occurred in or outside the wear area. This was used as the base condition to determine the high contribution of corrosion to total wear loss at acid concentrations between 0.5 percent (0.1 N) and 75 percent. Corrosion reached a maximum rate of 100 millimeters per year at 30 percent acid. At the same time, general corrosion outside the wear area was very low, in agreement with published information. It is clear that friction and wear greatly accelerated corrosion in the wear area. At dilute concentrations of 0.001 and 0.01 N, corrosion in the wear area was low, and general corrosion outside was also low, but local outside regions in the direction of the wear motion experienced some enhanced corrosion, apparently due to fluid motion of the acid.

Author

**N84-22734\*** National Aeronautics and Space Administration. Lewis Research Center, Cleveland, Ohio.

**METHOD OF MAKING A LIGHT-WEIGHT BATTERY PLAQUE**

Patent  
M. A. REID, R. E. POST, and D. G. SOLTIS, inventors (to NASA) 27 Mar. 1984 6 p Filed 19 Feb. 1982  
(NASA-CASE-LEW-13349-1; US-PATENT-4,439,465;  
US-PATENT-APPL-SN-350476; US-PATENT-CLASS-427-115;  
US-PATENT-CLASS-29-623.5; US-PATENT-CLASS-427-125;  
US-PATENT-CLASS-427-126.6; US-PATENT-CLASS-427-296;  
US-PATENT-CLASS-427-306; US-PATENT-CLASS-429-223;  
US-PATENT-CLASS-429-234) Avail: US Patent and Trademark Office CSCL 11F

A nickel plaque which may be coated with a suitable metal or compound to make an electrode for a fuel cell or battery is fabricated by directing nickel sensitizer, catalyst and plating solutions through a porous plastic substrate in the order named and at prescribed temperatures and flow rates. A boride compound dissolved in the plating solution decreases the electrical resistance of the plaque. Certain substrates may require treatment in an alkali solution to dissolve filler materials thereby increasing porosity to a required 65%.

Official Gazette of the U.S. Patent and Trademark Office

**N84-23897\*#** National Aeronautics and Space Administration. Lewis Research Center, Cleveland, Ohio.

**METALLIC ADHESION AND BONDING**

J. FERRANTE, J. R. SMITH (General Motors Research Labs.), and J. H. ROSE (Ames Lab.) *In its Tribology in the 80's*. Vol. 1 p 143-162 Apr. 1984 refs  
Avail: NTIS HC A22/MF A01 CSCL 11F

Although metallic adhesion has played a central part in much tribological speculation, few quantitative theoretical calculations are available. This is in part because of the difficulties involved in such calculations and in part because the theoretical physics community is not particularly involved with tribology. The calculations currently involved in metallic adhesion are summarized and shown that these can be generalized into a scaled universal relationship. Relationships exist to other types of covalent bonding, such as cohesive, chemisorptive, and molecular bonding. A simple relationship between surface energy and cohesive energy is offered.

Author

**N84-23898\*#** National Aeronautics and Space Administration. Lewis Research Center, Cleveland, Ohio.

**THE STRENGTH OF THE METAL ALUMINUM OXIDE INTERFACE**

S. V. PEPPER *In its Tribology in the 80's*. Vol. 1 p 165-175 Apr. 1984 refs  
Avail: NTIS HC A22/MF A01 CSCL 11F

The strength of the interface between metals and aluminum oxide is an important factor in the successful operation of devices found throughout modern technology. One finds the interface in machine tools, jet engines, and microelectronic integrated circuits. The strength of the interface, however, should be strong or weak depending on the application. The diverse technological demands have led to some general ideas concerning the origin of the interfacial strength, and have stimulated fundamental research on the problem. Present status of our understanding of the source of the strength of the metal - aluminum oxide interface in terms of interatomic bonds are reviewed. Some future directions for research are suggested.

Author

**N84-24772\*#** National Aeronautics and Space Administration. Lewis Research Center, Cleveland, Ohio.

**PERFORMANCE OF THERMAL BARRIER COATINGS IN HIGH HEAT FLUX ENVIRONMENTS**

R. A. MILLER and C. C. BERNDT (Cleveland State Univ.) 1984 13 p refs Presented at the Intern. Conf. on Metallurgical Coatings, San Diego, Calif., 9-13 Apr. 1984  
(NASA-TM-83663; E-2010; NAS 1.15:83663) Avail: NTIS HC A02/MF A01 CSCL 11F

Thermal barrier coatings were exposed to the high temperature and high heat flux produced by a 30 kW plasma torch. Analysis of the specimen heating rates indicates that the temperature drop across the thickness of the 0.038 cm ceramic layer was about 1100 C after 0.5 sec in the flame. An as-sprayed ZrO<sub>2</sub>-8%Y<sub>2</sub>O<sub>3</sub> specimens survived 3000 of the 0.5 sec cycles with failing. Surface spalling was observed when 2.5 sec cycles were employed but this was attributed to uneven heating caused by surface roughness. This surface spalling was prevented by smoothing the surface with silicon carbide paper or by laser glazing. A coated specimen with no surface modification but which was heat treated in argon also did not surface spall. Heat treatment in air led to spalling in as early as 2 cycle from heating stresses. Failures at edges were investigated and shown to be a minor source of concern. Ceramic coatings formed from ZrO<sub>2</sub>-12%Y<sub>2</sub>O<sub>3</sub> or ZrO<sub>2</sub>-20%Y<sub>2</sub>O<sub>3</sub> were shown to be unsuited for use under the high heat flux conditions of this study.

Author

**N84-24774\*#** General Electric Co., Evendale, Ohio.

**EFFECTS OF SURFACE CHEMISTRY ON HOT CORROSION LIFE Annual Report**

R. E. FRYXELL Jun. 1984 57 p refs  
(Contract NAS3-23926)  
(NASA-CR-174683; NAS 1.26:174683; R84AEB422; AR-1) Avail: NTIS HC A04/MF A01 CSCL 11F

Baseline burner rig hot corrosion with Udimet 700, Rene' 80; uncoated and with RT21, Codep, or NiCoCrAlY coatings were tested. Test conditions are: 900C, hourly thermal cycling, 0.5 ppm sodium as NaCl in the gas stream, velocity 0.3 Mach. The uncoated alloys exhibited substantial typical sulfidation in the range of 140 to 170 hours. The aluminide coatings show initial visual evidence of hot corrosion at about 400 hours, however, there is no such visual evidence for the NiCoCrAlY coatings. The turbine components show sulfidation. The extent of this distress appeared to be inversely related to the average length of mission which may, reflect greater percentage of operating time near ground level or greater percentage of operation time at takeoff conditions (higher temperatures). In some cases, however, the location of maximum distress did not exhibit the structural features of hot corrosion.

E.A.K.



**N84-25793\*#** National Aeronautics and Space Administration  
Lewis Research Center, Cleveland, Ohio  
**CREEP-RUPTURE BEHAVIOR OF CANDIDATE STIRLING  
ENGINE ALLOYS AFTER LONG-TERM AGING AT 760 DEG C  
IN LOW-PRESSURE HYDROGEN** Final Report  
R. H. TITRAN May 1984 45 p refs  
(Contract DE-AI01-77CS-51040)  
(NASA-TM-83676, DOE/NASA/51040-55; E-2124; NAS  
1.15:83676) Avail: NTIS HC A03/MF A01 CSCL 11F

Nine candidate Stirling automotive engine alloys were aged at 760 C for 3500 hr in low pressure hydrogen or argon to determine the resulting effects on mechanical behavior. Candidate heater head tube alloys were CG-27, W545, 12RN72, INCONEL-718, and HS-188 while candidate cast cylinder-regenerator housing alloys were SA-F11, CRM-6D, XF-818, and HS-31. Aging per se is detrimental to the creep rupture and tensile strengths of the iron base alloys. The presence of hydrogen does not significantly contribute to strength degradation. Based percent highway driving cycle; CG-27 has adequate 3500 hr - 870 C creep rupture strength and SA-F11, CRM-6D, and XF-818 have adequate 3500 hr - 775 C creep rupture strength. Author

**N84-26783\*#** National Aeronautics and Space Administration  
Lewis Research Center, Cleveland, Ohio.  
**EFFECTS OF ALLOY COMPOSITION ON CYCLIC FLAME  
HOT-CORROSION ATTACK OF CAST NICKEL-BASE  
SUPERALLOYS AT 900 DEG C**  
D. L. DEADMORE Jul. 1984 30 p refs  
(NASA-TP-2338; E-2009; NAS 1.60 2338) Avail: NTIS HC  
A03/MF A01 CSCL 11F

The effects of Cr, Al, Ti, Mo, Ta, Nb, and W content on the hot corrosion of nickel base alloys were investigated. The alloys were tested in a Mach 0.3 flame with 0.5 ppmw sodium at a temperature of 900 C. One nondestructive and three destructive tests were conducted. The best corrosion resistance was achieved when the Cr content was 12 wt %. However, some lower-Cr-content alloys (10 wt %) exhibited reasonable resistance provided that the Al content alloys (10 wt %) exhibited reasonable resistance provided that the Al content was 2.5 wt % and the Ti content was 1 wt %. The effect of W, Ta, Mo, and Nb contents on the hot-corrosion resistance varied depending on the Al and Ti contents. Several commercial alloy compositions were also tested and the corrosion attack was measured. Predicted attack was calculated for these alloys from derived regression equations and was in reasonable agreement with that experimentally measured. The regression equations were derived from measurements made on alloys in a one-quarter replicate of a 2(7) statistical design alloy composition experiment. These regression equations represent a simple linear model and are only a very preliminary analysis of the data needed to provide insights into the experimental method. A.R.H.

**N84-26785\*#** National Aeronautics and Space Administration.  
Lewis Research Center, Cleveland, Ohio.  
**P/M SUPERALLOYS: A TROUBLED ADOLESCENT?**  
R. L. DRESHFIELD and H. R. GRAY 1984 23 p refs  
Presented at P/M 1984, Toronto, 17-22 Jun. 1984; sponsored by Metal Powder Industries Federation  
(NASA-TM-83623; E-2057; NAS 1.15:83623) Avail: NTIS HC  
A02/MF A01 CSCL 11F

The history of powder metallurgy P/M superalloy technology is reviewed with a comment on the state of the art, and speculates on the technology's future potential growth and maturity. M.A.C.

**N84-26787\*#** National Aeronautics and Space Administration.  
Lewis Research Center, Cleveland, Ohio.  
**SOME FUNDAMENTAL ASPECTS OF SOLIDIFICATION IN A  
SUPERCOOLED MELT**  
V. LAXMANAN (Case Western Reserve Univ., Cleveland) 1983  
7 p refs To be presented at the 5th Conf. on Rapid Quenching  
and Solidification of Metals (RQ5), Wurzburg, West Germany, 3-7  
Sep 1984  
(NASA-TM-83714; E-2153; NAS 1.15:83714) Avail: NTIS-HC  
A02/MF A01 CSCL 11F

A model of dendritic growth in both supercooled pure and alloy melts is presented. In a pure melt, dendrite morphology is determined by the value of the dimensionless parameter  $\sigma = 2\alpha(L)d(o)/\sqrt{Rr(t)}$  whereas, in an alloy melt it is determined by the parameter  $\sigma = 2\lambda(c)D(L)/\sqrt{Rr(t)}$ . The application of the above analysis to cylindrical and spherical growth morphologies obtained in highly supercooled melts has been discussed. An upper and lower bound for the particle or tip radius in this case has been obtained in terms of the growth rate and the initial bath supercooling. Author

**N84-27855\*** National Aeronautics and Space Administration.  
Lewis Research Center, Cleveland, Ohio.  
**COATING WITH OVERLAY METALLIC-CERMET ALLOY  
SYSTEMS** Patent  
M. A. GEDWILL, S. R. LEVINE, and T. K. GLASGOW, inventors  
(to NASA) 29 May 1984 7 p Filed 7 Jan. 1983 Supersedes  
N83-17683 (21 - 08, p 1158) Division of  
US-Patent-Appl-SN-403378, US-Patent-4,446,199, filed 30 Jul.  
1982  
(NASA-CASE-LEW-13639-2; US-PATENT-4,451,496;  
US-PATENT-APPL-SN-456460; US-PATENT-CLASS-427-34;  
US-PATENT-CLASS-427-405; US-PATENT-CLASS-427-419.2;  
US-PATENT-CLASS-428-632) Avail: US Patent and Trademark  
Office CSCL 11F

A base layer of an oxide dispersed, metallic alloy (cermet) is arc plasma sprayed onto a substrate, such as a turbine blade, vane, or the like, which is subjected to high temperature use. A top layer of an oxidation, hot corrosion, erosion resistant alloy of nickel, cobalt, or iron is then arc plasma sprayed onto the base layer. A heat treatment is used to improve the bonding. The base layer serves as an inhibitor to interdiffusion between the protective top layer and the substrate. Otherwise, the 10 protective top layer would rapidly interact detrimentally with the substrate and degrade by spalling of the protective oxides formed on the outer surface at elevated temperatures.

Official Gazette of the U.S. Patent and Trademark Office

**N84-27857\*#** National Aeronautics and Space Administration.  
Lewis Research Center, Cleveland, Ohio.  
**INTERACTION OF SULFURIC ACID CORROSION AND  
MECHANICAL WEAR OF IRON**  
G. W. P. RENGSTORFF (Toledo Univ.), K. MIYOSHI, and D. H.  
BUCKLEY 1984 23 p refs Proposed for presentation at the  
Joint Lubrication Conf., San Diego, 22-24 Oct. 1984; sponsored  
by the American Society of Mechanical Engineers and the American  
Society of Lubrication Engineers  
(NASA-TM-83717; E-1985; NAS 1.15:83717) Avail: NTIS HC  
A02/MF A01 CSCL 11F

Friction and wear experiments were conducted with elemental iron sliding on aluminum oxide in aerated sulfuric acid at concentrations ranging from very dilute (0.00007 N; i.e., 4 ppm) to very concentrated (96 percent acid). Load and reciprocating sliding speed were kept constant. With the most dilute acid concentration of 0.00007 to 0.0002 N, a complex corrosion product formed that was friable and often increased friction and wear. At slightly higher concentrations of 0.001 N, metal losses were essentially by wear alone. Because no buildup of corrosion products occurred, this acid concentration became the standard from which to separate metal loss from direct corrosion and mechanical wear losses. When the acid concentration was increased to 5 percent (1 N), the well-established high corrosion rate of iron in sulfuric acid strongly dominated the total wear loss. This strong corrosion

increased to 30 percent acid and decreased somewhat to 50 percent acid in accordance with expectations. However, the low corrosion of iron expected at acid concentrations of 65 to 96 percent was not observed in the wear area. It was apparent that the normal passivating film was being worn away and a galvanic cell established that rapidly attacked the wear area. Under the conditions where direct corrosion losses were highest, the coefficient of friction was the lowest. Author

**N84-27858\*#** National Aeronautics and Space Administration. Lewis Research Center, Cleveland, Ohio.  
**MODELING DEGRADATION AND FAILURE OF NI-CR-AL OVERLAY COATINGS**  
J. A. NESBITT and R. W. HECKEL (Michigan Technological Univ.) 1984 11 p refs Presented at the 11th Intern. Conf. on Met. Coatings, San Diego, 9-13 Apr. 1984; sponsored by the American Vacuum Society (NASA-TM-83672; E-2116; NAS 1.15:83672) Avail: NTIS HC A02/MF A01 CSCL 11F

Degradation of a Ni-16Cr-25Al-0.06Zr overlay coating on a Ni-22Cr substrate was examined after oxidation accompanied by thermal cycling. Concentration/distance profiles were measured in the coating and substrate after various one-hour cycles at 1150 C. A numerical model was developed to simulate coating degradation by simultaneous oxidation and coating/substrate interdiffusion. The validity of the model was confirmed by comparison of predicted and measured concentration/distance profiles. The ability of the model to identify critical system parameters was demonstrated for the case of the initial Al and Cr content of the coating and substrate. M.G.

**N84-27859\*#** National Aeronautics and Space Administration. Lewis Research Center, Cleveland, Ohio.  
**IN-SITU MEASUREMENTS OF ALLOY OXIDATION/CORROSION/EROSION USING A VIDEO CAMERA AND PROXIMITY SENSOR WITH MICROCOMPUTER CONTROL**  
D. L. DEADMORE May 1984 16 p refs (NASA-TM-83673; E-2117; NAS 1.15:83673) Avail: NTIS HC A02/MF A01 CSCL 11F

Two noncontacting and nondestructive, remotely controlled methods of measuring the progress of oxidation/corrosion/erosion of metal alloys, exposed to flame test conditions, are described. The external diameter of a sample under test in a flame was measured by a video camera width measurement system. An eddy current proximity probe system, for measurements outside of the flame, was also developed and tested. The two techniques were applied to the measurement of the oxidation of 304 stainless steel at 910 C using a Mach 0.3 flame. The eddy current probe system yielded a recession rate of 0.41 mils diameter loss per hour and the video system gave 0.27. Author

**N84-28958\*#** National Aeronautics and Space Administration. Lewis Research Center, Cleveland, Ohio.  
**CHEMICAL MECHANISMS AND REACTION RATES FOR THE INITIATION OF HOT CORROSION OF IN-738**  
G. C. FRYBURG, F. J. KOHL, and C. A. STEARNS Jul. 1984 34 p Submitted for publication (NASA-TP-2319; E-1847; NAS 1.60:2319) Avail: NTIS HC A03/MF A01 CSCL 11F

Sodium-sulfate-induced hot corrosion of preoxidized IN-738 was studied at 975 C with special emphasis placed on the processes occurring during the long induction period. Thermogravimetric tests were run for predetermined periods of time, and then one set of specimens was washed with water. Chemical analysis of the wash solutions yielded information about water soluble metal salts and residual sulfate. A second set of samples was cross sectioned dry and polished in a nonaqueous medium. Element distributions within the oxide scale were obtained from electron microprobe X-ray micrographs. Evolution of SO was monitored throughout the thermogravimetric tests. Kinetic rate studies were performed for several pertinent processes; appropriate rate constants were obtained from the following chemical reactions:  $\text{Cr}_2\text{O}_3 + 2$

$\text{Na}_2\text{SO}_4(1) + 3/2 \text{O}_2$  yields  $2 \text{Na}_2\text{CrO}_4(1) + 2 \text{SO}_3(g)$   
 $\text{TiO}_2 + \text{Na}_2\text{SO}_4(1)$  yields  $\text{Na}_2\text{O}(\text{TiO}_2)_n + \text{SO}_3(g)$   
 $n \text{TiO}_2 + \text{Na}_2\text{CrO}_4(1)$  yields  $\text{Na}_2\text{O}(\text{TiO}_2)_n + \text{CrO}_3(g)$ . Author

**N84-28960\*#** Southwest Research Inst., San Antonio, Tex.  
**DEVELOPMENT OF CARBON SLURRY FUELS FOR TRANSPORTATION (HYBRID FUELS, PHASE 2)**  
T. W. RYAN, III and L. G. DODGE May 1984 174 p refs (Contract DEN3-263; DE-AI01-81CS-50006) (NASA-CR-174659; DOE/NASA/0263-1; NAS 1.26:174659; SWRI-6948) Avail: NTIS HC A08/MF A01 CSCL 11F

Slurry fuels of various forms of solids in diesel fuel are developed and evaluated for their relative potential as fuel for diesel engines. Thirteen test fuels with different solids concentrations are formulated using eight different materials. A variety of properties are examined including ash content, sulfur content, particle size distribution, and rheological properties. Attempts are made to determine the effects of these variations on these fuel properties on injection, atomization, and combustion processes. The slurries are also tested in a single cylinder CLR engine in both direct injection and prechamber configurations. The data includes the normal performance parameters as well as heat release rates and emissions. The slurries perform very much like the baseline fuel. The combustion data indicate that a large fraction (90 percent or more) of the solids are burning in the engine. It appears that the prechamber engine configuration is more tolerant of the slurries than the direct injection configuration. M.A.C.

**N84-28961\*#** IIT Research Inst., Chicago, Ill.  
**CREEP-RUPTURE BEHAVIOR OF CANDIDATE STIRLING ENGINE IRON SUPPERALLOYS IN HIGH-PRESSURE HYDROGEN. VOLUME 2: HYDROGEN CREEP-RUPTURE BEHAVIOR Final Report**  
S. BHATTACHARYA, W. PETERMAN, and C. HALES Jun. 1984 105 p refs (Contract DEN3-303; DE-AI01-77CS-51040) (NASA-CR-174705; NAS 1.26:174705; IITRI-M06116-15) Avail: NTIS HC A06/MF A01 CSCL 11F

The creep rupture behavior of nine iron base and one cobalt base candidate Stirling engine alloys is evaluated. Rupture life, minimum creep rate, and time to 1% strain data are analyzed. The 3500 h rupture life stress and stress to obtain 1% strain in 3500 h are also estimated. M.A.C.

**N84-28962\*#** National Aeronautics and Space Administration. Lewis Research Center, Cleveland, Ohio.  
**OXIDATION AND CORROSION RESISTANCE OF CANDIDATE STIRLING ENGINE HEATER-HEAD-TUBE ALLOYS**  
J. R. STEPHENS and C. A. BARRETT May 1984 33 p refs (Contract DE-AI01-77CS-51040) (NASA-TM-83609; DOE/NASA/51040-53; E-2028; NAS 1.15:83609) Avail: NTIS HC A03/MF A01 CSCL 11F

Sixteen candidate iron base Stirling engine heater head tube alloys are evaluated in a diesel fuel fired simulator materials test rig to determine their oxidation and corrosion resistance. Sheet specimens are tested at 820 C for 3500 hr in 5 hr heating cycles. Specific weight change data and an attack parameter are used to categorize the alloys into four groups; 10 alloys show excellent for good oxidation and corrosion resistance and six alloys exhibit poor or catastrophic resistance. Metallographic, X-ray, and electron microprobe analyses aid in further characterizing the oxidation and corrosion behavior of the alloys. Alloy compositions, especially the reactive elements aluminum, titanium, and chromium, play a major role in the excellent oxidation and corrosion behavior of the alloys. The best oxidation resistance is associated with the formation of an iron nickel aluminum outer oxide scale, an intermediate oxide scale rich in chromium and titanium, and an aluminum outer oxide scale adjacent to the metallic substrate, which exhibits a zone of internal oxidation of aluminum and to some extent titanium. M.A.C.

**N84-28963\*#** National Aeronautics and Space Administration. Lewis Research Center, Cleveland, Ohio.

**ADVANCED HIGH TEMPERATURE MATERIALS FOR THE ENERGY EFFICIENT AUTOMOTIVE STIRLING ENGINE**

R. H. TITRAN and J. R. STEPHENS 1984 22 p refs Presented at Conf. on Mater. for Future Energy Systems, Washington, D.C., 1-3 May 1984; sponsored by American Society for Metals (Contract DE-AI01-77CS-51040)

(NASA-TM-83659; E-2056; NAS 1.15:83659) Avail: NTIS HC A02/MF A01 CSCL 11F

The Stirling Engine is under investigation jointly by the Department of Energy and NASA Lewis as an alternative to the internal combustion engine for automotive applications. The Stirling Engine is an external combustion engine that offers the advantage of high fuel economy, low emissions, low noise, and low vibrations compared to current internal combustion automotive engines. The most critical component from a materials viewpoint is the heater head consisting of the cylinders, heating tubes, and regenerator housing. Materials requirements for the heater head include compatibility with hydrogen, resistance to hydrogen permeation, high temperature oxidation/corrosion resistance and high temperature creep-rupture and fatigue properties. A continuing supporting materials research and technology program has identified the wrought alloys CG-27 and 12RN72 and the cast alloys XF-818 and NASAUT 4G-A1 as candidate replacements for the cobalt containing alloys used in current prototype engines. Based on the materials research program in support of the automotive Stirling engine it is concluded that manufacture of the engine is feasible from low cost iron-base alloys rather than the cobalt alloys rather than the cobalt alloys used in prototype engines. This paper will present results of research that led to this conclusion.

Author

**N84-28965\*#** National Aeronautics and Space Administration. Lewis Research Center, Cleveland, Ohio.

**EROSION OF IRON-CHROMIUM ALLOYS BY GLASS PARTICLES**

J. SALIK and D. H. BUCKLEY Jul. 1984 10 p refs (NASA-TP-2354; E-1615; NAS 1.60:2354) Avail: NTIS HC A02/MF A01 CSCL 11F

The material loss upon erosion was measured for several iron-chromium alloys. Two types of erodent material were used, spherical glass beads and sharp particles of crushed glass. For erosion with glass beads the erosion resistance (defined as the reciprocal of material loss rate) was linearly dependent on hardness. This is in accordance with the erosion behavior of pure metals, but contrary to the erosion behavior of alloys of constant composition that were subjected to different heat treatments. For erosion with crushed glass, however, no correlation existed between hardness and erosion resistance. Instead, the erosion resistance depended on alloy composition rather than on hardness and increased with the chromium content of the alloy. The difference in erosion behavior for the two types of erodent particles suggested that two different material removal mechanisms were involved. This was confirmed by SEM micrographs of the eroded surfaces, which showed that for erosion with glass beads the mechanism of material removal was deformation-induced flaking of surface layers, or peening, whereas for erosion with crushed glass it was cutting or chopping.

Author

**N84-31344\*#** National Aeronautics and Space Administration. Lewis Research Center, Cleveland, Ohio.

**OVERLAY COATING DEGRADATION BY SIMULTANEOUS OXIDATION AND COATING/SUBSTRATE INTERDIFFUSION Ph.D. Thesis**

J. A. NESBITT Aug. 1983 207 p refs (Contract NAG3-244)

(NASA-TM-83738; E-2223; NAS 1.15:83738) Avail: NTIS HC A10/MF A01 CSCL 11F

Degradation of NiCrAlZr overlay coatings on various NiCrAl substrates was examined after cyclic oxidation. Concentration/distance profiles were measured in the coating and substrate after various oxidation exposures at 1150 C. For each

substrate, the Al content in the coating decreased rapidly. The concentration/distance profiles, and particularly that for Al, reflected the oxide spalling resistance of each coated substrate. A numerical model was developed to simulate diffusion associated with overlay-coating degradation by oxidation and coating/substrate interdiffusion. Input to the numerical model consisted of the Cr and Al content of the coating and substrate, ternary diffusivities, and various oxide spalling parameters. The model predicts the Cr and Al concentrations in the coating and substrate after any number of oxidation/thermal cycles. The numerical model also predicts coating failure based on the ability of the coating to supply sufficient Al to the oxide scale. The validity of the model was confirmed by comparison of the predicted and measured concentration/distance profiles. The model was subsequently used to identify the most critical system parameters affecting coating life.

B.W.

**N84-31345\*#** National Aeronautics and Space Administration. Lewis Research Center, Cleveland, Ohio.

**HIGH-TEMPERATURE CYCLIC OXIDATION DATA, VOLUME 1**

C. A. BARRETT, R. G. GARLICK, and C. E. LOWELL May 1984 188 p

(NASA-TM-83665; E-1499; NAS 1.15:83665) Avail: NTIS HC A09/MF A01 CSCL 11F

This first in a series of cyclic oxidation handbooks contains specific-weight-change-versus-time data and X-ray diffraction results derived from high-temperature cyclic tests on high-temperature, high-strength nickel-base gamma/gamma' and cobalt-base turbine alloys. Each page of data summarizes a complete test on a given alloy sample.

A.R.H.

**N84-31347\*#** National Aeronautics and Space Administration. Lewis Research Center, Cleveland, Ohio.

**FAILURE ANALYSIS OF PLASMA-SPRAYED THERMAL BARRIER COATINGS**

C. C. BERNDT (Cleveland State Univ.) and R. A. MILLER 1984 13 p refs Presented at the 11th Intern. Conf. on Met. Coatings, San Diego, Calif., 9-13 Apr. 1984; sponsored by American Vacuum Society

(NASA-TM-83777; E-2269; NAS 1.15:83777) Avail: NTIS HC A02/MF A01 CSCL 11F

Thermally induced failure processes of plasma-sprayed thermal barrier coatings are examined. Cracking processes give rise to noise which was monitored by acoustic emission (AE) techniques. The sequential failure of coatings was examined from samples which were thermally cycled. Coatings of yttria-stabilized zirconia with and without a NiCrAlZr bond coat were plasma-sprayed onto U700 alloy rod. In some cases the substrate was intentionally overheated during deposition of the thermal protection system to check how this process variable influenced the AE response of the specimen. In this way a qualitative appraisal of how process variables affect coating integrity could be discerned in terms of cracking behavior. Results from up to seven consecutive thermal cycles are reported here. Coating failure was observed in all cases. Failure of the thermal protection system is progressive, since cracking and crack growth were observed prior to ultimate failure. Thus catastrophic failure occurs at some stage when there is a transformation from the microcrack to a macrocrack network.

Author

**N84-31348\*#** National Aeronautics and Space Administration. Lewis Research Center, Cleveland, Ohio.

**EVALUATION OF THE EFFECT OF CRACK CLOSURE ON FATIGUE CRACK GROWTH OF SIMULATED SHORT CRACKS**

J. TELESMA and D. M. FISHER Aug. 1984 12 p refs (NASA-TM-83778; E-2063; NAS 1.15:83778) Avail: NTIS HC A02/MF A01 CSCL 11F

A test program was performed to determine the influence of crack closure on fatigue crack growth (FCG) rates of short cracks. By use of the standard compact tension specimen, test procedures were devised to evaluate closure loads in the wake of the crack behind its tip. The first procedure determined the magnitude of crack closure as a function of the fatigued crack wave by incrementally removing the contacting wake surfaces and

measuring closure load at each increment. The second procedure used a low-high loading sequence to simulate short crack behavior. Based on the results, it was concluded that crack closure is not the major reason for the more rapid growth of short cracks as compared to long crack growth. Author

**N84-31349\*#** National Aeronautics and Space Administration. Lewis Research Center, Cleveland, Ohio.

**EMPIRICAL RELATIONS FOR CAVITATION AND LIQUID IMPINGEMENT EROSION PROCESSES**

P. V. RAO and D. H. BUCKLEY Aug. 1984 27 p refs  
Submitted for publication  
(Contract NCC3-21)

(NASA-TP-2339; E-1872; NAS 1.60:2339) Avail: NTIS HC A03/MF A01 CSCL 11F

A unified power-law relationship between average erosion rate and cumulative erosion is presented. Extensive data analyses from venturi, magnetostriction (stationary and oscillating specimens), liquid drop, and jet impact devices appear to conform to this relation. A normalization technique using cavitation and liquid impingement erosion data is also presented to facilitate prediction. Attempts are made to understand the relationship between the coefficients in the power-law relationships and the material properties. Author

**N84-32503\*#** Syracuse Univ, N Y.

**CRACK TIP FIELD AND FATIGUE CRACK GROWTH IN GENERAL YIELDING AND LOW CYCLE FATIGUE Final Report**

Z. MINZHONG (Aircraft Strength Research Inst., Xian, China) and H. W. LIU Sep. 1984 94 p refs  
(Contract NAG3-348)

(NASA-CR-174686; NAS 1.26:174686) Avail: NTIS HC A05/MF A01 CSCL 11F

Fatigue life consists of crack nucleation and crack propagation periods. Fatigue crack nucleation period is shorter relative to the propagation period at higher stresses. Crack nucleation period of low cycle fatigue might even be shortened by material and fabrication defects and by environmental attack. In these cases, fatigue life is largely crack propagation period. The characteristic crack tip field was studied by the finite element method, and the crack tip field is related to the far field parameters: the deformation work density, and the product of applied stress and applied strain. The cyclic crack growth rates in specimens in general yielding as measured by Solomon are analyzed in terms of J-integral. A generalized crack behavior in terms of delta is developed. The relations between J and the far field parameters and the relation for the general cyclic crack growth behavior are used to analyze fatigue lives of specimens under general-yielding cyclic-load. Fatigue life is related to the applied stress and strain ranges, the deformation work density, crack nucleus size, fracture toughness, fatigue crack growth threshold, Young's modulus, and the cyclic yield stress and strain. The fatigue lives of two aluminum alloys correlate well with the deformation work density as depicted by the derived theory. The general relation is reduced to Coffin-Manson low cycle fatigue law in the high strain region. Author

**N84-32504\*#** United Technologies Corp., East Hartford, Conn. Engineering Div.

**MATERIALS FOR ADVANCED TURBINE ENGINES (MATE): PROJECT 3: DESIGN, FABRICATION AND EVALUATION OF AN OXIDE DISPERSION STRENGTHENED SHEET ALLOY COMBUSTOR LINER, VOLUME 1 Final Report**

R. J. HENRICKS and K. D. SHEFFLER Feb. 1984 274 p refs  
(Contract NAS3-20072)

(NASA-CR-174691; NAS 1.26:174691; PWA-5574-175-VOL-1) Avail: NTIS HC A12/MF A01 CSCL 11F

The suitability of wrought oxide dispersion strengthened (ODS) superalloy sheet for gas turbine engine combustor applications was evaluated. Incoloy MA 956 (FeCrAl base) and Haynes Developmental Alloy (HDA) 8077 (NiCrAl base) were evaluated. Preliminary tests showed both alloys to be potentially viable combustor materials, with neither alloy exhibiting a significant

advantage over the other. Both alloys demonstrated a +167C (300 F) advantage of creep and oxidation resistance with no improvement in thermal fatigue capability compared to a current generation combustor alloy (Hastelloy X). MA956 alloy was selected for further demonstration because it exhibited better manufacturing reproducibility than HDA8077. Additional property tests were conducted on MA956. To accommodate the limited thermal fatigue capability of ODS alloys, two segmented, mechanically attached, low strain ODS combustor design concepts having predicted fatigue lives or = 10,000 engine cycles were identified. One of these was a relatively conventional louvered geometry, while the other involved a transpiration cooled configuration. A series of 10,000 cycle combustor rig tests on subscale MA956 and Hastelloy X combustor components showed no cracking, thereby confirming the beneficial effect of the segmented design on thermal fatigue capability. These tests also confirmed the superior oxidation and thermal distortion resistance of the ODS alloy. A hybrid PW2037 inner burner liner containing MA956 and Hastelloy X components was designed and constructed. Author

**N84-32508\*#** National Aeronautics and Space Administration. Lewis Research Center, Cleveland, Ohio.

**MICROSTRUCTURE AND SURFACE CHEMISTRY OF AMORPHOUS ALLOYS IMPORTANT TO THEIR FRICTION AND WEAR BEHAVIOR**

K. MIYOSHI and D. H. BUCKLEY 1983 23 p refs To be presented at the Intern. Tribology Conf., Tokyo, 8-10 Jul. 1985; sponsored by the Japan Soc. of Lubrication  
(NASA-TM-83762; E-2213; NAS 1.15:83762) Avail: NTIS HC A02/MF A01 CSCL 11F

An investigation was conducted to examine the microstructure and surface chemistry of amorphous alloys, and their effects on tribological behavior. The results indicate that the surface oxide layers present on amorphous alloys are effective in providing low friction and a protective film against wear in air. Clustering and crystallization in amorphous alloys can be enhanced as a result of plastic flow during the sliding process at a low sliding velocity, at room temperature. Clusters or crystallites with sizes to 150 nm and a diffused honeycomb-shaped structure are produced on the wear surface. Temperature effects lead to drastic changes in surface chemistry and friction behavior of the alloys at temperatures to 750 C. Contaminants can come from the bulk of the alloys to the surface upon heating and impart to the surface oxides at 350 C and boron nitride above 500 C. The oxides increase friction while the boron nitride reduces friction drastically in vacuum. Author

**N84-33471\*#** National Aeronautics and Space Administration. Lewis Research Center, Cleveland, Ohio.

**UNDERSTANDING THE ROLES OF THE STRATEGIC ELEMENT COBALT IN NICKEL BASE SUPERALLOYS**

J. B. STEPHENS and R. L. DRESHFIELD In AGARD Mater. Substitution and Recycling 15 p Apr. 1984 refs  
Avail: NTIS HC A13/MF A01

Research progress in understanding the effects of cobalt and some possible substitute on microstructure, mechanical properties, and environmental resistance of turbine alloys is discussed. The United States imports over 90 percent of its cobalt, chromium, tantalum and columbium, all key elements in high temperature nickel base superalloys for aircraft gas turbine disks and airfoils. NASA, through joint government/industry/university teams, undertook a long range research program aimed at reducing or eliminating these strategic elements by examining their basic roles in superalloys and identifying viable substitutes. R.J.F.

**N84-33555\*** National Aeronautics and Space Administration. Lewis Research Center, Cleveland, Ohio.

**OVERLAY METALLIC-CERMET ALLOY COATING SYSTEMS Patent**

M. A. GEDWILL, S. R. LEVINE, and T. K. GLASGOW, inventors (to NASA) 1 May 1984 7 p Filed 30 Jul. 1982 Supersedes N82-33522 (20 - 24, p 3413)

(NASA-CASE-LEW-13639-1; NAS 1.71:LEW-13639-1; US-PATENT-4,446,199; US-PATENT-APPL-SN-403378; US-PATENT-CLASS-428-639, US-PATENT-CLASS-428-564; US-PATENT-CLASS-428-678; US-PATENT-CLASS-416-241R) Avail: US Patent and Trademark Office CSCL 11F

A substrate, such as a turbine blade, vane, or the like, which is subjected to high temperature use is coated with a base coating of an oxide dispersed, metallic alloy (cermet). A top-coating of an oxidation, hot corrosion, erosion resistant alloy of nickel, cobalt, or iron is then deposited on the base coating. A heat treatment is used to improve the bonding. The base coating serves as an inhibitor to interdiffusion between the protective top coating and the substrate. Otherwise, the protective top coating would rapidly interact detrimentally with the substrate and degrade by spalling of the protective oxides formed on the outer surface at elevated temperatures.

Official Gazette of the U.S. Patent and Trademark Office

**N84-33564\*#** National Aeronautics and Space Administration. Lewis Research Center, Cleveland, Ohio

**LOW CYCLE FATIGUE BEHAVIOR OF CONVENTIONALLY CAST MAR-M 200 AT 1000 DEG C**

W. W. MILLIGAN (Georgia Inst. of Technology) and R. C. BILL Sep. 1984 15 p refs

(NASA-TM-83769, E-2260; NAS 1.15.83769, USAVSCOM-TR-84-C-16) Avail: NTIS HC A02/MF A01 CSCL 11F

The low cycle fatigue behavior of the nickel-based superalloy MAR-M 200 in conventionally cast form was studied at 1000 C. Continuous cycling tests, without hold times, were conducted with inelastic strain ranges of from 0.04 to 0.33 percent. Tests were also conducted which included a hold time at peak strain in either tension or compression. For the conditions studied, it was determined that imposition of hold times did not significantly affect the fatigue life. Also, for continuous cycling tests, increasing or decreasing the cycle frequency did not affect life. Metallographic analysis revealed that the most significant damage mechanism involved environmentally assisted intergranular crack initiation and propagation, regardless of the cycle type. Changes in the gamma morphology (rafting and rod formation) were observed, but did not significantly affect the failure. Author

**N84-34589\*#** National Aeronautics and Space Administration. Lewis Research Center, Cleveland, Ohio.

**FUNDAMENTALS OF ALLOY SOLIDIFICATION APPLIED TO INDUSTRIAL PROCESSES**

Washington Sep. 1984 185 p refs Conf. held in Cleveland, 12-13 Sep. 1984 Sponsored in part by Case Western Reserve Univ.

(NASA-CP-2337; E-2235; NAS 1.55:2337) Avail: NTIS HC A09/MF A01 CSCL 11F

Solidification processes and phenomena, segregation, porosity, gravity effects, fluid flow, undercooling, as well as processing of materials in the microgravity environment of space, now available on space shuttle flights were discussed.

**N84-34603\*#** National Aeronautics and Space Administration. Lewis Research Center, Cleveland, Ohio.

**EVALUATION OF CANDIDATE STIRLING ENGINE HEATER TUBE ALLOYS AFTER 3500 HOURS EXPOSURE TO HIGH PRESSURE DOPED HYDROGEN OR HELIUM Final Report**

J. A. MISENICK and R. H. TITRAN Oct. 1984 46 p refs (Contract DE-AI01-77CS-51040)

(NASA-TM-83782; E-2276; DOE/NASA/51040-56; NAS 1.15:83782) Avail: NTIS HC A03/MF A01 CSCL 11F

The heater head tubes of current prototype automotive Stirling engines are fabricated from alloy N-155, an alloy which contains 20 percent cobalt. Because the United States imports over 90 percent of the cobalt used in this country and resource supplies could not meet the demand imposed by automotive applications of cobalt in the heater head (tubes plus cylinders and regenerator housings), it is imperative that substitute alloys free of cobalt be identified. The research described herein focused on the heater head tubes. Sixteen alloys (15 potential substitutes plus the 20 percent Co N-155 alloy) were evaluated in the form of thin wall tubing in the NASA Lewis Research Center Stirling simulator materials diesel fuel fired test rigs. Tubes filled with either hydrogen doped with 1 percent CO<sub>2</sub> or with helium at a gas pressure of 15 MPa and a temperature of 820 C were cyclic endurance tested for times up to 3500 hr. Results showed that two iron-nickel base superalloys, CG-27 and Pyromet 901 survived the 3500 hr endurance test. The remaining alloys failed by creep-rupture at times less than 3000 hr, however, several other alloys had superior lives to N-155. Results further showed that doping the hydrogen working fluid with 1 vol % CO<sub>2</sub> is an effective means of reducing hydrogen permeability through all the alloy tubes investigated.

Author

## 27

### NONMETALLIC MATERIALS

Includes physical, chemical, and mechanical properties of plastics, elastomers, lubricants, polymers, textiles, adhesives, and ceramic materials.

**A84-11676\*** National Aeronautics and Space Administration. Lewis Research Center, Cleveland, Ohio.

**DEVELOPMENT OF PLANE STRAIN FRACTURE TOUGHNESS TEST FOR CERAMICS USING CHEVRON NOTCHED SPECIMENS**

R. T. BUBSEY, J. L. SHANNON, JR. (NASA, Lewis Research Center, Cleveland, OH), and D. MUNZ (Deutsche Forschungs- und Versuchsanstalt fuer Luft- und Raumfahrt, Cologne, West Germany) IN: Ceramics for high-performance applications III: Reliability. New York, Plenum Press, 1983, p. 753-771. refs

Chevron-notched four-point-bend and short-bar specimens have been used to determine the fracture toughness of sintered aluminum oxide and hot-pressed silicon nitride ceramics. The fracture toughness for Si<sub>3</sub>N<sub>4</sub> is found to be essentially independent of the specimen size and chevron notch configuration, with values ranging from 4.6 to 4.9 MNm exp -3/2. In contrast, significant specimen size and notch geometry effects have been observed for Al<sub>2</sub>O<sub>3</sub>, with the fracture toughness ranging from 3.1 to 4.7 MNm exp -3/2. These effects are attributed to a rising crack growth resistance curve for the Al<sub>2</sub>O<sub>3</sub> tested. V.L.

**A84-13504\*** National Aeronautics and Space Administration. Lewis Research Center, Cleveland, Ohio.

**SHRINKAGE OF AMORPHOUS SILICA FIBERS**

I. ZAPLATYNSKY (NASA, Lewis Research Center, Cleveland, OH) Ceramic Engineering and Science Proceedings (ISSN 0196-6219), vol. 4, July-Aug. 1983, p. 492-501. refs

By the application of a new technique, the viscosity of amorphous silica fibers was determined in the 1100-1350 C temperature range. An equation was derived that describes the

## 27 NONMETALLIC MATERIALS

kinetics of shrinkage of the fibers in terms of their radius, viscosity, and surface tension. Author

**A84-13516\*** National Aeronautics and Space Administration. Lewis Research Center, Cleveland, Ohio.

### **SURFACE CHEMISTRY, FRICTION, AND WEAR OF NI-ZN AND MN-ZN FERRITES IN CONTACT WITH METALS**

K. MIYOSHI and D. H. BUCKLEY (NASA, Lewis Research Center, Cleveland, OH) Ceramic Engineering and Science Proceedings (ISSN 0196-6219), vol. 4, July-Aug. 1983, p. 674-693. refs

X-ray photoelectron and Auger electron spectroscopy analysis were used in sliding friction experiments. These experiments were conducted with hot-pressed polycrystalline Ni-Zn and Mn-Zn ferrites, and single-crystal Mn-Zn ferrite in contact with various transition metals at room temperature in both vacuum and argon. The results indicate that Ni<sub>2</sub>O<sub>3</sub> and Fe<sub>3</sub>O<sub>4</sub> were present on the Ni-Zn ferrite surface in addition to the nominal bulk constituents, while MnO<sub>2</sub> and Fe<sub>3</sub>O<sub>4</sub> were present on the Mn-Zn ferrite surface in addition to the nominal bulk constituents. The coefficients of friction for the ferrites in contact with metals were related to the relative chemical activity of these metals. The more active the metal, the higher is the coefficient of friction. The coefficients of friction for the ferrites were correlated with the free energy of formation of the lowest metal oxide. The interfacial bond can be regarded as a chemical bond between the metal atoms and the oxygen anions in the ferrite surfaces. The adsorption of oxygen on clean metal and ferrite does strengthen the metal-ferrite contact and increase the friction. The ferrites exhibit local cracking and fracture with sliding under adhesive conditions. All the metals transferred to the surfaces of the ferrites in sliding. Previously announced in STAR as N83-19901 Author

**A84-18044\*#** Army Aviation Research and Development Command, Cleveland, Ohio.

### **CERAMIC COMPOSITE LINER MATERIAL FOR GAS TURBINE COMBUSTORS**

D. B. ERCEGOVIC, C. L. WALKER (U.S. Army, Propulsion Laboratory, Cleveland, OH), and C. T. NORGREN (NASA, Lewis Research Center, Cleveland, OH) American Institute of Aeronautics and Astronautics, Aerospace Sciences Meeting, 22nd, Reno, NV, Jan. 9-12, 1984. 11 p. refs (AIAA PAPER 84-0363)

The application of ceramics to gas turbine combustor liners to reduce liner metal temperature was studied in an experiment in which yttria-stabilized zirconia plasma was sprayed on compliant metal substrates exposed to near stoichiometric combustion. The strain isolation pad materials chosen were Hoskins Alloy 875 and BRUNSLLOY 534 Fiber Metal of 0.25 and 0.38 cm thicknesses and 35 and 45 percent density levels. Combustor screening tests of all specimens showed no evidence of deterioration or failure. Specimens exposed to flame temperatures in excess of 2100 K were convectively or convective-transpiration cooled and were evaluated in a 10 cm sq flame tube at inlet air temperature of 533 K and pressure of 0.5 MPa. The results suggest the superiority of a system composed of the Hoskins Alloy 875 compliant pad with 0.25 cm thickness and 35 percent density coupled with a NiCrAlY bond coat and a 8 percent Y<sub>2</sub>O<sub>3</sub>-ZrO<sub>2</sub> ceramic top coat of 0.19 cm thickness. J.N.

**A84-18948\*** National Aeronautics and Space Administration. Lewis Research Center, Cleveland, Ohio.

### **PHASE DISTRIBUTIONS IN PLASMA-SPRAYED ZIRCONIA-YTRIA**

R. A. MILLER, R. G. GARLICK, and J. L. SMIALEK (NASA, Lewis Research Center, Cleveland, OH) American Ceramic Society Bulletin (ISSN 0002-7812), vol. 62, Dec. 1983, p. 1355-1358. refs

The distribution of phases in plasma-sprayed zirconia-ytria has been determined over a range of yttria levels from 0 to 26.1 molpct YO(1.5) using room temperature X-ray diffractometry. Pure, plasma-sprayed zirconia is composed almost entirely of the monoclinic phase. At levels of yttria between 4 and 10 percent, a quenched-in tetragonal phase predominates, and at higher levels

the cubic phase predominates. The phase distributions are compared with previously reported test lives of thermal barrier coatings formed from these materials. Regions of optimal lives were found to correlate with regions having high amounts of the tetragonal phase, small but nonzero amounts of the monoclinic phase, and little or none of the cubic phase. Possible relationships between phase composition and coating performance are discussed. Author

**A84-19781\*** State Univ. of New York, Stony Brook.

### **PHASE ANALYSIS OF PLASMA-SPRAYED ZIRCONIA-YTRIA COATINGS**

N. R. SHANKAR, C. G. BERNDT, and H. HERMAN (New York, State University, Stony Brook, NY) Ceramic Engineering and Science Proceedings (ISSN 0196-6219), vol. 4, Sept.-Oct. 1983, p. 784-787. refs (Contract NAG3-164)

Phase analysis of plasma-sprayed 8 wt pct-ytria-stabilized zirconia (YSZ) thermal barrier coatings and powders was carried out by X-ray diffraction. Step scanning was used for increased peak resolution. Plasma spraying of the YSZ powder into water or onto a steel substrate to form a coating reduced the cubic and monoclinic phases with a simultaneous increase in the tetragonal phase. Heat treatment of the coating at 1150 C for 10 h in an Ar atmosphere increased the amount of cubic and monoclinic phases. The implications of these transformations on coating performance and integrity are discussed. Author

**A84-19782\*** State Univ. of New York, Stony Brook.

### **ANISOTROPIC THERMAL EXPANSION EFFECTS IN PLASMA-SPRAYED ZRO2-8 PERCENT Y2O3 COATINGS**

C. C. BERNDT and H. HERMAN (New York, State University, Stony Brook, NY) Ceramic Engineering and Science Proceedings (ISSN 0196-6219), vol. 4, Sept.-Oct. 1983, p. 792-801. refs (Contract NAG3-164)

The thermal expansion properties of plasma-sprayed ZrO<sub>2</sub>-8 wt pct Y<sub>2</sub>O<sub>3</sub> coatings, detached from the substrate, have been examined. Coatings were heat-treated in air or in argon. Anisotropic effects in the longitudinal (planar to the substrate surface) and transverse (perpendicular to the substrate surface) directions were measured and related to the coating structure. The thermal expansion coefficient of the coating is discussed in terms of the material's properties, such as the crack network and interlamellar boundary distribution. A precise model for the expansion behavior of coatings still needs attention, since no description of all of the contributing variables exists. A quantitative analysis of thermal properties of coatings will aid in future design and modeling of coating systems. Author

**A84-19783\*** National Aeronautics and Space Administration. Lewis Research Center, Cleveland, Ohio.

### **RESIDUAL STRESS IN PLASMA-SPRAYED CERAMIC TURBINE TIP AND GAS-PATH SEAL SPECIMENS**

R. C. HENDRICKS, G. MCDONALD (NASA, Lewis Research Center, Cleveland, OH), and R. L. MULLEN (Case Western Reserve University, Cleveland, OH) Ceramic Engineering and Science Proceedings (ISSN 0196-6219), vol. 4, Sept.-Oct. 1983, p. 802-809. refs

The residual stresses in a ceramic sheet material used for turbine blade tip gas path seals, were estimated. These stresses result from the plasma spraying process which leaves the surface of the sheet in tension. To determine the properties of plasma sprayed ZrO<sub>2</sub>-Y<sub>2</sub>O<sub>3</sub> sheet material, its load deflection characteristics were measured. Estimates of the mechanical properties for sheet materials were found to differ from those reported for plasma sprayed bulk materials. Previously announced in STAR as N83-28380 Author



**A84-19784\*** Case Western Reserve Univ., Cleveland, Ohio.  
**CORRELATION OF COMPRESSIVE AND SHEAR STRESS WITH SPALLING OF PLASMA-SPRAYED CERAMIC MATERIALS**  
 R. L. MULLEN (Case Western Reserve University, Cleveland, OH), G. McDONALD, R. C. HENDRICKS (NASA, Lewis Research Center, Cleveland, OH), and M. M. HOFLE (Rensselaer Polytechnic Institute, Troy, NY) Ceramic Engineering and Science Proceedings (ISSN 0196-6219), vol. 4, Sept.-Oct. 1983, p. 810-818. refs

Ceramics on metal substrates for potential use as high temperature seals or other applications are exposed to forces originating from differences in thermal expansion between the ceramic and the metal substrate. This report develops a relationship between the difference in expansion of the ceramic and the substrate, defines conditions under which shear between the ceramic and the substrate occurs, and those under which bending forces are produced in the ceramic. The off-axis effect of compression forces resulting from high temperature plastic flow of the ceramic producing buckling of the ceramic is developed. Shear is associated with the edge or boundary stresses on the component while bending is associated with the distortion of an interior region. Both modes are significant in predicting life of the ceramic. Previously announced in STAR as N83-27016 Author

**A84-19785\*** National Aeronautics and Space Administration. Lewis Research Center, Cleveland, Ohio.

**THE EFFECT OF ANNEALING ON THE CREEP OF PLASMA-SPRAYED CERAMICS**

R. C. HENDRICKS, G. McDONALD (NASA, Lewis Research Center, Cleveland, OH), and R. L. MULLEN (Case Western Reserve University, Cleveland, OH) Ceramic Engineering and Science Proceedings (ISSN 0196-6219), vol. 4, Sept.-Oct. 1983, p. 819-827. refs

The creep of plasma sprayed ZrO<sub>2</sub>-8Y<sub>2</sub>O<sub>3</sub> was measured at temperatures from 98 to 1250 C (180 to 220 F), and compared to creep of identical samples after annealing at temperatures from 98 to 1316 C (1800 to 2400 F). Loads and temperatures which produced significant creep of as sprayed ceramics produced no creep after annealing. Previously announced in STAR as N83-24799 Author

**A84-19786\*** General Electric Co., Schenectady, N. Y.  
**MECHANICAL AND PHYSICAL PROPERTIES OF PLASMA-SPRAYED STABILIZED ZIRCONIA**

P. A. SIEMERS and R. L. MEHAN (General Electric Co., Schenectady, NY) Ceramic Engineering and Science Proceedings (ISSN 0196-6219), vol. 4, Sept.-Oct. 1983, p. 828-840. refs (Contract NAS3-21727)

Physical and mechanical properties were determined for plasma-sprayed MgO- or Y<sub>2</sub>O<sub>3</sub>-stabilized ZrO<sub>2</sub> thermal barrier coatings. Properties were determined for the ceramic coating in both the freestanding condition and as-bonded to a metal substrate. The properties of the NiCrAlY bond coating were also investigated. Author

**A84-19792\*** Florida Univ., Gainesville.  
**ANALYSIS OF GRAIN BOUNDARY PHASE DEVITRIFICATION OF Y<sub>2</sub>O<sub>3</sub>- AND Al<sub>2</sub>O<sub>3</sub>-DOPED Si<sub>3</sub>N<sub>4</sub>**

L. L. HENCH and P. N. VAIDYANATHAN (Florida, University, Gainesville, FL) Ceramic Engineering and Science Proceedings (ISSN 0196-6219), vol. 4, Sept.-Oct. 1983, p. 896-898. refs (Contract NSG-3254)

The present study has the objective to show that a Fourier Transform IR (FTIR) spectrometer in a single-beam reflection mode can be used for direct comparison of fractured vs nonfractured Si<sub>3</sub>N<sub>4</sub> surfaces. This can be done because the FTIR method permits a digital summation of nearly 1000 scans of the fracture surface. Commercial-grade Si<sub>3</sub>N<sub>4</sub>, Y<sub>2</sub>O<sub>3</sub>, and Al<sub>2</sub>O<sub>3</sub> were used in the study. The samples were heat treated in a vacuum induction heating furnace at either 1000 C for 10 h or 1200 C for 10 h each. Use of Fourier transform IR reflection spectroscopic analysis and X-ray diffraction shows that 10 h at 1200 C is sufficient to devitrify the amorphous grain boundary phase of Si<sub>3</sub>N<sub>4</sub> containing 15 percent Y<sub>2</sub>O<sub>3</sub> + 2 percent Al<sub>2</sub>O<sub>3</sub> densification aids. G.R.

**A84-19793\*** Missouri Univ., Rolla.  
**GRAIN-BOUNDARY PHASES IN HOT-PRESSED SILICON NITRIDE CONTAINING Y<sub>2</sub>O<sub>3</sub> AND CeO<sub>2</sub> ADDITIVES**

J. P. GUHA (Missouri-Rolla, University, Rolla, MO) and L. L. HENCH (Florida, University, Gainesville, FL) Ceramic Engineering and Science Proceedings (ISSN 0196-6219), vol. 4, Sept.-Oct. 1983, p. 901-906. refs (Contract NSG-3254)

Auger electron spectroscopy in conjunction with X-ray powder diffraction and scanning electron microscopy is used to analyze the grain-boundary phases of Y<sub>2</sub>O<sub>3</sub>- and CeO<sub>2</sub>-doped Si<sub>3</sub>N<sub>4</sub> hot-pressed materials in order to demonstrate that the additives concentrate predominantly in the grain boundaries of Si<sub>3</sub>N<sub>4</sub> in the form of various oxynitride phases. A high oxygen content observed in sample fracture surfaces was found to be consistent with the existence of an oxygen-enriched phase in the grain boundaries. The presence of yttrium and cerium in the fracture surfaces and an overall increase in the O/N ratio imply that the additive oxides are predominantly concentrated in the intergranular phases. J.N.

**A84-19794\*** Florida Univ., Gainesville.  
**COMPOSITIONAL EFFECTS ON Si<sub>3</sub>N<sub>4</sub> FRACTURE SURFACES**

L. L. HENCH (Florida, University, Gainesville, FL), F. OHUCHI (Du Pont de Nemours and Co., Wilmington, DE), P. N. VAIDYANATHAN (Warner and Swasey Co., Manchester Div., Akron, OH), and S. DUTTA (NASA, Lewis Research Center, Cleveland, OH) Ceramic Engineering and Science Proceedings (ISSN 0196-6219), vol. 4, Sept.-Oct. 1983, p. 907-917. refs (Contract NSG-3254)

Surface analysis techniques (X-ray, infrared reflection spectroscopy, Auger electron spectroscopy) applied to the same samples reveal that fracture surfaces of Si<sub>3</sub>N<sub>4</sub> with Y<sub>2</sub>O<sub>3</sub> densification aids possess a higher concentration of oxygen than the bulk. The oxide densification aids thus concentrate in the grain boundaries, and even low-temperature fracture is seen as occurring preferentially within the oxygen-enriched grain boundaries. It is found that increasing the concentrations of Y<sub>2</sub>O<sub>3</sub> and Al<sub>2</sub>O<sub>3</sub> increases the oxygen content of the fracture surface. A range of 13-15 percent Y<sub>2</sub>O<sub>3</sub> + 6 percent Al<sub>2</sub>O<sub>3</sub> gives an amorphous grain-boundary phase that is resistant to devitrification. Fracture occurs through the amorphous phase, and heat treatment at 1000 C has little effect on the amorphous phase. C.R.

**A84-19913\*** National Aeronautics and Space Administration. Lewis Research Center, Cleveland, Ohio.

**CHARACTERISTICS OF Si<sub>3</sub>N<sub>4</sub>-SiO<sub>2</sub>-Ce<sub>2</sub>O<sub>3</sub> COMPOSITIONS SINTERED IN HIGH-PRESSURE NITROGEN**

W. A. SANDERS and T. P. HERBELL (NASA, Lewis Research Center, Cleveland, OH) American Ceramic Society, Journal (ISSN 0002-7820), vol. 66, Dec. 1983, p. 835-841. refs

Full-density Si<sub>3</sub>N<sub>4</sub>-SiO<sub>2</sub>-Ce<sub>2</sub>O<sub>3</sub> compositions were prepared by sintering with 2.5 MPa nitrogen pressure at temperatures of 1900 and 2090 C. Room-temperature flexural strengths near 700 MPa for sintered material compared favorably with the strength of hot-pressed material. At 1370 C, where flexural strengths as high as 363 MPa were obtained, it was observed that the coarsest structure was the strongest and the finest structure was the weakest. One of the compositions tested, Si<sub>3</sub>N<sub>4</sub>-8.7 wt pct SiO<sub>2</sub>-8.3 wt pct-Ce<sub>2</sub>O<sub>3</sub>, was found to have excellent 200-h oxidation resistance at 700, 1000, and 1370 C, without incidence of 700 to 1000 C phase instability and cracking. Author

**A84-23689\*** National Aeronautics and Space Administration. Lewis Research Center, Cleveland, Ohio.

**BUBBLE FORMATION IN OXIDE SCALES ON SiC**

D. M. MIESKOWSKI (NASA, Lewis Research Center; Case Western Reserve University, Cleveland, OH), T. E. MITCHELL, and A. H. HEUER (Case Western Reserve University, Cleveland, OH) American Ceramic Society, Journal (ISSN 0002-7820), vol. 67, Jan. 1984, p. C-17, C-18. refs (Contract F49620-78-C-0053)

The oxidation of alpha-SiC single crystals and sintered alpha and beta-SiC polycrystals has been investigated at elevated



temperatures. Bubble formation is commonly observed in oxide scales on polycrystalline SiC, but is rarely found on single-crystal scales; bubbles result from the preferential oxidation of C inclusions, which are abundant in SiC polycrystals. The absence of bubbles on single crystals, in fact, implies that diffusion of the gaseous species formed on oxidation, CO (or possibly SiO), controls the rate of oxidation of SiC. Author

**A84-24553\*** Westinghouse Research and Development Center, Pittsburgh, Pa.

#### **THERMAL STRESS FRACTURE OF CERAMIC COATINGS**

C. A. ANDERSSON (Westinghouse Research and Development Center, Pittsburgh, PA) IN: Fracture mechanics of ceramics. Volume 6 - Measurements, transformations, and high-temperature fracture. New York, Plenum Press, 1983, p. 497-509. Research supported by the U.S. Department of Energy. refs (Contract DEN3-110)

Thermal stress failures of ceramic coatings are discussed in terms of fracture mechanics concepts. The effects of transient and residual stresses on single and multiple cycle failure mechanisms are considered. A specific example of a zirconia thermal barrier coating is presented and its endurance calculated using the proposed relationships. Author

**A84-25402\*** National Aeronautics and Space Administration. Lewis Research Center, Cleveland, Ohio.

#### **MICROSTRUCTURE, STRENGTH, AND OXIDATION OF A 10 WT PCT ZYTTRITE-Si3N4 CERAMIC**

S. DUTTA and B. BUZEK (NASA, Lewis Research Center, Cleveland, OH) American Ceramic Society, Journal (ISSN 0002-7820), vol. 67, Feb. 1984, p. 89-92. refs

Hot pressed Si3N4 doped with 10 wt pct zyttrite as a sintering aid was studied. An equiaxed, fine grained microstructure was predominant, with no apparent porosity. Bend strengths were determined at room temperature and high temperatures (up to 1370 C). Oxidation was measured by weight gain at 1370 C in air. The resulting material exhibited very good room temperature strength (755 MPa). The work showed that room temperature strength can be improved significantly by using controlled Si3N4 powder with 10 wt pct zyttrite. High temperature strength (514 MPa) at 1370 C was nearly double that of hot-pressed Si3N4 (NC-132). The oxidation resistance at 1370 C was also higher than that of NC-132. Author

**A84-28995\*** National Aeronautics and Space Administration. Lewis Research Center, Cleveland, Ohio.

#### **LIQUID CHROMATOGRAPHIC ANALYSIS OF A FORMULATED ESTER FROM A GAS-TURBINE ENGINE TEST**

W. R. JONES, JR. and W. MORALES (NASA, Lewis Research Center, Cleveland, OH) American Society of Lubrication Engineers and American Society of Mechanical Engineers, Lubrication Conference, Hartford, CT, Oct. 18-20, 1983. 6 p. refs (ASLE PREPRINT 83-LC-1A-1)

Size exclusion chromatography (SEC) utilizing mu-Bondagel and mu-Styragel columns with a tetrahydrofuran mobile phase was used to determine the chemical degradation of lubricant samples from a gas-turbine engine test. A MIL-L-27502 candidate, ester-based lubricant was run in a J57-29 engine at a bulk oil temperature of 216 C. In general, the analyses indicated a progressive loss of primary ester, additive depletion, and formation of higher molecular weight material. An oil sample taken at the conclusion of the test showed a reversal of this trend because of large additions of new oil. The high-molecular-weight product from the degraded ester absorbed strongly in the ultraviolet region at 254 nanometers. This would indicate the presence of chromophoric groups. An analysis of a similar ester lubricant from a separate high-temperature bearing test yielded qualitatively similar results. Author

**A84-30000\*** National Aeronautics and Space Administration. Lewis Research Center, Cleveland, Ohio.

#### **THERMAL OXIDATIVE DEGRADATION REACTIONS OF LINEAR PERFLUOROALKYL ETHERS**

W. R. JONES, JR. (NASA, Lewis Research Center, Cleveland, OH), K. J. L. PACLOREK, T. I. ITO, and R. H. KRATZER (NASA, Lewis Research Center, Cleveland, OH; Ultrasystems, Inc., Irvine, CA) I&EC - Industrial and Engineering Chemistry, Product Research and Development (ISSN 0196-4321), vol. 22, June 1983, p. 166-170. refs

Thermal and thermal oxidative stability studies were performed on linear perfluoroalkyl ether fluids. The effect on degradation by metal catalysts and degradation inhibitors is reported. The linear perfluoroalkyl ethers are inherently unstable at 316 C in an oxidizing atmosphere. The metal catalysts greatly increased the rate of degradation in oxidizing atmospheres. In the presence of these metals in an oxidizing atmosphere, the degradation inhibitors were highly effective in arresting degradation at 288 C. However, the inhibitors had only limited effectiveness at 316 C. The metals promote degradation by chain scission. Based on elemental analysis and oxygen consumption data, the linear perfluoroalkyl ether fluids have a structural arrangement based on difluoroformyl and tetrafluoroethylene oxide units, with the former predominating. Previously announced in STAR as N82-26468 S.L.

**A84-32306\*** National Aeronautics and Space Administration. Lewis Research Center, Cleveland, Ohio.

#### **SINTERABILITY, STRENGTH AND OXIDATION OF ALPHA SILICON CARBIDE POWDERS**

S. DUTTA (NASA, Lewis Research Center, Cleveland, OH) Journal of Materials Science (ISSN 0022-2461), vol. 19, April 1984, p. 1307-1313. refs

An investigation is made of pressureless sintering of commercially available alpha-SiC powders at temperatures between 1900 and 2150 C for periods of 10 to 240 min under one atmosphere of argon pressure. It is found that alpha-SiC powder containing boron and carbon sintering aids is sinterable at 2150 C for a period of 30 min to a high final density (greater than 96 percent of theoretical). In alpha-SiC powder containing aluminum and carbon sintering aids, the final density achieved is only about 80 percent of theoretical. Determinations are made of room temperature and high temperature (1370 C) flexure strength and oxidation resistance on sintered high density (more than 96 percent of theoretical) alpha-SiC (boron, carbon) material. It is found that both the strength and the resistance to oxidation are equivalent and comparable to those of the sintered alpha-SiC which represents the state of the art. C.R.

**A84-40594\*** National Aeronautics and Space Administration. Lewis Research Center, Cleveland, Ohio.

#### **POLYIMIDES FORMULATED FROM A PARTIALLY FLUORINATED DIAMINE FOR AEROSPACE TRIBOLOGICAL APPLICATIONS**

R. L. FUSARO (NASA, Lewis Research Center, Cleveland, OH) ASLE Transactions, vol. 27, July 1984, p. 189-196. refs

Preliminary tribological studies on polyimides formulated from the diamine 2,2-bis 4-(4-aminophenoxy)phenyl hexafluoropropane (4-BDAF) indicate that polyimides formulated from this diamine have excellent potential for high temperature tribological applications. The dianhydrides used to make the polyimides were pyromellitic (PMDA) and benzophenonetetracarboxylic acid (BTDA). Friction and wear studies at 25 and 200 C indicate that polyimides formulated using 50 mole percent of the PMDA dianhydride and 50 mole percent of the BTDA dianhydride perform better than polyimides formulated solely with the BTDA dianhydride. Graphite fiber reinforced polyimide composites were formulated with the polyimide made from the BTDA dianhydride and both graphitic and non-graphitic fibers were evaluated. Graphitic fibers produced better tribological results, since thin, flowing, 'layer-like' transfer films were produced which did not build up with long sliding durations. Non-graphitic fibers did not produce this type of transfer. Previously announced in STAR as N83-22423 M.G.

**A84-42668\*** Westinghouse Research and Development Center, Pittsburgh, Pa.

**DEGRADATION MECHANISMS OF CERAMIC THERMAL BARRIER COATINGS IN CORROSIVE ENVIRONMENTS**

S. K. LAU and R. J. BRATTON (Westinghouse Research and Development Center, Pittsburgh, PA) IN: High-temperature protective coatings; Proceedings of the Symposium, Atlanta, GA, March 7, 8, 1983. Warrendale, PA, Metallurgical Society of AIME, 1984, p. 305-317. Research sponsored by the Electric Power Research Institute. refs  
(Contract NAS3-21377)

Chemical as well as thermal-mechanical interactions between the ceramics and gas turbine combustion gases/condensates are found to play critical roles in the degradation of porous plasma-sprayed ceramic thermal barrier coatings. The detailed degradation mechanisms of several state-of-the-art ceramic thermal barrier coatings, including several zirconia compositions and a calcium silicate, in corrosive environments are examined in this paper. Approaches to extend coating lifetime are also described.

Author

**A84-44482\*** National Aeronautics and Space Administration. Lewis Research Center, Cleveland, Ohio.

**CERAMIC-COATED METALS CAN SURVIVE CONTACT WITH HOT WORKING FLUID**

S. R. LEVINE and R. A. MILLER (NASA, Lewis Research Center, Cleveland, OH) Research and Development (ISSN 0160-4074), vol. 26, March 1984, p. 122-125.

Thermal barrier coatings (TBCs) have been developed as a means of protecting turbine blades and other engine hot section components whose surfaces are exposed to the most extreme operating conditions. By adding a thin, insulating ceramic oxide layer to an air-cooled turbine blade, the difference between the gas temperature and the metal temperature is further increased as a function of ceramic coating thickness, heat flux, and oxide thermal conductivity. An 0.04-cm thick ceramic layer can typically yield a 100-300 C temperature drop. Of the various techniques available for the deposition of thermal barrier coatings, the most common is that of plasma spraying. Significant improvements have been made in TBC durability through the use of bond coat compositions with increased oxidation resistance.

O.C.

**N84-10310\*#** National Aeronautics and Space Administration. Lewis Research Center, Cleveland, Ohio.

**RESIN SELECTION CRITERIA FOR TOUGH COMPOSITE STRUCTURES**

C. C. CHAMIS and G. T. SMITH 4 May 1983 33 p refs Presented at 24th Structures, Structural Dyn. and Mater. Conf., Lake Tahoe, Nevada, 2-4 May 1983; sponsored by AIAA, ASME, ASCE and AHS Original language document previously announced as A83-29734

(NASA-TM-83449; E-1762; NAS 1.15:83449) Avail: NTIS HC A03/MF A01 CSCL 11G

Resin selection criteria are derived using a structured methodology consisting of an upward integrated mechanistic theory and its inverse (top-down structured theory). These criteria are expressed in a 'criteria selection space' which are used to identify resin bulk properties for improved composite 'toughness'. The resin selection criteria correlate with a variety of experimental data including laminate strength, elevated temperature effects and impact resistance.

Author

**N84-11295\*#** National Aeronautics and Space Administration. Lewis Research Center, Cleveland, Ohio.

**A REVIEW OF THE USE OF WEAR-RESISTANT COATINGS IN THE CUTTING-TOOL INDUSTRY**

J. SALIK Nov. 1983 11 p refs Presented at the Intern. Workshop on Industrial Applications of Plasma Chem., Ashkelon, Israel, Apr. 1981

(NASA-TM-83512; NAS 1.15:83512; E-1789) Avail: NTIS HC A02/MF A01 CSCL 11C

The main mechanisms involved in the wear of cutting tools are reviewed. Evaluation of the different coating properties required

for the reduction of the different kinds of wear was also reviewed. The types of coatings and their ranges of applicability are presented and discussed in view of their properties. Various coating processes as well as their advantages and shortcomings are described. Potential future developments in the field of wear-resistant coatings are discussed

Author

**N84-11296\*#** National Aeronautics and Space Administration. Lewis Research Center, Cleveland, Ohio.

**OVERVIEW OF LIQUID LUBRICANTS FOR ADVANCED AIRCRAFT**

W. R. LOOMIS 1982 19 p refs Presented at the Symp. on Lubricants for Extreme Environ. at the Joint Lubrication Conf., Washington, D.C., 4-6 Oct. 1982; sponsored by ASME and the American Society of Lubrication Engineers (NASA-TM-83529; E-1740; NAS 1.15:83529) Avail: NTIS HC A02/MF A01 CSCL 11H

An overall status report on liquid lubricants for use in high-performance turbojet engines is presented. Emphasis is placed on the oxidation and thermal stability requirements imposed upon the lubrication system. A brief history is given of the development of turbine engine lubricants which led to synthetic oils with their inherent modification advantages. The status and state of development of some nine candidate classes of fluids for use in advanced turbine engines are discussed. Published examples of fundamental studies to obtain a better understanding of the chemistry involved in fluid degradation are reviewed. Also, alternatives to high temperature fluid development are described. The importance of continuing work on improving high temperature lubricant candidates and encouraging development of fluid base stocks is discussed.

S.L.

**N84-12312\*#** Pratt and Whitney Aircraft Group, East Hartford, Conn. Engineering Div.

**DEVELOPMENT OF STRAIN TOLERANT THERMAL BARRIER COATING SYSTEMS, TASKS 1 - 3**

N. P. ANDERSON and K. D. SHEFFLER Sep. 1983 117 p refs  
(Contract NAS3-22548)

(NASA-CR-168251; NAS 1.26:168251; PWA-5777-29) Avail: NTIS HC A06/MF A01 CSCL 11B

Insulating ceramic thermal barrier coatings can reduce gas turbine airfoil metal temperatures as much as 170 C (about 300 F), providing fuel efficiency improvements greater than one percent and durability improvements of 2 to 3X. The objective was to increase the spalling resistance of zirconia based ceramic turbine coatings. To accomplish this, two baseline and 30 candidate duplex (layered MCrAlY/zirconia based ceramic) coatings were iteratively evaluated microstructurally and in four series of laboratory burner rig tests. This led to the selection of two candidate optimized 0.25 mm (0.010 inch) thick plasma sprayed partially stabilized zirconia ceramics containing six weight percent yttria and applied with two different sets of process parameters over a 0.13 mm (0.005 inch) thick low pressure chamber sprayed MCrAlY bond coat. Both of these coatings demonstrated at least 3X laboratory cyclic spalling life improvement over the baseline systems, as well as cyclic oxidation life equivalent to 15,000 commercial engine flight hours.

M.G.

**N84-13310\*#** Hughes Research Labs., Malibu, Calif.

**PLASMA POLYMERIZED HIGH ENERGY DENSITY DIELECTRIC FILMS FOR CAPACITORS Final Report, 28 Sep. - 31 Dec. 1982**

F. G. YAMAGISHI Oct. 1983 67 p refs  
(Contract NAS3-22828)

(NASA-CR-168233; NAS 1.26:168233) Avail: NTIS HC A04/MF A01 CSCL 11G

High energy density polymeric dielectric films were prepared by plasma polymerization of a variety of gaseous monomers. This technique gives thin, reproducible, pinhole free, conformable, adherent, and insoluble coatings and overcomes the processing problems found in the preparation of thin films with bulk polymers. Thus, devices are prepared completely in a vacuum environment.

The plasma polymerized films prepared all showed dielectric strengths of greater than 1000 kV/cm and in some cases values of greater than 4000 kV/cm were observed. The dielectric loss of all films was generally less than 1% at frequencies below 10 kHz, but this value increased at higher frequencies. All films were self healing. The dielectric strength was a function of the polymerization technique, whereas the dielectric constant varied with the structure of the starting material. Because of the thin films used (thickness in the submicron range) surface smoothness of the metal electrodes was found to be critical in obtaining high dielectric strengths. High dielectric strength graft copolymers were also prepared. Plasma polymerized ethane was found to be thermally stable up to 150 C in the presence of air and 250 C in the absence of air. No glass transitions were observed for this material. Author

**N84-16334\*#** National Aeronautics and Space Administration. Lewis Research Center, Cleveland, Ohio.

**FRICTION AND MORPHOLOGY OF MAGNETIC TAPES IN SLIDING CONTACT WITH NICKEL-ZINC FERRITE**

K. MIYOSHI, D. H. BUCKLEY, and B. BHUSHAN (IBM Corp.) Jan. 1984 18 p refs  
(NASA-TP-2267; NAS 1.60:2267; E-1720) Avail: NTIS HC A02/MF A01 CSCL 13I

Friction and morphological studies were conducted with magnetic tapes containing a Ni-Zn ferrite hemispherical pin in laboratory air at a relative humidity of 40 percent and at 23 C. The results indicate that the binder plays a significant role in the friction properties, morphology, and microstructure of the tape. Comparisons were made with four binders: nitrocellulose; poly(vinylidene) chloride; cellulose acetate; and hydroxyl-terminated, low molecular weight polyester added to the base polymer, polyester-polyurethane. The coefficient of friction was lowest for the tape with the nitrocellulose binder and increased in the order hydroxyl-terminated, low molecular weight polyester resin; poly(vinylidene) chloride, and cellulose acetate. The degree of enclosure of the oxide particles by the binder was highest for hydroxyl-terminated, low molecular weight polyester and decreased in the order cellulose acetate, poly(vinylidene) chloride, and nitrocellulose. The nature of deformation of the tape was a factor in controlling friction. The coefficient of friction under elastic contact conditions was considerably lower than under conditions that produced plastic contacts. Author

**N84-16337\*#** Pratt and Whitney Aircraft, East Hartford, Conn. Engineering Div.

**PROGRAM FOR DEVELOPMENT OF STRAIN TOLERANT THERMAL BARRIER COATING SYSTEM**

N. P. ANDERSON 30 Jan. 1984 20 p  
(Contract NAS3-22548)  
(NASA-CR-173214; NAS 1.26:173214; PWA-5777-30) Avail: NTIS HC A02/MF A01 CSCL 11B

The results of thermal conductivity, thermal expansion and high cycle fatigue tests conducted on coating systems are presented. These results show that the thermal conductivity of coating system 8 at approximately 982 C (1800 F) is substantially higher than system 3 while no significant differences were observed in the thermal expansion measurements up to approximately 1316 C (2400 F). High cycle fatigue (HCF) testing, which was conducted at room temperature and several stress levels, showed both coatings to be extremely resistant to spallation in HCF. S.L.

**N84-17389\*#** Cleveland State Univ., Ohio. Dept. of Chemical Engineering.

**CONSOLIDATION OF Si<sub>3</sub>N<sub>4</sub> WITHOUT ADDITIVES (BY HOT ISOSTATIC PRESSING) Final Technical Report**

H. C. YEY Sep. 1983 73 p refs  
(Contract NSG-3155)  
(NASA-CR-173279; NAS 1.26:173279) Avail: NTIS HC A04/MF A01 CSCL 11G

The potential of using hot isostatic pressing (HIP'ing) technique to produce dense silicon nitride materials without or with a reduced amount of additives (much less than 5 w/o) was investigated. Hot

isostatic pressing technique can provide higher pressure and temperature than hot pressing can, thus has the potential of requiring less densification aids to consolidate Si<sub>3</sub>N<sub>4</sub> materials. It was anticipated that if such dense materials could be fabricated, the high temperature strength of the material should be improved significantly. Observations on the phase transformation, densification behavior, and microstructures of the samples are also documented. Density, microhardness, four point bend strength (room temperature and 1370 C) were measured on selected densified materials. Author

**N84-18399\*#** National Aeronautics and Space Administration. Lewis Research Center, Cleveland, Ohio.

**WATER-VAPOR EFFECTS ON FRICTION OF MAGNETIC TAPE IN CONTACT WITH NICKEL-ZINC FERRITE**

K. MIYOSHI and D. H. BUCKLEY Feb. 1984 10 p refs  
(NASA-TP-2279; E-1768; NAS 1.60:2279) Avail: NTIS HC A02/MF A01 CSCL 11G

The effects of humidity of moist nitrogen on the friction and deformation behavior of magnetic tape in contact with a nickel-zinc ferrite spherical pin were studied. The results indicate that the coefficient of friction is markedly dependent on the ambient relative humidity. Although the coefficient of friction remains low below 40-percent relative humidity, it increases rapidly with increasing relative humidity above 40 percent. The general ambient environment of the tape does not have any effect on the friction behavior if the area where the tape is in sliding contact with the ferrite pin is flooded with controlled nitrogen. The response time for the friction of the tape to humidity changes is about 10 sec. The effect of friction as a function of relative humidity on dehumidifying is very similar to that on humidifying. A surface softening of the tape due to water vapor increases the friction of the tape. Author

**N84-18400\*#** National Aeronautics and Space Administration. Lewis Research Center, Cleveland, Ohio.

**BEAM IMPINGEMENT ANGLE EFFECTS ON SECONDARY ELECTRON EMISSION CHARACTERISTICS OF TEXTURED PYROLYTIC GRAPHITE**

A. N. CURREN and K. A. JENSEN Feb. 1984 16 p refs  
(NASA-TP-2285; E-1886; NAS 1.60:2285) Avail: NTIS HC A02/MF A01 CSCL 11G

Experimentally determined values of true secondary electron emission and relative values of reflected primary electron yield for untreated and ion-textured pyrolytic graphite over a range of primary electron energy levels and electron beam impingement angles are presented. Information required to develop high efficiency multistage depressed collectors (MDC's) for microwave amplifier traveling-wave tubes for space communication and aircraft applications is provided. To attain the highest possible MDC efficiencies, the electrode surfaces must have low secondary electron emission characteristics. Pyrolytic graphite, a chemically vapor-deposited material, is a particularly promising candidate for this application. The pyrolytic graphite surfaces studied were tested over a range of primary electron beam energies and beam impingement angles from 200 to 2000 eV and direct (0 deg) to near-grazing angles (85 deg), respectively. Surfaces both parallel to and normal to the planes of material deposition were examined. The true secondary electron emission and reflected primary electron yield characteristics of the pyrolytic graphite surfaces are compared to those of sooted control surfaces. S.L.

**N84-19566\*#** National Aeronautics and Space Administration. Lewis Research Center, Cleveland, Ohio.

**CERAMIC WEAR IN INDENTATION AND SLIDING**

K. MIYOSHI and D. H. BUCKLEY 1984 24 p refs Proposed for presentation at the 39th Ann. Meeting of the Am. Soc. of Lubrication Engr., Chicago, 7-10 May 1984  
(NASA-TM-83585; E-1884; NAS 1.15:83585) Avail: NTIS HC A02/MF A01 CSCL 11B

The various wear mechanisms involved with single-crystal ceramic materials in indentation and in sliding contacts. Experiments simulating interfacial events have been conducted

with hemispherical, conical and pyramidal indenters (riders). With spherical riders, under either abrasive or adhesive conditions, two types of fracture pits have been observed. First, spherical-shaped fracture pits and wear particles are found as a result of either indenting or sliding. These are shown to be due to a spherical-shaped fracture along the circular or spherical stress trajectories. Second, polyhedral fracture pits and debris, produced by anisotropic fracture, and also found both during indenting and sliding. These are primarily controlled by surface and subsurface cracking along cleavage planes. Several quantitative results have also been obtained from this work. For example, using a pyramidal diamond, crack length of Mn-Zn ferrite in the indentation process grows linearly with increasing normal load. Moreover, the critical load to fracture both in indentation and sliding is essentially isotropic and is found to be directly proportional to the indenter radius.

Author

**N84-19567\*#** National Aeronautics and Space Administration. Lewis Research Center, Cleveland, Ohio.

**DURABLE SOLID LUBRICANT COATINGS FOR FOIL GAS BEARINGS TO 315 DEG C**

R. C. WAGNER (Case Western Reserve Univ.) and H. E. SLINEY 1984 14 p refs Proposed for presentation at the 3rd Intern. Conf. on Solid Lubrication; Denver, 5-9 Aug. 1984; sponsored by Am. Soc. of Lubrication Engr.

(NASA-TM-83596; E-1904; NAS 1.15:83596) Avail: NTIS HC A02/MF A01 CSCL 11H

The durability and friction characteristics of bonded solid lubricant films on compliant gas bearings were measured. Coating compositions, which were judged to be suitable for use to at least 315 C, were selected for this study. Most of the data were obtained with polyimide-bonded graphite fluoride coatings and with silicate-bonded graphite coatings. These coatings were applied to the bore of Inconel 750 foil bearings. The journals were A286 stainless steel, with a rms surface finish of 0.2 microns. The foils were subjected to repeated start/stop cycles under a 14 kPa (2 psi) bearing unit load. Sliding contact occurred during lift-off and coast down at surface velocities less than 6 m/s (3000 rpm). Testing continued until 9000 cycles were accumulated or until a rise in starting torque indicated that the coating had failed. The coatings were evaluated in the temperature range from 25 C to 315 C. Comparisons in coating performance as well as discussions of their properties and methods of application are given. Author

**N84-20695\*#** Boeing Aerospace Co., Seattle, Wash. Engineering Technology.

**CHARACTERIZATION OF PMR POLYIMIDE RESIN AND PREPREG**

P. H. LINDENMEYER and C. H. SHEPPARD Mar. 1984 79 p (Contract NAS3-22523)

(NASA-CR-168217; NAS 1.26:168217; D180-26031-2) Avail: NTIS HC A05/MF A01 CSCL 11G

Procedures for the chemical characterization of PMR-15 resin solutions and graphite-reinforced prepreps were developed, and a chemical data base was established. In addition, a basic understanding of PMR-15 resin chemistry was gained; this was translated into effective processing procedures for the production of high quality graphite composites. During the program the PMR monomers and selected model compounds representative of postulated PMR-15 solution chemistry were acquired and characterized. Based on these data, a baseline PMR-15 resin was formulated and evaluated for processing characteristics and composite properties. Commercially available PMR-15 resins were then obtained and chemically characterized. Composite panels were fabricated and evaluated. Author

**N84-20699\*#** Boeing Aerospace Co., Seattle, Wash

**EVALUATION OF PROPELLANT TANK INSULATION CONCEPTS FOR LOW-THRUST CHEMICAL PROPULSION SYSTEMS: EXECUTIVE SUMMARY Final Report**

T. KRAMER, E. BROGREN, and B. SIEGEL Mar. 1984 37 p refs

(Contract NAS3-22824)

(NASA-CR-168321; NAS 1.26:168321; BAC-D180-28274-1)

Avail: NTIS HC A03/MF A01 CSCL 11G

Cryogenic propellant tank insulations or liquid oxygen/liquid hydrogen low-thrust 2224N (500 lbf) propulsion systems (LTPS) were assessed. The insulation studied consisted of combinations of N<sub>2</sub>-purged foam and multilayer insulation (MLI) as well as He-purged MLI-only. Heat leak and payload performance predictions were made for three shuttle-launched LTPS designed for shuttle bay packaged payload densities of 56 kg/cu m (3.5 lbm/cu ft), 40 kg/cu m (2.5 lbm/cu ft) and 24 kg/cu m (1.5 lbm/cu ft). Foam/MLI insulations were found to increase LTPS payload delivery capability when compared with He-purged MLI-only. An additional benefit of foam/MLI was reduced operational complexity because orbiter cargo bay N<sub>2</sub> purge gas could be used for MLI purging. Maximum payload mass benefit occurred when an enhanced convection, rather than natural convection, heat transfer was specified for the insulation purge enclosure. The enhanced convection environment allowed minimum insulation thickness to be used for the foam/MLI interface temperature selected to correspond to the moisture dew point in the N<sub>2</sub> purge gas. Experimental verification of foam/MLI benefits was recommended. A conservative program cost estimate for testing a MLI-foam insulated tank was 2.1 million dollars. This cost could be reduced significantly without increasing program risk. Author

**N84-21739\*#** National Aeronautics and Space Administration. Lewis Research Center, Cleveland, Ohio.

**CHARACTERIZATION AND MEASUREMENT OF POLYMER WEAR**

D. H. BUCKLEY and P. R. ARON 11 Apr. 1984 17 p refs Presented at Intern. Symp. on Polymer Wear and its Control, St. Louis, 9-11 Apr. 1984; sponsored by American Chemical Society (NASA-TM-83628; E-2033; NAS 1.15:83628) Avail: NTIS HC A02/MF A01 CSCL 11G

Analytical tools which characterize the polymer wear process are discussed. The devices discussed include: visual observation of polymer wear with SEM, the quantification with surface profilometry and ellipsometry, to study the chemistry with AES, XPS and SIMS, to establish interfacial polymer orientation and accordingly bonding with QUARTIR, polymer state with Raman spectroscopy and stresses that develop in polymer films using a X-ray double crystal camera technique. E.A.K.

**N84-21740\*#** National Aeronautics and Space Administration. Lewis Research Center, Cleveland, Ohio.

**OVERVIEW OF ZIRCONIA WITH RESPECT TO GAS TURBINE APPLICATIONS**

J. D. CAWLEY Mar. 1984 29 p refs (NASA-TP-2286; E-1726; NAS 1.60:2286) Avail: NTIS HC A03/MF A01 CSCL 11G

Phase relationships and the mechanical properties of zirconia are examined as well as the thermal conductivity, deformation, diffusion, and chemical reactivity of this refractory material. Observations from the literature particular to plasma-sprayed material and implications for gas turbine engine applications are discussed. The literature review indicates that Mg-PSZ (partially stabilized zirconia) and Ca-PSZ are unsuitable for advanced gas turbine applications; a thorough characterization of the microstructure of plasma-sprayed zirconia is needed. Transformation-toughened zirconia may be suitable for use in monolithic components. A.R.H.

**N84-22753\*#** California Univ., Los Angeles. Dept. of Materials Science and Engineering Science.

**CERAMIC-TO-METAL BONDING FOR PRESSURE TRANSDUCERS Final Report**

J. D. MACKENZIE Apr. 1984 29 p refs

(Contract NAG3-295)

(NASA-CR-173500; NAS 1.26:173500) Avail: NTIS HC A03/MF A01 CSCL 11A

A solid-state diffusion technique involving the placement of a gold foil between INCONEL X-750 and a machinable glass-ceramic 'MACOR' was shown to be successful in bonding these two materials. This technique was selected after an exhaustive literature search on ceramic-metal bonding methods. Small expansion mismatch between the Inconel and the MACOR resulted in fracture of the MACOR when the bonded body was subjected to tensile stress of 535 psi. The bonded parts were submitted to a cyclic loading test in an air atmosphere at 1 Hz from 0 to 60 KPa. Failure was observed after 700,000 cycles at 650 C. Ceramic-Inconel bonding was not achieved with this method for boron nitride and silica glass. Author

**N84-23764\*#** National Aeronautics and Space Administration. Lewis Research Center, Cleveland, Ohio.

**SIMULATION OF LUBRICATING BEHAVIOR OF A THIOETHER LIQUID LUBRICANT BY AN ELECTROCHEMICAL METHOD**

W. MORALES May 1984 12 p refs

(NASA-TP-2316; E-1808; NAS 1.60:2316) Avail: NTIS HC A02/MF A01 CSCL 11H

An electrochemical cell was constructed to explore the possible radical anion forming behavior of a thioether liquid lubricant. The electrochemical behavior of the thioether was compared with the electrochemical behavior of biphenyl, which is known to form radical anions. Under controlled conditions biphenyl undergoes a reversible reaction to a radical anion, whereas the thioether undergoes an irreversible reduction yielding several products. These results are discussed in relation to boundary lubrication. Author

**N84-23893\*#** National Aeronautics and Space Administration. Lewis Research Center, Cleveland, Ohio.

**IMPORTANCE AND DEFINITION OF MATERIALS IN TRIBOLOGY. STATUS OF UNDERSTANDING**

D. H. BUCKLEY *In its Tribology in the 80's*. Vol. 1 p 19-44 Apr. 1984 refs

Avail: NTIS HC A22/MF A01 CSCL 11H

In general, tribological systems consist of three basic components: the material surfaces in contact, the lubricant, and the environment. The materials in contact and the influence of both bulk and surface properties, indicating the importance of material characterization, on tribological behavior are addressed. Since metals and metallic alloys are the most widely used class of materials in practical devices, attention is focused principally on them. With respect to surface behavior, the effect of contaminants both from within the material and from the environment on adhesive behavior is addressed. The various surface events that alter adhesion, friction, and wear are discussed. These include surface reconstruction, segregation, chemisorption, and compound formation. Examples of these events are presented. Minor nuances in the structure of the outermost layers of solids have a pronounced effect on tribological properties. The importance of characterizing the materials of solids in contact in order to achieve a fundamental understanding of adhesion, friction, and wear and accordingly of methods for their control are addressed. Author

**N84-23907\*#** National Aeronautics and Space Administration. Lewis Research Center, Cleveland, Ohio.

**THERMAL AND OXIDATIVE STABILITIES OF LIQUID LUBRICANTS**

W. R. JONES, JR. *In its Tribology in the 80's*. Vol. 1 p 419-455 Apr. 1984 refs

Avail: NTIS HC A22/MF A01 CSCL 11H

The fundamental processes which occur during the thermal and oxidation degradation of hydrocarbons is reviewed. Various

classes of liquid lubricants such as mineral oils, esters, polyphenyl ethers, C-ethers, and fluorinated polyethers are emphasized. Techniques to determine thermal and oxidative stabilities of lubricants are discussed. The role of inhibitors and catalysis is examined. E.A.K.

**N84-24650\*#** National Aeronautics and Space Administration. Lewis Research Center, Cleveland, Ohio.

**ION-BEAM-TEXTURED AND COATED SURFACES EXPERIMENT (S1003)**

M. J. MIRTICH, JR. *In NASA. Langley Research Center Long Duration Exposure Facility (LDEF) p 62-65 Feb. 1984*

Avail: NTIS HC A09/MF A01; also available SOD HC CSCL 11G

The objective of this LDEF experiment is to measure the effects of exposure to the shuttle launch and near Earth space environments on the optical properties of ion beam textured high absorptance solar thermal control surfaces, the optical and electrical properties of ion beam sputtered conductive solar thermal control surfaces, and the weight loss of ion beam deposited oxide polymer films. The various types of surfaces to be tested include six major categories: (1) ion beam textured surfaces suitable for space solar thermal (solar concentration) application; (2) painted and/or state of the art solar thermal surfaces; (3) ion beam sputtered conductive coatings for thermal and space charge control (e.g., indium-oxide coated metalized FEP Teflon); (4) ion beam sputtered conductive coated solar sail materials for space charge control and cooling through emittance; (5) micrometeoroid sensitive samples whose optical properties change only as a result of micrometeoroid impact; and (6) Kapton coated with oxide polymer films to minimize oxygen degradation at near Earth orbit altitudes. M.G.

**N84-24808\*#** National Aeronautics and Space Administration. Lewis Research Center, Cleveland, Ohio.

**LOW WEAR PARTIALLY FLUORINATED POLYIMIDES**

R. L. FUSARO and W. F. HADY 1984 30 p refs To be presented at the Joint Lubrication Conf., San Diego, Calif., 22-24 Oct. 1984

(NASA-TM-83629; E-2066; NAS 1.15:83629) Avail: NTIS HC A03/MF A01 CSCL 11H

Tribological studies were conducted on five different polyimide solid bodies formulated from the diamine 2,2-bis 4-(4-aminophenoxy)phenyl hexafluoropropane (4-BDAF) and the dianhydrides pyromellitic acid (PMDA) and benzophenonetetracarboxylic acid (BTDA). The following polyimides were evaluated 4-BDAF/PMDA, 4-BDAF/BTDA, 4-BDAF/80 mole percent PMDA, 20 mole percent BTDA, 4-BDAF/60 mole percent BTDA. Friction coefficients, polyimide wear rates, polyimide surface morphology and transfer films were evaluated at sliding speeds of 0.31 to 11.6 m/s and at temperatures of 25 C to 300 C. The results indicate that the tribological properties are highly dependent on the composition of the polyimide and on the experimental conditions. Two polyimides were found which produced very low wear rates but very high friction coefficients (greater than 0.85) under ambient conditions. They offer considerable potential for high traction types of application such as brakes. Author

**N84-24809\*#** Pennsylvania State Univ., University Park. Dept. of Materials Science and Engineering.

**THE IMPACT RESISTANCE OF SiC AND OTHER MECHANICAL PROPERTIES OF SiC AND Si3N4 Final Report**

R. C. BRADT Apr. 1984 47 p refs

(Contract NSG-3016)

(NASA-CR-165325; NAS 1.26:165325) Avail: NTIS HC A03/MF A01 CSCL 11G

Studies focused on the impact and mechanical behavior of SiC and Si3N4 at high temperatures are summarized. Instrumented Charpy impact testing is analyzed by a compliance method and related to strength; slow crack growth is related to processing, and creep is discussed. The transient nature of flaw populations

during oxidation under load is emphasized for both SiC and Si<sub>3</sub>N<sub>4</sub>.  
Author

**N84-24810\*#** Texas A&M Univ., College Station Dept. of Mechanical Engineering.

**AN INVESTIGATION INTO THE INJECTION MOLDING OF PMR-15 POLYIMIDE Final Report**

M. A. COLALUCA Jun 1984 32 p refs

(Contract NAG3-129)

(NASA-CR-173550; NAS 1.26:173550) Avail. NTIS HC A03/MF A01 CSCL 11G

The chemorheological behavior of the PMR-15 molding compounds were characterized, the range of suitable processing parameters for injection molding in a reciprocating screw injection molding machine was determined, and the effects of the injection molding processing parameters on the mechanical properties of molded PMR-15 parts were studied. The apparatus and procedures for measuring viscosity and for determining the physical response of the material during heating are described. Results show that capillary rheometry can be effectively used with thermosets if the equipment is designed to overcome some of the inherent problems of these materials. A uniform temperature was provided in the barrel by using a circulating hot oil system. Standard capillary rheometry methods can provide the dependence of thermoset apparent viscosity on shear rate, temperature, and time. Process conditions resulting in complete imidization should be carefully defined. Specification of controlled oven temperature is inadequate and can result in incomplete imidization. For completely imidized PMR-15 heat at 15 C/min melt flow without gas evolution occurs in the temperature range of 325 C to 400 C. A.R.H.

**N84-25055\*#** National Aeronautics and Space Administration. Lewis Research Center, Cleveland, Ohio.

**STATUS AND NEW DIRECTIONS FOR SOLID LUBRICANT COATINGS AND COMPOSITE MATERIALS**

H. E. SLINEY *In its Tribology in the 80's*, vol. 2 p 665-680 Apr. 1984 refs

Avail. NTIS HC A17/MF A01 CSCL 11H

At one time, solid lubricants were used almost entirely in aerospace applications. Today there is a pronounced trend to use them over a much broader range of applications. For example, self-lubricating polymer-based composites have displaced traditional oil-lubricated, metallic composites for many journal bearings and thrust washers in applications as diverse as earth-moving machinery and snow blowers to aircraft applications. For moderate temperatures below 200 C, glass filament-wound epoxy bearings with PTFE lubricating liners are useful; for temperatures up to 350 C, graphite fiber reinforced polyimide bearing materials are finding applications. Advanced technology engines have severe lubrication and wear problems at temperatures beyond the capabilities of any of these lubricants. Here, self-lubricating ceramics and inorganic composites for use at 1000 C or higher are of interest. However, perhaps the most significant new direction for solid lubricant coatings and self-lubricating composites is their steadily increasing use in dry bearings for large volume, moderate temperature applications. This can be attributed to their simplicity of use (no supporting lubricant system needed), light weight, convenience, and general cost effectiveness. M.G.

**N84-25830\*#** National Aeronautics and Space Administration. Lewis Research Center, Cleveland, Ohio.

**DEPOSITION STRESS EFFECTS ON THERMAL BARRIER COATING BURNER RIG LIFE**

J. W. WATSON (Northwestern Univ.) and S. R. LEVINE 1984 15 p refs Presented at the 11th Intern. Conf. on Met. Coatings, San Diego, Calif., 9-13 Apr. 1984; sponsored by the American Vacuum Society

(NASA-TM-83670; E-2113; NAS 1.15:83670) Avail. NTIS HC A02/MF A01 CSCL 21B

A study of the effect of plasma spray processing parameters on the life of a two layer thermal barrier coating was conducted. The ceramic layer was plasma sprayed at plasma arc currents of

900 and 600 amps onto uncooled tubes, cooled tubes, and solid bars of Waspalloy in a lathe with 1 or 8 passes of the plasma gun. These processing changes affected the residual stress state of the coating. When the specimens were tested in a Mach 0.3 cyclic burner rig at 1130 deg C, a wide range of coating lives resulted. Processing factors which reduced the residual stress state in the coating, such as reduced plasma temperature and increased heat dissipation, significantly increased coating life. Author

**N84-25831\*#** National Aeronautics and Space Administration. Lewis Research Center, Cleveland, Ohio.

**EFFECT OF SUBSTRATE CHEMICAL PRETREATMENT ON THE TRIBOLOGICAL PROPERTIES OF GRAPHITE FILMS**

R. L. FUSARO 1984 21 p refs Presented at the 3rd Intern. Conf. on Solid Lubrication, Denver, 5-9 Aug. 1984; sponsored by the American Society of Lubrication Engineers

(NASA-TM-83574; E-1956; NAS 1.15:83574) Avail. NTIS HC A02/MF A01 CSCL 11G

Rubbed films of natural flake Madagascar graphite were applied to ASTM A-355(D) steel with chemical surface pretreatments of zinc phosphate, gas nitride, salt nitride, sulfo-nitride, and with mechanical pretreatment (sandblasting). SAE 1045 steel pins were slid against these films using a pin-on-disk tribometer. The results indicate that two different lubricating mechanisms can occur. In the chemical surface pretreatment, the graphite can mix together to form a surface layer of the two constituents and this plasticity flowing layer provides the lubrication. The longest endurance lives and the lowest pin wear rates were obtained with this mechanism. In the other, surface topography appeared to control the mechanism. A rough surface was necessary to serve as a reservoir to supply the graphite to the flat metallic plateaus where it was sheared in very thin films between the plateaus and the sliding pin surface. For this mechanism, chemical pretreatment seemed to do little more than serve as a means for roughening the surface. Mean friction was not significantly influenced by chemical pretreatment, but surface roughness effects were observed. Author

**N84-26803\*#** National Aeronautics and Space Administration. Lewis Research Center, Cleveland, Ohio.

**SPUTTERED COATINGS FOR PROTECTION OF SPACECRAFT POLYMERS**

B. A. BANKS, M. J. MIRTICH, S. K. RUTLEDGE, and D. M. SWEC 1983 13 p refs Presented at the 11th Intern. Conf. on Met. Coatings, San Diego, Calif., 9-13 Apr. 1984; sponsored by Am. Vacuum Soc.

(NASA-TM-83706; E-2092; NAS 1.15:83706) Avail. NTIS HC A02/MF A01 CSCL 11B

Kapton polyimide oxidizes at significant rates ( $4.3 \times 10^{-24}$  gram/incident oxygen atom) when exposed in low Earth orbit to the ram atomic oxygen flux. Ion beam sputter deposited thin films of Al<sub>2</sub>O<sub>3</sub> and SiO<sub>2</sub> as well as a codeposited mixture of predominantly SiO<sub>2</sub> with a small amount of polytetrafluoroethylene were evaluated and found to be effective in protecting Kapton from oxidation in both laboratory plasma ashing tests as well as in space on board shuttle flight STS-8. A protective film of  $\approx 96$  percent SiO<sub>2</sub> and  $\approx 4$  percent polytetrafluoroethylene was found to be very flexible compared to the pure metal oxide coatings and resulted in mass loss rates that were 0.2 percent of that of the unprotected Kapton. The optical properties of Kapton for wavelengths investigated between 0.33 and 2.2 microns were not significantly altered by the presence of the coatings or changed by exposure of the coated Kapton to the low Earth orbital ram environment. M.G.



**N84-27885\*** National Aeronautics and Space Administration. Lewis Research Center, Cleveland, Ohio.

**CHEMICAL APPROACH FOR CONTROLLING NADIMIDE CURE TEMPERATURE AND RATE Patent**

R. W. LAUVER, inventor (to NASA) 19 Jun 1984 9 p Filed 3 Aug 1982 Supersedes N83-13258 (21 - 04, p 0497) (NASA-CASE-LEW-13770-1; US-PATENT-4,455,418; US-PATENT-APPL-SN-404809; US-PATENT-CLASS-528-322; US-PATENT-CLASS-526-262; US-PATENT-CLASS-528-342) Avail: US Patent and Trademark Office CSCL 11G

Polyimide resins suitable for use as composite matrix materials are formed by copolymerization of maleic and norbornenyl endcapped monomers and oligomers. The copolymers can be cured at temperatures under about 300 C by controlling the available concentration of the maleic capped reactant. This control can be achieved by adding sufficient amounts of said maleic reactant, or by chemical modification of either copolymer, so as to either increase Diels-Alder retrogression of the norbornenyl capped reactant and/or holding initiation and polymerization to a rate compatible with the availability of the maleic capped reactant.

Official Gazette of the U.S. Patent and Trademark Office

**N84-27887\*#** National Aeronautics and Space Administration. Lewis Research Center, Cleveland, Ohio.

**EVALUATION OF TWO POLYIMIDES AND OF AN IMPROVED LINER RETENTION DESIGN FOR SELF-LUBRICATING BUSHINGS**

H. E. SLINEY 1984 17 p refs To be presented at the Joint Lubrication Conf., San Diego, 22-24 Oct. 1984 (NASA-TM-83719; E-2083; NAS 1.15:83719) Avail: NTIS HC A02/MF A01 CSCL 11H

Two different polyimide polymers were studied and the effectiveness of a design feature to improve retention of the self lubricating composite liners under high load was evaluated. The basic bearing design consisted of a molded layer of chopped graphite-fiber-reinforced-polyimide (GFRP) composite bonded to the bore of a steel bushing. The friction, wear, and load carrying ability of the bushings were determined in oscillating tests at 25, 260 and 315 C at radial unit loads up to 260 MPa. Friction coefficients were typically 0.15 to 0.25. Bushings with liners containing a new partially fluorinated polymer were functional, but had a lower load capacity and higher wear rate than those containing a more conventional, high temperature polyimide. The liner retention design feature reduced the tendency of the liners to crack and work out of the contact zone under high oscillating loads.

Author

**N84-28986\*#** National Aeronautics and Space Administration. Lewis Research Center, Cleveland, Ohio.

**DEPOSITION OF DIAMONDLIKE CARBON FILMS Patent Application**

M. J. MIRTICH, J. S. SOVEY, and B. A. BANKS, inventors (to NASA) 9 Jul. 1984 10 p (NASA-CASE-LEW-14080-1; US-PATENT-APPL-SN-628866) Avail: NTIS HC A02/MF A01 CSCL 11G

A diamondlike carbon film is deposited in the surface of a substrate by exposing the surface to an argon ion beam containing a hydrocarbon. The current density in the ion beam is low during initial deposition of the film. Subsequent to this initial low current condition, the ion beam is increased to full power. At the same time a second argon ion beam is directed toward the surface of the substrate. The second ion beam has an energy level much greater than that of the ion beam containing the hydrocarbon. This addition of energy to the system increases mobility of the condensing atoms and serves to remove lesser bound atoms.

NASA

**N84-28989\*#** National Aeronautics and Space Administration. Lewis Research Center, Cleveland, Ohio.

**SECONDARY ELECTRON EMISSION CHARACTERISTICS OF ION-TEXTURED COPPER AND HIGH-PURITY ISOTROPIC GRAPHITE SURFACES**

A. N. CURREN and K. A. JENSEN Jul. 1984 16 p refs (NASA-TP-2342; E-2064; NAS 1.60:2342) Avail: NTIS HC A02/MF A01 CSCL 11G

Experimentally determined values of true secondary electron emission and relative values of reflected primary electron yield for untreated and ion textured oxygen free high conductivity copper and untreated and ion textured high purity isotropic graphite surfaces are presented for a range of primary electron beam energies and beam impingement angles. This investigation was conducted to provide information that would improve the efficiency of multistage depressed collectors (MDC's) for microwave amplifier traveling wave tubes in space communications and aircraft applications. For high efficiency, MDC electrode surfaces must have low secondary electron emission characteristics. Although copper is a commonly used material for MDC electrodes, it exhibits relatively high levels of secondary electron emission if its surface is not treated for emission control. Recent studies demonstrated that high purity isotropic graphite is a promising material for MDC electrodes, particularly with ion textured surfaces. The materials were tested at primary electron beam energies of 200 to 2000 eV and at direct (0 deg) to near grazing (85 deg) beam impingement angles. True secondary electron emission and relative reflected primary electron yield characteristics of the ion textured surfaces were compared with each other and with those of untreated surfaces of the same materials. Both the untreated and ion textured graphite surfaces and the ion treated copper surface exhibited sharply reduced secondary electron emission characteristics relative to those of untreated copper. The ion treated graphite surface yielded the lowest emission levels.

Author

**N84-28990\*#** National Aeronautics and Space Administration. Lewis Research Center, Cleveland, Ohio.

**OXYGEN DIFFUSION IN ALPHA-AL<sub>2</sub>O<sub>3</sub> Ph.D. Thesis**

J. D. CAWLEY, J. W. HALLORAN (Case Western Reserve Univ.), and A. R. COOPER (Case Western Reserve Univ.) Jun. 1984 356 p refs

(Contract NSG-3291)

(NASA-TM-83622; E-1862; NAS 1.15:83622) Avail: NTIS HC A16/MF A01 CSCL 11G

Oxygen self diffusion coefficients were determined in single crystal alpha-Al<sub>2</sub>O<sub>3</sub> using the gas exchange technique. The samples were semi-infinite slabs cut from five different boules with varying background impurities. The diffusion direction was parallel to the c-axis. The tracer profiles were determined by two techniques, single spectrum proton activation and secondary ion mass spectrometry. The SIMS proved to be a more useful tool. The determined diffusion coefficients, which were insensitive to impurity levels and oxygen partial pressure, could be described by  $D = .00151 \exp(-572 \text{ kJ/RT}) \text{ sq m/s}$ . The insensitivities are discussed in terms of point defect clustering. Two independent models are consistent with the findings, the first considers the clusters as immobile point defect traps which buffer changes in the defect chemistry. The second considers clusters to be mobile and oxygen diffusion to be intrinsic behavior, the mechanism for oxygen transport involving neutral clusters of Schottky quintuplets.

Author



**N84-28994\*#** National Aeronautics and Space Administration. Lewis Research Center, Cleveland, Ohio.

**PROPERTIES OF FERRITES IMPORTANT TO THEIR FRICTION AND WEAR BEHAVIOR**

K. MIYOSHI and D. H. BUCKLEY 1983 29 p refs Prepared for presentation at the Joint Lubrication Conf., San Diego, Calif., 22-24 Oct. 1984; sponsored by ASME and Am. Soc. of Lubrication Engrs.

(NASA-TM-83718; E-2002; NAS 1.15:83718) Avail: NTIS HC A03/MF A01 CSCL 11G

Environmental, chemical and crystallographical effects on the fundamental nature on friction and wear of the ferrites in contact with metals, magnetic tapes and themselves are reviewed. The removal of adsorbed films from the surfaces of ferrites results in very strong interfacial adhesion and high friction in ferrite to metal and ferrite to magnetic tape contacts. The metal ferrite bond at the interface is primarily a chemical bond between the metal atoms and the large oxygen anions in the ferrite surface, and the strength of these bonds is related to the oxygen to metal bond strength in the metal oxide. The more active the metal, the higher is the coefficient of friction. Not only under adhesive conditions; but also under abrasive conditions the friction and wear properties of ferrites are related to the crystallographic orientation. With ferrite to ferrite contact the mating of highest atomic density (most closely packed) direction on matched crystallographic planes, that is, 110 directions on /110/planes, results in the lowest coefficient of friction.

Author

**N84-28995\*#** TRW, Inc., Redondo Beach, Calif. Energy Development Group.

**IMPROVED HIGH TEMPERATURE RESISTANT MATRIX RESINS**

G. E. CHANG, S. H. POWELL, and R. J. JONES Aug. 1983 71 p refs

(Contract NAS3-23274)

(NASA-CR-168210; NAS 1.26:168210; REPT-38945-6012-UT-00) Avail: NTIS HC A04/MF A01 CSCL 11D

The objective was to develop organic matrix resins suitable for service at temperatures up to 644 K (700 F) and at air pressures up to 0.4 MPa (60 psia) for time durations of a minimum of 100 hours. Matrix resins capable of withstanding these extreme oxidative environmental conditions would lead to increased use of polymer matrix composites in aircraft engines and provide significant weight and cost savings. Six linear condensation, aromatic/heterocyclic polymers containing fluorinated and/or diphenyl linkages were synthesized. The thermo-oxidative stability of the resins was determined at 644 K and compressed air pressures up to 0.4 MPa. Two formulations, both containing perfluoroisopropylidene linkages in the polymer backbone structure, exhibited potential for 644 K service to meet the program objectives. Two other formulations could not be fabricated into compression molded zero defect specimens.

Author

**N84-30072\*#** National Aeronautics and Space Administration. Lewis Research Center, Cleveland, Ohio.

**EFFECTS OF WATER-VAPOR ON FRICTION AND DEFORMATION OF POLYMERIC MAGNETIC MEDIA IN CONTACT WITH A CERAMIC OXIDE**

K. MIYOSHI and D. H. BUCKLEY 1984 28 p refs Proposed for presentation at the Joint Lubrication Conf., San Diego, Calif., 22-24 Oct. 1984; sponsored by the American Society of Mechanical Engineers and the American Society of Lubrication Engineers (NASA-TM-83727; E-1986; NAS 1.15:83727) Avail: NTIS HC A03/MF A01 CSCL 11C

The effects of humidity (water-vapor) in nitrogen on the friction and deformation behavior of magnetic tape in contact with a Ni-Zn ferrite spherical pin were studied. The coefficient of friction is markedly dependent on the ambient relative humidity. In elastic contacts the coefficient of friction increased linearly with increasing humidity; it decreased linearly when humidity was lowered. This effect is the result of changes in the chemistry and interaction of tape materials such as degradation of the lubricant. In plastic contacts there was no effect of humidity on friction below 40

percent relative humidity. There is no effect on friction associated with the breakthrough of the adsorbed water-vapor film at the interface of the tape and Ni-Zn ferrite. The coefficient of friction, however, increased rapidly with increasing relative humidity above 40 percent in plastic contacts.

Author

**N84-31379\*#** National Aeronautics and Space Administration. Lewis Research Center, Cleveland, Ohio.

**ADHESION BETWEEN POLYMERS AND EVAPORATED GOLD AND NICKEL FILMS**

Y. YAMADA, D. R. WHEELER, and D. H. BUCKLEY Aug. 1984 11 p refs

(NASA-TP-2360; E-2018; NAS 1.60:2360) Avail: NTIS HC A02/MF A01 CSCL 11B

To obtain information on the adhesion between metal films and polymeric solids, the adhesion force was measured by means of a tensile pull test. It was found that the adhesion strengths between polymeric solids and gold films evaporated on polymer substrates were  $(1.11 \pm 0.53)$  multiplied by  $10(6)$  N/m(2) on PTFE, about 5.49 multiplied by  $10(6)$  N/m(2) on UHMWPE, and  $6.54 \times 10(6)$  on 6/6 nylon. The adhesion strengths for nickel films evaporated on PTFE, UHMWPE, and 6/6 nylon were found to be a factor of 1.7 higher than those for the gold coated PTFE, UHMWPE, and 6/6 nylon. To confirm quantitatively the effect of electron irradiation on the adhesion strength between a PTFE solid and metal films, a tensile pull test was performed on the irradiated PTFE specimens, which were prepared by evaporating nickel or gold on PTFE surfaces irradiated by 2-keV electrons for various times. After irradiation, the adhesion strength increased to  $(4.92 \pm 0.92) \times 10(6)$  N/m(2) for nickel coated PTFE and  $(1.82 \pm 0.48) \times 10(6)$  N/m(2) for gold coated PTFE. The improvement in adhesion for nickel is higher than that for gold.

Author

**N84-32531\*#** National Aeronautics and Space Administration. Lewis Research Center, Cleveland, Ohio.

**THE FRICTION BEHAVIOR OF SEMICONDUCTORS SI AND GAAS IN CONTACT WITH PURE METALS**

H. MISHINA 1984 16 p refs Proposed for presentation at the Intern. Tribology Conf., Tokyo, 8-10 Jul. 1985; sponsored by the Japan Society of Lubrication Engineers

(NASA-TM-83779; E-2228; NAS 1.15:83779) Avail: NTIS HC A02/MF A01 CSCL 11G

The friction behavior of the semiconductors silicon and gallium arsenide in contact with pure metals was studied. Five transition and two nontransition metals, titanium, tantalum, nickel, palladium, platinum, copper, and silver, slid on a single crystal silicon (111) surface. Four metals, indium, nickel, copper and silver, slid on a single crystal gallium arsenide (100) surface. Experiments were conducted in room air and in a vacuum of 10 to the minus 7th power N/sq cm (10 to the minus 9th power torr). The results indicate that the sliding of silicon on the transition metals exhibits relatively higher friction than for the nontransition metals in contact with silicon. There is a clear correlation between friction and Schottky barrier height formed at the metal silicon interface for the transition metals. Transition metals with a higher barrier height on silicon had a lower friction. The same effect of barrier height was found for the friction of gallium arsenide in contact with metals.

Author

**N84-32536\*#** National Aeronautics and Space Administration. Lewis Research Center, Cleveland, Ohio.

**RF SPUTTERED SILICON AND HAFNIUM NITRIDES AS APPLIED TO 440C STEEL**

A. GRILL (Ben Gurion Univ. of the Negev, Beer Sheeva, Israel) and P. R. ARON Mar. 1984 28 p refs

(NASA-TM-86862; E-1993; NAS 1.15:86862) Avail: NTIS HC A03/MF A01 CSCL 11D

Silicon nitride and hafnium nitride coatings were deposited on oxidized and unoxidized 440C stainless steel substrates. Sputtering was done in mixtures of argon and nitrogen gases from pressed powder silicon nitride and from hafnium metal targets. The coatings and the interface between the coating and substrate were investigated by X-ray diffractometry, scanning electron microscopy,

energy dispersive X-ray analysis and Auger electron spectroscopy. Oxide was found at all interfaces with an interface width of at least 600 Å for the oxidized substrates and at least 300 Å for the unoxidized substrates. Scratch test results demonstrate that the adhesion of hafnium nitride to both oxidized and unoxidized 440C is superior to that of silicon nitride. Oxidized 440C is found to have increased adhesion, to both nitrides, over that of unoxidized 440C. Coatings of both nitrides deposited at 8 mtorr were found to have increased adhesion to both oxidized and unoxidized 440C over those deposited at 20 mtorr. A.R.H.

**N84-33590\*#** National Aeronautics and Space Administration. Lewis Research Center, Cleveland, Ohio.  
**FRICTION BEHAVIOR OF SILICON IN CONTACT WITH TITANIUM, NICKEL, SILVER AND COPPER**  
 H. MISHINA (Institute of Physical and Chemical Research) and D. H. BUCKLEY Sep. 1984 8 p refs  
 (NASA-TP-2362; E-2036; NAS 1.60:2362) Avail: NTIS HC A02/MF A01 CSCL 11G

Sliding friction experiments are conducted with the semiconductor silicon in contact with the metals titanium, nickel, copper, and silver. Sliding is on the (111) plane of single-crystal silicon in the 112 crystallographic direction both in dry and lubricated (mineral oil) sliding. The friction coefficient in dry sliding is controlled by adhesion and the surface chemical activity of the metal. The more active the metal the stronger the adhesion and the higher the friction. In lubricated sliding the lubricant absorbs to the surfaces and reduces the importance of metal chemical effects. In lubricated sliding, silicon ceases to behave in a brittle manner and undergoes plastic deformation under load. M.A.C.

**N84-33595\*#** National Aeronautics and Space Administration. Lewis Research Center, Cleveland, Ohio.  
**IMPROVED THERMAL BARRIER COATING SYSTEM Patent Application**  
 S. STECURA, inventor (to NASA) 14 Aug. 1984 8 p  
 (NASA-CASE-LEW-14057-1; NAS 1.71:LEW-14057-1; US-PATENT-APPL-SN-640712) Avail: NTIS HC A02/MF A01 CSCL 11G

An oxide thermal barrier coating is described which comprises  $ZrO_3$  -  $Yb_2O_3$  that is plasma sprayed onto a previously applied bond coating. The zirconia is partially stabilized with about 12.4 v/o ytterbia to insure cubic, monoclinic, and tetragonal phases. NASA

**N84-34619\*#** National Aeronautics and Space Administration. Lewis Research Center, Cleveland, Ohio.  
**THE ROLE OF MATERIAL PROPERTIES IN ADHESION**  
 D. H. BUCKLEY 1984 25 p refs Proposed for presentation at the 1984 Fall Meeting of the Mater. Res. Soc., Boston, 25-30 Nov. 1984  
 (NASA-TM-83792; E-2230; NAS 1.15:83792) Avail: NTIS HC A02/MF A01 CSCL 11B

When two solid surfaces are brought into contact strong adhesive bond forces can develop between the materials. The magnitude of the forces will depend upon the state of the surfaces, cleanliness and the fundamental properties of the two solids, both surface and bulk. Adhesion between solids is addressed from a theoretical consideration of the electronic nature of the surfaces and experimentally relating bond forces to the nature of the interface resulting from solid state contact. Surface properties correlated with adhesion include, atomic or molecular orientation, reconstruction and segregation as well as the chemistry of the surface specie. Where dissimilar solids are in contact the contribution of each is considered as is the role of their interactive chemistry on bond strength. Bulk properties examined include elastic and plastic behavior in the surficial regions, cohesive binding energies, crystal structure, crystallographic orientation and state. Materials examined with respect to interfacial adhesive interactions include metals, alloys, ceramics, polymers and diamond. They are reviewed both in single and polycrystalline form. The surfaces of the contacting solids are studied both in the atomic or molecularly

clean state and in the presence of selected surface contaminants. Author

**N84-34620\*#** National Aeronautics and Space Administration. Lewis Research Center, Cleveland, Ohio.  
**OPTICAL AND OTHER PROPERTY CHANGES OF M-50 BEARING STEEL SURFACES FOR DIFFERENT LUBRICANTS AND ADDITIVE PRIOR TO SCUFFING**  
 J. L. LAUER (Rensselaer Polytechnic Inst.) and N. MARXER (Rensselaer Polytechnic Inst.) 1984 25 p refs Presented at Joint Lubrication Conf., San Diego, Calif., 22-24 Oct. 1984; sponsored by ASME and American Society of Lubrication Engineers  
 (NASA-TM-83746; E-2234; NAS 1.15:83746) Avail: NTIS HC A02/MF A01 CSCL 11H

An ester lubricant base oil containing one or more standard additives to protect against wear, corrosion, and oxidation was used in an experimental ball/plate elastohydrodynamic contact under load and speed conditions such as to induce scuffing failure in short times. Both the ball and the plate were of identically treated M-50 steel. After various periods of operating time the wear track on the plate was examined with an interference microscope of plus or minus 30 Å depth resolution and sometimes also with a scanning ellipsometer and an Auger spectrometer. The optically deduced surface profiles varied with wavelength, indicating the presence of surface coatings, which were confirmed by the other instruments. As scuffing was approached, a thin (approximately Å) oxide layer and a carbide layer formed in the wear track in particular when tricresylphosphate antiwear additive was present in the lubricant. The rates of the formation of these layers and their reactivity toward dilute alcoholic HCl depended strongly on the lubricant and additives. Based on these results suggestions for improved formulations and a test method for bearing reliability could be proposed. R.J.F.

## 28

## PROPELLANTS AND FUELS

Includes rocket propellants, igniters, and oxidizers; storage and handling; and aircraft fuels.

**A84-18142\*#** United Technologies Research Center, East Hartford, Conn.  
**DEPOSIT FORMATION AND HEAT TRANSFER IN HYDROCARBON ROCKET FUELS**  
 A. J. GIOVANETTI, L. J. SPADACCINI, and E. J. SZETELA (United Technologies Research Center, East Hartford, CT) American Institute of Aeronautics and Astronautics, Aerospace Sciences Meeting, 22nd, Reno, NV, Jan. 9-12, 1984. 12 p. refs  
 (Contract NAS3-23344)  
 (AIAA PAPER 84-0512)

An experimental research program was undertaken to investigate the thermal stability and heat transfer characteristics of several hydrocarbon fuels under conditions that simulate high-pressure, rocket engine cooling systems. The rates of carbon deposition in heated copper and nickel-plated copper tubes were determined for RP-1, propane, and natural gas using a continuous flow test apparatus which permitted independent variation and evaluation of the effect on deposit formation of wall temperature, fuel pressure, and fuel velocity. In addition, the effects of fuel additives and contaminants, cryogenic fuel temperatures, and extended duration testing with intermittent operation were examined. Corrosion of the copper tube surface was detected for all fuels tested; however, plating the insides of the tubes with nickel reduced deposit formation and eliminated corrosion in most cases. The lowest rates of carbon deposition were obtained for natural gas, and the highest rates were obtained for propane. Forced-convection heat transfer film coefficients were satisfactorily

correlated using a Nusselt-Reynolds-Prandtl number equation for all the fuels tested. Author

**A84-26955\*#** National Aeronautics and Space Administration. Lewis Research Center, Cleveland, Ohio.

**HEATING EXPERIMENTS FOR FLOWABILITY IMPROVEMENT OF NEAR-FREEZING AVIATION FUEL**

R. FRIEDMAN (NASA, Lewis Research Center, Fuels Research Section, Cleveland, OH) and F. J. STOCKEMER Journal of Aircraft (ISSN 0021-8669), vol. 21, April 1984, p. 250-255. refs (Contract NAS3-21977)

An experimental jet fuel with a -33 C freezing point was chilled in a wing tank simulator with superimposed fuel heating to improve low temperature flowability. Heating consisted of circulating a portion of the fuel to an external heat exchanger and returning the heated fuel to the tank. Flowability was determined by the mass percent of unpumpable fuel (holdup) left in the simulator upon withdrawal of fuel at the conclusion of testing. The study demonstrated that fuel heating is feasible and improves flowability as compared to that of baseline, unheated tests. Delayed heating with initiation when the fuel reaches a prescribed low temperature limit, showed promise of being more efficient than continuous heating. Regardless of the mode or rate of heating, complete flowability (zero holdup) could not be restored by fuel heating. The severe, extreme-day environment imposed by the test caused a very small amount of subfreezing fuel to be retained near the tank surfaces even at high rates of heating. Correlations of flowability established for unheated fuel tests also could be applied to the heated test results if based on boundary-layer temperature or a solid index (subfreezing point) characteristic of the fuel. Previously announced in STAR as N82-26483 Author

**A84-35236\*#** United Technologies Research Center, East Hartford, Conn.

**ROLE OF FUEL CHEMICAL PROPERTIES ON COMBUSTOR RADIATIVE HEAT LOAD**

T. J. ROSFJORD (United Technologies Research Center, East Hartford, CT) AIAA, SAE, and ASME, Joint Propulsion Conference, 20th, Cincinnati, OH, June 11-13, 1984. 12 p. refs (Contract NAS3-23167) (AIAA PAPER 84-1493)

In an attempt to rigorously study the fuel chemical property influence on combustor radiative heat load, UTRC has conducted an experimental program using 25 test fuels. The burner was a 12.7-cm dia cylindrical device fueled by a single pressure-atomizing injector. Fuel physical properties were de-emphasized by selecting injectors which produced highly-atomized, and hence rapidly-vaporizing sprays. The fuels were specified to cover the following wide ranges of chemical properties: hydrogen, 9.1 to 15- (wt) pct; total aromatics, 0 to 100 (vol) pct; and naphthalene, 0 to 30 (vol) pct. They included standard fuels, specialty products and fuel blends. Fuel naphthalene content exhibited the strongest influence on radiation of the chemical properties investigated. Smoke point was a good global indicator of radiation severity.

Author

**N84-10332\*#** United Technologies Corp., East Hartford, Conn. **AN ASSESSMENT OF THE USE OF ANTIMISTING FUEL IN TURBOFAN ENGINES** Contractor Report, Sep. 1979 - Mar. 1982

A. J. FIORENTINO and J. R. PLANELL Oct. 1983 180 p refs (Contract NAS3-22045) (NASA-CR-168081; NAS 1 26:168081; PWA-5697-65) Avail: NTIS HC A09/MF A01 CSCL 21D

An evaluation was made on the effects of using antimisting kerosene (AMK) on the performance of the components from the fuel system and the combustor of current in service JT8D aircraft engines. The objectives were to identify if there were any problems associated with using antimisting kerosene and to determine the extent of shearing or degradation required to allow the engine components to achieve satisfactory operation. The program consisted of a literature survey and a test program which evaluated the antimisting kerosene fuel in laboratory and bench component

testing, and assessed the performance of the combustor in a high pressure facility and in an altitude reflight/cold ignition facility.

Author

**N84-13332\*#** Southwest Research Inst., San Antonio, Tex. **INVESTIGATION OF SOURCES, PROPERTIES AND PREPARATION OF DISTILLATE TEST FUELS**

J. N. BOWDEN and J. ERWIN Nov. 1983 69 p refs (Contract NAS3-22783) (NASA-CR-168227; NAS 1.26:168227; SWRI-6682/2) Avail: NTIS HC A04/MF A01 CSCL 21D

Distillate test fuel blends were generated for prescribed variations in composition and physical properties. Fuels covering a wide range in properties and composition which would provide a matrix of fuels for possible use in future combustion research programs were identified. Except for tetralin the blending components were all from typical refinery streams. Property variation blends span a boiling range within 150 C to 335 C, freezing point -23 C to -43 C, aromatic content 20 to 50 volume percent, hydrogen content 11.8 to 14.2 mass percent, viscosity 4 and 11 cSt (-20 C), and naphthalenes 8 and 16 volume percent. Composition variation blends were made with two base stocks, one paraffinic and the other naphthenic. To each base stock was added each of three aromatic type fuels (alkyl benzenes, tetralin, and naphthalenes) for assigned initial boiling point, final boiling point, and hydrogen content. The hydrogen content was 13.5 mass percent for the paraffinic base stock blends and 12.5 mass percent and 11.5 mass percent for the naphthenic base stock blends. Sample 5-gallon quantities of all blends were prepared and analyzed. Author

**N84-15283\*#** General Electric Co., Cincinnati, Ohio. Aircraft Engine Business Group.

**BROAD SPECIFICATION FUELS COMBUSTION TECHNOLOGY PROGRAM Final Report, Sep. 1979 - Feb. 1982**

W. J. DODDS and E. E. EKSTEDT Jan. 1984 341 p refs (Contract NAS3-22063) (NASA-CR-168179; NAS 1.26:168179) Avail: NTIS HC A15/MF A01 CSCL 21D

Design and development efforts to evolve promising aircraft gas turbine combustor configurations for burning broadened-properties fuels were discussed. Design and experimental evaluations of three different combustor concepts in sector combustor rig tests was conducted. The combustor concepts were a state of the art single-annular combustor, a staged double-annular combustor, and a short single-annular combustor with variable geometry to control primary zone stoichiometry. A total of 25 different configurations of the three combustor concepts were evaluated. Testing was conducted over the full range of CF6-80A engine combustor inlet conditions, using four fuels containing between 12% and 14% hydrogen by weight. Good progress was made toward meeting specific program emissions and performance goals with each of the three combustor concepts. The effects of reduced fuel hydrogen content, including increased flame radiation, liner metal temperature, smoke, and NOx emissions were documented. The most significant effect on the baseline combustor was a projected 33% life reduction, for a reduction from 14% to 13% fuel hydrogen content, due to increased liner temperatures. Author

**N84-17407\*#** United Technologies Research Center, East Hartford, Conn.

**AVIATION-FUEL PROPERTY EFFECTS ON COMBUSTION** Contractor Final Report

T. J. ROSFJORD Feb. 1984 147 p refs (Contract NAS3-23167) (NASA-CR-168334; NAS 1.26:168334; UTRC-884-915908-29) Avail: NTIS HC A07/MF A01 CSCL 21D

The fuel chemical property influence on a gas turbine combustor was studied using 25 test fuels. Fuel physical properties were de-emphasized by using fuel injectors which produce highly-atomized, and hence rapidly vaporizing sprays. A substantial fuel spray characterization effort was conducted to allow selection

of nozzles which assured that such sprays were achieved for all fuels. The fuels were specified to cover the following wide ranges of chemical properties: hydrogen, 9.1 to 15 (wt) pct; total aromatics, 0 to 100 (vol) pct; and naphthalene, 0 to 30 (vol) pct. standard fuels (e.g., Jet A, JP4), speciality products (e.g., decalin, xylene tower bottoms) and special fuel blends were included. The latter group included six, 4-component blends prepared to achieve parametric variations in fuel hydrogen, total aromatics and naphthalene contents. The principle influences of fuel chemical properties on the combustor behavior were reflected by the radiation, liner temperature, and exhaust smoke number (or equivalently, soot number density) data. Test results indicated that naphthalene content strongly influenced the radiative heat load while parametric variations in total aromatics did not. Author

**N84-17410\*#** Rensselaer Polytechnic Inst., Troy, N. Y. Dept. of Mechanical Engineering

**EMISSION FTIR ANALYSES OF THIN MICROSCOPIC PATCHES OF JET FUEL RESIDUE DEPOSITED ON HEATED METAL SURFACE** Interim Report

J. L. LAUER and P. VOGEL Jan. 1984 32 p refs  
(Contract NAG3-205; DAAG24-83-K-0058; AF-AFOSR-0005-81)  
(NASA-CR-168331; NAS 1.26:168331) Avail: NTIS HC A03/MF A01 CSCL 21D

Deposits laid down in patches on metal strips in a high pressure/high temperature fuel system simulator operated with aerated fuel at varying flow rates were analyzed by emission FTIR in terms of functional groups. Significant differences were found in the spectra and amounts of deposits derived from fuels to which small concentrations of oxygen-, nitrogen-, or sulfur-containing heterocyclics or metal naphthenates were added. The spectra of deposits generated on strips by heating fuels and air in a closed container were very different from those of the flowing fluid deposits. One such closed-container dodecane deposit on silver gave a strong surface-enhanced Raman spectrum.

Author

**N84-18420\*#** Case Western Reserve Univ., Cleveland, Ohio. Dept. of Electrical Engineering and Applied Physics.

**APPLICATIONS OF PHOTOACOUSTIC TECHNIQUES TO THE STUDY OF JET FUEL RESIDUE** Final Report, 22 Oct. 1980 - 20 May 1983

P. C. CLASPY 14 Nov. 1983 25 p refs  
(Contract NAG3-98)  
(NASA-CR-173322; NAS 1.26:173322) Avail: NTIS HC A02/MF A01 CSCL 21D

It has been known for many years that fuels for jet aircraft engines demonstrate thermal instability. One manifestation of this thermal instability is the formation of deleterious, fuel-derived thermally-induced deposits on surfaces of the aircraft's fuel-handling system. The results of an investigation of the feasibility of applying photoacoustic techniques to the study of the physical properties of these thermal deposits are presented. Both phase imaging and magnitude imaging and spectroscopy were investigated. It is concluded that the use of photoacoustic techniques in the study of films of the type encountered in this investigation is not practical. S.L.

**N84-23631\*#** National Aeronautics and Space Administration. Lewis Research Center, Cleveland, Ohio.

**TRENDS OF JET FUEL DEMAND AND PROPERTIES**

R. FRIEDMAN *In its* Assessment of Alternative Aircraft Fuels p 1-10 Apr. 1984 refs  
Avail: NTIS HC A09/MF A01 CSCL 21D

Petroleum industry forecasts predict an increasing demand for jet fuels, a decrease in the gasoline-to-distillate (heavier fuel) demand ratio, and a greater influx of poorer quality petroleum in the next two to three decades. These projections are important for refinery product analyses. The forecasts have not been accurate, however, in predicting the recent, short term fluctuations in jet fuel and competing product demand. Changes in petroleum quality can be assessed, in part, by a review of jet fuel property inspections. Surveys covering the last 10 years show that average

jet fuel freezing points, aromatic contents, and smoke points have trends toward their specification limits. Author

**N84-23642\*#** National Aeronautics and Space Administration. Lewis Research Center, Cleveland, Ohio.

**RESEARCH ON AVIATION FUEL INSTABILITY**

C. E. BAKER, D. A. BITTKER, S. M. COHEN, and G. T. SENG *In its* Assessment of Alternative Aircraft Fuels. p 121-130 Apr. 1984 refs

Avail: NTIS HC A09/MF A01 CSCL 21D

The problems associated with aircraft fuel instability are discussed. What is currently known about the problem is reviewed and a research program to identify those areas where more research is needed is discussed. The term fuel instability generally refers to the gums, sediments, or deposits which can form as a result of a set of complex chemical reactions when a fuel is stored for a long period at ambient conditions or when the fuel is thermally stressed inside the fuel system of an aircraft. R.J.F.

**N84-23643\*#** National Aeronautics and Space Administration. Lewis Research Center, Cleveland, Ohio.

**IN-FLIGHT ATMOSPHERIC AND FUEL TANK TEMPERATURE MEASUREMENTS**

R. SVEHLA *In its* Assessment of Alternative Aircraft Fuels p 131-140 Apr. 1984 refs

Avail: NTIS HC A09/MF A01 CSCL 21D

In order to maintain an adequate supply of aviation turbine fuels in the future, fuels may have properties different from those now currently produced. One possible change is an increase in the freezing point temperature. If this should occur, it will be necessary to know the low temperature flow characteristics of these fuels. Studies to date involved both the use of computer models and subscale fuel tank simulators. They indicate that steep temperature gradients occur near the upper and lower surfaces which can result in freezing at the bottom, even though the bulk fuel temperature is above the freezing point. In order to obtain flight data to verify computer model and simulator results, Lockheed L1011 research aircraft at Palmdale, California was instrumented with a vertical thermocouple rake in an inboard tank and an outboard tank. The tests were conducted with one of the two instrumented tanks maintained full for either two or five hours at altitudes of at least 10668 meters (35000 ft). Other flight parameters such as Mach number, air temperature, fuel quantity and heading were also recorded. R.J.F.

**N84-23774\*#** National Aeronautics and Space Administration. Lewis Research Center, Cleveland, Ohio.

**GROUP-TYPE HYDROCARBON STANDARDS FOR HIGH-PERFORMANCE LIQUID CHROMATOGRAPHIC ANALYSIS OF MIDDISTILLATE FUELS**

D. A. OTTERSON and G. T. SENG May 1984 18 p refs  
(NASA-TP-2317; E-1931; NAS 1.60:2317) Avail: NTIS HC A02/MF A01 CSCL 21D

A new high-performance liquid chromatographic (HPLC) method for group-type analysis of middistillate fuels is described. It uses a refractive index detector and standards that are prepared by reacting a portion of the fuel sample with sulfuric acid. A complete analysis of a middistillate fuel for saturates and aromatics (including the preparation of the standard) requires about 15 min if standard for several fuels are prepared simultaneously. From model fuel studies, the method was found to be accurate to within 0.4 vol% saturates or aromatics, and provides a precision of + or - 0. vol%. Olefin determinations require an additional 15 min of analysis time. However, this determination is needed only for those fuel displaying a significant olefin response at 200 nm (obtained routinely during the saturated/aromatics analysis procedure). The olefin determination uses the responses of the olefins and the corresponding saturates, as well as the average value of the refractive index sensitivity ratios (1.1). Studies indicated that although the relative error in the olefins result could reach 1 percent by using this average sensitivity ratio, it was 5 percent for the fuels used in this study. Olefin concentrations as low as 0. vol% have been determined using this method. Author

**N84-23775\*#** Purdue Univ., Lafayette, Ind. School of Mechanical Engineering.

**FLAME PROPAGATION IN HETEROGENEOUS MIXTURES OF FUEL DROPS AND AIR Final Report**

G. D. MYERS and A. H. LEFEBVRE May 1984 57 p refs  
(Contract NAG3-266; DE-AI01-81CS-50006)  
(NASA-CR-174644; DOE/NASA/0266-1; NAS 1.26:174644)  
Avail: NTIS HC A04/MF A01 CSCL 21D

Photographic methods are used to measure flame speeds in flowing mixtures of fuel props and air at atmospheric pressure. The fuels employed include a conventional fuel oil plus various blends JP 7 with stocks containing single-ring and multi-ring aromatics. The results for stoichiometric mixtures show that flame propagation cannot occur in mixtures containing mean drop sizes larger than 300 to 400 microns, depending on the fuel type. For smaller drop sizes, down to around 60 microns, flame speed is inversely proportional to drop size, indicating that evaporation rates are limiting to flame speed. Below around 60 microns, the curves of flame speed versus mean drop size flatten out, thereby demonstrating that for finely atomized sprays flame speeds are much less dependent on evaporation rates, and are governed primarily by mixing and/or chemical reaction rates. The fuels exhibiting the highest flame speeds are those containing multi-ring aromatics. This is attributed to the higher radiative heat flux emanating from their soot-bearing flames which enhances the rate of evaporation of the fuel drops approaching the flame front.

Author

**N84-24734\*#** National Aeronautics and Space Administration. Lewis Research Center, Cleveland, Ohio.

**RESEARCH ON AVIATION FUEL INSTABILITY**

C. E. BAKER, D. A. BITTKER, S. M. COHEN, and G. T. SENG  
*In* AGARD Combust. Probl. in Turbine Eng. 11p Jan. 1984  
refs

Avail: NTIS HC A19/MF A01 CSCL 21B

Current aircraft turbine fuels do not present a significant problem with fuel thermal stability. However, turbine fuels with broadened properties or nonpetroleum derived fuels may have reduced thermal stability because of their higher content of olefins, heteroatoms, and trace metals. Moreover, advanced turbine engines will increase the thermal stress on fuels because of their higher pressure ratios and combustion temperature. In recognition of the importance of this problem, NASA Lewis is currently engaged in a broadly based research effort to better understand the underlying causes of fuel thermal degradation. The progress and status of our various activities in this area are discussed. Topics covered include: nature of fuel instability and its temperature dependence, methods of measuring the instability, chemical mechanisms involved in deposit formation, and instrumental methods for characterizing fuel deposits. Finally, some preliminary thoughts on design approaches for minimizing the effects of lowered thermal stability are briefly discussed.

R.J.F.

**N84-25854\*#** Simmonds Precision Products, Inc., Vergennes, Vermont. Instrument Systems Div.

**STUDY OF EFFECTS OF FUEL PROPERTIES IN TURBINE-POWERED BUSINESS AIRCRAFT Final Report**

F. D. POWELL, R. J. BIEGEN, P. G. WEITZ, JR., and A. M. DUKE Apr. 1984 89 p refs  
(Contract NAS3-22827)  
(NASA-CR-174627; E-2470; NAS 1.26:174627) Avail: NTIS HC A05/MF A01 CSCL 21D

Increased interest in research and technology concerning aviation turbine fuels and their properties was prompted by recent changes in the supply and demand situation of these fuels. The most obvious change is the rapid increase in fuel price. For commercial airplanes, fuel costs now approach 50 percent of the direct operating costs. In addition, there were occasional local supply disruptions and gradual shifts in delivered values of certain fuel properties. Dwindling petroleum reserves and the politically sensitive nature of the major world suppliers make the continuation of these trends likely. A summary of the principal findings, and conclusions are presented. Much of the material, especially the

tables and graphs, is considered in greater detail later. The economic analysis and examination of operational considerations are described. Because some of the assumptions on which the economic analysis is founded are not easily verified, the sensitivity of the analysis to alternates for these assumptions is examined. The data base on which the analyses are founded is defined in a set of appendices.

Author

**N84-26813\*#** Pennsylvania State Univ., University Park  
**UTILIZATION OF ALTERNATIVE FUELS IN DIESEL ENGINES Final Report**

S. A. LESTZ May 1984 74 p refs  
(Contract NAG3-91; DE-AI01-81CS-50006)  
(NASA-CR-174669; DOE/NASA/0091-1; NAS 1.26:174669; CAES-700-84) Avail: NTIS HC A04/MF A01 CSCL 21D

Performance and emission data are collected for various candidate alternate fuels and compare these data to that for a certified petroleum based number two Diesel fuel oil. Results for methanol, ethanol, four vegetable oils, two shale derived oils, and two coal derived oils are reported. Alcohol fumigation does not appear to be a practical method for utilizing low combustion quality fuels in a Diesel engine. Alcohol fumigation enhances the bioactivity of the emitted exhaust particles. While it is possible to inject many synthetic fuels using the engine stock injection system, wholly acceptable performance is only obtained from a fuel whose specifications closely approach those of a finished petroleum based Diesel oil. This is illustrated by the contrast between the poor performance of the unupgraded coal derived fuel blends and the very good performance of the fully refined shale derived fuel.

M.A.C.

**N84-27908\*#** ICF, Inc., Washington, D. C.

**COMPUTER ANALYSIS OF EFFECTS OF ALTERING JET FUEL PROPERTIES ON REFINERY COSTS AND YIELDS Final Report**

T. BRETON and D. DUNBAR Jun. 1984 134 p  
(Contract NAS3-22780)  
(NASA-CR-174642; NAS 1.26:174642) Avail: NTIS HC A07/MF A01 CSCL 21D

This study was undertaken to evaluate the adequacy of future U.S. jet fuel supplies, the potential for large increases in the cost of jet fuel, and to what extent a relaxation in jet fuel properties would remedy these potential problems. The results of the study indicate that refiners should be able to meet jet fuel output requirements in all regions of the country within the current Jet A specifications during the 1990-2010 period. The results also indicate that it will be more difficult to meet Jet A specifications on the West Coast, because the feedstock quality is worse and the required jet fuel yield (jet fuel/crude refined) is higher than in the East. The results show that jet fuel production costs could be reduced by relaxing fuel properties. Potential cost savings in the East (PADDs I-IV) through property relaxation were found to be about 1.3 cents/liter (5 cents/gallon) in January 1, 1981 dollars between 1990 and 2010. However, the savings from property relaxation were all obtained within the range of current Jet A specifications, so there is no financial incentive to relax Jet A fuel specifications in the East. In the West (PADD V) the potential cost savings from lowering fuel quality were considerably greater than in the East. Cost savings from 2.7 to 3.7 cents/liter (10-14 cents/gallon) were found. In contrast to the East, on the West Coast a significant part of the savings was obtained through relaxation of the current Jet A fuel specifications.

B.W.

**N84-27909\*#** Texas A&M Univ., College Station  
**EVALUATION OF DISSOCIATED AND STEAM-REFORMED METHANOL AS AUTOMOTIVE ENGINE FUELS Final Report**

T. R. LALK, D. M. MCCALL, and J. M. MCCANLIES May 1984 145 p refs  
(Contract NAG3-142; DE-AI01-77CS-51044)  
(NASA-CR-168242; DOE/NASA/0142-1; NAS 1.26:168242)  
Avail: NTIS HC A07/MF A01 CSCL 21D

Dissociated and steam reformed methanol were evaluated as automotive engine fuels. Advantages and disadvantages in using

methanol in the reformed rather than liquid state were discussed. Engine dynamometer tests were conducted with a four cylinder, 2.3 liter, spark ignition automotive engine to determine performance and emission characteristics operating on simulated dissociated and steam reformed methanol ( $2H_2 + CO$  and  $3H_2 + CO_2$  respectively), and liquid methanol. Results are presented for engine performance and emissions as functions of equivalence ratio, at various throttle settings and engine speeds. Operation on dissociated and steam reformed methanol was characterized by flashback (violent propagation of a flame into the intake manifold) which limited operation to lower power output than was obtainable using liquid methanol. It was concluded that: an automobile could not be operated solely on dissociated or steam reformed methanol over the entire required power range - a supplementary fuel system or power source would be necessary to attain higher powers; the use of reformed methanol, compared to liquid methanol, may result in a small improvement in thermal efficiency in the low power range; dissociated methanol is a better fuel than steam reformed methanol for use in a spark ignition engine; and use of dissociated or steam reformed methanol may result in lower exhaust emissions compared to liquid methanol. Author

**N84-32552\*#** Utah Univ., Salt Lake City.  
**CARBON-13 AND PROTON NUCLEAR MAGNETIC RESONANCE ANALYSIS OF SHALE-DERIVED REFINERY PRODUCTS AND JET FUELS AND OF EXPERIMENTAL REFEREE BROADENED-SPECIFICATION JET FUELS** Final Report  
 D. K. DALLING, B. K. BAILEY, and R. J. PUGMIRE Sep. 1984 98 p refs  
 (Contract NAG3-27)  
 (NASA-CR-174761; NAS 1.26:174761) Avail: NTIS HC A05/MF A01 CSCL 21D

A proton and carbon-13 nuclear magnetic resonance (NMR) study was conducted of Ashland shale oil refinery products, experimental referee broadened-specification jet fuels, and of related isoprenoid model compounds. Supercritical fluid chromatography techniques using carbon dioxide were developed on a preparative scale, so that samples could be quantitatively separated into saturates and aromatic fractions for study by NMR. An optimized average parameter treatment was developed, and the NMR results were analyzed in terms of the resulting average parameters; formulation of model mixtures was demonstrated. Application of novel spectroscopic techniques to fuel samples was investigated. Author

**N84-33608\*#** National Aeronautics and Space Administration. Lewis Research Center, Cleveland, Ohio.  
**FTIR ANALYSIS OF AVIATION FUEL DEPOSITS**  
 L. S. HELMICK and G. T. SENG Sep. 1984 31 p refs  
 (NASA-TM-83773; E-2200; NAS 1.15:83773) Avail: NTIS HC A03/MF A01 CSCL 07D

Five modes of operation of the Nicolet 7199 Fourier Transform Infrared Spectrophotometer have been evaluated for application in analysis of the chemical structure of accelerated storage/thermal deposits produced by jet fuels. Using primarily the absorption and emission modes, the effects of fuel type, stress temperature, stress time, type of spiking agent, spiking agent concentration, fuel flow, and post-depositional treatment on the chemical nature of fuel deposits have been determined. Author

## ENGINEERING (GENERAL)

Includes vacuum technology; control engineering; display engineering; and cryogenics.

**A84-46965\*#** National Aeronautics and Space Administration. Lewis Research Center, Cleveland, Ohio.  
**COMPARISONS OF RATIONAL ENGINEERING CORRELATIONS OF THERMOPHORETICALLY-AUGMENTED PARTICLE MASS TRANSFER WITH STAN5-PREDICTIONS FOR DEVELOPING BOUNDARY LAYERS**  
 S. A. GOKOGLU (NASA, Lewis Research Center, Cleveland, OH) and D. E. ROSNER (Yale University, New Haven, CT) American Society of Mechanical Engineers, International Gas Turbine Conference and Exhibit, 29th, Amsterdam, Netherlands, June 4-7, 1984. 8 p. Previously announced in STAR as N84-19606. refs  
 (Contract NAS3-23293; NAG3-201)  
 (ASME PAPER 84-GT-158)

Modification of the code STAN5 to properly include thermophoretic mass transport, and examination of selected test cases developing boundary layers which include variable properties, viscous dissipation, transition to turbulence and transpiration cooling. Under conditions representative of current and projected GT operation, local application of  $St(M)/St(M)_o$  correlations evidently provides accurate and economical engineering design predictions, especially for suspended particles characterized by Schmidt numbers outside of the heavy vapor range. Author

**N84-16380\*#** National Aeronautics and Space Administration. Lewis Research Center, Cleveland, Ohio.  
**CHARACTERISTIC MORPHOLOGICAL AND FRICTIONAL CHANGES IN SPUTTERED MOS/SUB 2 FILMS**  
 T. SPALVINS 1984 16 p To be presented at the Intern. Solid Lubricants Conf., Denver, 6-9 Aug. 1984  
 (NASA-TM-83565; NAS 1.15:83565; E-1876) Avail: NTIS HC A02/MF A01 CSCL 20L

Three microstructural growth stages of sputtered MoS<sub>2</sub> films were identified with respect to film thickness: (1) ridge formation during nucleation, (2) an equiaxed transition zone, and (3) a columnar-fiber-like structure. Each of these growth stages are characterized in terms of microcrystallite size, shape, and orientation. The effective lubricating film thickness is established in terms of the microstructural growth stages during sliding experiments. The film has a tendency to break up within the columnar zone. Actual lubrication is performed by the remaining film which is 0.18 to 0.22 microns thick. Also a visual screening is proposed to evaluate the integrity of the as-sputtered MoS<sub>2</sub> film. The lubricating properties are identified with respect to optical changes before and after wiping. The orientation of the microcrystallites are responsible for the optical reflective changes observed. Author

**N84-16381\*#** Martin Marietta Aerospace, Denver, Colo.  
**CRYOGENIC FLUID MANAGEMENT EXPERIMENT (CFME) TRUNNION VERIFICATION TESTING** Final Report, Nov. 1981 - Sep. 1983  
 W. J. BAILEY and D. A. FESTER Dec. 1983 107 p refs  
 (Contract NAS3-23245)  
 (NASA-CR-168310; NAS 1.26:168310; MCR-83-624) Avail: NTIS HC A06/MF A01 CSCL 20L

The Cryogenic Fluid Management Experiment (CFME) was designed to characterize subcritical liquid hydrogen storage and expulsion in the low-g space environment. The CFME has now become the storage and supply tank for the Cryogenic Fluid Management Facility, which includes transfer line and receiver tanks, as well. The liquid hydrogen storage and supply vessel is supported within a vacuum jacket to two fiberglass/epoxy composite trunnions which were analyzed and designed. Analysis using the limited available data indicated the trunnion was the

C-2



most fatigue critical component in the storage vessel. Before committing the complete storage tank assembly to environmental testing, an experimental assessment was performed to verify the capability of the trunnion design to withstand expected vibration and loading conditions. Three tasks were conducted to evaluate trunnion integrity. The first determined the fatigue properties of the trunnion composite laminate materials. Tests at both ambient and liquid hydrogen temperatures showed composite material fatigue properties far in excess of those expected. Next, an assessment of the adequacy of the trunnion designs was performed (based on the tested material properties). S.L.

**N84-19606\*#** Yale Univ., New Haven, Conn. Dept. of Chemical Engineering.

**COMPARISONS OF RATIONAL ENGINEERING CORRELATIONS OF THERMOPHORETICALLY-AUGMENTED PARTICLE MASS TRANSFER WITH STAN5-PREDICTIONS FOR DEVELOPING BOUNDARY LAYERS Final Report**

S. A. GOEKOGLU (Analex Corp.) and D. E. ROSNER Jan 1984 17 p refs To be presented at the 29th Intern. Gas Turbine Conf., Amsterdam, 3-7 Jun. 1984

(Contract NAS3-23293; NAG3-201)

(NASA-CR-168221; E-1991; NAS 1.26:168221) Avail: NTIS HC A02/MF A01 CSCL 21E

Modification of the code STAN5 to properly include thermophoretic mass transport, and examination of selected test cases developing boundary layers which include variable properties, viscous dissipation, transition to turbulence and transpiration cooling. Under conditions representative of current and projected GT operation, local application of  $St(M)/St(M)_0$  correlations evidently provides accurate and economical engineering design predictions, especially for suspended particles characterized by Schmidt numbers outside of the heavy vapor range. Author

**N84-22771\*#** National Aeronautics and Space Administration. Lewis Research Center, Cleveland, Ohio.

**AERONAUTICS AND SPACE ENGINEERING BOARD: AERONAUTICS ASSESSMENT COMMITTEE**

1977 263 p refs Meeting held 16-17 Mar. 1977

(NASA-TM-85594; NAS 1.15:85594) Avail: NTIS HC A12/MF A01 CSCL 13B

High temperature engine materials, fatigue and fracture life prediction, composite materials, propulsion noise pollution, propulsion components, full-scale engine research, V/STOL propulsion, advanced engine concepts, and advanced general aviation propulsion research were discussed B.G.

## 32

### COMMUNICATIONS

Includes land and global communications; communications theory; and optical communications.

**A84-15626\*#** National Aeronautics and Space Administration. Lewis Research Center, Cleveland, Ohio.

**CONCEPT FOR ADVANCED SATELLITE COMMUNICATIONS AND REQUIRED TECHNOLOGIES**

J. R. RAMLER and J. A. SALZMAN (NASA, Lewis Research Center, Cleveland, OH) IN: NTC '82; National Telesystems Conference, Galveston, TX, November 7-10, 1982, Conference Record. New York, Institute of Electrical and Electronics Engineers, Inc., 1982, p. A2.1.1-A2.1.5.

The advanced communications technology satellite (ACTS) program of NASA is aimed at the development of high risk technologies that will enable exploiting higher frequency bands and techniques for improving frequency reuse. The technologies under development include multiple beam spacecraft antennas, on-board switching and processing, RF devices and components and advanced earth stations. The program focus is on the Ka-band

(30/20 GHz) as the implementing frequency since it has five times the bandwidth of either the C- or Ku-bands. However, the technology being developed is applicable to other frequency bands as well and will support a wide range of future communications systems required by NASA, other Government agencies and the commercial sector. An overview is presented of an operational 30/20 GHz satellite system that may evolve. How the system addresses service requirements is discussed, and the technology required and being developed is considered. Previously announced in STAR as N83-11210 A.R.H.

**A84-15627\* Ford Aerospace and Communications Corp., Palo Alto, Calif.**

**MULTIBEAM ANTENNA FOR 30/20 GHZ ADVANCED COMMUNICATIONS SATELLITE USING OFFSET SHAPED, DUAL REFLECTOR SURFACES**

A. E. SMOLL and H. S. LUH (Ford Aerospace and Communications Corp., Palo Alto, CA) IN: NTC '82; National Telesystems Conference, Galveston, TX, November 7-10, 1982, Conference Record. New York, Institute of Electrical and Electronics Engineers, Inc., 1982, p. A2.2.1-A2.2.4.

(Contract NAS3-22498)

Progress in the Antenna Technology Study being performed by NASA to characterize an antenna system with a scanning beam with a half-power beam diameter of around 0.3 deg and a minimum width over which the sidelobes stay below the -30 dB level is reported. Continuous U.S. (CONUS) coverage is desired by the satellite antenna system, with 10-20 fixed beams for trunk coverage and a rapidly scanned narrow beam for customer premises. The design specifies 24 beamwidths from east to west and 10 beamwidths from south to north. Reflector parameters have been identified to optimally focus all beams from a planar feed array. An example of coverage expected with the design demonstrates optimized beams for Seattle, Oklahoma City, and Miami, with -3 dB contours in circles 0.25 deg in diameter and a peak directivity of 55 dB. Experimental work was scheduled for 1983. M.S.K.

**A84-15628\* Motorola, Inc., Scottsdale, Ariz.**

**BASEBAND PROCESSOR DEVELOPMENT FOR THE ADVANCED COMMUNICATIONS SATELLITE PROGRAM**

D. MOAT, D. SABOURIN, J. STILWELL, R. MCCALLISTER, and M. BOROTA (Motorola, Inc., Government Electronics Group, Scottsdale, AZ) IN: NTC '82; National Telesystems Conference, Galveston, TX, November 7-10, 1982, Conference Record. New York, Institute of Electrical and Electronics Engineers, Inc., 1982, p. A2.4.1-A2.4.6. refs

(Contract NAS3-22502)

An onboard-baseband-processor concept for a satellite-switched time-division-multiple-access (SS-TDMA) communication system was developed for NASA Lewis Research Center. The baseband processor routes and controls traffic on an individual message basis while providing significant advantages in improved link margins and system flexibility. Key technology developments required to prove the flight readiness of the baseband-processor design are being verified in a baseband-processor proof-of-concept model. These technology developments include serial MSK modems, Clos-type baseband routing switch, a single-chip CMOS maximum-likelihood convolutional decoder, and custom LSL implementation of high-speed, low-power ECL building blocks. Author

**A84-15629\***

**SERIAL MSK MODEM FOR THE ADVANCED COMMUNICATIONS SATELLITE PROGRAM**

J. H. STILWELL (Motorola, Inc., Government Electronics Group, Gilbert, AZ) IN: NTC '82; National Telesystems Conference, Galveston, TX, November 7-10, 1982, Conference Record. New York, Institute of Electrical and Electronics Engineers, Inc., 1982, p. A2.5.1-A2.5.5. refs

(Contract NAS3-22502)

The design and test results of the 550-Mb/s, 110-Mb/s, and 27.5-Mb/s modems for the Advanced Communication Satellite Program are described. The TDMA/FDMA satellite environmental



constraints have resulted in several unique features which include total acquisition times of 100 bit times and modem degradation of less than 1.5 dB at 10 to the -6th Po. Key to the serial implementation of MSK is the resulting hardware simplicity and degradation insensitivity relative to conventionally implemented MSK and QPSK modems. The 110/27.5-Mb/s modems use an integrated circuit specifically developed for the program to perform the key carrier and clock-loop functions. Author

**A84-22141\*#** Mitre Corp., Bedford, Mass.

**A FREQUENCY-DIVISION MULTIPLE-ACCESS SYSTEM CONCEPT FOR 30/20 GHZ HIGH-CAPACITY DOMESTIC SATELLITE SERVICE**

G. BERK, P. N. JEAN, E. ROTHOLZ, and B. E. WHITE (Mitre Corp., Bedford, MA) IN: Communication Satellite Systems Conference, 9th, San Diego, CA, March 7-11, 1982, Collection of Technical Papers, p. 65-71) Journal of Spacecraft and Rockets (ISSN 0022-4650), vol. 20, Nov.-Dec. 1983, p. 619-625. refs (Contract NASA ORDER C-49029-D)

Previously cited in issue 09, p. 1357, Accession no. A82-23484

**A84-25256\*#** Ford Aerospace and Communications Corp., Palo Alto, Calif.

**A NEW MULTIPLE BEAM SATELLITE ANTENNA FOR 30/20 GHZ COMMUNICATIONS . COVERAGE OF CONUS-EXPERIMENTAL EVALUATION**

A. E. SMOLL, T. E. ROBERTS, E. W. MATTHEWS, E. A. LEE, and C. C. HAN (Ford Aerospace and Communications Corp., Palo Alto, CA) IN: Communication Satellite Systems Conference, 10th, Orlando, FL, March 19-22, 1984, Technical Papers . New York, American Institute of Aeronautics and Astronautics, 1984, p. 33-42.

(Contract NAS3-22498)

(AIAA PAPER 84-0655)

Additional frequency bands are needed to satisfy requirements related to the rapid growth of satellite communications, and the utilization of the 30/20 GHz frequencies is being considered. The present investigation is concerned with the experimental verification phase of an antenna technology study sponsored by NASA. The feasibility of narrow (0.3 degree) directive beam scanning over the entire continental U.S. (CONUS) from a single antenna at 30/20 GHz is demonstrated. The POC (Proof-of-Concept) model is based on an employment of an offset shaped dual reflector optics. The main reflector and the subreflector are both fabricated from aluminum. Attention is given to feed array and beam-forming network, multiple beam antenna range tests, an analysis, and test results. G.R.

**A84-25257\*#** National Aeronautics and Space Administration, Lewis Research Center, Cleveland, Ohio.

**MICROWAVE MONOLITHIC INTEGRATED CIRCUIT DEVELOPMENT FOR FUTURE SPACEBORNE PHASED ARRAY ANTENNAS**

G. ANZIC, T. J. KASCAK, A. N. DOWNEY, D. C. LIU, and D. J. CONNOLLY (NASA, Lewis Research Center, Cleveland, OH) IN: Communication Satellite Systems Conference, 10th, Orlando, FL, March 19-22, 1984, Technical Papers . New York, American Institute of Aeronautics and Astronautics, 1984, p. 43-53. refs (AIAA PAPER 84-0656)

The development of fully monolithic gallium arsenide (GaAs) receive and transmit modules suitable for phased array antenna applications in the 30/20 gigahertz bands is presented. Specifications and various design approaches to achieve the design goals are described. Initial design and performance of submodules and associated active and passive components are presented. A tradeoff study summary is presented, highlighting the advantages of a distributed amplifier approach compared to the conventional single power source designs. Previously announced in STAR as N84-13399 Author

**A84-25272\*#** National Aeronautics and Space Administration, Lewis Research Center, Cleveland, Ohio.

**A SYSTEM FOR THE SIMULATION AND EVALUATION OF SATELLITE COMMUNICATION NETWORKS**

J. W. BAGWELL (NASA, Lewis Research Center, Cleveland, OH) IN: Communication Satellite Systems Conference, 10th, Orlando, FL, March 19-22, 1984, Technical Papers . New York, American Institute of Aeronautics and Astronautics, 1984, p. 172-180. refs (AIAA PAPER 84-0680)

With the emergence of a new era in satellite communications, brought about by NASA's thrust into the Ka band with multibeam and onboard processing technologies, new and innovative techniques for evaluating these concepts and systems are required. To this end, NASA, in conjunction with its extensive program for advanced communications technology development, has undertaken to develop a concept for the simulation and evaluation of a complete communications network. Incorporated in this network will be proof-of-concept models of the latest technologies proposed for future satellite communications systems. These include low noise receivers, matrix switches, baseband processors, and solid state and tube type high power amplifiers. To accomplish this, numerous supporting technologies must be added to those aforementioned proof-of-concept models. These include controllers for synchronization, order wire, resource allocation, gain compensation, signal leveling, power augmentation, and rain fade and range delay simulation. Taken together, these will be assembled to comprise a system capable of addressing numerous design and performance questions. The simulation and evaluation system, as planned, will be modular in design and implementation, capable of modification and updating to track and evaluate a continuum of emerging concepts and technologies. Previously announced in STAR as N84-13400 Author

**A84-25274\*#** Communications Satellite Corp., Clarksburg, Md.

**ACTS TDMA NETWORK CONTROL**

T. INUKAI and S. J. CAMPANELLA (COMSAT Laboratories, Clarksburg, MD) IN: Communication Satellite Systems Conference, 10th, Orlando, FL, March 19-22, 1984, Technical Papers . New York, American Institute of Aeronautics and Astronautics, 1984, p. 188-195. Research sponsored by the Communications Satellite Corp. refs

(Contract NAS3-22905)

(AIAA PAPER 84-0682)

This paper presents basic network control concepts for the Advanced Communications Technology Satellite (ACTS) System. Two experimental systems, called the low-burst-rate and high-burst-rate systems, along with ACTS ground system features, are described. The network control issues addressed include frame structures, acquisition and synchronization procedures, coordinated station burst-time plan and satellite-time plan changes, on-board clock control based on ground drift measurements, rain fade control by means of adaptive forward-error-correction (FEC) coding and transmit power augmentation, and reassignment of channel capacities on demand. The NASA ground system, which includes a primary station, diversity station, and master control station, is also described. Author

**A84-25299\*#** National Aeronautics and Space Administration, Lewis Research Center, Cleveland, Ohio.

**ECONOMIC COMPARISON OF FDMA AND TDMA OPTIONS FOR COMMUNICATIONS BY KA-BAND MULTIPLE BEAM SATELLITES**

G. H. STEVENS (NASA, Lewis Research Center, Cleveland, OH) IN: Communication Satellite Systems Conference, 10th, Orlando, FL, March 19-22, 1984, Technical Papers . New York, American Institute of Aeronautics and Astronautics, 1984, p. 395-403. refs (AIAA PAPER 84-0740)

An assessment is made of the feasibility of providing low data rate service to small earth stations by satellite at Ka-band. Technological as well as economic factors are considered. The results of NASA-sponsored contractual studies are compared and results of internal NASA studies are presented. Several FDMA and TDMA scenarios are critically examined with the objective of

establishing the relative utility of such systems to end users. It is shown that FDMA has no advantage over TDMA in a multibeam scenario for 56 Kbs of data by voice, video, or the equivalent. For the same assumptions, significant weight and power advantages are realized in the space segment using TDMA.

C.D.

**A84-25324\*** National Aeronautics and Space Administration. Lewis Research Center, Cleveland, Ohio.

**RURAL LAND MOBILE RADIO MARKET ASSESSMENT AND SATELLITE AND TERRESTRIAL SYSTEM CONCEPTS**

S. STEVENSON and C. PROVENCHER (NASA, Lewis Research Center, Cleveland, OH) IN: Communication Satellite Systems Conference, 10th, Orlando, FL, March 19-22, 1984, Technical Papers. New York, American Institute of Aeronautics and Astronautics, 1984, p. 595-604.

(AIAA PAPER 84-0754)

The market for satellite-based mobile radio in the rural U.S. is evaluated, summarizing the results of two NASA-funded studies reported by Anderson et al. and Hornstein. The study aims are listed, and the results are presented in tables, graphs, and maps and discussed. Space systems are found to be competitive with land-based systems, providing superior service at lower subscriber charges, but having limited compatibility with urban cellular mobile-radio systems. Of the three system concepts evaluated from a technological standpoint (direct-to-mobile, mobile-translator, and hybrid), the mobile-translator concept is considered most cost effective, at least within the constraints assumed in the study.

D.G.

**A84-25326\*** National Aeronautics and Space Administration. Lewis Research Center, Cleveland, Ohio.

**NASA'S GEOSTATIONARY COMMUNICATIONS PLATFORM PROGRAM**

J. RAMLER (NASA, Lewis Research Center, Cleveland, OH) and R. DURRETT (NASA, Marshall Space Flight Center, Huntsville, AL) IN: Communication Satellite Systems Conference, 10th, Orlando, FL, March 19-22, 1984, Technical Papers. New York, American Institute of Aeronautics and Astronautics, 1984, p. 613-621. refs

(AIAA PAPER 84-0702)

This paper reviews recent trends in communications satellites and explains NASA's current interest in geostationary communications platforms. Large communications platforms capable of supporting multiple payloads with common utilities have been examined in a number of studies since 1974 and appear to offer a number of potential advantages. In 1981, an Industry Briefing and Workshop sponsored by NASA focused on the institutional, operational and technical issues that will influence the implementation of geostationary platforms. The workshop identified numerous issues and problem areas that needed more detailed study. To address the issues/problems identified, a NASA geostationary communications platform program has been developed. This program is described, focusing on the initial studies to be performed.

Author

**A84-39251\*** Motorola, Inc., Scottsdale, Ariz.

**30/20 GHZ COMMUNICATIONS SYSTEMS BASEBAND PROCESSOR DEVELOPMENT**

L. BROWN, D. SABOURIN, J. STILWELL, R. MCCALLISTER, and M. BOROTA (Motorola, Inc., Aerospace Payload Section, Scottsdale, AZ) IN: International Symposium on Space Technology and Science, 13th, Tokyo, Japan, June 28-July 3, 1982, Proceedings. Tokyo, AGNE Publishing, Inc., 1982, p. 923-929. refs

(Contract NAS3-22502)

The architecture and system design concepts for a commercial satellite communications system planned for the 1990's has been developed. The system provides data communications between the individual users via trunking and customer premise service terminals utilizing a central switching satellite operating in a time-division multiple-access mode. Baseband processing is employed to route and control traffic on an individual message

basis while providing significant advantages in improved link margins and system flexibility. Key technology developments required to prove the flight readiness of the baseband processor design are being verified in the baseband processor proof-of-concept model described herein.

Author

**A84-48452\*** Cleveland State Univ., Ohio.

**THE EFFECT OF VARIABLE S/N ON THE SUBJECTIVE EVALUATION OF PROTECTION RATIOS FOR DIRECT-TV SATELLITE SERVICES**

P. P. GROUMPOS, B. D. DIMITRIADIS (Cleveland State University, Cleveland, OH), and W. WHYTE (NASA, Lewis Research Center, Space Communications Div., Cleveland, OH) IN: Canadian Domestic and International Satellite Communications Conference, 1st, Ottawa, Canada, June 14-17, 1983, Proceedings. Amsterdam and New York, North Holland Publishing Co., 1984, p. 15.4.1-15.4.4. refs

(Contract NAG3-156)

Protection ratios, the ratio of wanted-to-unwanted signal power at the receiver input, for acceptable picture quality were experimentally evaluated for four different still pictures. The variation of carrier-to-interference, C/I, with picture impairment grade is investigated when different noise levels are present. Results are presented which show the relationship between the impairment grade and the C/I ratio for FM/TV co-channel systems under variable S/N conditions.

Author

**A84-49259\*** Toledo Univ., Ohio.

**NTSC COMPOSITE VIDEO AT 1.6 BITS/PEL**

S. C. KWATRA and H. FATMI (Toledo, University, Toledo, OH) IN: ICC '83 - Integrating communication for world progress; International Conference on Communications, Boston, MA, June 19-22, 1983, Conference Record. Volume 1. New York, Institute of Electrical and Electronics Engineers, 1983, p. 458-462. refs

(Contract NAG3-42)

An adaptive algorithm for intraframe compression of NTSC composite color video signal is described. With an average of 80 percent compression (1.6 bits/pixel) and a bit error rate of 0.0001, excellent broadcast quality pictures were obtained. This is confirmed by a subjective evaluation of processed pictures by five viewers. The algorithm and the results of the subjective evaluation are given in this paper.

Author

**A84-49303\*** Stanford Univ., Calif.

**INTERFERENCE PERFORMANCE ANALYSIS OF M-ARY CPSK AND M-ARY CAPK DIGITAL TRANSMISSION SYSTEMS AND THE COMPUTATION OF 'REQUIRED ISOLATION' FOR EFFICIENT UTILIZATION OF GEOSTATIONARY SATELLITE ORBIT/SPECTRUM**

R. CHEN and B. B. LUSIGNAN (Stanford University, Stanford, CA) IN: ICC '83 - Integrating communication for world progress; International Conference on Communications, Boston, MA, June 19-22, 1983, Conference Record. Volume 3. New York, Institute of Electrical and Electronics Engineers, 1983, p. 1426-1430. refs

(Contract NAS3-151)

**N84-10401\*** City Coll. of the City Univ. of New York. Communications Systems Lab.

**COMPUTER SIMULATOR FOR A MOBILE TELEPHONE SYSTEM Final Report, 21 Apr. 1982 - 19 Apr. 1983**

D. L. SCHILLING and C. ZIEGLER 1983 96 p

(Contract NAG3-277)

(NASA-CR-174533; NAS 1.26:174533) Avail. NTIS HC A05/MF A01 CSCL 17B

A software simulator to help NASA in the design of the LMSS was developed. The simulator will be used to study the characteristics of implementation requirements of the LMSS's configuration with specifications as outlined by NASA.

Author

**N84-10402\*#** General Electric Co., Schenectady, N. Y. Corporate Research and Development.

**MOBILE RADIO ALTERNATIVE SYSTEMS STUDY. VOLUME 1: TRAFFIC MODEL**

W. T. TUCKER and R. E. ANDERSON Jun. 1983 60 p refs (Contract NAS3-23244)

(NASA-CR-168062; NAS 1.26:168062; GE-CRD-83-SRD-037)

Avail: NTIS HC A04/MF A01 CSCL 17B

The markets for mobile radio services in non-urban areas of the United States are examined for the years 1985-2000. Three market categories are identified. New Services are defined as those for which there are different expressed ideas but which are not now met by any application of available technology. The complete fulfillment of the needs requires nationwide radio access to vehicles without knowledge of vehicle location, wideband data transmission from remote sites, one- and two way exchange of short data and control messages between vehicles and dispatch or control centers, and automatic vehicle location (surveillance). The commercial and public services market of interest to the study is drawn from existing users of mobile radio in non-urban areas who are dissatisfied with the geographical range or coverage of their systems. The mobile radio telephone market comprises potential users who require access to the public switched telephone network in areas that are not likely to be served by the traditional growth patterns of terrestrial mobile telephone services. Conservative, likely, and optimistic estimates of the markets are presented in terms of numbers of vehicles that will be served and the radio traffic they will generate. Author

**N84-10403\*#** General Electric Co., Schenectady, N. Y. Corporate Research and Development.

**MOBILE RADIO ALTERNATIVE SYSTEMS STUDY. VOLUME 2: TERRESTRIAL**

N. CROMWELL, H. L. LESTER, and R. E. ANDERSON Jun. 1983 76 p refs

(Contract NAS3-23244)

(NASA-CR-168063; NAS 1.26:168063; GEC-CRD-83-SRD-038)

Avail: NTIS HC A05/MF A01 CSCL 17B

Terrestrial systems for satisfying the markets for mobile radio services in non-urban areas of the United States in the years from 1985 to 2000 were investigated. Present day mobile communication technologies, systems and equipment are described for background in evaluating the concepts generated. Average propagation ranges are calculated for terrestrial installations in each of seven physiographic areas of the contiguous states to determine the number of installations that would be required for nationwide coverage. Four system concepts are defined and analyzed to determine how well terrestrial systems can fulfill the requirements at acceptable costs. Nationwide dispatch, telephone and data services would require terrestrial installations in many locations where they would be used infrequently and would not recover their investment. Access to a roaming vehicle requires that the vehicle location be known within the range limit of the terrestrial installation in which the vehicle is present at the time of the call. Access to that installation must be made through the public switched telephone network, usually involving a long-distance toll charge, and requiring costly means to track or locate the vehicle as it moved through the network of installations. A.R.H.

**N84-10404\*#** General Electric Co., Schenectady, N. Y. Corporate Research Development.

**MOBILE RADIO ALTERNATIVE SYSTEMS STUDY SATELLITE/TERRESTRIAL (HYBRID) SYSTEMS CONCEPTS**

J. D. KIESLING (General Electric Co., Philadelphia) and R. E. ANDERSON Jun. 1983 273 p refs

(Contract NAS3-23244)

(NASA-CR-168064; NAS 1.26:168064; GEC-CRD-83-SRD-039)

Avail: NTIS HC A12/MF A01 CSCL 17B

The use of satellites for mobile radio service in non-urban areas of the United States in the years from 1985 to 2000 was investigated. Several satellite concepts are considered: a system with single-beam coverage of the fifty United States and Puerto Rico, and multi-beam satellites with greater capacity. All of the

needed functions and services identified in the market study are provided by the satellite systems, including nationwide radio access to vehicles without knowledge of vehicle location wideband data transmission from remote sites, two way exchange of short data and control messages between vehicles and dispatch or control centers, and automatic vehicle location (surveillance). The costs of providing the services are within acceptable limits, and the desired returns to the system investors are attractive. The criteria by which the Federal Communication judges the competing demands for public radio spectrum are reviewed with comments on how the criteria might apply to the consideration of land mobile satellites. Institutional arrangements for operating a mobile satellite system are based on the present institutional arrangements in which the services are offered to the end users through wireline and radio common carriers, with direct access by large private and government users. Author

**N84-10405\*#** National Aeronautics and Space Administration. Lewis Research Center, Cleveland, Ohio.

**A COMPARISON OF THE DOMESTIC SATELLITE COMMUNICATIONS FORECAST TO THE YEAR 2000**

W. A. POLEY, J. F. LEKAN, J. A. SALZMAN, and S. M. STEVENSON Oct. 1983 33 p refs

(NASA-TM-83516; E-1859; NAS 1.15:83516) Avail: NTIS HC

A03/MF A01 CSCL 17B

The methodologies and results of three NASA-sponsored market demand assessment studies are presented and compared. Forecasts of future satellite addressable traffic (both trunking and customer premises services) were developed for the three main service categories of voice, data and video and subcategories thereof for the benchmark years of 1980, 1990 and 2000. The contractor results are presented on a service by service basis in two formats: equivalent 36 MHz transponders and basic transmission units (voice: half-voice circuits, data: megabits per second and video: video channels). It is shown that while considerable differences exist at the service category level, the overall forecasts by the two contractors are quite similar. ITT estimates the total potential satellite market to be 3594 transponders in the year 2000 with data service comprising 54 percent of this total. The WU outlook for the same time period is 2779 transponders with voice services accounting for 66 percent of the total. Author

**N84-11358\*#** National Aeronautics and Space Administration. Lewis Research Center, Cleveland, Ohio.

**GEOMETRIC MODELS, ANTENNA GAINS, AND PROTECTION RATIOS AS DEVELOPED FOR BC SAT-R2 CONFERENCE SOFTWARE**

E. F. MILLER 1982 16 p refs Presented at the BC SAT-R2 Seminar, Lima, 18-22 Apr. 1983; sponsored by the Intern. Frequency Registration Board

(NASA-TM-83381; E-1655; NAS 1.15:83381) Avail: NTIS HC

A02/MF A01 CSCL 20N

Mathematical models used in the software package developed for use at the 1983 Regional Administrative Radio Conference on broadcasting satellites. The models described are those used in the Spectrum Orbit Utilization Program (SOUP) analysis. The geometric relationships necessary to model broadcasting satellite systems are discussed. Antenna models represent copolarized and cross polarized performance as functions of the off axis angle. The protection ratio is modelled as a co-channel value and a template representing systems with frequency offsets. Author

**N84-11360\*#** National Aeronautics and Space Administration. Lewis Research Center, Cleveland, Ohio.

**THE SUBJECTIVE EFFECT OF MULTIPLE CO-CHANNEL FREQUENCY MODULATED TELEVISION INTERFERENCE**

W. A. WHYTE, JR., M. A. CAULEY (Cleveland State Univ.), and P. P. GROOMPOS (Cleveland State Univ.) Nov. 1983 14 p refs Presented at the GLOBECOM IEEE Telecommun. Conf., San Diego, Calif., 29 Nov. - 1 Dec. 1983

(NASA-TM-83415; NAS 1.15:83415; E-1703) Avail. NTIS HC A02/MF A01 CSCL 17B

As the geostationary orbit/spectrum becomes saturated, there is a need for the ability to reuse frequency assignments. Protection ratios (the ratio of wanted signal power to interfering signal power at the receiver) play a key role in determining efficient frequency reuse plans. A knowledge of the manner in which multiple sources of co-channel interference combine is vital in determining protection ratio requirements such that suitable margin may be allocated for multiple interfering signals. Results of tests examining the subjective assessment of multiple co-channel frequency modulated television signals interfering with another frequency modulated TV system are presented. Author

**N84-13398\*#** LNR Communications, Inc., Hauppauge, N. Y. **THE 30 GHZ COMMUNICATIONS SATELLITE LOW NOISE RECEIVER Final Report**

L. J. STEFFEK and D. W. SMITH Oct. 1983 67 p

(Contract NAS3-22494)

(NASA-CR-168254; NAS 1.26:168254; LNR-400) Avail. NTIS HC A04/MF A01 CSCL 17B

A Ka-band low noise front end in proof of concept (POC) model form for ultimate spaceborne communications receiver deployment was developed. The low noise receiver consists of a 27.5 to 30.0 GHz image enhanced mixer integrated with a 3.7 to 6.2 GHz FET low noise IF amplifier and driven by a self contained 23.8 GHz phase locked local oscillator source. The measured level of receiver performance over the 27.3 to 30.0 GHz RF/3.7 to 6.2 GHz IF band includes 5.5 to 6.5 dB (typ) SSB noise figure, 20.5 + or - 1.5 dB conversion gain and +23 dBm minimum third order two tone intermodulation output intercept point. M.G.

**N84-13399\*#** National Aeronautics and Space Administration. Lewis Research Center, Cleveland, Ohio.

**MICROWAVE MONOLITHIC INTEGRATED CIRCUIT DEVELOPMENT FOR FUTURE SPACEBORNE PHASED ARRAY ANTENNAS**

G. ANZIC, T. J. KASCAK, A. N. DOWNEY, D. C. LIU, and D. J. CONNOLLY Dec 1983 20 p refs To be presented at the 10th Ann. Commun. Satellite System Conf., Orlando, Fla., 18-22 Mar. 1984

(NASA-TM-83518; NAS 1.15:83518; E-1867) Avail. NTIS HC A02/MF A01 CSCL 17B

The development of fully monolithic gallium arsenide (GaAs) receive and transmit modules suitable for phased array antenna applications in the 30/20 gigahertz bands is presented. Specifications and various design approaches to achieve the design goals are described. Initial design and performance of submodules and associated active and passive components are presented. A tradeoff study summary is presented highlighting the advantages of distributed amplifier approach compared to the conventional single power source designs. Author

**N84-13400\*#** National Aeronautics and Space Administration. Lewis Research Center, Cleveland, Ohio.

**A SYSTEM FOR THE SIMULATION AND EVALUATION OF SATELLITE COMMUNICATION NETWORKS**

J. W. BAGWELL Dec. 1983 15 p refs To be presented at the 10th Commun. Satellite Systems Conf., Orlando, Fla., 18-22 Mar. 1984

(NASA-TM-83531; NAS 1.15:83531; E-1897) Avail. NTIS HC A02/MF A01 CSCL 17B

With the emergence of a new era in satellite communications brought about by NASA's thrust into the Ka band with multibeam and onboard processing technologies, new and innovative

techniques for evaluating these concepts and systems are required. To this end, NASA, in conjunction with its extensive program for advanced communications technology development, has undertaken to develop a concept for the simulation and evaluation of a complete communications network. Incorporated in this network will be proof of concept models of the latest technologies proposed for future satellite communications systems. These include low noise receivers, matrix switches, baseband processors, and solid state and tube type high power amplifiers. To accomplish this, numerous supporting technologies must be added to those aforementioned proof of concept models. These include controllers for synchronization, order wire, and resource allocation, gain compensation, signal leveling, power augmentation, and rain fade and range delay simulation. Taken together, these will be assembled to comprise a system capable of addressing numerous design and performance questions. The simulation and evaluation system as planned will be modular in design and implementation, capable of modification and updating to track and evaluate a continuum emerging concepts and technologies. Author

**N84-14376\*#** Sonalysts, Inc., Waterford, Conn. **COMMUNICATIONS NETWORK DESIGN AND COSTING MODEL TECHNICAL MANUAL Final Report**

K. P. LOGAN, S. S. SOMES, and C. A. CLARK 30 Sep. 1983 130 p refs

(Contract NAS3-23348)

(NASA-CR-168236; NAS 1.26:168236) Avail. NTIS HC A07/MF A01 CSCL 17B

This computer model provides the capability for analyzing long-haul trunking networks comprising a set of user-defined cities, traffic conditions, and tariff rates. Networks may consist of all terrestrial connectivity, all satellite connectivity, or a combination of terrestrial and satellite connectivity. Network solutions provide the least-cost routes between all cities, the least-cost network routing configuration, and terrestrial and satellite service cost totals. The CNDC model allows analyses involving three specific FCC-approved tariffs, which are uniquely structured and representative of most existing service connectivity and pricing philosophies. User-defined tariffs that can be variations of these three tariffs are accepted as input to the model and allow considerable flexibility in network problem specification. The resulting model extends the domain of network analysis from traditional fixed link cost (distance-sensitive) problems to more complex problems involving combinations of distance and traffic-sensitive tariffs. A.R.H.

**N84-14377\*#** Sonalysts, Inc., Waterford, Conn.

**COMMUNICATIONS NETWORK DESIGN AND COSTING MODEL PROGRAMMERS MANUAL Final Report**

K. P. LOGAN, S. S. SOMES, and C. A. CLARK 30 Sep. 1983 403 p

(Contract NAS3-23348)

(NASA-CR-168237; NAS 1.26:168237) Avail. NTIS HC A18/MF A01 CSCL 17B

Optimization algorithms and techniques used in the communications network design and costing model for least cost route and least cost network problems are examined from the programmer's point of view. All system program modules, the data structures within the model, and the files which make up the data base are described. A.R.H.

**N84-14378\*#** Sonalysts, Inc., Waterford, Conn. Space Communications Div.

**COMMUNICATIONS NETWORK DESIGN AND COSTING MODEL USERS MANUAL Final Report**

K. P. LOGAN, S. S. SOMES, and C. A. CLARK 30 Sep. 1983 158 p

(Contract NAS3-23348)

(NASA-CR-168238; NAS 1.26:168238) Avail. NTIS HC A08/MF A01 CSCL 17B

The information and procedures needed to exercise the communications network design and costing model for performing network analysis are presented. Specific procedures are included

## 32 COMMUNICATIONS

for executing the model on the NASA Lewis Research Center IBM 3033 computer. The concepts, functions, and data bases relating to the model are described. Model parameters and their format specifications for running the model are detailed. A.R.H.

**N84-15360\*#** Massachusetts Inst. of Tech., Cambridge. Gas Turbine and Plasma Dynamics Lab.

### **ASYMPTOTIC ANALYSIS OF NUMERICAL WAVE PROPAGATION IN FINITE DIFFERENCE EQUATIONS**

M. GILES and W. T. THOMPSON, JR. Mar. 1983 142 p refs (Contract NAG3-9)

(NASA-CR-175323; NAS 1.26:175323; GT/PDL-171) Avail: NTIS HC A07/MF A01 CSCL 20N

An asymptotic technique is developed for analyzing the propagation and dissipation of wave-like solutions to finite difference equations. It is shown that for each fixed complex frequency there are usually several wave solutions with different wavenumbers and the slowly varying amplitude of each satisfies an asymptotic amplitude equation which includes the effects of smoothly varying coefficients in the finite difference equations. The local group velocity appears in this equation as the velocity of convection of the amplitude. Asymptotic boundary conditions coupling the amplitudes of the different wave solutions are also derived. A wavepacket theory is developed which predicts the motion, and interaction at boundaries, of wavepackets, wave-like disturbances of finite length. Comparison with numerical experiments demonstrates the success and limitations of the theory. Finally an asymptotic global stability analysis is developed.

M.G.

**N84-16423\*#** Communications Satellite Corp., Clarksburg, Md. **PHASED-ARRAY-FED ANTENNA CONFIGURATION STUDY, VOLUME 1: TECHNOLOGY ASSESSMENT**

R. M. SORBELLO, A. I. ZAGHLOUL, B. S. LEE, S. SIDDIQI, B. D. GELLER, H. I. GERSON, and D. N. SRINIVAS Oct. 1983 158 p refs 2 Vol.

(Contract NAS3-23250)

(NASA-CR-168231; NAS 1.26:168231) Avail: NTIS HC A08/MF A01 CSCL 09C

The status of the technologies for phased-array-fed dual reflector systems is reviewed. The different aspects of these technologies, including optical performances, phased array systems, problems encountered in phased array design, beamforming networks, MMIC design and its incorporation into waveguide systems, reflector antenna structures, and reflector deployment mechanisms are addressed.

S.L.

**N84-16424\*#** Communications Satellite Corp., Clarksburg, Md. **PHASED-ARRAY-FED ANTENNA CONFIGURATION STUDY, VOLUME 2 Final Report**

R. M. SORBELLO, A. I. ZAGHLOUL, B. S. LEE, S. SIDDIQI, and B. D. GELLER Oct. 1983 493 p refs 2 Vol.

(Contract NAS3-23250)

(NASA-CR-168232; NAS 1.26:168232) Avail: NTIS HC A21/MF A01 CSCL 09C

Increased capacity in future satellite systems can be achieved through antenna systems which provide multiplicity of frequency reuses at K sub a band. A number of antenna configurations which can provide multiple fixed spot beams and multiple independent spot scanning beams at 20 GHz are addressed. Each design incorporates a phased array with distributed MMIC amplifiers and phase shifters feeding a two reflector optical system. The tradeoffs required for the design of these systems and the corresponding performances are presented. Five final designs are studied. In so doing, a type of MMIC/waveguide transition is described, and measured results of the breadboard model are presented. Other hardware components developed are described. This includes a square orthonode transducer, a subarray fed with a beamforming network to measure scanning performance, and another subarray used to study mutual coupling considerations. Discussions of the advantages and disadvantages of the final design are included.

S.L.

**N84-16425\*#** Analox Corp., Cleveland, Ohio.

### **MODULAR APPROACH FOR SATELLITE COMMUNICATION GROUND TERMINALS. Final Report**

G. R. GOULD Jan 1984 9 p Proposed for presentation at the 10th Commun. Satellite Systems Conf., Orlando, Fla., 18-22 Mar. 1984, sponsored by AIAA

(Contract NAS3-23923)

(NASA-CR-168327; E-1960; NAS 1.26:168327) Avail: NTIS HC A02/MF A01 CSCL 17B

The trend in satellite communications is toward completely digital, time division multiple access (TDMA) systems with uplink and downlink data rates dictated by the type of service offered. Trunking terminals will operate in the 550 MBPS (megabit per second) region uplink and downlink, whereas customer premise service (CPS) terminals will operate in the 25 to 10 MBPS region uplink and in the 200 MBPS region downlink. Additional criteria for the ground terminals will be to maintain clock synchronization with the system and burst time integrity to within a matter of nanoseconds, to process required order-fire information, to provide adaptive data scrambling, and to compensate for variations in the user input output data rates, and for changes in range in the satellite communications links resulting from satellite perturbations in orbit. To achieve the required adaptability of a ground terminal to the above mentioned variables, programmable building blocks can be developed that will meet all of these requirements. To maintain system synchronization, i.e., all burst data arriving at the satellite within assigned TDMA windows, ground terminal transmit data rates and burst timing must be maintained within tight tolerances. With a programmable synchronizer as the heart of the terminal timing generation, variable data rates and burst timing tolerances are achievable. In essence, the unit inputs microprocessor generated timing words and outputs discrete timing pulses.

S.L.

**N84-19620\*#** Illinois Univ., Urbana. Electromagnetics Lab.

### **NUMERICAL METHODS FOR ANALYZING ELECTROMAGNETIC SCATTERING Semiannual Report, 25 Sep. 1983 - 24 Mar. 1984**

Y. T. LO and S. W. LEE 23 Mar. 1984 21 p refs

(Contract NAG3-475)

(NASA-CR-175423; NAS 1.26:175423) Avail: NTIS HC A02/MF A01 CSCL 20N

The wave propagation inside a cylindrical waveguide, coated with lossy dielectric material due to the incidence of a plane wave at the open end of the guide, was studied. The general properties of the normal mode propagation were investigated.

N.W.

**N84-19640\*#** National Aeronautics and Space Administration. Lewis Research Center, Cleveland, Ohio.

### **BROADCASTING SATELLITES AT 12 GHZ FOR REGION 2: TECHNICAL CHARACTERISTICS**

E. F. MILLER Feb. 1984 23 p refs Presented at IEEE's GLOBECOM, San Diego, Calif., 29 Nov. - 1 Dec. 1983

(NASA-TM-83522; E-1834; NAS 1.15:83522) Avail: NTIS HC A02/MF A01 CSCL 17B

Technical parameters such as satellite antenna characteristics, Earth station requirements, bandwidths, channelization, and allowable carrier-to-interference ratios are discussed. An overview of the downlink plan is given, including a histogram of the transmitter power requirements. The plan includes satellite orbit positions, spacecraft transmitted powers, antennas beam sizes, channel assignments, and polarizations.

Author

**N84-19641\*#** National Aeronautics and Space Administration. Lewis Research Center, Cleveland, Ohio.

**RURAL LAND MOBILE RADIO MARKET ASSESSMENT AND SATELLITE AND TERRESTRIAL SYSTEM CONCEPTS**

S. M. STEVENSON and C. E. PROVENCHER 1984 29 p refs Presented at the 10th Communications Satellite Systems Conf., Orlando, Fla., 18-22 Mar. 1984 (NASA-TM-83591; E-1990; NAS 1.15:83591) Avail: NTIS-HC A03/MF A01 CSCL 17B

Market potential exists; the nature of the market in terms of service needs, usage characteristics, service requirements, and forecasting the demand to the year 2000; alternative system concepts that show promise in addressing the identified needs, in a cost effective manner; and advanced technology requirements associated with these concepts are considered. Author

**N84-20737\*#** Honeywell, Inc., Bloomington, Minn. Physical Sciences Center.

**THE 30-GHZ MONOLITHIC RECEIVE MODULE Annual Report, 3 Nov. 1982 - 31 Oct. 1983**

V. SOKOLOV, J. GEDDES, and P. BAUHAHN Dec. 1983 93 p refs

(Contract NAS3-23356) (NASA-CR-168326; NAS 1.26:168326; AR-1) Avail: NTIS HC A05/MF A01 CSCL 17B

Key requirements for a 30 GHz GaAs monolithic receive module for spaceborne communication antenna feed array applications include an overall receive module noise figure of 5 dB, a 30 dB RF to IF gain with six levels of intermediate gain control, a five-bit phase shifter, and a maximum power consumption of 250 mW. The RF designs for each of the four submodules (low noise amplifier, some gain control, phase shifter, and RF to IF sub-module) are presented. Except for the phase shifter, high frequency, low noise FETs with sub-half micron gate lengths are employed in the submodules. For the gain control, a two stage dual gate FET amplifier is used. The phase shifter is of the passive switched line type and consists of 5-bits. It uses relatively large gate width FETs (with zero drain to source bias) as the switching elements. A 20 GHz local oscillator buffer amplifier, a FET compatible balanced mixer, and a 5-8 GHz IF amplifier constitute the RF/IF sub-module. Phase shifter fabrication using ion implantation and a self-aligned gate technique is described. Preliminary RF results obtained on such phase shifters are included. A.R.H.

**N84-23807\*#** Illinois Univ., Urbana-Champaign. Electromagnetics Lab.

**THE STUDY OF MICROSTRIP ANTENNA ARRAYS AND RELATED PROBLEMS Semiannual Report, 22 Nov. 1983 - 21 May 1984**

R. Q. LO 25 May 1984 28 p refs

(Contract NAG3-418) (NASA-CR-173534; NAS 1.26:173534; SAR-2) Avail: NTIS HC A03/MF A01 CSCL 20N

The work on rectangular microstrip antennas for dual frequency operation is reported on. The principle of this approach is based on the excitation of a patch for two or more different modes which correspond to different frequencies. However, for a given geometry, the modal frequencies have a fixed relationship; therefore, the usefulness of such a design is greatly limited. In this study three different methods have been contrived to control the frequency ratio over a wide range. First, as found previously, if shorting pins are inserted at certain locations in the patch, the low frequency can be raised substantially. Second, if slots are cut in the patch, the high frequency can be lowered considerably. By using both techniques, the two frequency ratio can be varied approximately from 3 to 1.3. After that, the addition of more pins or slots becomes ineffective. B.W.

**N84-24918\*#** Case Western Reserve Univ., Cleveland, Ohio. Dept. of Electrical Engineering and Applied Physics.

**MILLIMETER WAVE TRANSMISSION SYSTEMS AND RELATED DEVICES Final Technical Report**

L. M. HEBERT 1984 119 p refs (Contract NAG3-288) (NASA-CR-173515; NAS 1.26:173515) Avail: NTIS HC A06/MF A01 CSCL 20N

A survey was made of the state-of-the-art in millimeter (20 GHz to 300 GHz) wave transmission systems and related devices. The survey includes summaries of analytical studies and theoretical results that were obtained for various transmission line structures. This material was supplemented by further analysis where appropriate. The transmission line structures are evaluated in terms of electrical performance, ease of manufacture, usefulness for building other devices and compatibility with solid state devices. Descriptions of waveguide transmission lines which have commonly been used in the microwave frequency range are provided along with special attention given to the problems that these guides face when their use is extended into the millimeter wave range. Also, guides which have been introduced specifically to satisfy the requirements of millimeter wave transmission are discussed in detail. Author

**N84-24924\*#** Ohio State Univ., Columbus. ElectroScience Lab. **ADAPTIVE ARRAYS FOR SATELLITE COMMUNICATIONS Final Report**

I. J. GUPTA and A. A. KSIENSKI Jun. 1984 49 p refs

(Contract NAG3-536) (NASA-CR-173548; NAS 1.26:173548; ESL-716111-1) Avail: NTIS HC A03/MF A01 CSCL 17B

The suppression of interfering signals in a satellite communication system was studied. Adaptive arrays are used to suppress interference at the reception site. It is required that the interference be suppressed to very low levels and a modified adaptive circuit is used which accomplishes the desired objective. Techniques for the modification of the transmit patterns to minimize interference with neighboring communication links are explored. E.A.K.

**N84-25908\*#** National Aeronautics and Space Administration. Lewis Research Center, Cleveland, Ohio.

**DETERMINATION OF THE KEY PARAMETERS AFFECTING HISTORIC COMMUNICATIONS SATELLITE TRENDS**

D. NAMKOONG Jun. 1984 13 p refs

(NASA-TM-83633; E-2072; NAS 1.15:83633) Avail: NTIS HC A02/MF A01 CSCL 17B

Data representing 13 series of commercial communications satellites procured between 1968 and 1982 were analyzed to determine the factors that have contributed to the general reduction over time of the per circuit cost of communications satellites. The model by which the data were analyzed was derived from a general telecommunications application and modified to be more directly applicable for communications satellites. In this model satellite mass, bandwidth-years, and technological change were the variable parameters. A linear, least squares, multiple regression routine was used to obtain the measure of significance of the model. Correlation was measured by coefficient of determination ( $R^2$  super 2) and t-statistic. The results showed that no correlation could be established with satellite mass. Bandwidth-year however, did show a significant correlation. Technological change in the bandwidth-year case was a significant factor in the model. This analysis and the conclusions derived are based on mature technologies, i.e., satellite designs that are evolutions of earlier designs rather than the first of a new generation. The findings, therefore, are appropriate to future satellites only if they are a continuation of design evolution. Author



**N84-25909\*#** National Aeronautics and Space Administration. Lewis Research Center, Cleveland, Ohio.

**SECONDARY PATTERN COMPUTATION OF AN ARBITRARILY SHAPED MAIN REFLECTOR**

P. T. C. LAM (Illinois Univ., Urbana), S. W. LEE (Illinois Univ., Urbana), and R. ACOSTA Apr. 1984 127 p refs (Contract NAG3-419)

(NASA-TM-85527; NAS 1.15:85527; ELSR-84-7;

UILU-ENG-84-2547) Avail: NTIS HC A07/MF A01 CSCL 20N

The secondary pattern of a perfectly conducting offset main reflector being illuminated by a point feed at an arbitrary location was studied. The method of analysis is based upon the application of the Fast Fourier Transform (FFT) to the aperture fields obtained using geometrical optics (GO) and geometrical theory of diffraction (GTD). Key features of the reflector surface is completely arbitrary, the incident field from the feed is most general with arbitrary polarization and location, and the edge diffraction is calculated by either UAT or by UTD. Comparison of this technique for an offset parabolic reflector with the Jacob-Bessel and Fourier-Bessel techniques shows good agreement. Near field, far field, and scan data of a large reflector are presented. Author

**N84-27954\*#** National Aeronautics and Space Administration. Lewis Research Center, Cleveland, Ohio.

**TEST RESULTS FOR 27.5- TO 30-GHZ COMMUNICATIONS SATELLITE RECEIVERS**

M. J. CONROY Jun. 1984 45 p refs

(NASA-TM-83662; E-1995; NAS 1.15:83662) Avail: NTIS HC A03/MF A01 CSCL 17B

Five proof of concept receivers are tested. The receivers operate in the 27.5 to 30 GHz uplink band for communications satellites and produce an output at C band. Receiver requirements and test results are given. Test methods are discussed and results are compared with the contractor's test results. M A.C.

**N84-30145\*#** Illinois Univ., Urbana-Champaign. Electromagnetics Lab.

**WAVE ATTENUATION AND MODE DISPERSION IN A WAVEGUIDE COATED WITH LOSSY DIELECTRIC MATERIAL**

C. S. LEE, S. L. CHUANG, S. W. LEE, and Y. T. LO Jul. 1984 65 p refs

(Contract NAG3-475)

(NASA-CR-173820; NAS 1.26:173820; EL-TR-84-13;

UILU-ENG-84-2552) Avail: NTIS HC A04/MF A01 CSCL 20N

The modal attenuation constants in a cylindrical waveguide coated with a lossy dielectric material are studied as functions of frequency, dielectric constant, and thickness of the dielectric layer. A dielectric material best suited for a large attenuation is suggested. Using Kirchhoff's approximation, the field attenuation in a coated waveguide which is illuminated by a normally incident plane wave is also studied. For a circular guide which has a diameter of two wavelengths and is coated with a thin lossy dielectric layer ( $\omega a/r = 9.1 - j2.3$ , thickness = 3% of the radius), a 3 dB attenuation is achieved within 16 diameters. M G.

**N84-30146\*#** National Aeronautics and Space Administration. Lewis Research Center, Cleveland, Ohio.

**SPECTRUM/ORBIT UTILIZATION PROGRAM FOR GEOSTATIONARY SATELLITES**

E. F. MILLER 1984 14 p refs Presented at the Mil. Commun. Conf. (MILCOM), Los Angeles, 21-24 Oct. 1984; sponsored by the Inst. of Electrical and Electronics Engineers (NASA-TM-83759; E-2247; NAS 1.15:83759) Avail: NTIS HC A02/MF A01 CSCL 17B

Mutual interferences among geostationary satellite communication systems determine the permitted spacing between satellites and the limits on the capacity of the orbit/spectrum resources available. This paper describes the computer program for analyzing the mutual interferences among communication satellite systems. Capabilities of the program are described. Inputs, models used, program operations, and program outputs are given. To show application of the program, an example scenario is

analyzed for fixed satellites providing domestic service to North America. Author

**N84-30147\*#** National Aeronautics and Space Administration. Lewis Research Center, Cleveland, Ohio.

**MMIC TECHNOLOGY FOR ADVANCED SPACE COMMUNICATIONS SYSTEMS**

A. N. DOWNEY, D. J. CONNOLLY, and G. ANZIC 1984 9 p refs Proposed for presentation at the 17th Ann. Electron. and Aerospace Conf. (EASCON), Washington, D.C., 10-12 Sep. 1984; sponsored by the Inst. of Electrical and Electronics Engineers (NASA-TM-83749; E-2236; NAS 1.15:83749) Avail: NTIS HC A02/MF A01 CSCL 17B

The current NASA program for 20 and 30 GHz monolithic microwave integrated circuit (MMIC) technology is reviewed. The advantages of MMIC are discussed. Millimeter wavelength MMIC applications and technology for communications systems are discussed. Passive and active MMIC compatible components for millimeter wavelength applications are investigated. The cost of a millimeter wavelength MMIC's is projected. Author

**N84-31460\*#** National Aeronautics and Space Administration. Lewis Research Center, Cleveland, Ohio.

**THE 20 AND 30 GHZ MMIC TECHNOLOGY FOR FUTURE SPACE COMMUNICATION ANTENNA SYSTEM**

G. ANZIC and D. J. CONNOLLY 25 Oct. 1984 9 p refs Presented at the Gallium Arsenide (GaAs) Integrated Circuits Symp., Boston, 23-25 Oct. 1984; sponsored by IEEE

(NASA-TM-83745; E-2227; NAS 1.15:83745) Avail: NTIS HC A02/MF A01 CSCL 17B

The development of fully monolithic gallium arsenide receive and transmit modules is described. These modules are slated for phased array antenna applications in future 30/20 gigahertz communications satellite systems. Performance goals and various approaches to achieve them are discussed. The latest design and performance results of components, submodules and modules are presented. Author

**N84-31461\*#** National Aeronautics and Space Administration. Lewis Research Center, Cleveland, Ohio.

**MONOLITHIC MICROWAVE INTEGRATED CIRCUITS: INTERCONNECTIONS AND PACKAGING CONSIDERATIONS**

K. B. BHASIN, A. N. DOWNEY, G. E. PONCHAK, R. R. ROMANOFKY, G. ANZIC, and D. J. CONNOLLY 1984 16 p refs Proposed for presentation at the 4th Ann. Intern. Electron. Packaging Conf., Baltimore, 29-31 Oct. 1984; sponsored by the International Electronics Packaging Society (NASA-TM-83774; E-2266; NAS 1.15:83774) Avail: NTIS HC A02/MF A01 CSCL 09C

Monolithic microwave integrated circuits (MMIC's) above 18 GHz were developed because of important potential system benefits in cost reliability, reproducibility, and control of circuit parameters. The importance of interconnection and packaging techniques that do not compromise these MMIC virtues is emphasized. Currently available microwave transmission media are evaluated to determine their suitability for MMIC interconnections. An antipodal inline type of microstrip waveguide transition's performance is presented. Packaging requirements for MMIC's are discussed for thermal, mechanical, and electrical parameters for optimum desired performance. E.A.K.

**N84-31464\*#** Chu Associates, Inc., Littleton, Mass.

**REFLECTOR ANTENNAS WITH LOW SIDELOBES, LOW CROSS POLARIZATION, AND HIGH APERTURE EFFICIENCY Final Report**

I. M. FAIGEN, C. F. REICHERT, C. J. SLETTEN, and R. A. SHORE Mar. 1984 123 p refs Prepared in cooperation with Solar Energy Technology, Inc., Bedford, Mass. (Contract NAS3-22343)

(NASA-CR-174670; NAS 1.26:174670) Avail: NTIS HC A06/MF A01 CSCL 20N

Techniques are presented for computing the horn near field patterns on the subreflectors and for correcting the phase center



errors of the horn pattern by shaping the subreflector surface. The diffraction pattern computations for scanned beams are described. The effects of dish aperture diffraction on pattern bandwidth are investigated. A model antenna consisting of a reflector, shaped subreflector, and corrugated feed horn is described. M.A.C.

**N84-32644\*#** National Aeronautics and Space Administration. Lewis Research Center, Cleveland, Ohio.

#### THE 20 X 20 HIGH SPEED MICROWAVE SWITCHES

A. SAUNDERS Sep. 1984 24 p refs

(NASA-TM-83775; E-2182; NAS 1.15:83775) Avail: NTIS HC A03/MF A01 CSCL 09A

Tests were conducted at NASA Lewis Research Center to characterize the proof-of-concept matrix switches built under NASA contract by Ford Aerospace and Aeronautics Corporation at Palo Alto, California, and the General Electric Company at Valley Forge, Pennsylvania. The contract requirements and goals are tabulated along with the results of the NASA tests. Characteristics examined are bandwidth, insertion loss, ripple, switching speed, isolation, standing wave ratio (input and output), deviation from linear phase, noise figure, reconfiguration rates, spurious responses, gain compression, and third order intermodulation distortion. A brief description of the testing method and a statistical analysis of the test results for each of the switches are provided. Author

**N84-32645\*#** Illinois Univ., Urbana. Electromagnetics Lab. NUMERICAL METHODS FOR ANALYZING ELECTROMAGNETIC SCATTERING Semiannual Report, 25 Mar. - 24 Sep. 1984

S. W. LEE, Y. T. LO, and S. L. CHUANG 24 Sep. 1984 45 p refs

(Contract NAG3-475)

(NASA-CR-173916; NAS 1.26:173916) Avail: NTIS HC A03/MF A01 CSCL 20N

The wave attenuation in a cylindrical waveguide coated with lossy dielectric material was studied. The scope was extended to the high frequency case for calculating attenuation coefficients and propagation constants of a dielectric coated circular waveguide. The magnetic material coating was studied. At low frequency a one way 3dB attenuation was achieved within a longitudinal distance of one diameter. A software program was generated to plot the field patterns of the lowest 30 modes in the cylindrical waveguides. E.R.

**N84-33642\*#** National Aeronautics and Space Administration. Lewis Research Center, Cleveland, Ohio.

#### PHOTOVOLTAIC POWER SYSTEM FOR SATELLITE EARTH STATIONS IN REMOTE AREAS: PROJECT STATUS AND DESIGN DESCRIPTION

R. DELOMBARD 1984 14 p refs Presented at the Intern. Telecommun. Energy Conf., New Orleans, 4-7 Nov. 1984; sponsored by the Communications Society of the Institute of Electrical and Electronics Engineers

(NASA-TM-83789; E-2285; NAS 1.15:83789) Avail: NTIS HC A02/MF A01 CSCL 20N

A photovoltaic power system which will be installed at a remote location in Indonesia to provide power for a satellite Earth station and a classroom for video and audio teleconferences are described. The Earth station may also provide telephone service to a nearby village. The use of satellite communications for development assistance applications and the suitability of a hybrid photovoltaic engine generator power system for remote satellite Earth stations are demonstrated. The Indonesian rural satellite project is discussed and the photovoltaic power system is described. E.A.K.

## ELECTRONICS AND ELECTRICAL ENGINEERING

Includes test equipment and maintainability; components, e.g., tunnel diodes and transistors; microminiaturization; and integrated circuitry.

**A84-12424\*** National Aeronautics and Space Administration. Lewis Research Center, Cleveland, Ohio.

#### EVALUATION OF THE EMISSION CAPABILITIES OF SPINDT-TYPE FIELD EMITTING CATHODES

R. FORMAN (NASA, Lewis Research Center, Cleveland, OH) Applications of Surface Science (ISSN 0378-5963), vol. 16, May-June 1983, p. 277-291. refs

The electron emitting capabilities of Spindt-type field emitting cathodes (FEC) are being studied at the Lewis Research Center, NASA. These cathodes, having 5000 emitting points in a 1 mm diameter, have been shown to be capable of emission current densities of 10 A/sq cm and higher. The purposes of this study are to (1) demonstrate that the cathodes can be processed and used in a tube-type configuration, (2) determine whether, at a sufficiently high current density, the cathode can operate in the space charge mode, and (3) evaluate failure mechanisms in this unique type of electron emitter. FEC's have been tested in a diode configuration, by the use of pulse techniques, up to current densities of 6 A/sq cm and anode potentials of 3000 V. Space charge effects have been observed in the range of 5 A/sq cm as an apparent linear increase of cathode current with anode voltage for a constant emitter-gate potential. Failed cathodes were studied by means of scanning electron-microscopy and the major failure modes encountered are attributed to gas evolution, followed by arcing, which destroys either individual emitters or a large segment of the cathode area. Author

**A84-18371\*** Honeywell Corporate Research Center, Bloomington, Minn.

#### A KA-BAND GAAS MONOLITHIC PHASE SHIFTER

V. SOKOLOV, J. J. GEDDES, A. CONTOLATIS, P. E. BAUHAHN, and C. CHAO (Honeywell Corporate Technology Center, Bloomington, MN) IEEE Transactions on Microwave Theory and Techniques (ISSN 0018-9480), vol. MTT-31, Dec. 1983, p. 1077-1083. refs

(Contract NAS3-23356)

The design and performance of a GaAs monolithic 180-degree one-bit switched line phase shifter test circuit for Ka-band operation is presented. A self-aligned gate (SAG) fabrication technique is also described that reduces resistive parasitics in the switching FET's. Over the 27.5-30 GHz band, typical measured differential insertion phase is within 10-20 deg of the ideal time delay characteristic. Over the same band, the insertion loss for the SAG phase shifter is about 2.5-3 dB per bit. The SAG fabrication technique holds promise in reducing phase shifter insertion loss to about 1.5 dB/bit for 30-GHz operation. Author

**A84-18403\*** Duke Univ., Durham, N. C.

#### PARAMETRIC STUDY OF MINIMUM CONVERTER LOSS IN AN ENERGY-STORAGE DC-TO-DC CONVERTER

R. C. WONG, H. A. OWEN, JR., and T. G. WILSON (Duke University, Durham, NC) IN: PESC '82; Annual Power Electronics Specialists Conference, 13th, Cambridge, MA, June 14-17, 1982, Record. New York, Institute of Electrical and Electronics Engineers, 1982, p. 411-425. refs

(Contract NSG-3157)

Through a combination of analytical and numerical minimization procedures, a converter design that results in the minimum total converter loss (including core loss, winding loss, capacitor and energy-storage-reactor loss, and various losses in the semiconductor switches) is obtained. Because the initial phase involves analytical minimization, the computation time required by the subsequent phase of numerical minimization is considerably

### 33 ELECTRONICS AND ELECTRICAL ENGINEERING

reduced in this combination approach. The effects of various loss parameters on the optimum values of the design variables are also examined. Author

**A84-18411\*** Virginia Polytechnic Inst. and State Univ., Blacksburg.  
**EXTENSIONS OF THE DISCRETE-AVERAGE MODELS FOR CONVERTER POWER STAGES**  
D. J. SHORTT (Burroughs Corp., Coral Springs, FL) and F. C. LEE (Virginia Polytechnic Institute and State University, Blacksburg, VA) IN: PESC '83; Annual Power Electronics Specialists Conference, 14th, Albuquerque, NM, June 6-9, 1983, Record. New York, Institute of Electrical and Electronics Engineers, 1983, p. 23-37. refs  
(Contract NAG3-274)

An improved power converter model is developed by combining the average and discrete modeling techniques. The parameter determination of the proposed discrete-average model is shown to be dependent on the type of duty cycle control law, and the accuracy of the model is shown to depend on the nature of the error processor used in the feedback loop. Author

**A84-18412\*** Bell Telephone Labs., Inc., Whippany, N. J.  
**STABILITY ANALYSIS OF A BUCK REGULATOR EMPLOYING INPUT FILTER COMPENSATION**  
S. S. KELKAR (Bell Telephone Laboratories, Inc., Whippany, NJ) and F. C. LEE (Virginia Polytechnic Institute and State University, Blacksburg, VA) IN: PESC '83; Annual Power Electronics Specialists Conference, 14th, Albuquerque, NM, June 6-9, 1983, Record. New York, Institute of Electrical and Electronics Engineers, 1983, p. 38-49. refs  
(Contract NAG3-220)

The interaction between the input filter and the regulator often causes serious degradation of performance. The reduction in loop gain due to input filter interaction can result in system instability. An exact stability analysis of the buck regulator system is presented. The input filter parameter values are varied and system instability is predicted for the case without feedforward. The eigenvalues of the system can be brought back into the unit circle and the system thus stabilized with the addition of the feedforward loop. Measurements made for the cases with and without feedforward confirm the analytical prediction. Author

**A84-18414\*** Virginia Polytechnic Inst. and State Univ., Blacksburg.  
**DESIGN CONSIDERATIONS FOR FET-GATED POWER TRANSISTORS**  
D. Y. CHEN and S. A. CHIN (Virginia Polytechnic Institute and State University, Blacksburg, VA) IN: PESC '83; Annual Power Electronics Specialists Conference, 14th, Albuquerque, NM, June 6-9, 1983, Record. New York, Institute of Electrical and Electronics Engineers, 1983, p. 144-149. refs  
(Contract NAG3-40)

An FET-bipolar combinational power transistor configuration (tested up to 300 V, 20 A at 100 kHz) is described. The critical parameters for integrating the chips in hybrid form are examined, and an effort to optimize the overall characteristics of the configuration is discussed. Chip considerations are examined with respect to the voltage and current rating of individual chips, the FET surge capability, the choice of triple diffused transistor or epitaxial transistor for the bipolar element, the current tailing effect, and the implementation of the bipolar transistor and an FET as single chip or separate chips. Package considerations are discussed with respect to package material and geometry, surge current capability of bipolar base terminal bonding, and power losses distribution. B.J.

**A84-20711\*** Systems Science and Software, La Jolla, Calif.  
**POTENTIALS IN A PLASMA OVER A BIASED PINHOLE**  
M. J. MANDELL and I. KATZ (Systems, Science and Software, La Jolla, CA) (IEEE, U.S. Defense Nuclear Agency, NASA, et al., Annual Conference on Nuclear and Space Radiation Effects, Gatlinburg, TN, July 18-21, 1983) IEEE Transactions on Nuclear Science (ISSN 0018-9499), vol. NS-30, Dec. 1983, p. 4307-4310. refs  
(Contract NAS3-23058)

The NASCAP/LEO code is used to simulate measurements taken at Jet Propulsion Laboratory of potentials near a simulated pinhole. The insulator near the high-voltage pinhole obeys an electric field boundary condition resulting from secondary electron hopping conductivity. The code predictions are in good agreement with the measurements. Author

**A84-22873\*#** Rockwell International Corp., Thousand Oaks, Calif.  
**A THREE-STAGE POWER AMPLIFIER FOR A 20 GHZ MONOLITHIC TRANSMIT MODULE**  
W. C. PETERSEN and A. K. GUPTA (Rockwell International Microelectronic Research and Development Center, Thousand Oaks, CA) Institute of Electrical and Electronics Engineers, GaAsIC Symposium, Phoenix, AZ, Oct. 25-27, 1983, Paper. 4 p.  
(Contract NAS3-23247)

Design, fabrication, and test results of a three-stage GaAs monolithic power amplifier covering the 17.7 to 20.2 GHz band are described. Intermediate results for single and two-stage amplifiers are also presented. The 1.5 x 3.1 millimeter three-stage amplifier chip has 15 dB gain from 16.5 to 20.2 GHz. Measured saturated output power is between +20 and +21 dBm with improvement expected from minor circuit and device changes. Author

**A84-22874\*#** Maxwell Labs., Inc., San Diego, Calif.  
**MATERIAL CONSIDERATIONS FOR HIGH FREQUENCY, HIGH POWER CAPACITORS**  
W. WHITE and J. GALPERIN (Maxwell Laboratories, Inc., San Diego, CA) Institute of Electrical and Electronics Engineers, Electrical Insulation and Dielectric Phenomenon Conference, Buck Falls, PA, Oct. 16-20, 1983, Paper. 8 p. refs  
(Contract NAS3-22668)

Dielectric materials chosen for use in this high frequency, high power capacitor must endure hard vacuum conditions, high currents (up to 125 A rms), and frequencies up to 40 kHz. Temperature requirements for this type of capacitor are that capacitor operation must be efficient up to 125 C. A more stringent requirement for the sold dielectric is that the temperature coefficient of dissipation factor should indicate self stabilization well below 125 C. In addition, the dielectric temperature coefficient of capacitance should be negative. Author

**A84-23255\*** Toledo Univ., Ohio.  
**INHERENT OVERLOAD PROTECTION FOR THE SERIES RESONANT CONVERTER**  
R. J. KING and T. A. STUART (Toledo, University, Toledo, OH) IEEE Transactions on Aerospace and Electronic Systems (ISSN 0018-9251), vol. AES-19, Nov. 1983, p. 820-830. refs  
(Contract NSG-3281)

The overload characteristics of the full bridge series resonant power converter are considered. This includes analyses of the two most common control methods presently in use. The first of these uses a current zero crossing detector to synchronize the control signals and is referred to as the alpha controller. The second is driven by a voltage controlled oscillator and is referred to as the gamma controller. It is shown that the gamma controller has certain reliability advantages in that it can be designed with inherent short circuit protection. Experimental results are included for an 86 kHz converter using power metal-oxide-semiconductor field-effect transistors (MOSFETs). Author

**A84-23258\*** Toledo Univ., Ohio.

**A LARGE-SIGNAL DYNAMIC SIMULATION FOR THE SERIES RESONANT CONVERTER**

R. J. KING and T. A. STUART (Toledo, University, Toledo, OH) IEEE Transactions on Aerospace and Electronic Systems (ISSN 0018-9251), vol. AES-19, Nov. 1983, p. 859-870. refs (Contract NSG-3281)

A simple nonlinear discrete-time dynamic model for the series resonant dc-dc converter is derived using approximations appropriate to most power converters. This model is useful for the dynamic simulation of a series resonant converter using only a desktop calculator. The model is compared with a laboratory converter for a large transient event. Author

**A84-24850\*#** Gould, Inc., Rolling Meadows, Ill.

**AN SCR INVERTER WITH AN INTEGRAL BATTERY CHARGER FOR ELECTRIC VEHICLES**

D. THIMMEACH (Gould Research Center, Rolling Meadows, Ill.) Institute of Electrical and Electronics Engineers, Annual Meeting, Mexico City, Mexico, Oct. 3-7, 1983, Paper. 8 p. Research supported by the U.S. Department of Energy. refs (Contract DEN3-249)

The feasibility of incorporating an onboard battery charger into the inverter previously developed under a NASA contract is successfully demonstrated. The rated output power of the resulting isolated battery charger is 3.6 kW at 220 Vac with an 86 percent efficiency and a 95 percent power factor. Also achieved are improved inverter efficiency (from 90 to 93 percent at 15 kW motor shaft power), inverter peak power capability (from 26 to 34 kW), and reduced weight and volume of the combined inverter/charger package (47 kg, 49 x 44 x 24 cm). Some major conclusions are that using the inverter commutation circuitry to perform the battery charging function is advantageous, and that the input-commutated thyristor inverter has the potential to be an excellent inverter and battery charger for use in electric vehicle applications. C.M.

**A84-25333\*#** National Aeronautics and Space Administration, Lewis Research Center, Cleveland, Ohio

**HIGH EFFICIENCY IMPATT DIODES FOR 60 GHZ INTERSATELLITE LINK APPLICATIONS**

E. J. HAUGLAND (NASA, Lewis Research Center, Cleveland, OH) IN: Communication Satellite Systems Conference, 10th, Orlando, FL, March 19-22, 1984, Technical Papers. New York, American Institute of Aeronautics and Astronautics, 1984, p. 679-684.

(AIAA PAPER 84-0767)

Intersatellite links are expected to play an increasingly important role in future satellite systems. Improved components are required to properly utilize the wide bandwidth allocated for intersatellite link applications around 60 GHz. IMPATT diodes offer the highest potential performance as solid state power sources for a 60 GHz transmitter. Presently available devices do not have the desired power and efficiency. High efficiency, high power IMPATT diodes for intersatellite link applications are being developed by NASA and other government agencies. This paper describes the development of high efficiency 60 GHz IMPATT diodes by NASA. These programs are cofunded by the U.S. Air Force, Space Division. Author

**A84-30209\*** National Aeronautics and Space Administration, Lewis Research Center, Cleveland, Ohio.

**NEW PROPULSION COMPONENTS FOR ELECTRIC VEHICLES**

R. R. SECUNDE (NASA, Lewis Research Center, Cleveland, OH) IN: IECEC '83; Proceedings of the Eighteenth Intersociety Energy Conversion Engineering Conference, Orlando, FL, August 21-26, 1983, Volume 5. New York, American Institute of Chemical Engineers, 1983, p. 2203-2211. refs

Improved component technology is described. This includes electronically commutated permanent magnet motors of both drum and disk configurations, an unconventional brush commutated motor, ac induction motors, various controllers, transmissions and complete systems. One or more of these approaches to electric

vehicle propulsion may eventually displace presently used controllers and brush commutated dc motors. Previously announced in STAR as N83-25982 S.L.

**A84-30857\*** Texas Instruments, Inc., Dallas.

**0.5 W 2-21 GHZ MONOLITHIC GAAS DISTRIBUTED AMPLIFIER**

B. KIM and H. Q. TSENG (Texas Instruments Central Research Laboratories, Dallas, TX) Electronics Letters (ISSN 0013-5194), vol. 20, March 29, 1984, p. 288, 289. refs (Contract NAS3-23781)

A novel circuit concept to reduce the gate loss using series capacitors on the gate feeding lines has been implemented for a distributed amplifier design. It has significantly increased the gate width of the amplifier with a resultant increase of the broadband output power and efficiency. A monolithic GaAs distributed amplifier using 6 x 300-micron FETs has achieved a record output power of 0.5 W over the 2 to 21 GHz frequency band with at least 4 dB gain. The power-added efficiency was 14 percent. The linear gain was 5 plus or minus 1 dB over the same frequency band.

Author

**A84-32029\*** Massachusetts Inst. of Tech., Cambridge.

**METAL VAPOR VACUUM ARC SWITCHING - APPLICATIONS AND RESULTS**

D. COPE (MIT, Cambridge, MA) and P. MONGEAU (Electromagnetic Launch Research, Inc., Cambridge, MA) (Institute of Electrical and Electronics Engineers, Symposium on Electromagnetic Launch Technology, 2nd, Boston, MA, Oct. 10-13, 1983) IEEE Transactions on Magnetics (ISSN 0018-9464), vol. MAG-20, March 1984, p. 316-319. refs (Contract NAG3-283)

The design of metal-vapor vacuum-arc switches (MVSs) for electromagnetic launchers is discussed, and preliminary results are presented for an experimental MVS. The general principles of triggered-vacuum-gap and vacuum-interrupter MVSs are reviewed, and the requirements of electromagnetic launchers are analyzed. High-current design problems such as electrode erosion, current sharing, magnetic effects, and thermal effects are examined. The experimental MVS employs stainless-steel flanges, a glass vacuum vessel, an adjustable electrode gap, autonomous internal magnetic-field coils, and a tungsten-pin trigger assembly. Some results from tests without magnetic augmentation are presented graphically. T.K.

**A84-32046\*** IAP Research, Inc., Dayton, Ohio.

**INVESTIGATION OF THE RESIDUE IN AN ELECTRIC RAIL GUN EMPLOYING A PLASMA ARMATURE**

D. P. BAUER and J. P. BARBER (IAP Research, Inc., Dayton, OH) (Institute of Electrical and Electronics Engineers, Symposium on Electromagnetic Launch Technology, 2nd, Boston, MA, Oct. 10-13, 1983) IEEE Transactions on Magnetics (ISSN 0018-9464), vol. MAG-20, March 1984, p. 385-388. refs (Contract NAS3-22819)

The performance of dc electric rail guns using plasma-armature-accelerated projectiles was studied. It was found that the initial rail launcher acceleration profile was consistent with the simulation, but that after the projectile had traveled approximately 25 to 30 cm along the gun, a considerable portion of the current in the projectile armature commutated into a secondary current path. Also noted were the lower than expected muzzle velocities. It was proposed that the secondary current path was a relatively high conductivity layer of residue on the launcher bore. C.M.

**A84-32281\*** Texas Instruments, Inc., Dallas.

**GAAS DUAL-GATE FET FOR OPERATION UP TO K-BAND**

B. KIM, H. Q. TSERNG, and P. SAUNIER (Texas Instruments Central Research Laboratories, Dallas, TX) IEEE Transactions on Microwave Theory and Techniques (ISSN 0018-9480), vol. MTT-32, March 1984, p. 256-261. refs (Contract NAS3-22886)

A high-frequency equivalent-circuit model of a GaAs dual-gate FET and analytical expressions for the input/output impedances, transconductance, unilateral gain, and stability factor are presented. It is found that the gain of a dual-gate FET is higher than of a single-gate FET at low frequency but decreases faster as frequency increases because of the capacitive shunting effect of the second gate. A dual-gate power FET suitable for variable-gain-amplifier applications up to K-band has been developed. At 10 GHz, a 1.2-mm-gatewidth device has achieved an output power of 1.1 W with 10.5-dB gain and 31-percent power-added efficiency. At 20 GHz, the same device delivered an output power of 340 mW with 5.3-dB gain. At K-band, a dynamic-gain control range of up to 45 dB was obtained with an insertion phase change of no more than  $\pm$  or 2 degrees for the first 10 dB of gain control. Author

**A84-32290\*** TRW Electronic Systems Group, Redondo Beach, Calif.

**A K-BAND GAAS FET AMPLIFIER WITH 8.2-W OUTPUT POWER**

J. GOEL (TRW, Inc., TRW Electronic Systems Group, Redondo Beach, CA) IEEE Transactions on Microwave Theory and Techniques (ISSN 0018-9480), vol. MTT-32, March 1984, p. 317-324. refs (Contract NAS3-22503)

An 8.2-W GaAs FET amplifier with 38.6  $\pm$  or - 0.5-dB gain over a 17.7-19.1-GHz frequency band has been developed. This amplifier combines the outputs of eight multistage amplifier modules utilizing a radial combiner. This state-of-the-art power level has been achieved with AM/PM of less than 2 deg/dB. The third-order intermodulation products at 1-dB gain compression were 20 dBc, and variation in group delay over the frequency band was less than  $\pm$  or - 0.25 ns. Tests show that the amplifier is unconditionally stable and follows the graceful-degradation principle. Author

**A84-32293\*** Virginia Polytechnic Inst. and State Univ., Blacksburg.

**A NEW FET-BIPOLAR COMBINATIONAL POWER SEMICONDUCTOR SWITCH**

D. Y. CHEN, S. CHANDRASEKARAN, and S. A. CHIN (Virginia Polytechnic Institute and State University, Blacksburg, VA) IEEE Transactions on Aerospace and Electronic Systems (ISSN 0018-9251), vol. AES-20, March 1984, p. 104-111. refs (Contract NAG3-340)

A novel FET-BJT combinational transistor configuration is proposed and demonstrated using discrete devices. This new transistor features fast switching, very simple drive requirement, elimination of reverse bias second breakdown, and good utilization of semiconductor chip area. Initial results indicate that power hybrid construction of the device is essential to enhance the current rating of the device. Author

**A84-33325\*** Tuskegee Inst., Ala.

**ENERGY PARTITIONING IN AN INDUCTIVELY DRIVEN RAIL GUN**

K. K. SEN and P. K. RAY (Tuskegee Institute, Tuskegee, AL) IEEE Proceedings, Part A - Physical Science, Measurement and Instrumentation, Management and Education, Reviews (ISSN 0143-702X), vol. 131, pt. A, no. 3, May 1984, p. 140-144. refs (Contract NAG3-76)

The equations describing the performance of an inductively driven rail are analyzed numerically. Friction between the projectile and rails is included through an empirical formulation. The equations are applied to the experiment of Rashleigh and Marshall to obtain an estimate of energy distribution in rail guns as a function of time. It is found that only 15 percent of energy delivered by the inductor to the gun is transformed into the kinetic energy of the

projectile. This study provides an insight into the nature of nonlinear coupling involved in the electromechanical interactions in a rail gun. Author

**A84-34521\*** Nebraska Univ., Lincoln.

**ELECTRONIC PROPERTIES OF CARBON FIBERS INTERCALATED WITH COPPER CHLORIDE**

H. OSHIMA (Nebraska, University, Lincoln, NE; Nihon University, Tokyo, Japan), V. NATARAJAN, J. A. WOOLLAM (Nebraska, University, Lincoln, NE), A. YAVROUIAN (California Institute of Technology, Jet Propulsion Laboratory, Pasadena, CA), E. J. HAUGLAND (NASA, Lewis Research Center, Cleveland, OH), and T. TSUZUKU (Nihon University, Tokyo, Japan) Japanese Journal of Applied Physics, Part 1 (ISSN 0021-4922), vol. 23, Jan. 1984, p. 40-43. Research supported by Nihon University. refs (Contract NAG3-95)

Copper chloride intercalated pitch-based carbon fibers are found to have electrical resistivities as low as 12.9 micro-ohm-cm, and are air- and thermally-stable at and above room temperature. This is therefore a good candidate system for conductor application. In addition, Shubnikov-deHaas quantum oscillatory effects were found, and electronic properties of the intercalated fiber are studied using magnetic fields to 20 tesla. Author

**A84-39197\*** Case Western Reserve Univ., Cleveland, Ohio.

**CIRCUIT EQUIVALENT TO THE ELASTIC SPHERICAL SHELL**

D. HAZONY (Case Western Reserve University, Cleveland, OH) Applied Physics Letters (ISSN 0003-6951), vol. 45, July 1, 1984, p. 22, 23.

(Contract NIH-EY-03251; NAG3-24)

The pulsating elastic spherical shell is investigated in detail. A possible equivalent circuit is shown to contain two capacitors, two inductors, a transmission line, and an ideal transformer. Author

**A84-41035\*#** National Aeronautics and Space Administration Lewis Research Center, Cleveland, Ohio.

**A TWT AMPLIFIER WITH A LINEAR POWER TRANSFER CHARACTERISTIC AND IMPROVED EFFICIENCY**

H. G. KOSMAHL (NASA, Lewis Research Center, Cleveland, OH) and J. C. PETERSON (Hughes Aircraft Co., Torrance, CA) IN: Communication Satellite Systems Conference, 10th, Orlando, FL, March 19-22, 1984, Technical Papers. New York, American Institute of Aeronautics and Astronautics, 1984, p. 488-492. (AIAA PAPER 84-0762)

A novel method called 'Dynamic Velocity Taper' to linearize the Pout versus Pin transfer characteristic that does not require any extraneous circuitry or tuning, has large bandwidth capabilities (10 percent) and offers also an increase in the intrinsic traveling wave tube (TWT) efficiency by 1 to 2 dB is described. In addition, the method permits the TWT to be operated at or near the synchronous voltage (b plus or minus o) which produces a flat small and large signal gain responses and low AM to PM conversion. The physics of the method and experimental verification are given. The implementation should have a significant impact on TWT performance and increase the channel capacity of communication satellites. Previously announced in STAR as N84-21803 R.J.F.

**A84-44912\*** National Aeronautics and Space Administration. Lewis Research Center, Cleveland, Ohio.

**NASA SEEKING HIGH-POWER 60-GHZ IMPATT DIODES**

E. J. HAUGLAND (NASA, Lewis Research Center, Cleveland, OH) Microwaves & RF (ISSN 0745-2993), vol. 23, Aug. 1984, p. 100-102, 107. refs

Recent progress in the development of high-power 60 GHz GaAs IMPATT diodes for communication links with high-data-rate satellites is discussed. One of the advantages of GaAs over Si as the material for the diodes are that GaAs is likely to have a higher output and efficiency than Si despite recent advances in Si technology. It is therefore in GaAs technology that research is currently concentrating. Some of the design strategies of the various companies working on the technology are described, including a pill process, MOCVD growth, and the use of diethy

zinc as a dopant. Reliability testing of the diodes will be performed by NASA. Some of the alternatives to solid state amplifiers are discussed, including optical and traveling wave tube technology (TWT). I.H.

**A84-49253\*** Ford Aerospace and Communications Corp., Palo Alto, Calif.

**HIGH-SPEED WIDE BAND 20 X 20 MICROWAVE SWITCH MATRIX**

E. COBAN, J. WISNIEWSKI, J. PELOSE, E. BALDERRAMA, N. CHIANG, and P. HO (Ford Aerospace and Communications Corp., Palo Alto, CA) IN: ICC '83 - Integrating communication for world progress; International Conference on Communications, Boston, MA, June 19-22, 1983, Conference Record. Volume 1. New York, Institute of Electrical and Electronics Engineers, 1983, p. 354-359.

(Contract NAS3-22501)

The use of a dynamic switching matrix for future communication satellites will significantly increase the communication channel capacity and improve the system capability and flexibility. This paper describes the design and development of a unique coupler crossbar 20 x 20 microwave switch matrix. This paper also presents the test results of the proof-of-concept model that meets the requirements for a high-speed satellite switched, time division multiple access (SS-TDMA) system. Author

**N84-10058\*** National Aeronautics and Space Administration. Lewis Research Center, Cleveland, Ohio.

**THREE-PHASE, HIGH-VOLTAGE, HIGH-FREQUENCY DISTRIBUTED BUS SYSTEM FOR ADVANCED AIRCRAFT**

R. C. FINKE IN: *its Aircraft Elect. Secondary Power* p 27-35 Jun. 1983

Avail: NTIS HC A09/MF A01 CSCL 09C

A three phase, high voltage, high frequency distributed bus system for advanced aircraft is discussed. A system model is given. Available components are described. Recommendations are given. R.J.F.

**N84-10064\*** National Aeronautics and Space Administration. Lewis Research Center, Cleveland, Ohio.

**INTERCALATED GRAPHITE ELECTRICAL CONDUCTORS**

B. A. BANKS IN: *its Aircraft Elect. Secondary Power* p 103-122 Jun. 1983 refs

Avail: NTIS HC A09/MF A01 CSCL 09A

For years NASA has wanted to reduce the weight of spacecraft and aircraft. Experiments are conducted to find a lightweight synthetic metal to replace copper. The subject of this paper, intercalated graphite, is such a material. Intercalated graphite is made by heating petroleum or coal to remove the hydrogen and to form more covalent bonds, thus increasing the molecular weight. The coal or petroleum eventually turns to pitch, which can then be drawn into a fiber. With continued heating the pitch-based fiber releases hydrogen and forms a carbon fiber. The carbon fiber, if heated sufficiently, becomes more organized in parallel layers of hexagonally arranged carbon atoms in the form of graphite. A conductor of intercalated graphite is potentially useful for spacecraft or aircraft applications because of its low weight.

B.W.

**N84-10065\*** National Aeronautics and Space Administration. Lewis Research Center, Cleveland, Ohio.

**NEW DEVELOPMENTS IN POWER SEMICONDUCTORS**

G. R. SUNDBERG IN: *its Aircraft Elect. Secondary Power* p 123-141 Jun. 1983

Avail: NTIS HC A09/MF A01 CSCL 09A

This paper represents an overview of some recent power semiconductor developments and spotlights new technologies that may have significant impact for aircraft electric secondary power. Primary emphasis will be on NASA-Lewis-supported developments in transistors, diodes, a new family of semiconductors, and solid-state remote power controllers. Several semiconductor companies that are moving into the power arena with devices

rated at 400 V and 50 A and above are listed, with a brief look at a few devices. Author

**N84-10066\*** National Aeronautics and Space Administration. Lewis Research Center, Cleveland, Ohio.

**LIGHTWEIGHT, HIGH-FREQUENCY TRANSFORMERS**

G. E. SCHWARZE IN: *its Aircraft Elect. Secondary Power* p 143-147 Jun. 1983

Avail: NTIS HC A09/MF A01 CSCL 09A

The 25-kVA space transformer was developed under contract by Thermal Technology Laboratory, Buffalo, N. Y. The NASA Lewis transformer technology program attempted to develop the baseline technology. For the 25-kVA transformer the input voltage was chosen as 200 V, the output voltage as 1500 V, the input voltage waveform as square wave, the duty cycle as continuous, the frequency range (within certain constraints) as 10 to 40 kHz, the operating temperatures as 85 deg. and 130 C, the baseplate temperature as 50 C, the equivalent leakage inductance as less than 10 micro-h, the operating environment as space, and the life expectancy as 10 years. Such a transformer can also be used for aircraft, ship and terrestrial applications. B.W.

**N84-10067\*** National Aeronautics and Space Administration. Lewis Research Center, Cleveland, Ohio.

**HIGH-CURRENT, HIGH-FREQUENCY CAPACITORS**

D. D. RENZ IN: *its Aircraft Elect. Secondary Power* p 149-158 Jun. 1983

Avail: NTIS HC A09/MF A01 CSCL 09A

The NASA Lewis high-current, high-frequency capacitor development program was conducted under a contract with Maxwell Laboratories, Inc., San Diego, California. The program was started to develop power components for space power systems. One of the components lacking was a high-power, high-frequency capacitor. Some of the technology developed in this program may be directly usable in an all-electric airplane. The materials used in the capacitor included the following: the film is polypropylene, the impregnant is monoisopropyl biphenyl, the conductive epoxy is Emerson and Cuming Stycast 2850 KT, the foil is aluminum, the case is stainless steel (304), and the electrode is a modified copper-ceramic. Author

**N84-10450\*** Virginia Polytechnic Inst. and State Univ., Blacksburg.

**IMPROVED TRANSISTOR-CONTROLLED AND COMMUTATED BRUSHLESS DC MOTORS FOR ELECTRIC VEHICLE PROPULSION Final Report**

N. A. DEMERDASH, R. H. MILLER, T. W. NEHL, and T. A. NYAMUSA 1 Jan. 1983 402 p refs

(Contract DEN3-65; DE-A101-77CS-51044)

(NASA-CR-168053; DOE/NASA/0065-83/1; NAS 1.26:168053)

Avail: NTIS HC A18/MF A01 CSCL 09C

The development, design, construction, and testing processes of two electronically (transistor) controlled and commutated permanent magnet brushless dc machine systems, for propulsion of electric vehicles are detailed. One machine system was designed and constructed using samarium cobalt for permanent magnets, which supply the rotor (field) excitation. Meanwhile, the other machine system was designed and constructed with strontium ferrite permanent magnets as the source of rotor (field) excitation. These machine systems were designed for continuous rated power output of 15 hp (11.2 kw), and a peak one minute rated power output of 35 hp (26.1 kw). Both power ratings are for a rated voltage of 115 volts dc, assuming a voltage drop in the source (battery) of about 5 volts. That is, an internal source voltage of 120 volts dc. Machine-power conditioner system computer-aided simulations were used extensively in the design process. These simulations relied heavily on the magnetic field analysis in these machines using the method of finite elements, as well as methods of modeling of the machine power conditioner system dynamic interaction. These simulation processes are detailed. Testing revealed that typical machine system efficiencies at 15 hp (11.2 kw) were about 88% and 84% for the samarium cobalt and

strontium ferrite based machine systems, respectively. Both systems met the peak one minute rating of 35 hp. S.L.

**N84-11385\*#** TRW Electronic Systems Group, Redondo Beach, Calif.

**A 20-GHZ IMPATT TRANSMITTER** Final Report, Aug. 1980 - Jul. 1982

J. L. CHAN and C. SUN Jun 1983 240 p refs

(Contract NAS3-22492)

(NASA-CR-168076; NAS 1.26:168076) Avail: NTIS HC A11/MF A01 CSCL 09A

The engineering development of a solid state transmitter amplifier operating in the 20 GHz frequency band. The development effort involved a variety of disciplines including IMPATT device development, circulator design, simple and multiple diode circuits designs, and amplifier integration and test.

**N84-11388\*#** Westinghouse Electric Corp., Pittsburgh, Pa.  
**DEVELOPMENT AND FABRICATION OF AN AUGMENTED POWER TRANSISTOR** Final Report, 22 Jul. 1981 - 21 Feb. 1983

M. J. GEISLER, F. E. HILL, and J. A. OSTOP 1 Aug. 1983 65 p refs

(Contract NAS3-22782)

(NASA-CR-168262; NAS 1.26:168262; DYD-10892-CE; REPT-83-9FS-ATRAN-R1) Avail: NTIS HC A04/MF A01 CSCL 09A

The development of device design and processing techniques for the fabrication of an augmented power transistor capable of fast switching and high voltage power conversion is discussed. The major device goals sustaining voltages in the range of 800 to 1000 V at 80 A and 50 A, respectively, at a gain of 14. The transistor switching rise and fall times were both to have been less than 0.5 microseconds. The development of a passivating glass technique to shield the device high voltage junction from moisture and ionic contaminants is discussed as well as the development of an isolated package that separates the thermal and electrical interfaces. A new method was found to alloy the transistors to the molybdenum disc at a relatively low temperature. The measured electrical performance compares well with the predicted optimum design specified in the original proposed design. A 40 mm diameter transistor was fabricated with seven times the emitter area of the earlier 23 mm diameter device. R.J.F.

**N84-11389\*#** National Aeronautics and Space Administration: Lewis Research Center, Cleveland, Ohio.

**HYBRID POWER SEMICONDUCTOR SWITCH** Patent Application

D. Y. CHEN, inventor (to NASA) 30 Sep. 1983 11 p

(NASA-CASE-LEW-13922-1; US-PATENT-APPL-SN-537614)

Avail: NTIS HC A02/MF A01 CSCL 09A

The voltage rating of a bipolar transistor may be greatly extended while at the same time reducing its switching time by operating it in conjunction with FETs in a hybrid circuit. One FET is used to drive the bipolar transistor and an inductive load. Both FETs are turned on or off by a single drive signal of load power, the second FET upon ceasing conduction, rendering one power electrode of the bipolar transistor open. Means provided to dissipate currents which flow after the bipolar transistor is rendered nonconducting. NASA

**N84-13443\*#** Allen-Bradley Co., Torrance, Calif. Power Transistor Components.

**DEVELOPMENT AND FABRICATION OF A HIGH CURRENT, FAST RECOVERY POWER DIODE** Final Report

A. H. BERMAN, V. BALODIS, D. C. DEVANCE, C. E. GAUGH, and E. A. KARLSSON Oct. 1983 70 p refs

(Contract NAS3-23280)

(NASA-CR-168196; NAS 1.26:168196) Avail: NTIS HC A04/MF A01 CSCL 09C

A high voltage ( $V_R = 1200$  V), high current ( $I_F = 150$  A), fast recovery ( $700$  ns) and low forward voltage drop ( $1.5$  V) silicon rectifier was designed and the process developed for its

fabrication. For maximum purity, uniformity and material characteristic stability, neutron transmutation n-type doped float zone silicon is used. The design features a hexagonal chip for maximum area utilization of space available in the DO-8 diode package, PIN diffused junction structure with deep diffused D(+) anode and a shallow high concentration n(+) cathode. With the high temperature glass passivated positive bevel mesa junction termination, the achieved blocking voltage is close to the theoretical limit of the starting material. Gold diffusion is used to control the lifetime and the resulting effect on switching speed and forward voltage tradeoff. For solder reflow assembly, trimetal (Al-Ti-Ni) contacts are used. The required major device electrical characteristics were achieved. Due to the tradeoff nature of forward voltage drop and reverse recovery time, a compromise was reached for these values. Author

**N84-14422\*** National Aeronautics and Space Administration. Lewis Research Center, Cleveland, Ohio.

**ADDITIVE FOR ZINC ELECTRODES** Patent

D. G. SOLTIS, D. W. SHEIBLEY, and W. J. NAGLE, inventors (to NASA) 29 Nov. 1983 4 p Filed 10 Jun. 1981 Supersedes N81-27597 (19 - 18, p 2506)

(NASA-CASE-LEW-13286-1; US-PATENT-4,418,130;

US-PATENT-APPL-SN-272406; US-PATENT-CLASS-429-206;

US-PATENT-CLASS-429-229; US-PATENT-CLASS-252-182.1)

Avail: US Patent and Trademark Office CSCL 10C

A zinc electrode for alkaline cells includes up to about ten percent by weight of  $Ba(OH)_2 \cdot 8H_2O$  with about five percent being preferred. The zinc electrode may or may not be amalgamated with mercury.

Official Gazette of the U.S. Patent and Trademark Office

**N84-15394\*#** National Aeronautics and Space Administration. Lewis Research Center, Cleveland, Ohio.

**PERFORMANCE OF COMPUTER-DESIGNED SMALL-SIZE MULTISTAGE DEPRESSED COLLECTORS FOR A HIGH-PERFORMANCE TRAVELING WAVE TUBE**

P. RAMINS Jan. 1984 24 p refs

(NASA-TP-2248; E-1700; NAS 1.60:2248) Avail: NTIS HC

A02/MF A01 CSCL 09A

Computer designed axisymmetric 2.4-cm-diameter three-, four-, and five-stage depressed collectors were evaluated in conjunction with an octave bandwidth, high-perveance, and high-electronic-efficiency, gridded-gun traveling wave tube (TWT). Spent-beam refocusing was used to condition the beam for optimum entry into the depressed collectors. Both the TWT and multistage depressed collector (MDC) efficiencies were measured, as well as the MDC current, dissipated thermal power, and DC input power distributions, for the TWT operating both at saturation over its bandwidth and over its full dynamic range. Relatively high collector efficiencies were obtained, leading to a very substantial improvement in the overall TWT efficiency. In spite of large fixed TWT body losses (due largely to the 6 to 8 percent beam interception), average overall efficiencies of 45 to 47 percent (for three to five collector stages) were obtained at saturation across the 2.5- to 5.5-GHz operating band. For operation below saturation the collector efficiencies improved steadily, leading to reasonable (20 percent) overall efficiencies as far as 6 dB below saturation. M.G.

**N84-16452\*** National Aeronautics and Space Administration. Lewis Research Center, Cleveland, Ohio.

**LADDER SUPPORTED RING BAR CIRCUIT** Patent

H. G. KOSMAHL, inventor (to NASA) 10 Dec. 1983 6 p Filed 3 Apr. 1981 Supersedes N81-24348 (19 - 15, p 2050)

(NASA-CASE-LEW-13570-1; US-PATENT-4,422,012;

US-PATENT-APPL-SN-251009; US-PATENT-CLASS-315-3.5;

US-PATENT-CLASS-315-3.6; US-PATENT-CLASS-315-39.3;

US-PATENT-CLASS-333-162) Avail: US Patent and Trademark Office CSCL 09C

An improved slow wave circuit especially useful in backward wave oscillators includes a slow wave circuit in a waveguide. The slow wave circuit is comprised of rings disposed between and

attached to respective stubs. The stubs are attached to opposing sidewalls of the waveguide. To the end that opposed, interacting magnetic fields will be established to provide a very high coupling impedance for the slow wave structure, axially orientated bars are connected between rings in alternate spaces and adjacent to the attachment points of stubs. Similarly, axial bars are connected between rings in the spaces which do not include bars and at points adjacent to the attachment of bars.

Official Gazette of the U.S. Patent and Trademark Office

**N84-16458\*#** Texas Univ., Austin. Center for Electromechanics.

**ENERGY STORES AND SWITCHES FOR RAIL-LAUNCHER SYSTEMS Final Report**

W. F. WELDON, R. C. ZOWARKA, and R. A. MARSHALL 1983 95 p refs Original contains color illustrations

(Contract NAG3-303)

(NASA-CR-173249; NAS 1.26:173249) Avail: NTIS HC A05/MF A01 CSCL 09C

An overview of existing switch and power supply technology applicable to space launch, a new candidate pulsed power supply for Earth-to-space rail launcher duty, the inverse railgun flux compressor, and a set of switching experiments to study further the feasibility of Earth-to-space launch are discussed. Author

**N84-16459\*#** Virginia Polytechnic Inst. and State Univ., Blacksburg. Dept. of Electrical Engineering.

**INPUT FILTER COMPENSATION FOR SWITCHING REGULATORS Final Report**

S. S. KELKAR and F. C. LEE 8 Aug. 1983 374 p refs

(Contract NAG3-220)

(NASA-CR-173247; NAS 1.26:173247) Avail: NTIS HC A16/MF A01 CSCL 09A

A novel input filter compensation scheme for a buck regulator that eliminates the interaction between the input filter output impedance and the regulator control loop is presented. The scheme is implemented using a feedforward loop that senses the input filter state variables and uses this information to modulate the duty cycle signal. The feedforward design process presented is seen to be straightforward and the feedforward easy to implement. Extensive experimental data supported by analytical results show that significant performance improvement is achieved with the use of feedforward in the following performance categories: loop stability, audiosusceptibility, output impedance and transient response. The use of feedforward results in isolating the switching regulator from its power source thus eliminating all interaction between the regulator and equipment upstream. In addition the use of feedforward removes some of the input filter design constraints and makes the input filter design process simpler thus making it possible to optimize the input filter. The concept of feedforward compensation can also be extended to other types of switching regulators. Author

**N84-16461\*#** National Aeronautics and Space Administration. Lewis Research Center, Cleveland, Ohio.

**DEVELOPMENT OF AN INSTRUMENT FOR REAL-TIME COMPUTATION OF INDICATED MEAN EFFECTIVE PRESSURE**

W. J. RICE Jan. 1984 22 p refs

(NASA-TP-2238; E-1650; NAS 1.60:2238) Avail: NTIS HC A02/MF A01 CSCL 14B

A new instrument capable of computing in real time the per-cycle indicated mean effective pressure (IMEP) of internal combustion engines and compressors was designed and tested. The values of IMEP obtained with the new instrument were found to be in excellent agreement with values obtained by previous post-run data reduction techniques. Author

**N84-16463\*#** Texas Instruments, Inc., Dallas. Central Research Labs.

**30/20 GHZ SPACECRAFT GAAS FET SOLID STATE TRANSMITTER FOR TRUNKING AND CUSTOMER-PREMISE-SERVICE APPLICATION Final Technical Report, Jul. 1980 - Sep. 1983**

P. SAUNIER and S. NELSON 1 Oct. 1983 84 p

(Contract NAS3-22504)

(NASA-CR-168276; NAS 1.26:168276; TI-08-83-42) Avail: NTIS HC A05/MF A01 CSCL 09C

Sixteen 30 dB 0.5 W amplifier modules were combined to satisfy the requirement for a graceful degradation. If one module fails, the output power drops by only 0.43 dB. Also, by incorporating all the gain stages within the combiner the overall combining efficiency is maximized. A 16 way waveguide divider combiner was developed to minimize the insertion loss associated with such a large corporate feed structure. Tests showed that the 16 way insertion loss was less than 0.5 dB. To minimize loss, a direct transition from waveguide to microstrip, using a finline on duroid substrate, was developed. The FETs fabricated on MBE grown material, demonstrated superior performances. For example, a 600 micrometer device was capable of 320 mW output power with 5 dB gain and 26.6% efficiency at 21 GHz. The 16 module amplifier gave 8.95 W saturated output power with 30 dB gain. The overall efficiency was 9%. The 3 dB bandwidth was 2.5 GHz. At 17.7 GHz the amplifier had 5 W output power and at 20.2 GHz it still had 4.4 W. A.R.H.

**N84-17477\*#** TRW Electronic Systems Group, Redondo Beach, Calif.

**THE 20 GHZ SPACECRAFT FET SOLID STATE TRANSMITTER Final Report**

Jul. 1983 181 p refs

(Contract NAS3-22503)

(NASA-CR-168240; NAS 1.26:168240) Avail: NTIS HC A09/MF A01 CSCL 09A

The engineering development of a solid state transmitter amplifier operating in the 20 GHz frequency band using GaAs field effect transistors (FETs) was detailed. The major efforts include GaAs FET device development, single-ended amplifier stage, balanced amplifier stage, cascaded stage and radial combiner designs, and amplifier integration and test. A multistage GaAs FET amplifier capable of 8.2 W CW output over the 17.9 to 19.1 GHz frequency band was developed. The GaAs FET devices developed represent state of the art FET power device technology. Further device improvements are necessary to increase the bandwidth to 2.5 GHz, improve dc-to-RF efficiency, and increase power capability at the device level. Higher power devices will simplify the amplifier combining scheme, reducing the size and weight of the overall amplifier. Author

**N84-17479\*#** National Aeronautics and Space Administration. Lewis Research Center, Cleveland, Ohio.

**A MATHEMATICAL MODEL FOR THE DOUBLY-FED WOUND ROTOR GENERATOR, PART 2**

F. J. BRADY 1984 8 p refs Proposed for presentation at the Summer Meeting of the Power Eng. Soc., Seattle, 15-20 Jul. 1984; sponsored by IEEE

(Contract DE-AI01-76ET-20320)

(NASA-TM-83581; DOE/NASA/20320-57-PT-2; E-1972-PT-2; NAS 1.15:83581) Avail: NTIS HC A02/MF A01 CSCL 09A

A mathematical analysis of a doubly-fed wound rotor generator is presented. The constraints of constant stator voltage and frequency to the circuit equations were applied and expressions for the currents and voltages in the machine obtained. The derived variables are redefined as direct and quadrature components. In addition, the apparent (complex) power for both the rotor and the stator are derived in terms of these redefined components. S.L.



**N84-17481\*#** Hughes Research Labs., Malibu, Calif.  
**THE 25 KW RESONANT DC/DC POWER CONVERTER Final Report, 28 Sep. 1981 - 28 Oct. 1983**  
 R. R. ROBSON Sep. 1983 147 p refs  
 (Contract NAS3-23159)  
 (NASA-CR-168273; NAS 1.26:168273) Avail: NTIS HC A07/MF A01 CSCL 09C

The feasibility of processing 25-kW of power with a single, transistorized, series resonant converter stage was demonstrated by the successful design, development, fabrication, and testing of such a device which employs four Westinghouse D7ST transistors in a full-bridge configuration and operates from a 250-to-350 Vdc input bus. The unit has an overall worst-case efficiency of 93.5% at its full rated output of 1000 V and 25 A dc. A solid-state dc input circuit breaker and output-transient-current limiters are included in and integrated into the design. Full circuit details of the converter are presented along with the test data. Author

**N84-18536\*#** Westinghouse Research and Development Center, Pittsburgh, Pa.  
**DOUBLE-INJECTION, DEEP-IMPURITY SWITCH DEVELOPMENT Final Report, 23 Dec. 1982 - 23 Oct. 1983**  
 F. A. SELIM and D. W. WHITSON 3 Nov. 1983 39 p refs  
 (Contract NAS3-22247)  
 (NASA-CR-168335; NAS 1.26:168335; REPT-83-9F5-DISQR-R1)  
 Avail: NTIS HC A03/MF A01 CSCL 09A

The overall objective of this program is the development of device design and process techniques for the fabrication of a double-injection, deep-impurity (DI)(2) silicon switch that operates in the 1-10 kV range with conduction current of 10 and 1A, respectively. Other major specifications include a holding voltage of 0 to 5 volts at 1 A anode current, 10 microsecond switching time, and power dissipation of 50 W at 75 C. This report describes work that shows how the results obtained at the University of Cincinnati under NASA Grant NSG-3022 have been applied to larger area and higher voltage devices. The investigations include theoretical, analytical, and experimental studies of device design and processing. Methods to introduce deep levels, such as Au diffusion and electron irradiation, have been carried out to 'pin down' the Fermi level and control device-switching characteristics. Different anode, cathode, and gate configurations are presented. Techniques to control the surface electric field of planar structures used for (DI)(2) switches are examined. Various sections of this report describe the device design, wafer-processing techniques, and various measurements which include ac and dc characteristics, 4-point probe, and spreading resistance. Author

**N84-19708\*#** National Aeronautics and Space Administration, Lewis Research Center, Cleveland, Ohio.  
**HIGH EFFICIENCY IMPATT DIODES FOR 60 GHZ INTERSATELLITE LINK APPLICATIONS**  
 E. J. HAUGLAND 1984 14 p refs Presented at the 10th Communications Satellite Systems Conf., Orlando, Fla., 18-22 Mar. 1984 Sponsored in part by U.S. Air Force Space Div.  
 (NASA-TM-83584; E-1974; NAS 1.15:83584) Avail: NTIS HC A02/MF A01 CSCL 09A

Intersatellite links are expected to play an increasingly important role in future satellite systems. Improved components are required to properly utilize the wide bandwidth allocated for intersatellite link applications around 60 GHz. IMPATT diodes offer the highest potential performance as solid state power sources for a 60 GHz transmitter. Presently available devices do not have the desired power and efficiency. High efficiency, high power IMPATT diodes for intersatellite link applications are being developed by NASA and other government agencies. The development of high efficiency 60 GHz IMPATT diodes by NASA is described. Author

**N84-19709\*#** Oregon Graduate Center for Study and Research, Beaverton.  
**EVALUATION OF SINGLE CRYSTAL LAB6 CATHODES FOR USE IN A HIGH FREQUENCY BACKWARD WAVE OSCILLATOR TUBE Interim Report, 1 Jul. 1983 - 1 Jan. 1984**  
 L. W. SWANSON, P. R. DAVIS, and G. A. SCHWIND 1 Jan. 1984 61 p refs  
 (Contract NAG3-434)  
 (NASA-CR-173343; NAS 1.26:173343) Avail: NTIS HC A04/MF A01 CSCL 09C

The results of thermionic emission and evaporation studies of single crystal LaB6 cathodes are given. A comparison between the (100), (210) and (310) crystal planes shows the (310) and (210) planes to possess a work function approx 0.2 eV lower than (100). This translates into a significant increase in current density, J, at a specified temperature. Comparison with a state-of-the-art impregnated dispenser cathode shows that LaB6 (310) is a superior cathode in nearly all respects except operating temperature at j 10 A/sq cm. The 1600 K thermionic and room temperature retarding potential work functions for LaB6 (310) are 2.42 and 2.50 respectively. Author

**N84-21376\*#** EIC, Inc., Newton, Mass.  
**MODERATE TEMPERATURE RECHARGEABLE NANIS2 CELLS**  
 K. M. ABRAHAM -/n Brookhaven National Lab. Proc. of the Conf. on High Temp Solid Oxide Electrolytes, Vol. 2 p 95-105 Oct. 1983 refs  
 (Contract NAS3-21726)  
 Avail: NTIS HC A07/MF A01 CSCL 09C

A rechargeable sodium battery of the configuration, liquid Na/beta double prime -Al2O3/molten NaAlCl4, NiS2, operating in the temperature range of 170 to 190 C, is described. This battery is capable of delivering or = to 50 W-hr/lb and 1000 deep discharge/charge cycles. Author

**N84-21803\*#** National Aeronautics and Space Administration, Lewis Research Center, Cleveland, Ohio.  
**A TWT AMPLIFIER WITH A LINEAR POWER TRANSFER CHARACTERISTIC AND IMPROVED EFFICIENCY**  
 H. G. KOSMAHL and J. C. PETERSON (Hughes Aircraft Co., Torrance, Calif.) 1984 12 p refs Proposed for presentation at the 10th Commun. Satellite Systems Conf., Orlando, Fla., 18-22 Mar. 1984; sponsored by AIAA  
 (NASA-TM-83590; E-1793; NAS 1.15:83590) Avail: NTIS HC A02/MF A01 CSCL 09A

A novel method called 'Dynamic Velocity Taper' to linearize the Pout versus Pin transfer characteristic that does not require any extraneous circuitry or tuning, has large bandwidth capabilities (10 percent) and offers also an increase in the intrinsic traveling wave tube (TWT) efficiency by 1 to 2 dB is described. In addition, the method permits the TWT to be operated at or near the synchronous voltage (b plus or minus o) which produces a flat small and large signal gain responses and low AM to PM conversion. The physics of the method and experimental verification are given. The implementation should have a significant impact on TWT performance and increase the channel capacity of communication satellites. R.J.F.

**N84-22889\*#** Hughes Aircraft Co., El Segundo, Calif. Space Communications Group.  
**ADVANCED NICKEL-HYDROGEN CELL CONFIGURATION STUDY Final Report**  
 Sep. 1983 77 p refs  
 (Contract NAS3-22249)  
 (NASA-CR-173417; NAS 1.26:173417) Avail: NTIS HC A05/MF A01 CSCL 10C

Long-term trends in the evolution of space power technology point toward increased payload power demand which in turn translates into both higher battery system charge storage capability and higher operating voltages. State of the art nickel-hydrogen cells of the 50 to 60 Wh size, packaged in individual pressure vessels, are capable of meeting the required cycle life for a wide range of anticipated operating conditions; however, they provided

several drawbacks to battery system integrated efforts. Because of size, high voltage/high power systems require integrating hundreds of cells into the operating system. Packaging related weight and volume inefficiencies degrade the energy density and specific energy of individual cells currently at 30 Wh/cudm and 40 Wh/kg respectively. In addition, the increased parts count and associated handling significantly affect the overall battery related costs. Spacecraft battery systems designers within industry and Government realize that to reduce weight, volume, and cost requires increases in the capacity of nickel-hydrogen cells.

Author

**N84-22890\*#** National Aeronautics and Space Administration. Lewis Research Center, Cleveland, Ohio.

**RADIATION DAMAGE AND DEFECT BEHAVIOR IN ION-IMPLANTED, LITHIUM COUNTERDOPED SILICON SOLAR CELLS**

I. WEINBERG, S. MEHTA, and C. K. SWARTZ 1984 11 p refs Presented at the 17th Photovoltaic Spec. Conf., Kissimmee, Fla., 1-4 May 1984; sponsored by IEEE (NASA-TM-83646; E-2091; NAS 1.15:83646) Avail: NTIS HC A02/MF A01 CSCL 10A

Boron doped silicon n+p solar cells were counterdoped with lithium by ion implantation and the resultant n+p cells irradiated by 1 MeV electrons. The function of fluence and a Deep Level Transient Spectroscopy (DLTS) was studied to correlate defect behavior with cell performance. It was found that the lithium counterdoped cells exhibited significantly increased radiation resistance when compared to boron doped control cells. It is concluded that the annealing behavior is controlled by dissociation and recombination of defects. The DLTS studies show that counterdoping with lithium eliminates at least three deep level defects and results in three new defects. It is speculated that the increased radiation resistance of the counterdoped cells is due primarily to the interaction of lithium with oxygen, single vacancies and divacancies and that the lithium-oxygen interaction is the most effective in contributing to the increased radiation resistance

E.A.K.

**N84-22891\*#** National Aeronautics and Space Administration. Lewis Research Center, Cleveland, Ohio.

**ADVANCES IN SOLID STATE SWITCHGEAR TECHNOLOGY FOR LARGE SPACE POWER SYSTEMS**

G. R. SUNDBERG 1984 20 p refs To be presented at the 19th Intersoc. Energy Conversion Eng. Conf., San Francisco, 19-24 Aug. 1984

(NASA-TM-83652; E-2096; NAS 1.15:83652) Avail: NTIS HC A02/MF A01 CSCL 09C

High voltage solid state remote power controllers (RPC's) and the required semiconductor power switches to provide baseline technology for large, high power distribution systems in the space station, all electric airplane and other advanced aerospace applications were developed. The RPC's were developed for dc voltages from 28 to 1200 V and ac voltages of 115, 230, and 440 V at frequencies of 400 Hz to 20 kHz. The benefits and operation of solid state RPC's and highlights of several developments to bring the RPC to technology readiness for future aerospace needs are examined. The 28 V dc Space Shuttle units, three RPC types at 120 V dc, two at 270/300 V dc, two at 230 V ac and several high power RPC models at voltages up to 1200 V dc with current ratings up to 100 A are reviewed. New technology programs to develop a new family of (DI)2 semiconductor switches and 20 kHz, 440 V ac RPC's are described.

E.A.K.

**N84-22892\*#** National Aeronautics and Space Administration. Lewis Research Center, Cleveland, Ohio.

**DEVELOPMENT OF HIGH FREQUENCY LOW WEIGHT POWER MAGNETICS FOR AEROSPACE POWER SYSTEMS**

G. E. SCHWARZE 1984 13 p refs To be presented at the 19th Intersoc. Energy Conversion Eng. Conf., San Francisco, 19-24 Aug. 1984

(NASA-TM-83656; E-2043; NAS 1.15:83656) Avail: NTIS HC A02/MF A01 CSCL 09C

A dominant design consideration in the development of space type power magnetic devices is the application of reliable thermal control methods to prevent device failure which is due to excessive temperature rises and hot temperatures in critical areas. The resultant design must also yield low weight, high efficiency, high reliability and maintainability, and long life. The weight savings and high efficiency that results by going to high frequency and unique thermal control techniques is demonstrated by the development of a 25 kVA, 20 kHz space type transformer under the power magnetics technology program. Work in the area of power rotary transformer is also discussed.

E.A.K.

**N84-23841\*#** Analox Corp., Cleveland, Ohio.

**USERS' MANUAL FOR COMPUTER PROGRAM FOR THREE-DIMENSIONAL ANALYSIS OF COUPLER-CAVITY TRAVELING WAVE TUBES Final Report**

T. A. O'MALLEY Jan. 1984 66 p refs

(Contract NAS3-23293)

(NASA-CR-168269; E-1930; NAS 1.26:168269) Avail: NTIS HC A04/MF A01 CSCL 09A

The use of the coupled cavity traveling wave tube for space communications has led to an increased interest in improving the efficiency of the basic interaction process in these devices through velocity resynchronization and other methods. A flexible, three dimensional, axially symmetric, large signal computer program was developed for use on the IBM 370 time sharing system. A users' manual for this program is included.

M.A.C.

**N84-24973\*#** TRW Electronic Systems Group, Redondo Beach, Calif.

**K-BAND LATCHING SWITCHES Final Report**

W. S. PIOTROWSKI and J. E. RAUE May 1984 77 p

(Contract NAS3-22336)

(NASA-CR-168253; NAS 1.26:168253; REPT-11982) Avail: NTIS HC A05/MF A01 CSCL 09A

Design, development, and tests are described for two single-pole-double-throw latching waveguide ferrite switches: a K-band switch in WR-42 waveguide and a Ka-band switch in WR-28 waveguide. Both switches have structurally simple junctions, mechanically interlocked without the use of bonding materials; they are impervious to the effects of thermal, shock, and vibration stresses. Ferrite material for the Ka-band switch with a proper combination of magnetic and dielectric properties was available and resulted in excellent low loss, wideband performance. The high power handling requirement of the K-band switch limited the choice of ferrite to nickel-zinc compositions with adequate magnetic properties, but with too low relative dielectric constant. The relative dielectric constant determines the junction dimensions for given frequency responses. In this case the too low value unavoidably leads to a larger than optimum junction volume, increasing the insertion loss and restricting the operating bandwidth. Efforts to overcome the materials-related difficulties through the design of a composite junction with increased effective dielectric properties efforts to modify the relative dielectric constant of nickel-zinc ferrite are examined.

A.R.H.

**N84-24974\*#** Virginia Univ., Charlottesville. Dept. of Electrical Engineering.

**DESIGN CONSIDERATIONS FOR A MONOLITHIC, GAAS, DUAL-MODE, QPSK/QASK, HIGH-THROUGHPUT RATE TRANSCIVER M.S. Thesis**

R. A. KOT, J. D. OLIVER, and S. G. WILSON Jun. 1984 207 p refs

(Contract NAG3-316)

(NASA-CR-173560; NAS 1.26:173560; UVA/528219/EE84103)

Avail: NTIS HC A10/MF A01 CSCL 09C

A monolithic, GaAs, dual mode, quadrature amplitude shift keying and quadrature phase shift keying transceiver with one and two billion bits per second data rate is being considered to achieve a low power, small and ultra high speed communication system for satellite as well as terrestrial purposes. Recent GaAs integrated circuit achievements are surveyed and their constituent device types are evaluated. Design considerations, on an elemental level, of the entire modem are further included for monolithic realization with practical fabrication techniques. Numerous device types, with practical monolithic compatibility, are used in the design of functional blocks with sufficient performances for realization of the transceiver. A.R.H.

**N84-24975\*#** Virginia Polytechnic Inst. and State Univ., Blacksburg. Dept. of Electrical Engineering.

**INPUT FILTER COMPENSATION FOR SWITCHING REGULATORS Final Report**

F. C. LEE 1984 368 p refs

(Contract NAG3-220)

(NASA-CR-173557; NAS 1.26:173557) Avail: NTIS HC A16/MF A01 CSCL 09C

Problems caused by input filter interaction and conventional input filter design techniques are discussed. The concept of feedforward control is modeled with an input filter and a buck regulator. Experimental measurement and comparison to the analytical predictions is carried out. Transient response and the use of a feedforward loop to stabilize the regulator system is described. Other possible applications for feedforward control are included. M.A.C.

**N84-25926\*#** National Aeronautics and Space Administration. Lewis Research Center, Cleveland, Ohio.

**LOW-FREQUENCY SWITCHING VOLTAGE REGULATORS FOR TERRESTRIAL PHOTOVOLTAIC SYSTEMS**

R. DELOMBARD May 1984 27 p refs

(Contract DE-A101-79ET-20485)

(NASA-TM-83625; E-2060; DOE/NASA/20485-16; NAS 1.15:83625) Avail: NTIS HC A03/MF A01 CSCL 09A

The photovoltaic technology project and the stand alone applications project are discussed. Two types of low frequency switching type regulators were investigated. The design, operating characteristics and field application of these regulators is described. The regulators are small in size, low in cost, very low in power dissipation, reliable and allow considerable flexibility in system design. E.A.K.

**N84-27974\*** National Aeronautics and Space Administration. Lewis Research Center, Cleveland, Ohio.

**DIELECTRIC BASED SUBMILLIMETER BACKWARD WAVE OSCILLATOR CIRCUIT Patent**

H. G. KOSMAHL, inventor (to NASA) 10 Jul. 1984 6 p Filed 13 Oct. 1982 Supersedes N83-17802 (21 - 08, p 1176)

(NASA-CASE-LEW-13736-1; US-PATENT-4,459,562;

US-PATENT-APPL-SN-434084; US-PATENT-CLASS-331-82;

US-PATENT-CLASS-315-3.6; US-PATENT-CLASS-315-39.3;

US-PATENT-CLASS-333-162) Avail: US Patent and Trademark Office CSCL 09C

A ladder circuit especially useful in backward wave oscillators operating in the 500 GHz to 2000 GHz range has a waveguide with transversely orientated slabs which contact an upper wall of the waveguide. The edges of the slabs adjacent to the physical center of waveguide are curved segments and stubs of electrically conductive, nonmagnetic material. The ends of slabs include metal

layers at opposite ends to provide a conductive leakage path. A ridge bar is attached to the inside of the bottom wall of the waveguide and includes a concave upper surface which partially straddles the electron beam. The novelty of the invention lies in the ladder structure compared of thin, vapor deposited rungs supported on the edge of diamond slabs; each rung having a curved segment which straddles the electron beam together with a ridge bar which also straddles the electron-beam.

Official Gazette of the U.S. Patent and Trademark Office

**N84-29084\*#** National Aeronautics and Space Administration. Lewis Research Center, Cleveland, Ohio.

**OXYGEN RECOMBINATION IN INDIVIDUAL PRESSURE VESSEL NICKEL-HYDROGEN BATTERIES Patent Application**

J. J. SMITHRICK, inventor (to NASA) 27 Jun. 1984 12 p

(NASA-CASE-LEW-13822-1; US-PATENT-APPL-SN-625077)

Avail: NTIS HC A02/MF A01 CSCL 10C

In a metal hydrogen cell of the type including a number of electrical cell units in back-to-back relationship and which may be lined with a wick, one or more catalyzed sites are provided on the inner surface of the cell. Separators between the respective metal and hydrogen electrodes of each cell unit have gas directing notches around their peripheries to facilitate the desired movement of gasses within the metal-hydrogen cell. Any two metal electrodes separated by a gas screen and including apertures which may be required to accommodate compression means such as bolts, are provided with gas tight seals between the electrodes at each aperture. The sealing means may be ring of rubber or elastomeric material which is somewhat compressible but non-reactive with other materials in the cell. NASA

**N84-31512\*#** National Aeronautics and Space Administration. Lewis Research Center, Cleveland, Ohio.

**DUAL ION BEAM DEPOSITION OF CARBON FILMS WITH DIAMONDLIKE PROPERTIES**

M. J. MIRTICH, D. M. SWEC, and J. C. ANGUS (Case Western Reserve Univ.) 1984 20 p refs Presented at the 11th Intern. Conf. on Met. Coatings, San Diego, Calif., 9-13 Apr. 1984 sponsored by the American Vacuum Society

(NASA-TM-83743; E-2080; NAS 1.15:83743) Avail: NTIS HC A02/MF A01 CSCL 09C

A single and dual ion beam system was used to generate amorphous carbon films with diamond like properties. A methane/argon mixture at a molar ratio of 0.28 was ionized in the low pressure discharge chamber of a 30-cm-diameter ion source. A second ion source, 8 cm in diameter was used to direct a beam of 600 eV Argon ions on the substrates (fused silica or silicon) while the deposition from the 30-cm ion source was taking place. Nuclear reaction and combustion analysis indicate H/C ratios for the films to be 1.00. This high value of H/C, it is felt, allows the films to have good transmittance. The films were impervious to reagents which dissolve graphitic and polymeric carbon structures. Although the measured density of the films was approximately 1.8 gm/cu cm, a value lower than diamond, the films exhibited other properties that were relatively close to diamond. These films were compared with diamondlike films generated by sputtering a graphite target. Autho

**N84-31513\*#** National Aeronautics and Space Administration. Lewis Research Center, Cleveland, Ohio.

**THE EFFECTS OF LITHIUM COUNTERDOPING ON RADIATION DAMAGE AND ANNEALING IN N(+)-P SILICON SOLAR CELLS**

I. WEINBERG, H. W. BRANDHORST, JR., S. MEHTA (Cleveland State Univ., Ohio), and C. K. SWARTZ 1984 12 p refs Presented at the 4th European Symp. on Photovoltaic Generators in Space, Cannes, France, 18-20 Sep. 1984

(NASA-TM-83755; E-2243; NAS 1.15:83755) Avail: NTIS HC A02/MF A01 CSCL 09A

Boron-doped silicon n(+)-p solar cells were counterdoped with lithium by ion implantation and the resultant n(+)-p cells irradiated by 1 MeV electrons. Performance parameters were determined as a function of fluence and a deep level transient spectroscopy (DLTS) study was conducted. The lithium counterdoped cell:

exhibited significantly increased radiation resistance when compared to boron doped control cells. Isochronal annealing studies of cell performance indicate that significant annealing occurs at 100 C. Isochronal annealing of the deep level defects showed a correlation between a single defect at  $E_{\text{sub}} \approx 0.43$  eV and the annealing behavior of short circuit current in the counterdoped cells. The annealing behavior was controlled by dissociation and recombination of this defect. The DLTS studies showed that counterdoping with lithium eliminated three deep level defects and resulted in three new defects. The increased radiation resistance of the counterdoped cells is due to the interaction of lithium with oxygen, single vacancies and divacancies. The lithium-oxygen interaction is the most effective in contributing to the increased radiation resistance. Author

**N84-31514\***# Eaton Corp., Southfield, Mich. Engineering and Research Center.  
**AC PROPULSION SYSTEM FOR AN ELECTRIC VEHICLE, PHASE 2 Interim Report**  
 J. M. SLICKER Jun. 1983 287 p  
 (Contract DEN3-211)  
 (NASA-CR-168244; DOE/NASA/0211-1; NAS 1.26:168244; ERC-TR-83024) Avail: NTIS HC A13/MF A01 CSCL 09C

A second-generation prototype ac propulsion system for a passenger electric vehicle was designed, fabricated, tested, installed in a modified Mercury Lynx vehicle and track tested at the Contractor's site. The system consisted of a Phase 2, 18.7 kw rated ac induction traction motor, a 192-volt, battery powered, pulse-width-modulated, transistorized inverter packaged for under rear seat installation, a 2-axis, 2-speed, automatically-shifted mechanical transaxle and a microprocessor-based powertrain/vehicle controller. A diagnostics computer to assist tuning and fault finding was fabricated. Dc-to-mechanical-system efficiency varied from 78% to 82% as axle speed/torque ranged from 159 rpm/788 nm to 65 rpm/328 nm. Track test efficiency results suggest that the ac system will be equal or superior to dc systems when driving urban cycles. Additional short-term work is being performed under a third contract phase (AC-3) to raise transaxle efficiency to predicted levels, and to improve starting and shifting characteristics. However, the long-term challenge to the system's viability remains inverter cost. A final report on the Phase 2 system, describing Phase 3 modifications, will be issued at the conclusion of AC-3. Author

**N84-32678\***# National Aeronautics and Space Administration. Lewis Research Center, Cleveland, Ohio. Dept. of Electrical Engineering.  
**A STUDY OF THE HIGH FREQUENCY LIMITATIONS OF SERIES RESONANT CONVERTERS** Technical Report, 1 Sep. 1981 - 31 Aug. 1982  
 T. A. STUART and R. J. KING 20 Sep. 1982 78 p refs  
 (Contract NSG-3281)  
 (NASA-CR-173868; NAS 1.26:173868) Avail: NTIS HC A05/MF A01 CSCL 09C

A transformer induced oscillation in series resonant (SR) converters is studied. It may occur in the discontinuous current mode. The source of the oscillation is an unexpected resonant circuit formed by normal resonance components in series with the magnetizing inductance of the output transformers. The methods for achieving cyclic stability are: to use a half bridge SR converter where  $Q \geq 0.5$ .  $Q$  should be as close to 1.0 as possible. If  $0.5 < Q < 1.0$ , the instability will be avoided if  $\psi \leq 2/3$ . The second objective was to investigate a power field effect transistor (FET) version of the SR converter capable of operating at frequencies above 100 KHz, to study component stress and losses at various frequencies. S.B.

**N84-32682\***# Michigan State Univ., East Lansing. Coll. of Engineering  
**SPATIAL ELECTRON DENSITY AND ELECTRIC FIELD STRENGTH MEASUREMENTS IN MICROWAVE CAVITY EXPERIMENTS**  
 M. PETERS, J. ROGERS (Lincoln Lab., MIT), S. WHITEHAIR, J. ASMUSSEN, and R. KERBER 1984 6 p refs  
 (Contract NAG3-305)  
 (NASA-CR-173907; NAS 1.26:173907) Avail: NTIS HC A02/MF A01 CSCL 09C

Measurements of electron density and electric field strength have been made in an argon plasma contained in a resonant microwave cavity at 2.45 GHz. Spatial measurements of electron density,  $n_{\text{sub e}}$ , are correlated with fluorescence observations of the discharge. Measurements of  $n_{\text{sub e}}$  were made with Stark broadening and compared with  $n_{\text{sub 3}}$  calculated from measured plasma conductivity. Additional measurements of  $n_{\text{sub 3}}$  as a function of pressure and in mixtures of argon and oxygen are presented for pressures from 10 Torr to 1 atm. Measurements in flowing gases and in static systems are presented. In addition, limitations of these measurements are identified. Author

**N84-33663\*** National Aeronautics and Space Administration. Lewis Research Center, Cleveland, Ohio.  
**SIMPLIFIED DC TO DC CONVERTER Patent**  
 R. P. GRUBER, inventor (to NASA) 7 Aug. 1984 9 p Filed 14 Apr. 1982 Supersedes N82-24432 (20 - 15, p 2079)  
 (NASA-CASE-LEW-13495-1; NAS 1.71:LEW-13495-1; US-PATENT-4,464,710; US-PATENT-APPL-SN-368188; US-PATENT-CLASS-363-22; US-PATENT-CLASS-363-49; US-PATENT-CLASS-323-901) Avail: US Patent and Trademark Office CSCL 09A

A dc to dc converter which can start with a shorted output and which regulates output voltage and current is described. Voltage controlled switches directed current through the primary of a transformer the secondary of which includes virtual reactance. The switching frequency of the switches is appropriately varied to increase the voltage drop across the virtual reactance in the secondary winding to which there is connected a low impedance load. A starting circuit suitable for voltage switching devices is provided.

Official Gazette of the U.S. Patent and Trademark Office

**N84-33670\***# National Aeronautics and Space Administration. Lewis Research Center, Cleveland, Ohio.  
**REGENERATIVE HYDROGEN-OXYGEN FUEL CELL-ELECTROLYZER SYSTEMS FOR ORBITAL ENERGY STORAGE**  
 D. W. SHEIBLEY In NASA. Goddard Space Flight Center The 1983 Goddard Space Flight Center Battery Workshop p 23-42 Sep. 1984 refs  
 Avail: NTIS HC A23/MF A01 CSCL 10C

Fuel cells have found application in space since Gemini. Over the years technology advances have been factored into the mainstream hardware programs. Performance levels and service lives have been gradually improving. More recently, the storage application for fuel cell-electrolyzer combinations are receiving considerable emphasis. The regenerative system application described here is part of a NASA Fuel Cell Program which was developed to advance the fuel cell and electrolyzer technology required to satisfy the identified power generation and energy storage need of the Agency for space transportation and orbital applications to the year 2000. Author

**N84-33702\*#** National Aeronautics and Space Administration. Lewis Research Center, Cleveland, Ohio.

**TEST RESULTS OF A TEN CELL BIPOLAR NICKEL-HYDROGEN BATTERY**

R. L. CATALDO *In* NASA. Goddard Space Flight Center The 1983 Goddard Space Flight Center Battery Workshop p 507-521 Sep. 1984 refs

Avail: NTIS HC A23/MF A01 CSCL 10C

A study was initiated to design and evaluate a new design concept for nickel-hydrogen cells. This concept involved constructing a battery in a bipolar stack with cells consisting of a one plate for each nickel and hydrogen electrode. Preliminary designs at the system level of this concept promised improvements in both volumetric and gravimetric energy densities, thermal management, life extension, costs, and peak power capability over more conventional designs. Test results were most encouraging. This prototype battery, built with less than ideal components and hardware, exceeded expectations. A total of 2000 LEO cycles at 80 percent depth of discharge were accrued. A cycle life goal of 30,000 cycles appears achievable with minor design changes. These improvements include advanced technology nickel electrodes, insulated bipolar plates and specifically designed frames to minimize shunt currents. The discharge rate capability of this design exceeds 25C. At the 10C discharge rate, 80% of the battery capacity can be withdrawn in six minutes. This data shows that the bipolar design is well suited for those applications requiring high peak power pulses. R.J.F.

**N84-33715\*#** LNR Communications, Inc., Hauppauge, N. Y. **THE 20 GHZ SOLID STATE TRANSMITTER DESIGN, IMPATT DIODE DEVELOPMENT AND RELIABILITY ASSESSMENT Final Report**

S. PICONE, Y. CHO, and J. R. ASMUS Jun. 1984 503 p (Contract NAS3-22491)

(NASA-CR-174716; NAS 1.26:174716, LNR-300) Avail: NTIS HC A22/MF A01 CSCL 09A

A single drift gallium arsenide (GaAs) Schottky barrier IMPATT diode and related components were developed. The IMPATT diode reliability was assessed. A proof of concept solid state transmitter design and a technology assessment study were performed. The transmitter design utilizes technology which, upon implementation, will demonstrate readiness for development of a POC model within the 1982 time frame and will provide an information base for flight hardware capable of deployment in a 1985 to 1990 demonstrational 30/20 GHz satellite communication system. Life test data for Schottky barrier GaAs diodes and grown junction GaAs diodes are described. The results demonstrate the viability of GaAs IMPATTs as high performance, reliable RF power sources which, based on the recommendation made herein, will surpass device reliability requirements consistent with a ten year spaceborne solid state power amplifier mission. B.G.

**N84-34675\*#** Illinois Univ., Urbana. Electromagnetic Communications Lab.

**MONOLITHIC MICROWAVE INTEGRATED CIRCUIT DEVICES FOR ACTIVE ARRAY ANTENNAS Final Report, 21 May - 20 Aug. 1984**

R. MITTRA 20 Aug. 1984 36 p refs

(Contract NAG3-420)

(NASA-CR-173981; NAS 1.26:173981) Avail: NTIS HC A03/MF A01 CSCL 09C

Two different aspects of active antenna array design were investigated. The transition between monolithic microwave integrated circuits and rectangular waveguides was studied along with crosstalk in multiconductor transmission lines. The boundary value problem associated with a discontinuity in a microstrip line is formulated. This entailed, as a first step, the derivation of the propagating as well as evanescent modes of a microstrip line. The solution is derived to a simple discontinuity problem: change in width of the center strip. As for the multiconductor transmission line problem. A computer algorithm was developed for computing the crosstalk noise from the signal to the sense lines. The

computation is based on the assumption that these lines are terminated in passive loads. R.S.F.

## 34

## FLUID MECHANICS AND HEAT TRANSFER

Includes boundary layers; hydrodynamics; fluidics; mass transfer; and ablation cooling.

**A84-13237\*#** Michigan State Univ., East Lansing.

**MODELING OF TRANSIENT TWO-COMPONENT FLOW USING A FOUR-POINT IMPLICIT METHOD**

D. C. WIGGERT (Michigan State University, East Lansing, MI), C. S. MARTIN, M. NAGHASH (Georgia Institute of Technology, Atlanta, GA), and P. V. RAO (NASA, Lewis Research Center, Cleveland, OH) *IN*: Numerical methods for fluid transient analysis; Proceedings of the Applied Mechanics, Bioengineering, and Fluids Engineering Conference, Houston, TX, June 20-22, 1983. New York, American Society of Mechanical Engineers, 1983, p. 23-28. Research supported by the Electric Power Research Institute. refs

The four-point, centered implicit scheme that is extensively used in open channel flow simulation is shown to be applicable to rapid and slow pressure transient problems in conduits with nearly single phase and two-phase flows. It is only necessary to choose the proper weighting factor value, theta, of the Courant number. For rapid pressure transients such as waterhammer, the implicit method can yield reasonable results with limited numerical dispersion and attenuation if theta is only slightly greater than the critical value of 0.5. For slower pressure gradients in single and two-phase flows, reasonable numerical solutions may be achieved for Courant number values as high as 20. O.C.

**A84-13239\*#** Case Western Reserve Univ., Cleveland, Ohio.

**INTERNAL HEAT TRANSFER COEFFICIENTS OF POROUS METALS**

K. K. KAR and A. DYBBS (Case Western Reserve University, Cleveland, OH) *IN*: Heat transfer in porous media; Proceedings of the Winter Annual Meeting, Phoenix, AZ, November 14-19, 1982. New York, American Society of Mechanical Engineers (Heat Transfer Symposia Series. HTD Volume 22), 1982, p. 81-91. refs

(Contract NSG-3040; NSF ENG-78-17782)

The internal heat transfer coefficients of porous metals have been experimentally determined in order to develop correlations between approximately defined Nusselt and Reynolds numbers. Scaled-up models of porous materials, and actual porous metal specimens, were subjected to countercurrent heat and mass transfer boundary conditions. Solid and gas phase temperatures were measured for both the scaled-up models and the actual porous metal specimens. On the basis of these measurements, the average internal heat transfer coefficient was evaluated, and a correlation between the Nusselt and Reynolds numbers was derived. O.C.

**A84-13311\*** Carnegie-Mellon Univ., Pittsburgh, Pa.

**TURBULENT FLOW FIELD CALCULATIONS IN AN INTERNAL COMBUSTION ENGINE EQUIPPED WITH TWO VALVES**

J. I. RAMOS (Carnegie-Mellon University, Pittsburgh, PA) and M. H. CARPENTER *IN*: Numerical methods in laminar and turbulent flow; Proceedings of the Third International Conference, Seattle, WA, August 8-11, 1983. Swansea, Wales, Pineridge Press, 1983, p. 1137-1147. refs

(Contract NAG3-21)

**A84-13495\*** National Aeronautics and Space Administration. Lewis Research Center, Cleveland, Ohio.

**BOUNDARY CONDITIONS FOR THE SOLUTION OF COMPRESSIBLE NAVIER-STOKES EQUATIONS BY AN IMPLICIT FACTORED METHOD**

T. I.-P. SHIH (NASA, Lewis Research Center, Cleveland, OH), G. E. SMITH, G. S. SPRINGER (Michigan, University, Ann Arbor, MI), and Y. RIMON (Ministry of Defence, Computer Science Dept., Haifa, Israel) *Journal of Computational Physics* (ISSN 0021-9991), vol. 52, Oct. 1983, p. 54-79. refs

A method is presented for formulating the boundary conditions in implicit finite-difference form needed for obtaining solutions to the compressible Navier-Stokes equations by the Beam and Warming implicit factored method. The usefulness of the method was demonstrated (a) by establishing the boundary conditions applicable to the analysis of the flow inside an axisymmetric piston-cylinder configuration and (b) by calculating velocities and mass fractions inside the cylinder for different geometries and different operating conditions. Stability, selection of time step and grid sizes, and computer time requirements are discussed in reference to the piston-cylinder problem analyzed. Author

**A84-13564\*#** Dynamics Technology, Inc., Torrance, Calif.

**TURBULENCE MEASUREMENTS IN CONFINED JETS USING A ROTATING SINGLE-WIRE PROBE TECHNIQUE**

S. I. JANJUA, D. K. MCLAUGHLIN (Dynamics Technology, Inc., Torrance, CA), D. G. LILLEY (Oklahoma State University, Stillwater, OK), and T. W. JACKSON *AIAA Journal* (ISSN 0001-1452), vol. 21, Dec. 1983, p. 1609, 1610. USAF-supported research. (Contract NAG3-74)

Previously cited in issue 18, p. 2885, Accession no. A82-37710

**A84-16828\*** Wichita State Univ., Kans.

**STREAMWISE COMPUTATION OF THREE-DIMENSIONAL PARABOLIC FLOWS**

M. S. GREYWALL (Wichita State University, Wichita, KS) *Computer Methods in Applied Mechanics and Engineering* (ISSN 0045-7825), vol. 36, Jan. 1983, p. 71-93. refs (Contract NSG-3186)

A new approach to calculate three-dimensional parabolic flows is presented. The flow field is computed by calculating velocity along a set of streamlines. The dependent variables commonly used in the computation of three-dimensional flows are the three velocity components. In contrast, the dependent variables in the present approach are the streamwise velocity and the two coordinates, in the cross-stream plane, of the chosen streamlines. The streamwise velocity is calculated from the finite difference equations obtained by applying Euler's momentum theorem to streamtubes constructed around the chosen streamlines; the streamline coordinates are calculated from the conservation of mass. Results of the calculations, based on the present approach, are compared with the experimental data for flow through rectangular ducts; the agreement is satisfactory. Author

**A84-17834\*#** National Aeronautics and Space Administration. Lewis Research Center, Cleveland, Ohio.

**HEAT TRANSFER DISTRIBUTIONS AROUND NOMINAL ICE ACCRETION SHAPES FORMED ON A CYLINDER IN THE NASA LEWIS ICING RESEARCH TUNNEL**

G. J. VAN-FOSSSEN, R. J. SIMONEAU, W. A. OLSEN, and R. J. SHAW (NASA, Lewis Research Center, Cleveland, OH) *American Institute of Aeronautics and Astronautics, Aerospace Sciences Meeting, 22nd, Reno, NV, Jan. 9-12, 1984. 18 p. refs* (AIAA PAPER 84-0017)

Local heat transfer coefficients were obtained on irregular cylindrical shapes which typify the accretion of ice on circular cylinders in cross flow. The shapes were 2, 5, and 15 min accumulations of glaze ice and 15 min accumulation of rime ice. These icing shapes were averaged axially to obtain a nominal shape of constant cross section for the heat transfer tests. Heat transfer coefficients were also measured around the cylinder with no ice accretion. The models were run in a 15.2 x 68.6 cm (6 x

27 in.) wind tunnel at several velocities. The models were also run with a turbulence producing grid which gave about 3.5 percent turbulence. The effect of roughness was also simulated with sand grains glued to the surface. Results are presented as Nusselt number versus angle from the stagnation line for the smooth and rough models for both high and low levels of free stream turbulence. Roughness of the surface in the region prior to flow separation plays a major role in determining the heat transfer distribution. Free stream turbulence does not affect the distribution of heat transfer in this region but raises the level by a nearly uniform amount. For the rime shape, roughness had a larger effect in the near wedge shaped region past the initial separation point. Author

**A84-17835\*#** Tennessee Univ., Knoxville.

**MEASUREMENTS OF LOCAL CONVECTIVE HEAT TRANSFER COEFFICIENTS ON ICE ACCRETION SHAPES**

R. V. ARIMILLI, E. G. KESHOCK (Tennessee, University, Knoxville, TN), and M. E. SMITH (USAF, Arnold Engineering and Development Center, Arnold Air Force Station, TN) *American Institute of Aeronautics and Astronautics, Aerospace Sciences Meeting, 22nd, Reno, NV, Jan. 9-12, 1984. 13 p. refs*

(Contract NAG3-83)

(AIAA PAPER 84-0018)

The thin-skin heat rate technique was used to determine local convective heat transfer coefficients for four representative ice accretion shapes. The shapes represented three stages of glaze ice formation and one rime ice formation; the ice models had varying degrees of surface roughness. In general, convective heat transfer was higher in regions where the model's surfaces were convex and lower in regions where the surfaces were concave. The effect of roughness was different for the glaze and rime ice shapes. On the glaze ice shapes, roughness increased the maximum Nu by 80 percent, but the other Nu values were virtually unchanged. On the rime ice shape, the Nu numbers near the stagnation point were unchanged. The maximum Nu value increased by 45 percent, and the Nu number downstream of the peak increased by approximately 150 percent. V.L.

**A84-17842\*#** Pennsylvania State Univ., University Park.

**STRUCTURE OF PARTICLE-LADEN JETS - MEASUREMENTS AND PREDICTIONS**

J.-S. SHUEN, A. S. P. SOLOMON, G. M. FAETH (Pennsylvania State University, University Park, PA), and Q.-F. ZHANG *American Institute of Aeronautics and Astronautics, Aerospace Sciences Meeting, 22nd, Reno, NV, Jan. 9-12, 1984. 11 p. refs* (Contract NAG3-190)

(AIAA PAPER 84-0038)

Measurements of mean and fluctuating velocities of both phases as well as particle mass fluxes were completed in turbulent, particle-laden jets containing monodisperse particles with well-defined initial and boundary conditions. The new measurements were used to evaluate a stochastic separated flow model of the process which treated effects of interphase slip and turbulent dispersion using random-walk computations for particle motion. The continuous phase was treated using a modified k-epsilon model allowing for direct contributions of interphase transport to both mean and turbulence properties. The model performed reasonably well over the new data base, with all empirical parameters fixed from earlier work. In contrast, simplified models ignoring either interphase slip or turbulent dispersion yielded poor agreement with the measurements. Author

**A84-17897\*#** Pennsylvania State Univ., University Park.  
**STRUCTURE OF NONEVAPORATING SPRAYS - MEASUREMENTS AND PREDICTIONS**

A. S. P. SOLOMON, J.-S. SHUEN, Q.-F. ZHANG (Pennsylvania State University, University Park, PA), and G. M. FAETH American Institute of Aeronautics and Astronautics, Aerospace Sciences Meeting, 22nd, Reno, NV, Jan. 9-12, 1984. 12 p. refs (Contract NAG3-190)  
 (AIAA PAPER 84-0125)

Structure measurements were completed within the dilute portion of axisymmetric nonevaporating sprays (SMD of 30 and 87 microns) injected into a still air environment, including: mean and fluctuating gas velocities and Reynolds stress using laser-Doppler anemometry; mean liquid fluxes using isokinetic sampling; drop sizes using slide impaction; and drop sizes and velocities using multiframe photography. The new measurements were used to evaluate three representative models of sprays: (1) a locally homogeneous flow (LHF) model, where slip between the phases was neglected; (2) a deterministic separated flow (DSF) model, where slip was considered but effects of drop interaction with turbulent fluctuations were ignored; and (3) a stochastic separated flow (SSF) model, where effects of both interphase slip and turbulent fluctuations were considered using random sampling for turbulence properties in conjunction with random-walk computations for drop motion. The LHF and DSF models were unsatisfactory for present test conditions-both underestimating flow widths and the rate of spread of drops. In contrast, the SSF model provided reasonably accurate predictions, including effects of enhanced spreading rates of sprays due to drop dispersion by turbulence, with all empirical parameters fixed from earlier work.

Author

**A84-17979\*#** National Aeronautics and Space Administration.  
 Lewis Research Center, Cleveland, Ohio.

**COMPUTATION OF VISCOUS FLOW IN PLANAR AND AXISYMMETRIC DUCTS BY AN IMPLICIT MARCHING PROCEDURE**

C. E. TOWNE (NASA, Lewis Research Center, Cleveland, OH) and J. D. HOFFMAN (Purdue University, West Lafayette, IN) American Institute of Aeronautics and Astronautics, Aerospace Sciences Meeting, 22nd, Reno, NV, Jan. 9-12, 1984. 33 p. refs (AIAA PAPER 84-0256)

A streamwise marching procedure, approximately 200 times faster than a full Navier-Stokes procedure with comparable accuracy, is presented for solving problems of compressible viscous subsonic flow. Results are presented and compared with experimental data for the cases of developing turbulent flow in a circular pipe; turbulent flow in a two-dimensional S-duct; and turbulent flow in a typical subsonic diffuser. Prior to each main marching step, a preliminary marching step is taken in which the integral continuity equation and an uncoupled form of the streamwise momentum equation are solved simultaneously to obtain the viscous pressure correction. During the main marching step the equations for continuity, streamwise momentum, cross-flow momentum, and energy are solved simultaneously as a coupled system using an implicit finite-difference method, with the viscous pressure correction treated as a source term. The analysis may be used for flows with both favorable and adverse pressure gradients and to predict the location of flow separation. J.N.

**A84-18048\*#** United Technologies Corp., East Hartford, Conn.  
**CALCULATIONS OF TURBULENT MASS TRANSPORT IN A BLUFF-BODY DIFFUSION-FLAME COMBUSTOR**

G. J. STURGEON and K. R. MCANUS (United Technologies Corp., Pratt and Whitney Aircraft Group, East Hartford, CT) American Institute of Aeronautics and Astronautics, Aerospace Sciences Meeting, 22nd, Reno, NV, Jan. 9-12, 1984. 12 p. refs (Contract NAS3-23524)  
 (AIAA PAPER 84-0372)

Experimental measurements of turbulent mass transit in a bluff-body diffusion-flame combustor (using CO<sub>2</sub> instead of fuel) are analyzed to evaluate the accuracy of physical models used in flow computations. The data of Lightman and Magill (1981),

Lightman et al. (1983), and Roquemore et al. (1983) are used to calculate apparent turbulent Schmidt numbers (TSN) for a series of flow conditions by a modified TEACH viscous-flow code. The modeling principles, calculation grid, and boundary conditions are discussed, and the results are presented in graphs comparing calculated and measured values. It is shown that models such as the two-equation (K - epsilon) model which use a single value of the TSN are inappropriate for conditions typical of gas-turbine combustors: local TSN variations due to turbulence behavior must be taken into account in improved models. D.G.

**A84-18096\*#** Oklahoma State Univ., Stillwater.  
**LIMITATIONS AND EMPIRICAL EXTENSIONS OF THE K-EPSILON MODEL AS APPLIED TO TURBULENT CONFINED SWIRLING FLOWS**

D. G. LILLEY (Oklahoma State University, Stillwater, OK) and M. T. ABUJELALA American Institute of Aeronautics and Astronautics, Aerospace Sciences Meeting, 22nd, Reno, NV, Jan. 9-12, 1984. 10 p. USAF-supported research. refs (Contract NAG3-74)  
 (AIAA PAPER 84-0441)

Shortcomings and recommended corrections to the standard two-equation k-epsilon turbulence model suggested by previous investigators are presented. They are assessed regarding their applicability to turbulent swirling recirculating flow. Recent experimental data on swirling confined flows, obtained with a five-hole pitot probe and a six-orientation hot-wire probe, are used to obtain optimum values of the turbulence parameters C- $\mu$ , C<sub>2</sub>, and sigma-epsilon for swirling flows. General predictions of moderately and strongly swirling flows with these values are more accurate than predictions with the standard or previous simple extensions of the k-epsilon turbulence model. Author

**A84-18171\*#** California Univ., Berkeley.  
**FORMATION AND INFLAMMATION OF A TURBULENT JET**

A. F. GHONIEM (California, University, Berkeley, CA; MIT, Cambridge, MA), D. Y. CHEN (California, University, Berkeley, CA; Allison Gas Turbine Operations, Indianapolis, IN), and A. K. OPPENHEIM (California, University, Berkeley, CA) American Institute of Aeronautics and Astronautics, Aerospace Sciences Meeting, 22nd, Reno, NV, Jan. 9-12, 1984. 11 p. refs (Contract W-7405-ENG-48; NSF CPE-81-15163; NAG3-131)  
 (AIAA PAPER 84-0572)

The formation and inflammation of a planar, turbulent jet in an incompressible medium is modeled numerically by the use of the random vortex method amended by a flame propagation algorithm. The results demonstrate the dominant influence of turbulent eddies and their interactions upon the development of the jet. Its growth is shown to consist of three stages: formation of small eddies, pairing of eddies with the same sign of circulation, and pairing of eddies of opposite signs. On this basis a number of features of the jet mechanism are revealed, namely penetration, engulfment, entrainment, and intermittency. Two cases of inflammation are considered. In one, the jet is ignited at the center of the orifice, the solution tracing its own inflammation. In the other, combustion is initiated across its full cross section, the results modeling the action of a turbulent torch as it spreads the flame into the combustible surroundings. In both cases the flow field is still dominated by the turbulent eddies and their interactions. However, the coherence among them is encumbered as a consequence of expansion due to the exothermicity of the combustion process.

Author



**A84-18357\*** British Columbia Univ., Vancouver.

**THE PRODUCTION OF TURBULENT STRESS IN A SHEAR FLOW BY IRRATIONAL FLUCTUATIONS**

I. S. GARTSHORE (British Columbia, University, Vancouver, Canada), P. A. DURBIN (NASA, Lewis Research Center, Cleveland, OH), and J. C. R. HUNT (Cambridge University, Cambridge, England) IN: Structure of complex turbulent shear flow; Proceedings of the Symposium, Marseille, France, August 31-September 3, 1982. Berlin, Springer-Verlag, 1983, p. 388-398.

This paper examines, both theoretically and experimentally, the effect produced by irrotational fluctuations, associated with a nearby turbulent field, in a region where the turbulence is initially very low but where there is a mean shear. Calculations are based on rapid distortion theory and experiments use linearized hot wire anemometers in an open circuit wind tunnel. Turbulent shear stress is observed to grow from zero to significant values in the interaction region. The magnitude and extent of this observed shear stress agree reasonably well with predictions of the analysis, when intermittency effects are included. It is concluded that turbulent stresses can be produced by irrotational fluctuations in a region of mean shear and that this effect can be estimated using rapid distortion theory if the overall strain ratio is not large. Author

**A84-21303\*#** National Aeronautics and Space Administration, Lewis Research Center, Cleveland, Ohio.

**COMPUTATION OF VISCOUS FLOW IN CURVED DUCTS AND COMPARISON WITH EXPERIMENTAL DATA**

C. E. TOWNE (NASA, Lewis Research Center, Cleveland, OH) American Institute of Aeronautics and Astronautics, Aerospace Sciences Meeting, 22nd, Reno, NV, Jan. 9-12, 1984. 22 p. refs (AIAA PAPER 84-0531)

A three dimensional analysis for fully viscous subsonic internal flow is evaluated. The analysis, designated PEPSIG, solves an approximate form of the Navier-Stokes equations by an implicit spatial marching procedure. Results of calculations are presented for laminar flow through two different circular cross-sectioned 180 degree bends, and for laminar and turbulent flow through circular and square cross-sectioned 22.5 to 22.5 degree S-ducts. Quantitative comparisons with experimental data are shown for all cases. Special emphasis is placed on verifying the ability of the analysis to accurately predict the distorted flow fields resulting from pressure-driven secondary flows. Previously announced in STAR as N84-13404 Author

**A84-21378\*** Levy (Salomon), Inc., Campbell, Calif.

**TURBULENT BOUNDARY-LAYER FLOW AND STRUCTURE ON A CONVEX WALL AND ITS REDEVELOPMENT ON A FLAT WALL**

J. C. GILLIS (S. Levy, Inc., Campbell, CA) and J. P. JOHNSTON (Stanford University, Stanford, CA) Journal of Fluid Mechanics (ISSN 0022-1120), vol. 135, Oct. 1983, p. 123-153. refs (Contract NSG-3124; NAG3-3)

Although the number of data sets which show the effects of convex curvature on turbulence has increased in the last 10 years, the development of really good calculational models is being held back by a lack of reliable data. The present investigation is concerned with a set of experiments which provide a little more information regarding the response of a boundary-layer flow to convex curvature. Careful measurements were conducted to show the response of the boundary layer to a sudden change from flat wall to curvature, and from curvature to flat wall. It was found that curvature effects were clearly apparent one or two boundary-layer thicknesses downstream of the start of curvature, while the disappearance of the curvature effects on a flat wall was an extremely slow process. G.R.

**A84-21390\*** British Columbia Univ., Vancouver.

**THE PRODUCTION OF TURBULENT STRESS IN A SHEAR FLOW BY IRRATIONAL FLUCTUATIONS**

I. S. GARTSHORE (British Columbia, University, Vancouver, Canada), P. A. DURBIN (NASA, Lewis Research Center, Cleveland, OH), and J. C. R. HUNT (Cambridge University, Cambridge, England) Journal of Fluid Mechanics (ISSN 0022-1120), vol. 137, Dec. 1983, p. 307-329. Research supported by the Killam Foundation and Natural Sciences and Engineering Research Council of Canada. refs

Attention is given to the way in which external turbulence affects an initially turbulence-free region in which there is a mean velocity gradient. External turbulence induces irrotational fluctuations in the sheared region which interact with the shear to produce rotational velocity fluctuations and mean Reynolds stresses. Since the actual front between the initial external turbulence and the shear flow is a randomly contorted surface, the turbulence near the front is intermittent, and is presently included in the form of a simple statistical model. In wind tunnel tests, turbulent shear stress was found to grow from zero to significant values in the interaction region. Observed stress magnitude and extent agrees with predictions, and it is concluded that turbulent stresses can be produced by irrotational fluctuations in a region of mean shear. O.C.

**A84-22922\*#** Illinois Inst. of Tech., Chicago.

**ON THE DESIGN OF CONTRACTIONS AND SETTLING CHAMBERS FOR OPTIMAL TURBULENCE MANIPULATIONS IN WIND TUNNELS**

H. M. NAGIB, A. MARION, and J. TAN-ATICHAT (Illinois Institute of Technology, Chicago, IL) American Institute of Aeronautics and Astronautics, Aerospace Sciences Meeting, 22nd, Reno, NV, Jan. 9-12, 1984. 10 p. refs (Contract NAG1-74; NSG-3220) (AIAA PAPER 84-0536)

The sensitivity of a moderate axisymmetric contraction of turbulence to upstream conditions is parametrically investigated in terms of turbulence intensities and integral length scales. Semi-empirical correlations are derived to characterize the development of turbulence intensities and integral length scales downstream of typical wind-tunnel turbulence manipulators. A new approach is described, permitting wind-tunnel designers to select the characteristic mesh of the turbulence manipulators, as well as the distance from them to the contraction, in order to obtain certain required turbulence characteristics in the test section at the exit of the contraction. The design charts strongly suggest that it may not be possible to achieve small scales and low intensities simultaneously, when using a contraction ratio of nine or larger. The results also confirm that the rapid distortion theory is only valid, with a proper viscous dissipation correction, up to the 'critical point' of a contraction. At that point, the scales of the various components of the velocity are equal and intercomponent transfer from the lateral to the streamwise velocities commences. Author

**A84-23591\*** National Aeronautics and Space Administration, Lewis Research Center, Cleveland, Ohio.

**SHAPE OF POROUS REGION TO CONTROL COOLING ALONG CURVED EXIT BOUNDARY**

R. SIEGEL, and A. SNYDER (NASA, Lewis Research Center, Cleveland, OH) International Journal of Heat and Mass Transfer (ISSN 0017-9310), vol. 27, Feb. 1984, p. 243-252. refs

A cooled porous insert in a curved wall has a specified spatially varying heat flux applied to one side. It is desired to control the distribution of coolant flow out through this curved surface so that the surface will be kept at a desired uniform temperature. The flow regulation is accomplished by shaping the surface through which the coolant enters the region to obtain the required variation of flow resistance within the region. The proper surface shape is found by solving a Cauchy boundary value problem. Analytical solutions are given in two dimensions for various shapes of the heated boundary subjected to different heating distributions. Author

**A84-23950\*** National Aeronautics and Space Administration. Lewis Research Center, Cleveland, Ohio.

**MULTIPLE-GRID CONVERGENCE ACCELERATION OF VISCOUS AND INVISCID FLOW COMPUTATIONS**

G. M. JOHNSON (NASA, Lewis Research Center, Cleveland, OH) Applied Mathematics and Computation (ISSN 0096-3003), vol. 13, Nov. 1983, p. 375-398. refs

A multiple-grid algorithm for use in efficiently obtaining steady solution to the Euler and Navier-Stokes equations is presented. The convergence of a simple, explicit-fine-grid solution procedure is accelerated on a sequence of successively coarser grids by a coarse-grid information propagation method which rapidly eliminates transients from the computational domain. This use of multiple-gridding to increase the convergence rate results in substantially reduced work requirements for the numerical solution of a wide range of flow problems. Computational results are presented for subsonic and transonic inviscid flows and for laminar and turbulent, attached and separated, subsonic viscous flows. Work reduction factors as large as eight, in comparison to the basic fine-grid algorithm, were obtained. Possibilities for further performance improvement are discussed. Previously announced in STAR as N83-21847 M.G.

**A84-24892\*** National Aeronautics and Space Administration. Lewis Research Center, Cleveland, Ohio.

**SMALL-AMPLITUDE VISCOUS MOTION ON ARBITRARY POTENTIAL FLOWS**

M. E. GOLDSTEIN (NASA, Lewis Research Center, Cleveland, OH) Quarterly Journal of Mechanics and Applied Mathematics (ISSN 0033-5614), vol. 37, Feb. 1984, p. 1-31. refs

This paper is concerned with small-amplitude, unsteady, vortical and entropic motion imposed on steady potential flows. It is restricted to the case where the spatial scale of the unsteady motion is small compared to that of the mean flow. Under such conditions, the unsteady motion may be influenced by viscosity even if the mean flow is not. An exact high-frequency (small-wavelength) solution is obtained for the small-amplitude viscous motion imposed on a steady potential flow. It generalizes the one obtained by Pearson (1959) for the homogeneous-strain case to the case of quasi-homogeneous strain. This result is used to study the effect of viscosity on rapidly distorted turbulent flows. Specific numerical results are given for a turbulent flow near a two-dimensional stagnation point. Author

**A84-25807\*** Iowa Univ., Iowa City.

**FINITE-ANALYTIC NUMERICAL METHOD FOR UNSTEADY TWO-DIMENSIONAL NAVIER-STOKES EQUATIONS**

C.-J. CHEN (Iowa, University, Iowa City, IA) and H.-C. CHEN Journal of Computational Physics (ISSN 0021-9991), vol. 53, Feb. 1984, p. 209-226. refs

(Contract NSG-3305; DE-AC02-79ER-10515-A000)

A finite analytic (FA) numerical solution is developed for unsteady two-dimensional Navier-Stokes equations. The FA method utilizes the analytic solution in a small local element to formulate the algebraic representation of partial differential equations. The combination of linear and exponential functions that satisfy the governing equation is adopted as the boundary function, thereby improving the accuracy of the finite analytic solution. Two flows, one a starting cavity flow and the other a vortex shedding flow behind a rectangular block, are solved by the FA method. The starting square cavity flow is solved for Reynolds number of 400, 1000, and 2000 to show the accuracy and stability of the FA solution. The FA solution for flow over a rectangular block ( $H \times H/4$ ) predicts the Strouhal number for Reynolds numbers of 100 and 500 to be 0.156 and 0.125. Details of the flow patterns are given. In addition to streamlines and vorticity distribution, rest-streamlines are given to illustrate the vortex motion downstream of the block. Author

**A84-25859\*** Purdue Univ. School of Science at Indianapolis, Ind.

**FINITE ELEMENT FORMULATION OF TRANSONIC FLOW PROBLEMS**

H. U. AKAY and A. ECER (Purdue University, Indianapolis, IN) IN: Finite element flow analysis; Proceedings of the Fourth International Symposium on Finite Element Methods in Flow Problems, Tokyo, Japan, July 26-29, 1982. Tokyo/Amsterdam, University of Tokyo Press/North-Holland Publishing Co., 1982, p. 403-410. refs

(Contract NSG-3294)

Reference is made to the study by Akay and Ecer (1982), which treated the solution of full Euler equations for transonic, rotational, inviscid flows. Attention is given here to some of the important features of a general finite element formulation for transonic flows. Both rotational and irrotational cases are treated: Transonic flow through a parallel channel with a 4.2 percent thick circular bump is analyzed for an upstream Mach number of 0.85. A figure is included showing the computational grid of  $44 \times 8$  elements. In this case, the distance between the walls of the channel is 2.073 times the chord length of the bump. The pressure distributions over the bump for rotational assumptions are presented. C.R.

**A84-27138\*#** Oklahoma State Univ., Stillwater.

**FURTHER TIME-MEAN MEASUREMENTS IN CONFINED SWIRLING FLOWS**

D. G. LILLEY (Oklahoma State University, Stillwater, OK) and H. K. YOON AIAA Journal (ISSN 0001-1452), vol. 22, April 1984, p. 514, 515. Abridged. USAF-supported research.

(Contract NAG3-74)

Previously cited in issue 05, p. 634, Accession no. A83-16645

**A84-28379\*#** California Univ., Berkeley.

**SELF-SIMILAR BLAST WAVES INCORPORATING DEFLAGRATIONS OF VARIABLE SPEED**

R. H. GUIRGUIS, M. M. KAMEL (California, University, Berkeley, CA), and A. K. OPPENHEIM (California, University, Berkeley, CA; Cairo, University, Giza, Egypt) IN: Shock waves, explosions, and detonations. New York, American Institute of Aeronautics and Astronautics, Inc., 1983, p. 121-156. refs

(Contract W-7405-ENG-48; NSF ENG-78-712372; NAG3-131)

The present investigation is concerned with the development of a systematic approach to the problem of self-similar blast waves incorporating nonsteady flames. The regime covered by the presented solutions is bounded on one side by an adiabatic strong explosion and, on the other, by deflagration propagating at an infinite acceleration. Results for a representative set of accelerations are displayed, taking into account the full range of propagation speeds from zero to velocities corresponding to the Chapman-Jouguet deflagration. It is found that the distribution of stored energy in the undisturbed medium determines the acceleration of the deflagration-shock wave system. The obtained results reveal the existence of a simple relation between the location of the deflagration and its Mach number. G.R.

**A84-28709\*#** National Aeronautics and Space Administration. Lewis Research Center, Cleveland, Ohio.

**DEVELOPING FLOW IN S-SHAPED DUCTS**

B. H. ANDERSON (NASA, Lewis Research Center, Propulsion Systems Div., Cleveland, OH), A. M. K. P. TAYLOR, J. H. WHITELAW, and M. YIANNESKIS (Imperial College of Science and Technology, London, England) IN: International Symposium on Applications of Laser-Doppler Anemometry to Fluid Mechanics, Lisbon, Portugal, July 5-7, 1982, Proceedings. Lisbon, Instituto Superior Tecnico, 1982, p. 4.2.1-4.2.17. NASA-supported research. refs

The velocity characteristics of laminar and turbulent developing flow in an S-duct formed from two 22.5-deg bends of rectangular cross-section have been studied experimentally using laser Doppler velocimetry. It is shown that pressure-driven secondary flows arise in the first bend of the duct and reach maxima of 0.22 and 0.15 of the bulk velocity in the laminar and turbulent flows, respectively.

The velocities are greater in the laminar flow, mainly because of the thicker inlet boundary layers. On passing through the second half of the S-duct, a secondary flow is established over most of the section in the direction opposite to that in the first half. Near the outer wall of the second bend, however, the secondary flow generated in the first bend is sustained because of the local sign of radial vorticity. This effect contributes to a redistribution of the streamwise isotachs, by the end of the duct, comparable with that in unidirectional bends. V.L.

**A84-28738\*#** Case Western Reserve Univ., Cleveland, Ohio.  
**OUTPUT STATISTICS OF LASER ANEMOMETERS IN SPARSELY SEEDED FLOWS**

R. V. EDWARDS (Case Western Reserve University, Cleveland, OH) and A. S. JENSEN (Forsøgsanlæg Riso, Roskilde, Denmark) IN: International Symposium on Applications of Laser-Doppler Anemometry to Fluid Mechanics, Lisbon, Portugal, July 5-7, 1982, Proceedings. Lisbon, Instituto Superior Tecnico, 1982, p. 16.5.1-16.5.10. refs  
 (Contract NSF CPE-80-17868; NAG3-2)

It is noted that until very recently, research on this topic concentrated on the particle arrival statistics and the influence of the optical parameters on them. Little attention has been paid to the influence of subsequent processing on the measurement statistics. There is also controversy over whether the effects of the particle statistics can be measured. It is shown here that some of the confusion derives from a lack of understanding of the experimental parameters that are to be controlled or known. A rigorous framework is presented for examining the measurement statistics of such systems. To provide examples, two problems are then addressed. The first has to do with a sample and hold processor, the second with what is called a saturable processor. The sample and hold processor converts the output to a continuous signal by holding the last reading until a new one is obtained. The saturable system is one where the maximum processable rate is arrived at by the dead time of some unit in the system. At high particle rates, the processed rate is determined through the dead time. C.R.

**A84-29798\*** California Inst. of Tech., Pasadena.

**STABILITY AND STRUCTURE OF STRETCHED VORTICES**

A. C. ROBINSON and P. G. SAFFMAN (California Institute of Technology, Pasadena, CA) Studies in Applied Mathematics (ISSN 0022-2526), vol. 70, April 1984, p. 163-181. Navy-supported research. refs  
 (Contract NAG3-179)  
 (AD-A142913)

The linear stability of the symmetric Burgers vortex to a class of two-dimensional perturbations is demonstrated. The linear stability of the axially symmetric Burgers vortex to two-dimensional low-Reynolds number disturbances is first discussed. The analysis describes the connection of the normal modes with a classical set of special functions. An expansion in Reynolds number gives the variation of the temporal eigenvalues of the normal modes. Then, Burgers-type solutions are sought where the radially inward-straining field is not axially symmetric. A rational perturbation procedure is used to obtain a new class of nonsymmetric Burgers vortices valid when the Reynolds number and the asymmetry in the external strain are small. Finally, the perturbation solutions are numerically extended to larger values of the parameters. C.D.

**A84-32323\*** National Aeronautics and Space Administration. Lewis Research Center, Cleveland, Ohio.

**CORRELATION OF THERMOPHORETICALLY-MODIFIED SMALL PARTICLE DIFFUSIONAL DEPOSITION RATES IN FORCED CONVECTION SYSTEMS WITH VARIABLE PROPERTIES, TRANSPIRATION COOLING AND/OR VISCOUS DISSIPATION**

S. A. GOKOGLU (NASA, Lewis Research Center, Cleveland, OH; Yale University, New Haven, CT) and D. E. ROSNER (Yale University, New Haven, CT) International Journal of Heat and Mass Transfer (ISSN 0017-9310), vol. 27, May 1984, p. 639-646. refs  
 (Contract F49620-82-K-0020; NAG3-201)

A cooled object (heat exchanger tube or turbine blade) is considered to be immersed in a hot fluid stream containing trace amounts of suspended vapors and/or small particles. Numerical prediction calculations were done for self-similar laminar boundary layers and law-of-the-wall turbulent boundary layers. Correlations are presented for the effect of thermophoresis in the absence of transpiration cooling and viscous dissipation; the effect of real suction and blowing in the absence of thermophoresis; the effect of viscous dissipation on thermophoresis in the absence of transpiration cooling, and the combined effect of viscous dissipation and transpiration cooling on thermophoresis. The final correlation,  $St/St_{\text{sub-zero}}$ , is insensitive to particle properties, Euler number, and local mainstream temperature J.N.

**A84-33703\*** National Aeronautics and Space Administration. Lewis Research Center, Cleveland, Ohio.

**COMPARISON OF VISUALIZED TURBINE ENDWALL SECONDARY FLOWS AND MEASURED HEAT TRANSFER PATTERNS**

R. E. GAUGLER and L. M. RUSSELL (NASA, Lewis Research Center, Cleveland, OH) ASME, Transactions, Journal of Engineering for Gas Turbines and Power (ISSN 0022-0825), vol. 106, Jan. 1984, p. 168-172. refs  
 (ASME PAPER 83-GT-83)

Various flow visualization techniques were used to define the secondary flows near the endwall in a large heat transfer data. A comparison of the visualized flow patterns and the measured Stanton number distribution was made for cases where the inlet Reynolds number and exit Mach number were matched. Flows were visualized by using neutrally buoyant helium-filled soap bubbles, by using smoke from oil soaked cigars, and by a few techniques using permanent marker pen ink dots and synthetic wintergreen oil. Details of the horseshoe vortex and secondary flows can be directly compared with heat transfer distribution. Near the cascade entrance there is an obvious correlation between the two sets of data, but well into the passage the effect of secondary flow is not as obvious. Previously announced in STAR as N83-14435 M.G.

**A84-33705\*** Rensselaer Polytechnic Inst., Troy, N. Y.

**EFFECT OF AN OSCILLATING FLOW DIRECTION ON LEADING EDGE HEAT TRANSFER**

M. L. MARZIALE (Westvaco Corp., Covington, VA) and R. E. MAYLE (Rensselaer Polytechnic Institute, Troy, NY) (Tokyo International Gas Turbine Congress, Tokyo, Japan, Oct. 24-28, 1983) ASME, Transactions, Journal of Engineering for Gas Turbines and Power (ISSN 0022-0825), vol. 106, Jan. 1984, p. 222-228. refs  
 (Contract NSG-3262)

An experimental investigation was conducted to examine the effect of a periodic variation in the angle of attack on heat transfer at the leading edge of a gas turbine blade. A circular cylinder was used as a large-scale model of the leading edge region. The cylinder was placed in a wind tunnel and was oscillated rotationally about its axis. The incident flow Reynolds number and the Strouhal number of oscillation were chosen to model an actual turbine condition. Incident turbulence levels up to 4.9 percent were produced by grids placed upstream of the cylinder. The transfer rate was measured using a mass transfer technique and heat transfer rates inferred from the results. A direct comparison of

the unsteady and steady results indicate that the effect is dependent on the Strouhal number, turbulence level, and the turbulence length scale, but that the largest observed effect was only a 10 percent augmentation at the nominal stagnation position. Author

**A84-33706\*** National Aeronautics and Space Administration. Lewis Research Center, Cleveland, Ohio.

## LENGTH TO DIAMETER RATIO AND ROW NUMBER EFFECTS IN SHORT PIN-FIN HEAT TRANSFER

B. A. BRIGHAM and G. J. VANFOSSEN (NASA, Lewis Research Center, Cleveland, OH) ASME, Transactions, Journal of Engineering for Gas Turbines and Power (ISSN 0022-0825), vol. 106, Jan. 1984, p. 241-245. refs (ASME PAPER 83-GT-54)

The relative effects of pin length to diameter ratio and of pin row geometry on the heat transfer from pin fins, was determined. Array averaged heat transfer coefficients on pin and endwall surfaces were measured for two configurations of staggered arrays of short pin fins (length to diameter ratio of 4). One configuration contained eight streamwise rows of pins, while the other contained only four rows. Results showed that both the 8-row and the 4-row configurations for an L sub p/D of 4, exhibit higher heat transfer than in similar tests on shorter pin fins (L sub p/D of 1/2 and 2). It was also found that for this L sub p/D ratio, the array averaged heat transfer was slightly higher with eight rows of staggered pins than with only four rows. Previously announced in STAR as N83-14431 J.D.

**A84-35168\*#** Science Applications, Inc., Chatsworth, Calif.

## ANALYTIC MODELING OF A SPRAY DIFFUSION FLAME

P. T. HARSHA and R. B. EDELMAN (Science Applications, Inc., Chatsworth, CA) AIAA, SAE, and ASME, Joint Propulsion Conference, 20th, Cincinnati, OH, June 11-13, 1984. 9 p. refs (Contract F49620-80-C-0082; DE-AC22-81PC-40276; NAS3-22822) (AIAA PAPER 84-1317)

A detailed model for a spray diffusion flame is described. The model is based on the boundary layer form of the equations of motion, with droplet transport accounted for using a discretized droplet size distribution function. Interphase transport of mass and energy are accounted for, with a flame-sheet model used to describe the combustion process on a droplet scale. Near dynamic equilibrium is assumed for the description of droplet transport; droplets can diffuse relative to the gas phase. Gas-phase mixing is accounted for using a two-equation turbulence model; buoyancy effects are included, with a temperature fluctuation equation used to account for buoyancy effects on turbulence structure. Thermal radiation from gas-phase CO<sub>2</sub> and H<sub>2</sub>O is included. Gas-phase chemical kinetics are modeled using a 20-reaction, 10-species version of the advanced quasi-global chemical kinetics formulation. Results are compared with data for a vaporizing Freon spray and a pentane spray flame. It is shown that the computational approach provides a reasonably valid picture of the overall development of a spray diffusion flame, and, furthermore, provides a useful tool for the parametric examination of the spray combustion process. Author

**A84-35171\*#** Pratt and Whitney Aircraft Group, East Hartford, Conn.

## CALCULATION OF A HOLLOW-CONE LIQUID SPRAY IN A UNIFORM AIR STREAM

G. J. STURGES, S. A. SYED, and K. R. MCMANUS (United Technologies Corp., Pratt and Whitney Group, East Hartford, CT) AIAA, SAE, and ASME, Joint Propulsion Conference, 20th, Cincinnati, OH, June 11-13, 1984. 18 p. refs (Contract NAS3-235924) (AIAA PAPER 84-1322)

Fluid dynamic computer codes for the simulation of flows in gas turbine engine combustion systems are being developed. NASA is currently sponsoring a two-phase program for the evaluation of the performance of current codes, taking into account also an improvement of accuracy, if needed. The present investigation

forms a part of this program. The numerical technique used includes a Lagrangian spray model for liquid fuels. The spray model, in conjunction with the turbulence model, determines the distribution of fuel in the burning zone of the combustor. The numerical technique was applied to a hollow-cone pressure atomizer spraying water into a coflowing confined airstream. G.R.

**A84-35196\*#** Oklahoma State Univ., Stillwater.

## SWIRL FLOW TURBULENCE MODELING

M. T. ABUJELALA, T. W. JACKSON, and D. G. LILLEY (Oklahoma State University, Stillwater, OK) AIAA, SAE, and ASME, Joint Propulsion Conference, 20th, Cincinnati, OH, June 11-13, 1984. 13 p. refs

(Contract NAG3-74)

(AIAA PAPER 84-1376)

Confined turbulent swirling flow data obtained from a single hot-wire using a six-orientation technique are analyzed numerically. The effects of swirl strength and the presence of a strong contraction nozzle further downstream on deduced parameters is also presented and discussed for the case of chamber-to-inlet diameter ratio D/d = 2. Three swirl strengths are considered with inlet swirl vane angles of 0, 45 and 70 deg. A strong contraction nozzle with an area ratio of 4 is located two chamber-diameters downstream of the inlet to the flowfield. It is found that both the swirl strength and the contraction have strong effects on the turbulence parameters. Generally, the most dramatic effect of increase of swirl strength is the considerable increase in values of all the parameters considered, (rx-viscosity, kinetic energy of turbulence, length scales, and degree of nonisotropy). The presence of a strong contraction nozzle tends to increase the turbulence parameter values in regions of acceleration and to reduce them in deceleration regions. Based on similarity of viscosity and length scale profiles, a C sub mu formulation is deduced which is shown to improve the predictive capability of the standard k-epsilon turbulence model in swirling recirculating flows. Author

**A84-35197\*#** Oklahoma State Univ., Stillwater.

## SWIRL, CONFINEMENT AND NOZZLE EFFECTS ON CONFINED TURBULENT FLOW

M. T. ABUJELALA and D. G. LILLEY (Oklahoma State University, Stillwater, OK) AIAA, SAE, and ASME, Joint Propulsion Conference, 20th, Cincinnati, OH, June 11-13, 1984. 10 p. refs (Contract NAG3-74)

(AIAA PAPER 84-1377)

Predictions of swirl, confinement and nozzle effects on confined turbulent flow are exhibited and compared with five-hole pitot-probe time-mean velocity measurements. Two sets of computations are given, one using the standard k-epsilon turbulence model and the other using a C sub mu formulation model deduced from recent six-orientation single-wire hot-wire measurements. Results confirm that the accuracy of the latter model is superior. To highlight the effects of confinement and exit nozzle area on this flow, three expansion ratios and two contraction ratios are used. Predictions are given for a full range of swirl strengths using measured inlet conditions for axial, radial and swirl velocity profiles. The predicted velocity profiles illustrate the large-scale effects of inlet swirl on flowfields. It appears that a strong contraction nozzle has a pronounced effect, on swirl flow cases, with discouragement of central recirculation zones, and forward flow in highly swirled vortex core regions. The expansion ratio value has large-scale effects on the size and location of the recirculation zones. Author

**A84-35233\*#** Centro Tecnico Aeroespacial, San Jose dos Campos (Brazil).

**CONVECTIVE HEAT TRANSFER STUDIES AT HIGH TEMPERATURES WITH PRESSURE GRADIENT FOR INLET FLOW MACH NUMBER OF 0.45**

A. C. F. PEDROSA (Centro Tecnico Aeroespacial, Sao Jose dos Campos, Sao Paulo, Brazil), H. T. NAGAMATSU (Rensselaer Polytechnic Institute, Troy, NY), and J. A. HINCKEL (AIAA, SAE, and ASME, Joint Propulsion Conference, 20th, Cincinnati, OH, June 11-13, 1984. 8 p. refs

(Contract NSF MEA-80-06806; NAG3-292)

(AIAA PAPER 84-1487)

Heat transfer measurements were determined for a flat plate with and without pressure gradient for various free stream temperatures, wall temperature ratios, and Reynolds numbers for an inlet flow Mach number of 0.45, which is a representative inlet Mach number for gas turbine rotor blades. A shock tube generated the high temperature and pressure air flow, and a variable geometry test section was used to produce inlet flow Mach number of 0.45 and accelerate the flow over the plate to sonic velocity. Thin-film platinum heat gages recorded the local heat flux for laminar, transition, and turbulent boundary layers. The free stream temperatures varied from 611 R (339 K) to 3840 R (2133 K) for a  $T(w)/T(r,g)$  temperature ratio of 0.87 to 0.14. The Reynolds number over the heat gages varied from 3000 to 690,000. The experimental heat transfer data were correlated with laminar and turbulent boundary layer theories for the range of temperatures and Reynolds numbers and the transition phenomenon was examined. Author

**A84-35318\*** California Univ., Berkeley.  
**RANDOM ELEMENT METHOD FOR NUMERICAL MODELING OF DIFFUSIONAL PROCESSES**

A. F. GHONIEM and A. K. OPPENHEIM (California, University, Berkeley, CA) IN: International Conference on Numerical Methods in Fluid Dynamics, 8th, Aachen, West Germany, June 28-July 2, 1982, Proceedings. Berlin, Springer-Verlag, 1982, p. 224-232. refs

(Contract NAG3-131; W-7405-ENG-48)

The random element method is a generalization of the random vortex method that was developed for the numerical modeling of momentum transport processes as expressed in terms of the Navier-Stokes equations. The method is based on the concept that random walk, as exemplified by Brownian motion, is the stochastic manifestation of diffusional processes. The algorithm based on this method is grid-free and does not require the diffusion equation to be discretized over a mesh, it is thus devoid of numerical diffusion associated with finite difference methods. Moreover, the algorithm is self-adaptive in space and explicit in time, resulting in an improved numerical resolution of gradients as well as a simple and efficient computational procedure. The method is applied here to an assortment of problems of diffusion of momentum and energy in one-dimension as well as heat conduction in two-dimensions in order to assess its validity and accuracy. The numerical solutions obtained are found to be in good agreement with exact solution except for a statistical error introduced by using a finite number of elements, the error can be reduced by increasing the number of elements or by using ensemble averaging over a number of solutions. Author

**A84-35323\*** National Aeronautics and Space Administration, Lewis Research Center, Cleveland, Ohio.

**RELAXATION SOLUTION OF THE FULL EULER EQUATIONS**

G. M. JOHNSON (NASA, Lewis Research Center, Cleveland, OH) IN: International Conference on Numerical Methods in Fluid Dynamics, 8th, Aachen, West Germany, June 28-July 2, 1982, Proceedings. Berlin, Springer-Verlag, 1982, p. 273-279. refs

A numerical procedure for the relaxation solution of the full steady Euler equations is described. By embedding the Euler system in a second order surrogate system, central differencing may be used in subsonic regions while retaining matrix forms well suited to iterative solution procedures and convergence acceleration techniques. Hence, this method allows the development of stable, fully conservative differencing schemes for

the solution of quite general inviscid flow problems. Results are presented for both subcritical and shocked supercritical internal flows. Comparisons are made with a standard time dependent solution algorithm. Previously announced in STAR as N82-24859

Author

**A84-35349\*** General Electric Co., Cincinnati, Ohio  
**APPLICATION OF A POLYNOMIAL SPLINE IN HIGHER-ORDER ACCURATE VISCOUS-FLOW COMPUTATIONS**

M. G. TURNER, J. S. KEITH (General Electric Co., Cincinnati, OH), K. N. GHIA, and U. GHIA (Cincinnati, University, Cincinnati, OH) IN: International Conference on Numerical Methods in Fluid Dynamics, 8th, Aachen, West Germany, June 28-July 2, 1982, Proceedings. Berlin, Springer-Verlag, 1982, p. 499-506. refs (Contract NSG-3267)

A quartic spline,  $S(4,2)$ , is proposed which overcomes some of the difficulties associated with the use of splines  $S(5,3)$  and  $S(3,1)$  and provides fourth-order accurate results with relatively few grid points. The accuracy of spline  $S(4,2)$  is comparable to or better than that of the fourth-order box scheme and the compact differencing scheme. The use of spline  $S(4,2)$  is suggested as a possible way of obtaining fourth-order accurate solutions to Navier-Stokes equations. V.L.

**A84-35664\*#** United Technologies Research Center, East Hartford, Conn.

**MASS AND MOMENTUM TURBULENT TRANSPORT EXPERIMENTS WITH CONFINED SWIRLING COAXIAL JETS. I**

B. V. JOHNSON and R. ROBACK (United Technologies Research Center, East Hartford, CT) AIAA, SAE, and ASME, Joint Propulsion Conference, 20th, Cincinnati, OH, June 11-13, 1984. 10 p. (Contract NAS3-22771)

(AIAA PAPER 84-1380)

An experimental study of mixing downstream of swirling coaxial jets discharging into an expanded duct was conducted to obtain data for the evaluation and improvement of turbulent transport models currently used in a variety of computational procedures throughout the combustion community. A combination of laser velocimeter and laser induced fluorescence techniques was employed to obtain mean and fluctuating velocity and concentration distributions which were used to derive mass and momentum turbulent transport parameters currently incorporated into various combustor flow models. Flow visualization techniques were also employed to determine qualitatively the time dependent characteristics of the flow and the scale of turbulence. Mean and fluctuating velocity profiles and probability density functions were obtained at selected axial and radial locations throughout the flow field. Mixing occurred in several steps of axial and radial mass transport and was coupled with a large radial mean convective flux. Major mixing regions were observed to occur (1) at the interface between the inner stream and the centerline recirculation zone, and (2) at the interface between the inner jet and the annular jet streams. Mixing for swirling flow was completed in one-third the length required for nonswirling flow. Author

**A84-35150\*#** National Aeronautics and Space Administration, Lewis Research Center, Cleveland, Ohio.

**EFFECT OF LOCATION IN AN ARRAY ON HEAT TRANSFER TO A SHORT CYLINDER IN CROSSFLOW**

R. J. SIMONEAU and G. J. VANFOSSEN, JR. (NASA, Lewis Research Center, Cleveland, OH) ASME, Transactions, Journal of Heat Transfer (ISSN 0022-1481), vol. 106, Feb. 1984, p. 42-48. refs

An experiment was conducted to measure the heat transfer from a heated cylinder in crossflow in an array of circular cylinders. All cylinders had a length-to-diameter ratio of 3.0. Both in-line and staggered array patterns were studied. The cylinders were spaced 2.67 diameters apart center-to-center in both the axial and transverse directions to the flow. The row containing the heated cylinder remained in a fixed position in the channel and the relative location of this row within the array was changed by adding up to five upstream rows. The working fluid was nitrogen gas at pressures from 100 to 600 kPa. The Reynolds number range based on

cylinder diameter and average unobstructed channel velocity was from 5,000 to 125,000. Turbulence intensity profiles were measured for each case at a point one half space upstream of the row containing the heated cylinder. The basis of comparison for all the heat transfer data was the single row with the heated cylinder. For the in-line cases the addition of a single row of cylinders upstream of the row containing the heated cylinder increased the heat transfer by an average of 50 percent above the base case. Adding up to five more-rows caused no increase or decrease in heat transfer. Adding rows in the staggered array cases resulted in average increases in heat transfer of 21, 64, 58, 46, and 46 percent for one to five upstream rows, respectively. Previously announced in STAR as N82-19493 Author

**A84-36973\*#** National Aeronautics and Space Administration. Lewis Research Center, Cleveland, Ohio.

## **AERODYNAMIC EFFECT OF COMBUSTOR INLET-AIR PRESSURE ON FUEL JET ATOMIZATION**

R. D. INGEBO (NASA, Lewis Research Center, Cleveland, OH) AIAA, SAE, and ASME, Joint Propulsion Conference, 20th, Cincinnati, OH, June 11-13, 1984. 11 p. refs (AIAA PAPER 84-1320)

Mean drop diameters were measured with a recently developed scanning radiometer in a study of the atomization of liquid jets injected cross stream in high velocity and high pressure airflows. At constant inlet air pressure, reciprocal mean drop diameter was correlated with airflow mass velocity. Over a combustor inlet-air pressure range of 1 to 21 atmospheres, the ratio of orifice to mean drop diameter,  $D(O)/D(M)$ , was correlated with the product of Weber and Reynolds number,  $WeRe$ , and with the molecular scale momentum transfer ratio of gravitational to inertial forces. Previously announced in STAR as N84-22910 M.A.C.

**A84-37467\*#** National Aeronautics and Space Administration. Lewis Research Center, Cleveland, Ohio.

## **FLAT PLATE HEAT TRANSFER FOR LAMINAR TRANSITION AND TURBULENT BOUNDARY LAYERS USING A SHOCK TUBE**

J. D. BROSTMAYER (NASA, Lewis Research Center, Cleveland, OH) and H. T. NAGAMATSU (Rensselaer Polytechnic Institute, Troy, NY) American Institute of Aeronautics and Astronautics, Thermophysics Conference, 19th, Snowmass, CO, June 25-28, 1984. 6 p. refs (Contract NAG3-292; NSF 80-06806)

(AIAA PAPER 84-1726)

Heat transfer results are presented for laminar, transition, and turbulent boundary layers for a Mach number of 0.12 with gas temperatures of 425 K and 1000 K over a flat plate at room temperature. The measurements were made in air for a Reynolds number range of 600 to 6 million. The heat transfer measurements were conducted in a 70-ft long, 4 in. diameter shock tube. Reflecting wedges were used to reflect the incident shock wave to produce a flow Mach number of 0.12 behind the reflected shock wave. Thin film platinum heat gages were mounted on the plate surface to measure the local heat flux. The laminar results for gas temperatures of 425 K to 1000 K agree well with theory. The turbulent results are also close to incompressible theory, with the 1000 K flow case being slightly higher. The transition results lie between the laminar and turbulent predictions. Author

**A84-38000\*#** Oklahoma State Univ., Stillwater.

## **FIVE-HOLE PITOT PROBE MEASUREMENTS OF SWIRL, CONFINEMENT AND NOZZLE EFFECTS ON CONFINED TURBULENT FLOW**

D. G. LILLEY (Oklahoma State University, Stillwater, OK) and G. L. SCHARRER American Institute of Aeronautics and Astronautics, Fluid Dynamics, Plasma Dynamics, and Lasers Conference, 17th, Snowmass, CO, June 25-27, 1984. 15 p. USAF-supported research. refs (Contract NAG3-74)

(AIAA PAPER 84-1605)

The results of a time-mean flow characterization of nonswirling and swirling inert flows in a combustor are reported. The five-hole

pilot probe technique was used in axisymmetric test sections with expansion ratios of 1 and 1.5. A prominent corner recirculation zone identified in nonswirling expanding flows decreased in size with swirling flows. The presence of a downstream nozzle led to an adverse pressure gradient at the wall and a favorable gradient near the centerline. Reducing the expansion ratio reduced the central recirculation length. No significant effect was introduced in the flowfield by a gradual expansion. M.S.K.

**A84-38030\*#** Massachusetts Inst. of Tech., Cambridge.

## **CONSERVATIVE STREAMTUBE SOLUTION OF STEADY-STATE EULER EQUATIONS**

M. DRELA, M. GILES, and W. T. THOMPSON, JR. (MIT, Cambridge, MA) American Institute of Aeronautics and Astronautics, Fluid Dynamics, Plasma Dynamics, and Lasers Conference, 17th, Snowmass, CO, June 25-27, 1984. 8 p. refs (Contract F49620-78-C-0084; NAG3-9) (AIAA PAPER 84-1643)

This paper presents a new method for solving the steady state Euler equations. The method is similar to streamline curvature methods but has a conservative finite volume formulation which ensures correct shock capturing. Either wall position or wall pressure may be prescribed as boundary conditions, permitting both direct and inverse calculations. In supersonic applications the solution is obtained by space-marching while in subsonic and transonic applications iterative relaxation methods are used. Numerical results are given for: (1) supersonic diffuser with oblique shocks (direct calculation); (2) supersonic jet entering still reservoir (inverse calculation); (3) subsonic bump in a channel with 25 percent blockage (direct and inverse); (4) subsonic high-work turbine cascade (direct); and (5) transonic bump in a channel with 12 percent blockage (direct calculation). Author

**A84-38557\*** California Inst. of Tech., Pasadena.

## **THREE-DIMENSIONAL STABILITY OF AN ELLIPTICAL VORTEX IN A STRAINING FIELD**

A. C. ROBINSON and P. G. SAFFMAN (California Institute of Technology, Pasadena, CA) Journal of Fluid Mechanics (ISSN 0022-1120), vol. 142, May 1984, p. 451-466. Navy-supported research. refs (Contract NAG3-179) (AD-A146317)

The three-dimensional linear stability of a rectilinear vortex of elliptical cross-section existing as a steady state in an irrotational straining field is studied numerically in the case of finite strain. It is shown that the instability predicted analytically for weak strain persists for finite strain and that the weak-strain results continue to be quantitatively valid for finite strain. The dependence of the growth rates of the unstable modes on the strain and the axial-disturbance wavelength is discussed. It is also shown that a three-dimensional instability is always more unstable than a two-dimensional instability in the range of parameters of most interest. Author

**A84-38857\*#** Tennessee Univ., Knoxville.

## **THERMOACOUSTIC CONVECTION HEAT-TRANSFER PHENOMENON**

M. PARANG (Tennessee, University, Knoxville, TN) and A. SALAH-EDDINE AIAA Journal (ISSN 0001-1452), vol. 22, July 1984, p. 1020-1022. refs (Contract NAG3-239)

Previously cited in issue 14, p. 2009, Accession no. A83-32701



**A84-40242\*#** National Aeronautics and Space Administration. Lewis Research Center, Cleveland, Ohio.

**A REVIEW OF INTERNAL COMBUSTION ENGINE COMBUSTION CHAMBER PROCESS STUDIES AT NASA LEWIS RESEARCH CENTER**

H. J. SCHOCK (NASA, Lewis Research Center, Cleveland, OH) AIAA, SAE, and ASME, Joint Propulsion Conference, 20th, Cincinnati, OH, June 11-13, 1984. 13 p. refs (AIAA PAPER 84-1316)

The performance of internal combustion stratified-charge engines is highly dependent on the in-cylinder fuel-air mixing processes occurring in these engines. Current research concerning the in-cylinder airflow characteristics of rotary and piston engines is presented. Results showing the output of multidimensional models, laser velocimetry measurements and the application of a holographic optical element are described. Models which simulate the four-stroke cycle and seal dynamics of rotary engines are also discussed. Previously announced in STAR as N84-24999

R.S.F.

**A84-40243\*#** National Aeronautics and Space Administration. Lewis Research Center, Cleveland, Ohio.

**COMPUTATIONAL MODELING OF JET INDUCED MIXING OF CRYOGENIC PROPELLANTS IN LOW-G**

J. I. HOCHSTEIN, P. M. GERHART (Akron, University, Akron, OH), and J. C. AYDELOTT (NASA, Lewis Research Center, Cleveland, OH) AIAA, SAE, and ASME, Joint Propulsion Conference, 20th, Cincinnati, OH, June 11-13, 1984. 14 p. refs (AIAA PAPER 84-1344)

The SOLA-ECLIPSE Code is being developed to enable computational prediction of jet induced mixing in cryogenic propellant tanks in a low-gravity environment. Velocity fields, predicted for scale model tanks, are presented which compare favorably with the available experimental data. A full scale liquid hydrogen tank for a typical Orbit Transfer Vehicle is analyzed with the conclusion that coupling an axial mixing jet with a thermodynamic vent system appears to be a viable concept for the control of tank pressure. Previously announced in STAR as N84-25000

Author

**A84-41156\*** National Aeronautics and Space Administration. Lewis Research Center, Cleveland, Ohio.

**TURBULENT SOLUTIONS OF THE EQUATIONS OF FLUID MOTION**

R. G. DEISSLER (NASA, Lewis Research Center, Cleveland, OH) Reviews of Modern Physics (ISSN 0034-6861), vol. 56, April 1984, p. 223-254. refs

Some turbulent solutions of the unaveraged Navier-Stokes equations (equations of fluid motion) are reviewed. Those equations are solved numerically in order to study the nonlinear physics of incompressible turbulent flow. Initial three-dimensional cosine velocity fluctuations and periodic boundary conditions are used in most of the work considered. The three components of the mean-square velocity fluctuations are initially equal for the conditions chosen. The resulting solutions show characteristics of turbulence such as the linear and nonlinear excitation of small-scale fluctuations. For the stronger fluctuations, the initially nonrandom flow develops into an apparently random turbulence. Thus randomness or turbulence can arise as a consequence of the structure of the Navier-Stokes equations. The cases considered include turbulence which is statistically homogeneous or inhomogeneous and isotropic or anisotropic. A mean shear is present in some cases. A statistically steady-state turbulence is obtained by using a spatially periodic body force. Various turbulence processes, including the transfer of energy between eddy sizes and between directional components, and the production, dissipation, and spatial diffusion of turbulence, are considered. It is concluded that the physical processes occurring in turbulence can be profitably studied numerically.

Author

**A84-43546\*** Southwest Research Inst., San Antonio, Tex.

**GAS FLOW ACROSS A WET SCREEN - ANALOGY TO A RELIEF VALVE WITH HYSTERESIS**

A. NACHMAN and F. T. DODGE (Southwest Research Institute, San Antonio, TX) Applied Mathematical Modelling (ISSN 0307-904X), vol. 7, Aug. 1983, p. 288-290. (Contract NAS3-22664)

The flow of gas through a wet fine-mesh screen is analyzed in terms of the capillary forces of the liquid wetting the screen and the pressure difference across the screen thickness driving the gas flow. Several different types of time-dependent flow are shown to be possible. The most interesting type is one in which the pressure difference opens small channels in the liquid, which are then closed rapidly by the wetting action of the liquid. The opening and closing exhibit hysteresis, and the flow is highly oscillatory.

Author

**A84-44183\*#** National Aeronautics and Space Administration. Lewis Research Center, Cleveland, Ohio.

**ON MODELING DILUTION JET FLOWFIELDS**

J. D. HOLDEMAN (NASA, Lewis Research Center, Cleveland, OH) and R. SRINIVASAN (Garrett Turbine Engine Co., Phoenix, AZ) AIAA, SAE, and ASME, Joint Propulsion Conference, 20th, Cincinnati, OH, June 11-13, 1984. 13 p. Previously announced in STAR as N84-25713. refs (AIAA PAPER 84-1379)

This paper compares temperature field measurements from selected experiments on a single row, and opposed rows, of jets injected into a ducted crossflow with profiles calculated using an empirical model based on assumed vertical profile similarity and superposition, and distributions calculated with a 3-D elliptic code using a standard K-E turbulence model. The empirical model predictions are very good within the range of the generating experiments, and the numerical model results, although exhibiting too little mixing, correctly describe the effects of the principal flow and geometric variables.

Author

**A84-46900\*#** Virginia Univ., Charlottesville.

**PENALTY FUNCTION FINITE ELEMENT ANALYSIS OF STEADY VISCOUS INCOMPRESSIBLE FLOW IN ROTATING COORDINATES**

M. C. ROSEN, P. E. ALLAI, and J. G. RICE (Virginia, University, Charlottesville, VA) American Society of Mechanical Engineers, International Gas Turbine Conference and Exhibit, 29th, Amsterdam, Netherlands, June 4-7, 1984. 10 p. refs (Contract NAG3-180) (ASME PAPER 84-GT-36)

Finite element methods for incompressible viscous flow in turbomachines have not been presented in the literature previously. This paper develops a penalty function primitive variable method including Coriolis and centrifugal force terms for steady flow in a rotating coordinate system. Simplex elements are used with the result of solution times comparable to equivalent finite difference solutions. Example cases considered are Couette flow, Poiseuille flow, flow over a step and flow in a rotating channel. Both laminar and turbulent flows are discussed. The accuracy of computed solutions compares well with theoretical solutions and experimental measurements.

Author

**A84-46982\*#** Akron Univ., Ohio.

**HEAT TRANSFER IN THERMAL BARRIER COATED RODS WITH CIRCUMFERENTIAL AND RADIAL TEMPERATURE GRADIENTS**

B. T. F. CHUNG, M. M. KERMANI, M. J. BRAUN, J. PADOVAN (Akron, University, Akron, OH), and R. HENDRICKS (NASA, Lewis Research Center, Cleveland, OH) American Society of Mechanical Engineers, International Gas Turbine Conference and Exhibit, 29th, Amsterdam, Netherlands, June 4-7, 1984. 7 p. refs (Contract NAG3-265) (ASME PAPER 84-GT-181)

To study the heat transfer in ceramic coatings applied to the heated side of internally cooled hot section components of the gas turbine engine, a mathematical model is developed for the



thermal response of plasma-sprayed ZrO<sub>2</sub>-Y<sub>2</sub>O<sub>3</sub> ceramic materials with a Ni-Cr-AL-Y bond coat on a Rene 41 rod substrate subject to thermal cycling. This multilayered cylinder with temperature dependent thermal properties is heated in a cross-flow by a high velocity flame and then cooled by ambient air. Due to high temperature and high velocity of the flame, both gas radiation and forced convection are taken into consideration. Furthermore, the local turbulent heat transfer coefficient is employed which varies with angular position as well as the surface temperature. The transient two-dimensional (heat transfer along axial direction is neglected) temperature distribution of the composite cylinder is determined numerically. Author

**A84-48138\*#** Pennsylvania State Univ., University Park.  
**TURBULENCE MODELING FOR THREE-DIMENSIONAL SHEAR FLOWS OVER CURVED ROTATING BODIES**  
J. M. GAMES and B. LAKSHMINARAYANA (Pennsylvania State University, University Park, PA) AIAA Journal (ISSN 0001-1452), vol. 22, Oct. 1984, p. 1420-1428. Previously cited in issue 05, p. 637, Accession no. A83-16787. refs  
(Contract NSG-3266)

**A84-48140\*#** National Aeronautics and Space Administration. Lewis Research Center, Cleveland, Ohio.  
**EXPERIMENTS IN DILUTION JET MIXING**  
J. D. HOLDEMAN (NASA, Lewis Research Center, Cleveland, OH), R. SRINIVASAN, and A. BERENFELD (Garrett Turbine Engine Co., Phoenix, AZ) AIAA Journal (ISSN 0001-1452), vol. 22, Oct. 1984, p. 1436-1443. Previously cited in issue 16, p. 2352, Accession no. A83-36277. refs

**A84-49112\*#** Cincinnati Univ., Ohio.  
**ON NUMERICAL SIMULATION OF VISCOUS FLOWS**  
K. N. GHIA and U. GHIA (Cincinnati, University, Cincinnati, OH) IN: Developments in mechanics. Volume 12 - Midwestern Mechanics Conference, 18th, Iowa City, IA, May 16-18, 1983, Proceedings. Iowa City, IA, University of Iowa, 1983, p. 207-210. refs  
(Contract AF-AFOSR-80-0160; NAG3-194)

Numerical simulation methods for viscous incompressible laminar flows are reviewed, with a focus on finite-difference schemes. The approaches to high/moderate-Reynolds-number flows (strong-viscous-interaction model or single sets of equations) and the factors affecting the versatility, reliability, and accuracy of the analysis algorithms are considered; approximate-factorization implicit solution techniques for low-Reynolds-number flows are discussed; and the procedures used in a number of specific problems are indicated. T.K.

**A84-49192\*#** Georgia Inst. of Tech., Atlanta.  
**APPLICATION OF SIGNAL ANALYSIS TO CAVITATION**  
C. S. MARTIN (Georgia Institute of Technology, Atlanta, GA) and P. VEERABHADRA RAO (NASA, Lewis Research Center, Cleveland, OH) ASME, Transactions, Journal of Fluids Engineering (ISSN 0098-2202), vol. 106, Sept. 1984, p. 342-346. refs  
(Contract F33615-77-C-2036)

The diagnostic facilities of the cross power spectrum and the coherence function have been employed to enhance the identification of not only the inception of cavitation, but also its level. Two piezoelectric pressure transducers placed in the downstream chamber of a model spool valve undergoing various levels of cavitation allowed for the use of both functions - the phase angle of the complex cross spectrum and the dimensionless coherence function - to sense clearly the difference between noise levels associated with a noncavitating jet from those once cavitation inception is attained. The cavitation noise within the chamber exhibited quite a regular character in terms of the phase difference between instruments for limited cavitation. Varying cavitation levels clearly illustrated the effect of bubble size on the attendant frequency range for which there was an extremely high coherence or nearly perfect causality. Author

**N84-13490\*#** Toledo Univ., Ohio. Dept. of Chemical Engineering.  
**NUMERICAL SIMULATION OF TWO-DIMENSIONAL HEAT TRANSFER IN COMPOSITE BODIES WITH APPLICATION TO DE-ICING OF AIRCRAFT COMPONENTS** Ph.D. Thesis. Final Report  
D. F. K. CHAO Nov. 1983 125 p refs  
(Contract NAG3-72)  
(NASA-CR-168283; NAS 1.26:168283) Avail: NTIS HC A06/MF A01 CSCL 20D

Transient, numerical simulations of the de-icing of composite aircraft components by electrothermal heating were performed for a two dimensional rectangular geometry. The implicit Crank-Nicolson formulation was used to insure stability of the finite-difference heat conduction equations and the phase change in the ice layer was simulated using the Enthalpy method. The Gauss-Seidel point iterative method was used to solve the system of difference equations. Numerical solutions illustrating de-icer performance for various composite aircraft structures and environmental conditions are presented. Comparisons are made with previous studies. The simulation can also be used to solve a variety of other heat conduction problems involving composite bodies. Author

**N84-13494\*#** National Aeronautics and Space Administration. Lewis Research Center, Cleveland, Ohio.  
**COMPUTATION OF VISCOUS FLOW IN CURVED DUCTS AND COMPARISON WITH EXPERIMENTAL DATA**  
C. E. TOWNE Dec. 1983 22 p refs Presented at the 21st Aerospace Sci. Conf., Reno, Nev., 9-12 Jan. 1984  
(NASA-TM-83548; NAS 1.15:83548; AIAA-84-0531; E-1922)  
Avail: NTIS HC A02/MF A01 CSCL 20D

A three dimensional analysis for fully viscous subsonic internal flow is evaluated. The analysis, designated PEP SIG, solves an approximate form of the Navier-Stokes equations by an implicit spatial marching procedure. Results of calculations are presented for laminar flow through two different circular cross-sectioned 180 degree bends, and for laminar and turbulent flow through circular and square cross-sectioned 22.5 to 22.5 degree S-ducts. Quantitative comparisons with experimental data are shown for all cases. Special emphasis is placed on verifying the ability of the analysis to accurately predict the distorted flow fields resulting from pressure-driven secondary flows. Author

**N84-14462\*#** Scientific Research Associates, Inc., Glastonbury, Conn.  
**FURTHER DEVELOPMENT OF A METHOD FOR COMPUTING THREE-DIMENSIONAL SUBSONIC VISCOUS FLOWS IN TURBOFAN LOBE MIXERS** Final Report  
S. J. LIN, J. P. KRESKOVSKY, W. R. BRILEY, and H. MCDONALD Nov. 1983 66 p refs  
(Contract NAS3-22758)  
(NASA-CR-168304; NAS 1.26:168304; R83-900011-F) Avail: NTIS HC A04/MF A01 CSCL 20D

Procedure for computing subsonic, turbulent flow in turbofan lobe mixers was extended to allow consideration of flow fields in which a swirl component of velocity may be present. Additional, an optional k-lambda turbulence model was added to the procedure. The method of specifying the initial flow field was also modified, allowing parametric specification or radial secondary flow velocities, and making it possible to consider initial flow fields which have significant inlet secondary flow vorticity. A series of example calculations was performed which demonstrate the various capabilities of the modified code. These calculations demonstrate the effects of initial secondary flows of various magnitudes, the effects of swirl, and the effects of turbulence model on the mixing process. The results of these calculations indicate that the initial secondary flows, presumed to be generated within the lobes, play a dominant role in the mixing process, and that the predicted results are relatively insensitive to the turbulence model used. Author

**N84-14463\*#** National Aeronautics and Space Administration. Lewis Research Center, Cleveland, Ohio.

**HEAT TRANSFER DISTRIBUTIONS AROUND NOMINAL ICE ACCRETION SHAPES FORMED ON A CYLINDER IN THE NASA LEWIS ICING RESEARCH TUNNEL**

G. J. VANFOSSEN, R. J. SIMONEAU, W. A. OLSEN, and R. J. SHAW 1984 19 p refs Presented at the 22nd Aerospace Sci. Meeting, Reno, Nev., 9-12 Jan. 1984; sponsored by AIAA (NASA-TM-83557; E-1905; NAS 1.15:83557) Avail: NTIS HC A02/MF A01 CSCL 20D

Local heat transfer coefficients were obtained on irregular cylindrical shapes which typify the accretion of ice on circular cylinders in cross flow. The ice shapes were grown on a 5.1 cm (2.0 in.) diameter cylinder in the NASA Lewis Icing Research Tunnel. The shapes were 2, 5, and 15 min accumulations of glaze ice and 15 min accumulation of rime ice. Heat transfer coefficients were also measured around the cylinder with no ice accretion. These icing shapes were averaged axially to obtain a nominal shape of constant cross section for the heat transfer tests. Heat transfer coefficients around the perimeter of each shape were measured with electrically heated copper strips embedded in the surface of the model which was cast from polyurethane foam. Each strip contained a thermocouple to measure the local surface temperature. The models were run in a 15.2 x 68.6 cm (6 x 27 in.) wind tunnel at several velocities. Background turbulence in the wind tunnel was less than 0.5 percent. The models were also run with a turbulence producing grid which gave about 3.5 percent turbulence at the model location with the model removed. The effect of roughness was also simulated with sand grains glued to the surface. Results are presented as Nusselt number versus angle from the stagnation line for the smooth and rough models for both high and low levels of free stream turbulence. Roughness of the surface in the region prior to flow separation plays a major role in determining the heat transfer distribution. R.J.F.

**N84-16488\*#** Arizona State Univ., Tempe. Dept. of Mechanical and Aerospace Engineering.

**FORCED CONVECTION HEAT TRANSFER TO AIR/WATER VAPOR MIXTURES Final Report**

D. R. RICHARDS and L. W. FLORSCHUETZ Washington NASA Jan. 1984 80 p refs (Contract NSG-3075) (NASA-CR-3769; E-1889; NAS 1.26:3769; CR-R-83036) Avail: NTIS HC A05/MF A01 CSCL 20D

Heat transfer coefficients were measured using both dry and humid air in the same forced convection cooling scheme and were compared using appropriate nondimensional parameters (Nusselt, Prandtl and Reynolds numbers). A forced convection scheme with a complex flow field, two dimensional arrays of circular jets with crossflow, was utilized with humidity ratios (mass ratio of water vapor to air) up to 0.23. The dynamic viscosity, thermal conductivity and specific heat of air, steam and air/steam mixtures are examined. Methods for determining gaseous mixture properties from the properties of their pure components are reviewed as well as methods for determining these properties with good confidence. The need for more experimentally determined property data for humid air is discussed. It is concluded that dimensionless forms of forced convection heat transfer data and empirical correlations based on measurements with dry air may be applied to conditions involving humid air with the same confidence as for the dry air case itself, provided that the thermophysical properties of the humid air mixtures are known with the same confidence as their dry air counterparts. A.R.H.

**N84-16492\*#** National Aeronautics and Space Administration. Lewis Research Center, Cleveland, Ohio.

**SOME INELASTIC EFFECTS OF THERMAL CYCLING ON YTTRIA-STABILIZED ZIRCONIA**

R. C. HENDRICKS, G. MCDONALD, and R. C. BILL (AVRADCOM Research and Technology Labs.) 1982 13 p refs Presented at the 84th Ann. Meeting and Exposition of the American Ceramic Society, Cincinnati, 2-5 May 1982 (NASA-TM-83488; E-1812; NAS 1.15:83488; AVRADCOM-TR-83-C-10) Avail: NTIS HC A02/MF A01 CSCL 20D

The effects of inelastic behavior of yttria-stabilized zirconia (YSZ) materials were analyzed. The results show these materials to be sensitive to small changes in temperature and are supported by measurements of inelastic behavior in disc and bar specimens at temperatures as low as 1010 C (1850 F). At higher thermomechanical loadings, the test specimens can deform to strains above 1 percent. M.G.

**N84-16493\*#** National Aeronautics and Space Administration. Lewis Research Center, Cleveland, Ohio.

**ADVANCED HIGH TEMPERATURE HEAT FLUX SENSORS**

W. ATKINSON (Pratt and Whitney Aircraft Group, East Hartford, Conn.), H. F. HOBART, and R. R. STRANGE 1983 22 p refs Presented at the Intern. Conf. of the Instrument Society of America, ISA '83, Houston, Tex., 10-13 Oct. 1983 (NASA-TM-83526; E-1891; NAS 1.15:83526) Avail: NTIS HC A02/MF A01 CSCL 14B

To fully characterize advanced high temperature heat flux sensors, calibration and testing is required at full engine temperature. This required the development of unique high temperature heat flux test facilities. These facilities were developed, are in place, and are being used for advanced heat flux sensor development. Author

**N84-16494\*#** National Aeronautics and Space Administration. Lewis Research Center, Cleveland, Ohio.

**EFFECTS OF BROADENED PROPERTY FUELS ON RADIANT HEAT FLUX TO GAS TURBINE COMBUSTOR LINERS**

J. B. HAGGARD, JR. Dec. 1983 27 p refs (NASA-TM-83537; E-1906; NAS 1.15:83537) Avail: NTIS HC A03/MF A01 CSCL 20D

The effects of fuel type, inlet air pressure, inlet air temperature, and fuel/air ratio on the combustor radiation were investigated. Combustor liner radiant heat flux measurements were made in the spectral region between 0.14 and 6.5 microns at three locations in a modified commercial aviation can combustor. Two fuels, Jet A and a heavier distillate research fuel called ERBS were used. The use of ERBS fuel as opposed to Jet A under similar operating conditions resulted in increased radiation to the combustor liner and hence increased backside liner temperature. This increased radiation resulted in liner temperature increases always less than 73 C. The increased radiation is shown by way of calculations to be the result of increased soot concentrations in the combustor. The increased liner temperatures indicated can substantially affect engine maintenance costs by reducing combustor liner life up to 1/3 because of the rapid decay in liner material properties when operated beyond their design conditions. M.G.

**N84-17525\*#** National Aeronautics and Space Administration. Lewis Research Center, Cleveland, Ohio.

**HOT-FLOW TESTS OF A SERIES OF 10-PERCENT-SCALE TURBOFAN FORCED MIXING NOZZLES**

V. L. HEAD, L. A. POVINELLI, and W. H. GERSTENMAIER Jan. 1984 95 p refs (NASA-TP-2268; E-1746; NAS 1.60:2268) Avail: NTIS HC A05/MF A01 CSCL 20D

An approximately 1/10-scale model of a mixed-flow exhaust system was tested in a static facility with fully simulated hot-flow cruise and takeoff conditions. Nine mixer geometries with 12 to 24 lobes were tested. The areas of the core and fan stream were held constant to maintain a bypass ratio of approximately 5. The research results presented in this report were obtained as part of

a program directed toward developing an improved mixer design methodology by using a combined analytical and experimental approach. The effects of lobe spacing, lobe penetration, lobe-to-centerbody gap, lobe contour, and scalloping of the radial side walls were investigated. Test measurements included total pressure and temperature surveys, flow angularity surveys, and wall and centerbody surface static pressure measurements. Contour plots at various stations in the mixing region are presented to show the mixing effectiveness for the various lobe geometries.

Author

**N84-17530\*#** United Technologies Research Center, East Hartford, Conn.

**MASS AND MOMENTUM TURBULENT TRANSPORT EXPERIMENTS WITH CONFINED SWIRLING COAXIAL JETS**  
Interim Report, 18 Oct. 1981 - 31 Aug. 1983

R. ROBACK and B. V. JOHNSON Aug. 1983 260 p refs  
(Contract NAS3-2271)

(NASA-CR-168252; NAS 1.26:168252; R83-915540-26) Avail:  
NTIS HC A12/MF A01, CSCL 20D

Swirling coaxial jets mixing downstream, discharging into an expanded duct was conducted to obtain data for the evaluation and improvement of turbulent transport models currently used in a variety of computational procedures throughout the combustion community. A combination of laser velocimeter (LV) and laser induced fluorescence (LIF) techniques was employed to obtain mean and fluctuating velocity and concentration distributions which were used to derive mass and momentum turbulent transport parameters currently incorporated into various combustor flow models. Flow visualization techniques were also employed to determine qualitatively the time dependent characteristics of the flow and the scale of turbulence. The results of these measurements indicated that the largest momentum turbulent transport was in the r-z plane. Peak momentum turbulent transport rates were approximately the same as those for the nonswirling flow condition. The mass turbulent transport process for swirling flow was complicated. Mixing occurred in several steps of axial and radial mass transport and was coupled with a large radial mean convective flux. Mixing for swirling flow was completed in one-third the length required for nonswirling flow.

Author

**N84-17533\*#** National Aeronautics and Space Administration, Lewis Research Center, Cleveland, Ohio.

**EXPERIMENTAL STUDY OF BUBBLE CAVITIES ATTACHED TO A ROTATING SHAFT IN A RESERVOIR**

R. C. HENDRICKS, M. J. BRAUN (Akron Univ.), and R. L. MULLEN (Case Western Reserve Univ.) 1984 7 p refs Presented at the Cavitation and Multiphase Flow Forum, New Orleans, 11-17 Feb. 1984

(NASA-TM-83586; NAS 1.15:83586; E-1975) Avail: NTIS HC A02/MF A01 CSCL 20D

Bubble cavities formed by air entrainment and attached to a rotating shaft in an oil reservoir were studied. The cavities appear to the unaided eye as toroidal. High speed photography, however, reveals the individuality of the bubble cavities and their near solid body rotational characteristics. The cavities are distorted by the rotation effects but remain attached and tend to merge because of edge effects in the axial direction. The flow field within the reservoir is influenced by the unusual character of the two phase fluid found there; the vorticity is readily visualized. Other examples of vapor entrapment at the inlet of an eccentric rotor are also discussed. A simplified analytical method is provided, and a numerical analysis is being investigated. Vapor (void) entrainment and generation can significantly alter leakage rates and stability of seals, bearings, and dampers. Recognition of these effects in the component design systems will result only after detailed studies of the above phenomena.

S.L.

**N84-18578\*#** Analox Corp., Cleveland, Ohio.

**ENGINEERING CORRELATIONS OF VARIABLE-PROPERTY EFFECTS ON LAMINAR FORCED CONVECTION MASS TRANSFER FOR DILUTE VAPOR SPECIES AND SMALL PARTICLES IN AIR** Final Report

S. A. GOEKOGLU and D. E. ROSNER (Yale Univ, New Haven, Conn.) Jan. 1984 16 p refs

(Contract NAS3-23293; NAG3-201)

(NASA-CR-168322; NAS 1.26:168322) Avail: NTIS HC A02/MF A01 CSCL 20D

A simple engineering correlation scheme is developed to predict the variable property effects on dilute species laminar forced convection mass transfer applicable to all vapor molecules or Brownian diffusing small particle, covering the surface to mainstream temperature ratio of 0.25 T sub W/T sub e 4. The accuracy of the correlation is checked against rigorous numerical forced convection laminar boundary layer calculations of flat plate and stagnation point flows of air containing trace species of Na, NaCl, NaOH, Na2SO4, K, KCl, KOH, or K2SO4 vapor species or their clusters. For the cases reported here the correlation had an average absolute error of only 1 percent (maximum 13 percent) as compared to an average absolute error of 18 percent (maximum 54 percent) one would have made by using the constant-property results.

Author

**N84-19741\*#** National Aeronautics and Space Administration, Langley Research Center, Hampton, Va.

**EXPERIMENTAL AND THEORETICAL DEPOSITION RATES FROM SALT-SEEDING COMBUSTION GASES OF A MACH 0.3 BURNER RIG**

G. J. SANTORO, F. J. KOHL, C. A. STEARNS, S. A. GOEKOGLU (Analox Corp.), and D. E. ROSNER (Yale Univ.) Mar. 1984 46 p refs

(Contract NAS3-23293; NAG3-201)

(NASA-TP-2225; E-1752, NAS 1.60:2225) Avail: NTIS HC A03/MF A01 CSCL 20D

Deposition rates on platinum-rhodium cylindrical collectors rotating in the cross streams of the combustion gases of a salt-seeded Mach 0.3 burner rig were determined. The collectors were internally air cooled so that their surface temperatures could be widely varied while they were exposed to constant combustion gas temperatures. The deposition rates were compared with those predicted by the chemically frozen boundary layer (CFBL) computer program, which is based on multicomponent vapor transport through the boundary layer. Excellent agreement was obtained between theory and experiment for the NaCl-seeded case, but the agreement lessened as the seed was changed to synthetic sea salt, NaNO3, and K2SO4, respectively, and was particularly poor in the case of Na2SO4. However, when inertial impaction was assumed to be the deposition mechanism for the Na2SO4 case, the predicted rates agreed well with the experimental rates. The former were calculated from a mean particle diameter that was derived from the measured initial droplet size distribution of the solution spray. Critical experiments showed that liquid phase deposits were blown off the smooth surface of the platinum-rhodium collectors by the aerodynamic shear forces of the high-velocity combustion gases but that rough or porous surfaces retained their liquid deposits.

Author

**N84-19744\*#** Oklahoma State Univ., Stillwater.

**TURBULENCE CHARACTERISTICS OF SWIRLING FLOWFIELDS** Ph.D. Thesis

T. W. JACKSON Dec. 1983 277 p refs

(Contract NAG3-74)

(NASA-CR-175392; NAS 1.26:175392) Avail: NTIS HC A13/MF A01 CSCL 20D

Combustor design phenomena; recirculating flows research; single-wire, six-orientation, eddy dissipation rate, and turbulence modeling measurement; directional sensitivity (DS); calibration equipment, confined jet facility, and hot-wire instrumentation; effects of swirl, strong contraction nozzle, and expansion ratio; and turbulence parameters; uncertain; and DS in laminar jets; turbulent nonswirling jets, and turbulent swirling jets are discussed. N.W.

**N84-19745\*#** Oklahoma State Univ., Stillwater. School of Mechanical and Aerospace Engineering.

**CONFINED TURBULENT SWIRLING RECIRCULATING FLOW PREDICTIONS** Ph.D. Thesis

M. T. ABUJELALA May 1984 237 p refs

(Contract NAG3-74)

(NASA-CR-175397; NAS 1.26:175397) Avail: NTIS HC A11/MF A01 CSCL 20D

Turbulent swirling flow, the STARPIC computer code, turbulence modeling of turbulent flows, the k- $\epsilon$  turbulence model and extensions, turbulence parameters deduction from swirling confined flow measurements, extension of the k- $\epsilon$  to confined swirling recirculating flows, and general predictions for confined turbulent swirling flow are discussed. N.W.

**N84-19746\*#** University of Northern Arizona, Flagstaff.

**SWIRL, EXPANSION RATIO AND BLOCKAGE EFFECTS ON CONFINED TURBULENT FLOW** M.S. Thesis

G. L. SCHARRE 1982 175 p refs

(Contract NAG3-74)

(NASA-CR-175391; NAS 1.26:175391) Avail: NTIS HC A08/MF A01 CSCL 20D

A confined jet test facility, a swirls, flow visualization equipment, five-hole pitot probe instrumentation; flow visualization; and effects of swirl on open-ended flows, of gradual expansion on open-ended flows, and blockages of flows are addressed. N.W.

**N84-20527\*#** National Aeronautics and Space Administration. Lewis Research Center, Cleveland, Ohio.

**FUEL SPRAY DIAGNOSTICS**

M. A. BOSQUE *In its* Combust. Fundamentals Res. p 17-21 Apr. 1984 refs

Avail: NTIS HC A14/MF A01 CSCL 20D

Several laser measurement methods are being studied to provide the capability to make droplet size and velocity measurements under a variety of spray conditions. The droplet sizing interferometer (DSI) promises to be a successful technique because of its capability for rapid data acquisition, compilation and analysis. Its main advantage is the ability to obtain size and velocity measurements in air-fuel mixing studies and hot flows. The existing DSI at NASA Lewis is a two-color, two-component system. Two independent orthogonal measurements of size and velocity components can be made simultaneously. It also uses an off-axis large-angle light scatter detection. The fundamental features of the system are optics, signal processing and data management system. The major component includes a transmitter unit, two receiver units, two signal processors, two data management systems, two Bragg cell systems, two printer/plotters, a laser, power supply and color monitor. A.R.H.

**N84-20531\*#** Aerodyne Research, Inc., Bedford, Mass. Center for Chemical and Environmental Physics

**AUTOMATIC HOLOGRAPHIC DROPLET ANALYSIS FOR LIQUID FUEL SPRAYS**

A. C. STANTON, G. W. STEWART, and H. J. CAULFIELD *In* NASA. Lewis Research Center Combust. Fundamentals Res. p 51-54 Apr. 1984 refs

(Contract NAS3-24094)

Avail: NTIS HC A14/MF A01 CSCL 20D

The basic scheme for automated holographic analysis involves an optical system for reconstruction of the three dimensional real image of the droplet field, a spatial scanning system to transport a digitizing X-y image sensor through the real image, and processing algorithms for droplet recognition which establish the droplet sizes and positions. The hardware for system demonstrated includes the expanded and collimated beam from a 5 mW helium-neon laser for hologram reconstruction, an imaging lens for magnification of the real image field, and a video camera and digitizer providing 512-by-512 pixel resolution with 8-bit digitization. A mechanical stage is used to scan the hologram in three dimensional space, maintaining constant image magnification. A test droplet hologram is used for development and testing of the image processing algorithms. A.R.H.

**N84-20538\*#** National Aeronautics and Space Administration. Lewis Research Center, Cleveland, Ohio

**NUMERICAL MODELING OF TURBULENT FLOW**

R. W. CLAUS *In its* Combust. Fundamentals Res. p 97 Apr. 1984 refs

Avail: NTIS HC A14/MF A01 CSCL 20D

Three dimensional combustor calculations are currently stretching the computer hardware capabilities and the computing budgets of gas turbine manufacturers. One of the main reasons for this relates to the large number of complex physical processes occurring in the combustor. Airflow, fuel spray, reaction kinetics, flame radiation, and not the least of which, turbulence must be modeled and the related differential equations solved. Discussions in this conference will address methods to improve the accuracy of combustor flow field calculations and methods to speed the convergence of the modeled equations. This report will focus on aspects of merging these two new technologies. The improved accuracy discretization schemes have a negative impact on the speed of convergence of the modeled equations that the improved solution algorithms may not overcome. A description of the causes of this problem and potential solutions will be examined. B.W.

**N84-20542\*#** Connecticut Univ., Storrs. Dept. of Mechanical Engineering.

**THE INFLUENCE OF LARGE-SCALE MOTION ON TURBULENT TRANSPORT FOR CONFINED COAXIAL JETS**

D. C. BRONDUM and J. C. BENNETT *In* NASA. Lewis Research Center Combust. Fundamentals Res. p 125-129 Apr. 1984 refs

(Contract NAG3-350)

Avail: NTIS HC A14/MF A01 CSCL 20D

The existence of large-scale coherent structures in turbulent shear flows has been well documented in the literature. The importance of these structures in flow entrainment, momentum transport and mass transport in the shear layer has been suggested by several researchers. Comparisons between existing models and experimental data for shear flow in confined coaxial jets reinforce the necessity of further investigation of the large scale structures. These comparisons show the greatest discrepancy between prediction and actual results in the developing flow region where the large scales exist. It was also observed that the momentum transport rate comparisons were very bad. Finally, Schetz has reviewed mixing flows and concluded that large-scale structures were essential aspects of future modeling efforts. Author

**N84-20546\*#** Michigan State Univ., East Lansing. Dept. of Mechanical Engineering.

**FREE STREAM TURBULENCE AND DENSITY RATIO EFFECTS ON THE INTERACTION REGION OF A JET IN A CROSS FLOW**

C. E. WARK and J. F. FOSS *In* NASA. Lewis Research Center Combust. Fundamentals Res. p 163-174 Apr. 1984

(Contract NAG3-245)

Avail: NTIS HC A14/MF A01 CSCL 20D

Jets of low temperature air are introduced into the aft sections of gas turbine combustors for the purpose of cooling the high temperature gases and quenching the combustion reactions. Research studies, motivated by this complex flow field, have been executed by introducing a heated jet into the cross stream of a wind tunnel. The investigation by Kamotani and Greber stands as a prime example of such investigations and it serves as the principal reference for the present study. The low disturbance level of the cross stream, in their study and in similar research investigations, is compatible with an interest in identifying the basic features of this flow field. The influence of the prototypes' strongly disturbed cross flow is not, however, made apparent in these prior investigations. B.W.

**N84-20547\*#** National Aeronautics and Space Administration. Lewis Research Center, Cleveland, Ohio.

## MODELING OF DILUTION JET FLOWFIELDS

J. D. HOLDEMAN and R. SRINIVASAN (Garrett Turbine Engine Co.) *In its Combust. Fundamentals Res.* p 175-187 Apr. 1984 refs

Avail: NTIS HC A14/MF A01 CSCL 20D

The present paper will compare temperature field measurements from selected cases in these investigations with distributions calculated with an empirical model based on assumed vertical profile similarity and superposition and with a 3-D elliptic code using a standard K-E turbulence model. The results will show the capability (or lack thereof) of the models to predict the effects of the principle flow and geometric variables. Author

**N84-20782\*#** National Aeronautics and Space Administration. Lewis Research Center, Cleveland, Ohio.

## VORTEX GENERATING FLOW PASSAGE DESIGN FOR INCREASED FILM COOLING EFFECTIVENESS Patent Application

S. S. PAPELL, inventor (to NASA) 15 Feb. 1984 15 p (NASA-CASE-LEW-14039-1; US-PATENT-APPL-SN-580419)

Avail: NTIS HC A02/MF A01 CSCL 20D

A cooling fluid is injected into a hot flowing gas through a passageway in a wall which contains and is subject to the hot gas. The passageway is slanted in a downstream direction at an acute angle to the wall. A cusp shape is provided in the passageway to generate vortices in the injected cooling fluid thereby reducing the energy extracted from the hot gas for that purpose. The cusp shape increases both film cooling effectiveness and wall area coverage. The cusp may be at either the downstream or upstream side of the passageway, the former substantially eliminating flow separation of the cooling fluid from the wall immediately downstream of the passageway. NASA

**N84-21828\*#** National Aeronautics and Space Administration. Lewis Research Center, Cleveland, Ohio.

## REVIEW AND STATUS OF HEAT-TRANSFER TECHNOLOGY FOR INTERNAL PASSAGES OF AIR-COOLED TURBINE BLADES

F. C. YEH and F. S. STEPKA Apr. 1984 36 p refs (NASA-TP-2232; E-1373; NAS 1.60:2232) Avail: NTIS HC A03/MF A01 CSCL 20D

Selected literature on heat-transfer and pressure losses for airflow through passages for several cooling methods generally applicable to gas turbine blades is reviewed. Some useful correlating equations are highlighted. The status of turbine-blade internal air-cooling technology for both nonrotating and rotating blades is discussed and the areas where further research is needed are indicated. The cooling methods considered include convection cooling in passages, impingement cooling at the leading edge and at the midchord, and convection cooling in passages, augmented by pin fins and the use of roughened internal walls. A.R.H.

**N84-21832\*#** National Aeronautics and Space Administration. Lewis Research Center, Cleveland, Ohio.

## EFFECT OF A ROTOR WAKE ON HEAT TRANSFER FROM A CIRCULAR CYLINDER

R. J. SIMONEAU, K. A. MOREHOUSE, G. J. VANFOSSEN, and F. P. BEHNING 8 Aug. 1984 18 p refs Proposed for presentation at 22nd Natl. Heat Transfer Conf., New York, 5-8 Aug. 1984; sponsored by ASME and Aiche (NASA-TM-83613; E-2039; NAS 1.15:83613) Avail: NTIS HC A02/MF A01 CSCL 20D

The effect of a rotor wake on heat transfer to a downstream stator was investigated. The rotor was modeled with a spoked wheel of 24 circular pins 1.59 mm in diameter. One of the stator pins was electrically heated in the midspan region and circumferentially averaged heat transfer coefficients were obtained. The experiment was run in an annular flow wind tunnel using air at ambient temperature and pressure. Reynolds numbers based on stator cylinder diameter ranged from .001 to .00001. Rotor

blade passing frequencies ranged from zero to 2500 Hz. Stationary grids were used to vary the rotor inlet turbulence from one to four percent. The rotor-stator spacings were one and two stator pin diameters. In addition to the heat transfer coefficients, turbulence spectra and ensemble averaged wake profiles were measured. At the higher Reynolds numbers, which is the primary range of interest for turbulent heat transfer, the rotor wakes increased Nusselt number from 10 to 45 percent depending on conditions. At lower Reynolds numbers the effect was as much as a factor of two. Author

**N84-22909\*#** National Aeronautics and Space Administration. Lewis Research Center, Cleveland, Ohio.

## VORTEX GENERATING FLOW PASSAGE DESIGN FOR INCREASED FILM-COOLING EFFECTIVENESS AND SURFACE COVERAGE

S. S. PAPELL 1984 21 p refs Presented at the 22nd Natl. Heat Transfer Conf., Niagara Falls, N.Y., 5-8 Aug. 1984; sponsored by ASME and the American Inst. for Chemical Engineering. (NASA-TM-83617; E-2048; NAS 1.15:83617) Avail: NTIS HC A02/MF A01 CSCL 20D

The fluid mechanics of the basic discrete hole film cooling process is described as an inclined jet in crossflow and a cusp shaped coolant flow channel contour that increases the efficiency of the film cooling process is hypothesized. The design concept requires the channel to generate a counter rotating vortex pair secondary flow within the jet stream by virtue of flow passage geometry. The interaction of the vortex structures generated by both geometry and crossflow was examined in terms of film cooling effectiveness and surface coverage. Comparative data obtained with this vortex generating coolant passage showed up to factors of four increases in both effectiveness and surface coverage over that obtained with a standard round cross section flow passage. A streakline flow visualization technique was used to support the concept of the counter rotating vortex pair generating capability of the flow passage design. M.G.

**N84-22910\*#** National Aeronautics and Space Administration. Lewis Research Center, Cleveland, Ohio.

## AERODYNAMIC EFFECT OF COMBUSTOR INLET-AIR PRESSURE ON FUEL JET ATOMIZATION

R. D. INGEBO 1984 18 p refs Proposed for presentation at the 20th Joint Propulsion Conf., Cincinnati, 11-13 Jun. 1984 sponsored by AIAA, SAE, and ASME (NASA-TM-83611; E-2034; NAS 1.15:83611) Avail: NTIS HC A02/MF A01 CSCL 20D

Mean drop diameters were measured with a recently developed scanning radiometer in a study of the atomization of liquid jet injected cross stream in high velocity and high pressure airflows. At constant inlet air pressure, reciprocal mean drop diameter, was correlated with airflow mass velocity. Over a combustor inlet-air pressure range of 1 to 21 atmospheres, the ratio of orifice to mean drop diameter,  $D(O)/D(M)$ , was correlated with the product of Weber and Reynolds number,  $WeRe$ , and with the molecular scale momentum transfer ratio of gravitational to inertial forces. M.A.C.

**N84-22911\*#** National Aeronautics and Space Administration. Lewis Research Center, Cleveland, Ohio.

## HEAT TRANSFER IN SERPENTINE PASSAGES WITH TURBULENCE PROMOTERS

R. J. BOYLE 1984 16 p refs Proposed for presentation at the 22nd Natl. Heat Transfer Conf., 5-8 Aug. 1984; sponsored by ASME and Aiche (NASA-TM-83614; E-2040; NAS 1.15:83614) Avail: NTIS HC A02/MF A01 CSCL 20D

Local heat transfer rates and overall pressure losses were determined for serpentine passages of square cross section. The flow entered an inlet leg, turned 180 deg and then passed through an outlet leg. Results were obtained for a passage with smooth walls for three different bend geometries and the effect of turbulence promoters was investigated. Turbulence promoter between 0.6 and 15% of the passage height were tested. Local

heat transfer rates are determined from thermocouple measurements on a thin electrically heated Inconel foil and pressure drop is measured along the flow path. E.A.K.

**N84-23854\*#** Michigan Univ., Ann Arbor. Heat Transfer Lab.  
**MODELING OF ZERO GRAVITY VENTING Interim Report**  
H. MERTE, JR. May 1984 42 p refs  
(Contract NAS3-403)  
(NASA-CR-173503; NAS 1.26:173503; REPT-020547-IR-1) Avail:  
NTIS HC A03/MF A01 CSCL 20D

The venting of cylindrical containers partially filled with initially saturated liquids was conducted under zero gravity conditions and compared with an analytical model which determined the effect of interfacial mass transfer on the ullage pressure response during venting. A model is proposed to improve the estimation of the interfacial mass transfer. Duhammel's superposition integral is incorporated in this analysis to approximate the transient temperature response of the interface, treating the liquid as a semiinfinite solid with conduction heat transfer. This approach to estimating interfacial mass transfer gives improved response when compared to previous models. The model still predicts a pressure decrease greater than those in the experiments reported. M.A.C.

**N84-24747\*#** National Aeronautics and Space Administration.  
Lewis Research Center, Cleveland, Ohio.  
**DETAILED FUEL SPRAY ANALYSIS TECHNIQUES**  
E. J. MULARZ (AVRADCOM), M. A. BOSQUE, and F. M. HUMENIK In AGARD Combust. Probl. in Turbine Eng. 10p  
Jan. 1984 refs Previously announced as N83-34943  
Avail: NTIS HC A19/MF A01 CSCL 20D

Fuel spray analyses which are a necessary input to the analytical modeling of the complex mixing and combustion processes which occur in advanced combustor systems are discussed. It is anticipated that by controlling fuel air reaction conditions, combustor temperatures can be better controlled, leading to improved combustion system durability. The capability to measure liquid droplet size, velocity, and number density throughout a fuel spray and to utilize this measurement technique in laboratory benchmark experiments was demonstrated. The experiment to characterize fuel sprays is described. The experiments and data are useful for application to and validation of turbulent flow modeling to improve the design systems of future advanced technology engines. E.A.K.

**N84-24999\*#** National Aeronautics and Space Administration.  
Lewis Research Center, Cleveland, Ohio.  
**A REVIEW OF INTERNAL COMBUSTION ENGINE COMBUSTION CHAMBER PROCESS STUDIES AT NASA LEWIS RESEARCH CENTER**

H. J. SCHOCK 1984 12 p refs Presented at the 20th Joint Propulsion Conf., Cincinnati, 11-13 Jun 1984; sponsored by AIAA, SAE and ASME  
(NASA-TM-83666; E-2085; NAS 1.15:83666) Avail: NTIS HC A02/MF A01 CSCL 20D

The performance of internal combustion stratified-charge engines is highly dependent on the in-cylinder fuel-air mixing processes occurring in these engines. Current research concerning the in-cylinder airflow characteristics of rotary and piston engines is presented. Results showing the output of multidimensional models, laser velocimetry measurements and the application of a holographic optical element are described. Models which simulate the four-stroke cycle and seal dynamics of rotary engines are also discussed. R.S.F.

**N84-25000\*#** National Aeronautics and Space Administration.  
Lewis Research Center, Cleveland, Ohio.

**COMPUTATIONAL MODELING OF JET INDUCED MIXING OF CRYOGENIC PROPELLANTS IN LOW-G**

J. I. HOCHSTEIN (Akron Univ.), P. M. GERHART (Akron Univ.), and J. C. AYDELOT May 1984 13 p refs Presented at the 20th Joint Propulsion Conf., Cincinnati, 11-13 Jun. 1984; sponsored by AIAA, SAE and ASME

(Contract NAG3-318)  
(NASA-TM-83703; E-2161; NAS 1.15:83703; AIAA-84-1344)  
Avail: NTIS HC A02/MF A01 CSCL 20D

The SOLA-ECLIPSE Code is being developed to enable computational prediction of jet induced mixing in cryogenic propellant tanks in a low-gravity environment. Velocity fields, predicted for scale model tanks, are presented which compare favorably with the available experimental data. A full scale liquid hydrogen tank for a typical Orbit Transfer Vehicle is analyzed with the conclusion that coupling an axial mixing jet with a thermodynamic vent system appears to be a viable concept for the control of tank pressure. Author

**N84-25001\*#** Pennsylvania State Univ., State College. Applied Research Lab.

**THE BOUNDARY LAYER ON COMPRESSOR CASCADE BLADES Semiannual Progress Report, 1 Dec. 1983 - 1 Jun. 1984**

S. DEUTSCH and W. C. ZIERKE 1984 76 p refs

(Contract NSG-3264)  
(NASA-CR-173514; NAS 1.26:173514) Avail: NTIS HC A05/MF A01 CSCL 20D

The characteristics of the flow field about highly loaded turbocompressor blades in a cascade wind tunnel were investigated. Experimental tests were conducted at chord Reynolds number ( $R_{sub c}$ ) near 500,000. A laser Doppler anemometer was employed in flow velocity measurement. Suction surface mean velocity and turbulence intensity profiles at a single incidence angle are presented. These data contribute to further understanding of two-dimensional boundary layer profiles, points of separation, and transition zones for turbomachine blades, and concomitantly, to compressor cascade predictive models. R.S.F.

**N84-25941\*#** Case Western Reserve Univ., Cleveland, Ohio.  
Dept. of Mechanical and Aerospace Engineering.

**SCALING AND MODELING OF THREE-DIMENSIONAL, END-WALL, TURBULENT BOUNDARY LAYERS Ph.D. Thesis - Final Report**

U. C. GOLDBERG and E. RESHOTKO Washington NASA Jun. 1984 135 p refs

(Contract NAG3-270)  
(NASA-CR-3792; E-2024; NAS 1.26:3792) Avail: NTIS HC A07/MF A01 CSCL 20D

The method of matched asymptotic expansion was employed to identify the various subregions in three dimensional, turbomachinery end wall turbulent boundary layers, and to determine the proper scaling of these regions. The two parts of the b.l. investigated are the 3D pressure driven part over the endwall, and the 3D part located at the blade/end wall juncture. Models are proposed for the 3d law of the wall and law of the wake. These models and the data of van den Berg and Elsenaar and of Mueller are compared and show good agreement between models and experiments. E.A.K.

**N84-25943\*#** Cleveland State Univ., Ohio. Dept. of Mechanical Engineering.

**EFFECTS OF UNSTEADY FREE STREAM VELOCITY AND FREE STREAM TURBULENCE ON STAGNATION POINT HEAT TRANSFER Final Report**

R. S. R. GORLA Washington NASA Jun. 1984 39 p refs  
(Contract NCC3-3)

(NASA-CR-3804; E-2100; NAS 1.26:3804) Avail: NTIS HC A03/MF A01 CSCL 20D

The combined effects of transient free stream velocity and free stream turbulence on heat transfer at a stagnation point over a cylinder situated in a crossflow are studied. An eddy diffusivity



model was formulated and the governing momentum and energy equations are integrated by means of the steepest descent method. The numerical results for the wall shear stress and heat transfer rate are correlated by a turbulence parameter. The wall friction and heat transfer rate increase with increasing free stream turbulence intensity. Author

**N84-25946\*#** National Aeronautics and Space Administration. Lewis Research Center, Cleveland, Ohio.

## A SEMI-DIRECT PROCEDURE USING A LOCAL RELAXATION FACTOR AND ITS APPLICATION TO AN INTERNAL FLOW PROBLEM

S. C. CHANG 1984 9 p refs Presented at the 9th Intern. Conf. on Numerical Methods in Fluid Dyn., Saclay, France, 25-29 Jun. 1984; sponsored by CEA, CISE, DRET, CNES, EDF, Framatome and Novatome (NASA-TM-83704; E-2162; NAS 1.15:83704) Avail: NTIS HC A02/MF A01 CSCL 20D

Generally, fast direct solvers are not directly applicable to a nonseparable elliptic partial differential equation. This limitation, however, is circumvented by a semi-direct procedure, i.e., an iterative procedure using fast direct solvers. An efficient semi-direct procedure which is easy to implement and applicable to a variety of boundary conditions is presented. The current procedure also possesses other highly desirable properties, i.e.: (1) the convergence rate does not decrease with an increase of grid cell aspect ratio, and (2) the convergence rate is estimated using the coefficients of the partial differential equation being solved.

Author

**N84-25961\*#** National Aeronautics and Space Administration. Lewis Research Center, Cleveland, Ohio.

## UNSTEADY FLOW IN TURBOMACHINERY: AN OVERVIEW

/n Von Karman Inst. for Fluid Dynamics Unsteady Flow in Turbomachines, Vol. 1 p 1-20 1984 refs Avail: NTIS HC A14/MF A01

The importance of understanding and modeling the unsteady flow phenomena in turbomachinery is discussed. Historical events in the application and development of gas turbines for aircraft propulsion are traced. Technology advancements over the years are highlighted with focus on the compression system components. Trends in compressor research within the National Advisory Committee for Aeronautics (NACA)/National Aeronautics and Space Administration (NASA) are noted. The impact of technology advancements on the increased occurrences of unsteady flow related problems in advanced engine development programs is discussed. The impact of the new and more demanding requirements being imposed on the propulsion system to meet advanced aircraft mission needs are also noted. Brief discussions on the present day understanding and modeling capability of the unsteady flow phenomena are presented to include discussions on rotating stall, surge, flutter, forced response and noise generation. Author

**N84-25968\*#** National Aeronautics and Space Administration. Lewis Research Center, Cleveland, Ohio.

## NUMERICAL ASPECTS OF UNSTEADY FLOW CALCULATIONS

J. J. ADAMCZYK /n Von Karman Inst. for Fluid Dynamics Unsteady Flow in Turbomachines, Vol. 2 75 p 1984 refs Avail: NTIS HC A16/MF A01 CSCL 20D

The numerical aspects of simulation unsteady flows which arise in turbomachinery are addressed. In particular the simulation of rotating stall and surge is discussed. Author

**N84-29155\*#** Pennsylvania State Univ., University Park. Dept. of Mechanical Engineering.

## THE STRUCTURE OF EVAPORATING AND COMBUSTING SPRAYS: MEASUREMENTS AND PREDICTIONS Semiannual Status Report, 1 Jan. - 30 Jun. 1984

J. S. SHUEN, A. S. P. SOLOMON, and G. M. FAETH Jul. 1984 33 p refs (Contract NAG3-190) (NASA-CR-173778; NAS 1:26:173778) Avail: NTIS HC A03/MF A01 CSCL 20D

An apparatus developed, to allow observations of monodisperse sprays, consists of a methane-fueled turbulent jet diffusion flame with monodisperse methanol drops injected at the burner exit. Mean and fluctuating-phase velocities, drop sizes, drop-mass fluxes and mean-gas temperatures were measured. Initial drop diameters of 100 and 180 microns are being considered in order to vary drop penetration in the flow and effects of turbulent dispersion. Baseline tests of the burner flame with no drops present were also conducted. Calibration tests, needed to establish methods for predicting drop transport, involve drops supported in the post-flame region of a flat-flame burner operated at various mixture ratios. Spray models which are being evaluated include: (1) locally homogeneous flow (LFH) analysis, (2) deterministic separated flow (DSF) analysis and (3) stochastic separated flow (SSF) analysis. A.R.H.

**N84-29157\*#** National Aeronautics and Space Administration. Lewis Research Center, Cleveland, Ohio.

## TURBULENCE AND SURFACE HEAT TRANSFER NEAR THE STAGNATION POINT OF A CIRCULAR CYLINDER IN TURBULENT FLOW

C. R. WANG 1983 17 p refs Prepared for presentation at the Winter Ann. Meeting of the ASME, New Orleans, 9-14 Dec. 1984

(NASA-TM-83732; E-2210; NAS 1.15:83732) Avail: NTIS HC A02/MF A01 CSCL 20D

A turbulent boundary layer flow analysis of the momentum and thermal flow fields near the forward stagnation point due to a circular cylinder in turbulent cross flow is presented. Turbulence modeling length scale, anisotropic turbulence initial profiles and boundary conditions were identified as functions of the cross flow turbulence intensity and the boundary layer flow far field velocity. These parameters were used in a numerical computational procedure to calculate the mean velocity, mean temperature, and turbulence double correlation profiles within the flow field. The effects of the cross flow turbulence on the stagnation region momentum and thermal flow fields were investigated. This analysis predicted the existing measurements of the stagnation region mean velocity and surface heat transfer rate with cross flow Reynolds number and turbulence intensity less than 250,000 and 0.05, respectively. Author

**N84-30223\*#** National Aeronautics and Space Administration. Lewis Research Center, Cleveland, Ohio.

## ATOMIZATION OF LIQUID SHEETS IN HIGH PRESSURE AIRFLOW

R. D. INGEBO 1984 18 p refs Proposed for presentation at the Winter Ann. Meeting of the American Society of Mechanical Engineers, New Orleans, 9-14 Dec. 1984

(NASA-TM-83731; E-2207; NAS 1.15:83731) Avail: NTIS HC A02/MF A01 CSCL 20D

An investigation of liquid sheet atomization is made with combustor simulated inlet air pressures varied from 0.10 to 2.1 MPa. Mean drop diameters are measured with an improved scanning radiometer and correlated with the liquid and air stream Reynolds numbers, RE(1) and RE(A) and the airstream pressure sensitive group GC(2). These data are used in the modeling of the combustion process. M.A.C.



**N84-30224\*#** National Aeronautics and Space Administration. Lewis Research Center, Cleveland, Ohio.

**ACOUSTIC PRESSURES EMANATING FROM A TURBOMACHINE STAGE**

S. M. RAMACHANDRA 1984 16 p refs Proposed for presentation at the 9th Aeroacoustics Meeting, Williamsburg, Va., 15-17 Oct. 1984; sponsored by NASA and the American Inst. of Aeronautics and Astronautics (NASA-TM-83734; E-2217; NAS 1.15:83734) Avail: NTIS HC A02/MF A01 CSCL 20D

A knowledge of the acoustic energy emission of each blade row of a turbomachine is useful for estimating the overall noise level of the machine and for determining its discrete frequency noise content. Because of the close spacing between the rotor and stator of a compressor stage, the strong aerodynamic interactions between them have to be included in obtaining the resultant flow field. A three dimensional theory for determining the discrete frequency noise content of an axial compressor consisting of a rotor and a stator each with a finite number of blades are outlined. The lifting surface theory and the linearized equation of an ideal, nonsteady compressible fluid motion are used for thin blades of arbitrary cross section. The combined pressure field at a point of the fluid is constructed by linear addition of the rotor and stator solutions together with an interference factor obtained by matching them for net zero vorticity behind the stage.

Author

**N84-31558\*#** National Aeronautics and Space Administration. Lewis Research Center, Cleveland, Ohio.

**DEPOSITION OF  $\text{Na}_2\text{SO}_4$  FROM SALT-SEEDED COMBUSTION GASES OF A HIGH VELOCITY BURNER RIG**

G. J. SANTORO, S. A. GOEKOGLU (Analox Corp.), F. J. KOHL, C. A. STEARNS, and D. E. ROSNER (Yale Univ.) 1984 24 p refs Proposed for presentation at the TMS-AIME Fall Meeting, Detroit, 17-19 Sep. 1984 (NASA-TM-83751; E-2237; NAS 1.15:83751) Avail: NTIS HC A02/MF A01 CSCL 20D

The mechanism of deposition of  $\text{Na}_2\text{SO}_4$  was studied under controlled laboratory conditions and the results have been compared to a recently developed comprehensive theory of vapor deposition. Thus  $\text{Na}_2\text{SO}_4$ ,  $\text{NaCl}$ ,  $\text{NaNO}_3$  and simulated sea salt solutions were injected into the combustor of a nominal Mach.0.3 burner rig burning jet fuel at constant fuel/air ratios. The deposits formed on inert collectors, rotation in the cross flow of the combustion gases, were weighed and analyzed. Collector temperature was uniform and could be varied over a large range by internal air cooling. Deposition rates and dew point temperatures were determined. Supplemental testing included droplet size measurements of the atomized salt solutions. These tests along with thermodynamic and transport calculations were utilized in the interpretation of the deposition results.

Author

**N84-32751\*#** Rensselaer Polytechnic Inst., Troy, N. Y.

**MASS TRANSFER FROM A CIRCULAR CYLINDER: EFFECTS OF FLOW UNSTEADINESS AND SLIGHT NONUNIFORMITIES**  
**Final Report**

M. L. MARZIALE and R. E. MAYLE Sep. 1984 244 p refs (Contract NSG-3262) (NASA-CR-174759; E-126:174759) Avail: NTIS HC A11/MF A01 CSCL 20D

Experiments were performed to determine the effect of periodic variations in the angle of the flow incident to a turbine blade on its leading edge heat load. To model this situation, measurements were made on a circular cylinder oscillating rotationally in a uniform steady flow. A naphthalene mass transfer technique was developed and used in the experiments and heat transfer rates are inferred from the results. The investigation consisted of two parts. In the first, a stationary cylinder was used and the transfer rate was measured for  $\text{Re} = 75,000$  to  $110,000$  and turbulence levels from .34 percent to 4.9 percent. Comparisons with both theory and the results of others demonstrate that the accuracy and repeatability of the developed mass transfer technique is about  $\pm$  or  $\pm$  2 percent, a large improvement over similar methods. In the second part

identical flow conditions were used but the cylinder was oscillated. A Strouhal number range from .0071 to .1406 was covered. Comparisons of the unsteady and steady results indicate that the magnitude of the effect of oscillation is small and dependent on the incident turbulence conditions.

Author

## 35

### INSTRUMENTATION AND PHOTOGRAPHY

Includes remote sensors; measuring instruments and gages; detectors; cameras and photographic supplies; and holography.

**A84-13125\***

**THE PRESSURE MULTIPLIER REVISITED**

B. R. F. KENDALL (Pennsylvania State University, University Park, PA) Journal of Vacuum Science and Technology A (ISSN 0734-2101), vol. 1, Oct.-Dec. 1983, p. 1875-1877. refs (Contract NSG-3301)

Pressure multipliers, which were originally intended to continuously sample an unknown pressure and increase it by a known factor, so that measurements could be conducted at low pressures with liquid-in-gas gauges, may be usefully applied to the increasing number of components available for use in molecular flow networks. An intriguing possibility involves the electric control of pressure multiplier gain by means of a piezoelectric valve.

O.C.

**A84-13192\*** Riso National Lab., Roskilde (Denmark).

**ESTIMATING TIME AND TIME-LAG IN TIME-OF-FLIGHT VELOCIMETRY**

L. LADING (Atomenergikommissionens, Forsogsanlaeg Riso, Roskilde, Denmark) Applied Optics (ISSN 0003-6935), vol. 22, Nov. 15, 1983, p. 3637-3643. Research supported by the Statens Naturvidenskabelige Forskningsrad. refs (Contract NAG3-2)

Estimating time and time-lag in time-of-flight velocimeters is investigated. Statistics of a filtered Poisson point process is given. A Maximum Likelihood Estimator is compared with suboptimum estimators in terms of robustness. For a dominating background combined spatial and temporal processing can improve the robustness compared with purely temporal processing. Schemes for the spatial filters are given.

Author

**A84-17946\*#** Spectron Development Labs., Inc., Costa Mesa, Calif.

**A TECHNIQUE COMBINING THE VISIBILITY OF A DOPPLER SIGNAL WITH THE PEAK INTENSITY OF THE PEDESTAL TO MEASURE THE SIZE AND VELOCITY OF DROPLETS IN A SPRAY**

C. F. HESS (Spectron Development Laboratories, Inc., Costa Mesa, CA) American Institute of Aeronautics and Astronautics, Aerospace Sciences Meeting, 22nd, Reno, NV, Jan. 9-12, 1984. 8 p. refs (Contract NAS3-23538; F49620-83-C-0060) (AIAA PAPER 84-0203)

A technique combining the visibility of a Doppler signal and the intensity of the scattered light to measure the size and velocity of particles is presented. It is shown that using only the visibility technique can lead to large errors under many conditions such as dense sprays. It is also shown that this error is considerably reduced and very high resolution is obtained by combining the visibility with the intensity of the scattered light. An instrument was developed using this new concept and measurements were performed in sprays of known characteristics. The results of monodispersed, bimodal and trimodal sprays are reported.

Author

**A84-18047\*#** Oklahoma State Univ., Stillwater.  
**ACCURACY AND DIRECTIONAL SENSITIVITY OF THE SINGLE-WIRE TECHNIQUE**

D. G. LILLEY (Oklahoma State University, Stillwater, OK) and T. W. JACKSON (American Institute of Aeronautics and Astronautics, Aerospace Sciences Meeting, 22nd, Reno, NV, Jan. 9-12, 1984, 17 p. refs  
 (Contract NAG3-74)  
 (AIAA PAPER 84-0367)

Multi-orientation of a single-hot-wire is a novel way to measure the three time-mean velocities, the three turbulent normal stresses, and the three turbulent shear stresses. The present study focuses on the accuracy and directional sensitivity of the technique with respect to mean flow velocity orientation to the probe. Results demonstrate relative insensitivity, indicating that the method is a useful cost-effective tool for turbulent flows of unknown dominant flow direction. Author

**A84-22872\*#** National Aeronautics and Space Administration, Lewis Research Center, Cleveland, Ohio.  
**APPLICATION OF LASER ANEMOMETRY IN TURBINE ENGINE RESEARCH**

R. G. SEASHOLTZ (NASA, Lewis Research Center, Cleveland, OH) Cleveland Electrical/Electronics Conference and Exposition, Cleveland, OH, Oct. 4-6, 1983, Paper. 7 p. refs

The application of laser anemometry to the study of flow fields in turbine engine components is reviewed. Included are discussions of optical configurations, seeding requirements, electronic signal processing, and data processing. Some typical results are presented along with a discussion of ongoing work. Author

**A84-28623\*** United Technologies Research Center, East Hartford, Conn.

**THE USE OF HETERODYNE SPECKLE PHOTOGRAMMETRY TO MEASURE HIGH-TEMPERATURE STRAIN DISTRIBUTIONS**

K. A. STETSON (United Technologies Research Center, East Hartford, CT) IN: Holographic data nondestructive testing; Proceedings of the Meeting, Dubrovnik, Yugoslavia, October 4-8, 1982. Bellingham, WA, SPIE - The International Society for Optical Engineering, 1983, p. 46-55.  
 (Contract NAS3-22126)

Thermal and mechanical strains have been measured on samples of a common material used in jet engine burner liners, which were heated from room temperature to 870 C and cooled back to 220 C, in a laboratory furnace. The physical geometry of the sample surface was recorded to select temperatures by means of a set of twelve single-exposure specklegrams. Sequential pairs of specklegrams were compared in a heterodyne interferometer which allowed high-precision measurement of differential displacements. Good speckle correlation was observed between the first and last specklegrams also, which showed the durability of the surface microstructure, and permitted a check on accumulated errors. Agreement with calculated thermal expansion was to within a few hundred microstrain over a range of fourteen thousand. Author

**A84-28739\*#** Case Western Reserve Univ., Cleveland, Ohio.  
**OPTIMIZING AND COMPARING LASER ANEMOMETERS**

R. V. EDWARDS (Case Western Reserve University, Cleveland, OH), L. LADING, and A. S. JENSEN (Forsøgsanlaeg Riso, Roskilde, Denmark) IN: International Symposium on Applications of Laser-Doppler Anemometry to Fluid Mechanics, Lisbon, Portugal, July 5-7, 1982, Proceedings. Lisbon, Instituto Superior Tecnico, 1982, p. 17.2.1-17.2.11.  
 (Contract NAG3-2)

Comparisons can be made only if some single valued measure of the quality of each system can be defined. This concept is illustrated here by specifying the quality variable to be the measurement uncertainty in the mean velocity of a turbulent flow in the presence of a large background noise. The Fisher number is used as a figure of merit for some parts of the system. It is noted that in many cases of practical interest, the reciprocal Fisher number gives the actual variance of an estimator. Its principal

advantage here is that it can be computed without detailed assumptions about the statistics of the estimated quantities. The concept of a Fisher number is related to the concept of information gain in a measurement. The variance of the measured mean velocity is expressed in terms of the uncertainty for the individual measurements, the measurement rate, and the velocity correlation time. Conditions are given under which the fringe and the two-spot anemometer are optimized. C.R.

**A84-28797\*** Colorado State Univ., Fort Collins.  
**STRESS MEASUREMENT IN THIN FILMS BY GEOMETRICAL OPTICS**

S. M. ROSSNAGEL, P. GILSTRAP, and R. RUJKORAKARN (Colorado State University, Fort Collins, CO) Journal of Vacuum Science and Technology (ISSN 0022-5355), vol. 21, Nov.-Dec. 1982, p. 1045, 1046. refs  
 (Contract NAG3-209; F29601-82-K-0009)

A variation of Newton's rings experiment is proposed for measuring film stress. The procedure described, the geometrical optics method, is used to measure radii of curvature for a series of film depositions with Ta, Al, and Mo films. The method has a sensitivity of  $1 \times 10$  to the 9th dyn/sq cm, corresponding to the practical radius limit of about 50 m, and a repeatability usually within five percent. For the purposes of comparison, radii are also measured by Newton's rings method and the Talysurf method; all results are found to be in general agreement. Measurement times are also compared: the geometrical optics method requires only 1/2-1 minute. It is concluded that the geometrical optics method provides an inexpensive, fast, and a reasonably correct technique with which to measure stresses in film. C.M.

**A84-34528\*#** National Aeronautics and Space Administration, Lewis Research Center, Cleveland, Ohio.  
**LARGE-APERTURE INTERFEROMETER WITH LOCAL REFERENCE BEAM**

W. L. HOWES (NASA, Lewis Research Center, Cleveland, OH) Applied Optics (ISSN 0003-6935), vol. 23, May 15, 1984, p. 1467-1473. refs

A large-aperture interferometer was devised by adding a local-reference-beam-generating optical system to a schlieren system. Two versions of the interferometer are demonstrated, one employing 12.7 cm (5 in.) diameter schlieren optics, the other employing 30.48 cm (12 in.) diameter parabolic mirrors in an off-axis system. In the latter configuration a cylindrical lens is introduced near the light source to correct for astigmatism. A zone plate is a satisfactory decollimating element in the reference-beam arm of the interferometer. Attempts to increase the flux and uniformity of irradiance in the reference beam by using a diffuser are discussed. Previously announced in STAR as N83-13979 R.J.F.

**A84-35223\*#** National Aeronautics and Space Administration, Lewis Research Center, Cleveland, Ohio.

**MEASUREMENT OF FLUID PROPERTIES USING RAPID-DOUBLE-EXPOSURE AND TIME-AVERAGE HOLOGRAPHIC INTERFEROMETRY**

A. J. DECKER (NASA, Lewis Research Center, Cleveland, OH) AIAA, SAE, and ASME, Joint Propulsion Conference, 20th, Cincinnati, OH, June 11-13, 1984, 9 p. refs  
 (AIAA PAPER 84-1461)

The holographic recording of the time history of a flow feature in three dimensions is discussed. The use of diffuse illumination holographic interferometry or the three-dimensional visualization of flow features such as shock waves and turbulent eddies is described. The double-exposure and time-average methods are compared using the characteristic function and the results from a flow simulator. A time history requires a large hologram recording rate. Results of holographic cinematography of the shock waves in a flutter cascade are presented as an example. Future directions of this effort, including the availability and development of suitable lasers, are discussed. Previously announced in STAR as N84-21849 Author

**A84-36958\*# Aerometrics, Inc., Mountain View, Calif.  
DEVELOPMENT OF THE PHASE/DOPPLER SPRAY ANALYZER  
FOR LIQUID DROP SIZE AND VELOCITY  
CHARACTERIZATIONS**

W. D. BACHALO and M. J. HOUSER (Aerometrics, Inc., Mountain View, CA) AIAA, SAE, and ASME, Joint Propulsion Conference, 20th, Cincinnati, OH, June 11-13, 1984. 14 p. refs  
(Contract NAS3-23684; F49620-84-C-0023)  
(AIAA PAPER 84-1199)

The present novel method for spray drop size and velocity measurement is analogous to a laser Doppler velocimeter, obtaining data from the spatial frequency of the interference fringe pattern produced by light scattering. Monodisperse droplet streams were used as a basic test of the theory, as well as of the susceptibility of the method to effects involved in actual application. Either beam intersection angle or detector spacing can be changed to achieve the same result. Polydispersed sprays were also measured. O.C.

**A84-36981\*# General Electric Co., Schenectady, N. Y.  
ACOUSTICALLY-INDUCED MODULATION SPECTROSCOPY  
FOR ULTRA-SENSITIVE GAS ANALYSIS**

R. W. FITZ, C. M. PENNEY, and M. LAPP (General Electric Co., Schenectady, NY) AIAA, SAE, and ASME, Joint Propulsion Conference, 20th, Cincinnati, OH, June 11-13, 1984. 7 p. refs  
(Contract NAS3-23532; NAS3-24084)  
(AIAA PAPER 84-1460)

A new optical technique has been developed for ultra-sensitive attenuation measurements in gaseous media and, in particular, for determination of low levels of smoke emitted from jet engines. It is a variation on direct light transmission where the sample gas density in a cell is modulated acoustically by a speaker. The amplitude variation of the light transmission is proportional to the gas density and is insensitive to window contamination and detector instabilities. Preliminary analysis and experiments indicate that the instrument promises to measure light absorption to less than 1 percent per meter and allow measurement of smoke emissions from 1 to 100 mg/cu m. The technique has been demonstrated through the use of an absorbing gas, viz., 200 ppm of NO<sub>2</sub> in N<sub>2</sub> which produces 25 percent per meter absorption. Author

**A84-37999\*# Oklahoma State Univ., Stillwater.  
TURBULENCE MEASUREMENTS IN A COMPLEX FLOWFIELD  
USING A CROSSED HOT-WIRE**

D. G. LILLEY (Oklahoma State University, Stillwater, OK) and B. E. MCKILLOP (American Institute of Aeronautics and Astronautics, Fluid Dynamics, Plasma Dynamics, and Lasers Conference, 17th, Snowmass, CO, June 25-27, 1984. 11 p. USAF-supported research. refs  
(Contract NAG3-74)  
(AIAA PAPER 84-1604)

An X-wire probe was used to measure the time-mean and fluctuating velocities and shear stress in nonswirling nonreacting confined jet flows. Data were taken from an axisymmetric confined jet with an expansion ratio of 2 and an expansion angle of 90 deg, and from the same segment with a contraction nozzle. Velocity profiles developed faster in the confined jet than in the free jet, with the former experiencing higher turbulence levels and larger time-mean velocities. The X-wire is concluded to furnish more accurate results for the turbulent shear stress than a multioriented single-wire technique. M.S.K.

**A84-40248\*# National Aeronautics and Space Administration.  
Lewis Research Center, Cleveland, Ohio.**

**OPTIMIZATION OF FRINGE-TYPE LASER ANEMOMETERS FOR  
TURBINE ENGINE COMPONENT TESTING**

R. G. SEASHOLTZ, L. G. OBERLE, and D. H. WEIKLE (NASA, Lewis Research Center, Cleveland, OH) AIAA, SAE, and ASME, Joint Propulsion Conference, 20th, Cincinnati, OH, June 11-13, 1984. 17 p. refs  
(AIAA PAPER 84-1459)

The fringe type laser anemometer is analyzed using the Cramer-Rao bound for the variance of the estimate of the Doppler frequency as a figure of merit. Mie scattering theory is used to

calculate the Doppler signal wherein both the amplitude and phase of the scattered light are taken into account. The noise from wall scatter is calculated using the wall bidirectional reflectivity and the irradiance of the incident beams. A procedure is described to determine the optimum aperture mask for the probe volume located a given distance from a wall. The expected performance of counter type processors is also discussed in relation to the Cramer-Rao bound. Numerical examples are presented for a coaxial backscatter anemometer. Previously announced in STAR as N84-25019

Author

**A84-40736\* Southwest Research Inst., San Antonio, Tex.  
CALIBRATION OF THE MALVERN PARTICLE SIZER**

L. G. DODGE (Southwest Research Institute, San Antonio, TX) Applied Optics (ISSN 0003-6935), vol. 23, July 15, 1984, p. 2415-2419. refs  
(Contract N00014-80-K-0460; NAS3-24090)

A relatively simple technique has been developed to calibrate particle- and droplet-sizing instruments manufactured by Malvern and other similar Fraunhofer diffraction particle-sizing instruments. Measurements of standard reticles using an instrument calibrated in this manner demonstrate the effectiveness of the procedure. In addition, guidelines are presented to avoid errors due to vignetting of the scattered light signal. Author

**A84-40738\*# National Aeronautics and Space Administration  
Lewis Research Center, Cleveland, Ohio.**

**RAINBOW SCHLIEREN AND ITS APPLICATIONS**

W. L. HOWES (NASA, Lewis Research Center, Cleveland, OH) Applied Optics (ISSN 0003-6935), vol. 23, July 15, 1984, p. 2449-2460. refs

In this modification of the schlieren apparatus the knife-edge is replaced by a radial-rainbow filter with a transparent center and opaque surround. Consequently, refractive-index inhomogeneities in the test section appear varicolored, whereas uniformities appear white. The rainbow schlieren is simple, is easy to use, and accentuates detail regarding inhomogeneities more than the ordinary schlieren. The rainbow schlieren permits quantitative evaluation of certain refractive-index distributions, including turbulence, by simple calculations from observations of hue rather than irradiance. Author

**N84-11456\*# National Aeronautics and Space Administration.  
Lewis Research Center, Cleveland, Ohio.**

**APPLICATION OF LASER ANEMOMETRY IN TURBINE ENGINE  
RESEARCH**

R. G. SEASHOLTZ 1982 9 p. refs Presented at the Electron. Conf., Cleveland, 4-6 Oct. 1983; sponsored by Inst. of Elec. and Electron. Engr., Inc.  
(NASA-TM-83513; E-1860; NAS 1.15:83513) Avail: NTIS HC A02/MF A01 CSCL 14B

The application of laser anemometry to the study of flow fields in turbine engine components is reviewed. Included are discussions of optical configurations, seeding requirements, electronic signal processing, and data processing. Some typical results are presented along with a discussion of ongoing work. Author

**N84-12447\*# National Aeronautics and Space Administration.  
Lewis Research Center, Cleveland, Ohio.**

**A MULTISTAGE SPENT PARTICLE COLLECTOR AND A  
METHOD FOR MAKING SAME Patent Application**

B. T. EBHARA, inventor (to NASA) 30 Sep. 1983 12 p  
(NASA-CASE-LEW-13914-1; US-PATENT-APPL-SN-537615)  
Avail: NTIS HC A02/MF A01 CSCL 14B

A spent particle collector is comprised of one or more axisymmetric stages, each stage comprising a subassembly having an inner pyrolytic graphite ring, a transition ring, a ceramic insulator ring, and an outer metal ring which forms part of the wall of the collector. Each transition ring is of a ductile metal having high thermal conductivity and is provided with an annular sputter shield wall extending toward the source of spent particles and, where necessary, a trough in the other surface to enclose the sputter shield of the next adjacent transition ring. Radial extending slots

are provided in a transition ring to form segments which are retained in their position by the sputter shield. This arrangement with the ceramic ring outwardly of the transition ring keeps the latter in contact with the inner pyrolytic graphite ring. This multistage collector can be assembled with high accuracy. The collector is attached by welding to a flange attached to a source of spent particles such as a traveling wave tube. NASA

**N84-16529\*#** Pratt and Whitney Aircraft, West Palm Beach, Fla.  
**DYNAMIC GAS TEMPERATURE MEASUREMENT SYSTEM, VOLUME 1**  
 D. L. ELMORE, W. W. ROBINSON, and W. B. WATKINS 10 May 1983 138 p refs  
 (Contract NAS3-23154)  
 (NASA-CR-168267-VOL-1; NAS 1.26:168267-VOL-1; PWA/GPD-FR-17145-VOL-1) Avail: NTIS HC A07/MF A01 CSCL 14B

A gas temperature measurement system with compensated frequency response of 1 kHz and capability to operate in the exhaust of a gas turbine engine combustor was developed. A review of available technologies which could attain this objective was done. The most promising method was identified as a two wire thermocouple, with a compensation method based on the responses of the two different diameter thermocouples to the fluctuating gas temperature field. In a detailed design of the probe, transient conduction effects were identified as significant. A compensation scheme was derived to include the effects of gas convection and wire conduction. The two wire thermocouple concept was tested in a laboratory burner exhaust to temperatures of about 3000 F and in a gas turbine engine to combustor exhaust temperatures of about 2400 F. Uncompensated and compensated waveforms and compensation spectra are presented. S.L.

**N84-19787\*#** National Aeronautics and Space Administration, Lewis Research Center, Cleveland, Ohio.  
**THE INFINITE LINE PRESSURE PROBE**  
 D. R. ENGLUND and W. B. RICHARDS (Oberlin Coll., Ohio) 1984 17 p refs Proposed for presentation at the 30th Intern. Instrumentation Symp., Denver, 7-10 May 1984  
 (NASA-TM-83582; E-1973; NAS 1.15:83582) Avail: NTIS HC A02/MF A01 CSCL 14B

The infinite line pressure probe provides a means for measuring high frequency fluctuating pressures in difficult environments. A properly designed infinite line probe does not resonate; thus its frequency response is not limited by acoustic resonance in the probe tubing, as in conventional probes. The characteristics of infinite line pressure probes are reviewed and some applications in turbine engine research are described. A probe with a flat-oval cross section, permitting a constant-impedance pressure transducer installation, is described. Techniques for predicting the frequency response of probes with both circular and flat-oval cross sections are also cited. Author

**N84-20528\*#** Spectron Development Labs., Inc., Costa Mesa, Calif.  
**DEVELOPMENT AND IMPLEMENTATION OF ADVANCED DIAGNOSTIC TECHNIQUES**  
 C. F. HESS /n NASA, Lewis Research Center Combust. Fundamentals Res. p 23-29 Apr. 1984  
 (Contract NAS3-23538)  
 Avail: NTIS HC A14/MF A01 CSCL 14B

Two techniques were identified which offer great potential in the measurement of sprays. The first is referred to as IMAX, and it consists of a nonintrusive pulse height analyzer. The second is referred to as Visibility/Intensity (V/I) and it performs a size measurement by examining the visibility and the pedestal intensity that the IMAX technique provides a larger dynamic range and higher accuracy than V/I. It also shows that the two-color IMAX concept provides a higher S/N primarily because of the high efficiency in spectrally separating the two signals. The size distribution of two kinds of sprays are reported. The first spray was produced by a Berglund-Liu droplet generator with dispersion

air. The second spray was produced by a pressure nozzle.

A.R.H.

**N84-21849\*#** National Aeronautics and Space Administration, Lewis Research Center, Cleveland, Ohio.  
**MEASUREMENT OF FLUID PROPERTIES USING RAPID-DOUBLE-EXPOSURE AND TIME-AVERAGE HOLOGRAPHIC INTERFEROMETRY**  
 A. J. DECKER 13 Jun. 1984 12 p refs Proposed for presentation at 20th Joint Propulsion Conf., Cincinnati, 11-13 Jun. 1984; sponsored by AIAA and SAE and ASME  
 (NASA-TM-83630; E-2067; NAS 1.15:83630) Avail: NTIS HC A02/MF A01 CSCL 14B

The holographic recording of the time history of a flow feature in three dimensions is discussed. The use of diffuse illumination holographic interferometry or the three dimensional visualization of flow features such as shock waves and turbulent eddies is described. The double-exposure and time-average methods are compared using the characteristic function and the results from a flow simulator. A time history requires a large hologram recording rate. Results of holographic cinematography of the shock waves in a flutter cascade are presented as an example. Future directions of this effort, including the availability and development of suitable lasers, are discussed. Author

**N84-22930\*** National Aeronautics and Space Administration, Lewis Research Center, Cleveland, Ohio.  
**MULTICOLOR PRINTING PLATE JOINING Patent**  
 W. J. WATERS, inventor (to NASA) 20 Mar. 1984 6 p Filed 28 Sep. 1982  
 (NASA-CASE-LEW-13598-1; US-PATENT-4,437,923; US-PATENT-APPL-SN-425203; US-PATENT-CLASS-156-630, US-PATENT-CLASS-101-395; US-PATENT-CLASS-156-654; US-PATENT-CLASS-156-905; US-PATENT-CLASS-228-165)  
 Avail: US Patent and Trademark Office CSCL 14E

An upper plate having ink flow channels and a lower plate having a multicolored pattern are joined. The joining is accomplished without clogging any ink flow paths. A pattern having different colored parts and apertures is formed in a lower plate. Ink flow channels each having respective ink input ports are formed in an upper plate. The ink flow channels are coated with solder mask and the bottom of the upper plate is then coated with solder. The upper and lower plates are pressed together at from 2 to 5 psi and heated to a temperature of from 295 F to 750 F or enough to melt the solder. After the plates have cooled and the pressure is released, the solder mask is removed from the interior passageways by means of a liquid solvent.

Official Gazette of the U.S. Patent and Trademark Office

**N84-25017\*#** National Aeronautics and Space Administration, Lewis Research Center, Cleveland, Ohio.  
**HOLOGRAPHIC AIDS FOR INTERNAL COMBUSTION ENGINE FLOW STUDIES**  
 C. REGAN 1984 12 p refs Presented at the 7th Intern. Conf. of Women Engr. and Scientists, Washington, 17-24 Jun 1984  
 (NASA-TM-83681; E-2070; NAS 1.15:83681) Avail: NTIS HC A02/MF A01 CSCL 14E

Worldwide interest in improving the fuel efficiency of internal combustion (I.C.) engines has sparked research efforts designed to learn more about the flow processes of these engines. The flow fields must be understood prior to fuel injection in order to design efficient valves, piston geometries, and fuel injectors. Knowledge of the flow field is also necessary to determine the heat transfer to combustion chamber surfaces. Computational codes can predict velocity and turbulence patterns, but experimental verification is mandatory to justify their basic assumptions. Due to their nonintrusive nature, optical methods are ideally suited to provide the necessary velocity verification data. Optical systems such as Schlieren photography, laser velocimetry, and illuminated particle visualization are used in I.C. engines, and now their versatility is improved by employing holography. These holographically enhanced optical techniques are

described with emphasis on their applications in I.C. engines.

Author

**N84-25019\*#** National Aeronautics and Space Administration. Lewis Research Center, Cleveland, Ohio.

**OPTIMIZATION OF FRINGE-TYPE LASER ANEMOMETERS FOR TURBINE ENGINE COMPONENT TESTING**

R. G. SEASHOLTZ, L. G. OBERLE, and D. H. WEIKLE 1984 16 p refs Presented at the 20th Joint Propulsion Conf., Cincinnati, 11-13 Jun. 1984; sponsored by AIAA, SAE and ASME (NASA-TM-83658; E-2099; NAS 1.15:83658; AIAA-84-1459) Avail: NTIS HC A02/MF A01 CSCL 14B

The fringe type laser anemometer is analyzed using the Cramer-Rao bound for the variance of the estimate of the Doppler frequency as a figure of merit. Mie scattering theory is used to calculate the Doppler signal wherein both the amplitude and phase of the scattered light are taken into account. The noise from wall scatter is calculated using the wall bidirectional reflectivity and the irradiance of the incident beams. A procedure is described to determine the optimum aperture mask for the probe volume located a given distance from a wall. The expected performance of counter type processors is also discussed in relation to the Cramer-Rao bound. Numerical examples are presented for a coaxial backscatter anemometer.

Author

**N84-26010\*#** National Aeronautics and Space Administration. Lewis Research Center, Cleveland, Ohio.

**THREE COMPONENT VELOCITY MEASUREMENTS USING FABRY-PEROT INTERFEROMETER**

R. G. SEASHOLTZ and L. J. GOLDMAN 1984 8 p refs Presented at the 2nd Intern. Symp. on Appl. of Laser Anemometry to Fluid Mech., Lisbon, 2-4 Jul. 1984 (NASA-TM-83692; E-2148; NAS 1.15:83692) Avail: NTIS HC A02/MF A01 CSCL 14B

A method for measuring the three components of mean flow velocity using a backscatter optical system based on a confocal Fabry-Perot interferometer is described. An analysis of the expected uncertainties in the velocity component measurements is presented along with experimental data taken in a free jet at two flow velocities (100 and 300 m/s).

Author

**N84-31595\*#** Aerometrics, Inc., Mountain View, Calif.

**ANALYSIS AND TESTING OF A NEW METHOD FOR DROP SIZE MEASUREMENT USING LASER SCATTER INTERFEROMETRY Final Report**

W. D. BACHALO and M. J. HOUSER Aug. 1984 68 p refs (Contract NAS3-23684) (NASA-CR-174636; NAS 1.26:174636) Avail: NTIS HC A04/MF A01 CSCL 14B

Research was conducted on a laser light scatter detection method for measuring the size and velocity of spherical particles. The method is based upon the measurement of the interference fringe pattern produced by spheres passing through the intersection of two laser beams. A theoretical analysis of the method was carried out using the geometrical optics theory. Experimental verification of the theory was obtained by using monodisperse droplet streams. Several optical configurations were tested to identify all of the parametric effects upon the size measurements. Both off-axis forward and backscatter light detection were utilized. Simulated spray environments and fuel spray nozzles were used in the evaluation of the method. The measurements of the monodisperse drops showed complete agreement with the theoretical predictions. The method was demonstrated to be independent of the beam intensity and extinction resulting from the surrounding drops. Signal processing concepts were considered and a method was selected for development.

Author

**N84-32782\*#** National Aeronautics and Space Administration. Lewis Research Center, Cleveland, Ohio.

**PIEZOELECTRIC DEICING DEVICE Patent Application**

R. FINKE and B. BANKS, inventors (to NASA) 7 Aug. 1984 9 p Continuation of US-Patent-Appl-SN-469867, filed 25 Feb. 1983 (NASA-CASE-LEW-13773-2; NAS 1.71:LEW-13773-2; US-PATENT-APPL-SN-638541) Avail: NTIS HC A02/MF A01 CSCL 14B

A fast voltage pulse is applied to a transducer which comprises a composite of multiple layers of alternately polarized piezoelectric material. These layers are bonded together and positioned over the curved leading edge of an aircraft wing structure. Each layer is relatively thin and metallized on both sides. The strain produced in the transducer causes the composite to push forward resulting in detachment and breakup of ice on the leading edge of the aircraft wing.

NASA

**N84-32783\*#** National Aeronautics and Space Administration. Lewis Research Center, Cleveland, Ohio.

**STRUCTURAL DESIGN OF A VERTICAL ANTENNA BORESIGHT 18.3 BY 18.3-M PLANAR NEAR-FIELD ANTENNA MEASUREMENT SYSTEM**

G. R. SHARP, P. A. TRIMARCHI, and J. S. WANHAINE 1984 26 p refs Proposed for presentation at the Meeting of the Antenna Measurement Techniques Association, San Diego, Calif., 2-4 Oct. 1984 (NASA-TM-83781; E-2274; NAS 1.15:83781) Avail: NTIS HC A03/MF A01 CSCL 14B

A large very precise near-field planar scanner was proposed for NASA Lewis Research Center. This scanner would permit near-field measurements over a horizontal scan plane measuring 18.3 m by 18.3 m. Large aperture antennas mounted with antenna boresight vertical could be tested up to 60 GHz. When such a large near field scanner is used for pattern testing, the antenna or antenna system under test does not have to be moved. Hence, such antennas and antenna systems can be positioned and supported to simulate configuration in zero g. Thus, very large and heavy machinery that would be needed to accurately move the antennas are avoided. A preliminary investigation was undertaken to address the mechanical design of such a challenging near-field antenna scanner. The configuration, structural design and results of a parametric NASTRAN structural optimization analysis are contained. Further, the resulting design was dynamically analyzed in order to provide resonant frequency information to the scanner mechanical drive system designers. If other large near field scanners of comparable dimensions are to be constructed, the information can be used for design optimization of these also.

Author

**N84-32789\*#** National Aeronautics and Space Administration. Lewis Research Center, Cleveland, Ohio.

**CHARACTERISTICS AND CAPACITIES OF THE NASA LEWIS RESEARCH CENTER HIGH PRECISION 6.7- BY 6.7-M PLANAR NEAR-FIELD SCANNER**

G. R. SHARP, R. J. ZAKRAJSEK, R. R. KUNATH, C. A. RAQUET, and R. E. ALEXOVICH 1984 27 p refs Presented at the Meeting of the Antenna Meas. Tech. Assoc., San Diego, Calif., 2-4 Oct. 1984 (NASA-TM-83785; E-2281; NAS 1.15:83785) Avail: NTIS HC A03/MF A01 CSCL 14B

A very precise 6.7- by 6.7-m planar near-field scanner has recently become operational at the NASA Lewis Research Center. The scanner acquires amplitude and phase data at discrete points over a vertical rectangular grid. During the design phase for this scanner, special emphasis was given to the dimensional stability of the structures and the ease of adjustment of the rails that determine the accuracy of the scan plane. A laser measurement system is used for rail alignment and probe positioning. This has resulted in very repeatable horizontal and vertical motion of the probe cart and hence precise positioning in the plane described by the probe tip. The resulting accuracy will support near-field measurements at 60 GHz without corrections. Subsystem design

including laser, electronic and mechanical and their performance is described. Summary data are presented on the scan plane flatness and environmental temperature stability. Representative near-field data and calculated far-field test results are presented. Prospective scanner improvements to increase test capability are also discussed. Author

**N84-32790\*#** Pratt and Whitney Aircraft, East Hartford, Conn. Engineering Div.

**TURBINE BLADE AND VANE HEAT FLUX SENSOR DEVELOPMENT, PHASE 1 Final Report**

W. H. ATKINSON, M. A. CYR, and R. R. STRANGE Aug. 1984 88 p refs

(Contract NAS3-23529)

(NASA-CR-168297; NAS 1.26:168297; PWA-5914-21) Avail:

NTIS HC A05/MF A01 CSCL 14B

Heat flux sensors available for installation in the hot section airfoils of advanced aircraft gas turbine engines were developed. Two heat flux sensors were designed, fabricated, calibrated, and tested. Measurement techniques are compared in an atmospheric pressure combustor rig test. Sensors, embedded thermocouple and the Gordon gauge, were fabricated that met the geometric and fabricability requirements and could withstand the hot section environmental conditions. Calibration data indicate that these sensors yielded repeatable results and have the potential to meet the accuracy goal of measuring local heat flux to within 5%. Thermal cycle tests and thermal soak tests indicated that the sensors are capable of surviving extended periods of exposure to the environment conditions in the turbine. Problems in calibration of the sensors caused by severe non-one dimensional heat flow were encountered. Modifications to the calibration techniques are needed to minimize this problem and proof testing of the sensors in an engine is needed to verify the designs. Author

## 36

## LASERS AND MASERS

Includes parametric amplifiers.

**A84-24663\*#** National Aeronautics and Space Administration. Lewis Research Center, Cleveland, Ohio.

**WINDOW ABERRATION CORRECTION IN LASER VELOCIMETRY USING MULTIFACETED HOLOGRAPHIC OPTICAL ELEMENTS**

H. J. SCHOCK (NASA, Lewis Research Center, Cleveland, OH), S. CASE, and L. KONICEK (Spectral Sciences, Inc., Minneapolis, MN) Applied Optics (ISSN 0003-6935), vol. 23, March 1, 1984, p. 752-756. refs

**N84-18620\*#** Westinghouse Research and Development Center, Pittsburgh, Pa.

**MEASUREMENT OF HEAT PUMP PROCESSES INDUCED BY LASER RADIATION**

M. GARBUNY and T. HENNINGSSEN Nov. 1983 50 p refs

(Contract NAS3-22877)

(NASA-CR-168324; NAS 1.26:168324; W-R/D-83-9C1-LK00L-R1)

Avail: NTIS HC A03/MF A01 CSCL 20E

A series of experiments was performed in which a suitably tuned CO<sub>2</sub> laser, frequency doubled by a Ti:AsSe<sub>3</sub> crystal, was brought into resonance with a P-line or two R-lines in the fundamental vibration spectrum of CO. Cooling or heating produced by absorption in CO was measured in a gas-thermometer arrangement. P-line cooling and R-line heating could be demonstrated, measured, and compared. The experiments were continued with CO mixed with N<sub>2</sub> added in partial pressures from 9 to 200 Torr. It was found that an efficient collisional resonance energy transfer from CO to N<sub>2</sub> existed which increased the cooling effects by one to two orders of magnitude over those in pure CO. Temperature reductions in the order of tens of degrees Kelvin

were obtained by a single pulse in the core of the irradiated volume. These measurements followed predicted values rather closely, and it is expected that increase of pulse energies and durations will enhance the heat pump effects. The experiments confirm the feasibility of quasi-isentropic engines which convert laser power into work without the need for heat rejection. Of more immediate potential interest is the possibility of remotely powered heat pumps for cryogenic use, such applications are discussed to the extent possible at the present stage. Author

**N84-22944\*** National Aeronautics and Space Administration. Lewis Research Center, Cleveland, Ohio.

**METHOD AND APPARATUS FOR COATING SUBSTRATES USING A LASER Patent**

I. ZAPLATYNSKY, inventor (to NASA) 28 Feb. 1984 5 p Filed 15 Mar. 1982

(NASA-CASE-LEW-13526-1; US-PATENT-4,434,189;

US-PATENT-APPL-SN-358398; US-PATENT-CLASS-427-53.1;

US-PATENT-CLASS-118-50.1; US-PATENT-CLASS-118-624;

US-PATENT-CLASS-118-641; US-PATENT-CLASS-427-399)

Avail: US Patent and Trademark Office CSCL 20E

Metal substrates, preferably of titanium and titanium alloys, are coated by alloying or forming TiN on a substrate surface. A laser beam strikes the surface of a moving substrate in the presence of purified nitrogen gas. A small area of the substrate surface is quickly heated without melting. This heated area reacts with the nitrogen to form a solid solution. The alloying or formation of TiN occurs by diffusion of nitrogen into the titanium. Only the surface layer of the substrate is heated because of the high power density of the laser beam and short exposure time. The bulk of the substrate is not affected, and melting of the substrate is avoided because it would be detrimental.

Official Gazette of the U.S. Patent and Trademark Office

**N84-30273\*#** National Aeronautics and Space Administration. Lewis Research Center, Cleveland, Ohio

**ORBITAL STABILITY IN COMBINED UNIFORM AXIAL AND THREE-DIMENSIONAL WIGGLER MAGNETIC FIELDS FOR FREE-ELECTRON LASERS**

S. JOHNSTON Aug. 1984 29 p refs

(NASA-TM-83753; E-2241; NAS 1.15:83753) Avail: NTIS HC

A03/MF A01 CSCL 20E

Zachary Phys. Rev. A 29 (6), 3224 (1984) recently analyzed the instability of relativistic-electron helical trajectories in combined uniform axial and helical wiggler magnetic fields when the radial variation of the wiggler field is taken into account. It is shown here that the type 2 instability comprised of secular terms growing linearly in time, identified by Zachary and earlier by Diamant Phys. Rev. A 23 (5), 2537 (1981), is an artifact of simple perturbation theory. A multiple-time-scale perturbation analysis reveals a nonsecular evolution on a slower time scale which accommodates an arbitrary initial perturbation. It is shown that, in the absence of exponential instability, the electron seeks a modified helical orbit more appropriate to its perturbed state and oscillates stably about it. Thus, the perturbed motion is oscillatory but nonsecular, and hence the helical orbits are stable. Author



## MECHANICAL ENGINEERING

Includes auxiliary systems (non-power); machine elements and processes; and mechanical equipment.

**A84-10499\*#** General Motors Corp., Indianapolis, Ind.  
**COMBUSTOR DEVELOPMENT FOR AUTOMOTIVE GAS TURBINES**

P. T. ROSS, J. R. WILLIAMS (General Motors Corp., Detroit Diesel Allison Div., Indianapolis, IN), and D. N. ANDERSON (NASA, Lewis Research Center, Cleveland, OH). *Journal of Energy* (ISSN 0146-0412), vol. 7, Sept.-Oct. 1983, p. 429-435. Research supported by the U.S. Department of Energy. refs (Contract DEN3-168)

Previously cited in issue 17, p. 2742, Accession no. A82-35062

**A84-11273\*** National Aeronautics and Space Administration, Lewis Research Center, Cleveland, Ohio.  
**FERROGRAPHIC AND SPECTROMETER OIL ANALYSIS FROM A FAILED GAS TURBINE ENGINE**

W. R. JONES, JR. (NASA, Lewis Research Center, Cleveland, OH) (International Conference on Advances in Ferrography, 1st, University College of Swansea, Swansea, Wales, Sept. 22-24, 1982) *Wear* (ISSN 0043-1648), vol. 90, Oct. 1, 1983, p. 239-249. refs

An experimental gas turbine engine was destroyed as a result of the combustion of its titanium components. It was concluded that a severe surge may have caused interference between rotating and stationary compressor parts that either directly or indirectly ignited the titanium components. Several engine oil samples (before and after the failure) were analyzed with a Ferrograph, and with plasma, atomic absorption, and emission spectrometers to see if this information would aid in the engine failure diagnosis. The analyses indicated that a lubrication system failure was not a causative factor in the engine failure. Neither an abnormal wear mechanism nor a high level of wear debris was detected in the engine oil sample taken just prior to the test in which the failure occurred. However, low concentrations (0.2 to 0.5 ppm) of titanium were evident in this sample and samples taken earlier. After the failure, higher titanium concentrations (2 ppm) were detected in oil samples taken from different engine locations. Ferrographic analysis indicated that most of the titanium was contained in spherical metallic debris after the failure. The oil analyses eliminated a lubrication system bearing or shaft seal failure as the cause of the engine failure. Previously announced in STAR as N83-12433

Author

**A84-13228\*#** Westinghouse Research and Development Center, Pittsburgh, Pa.

**LABYRINTH SEAL FORCES ON A WHIRLING ROTOR**

D. V. WRIGHT (Westinghouse Research and Development Center, Pittsburgh, PA) IN: Rotor dynamical instability; Proceedings of the Applied Mechanics, Bioengineering, and Fluids Engineering Conference, Houston, TX, June 20-22, 1983. New York, American Society of Mechanical Engineers, 1983, p. 19-31. refs (Contract NAS3-20825)

An experimental investigation of air labyrinth seal forces on a subsynchronously whirling model rotor is described and test results are given for diverging, converging, and straight two-strip seals. The effects of pressure drop, back pressure, whirl direction, and whirl frequency are shown. These results provide basic experimental data needed in the development of design methods for predicting and preventing self-excited whirl of turbine rotors and other machines having labyrinth seals. The total dynamic seal forces on the whirling model rotor are measured accurately by means of a novel active damping and stiffness system that is adjusted to obtain neutral whirl stability of the model rotor system. In addition, the whirling pressure pattern in the seal annulus is measured for a few test conditions and the corresponding pressure

forces on the rotor are compared with the total measured forces. This comparison shows that either radial and axial pressure gradients in the seal annulus or drag forces on the rotor are significant.

Author

**A84-15575\*** Detroit Diesel Allison, Indianapolis, Ind.  
**MATERIAL REMOVAL CONSIDERATIONS FOR METAL-CERAMIC ABRADABLE TURBINE SEAL SYSTEMS**

D. L. CLINGMAN, B. SCHECHTER, K. R. CROSS, and J. R. CAVANAGH (General Motors Corp., Detroit Diesel Allison Div., Indianapolis, IN) *Lubrication Engineering* (ISSN 0024-7154), vol. 39, Nov. 1983, p. 712-716. (Contract NAS3-22012)

Possible interaction mechanisms between turbine blade tips and ceramic seal elements have been considered and preferred mechanism defined. The influence of porosity in the seal structure is qualitatively assessed and a preferred form determined. A dual-density plasma-sprayed ceramic seal system encompassing the desired characteristics is described and test results, including engine tests, are reported. Possible remedies to correct performance deficiencies are presented.

Author

**A84-15950\*#** Illinois Univ., Chicago.  
**PRECISION OF SPIRAL-BEVEL GEARS**

F. L. LITVIN, R. N. GOLDRICH (Illinois, University, Chicago, IL), J. J. COY (U.S. Army, Propulsion Laboratory, Cleveland, OH), and E. V. ZARETSKY (NASA, Lewis Research Center, Cleveland, OH) *ASME, Transactions, Journal of Mechanisms, Transmission, and Automation in Design*, vol. 105, Sept. 1983, p. 310-316. refs (ASME PAPER 82-WA/DE-33)

The kinematic errors in spiral bevel gear trains caused by the generation of nonconjugate surfaces, by axial displacements of the gears during assembly, and by eccentricity of the assembled gears were determined. One mathematical model corresponds to the motion of the contact ellipse across the tooth surface, (geometry I) and the other along the tooth surface (geometry II). The following results were obtained: (1) kinematic errors induced by errors of manufacture may be minimized by applying special machine settings, the original error may be reduced by order of magnitude, the procedure is most effective for geometry 2 gears, (2) when trying to adjust the bearing contact pattern between the gear teeth for geometry I gears, it is more desirable to shim the gear axially; for geometry II gears, shim the pinion axially; (3) the kinematic accuracy of spiral bevel drives are most sensitive to eccentricities of the gear and less sensitive to eccentricities of the pinion. The precision of mounting accuracy and manufacture are most crucial for the gear, and less so for the pinion. Previously announced in STAR as N82-30552

Author

**A84-15951\*#** Illinois Univ., Chicago.  
**KINEMATIC PRECISION OF GEAR TRAINS**

F. L. LITVIN, R. N. GOLDRICH (Illinois, University, Chicago, IL), J. J. COY (U.S. Army, Propulsion Laboratory, Cleveland, OH), and E. V. ZARETSKY (NASA, Lewis Research Center, Cleveland, OH) *ASME, Transactions, Journal of Mechanisms, Transmission, and Automation in Design*, vol. 105, Sept. 1983, p. 317-326. refs (ASME PAPER 82-WA/DE-34)

Kinematic precision is affected by errors which are the result of either intentional adjustments or accidental defects in manufacturing and assembly of gear trains. A method for the determination of kinematic precision of gear trains is described. The method is based on the exact kinematic relations for the contact point motions of the gear tooth surfaces under the influence of errors. An approximate method is also explained. Example applications of the general approximate methods are demonstrated for gear trains consisting of involute (spur and helical) gears, circular arc (Wildhaber-Novikov) gears, and spiral bevel gears. Gear noise measurements from a helicopter transmission are presented and discussed with relation to the kinematic precision theory. Previously announced in STAR as N82-32733

Author



**A84-20580\*** Akron Univ., Ohio.

**NONLINEAR TRANSIENT FINITE ELEMENT ANALYSIS OF ROTOR-BEARING-STATOR SYSTEMS**

J. PADOVAN, M. ADAMS, D. FERTIS, I. ZEID, and P. LAM (Akron, University, Akron, OH) Computers and Structures (ISSN 0045-7949), vol 18, no. 4, 1984, p. 629-639. refs (Contract NSG-3283)

This paper extends the finite element scheme to handle the highly nonlinear interfacial fields generated in the fluid filled annuli of squeeze film and journal bearings so as to model the transient response of rotor-bearing-stator systems. Since such simulations are highly nonlinear, direct numerical integration schemes are employed to generate the overall response. In this context, the paper gives consideration to such items as (1) numerical efficiency/stability, (2) comparison of implicit and explicit schemes, (3) determines extent of response nonlinearity as well as (4) extensively benchmarks the overall concept/methodologies.

Author

**A84-22316\*#** Virginia Univ., Charlottesville.

**EFFECTS OF VOLUTE GEOMETRY AND IMPELLER ORBIT ON THE HYDRAULIC PERFORMANCE OF A CENTRIFUGAL PUMP**

R. D. FLACK (Virginia, University, Charlottesville, VA) and R. F. LANES (General Dynamics Corp., St. Louis, MO) IN: Performance characteristics of hydraulic turbines and pumps; Proceedings of the Winter Annual Meeting, Boston, MA, November 13-18, 1983. New York, American Society of Mechanical Engineers, 1983, p. 127-133. Research sponsored by the University of Virginia. refs (Contract NAG3-180)

Overall performance data was taken for a Plexiglas water pump with a logarithmic spiral volute and rectangular cross sectioned flow channels. Parametric studies were made in which the center of the impeller was offset from the design center of the volute. The rig was also designed such that the impeller was allowed to synchronously orbit by a fixed amount about any center. The studies indicate that decreasing the tongue clearance decreases the head at low flowrates and increases the head at high flowrates. Also, decreasing the volute area in the first half of the volute and holding the tongue clearance the same, resulted in a decreased head for low flowrates but performance at high flowrates was not affected. Finally, the overall hydraulic performance was not affected by the impeller orbiting about the volute center.

Author

**A84-22864\*#** Mechanical Technology, Inc., Latham, N. Y.

**FREE-PISTON STIRLING ENGINE ENDURANCE TEST PROGRAM**

G. DOCHAT, J. RAUCH, and G. ANTONELLI (Mechanical Technology, Inc., Stirling Engine Systems Div., Latham, NY) Automotive Technology Development Contractors' Coordination Meeting, 21st, Dearborn, MI, Nov. 14-19, 1983, Paper. 9 p. Research supported by U.S. Department of Energy. (Contract DEN3-333)

The Free-Piston Stirling Engine (FPSE) has the potential to be a long-lived, highly reliable, power conversion device attractive for many product applications such as space, residential, or remote-site power. The purpose of endurance testing the FPSE is to demonstrate its potential for long life. The endurance program was directed at obtaining 1000 operational hours under various test conditions: low power, full stroke, duty cycle, and stop/start. Critical performance parameters were measured to note any change and/or trend. Inspections were conducted to measure and compare critical seal/bearing clearance. The engine performed well throughout the program, completing the 1000 hours. Hardware inspection, including the critical clearances, showed no significant change in hardware or clearance dimensions. The performance parameters did not exhibit any increasing or decreasing trends. The test program confirms the potential for long-life FPSE applications. Additional testing is planned to increase the test hours to 10,000.

Author

**A84-22878\*#** Detroit Diesel Allison, Indianapolis, Ind.

**CERAMIC COMPONENTS FOR THE AGT 100 ENGINE**

H. E. HELMS and P. W. HEITMAN (General Motors Corp., Detroit Diesel Allison Div., Indianapolis, IN) International Symposium on Ceramic Components for Engines, Hakone, Japan, Oct 17-21, 1983, Paper. 13 p. Research supported by the U.S. Department of Energy.

(Contract DEN3-168)

Historically, automotive gas turbines have not been able to meet requirements of the marketplace with respect to cost, performance, and reliability. However, the development of appropriate ceramic materials has overcome problems related to a need for expensive superalloy components and to limitations regarding the operating temperature. An automotive gas turbine utilizing ceramic components has been developed by a U.S. automobile manufacturer. A 100-horsepower, two-shaft, regenerative engine geometry was selected because it is compatible with manual, automatic, and continuously variable transmissions. Attention is given to the ceramic components, the ceramic gasifier turbine rotor development, the ceramic gasifier scroll, ceramic component testing, and the use of advanced nondestructive techniques for the evaluation of the engine components.

G.R.

**A84-23522\*#** National Aeronautics and Space Administration. Lewis Research Center, Cleveland, Ohio.

**HOSTILE ENVIRONMENTAL CONDITIONS FACING CANDIDATE ALLOYS FOR THE AUTOMOTIVE STIRLING ENGINE**

J. R. STEPHENS (NASA, Lewis Research Center, Cleveland, OH) IN: Environmental degradation of engineering materials in hydrogen. Blacksburg, VA, Virginia Polytechnic Institute and State University, 1981, p. 123-132. refs

The materials research program in support of the Automotive Stirling Engine Project focuses on the hot heater head of the engine including the heater head tubes, cylinders, and regenerator housings, which are considered to be the most critical components from a materials viewpoint. The specific areas of investigation in the program involve hydrogen permeability testing, doping of the hydrogen working fluid to reduce permeability rates, oxidation/corrosion studies, creep-rupture evaluation, and assessing effects of hydrogen environment on mechanical properties. Emphasis is placed on the materials challenges that result from the use of hydrogen as the working fluid. Previously announced in STAR as N81-26236

S.F.

**A84-28791\*** National Aeronautics and Space Administration. Lewis Research Center, Cleveland, Ohio.

**ELASTIC MODEL OF THE TRACTION BEHAVIOR OF TWO TRACTION LUBRICANTS**

S. H. LOEWENTHAL and D. A. ROHN (NASA, Lewis Research Center, Cleveland, OH) ASLE Transactions, vol. 27, April 1984, p. 129-137; Discussion, p. 137; Authors' Closure, p. 137. refs

In the analysis of rolling-sliding concentrated contacts, such as gears, bearings and traction drives, the traction characteristics of the lubricant are of prime importance. The elastic shear modulus and limiting shear stress properties of the lubricant dictate the traction/slip characteristics and power loss associated with an EHD contact undergoing slip and/or spin. These properties can be deduced directly from the initial slope  $m$  and maximum traction coefficient micron of an experimental traction curve. In this investigation, correlation equations are presented to predict  $m$  and micron for two modern traction fluids based on the regression analysis of 334 separate traction disk machine experiments. The effects of contact pressure, temperature, surface velocity, ellipticity ratio are examined. Problems in deducing lubricant shear moduli from disk machine tests are discussed. Previously announced in STAR as N83-20116

Author

**A84-28792\*** Carnegie-Mellon Univ., Pittsburgh, Pa.

**DYNAMICS OF TWO-PHASE FACE SEALS**

R. M. BEELER and W. F. HUGHES (Carnegie-Mellon University, Pittsburgh, PA) ASLE Transactions, vol. 27, April 1984, p. 146-153; Discussion, p. 153; Authors' Closure, p. 153. refs (Contract NAG3-166)

An analytic study is presented of the effects of phase change on load support for parallel and tapered face seals. Consideration is given to an adiabatic model for low Reynolds number flow. Numerical integration is carried out of the descriptive fluid equations, giving the opening force due to fluid film pressure. The loci of steady-state solutions are then plotted for water to provide curves of load support as a function of film thickness. For axial excursions of the seal rings, a quasi-steady transient analysis is made. It is found that the load support generated by fluid pressure can be multivalued for a given film thickness. Another finding is that axial disturbances of the seal rings may lead to sudden drops in load support generated by fluid pressure with three possible results. The first is that sufficient damping may permit the seal to return to the previous equilibrium operating position. The second is that the seal may collapse to an equilibrium position of smaller film thickness where face contact is more likely and a significantly higher operating temperature is assured. The third is that a limit cycle of self-sustained oscillation in the axial direction may occur if damping is sufficiently low. C.R.

**A84-28987\*** Illinois Univ., Urbana.

**SURFACE ROUGHNESS EFFECTS WITH SOLID LUBRICANTS DISPERSED IN MINERAL OILS**

C. CUSANO, P. R. GOGLIA (Illinois University, Urbana, IL), and H. E. SLINNEY (NASA, Lewis Research Center, Cleveland, OH) American Society of Lubrication Engineers and American Society of Mechanical Engineers, Lubrication Conference, Hartford, CT, Oct. 18-20, 1983. 9 p. refs (Contract NAG3-153) (ASLE PREPRINT 83-LC-4C-1)

The lubricating effectiveness of solid-lubricant dispersions are investigated in both point and line contacts using surfaces with both random and directional roughness characteristics. Friction and wear data obtained at relatively low speeds and at room temperature, indicate that the existence of solid lubricants such as graphite, MoS<sub>2</sub>, and PTFE in a plain mineral oil generally will not improve the effectiveness of the oil as a lubricant for such surfaces. Under boundary lubrication conditions, the friction force, as a function of time, initially depends upon the directional roughness properties of the contacting surfaces irrespective of whether the base oil or dispersions are used as lubricants.

Author

**A84-28989\*** Mechanical Technology, Inc., Latham, N. Y.

**DESIGN ANALYSIS OF RAYLEIGH-STEP FLOATING-RING SEALS**

A. ARTILES, W. SHAPIRO, and H. F. JONES (Mechanical Technology, Inc., Latham, NY) American Society of Lubrication Engineers and American Society of Mechanical Engineers, Lubrication Conference, Hartford, CT, Oct. 18-20, 1983. 10 p. (Contract NAS3-23260) (ASLE PREPRINT 83-LC-3B-2)

The analysis and design of a 50-mm diameter floating-ring helium buffer seal are described. The seal rings incorporated Rayleigh-step lift pads to provide hydrodynamic forces to separate the rings from the shaft. Maximum surface speed is 183 m/s (600 fps) and maximum buffer gas pressure is 1389 kPa (200 psia). An operating range map was computed as a function of speed and pressure. Contradictory problems arise due to excessive friction preventing ring tracking at low-speed, high-pressure conditions and insufficient friction to retard inertia driven motions at high-speed, low-pressure conditions. Steady-state and dynamic analyses and performance are described, as well as the results of thermal studies. Author

**A84-29092\*#** Akron Univ., Ohio.

**A THERMOMECHANICAL MODEL FOR ENERGY PROPAGATION IN A SOLID-FLUID-SOLID SYSTEM WITH ONE BOUNDARY IN RELATIVE MOTION**

M. J. BRAUN (Akron University, Akron, OH), R. L. MULLEN (Case Western Reserve University, Cleveland, OH), and R. C. HENDRICKS (NASA, Lewis Research Center, Cleveland, OH) American Society of Mechanical Engineers and American Institute of Chemical Engineers, Heat Transfer Conference, Seattle, WA, July 24-28, 1983. 9 p. refs (ASME PAPER 83-HT-97)

A model is developed to predict the behavior of a thin fluid film in the wake of a tool in relative motion with respect to the table. Computational procedures are developed and limitations of the model are discussed. In general the fluid-interface temperature is controlled by conduction into the table. From the numerical results four regimes are identified: convective cooling, partial evaporation of the fluid film, extended evaporation due to a limiting evaporative heat flux, and surface dryout due to total evaporation of the fluid layer. These regimes are qualitatively illustrated in terms of the parameters film thickness, viscosity, and relative velocity. Author

**A84-29097\*#** Toledo Univ., Ohio.

**ASSESSMENT OF TWO NEGLECTED EFFECTS IN THE ANALYSIS OF AN OIL PUMPING RING SEAL**

T. G. KEITH (Toledo University, Toledo, OH) and P. J. SMITH (American Society of Mechanical Engineers and American Society of Lubrication Engineers, Joint Lubrication Conference, Hartford, CT, Oct. 18-20, 1983. 6 p. refs (Contract NAS3-156) (ASME PAPER 83-LUB-16)

Many factors have been found to affect the performance of a pumping ring seal. In this paper, two effects (elevated reservoir temperature and rod deformation), both heretofore neglected, are assessed through the use of a thermoelastohydrodynamic numerical model of the pumping ring. Elevated reservoir temperatures are found to result in an increase in the amount of lubricant pumped while deformation of the translating rod is shown to cause a reduction in the lubricant pumped. Author

**A84-29099\*#** Battelle Columbus Labs., Ohio.

**SUBSURFACE STRESS EVALUATIONS UNDER ROLLING/SLIDING CONTACTS**

J. W. KANNEL and J. L. TEVAARWERK (Battelle Columbus Laboratories, Columbus, OH) American Society of Mechanical Engineers and American Society of Lubrication Engineers, Joint Lubrication Conference, Hartford, CT, Oct. 18-20, 1983. 8 p. refs (Contract NAS3-22808) (ASME PAPER 83-LUB-18)

A computer model has been developed for evaluating the subsurface stresses incurred within rolling/sliding (elastic) contacts. The model involves first defining the stress tensor at any point (x, y, or z) beneath the surface in terms of the surface stresses. The stress tensors are analyzed to determine the maximum shear stresses and stress reversals. As a result of computations with the model, several observations were made. For example, the maximum reversing shear stresses are on the plane of the orthogonal shear stress. Further, the magnitude of these stresses is not altered by friction. However, under very high friction (typical of dry contact) surface stresses can dominate over subsurface stresses. Author

**A84-30061\*** Santa Clara Univ., Calif.

**ALCOHOL COLD STARTING - A THEORETICAL STUDY**

L. H. BROWNING (Santa Clara University, Santa Clara, CA) IN: IECEC '83; Proceedings of the Eighteenth Intersociety Energy Conversion Engineering Conference, Orlando, FL, August 21-26, 1983. Volume 2. New York, American Institute of Chemical Engineers, 1983, p. 586-591. Research supported by the U.S. Department of Energy. refs  
(Contract NAG3-143)

Two theoretical computer models have been developed to study cold-starting problems with alcohol fuels. The first model, a droplet fall-out and sling-out model, shows that droplets must be smaller than 50 microns to enter the cylinder under cranking conditions without being slung-out in the intake manifold. The second model, which examines the fate of droplets during the compression process, shows that the heat of compression can be used to vaporize small droplets (less than 50 microns) producing flammable mixtures below freezing ambient temperatures. While droplet size has the greater effect on startability, a very high compression ratio can also aid cold starting. Author

**A84-30062\*** Cummins Engine Co., Inc., Columbus, Ind.  
**NEW PERSPECTIVES FOR ADVANCED AUTOMOBILE DIESEL ENGINES**

L. TOZZI, R. SEKAR, R. KAMO (Cummins Engine Co., Inc., Columbus, IN), and J. C. WOOD (NASA, Lewis Research Center, Cleveland, OH) IN: IECEC '83; Proceedings of the Eighteenth Intersociety Energy Conversion Engineering Conference, Orlando, FL, August 21-26, 1983. Volume 2. New York, American Institute of Chemical Engineers, 1983, p. 600-608. Research supported by the U.S. Department of Energy. refs  
(Contract DEN3-261)

Computer simulation results are presented for advanced automobile diesel engine performance. Four critical factors for performance enhancement were identified: (1) part load preheating and exhaust gas energy recovery, (2) fast heat release combustion process, (3) reduction in friction, and (4) air handling system efficiency. Four different technology levels were considered in the analysis. Simulation results are compared in terms of brake specific fuel consumption and vehicle fuel economy in km/liter (miles per gallon). Major critical performance sensitivity areas are: (1) combustion process, (2) expander and compressor efficiency, and (3) part load preheating and compound system. When compared to the state of the art direct injection, cooled, automobile diesel engine, the advanced adiabatic compound engine concept showed the unique potential of doubling the fuel economy. Other important performance criteria such as acceleration, emissions, reliability, durability and multifuel capability are comparable to or better than current passenger car diesel engines. Author

**A84-30069\*** National Aeronautics and Space Administration.  
Lewis Research Center, Cleveland, Ohio.  
**DOE/NASA AUTOMOTIVE STIRLING ENGINE PROJECT OVERVIEW 83**

D. G. BEREMAND (NASA, Lewis Research Center, Cleveland, OH) IN: IECEC '83; Proceedings of the Eighteenth Intersociety Energy Conversion Engineering Conference, Orlando, FL, August 21-26, 1983. Volume 2. New York, American Institute of Chemical Engineers, 1983, p. 681-688. refs

An overview of the DOE/NASA Automotive Stirling Engine Project is presented. The background and objectives of the project are reviewed. Project activities are described and technical progress and status are presented and assessed. Prospects for achieving the objective 30 percent fuel economy improvement are considered good. The key remaining technology issues are primarily related to life, reliability and cost, such as piston rod seals, and low cost heat exchangers. Previously announced in STAR as N83-27924

Author

**A84-30085\*** Carnegie-Mellon Univ., Pittsburgh, Pa.  
**THERMAL AND ELASTOHYDRODYNAMIC ANALYSIS OF RECIPROCATING ROD SEALS IN THE STIRLING ENGINE**

Y. YANG and W. F. HUGHES (Carnegie-Mellon University, Pittsburgh, PA) IN: IECEC '83; Proceedings of the Eighteenth Intersociety Energy Conversion Engineering Conference, Orlando, FL, August 21-26, 1983. Volume 2. New York, American Institute of Chemical Engineers, 1983, p. 812-817. refs  
(Contract NSG-3202)

Sliding seals and pumping rings for use in Stirling engines are analyzed from an elastohydrodynamic point of view. The oil film thickness and pressure distribution are found by a finite element method and then used to determine the operating temperature of sliding seals. Thermal aspects of dry seals (cap seals) are also discussed. A parametric study has been made and the results summarized in a set of curves. Author

**A84-30091\*** Mechanical Technology, Inc., Latham, N. Y.  
**AUTOMOTIVE STIRLING ENGINE DEVELOPMENT PROGRAM MOD I STIRLING ENGINE DEVELOPMENT**

M. A. SIMETKOSKY (Mechanical Technology, Inc., Latham, NY) IN: IECEC '83; Proceedings of the Eighteenth Intersociety Energy Conversion Engineering Conference, Orlando, FL, August 21-26, 1983. Volume 2. New York, American Institute of Chemical Engineers, 1983, p. 856-862. Research supported by the U.S. Department of Energy.  
(Contract DEN3-32)

The development of the Mod I 4-cylinder automotive Stirling engine is discussed and illustrated with drawings, block diagrams, photographs, and graphs and tables of preliminary test data. The engine and its drive, cold-engine, hot-engine, external-heat, air/fuel power-control, electronic-control, and auxiliary systems are characterized. Performance results from a total of 1900 h of test on 4 prototype engines include average maximum efficiency (at 2000 rpm) 34.5 percent and maximum output power 54.4 kW. The modifications introduced in an upgraded version of the Mod are explained; this engine has maximum efficiency 40.4 percent and maximum power output 69.2 kW. D.G.

**A84-30092\*** Mechanical Technology, Inc., Latham, N. Y.  
**AUTOMOTIVE STIRLING ENGINE DEVELOPMENT PROGRAM - OVERVIEW AND STATUS REPORT**

N. P. NIGHTINGALE (Mechanical Technology, Inc., Latham, NY) IN: IECEC '83; Proceedings of the Eighteenth Intersociety Energy Conversion Engineering Conference, Orlando, FL, August 21-26, 1983. Volume 2. New York, American Institute of Chemical Engineers, 1983, p. 863-871. Research supported by the U.S. Department of Energy.  
(Contract DEN3-32)

The current status of the automotive-Stirling-engine development program being undertaken by DOE and NASA Lewis is reviewed. The program goals and the reference-engine design are explained, and the modifications introduced to improve performance and lower manufacturing costs are discussed and illustrated, including part-power optimization; increased operating temperature (from 720 to 820 C); 45.4-kg weight reduction; elimination of Co and reduction of Cr used; and improved seal; ceramic components, and high-temperature alloys. The test program, some difficulties encountered, and results after 2042 h are summarized. D.G.

**A84-30095\*** National Aeronautics and Space Administration.  
Lewis Research Center, Cleveland, Ohio.

**TEST RESULTS AND DESCRIPTION OF A 1 KW FREE-PISTON STIRLING ENGINE WITH A DASHPOT LOAD**

J. SCHREIBER (NASA, Lewis Research Center, Cleveland, OH) IN: IECEC '83; Proceedings of the Eighteenth Intersociety Energy Conversion Engineering Conference, Orlando, FL, August 21-26, 1983. Volume 2. New York, American Institute of Chemical Engineers, 1983, p. 887-896.  
(Contract DE-AC05-82OR-21005)

A 1 kW (1.33 hp) single cylinder free piston Stirling engine was installed in the test facilities at the Lewis laboratory. The

engine was designed specifically for research of the dynamics of its operation. A more complete description of the engine and its instrumentation is provided in a prior NASA paper TM-82999 by J. G. Schreiber. Initial tests at Lewis showed the power level and efficiency of the engine to be below design level. Tests were performed to help determine the specific problems in the engine causing the below design level performance. Modifications to engine hardware and to the facility where performed in an effort to bring the power output and efficiency to their design values. As finally configured the engine generated more than 1250 watts of output power at an engine efficiency greater than 32 percent. This report presents the tests performed to help determine the specific problems, the results if the problem was eliminated, the fix performed to the hardware, and the test results after the engine was tested. In cases where the fix did not cause the anticipated effects, a possible explanation is given. Previously announced in STAR as N83-27346 Author

**A84-38838\*#** National Aeronautics and Space Administration. Lewis Research Center, Cleveland, Ohio.  
**FORMATION AND DESTRUCTION OF VORTICES IN A MOTORED FOUR-STROKE PISTON-CYLINDER CONFIGURATION**

H. J. SCHOCK, D. J. SOSOKA (NASA, Lewis Research Center, Cleveland, OH), and J. I. RAMOS (Carnegie-Mellon University, Pittsburgh, PA) AIAA Journal (ISSN 0001-1452), vol. 22, July 1984, p. 948, 949; Abndged.

Previously cited in issue 05, p. 652, Accession no. A83-16749

**A84-40595\*** National Aeronautics and Space Administration. Lewis Research Center, Cleveland, Ohio.

**PIVOTING AND SLIP IN AN ANGULAR CONTACT BEARING**  
E. KINGSBURY (NASA, Lewis Research Center, Cleveland, OH; Charles Stark Draper Laboratory, Inc., Cambridge, MA) ASLE Transactions, vol. 27, July 1984, p. 259-262 refs

Pivoting slips are calculated for the ball-race and ball-ball contacts in a retainerless bearing. The calculation is kinematic, ignoring all inertial loadings. Pure spin and uniform precession of the balls are considered. Pivoting slip magnitudes are compared with several other kinds of slip which were previously reported in an R4 size bearing. Previously announced in STAR as N83-26079

Author

**A84-44300\*#** Lulea Univ. (Sweden).

**NON-NEWTONIAN FLUID MODEL INCORPORATED INTO ELASTOHYDRODYNAMIC LUBRICATION OF RECTANGULAR CONTACTS**

B. O. JACOBSON (Lulea, Hogskolan, Lulea, Sweden) and B. J. HAMROCK (NASA, Lewis Research Center, Cleveland, OH) ASME, Transactions, Journal of Tribology (ISSN 0022-2305), vol. 106, April 1984, p. 275-282; Discussion, p. 282-284; Authors' Closure, p. 284. Previously announced in STAR as N83-28454. refs (ASME PAPER 83-LUB-15)

A procedure is outlined for the numerical solution of the complete elastohydrodynamic lubrication of rectangular contacts incorporating a non-Newtonian fluid model. The approach uses a Newtonian model as long as the shear stress is less than a limiting shear stress. If the shear stress exceeds the limiting value, the shear stress is set equal to the limiting value. The numerical solution requires the coupled solution of the pressure, film shape, and fluid rheology equations from the inlet to the outlet. Isothermal and no-side-leakage assumptions were imposed in the analysis. The influence of dimensionless speed, load, materials, and sliding velocity and limiting-shear-strength proportionality constant on dimensionless minimum film thickness was investigated. Fourteen cases were used in obtaining the minimum-film-thickness equation for an elastohydrodynamically lubricated rectangular contact incorporating a non-Newtonian fluid model. Computer plots are also presented that indicate in detail pressure distribution, film shape, shear stress at the surfaces, and flow throughout the conjunction. Author

**A84-44918\*#** National Aeronautics and Space Administration. Lewis Research Center, Cleveland, Ohio.

**TWO-REGION ANALYSIS OF INTERFACE SHAPE IN CONTINUOUS CASTING WITH SUPERHEATED LIQUID**

R. SIEGEL (NASA, Lewis Research Center, Cleveland, OH) ASME, Transactions, Journal of Heat Transfer (ISSN 0022-1481), vol. 106, Aug. 1984, p. 506-511.

A slab ingot is being formed as a continuous casting by withdrawal from a mold with parallel walls. The sides of the ingot below the mold are cooled to remove heat of fusion and energy transferred to the solidification interface by superheated liquid metal in the mold. A two-region analysis is made to determine the non-uniform heat conduction from the liquid metal to the interface, and then from the interface to the cooled ingot sides. The solidification interface shape is found that is compatible with the removal of fusion energy and nonuniform heating from the liquid. The solution is obtained by two applications of a Cauchy boundary value method. Author

**A84-45965\*#** National Aeronautics and Space Administration. Lewis Research Center, Cleveland, Ohio.

**FEASIBILITY ANALYSIS OF A SPIRAL GROOVE RING SEAL FOR COUNTER-ROTATING SHAFTS**

E. DIRUSSO (NASA, Lewis Research Center, Cleveland, OH) Journal of Aircraft (ISSN 0021-8669), vol. 21, Aug. 1984, p. 618-622. Previously cited in issue 16, p. 2361, Accession no. A83-36239.

**A84-46355\*#** National Aeronautics and Space Administration. Lewis Research Center, Cleveland, Ohio.

**NASA TRANSMISSION RESEARCH AND ITS PROBABLE EFFECTS ON HELICOPTER TRANSMISSION DESIGN**

E. V. ZARETSKY, J. J. COY, and D. P. TOWNSEND (NASA, Lewis Research Center, Cleveland, OH) IN: American Helicopter Society, Annual Forum, 39th, St. Louis, MO, May 9-11, 1983, Proceedings. Alexandria, VA, American Helicopter Society, 1984, p. 303-320. Previously announced in STAR as N83-24858. refs

Transmissions studied for application to helicopters in addition to the more conventional geared transmissions include hybrid (traction/gear), bearingless planetary, and split torque transmissions. Research is being performed to establish the validity of analysis and computer codes developed to predict the performance, efficiency, life, and reliability of these transmissions. Results of this research should provide the transmission designer with analytical tools to design for minimum weight and noise with maximum life and efficiency. In addition, the advantages and limitations of drive systems as well as the more conventional systems will be defined. S.L.

**A84-46893\*#** Arizona State Univ., Tempe.

**A BLADE LOSS RESPONSE SPECTRUM FOR FLEXIBLE ROTOR SYSTEMS**

H. D. NELSON (Arizona State University, Tempe, AZ) and M. ALAM American Society of Mechanical Engineers, International Gas Turbine Conference and Exhibit, 29th, Amsterdam, Netherlands, June 4-7, 1984. 8 p. refs (Contract NAG3-6) (ASME PAPER 84-GT-29)

A shock spectrum procedure is developed to estimate the peak displacement response of linear flexible rotor-bearing systems subjected to a step change in unbalance (i.e., a blade loss). A progressive and a retrograde response spectrum are established. These blade loss response spectra are expressed in a unique non-dimensional form and are functions of the modal damping ratio and the ratio of rotor spin speed to modal damped whirl speed. Modal decomposition using complex modes is utilized to make use of the unique feature of the spectra for the calculation of the peak blade loss displacement response of the rotor system. The procedure is applied to three example systems using several modal superposition strategies. The results of each are compared to true peak displacement obtained by a separate transient response program. Author

**A84-46896\*#** Texas A&M Univ., College Station.  
**ANALYSIS FOR LEAKAGE AND ROTORDYNAMIC COEFFICIENTS OF SURFACE-ROUGHENED TAPERED ANNULAR GAS SEALS**  
 C. C. NELSON (Texas A&M University, College Station, TX) American Society of Mechanical Engineers, International Gas Turbine Conference and Exhibit, 29th, Amsterdam, Netherlands, June 4-7, 1984. 8 p. refs  
 (Contract NAG3-181)  
 (ASME PAPER 84-GT-32)

The present analysis calculates the leakage and rotor-dynamic coefficients for tapered annular gas seals whose rotor and stator have been subjected to different surface roughness treatments. The analysis is demonstrated for the effects of changes in the Space Shuttle Main Engine High Pressure Oxygen Turbopump's turbine interstage seal length, taper, clearance, and fluid prerotation. It is noted that changes in these parameters generally resulted in major changes in leakage and rotordynamic coefficients. O.C.

**A84-46954\*#** Carborundum Co., Niagara Falls, N. Y.  
**PROCESSING OF SINTERED ALPHA SiC**  
 R. S. STORM (Carborundum Co., Advanced Materials Div., Niagara Falls, NY) American Society of Mechanical Engineers, International Gas Turbine Conference and Exhibit, 29th, Amsterdam, Netherlands, June 4-7, 1984. 13 p. Research supported by the U.S. Department of Energy. refs  
 (Contract DEN3-17; DEN3-168; DEN3-167)  
 (ASME PAPER 84-GT-127)

Processing methods of sintered alpha SiC for engine applications are developed in a cost effective manner, using a submicron sized powder blended with sintering aids (boron and carbon). The processes for forming a green powder compact, such as dry pressing, cold isostatic pressing and green machining, slip casting, aqueous extrusion, plastic extrusion, and injection molding, are described. Dry pressing is the simplest route to component fabrication, and is carried out at approximately 10,000 psi pressure, while in the cold isostatic method the pressure could go as high as 20,000 psi. Surfactants are added to control settling rates and casting characteristics in the slip casting. The aqueous extrusion process is accomplished by a hydraulic ram forcing the aqueous mixture through a die. The plastic forming processes of extrusion and injection molding offer the potential of greater diversity in shape capacity. The physical properties of sintered alpha SiC (hardness, Young's modulus, shear modulus, and thermal diffusivity) are extensively tested. Corrosion resistance test results of silicon carbide are included. S.H.

**A84-47036\*#** Carborundum Co., Niagara Falls, N. Y.  
**PROGRESS IN NET SHAPE FABRICATION OF ALPHA SiC TURBINE COMPONENTS**  
 T. B. SWEETING, F. J. FRECHETTE, and J. W. MACBETH (Carborundum Co., Niagara Falls, NY) American Society of Mechanical Engineers, International Gas Turbine Conference and Exhibit, 29th, Amsterdam, Netherlands, June 4-7, 1984. 7 p. refs  
 (Contract DEN3-17; DEN3-168; DEN3-167)  
 (ASME PAPER 84-GT-273)

An update of the status of ceramic component development of the AGT Programs is presented. Activity on AGTO Program focussed on the following: successful transition from the prototype to engine configuration rotor, investigation of alternate rotor molding techniques, and completion of scroll assemblies. Progress on the Garrett AGT Program was highlighted by the introduction of plastic molding and extrusion to parts which were previously fabricated by slip casting and isopressing respectively. Author

**A84-47046\*#** National Aeronautics and Space Administration.  
 Lewis Research Center, Cleveland, Ohio.  
**ACOUSTIC EMISSION EVALUATION OF PLASMA-SPRAYED THERMAL BARRIER COATINGS**  
 C. C. BERNDT (NASA, Lewis Research Center, Cleveland, OH) American Society of Mechanical Engineers, International Gas Turbine Conference and Exhibit, 29th, Amsterdam, Netherlands, June 4-7, 1984. 5 p. refs  
 (Contract NAG3-164; NCC3-27)  
 (ASME PAPER 84-GT-292)

Acoustic emission techniques have recently been used in a number of studies to investigate the performance and failure behavior of plasma-sprayed thermal barrier coatings. Failure of the coating is a complex phenomena, especially when the composite nature of the coating is considered in the light of possible failure mechanisms. Thus it can be expected that both the metal and ceramic components (i.e., the bond coat and ceramic overlay) of a composite thermal protection system influence the macroscopic behavior and performance of the coating. The aim of the present work is to summarize the 'state-of-the-art' in terms of this initial work and indicate where future progress may be made. Author

**A84-48996\*#** Dartmouth Coll., Hanover, N.H.  
**DETERMINATION OF NEAR-SURFACE PLASTIC DEFORMATION IN SLIDING CONTACTS**  
 F. E. KENNEDY, JR. (Dartmouth College, Hanover, NH) and L. P. GROTELUESCHEN (Union Carbide Corp., Indianapolis, IN) (U.S. National Congress of Applied Mechanics, 9th, Ithaca, NY, June 1982) ASME, Transactions, Journal of Applied Mechanics (ISSN 0021-8936), vol. 51, Sept. 1984, p. 687-689. refs  
 (Contract NSG-3253)

It is pointed out that substantial plastic deformation occurs on and near the contact surfaces, when two solid bodies slide against each other without lubrication. It has been found that this deformation plays an important role in the tribological behavior of the sliding contact. The present investigation has the objective to develop an analytical model to predict the near-surface plastic deformation resulting from a single pass of one metallic surface over another. A finite element viscoplasticity program was written relating velocities to forces in a two-dimensional domain. The program was employed in the study of plastic deformation during a single pass of a hardened tool steel slider over a copper rub specimen. It was found that essentially the only material set in motion by the slider was directly under the contact zone. The agreement between values obtained in the analysis and experimental data is reasonably good. G.R.

**N84-10581\*#** Detroit Diesel Allison, Indianapolis, Ind.  
**ADVANCED GAS TURBINE (AGT): POWER-TRAIN SYSTEM DEVELOPMENT** Semiannual Report, Jan. - Jun. 1982  
 H. E. HELMS, R. A. JOHNSON, R. K. GIBSON, and L. B. SMITH  
 Aug. 1983 64 p  
 (Contract DEN3-168; DE-AI01-77CS-51040)  
 (NASA-CR-168056; DOE/NASA/0168-5; NAS 1.26:168056; DDA-EDR-11185; SAR-5) Avail: NTIS HC A04/MF A01 CSCI 07E

Technical work on the design and effort leading to the testing of a 74.5 kW (100 hp) automotive gas turbine is described. The general effort was concentrated on building an engine for test starting in July. The buildup progressed with only routine problems and the engine was delivered to the test stand 9 July. In addition to the engine build effort, work continued in selected component areas. Ceramic turbine parts were built and tested. Burst tests of ceramic rotors show strengths are approaching that achieved in test bars; proof testing is required for acceptable strength ceramic vanes. Over 25 hours was accumulated on the combustor rig in three test modes: pilot nozzle only, start nozzle, and main nozzle operation. Satisfactory ignition was achieved for a wide range of starting speeds and the lean blowout limit was as low as 0.06 kg/b (0.14 lb/hr). Lean blowout was more a function of nozzle atomization than fuel/air ratio. A variety of cycle points were tested. Transition from start nozzle flow to main nozzle flow was done

manually without difficulty. Regenerator parts were qualification tested without incident and the parts were assembled on schedule. Rig based performance matched first build requirements. Repeated failures in the harmonic drive gearbox during rig testing resulted in that concept being abandoned for an alternate scheme.

Author

**N84-11498\*#** National Aeronautics and Space Administration. Lewis Research Center, Cleveland, Ohio.

**NUMERICAL METHODS AND COMPUTERS USED IN ELASTOHYDRODYNAMIC LUBRICATION**

B. J. HAMROCK and J. H. TRIPP (Case Western Research Univ., Cleveland) 1982 21 p refs Presented at the 10th Leeds-Lyon Symp. on Tribology, Lyon, 6-9 Sep. 1983 (NASA-TM-83524; E-1797, NAS 1.15:83524) Avail: NTIS HC A02/MF A01 CSCL 11H

Some of the methods of obtaining approximate numerical solutions to boundary value problems that arise in elastohydrodynamic lubrication are reviewed. The highlights of four general approaches (direct, inverse, quasi-inverse, and Newton-Raphson) are sketched. Advantages and disadvantages of these approaches are presented along with a flow chart showing some of the details of each. The basic question of numerical stability of the elastohydrodynamic lubrication solutions, especially in the pressure spike region, is considered. Computers used to solve this important class of lubrication problems are briefly described, with emphasis on supercomputers. S.L.

**N84-11500\*#** National Aeronautics and Space Administration. Lewis Research Center, Cleveland, Ohio.

**SPECIAL CASES OF FRICTION AND APPLICATIONS**

F. L. LITVIN (Illinois Univ.) and J. J. COY Nov. 1983 18 p refs To be presented at the Design Eng. Show and Conf., Chicago, 26-29 Mar. 1984 (NASA-TM-83523; NAS 1.15:83523; AVRADCOM-TR-83-C-9; E-1857) Avail: NTIS HC A02/MF A01 CSCL 20K

Two techniques for reducing friction forces are presented. The techniques are applied to the generalized problem of reducing the friction between kinematic pairs which connect a moveable link to a frame. The basic principles are: (1) Let the moveable link be supported by two bearings where the relative velocities of the link with respect to each bearing are of opposite directions. Thus the resultant force (torque) of friction acting on the link due to the bearings is approximately zero. Then, additional perturbation of motion parallel to the main motion of the moveable link will require only a very small force; (2) Let the perturbation in motion be perpendicular to the main motion. Equations are developed which explain these two methods. The results are discussed in relation to friction in geared couplings, gyroscope gimbal bearings and a rotary conveyor system. Design examples are presented. Author

**N84-13577\*#** National Aeronautics and Space Administration. Lewis Research Center, Cleveland, Ohio.

**MEASUREMENT OF ROLLING FRICTION BY A DAMPED OSCILLATOR**

M. DAYAN and D. H. BUCKLEY Dec. 1983 8 p refs (NASA-TP-2257; E-1583; NAS 1.60:2257) Avail: NTIS HC A02/MF A01 CSCL 20K

An experimental method for measuring rolling friction is proposed. The method is mechanically simple. It is based on an oscillator in a uniform magnetic field and does not involve any mechanical forces except for the measured friction. The measured pickup voltage is Fourier analyzed and yields the friction spectral response. The proposed experiment is not tailored for a particular case. Instead, various modes of operation, suitable to different experimental conditions, are discussed. Author

**N84-14519\*#** National Aeronautics and Space Administration. Lewis Research Center, Cleveland, Ohio.

**A DYNAMIC ANALYSIS OF ROTARY COMBUSTION ENGINE SEALS**

J. KNOLL (Michigan Technological Univ.), C. R. VILMANN (Michigan Technological Univ.), H. J. SCHOCK, and R. P. STUMPF 1984 15 p refs Proposed for presentation at the Ann. Congr. and Exposition, Detroit, 27 Feb. - 2 Mar. 1984; sponsored by SAE (NASA-TM-83536; E-1902; NAS 1.15:83536) Avail: NTIS HC A02/MF A01 CSCL 11A

Real time work cell pressures are incorporated into a dynamic analysis of the gas sealing grid in Rotary Combustion Engines. The analysis which utilizes only first principal concepts accounts for apex seal separation from the trochoidal bore, apex seal shifting between the sides of its restraining channel, and apex seal rotation within the restraining channel. The results predict that apex seals do separate from the trochoidal bore and shift between the sides of their channels. The results also show that these two motions are regularly initiated by a seal rotation. The predicted motion of the apex seals compares favorably with experimental results. Frictional losses associated with the sealing grid are also calculated and compare well with measurements obtained in a similar engine. A comparison of frictional losses when using steel and carbon apex seals has also been made as well as friction losses for single and dual side sealing. Author

**N84-15554\*#** General Motors Corp., Indianapolis, Ind. Engineering Dept.

**ADVANCED GAS TURBINE (AGT) TECHNOLOGY DEVELOPMENT Semiannual Report**

May 1983 49 p refs (Contract DEN3-168, DE-AI01-77CS-1040) (NASA-CR-168235; DOE/NASA/0168-6; NAS 1.26:168235; EDR-11443) Avail: NTIS HC A03/MF A01 CSCL 21A

A 74.5 kW (100 hp) automotive gas turbine was evaluated. The engine structure, bearings, oil system, and electronics were demonstrated and no shaft dynamics or other vibration problem were encountered. Areas identified during the five tests are the scroll retention features, and transient thermal deflection of turbine backplates. Modifications were designed. Scroll retention is addressed by modifying the seal arrangement in front of the gasifier turbine assembly, which will increase the pressure load on the scroll in the forward direction and thereby increase the retention forces. The backplate thermal deflection is addressed by geometric changes and thermal insulation to reduce heat input. Combustor rig proof testing of two ceramic combustor assemblies was completed. The combustor was modified to incorporate slots and reduce sharp edges, which should reduce thermal stresses. The development work focused on techniques to sinter these barrier materials onto the ceramic rotors with successes for both material systems. Silicon carbide structural parts, including engine configuration gasifier rotors (ECRs), preliminary gasifier scroll parts, and gasifier and power turbine vanes are fabricated. E.A.K.

**N84-16562\*#** Virginia Univ., Charlottesville. Rotor Dynamics Lab.

**DESIGN STUDY OF MAGNETIC EDDY-CURRENT VIBRATION SUPPRESSION DAMPERS FOR APPLICATION TO CRYOGENIC TURBOMACHINERY Final Report**

E. J. GUNTER, R. R. HUMPHRIS, and S. J. SEVERSON Dec. 1983 142 p refs (Contract NAG3-263) (NASA-CR-173273; NAS 1.26:173273; UVA/52810/MAE84/101) Avail: NTIS HC A07/MF A01 CSCL 13I

Cryogenic turbomachinery used to pump high pressure fuel (liquid H<sub>2</sub>) and oxidizer (liquid O<sub>2</sub>) to the main engines of the Space Shuttle have experienced rotor instabilities. Subsynchronous whirl, an extremely destructive instability, has caused bearing failures and severe rubs in the seals. These failures have resulted in premature engine shutdowns or, in many instances, have limited the power level to which the turbopumps could be operated. The



feasibility of using an eddy current type of damping mechanism for the Space Shuttle Main Engine is outlined. Author

**N84-17590\*#** National Aeronautics and Space Administration. Lewis Research Center, Cleveland, Ohio.

**EFFECTS OF DIFFERENT RUB MODELS ON SIMULATED ROTOR DYNAMICS**

A. F. KASCAK and J. J. TOMKO Feb. 1984 12 p refs Presented at the ASME Appl. Mech., Bioeng., and Fluids Eng. Conf., Houston, Tex., 20-22 Jun. 1983 Prepared in cooperation with Army Research and Technology Labs., Cleveland (NASA-TP-2220; E-1801; NAS 1.60:2220; AFSCOM-TR-83-C-8; AD-A138495) Avail: NTIS HC A02/MF A01 CSCL 131

Using a direct integration, transient response rotor dynamics computer code, the response of turbine engine rotors to two different blade tip - seal interference rub models was studied. The first model, an abradable seal rub model, is based on an energy-loss-per-unit-volume theory (applicable to a ceramic turbine blade tip seal). The second, a smearin model, is based on viscous hydrodynamic theory (applicable to a metallic blade tip seal). The results from these two models were compared with those from a previously studied model based on dry friction theory. The abradable model was very sensitive to small changes in the energy per unit volume, and once a threshold was exceeded, the rotor went into a backward whirl. The amplitude seemed to grow without limit. This was similar to the dry friction model when the coefficient of friction exceeded a particular threshold. The smearing model was not as sensitive to small changes in the viscosity, but a threshold viscosity was found. When it was exceeded, the rotor went into backward whirl, but the amplitude seemed to grow to a finite limit. Author

**N84-17591\*#** National Aeronautics and Space Administration. Lewis Research Center, Cleveland, Ohio.

**THE BALL BEARING AS A RHEOLOGICAL TEST DEVICE**

E. KINGSBURY (Draper, Charles S. Lab.) 1984 13 p refs Presented at the 10th Leeds-Lyon Symp. on Tribology, Lyon, 6-9 Sep. 1983

(NASA-TM-83570; NAS 1.15:83570; E-1814) Avail: NTIS HC A02/MF A01 CSCL 131

An angular-contact ball bearing provides an easily obtainable, precise mechanical system for rheological tests on thin films under high pressure. The test conditions are by definition similar to those found in practice. Accessible independent variables include size, pressure, bulk temperature, roughness, adsorbed surfactant, fluid type, fluid quantity, fluid supply rate, film thickness, entrainment velocity, transit time, and combined strain. Easily measured or inferred variables include slip, changes in film thickness with time (transients), strain rate, lubricant elastic modulus (thin film, high pressure), tractive force, lubricant chemical degradation rate, and lubricant degradation product. Methods for setting and obtaining these quantities in a bearing are discussed, together with experimental limitations on them. Author

**N84-17592\*#** National Aeronautics and Space Administration. Lewis Research Center, Cleveland, Ohio.

**HYDRODYNAMIC LUBRICATION OF RIGID NONCONFORMAL CONTACTS IN COMBINED ROLLING AND NORMAL MOTION**

M. K. GHOSH (Banaras Hindu Univ.), B. J. HAMROCK, and D. E. BREWE 1984 28 p refs Proposed for presentation at the Joint Lubrication Conf., San Diego, Calif., 22-24 Oct. 1984; sponsored by ASME and American Society of Lubrication Engineers Prepared in cooperation with Army Research and Technology Labs., Cleveland (NASA-TM-83578; E-1926; NAS 1.15:83578; AVRADCOM-TR-84-C-2) Avail: NTIS HC A03/MF A01 CSCL 131

A numerical solution to the problem of hydrodynamic lubrication of rigid point contacts with an isoviscous, incompressible lubricant was obtained. The hydrodynamic load-carrying capacity under unsteady (or dynamic) conditions arising from the combined effects of squeeze motion superposed upon the entraining motion was determined for both normal approach and separation. Superposed

normal motion considerably increases net load-carrying capacity during normal approach and substantially reduces net load-carrying capacity during separation. Geometry was also found to have a significant influence on the dynamic load-carrying capacity. The ratio of dynamic to steady state load-carrying capacity increases with increasing geometry parameter for normal approach and decreases during separation. The cavitation (film rupture) boundary is also influenced significantly by the normal motion, moving downstream during approach and upstream during separation. For sufficiently high normal separation velocity the rupture boundary may even move upstream of the minimum-film-thickness position. Sixty-three cases were used to derive a functional relationship for the ratio of the dynamic to steady state load-carrying capacity in terms of the dimensionless normal velocity parameter (incorporating normal velocity, entraining velocity, and film thickness) and the geometry parameter. M.G.

**N84-18653\*#** National Aeronautics and Space Administration. Lewis Research Center, Cleveland, Ohio.

**MECHANISM OF LUBRICATION BY TRICRESYLPHOSPHATE (TCP)**

O. D. FAUT (Wilkes Coll., Wilkes-Barre, Pa.) and D. H. BUCKLEY Feb. 1984 13 p refs

(NASA-TP-2274; E-1846; NAS 1.60:2274) Avail: NTIS HC A02/MF A01 CSCL 11H

The coefficient of friction was measured as a function of temperature on a pin-on-disk tribometer. Pins and disks of 440C and 52100 steels were lubricated with trisecylphosphate (TCP), 3.45 percent TCP in squalene, and pure squalene. The M-50 pins and disks were lubricated with 3.45 percent TCP in squalene and pure squalene. Experiments were conducted under limited lubrication conditions in dry (100 ppm H<sub>2</sub>O) air and dry (pp H<sub>2</sub>O) nitrogen at 50 rpm (equivalent to a sliding velocity of 13 cm/sec) and a constant load of 9.8 N (1 kg). Characteristic temperatures T<sub>sub r</sub> were identified for TCP on 52100 steel and for squalene on M-50 and 52100 steels, where the friction decreased because of a chemical reaction between the lubricant and the metal surface. The behavior of squalene obscured the influence of 3.45 percent TCP solute on the friction of the system. Wear volume measurements demonstrated that wear was lowest at temperatures just above T<sub>sub r</sub>. Comparing the behavior of TCP on M-50, 440C, and 52100 steels revealed that the TCP either reacted to give T<sub>sub r</sub> behavior or produced initial failure in the temperature range 223 ± or - 5 C. S.L.

**N84-18654\*#** National Aeronautics and Space Administration. Lewis Research Center, Cleveland, Ohio.

**COMPARISON OF PREDICTED AND EXPERIMENTAL THERMAL PERFORMANCE OF ANGULAR-CONTACT BALL BEARINGS**

R. J. PARKER Feb. 1984 19 p refs

(NASA-TP-2275; E-1751; NAS 1.60:2275) Avail: NTIS HC A02/MF A01 CSCL 131

Predicted bearing heat generation and bearing temperature were verified by experimental data for ball bearings over a range of sizes, shaft speeds, and lubricant flow rates. The computer program Shaberth requires, as input, a factor which describes the air-oil mixture in the bearing cavity for calculation of the ball drag contribution to bearing heat generation. An equation for this lubricant percent volume in the bearing cavity was derived and appears to be valid over the range of test conditions including bearing bore sizes from 35 to 167 mm and shaft speeds from 1.0 to 3.0 million DN. Author

**N84-19816\*#** National Aeronautics and Space Administration. Lewis Research Center, Cleveland, Ohio.

**FIRST ORDER BALL BEARING KINEMATICS**

E. KINGBURY (Draper (Charles Stark) Lab.) 1984 17 p refs To be presented at the Ann. Meeting of the Am. Soc. of Lubrication Engr., Chicago, 7-10 May 1984

(NASA-TM-83592; E-1918; NAS 1.15:83592) Avail: NTIS HC A02/MF A01 CSCL 131

Two first order equations are given connecting geometry and internal motions in an angular contact ball bearing. Total speed,



kinematic equivalence, basic speed ratio, and modal speed ratio are defined and discussed; charts are given for the speed ratios covering all bearings and all rotational modes. Instances where specific first order assumptions might fail are discussed, and the resulting effects on bearing performance reviewed. Author

**N84-20858\*#** National Aeronautics and Space Administration. Lewis Research Center, Cleveland, Ohio.  
**FRictionAL AND MORPHOLOGICAL PROPERTIES OF AU-MOS2 FILMS SPUTTERED FROM A COMPACT TARGET**  
 T. SPALVINS 13 Apr. 1984 19 p refs Presented at 11th Intern. Conf. on Metallurg. Coatings, San-Diego, Calif., 9-13 Apr. 1984; sponsored by American Vacuum Society (NASA-TM-83604; E-2004; NAS 1.15:83604) Avail: NTIS HC A02/MF A01 CSCL 11H

AuMoS<sub>2</sub> films 0.02 to 1.2 microns thick were sputtered from target compacted from 5 wt % Au + 95 wt % MoS<sub>2</sub>, to investigate the frictional and morphological film growth characteristics. The gold dispersion effects in MoS<sub>2</sub> films are of interest to increase the densification and strengthening of the film structure. Three microstructural growth stages were identified on the nano-micro-macrostructural level. During sliding both sputtered Au-MoS<sub>2</sub> and MoS<sub>2</sub> films have a tendency to break within the columnar region. The remaining or effective film, about 0.2 microns thick, performs the lubrication. The Au-MoS<sub>2</sub> films displayed a lower friction coefficient with a high degree of frictional stability and less wear debris generation as compared to pure MoS<sub>2</sub> films. The more favorable frictional characteristics of the Au-MoS<sub>2</sub> films are attributed to the effective film thickness and the high density packed columnar zone which has a reduced effect on the fragmentation of the tapered crystallites during fracture. M.G.

**N84-21877\*#** Department of Energy, Washington, D. C. Office of Vehicle and Engine Research and Development.  
**PROCEEDINGS OF THE 20TH AUTOMOTIVE TECHNOLOGY DEVELOPMENT CONTRACTORS' COORDINATION MEETING**  
 Warrendale, Pa. Society of Automotive Engineers, Inc. Apr. 1983 366 p refs Proc. held in Dearborn, Mich., 25-28 Oct. 1982

(Contract DEN3-287)  
 (NASA-CR-173412; NAS 1.26:173412; DE83-016840; CONF-821055; ISBN-0-89883-081-8; P-120) Avail: NTIS HC A16/MF A01 CSCL 13I

Thirty-four papers are included which cover the following topics: stirring technology, gas turbines, ceramics, heavy duty transport, industry perspectives, and alternative fuels. B.G.

**N84-21879\*#** Garrett Turbine Engine Co., Phoenix, Ariz.  
**ADVANCED TURBOCHARGER DESIGN STUDY PROGRAM Final Report**  
 D. G. CULY, R. W. HELDENBRAND, and N. R. RICHARDSON (Garrett Automotive Products Co., Torrance, Calif.) 1 Jan. 1984 193 p refs  
 (Contract NAS3-22750)  
 (NASA-CR-174633; NAS 1.26:174633; GTEC-21-4498) Avail: NTIS HC A09/MF A01 CSCL 21G

The advanced Turbocharger Design Study consisted of: (1) the evaluation of three advanced engine designs to determine their turbocharging requirements, and of technologies applicable to advanced turbocharger designs; (2) trade-off studies to define a turbocharger conceptual design and select the engine with the most representative requirements for turbocharging; (3) the preparation of a turbocharger conceptual design for the Curtiss Wright RC2-32 engine selected in the trade-off studies; and (4) the assessment of market impact and the preparation of a technology demonstration plan for the advanced turbocharger. Author

**N84-22957\*** National Aeronautics and Space Administration. Lewis Research Center, Cleveland, Ohio.

**METHOD OF FABRICATING AN ABRADABLE GAS PATH SEAL Patent**

R. C. BILL and D. W. WISANDER, inventors (to NASA) 7 Feb. 1984 6 p Filed 30 Sep. 1982 Division of US Patent No 4,377,371, US Patent Appl. SN-242795, filed 11 Mar. 1981 (NASA-CASE-LEW-13269-2; US-PATENT-4,430,360; US-PATENT-4,377,371; US-PATENT-APPL-SN-431448; US-PATENT-APPL-SN-242795; US-PATENT-CLASS-427-34; US-PATENT-CLASS-415-174; US-PATENT-CLASS-427-53.1; US-PATENT-CLASS-427-423; US-PATENT-CLASS-428-155) Avail: US Patent and Trademark Office CSCL 11A

The thermal shock resistance of a ceramic layer is improved. The invention is particularly directed to an improved abradable lining that is deposited on shroud forming a gas path in turbomachinery. Improved thermal shock resistance of a shroud is effected through the deliberate introduction of benign cracks. These are microcracks which will not propagate appreciably upon exposure to the thermal shock environment in which a turbine seal must function. Laser surface fusion treatment is used to introduce these microcracks. The ceramic surface is laser scanned to form a continuous dense layer. As this layer cools and solidifies, shrinkage results in the formation of a very fine crack network. The presence of this deliberately introduced fine crack network precludes the formation of a catastrophic crack during thermal shock exposure.

Official Gazette of the U.S. Patent and Trademark Office

**N84-22958\*** National Aeronautics and Space Administration. Lewis Research Center, Cleveland, Ohio.

**HEAT PIPES TO REDUCE ENGINE EXHAUST EMISSIONS Patent**

D. F. SCHULTZ, inventor (to NASA) 7 Feb. 1984 8 p Filed 30 Jan. 1981 (NASA-CASE-LEW-12590-1; US-PATENT-4,429,537; US-PATENT-APPL-SN-229693, US-PATENT-CLASS-60-730; US-PATENT-CLASS-60-736) Avail: US Patent and Trademark Office CSCL 21A

A fuel combustor is presented that consists of an elongated casing with an air inlet conduit portion at one end, and having an opposite exit end. An elongated heat pipe is mounted longitudinally in the casing and is offset from and extends alongside the combustion space. The heat pipe is in heat transmitting relationship with the air intake conduit for heating incoming air. A guide conduit structure is provided for conveying the heated air from the intake conduit into the combustion space. A fuel discharge nozzle is provided to inject fuel into the combustion space. A fuel conduit from a fuel supply source has a portion engaged in heat transfer relationship of the heat pipe for preheating the fuel. The downstream end of the heat pipe is in heat transfer relationship with the casing and is located adjacent to the downstream end of the combustion space. The offset position of the heat pipe relative to the combustion space minimizes the quenching effect of the heat pipe on the gaseous products of combustion, as well as reducing coking of the fuel on the heat pipe, thereby improving the efficiency of the combustor.

Official Gazette of the U.S. Patent and Trademark Office

**N84-22959\*#** National Aeronautics and Space Administration. Lewis Research Center, Cleveland, Ohio.

**IMPROVED COMPLIANT HYDRODYNAMIC FLUID JOURNAL BEARING Patent Application**

E. L. WARREN, inventor (to NASA) 2 Apr. 1984 11 p (NASA-CASE-LEW-13670-1; US-PATENT-APPL-SN-603374) Avail: NTIS HC A02/MF A01 CSCL 13I

An arc heating structure is described that prevents destructive bending moments within the top foil. Welds are eliminated by mounting the top bearing foil in the bearing cartridge sleeve without using a space block. Tabs or pins at the end of the top bearing foil are restrained by slots or stops formed in the cartridge sleeve. These structural members are free to move in a direction normal

to the shaft while being restrained from movement in the direction of shaft rotation. NASA

**N84-23891\*#** National Aeronautics and Space Administration. Lewis Research Center, Cleveland, Ohio.

## TRIBOLOGY IN THE 80'S. VOLUME 1: SESSIONS 1 TO 4

Apr. 1984 508 p refs Conf. held at NASA. Lewis Research Center, 18-21 Apr. 1983 2 Vol (NASA-CP-2300-VOL-1; E-1559; NAS 1.55:2300-VOL-1) Avail: NTIS HC A22/MF A01 CSCL 11H

A wide range of subjects extending from fundamental research with tribological materials and their surface effects up to the final applications in mechanical components were covered.

**N84-23903\*#** National Aeronautics and Space Administration. Lewis Research Center, Cleveland, Ohio.

## CONSIDERATIONS IN FRICTION AND WEAR

K. MIYOSHI and D. H. BUCKLEY *In its* Tribology in the 80's. Vol. 1 p 291-320 Apr. 1984 refs Avail: NTIS HC A22/MF A01 CSCL 11H

The abrasion of ceramic materials is discussed. The friction and wear properties of ceramics which arise primarily from adhesion between sliding surfaces in contact was examined. The role of chemical bonding in adhesion and friction and the influence of surface films, temperature, and crystallographic orientation effects on tribological response with respect to adhesion, friction, and wear are discussed. The complex interaction of various deformation and fracture mechanisms in ceramics, the effect of crystallographic orientation on abrasion, friction, and fracture behavior is addressed. E.A.K.

**N84-24895\*#** National Aeronautics and Space Administration. Lewis Research Center, Cleveland, Ohio.

## ELASTOHYDRODYNAMIC LUBRICATION OF SMOOTH SURFACES Abstract Only

B. J. HAMROCK *In* Delaware Univ. Abstr. of the 20th Ann. Meeting, Society of Engineering Science, Inc. p 141-142 1983 refs Avail: NTIS HC A16/MF A01 CSCL 13I

Fully flooded, elastohydrodynamically lubricated contacts are considered. Elastohydrodynamic lubrication (EHL) analysis requires the simultaneous solution of the elasticity, viscosity, density, and Reynolds equations. The most important practical aspect of elastohydrodynamic lubrication theory is the determination of the minimum film thickness within the conjunction. The maintenance of a fluid film of adequate magnitude is an essential feature of the correct operation of lubricated machine elements. The results show the influence of contact geometry on minimum film thickness as expressed by the ellipticity parameter and the dimensionless speed, load, and materials parameters. Film thickness equations are developed for materials of high elastic modulus, such as metal, and for materials of low elastic modulus, such as rubber. A.R.H.

**N84-24898#** National Aeronautics and Space Administration. Lewis Research Center, Cleveland, Ohio.

## SURFACE TOPOGRAPHY-CONNECTIONS BETWEEN LUBRICATION AND FAILURE INITIATION Abstract Only

L. D. WEDEVEN *In* Delaware Univ. Abstr. of the 20th Ann. Meeting, Society of Engineering Science, Inc. p 146-147 1983 Avail: NTIS HC A16/MF A01 CSCL 13H

The characteristics of the initial surface topography is intimately connected to the machining process by which it is produced. Both processes create a near surface region of residual stresses, microstructure and hardness that is different from the bulk. The material properties in this rather undefined region can significantly influence the mode of failure, such as wear, scuffing or fatigue, as well as the degree of failure resistance for a given material. Under full film elastohydrodynamic (EHD) conditions, where shear is accommodated within a relatively thick lubricant film, the normal and shear stresses are distributed uniformly over the near surface region, and the surface topography has little influence on the lubrication or failure process. Under more typical conditions where surface roughness and lubricant film thickness are of the same

order of magnitude, the surface topography not only emerges as an important parameter in failure initiation, but it also becomes intimately involved in the lubrication process itself. B.W.

**N84-25047\*#** National Aeronautics and Space Administration. Lewis Research Center, Cleveland, Ohio.

## TRIBOLOGY IN THE 80'S. VOLUME 2: SESSIONS 5 - 8

Aug. 1984 377 p refs Conf. held in Cleveland, 18-21 Apr. 1983 2-Vol. (NASA-CP-2300-VOL-2; E-1559; NAS 1.55:2300-VOL-2) Avail: NTIS HC A17/MF A01 CSCL 13I

Tender standing and technical advancement of various disciplines and subdisciplines on tribology were discussed. Topics discussed included importance and definition of materials in tribology; directions of research in adhesion and friction; research in wear and wear resistant materials; liquid lubricants and additives; solid lubricants; and tribological materials for mechanical components of the future.

**N84-25048\*#** National Aeronautics and Space Administration. Lewis Research Center, Cleveland, Ohio.

## ELASTOHYDRODYNAMIC LUBRICATION. STATUS OF UNDERSTANDING

B. J. HAMROCK *In its* Tribology in the 80's, vol. 2 p 507-531 Apr. 1984 refs Avail: NTIS HC A17/MF A01 CSCL 13I

The development of elastohydrodynamic lubrication which was divided into three main stages is discussed. The first stage is the development of the idealized form of elastohydrodynamic lubrication, where the surfaces are smooth, the fluid behavior is assumed to be Newtonian, and isothermal considerations are assumed. The complete spectrum of contact geometries contact materials and lubricant availability are presented. The second state of development incorporates the effects of a nonNewtonian fluid model, thermal effects, and surface roughness effects into the elastohydrodynamic lubrication model developed in stage one. Recent developments in this stage are presented. The third stage considers the items considered in stage two, the lubrication of real surfaces in their operating environments is examined. E.A.K.

**N84-25061\*#** National Aeronautics and Space Administration. Lewis Research Center, Cleveland, Ohio.

## STATUS OF UNDERSTANDING FOR GEAR MATERIALS

D. P. TOWNSEND *In its* Tribology in the 80's, vol. 2 p 795-809 Apr. 1984 refs Avail: NTIS HC A17/MF A01 CSCL 13I

A wide variety of gear materials is available today for the gear designer. The choice of which material to use should be based on the requirements of the application and will include the operating conditions of load, speed, and temperature in addition to reliability, weight, noise limitation, accuracy, and cost. In aircraft applications such as helicopters, V/STOL aircraft, and turboprops, the dominant factors to be considered are reliability and weight. The following gear materials are reviewed herein with an emphasis upon mechanical properties, cost, and durability: plastics, nonferrous metals, copper alloys, iron alloys, metal powders, and steels. R.S.F.

**N84-25064\*#** National Aeronautics and Space Administration. Lewis Research Center, Cleveland, Ohio.

## DUAL CLEARANCE SQUEEZE FILM DAMPER FOR HIGH LOAD CONDITIONS

D. P. FLEMING 1984 14 p refs Presented at the Joint Lubrication Conf., San Diego, Calif., 22-24 Oct. 1984; sponsored by ASME and the American Society of Lubrication Engineers (NASA-TM-83619; E-2053; NAS 1.15:83619) Avail: NTIS HC A02/MF A01 CSCL 13I

Squeeze film dampers are widely used to control vibrations in aircraft turbine engines and other rotating machinery. However, if shaft unbalance rises appreciably above the design value (e.g., due to a turbine blade loss), a conventional squeeze film becomes overloaded, and is no longer effective in controlling vibration amplitudes and bearing forces. A damper concept characterized

by two oil films is described. Under normal conditions, only one low-clearance film is active, allowing precise location of the shaft centerline. Under high unbalance conditions, both films are active, controlling shaft vibration in a near-optimum manner, and allowing continued operation until a safe shutdown can be made. Author

**N84-25065\*#** United Technologies Research Center, East Hartford, Conn.

**ABRASIVE TIP TREATMENT FOR USE ON COMPRESSOR BLADES Final Report**

H. C. PEDERSEN Jan. 1984 73 p  
(Contract NAS3-22813; DA PROJ. 1L1-61102-AH-45)  
(NASA-CR-174666; NAS 1.26:174666; PWA-5833-37) Avail.  
NTIS HC A04/MF A01 CSCL 13I

A co-spray process was used which simultaneously but separately introduces abrasive grits and metal matrix powder into the plasma stream and entraps the abrasive grits within a molten matrix to form an abrasive coating as the matrix material solidifies on test specimen surfaces. Spray trials were conducted to optimize spray parameter settings for the various matrix/grit combinations before actual spraying of the test specimens. Rub, erosion, and bond adhesion tests were conducted on the coated specimens in the as-sprayed condition as well as on coated specimens that were aged for 100 hours at a temperature of 866K (1100 F). Microscopic examinations were performed to determine the coating abrasive-particle content, the size and shape of the adhesive particles in the coating, and the extent of compositional or morphological changes resulting from the aging process. A nickel chromium/aluminum composite with No. 150 size (0.002 to 0.005 inch) silicon carbide grits was selected as the best matrix/abrasive combination of the candidates surveyed for coating compressor blade tips. A.R.H.

**N84-26027\*#** Cleveland State Univ., Ohio.

**DYNAMICS OF EARLY PLANETARY GEAR TRAINS Final Report**

R. AUGUST, R. KASUBA, J. L. FRATER, and A. PINTZ  
Washington NASA Jun 1984 233 p refs  
(Contract NAG3-186)  
(NASA-CR-3793; NAS 1 26:3793) Avail: NTIS HC A11/MF A01 CSCL 13I

A method to analyze the static and dynamic loads in a planetary gear train was developed. A variable-variable mesh stiffness (VVMS) model was used to simulate the external and internal spur gear mesh behavior, and an equivalent conventional gear train concept was adapted for the dynamic studies. The analysis can be applied either involute or noninvolute spur gearing. By utilizing the equivalent gear train concept, the developed method may be extended for use for all types of epicyclic gearing. The method is incorporated into a computer program so that the static and dynamic behavior of individual components can be examined. Items considered in the analysis are: (1) static and dynamic load sharing among the planets; (2) floating or fixed Sun gear; (3) actual tooth geometry, including errors and modifications; (4) positioning errors of the planet gears; (5) torque variations due to noninvolute gear action. A mathematical model comprised of power source, load, and planetary transmission is used to determine the instantaneous loads to which the components are subjected. It considers fluctuating output torque, elastic behavior in the system, and loss of contact between gear teeth. The dynamic model has nine degrees of freedom resulting in a set of simultaneous second order differential equations with time varying coefficients, which are solved numerically. The computer program was used to determine the effect of manufacturing errors, damping and component stiffness, and transmitted load on dynamic behavior. It is indicated that this methodology offers the designer/analyst a comprehensive tool with which planetary drives may be quickly and effectively evaluated. E.A.K.

**N84-26029\*#** National Aeronautics and Space Administration. Lewis Research Center, Cleveland, Ohio.

**FACTORS THAT AFFECT THE FATIGUE STRENGTH OF POWER TRANSMISSION SHAFTING**

S. H. LOEWENTHAL 1984 28 p refs Proposed for presentation at the 4th Intern. Power Transmission and Gearing Conf., Cambridge, Mass., 8-12 Oct. 1984; sponsored by ASME (NASA-TM-83608; E-1984; NAS 1.15:83608) Avail: NTIS HC A03/MF A01 CSCL 13I

A long standing objective in the design of power transmission shafting is to eliminate excess shaft material without compromising operational reliability. A shaft design method is presented which accounts for variable amplitude loading histories and their influence on limited life designs. The effects of combined bending and torsional loading are considered along with a number of application factors known to influence the fatigue strength of shafting materials. Among the factors examined are surface condition, size, stress concentration, residual stress and corrosion fatigue. Author

**N84-27041\*#** National Aeronautics and Space Administration. Lewis Research Center, Cleveland, Ohio

**DESIGN OF POWER-TRANSMITTING SHIFTS**

S. H. LOEWENTHAL Jul. 1984 26 p refs Submitted for publication  
(NASA-RP-1123; E-1899; NAS 1.61:1123) Avail: NTIS HC A03/MF A01 CSCL 13I

Power transmission shafting which is a vital element of all rotating machinery is discussed. Design methods, based on strength considerations for sizing shafts and axles to withstand both steady and fluctuating loads are summarized. The effects of combined bending, torsional, and axial loads are considered along with many application factors that are known to influence the fatigue strength of shafting materials. Methods are presented to account for variable amplitude loading histories and their influence on limited life designs. The influences of shaft rigidity, materials, and vibration on the design are discussed. E.A.K.

**N84-27042\*#** National Aeronautics and Space Administration. Lewis Research Center, Cleveland, Ohio.

**SPIN ANALYSIS OF CONCENTRATED TRACTION CONTACTS**

S. H. LOEWENTHAL 1983 31 p refs To be presented at the 4th Intern. Power Transmission and Gearing Conf., Cambridge, Mass., 8-12 Oct. 1984; sponsored by ASME (NASA-TM-83713; E-2103; NAS 1.15:83713) Avail: NTIS HC A03/MF A01 CSCL 13I

Spin, the result of a mismatch in contact radii on either side of the point of rolling, has a detrimental effect on traction contact performance. It occurs in concentrated contacts having conical or contoured rolling elements, such as those in traction drives or angular contact bearings, and is responsible for an increase in contact heating and power loss. The kinematics of spin producing contact geometries and the subsequent effect on traction and power loss are investigated. The influence of lubricant traction characteristics and contact geometries that minimize spin are also addressed. Author

**N84-27043\*#** National Aeronautics and Space Administration. Lewis Research Center, Cleveland, Ohio.

**AN ANALYSIS OF TRACTION DRIVE TORSIONAL STIFFNESS**

D. A. ROHN and S. H. LOEWENTHAL 1983 38 p refs To be presented at the 4th Intern. Power Transmission and Gearing Conf., Cambridge, Mass., 8-12 Oct. 1984; sponsored by ASME (NASA-TM-83712; E-2118; NAS 1.15:83712) Avail: NTIS HC A03/MF A01 CSCL 13I

The tangential compliance of elastic bodies in concentrated contact applied to traction drive elements to determine their torsional stiffness was analyzed. Static loading and rotating conditions are considered. The effects of several design variables are shown. The theoretical torsional stiffness of a fixed ratio multiroller drive is computed and compared to experimental values. It is shown that the torsional compliance of the traction contacts themselves is a relatively small portion of the overall drive system compliance. E.A.K.

**N84-28087\*#** National Aeronautics and Space Administration. Lewis Research Center, Cleveland, Ohio.

**PARAMETER STUDIES OF GEAR COOLING USING AN AUTOMATIC FINITE ELEMENT MESH GENERATOR**

L. E. EL-BAYOUMY (California State Univ., Long Beach), L. S. AKIN (California State Univ., Long Beach), and D. P. TOWNSEND 1984 15 p refs Proposed for presentation at the 4th Intern. Power Transmission and Gearing Conf., Cambridge, Mass., 10-12 Oct. 1984; sponsored by the American Society of Mechanical Engineers

(NASA-TM-83721; E-2187; NAS 1.15:83721) Avail: NTIS HC A02/MF A01 CSCL 131

The range of accuracies achieved in the gear tooth temperature using an automatic finite element mesh generator were investigated. Gear web contribution to the gear cooling process was studied by introducing a varying size hole at the center of the gear because of the versatility of program TARG in allowing different heat transfer coefficients in different areas of the gear tooth. A study was carried out to evaluate the contribution of the loaded and unloaded faces as well as the top and bottom lands. A general purpose two-dimensional finite element preprocessor ATOGEN has been developed for automatic generation of a finite element mesh over a pie-shaped sector of a gear. The program was used for facilitating the input to an upgraded version of a previously developed program for the thermal analysis of running gears (TARG). The latter program determined the steady state temperature distribution throughout the specified gear. The automatic mesh generator program includes a band width minimization routine for reducing computer cost. M.G.

**N84-28088\*#** National Aeronautics and Space Administration. Lewis Research Center, Cleveland, Ohio.

**AN INVESTIGATION OF THE TRANSIENT THERMAL ANALYSIS OF SPUR GEARS**

L. E. EL-BAYOUMY (California State Univ., Long Beach), L. S. AKIN (California State Univ., Long Beach), and D. P. TOWNSEND 1984 21 p refs To be presented at the 4th Intern. Power Transmission and Gearing Conf., Cambridge, 10-12 Oct. 1984

(NASA-TM-83724; E-2192; NAS 1.15:83724) Avail: NTIS HC A02/MF A01 CSCL 131

A finite element computer program is developed for evaluating the transient behavior of surface temperature in high performance spur gears. The time dimension is implemented using two and three point finite difference schemes. The different schemes are provided for the purpose of numerical stability and convergence studies. A detailed explanation of the gear cooling process leading to the establishment of a modified Blok model is also included. Other conventional models for approximating the heat transfer coefficients are available for comparison. Preliminary results are given showing snap shots of gear temperature contours at the initial stages of tooth engagement. M.A.C.

**N84-28089\*#** General Motors Corp., Indianapolis, Ind. **ADVANCED GAS TURBINE (AGT) TECHNOLOGY PROJECT Semiannual Report, 1 Jan. - 30 Jun. 1983**

Jun. 1984 69 p

(Contract DEN3-168; DE-AI01-77CS-51040)

(NASA-CR-174629; DOE/NASA/0168-7; NAS 1.26:174629;

EDR-11577; SAR-7) Avail: NTIS HC A04/MF A01 CSCL 21E

Technical work on the design and effort leading to the testing of a 74.5 kW (100 hp) automotive gas turbine engine is reviewed. Development of the engine compressor, gasifier turbine, power turbine, combustor, regenerator, and secondary system is discussed. Ceramic materials development and the application of such materials in the gas turbine engine components is described. R.S.F.

**N84-28231\*#** National Aeronautics and Space Administration. Lewis Research Center, Cleveland, Ohio.

**OVERVIEW OF ADVANCED STIRLING AND GAS TURBINE ENGINE DEVELOPMENT PROGRAMS AND IMPLICATIONS FOR SOLAR THERMAL ELECTRICAL APPLICATIONS Abstract Only**

D. ALGER In JPL Proc. of the 5th Parabolic Dish Solar Thermal Power Program p 49 1 Mar. 1984

Avail: NTIS HC A15/MF A01 CSCL 10B

The DOE automotive advanced engine development projects managed by the NASA Lewis Research Center were described. These included one Stirling cycle engine development and two air Brayton cycle development. Other engine research activities included: (1) an air Brayton engine development sponsored by the Gas Research Institute, and (2) plans for development of a Stirling cycle engine for space use. Current and potential use of these various engines with solar parabolic dishes were discussed.

Author

**N84-29223\*#** National Aeronautics and Space Administration. Lewis Research Center, Cleveland, Ohio.

**EFFICIENCY OF NONSTANDARD AND HIGH CONTACT RATIO INVOLUTE SPUR GEARS**

N. E. ANDERSON and S. H. LOEWENTHAL 1984 35 p refs Proposed for presentation at the 4th Intern. Power Transmission and Gearing Conf., Cambridge, Mass., 10-12 Oct. 1984; sponsored by ASME Prepared in cooperation with Army Research and Technology Labs., Cleveland

(NASA-TM-83725; E-2173; NAS 1.15:83725; USAVSCOM-TR-84-C-9) Avail: NTIS HC A03/MF A01 CSCL 131

A power loss prediction was extended to include involute spur gears of nonstandard proportions. The method is used to analyze the effects of modified addendum, tooth thickness, and gear center distance in addition to the parameters previously considered which included gear diameter, pitch, pressure angle, face width, oil viscosity, speed, and torque. Particular emphasis was placed on high contact ratio gearing (contact ratios greater than two). Despite their higher sliding velocities, high contact ratio gears are designed to levels of efficiency comparable to those of conventional gears while retaining their advantages through proper selection of gear geometry. Author

**N84-29224\*#** National Aeronautics and Space Administration. Lewis Research Center, Cleveland, Ohio.

**LUBRICANT JET FLOW PHENOMENA IN SPUR AND HELICAL GEARS WITH MODIFIED CENTER DISTANCES AND/OR ADDENDUMS FOR OUT-OF-MESH CONDITIONS**

L. S. AKIN and D. P. TOWNSEND 1983 27 p refs Prepared for presentation at the 4th Intern. Power Transmission and Gearing Conf., Cambridge, Mass., 10-12 Oct. 1984; sponsored by ASME (NASA-TM-83723; E-2190; NAS 1.15:83723) Avail: NTIS HC A03/MF A01 CSCL 131

Out-of-mesh jet lubrication of gears was examined. The pinion impingement cycle was described briefly. An analysis was developed for the lubricant jet flow in the out-of-mesh condition. The analysis provides for the inclusion of modified center distances and modified addendums. Equations were generated for the limit values of variables necessary to remove the severe limitations to facilitate computer analysis. A computer program was designed using these limit formulas to prevent negative impingement (missing) on the pinion. R.S.F.

**N84-29226\*#** National Aeronautics and Space Administration. Lewis Research Center, Cleveland, Ohio.

**OPERATING CHARACTERISTICS OF A THREE-PIECE-INNER-RING LARGE-BORE ROLLER BEARING TO SPEEDS OF 3 MILLION DN**

F. T. SCHULLER Aug. 1984 21 p refs (NASA-TP-2355; E-1806; NAS 1.60:2355) Avail: NTIS HC A02/MF A01 CSCL 131

A 118 mm bore roller bearing with a three piece inner ring ran successfully at 300,000 DN for 20 hr. Provisions were made for

lubrication and cooling through the inner ring. In some tests the outer ring was also cooled. Power loss within the bearing increased with both speed and total oil flow rate to the inner ring. Outer ring temperature decreased by as much as 22 K (40 F) when outer ring cooling was employed whereas inner ring temperature remained essentially constant. Cage slip was greatly reduced or even eliminated by using a bearing with a very tight clearance at operating speed. A three piece inner ring bearing had higher inner ring temperatures and less temperature difference between the inner and outer rings than a conventional one piece inner ring bearing. Author

**N84-30293\*#** National Aeronautics and Space Administration. Lewis Research Center, Cleveland, Ohio.

**TRANSMISSION EFFICIENCY MEASUREMENTS AND CORRELATIONS WITH PHYSICAL CHARACTERISTICS OF THE LUBRICANT**

J. J. COY, A. M. MITCHELL, and B. J. HAMROCK 1984 20 p refs Proposed for presentation at the 64th Symp. of the Propulsion and Energetics Panel on Gears and Transmission Systems for Helicopters and Turboprops, Lisbon, 8-12 Oct. 1984; sponsored by AGARD Prepared in cooperation with Army Research and Technology Labs.

(NASA-TM-83740; E-2167; NAS 1.15:83740; USAAVSCOM-TR-84-C-11) Avail: NTIS HC A02/MF A01 CSCL 11H

Data from helicopter transmission efficiency tests were compared to physical properties of the eleven lubricants used in those tests. The tests were conducted with the OH-58 helicopter main rotor transmission. Efficiencies ranged from 98.3 to 98.8 percent. The data was examined for correlation of physical properties with efficiency. There was a reasonable correlation of efficiency with absolute viscosity if the viscosity was first corrected for temperature and pressure in the lubricated contact. Between lubricants, efficiency did not correlate well with viscosity at atmospheric pressure. Between lubricants, efficiency did not correlate well with calculated lubricant film forming capacity. Bench type sliding friction and wear measurements could not be correlated to transmission efficiency and component wear. Author

**N84-30294\*#** National Aeronautics and Space Administration. Lewis Research Center, Cleveland, Ohio.

**SUMMARY OF DRIVE-TRAIN COMPONENT TECHNOLOGY IN HELICOPTERS**

G. J. WEDEN and J. J. COY 1984 24 p refs Proposed for presentation at the NATO-AGARD PEP 64th Symp. on Gears and Power Transmissions for Helicopters and Turboprops, Lisbon, 8-12 Oct. 1984 Prepared in cooperation with Army Research and Technology Labs.

(Contract DA PROJ. 1L1-61101-AH-45) (NASA-TM-83726; E-1296; NAS 1.15:83726; USAAVSCOM-TR-84-C-10) Avail: NTIS HC A02/MF A01 CSCL 13I

A review of current helicopters was conducted to determine the technology in the drive-train systems. The design features are highlighted including reliability characteristics in transmission systems for the OH-58, UH-1, CH-47, and UH-60 helicopters. In addition, trade-offs involving cost, reliability and life are discussed. Author

**N84-31640\*#** National Aeronautics and Space Administration. Lewis Research Center, Cleveland, Ohio.

**LUBRICATION OF MACHINE ELEMENTS**

B. J. HAMROCK Aug. 1984 92 p refs Submitted for publication

(NASA-RP-1126; E-1949; NAS 1.61:1126) Avail: NTIS HC A05/MF A01 CSCL 13I

The understanding of hydrodynamic lubrication began with the classical experiments of Tower and Petrov. Reynolds used a reduced form of the Navier-Stokes equations and the continuity equation to generate a second order differential equation for the pressure in the narrow, converging gap of a bearing contact. Such a pressure enables a load to be transmitted between the surfaces

with very low friction since the surfaces are completely separated by a film of fluid. In such a situation it is the physical properties of the lubricant, notably the dynamic viscosity, that dictate the behavior of the contact. The understanding of boundary lubrication is normally attributed to Hardy and Doubleday. In boundary lubrication it is the physical and chemical properties of thin films of molecular proportions and the surfaces to which they are attached that determine contact behavior. The lubricant viscosity is not an influential parameter. Research is devoted to a better understanding and more precise definition of other lubrication regimes between these extremes. One such regime, elastohydrodynamic lubrication, occurs in nonconformal contacts, where the pressures are high and the bearing surfaces deform elastically. In this situation the viscosity of the lubricant may raise considerably, and this further assists the formation of an effective fluid film. The science of these three lubrication regimes (hydrodynamic, elastohydrodynamic, and boundary) are described and the manner in which this science is used in the design of machine elements is examined. M.A.C.

**N84-32824\*#** National Aeronautics and Space Administration. Lewis Research Center, Cleveland, Ohio.

**THERMAL ANALYSIS OF A PLANETARY TRANSMISSION WITH SPHERICAL ROLLER BEARINGS OPERATING AFTER COMPLETE LOSS OF OIL**

H. H. COE Sep. 1984 14 p refs (NASA-TP-2367; E-2008; NAS 1.60:2367) Avail: NTIS HC A02/MF A01 CSCL 13I

Planetsys and Spherbean, two computer programs developed for the analysis of rolling element bearings, were used to simulate the thermal performance of an OH-58 helicopter main rotor transmission. A steady state and a transient thermal analysis were made and temperatures thus calculated were compared with experimental data obtained from a transmission that was operated to destruction, which occurred about 30 min after all the oil was drained from the transmission. Temperatures predicted by Spherbean were within 3% of the corresponding measured values at 15 min elapsed time and within 9% at 25 min. Spherbean also indicates a potential for high bearing cage temperatures with misalignment and outer ring rotation. E.A.K.

**N84-32825\*#** National Aeronautics and Space Administration. Lewis Research Center, Cleveland, Ohio.

**CHARACTERIZATION OF EROSION OF METALLIC MATERIALS UNDER CAVITATION ATTACK IN A MINERAL OIL**

B. C. S. RAO (Indian Inst. of Science, Bangalore, India) and D. H. BUCKLEY Sep. 1984 14 p refs (NASA-TP-2368; E-2049; NAS 1.60:2368) Avail: NTIS HC A02/MF A01 CSCL 11F

Cavitation erosion and erosion rates of eight metallic materials representing three crystal structures were studied using a 20-kHz ultrasonic magnetostrictive oscillator in viscous mineral oil. The erosion rates of the metals with an fcc matrix were 10 to 100 times higher than that of an hcp-matrix titanium alloy. The erosion rates of iron and molybdenum, with bcc matrices, were higher than that of the titanium alloy but lower than those of the fcc metals. Scanning electron microscopy indicates that the cavitation pits are initially formed at the grain boundaries and precipitates and that the pits that formed at the triple points grew faster than the others. Transcrystalline craters formed by cavitation attack over the surface of grains and roughened the surfaces by multiple slip and twinning. Surface roughness measurements show that the pits that formed over the grain boundaries deepened faster than other pits. Computer analysis revealed that a geometric expression describes the nondimensional erosion curves during the time period  $0.5 t(0) \leq t \leq 2.5 t(0)$ , where  $t(0)$  is the incubation period. The fcc metals had very short incubation periods; the titanium alloy had the longest incubation period. A.R.H.

**N84-32828\*#** TRW, Inc., Redondo Beach, Calif. Energy Development Group.  
**DEVELOPMENT OF PARTIALLY FLUORINATED RESIN APEX SEALS** Final Report  
 H. E. GREEN, G. E. C. CHANG, S. H. POWELL, and K. YATES  
 1 Mar. 1984 33 p  
 (Contract NAS3-23054)  
 (NASA-CR-174706; NAS 1.26:174706; TRW-38603-6009-UT-00)  
 Avail: NTIS HC A03/MF A01 CSDL 11A

Partially fluorinated polyimides were prepared and molded in the form of discs and pins for test as potential apex seal materials for advanced rotary combustion engines. The polyimides were formulated from the diamine 2,2-bis 4-(4-aminophenoxy)phenyl hexafluoropropane (4-BDAF) and the dianhydrides of pyromellitic acid (PMDA) and benzophenonetetracarboxylic acid (BTDA). Tribological testing was performed at sliding speeds of 0.31 to 11.6 m/s and at temperatures of from 298K to 573K. It is shown that the carbon fiber filled polyimides, particularly the 80/20 compositions, have an excellent balance of wear/friction at 573K. The unfilled, 80/20 and 60/40 compositions indicate an unusual combination of high friction and low wear which may be advantageous in such applications as brakes and traction drives.

E.A.K.

**N84-33808\*** National Aeronautics and Space Administration. Lewis Research Center, Cleveland, Ohio.  
**DIESEL ENGINE CATALYTIC COMBUSTOR SYSTEM** Patent  
 L. W. REAM, inventor (to NASA) 22 May 1984 7 p Filed 6 Jun. 1980 Supersedes N80-26659 (18 - 17, p 2274)  
 (NASA-CASE-LEW-12995-1; NAS 1.71:LEW-12995-1;  
 US-PATENT-4,449,370; US-PATENT-APPL-SN-157150;  
 US-PATENT-CLASS-60-606; US-PATENT-CLASS-60-303) Avail:  
 US Patent and Trademark Office CSDL 20A

A low compression turbocharged diesel engine is provided in which the turbocharger can be operated independently of the engine to power auxiliary equipment. Fuel and air are burned in a catalytic combustor to drive the turbine wheel of turbine section which is initially caused to rotate by starter motor. By opening a flapper valve, compressed air from the blower section is directed to catalytic combustor when it is heated and expanded, serving to drive the turbine wheel and also to heat the catalytic element. To start, engine valve is closed, combustion is terminated in catalytic combustor, and the valve is then opened to utilize air from the blower for the air driven motor. When the engine starts, the constituents in its exhaust gas react in the catalytic element and the heat generated provides additional energy for the turbine section.

Official Gazette of the U.S. Patent and Trademark Office

**N84-33811\*#** Rocketdyne, Canoga Park, Calif.  
**RESEARCH STUDY FOR EFFECTS OF CASE FLEXIBILITY ON BEARING LOADS AND ROTOR STABILITY** Final Report  
 J. R. FENWICK and R. B. TARN 31 Aug. 1984 255 p  
 (Contract NAS3-34964)  
 (NASA-CR-171147; NAS 1.26:171147; RI/RD84-191) Avail:  
 NTIS HC A12/MF A01 CSDL 13K

Methods to evaluate the effect of casing flexibility on rotor stability and component loads were developed. Recent Rocketdyne turbomachinery was surveyed to determine typical properties and frequencies versus running speed. A small generic rotor was run with a flexible case with parametric variations in casing properties for comparison with a rotor attached to rigid supports. A program for the IBM personal computer for interactive evaluation of rotors and casings is developed. The Root locus method is extended for use in rotor dynamics for symmetrical systems by transforming all motion and coupling into a single plane and using a 90 degree criterion when plotting loci.

E.A.K.

## QUALITY ASSURANCE AND RELIABILITY

Includes product sampling procedures and techniques; and quality control.

**A84-17546\*** National Aeronautics and Space Administration. Lewis Research Center, Cleveland, Ohio.

**FAILURE ANALYSIS OF A TOOL STEEL TORQUE SHAFT**

J. R. REAGAN (NASA, Lewis Research Center, Cleveland, OH)  
 IN: Technology advances in engineering and their impact on detection, diagnosis and prognosis methods; Proceedings of the Thirty-sixth Meeting, Scottsdale, AZ, December 6-10, 1982. Cambridge and New York, Cambridge University Press, 1983, p. 287-291.

A low design load drive shaft used to deliver power from an experimental exhaust heat recovery system to the crankshaft of an experimental diesel truck engine failed during highway testing. An independent testing laboratory analyzed the failure by routine metallography and attributed the failure to fatigue induced by a banded microstructure. Visual examination by NASA of the failed shaft plus the knowledge of the torsional load that it carried pointed to a 100 percent ductile failure with no evidence of fatigue. Scanning electron microscopy confirmed this. Previously announced in STAR as N82-11184

A.R.H.

**N84-14525\*#** Ohio State Univ., Columbus.  
**VOLUME INTEGRALS ASSOCIATED WITH THE INHOMOGENEOUS HELMHOLTZ EQUATION. PART 1: ELLIPSOIDAL REGION** Final Report

L. S. FU and T. MURA Washington NASA Dec. 1983 19 p refs

(Contract NSG-3269)

(NASA-CR-3749; NAS 1.26:3749) Avail: NTIS HC A02/MF A01 CSDL 14D

Problems of wave phenomena in fields of acoustics, electromagnetics and elasticity are often reduced to an integration of the inhomogeneous Helmholtz equation. Results are presented for volume integrals associated with the Helmholtz operator,  $\nabla^2$  to  $\alpha^2$ , for the case of an ellipsoidal region. By using appropriate Taylor series expansions and multinomial theorem, these volume integrals are obtained in series form for regions  $r^4$  and  $r^2$ , where  $r$  and  $r'$  are distances from the origin to the point of observation and source, respectively. Derivatives of these integrals are easily evaluated. When the wave number approaches zero, the results reduce directly to the potentials of variable densities.

M.G.

**N84-14526\*#** Ohio State Univ., Columbus.  
**VOLUME INTEGRALS ASSOCIATED WITH THE INHOMOGENEOUS HELMHOLTZ EQUATION. PART 2: CYLINDRICAL REGION; RECTANGULAR REGION** Final Report

W. F. ZHONG and L. S. FU Dec. 1983 22 p refs

(Contract NAG3-340)

(NASA-CR-3750; NAS 1.26:3750) Avail: NTIS HC A02/MF A01 CSDL 20K

Results are presented for volume integrals associated with the Helmholtz operator,  $\nabla^2 + \alpha^2$ , for the cases of a finite cylindrical region and a region of rectangular parallelepiped. By using appropriate Taylor series expansions and multinomial theorem, these volume integrals are obtained in series form for regions  $r^4$  and  $r^2$ , where  $r$  and  $r'$  are distances from the origin to the point of observation and source, respectively. When the wave number approaches zero, the results reduce directly to the potentials of variable densities.

M.G.



**N84-15565\*#** Massachusetts Inst. of Tech., Cambridge. Dept. of Mechanical Engineering.

**INPUT-OUTPUT CHARACTERIZATION OF AN ULTRASONIC TESTING SYSTEM BY DIGITAL SIGNAL ANALYSIS Final Report**

H. KARAGUELLE, S. S. LEE, and J. WILLIAMS, JR  
Washington NASA Jan. 1984 46 p refs  
(Contract NAG3-328)

(NASA-CR-3756; E-1873; NAS 1.26:3756) Avail: NTIS HC A03/MF A01 CSCL 14D

The input/output characteristics of an ultrasonic testing system used for stress wave factor measurements were studied. The fundamentals of digital signal processing are summarized. The inputs and outputs are digitized and processed in a microcomputer using digital signal processing techniques. The entire ultrasonic test system, including transducers and all electronic components, is modeled as a discrete-time linear shift-invariant system. Then the impulse response and frequency response of the continuous time ultrasonic test system are estimated by interpolating the defining points in the unit sample response and frequency response of the discrete time system. It is found that the ultrasonic test system behaves as a linear phase bandpass filter. Good results were obtained for rectangular pulse inputs of various amplitudes and durations and for tone burst inputs whose center frequencies are within the passband of the test system and for single cycle inputs of various amplitudes. The input/output limits on the linearity of the system are determined. E.A.K.

**N84-34769\*#** National Aeronautics and Space Administration. Lewis Research Center, Cleveland, Ohio.

**ULTRASONIC VELOCITY MEASUREMENT USING PHASE-SLOPE CROSS-CORRELATION METHODS**

D. R. HULL, H. E. KAUTZ, and A. VARY 1984 20 p refs  
Presented at 1984 Spring Conf. of the Am. Soc. for Nondestructive Testing, Denver, 21-24 May 1984

(NASA-TM-83794; E-2290; NAS 1.15:83794) Avail: NTIS HC A02/MF A01 CSCL 14D

Computer implemented phase-slope and cross-correlation methods are introduced for measuring time delays between pairs of broadband ultrasonic pulse-echo signals for determining velocity in engineering materials. The phase-slope and cross-correlation methods are compared with the overlap method which is currently in wide use. Comparison of digital versions of the three methods shows similar results for most materials having low ultrasonic attenuation. However, the cross-correlation method is preferred for highly attenuating materials. An analytical basis for the cross-correlation method is presented. Examples are given for the three methods investigated to measure velocity in representative materials in the megahertz range. Author

## 39

## STRUCTURAL MECHANICS

Includes structural element design and weight analysis; fatigue; and thermal stress.

**N84-17606\*#** Cleveland State Univ., Ohio. Coll. of Engineering. **PRELIMINARY INVESTIGATION OF AN ELECTRICAL NETWORK MODEL FOR ULTRASONIC SCATTERING Final Report**

J. E. MAISEL Washington NASA Jan. 1984 46 p refs  
(Contract NAG3-362)

(NASA-CR-3770; E-1895; NAS 1.26:3770) Avail: NTIS HC A03/MF A01 CSCL 14D

The behavior of acoustic attenuation in a solid is related to the electrical transmission line model where the electrical shunt conductance, which is frequency dependent, represents the loss due to the scattering sites in the solid. Results indicate that the absolute value of attenuation at a given frequency depends on both the normalized mean square deviation of the density and bulk modulus of the scattering sites from the ambient medium and the spatial scattering correlation function. Besides establishing the absolute value of attenuation, the spatial correlation function determines the attenuation profile as a function of frequency.

S. L.

**A84-11039\*#** National Aeronautics and Space Administration. Lewis Research Center, Cleveland, Ohio.

**TENSILE BUCKLING OF ADVANCED TURBOPROPS**

C. C. CHAMIS and R. A. AIELLO (NASA, Lewis Research Center, Cleveland, OH) Journal of Aircraft (ISSN 0021-8669), vol. 20, Nov. 1983, p. 907-912. refs

Previously cited in issue 01, p. 60, Accession no. A83-10900.

**A84-13248\*#** Georgia Inst. of Tech., Atlanta.

**INELASTIC STRESS ANALYSES AT FINITE DEFORMATION THROUGH COMPLEMENTARY ENERGY APPROACHES**

S. N. ATLURI (Georgia Institute of Technology, Atlanta, GA) and K. W. REED IN: Computer methods for nonlinear solids and structural mechanics; Proceedings of the Applied Mechanics, Bioengineering, and Fluids Engineering Conference, Houston, TX, June 20-22, 1983. New York, American Society of Mechanical Engineers, 1983, p. 191-226. refs  
(Contract NAG3-346)

A new hybrid-stress finite element algorithm, suitable for analyses of large, quasistatic, inelastic deformations, is presented. The algorithm is based upon a generalization of de Veubeke's (1972) complementary energy principle. The principal variables in the formulation are the nominal stress rate and spin, and the resulting finite element equations are discrete versions of the equations of compatibility and angular momentum balance. The algorithm produces true rates, time derivatives, as opposed to 'increments'. There results a boundary value problem (for stress rate and velocity) and an initial value problem (for total stress and deformation). A discussion of the numerical treatment of the boundary value problem is followed by a detailed examination of the numerical treatment of the initial value problem, covering the topics of efficiency, stability, and objectivity. The paper is closed with a set of examples, finite homogeneous deformation problems, which serve to bring out important aspects of the algorithm.

Author

**N84-32849\*#** National Aeronautics and Space Administration. Lewis Research Center, Cleveland, Ohio.

**THE ROLE OF THE REFLECTION COEFFICIENT IN PRECISION MEASUREMENT OF ULTRASONIC ATTENUATION**

E. R. GENERAZIO 1984 30 p refs Presented at the Ann. Rev. of Progr. in Quantitative Nondestructive Evaluation, La Jolla, Calif., 8-13 Jul. 1984; sponsored by DARPA

(NASA-TM-83788; E-2185; NAS 1.15:83788) Avail: NTIS HC A03/MF A01 CSCL 14D

Ultrasonic attenuation measurements using contact, pulse-echo techniques are sensitive to surface roughness and couplant thickness variations. This can reduce considerable inaccuracies in the measurement of the attenuation coefficient for broadband pulses. Inaccuracies arise from variations in the reflection coefficient at the buffer-couplant-sample interface. The reflection coefficient is examined as a function of the surface roughness and corresponding couplant thickness variations. Interrelations with ultrasonic frequency are illustrated. Reliable attenuation measurements are obtained only when the frequency dependence of the reflection coefficient is incorporated in signal analysis. Data are given for nickel 200 samples and a silicon nitride ceramic bar having surface roughness variations in the 0.3 to 3.0 microns range for signal bandwidths in the 50 to 100 MHz range. Author



**A84-13545\*** Texas Univ., Austin.

## COMMENTS ON SOME PROBLEMS IN COMPUTATIONAL PENETRATION MECHANICS

J. T. ODEN (Texas, University, Austin, TX) IN: Computational aspects of penetration mechanics; Proceedings of the Workshop, Aberdeen Proving Ground, MD, April 27-29, 1982. Berlin, Springer-Verlag, 1983, p. 149-165. refs  
(Contract NAG3-329; F49620-78-C-0083)

Three problem areas in the computer simulation of large-scale penetration mechanics problems are briefly discussed. These are numerical instabilities due to incomplete integration of the momentum or continuity equations, constitutive modelling, and friction effects. Author

**A84-16874\*** Georgia Inst. of Tech., Atlanta.

## ANALYSES OF LARGE QUASISTATIC DEFORMATIONS OF INELASTIC BODIES BY A NEW HYBRID-STRESS FINITE ELEMENT ALGORITHM

K. W. REED and S. N. ATLURI (Georgia Institute of Technology, Atlanta, GA) Computer Methods in Applied Mechanics and Engineering (ISSN 0045-7825), vol. 39, Sept 1983, p. 245-295. refs  
(Contract NAG3-38)

A new hybrid-stress finite element algorithm, suitable for analyses of large, quasistatic, inelastic deformations, is presented. The algorithm is based upon a generalization of de Veubeke's complementary energy principle. The principal variables in the formulation are the nominal stress rate and spin, and the resulting finite element equations are discrete versions of the equations of compatibility and angular momentum balance. The algorithm produces true rates, time derivatives, as opposed to 'increments'. There results a complete separation of the boundary value problem (for stress rate and velocity) and the initial value problem (for total stress and deformation); hence, their numerical treatments are essentially independent. After a fairly comprehensive discussion of the numerical treatment of the boundary value problem, we launch into a detailed examination of the numerical treatment of the initial value problem, covering the topics of efficiency, stability and objectivity. The paper is closed with a set of examples, finite homogeneous deformation problems, which serve to bring out important aspects of the algorithm. Author

**A84-16884\*** Georgia Inst. of Tech., Atlanta

## ANALYSES OF LARGE QUASISTATIC DEFORMATIONS OF INELASTIC BODIES BY A NEW HYBRID-STRESS FINITE ELEMENT ALGORITHM - APPLICATIONS

K. W. REED and S. N. ATLURI (Georgia Institute of Technology, Atlanta, GA) Computer Methods in Applied Mechanics and Engineering (ISSN 0045-7825), vol. 40, Oct. 1983, p. 171-198. refs  
(Contract NAG3-38)

A new hybrid-stress finite element algorithm suitable for analyzing large quasistatic deformations of inelastic solids is presented and its feasibility and performance are demonstrated with examples. The algorithm provides extremely accurate bifurcation analysis which is stable with respect to variation in the finite element mesh, so long as the same type of element is used in every mesh. When the mesh element is varied, the result changes in a predictable manner. The method does not necessarily lead to an upper or lower bound for the critical load. An explicit forward gradient scheme is used to improve stability and is shown to be useful also for elongation-dominated deformations. The application of the method to the onset of necking in plane extension and to deformation and stress in plane extension of an elasticoviscous fluid with an array of cylindrical voids is given in detail. C.D.

**A84-18691\*** National Aeronautics and Space Administration. Lewis Research Center, Cleveland, Ohio.

## ANALYSIS OF AN INTERNALLY RADIALLY CRACKED RING SEGMENT SUBJECT TO THREE-POINT RADIAL LOADING

B. GROSS and J. E. SRAWLEY (NASA, Lewis Research Center, Cleveland, OH) Journal of Testing and Evaluation (ISSN 0090-3973), vol. 11, Nov. 1983, p. 357-359. refs

The boundary collocation method was used to generate Mode I stress intensity and crack mouth opening displacement coefficients for externally radially cracked ring segments subjected to three point radial loading. Numerical results were obtained for ring segment outer-to-inner radius ratios ( $R_{\text{sub } o}/R_{\text{sub } i}$ ) ranging from 1.10 to 2.50 and crack length to segment width ratios ( $a/W$ ) ranging from 0.1 to 0.8. Stress intensity and crack mouth displacement coefficients were found to depend on the ratios  $R_{\text{sub } o}/R_{\text{sub } i}$  and  $a/W$  as well as the included angle between the directions of the reaction forces. Previously announced in STAR as N83-35413 Author

**A84-21267\*** Princeton Univ., N. J.

## FORCED RESPONSE OF A CANTILEVER BEAM WITH A DRY FRICTION DAMPER ATTACHED. I - THEORY. II - EXPERIMENT

E. H. DOWELL and H. B. SCHWARTZ (Princeton University, Princeton, NJ) Journal of Sound and Vibration (ISSN 0022-460X), vol. 91, Nov. 22, 1983, p. 255-267, 269-291. refs  
(Contract NAG3-221)

A theoretical and experimental study of the forced vibration response of a cantilevered beam with Coulomb damping nonlinearity is described. Viscous damping in the beam is neglected. Beam and dry friction damper configurations of interest for applications to turbine blade vibrations are considered. It is shown that the basic phenomena found by Dowell (1983) for a simply supported beam with an attached dry friction damper of specific geometry also apply to a cantilevered beam and a more general representation of the dry friction damper and its associated mass and stiffness. C.D.

**A84-21541\*** Massachusetts Inst. of Tech., Cambridge.

## ON THE SUPPRESSION OF ZERO ENERGY DEFORMATION MODES

T. H. H. PIAN (MIT, Cambridge, MA) and D. CHEN International Journal for Numerical Methods in Engineering (ISSN 0029-5981), vol. 19, Dec. 1983, p. 1741-1752. refs  
(Contract NAG3-33)

Based on the Hellinger-Reissner principle and the deformation energy due to assumed stresses and displacements, the problem of the kinematic deformation modes in assumed stress hybrid/mixed finite elements has been examined. Basic schemes are developed for the choice of assumed stress terms that will suppress all kinematic deformation modes. Quadrilateral membrane and axisymmetric elements, and three-dimensional hexahedral elements, are used to illustrate the suggested procedure. Author

**A84-27370\*** Texas Univ., Austin.

## A NUMERICAL ANALYSIS OF CONTACT AND LIMIT-POINT BEHAVIOR IN A CLASS OF PROBLEMS OF FINITE ELASTIC DEFORMATION

T. ENDO, J. T. ODEN, E. B. BECKER, and T. MILLER (Texas, University, Austin, TX) Computers and Structures (ISSN 0045-7949), vol. 18, no. 5, 1984, p. 899-910. refs  
(Contract NAG3-329)

Finite element methods for the analysis of bifurcations, limit-point behavior, and unilateral frictionless contact of elastic bodies undergoing finite deformation are presented. Particular attention is given to the development and application of Riks-type algorithms for the analysis of limit points and exterior penalty methods for handling the unilateral constraints. Applications focus on the problem of finite axisymmetric deformations, snap-through, and inflation of thick rubber spherical shells. Author

**A84-29103\*#** Textron Bell Aerospace Co., Buffalo, N. Y.  
**NASTRAN FORCED VIBRATION ANALYSIS OF ROTATING CYCLIC STRUCTURES**

V. ELCHURI, G. C. C. SMITH, and A. M. GALLO (Bell Aerospace Textron, Buffalo, NY) American Society of Mechanical Engineers, Design and Production Engineering Technical Conference, Dearborn, MI, Sept. 11-14, 1983. 11 p. refs  
 (Contract NAS3-22533)  
 (ASME PAPER 83-DET-20)

Theoretical aspects of a new capability, developed and added to the general purpose finite element program NASTRAN Level 17.7, to conduct forced vibration analysis of turned cyclic structures rotating about their axis of symmetry, are presented. The effects of Coriolis and centripetal accelerations as well as those due to the translational acceleration of the axis of rotation, are included. The equations of motion are first derived for an arbitrary grid point of the cyclic sector finite element model and then extended for the complete model. The equations are solved by four principal steps: (1) transformation of applied loads at frequency-dependent circumferential harmonic components; (2) application of circumferential harmonic-dependent intersegment compatibility constraints; (3) solution of frequency-dependent circumferential harmonic components of displacements; and (4) recovery of frequency-dependent response in various segments of the total structure. Five interrelated examples are presented to illustrate the various features of the development. C.D.

**A84-31596\*** Arizona Univ., Tucson.

**ADVANCED RELIABILITY METHOD FOR FATIGUE ANALYSIS**  
 Y.-T. WU and P. H. WIRSCHING (Arizona, University, Tucson, AZ) Journal of Engineering Mechanics (ISSN 0733-9399), vol. 110, April 1984, p. 536-553. Research supported by the Cummins Engine Co. refs  
 (Contract NAG3-41)

When design factors are considered as random variables and the failure condition cannot be expressed by a closed form algebraic inequality, computations of risk (or probability of failure) may become extremely difficult or very inefficient. This study suggests using a simple and easily constructed second degree polynomial to approximate the complicated limit state in the neighborhood of the design point; a computer analysis relates the design variables at selected points. Then a fast probability integration technique (i.e., the Rackwitz-Fiessler algorithm) can be used to estimate risk. The capability of the proposed method is demonstrated in an example of a low cycle fatigue problem for which a computer analysis is required to perform local strain analysis to relate the design variables. A comparison of the performance of this method is made with a far more costly Monte Carlo solution. Agreement of the proposed method with Monte Carlo is considered to be good. Author

**A84-31903\*#** Massachusetts Inst. of Tech., Cambridge.  
**STAGGER ANGLE DEPENDENCE OF INERTIAL AND ELASTIC COUPLING IN BLADED DISKS**

E. F. CRAWLEY and D. R. MOKADAM (MIT, Cambridge, MA) ASME, Transactions, Journal of Vibration, Acoustics, Stress and Reliability in Design (ISSN 0739-3717), vol. 106, April 1984, p. 181-188. refs  
 (Contract NAG3-200; F33615-81-K-2036)

Conditions which necessitate the inclusion of disk and shaft flexibility in the analysis of blade response in rotating blade-disk-shaft systems are derived in terms of nondimensional parameters. A simple semianalytical Rayleigh-Ritz model is derived in which the disk possesses all six rigid body degrees of freedom, which are elastically constrained by the shaft. Inertial coupling by the rigid body motion of the disk on a flexible shaft and out-of-plane elastic coupling due to disk flexure are included. Frequency ratios and mass ratios, which depend on the stagger angle, are determined for three typical rotors: a first stage high-pressure core compressor, a high bypass ratio fan, and an advanced turboprop. The stagger angle controls the degree of coupling in the blade-disk system. In the blade-disk-shaft system, the stagger angle determines whether blade-disk motion couples principally to the

out-of-plane or in-plane motion of the disk on the shaft. The Ritz analysis shows excellent agreement with experimental results.

J.N

**A84-32039\*** National Aeronautics and Space Administration  
 Lewis Research Center, Cleveland, Ohio.

**THE STRUCTURAL RESPONSE OF A RAIL ACCELERATION**  
 S. Y. WANG (NASA, Lewis Research Center, Cleveland, OH) (Institute of Electrical and Electronics Engineers, Symposium on Electromagnetic Launch Technology, 2nd, Boston, MA, Oct. 10-13, 1983) IEEE Transactions on Magnetics (ISSN 0018-9464), vol. MAG-20, March 1984, p. 356-359. refs

The transient response of a 0.4 by 0.6 cm rectangular bore rail accelerator was analyzed by a three dimensional finite element code. The copper rail deflected to a peak value of 0.08 mm in compression and then oscillated at an amplitude of 0.02 mm. Simultaneously the insulating side wall of glass fabric base, epoxy resin laminate (G-10) was compressed to a peak value of 0.13 mm and rebounded to a steady state in extension. Projectile pinch or blowby due to the rail extension or compression, respectively, can be identified by examining the time history of the rail displacement. The effect of blowby was most significant at the side wall characterized by mm size displacement in compression. Dynamic stress calculations indicate that the G-10 supporting material behind the rail is subjected to over 21 MPa at which the G-10 could fail if the laminate was not carefully oriented. Results for a polycarbonate resin (Lexan) side wall show much larger displacements and stresses than for G-10. The tradeoff between the transparency of Lexan and the mechanical strength of G-10 for sidewall material is obvious. Displacement calculations from the modal method are smaller than the results from the direct integration method by almost an order of magnitude, because the high frequency effect is neglected. Previously announced in STAR as N83-35412 E.A.K.

**A84-33701\*** National Aeronautics and Space Administration.  
 Lewis Research Center, Cleveland, Ohio.

**EFFECTS OF STRUCTURAL COUPLING ON MISTUNED CASCADE FLUTTER AND RESPONSE**  
 R. E. KIELB and K. R. V. KAZA (NASA, Lewis Research Center, Cleveland, OH) ASME, Transactions, Journal of Engineering for Gas Turbines and Power (ISSN 0022-0825), vol. 106, Jan. 1984, p. 17-24. refs  
 (ASME PAPER 83-GT-117)

The effects of structural coupling on mistuned cascade flutter and response are analytically investigated using an extended typical section model. This model includes both structural and aerodynamic coupling between the blades. The model assumes that the structurally coupled system natural modes were determined and are represented in the form of N bending and N torsional uncoupled modes for each blade, where N is the number of blades and, hence, is only valid for blade dominated motion. The aerodynamic loads are calculated by using two dimensional unsteady cascade theories in the subsonic and supersonic flow regimes. The results show that the addition of structural coupling can affect both the aeroelastic stability and frequency. The stability is significantly affected only when the system is mistuned. The resonant frequencies can be significantly changed by structural coupling in both tuned and mistuned systems, however, the peak response is significantly affected only in the latter. Previously announced in STAR as N83-15672 S.L.

**A84-33702\*** National Aeronautics and Space Administration.  
 Lewis Research Center, Cleveland, Ohio.

**MEASUREMENTS OF SELF-EXCITED ROTOR-BLADE VIBRATIONS USING OPTICAL DISPLACEMENTS**  
 A. P. KURKOV (NASA, Lewis Research Center, Cleveland, OH) ASME, Transactions, Journal of Engineering for Gas Turbines and Power (ISSN 0022-0825), vol. 106, Jan. 1984, p. 44-49. refs  
 (ASME PAPER 83-GT-132)

The characteristics of optical displacement spectra and their role of monitoring rotor blade vibrations are discussed. During the operation of a turbofan engine at part speed, near stall, and

elevated inlet pressure and temperature, several vibratory instabilities were excited simultaneously on the first fan rotor. The torsional and bending contributions to the main flutter mode were resolved by using casing-mounted optical displacement sensors. Other instabilities in the blade deflection spectra were identified. Previously announced in STAR as N83-14523 E.A.K.

**A84-36492\*#** Bell Aerospace Co., Buffalo, N. Y.  
**FLUTTER ANALYSIS OF ADVANCED TURBOPROPELLERS**  
 V. ELCHURI and G. C. C. SMITH (Bell Aerospace Textron, Buffalo, NY) (Structures, Structural Dynamics and Materials Conference, 24th, Lake Tahoe, NV, May 2-4, 1983, Collection of Technical Papers. Part 2, p. 160-165) AIAA Journal (ISSN 0001-1452), vol. 22, June 1984, p. 801, 802. refs  
 (Contract NAS3-22533)  
 Previously cited in issue 12, p. 1742, Accession no. A83-29824

**A84-38480\*** Akron Univ., Ohio.  
**ALGORITHMS FOR ELASTO-PLASTIC-CREEP POSTBUCKLING**  
 J. PADOVAN (Akron, University, Akron, OH) and S. TOVICHAKCHAIKUL (IBM, Thailand) Journal of Engineering Mechanics (ISSN 0733-9399), vol. 110, June 1984, p. 911-929. refs  
 (Contract NAG3-54)

This paper considers the development of an improved constrained time stepping scheme which can efficiently and stably handle the pre-post-buckling behavior of general structure subject to high temperature environments. Due to the generality of the scheme, the combined influence of elastic-plastic behavior can be handled in addition to time dependent creep effects. This includes structural problems exhibiting indefinite tangent properties. To illustrate the capability of the procedure, several benchmark problems employing finite element analyses are presented. These demonstrate the numerical efficiency and stability of the scheme. Additionally, the potential influence of complex creep histories on the buckling characteristics is considered. Author

**A84-45994\*** Virginia Polytechnic Inst. and State Univ., Blacksburg.  
**A MIXED SHEAR FLEXIBLE FINITE ELEMENT FOR THE ANALYSIS OF LAMINATED PLATES**  
 N. S. PUTCHA and J. N. REDDY (Virginia Polytechnic Institute and State University, Blacksburg, VA) Computer Methods in Applied Mechanics and Engineering (ISSN 0045-7825), vol. 44, July 1984, p. 213-227. refs  
 (Contract NAG3-208; AF-AFOSR-81-0142)

A mixed shear flexible finite element based on the Hencky-Mindlin type shear deformation theory of laminated plates is presented and their behavior in bending is investigated. The element consists of three displacements, two rotations, and three moments as the generalized degrees of freedom per node. The numerical convergence and accuracy characteristics of the element are investigated by comparing the finite element solutions with the exact solutions. The present study shows that reduced-order integration of the stiffness coefficients due to shear is necessary to obtain accurate results for thin plates. Author

**A84-46937\*#** Air Force Aero Propulsion Lab., Wright-Patterson AFB, Ohio.  
**VIBRATIONS OF TWISTED CANTILEVERED PLATES - EXPERIMENTAL INVESTIGATION**  
 J. C. MACBAIN (USAF, Aero Propulsion Laboratory, Wright-Patterson AFB, OH), R. E. KIELB (NASA, Lewis Research Center, Structural and Mechanical Technology Div., Cleveland, OH), and A. W. LEISSA (Ohio State University, Columbus, OH) American Society of Mechanical Engineers, International Gas Turbine Conference and Exhibit, 29th, Amsterdam, Netherlands, June 4-7, 1984. 10 p. refs  
 (ASME PAPER 84-GT-96)

The experimental portion of a joint government/industry/university research study on the vibrational

characteristics of twisted cantilevered plates is presented. The overall purpose of the research study was to assess the capabilities and limitations of existing analytical methods in predicting the vibratory characteristics of twisted plates. Thirty cantilevered plates were precision machined at the Air Force's Aero Propulsion Laboratory. These plates, having five different degrees of twist, two thicknesses, and three aspect ratios representative of turbine engine blade geometries, were tested for their vibration mode shapes and frequencies. The resulting nondimensional frequencies and selected mode shapes are presented as a function of plate tip twist. The trends of the natural frequencies as a function of the governing geometric parameters are discussed. The effect of support compliance on the plate natural frequency and its impact on numerically modeling twisted plates is also presented. Author

**A84-46957\*#** Carnegie-Mellon Univ., Pittsburgh, Pa.  
**THE INTERACTION BETWEEN MISTUNING AND FRICTION IN THE FORCED RESPONSE OF BLADED DISK ASSEMBLIES**  
 J. H. GRIFFIN (Carnegie-Mellon University, Pittsburgh, PA) and A. SINHA (Pennsylvania State University, University Park, PA) American Society of Mechanical Engineers, International Gas Turbine Conference and Exhibit, 29th, Amsterdam, Netherlands, June 4-7, 1984. 7 p. refs  
 (Contract NAG3-231)  
 (ASME PAPER 84-GT-139)

This paper summarizes the results of an investigation to establish the impact of mistuning on the performance and design of blade-to-blade friction dampers of the type used to control the resonant response of turbine blades in gas turbine engines. In addition, it discusses the importance of friction slip force variations on the dynamic response of shrouded fan blades. Author

**A84-48565\*** Akron Univ., Ohio.  
**HIGH TEMPERATURE THERMOMECHANICAL ANALYSIS OF CERAMIC COATINGS**  
 J. PADOVAN, M. J. BRAUN, B. T. F. CHUNG (Akron, University, Akron, OH), D. DOUGHERTY (General Tire and Rubber Co., Akron, OH), and R. HENDRICKS (NASA, Lewis Research Center, Cleveland, OH) Journal of Thermal Stresses (ISSN 0149-5739), vol. 7, no. 1, 1984, p. 51-74. refs  
 (Contract NAG3-265)

This paper investigates the thermomechanical response of ceramically coated metal parts in elevated thermal environments. This is made possible through the development of an improved finite element algorithm that enables the efficient and stable solution of the inherently nonlinear elastic-creep (inelastic) type thermomechanical field equations associated with high temperature. Based on the improved algorithm, the results of several numerical experiments are presented. These illustrate the significant influence of inelastic behavior in generating residual stress fields. Author

**N84-10612\*#** Dayton Univ., Ohio. Aerospace Mechanics Div.  
**A TOTAL LIFE PREDICTION MODEL FOR STRESS CONCENTRATION SITES** Final Report  
 G. A. HARTMAN and D. S. DAWICKE Sep. 1983 33 p refs  
 (Contract NAG3-246)  
 (NASA-CR-168225; NAS 1.26:168225; UDR-TR-83-57) Avail: NTIS HC A03/MF A01 CSCL 20K

Fatigue crack growth tests were performed on center crack panels and radial crack hole samples. The data were reduced and correlated with the elastic parameter K taking into account finite width and corner crack corrections. The anomalous behavior normally associated with short cracks was not observed. Total life estimates for notches were made by coupling an initiation life estimate with a propagation life estimate. Author

**N84-10613\*#** United Technologies Research Center, East Hartford, Conn.

**RESEARCH AND DEVELOPMENT PROGRAM FOR THE DEVELOPMENT OF ADVANCED TIME-TEMPERATURE DEPENDENT CONSTITUTIVE RELATIONSHIPS. VOLUME 1: THEORETICAL DISCUSSION Final Report**

B. N. CASSENTI Jul. 1983 127 p. refs

(Contract NAS3-23273).

(NASA-CR-168191-VOL-1; NAS 1.26:168191-VOL-1;

R83-956077-1) Avail: NTIS HC A07/MF A01

The results of a 10-month research and development program for the development of advanced time-temperature constitutive relationships are presented. The program included (1) the effect of rate of change of temperature, (2) the development of a term to include time independent effects, and (3) improvements in computational efficiency. It was shown that rate of change of temperature could have a substantial effect on the predicted material response. A modification to include time-independent effects, applicable to many viscoplastic constitutive theories, was shown to reduce to classical plasticity. The computation time can be reduced by a factor of two if self-adaptive integration is used when compared to an integration using ordinary forward differences. During the course of the investigation, it was demonstrated that the most important single factor affecting the theoretical accuracy was the choice of material parameters. Author

**N84-10614\*#** United Technologies Research Center, East Hartford, Conn.

**RESEARCH AND DEVELOPMENT PROGRAM FOR THE DEVELOPMENT OF ADVANCED TIME-TEMPERATURE DEPENDENT CONSTITUTIVE RELATIONSHIPS. VOLUME 2: PROGRAMMING MANUAL Final Report**

B. N. CASSENTI Jul. 1983 58 p. refs

(Contract NAS3-23273)

(NASA-CR-168191-VOL-2; NAS 1.26:168191-VOL-2;

R83-956077-2) Avail: NTIS-HC A04/MF A01

The results of a 10-month research and development program for nonlinear structural modeling with advanced time-temperature constitutive relationships are presented. The implementation of the theory in the MARC nonlinear finite element code is discussed, and instructions for the computational application of the theory are provided. Author

**N84-11512\*#** National Aeronautics and Space Administration. Lewis Research Center, Cleveland, Ohio.

**WIDE RANGE WEIGHT FUNCTIONS FOR THE STRIP WITH A SINGLE EDGE CRACK**

T. W. ORANGE 1982 12 p. refs Presented at the 16th Natl. Symp. on Fracture Mech., Columbus, Ohio, 15-18 Aug. 1983; sponsored by the Am. Soc. for Testing and Mater.

(NASA-TM-83478; E-1794; NAS 1.15:83478) Avail: NTIS HC A02/MF A01 CSCL 20K

A closed form expression for the weight function for a strip with a single edge crack is presented. The expression is valid for relative crack lengths from zero to unity. It is based on the assumption that the shape of an opened edge crack can be approximated by a conic section. The results agree well with published values for weight functions, stress intensity factors, and crack mouth opening displacements. S.L.

**N84-11513\*#** Case Western Reserve Univ., Cleveland, Ohio.  
**EFFECT OF CRACK CURVATURE ON STRESS INTENSITY FACTORS FOR ASTM STANDARD COMPACT TENSION SPECIMENS Final Report**

J. ALAM and A. MENDELSON Oct. 1983 19 p. refs

(Contract NSG-3251)

(NASA-CR-168280; NAS 1.26:168280) Avail: NTIS HC A02/MF A01 CSCL 20K

The stress intensity factors (SIF) are calculated using the method of lines for the compact tension specimen in tensile and shear loading for curved crack fronts. For the purely elastic case, it was found that as the crack front curvature increases, the SIF value at the center of the specimen decreases while increasing

at the surface. For the higher values of crack front curvatures, the maximum value of the SIF occurs at an interior point located adjacent to the surface. A thickness average SIF was computed for parabolically applied shear loading. These results were used to assess the requirements of ASTM standards E399-71 and E399-81 on the shape of crack fronts. The SIF is assumed to reflect the average stress environment near the crack edge.

Author

**N84-11514\*#** Textron Bell Aerospace Co., Buffalo, N. Y.  
**FORCED VIBRATION ANALYSIS OF ROTATING CYCLIC STRUCTURES IN NASTRAN Final Report**

V. ELCHURI, A. M. GALLO, and S. C. SKALSKI Dec. 1981 176 p

(Contract NAS3-22533)

(NASA-CR-165429; NAS 1.26:165429; D2536-941007) Avail:

NTIS HC A09/MF A01 CSCL 20K

A new capability was added to the general purpose finite element program NASTRAN Level 17.7 to conduct forced vibration analysis of tuned cyclic structures rotating about their axis of symmetry. The effects of Coriolis and centripetal accelerations together with those due to linear acceleration of the axis of rotation were included. The theoretical, user's, programmer's and demonstration manuals for this new capability are presented.

Author

**N84-11515\*#** Textron Bell Aerospace Co., Buffalo, N. Y.  
**FINITE ELEMENT FORCED VIBRATION ANALYSIS OF ROTATING CYCLIC STRUCTURES Final Technical Report**

V. ELCHURI and G. C. C. SMITH Dec. 1981 73 p. refs

(Contract NAS3-22533)

(NASA-CR-165430; NAS 1.26:165430; D2536-941008) Avail:

NTIS HC A04/MF A01 CSCL 20K

A capability was added to the general purpose finite element program NASTRAN Level 17.7 to conduct forced vibration analysis of tuned cyclic structures rotating about their axes of symmetry. The effects of Coriolis and centripetal accelerations together with those due to linear acceleration of the axis of rotation were included. The theoretical development of this capability is presented. S.L.

**N84-12530\*#** United Technologies Research Center, East Hartford, Conn.

**AEROELASTIC ANALYSIS FOR PROPELLERS - MATHEMATICAL FORMULATIONS AND PROGRAM USER'S MANUAL Final Report**

R. L. BIELAWA, S. A. JOHNSON, R. M. CHI, and S. T. GANGWANI Washington NASA Dec. 1983 255 p. refs

(Contract NAS3-22753)

(NASA-CR-3729; NAS 1.26:3729; UTRC83-6) Avail: NTIS HC A12/MF A01 CSCL 20K

Mathematical development is presented for a specialized propeller dedicated version of the G400 rotor aeroelastic analysis. The G400PROP analysis simulates aeroelastic characteristics particular to propellers such as structural sweep, aerodynamic sweep and high subsonic unsteady airloads (both stalled and unstalled). Formulations are presented for these expanded propeller related methodologies. Results of limited application of the analysis to realistic blade configurations and operating conditions which include stable and unstable stall flutter test conditions are given. Sections included for enhanced program user efficiency and expanded utilization include descriptions of: (1) the structuring of the G400PROP FORTRAN coding; (2) the required input data; and (3) the output results. General information to facilitate operation and improve efficiency is also provided. Author

**N84-13610\*#** National Aeronautics and Space Administration. Lewis Research Center, Cleveland, Ohio.

## **AN IMPROVED FINITE-DIFFERENCE ANALYSIS OF UNCOUPLED VIBRATIONS OF TAPERED CANTILEVER BEAMS**

K. B. SUBRAHMANYAM (NBKR Inst. of Science and Technology) and K. R. V. KAZA Sep. 1983 39 p refs (NASA-TM-83495; E-1828; NAS 1.15:83495) Avail: NTIS HC A03/MF A01 CSCL 20K

An improved finite difference procedure for determining the natural frequencies and mode shapes of tapered cantilever beams undergoing uncoupled vibrations is presented. Boundary conditions are derived in the form of simple recursive relations involving the second order central differences. Results obtained by using the conventional first order central differences and the present second order central differences are compared, and it is observed that the present second order scheme is more efficient than the conventional approach. An important advantage offered by the present approach is that the results converge to exact values rapidly, and thus the extrapolation of the results is not necessary. Consequently, the basic handicap with the classical finite difference method of solution that requires the Richardson's extrapolation procedure is eliminated. Furthermore, for the cases considered herein, the present approach produces consistent lower bound solutions. Author

**N84-14541\*#** National Aeronautics and Space Administration. Lewis Research Center, Cleveland, Ohio.

## **COMPLEXITIES OF HIGH TEMPERATURE METAL FATIGUE: SOME STEPS TOWARD UNDERSTANDING**

S. S. MANSON and G. R. HALFORD 1983 47 p refs Presented at the 25th Ann. Conf. on Aeronautics and Astronautics, Haifa, Israel, 23-25 Feb. 1983 (NASA-TM-83507; E-1852; NAS 1.15:83507) Avail: NTIS HC A03/MF A01 CSCL 20K

After pointing out many of the complexities that attend high temperature metal fatigue beyond those already studied in the sub-creep range, a description of the micromechanisms of deformation and fracture is presented for several classes of materials that were studied over the past dozen years. Strainrange Partitioning (SRP) is used as a framework for interpreting the results. Several generic types of behavior were observed with regard both to deformation and fracture and each is discussed in the context of the micromechanisms involved. Treatment of cumulative fatigue damage and the possibility of "healing" of damage in successive loading loops, has led to a new interpretation of the Interaction Damage Rule of SRP. Using the concept of "equivalent micromechanistic damage" -- that the same damage on a microscopic scale is induced if the same hysteresis loops are generated, element for element -- it turns out the Interaction Damage Rule essentially compounds a number of variants of hysteresis loops, all of which have the same damage according to SRP concepts, into a set of loops each containing only one of the generic SRP strainranges. Thus the damage associated with complex loops comprising several types of strainrange is analyzed by considering a combination of loops each containing only one type of strainrange. This concept is expanded to show how several independent loops can combine to "heal" creep damage in a complex loading history. Author

**N84-14542\*#** National Aeronautics and Space Administration. Lewis Research Center, Cleveland, Ohio.

## **A SIMPLIFIED METHOD FOR ELASTIC-PLASTIC-CREEP STRUCTURAL ANALYSIS**

A. KAUFMAN 1984 19 p refs Proposed for presentation at the 29th Ann. Intern. Gas Turbine Conf., Amsterdam, 3-7 Jun. 1984; sponsored by ASME (NASA-TM-83509; E-1855-1; NAS 1.15:83509) Avail: NTIS HC A02/MF A01 CSCL 20K

A simplified inelastic analysis computer program (ANSYPM) was developed for predicting the stress-strain history at the critical location of a thermomechanically cycled structure from an elastic solution. The program uses an iterative and incremental procedure

to estimate the plastic strains from the material stress-strain properties and a plasticity hardening model. Creep effects are calculated on the basis of stress relaxation at constant strain, creep at constant stress or a combination of stress relaxation and creep accumulation. The simplified method was exercised on a number of problems involving uniaxial and multiaxial loading, isothermal and nonisothermal conditions, dwell times at various points in the cycles, different materials and kinematic hardening. Good agreement was found between these analytical results and nonlinear finite element solutions for these problems. The simplified analysis program used less than 1 percent of the CPU time required for a nonlinear finite element analysis. Author

**N84-15589\*#** Kansas Univ., Lawrence. Structural Engineering and Engineering Materials.

## **THEORETICAL AND SOFTWARE CONSIDERATIONS FOR NONLINEAR DYNAMIC ANALYSIS Interim Report**

R. J. SCHMIDT and R. H. DODDS, JR. Feb. 1983 299 p refs (Contract NAG3-32) (NASA-CR-174504; NAS 1.26:174504; SM-8) Avail: NTIS HC A13/MF A01 CSCL 20K

In the finite element method for structural analysis, it is generally necessary to discretize the structural model into a very large number of elements to accurately evaluate displacements, strains, and stresses. As the complexity of the model increases, the number of degrees of freedom can easily exceed the capacity of present-day software system. Improvements of structural analysis software including more efficient use of existing hardware and improved structural modeling techniques are discussed. One modeling technique that is used successfully in static linear and nonlinear analysis is multilevel substructuring. This research extends the use of multilevel substructure modeling to include dynamic analysis and defines the requirements for a general purpose software system capable of efficient nonlinear dynamic analysis. The multilevel substructuring technique is presented, the analytical formulations and computational procedures for dynamic analysis and nonlinear mechanics are reviewed, and an approach to the design and implementation of a general purpose structural software system is presented. E.A.K.

**N84-16587\*#** National Aeronautics and Space Administration. Lewis Research Center, Cleveland, Ohio.

## **FLUTTER OF SWEEPED FAN BLADES**

R. E. KIELB and K. R. V. KAZA 1984 12 p refs Proposed for presentation at the 29th Intern. Gas Turbine Conf., Amsterdam, 3-7 Jun. 1984, sponsored by ASME (NASA-TM-83547; E-1921; NAS 1.15:83547) Avail: NTIS HC A02/MF A01 CSCL 20K

The effect of sweep on fan blade flutter is studied by applying the analytical methods developed for aeroelastic analysis of advance turboprops. Two methods are used. The first method utilizes an approximate structural model in which the blade is represented by a swept, nonuniform beam. The second method utilizes a finite element technique to conduct modal flutter analysis. For both methods the unsteady aerodynamic loads are calculated using two dimensional cascade theories which are modified to account for sweep. An advanced fan stage is analyzed with 0, 15 and 30 degrees of sweep. It is shown that sweep has a beneficial effect on predominantly torsional flutter and a detrimental effect on predominantly bending flutter. This detrimental effect is shown to be significantly destabilizing for 30 degrees of sweep. M.G.

**N84-16588\*#** National Aeronautics and Space Administration. Lewis Research Center, Cleveland, Ohio.

## **IMPROVED FINITE-DIFFERENCE VIBRATION ANALYSIS OF PRETWISTED, TAPERED BEAMS**

K. B. SUBRAHMANYAM and K. R. V. KAZA 1984 13 p refs To be presented at the Southeastern Conf. on Theoretical and Appl. Mech. (SECTAM 12), Pine Mountain, Ga., 10-11 May 1984 (NASA-TM-83549; NAS 1.15:83549, E-1923) Avail: NTIS HC A02/MF A01 CSCL 20K

An improved finite difference procedure based upon second order central differences is developed. Several difficulties

encountered in earlier works with fictitious stations that arise in using second order central differences, are eliminated by developing certain recursive relations. The need for forward or backward differences at the beam boundaries or other similar procedures is eliminated in the present theory. By using this improved theory, the vibration characteristics of pretwisted and tapered blades are calculated. Results of the second order theory are compared with published theoretical and experimental results and are found to be in good agreement. The present method generally produces close lower bound solutions and shows fast convergence. Thus, extrapolation procedures that are customary with first order finite-difference methods are unnecessary. Furthermore, the computational time and effort needed for this improved method are almost the same as required for the conventional first order finite-difference approach. M.G.

**N84-16589\*#** National Aeronautics and Space Administration. Lewis Research Center, Cleveland, Ohio.  
**BENDING FATIGUE OF ELECTRON-BEAM-WELDED FOILS. APPLICATION TO A HYDRODYNAMIC AIR BEARING IN THE CHRYSLER/DOE UPGRADED AUTOMOTIVE GAS TURBINE ENGINE** Final Report

J. F. SALTSMAN and G. R. HALFORD Jan. 1984 27 p refs (Contract DE-AI01-77CS-51040)  
 (NASA-TM-83539; DOE/NASA/51040-51; E-1910; NAS 1.15:83539) Avail: NTIS HC A03/MF A01 CSCL 20K

A hydrodynamic air bearing with a compliant surface is used in the gas generator of an upgraded automotive gas turbine engine. In the prototype design, the compliant surface is a thin foil spot welded at one end to the bearing cartridge. During operation, the foil failed along the line of spot welds which acted as a series of stress concentrators. Because of its higher degree of geometric uniformity, electron beam welding of the foil was selected as an alternative to spot welding. Room temperature bending fatigue tests were conducted to determine the fatigue resistance of the electron beam welded foils. Equations were determined relating cycles to crack initiation and cycles to failure to nominal total strain range. A scaling procedure is presented for estimating the reduction in cyclic life when the foil is at its normal operating temperature of 260 C (500 F). S.L.

**N84-18683\*#** National Aeronautics and Space Administration. Lewis Research Center, Cleveland, Ohio.  
**ENGINE CYCLIC DURABILITY BY ANALYSIS AND MATERIAL TESTING**

A. KAUFMAN and G. R. HALFORD 1983 19 p refs To be presented at the 61st Meeting of the Propulsion and Energetics Panel, Lisse, Netherlands, 30 May - 1 Jun. 1984; sponsored by AGARD  
 (NASA-TM-83577; E-1964; NAS 1.15:83577) Avail: NTIS HC A02/MF A01 CSCL 20K

The problem of calculating turbine engine component durability is addressed. Nonlinear, finite-element structural analyses, cyclic constitutive behavior models, and an advanced creep-fatigue life prediction method called strainrange partitioning were assessed for their applicability to the solution of durability problems in hot-section components of gas turbine engines. Three different component or subcomponent geometries are examined: a stress concentration in a turbine disk; a louver lip of a half-scale combustor liner; and a squealer tip of a first-stage high-pressure turbine blade. Cyclic structural analyses were performed for all three problems. The computed strain-temperature histories at the critical locations of the combustor linear and turbine blade components were imposed on smooth specimens in uniaxial, strain-controlled, thermomechanical fatigue tests to evaluate the structural and life analysis methods. Author

**N84-19925\*#** Arizona Univ., Tucson Dept. of Aerospace and Mechanical Engineering.

**CREEP-RUPTURE RELIABILITY ANALYSIS** Final Report

A. PERALTA-DURAN and P. H. WIRSCHING Washington NASA Mar. 1984 31 p refs (Contract NAG3-41)  
 (NASA-CR-3790; E-1982; NAS 1.26:3790) Avail: NTIS HC A03/MF A01 CSCL 20K

A probabilistic approach to the correlation and extrapolation of creep-rupture data is presented. Time temperature parameters (TTP) are used to correlate the data, and an analytical expression for the master curve is developed. The expression provides a simple model for the statistical distribution of strength and fits neatly into a probabilistic design format. The analysis focuses on the Larson-Miller and on the Manson-Haferd parameters, but it can be applied to any of the TTP's. A method is developed for evaluating material dependent constants for TTP's. It is shown that optimized constants can provide a significant improvement in the correlation of the data, thereby reducing modelling error. Attempts were made to quantify the performance of the proposed method in predicting long term behavior. Uncertainty in predicting long term behavior from short term tests was derived for several sets of data. Examples are presented which illustrate the theory and demonstrate the application of state of the art reliability methods to the design of components under creep. Author

**N84-19927\*#** Akron Univ., Ohio. Dept. of Mechanical Engineering.

**EXPERIMENTAL STUDY OF UNCENTRALIZED SQUEEZE FILM DAMPERS**

R. D. QUINN Dec. 1983 127 p refs (Contract NSG-3283; NAG3-50)  
 (NASA-CR-168317; NAS 1.26:168317; NAUFP-202-2) Avail: NTIS HC A07/MF A01 CSCL 20K

The vibration response of a rotor system supported by a squeeze film damper (SFD) was experimentally investigated in order to provide experimental data in support of the Rotor/Stator Interactive Finite Element theoretical development. Part of the investigation required the designing and building of a rotor/SFD system that could operate with or without end seals in order to accommodate different SFD lengths. SFD variables investigated included clearance, eccentricity mass, fluid pressure, and viscosity and temperature. The results show inlet pressure, viscosity and clearance have significant influence on the damper performance and accompanying rotor response. Author

**N84-20878\*#** National Aeronautics and Space Administration. Lewis Research Center, Cleveland, Ohio.

**DEVELOPMENT OF A SIMPLIFIED PROCEDURE FOR CYCLIC STRUCTURAL ANALYSIS**

A. KAUFMAN Mar. 1984 20 p refs Proposed for presentation at the 29th ASME Intern Gas Turbine Conf., Amsterdam, 3-7 Jun. 1984  
 (NASA-TP-2243; E-1855; NAS 1.60:2243) Avail: NTIS HC A02/MF A01 CSCL 20K

Development was extended of a simplified inelastic analysis computer program (ANSYMP) for predicting the stress-strain history at the critical location of a thermomechanically cycled structure from an elastic solution. The program uses an iterative and incremental procedure to estimate the plastic strains from the material stress-strain properties and a plasticity hardening model. Creep effects can be calculated on the basis of stress relaxation at constant strain, creep at constant stress, or a combination of stress relaxation and creep accumulation. The simplified method was exercised on a number of problems involving uniaxial and multiaxial loading, isothermal and nonisothermal conditions, dwell times at various points in the cycles, different materials, and kinematic hardening. Good agreement was found between these analytical results and nonlinear finite-element solutions for these problems. The simplified analysis program used less than 1 percent of the CPU time required for a nonlinear finite-element analysis. Author

**N84-21903\*#** Toledo Univ., Ohio. Dept. of Civil Engineering.  
**THERMAL STRESS ANALYSIS FOR A WOOD COMPOSITE BLADE** Report, 5 Dec. 1982 - 4 Apr. 1984  
 K. C. FU and A. HARB 4 Apr. 1984 117 p refs  
 (Contract NAG3-373)  
 (NASA-CR-173394; NAS 1.26:173394) Avail: NTIS HC A06/MF A01 CSCL 20K

Heat conduction throughout the blade and the distribution of thermal stresses caused by the temperature distribution were determined for a laminated wood wind turbine blade in both the horizontal and vertical positions. Results show that blade cracking is not due to thermal stresses induced by insulation. A method and practical example of thermal stress analysis for an engineering body of orthotropic materials is presented. A.R.H.

**N84-21905\*#** Connecticut Univ., Storrs. Dept. of Mechanical Engineering.  
**ELEVATED TEMPERATURE BIAXIAL FATIGUE** Semiannual Status Report, 15 Feb. - 15 Aug. 1983  
 E. H. JORDAN 15 Aug. 1983 21 p  
 (Contract NAG3-160)  
 (NASA-CR-173473; NAS 1.26:173473) Avail: NTIS HC A02/MF A01 CSCL 20K

Biaxial fatigue is often encountered in the complex thermo-mechanical loadings present in gas turbine engines. Engine strain histories can involve non-constant temperature, mean stress, creep, environmental effects, both isotropic and anisotropic materials and non-proportional loading. Life prediction for the general case involving all the above factors is not a practicable research project. The current research program is limited to isothermal fatigue at room temperature and 1200 F of Hastalloy-X for both proportional and non-proportional loading. An improved method for predicting the fatigue life and deformation response under biaxial cycle loading is sought. Author

**N84-22980\*#** Case Western Reserve Univ., Cleveland, Ohio. Dept. of Civil Engineering.  
**CRACK LAYER THEORY**  
 A. CHUDNOVSKY Mar. 1984 43 p refs  
 (Contract NAG3-23)  
 (NASA-CR-174634; NAS 1.26:174634) Avail: NTIS HC A03/MF A01 CSCL 20K

A damage parameter is introduced in addition to conventional parameters of continuum mechanics and consider a crack surrounded by an array of microdefects within the continuum mechanics framework. A system consisting of the main crack and surrounding damage is called crack layer (CL). Crack layer propagation is an irreversible process. The general framework of the thermodynamics of irreversible processes are employed to identify the driving forces (causes) and to derive the constitutive equation of CL propagation, that is, the relationship between the rates of the crack growth and damage dissemination from one side and the conjugated thermodynamic forces from another. The proposed law of CL propagation is in good agreement with the experimental data on fatigue CL propagation in various materials. The theory also elaborates material toughness characterization. M.A.C.

**N84-23923\*#** National Aeronautics and Space Administration. Lewis Research Center, Cleveland, Ohio.  
**VIBRATION AND FLUTTER OF MISTUNED BLADED-DISK ASSEMBLIES**  
 K. R. V. KAZA and R. E. KIELB 1984 17 p refs Presented at the 25th Struct., Struct. Dyn. and Mater. Conf., Palm Springs, Calif., 14-16 May 1984; sponsored by the AIAA, ASME, ASCE and AHS  
 (NASA-TM-83634; E-2074; NAS 1.15:83634; AIAA-84-0991)  
 Avail: NTIS HC A02/MF A01 CSCL 20K

An analytical model for investigating vibration and flutter of mistuned bladed disk assemblies is presented. This model accounts for elastic, inertial and aerodynamic coupling between bending and torsional motions of each individual blade, elastic and inertial couplings between the blades and the disk, and aerodynamic

coupling among the blades. The disk was modeled as a circular plate with constant thickness and each blade was represented by a twisted, slender, straight, nonuniform, elastic beam with a symmetric cross section. The elastic axis, inertia axis, and the tension axis were taken to be noncoincident and the structural warping of the section was explicitly considered. The blade aerodynamic loading in the subsonic and-supersonic flow regimes was obtained from two-dimensional unsteady, cascade theories. All the possible standing wave modes of the disk and traveling wave modes of the blades were included. The equations of motion were derived by using the energy method in conjunction with the assumed mode shapes for the disk and the blades. Continuities of displacement and slope at the blade-disk junction were maintained. The equations were solved to investigate the effects of blade-disk coupling and blade frequency mistuning on vibration and flutter. Results showed that the flexibility of practical disks such as those used for current generation turbopumps did not have a significant influence on either the tuned or mistuned flutter characteristics. However, the disk flexibility may have a strong influence on some of the system frequencies and on forced response. Author

**N84-29247\*#** National Aeronautics and Space Administration. Lewis Research Center, Cleveland, Ohio.  
**A COMPUTER PROGRAM FOR PREDICTING NONLINEAR UNIAXIAL MATERIAL RESPONSES USING VISCOPLASTIC MODELS**  
 T. Y. CHANG (Akron Univ., Ohio) and R. L. THOMPSON Jul. 1984 65 p refs  
 (NASA-TM-83675; E-2120; NAS 1.15:83675) Avail: NTIS HC A04/MF A01 CSCL 20K

A computer program was developed for predicting nonlinear uniaxial material responses using viscoplastic constitutive models. Four specific models, i.e., those due to Miller, Walker, Kneeg-Swearengen-Rhode, and Robinson, are included. Any other unified model is easily implemented into the program in the form of subroutines. Analysis features include stress-strain cycling, creep response, stress relaxation, thermomechanical fatigue loop, or any combination of these responses. An outline is given on the theoretical background of uniaxial constitutive models, analysis procedure, and numerical integration methods for solving the nonlinear constitutive equations. In addition, a discussion on the computer program implementation is also given. Finally, seven numerical examples are included to demonstrate the versatility of the computer program developed. Author

**N84-29248\*#** National Aeronautics and Space Administration. Lewis Research Center, Cleveland, Ohio.  
**MODE 2 FATIGUE CRACK GROWTH SPECIMEN DEVELOPMENT**  
 R. J. BUZZARD, B. GROSS, and J. E. SRAWLEY 1983 18 p refs Presented at the 17th Natl. Symp. on Fracture Mech., Albany, N.Y., 7-9 Aug. 1984; sponsored by Am. Soc. for Testing and Mater.  
 (NASA-TM-83722; E-2108; NAS 1.15:83722) Avail: NTIS HC A02/MF A01 CSCL 20K

A Mode II test specimen was developed which has potential application in understanding phenomena associated with mixed mode fatigue failures in high performance aircraft engine bearing races. The attributes of the specimen are: it contains one single ended notch, which simplifies data gathering and reduction; the fatigue crack grows in-line with the direction of load application; a single axis test machine is sufficient to perform testing; and the Mode I component is vanishingly small. Author



**N84-29252\*#** Textron Bell Aerospace Co., Buffalo, N. Y. Structural Dynamics.

**NASTRAN FORCED VIBRATION ANALYSIS OF ROTATING CYCLIC STRUCTURES Final Report**

V. ELCHURI, G. C. C. SMITH, and A. M. GALLO 1983 31 p refs Presented at the ASME Conf on Mech. Vibration and Noise, Dearborn, Mich., Sep. 1983

(Contract NAS3-22533)

(NASA-CR-173821; NAS 1.26:173821) Avail. NTIS HC A03/MF A01 CSCL 20K

Theoretical aspects of a new capability developed and implemented in NASTRAN level 17.7 to analyze forced vibration of a cyclic structure rotating about its axis of symmetry are presented. Fans, propellers, and bladed shrouded discs of turbomachines are some examples of such structures. The capability includes the effects of Coriolis and centripetal accelerations on the rotating structure which can be loaded with: (1) directly applied loads moving with the structure and (2) inertial loads due to the translational acceleration of the axis of rotation ("base" acceleration). Steady-state sinusoidal or general periodic loads are specified to represent: (1) the physical loads on various segments of the complete structure, or (2) the circumferential harmonic components of the loads in (1). The cyclic symmetry feature of the rotating structure is used in deriving and solving the equations of forced motion. Consequently, only one of the cyclic sectors is modelled and analyzed using finite elements, yielding substantial savings in the analysis cost. Results, however, are obtained for the entire structure. A tuned twelve bladed disc example is used to demonstrate the various features of the capability. M.G.

**N84-30329\*#** National Aeronautics and Space Administration. Lewis Research Center, Cleveland, Ohio.

**IMPROVED METHODS OF VIBRATION ANALYSIS OF PRETWISTED, AIRFOIL BLADES**

K. B. SUBRAHMANYAM and K. R. V. KAZA 1984 37 p refs Presented at the 16th Intern. Congr. of Theoretical and Appl. Mech., Lyngby, Denmark, 19-25 Aug. 1984; sponsored by the International Union of Theoretical and Applied Mechanics and the Technical Univ. of Denmark

(NASA-TM-83735; E-2175; NAS 1.15:83735) Avail. NTIS HC A03/MF A01 CSCL 20K

Vibration analysis of pretwisted blades of asymmetric airfoil cross section is performed by using two mixed variational approaches. Numerical results obtained from these two methods are compared to those obtained from an improved finite difference method and also to those given by the ordinary finite difference method. The relative merits, convergence properties and accuracies of all four methods are studied and discussed. The effects of asymmetry and pretwist on natural frequencies and mode shapes are investigated. The improved finite difference method is shown to be far superior to the conventional finite difference method in several respects. Close lower bound solutions are provided by the improved finite difference method for untwisted blades with a relatively coarse mesh while the mixed methods have not indicated any specific bound. Author

**N84-31683\*#** National Aeronautics and Space Administration. Lewis Research Center, Cleveland, Ohio.

**NONLINEAR DISPLACEMENT ANALYSIS OF ADVANCED PROPELLER STRUCTURES USING NASTRAN**

C. LAWRENCE and R. E. KIELB Aug. 1984 12 p refs (NASA-TM-83737; E-2222; NAS 1.15:83737) Avail. NTIS HC A02/MF A01 CSCL 20K

The steady state displacements of a rotating advanced turboprop are computed using the geometrically nonlinear capabilities of COSMIC NASTRAN Rigid Format 4 and MSC NASTRAN Solution 64. A description of the modified Newton-Raphson algorithm used by Solution 64 and the iterative scheme used by Rigid Format 4 is provided. A representative advanced turboprop, SR3, was used for the study. Displacements for SR3 are computed for rotational speeds up to 10,000 rpm. The results show Solution 64 to be superior for computing

displacements of flexible rotating structures. This is attributed to its ability to update the displacement dependent centrifugal force during the solution process. Author

**N84-31685\*#** Toledo Univ., Ohio. Dept. of Civil Engineering.

**THERMAL-STRESS ANALYSIS FOR WOOD COMPOSITE BLADE Report, 5 Dec. 1982 - 4 Apr. 1984**

K. C. FU and A. HARB 20 Jul. 1984 117 p refs

(Contract NAG3-373)

(NASA-CR-173830; NAS 1.26:173830) Avail. NTIS HC A06/MF A01 CSCL 20K

The thermal-stress induced by solar insolation on a wood composite blade of a Mod-OA wind turbine was investigated. The temperature distribution throughout the blade (a heat conduction problem) was analyzed and the thermal-stress distribution of the blades caused by the temperature distribution (a thermal-stress analysis problem) was then determined. The computer programs used for both problems are included along with output examples. A.R.H.

**N84-31687\*#** National Aeronautics and Space Administration. Lewis Research Center, Cleveland, Ohio.

**CYCLIC TORSION TESTING**

G. E. LEESE Aug. 1984 21 p refs Submitted for publication (NASA-TM-83756; E-2232; NAS 1.15:83756) Avail. NTIS HC A02/MF A01 CSCL 20K

Torsional fatigue testing and data analysis procedures are described. Since there are no standards governing cyclic torsion testing that are generally accepted on a widespread basis by the technical community, the different approaches that dominate current experimental activity, and the ramifications of each are discussed. Particular attention is given to the theoretical and experimental difficulties that have paced refinement and general acceptance of test procedures. Finally, specific quantities and nomenclature modelled after analogous axial fatigue properties are suggested as an effective way to communicate torsional fatigue results until accepted standards are established. Author

**N84-31688\*#** National Aeronautics and Space Administration. Lewis Research Center, Cleveland, Ohio.

**NONLINEAR STRUCTURAL ANALYSIS**

Washington Jun. 1984 168 p Workshop held in Cleveland, 19-20 Apr. 1983

(NASA-CP-2297; E-1903; NAS 1.55:2297) Avail. NTIS HC A08/MF A01 CSCL 20K

Nonlinear structural analysis techniques for engine structures and components are addressed. The finite element method and boundary element method are discussed in terms of stress and structural analyses of shells, plates, and laminates.

**N84-31689\*#** Textron Bell Aerospace Co., Buffalo, N. Y.

**SLAVE FINITE ELEMENTS: THE TEMPORAL ELEMENT APPROACH TO NONLINEAR ANALYSIS**

S. GELLIN in NASA. Lewis Research Center Nonlinear Struct. Anal. p 1-16 Jun. 1984 refs (Contract NAS3-23279)

Avail. NTIS HC A08/MF A01 CSCL 20K

A formulation method for finite elements in space and time incorporating nonlinear geometric and material behavior is presented. The method uses interpolation polynomials for approximating the behavior of various quantities over the element domain, and only explicit integration over space and time. While applications are general, the plate and shell elements that are currently being programmed are appropriate to model turbine blades, vanes, and combustor liners. Author

**N84-31690\*#** Massachusetts Inst. of Tech., Cambridge.  
**NEW VARIATIONAL FORMULATIONS OF HYBRID STRESS ELEMENTS**

T. H. H. PIAN, K. SUMIHARA, and D. KANG *In* NASA. Lewis Research Center Nonlinear Struct. Anal. p 17-29 Jun. 1984 refs

(Contract NAG3-33)

Avail: NTIS HC A08/MF A01 CSCL 20K

In the variational formulations of finite elements by the Hu-Washizu and Hellinger-Reissner principles the stress equilibrium condition is maintained by the inclusion of internal displacements which function as the Lagrange multipliers for the constraints. These versions permit the use of natural coordinates and the relaxation of the equilibrium conditions and render considerable improvements in the assumed stress hybrid elements. These include the derivation of invariant hybrid elements which possess the ideal qualities such as minimum sensitivity to geometric distortions, minimum number of independent stress parameters, rank sufficient, and ability to represent constant strain states and bending moments. Another application is the formulation of semiLoof thin shell elements which can yield excellent results for many severe test cases because the rigid body nodes, the momentless membrane strains, and the inextensional bending modes are all represented. Author

**N84-31692\*#** Akron Univ., Ohio.  
**NONLINEAR FINITE ELEMENT ANALYSIS OF SHELLS WITH LARGE ASPECT RATIO**

T. Y. CHANG and K. SAWAMIPHAUDI *In* NASA. Lewis Research Center Nonlinear Struct. Anal. p 45-54 Jun. 1984 refs

(Contract NAG3-317)

Avail: NTIS HC A08/MF A01 CSCL 20K

A higher order degenerated shell element with nine nodes was selected for large deformation and post-buckling analysis of thick or thin shells. Elastic-plastic material properties are also included. The post-buckling analysis algorithm is given Using a square plate, it was demonstrated that the nine-node element does not have shear locking effect even if its aspect ratio was increased to the order 10 to the 8th power. Two sample problems are given to illustrate the analysis capability of the shell element. Author

**N84-31693\*#** Akron Univ., Ohio.  
**SELF-ADAPTIVE SOLUTION STRATEGIES**

J. PADOVAN *In* NASA. Lewis Research Center Nonlinear Struct. Anal. p 55-63 Jun. 1984 refs

(Contract NAG3-54)

Avail: NTIS HC A08/MF A01 CSCL 20K

The development of enhancements to current generation nonlinear finite element algorithms of the incremental Newton-Raphson type was overviewed. Work was introduced on alternative formulations which lead to improve algorithms that avoid the need for global level updating and inversion. To quantify the enhanced Newton-Raphson scheme and the new alternative algorithm, the results of several benchmarks are presented. Author

**N84-31694\*#** Stanford Univ., Calif.  
**ELEMENT-BY-ELEMENT SOLUTION PROCEDURES FOR NONLINEAR STRUCTURAL ANALYSIS**

T. J. R. HUGHES, J. M. WINGET, and I. LEVIT *In* NASA. Lewis Research Center Nonlinear Struct. Anal. p 65-84 Jun. 1984 refs

(Contract NAG3-319)

Avail: NTIS HC A08/MF A01 CSCL 20K

Element-by-element approximate factorization procedures are proposed for solving the large finite element equation systems which arise in nonlinear structural mechanics. Architectural and data base advantages of the present algorithms over traditional direct elimination schemes are noted. Results of calculations suggest considerable potential for the methods described. Author

**N84-31695\*#** Kent State Univ., Ohio. Dept. of Mathematical Sciences.

**AUTOMATIC FINITE ELEMENT GENERATORS**

P. S. WANG *In* NASA. Lewis Research Center Nonlinear Struct. Anal. p 85-94 Jun. 1984 refs

(Contract NAG3-298)

Avail: NTIS HC A08/MF A01 CSCL 20K

The design and implementation of a software system for generating finite elements and related computations are described. Exact symbolic computational techniques are employed to derive strain-displacement matrices and element stiffness matrices. Methods for dealing with the excessive growth of symbolic expressions are discussed. Automatic FORTRAN code generation is described with emphasis on improving the efficiency of the resultant code. Author

**N84-31696\*#** Texas Univ., Austin.  
**STABILITY AND CONVERGENCE OF UNDERINTEGRATED FINITE ELEMENT APPROXIMATIONS**

J. T. ODEN *In* NASA. Lewis Research Center Nonlinear Struct. Anal. p 95-103 Jun. 1984 refs

(Contract NAG3-329)

Avail: NTIS HC A08/MF A01 CSCL 20K

The effects of underintegration on the numerical stability and convergence characteristics of certain classes of finite element approximations were analyzed. Particular attention is given to hourglassing instabilities that arise from underintegrating the stiffness matrix entries and checkerboard instabilities that arise from underintegrating constrain terms such as those arising from incompressibility conditions. A fundamental result reported here is the proof that the fully integrated stiffness is restored in some cases through a post-processing operation. Author

**N84-31697\*#** Georgia Inst. of Tech., Atlanta.  
**INELASTIC AND DYNAMIC FRACTURE AND STRESS ANALYSES**

S. N. ATLURI *In* NASA. Lewis Research Center Nonlinear Struct. Anal. p 105-118 Jun. 1984 refs

(Contract NAG3-346)

Avail: NTIS HC A08/MF A01 CSCL 20K

Large deformation inelastic stress analysis and inelastic and dynamic crack propagation research work is summarized. The salient topics of interest in engine structure analysis that are discussed herein include: (1) a path-independent integral (T) in inelastic fracture mechanics, (2) analysis of dynamic crack propagation, (3) generalization of constitutive relations of inelasticity for finite deformations, (4) complementary energy approaches in inelastic analyses, and (5) objectivity of time integration schemes in inelastic stress analysis. Author

**N84-31699\*#** National Aeronautics and Space Administration. Lewis Research Center, Cleveland, Ohio.

**NONLINEAR ANALYSIS FOR HIGH-TEMPERATURE COMPOSITES: TURBINE BLADES/VANES**

D. A. HOPKINS and C. C. CHAMIS *In* its Nonlinear Struct. Anal. p 131-147 Jun. 1984 refs

Avail: NTIS HC A08/MF A01 CSCL 20K

An integrated approach to nonlinear analysis of high-temperature composites in turbine blade/vane applications is presented. The overall strategy of this approach and the key elements comprising this approach are summarized. Preliminary results for a tungsten-fiber-reinforced superalloy (TFRS) composite are discussed. Author

**N84-31700\*#** Pratt and Whitney Aircraft, East Hartford, Conn.  
**THREE-DIMENSIONAL STRESS ANALYSIS USING THE  
 BOUNDARY ELEMENT METHOD**

R. B. WILSON and P. K. BANERJEE (State Univ. of New York, Buffalo) In NASA. Lewis Research Center Nonlinear Struct. Anal. p 149-160 Jun. 1984 refs  
 (Contract NAS3-23697)

Avail: NTIS HC A08/MF A01 CSCL 20K

The boundary element method is to be extended (as part of the NASA Inelastic Analysis Methods program) to the three-dimensional stress analysis of gas turbine engine hot section components. The analytical basis of the method (as developed in elasticity) is outlined, its numerical implementation is summarized, and the approaches to be followed in extending the method to include inelastic material response indicated. Author

**N84-34774\*#** Case Western Reserve Univ., Cleveland, Ohio.  
 Dept. of Civil Engineering.

**ON STRESS ANALYSIS OF A CRACK-LAYER Final Report**

A. CHUDNOVSKY, A. DOLGOPOLSKY (Delaware Univ., Newark), and M. KACHANOV (Tufts Univ., Medford, Mass.) Oct. 1984 95 p refs

(Contract NAG3-223)

(NASA-CR-174774; NAS 1.26:174774) Avail: NTIS HC A05/MF A01 CSCL 20K

This work considers the problem of elastic interaction of a macrocrack with an array of microcracks in the vicinity of the macrocrack tip. Using the double layer potential techniques, the solution to the problem within the framework of the plane problem of elastostatics has been obtained. Three particular problems of interest to fracture mechanics have been analyzed. It follows from analysis that microcrack array can either amplify or reduce the resulting stress field of the macrocrack-microcrack array system depending on the array's configuration. Using the obtained elastic solution the energy release rate associated with the translational motion of the macrocrack-microcrack array system has been evaluated. Author

## 43

## EARTH RESOURCES

Includes remote sensing of earth resources by aircraft and spacecraft; photogrammetry; and aerial photography.

**A84-31608\*** National Aeronautics and Space Administration.  
 Lewis Research Center, Cleveland, Ohio.

**A LASER SYSTEM TO REMOTELY SENSE BIRD MOVEMENTS**

C. E. KORSCHGEN, W. L. GREEN (U.S. Fish and Wildlife Service, Northern Prairie Wildlife Research Center, La Crosse, WI), and R. G. SEASHOLTZ (NASA, Lewis Research Center, Cleveland, OH) Journal of Wildlife Management (ISSN 0022-541X), vol. 47, no. 4, 1983, p. 1159-1162. refs

The design and operation of a laser detection system for migrating birds are presented. A battery-powered class-III laser (operating at 904 nm, pulse-repetition rate 5 kHz, pulse duration 100 nsec, and peak power 25 W) and a photodiode receiver are mounted on poles at height 10 m and distance 850 m and equipped with 135-mm f/2.8 collimating lenses; beam diameter at the receiver is 1.7 m. The microprocessor-controlled system is found to detect the passing of an object as small as 30 sq cm in cross section at a distance of 425 m. T.K.

**N84-27258\*#** Environmental Research Inst. of Michigan, Ann Arbor. Applications Div.

**DEVELOPMENT OF GREAT LAKES ALGORITHMS FOR THE  
 NIMBUS-G COASTAL ZONE COLOR SCANNER Final Report**

F. J. TANIS and D. R. LYZENGA Jun. 1981 95 p refs

(Contract NAS3-22442)

(NASA-CR-173511; NAS 1.26:173511; ERIM-150000-11-F) Avail: NTIS HC A05/MF A01 CSCL 05B

A series of experiments in the Great Lakes designed to evaluate the application of the Nimbus G satellite Coastal Zone Color Scanner (CZCS) were conducted. Absorption and scattering measurement data were reduced to obtain a preliminary optical model for the Great Lakes. Available optical models were used in turn to calculate subsurface reflectances for expected concentrations of chlorophyll-a pigment and suspended minerals. Multiple nonlinear regression techniques were used to derive CZCS water quality prediction equations from Great Lakes simulation data. An existing atmospheric model was combined with a water model to provide the necessary simulation data for evaluation of the preliminary CZCS algorithms. A CZCS scanner model was developed which accounts for image distorting scanner and satellite motions. This model was used in turn to generate mapping polynomials that define the transformation from the original image to one configured in a polyconic projection. Four computer programs (FORTRAN IV) for image transformation are presented. R.S.F.

## 44

## ENERGY PRODUCTION AND CONVERSION

Includes specific energy conversion systems, e.g., fuel cells and batteries; global sources of energy; fossil fuels; geophysical conversion; hydroelectric power; and wind power.

**A84-16395\*** National Aeronautics and Space Administration.  
 Lewis Research Center, Cleveland, Ohio.

**HARNESSING SURFACE PLASMONS FOR SOLAR ENERGY  
 CONVERSION**

L. M. ANDERSON (NASA, Lewis Research Center, Cleveland, OH) IN: Integrated optics III; Proceedings of the Conference, Arlington, VA, April 5, 6, 1983. Bellingham, WA, SPIE - The International Society for Optical Engineering, 1983, p. 172-178. refs

NASA research on the feasibility of solar-energy conversion using surface plasmons is reviewed, with a focus on inelastic-tunnel-diode techniques for power extraction. The need for more efficient solar converters for planned space missions is indicated, and it is shown that a device with 50-percent efficiency could cost up to 40 times as much per sq cm as current Si cells and still be competitive. The parallel-processing approach using broadband carriers and tunable diodes is explained, and the physics of surface plasmons on metal surfaces is outlined. Technical problems being addressed include phase-matching sunlight to surface plasmons, minimizing ohmic losses and reradiation in energy transport, coupling into the tunnels by mode conversion, and gaining an understanding of the tunnel-diode energy-conversion process. Diagrams illustrating the design concepts are provided. T.K.

**A84-22981\*** Applied Solar Energy Corp., City of Industry, Calif.  
**RECENT ADVANCES IN THIN SILICON SOLAR CELLS**  
 F. HO, P. A. ILES (Applied Solar Energy Corp., City of Industry, CA), H. CURTIS, and C. BARAONA (NASA, Lewis Research Center, Cleveland, OH) IN: Photovoltaic Specialists Conference, 16th, San Diego, CA, September 27-30, 1982, Conference Record . New York, Institute of Electrical and Electronics Engineers, 1982, p. 156-159. refs  
 (Contract NAS3-22229; NAS3-22228)

Recent progress in thin (2-4 mils, 50-100 microns)-silicon-solar cells-which extends the capability of the cells into areas of use for possible space missions is reviewed. The production of thin flexible arrays using wrapped-around junction and wrapped-around contact cells is considered. Attention is also given to the formation of cells with very low solar absorptance (alpha-s less than 0.66) through changes in the AR coating, changes in front contact area, and maximizing cell efficiency. J.N.

**A84-22987\*#** National Aeronautics and Space Administration. Lewis Research Center, Cleveland, Ohio.  
**EFFECTS OF INDIRECT BANDGAP TOP CELLS IN A MONOLITHIC CASCADE CELL STRUCTURE**  
 H. B. CURTIS and M. P. GODLEWSKI (NASA, Lewis Research Center, Cleveland, OH) IN: Photovoltaic Specialists Conference, 16th, San Diego, CA, September 27-30, 1982, Conference Record . New York, Institute of Electrical and Electronics Engineers, 1982, p. 231-235. refs

The effect of having a slightly indirect top cell in a three junction cascade monolithic stack is calculated. The minority carrier continuity equations are utilized to calculate individual junction performance. Absorption coefficient curves for general III-V compounds are calculated for a variety of direct and indirect gap materials. The results indicate that for a small excursion into the indirect region, (about 0.1 eV), the loss of efficiency is acceptably small (less than 2.5 percent) and considerably less than attempting to make the top junction a smaller direct bandgap. Author

**A84-22993\*** National Aeronautics and Space Administration. Lewis Research Center, Cleveland, Ohio.  
**INVESTIGATION OF ENERGY MANAGEMENT STRATEGIES FOR PHOTOVOLTAIC SYSTEMS - AN ANALYSIS TECHNIQUE**  
 R. C. CULL (NASA, Lewis Research Center, Cleveland, OH) and A. H. ELTIMSAHY (Toledo, University, Toledo, OH) IN: Photovoltaic Specialists Conference, 16th, San Diego, CA, September 27-30, 1982, Conference Record . New York, Institute of Electrical and Electronics Engineers, 1982, p. 270-275. NASA-supported research.

Progress is reported in formulating energy management strategies for stand-alone PV systems, developing an analytical tool that can be used to investigate these strategies, applying this tool to determine the proper control algorithms and control variables (controller inputs and outputs) for a range of applications, and quantifying the relative performance and economics when compared to systems that do not apply energy management. The analysis technique developed may be broadly applied to a variety of systems to determine the most appropriate energy management strategies, control variables and algorithms. The only inputs required are statistical distributions for stochastic energy inputs and outputs of the system and the system's device characteristics (efficiency and ratings). Although the formulation was originally driven by stand-alone PV system needs, the techniques are also applicable to hybrid and grid connected systems. Author

**A84-22998\*** Hughes Research Labs., Malibu, Calif.  
**EFFECT OF ELECTRON FLUX ON RADIATION DAMAGE IN GAAS SOLAR CELLS**  
 R. Y. LOO, G. S. KAMATH, and R. C. KNECHTLI (Hughes Research Laboratories, Malibu, CA) IN: Photovoltaic Specialists Conference, 16th, San Diego, CA, September 27-30, 1982, Conference Record . New York, Institute of Electrical and Electronics Engineers, 1982, p. 307-309.  
 (Contract NAS3-22227)

The objective of this work was to evaluate the effect of electron flux and temperature on radiation damage in GaAs solar cells. The defect levels and the power ratio of the GaAs solar cells under various irradiation conditions are compared. In a 200 C continuous annealing experiment, the GaAs solar cells which were irradiated at a flux of  $2 \times 10$  to the 9th e/sq cm s suffered less power degradation than the cells which were irradiated at the same temperature at a higher flux of  $4 \times 10$  to the 10th e/sq cm s. After the continuous annealing experiment, a single-step post annealing at 200 C was performed for 40 hr on these irradiated cells. An additional improvement in power recovery was observed only on those cells irradiated at the high flux of  $4 \times 10$  to the 10th e/sq cm s. DLTS data indicate that the defect density decreases with lower electron flux. Both of these observations strongly suggest that the continuous annealing in GaAs cells can be effective at temperatures as low as 150 C, or even less in a space environment such as geosynchronous orbit. Author

**A84-23002\*** Communications Satellite Corp., Clarksburg, Md.  
**SURFACE EFFECTS IN HIGH VOLTAGE SILICON SOLAR CELLS**  
 A. MEULENBERG and R. A. ARNDT (COMSAT Laboratories, Clarksburg, MD) IN: Photovoltaic Specialists Conference, 16th, San Diego, CA, September 27-30, 1982, Conference Record . New York, Institute of Electrical and Electronics Engineers, 1982, p. 348-354. Research sponsored by the Communications Satellite Corp. refs  
 (Contract NAS3-22227)

The surface of low-resistivity silicon solar cells appears to be a major source of dark diffusion current. This region, consisting of the interface and the adjacent heavily doped layer, therefore, prevents attainment of the high open-circuit voltages expected from these cells. This paper describes the experimental effort carried out to reduce the various contributions of dark current from the surface. Analysis of results from this effort points to means of improving cell voltages by changing processing and structures. Author

**A84-23006\*#** National Aeronautics and Space Administration. Lewis Research Center, Cleveland, Ohio.  
**PARALLEL-PROCESSING WITH SURFACE PLASMONS, A NEW STRATEGY FOR CONVERTING THE BROAD SOLAR SPECTRUM**  
 L. M. ANDERSON (NASA, Lewis Research Center, Cleveland, OH) IN: Photovoltaic Specialists Conference, 16th, San Diego, CA, September 27-30, 1982, Conference Record . New York, Institute of Electrical and Electronics Engineers, 1982, p. 371-377. refs

A new strategy for efficient solar-energy conversion is based on parallel processing with surface plasmons: guided electromagnetic waves supported on thin films of common metals like aluminum or silver. The approach is unique in identifying a broadband carrier with suitable range for energy transport and an inelastic tunneling process which can be used to extract more energy from the more energetic carriers without requiring different materials for each frequency band. The aim is to overcome the fundamental 56-percent loss associated with mismatch between the broad solar spectrum and the monoenergetic conduction electrons used to transport energy in conventional silicon solar cells. This paper presents a qualitative discussion of the unknowns and barrier problems, including ideas for coupling surface plasmons into the tunnels, a step which has been the weak link in the efficiency chain. Author

**A84-23059\*** Spire Corp., Bedford, Mass.

**NEW IMPLANTATION TECHNIQUES FOR IMPROVED SOLAR CELL JUNCTIONS**

M. B. SPITZER and S. N. BUNKER (Spire Corp., Bedford, MA) IN: Photovoltaic Specialists Conference, 16th, San Diego, CA, September 27-30, 1982, Conference Record. New York, Institute of Electrical and Electronics Engineers, 1982, p. 764-769. refs (Contract NAS7-100; NAS3-22236)

Ion implantation techniques offering improved cell performance and reduced cost have been studied. These techniques include non-mass-analyzed phosphorus implantation, argon implantation gettering, and low temperature boron annealing. It is found that cells produced by non-mass-analyzed implantation perform as well as mass-analyzed controls, and that the cell performance is largely independent of process parameters. A study of argon implantation gettering shows no improvement over non-gettered controls. Results of low temperature boron annealing experiments are presented. Author

**A84-23115\*** Rensselaer Polytechnic Inst., Troy, N. Y.

**PHOTOVOLTAIC CHARACTERISTICS OF DIFFUSED P/+N BULK GAAS SOLAR CELLS**

J. M. BORREGO, R. P. KEENEY, I. B. BHAT, K. N. BHAT, L. G. SUNDARAM, and S. K. GHANDHI (Rensselaer Polytechnic Institute, Troy, NY) IN: Photovoltaic Specialists Conference, 16th, San Diego, CA, September 27-30, 1982, Conference Record. New York, Institute of Electrical and Electronics Engineers, 1982, p. 1157-1160. (Contract NAG3-188)

The photovoltaic characteristics of P(+)-N junction solar cells fabricated on bulk GaAs by an open tube diffusion technique are described in this paper. Spectral response measurements were analyzed in detail and compared to a computer simulation in order to determine important material parameters. It is projected that proper optimization of the cell parameters can increase the efficiency of the cells from 12.2 percent to close to 20 percent. Author

**A84-23135\*#** National Aeronautics and Space Administration. Lewis Research Center, Cleveland, Ohio.

**THE WORLDWIDE MARKET FOR PHOTOVOLTAICS IN THE RURAL SECTOR**

W. A. BRAINARD (NASA, Lewis Research Center, Cleveland, OH) IN: Photovoltaic Specialists Conference, 16th, San Diego, CA, September 27-30, 1982, Conference Record. New York, Institute of Electrical and Electronics Engineers, 1982, p. 1308-1313. refs

Attention is given to the assessment of results obtained by three NASA studies aimed at determining the global market for stand-alone photovoltaic (PV) power systems in the village power, cottage industry, and agricultural applications areas of the rural sector. An attempt was made to identify technical, social, and institutional barriers to PV system implementation, as well as the funding sources available to potential users. Country- and sector-specific results are discussed, and marketing strategies appropriate for each sector are suggested for the benefit of American PV products manufacturers. O.C.

**A84-25468\*** National Aeronautics and Space Administration. Lewis Research Center, Cleveland, Ohio.

**INVESTIGATION OF ENERGY MANAGEMENT STRATEGIES FOR PHOTOVOLTAIC SYSTEMS - A PREDICTIVE CONTROL ALGORITHM**

R. C. CULL (NASA, Lewis Research Center, Cleveland, OH) and A. H. ELTIMSAHY (Toledo, University, Toledo, OH) IN: American Control Conference, San Francisco, CA, June 22-24, 1983, Proceedings, Volume 2. New York, Institute of Electrical and Electronics Engineers, 1983, p. 393-398. NASA-supported research.

The present investigation is concerned with the formulation of energy management strategies for stand-alone photovoltaic (PV) systems, taking into account a basic control algorithm for a possible predictive, (and adaptive) controller. The control system controls

the flow of energy in the system according to the amount of energy available, and predicts the appropriate control set-points based on the energy (insolation) available by using an appropriate system model. Aspects of adaptation to the conditions of the system are also considered. Attention is given to a statistical analysis technique, the analysis inputs, the analysis procedure, and details regarding the basic control algorithm. G.R.

**A84-26027\*** Rensselaer Polytechnic Inst., Troy, N. Y.

**DIFFUSED JUNCTION P(+)-N SOLAR CELLS IN BULK GAAS. I FABRICATION AND CELL PERFORMANCE**

I. BHAT, K. N. BHAT, G. MATHUR, J. M. BORREGO, and S. K. GHANDHI (Rensselaer Polytechnic Institute, Troy, NY) Solid-State Electronics (ISSN 0038-1101), vol. 27, Feb. 1984, p. 121-125. refs (Contract NAG3-188)

This paper describes the fabrication of solar cells made by a simple open tube p(+)-diffusion into bulk n-GaAs. In addition, cell performance is provided as an indicator of the quality of bulk GaAs for this application. Initial results using this technique (12.2 percent efficiency at AM1 for 0.5 sq cm cells) are promising, and indicate directions for materials improvement. It is shown that the introduction of the diffusant (zinc) with point defects significantly affects the material properties and results in an increase in current capability. Author

**A84-26028\*** Rensselaer Polytechnic Inst., Troy, N. Y.

**DIFFUSED JUNCTION P(+)-N SOLAR CELLS IN BULK GAAS. II - DEVICE CHARACTERIZATION AND MODELLING**

R. KEENEY, L. M. G. SUNDARAM, H. RODE, I. BHAT, S. K. GHANDHI, and J. M. BORREGO (Rensselaer Polytechnic Institute, Troy, NY) Solid-State Electronics (ISSN 0038-1101), vol. 27, Feb. 1984, p. 127-130. refs (Contract NAG3-188)

The photovoltaic characteristics of p(+)-n junction solar cells fabricated on bulk GaAs by an open tube diffusion technique are presented in detail. Quantum efficiency measurements were analyzed and compared to computer simulations of the cell structure in order to determine material parameters such as diffusion length, surface recombination velocity and junction depth. From the results obtained it is projected that proper optimization of the cell parameters can increase the efficiency of the cells to close to 20 percent. Author

**A84-30162\*** General Dynamics Corp., San Diego, Calif.

**MULTIBANDGAP PHOTOVOLTAIC RECEIVER USING BACK SURFACE REFLECTORS**

T. G. STERN (General Dynamics Corp., Convair Div., San Diego, CA) IN: IECEC '83; Proceedings of the Eighteenth Intersociety Energy Conversion Engineering Conference, Orlando, FL, August 21-26, 1983, Volume 3. New York, American Institute of Chemical Engineers, 1983, p. 1334-1338. refs (Contract NAS3-22252)

Requirements for prime power generation from solar arrays are expected to increase for the next generation of spacecraft power systems. An enhancement of the efficiency of the conversion of incident sunlight to electricity would have a number of advantages, provided the cost involved in achieving this enhancement would not be too great. Solar input response can be improved by splitting the solar spectrum into component wavelength bands and directing these bands to solar cells of different bandgaps. Two approaches have been proposed for achieving spectrum splitting photovoltaics. One approach involves multiple-cell systems using dichroic mirrors, while the other employs monolithic multibandgap solar cells. The present investigation is concerned with a procedure which has the advantages of both approaches, while avoiding many of the drawbacks of each. G.R.

**A84-30183\*** United Technologies Corp., South Windsor, Conn.  
**ALKALINE FUEL CELLS FOR THE REGENERATIVE FUEL CELL ENERGY STORAGE SYSTEM**

R. E. MARTIN (United Technologies Corp., Power Systems Div., South Windsor, CT) IN: IECEC '83; Proceedings of the Eighteenth Intersociety Energy Conversion Engineering Conference, Orlando, FL, August 21-26, 1983. Volume 4. New York, American Institute of Chemical Engineers, 1983, p. 1525-1529. refs  
 (Contract NAS3-22234)

The development of the alkaline Regenerative Fuel Cell-System, whose fuel cell module would be a derivative of the 12-kW fuel cell power plant currently being produced for the Space Shuttle Orbiter, is reviewed. Long-term endurance testing of full-size fuel cell modules has demonstrated. (1) the extended endurance capability of potassium titanate matrix cells, (2) the long-term performance stability of the anode catalyst, and (3) the suitability of a lightweight graphite structure for use at the anode. These approaches, developed in the NASA-sponsored fuel cell technology advancement program, would also reduce cell weight by nearly one half. J.N.

**A84-30185\*** National Aeronautics and Space Administration.  
 Lewis Research Center, Cleveland, Ohio.

**CYCLE LIFE TEST AND FAILURE MODEL OF NICKEL-HYDROGEN CELLS**

J. J. SMITHRICK (NASA, Lewis Research Center, Cleveland, OH) IN: IECEC '83; Proceedings of the Eighteenth Intersociety Energy Conversion Engineering Conference, Orlando, FL, August 21-26, 1983. Volume 4. New York, American Institute of Chemical Engineers, 1983, p. 1535-1542. refs

Six ampere hour individual pressure vessel nickel hydrogen cells were charge/discharge cycled to failure. Failure as used here is defined to occur when the end of discharge voltage degraded to 0.9 volts. They were cycled under a low earth orbit cycle regime to a deep depth of discharge (80 percent of rated ampere hour capacity). Both cell designs were fabricated by the same manufacturer and represent current state of the art. A failure model was advanced which suggests both cell designs have inadequate volume tolerance characteristics. The limited existing data base at a deep depth of discharge (DOD) was expanded. Two cells of each design were cycled. One COMSAT cell failed at cycle 1712 and the other failed at cycle 1875. For the Air Force/Hughes cells, one cell failed at cycle 2250 and the other failed at cycle 2638. All cells, of both designs, failed due to low end of discharge voltage (0.9 volts). No cell failed due to electrical shorts. After cell failure, three different reconditioning tests (deep discharge, physical reorientation, and open circuit voltage stand) were conducted on all cells of each design. A fourth reconditioning test (electrolyte addition) was conducted on one cell of each design. In addition post cycle cell teardown and failure analysis were performed on the one cell of each design which did not have electrolyte added after failure. Previously announced in STAR as N83-25038 Author

**A84-30186\*** Hughes Research Labs., Malibu, Calif.  
**LONG LIFE NICKEL ELECTRODES FOR A NICKEL-HYDROGEN CELL. I INITIAL PERFORMANCE**

H. S. LIM, S. A. VERZWYVELT (Hughes Research Laboratories, Malibu, CA), C. BLASER, and K. M. KEENER (Eagle-Picher Industries, Inc., Colorado Springs, Co) IN: IECEC '83; Proceedings of the Eighteenth Intersociety Energy Conversion Engineering Conference, Orlando, FL, August 21-26, 1983. Volume 4. New York, American Institute of Chemical Engineers, 1983, p. 1543-1551. refs  
 (Contract NAS3-22238)

In order to develop a long life nickel electrode for a Ni/H<sub>2</sub> cell, an investigation was begun to study the effects of sinter structure and active material loading level on the long life performance of nickel electrodes. This paper is a report on the initial performance of these electrodes as a part of an accelerated life test program. Seven different types of nickel plaques were made which included three levels of both their mechanical strength and median pore size. These plaques were impregnated with three

levels of active material loading. The resultant electrodes were tested by a 200-cycle stress test which was conducted in flooded electrolyte, and also for initial performance in a Ni/H<sub>2</sub> boiler plate cell. An interesting and unexpected observation was that an increased initial utilization of the active material was due more to its complete discharge to the lower average oxidation state than its increased charge acceptance in the charged state. Author

**A84-30187\*** National Aeronautics and Space Administration.  
 Lewis Research Center, Cleveland, Ohio.

**PORE SIZE ENGINEERING APPLIED TO THE DESIGN OF SEPARATORS FOR NICKEL-HYDROGEN CELLS AND BATTERIES**

K. M. ABBEY and D. L. BRITTON (NASA, Lewis Research Center, Cleveland, OH) IN: IECEC '83; Proceedings of the Eighteenth Intersociety Energy Conversion Engineering Conference, Orlando, FL, August 21-26, 1983. Volume 4. New York, American Institute of Chemical Engineers, 1983, p. 1552-1560. refs

Pore size engineering in starved alkaline multiplate cells involves adopting techniques to widen the volume tolerance of individual cells. Separators with appropriate pore size distributions and wettability characteristics (capillary pressure considerations) to have wider volume tolerances and an ability to resist dimensional changes in the electrodes were designed. The separators studied for potential use in nickel-hydrogen cells consist of polymeric membranes as well as inorganic microporous mats. In addition to standard measurements, the resistance and distribution of electrolyte as a function of total cell electrolyte content were determined. New composite separators consisting of fibers, particles and/or binders deposited on Zircar cloth were developed in order to engineer the proper capillary pressure characteristics in the separator. These asymmetric separators were prepared from a variety of fibers, particles and binders. Previously announced in STAR as N83-24571 Author

**A84-30188\*** National Aeronautics and Space Administration.  
 Lewis Research Center, Cleveland, Ohio

**TEST RESULTS OF A TEN CELL BIPOLAR NICKEL-HYDROGEN BATTERY**

R. L. CATALDO (NASA, Lewis Research Center, Cleveland, OH) IN: IECEC '83; Proceedings of the Eighteenth Intersociety Energy Conversion Engineering Conference, Orlando, FL, August 21-26, 1983. Volume 4. New York, American Institute of Chemical Engineers, 1983, p. 1561-1567.

A ten cell bipolar nickel hydrogen 6.5 ampere-hour battery demonstrated over 2000 low earth orbit cycles at an 80 percent depth-of-discharge. Charge/discharge cyclic ampere-hour and watt-hour efficiencies of 88 and 76 percent, respectively, observed. Peak power capability was determined at 1.1 kW. A 10C discharge rate yields 83 percent of the nominal stark capacity to the 1.0 volt cut off in just under 6 minutes. Previously announced in STAR as N83-26253 Author

**A84-30189\*** Hughes Aircraft Co., El Segundo, Calif.  
**DEVELOPMENT OF A LARGE SCALE BIPOLAR NIH<sub>2</sub> BATTERY**

E. ADLER and F. PEREZ (Hughes Aircraft Co., El Segundo, CA) IN: IECEC '83; Proceedings of the Eighteenth Intersociety Energy Conversion Engineering Conference, Orlando, FL, August 21-26, 1983. Volume 4. New York, American Institute of Chemical Engineers, 1983, p. 1568-1573. refs  
 (Contract NAS3-22249)

The bipolar battery concept, developed in cooperation with NASA, is described in the context of the advantages afforded by near-term IPV and CVP cell technology. The projected performance, development requirements, and a possible approach to bipolar battery design are outlined. Consideration is given to packaging electrodes within a common hydrophobic plastic frame, electrode technology that involves a photochemically etched 0.1 mm thick nickel substrate coated with a 10 mg/sq cm mixture of platinum powder and TFE<sub>3</sub>O, and an electrode design that eliminates the screen and doubles the electrode thickness (from the currently used 0.8 mm) while retaining the active material loading of 1.6-1.8

gm/cu cm. Also covered are thermal management, and electrolyte and oxygen management. It is concluded that a high voltage, high capacity, bipolar  $\text{NiH}_2$  cell can be configured with proper development for use in large power systems, and that it can provide considerable weight savings. C.M.

**A84-30191\*** Energy Research Corp., Danbury, Conn.  
**EVALUATION OF GAS COOLING FOR PRESSURIZED PHOSPHORIC ACID FUEL CELL STACKS**

M. FAROQUE, A. J. SKOK, H. C. MARU (Energy Research Corp., Danbury, CT), R. E. KOTHMANN (Westinghouse R&D Center, Pittsburgh, PA), and R. W. HARRY (Westinghouse Electric Corp., Pittsburgh, PA) IN: IECEC '83; Proceedings of the Eighteenth Intersociety Energy Conversion Engineering Conference, Orlando, FL, August 21-26, 1983, Volume 4. New York, American Institute of Chemical Engineers, 1983, p. 1607-1612. refs (Contract DEN3-201)

Gas cooling is a more reliable, less expensive and a more simple alternative to conventional liquid cooling for heat removal from the phosphoric acid fuel cell (PAFC). The feasibility of gas cooling has already been demonstrated in atmospheric pressure stacks. This paper presents theoretical and experimental investigation of gas cooling for pressurized PAFC. Two approaches to gas cooling, Distributed Gas Cooling (DIGAS) and Separated Gas Cooling (SGC) were considered, and a theoretical comparison on the basis of cell performance indicated SGC to be superior to DIGAS. The feasibility of SGC was experimentally demonstrated by operating a 45-cell stack for 700 hours at pressure, and determining thermal response and the effect of other related parameters. Author

**A84-30194\*** National Aeronautics and Space Administration. Lewis Research Center, Cleveland, Ohio.

**SINGLE CELL PERFORMANCE STUDIES ON THE FE/CR REDOX ENERGY STORAGE SYSTEM USING MIXED REACTANT SOLUTIONS AT ELEVATED TEMPERATURE**

R. F. GAHN, N. H. HAGEDORN, and J. S. LING (NASA, Lewis Research Center, Cleveland, OH) IN: IECEC '83; Proceedings of the Eighteenth Intersociety Energy Conversion Engineering Conference, Orlando, FL, August 21-26, 1983, Volume 4. New York, American Institute of Chemical Engineers, 1983, p. 1647-1652. refs

Experimental studies in a 14.5 sq cm single cell system using mixed reactant solutions at 65 C are described. Systems were tested under isothermal conditions, i.e., reactants and the cell were at the same temperature. Charging and discharging performance were evaluated by measuring watt-hour and coulombic efficiencies, voltage-current relationships, hydrogen evolution and membrane resistivity. Watt-hour efficiencies ranged from 86 percent at 43 ma/sq cm to 75 percent at 129 ma/sq cm with corresponding coulombic efficiencies of 92 percent and 97 percent, respectively. Hydrogen evolution was less than 1 percent of the charge coulombic capacity during charge-discharge cycling. Bismuth and bismuth-lead catalyzed chromium electrodes maintained reversible performance and low hydrogen evolution under normal and adverse cycling conditions. Reblending of the anode and cathode solutions was successfully demonstrated to compensate for osmotic volume changes. Improved performance was obtained with mixed reactant systems in comparison to the unmixed reactant systems. Previously announced in STAR as N83-25042 Author

**A84-33766\*** National Aeronautics and Space Administration. Lewis Research Center, Cleveland, Ohio.

**REVIEW OF THE DOE/NASA WIND TURBINE ENGINEERING INFORMATION SYSTEM**

H. E. NEUSTADTER and D. A. SPERA (NASA, Lewis Research Center, Cleveland, OH) Solar Energy (ISSN 0038-092X), vol. 32, no. 5, 1984, p. 591-596. Research supported by the University of California and NSF. refs

A statistical analysis of data obtained from the Technology and Engineering Information Systems was made. The systems analyzed consist of the following elements: (1) sensors which measure critical parameters (e.g., wind speed and direction, output

power, blade loads and component vibrations); (2) remote multiplexing units (RMUs) on each wind turbine which frequency-modulate, multiplex and transmit sensor outputs; (3) on-site instrumentation to record, process and display the sensor output; and (4) statistical analysis of data. Two examples of the capabilities of these systems are presented. The first illustrates the standardized format for application of statistical analysis to each directly measured parameter. The second shows the use of a model to estimate the variability of the rotor thrust loading, which is a derived parameter. Previously announced in STAR as N82-23696 Author

**A84-34846\*** National Aeronautics and Space Administration. Lewis Research Center, Cleveland, Ohio.

**INCREASED RADIATION RESISTANCE IN LITHIUM-COUNTERDOPED SILICON SOLAR CELLS**

I. WEINBERG, C. K. SWARTZ (NASA, Lewis Research Center, Cleveland, OH), and S. MEHTA (Cleveland State University, Cleveland, OH) Applied Physics Letters (ISSN 0003-6951), vol. 44, June 1, 1984, p. 1071-1073. refs

Lithium-counter-doped  $n(+)$ p silicon solar cells are found to exhibit significantly increased radiation resistance to 1-MeV electron irradiation when compared to boron-doped  $n(+)$ p silicon solar cells. In addition to improved radiation resistance, considerable damage recovery by annealing is observed in the counter-doped cells at T less than or equal to 100 C. Deep level transient spectroscopy measurements are used to identify the defect whose removal results in the low-temperature anneal. It is suggested that the increased radiation resistance of the counter-doped cells is primarily due to interaction of the lithium with interstitial oxygen. Author

**N84-10661#** University of Southern Illinois, Carbondale. Coll. of Engineering and Technology.

**HOW TO PROTECT A WIND TURBINE FROM LIGHTNING Final Report**

C. W. DODD, T. MCCALLA, JR., and J. G. WOOD Sep. 1983 111 p refs

(Contract NCC3-7; DE-AI01-76ET-20320)

(NASA-CR-168229; DOE/NASA/0007-1; NAS 1 26:168229)

Avail: NTIS HC A06/MF A01 CSCL 10A

Techniques for reducing the chances of lightning damage to wind turbines are discussed. The methods of providing a ground for a lightning strike are discussed. Then details are given on ways to protect electronic systems, generating and power equipment, blades, and mechanical components from direct and nearby lightning strikes. Author

**N84-10664#** National Aeronautics and Space Administration. Lewis Research Center, Cleveland, Ohio.

**EXAMINATION, EVALUATION AND REPAIR OF LAMINATED WOOD BLADES AFTER SERVICE ON THE MOD-OA WIND TURBINE**

J. R. FADDOUL 1983 46 p refs Presented at the Natl. Conf. of the American Wind Energy Association, San Francisco, 16-19 Oct. 1983

(Contract DE-AI01-79ET-20320)

(NASA-TM-83483; E-1805; DOE/NASA/20320-53; NAS

1.15-83483) Avail: NTIS HC A03/MF A01 CSCL 10A

Laminated wood blades were designed, fabricated, and installed on a 200-KW wind turbine (Mod-OA). The machine uses a two-blade rotor with a diameter of 38.1 m (125 ft). Each blade weighs less than 1361 kg (3000 lb). After operating in the field, two blade sets were returned for inspection. One set had been in Hawaii for 17 months (7844 hr of operation) and the other had been at Block Island, Rhode Island, for 26 months (22 months operating - 7564 hr). The Hawaii set was returned because of one of the studs that holds the blade to the hub had failed. This was found to be caused by a combination of improper installation and inadequate corrosion protection. No other problems were found. The broken stud (along with four others that were badly corroded) was replaced and the blades are now in storage. The Block Island set of blades was returned at the completion of the test program, but one blade was found to have developed a crack in the leading



## 44 ENERGY PRODUCTION AND CONVERSION

edge along the entire span. This crack was found to be the result of a manufacturing process problem but was not structurally critical. When a load-deflection test was conducted on the cracked blade, the response was identical to that measured before installation. In general, the laminate quality of both blade sets was excellent. No significant internal delamination or structural defects were found in any blade. The stud bonding process requires close tolerance control and adequate corrosion protection, but studs can be removed and replaced without major problems. Moisture content stabilization does not appear to be a problem, and laminated wood blades are satisfactory for long-term operation on Mod-OA wind turbines. Author

**N84-10665\*#** National Aeronautics and Space Administration. Lewis Research Center, Cleveland, Ohio.

### **ECONOMIC COMPETITIVENESS OF FUEL CELL ONSITE INTEGRATED ENERGY SYSTEMS Final Report**

G. BOLLENBACHER Aug 1983 69 p refs

(Contract DE-AI01-80ET-17088)

(NASA-TM-83403; E-1681; DOE/NASA/17088-4; NAS 1.15:83403) Avail: NTIS HC A04/MF A01 CSCL 10A

The economic competitiveness of fuel cell onsite integrated energy systems (OS/IES) in residential and commercial buildings is examined. The analysis is carried out for three different buildings with each building assumed to be at three geographic locations spanning a range of climatic conditions. Numerous design options and operating strategies are evaluated and two economic criteria are used to measure economic performance. In general the results show that fuel cell OS/IES's are competitive in most regions of the country if the OS/IES is properly designed. The preferred design is grid connected, makes effective use of the fuel cell's thermal output, and has a fuel cell powerplant sized for the building's base electrical load. Author

**N84-11579\*#** National Aeronautics and Space Administration. Lewis Research Center, Cleveland, Ohio.

### **NASA REDOX STORAGE SYSTEM DEVELOPMENT PROJECT, CALENDAR YEAR 1982 Annual Report**

Oct. 1983 28 p refs

(Contract DE-AI04-80AL-12726)

(NASA-TM-83469; E-1784; NAS 1.15:83469;

DOE/NASA/12726-23) Avail: NTIS HC A03/MF A01 CSCL 10C

Development was continued for iron-chromium battery operation at 65 C. Membranes that were adequate at 25 C were shown to be unacceptable at 65 C with regard to selectivity. This led to the elevated-temperature, mixed-reactant mode of operation, in which each reactant solution, when discharged, contains both ferrous and chromic chlorides. This operating mode allows the use of very low-resistivity membranes, resulting in high energy efficiencies at current densities. It also allows the use of very simple techniques to correct for solvent or reactant transfer through cell membranes. Screening of candidate catalysts for the chromium electrode led to the development of a bismuth-lead candidate having several attractive characteristics. Author

**N84-11580\*#** Allied Chemical Corp., Solvay, N. Y. Syracuse Research Lab.

### **STUDY TO ESTABLISH COST PROJECTIONS FOR PRODUCTION OF REDOX CHEMICALS Final Report**

J. F. WALTHER, C. C. GRECO, R. N. RUSINKO, and A. L. WADSWORTH, III Nov. 1982 36 p refs

(Contract DEN3-250; DE-AI04-80AL-12726)

(NASA-CR-167881; DOE/NASA/0250-1; NAS 1.26:167881)

Avail: NTIS HC A03/MF A01 CSCL 10B

A cost study of four proposed manufacturing processes for redox chemicals for the NASA REDOX Energy Storage System yielded favorable selling prices in the range \$0.99 to \$1.91/kg of chromic chloride, anhydrous basis, including ferrous chloride. The prices corresponded to specific energy storage costs from under \$9 to \$17/kWh. A refined and expanded cost analysis of the most favored process yielded a price estimate corresponding to a

storage cost of \$11/kWh. The findings supported the potential economic viability of the NASA REDOX system. Author

### **N84-11581\*#** Engelhard Industries, Inc., Edison, N.J. **DEVELOP AND TEST FUEL CELL POWERED ON-SITE INTEGRATED TOTAL ENERGY SYSTEM Quarterly Report, Aug. - Oct. 1982**

7 Sep. 1983 23 p

(Contract DEN3-241; DE-AI01-80ET-17088)

(NASA-CR-168159; DOE/NASA/0241-7; NAS 1.26:168159; QR-7)

Avail: NTIS HC A02/MF A01 CSCL 10C

Test results are given for a 5 kW stack and initial results for an integrated, grid connected system operating from methanol fuel. Site selection criteria are presented for future demonstration of a 50 or 100 kW OS/IES. Preliminary results are also given with approximate internal rates of return to the building owner. Progress in development and construction of a 50 kW modular methanol/steam reformer is reported. Author

**N84-13670\*#** National Aeronautics and Space Administration. Lewis Research Center, Cleveland, Ohio.

### **MOD-2 WIND TURBINE DEVELOPMENT**

L. H. GORDON, J. S. ANDREWS (Boeing Engineering and Construction Co., Tukwila, Wash.), and D. K. ZIMMERMAN (Boeing Engineering and Construction Co., Tukwila, Wash.) 1983 28 p refs Presented at the 6th Wind Workshop, Minneapolis, 1-3 Jun. 1983

(Contract DE-AI01-79ET-20305)

(NASA-TM-83460; E-1776; NAS 1.15:83460;

DOE/NASA/20305-9) Avail: NTIS HC A03/MF A01 CSCL 10A

The development of the Mod-2 turbine, designed to achieve a cost of electricity for the 100th production unit that will be competitive with conventional electric power generation is discussed. The Mod-2 wind turbine system (WTS) background, project flow, and a chronology of events and problem areas leading to Mod-2 acceptance are addressed. The role of the participating utility during site preparation, turbine erection and testing, remote operation, and routine operation and maintenance activity is reviewed. The technical areas discussed pertain to system performance, loads, and controls. Research and technical development of multimegawatt turbines is summarized. Author

**N84-13672\*#** Engelhard Corp., Menlo Park, Calif. Industries Div.

### **DEVELOP AND TEST FUEL CELL POWERED ON-SITE INTEGRATED TOTAL ENERGY SYSTEMS. PHASE 3: FULL-SCALE POWER PLANT DEVELOPMENT Quarterly Report, May - Jul. 1983**

H. FEIGENBAUM, A. KAUFMAN, C. L. WANG, J. WERTH, and J. A. WHELAN 31 Oct. 1983 25 p refs

(Contract DEN3-241; DE-AI01-80ET-17088)

(NASA-CR-168294; DOE/NASA/0241-10; NAS 1.26:168294;

QR-10) Avail: NTIS HC A02/MF A01 CSCL 10A

Operating experience with a 5kW methanol-air integrated system is described. On-going test results for a 24-cell, two-sq ft (4kW) stack are reported. The main activity for this stack is currently the evaluation of developmental non-metallic cooling plates. Single-cell test results are presented for a promising developmental cathode catalyst. Author

**N84-13673\*#** Engelhard Industries, Inc., Edison, N.J.

### **DEVELOP AND TEST FUEL CELL POWERED ON-SITE INTEGRATED TOTAL ENERGY SYSTEM Quarterly Report, Feb. - Apr. 1983**

A. KAUFMAN, H. FEIGENBAUM, C. L. WANG, J. WERTH, and J. A. WHELAN 5 Jul. 1983 42 p refs

(Contract DEN3-241; DE-AI01-80ET-17088)

(NASA-CR-168239; DOE/NASA/0241-5; NAS 1.26:168239; QR-9)

Avail: NTIS HC A03/MF A01 CSCL 10A

Test results are presented for a 24 cell, two sq ft (4kW) stack. This stack is a precursor to a 25kW stack that is a key milestone. Results are discussed in terms of cell performance, electrolyte

management, thermal management, and reactant gas manifold. The results obtained in preliminary testing of a 50kW methanol processing subsystem are discussed. Subcontracting activities involving application analysis for fuel cell on site integrated energy systems are updated. S.C.L.

**N84-14585\*#** Chronos Research Labs, Inc., Olivehain, Calif.  
**PYROELECTRIC CONVERSION IN SPACE: A CONCEPTUAL DESIGN STUDY** Final Report, 21 Sep. 1982 - 20 Sep. 1983  
 R. B. OLSEN Sep. 1983 78 p refs  
 (Contract NAS3-23052)  
 (NASA-CR-168272; NAS 1.26:168272) Avail: NTIS HC A05/MF A01 CSCL 10A

Pyroelectric conversion is potentially a very lightweight means of providing electrical power generation in space. Two conceptualized systems approaches for the direct conversion of heat (from sunlight) into electrical energy using the pyroelectric effect of a new class of polar polymers were evaluated. Both of the approaches involved large area thin sheets of plastic which are thermally cycled by radiative input and output of thermal energy. The systems studied are expected to eventually achieve efficiencies of the order of 8% and may deliver as much as one half kilowatt per kilogram. In addition to potentially very high specific power, the pyroelectric conversion approaches outlined appear to offer low cost per watt in the form of an easily deployed, flexible, strong, electrically "self-healing", and high voltage sheet. This study assessed several potential problems such as plasma interactions and radiation degradation and suggests approaches to overcome them. The fundamental technological issues for space pyroelectric conversion are: (1) demonstration of the conversion cycle with the proposed class of polymers, (2) achievement of improved dielectric strength of the material, (3) demonstration of acceptable plasma power losses for low altitude, and (4) establishment of reasonable lifetime for the pyroelectric material in the space environment. Recommendations include an experimental demonstration of the pyroelectric conversion cycle followed by studies to improve the dielectric strength of the polymer and basic studies to discover additional pyroelectric materials. Author

**N84-14586\*#** National Aeronautics and Space Administration, Lewis Research Center, Cleveland, Ohio.

**USE OF THE WEST-1 WIND TURBINE SIMULATOR TO PREDICT BLADE FATIGUE LOAD DISTRIBUTION**

D. C. JANETZKE 1983 13 p refs Presented at the 6th Bien. Wind Energy Conf. and Workshop, Minneapolis, 1-3 Jun 1983

(Contract DE-AI01-76ET-20320)

(NASA-TM-83532; E-1898; NASA/DOE/20320-56, NAS 1.15:83532) Avail: NTIS HC A02/MF A01 CSCL 10A

To test the ability of WEST-1 to predict blade fatigue load distribution, actual wind signals were fed into the simulator and the response data were recorded and processed in the same manner as actual wind turbine data. The WEST-1 simulator was operated in a stable, unattended mode for six hours. The probability distribution of the cyclic flatwise bending moment for the blade was comparable to that for an actual wind turbine in winds with low turbulence. The input from a stationary anemometer was found to be inadequate for use in the prediction of fatigue load distribution for blade design purposes and modifications are necessary. Author

**N84-14587\*#** Faucett (Jack) Associates, Inc., Chevy Chase, Md

**ASSESSMENT OF INSTITUTIONAL BARRIERS TO THE USE OF NATURAL GAS FUEL IN AUTOMOTIVE VEHICLE FLEETS** Final Report

J. JABLONSKI, L. LENT, M. LAWRENCE, and L. WHITE (Safety Sciences, Inc., Washington, D.C.) Aug. 1983 90 p refs  
 (Contract DEN3-295; DE-AI01-81CS-50006)

(NASA-CR-168183; DOE/NASA/0295-1; NAS 1.26:168183; JACKFAU-83-302) Avail: NTIS HC A05/MF A01 CSCL 21D

Institutional barriers to the use of natural gas as a fuel for motor vehicle fleets were identified. Recommendations for barrier

removal were developed. Eight types of institutional barriers were assessed: (1) lack of a national standard for the safe design and certification of natural gas vehicles and refueling stations; (2) excessively conservative or misapplied state and local regulations, including bridge and tunnel restrictions, restrictions on types of vehicles that may be fueled by natural gas, zoning regulations that prohibit operation of refueling stations, parking restrictions, application of LPG standards to LNG vehicles, and unintentionally unsafe vehicle or refueling station requirements; (3) need for clarification of EPA's tampering enforcement policy; (4) the U.S. hydrocarbon standard; (5) uncertainty concerning state utility commission jurisdiction; (6) sale for resale prohibitions imposed by natural gas utility companies or state utility commissions; (7) uncertainty of the effects of conversions to natural gas on vehicle manufacturers warranties, and (8) need for a natural gas to gasoline equivalent units conversion factor for use in calculation of state road use taxes. E.A.K.

**N84-15679\*#** Institute of Gas Technology, Chicago, Ill.  
**HIGH-TEMPERATURE MOLTEN SALT THERMAL ENERGY STORAGE SYSTEMS FOR SOLAR APPLICATIONS**

R. J. PETRI, T. D. CLAAR, and E. ONG Jul. 1983 171 p refs  
 (Contract DEN3-156)

(NASA-CR-167916; DOE/NASA/0156-83/1; NAS 1.26:167916)

Avail: NTIS HC A08/MF A01 CSCL 10C

Experimental results of compatibility screening studies of 100 salt/containment/thermal conductivity enhancement (TCE) combinations for the high temperature solar thermal application range of 704 deg to 871 C (1300 to 1600 F) are presented. Nine candidate containment/HX alloy materials and two TCE materials were tested with six candidate solar thermal alkali and alkaline earth carbonate storage salts (both reagent and technical grade of each). Compatibility tests were conducted with salt encapsulated in approx. 6.0 inch x 1 inch welded containers of test material from 300 to 3000 hours. Compatibility evaluations were end application oriented, considering the potential 30 year lifetime requirement of solar thermal power plant components. Analyses were based on depth and nature of salt side corrosion of materials, containment alloy thermal aging effects, weld integrity in salt environment, air side containment oxidation, and chemical and physical analyses of the salt. A need for more reliable, and in some cases first time determined thermophysical and transport property data was also identified for molten carbonates in the 704 to 871 C temperature range. In particular, accurate melting point (mp) measurements were performed for Li<sub>2</sub>CO<sub>3</sub> and Na<sub>2</sub>CO<sub>3</sub> while melting point, heat of fusion, and specific heat determinations were conducted on 81.3 weight percent Na<sub>2</sub>CO<sub>3</sub>-18.7 weight percent K<sub>2</sub>CO<sub>3</sub> and 52.2 weight percent BaCO<sub>3</sub>-47.8 weight percent Na<sub>2</sub>CO<sub>3</sub> to support future TES system design and ultimate scale up of solar thermal energy storage (TES) subsystems. Author

**N84-15681\*#** Case Western Reserve Univ., Cleveland, Ohio, Center for Electrochemical Sciences.

**ELECTROCHEMICAL STUDIES OF REDOX SYSTEMS FOR ENERGY STORAGE** Semiannual Report, 4 Dec. 1982 - 31 May 1983

C. D. WU, E. J. CALVO, and E. YEAGER 30 Sep. 1983 74 p refs

(Contract NAG3-219)

(NASA-CR-174503; NAS 1.26:174503; SAR-3) Avail: NTIS HC A04/MF A01 CSCL 10C

Particular attention was paid to the Cr(II)/Cr(III) redox couple in aqueous solutions in the presence of Cl<sup>-</sup> ions. The aim of this research has been to unravel the electrode kinetics of this redox couple and the effect of Cl<sup>-</sup> and electrode substrate. Gold and silver were studied as electrodes and the results show distinctive differences; this is probably due to the role Cl<sup>-</sup> ion may play as a mediator in the reaction and the difference in state of electrical charge on these two metals (difference in the potential of zero charge, pzc). The competition of hydrogen evolution with CrCl<sub>3</sub> reduction on these surfaces was studied by means of the rotating ring disk electrode (RRDE). The ring downstream measures the

## 44 ENERGY PRODUCTION AND CONVERSION

flux of chromous ions from the disk and therefore separation of both Cr(III) and H<sub>2</sub> generation can be achieved by analyzing ring and disk currents. The conditions for the quantitative detection of Cr(2+) at the ring electrode were established. Underpotential deposition of Pb on Ag and its effect on the electrokinetics of Cr(II)/Cr(III) reaction was studied. Author

**N84-15682\*#** Communications Satellite Corp., Clarksburg, Md.  
**THIN N-I-P RADIATION RESISTANT SOLAR CELLS**  
A. MEULENBERG Jul. 1983. 36 p refs  
(Contract NAS3-22245)  
(NASA-CR-168284; NAS 1.26:168284) Avail: NTIS HC A03/MF A01 CSDL 10A

Several sets of N-I-P solar cells were fabricated from high resistivity silicon to test the effectiveness of various methods for hardening these devices against radiation. Different substrate materials were used to provide information on the effects of dopant concentration, silicon type, and the presence of oxygen. In some cells, P-type float-zone refined silicon of 800, 8000 and 15,000 ohm-cm resistivity was used to provide a basis for studying resistivity and purity effects. In other cells, N-type silicon (approximately 800 ohm-cm) was used to allow a comparison of dopant type. Oxygen-rich, crucible-grown, silicon (approximately 100 ohm-cm, p-type) will provide information on purity effects and defect gettering. Lithium was introduced into different types of silicon to determine if mobile ions can reduce radiation induced defects in high resistivity material. Thin cells (2 mil) were fabricated to study the effects of cell thickness and carrier injection on radiation damage. The electrical characteristics of the different sets of cells were measured, analyzed, and compared prior to shipment of the cells to NASA/Lewis for irradiation. R J.F.

**N84-18757\*#** Little (Arthur D.), Inc., Cambridge, Mass.  
**NEW APPLICATIONS FOR PHOSPHORIC ACID FUEL CELLS Final Report**  
R. P. STICKLES and C. T. BREUER Nov. 1983 225 p refs  
(Contract DEN3-291; DE-AI21-80ET-17088)  
(NASA-CR-168203; DOE/NASA/0291-1; NAS 1.26:168203; ADL-88036) Avail: NTIS HC A10/MF A01 CSDL 10A

New applications for phosphoric acid fuel cells were identified and evaluated. Candidates considered included all possibilities except grid connected electric utility applications, on site total energy systems, industrial cogeneration, opportunistic use of waste hydrogen, space and military applications, and applications smaller than 10 kW. Applications identified were screened, with the most promising subjected to technical and economic evaluation using a fuel cell and conventional power system data base developed in the study. The most promising applications appear to be the underground mine locomotive and the railroad locomotive. Also interesting are power for robotic submersibles and Arctic villages. The mine locomotive is particularly attractive since it is expected that the fuel cell could command a very high price and still be competitive with the conventionally used battery system. The railroad locomotive's attractiveness results from the (smaller) premium price which the fuel cell could command over the conventional diesel electric system based on its superior fuel efficiency, and on the large size of this market and the accompanying opportunities for manufacturing economy. Author

**N84-20014\*#** Eaton Corp., Southfield, Mich.  
**DEVELOPMENT OF A DC PROPULSION SYSTEM FOR AN ELECTRIC VEHICLE Final Report**  
W. L. KELLEDES Jan. 1984 138 p refs  
(Contract DEN3-258; DE-AI01-77CS-51044)  
(NASA-CR-168306; DOE/NASA/0258-1; NAS 1.26:168306; ERC-TR-83020) Avail: NTIS HC A07/MF A01 CSDL 10B

The suitability of the Eaton automatically shifted mechanical transaxle concept for use in a near-term dc powered electric vehicle is evaluated. A prototype dc propulsion system for a passenger electric vehicle was designed, fabricated, tested, installed in a modified Mercury Lynx vehicle and track tested at the contractor's site. The system consisted of a two-axis, three-speed, automatically-shifted mechanical transaxle, 15.2 Kw rated,

separately excited traction motor, and a transistorized motor controller with a single chopper providing limited armature current below motor base speed and full range field control above base speed at up to twice rated motor current. The controller utilized a microprocessor to perform motor and vehicle speed monitoring and shift sequencing by means of solenoids applying hydraulic pressure to the transaxle clutches. Bench dynamometer and track testing was performed. Track testing showed best system efficiency for steady-state cruising speeds of 65-80 Km/Hr (40-50 mph). Test results include acceleration, steady speed and SAE J227A/D cycle energy consumption, braking tests and coast down to characterize the vehicle road load. Author

**N84-20016\*#** National Aeronautics and Space Administration. Lewis Research Center, Cleveland, Ohio.  
**ROAD LOAD SIMULATOR TESTS OF THE GOULD PHASE 1 FUNCTIONAL MODEL SILICON CONTROLLED RECTIFIER AC MOTOR CONTROLLER FOR ELECTRIC VEHICLES Final Report**  
F. GOURASH Feb. 1984 70 p refs  
(Contract DE-AI01-77CS-51044)  
(NASA-TM-83497; E-1831; NAS 1.15:83497; DOE/NASA/51044-34) Avail: NTIS HC A04/MF A01 CSDL 10B

The test results for a functional model ac motor controller for electric vehicles and a three-phase induction motor which were dynamically tested on the Lewis Research Center road load simulator are presented. Results show that the controller has the capability to meet the SAE-J227a D cycle test schedule and to accelerate a 1576-kg (3456-lb) simulated vehicle to a cruise speed of 88.5 km/hr (55 mph). Combined motor controller efficiency is 72 percent and the power inverter efficiency alone is 89 percent for the cruise region of the D cycle. Steady state test results for motoring, regeneration, and thermal data obtained by operating the simulator as a conventional dynamometer are in agreement with the contractor's previously reported data. The regeneration test results indicate that a reduction in energy requirements for urban driving cycles is attainable with regenerative braking. Test results and data in this report serve as a data base for further development of ac motor controllers and propulsion systems for electric vehicles. The controller uses state-of-the-art silicon controlled rectifier (SCR) power semiconductors and microprocessor-based logic and control circuitry. The controller was developed by Gould Laboratories under a Lewis contract for the Department of Energy's Electric and Hybrid Vehicle program. Author

**N84-20017\*#** National Aeronautics and Space Administration. Lewis Research Center, Cleveland, Ohio.  
**ELECTRIC VEHICLE PROPULSION ALTERNATIVES Final Report**  
R. R. SECUNDE, R. M. SCHUH, and R. F. BEACH Nov. 1983 65 p refs  
(Contract DE-AI01-77CS-51044)  
(NASA-TM-83504; E-1845; DOE/NASA/51044-33; NAS 1.15:83504) Avail: NTIS HC A04/MF A01 CSDL 10B

Propulsion technology development for electric vehicles is summarized. Analytical studies, technology evaluation, and the development of technology for motors, controllers, transmissions, and complete propulsion systems are included. Author

**N84-20915\*#** Trane Co., LaCrosse, Wis.  
**HEAT RECOVERY SUBSYSTEM AND OVERALL SYSTEM INTEGRATION OF FUEL CELL ON-SITE INTEGRATED ENERGY SYSTEMS Final Report**  
L. J. MOUGIN 15 Jul. 1983 134 p  
(Contract DEN3-241)  
(NASA-CR-168309; DOE/NASA/0241-12; NAS 1.26:168309) Avail: NTIS HC A07/MF A01 CSDL 10A

The best HVAC (heating, ventilating and air conditioning) subsystem to interface with the Engelhard fuel cell system for application in commercial buildings was determined. To accomplish this objective, the effects of several system and site specific

parameters on the economic feasibility of fuel cell/HVAC systems were investigated. An energy flow diagram of a fuel cell/HVAC system is shown. The fuel cell system provides electricity for an electric water chiller and for domestic electric needs. Supplemental electricity is purchased from the utility if needed. An excess of electricity generated by the fuel cell system can be sold to the utility. The fuel cell system also provides thermal energy which can be used for absorption cooling, space heating and domestic hot water. Thermal storage can be incorporated into the system. Thermal energy is also provided by an auxiliary boiler if needed to supplement the fuel cell system output. Fuel cell/HVAC systems were analyzed with the TRACE computer program. S.L.

**N84-20916\*** National Aeronautics and Space Administration. Lewis Research Center, Cleveland, Ohio.  
**VOLTAGE CONTROLLING MECHANISMS IN LOW RESISTIVITY SILICON SOLAR CELLS: A UNIFIED APPROACH**  
 V. G. WEIZER, C. K. SWARTZ, R. E. HART, and M. P. GODLEWSKI 4 May 1984 13 p refs Presented at 17th Photovoltaic Specialists Conf., Kissimmee, Fla., 1-4 May 1984; sponsored by IEEE  
 (NASA-TM-83612; NAS 1.15:83612) Avail: NTIS HC A02/MF A01 CSCL 10A

An experimental technique capable of resolving the dark saturation current into its base and emitter components is used as the basis of an analysis in which the voltage limiting mechanisms were determined for a variety of high voltage, low resistivity silicon solar cells. The cells studied include the University of Florida hi-low emitter cell, the NASA and the COMSAT multi-step diffused cells, the Spire Corporation ion-implanted emitter cell, and the University of New South Wales MINMIS and MINP cells. The results proved to be, in general, at variance with prior expectations. Most surprising was the finding that the MINP and the MINMIS voltage improvements are due, to a considerable extent, to a previously unrecognized optimization of the base component of the saturation current. This result is substantiated by an independent analysis of the material used to fabricate these devices. Author

**N84-20918\*** National Aeronautics and Space Administration. Lewis Research Center, Cleveland, Ohio.  
**THERMIONIC-PHOTOVOLTAIC ENERGY CONVERTER Patent Application**  
 D. L. CHUBB, inventor (to NASA) 15 Feb. 1984 10 p  
 (NASA-CASE-LEW-14077-1; US-PATENT-APPL-SN-580573)  
 Avail: NTIS HC A02/MF A01 CSCL 10A

A thermionic photovoltaic energy conversion device comprised of a thermionic diode mounted within a hollow tubular photovoltaic converter is described. The thermionic diode maintains a cesium discharge for producing excited atoms that emit line radiation in the wave length region of 850 nm to 890 nm. The photovoltaic converter is a silicon or gallium arsenide photovoltaic cell having bandgap energies in this same wavelength region for optimum cell efficiency. NASA

**N84-22001\*** Jet Propulsion Lab., California Inst. of Tech., Pasadena.  
**AN ASSESSMENT OF ADVANCED TECHNOLOGY FOR INDUSTRIAL COGENERATION Report, Nov. 1982 - May 1983**  
 N. MOORE Jun. 1983 139 p refs  
 (Contract NAS7-918; NASA ORDER C-2742911)  
 (NASA-CR-173456; JPL-PUB-83-66; NAS 1.26:173456) Avail: NTIS HC A07/MF A01 CSCL 10B

The potential of advanced fuel utilization and energy conversion technologies to enhance the outlook for the increased use of industrial cogeneration was assessed. The attributes of advanced cogeneration systems that served as the basis for the assessment included their fuel flexibility and potential for low emissions, efficiency of fuel or energy utilization, capital equipment and operating costs, and state of technological development. Over thirty advanced cogeneration systems were evaluated. These cogeneration system options were based on Rankine cycle, gas turbine engine, reciprocating engine, Stirling engine, and fuel cell energy conversion systems. The alternatives for fuel utilization

included atmospheric and pressurized fluidized bed combustors, gasifiers, conventional combustion systems, alternative energy sources, and waste heat recovery. Two advanced cogeneration systems with mid-term (3 to 5 year) potential were found to offer low emissions, multi-fuel capability, and a low cost of producing electricity. Both advanced cogeneration systems are based on conventional gas turbine engine/exhaust heat recovery technology; however, they incorporate advanced fuel utilization systems.

Author

**N84-23021\*** TRW Space Technology Labs., Redondo Beach, Calif.  
**STUDY OF SOLAR ARRAY SWITCHING POWER MANAGEMENT TECHNOLOGY FOR SPACE POWER SYSTEM Progress Report, Oct. 1980 - Sep. 1981**  
 J. E. CASSINELLI Sep. 1982 33 p  
 (Contract NAS3-22656)  
 (NASA-CR-167890-EXEC-SUM; NAS 1.26:167890-EXEC-SUM; TRW-37243-EXEC-SUM) Avail: NTIS HC A03/MF A01 CSCL 10A

This report documents work performed on the Solar Array Switching Power Management Study. Mission characteristics for three missions were defined to the depth necessary to determine their power management requirements. Solar array switching concepts were identified that could satisfy the mission requirements. These switching concepts were compared with a conventional buck regulator system on the basis of cost, weight and volume, reliability, efficiency and thermal control. For the missions reviewed, solar array switching provided significant advantages in all areas of comparison. Author

**N84-23022\*** National Aeronautics and Space Administration. Lewis Research Center, Cleveland, Ohio.  
**A 37.5-KW POINT DESIGN COMPARISON OF THE NICKEL-CADMIUM BATTERY, BIPOLAR NICKEL-HYDROGEN BATTERY, AND REGENERATIVE HYDROGEN-OXYGEN FUEL CELL ENERGY STORAGE SUBSYSTEMS FOR LOW EARTH ORBIT**  
 M. A. MANZO and M. A. HOBERECHT 1984 11 p Proposed for presentation at the 19th Intersoc. Energy Conversion Eng. Conf., San Francisco, 19-24 Aug. 1984; sponsored by ANS, ASME, SAE, IEEE, AIAA, ACS, and American Inst. for Chemical Engineering (NASA-TM-83651; E-2016; NAS 1.15:83651) Avail: NTIS HC A02/MF A01 CSCL 10C

Nickel-cadmium batteries, bipolar nickel-hydrogen batteries, and regenerative fuel cell storage subsystems were evaluated for use as the storage subsystem in a 37.5 kW power system for space station. Design requirements were set in order to establish a common baseline for comparison purposes. The storage subsystems were compared on the basis of effective energy density, round trip electrical efficiency, total subsystem weight and volume, and life. Author

**N84-23023\*** National Aeronautics and Space Administration. Lewis Research Center, Cleveland, Ohio.  
**DESIGN CONSIDERATIONS FOR A 10-KW INTEGRATED HYDROGEN-OXYGEN REGENERATIVE FUEL CELL SYSTEM**  
 M. A. HOBERECHT, T. B. MILLER, L. L. RIEKER, and O. D. GONZALEZ-SANABRIA 1984 13 p refs Proposed for presentation at the 19th Intersoc. Energy Conversion Eng. Conf., San Francisco, 19-24 Aug. 1984; sponsored by ANS, ASME, SAE, IEEE, AIAA, ACS and AIChE  
 (NASA-TM-83664; E-2041; NAS 1.15:83664) Avail: NTIS HC A02/MF A01 CSCL 10B

Integration of an alkaline fuel cell subsystem with an alkaline electrolysis subsystem to form a regenerative fuel cell (RFC) system for low earth orbit (LEO) applications characterized by relatively high overall round trip electrical efficiency, long life, and high reliability is possible with present state of the art technology. A hypothetical 10 kW system computer modeled and studied based on data from ongoing contractual efforts in both the alkaline fuel cell and alkaline water electrolysis areas. The alkaline fuel cell technology is under development utilizing advanced cell

## 44 ENERGY PRODUCTION AND CONVERSION

components and standard Shuttle Orbiter system hardware. The alkaline electrolysis technology uses a static water vapor feed technique and scaled up cell hardware is developed. The computer aided study of the performance, operating, and design parameters of the hypothetical system is addressed. E.A K.

**N84-23024\*#** National Aeronautics and Space Administration. Lewis Research Center, Cleveland, Ohio.

### **DESIGN OF A 1-KWH BIPOLAR NICKEL HYDROGEN BATTERY**

R. L. CATALDO 1984 9 p refs Proposed for presentation at the 19th Intersoc. Energy Conversion Eng. Conf., San Francisco, 19-14 Aug. 1984; sponsored by ANS, ASME, SAE, IEEE, AIAA, ACS and AIChE

(NASA-TM-83647; E-2037; NAS 1.15:83647) Avail: NTIS HC A02/MF A01 CSCL 10C

The design of a nickel hydrogen battery utilizing bipolar construction in a common pressure vessel is discussed. Design features are as follows: 40 ampere-hour capacity, 1 kWh stored energy as a 24 cell battery, 1.8 kW delivered in a LEO Cycle and maximum pulse power of 18.0 kW. Author

**N84-23025\*#** National Aeronautics and Space Administration. Lewis Research Center, Cleveland, Ohio.

### **ADVANCED DESIGNS FOR IPV NICKEL-HYDROGEN CELLS**

J. J. SMITHRICK, M. A. MANZO, and O. D. GONZALEZ-SANABRIA 1984 8 p refs To be presented at the 19th Intersoc. Energy Conversion Eng. Conf., San Francisco, 19-24 Aug. 1984

(NASA-TM-83643; E-2052; NAS 1.15:83643) Avail: NTIS HC A02/MF A01 CSCL 10C

Advanced designs for individual pressure vessel nickel-hydrogen cells have been conceived which should improve the cycle life at deep depths-of-discharge. Features of the designs which are new and not incorporated in either of the contemporary cells (Air Force/Hughes, Comsat) are: (1) use of alternate methods of oxygen recombination, (2) use of serrated edge separators to facilitate movement of gas within the cell while still maintaining required physical contact with the wall wick, and (3) use of an expandable stack to accommodate some of the nickel electrode expansion. The designs also consider electrolyte volume requirements over the life of the cells, and are fully compatible with the Air Force/Hughes design. Author

**N84-23026\*#** National Aeronautics and Space Administration. Lewis Research Center, Cleveland, Ohio.

### **TEARDOWN ANALYSIS OF A TEN CELL BIPOLAR NICKEL-HYDROGEN BATTERY**

M. A. MANZO, O. D. GONZALEZ-SANABRIA, J. S. HERZAU, and L. J. SCAGLIONE 1984 13 p refs To be presented at the 19th Intersoc. Energy Conversion Eng. Conf., San Francisco, 19-24 Aug. 1984

(NASA-TM-83618; E-2051; NAS 1.15:83618) Avail: NTIS HC A02/MF A01 CSCL 10C

Design studies have identified bipolar nickel-hydrogen batteries as an attractive storage option for high power, high voltage applications. A pre-prototype Ni-H<sub>2</sub> battery was designed, assembled and tested in the early phases of a concept verification program. The initial stack was built with available hardware and components from past programs. The stack performed well. After 2000 low-earth-orbit cycles the stack was dismantled in order to allow evaluation and analysis of the design and components. The results of the teardown analysis and recommended modifications are discussed. Author

**N84-23027\*#** National Aeronautics and Space Administration. Lewis Research Center, Cleveland, Ohio.

### **THE EFFECT OF DIFFUSION INDUCED LATTICE STRESS ON THE OPEN-CIRCUIT VOLTAGE IN SILICON SOLAR CELLS**

V. G. WEIZER and M. P. GODLEWSKI 1984 10 p refs Presented at the 17th Photovoltaic Specialists Conf., Kissimmee, Fla., 1-4 May 1984

(NASA-TM-83667; E-2110; NAS 1.15:83667) Avail: NTIS HC A02/MF A01 CSCL 10C

It is demonstrated that diffusion induced stresses in low resistivity silicon solar cells can significantly reduce both the open-circuit voltage and collection efficiency. The degradation mechanism involves stress induced changes in both the minority carrier mobility and the diffusion length. Thermal recovery characteristics indicate that the stresses are relieved at higher temperatures by divacancy flow (silicon self diffusion). The level of residual stress in as-fabricated cells was found to be negligible in the cells tested. Author

**N84-24656\*#** National Aeronautics and Space Administration. Marshall Space Flight Center, Huntsville, Ala.

### **SOLAR-ARRAY-MATERIALS PASSIVE LDEF EXPERIMENT (A0171)**

A. F. WHITAKER, C. F. SMITH, JR., L. E. YOUNG, H. W. BRANDHORST, JR., A. F. FORESTIERI, E. M. GADDY, J. A. BASS, and P. M. STELLA In NASA. Langley Research Center Long Duration Exposure Facility (LDEF) p 86-87 Feb. 1984 Prepared in cooperation with NASA. Lewis Research Center and NASA. Goddard Space Flight Center and JPL

Avail: NTIS HC A09/MF A01; also available SOD HC CSCL 10A

The objective of this experiment is to evaluate the synergistic effects of the space environment on various solar-array materials, including solar cells, cover slips with various antireflectance coatings, adhesive, encapsulants, reflector materials, substrate strength materials, mast and harness materials, structural composites, and thermal control treatments. The experiment is passive and consists of an arrangement of material specimens mounted in a 3-in.-deep peripheral tray. The effects of the space environment on the specimens will be determined by comparison of preflight and postflight measurements of mechanical, electrical, and optical properties. M.G.

**N84-24657\*#** National Aeronautics and Space Administration. Lewis Research Center, Cleveland, Ohio.

### **ADVANCED PHOTOVOLTAIC EXPERIMENT (S0014)**

H. W. BRADHORST, JR. and A. F. FORESTIERI In NASA. Langley Research Center Long Duration Exposure Facility (LDEF) p 88-90 Feb. 1984

Avail: NTIS HC A09/MF A01; also available SOD HC CSCL 10A

The advanced photovoltaics-related experiments for investigating a portion of the solar spectrum and the effect of the space environment on photovoltaics. The information will be used to provide correlation between space and ground testing and also to provide for more accurate performance measurement in the laboratory. Specific objectives of these experiments are to provide information on the performance and endurance of advanced and conventional solar cells, to improve reference standards for photovoltaic measurements, and to measure the energy distribution in the extraterrestrial solar spectrum. Data to be obtained will include temperatures and short-circuit current of the samples. Six-point current-voltage (I-V) characteristics will be obtained for selected samples. These data will be recorded once a day during the flight. Orbit data will be correlated with preflight and postflight measurement of the samples. M.G.

**N84-25162\*#** Motorola, Inc., Phoenix, Ariz.  
**QUALIFICATION TESTING OF SOLAR PHOTOVOLTAIC POWERED REFRIGERATOR FREEZERS FOR MEDICAL USE IN REMOTE GEOGRAPHIC LOCATIONS** Final Report  
 W. J. KASZETA Dec. 1982 58 p  
 (Contract DEN3-240)  
 (NASA-CR-168181; NAS 1.26:168181) Avail: NTIS HC A04/MF A01 CSCL 10B

One of the primary obstacles to the application of vaccination in developing countries is the lack of refrigerated storage. Vaccines exposed to elevated temperatures suffer a permanent loss of potency. Photovoltaic (PV) powered refrigerator/freezer (R/F) units could surmount the problem of refrigeration in remote areas where no reliable commercial power supply is available. The performance measurements of two different models of PV powered R/F units for medical use are presented. Qualification testing consisted of four major procedures: no-load pull down, ice making, steady-state (maintenance), and holdover. Both R/F units met the major World Health Organization (WHO) requirements. However, the testing performed does not provide complete characterization of the two units; such information could be derived only from further extensive test procedures. R.S.F.

**N84-25163\*#** Solar Power Corp., Woburn, Mass.  
**SOLAR PHOTOVOLTAIC POWERED REFRIGERATORS/FREEZERS FOR MEDICAL USE IN REMOTE GEOGRAPHIC LOCATIONS** Final Report  
 G. DARKAZALLI and G. F. HEIN Oct. 1983 98 p  
 (Contract DEN3-238)  
 (NASA-CR-168268; NAS 1.26:168268) Avail: NTIS HC A05/MF A01 CSCL 10B

One of the obstacles preventing widespread immunization against disease is the virtual absence of reliable, low maintenance refrigeration systems for storage of vaccines in remote geographic locations. A system which consists of a solar photovoltaic cell array and an integrated refrigerator/freezer-energy storage unit is discussed herein. The array converts solar radiation into direct current (DC) electricity with no moving parts and no intermediate steps. A detailed description of the refrigeration system, its design and an analysis thereof, performance test procedures, and test results are presented. A system schematic is also provided. R.S.F.

**N84-25166\*#** National Aeronautics and Space Administration. Lewis Research Center, Cleveland, Ohio.  
**RESULTS OF ELECTRIC-VEHICLE PROPULSION SYSTEM PERFORMANCE ON THREE LEAD-ACID BATTERY SYSTEMS**  
 J. G. EWASHINKA 1984 16 p refs Presented at the 19th Intersoc. Energy Conversion Eng. Conf., San Francisco, 19-24 Aug. 1984  
 (Contract DE-AI01-77CS-51044)  
 (NASA-TM-83657; E-2015; NAS 1.15:83657; DOE/NASA/51044-36) Avail: NTIS HC A02/MF A01 CSCL 10C

Three types of state of the art 6 V lead acid batteries were tested. The cycle life of lead acid batteries as a function of the electric vehicle propulsion system design was determined. Cycle life, degradation rate and failure modes with different battery types (baseline versus state of the art tubular and thin plate batteries) were compared. The effects of testing strings of three versus six series connected batteries on overall performance were investigated. All three types do not seem to have an economically feasible battery system for the propulsion systems. The tubular plate batteries on the load leveled profile attained 235 cycles with no signs of degradation and minimal capacity loss. E.A.K.

**N84-25168\*#** Washington Univ., Seattle.  
**BASIC AND APPLIED RESEARCH RELATED TO THE TECHNOLOGY OF SPACE ENERGY CONVERSION SYSTEMS, 1982 - 1983** Final Report  
 A. HERTZBERG 1983 12 p refs  
 (Contract NAG3-16)  
 (NASA-CR-173554; NAS 1.26:173554) Avail: NTIS HC A02/MF A01 CSCL 10A

Topics on solar energy conversion concepts and applications are discussed. An overview of the current status and future utilization of radiation receivers for electrical energy generation, liquid droplet radiation systems, and liquid droplet heat exchangers is presented. M.A.C.

**N84-25169\*#** Energy Research Corp., Danbury, Conn.  
**EVALUATION OF GAS-COOLED PRESSURIZED PHOSPHORIC ACID FUEL CELLS FOR ELECTRIC UTILITY POWER GENERATION** Final Report  
 M. FAROQUE Sep 1983 84 p refs  
 (Contract DEN3-201; DE-AI21-80ET-17088)  
 (NASA-CR-168298; DOE/NASA/0201-4; NAS 1.26:168298)  
 Avail: NTIS HC A05/MF A01 CSCL 10A

Gas cooling is a more reliable, less expensive and a more simple alternative to conventional liquid cooling for heat removal from the phosphoric acid fuel cell (PAFC). The feasibility of gas-cooling was already demonstrated in atmospheric pressure stacks. Theoretical and experimental investigations of gas-cooling for pressurized PAFC are presented. Two approaches to gas cooling, Distributed Gas-Cooling (DIGAS) and Separated Gas-Cooling (SGC) were considered, and a theoretical comparison on the basis of cell performance indicated SGC to be superior to DIGAS. The feasibility of SGC was experimentally demonstrated by operating a 45-cell stack for 700 hours at pressure, and determining thermal response and the effect of other related parameters. Author

**N84-26165\*#** Energy Research Corp., Danbury, Conn.  
**FULL SCALE PHOSPHORIC ACID FUEL CELL STACK TECHNOLOGY DEVELOPMENT** Final Technical Report  
 L. CHRISTNER and M. FAROQUE Mar. 1984 99 p refs  
 (Contract DEN3-205; DE-AI21-80ET-17088)  
 (NASA-CR-174660; DOE/NASA/0205-8; NAS 1.26:174660)  
 Avail: NTIS HC A05/MF A01 CSCL 10A

The technology development for phosphoric acid fuel cells is summarized. The preparation, heat treatment, and characterization of carbon composites used as bipolar separator plates are described. Characterization included resistivity, porosity, and electrochemical corrosion. High density glassy carbon/graphite composites performed well in long-term fuel cell endurance tests. Platinum alloy cathode catalysts and low-loaded platinum electrodes were evaluated in 25 sq cm cells. Although the alloys displayed an initial improvement, some of this improvement diminished after a few thousand hours of testing. Low platinum loading (0.12 mg/sq cm anodes and 0.3 mg/sq cm cathodes) performed nearly as well as twice this loading. A selectively wetproofed anode backing paper was tested in a 5 by 15 inch three-cell stack. This material may provide for acid volume expansion, acid storage, and acid lateral distribution. R.S.F.

**N84-27327\*#** National Aeronautics and Space Administration. Lewis Research Center, Cleveland, Ohio.  
**LARGE, HORIZONTAL-AXIS WIND TURBINES** Final Report  
 B. S. LINSKOTT, P. PERKINS (Analex Corp.), and J. T. DENNETT (RDD Consultants, Inc.) Mar. 1984 73 p refs  
 (Contract DE-AI01-76ET-20320)  
 (NASA-TM-83546; DOE/NASA/20320-58, E-1920; NAS 1.15:83546) Avail: NTIS HC A04/MF A01 CSCL 10B

Development of the technology for safe, reliable, environmentally acceptable large wind turbines that have the potential to generate a significant amount of electricity at costs competitive with conventional electric generating systems are presented. In addition, these large wind turbines must be fully compatible with electric utility operations and interface



## 44 ENERGY PRODUCTION AND CONVERSION

requirements. There are several ongoing large wind system development projects and applied research efforts directed toward meeting the technology requirements for utility applications. Detailed information on these projects is provided. The Mod-O research facility and current applied research effort in aerodynamics, structural dynamics and aeroelasticity, composite and hybrid composite materials, and multiple system interaction are described. A chronology of component research and technology development for large, horizontal axis wind turbines is presented. Wind characteristics, wind-turbine economics, and the impact of wind turbines on the environment are reported. The need for continued wind turbine research and technology development is explored. Over 40 references are cited and a bibliography is included.

Author

**N84-27329\*** Engelhard Minerals and Chemicals Corp., Edison, N. J.

**DEVELOP AND TEST FUEL CELL POWERED ON-SITE INTEGRATED TOTAL ENERGY SYSTEMS Quarterly Report, Feb. - Apr. 1984**

A. KAUFMAN, S. PUDICK, C. L. WANG, J. WERTH, and J. A. WHELAN 31 May 1984 25 p  
(Contract DEN3-241; DE-AI01-80ET-17088)  
(NASA-CR-174714; DOE/NASA/0241-13; NAS 1.26:174714; QR-12) Avail: NTIS HC A02/MF A01 CSCL 10B

On-going testing of an 11 cell, 10.7 in. x 14 in. stack (about 1 kW) reached 2600 hours on steady load. Nonmetallic cooling plates and an automated electrolyte replenishment system continued to perform well. A 10 cell, 10.7 in. x 14 in. stack was constructed with a modified electrolyte matrix configuration for the purpose of reducing cell IR loss. The desired effect was achieved, but the general cell performance level was irregular. Evaluation is continuing. Preparations for a long term 25 cell, 13 in. x 23 in. test stack (about 4 kW) approached completion. Start up in early May 1984 is expected.

Author

**N84-28205\*** National Aeronautics and Space Administration. Lewis Research Center, Cleveland, Ohio.

**CHROMIUM ELECTRODES FOR REDOX CELLS Patent**

V. JALAN, M. A. REID, and A. CHARLESTON, inventors (to NASA) 19 Jun. 1984 8 p Filed 26 Feb. 1982 Supersedes N82-22672 (20 - 13, p 1822)

(NASA-CASE-LEW-13653-1; US-PATENT-4,454,649; US-PATENT-APPL-SN-352821; US-PATENT-CLASS-29-623.5; US-PATENT-CLASS-29-825; US-PATENT-CLASS-427-113; US-PATENT-CLASS-427-115; US-PATENT-CLASS-427-125; US-PATENT-CLASS-427-226; US-PATENT-CLASS-427-379; US-PATENT-CLASS-427-380; US-PATENT-CLASS-427-372.2; US-PATENT-CLASS-427-443; US-PATENT-CLASS-429-44; US-PATENT-CLASS-204-290) Avail: US Patent and Trademark Office CSCL 10C

An improved electrode having a gold coating for use in the anode compartment of a REDOX cell is described. The anode fluid utilizes a chromic/chromous couple. A carbon felt is soaked in methanol, rinsed in water, dried and then heated in KOH after which it is again washed in deionized water and dried. The felt is then moistened with a methanol water solution containing chloroauric acid and is stored in a dark place while still in contact with the gold-containing solution. After all the gold-containing solution is absorbed in the felt, the latter is dried by heat and then heat treated at a substantially greater temperature. The felt is then suitable for use as an electrode and is wetted with water or up to two molar HCl prior to installation in a REDOX cell. The novelty of the invention lies in the use of KOH for cleaning the felt and the use of alcohol as a carrier for the gold together with the heat treating procedure.

Official Gazette of the U.S. Patent and Trademark Office

**N84-29307\*** National Aeronautics and Space Administration. Lewis Research Center, Cleveland, Ohio.

**SPACE PHOTOVOLTAIC RESEARCH AND TECHNOLOGY 1983. HIGH EFFICIENCY, RADIATION DAMAGE, AND BLANKET TECHNOLOGY**

Washington, D.C. 1984 266 p refs Conf. held in Cleveland, 18-20 Oct. 1983

(NASA-CP-2314; E-2005; NAS 1.55:2314) Avail: NTIS HC A12/MF A01 CSCL 10A

This three day conference, sixth in a series that began in 1974, was held at the NASA Lewis Research Center on October 18-20, 1983. The conference provided a forum for the discussion of space photovoltaic systems, their research status, and program goals. Papers were presented and workshops were held in a variety of technology areas, including basic cell research, advanced blanket technology, and radiation damage.

**N84-29312\*** National Aeronautics and Space Administration. Lewis Research Center, Cleveland, Ohio.

**OPTIMAL DESIGN OF GAAS-BASED CONCENTRATOR SPACE SOLAR CELLS FOR 100 AMO, 80 DEG C OPERATION**

C. GORADIA (Cleveland State Univ.), M. GHALLA-GORADIA (Cleveland State Univ.), and H. CURTIS *In its* Space Photovoltaic Res. and Technol. 1983 p 25-33 1984  
(Contract NAG3-249)

Avail: NTIS HC A12/MF A01 CSCL 10A

Using a detailed computer code and reasonable values of electrical and optical material parameters from current published literature, parameter optimization studies were performed on three configurations of GaAs-based concentrator solar cells for 100 AMO, 80 C operation. These studies show the possibility of designing GaAs-based solar cells with efficiencies exceeding 22% at 100 AMO 80 C and probable efficiency degradation of less than 15% after a 70% reduction in diffusion length in each cell region.

Author

**N84-29318\*** National Aeronautics and Space Administration. Lewis Research Center, Cleveland, Ohio.

**RADIATION TOLERANCE OF LOW RESISTIVITY, HIGH VOLTAGE SILICON SOLAR CELLS**

V. G. WEIZER, I. WEINBERG, and C. K. SWARTZ *In its* Space Photovoltaic Res. and Technol. 1983 p 74-80 1984 refs

Avail: NTIS HC A12/MF A01 CSCL 10A

The radiation tolerance of the following three low resistivity, high voltage silicon solar cells was investigated: (1) the COMSAT MSD (multi-step diffused) cell, (2) the MinMIS cell, and (3) the MIND cell. A description of these solar cells is given along with drawings of their configurations. The diffusion length damage coefficients for the cells were calculated and presented. Solar cell spectral response was also discussed. Cells of the MinMIS type were judged to be unsuitable for use in the space radiation environment.

R.S.F.

**N84-29322\*** National Aeronautics and Space Administration. Lewis Research Center, Cleveland, Ohio.

**CELL AND DEFECT BEHAVIOR IN LITHIUM-COUNTERDOPED SOLAR CELLS**

I. WEINBERG, S. MEHTA (Cleveland State Univ.), and C. K. SWARTZ *In its* Space Photovoltaic Res. and Technol. 1983 p 102-110 1984 refs

Avail: NTIS HC A12/MF A01 CSCL 10A

Some n(+)/p cells in which lithium is introduced as a counterdopant, by ion-implantation, into the cell's boron-doped p-region were studied. To determine if the cells radiation resistance could be significantly improved by lithium counterdoping. Defect behavior was related to cell performance using deep level transient spectroscopy. Results indicate a significantly increased radiation resistance for the lithium counterdoped cells when compared to the boron doped 1 ohm-cm control cell. The increased radiation resistance of the lithium counterdoped cells is due to the complexing of lithium with divacancies and boron. It is speculated that complexing with oxygen and single vacancies also contributes



to the increased radiation resistance. Counterdoping silicon with lithium results in a different set of defects. A.R.H.

**N84-29328\*#** Varian Associates, Palo Alto, Calif.  
**DEVELOPMENT OF A 30 PERCENT EFFICIENT 3-JUNCTION MONOLITHIC CASCADE SOLAR CELL**

C. R. LEWIS, W. T. DIETZE, and M. J. LUDOWISE *In* NASA. Lewis Research Center Space Photovoltaic Res. and Technol. 1983 p 140-147 1984 refs Sponsored in part by SERI (Contract NAS3-22232)

Avail: NTIS HC A12/MF A01 CSCL 10A

The individual subcells of the 3-junction monolithic cascade concentrator cell are grown lattice mismatched with respect to each other, if appropriate grading layers are inserted between the mismatched layers. Under these conditions, negligible degradation of the properties of either underlying or overlying material results, and high-efficiency subcells are produced by this technique.

Author

**N84-29330\*#** National Aeronautics and Space Administration. Lewis Research Center, Cleveland, Ohio.

**PLASMON DEVICE DESIGN: CONVERSION FROM SURFACE TO JUNCTION PLASMONS WITH GRATING-COUPLEDERS Abstract Only**

L. M. ANDERSON *In its* Space Photovoltaic Res. and Technol. 1983 p 155 1984

Avail: NTIS HC A12/MF A01 CSCL 10A

Scaling calculations and numerical studies are used to show that grating couplers provide effective energy transfer between surface plasmons and slower modes localized in the tunnel diodes. Within first order perturbation theory in grating amplitude, 90% efficiency energy transfer occurs within micrometers for realistic structures and materials parameters. Scaling laws are derived. Seventy to 90% of the electromagnetic field energy is concentrated in the oxide layer of an MOM diode after the energy is distributed by longer range modes that have less than 0.1% overlap with the tunneling region. The mode conversion allows the requirements separation for energy transport and power production by inelastic tunneling. M.A.C.

**N84-29340\*#** National Aeronautics and Space Administration. Lewis Research Center, Cleveland, Ohio.

**HIGH SPEED, LOW COST, LEO-THERMAL-CYCLING FACILITY**  
 R. E. HART, JR. and L. G. SIDORAK *In its* Space Photovoltaic Res. and Technol. 1983 p 223-227 1984

Avail: NTIS HC A12/MF A01 CSCL 10A

The design and operations of a low cost, high rate thermal cycling facility designed for LEO conditions is described. Thermal cycling facilities were constructed with various design criteria. Some were designed to duplicate as closely as possible the conditions a cell or module would encounter while in orbit about the Earth. A typical facility to perform this type of cycling was a large vacuum system with liquid nitrogen cooled walls. The cells were heated by an AMO spectrum solar simulator, then a shutter was closed allowing the cells to give up their heat to the cold walls. This system was good at duplicating the orbital conditions but was slow and very costly to operate. Other systems used a gas atmosphere and heated the cells with radiant heat and cooled the cells by moving them into close proximity to a cold plate. The systems greatly increased the cycle times. Other systems moved the heating and cooling atmosphere into and out of the test areas and achieved reasonable cycle rates. All these systems, however, are expensive to operate. E.A.K.

**N84-29342\*#** National Aeronautics and Space Administration. Lewis Research Center, Cleveland, Ohio.

**ELECTROCHEMICAL STORAGE Abstract Only**

L. H. THALLER *In its* Space Photovoltaic Res. and Technol. 1983 p 235 1984

Avail: NTIS HC A12/MF A01 CSCL 10C

The source of the problem within the individual single cell which is related to the stochastic properties of cell populations and to the actual electrochemistry and chemistry taking place is described.

The complications which arise in multicell batteries to show how different electrochemistries might alleviate or accentuate these problems is described. The concept of the electrochemical system is introduced to show how certain shortcomings of the single cell/battery string concept can be circumvented. Some of these electrochemical systems permit performance characteristics that are impossible by using conventional battery design philosophies. Projections for energy density and performance characteristics of the concepts are addressed. E.A.K.

**N84-29343\*#** National Aeronautics and Space Administration. Lewis Research Center, Cleveland, Ohio.

**SOLAR ARRAY: PLASMA INTERACTIONS Abstract Only**

C. K. PURVIS *In its* Space Photovoltaic Res. and Technol. 1983 p 236 1984

Avail: NTIS HC A12/MF A01 CSCL 10A

Interactions between space systems and their orbital particle and field environments have significant impact on the system's operation and life. Interactions such as radiation damage and aerodynamic drag are considered in designing space systems. There are, however, a number of orbital environmental interactions which become important design considerations only for large or high power systems. Their impact is assessed to ensure successful design. Interactions between higher voltage solar arrays and the space plasma which are of critical concern in designing large orbital photovoltaic power systems are outlined. E.A.K.

**N84-29347\*#** National Aeronautics and Space Administration. Lewis Research Center, Cleveland, Ohio.

**EFFECT OF VORTEX GENERATORS ON THE POWER CONVERSION PERFORMANCE AND STRUCTURAL DYNAMIC LOADS OF THE MOD-2 WIND TURBINE Final Report**

T. L. SULLIVAN Jun. 1984 29 p refs

(Contract DE-A101-76ET-20320)

(NASA-TM-83680; E-2131; DOE/NASA/20320-59; NAS

1.15:83680) Avail: NTIS HC A03/MF A01 CSCL 10A

Applying vortex generators from 20 to 100 percent span of the Mod-2 rotor resulted in a projected increase in annual energy capture of 20 percent and reduced the wind speed at which rated power is reached by nearly 3 m/sec. Application of vortex generators from 20 to 70 percent span, the fixed portion of the Mod-2 rotor, resulted in a projected increase in annual energy capture of about half this. This improved performance came at the cost of a small increase in cyclic blade loads in below rated power conditions. Cyclic blade loads were found to correlate well with the change in wind speed during one rotor revolution.

Author

**N84-29357\*#** Westinghouse Electric Corp., Pittsburgh, Pa. Advanced Systems Technology.

**WIND TURBINE GENERATOR INTERACTION WITH CONVENTIONAL DIESEL GENERATORS ON BLOCK ISLAND, RHODE ISLAND. VOLUME 1: EXECUTIVE SUMMARY Final Report**

V. F. WILREKER, P. H. STILLER, G. W. SCOTT, V. J. KRUSE, and R. F. SMITH Feb. 1984 47 p refs

(Contract DEN3-275; DEN3-354; DE-A101-76ET-20320)

(NASA-CR-168318; DOE/NASA/0354-1; NAS 1.26:168318;

AST-84-1808) Avail: NTIS HC A03/MF A01 CSCL 10B

Primary results are summarized for a three-part study involving the effects of connecting a MOD-OA wind turbine generator to an isolated diesel power system. The MOD-OA installation considered was the third of four experimental nominal 200 kW wind turbines connected to various utilities under the Federal Wind Energy Program and was characterized by the highest wind energy penetration levels of four sites. The study analyses address: fuel displacement, dynamic interaction, and three modes of reactive power control. These analyses all have as their basis the results of the data acquisition program conducted on Block Island, Rhode Island. A.R.H.

## 44 ENERGY PRODUCTION AND CONVERSION

**N84-29358\*#** Ionics, Inc., Watertown, Mass. Research Div.  
**ANION PERMSELECTIVE MEMBRANE Final Report**  
R. B. HODGDON, W. A. WAITE, and S. S. ALEXANDER 17 Jul. 1984 48 p  
(Contract DEN3-264; DE-AI04-80AL-12726)  
(NASA-CR-174725; DOE/NASA/0264-1; NAS 1.26:174725)  
Avail: NTIS HC A03/MF A01 CSCL 10A

Two polymer ion exchange membranes were synthesized to fulfill the needs of both electrical resistivity and anolyte/catholyte separation for utility load leveling utilizing the DOE/NASA mixed electrolyte REDOX battery. Both membranes were shown to meet mixed electrolyte utility load leveling criteria. Several modifications of an anion exchange membrane failed to meet utility load leveling REDOX battery criteria using the unmixed electrolyte REDOX cell.

Author

**N84-30528\*#** National Aeronautics and Space Administration  
Lewis Research Center, Cleveland, Ohio.  
**DEVELOPMENT OF A LIGHTWEIGHT NICKEL ELECTRODE**  
D. L. BRITTON and M. A. REID Aug. 1984 20 p refs  
(NASA-TM-86861; E-1967; NAS 1.15:86861) Avail: NTIS HC A02/MF A01 CSCL 10C

Nickel electrodes made using lightweight plastic plaque are about half the weight of electrodes made from state of the art sintered nickel plaque. This weight reduction would result in a significant improvement in the energy density of batteries using nickel electrodes (nickel hydrogen, nickel cadmium and nickel zinc). These lightweight electrodes are suitably conductive and yield comparable capacities (as high as 0.25 AH/gm (0.048 AH/sq cm)) after formation. These lightweight electrodes also show excellent discharge performance at high rates.

Author

**N84-31782\*#** National Aeronautics and Space Administration.  
Lewis Research Center, Cleveland, Ohio.  
**PHOTOVOLTAICS: THE ENDLESS SPRING**  
H. W. BRANDHORST, JR. 1984 15 p Presented at the 17th Photovoltaic Spec. Conf., Kissimmee, Fla., 1-4 May 1984; sponsored by the Institute of Electrical and Electronic Engineers (NASA-TM-83684; E-2121; NAS 1.15:83684) Avail: NTIS HC A02/MF A01 CSCL 10A

An overview of the developments in the photovoltaic field over the past decade or two is presented. Accomplishments in the terrestrial field are reviewed along with projections and challenges toward meeting cost goals. The contrasts and commonality of space and terrestrial photovoltaics are presented. Finally, a strategic philosophy of photovoltaics research highlighting critical factors, appropriate directions, emerging opportunities, and challenges of the future is given.

Author

**N84-31783\*#** Westinghouse Electric Corp., Pittsburgh, Pa.  
Advanced Systems Technology.  
**WIND TURBINE GENERATOR INTERACTION WITH CONVENTIONAL DIESEL GENERATORS ON BLOCK ISLAND, RHODE ISLAND. VOLUME 2: DATA ANALYSIS Final Report**  
V. F. WILREKER, P. H. STILLER, G. W. SCOTT, V. J. KRUSE, and R. F. SMITH Feb. 1984 140 p refs  
(Contract DEN3-954; DE-AI01-76ET-20320)  
(NASA-CR-168319; DOE/NASA/0354-2; NAS 1.26:168319; AST-84-1808-VOL-2) Avail: NTIS HC A07/MF A01 CSCL 10A

Assessing the performance of a MOD-OA horizontal axis wind turbine connected to an isolated diesel utility, a comprehensive data measurement program was conducted on the Block Island Power Company installation on Block Island, Rhode Island. The detailed results of that program focusing on three principal areas of (1) fuel displacement (savings), (2) dynamic interaction between the diesel utility and the wind turbine, (3) effects of three models of wind turbine reactive power control are presented. The approximate two month duration of the data acquisition program conducted in the winter months (February into April 1982) revealed performance during periods of highest wind energy penetration and hence severity of operation. Even under such conditions fuel savings were significant resulting in a fuel reduction of 6.7% while the MOD-OA was generating 10.7% of the total electrical energy.

Also, electrical disturbance and interactive effects were of an acceptable level.

Author

**N84-31784\*#** Catalytic, Inc., Philadelphia, Pa.  
**AFB/OPEN CYCLE GAS TURBINE CONCEPTUAL DESIGN STUDY Final Report**

T. W. DICKINSON and R. TASHJIAN Sep. 1983 422 p refs  
(Contract DEN3-257; DE-AI01-77ET-13111)  
(NASA-CR-168135; DOE/NASA/0257-1; NAS 1.26:168135; CATALYTIC-43790) Avail: NTIS HC A18/MF A01 CSCL 10B

Applications of coal fired atmospheric fluidized bed gas turbine systems in industrial cogeneration are identified. Based on site-specific conceptual designs, the potential benefits of the AFB/gas turbine system were compared with an atmospheric fluidized design steam boiler/steam turbine system. The application of these cogeneration systems at four industrial plant sites is reviewed. A performance and benefit analysis was made along with a study of the representativeness of the sites both in regard to their own industry and compared to industry as a whole. A site was selected for the conceptual design, which included detailed site definition, AFB/gas turbine and AFB/steam turbine cogeneration system designs, detailed cost estimates, and comparative performance and benefit analysis. Market and benefit analyses identified the potential market penetration for the cogeneration technologies and quantified the potential benefits.

Author

**N84-32909\*#** National Aeronautics and Space Administration.  
Lewis Research Center, Cleveland, Ohio.  
**NEGATIVE ELECTRODE CATALYST FOR THE IRON-CHROMIUM REDOX ENERGY STORAGE SYSTEM Patent Application**

R. F. GAHN and N. H. HAGEDORN, inventors (to NASA) 20 Aug. 1984 14 p  
(NASA-CASE-LEW-14028-1; NAS 1.71:LEW-14028-1; US-PATENT-APPL-SN-642310) Avail: NTIS HC A02/MF A01 CSCL 10C

A redox cell which operates at elevated temperatures and which utilizes the same two metal couples in each of the two reactant fluids is disclosed. Each fluid includes a bismuth salt and may also include a lead salt. A low cost, cation permselective membrane separates the reactant fluids.

NASA

**N84-34036\*#** Institute of Gas Technology, Chicago, Ill.  
Engineering Research Div.

**ADVANCED ONBOARD STORAGE CONCEPTS FOR NATURAL GAS-FUELED AUTOMOTIVE VEHICLES Final Report**

R. J. REMICK, R. H. ELKINS, E. H. CAMARA, and T. BULICZ Jun. 1984 139 p refs  
(Contract DEN3-327; DE-AI01-81CS-50006)  
(NASA-CR-174655; DOE/NASA/0327-1; NAS 1.26:174655)  
Avail: NTIS HC A07/MF A01 CSCL 10B

The evaluation of several advanced concepts for storing natural gas at reduced pressure is presented. The advanced concepts include adsorption on high surface area carbon, adsorption in high porosity zeolite, storage in clathration compounds, and storage by dissolution in liquid solvents. High surface area carbons with high packing density are the best low pressure storage mediums. A simple mathematical model is used to compare adsorption storage on a state of the art carbon with compression storage. The model indicates that a vehicle using adsorption storage of natural gas at 3.6 MPa will have 36 percent of the range, on the EPA city cycle, of a vehicle operating on a compression storage system having the same physical size and a peak storage pressure of 21 MPa. Preliminary experiments and current literature suggest that the storage capacity of state of the art carbons could be improved by as much as 50 percent, and that adsorption systems having a capacity equal to compression storage at 14 MPa are possible without exceeding a maximum pressure of 3.6 MPa.

M.A.C.

**N84-34037\*#** Cleveland State Univ., Ohio.  
**MANUAL OF PHOSPHORIC ACID FUEL CELL POWER PLANT COST MODEL AND COMPUTER PROGRAM Final Report**  
 C. Y. LU and K. A. ALKASAB May 1984 39 p refs  
 (Contract NCC3-17; DE-AI21-80ET-17088)  
 (NASA-CR-174720; DOE/NASA/0017-2; NAS 1.26:174720)  
 Avail: NTIS HC A03/MF A01 CSCL 10B

Cost analysis of phosphoric acid fuel cell power plant includes two parts: a method for estimation of system capital costs, and an economic analysis which determines the levelized annual cost of operating the system used in the capital cost estimation. A FORTRAN computer has been developed for this cost analysis.

Author

**N84-34038\*#** National Aeronautics and Space Administration, Lewis Research Center, Cleveland, Ohio.  
**COGENERATION TECHNOLOGY ALTERNATIVES STUDY (CTAS). VOLUME 2: COMPARISON AND EVALUATION OF RESULTS**

Aug. 1984 394 p refs  
 (Contract DE-AI01-77ET-13111)  
 (NASA-TM-81401; E-311; DOE/NASA/13111-14; NAS 1.15:81401) Avail: NTIS HC A17/MF A01 CSCL 10B

CTAS compared and evaluated various advanced energy conversion systems that can use coal or coal-derived fuels for industrial cogeneration applications. The principal aim of the study was to provide information needed by DOE to establish research and development (R&D) funding priorities for advanced-technology systems that could significantly advance the use of coal or coal-derived fuels in industrial cogeneration. Steam turbines, diesel engines, open-cycle gas turbines, combined cycles, closed-cycle gas turbines, Stirling engines, phosphoric acid fuel cells, molten carbonate fuel cells, and thermionics were studied with technology advancements appropriate for the 1985-2000 time period. The various advanced systems were compared and evaluated for a wide diversity of representative industrial plants on the basis of fuel energy savings, annual energy cost savings, emissions savings, and rate of return on investment (ROI) as compared with purchasing electricity from a utility and providing process heat with an on-site boiler.

B.W.

## 45

### ENVIRONMENT POLLUTION

Includes air, noise, thermal and water pollution; environment monitoring; and contamination control.

**A84-41044\*** Mechanical Technology, Inc., Latham, N. Y.  
**COMPARISON OF STEADY-STATE AND TRANSIENT CVS CYCLE EMISSION OF AN AUTOMOTIVE STIRLING ENGINE**  
 R. A. FARRELL and R. J. BOLTON (Mechanical Technology, Inc., Latham, NY) Society of Automotive Engineers, Fuels and Lubrication Conference, San Francisco, CA, Oct. 31-Nov. 4, 1983, Paper. 8 p. Research sponsored by the U.S. Department of Energy. refs  
 (Contract DEN3-32)

The Automotive Stirling Engine Development Program is to demonstrate a number of goals for a Stirling-powered vehicle. These goals are related to an achievement of specified maximum emission rates, a combined cycle fuel economy 30 percent better than a comparable internal-combustion engine-powered automobile, multifuel capability, competitive cost and reliability, and a meeting of Federal standards concerning noise and safety. The present investigation is concerned with efforts related to meeting the stringent emission goals. Attention is given to the initial development of a procedure for predicting transient CVS urban cycle gaseous emissions from steady-state engine data, taking into account the employment of the test data from the first-generation automotive Stirling engine. A large amount of

steady-state data from three Mod I automotive Stirling engines were used to predict urban CVS cycle emissions for the Mod I Lerma vehicle.

G.R.

**N84-11594\*#** National Aeronautics and Space Administration, Lewis Research Center, Cleveland, Ohio.  
**BACTERIAL DEGRADATION OF POLYCHLORINATED BIPHENYLS IN SLUDGE FROM AN INDUSTRIAL SEWER LAGOON**

W. S. KIM, A. M. TAKACS (Case Western Reserve Univ.), and D. E. KUIVINEN 1983 13 p Presented at the PCB Seminar, Atlanta, 6-8 Dec. 1983; sponsored by EPRI  
 (NASA-TM-83543; E-1915; NAS 1.15:83543) Avail: NTIS HC A02/MF A01 CSCL 13B

A laboratory experiment was conducted to determine if polychlorinated biphenyls (PCB's) found in an industrial sewer sludge can be effectively degraded by mutant bacteria. The aerated sludge was inoculated daily with mutant bacteria in order to augment the existing bacteria with bacteria that were considered to be capable of degrading PCB's. The pH, nitrogen, and phosphorus levels were monitored daily to maintain an optimum growing medium for the bacteria. A gas chromatographic method was used to determine the PCB concentrations of the sludge initially and also throughout the experiment. Results and discussion of the bacterial treatment of polychlorinated biphenyls are presented.

Author

## 46

### GEOPHYSICS

Includes aeronomy; upper and lower atmosphere studies; ionospheric and magnetospheric physics; and geomagnetism.

**N84-25204\*#** National Aeronautics and Space Administration, Washington, D. C.  
**EFFECTS OF CHEMICAL RELEASES BY THE STS-3 ORBITER ON THE IONOSPHERE Final Report**

J. S. PICKETT (Iowa Univ., Iowa City), G. B. MURPHY (Iowa Univ., Iowa City), W. S. KURTH (Iowa Univ., Iowa City), C. K. GOERTZ (Iowa Univ., Iowa City), and S. D. SHAWHAN Dec. 1983 43 p refs Submitted for publication  
 (Contract NAS8-32807; NAG3-449)  
 (NASA-CR-171032; NAS 1.26:171032; U-OF-IOWA-84-5) Avail: NTIS HC A03/MF A01 CSCL 04A

The Plasma Diagnostics Package, flown aboard STS-3 as part of the first Shuttle payload (OSS-1), recorded the effects of various chemical releases from the Orbiter. Changes in the plasma environment was observed during flash evaporator system releases, water dumps and maneuvering thruster operations. During flash evaporator operations, broadband Orbiter-generated electrostatic noise was enhanced and plasma density irregularities were observed to increase by 3 to 30 times with a spectrum which rose steeply and peaked below 6 Hz. In the case of water dumps, background electrostatic noise was enhanced at frequencies below about 3 kHz and suppressed at frequencies above 2 kHz. Thruster activity also stimulated electrostatic noise with a spectrum which peaked at approximately 0.5 kHz. In addition, ions with energies up to 1 keV were seen during some thruster events.

Author

## METEOROLOGY AND CLIMATOLOGY

Includes weather forecasting and modification.

**A84-23424\*** National Aeronautics and Space Administration. Marshall Space Flight Center, Huntsville, Ala.

**SIXTH ANNUAL WORKSHOP ON METEOROLOGICAL AND ENVIRONMENTAL INPUTS TO AVIATION SYSTEMS, 26-28 OCTOBER 1982, TULLAHOMA, TENN**

D. W. CAMP (NASA, Marshall Space Flight Center, Huntsville, AL), W. FROST (Tennessee University, Tullahoma, TN), F. COONS (FAA, Washington, DC), P. EVANICH (NASA, Lewis Research Center, Cleveland, OH), and C. H. SPRINKLE (NOAA, National Weather Service, Silver Spring, MD) American Meteorological Society, Bulletin (ISSN 0003-0007), vol. 65, Jan. 1984, p. 44-47. refs

The six workshops whose proceedings are presently reported considered the subject of meteorological and environmental information inputs to aviation, in order to satisfy workshop-sponsoring agencies' requirements for (1) greater knowledge of the interaction of the atmosphere with aircraft and airport operators, (2) a better definition and implementation of meteorological services to operators, and (3) the collection and interpretation of data useful in establishing operational criteria that relate the atmospheric science input to aviation community operations. Workshop topics included: equipment and instrumentation, forecasts and information updates, training and simulation facilities, and severe weather, icing and wind shear.

O.C.

**A84-40399\*** National Aeronautics and Space Administration. Lewis Research Center, Cleveland, Ohio.

**TROPICAL RESPONSE TO LATERAL FORCING WITH A LATITUDINALLY AND ZONALLY NONUNIFORM BASIC STATE**  
J. D. WILSON (NASA, Lewis Research Center, Cleveland, OH; Illinois University, Urbana-Champaign, IL) and M. MAK (Illinois University, Urbana-Champaign, IL) Journal of the Atmospheric Sciences (ISSN 0022-4928), vol. 41, April 1, 1984, p. 1187-1201. refs

(Contract NSF ATM-80-19423)

The dynamics of lateral forcing of a stable tropical atmosphere by incident waves from the midlatitudes are examined. Attention is focused on conditions where the WKB method is invalid, and only given to barotropic flows. The tropical atmosphere is treated as a steady planetary wave and a zonal shear flow. The 200 mb level is investigated in terms of a midlatitude wave with self-compatible parametric values that is constrained to satisfy the radiation conditions at the boundary. Wave modes are found to be susceptible to trapping between two turning points in the equatorial zone in the presence of a zonal shear flow. Quasi-resonant waves can then appear over a wide range of parametric conditions of the forcing wave and the basic state. The zonal wind structure determines the resonance conditions.

M.S.K.

**N84-18806\*** National Aeronautics and Space Administration. Lewis Research Center, Cleveland, Ohio.

**TABULATIONS OF AMBIENT OZONE DATA OBTAINED BY GASP (GLOBAL AIR SAMPLING PROGRAM) AIRLINERS, MARCH 1975 TO JULY 1979**

W. H. JASPERSON (Control Data Corp., Minneapolis) and J. D. HOLDEMAN Jan. 1984 141 p refs

(Contract DOT-FA78WAI-893)

(NASA-TM-82742; E-1055; NAS 1.15:82742) Avail: NTIS HC A07/MF A01 CSCL 04B

Tabulations are given of GASP ambient ozone mean, standard deviation, median, 84th percentile, and 98th percentile values, by month, flight level, and geographical region. These data are tabulated to conform to the temporal and spatial resolution required

by FAA Advisory Circular 120-38 (monthly by 2000 ft in altitude by 5 deg in latitude) for climatological data used to show compliance with cabin ozone regulations. In addition seasonal x 10 deg latitude tabulations are included which are directly comparable to and supersede the interim GASP ambient ozone tabulations given in appendix B of FAA-EE-80-43 (NASA TM-81528). Selected probability variations are highlighted to illustrate the spatial and temporal variability of ambient ozone and to compare results from the coarse-and-fine gnd analyses.

Author

**N84-27375\*# Control Data Corp., Minneapolis, Minn. TABULATIONS OF OZONESONDE DATA, 1963 - 1980 Final Report**

W. H. JASPERSON and R. W. WILCOX Mar. 1984 345 p refs

(Contract NAS3-21249; DOT-FA78WAI-893)

(NASA-CR-174631; NAS 1.26:174631; FAA-EE-83-13) Avail:

NTIS HC A15/MF A01 CSCL 04B

Ozonesonde data available from the period 1962 to 1980 were compiled and statistics computed. Seasonal and monthly statistics of the mean, standard deviation and the empirical 50th, 84th, and 98th percentiles of ozone are presented as a function of height. The gridded format parallels the format of the GASP data summaries to make an easy comparison.

E.A.K.

**N84-31865\*# National Aeronautics and Space Administration. Lewis Research Center, Cleveland, Ohio.**

**CLIMATOLOGY OF OZONE AT ALTITUDES FROM 19,000 AT 59,000 FEET BASED ON COMBINED GASP AND OZONESONDE DATA**

W. H. JASPERSON (Control Data Corp.), G. D. NASTROM (Control Data Corp.), and J. D. HOLDEMAN Aug. 1984 363 p refs

(Contract DOT-FA78WAI-893)

(NASA-TP-2303; E-1626; NAS 1.60:2303) Avail: NTIS HC

A16/MF A01 CSCL 04B

A climatology of ozone for altitudes from FL190 to FL590 (19,000 to 59,000 ft) is presented. Climatological tables are given in two appendixes: one with 1 deg latitude resolution on a monthly basis, and one with 10 deg latitude resolution on a seasonal basis. Data were taken from 11,472 balloon-borne ozonesondes launched at 60 stations from 1963 to 1980 and from over 160,000 observations made by the Global Atmospheric Sampling Program on 4417 commercial airliner flights from 1975 to 1979. Case study and statistical comparisons of results from these two data sets showed that they are compatible and can be combined. Several examples of analyses that can be made by using the tabulated data are given and discussed.

Author

## AEROSPACE MEDICINE

Includes physiological factors; biological effects of radiation; and weightlessness.

**N84-23095\*** National Aeronautics and Space Administration. Lewis Research Center, Cleveland, Ohio.

**METHOD OF MAKING AN ION BEAM SPUTTER-ETCHED VENTRICULAR CATHETER FOR HYDROCEPHALUS SHUNT Patent**

B. A. BANKS, inventor (to NASA) 21 Feb. 1984 8 p Filed 24 Nov. 1982 Division of Serial No. 272407, filed 10 Jun. 1981, Patent No. 4,377,169

(NASA-CASE-LEW-13107-2; US-PATENT-4,432,853;

US-PATENT-APPL-SN-444124; US-PATENT-CLASS-204-192E;

US-PATENT-CLASS-156-643; US-PATENT-CLASS-156-644;

US-PATENT-CLASS-156-668) Avail: US Patent and Trademark

Office CSCL 06B

The centricular catheter comprises a multiplicity of inlet microtubules. Each microtubule has both a large opening at its

inlet end and a multiplicity of microscopic openings along its lateral surfaces. The microtubules are perforated by an ion beam sputter etch technique. The holes are etched in each microtubule by directing an ion beam through an electro formed mesh mask producing perforations having diameters ranging from about 14 microns to about 150 microns. This structure assures a reliable means for shunting cerebrospinal fluid from the cerebral ventricles to selected areas of the body.

Official Gazette of the U.S. Patent and Trademark Office

## 54

### MAN/SYSTEM TECHNOLOGY AND LIFE SUPPORT

Includes human engineering, biotechnology; and space suits and protective clothing.

**A84-49108\*** Iowa Univ., Iowa City.  
**PREDICTION OF TURBULENT FLOW PAST A PROSTHETIC HEART VALVE**  
 C. H. YU, C. J. CHEN, and K. B. CHANDRAN (Iowa, University, Iowa City, IA) IN: Developments in mechanics. Volume 12 - Midwestern Mechanics Conference, 18th, Iowa City, IA, May 16-18, 1983, Proceedings. Iowa City, IA, University of Iowa, 1983, p. 107-110. refs  
 (Contract PHS-HL-26269; NSG-3305)

## 60

### COMPUTER OPERATIONS AND HARDWARE

Includes computer graphics and data processing

**A84-11876\*** California Univ., Los Angeles.  
**PARALLELISM AND PIPELINING IN HIGH-SPEED DIGITAL SIMULATORS**  
 W. J. KARPLUS (California, University, Los Angeles, CA) IN: World Congress on System Simulation and Scientific Computation, 10th, Montreal, Canada, August 8-13, 1982, Proceedings. Volume 1. Montreal, International Association for Mathematics and Computers in Simulation, 1983, p. 272-274. refs  
 (Contract NAG3-132)

The attainment of high computing speed as measured by the computational throughput is seen as one of the most challenging requirements. It is noted that high speed is cardinal in several distinct classes of applications. These classes are then discussed; they comprise (1) the real-time simulation of dynamic systems, (2) distributed parameter systems, and (3) mixed lumped and distributed systems. From the 1950s on, the quest for high speed in digital simulators concentrated on overcoming the limitations imposed by the so-called von Neumann bottleneck. Two major architectural approaches have made it possible to circumvent this bottleneck and attain high speeds. These are pipelining and parallelism. Supercomputers, peripheral array processors, and microcomputer networks are then discussed. C.R.

**A84-39972\*** TRW, Inc., El Segundo, Calif.

### A SCHEME FOR HANDLING ARRAYS IN DATA-FLOW SYSTEMS

J.-L. GAUDIOT (TRW Technology Research Center, El Segundo, CA) and M. D. ERCEGOVAC (California, University, Los Angeles, CA) IN: Institute of Electrical and Electronics Engineers, International Conference on Distributed Computing Systems, 3rd, Hollywood, FL, October 17-21, 1982, Proceedings New York, Institute of Electrical and Electronics Engineers, 1982, p. 724-729. refs  
 (Contract NAG3-132)

An examination of the effects of atomicity (higher resolution) on the performance of array processors (data-flow computers) is presented. Data-flow principles are reviewed, noting the reliance on parallel processing using functional languages to specify sequencing of the operations. Techniques are described for eliminating the necessity of copying whole arrays between processing steps, thereby reducing the number of store cycles. The method involves setting whole columns to specific values rather than individual elements. The individual column values can be processed in parallel, i.e., a locally optimized condition exists. A drawback of the system is the need for more low level arguments, to identify the appropriate processing sequences, and high system complexity. M.S.K.

**A84-40266\*** Carnegie-Mellon Univ., Pittsburgh, Pa.  
**ACOUSTOOPTIC LINEAR ALGEBRA PROCESSORS - ARCHITECTURES, ALGORITHMS, AND APPLICATIONS**  
 D. CASASSENT (Carnegie-Mellon University, Pittsburgh, PA) IEEE, Proceedings (ISSN 0018-9219), vol. 72, July 1984, p. 831-849  
 Research supported by the Unicorn Systems, Inc refs  
 (Contract NAG3-5; AF-AFOSR-79-0091; NAG1-409)

Architectures, algorithms, and applications for systolic processors are described with attention to the realization of parallel algorithms on various optical systolic array processors. Systolic processors for matrices with special structure and matrices of general structure, and the realization of matrix-vector, matrix-matrix, and triple-matrix products and such architectures are described. Parallel algorithms for direct and indirect solutions to systems of linear algebraic equations and their implementation on optical systolic processors are detailed with attention to the pipelining and flow of data and operations. Parallel algorithms and their optical realization for LU and QR matrix decomposition are specifically detailed. These represent the fundamental operations necessary in the implementation of least squares, eigenvalue, and SVD solutions. Specific applications (e.g., the solution of partial differential equations, adaptive noise cancellation, and optimal control) are described to typify the use of matrix processors in modern advanced signal processing. Author

**N84-12730\*** National Aeronautics and Space Administration. Lewis Research Center, Cleveland, Ohio.  
**A GRAPHICS SUBSYSTEM RETROFIT DESIGN FOR THE BLADED-DISK DATA ACQUISITION SYSTEM M.S. Thesis**  
 R. R. CARNEY Jan. 1983 74 p refs  
 (NASA-TM-83510; E-1760; NAS 1.15:83510) Avail: NTIS HC A04/MF A01 CSCL 09B

A graphics subsystem retrofit design for the turbojet blade vibration data acquisition system is presented. The graphics subsystem will operate in two modes permitting the system operator to view blade vibrations on an oscilloscope type of display. The first mode is a real-time mode that displays only gross blade characteristics, such as maximum deflections and standing waves. This mode is used to aid the operator in determining when to collect detailed blade vibration data. The second mode of operation is a post-processing mode that will animate the actual blade vibrations using the detailed data collected on an earlier data collection run. The operator can vary the rate of playback to view differing characteristics of blade vibrations. The heart of the graphics subsystem is a modified version of AMD's "super sixteen" computer, called the graphics preprocessor computer (GPC). This computer is based on AMD's 2900 series of bit-slice components. Author

**N84-16812\*#** National Aeronautics and Space Administration  
Lewis Research Center, Cleveland, Ohio.

**A REAL-TIME, PORTABLE, MICROCOMPUTER-BASED JET ENGINE SIMULATOR**

R. A. BLECH, J. F. SOEDER, and J. R. MIHALOEW 1984 12 p refs Presented at the 1984 Simulators Mini-Conf., Norfolk, Va., 18-20 Apr. 1984; sponsored by the Society for Computer Simulation

(NASA-TM-83550, E-1925; NAS 1.15:83550) Avail: NTIS HC A02/MF A01 CSCL 09B

Modern piloted flight simulators require detailed models of many aircraft components, such as the airframe, propulsion system, flight deck controls and instrumentation, as well as motion drive and visual display systems. The amount of computing power necessary to implement these systems can exceed that offered by dedicated mainframe computers. One approach to this problem is through the use of distributed computing, where parts of the simulation are assigned to computing subsystems, such as microcomputers. One such subsystem, such as microcomputers. One such subsystem, a real-time, portable, microcomputer-based jet engine simulator, is described in this paper. The simulator will be used at the NASA Ames Vertical Motion Simulator facility to perform calculations previously done on the facility's mainframe computer. The mainframe will continue to do all other system calculations and will interface to the engine simulator through analog I/O. The engine simulator hardware includes a 16-bit microcomputer and floating-point coprocessor. There is an 8 channel analog input board and an 8 channel analog output board. A model of a small turboshaft engine/control is coded in floating-point FORTRAN. The FORTRAN code and a data monitoring program run under the control of an assembly language real-time executive. The monitoring program allows the user to display and/or modify simulator variables on-line through a data terminal. A dual disk drive system is used for mass storage of programs and data. The CP/M-86 operating system provides file management and overall system control. The frame time for the simulator is 30 milliseconds, which includes all analog I/O operations. Author

## 61

## COMPUTER PROGRAMMING AND SOFTWARE

Includes computer programs, routines, and algorithms

**A84-10905\* College of William and Mary, Williamsburg, Va. ADA AND MULTI-MICROPROCESSOR REAL-TIME SIMULATION**

S. FEYOCK and W. R. COLLINS (College of William and Mary, Williamsburg, VA) IN: Annual Simulation Symposium, 16th, Tampa, FL, March 16-18, 1983, Record of Proceedings. Silver Spring, MD, IEEE Computer Society Press, 1983, p. 211-228. refs (Contract NAG3-232)

The selection of a high-order programming language for a real-time distributed network simulation is described. The additional problem of implementing a language on a possibly changing network is addressed. The recently designed language ADA (trademarked by DoD) was chosen since it provides the best model of the underlying application to be simulated. Author

**A84-11892\* Arizona State Univ., Tempe. SOFTWARE SIMULATOR FOR MULTIPLE COMPUTER SIMULATION SYSTEM**

E. P. OGRADY (Arizona State University, Tempe, AZ) IN: World Congress on System Simulation and Scientific Computation, 10th, Montreal, Canada, August 8-13, 1982, Proceedings. Volume 1. Montreal, International Association for Mathematics and Computers in Simulation, 1983, p. 352-354. refs (Contract NAG3-112)

A description is given of the structure and use of a computer program that simulates the operation of a parallel processor

simulation system. The program is part of an investigation to determine algorithms that are suitable for simulating continuous systems on a parallel processor configuration. The simulator is designed to accurately simulate the problem-solving phase of a simulation study. Care has been taken to ensure the integrity and correctness of data exchanges and to correctly sequence periods of computation and periods of data exchange. It is pointed out that the functions performed during a problem-setup phase or a reset phase are not simulated. In particular, there is no attempt to simulate the downloading process that loads object code into the local, transfer, and mapping memories of processing elements or the memories of the run control processor and the system control processor. The main program of the simulator carries out some problem-setup functions of the system control processor in that it requests the user to enter values for simulation system parameters and problem parameters. The method by which these values are transferred to the other processors, however, is not simulated. C.R.

**A84-21305\*#** National Aeronautics and Space Administration. Lewis Research Center, Cleveland, Ohio.

**A REAL-TIME IMPLEMENTATION OF AN ADVANCED SENSOR FAILURE DETECTION, ISOLATION, AND ACCOMMODATION ALGORITHM**

J. C. DELAAT and W. C. MERRILL (NASA, Lewis Research Center, Cleveland, OH) American Institute of Aeronautics and Astronautics, Aerospace Sciences Meeting, 22nd, Reno, NV, Jan. 9-12, 1984. 12 p. refs (AIAA PAPER 84-0569)

A sensor failure detection, isolation, and accommodation algorithm was developed which incorporates analytic sensor redundancy through software. This algorithm was implemented in a high level language on a microprocessor based controls computer. Parallel processing and state-of-the-art 16-bit microprocessors are used along with efficient programming practices to achieve real-time operation. Previously announced in STAR as N84-13140 Author

**N84-13812\*#** National Aeronautics and Space Administration. Lewis Research Center, Cleveland, Ohio.

**PREWATE: AN INTERACTIVE PREPROCESSING COMPUTER CODE TO THE WEIGHT ANALYSIS OF TURBINE ENGINES (WATE) COMPUTER CODE**

L. H. FISHBACH Dec. 1983 53 p refs (NASA-TM-83545; E-1917; NAS 1.15:83545) Avail: NTIS HC A04/MF A01 CSCL 09B

The Weight Analysis of Turbine Engines (WATE) computer code was developed by Boeing under contract to NASA Lewis. It was designed to function as an adjunct to the Navy/NASA Engine Program (NNEP). NNEP calculates the design and off-design thrust and sfc performance of User defined engine cycles. The thermodynamic parameters throughout the engine as generated by NNEP are then combined with input parameters defining the component characteristics in WATE to calculate the bare engine weight of this User defined engine. Preprocessor programs for NNEP were previously developed to simplify the task of creating input datasets. This report describes a similar preprocessor for the WATE code. Author

**N84-25336\*# California Univ., Los Angeles. DATAFLOW COMPUTING APPROACH IN HIGH-SPEED DIGITAL SIMULATION Final Report, 15 Dec. 1980 - 14 Dec. 1982**

M. D. ERCEGOVAC and W. J. KARPLUS Jun. 1984 5 p refs (Contract NAG3-132) (NASA-CR-173552; NAS 1.26:173552) Avail: NTIS HC A02/MF A01 CSCL 09B

New computational tools and methodologies for the digital simulation of continuous systems were explored. Programmability, and cost effective performance in multiprocessor organizations for real time simulation was investigated. Approach is based on functional style languages and data flow computing principles, which allow for the natural representation of parallelism in algorithms and provides a suitable basis for the design of cost

effective high performance distributed systems. The objectives of this research are to. (1) perform comparative evaluation of several existing data flow languages and develop an experimental data flow language suitable for real time simulation using multiprocessor systems; (2) investigate the main issues that arise in the architecture and organization of data flow multiprocessors for real time simulation; and (3) develop and apply performance evaluation models in typical applications.

**N84-26209\*#** National Aeronautics and Space Administration. Lewis Research Center, Cleveland, Ohio.

**HIGH VOLTAGE SOLAR ARRAY MODELS AND SHUTTLE TILE CHARGING**

A. G. RUBIN and N. J. STEVENS *in* AFGL Proc. of the AFGL Workshop on Nat. Charging of Large Space Struct. in Near Earth Polar Orbit p 333-336 25 Jan. 1983 Prepared in cooperation with AFGL, Hanscom AFB, Mass  
(AD-P002123) Avail: NTIS HC A18/MF A01 CSCL 09B

This paper described NASCAP/LEO (NASA Charging Analyzer Program/Low Earth Orbit) a 3-D computer code that simulates the interaction of space plasma with high-voltage solar arrays in the thin plasma sheath regime. The code requires information about the object and the ambient plasma. The geometric description, the material composition and the voltage distribution versus time of a solar array are the data required about the object. The plasma properties needed are the composition, density, and temperature. NASCAP/LEO will then provide the time-dependent current to each element of area of the array from the external plasma. The NASCAP/LEO output is provided in both three dimensional computer graphics and in numerical form. NASCAP/LEO is user oriented and will provide potential distributions around the object, the currents to each of the conductors, and graphical details of the sheaths and particle trajectories

GRA

## 62

### COMPUTER SYSTEMS

Includes computer networks.

**A84-10010\*#** General Dynamics/Convair, San Diego, Calif.  
**GRAPHICS ENHANCED COMPUTER EMULATION FOR IMPROVED TIMING-RACE AND FAULT TOLERANCE CONTROL SYSTEM ANALYSIS**

G. P. SZATKOWSKI (General Dynamics Corp., Convair Div., San Diego, CA) *IN: Computers in Aerospace Conference, 4th, Hartford, CT, October 24-26, 1983, Collection of Technical Papers*. New York, American Institute of Aeronautics and Astronautics, 1983, p. 55-63.

(Contract NAS3-22324)

(AIAA PAPER 83-2328)

A computer simulation system has been developed for the Space Shuttle's advanced-Centaur liquid fuel booster rocket, in order to conduct systems safety verification and flight operations training. This simulation utility is designed to analyze functional system behavior by integrating control avionics with mechanical and fluid elements, and is able to emulate any system operation, from simple relay logic to complex VLSI components, with wire-by-wire detail. A novel graphics data entry system offers a pseudo-wire wrap data base that can be easily updated. Visual subsystem operations can be selected and displayed in color on a six-monitor graphics processor. System timing and fault verification analyses are conducted by injecting component fault modes and min/max timing delays, and then observing system operation through a red line monitor.

O.C.

**N84-20258\*#** National Aeronautics and Space Administration. Lewis Research Center, Cleveland, Ohio.

**OPERATING SYSTEM FOR A REAL-TIME MULTIPROCESSOR PROPULSION SYSTEM SIMULATOR**

G. L. COLE 1984 11 p refs To be presented at the Summer Computer Simulation Conf., Boston, 23-25 Jul. 1984 (NASA-TM-83605; E-2023; NAS 1.15:83605) Avail: NTIS HC A02/MF A01 CSCL 09B

The success of the Real Time Multiprocessor Operating System (RTMPOS) in the development and evaluation of experimental hardware and software systems for real time interactive simulation of air breathing propulsion systems was evaluated. The Real Time Multiprocessor Operating System (RTMPOS) provides the user with a versatile, interactive means for loading, running, debugging and obtaining results from a multiprocessor based simulator. A front end processor (FEP) serves as the simulator controller and interface between the user and the simulator. These functions are facilitated by the RTMPOS which resides on the FEP. The RTMPOS acts in conjunction with the FEP's manufacturer supplied disk operating system that provides typical utilities like an assembler, linkage editor, text editor, file handling services, etc. Once a simulation is formulated, the RTMPOS provides for engineering level, run time operations such as loading, modifying and specifying computation flow of programs, simulator mode control, data handling and run time monitoring. Run time monitoring is a powerful feature of RTMPOS that allows the user to record all actions taken during a simulation session and to receive advisories from the simulator via the FEP. The RTMPOS is programmed mainly in PASCAL along with some assembly language routines. The RTMPOS software is easily modified to be applicable to hardware from different manufacturers. M.A.C.

**N84-20259\*#** National Aeronautics and Space Administration. Lewis Research Center, Cleveland, Ohio.

**RTMPL: A STRUCTURED PROGRAMMING AND DOCUMENTATION UTILITY FOR REAL-TIME MULTIPROCESSOR SIMULATIONS**

D. J. ARPASI 1984 8 p refs To be presented at the Summer Computer Simulation Conf., Boston, 23-25 Jul. 1984 (NASA-TM-83606; E-2025; NAS 1.15:83606) Avail: NTIS HC A02/MF A01 CSCL 09B

The NASA Lewis Research Center is developing and evaluating experimental hardware and software systems to help meet future needs for real time simulations of air-breathing propulsion systems. The Real Time Multiprocessor Simulator (RTMPS) project is aimed at developing a prototype simulator system that uses multiple microprocessors to achieve the desired computing speed and accuracy at relatively low cost. Software utilities are being developed to provide engineering-level programming and interactive operation of the simulator. Two major software development efforts were undertaken in the RTMPS project. A real time multiprocessor operating system was developed to provide for interactive operation of the simulator. The second effort was aimed at developing a structured, high-level, engineering-oriented programming language and translator that would facilitate the programming of the simulator. The Real Time Multiprocessor Programming Language (RTMPL) allows the user to describe simulation tasks for each processor in a straight-forward, structured manner. The RTMPL utility acts as an assembly language programmer, translating the high-level simulation description into time-efficient assembly language code for the processors. The utility sets up all of the interfaces between the simulator hardware, firmware, and operating system. Author



## CYBERNETICS

Includes feedback and control theory.

**A84-23602\*** Carnegie-Mellon Univ., Pittsburgh, Pa.  
**STATE ESTIMATION KALMAN FILTER USING OPTICAL PROCESSINGS-NOISE STATISTICS KNOWN**  
J. JACKSON and D. CASASANT (Carnegie-Mellon University, Pittsburgh, PA) Applied Optics (ISSN 0003-6935), vol. 23, Feb. 1, 1984, p. 376-378. refs  
(Contract AF-AFOSR-79-0091; NAG3-5)

Reference is made to a study by Casasent et al. (1983), which gave a description of a frequency-multiplexed acoustooptic processor and showed how it was capable of performing all the individual operations required in Kalman filtering. The data flow and organization of all required operations however, were not detailed in that study. Consideration is given here to a simpler Kalman filter state estimation problem. Equally spaced time-sampled intervals ( $k$  times  $T$  sub  $s$ , with  $k$  the iterative time index) are assumed. It is further assumed that the system noise vector  $w$  and the measurement noise vector  $v$  are uncorrelated and Gaussian distributed and that the noise statistics ( $Q$  and  $R$ ) and the system model ( $\Phi$ ,  $\Gamma$ ,  $H$ ) are known. The error covariance matrix  $P$  and the extrapolated error covariance matrix  $M$  can thus be precomputed and the Kalman gain matrix  $K$  sub  $k$  can be precomputed and stored for each input time sample.

C.R.

**A84-38596\*** Carnegie-Mellon Univ., Pittsburgh, Pa.  
**OPTICAL KALMAN FILTERING FOR MISSILE GUIDANCE**  
D. CASASANT, C. P. NEUMAN, and J. LYCAS (Carnegie-Mellon University, Pittsburgh, PA) Applied Optics (ISSN 0003-6935), vol. 23, June 15, 1984, p. 1960-1966. refs  
(Contract NAG3-5; AF-AFOSR-79-0091)

Optical systolic array processors constitute a powerful and general-purpose set of optical architectures with high computational rates. In this paper, Kalman filtering, a novel application for these architectures, is investigated. All required operations are detailed; their realization by optical and special-purpose analog electronics are specified; and the processing time of the system is quantified. The specific Kalman filter application chosen is for an air-to-air missile guidance controller. The architecture realized in this paper meets the design goal of a fully adaptive Kalman filter which processes a measurement every 1 msec. The vital issue of flow and pipelining of data and operations in a systolic array processor is addressed. The approach is sufficiently general and can be realized on an optical or digital systolic array processor. Author

**N84-16843\*#** National Aeronautics and Space Administration. Lewis Research Center, Cleveland, Ohio.  
**AESOP: AN INTERACTIVE COMPUTER PROGRAM FOR THE DESIGN OF LINEAR QUADRATIC REGULATORS AND KALMAN FILTERS**  
B. LEHTINEN and L. C. GEYSER Jan. 1984 115 p refs  
(NASA-TP-2221; E-1686; NAS 1.60-2221) Avail: NTIS HC A06/MF A01 CSCL 09B

AESOP is a computer program for use in designing feedback controls and state estimators for linear multivariable systems. AESOP is meant to be used in an interactive manner. Each design task that the program performs is assigned a 'function' number. The user accesses these functions either (1) by inputting a list of desired function numbers or (2) by inputting a single function number. In the latter case the choice of the function will in general depend on the results obtained by the previously executed function. The most important of the AESOP functions are those that design linear quadratic regulators and Kalman filters. The user interacts with the program when using these design functions by inputting design weighting parameters and by viewing graphic displays of designed system responses Supporting functions are

provided that obtain system transient and frequency responses, transfer functions, and covariance matrices. The program can also compute open-loop system information such as stability (eigenvalues), eigenvectors, controllability, and observability. The program is written in ANSI-66 FORTRAN for use on an IBM 3033 using TSS 370. Descriptions of all subroutines and results of two test cases are included in the appendixes. Author

## NUMERICAL ANALYSIS

Includes iteration, difference equations, and numerical approximation.

**N84-11831\*#** National Aeronautics and Space Administration. Lewis Research Center, Cleveland, Ohio.  
**EMBEDDING METHODS FOR THE STEADY EULER EQUATIONS**  
S. H. CHANG and G. M. JOHNSON Jul. 1983 12 p refs  
(Contract NAG3-339)  
(NASA-TM-83481; E-1803; NAS 1.15:83481) Avail: NTIS HC A02/MF A01 CSCL 12A

An approach to the numerical solution of the steady Euler equations is to embed the first-order Euler system in a second-order system and then to recapture the original solution by imposing additional boundary conditions. Initial development of this approach and computational experimentation with it were previously based on heuristic physical reasoning. This has led to the construction of a relaxation procedure for the solution of two-dimensional steady flow problems. The theoretical justification for the embedding approach is addressed. It is proven that, with the appropriate choice of embedding operator and additional boundary conditions, the solution to the embedded system is exactly the one to the original Euler equations. Hence, solving the embedded version of the Euler equations will not produce extraneous solutions. M.G.

**N84-13885\*#** National Aeronautics and Space Administration. Lewis Research Center, Cleveland, Ohio.  
**ACCELERATION OF CONVERGENCE OF VECTOR SEQUENCES**  
A. SIDI, W. F. FORD, and D. A. SMITH (Duke Univ., Durham, N.C.) Dec. 1983 27 p refs  
(Contract NAS3-23606; NSG-3160)  
(NASA-TP-2193; E-1719; NAS 1.60-2193) Avail: NTIS HC A03/MF A01 CSCL 12A

A general approach to the construction of convergence acceleration methods for vector sequence is proposed. Using this approach, one can generate some known methods, such as the minimal polynomial extrapolation, the reduced rank extrapolation, and the topological epsilon algorithm, and also some new ones. Some of the new methods are easier to implement than the known methods and are observed to have similar numerical properties. The convergence analysis of these new methods is carried out, and it is shown that they are especially suitable for accelerating the convergence of vector sequences that are obtained when one solves linear systems of equations iteratively. A stability analysis is also given, and numerical examples are provided. The convergence and stability properties of the topological epsilon algorithm are likewise given. Author

**N84-20537\*#** National Aeronautics and Space Administration. Lewis Research Center, Cleveland, Ohio.  
**APPLICATION OF IMPROVED NUMERICAL SCHEMES**  
G. H. NEELY In its Combust. Fundamentals Res. p 95-96  
Apr. 1984 refs  
Avail: NTIS HC A14/MF A01 CSCL 12A

Two approaches which accelerate the solution of the steady state Navier-Stokes equations are discussed. The SIMPLER algorithm, a revised version of SIMPLE, provides a more accurate

pressure field for each iteration through the momentum equations, thereby speeding convergence. PISO (Pressure Implicit Split Operator), performs a secondary correction of the velocity and pressure fields (after the typical pressure correction) which enhances convergence. Both schemes account for terms neglected in the SIMPLE approach, but do so in slightly different ways. Two dimensional driven cavity flow and flow over a step were calculated to examine the effect of geometry on the performance of these schemes. Computations were carried out on a series of progressively finer grids. The effect of relaxation number on convergence rate was analyzed, using results from SIMPLE as criteria for performance correlation. Results show: (1) the improved schemes promoted convergence by up to 60% for the driven cavity and 40% for flow over a step; (2) for the driven cavity problem, the efficiency of PISO and SIMPLER increased as the number of nodes increased; and (3) to ensure faster convergence, higher relaxation numbers must be applied. A.R.H.

**N84-31279\***# Seattle Univ., Wash.

**EXPONENTIAL-FITTED METHODS FOR INTEGRATING STIFF SYSTEMS OF ORDINARY DIFFERENTIAL EQUATIONS: APPLICATIONS TO HOMOGENEOUS GAS-PHASE CHEMICAL KINETICS**

D. T. PRATT *In* APL Computational Methods. 1984 JPM Spec. Session p 53-68 Feb. 1984 refs  
(Contract NAG3-227)

Avail: NTIS HC A05/MF A01 CSCL 12A

Conventional algorithms for the numerical integration of ordinary differential equations (ODEs) are based on the use of polynomial functions as interpolants. However, the exact solutions of stiff ODEs behave like decaying exponential functions, which are poorly approximated by polynomials. An obvious choice of interpolant are the exponential functions themselves, or their low-order diagonal Padé (rational function) approximants. A number of explicit, A-stable, integration algorithms were derived from the use of a three-parameter exponential function as interpolant, and their relationship to low-order, polynomial-based and rational-function-based implicit and explicit methods were shown by examining their low-order diagonal Padé approximants. A robust implicit formula was derived by exponential fitting the trapezoidal rule. Application of these algorithms to integration of the ODEs governing homogenous, gas-phase chemical kinetics was demonstrated in a developmental code CREK1D, which compares favorably with the Gear-Hindmarsh code LSODE in spite of the use of a primitive stepsize control strategy. Author

## 65

### STATISTICS AND PROBABILITY

Includes data sampling and smoothing; Monte Carlo method; and stochastic processes.

**N84-17982\***# National Aeronautics and Space Administration. Lewis Research Center, Cleveland, Ohio.

**A STUDY OF NUCLEATION AND GROWTH OF THIN FILMS BY MEANS OF COMPUTER SIMULATION: GENERAL FEATURES**

J. SALIK 1984 14 p refs Proposed for presentation at the 11th Intern. Conf. on Metall. Coatings, San Diego, Calif., 9-13 Apr. 1984; sponsored by Am. Vacuum Soc.  
(NASA-TM-83559; E-1869; NAS 1.15:83559) Avail: NTIS HC A02/MF A01 CSCL 12A

Some of the processes involved in the nucleation and growth of thin films were simulated by means of a digital computer. The simulation results were used to study the nucleation and growth kinetics resulting from the various processes. Kinetic results obtained for impingement, surface migration, impingement combined with surface migration, and with reevaporation are presented. A substantial fraction of the clusters may form directly

upon impingement. Surface migration results in a decrease in cluster density, and reevaporation of atoms from the surface causes a further reduction in cluster density. Author

## 70

### PHYSICS (GENERAL)

**A84-24410\*** California Univ., Irvine.

**INTERFERENCE PHENOMENA IN THE REFRACTION OF A SURFACE POLARITON BY VERTICAL DIELECTRIC BARRIERS**

T. P. SHEN, R. F. WALLIS, A. A. MARADUDIN (California, University, Irvine, CA), and G. I. STEGEMAN (Arizona, University, Tucson, AZ) Applied Optics (ISSN 0003-6935), vol. 23, Feb. 15, 1984, p. 607-611. refs

(Contract DAAG29-82-K-0018; NAG3-392)

A normal mode analysis is used to calculate the transmission and reflection coefficients for a surface polariton propagating along the interface between a surface active medium and a dielectric and incident normally on a vertical dielectric barrier of finite thickness or a thin dielectric film of finite length. The efficiencies of conversion of the surface polariton into transmitted and reflected bulk waves are also determined. The radiation patterns associated with the latter waves are presented. Author

**N84-28565\*** National Aeronautics and Space Administration. Lewis Research Center, Cleveland, Ohio.

**ION SPUTTER TEXTURED GRAPHITE ELECTRODE PLATES Patent**

A. N. CURREN, R. FORMAN, J. S. SOVEY, and E. G. WINTUCKY, inventors (to NASA) 22 Nov. 1983 7 p Filed 31 Mar. 1982 Supersedes N82-26386 (20 - 17, p 2370) Division of US Patent Application SN-264378, US Patent-4,349,424, filed 15 May 1981 (NASA-CASE-LEW-12919-2; US-PATENT-4,417,175; US-PATENT-4,349,424; US-PATENT-APPL-SN-364072; US-PATENT-APPL-SN-264378, US-PATENT-CLASS-315-5.38; US-PATENT-CLASS-313-106; US-PATENT-CLASS-313-107; US-PATENT-CLASS-313-351) Avail: US Patent and Trademark Office CSCL 20C

A specially textured surface of pyrolytic graphite exhibits extremely low yields of secondary electrons and reduced numbers of reflected primary electrons after impingement of high energy primary electrons. Electrode plates of this material are used in multistage depressed collectors. An ion flux having an energy between 500 eV and 1000 eV and a current density between 1.0 mA/sq cm and 6.0 mA/sq cm produces surface roughening or texturing which is in the form of needles or spires. Such textured surfaces are especially useful as anode collector plates in high tube devices.

Official Gazette of the U.S. Patent and Trademark Office

## 71

### ACOUSTICS

Includes sound generation, transmission, and attenuation.

**A84-10136\***# North Carolina State Univ., Raleigh.

**SUPERSONIC JET SCREECH TONE CANCELLATION**

R. T. NAGEL, J. W. DENHAM, and A. G. PAPATHANASIOU (North Carolina State University, Raleigh, NC) AIAA Journal (ISSN 0001-1452), vol. 21, Nov. 1983, p. 1541-1545. refs  
(Contract NAG3-189)

A new method of supersonic jet screech tone reduction is presented. The method utilizes a sound reflecting surface

positioned upstream of the nozzle exit a distance of one-quarter wavelength of the fundamental screech tone. The reflector establishes a standing wave pattern of acoustic waves with a node at the nozzle exit plane. The pressure minimum at the exit halts the screech tone feedback mechanism. Experimental results indicate that the method eliminates supersonic jet screech as effectively as the currently accepted technique using an intrusive tab, but without distortion of the jet flow. The change in shock cell spacing, which occurs with an intrusive tab, does not occur when screech is cancelled with the new technique. The broadband shock-associated noise is also influenced much less when the jet screech tones are eliminated by the new method. Author

**A84-18131\*** Georgia Inst. of Tech., Atlanta.

**A PARAMETRIC STUDY OF THE EFFECT OF INLET LIP SHAPE UPON THE RADIATED SOUND FIELD**

W. L. MEYER and B. T. ZINN (Georgia Institute of Technology, Atlanta, GA) American Institute of Aeronautics and Astronautics, Aerospace Sciences Meeting, 22nd, Reno, NV, Jan. 9-12, 1984. 6 p. refs

(Contract NAG3-67)

(AIAA PAPER 84-0498)

Far field sound radiation predictions for four different axisymmetric inlet lips excited by different tangential acoustic modes at several cut-off ratios are presented. These results were obtained by numerical integration of a special cylindrically symmetric integral representation of the external solutions of the Helmholtz equation which yields unique solutions at all wave numbers. The paper presents plots which detail the dependence of the relative SPL (dB) in the field upon the engine inlet lip shape, the modal input, and the cut-off ratio. Examination of these data indicate that: (1) as the inlet lip becomes larger the predominant acoustic radiation peak in the field becomes narrower and moves towards the centerline of the inlet; (2) as the order of the tangential acoustic mode of the driver increases the radiated sound peak again becomes narrower but moves away from the inlet centerline; and (3) as the cut-off ratio is increased for a specific tangential acoustic mode the predominant radiation peak becomes narrower and moves towards the centerline of the inlet.

Author

**A84-21184\*** Georgia Inst. of Tech., Atlanta.

**A FINITE ELEMENT APPROACH FOR PREDICTING NOZZLE ADMITTANCES**

R. K. SIGMAN and B. T. ZINN (Georgia Institute of Technology, Atlanta, GA) Journal of Sound and Vibration (ISSN 0022-460X), vol. 88, May 8, 1983, p. 117-131. refs

(Contract NSG-3036)

A finite element method is used to predict the admittances of axisymmetric nozzles. It is assumed that the flow in the nozzle is isentropic and the disturbances are small so that linear analyses apply. An approximate, two dimensional compressible model is used to describe the steady flow in the nozzle. The propagation of acoustic disturbances is governed by the complete linear wave equation. The differential form of the acoustic equation is transformed to an integral equation by using Galerkin's method, and Green's theorem is applied so that the acoustic boundary conditions can be introduced through the boundary residuals. The boundary conditions are described for both straight and curved sonic lines. A two dimensional FEM with linear elements is used to solve the acoustic equation. A one dimensional FEM is also used to solve the reduced equation of Crocco, and the solution verifies the sufficiency of the boundary residual formulation. Comparison between computed admittances and experimental data is shown to be quite good. Author

**A84-21250\*** Missouri Univ., Rolla.

**A NUMERICAL MODEL OF ACOUSTIC CHOKING. I - SHOCK FREE SOLUTIONS**

N. J. WALKINGTON and W. EVERSMAN (Missouri-Rolla, University, Rolla, MO) Journal of Sound and Vibration (ISSN 0022-460X), vol. 90, Oct. 22, 1983, p. 509-526. refs

(Contract NAG3-178)

The phenomenon of acoustic choking in near sonic flows is investigated using the one-dimensional gasdynamic equations for an ideal gas. It is pointed out that this approach eliminates the need to make the classical small disturbance assumption. A finite difference scheme is elaborated to approximate these equations. Boundary conditions that correctly model the physics of the acoustics problems are chosen. The use of a fast Fourier transform routine allows the results to be compared with those obtained by using the conventional harmonic assumptions. Only solutions in which shocks have not fully developed are reported. Continuous solutions are sought, and these are compared with the Fubini solution and with certain results of Myers and Callegari (1977, 1978, 1979). C.R.

**A84-21272\*** Lockheed-Georgia Co., Marietta.

**ACOUSTIC POWER DISSIPATION ON RADIATION THROUGH DUCT TERMINATIONS - EXPERIMENTS**

M. SALIKUDDIN and K. K. AHUJA (Lockheed-Georgia Co., Marietta, GA) Journal of Sound and Vibration (ISSN 0022-460X), vol. 91, Dec 22, 1983, p. 479-502. Research sponsored by the Lockheed Independent Research and Development Program. refs

(Contract NAS3-20797)

This paper describes the acoustic transmission characteristics of ducts, nozzles, orifices, and perforated plates, studied under an experimental program using an acoustic impulse technique. In this technique high intensity pulses, generated by discharging a capacitor across a spark gap, were used as the sound source. The test conditions include heated and unheated flows, with and without simulated flight. Results for a straight round duct, three convergent nozzles, a suppressor nozzle, 12 orifice plates, and 10 perforated plates are presented. A low frequency acoustic power loss phenomenon was observed for all configurations at all test conditions including the no flow condition. It was suspected that the power loss phenomenon at the no flow condition could be due to the conversion of acoustic energy into vortical energy due to non-linear propagation of high intensity pulses. However, a small amount of low frequency power loss was noticed even when tests were repeated with a low intensity sound. Detailed flow visualization results were also obtained to complement the acoustic results.

Author

**A84-21273\*** National Aeronautics and Space Administration. Lewis Research Center, Cleveland, Ohio.

**HIGH FREQUENCY GREEN FUNCTION FOR AERODYNAMIC NOISE IN MOVING MEDIA. I - GENERAL THEORY. II - NOISE FROM A SPREADING JET**

P. A. DURBIN (NASA, Lewis Research Center, Cleveland, OH) Journal of Sound and Vibration (ISSN 0022-460X), vol. 91, Dec 22, 1983, p. 519-525, 527-538. refs

It is shown how a high frequency analysis can be made for general problems involving flow-generated noise. In the parallel shear flow problem treated by Balsa (1976) and Goldstein (1982), the equation governing sound propagation in the moving medium could be transformed into a wave equation for a stationary medium with an inhomogeneous index of refraction. It is noted that the procedure of Avila and Keller (1963) was then used to construct a high frequency Green function. This procedure involves matching a solution valid in an inner region around the point source to an outer, ray-acoustics solution. This same procedure is used here to construct the Green function for a source in an arbitrary mean flow. In view of the fact that there is no restriction to parallel flow, the governing equations cannot be transformed into a wave equation; the analysis therefore proceeds from the equations of motion themselves. C.R.

**A84-21304\*#** National Aeronautics and Space Administration. Lewis Research Center, Cleveland, Ohio.

**ON SOME FLOW CHARACTERISTICS OF CONVENTIONAL AND EXCITED JETS**

U. H. VON GLAHN (NASA, Lewis Research Center, Cleveland, OH) American Institute of Aeronautics and Astronautics, Aerospace Sciences Meeting, 22nd, Reno, NV, Jan. 9-12, 1984. 13 p. refs  
(AIAA PAPER 84-0532)

Improved correlations of jet centerline velocity and static temperature decay data for convergent nozzles are developed. From these empirical correlations, a relationship was devised by which the static temperature decay for a nonisothermal jet plume can be determined from cold-flow jet centerline velocity decay data or prediction. This relationship is shown to apply as well to jet plumes for various nozzle shapes. It is assumed, by analogy, that this relationship also applies to acoustically excited jet plumes. Jet plume spreading with and without excitation is discussed. Finally, the radial velocity and temperature profiles for conventional and enhanced mixing jet flows are shown and their implication for excited flows is discussed. Previously announced in STAR as N84-13922 Author

**A84-22584\*#** National Aeronautics and Space Administration. Lewis Research Center, Cleveland, Ohio.

**AEROACOUSTICS OF TURBULENT SHEAR FLOWS**

M. E. GOLDSTEIN (NASA, Lewis Research Center, Cleveland, OH) IN: Annual review of fluid mechanics Volume 16. Palo Alto, CA, Annual Reviews, Inc., 1984, p. 263-285. refs

Recent analytical, numerical-simulation and experimental studies of sound generation by high-Reynolds-number turbulent shear flows are reviewed, with a focus on the application of linear rapid-distortion theory to the calculation of the unsteady flow field producing the sound. This approach is considered the most important alternative to acoustic-analogy methods. Topics surveyed include the linear theory of solid-surface interactions, the jet-noise problem, extensions to more complex turbulent flows, and supersonic flows. Graphs comparing theoretical and experimental results are shown. D.G.

**A84-23355\*#** Houston Univ., Tex.

**JET NOISE MODIFICATION BY THE 'WHISTLER NOZZLE'**

M. A. Z. HASAN, O. ISLAM, and A. K. M. F. HUSSAIN (Houston, University, Houston, TX) AIAA Journal (ISSN 0001-1452), vol. 22, March 1984, p. 340-347. refs  
(Contract NSF MEA-81-11676; NAG3-198)

The farfield noise characteristics of a subsonic whistler nozzle jet are measured as a function of Mach number (0.25, 0.37, and, 0.51), emission angle, and excitation mode. It is shown that a whistler nozzle has greater total and broadband acoustic power than an excited contraction nozzle; and that the intensity of far-field noise is a function of emission angle, Mach number, and whistler excitation stage. The whistler nozzle excitation produces broadband noise amplification with constant spectral shape; the broadband noise amplification (without associated whistler tones and harmonics) increases omnidirectionally with emission angle at all Mach numbers; and the broadband amplification factor decreases as Mach number and emission angle increase. Finally the whistler nozzle is described as a very efficient but inexpensive siren with applications in not only jet excitation but also acoustics. C.M.

**A84-24597\*** Florida State Dept. of Education, Tallahassee. **SOUND GENERATED BY INSTABILITY WAVES OF SUPERSONIC FLOWS. I TWO-DIMENSIONAL MIXING LAYERS. II - AXISYMMETRIC JETS**

C. K. W. TAM and D. E. BURTON (Florida State University, Tallahassee, FL) Journal of Fluid Mechanics (ISSN 0022-1120), vol. 138, Jan. 1984, p. 249-271, 273-295. refs  
(Contract NSF CME-78-05122-A01; NAG3-182)

An investigation is conducted of the phenomenon of sound generation by spatially growing instability waves in high-speed flows. It is pointed out that this process of noise generation is most effective when the flow is supersonic relative to the ambient speed

of sound. The inner and outer asymptotic expansions corresponding to an excited instability wave in a two-dimensional mixing layer and its associated acoustic fields are constructed in terms of the inner and outer spatial variables. In matching the solutions, the intermediate matching principle of Van Dyke and Cole is followed. The validity of the theory is tested by applying it to an axisymmetric supersonic jet and comparing the calculated results with experimental measurements. Very favorable agreements are found both in the calculated instability-wave amplitude distribution (the inner solution) and the near pressure field level contours (the outer solution) in each case. G.R.

**A84-31103\*** Virginia Polytechnic Inst., Blacksburg.

**A TEMPERATURE CORRELATION FOR THE RADIATION RESISTANCE OF A THICK-WALLED CIRCULAR DUCT EXHAUSTING A HOT GAS**

J. R. MAHAN, J. G. CLINE, and J. D. JONES (Virginia Polytechnic Institute and State University, Blacksburg, VA) Acoustical Society of America, Journal (ISSN 0001-4966), vol. 75, Jan. 1984, p. 63-71. Research supported by the General Electric Co. refs  
(Contract NAG3-124)

It is often useful to know the radiation impedance of an unflanged but thick-walled circular duct exhausting a hot gas into relatively cold surroundings. The reactive component is shown to be insensitive to temperature, but the resistive component is shown to be temperature dependent. A temperature correlation is developed permitting prediction of the radiation resistance from a knowledge of the temperature difference between the ambient air and the gas flowing from the duct, and a physical basis for this correlation is presented. Author

**A84-32609\*#** Virginia Polytechnic Inst. and State Univ., Blacksburg.

**RECOVERY OF BURNER ACOUSTIC SOURCE STRUCTURE FROM FAR-FIELD SOUND SPECTRA**

J. R. MAHAN and J. D. JONES (Virginia Polytechnic Institute and State University, Blacksburg, VA) AIAA Journal (ISSN 0001-1452), vol. 22, May 1984, p. 631-637. refs  
(Contract NAG3-124)  
(AIAA PAPER 83-0763)

A method is presented that permits the thermal-acoustic efficiency spectrum in a long turbulent burner to be recovered from the corresponding far-field sound spectrum. An acoustic source/propagation model is used based on the perturbation solution of the equations describing the unsteady one-dimensional flow of an inviscid ideal gas with a distributed heat source. The technique is applied to a long cylindrical hydrogen-flame burner operating over power levels of 4.5-22.3 kW. The results show that the thermal-acoustic efficiency at a given frequency, defined as the fraction of the total burner power converted to acoustic energy at that frequency, is rather insensitive to burner power, having a maximum value on the order of 10 to the -4th at 150 Hz and rolling off steeply with increasing frequency. Evidence is presented that acoustic agitation of the flame at low frequencies enhances the mixing of the unburned fuel and air with the hot products of combustion. The paper establishes the potential of the technique as a useful tool for characterizing the acoustic source structure in any burner, such as a gas turbine combustor, for which a reasonable acoustic propagation model can be postulated. Author

**A84-38091\*** National Aeronautics and Space Administration. Lewis Research Center, Cleveland, Ohio.

**WHY CREDIBLE PROPELLER NOISE MEASUREMENTS ARE POSSIBLE IN THE ACOUSTICALLY UNTREATED NASA LEWIS 8 FT BY 6 FT WIND TUNNEL**

J. H. DITTMAR (NASA, Lewis Research Center, Cleveland, OH) Acoustical Society of America, Journal (ISSN 0001-4966), vol. 75, June 1984, p. 1913, 1914. refs

An explanation is presented for the lack of acoustic reflections in noise studies of propfan models in the NASA-Lewis, 8 x 6 ft wind tunnel, where trials were run at Mach numbers 0.5-0.85. The highly directional propeller noise, i.e., mainly in the plane of rotation,

experiences a convective effect due to the high subsonic axial Mach number. Reflected sounds are carried downstream, out of range of the acoustic sensors in the tunnel. Furthermore, reflected noise is less audible, and therefore does not affect measurements near peak values. It is suggested that some data contamination may occur below Mach 0.6, and that measurements be performed on higher harmonics generated by low level reflected noise.

M.S.K.

**A84-41132\*#** National Aeronautics and Space Administration. Lewis Research Center, Cleveland, Ohio.  
**FINITE ELEMENT-INTEGRAL ACOUSTIC SIMULATION OF JT15D TURBOFAN ENGINE**

K. J. BAUMEISTER (NASA, Lewis Research Center, Cleveland, OH) and S. J. HOROWITZ (USAF, Washington, DC) ASME, Transactions, Journal of Vibration, Acoustics, Stress and Reliability in Design (ISSN 0739-3717), vol. 106, July 1984, p. 405-413. refs

An iterative finite element integral technique is used to predict the sound field radiated from the JT15D turbofan inlet. The sound field is divided into two regions: the sound field within and near the inlet which is computed using the finite element method and the radiation field beyond the inlet which is calculated using an integral solution technique. The velocity potential formulation of the acoustic wave equation was employed in the program. For some single mode JT15D data, the theory and experiment are in good agreement for the far field radiation pattern as well as suppressor attenuation. Also, the computer program is used to simulate flight effects that cannot be performed on a ground static test stand.

Author

**A84-44508\*#** National Aeronautics and Space Administration. Lewis Research Center, Cleveland, Ohio.

**LOW FLIGHT SPEED FAN NOISE FROM A SUPERSONIC INLET**

R. P. WOODWARD, F. W. GLASER, and J. G. LUCAS (NASA, Lewis Research Center, Cleveland, OH) Journal of Aircraft (ISSN 0021-8669), vol. 21, Sept. 1984, p. 665-672. Previously cited in issue 21, p. 3201, Accession no. A83-45517. refs

**N84-11883\*#** National Aeronautics and Space Administration. Lewis Research Center, Cleveland, Ohio.

**CORRELATION OF FLIGHT EFFECTS ON CENTERLINE VELOCITY DECAY FOR COLD-FLOW ACOUSTICALLY EXCITED JETS**

U. H. VONGLAHN 1982 17 p refs Presented at the 106th Meeting of the Acoustical Soc of Am, San Diego, Calif., 7-11 Nov. 1983

(NASA-TM-83502; E-1842; NAS 1.15:83502) Avail: NTIS HC A02/MF A01 CSCL 20A

Acoustic excitation can influence the large scale shear layer structure of jet flow, thereby causing the jet centerline velocity to decay more rapidly. This phenomena has numerous practical applications, such as the reduction of jet/flap impingement velocity in order to reduce flap structural loads for under-the-wing STOL aircraft concepts. Cold flow centerline velocity decay data obtained with acoustic excitation of the jet exhaust flow are correlated with and without flight effects. Initially, static data are correlated in terms of an acoustic parameter involving the threshold sound level needed to initiate acoustic excitation of the jet plume. It is shown that for a given flight speed, the same acoustic excitation parameter as that developed for the static condition is valid. Finally, an aerodynamic flight effects parameter is included to correlate the static and flight centerline velocity decay data with and without acoustic excitation.

S.L.

**N84-11885\*#** National Aeronautics and Space Administration. Lewis Research Center, Cleveland, Ohio.

**CROSS SPECTRA BETWEEN PRESSURE AND TEMPERATURE IN A CONSTANT-AREA DUCT DOWNSTREAM OF A HYDROGEN-FUELED COMBUSTOR**

J. H. MILES, C. A. WASSERBAUER, and E. A. KREJSA Nov. 1983 30 p refs Presented at the 150th Meeting of the Acoustical Soc. of Am., Cincinnati, 10-13 May 1983

(NASA-TM-83463; E-1779; NAS 1.15:83463) Avail: NTIS HC A03/MF A01 CSCL 20A

Pressure temperature cross spectra are necessary in predicting noise propagation in regions of velocity gradients downstream of combustors if the effect of convective entropy disturbances is included. Pressure temperature cross spectra and coherences were measured at spatially separated points in a combustion rig fueled with hydrogen. Temperature-temperature and pressure-pressure cross spectra and coherences between the spatially separated points as well as temperature and pressure autospectra were measured. These test results were compared with previous results obtained in the same combustion rig using Jet A fuel in order to investigate their dependence on the type of combustion process. The phase relationships are not consistent with a simple source model that assumes that pressure and temperature are in phase at a point in the combustor and at all other points downstream are related to one another by only a time delay due to convection of temperature disturbances. Thus these test results indicate that a more complex model of the source is required.

Author

**N84-13922\*#** National Aeronautics and Space Administration. Lewis Research Center, Cleveland, Ohio.

**ON SOME FLOW CHARACTERISTICS OF CONVENTIONAL AND EXCITED JETS**

U. H. VONGLAHN 1983 22 p refs Proposed for presentation at the 22nd Aerospace Sci. Meeting, Reno, Nev., 9-12 Jan. 1984; sponsored by AIAA

(NASA-TM-83503; E-1843; NAS 1.15:83503) Avail: NTIS HC A02/MF A01 CSCL 20A

Improved correlations of jet centerline velocity and static temperature decay data for convergent nozzles are developed. From these empirical correlations, a relationship was devised by which the static temperature decay for a nonisothermal jet plume can be determined from cold-flow jet centerline velocity decay data or prediction. This relationship is shown to apply as well to jet plumes for various nozzle shapes. It is assumed, by analogy, that this relationship also applies to acoustically excited jet plumes. Jet plume spreading with and without excitation is discussed. Finally, the radial velocity and temperature profiles for conventional and enhanced mixing jet flows are shown and their implication for excited flows is discussed.

Author

**N84-13924\*#** National Aeronautics and Space Administration. Lewis Research Center, Cleveland, Ohio.

**INVERTED VELOCITY PROFILE SEMI-ANNULAR NOZZLE JET EXHAUST NOISE EXPERIMENTS**

J. H. GOODYKOONTZ Dec 1983 23 p refs

(NASA-TM-83525; E-1890; NAS 1.15:83525) Avail: NTIS HC A02/MF A01 CSCL 20A

Experimental noise data are shown for a conical nozzle with a semi-annular secondary flow passage having secondary to primary velocity ratios ranging from 1.0 to 1.4. Spectral data are presented at different directivity angles in the flyover plane with the semi-annular flow passage located either on the same side or opposite side relative to an observer. A 10.0 cm diameter primary conical nozzle was used with a 2.59 cm and 5.07 cm wide annular gap secondary nozzle. Similar trends were observed for both nozzle configurations. In general, near the peak noise location and at velocity ratios greater than 1.0, noise levels were larger on the side where the secondary passage was closest to an observer. At velocity ratios near 1.0 the opposite was true. When compared to predicted noise levels for a conical nozzle alone operating at the same ideal thrust, the semi-annular configuration showed no benefit in terms of noise attenuation.

Author

**N84-14874\*#** National Aeronautics and Space Administration. Lewis Research Center, Cleveland, Ohio.

**A POSSIBLE EXPLANATION FOR THE PRESENT DIFFERENCE BETWEEN LINEAR NOISE THEORY AND EXPERIMENTAL DATA FOR SUPERSONIC HELICAL TIP SPEED PROPELLERS**

J. H. DITTMAR Nov. 1983 18 p refs  
(NASA-TM-83467; E-1781; NAS 1.15:83467) Avail: NTIS HC A02/MF A01 CSCL 20F

High speed turboprops are attractive candidates for future aircraft because of their high propulsive efficiency. However, the noise of their propellers may create a cabin environment problem for the aircraft powered by these propellers. The noise of some propeller models was measured, and predictions of the noise using a method based on the Flowcs Williams-Hawkins equation were made. The predictions and data agree well at lower helical tip Mach numbers but deviate above Mach 1.0. Some possible reasons why the theory does not predict the data and focuses on improvement of the aerodynamic inputs as the most likely remedy are investigated. In particular, it is proposed that an increase in the drag and a decrease in the lift near the tip of the blade where the majority of the noise is generated, is warranted in the input to the theory. Author

**N84-15031\*#** National Aeronautics and Space Administration. Lewis Research Center, Cleveland, Ohio.

**GENERATION OF SOUND IN TURBULENT SHEAR FLOWS**

M. E. GOLDSTEIN In Von Karman Inst. for Fluid Dynamics Aeroacoustics: Ten Years of Res. 72 p 1983 refs  
Avail: NTIS HC A14/MF A01

An alternative to the Lighthill acoustic analogy for jet noise is discussed. It involves calculating the unsteady flow that produces the sound along with its resulting sound field starting from a prescribed upstream state that, ideally, is specified just ahead of the region where the sound generation takes place. Sound generation by turbulence interacting with solid obstacles is considered. It is shown that the process can be described by linear theory. Sound generated by turbulence interacting with itself is discussed. The processes are nonlinear and the theory is incomplete. Theories of sound generation are compared with experiment and the inadequacies of each are indicated. Additional mechanisms that appear at supersonic speeds are discussed.

Author (ESA)

**N84-15894\*#** National Aeronautics and Space Administration. Lewis Research Center, Cleveland, Ohio.

**FLUID SHIELDING OF HIGH-VELOCITY JET NOISE**

J. H. GOODYKOONTZ Jan. 1984 22 p refs  
(NASA-TP-2259; E-1705; NAS 1.60:2259) Avail: NTIS HC A02/MF A01 CSCL 20A

Experimental noise data for a nozzle exhaust system incorporating a thermal acoustic shield (TAS) are presented to show the effect of changes in geometric and flow parameters on attenuation of high-velocity jet exhaust noise in the flyover plane. The results are presented for a 10.00-cm-diameter primary conical nozzle with a TAS configuration consisting of a 2.59- or 5.07-cm-wide annular gap. Shield-stream exhaust velocity was varied from 157 to 248 m/sec to investigate the effect of velocity ratio. The results showed that increasing the annular gap width increases attenuation of high-frequency noise when comparisons are made on the same ideal thrust basis. Varying the velocity ratio had a minor effect on the noise characteristics of the nozzles investigated. Author

**N84-16946\*#** National Aeronautics and Space Administration. Lewis Research Center, Cleveland, Ohio.

**NOISE OF THE SR-6 PROPELLER MODEL AT 2 DEG AND 4 DEG ANGLES OF ATTACK**

J. H. DITTMAR and G. L. STEFKO Nov. 1983 18 p refs  
(NASA-TM-83515; E-1864; NAS 1.15:83515) Avail: NTIS HC A02/MF A01 CSCL 20A

The noise generated by supersonic-tip-speed propellers creates a cabin noise problem for future airplanes powered by these propellers. Noise of a number of propeller models were measured

in the NASA Lewis 8- by 6-Foot Wind Tunnel with flow parallel to the propeller axis. In flight, as a result of the induced upwash from the airplane wing, the propeller is at an angle of attack with respect to the incoming flow. Therefore, the 10-blade SR-6 propeller was operated at angle of attack to determine its noise behavior. Higher blade passage tones were observed for the propeller operating at angle of attack in a 0.6 axial Mach number flow. The noise increase was not symmetrical, with one wall of the wind tunnel showing a larger noise increase than the other wall. No noise increase was observed at angle of attack in a 0.8 axial Mach number flow. For this propeller the dominance of thickness noise, which does not increase with angle of attack, explains the lack of noise increase at the higher 0.8 Mach number. Author

**N84-19049\*#** National Aeronautics and Space Administration. Lewis Research Center, Cleveland, Ohio.

**SIMPLIFIED COMBUSTION NOISE THEORY YIELDING A PREDICTION OF FLUCTUATING PRESSURE LEVEL**

R. G. HUFF Feb. 1984 17 p refs  
(NASA-TP-2237; E-1856; NAS 1.60:2237) Avail: NTIS HC A02/MF A01 CSCL 20A

The first order equations for the conservation of mass and momentum in differential form are combined for an ideal gas to yield a single second order partial differential equation in one dimension and time. Small perturbation analysis is applied. A Fourier transformation is performed that results in a second order, constant coefficient, nonhomogeneous equation. The driving function is taken to be the source of combustion noise. A simplified model describing the energy addition via the combustion process gives the required source information for substitution in the driving function. This enables the particular integral solution of the nonhomogeneous equation to be found. This solution multiplied by the acoustic pressure efficiency predicts the acoustic pressure spectrum measured in turbine engine combustors. The prediction was compared with the overall sound pressure levels measured in a CF6-50 turbofan engine combustor and found to be in excellent agreement. Author

**N84-20320\*#** National Aeronautics and Space Administration. Lewis Research Center, Cleveland, Ohio

**LOW FREQUENCY NOISE IN A QUIET, CLEAN, GENERAL AVIATION TURBOFAN ENGINE**

R. G. HUFF, D. E. GROESBECK, and J. H. GOODYKOONTZ Jan. 1984 55 p refs  
(NASA-TM-83520; E-1879; NAS 1.15:83520) Avail: NTIS HC A04/MF A01 CSCL 20A

A quiet, clean, general aviation, turbofan engine was instrumented to measure the fluctuating pressures in the combustor, turbine exit duct, engine nozzle and the far field. Both a separate flow nozzle and an internal mixer nozzle were tested. The fluctuating pressure data are presented in overall pressure and power levels and in spectral plots. The combustor data are compared to recent theory and found to be in excellent agreement. The results indicate that microphone correction procedures for elevated mean pressures are questionable. Ordinary coherence function analysis suggests the presence of an additional low frequency noise source downstream of the turbine that is due to the turbine itself. Low frequency narrowband data and coherence function analysis are presented. Author

**N84-21275\*#** Lockheed-Georgia Co., Marietta.

**BASIC EXPERIMENTAL STUDY OF THE COUPLING BETWEEN FLOW INSTABILITIES AND INCIDENT SOUND** Final Report

K. K. AHUJA Washington NASA Mar. 1984 101 p refs  
(Contract NAS3-23286)  
(NASA-CR-3789; NAS 1.26:3789; LG83ER0137) Avail: NTIS HC A06/MF A01 CSCL 20A

Whether a solid trailing edge is required to produce efficient coupling between sound and instability waves in a shear layer was investigated. The differences found in the literature on the theoretical notions about receptivity, and a need to resolve them by way of well-planned experiments are discussed. Instability waves in the shear layer of a subsonic jet, excited by a point sound

source located external to the jet, were first visualized using an ensemble averaging technique. Various means were adopted to shield the sound reaching the nozzle lip. It was found that the low frequency sound couples more efficiently at distances downstream of the nozzle. To substantiate the findings further, a supersonic screeching jet was tested such that it passed through a small opening in a baffle placed parallel to the exit plane. The measured feedback or screech frequencies and also the excited flow disturbances changed drastically on traversing the baffle axially thus providing a strong indication that a trailing edge is not necessary for efficient coupling between sound and flow. A.R.H.

**N84-23235\*#** National Aeronautics and Space Administration. Lewis Research Center, Cleveland, Ohio.

**FAN NOISE REDUCTION ACHIEVED BY REMOVING TIP FLOW IRREGULARITIES BEHIND THE ROTOR - FORWARD ARC TEST CONFIGURATIONS**

J. H. DITTMAR, R. P. WOODWARD, and M. J. MACKINNON  
1984 17 p refs Presented at the 107th Meeting of the Acoustical Soc of Am., Norfolk, Va. 7-10 May 1984  
(NASA-TM-83616; E-2047; NAS 1.15:83616) Avail: NTIS HC A02/MF A01 CSCL 20A

The noise source caused by the interaction of the rotor tip flow irregularities (vortices and velocity defects) with the downstream stator vanes was studied. Fan flow was removed behind a 0.508 meter (20 in.) diameter model turbopump through an outer wall slot between the rotor and stator. Noise measurements were made with far-field microphones positioned in an arc about the fan inlet and with a pressure transducer in the duct behind the stator. Little tone noise reduction was observed in the forward arc during flow removal; possibly because the rotor-stator interaction noise did not propagate upstream through the rotor. Noise reductions were made in the duct behind the stator and the largest decrease occurred with the first increment of flow removal. This result indicates that the rotor tip flow irregularity-stator interaction is as important a noise producing mechanism as the normally considered rotor wake-stator interaction. Author

**N84-24323\*#** General Electric Co., Cincinnati, Ohio. Aircraft Engine Business Group.

**EXPERIMENTAL INVESTIGATION OF SHOCK-CELL NOISE REDUCTION FOR DUAL-STREAM NOZZLES IN SIMULATED FLIGHT COMPREHENSIVE DATA REPORT. VOLUME 1: TEST NOZZLES AND ACOUSTIC DATA**

K. YAMAMOTO, B. A. JANARDAN, J. F. BRAUSCH, D. J. HOERST, and A. O. PRICE Feb. 1984 533 p 2 Vol.  
(Contract NAS3-23166)  
(NASA-CR-168336-VOL-1; NAS 1.26:168336-VOL-1; R83AEB358-VOL-1) Avail: NTIS HC A23/MF A01 CSCL 20A

Parameters which contribute to supersonic jet shock noise were investigated for the purpose of determining means to reduce such noise generation to acceptable levels. Six dual-stream test nozzles with varying flow passage and plug closure designs were evaluated under simulated flight conditions in an anechoic chamber. All nozzles had combined convergent-divergent or convergent flow passages. Acoustic behavior as a function of nozzle flow passage geometry was measured. The acoustic data consist primarily of 1/3 octave band sound pressure levels and overall sound pressure levels. Detailed schematics and geometric characteristics of the six scale model nozzle configurations and acoustic test point definitions are presented. Tabulation of aerodynamic test conditions and a computer listing of the measured acoustic data are displayed. R.S.F.

**N84-24324\*#** General Electric Co., Cincinnati, Ohio. Aircraft Engine Business Group.

**EXPERIMENTAL INVESTIGATION OF SHOCK-CELL NOISE REDUCTION FOR DUAL-STREAM NOZZLES IN SIMULATED FLIGHT COMPREHENSIVE DATA REPORT. VOLUME 2: LASER VELOCIMETER DATA, STATIC PRESSURES AND SHADOWGRAPH PHOTOS**

K. YAMAMOTO, B. A. JANARDAN, J. F. BRAUSCH, D. J. HOERST, and A. O. PRICE Feb. 1984 525 p 2 Vol.

(Contract NAS3-23166)  
(NASA-CR-168336-VOL-2; NAS 1.26:168336-VOL-2; R83AEB358-VOL-2) Avail: NTIS HC A22/MF A01 CSCL 20A

Parameters which contribute to supersonic jet shock noise were investigated for the purpose of determining means to reduce such noise generation to acceptable levels. Six dual-stream test nozzles with varying flow passage and plug closure designs were evaluated under simulated flight conditions in an anechoic chamber. All nozzles had combined convergent-divergent or convergent flow passages. Mean velocity and turbulence velocity measurements of 25 selected flow conditions were performed employing a laser Doppler velocimeter. Static pressure measurements were made to define the actual convergence-divergence condition. Test point definition, tabulation of aerodynamic test conditions, velocity histograms, and shadowgraph photographs are presented. Flow visualization through shadowgraph photography can contribute to the development of an analytical prediction model for shock noise from coannular plug nozzles. R.S.F.

**N84-26383\*#** National Aeronautics and Space Administration. Lewis Research Center, Cleveland, Ohio.

**A THEORETICAL PREDICTION OF THE ACOUSTIC PRESSURE GENERATED BY TURBULENCE-FLAME FRONT INTERACTIONS**

R. G. HUFF 1984 13 p refs Presented at the Winter Ann. Meeting of the Am. Soc. of Mech. Engr., New Orleans, 9-13 Dec. 1984

(NASA-TM-83587; E-1962; NAS 1.15:83587) Avail: NTIS HC A02/MF A01 CSCL 20A

The equations of momentum and continuity are combined and linearized yielding the one dimensional nonhomogeneous acoustic wave equation. Three terms in the non-homogeneous equation act as acoustic sources and are taken to be forcing functions acting on the homogeneous wave equation. The three source terms are: fluctuating entropy, turbulence gradients, and turbulence-flame interactions. Each source term is discussed. The turbulence-flame interaction source is used as the basis for computing the source acoustic pressure from the Fourier transformed wave equation. Pressure fluctuations created in turbopump gas generators and turbines may act as a forcing function for turbine and propellant tube vibrations in Earth to orbit space propulsion systems and could reduce their life expectancy. A preliminary assessment of the acoustic pressure fluctuations in such systems is presented. Author

**N84-26384\*#** Virginia Polytechnic Inst. and State Univ., Blacksburg. Dept. of Mechanical Engineering.

**A CRITICAL REVIEW OF NOISE PRODUCTION MODELS FOR TURBULENT, GAS-FUELED BURNERS Final Report**

J. R. MAHAN Jun. 1984 56 p refs

(Contract NAG3-124)  
(NASA-CR-3803; NAS 1.26:3803) Avail: NTIS HC A04/MF A01 CSCL 20A

The combustion noise literature for the period between 1952 and early 1984 is critically reviewed. Primary emphasis is placed on past theoretical and semi-empirical attempts to predict or explain observed direct combustion noise characteristics of turbulent, gas-fueled burners; works involving liquid-fueled burners are reviewed only when ideas equally applicable to gas-fueled burners are presented. The historical development of the most important contemporary direct combustion noise theories is traced, and the theories themselves are compared and criticized. While most theories explain combustion noise production by turbulent flames in terms of randomly distributed acoustic monopoles produced by



turbulent mixing of products and reactants, none is able to predict the sound pressure in the acoustic farfield of a practical burner because of the lack of a proven model which relates the combustion noise source strength at a given frequency to the design and operating parameters of the burner. Recommendations are given for establishing a benchmark-quality data base needed to support the development of such a model. A R H.

**N84-27544\*** Minnesota Univ., Minneapolis. Dept. of Electrical Engineering.

**STUDIES OF ACOUSTICAL PROPERTIES OF BULK POROUS FLEXIBLE MATERIALS Final Report**

R. F. LAMBERT 30 Jun. 1984 29 p refs  
(Contract NAG3-161)

(NASA-CR-173622; NAS 1.26 173622) Avail: NTIS HC A03  
CSCL 20A

Acoustic prediction and measurement of bulk porous materials with flexible frames is investigated. The acoustic properties of Kevlar 29 are examined. Various acoustic tests are employed to determine impedance, sound wave propagation, and wave pressure equations for the highly porous fiber composites. The derivation of design equations and future research goals are included.

**N84-29661\*#** General Electric Co., Cincinnati, Ohio. Aircraft Engine Business Group.

**FREE JET FEASIBILITY STUDY OF A THERMAL ACOUSTIC SHIELD CONCEPT FOR AST/VCE APPLICATION: SINGLE STREAM NOZZLES Final Report**

R. K. MAJJIGI, J. F. BRAUSCH, B. A. JANARDAN, T. F. BALSAL, P. R. KNOTT, and N. PICKUP Washington NASA Jul. 1984 354 p refs

(Contract NAS3-22137)  
(NASA-CR-3758; E-2132; NAS 1.26:3758; R82AEB494) Avail:  
NTIS HC A16/MF A01 CSCL 20A

A technology base for the thermal acoustic shield concept as a noise suppression device for single stream exhaust nozzles was developed. Acoustic data for 314 test points for 9 scale model nozzle configurations were obtained. Five of these configurations employed an unsuppressed annular plug core jet and the remaining four nozzles employed a 32 chute suppressor core nozzle. Influence of simulated flight and selected geometric and aerodynamic flow variables on the acoustic behavior of the thermal acoustic shield was determined. Laser velocimeter and aerodynamic measurements were employed to yield valuable diagnostic information regarding the flow field characteristics of these nozzles. An existing theoretical aeroacoustic prediction method was modified to predict the acoustic characteristics of partial thermal acoustic shields. B.G.

**N84-29676\*#** National Aeronautics and Space Administration. Lewis Research Center, Cleveland, Ohio.

**HELICOPTER ENGINE CORE NOISE**

U. H. VONGLAHN in NASA. Langley Research Center Rotorcraft Noise p 261-284 Jul. 1982 refs

Avail: NTIS HC A18/MF A01 CSCL 20A

Calculated engine core noise levels, based on NASA Lewis prediction procedures, for five representative helicopter engines are compared with measured total helicopter noise levels and ICAO helicopter noise certification requirements. Comparisons are made for level flyover and approach procedures. The measured noise levels are generally significantly greater than those predicted for the core noise levels, except for the Sikorsky S-61 and S-64 helicopters. However, the predicted engine core noise levels are generally at or within 3 dB of the ICAO noise rules. Consequently, helicopter engine core noise can be a significant contributor to the overall helicopter noise signature. Author

**N84-32118\*#** National Aeronautics and Space Administration. Lewis Research Center, Cleveland, Ohio.

**TIME DEPENDENT WAVE ENVELOPE FINITE DIFFERENCE ANALYSIS OF SOUND PROPAGATION**

K. J. BAUMEISTER 1984 14 p refs Proposed for presentation at the 9th Aeroacoustics Conf., Williamsburg, Va, 15-17 Oct. 1984; sponsored by the American Inst. of Aeronautics and Astronautics (NASA-TM-83744; E-2233; NAS 1.15:83744) Avail: NTIS HC A02/MF A01 CSCL 20A

A transient finite difference wave envelope formulation is presented for sound propagation, without steady flow. Before the finite difference equations are formulated, the governing wave equation is first transformed to a form whose solution tends not to oscillate along the propagation direction. This transformation reduces the required number of grid points by an order of magnitude. Physically, the transformed pressure represents the amplitude of the conventional sound wave. The derivation for the wave envelope transient wave equation and appropriate boundary conditions are presented as well as the difference equations and stability requirements. To illustrate the method, example solutions are presented for sound propagation in a straight hard wall duct and in a two dimensional straight soft wall duct. The numerical results are in good agreement with exact analytical results.

Author

**N84-32122\*#** National Aeronautics and Space Administration. Lewis Research Center, Cleveland, Ohio.

**ANALYSIS OF THE EFFECT ON COMBUSTOR NOISE MEASUREMENTS OF ACOUSTIC WAVES REFLECTED BY THE TURBINE AND COMBUSTOR INLET**

R. G. HUFF 1984 14 p refs Presented at the 9th Aeroacoustics Conf., Williamsburg, Va, 15-17 Oct. 1984; sponsored by NASA and AIAA

(NASA-TM-83760; E-2250; NAS 1.15:83760) Avail: NTIS HC A02/MF A01 CSCL 20A

Spectral analyses of static pressure fluctuations measured in turbine engine combustors at low engine speed show good agreement with theory. At idle speed the high pressure turbine is choked. Above idle speed the turbine chokes and a significant change in the shape of the measured combustor pressure spectrum is observed. A simplified theoretical model of the acoustic pressure generated in the combustor due to the turbulence-flame front interaction did not account for acoustic waves reflected from the turbine. By retaining this simplified combustion noise source model and adding a partial reflecting plane at the turbine and combustor inlet, a simple theoretical model was developed that reproduces the undulations in the combustor fluctuating pressure spectra. Plots of the theoretical combustor fluctuating pressure spectra are compared to the measured pressure spectra obtained from the CF6-50 turbofan engine over a range of engine operating speeds. The simplified combustion noise theory when modified by a simple turbine reflecting plane adequately accounts for the changes in measured combustor pressure spectra. It is further concluded that the shape of the pressure spectra downstream of the turbine, neglecting noise generated by the turbine itself, will be the combustion noise spectra unchanged except for the level reduction due to the energy blocked by the turbine. Author

**N84-33148\*#** General Electric Co., Cincinnati, Ohio. Aircraft Engine Group.

**EXPERIMENTAL INVESTIGATION OF SHOCK-CELL NOISE REDUCTION FOR SINGLE-STREAM NOZZLES IN SIMULATED FLIGHT, COMPREHENSIVE DATA REPORT. VOLUME 1: TEST NOZZLES AND ACOUSTIC DATA**

K. YAMAMOTO, J. F. BRAUSCH, B. A. JANARDAN, D. J. HOERST, A. O. PRICE, and P. R. KNOTT May 1984 600 p refs 3 Vol

(Contract NAS3-22514)  
(NASA-CR-168234-VOL-1; NAS 1.26:168234-VOL-1;  
R82AEB491-VOL-1) Avail: NTIS HC A25/MF A01 CSCL 20A

The model nozzle configurations, acoustic test conditions, and detailed test results from the hot static and simulated flight acoustic

tests at the General Electric Anechoic Chamber are described.

B.G.

**N84-33149\*#** General Electric Co., Cincinnati, Ohio. Aircraft Engine Group.

## EXPERIMENTAL INVESTIGATION OF SHOCK-CELL NOISE REDUCTION FOR SINGLE-STREAM NOZZLES IN SIMULATED FLIGHT, COMPREHENSIVE DATA REPORT. VOLUME 2: LASER VELOCIMETER DATA

K. YAMAMOTO, J. F. BRAUSCH, B. A. JANARDAN, D. J. HOERST, A. O. PRICE, and P. R. KNOTT May 1984 780 p refs 3 Vol.

(Contract NAS3-22514)

(NASA-CR-168234-VOL-2; NAS 1.26:168234-VOL-2;

R82AEB491-VOL-2) Avail: NTIS HC A99/MF A01 CSCL 20A

Mean velocity (axial component) and turbulent velocity (axial component) measurements for thirty one selected flow conditions of six models were performed employing the Laser Doppler Velocimeter Aerodynamic conditions which define the test points are given. Tabulations which explain the scope of mean velocity traverses and turbulence histogram measurements are also presented. The actual LV position, the type of traverse, and measured mean and turbulent velocities along copies of the LV mean velocity traces are contained.

Author

**N84-33150\*#** General Electric Co., Cincinnati, Ohio. Aircraft Engine Group.

## EXPERIMENTAL INVESTIGATION OF SHOCK-CELL NOISE REDUCTION FOR SINGLE-STREAM NOZZLES IN SIMULATED FLIGHT, COMPREHENSIVE DATA REPORT. VOLUME 3: SHADOWGRAPH PHOTOS AND FACILITY DESCRIPTION

K. YAMAMOTO, J. F. BRAUSCH, B. A. JANARDAN, D. J. HOERST, A. O. PRICE, and P. R. KNOTT May 1984 208 p refs 3 Vol.

(Contract NAS3-22514)

(NASA-CR-168234-VOL-3; NAS 1.26:168234-VOL-3;

R82AEB491-VOL-3) Avail: NTIS HC A10/MF A01 CSCL 20A

A total of 142 shadowgraph photographs were taken on 43 different plumes that were distributed over the six nozzle configurations using the 9.5 inch diameter collimated light beam of the shadowgraph setup. Aerodynamic flow conditions of the shadowgraph test points, the location and identification of each of the photographs, and copies of the pictures are presented.

Author

**N84-34230\*#** National Aeronautics and Space Administration. Lewis Research Center, Cleveland, Ohio.

## AN EXPERIMENTAL INVESTIGATION OF THE EFFECT OF BOUNDARY LAYER REFRACTION ON THE NOISE FROM A HIGH-SPEED PROPELLER

J. H. DITTMAR, R. J. BURNS, and D. J. LECIEJEWSKI Sep. 1984 31 p refs

(NASA-TM-83764; E-2257; NAS 1.15:83764) Avail: NTIS HC

A03/MF A01 CSCL 20A

Models of supersonic propellers were previously tested for acoustics in the Lewis 8- by 6-Foot Wind Tunnel using pressure transducers mounted in the tunnel ceiling. The boundary layer on the tunnel ceiling is believed to refract some of the propeller noise away from the measurement transducers. Measurements were made on a plate installed in the wind tunnel which had a thinner boundary layer than the ceiling boundary layer. The plate was installed in two locations for comparison with tunnel ceiling noise data and with fuselage data taken on the NASA Dryden Jetstar airplane. Analysis of the data indicates that the refraction increases with: increasing boundary layer thickness; increasing free stream Mach number; increasing frequency; and decreasing sound radiation angle (toward the inlet axis). At aft radiation angles greater than about 100 deg there was little or no refraction. Comparisons with the airplane data indicated that not only is the boundary layer thickness important but also the shape of the velocity profile. Comparisons with an existing two-dimensional theory, using an idealized shear layer to approximate the boundary layer, showed that the theory and data had the same trends. Analysis of the

data taken in the tunnel at two different distances from the propeller indicates a decay with distance in the wind tunnel at high Mach numbers but the decay at low Mach numbers is not as clear.

Author

**N84-34231\*#** National Aeronautics and Space Administration. Lewis Research Center, Cleveland, Ohio.

## A THEORETICAL MODEL FOR THE CROSS SPECTRA BETWEEN PRESSURE AND TEMPERATURE DOWNSTREAM OF A COMBUSTOR

J. H. MILES and E. A. KREJSA 1984 61 p refs Presented at the 107th Meeting of the Acoustical Society of America, Norfolk, Vir., 6-10 May 1984

(NASA-TM-83671; E-2114; NAS 1.15:83671) Avail: NTIS HC

A04/MF A01 CSCL 20A

A theoretical model developed to calculate pressure-temperature cross spectra, pressure spectra, temperature spectra and pressure cross spectra in a ducted combustion system is presented. The model assumes the presence of a fluctuating-volumetric-heat-release-rate disk source and takes into account the spatial distribution of the steady-state volumetric-heat flux. Using the model, pressure, velocity, and temperature perturbation relationships can be obtained. The theoretical results show that, at a given air mass flow rate, the calculated pressure-temperature cross spectra phase angle at the combustor exit depends on the model selected for the steady-state volumetric-heat flux in the combustor. Using measurements of the phase angle, an appropriate source region model was selected. The model calculations are compared with the data. The comparison shows good agreement and indicates that with the use of this model the pressure-temperature cross spectra measurements provide useful information on the physical mechanisms active at the combustion noise source.

Author

**N84-35085\*#** National Aeronautics and Space Administration. Lewis Research Center, Cleveland, Ohio.

## SUPERSONIC JET SHOCK NOISE REDUCTION

J. R. STONE 1984 45 p refs Presented at 9th Aeroacoust. Conf., Williamsburg, Va., 15-17 Oct. 1984

(NASA-TM-83799; E-2299; NAS 1.15:83799) Avail: NTIS HC

A03/MF A01 CSCL 20A

Shock-cell noise is identified to be a potentially significant problem for advanced supersonic aircraft at takeoff. Therefore NASA conducted fundamental studies of the phenomena involved and model-scale experiments aimed at developing means of noise reduction. The results of a series of studies conducted to determine means by which supersonic jet shock noise can be reduced to acceptable levels for advanced supersonic cruise aircraft are reviewed. Theoretical studies were conducted on the shock associated noise of supersonic jets from convergent-divergent (C-D) nozzles. Laboratory studies were conducted on the influence of narrowband shock screech on broadband noise and on means of screech reduction. The usefulness of C-D nozzle passages was investigated at model scale for single-stream and dual-stream nozzles. The effect of off-design pressure ratio was determined under static and simulated flight conditions for jet temperatures up to 960 K. Annular and conical flow passages with center plugs and multi-element suppressor nozzles were evaluated, and the effect of plug tip geometry was established. In addition to the far-field acoustic data, mean and turbulent velocity distributions were measured with a laser velocimeter, and shadowgraph images of the flow field were obtained.

Author

## ATOMIC AND MOLECULAR PHYSICS

Includes atomic structure and molecular spectra.

**N84-10923\*#** National Aeronautics and Space Administration. Lewis Research Center, Cleveland, Ohio.

**MATRIX EFFECTS IN ION-INDUCED EMISSION AS OBSERVED IN NE COLLISIONS WITH CU-MG AND CU-AL ALLOYS**

J. FERRANTE and S. V. PEPPER Sep. 1983 9 p refs (NASA-TM-83061; E-1532; NAS 1.15:83061) Avail: NTIS HC A02/MF A01 CSCL 20H

Ion induced Auger electron emission is used to study the surfaces of Al, Mg, Cu - 10 at. % Al, Cu - 19.6 at. % Al, and Cu - 7.4 at. % Mg. A neon (Ne) ion beam whose energy is varied from 0.5 to 3 keV is directed at the surface. Excitation of the lighter Ne occurs by the promotion mechanism of Barat and Lichten in asymmetric collisions with Al or Mg atoms. Two principal Auger peaks are observed in the Ne spectrum: one at 22 eV and one at 25 eV. Strong matrix effects are observed in the alloys as a function of energy in which the population of the second peak is greatly enhanced relative to the first over the pure materials. For the pure material over this energy range this ratio is 1.0. For the alloys it can rise to the electronic structure of alloys and to other surface tools such as secondary ion mass spectroscopy. Author

**N84-26189\*#** National Aeronautics and Space Administration. Lewis Research Center, Cleveland, Ohio.

**CHARGED PARTICLE EFFECTS ON SPACE SYSTEMS**

W. N. HALL and N. J. STEVENS In AFGL Proc. of the AFGL Workshop on Nat. Charging of Large Space Struct. in Near Earth Polar Orbit p 79-106 25 Jan. 1983 refs Prepared in cooperation with AFGL, Hanscom AFB, Mass. (AD-P002103) Avail: NTIS HC A18/MF A01 CSCL 20H

There is a growing tendency to plan space missions that will incorporate very large space power systems. These space power systems must function in a space plasma environment that can impose operational limitations. As the power output increases, the operating voltage must also increase and this voltage, exposed at solar array interconnects, interacts with the local plasma. The implications of such interactions are considered here. The available laboratory data for biased array segment tests are reviewed to demonstrate the basic interactions considered. A data set for a test of a floating high voltage array illuminated in a solar simulator test is used to generate approximate relationships for positive and negative current collection from plasma. These relationships are applied to a hypothetical 100 kW power system operating in a 400 km, near-equatorial, orbit. It is found that discharges from the negative regions of the array are the most probable limiting factor for array operation. Author

**N84-34484\*#** National Aeronautics and Space Administration. Lewis Research Center, Cleveland, Ohio.

**THE ENERGY DEPENDENCE AND SURFACE MORPHOLOGY OF KAPTON (TRADEMARK) DEGRADATION UNDER ATOMIC OXYGEN BOMBARDMENT**

D. C. FERGUSON In NASA. Goddard Space Flight Center 13th Space Simulation Conf. p 205-221 1984 refs Avail: NTIS HC A13/MF A01 CSCL 20H

Data from laboratory simulations and from samples returned from STS-8 are used to derive the energy dependence of the mass loss rate of Kapton under atomic oxygen bombardment and to discuss the development of surface structure and its effect on erosion rates. It is concluded that all the laboratory data from discharge and flow tubes and from accelerated beams, along with the orbital data from STS-3 through STS-8, can be accommodated by a rate of mass loss that varies with impact energy normal to the surface. It is hypothesized that increases of mass loss rate with exposure time may be due to trapping of the incoming atoms by the surface structure which develops. Author

## OPTICS

Includes light phenomena.

**A84-13184\*** Carnegie-Mellon Univ., Pittsburgh, Pa.

**DIRECT AND IMPLICIT OPTICAL MATRIX-VECTOR ALGORITHMS**

D. CASASANT and A. GHOSH (Carnegie-Mellon University, Pittsburgh, PA) Applied Optics (ISSN 0003-6935), vol. 22, Nov. 15, 1983, p. 3572-3578. refs (Contract NAG3-5; AF-AFOSR-79-0091)

New direct and implicit algorithms for optical matrix-vector and systolic array processors are considered. Direct rather than indirect algorithms to solve linear systems and implicit rather than explicit solutions to solve second-order partial differential equations are discussed. In many cases, such approaches more properly utilize the advantageous features of optical systolic array processors. The matrix-decomposition operation (rather than solution of the simplified matrix-vector equation that results) is recognized as the computationally burdensome aspect of such problems that should be computed on an optical system. The Householder QR matrix-decomposition algorithm is considered as a specific example of a direct solution. Extensions to eigenvalue computation and formation of matrices of special structure are also noted. Author

**A84-16397\*** Rochester Univ., N. Y.

**COUPLING OF RADIATION INTO THIN FILM MODES BY MEANS OF LOCALIZED PLASMA RESONANCES**

W. R. HOLLAND and D. G. HALL (Rochester University, Rochester, NY) IN: Integrated optics III; Proceedings of the Conference, Arlington, VA, April 5, 6, 1983. Bellingham, WA, SPIE - The International Society for Optical Engineering, 1983, p. 188-190. refs (Contract DAAG29-81-K-0134; NAG3-414)

The interaction between the surface plasmon mode that propagates at a metal dielectric interface and the localized plasma resonances (LPR) is investigated experimentally in Ag-island films. A stair-stepped sample geometry comprising a glass substrate, a continuous 50-nm Ag film, an LiF spacer film of thickness  $d = 5-60$  nm, and an Ag-island film of mass thickness 3 nm is used in near-normal-reflectivity and plasmon-propagation-constant ( $k$ ) determinations. The results are presented graphically and discussed. The overall shape of the reflectivity curves is found to be characteristic of Ag films, but with a dip at about 400 nm (corresponding to the absorption resonance of the island film) which is most pronounced with  $d = 25$  nm. It is inferred that the island resonances are strongly coupled to a continuous-film dissipative mechanism at this  $d$  value. This inference is supported by the fact that the variation in  $k$ , corrected for LiF effects and plotted as a function of  $d$ , is greatest at around  $d = 25$  nm. The implications of this finding for broad-band coupling into a thin-film mode, LPR enhancement of waveguide nonlinear effects, and new surface-enhanced-Raman-scattering geometries are indicated. T.K.

**A84-28485\*** Carnegie-Mellon Univ., Pittsburgh, Pa.

**ADVANCED ACOUSTO-OPTIC SIGNAL PROCESSORS**

D. CASASANT (Carnegie-Mellon University, Pittsburgh, PA) IN: Bragg signal processing and output devices; Proceedings of the Meeting, San Diego, CA, August 24, 25, 1982. Bellingham, WA, SPIE - The International Society for Optical Engineering, 1983, p. 50-58. refs (Contract NSF ECS-81-14344; NAG3-5)

The basic acousto-optic signal processing architectures (spectrum analyzer, space-integrating, time-integrating, and triple product processor) systems and algorithms such as the chirp-Z transform are reviewed. New acousto-optic data processing systems and applications that utilize these basic architectures and new ones are described. These include a matched spatial filter

acousto-optic processor, two new hybrid time and space-integrating systems, a triple product processor, and four new matrix-vector iterative feedback systems. Author

**A84-40332\*** Ohio State Univ., Columbus.  
**OPTICAL FLIP-FLOPS AND SEQUENTIAL LOGIC CIRCUITS USING A LIQUID CRYSTAL LIGHT VALVE**

M. T. FATEHI, S. A. COLLINS, JR. (Ohio State University, Columbus, OH), and K. C. WASMUNDT (Colorado, University, Denver, CO) *Applied Optics* (ISSN-0003-6935), vol. 23, July 1, 1984, p. 2163-2171. refs  
 (Contract NSG-3302)

This paper is concerned with the application of optics to digital computing. A Hughes liquid crystal light valve is used as an active optical element where a weak light beam can control a strong light beam with either a positive or negative gain characteristic. With this device as the central element the ability to produce bistable states from which different types of flip-flop can be implemented is demonstrated. In this paper, some general comments are first presented on digital computing as applied to optics. This is followed by a discussion of optical implementation of various types of flip-flop. These flip-flops are then used in the design of optical equivalents to a few simple sequential circuits such as shift registers and accumulators. As a typical sequential machine, a schematic layout for an optical binary temporal integrator is presented. Finally, a suggested experimental configuration for an optical master-slave flip-flop array is given.

Author

**N84-16984\*#** Rensselaer Polytechnic Inst., Troy, N. Y. Dept. of Mechanical Engineering.

**SURFACE TOPOGRAPHICAL CHANGES MEASURED BY PHASE-LOCKED INTERFEROMETRY Final Report**

J. L. LAUER and S. S. FUNG Jan. 1984 103 p refs  
 (Contract NAG3-222)

(NASA-CR-3757; NAS 1.26:3757) Avail: NTIS HC A06/MF A01 CSCL 20F

An electronic optical laser interferometer capable of resolving depth differences of as low as 30 Å and planar displacements of 6000 Å was constructed to examine surface profiles of bearing surfaces without physical contact. Topological chemical reactivity was determined by applying a drop of dilute alcoholic hydrochloric acid and measuring the profile of the solid surface before and after application of this probe. Scuffed bearing surfaces reacted much faster than virgin ones but that bearing surfaces exposed to lubricants containing an organic chloride reacted much more slowly. The reactivity of stainless steel plates, heated in a nitrogen atmosphere to different temperatures, were examined later at ambient temperature. The change of surface contour as a result of the probe reaction followed Arrhenius-type relation with respect to heat treatment temperature. The contact area of the plate of a ball/plate sliding elastohydrodynamic contact run on trimethylpropane triheptanoate with or without additives was optically profiled periodically. As scuffing was approached, the change of profile within the contact region changed much more rapidly by the acid probe and assumed a constant high value after scuffing. A nonetching metallurgical phase was found in the scuff mark, which was apparently responsible for the high reactivity.

A.R.H.

**N84-22405\*#** Carnegie-Mellon Univ., Pittsburgh, Pa. Dept. of Electrical and Computer Engineering.

**OPTICAL SYSTOLIC SOLUTIONS OF LINEAR ALGEBRAIC EQUATIONS**

C. P. NEUMAN and D. CASASENT *In* NASA. Langley Research Center Opt. Inform. Process. for Aerospace Appl. 2 p 35-51 Mar. 1984 refs

(Contract NAG3-5; AF-AFSR-0091-79)

Avail: NTIS HC A12/MF A01 CSCL 20F

The philosophy and data encoding possible in systolic array optical processor (SAOP) were reviewed. The multitude of linear algebraic operations achievable on this architecture is examined. These operations include such linear algebraic algorithms as:

matrix-decomposition, direct and indirect solutions, implicit and explicit methods for partial differential equations, eigenvalue and eigenvector calculations, and singular value decomposition. This architecture can be utilized to realize general techniques for solving matrix linear and nonlinear algebraic equations, least mean square error solutions, FIR filters, and nested-loop algorithms for control engineering applications. The data flow and pipelining of operations, design of parallel algorithms and flexible architectures, application of these architectures to computationally intensive physical problems, error source modeling of optical processors, and matching of the computational needs of practical engineering problems to the capabilities of optical processors are emphasized. E.A.K.

**N84-22414\*#** Ohio State Univ., Columbus. Electroscience Lab.  
**OPTICAL PULSE GENERATOR USING LIQUID CRYSTAL LIGHT VALVE**

S. A. COLLINS, JR. *In* NASA. Langley Research Center Opt. Inform. Process. for Aerospace Appl. 2 p 179-189 Mar. 1984 refs

(Contract NSG-3302)

Avail: NTIS HC A12/MF A01 CSCL 20F

Numerical optical computing is discussed. A design for an optical pulse generator using a Hughes Liquid crystal light valve and intended for application as an optical clock in a numerical optical computer is considered. The pulse generator is similar in concept to the familiar electronic multivibrator, having a flip-flop and delay units. R.J.F.

**N84-22417\*#** Ohio State Univ., Columbus. Electroscience Lab.  
**OPTICAL RESIDUE ADDITION AND STORAGE UNITS USING A HUGHES LIQUID CRYSTAL LIGHT VALVE**

S. F. HABIBY and S. A. COLLINS, JR. *In* NASA. Langley Research Center Opt. Inform. Process. for Aerospace Appl. 2 p 215-229 Mar. 1984 refs

(Contract NSG-3302)

Avail: NTIS HC A12/MF A01 CSCL 20F

Optical addition and storage units are described in this paper. These units are implemented using the Hughes Liquid Crystal Light Valve (LCLV) as a spatial light modulator using residue arithmetic for a numerical representation. The main hardware components of the design, besides the light valve, include an array of single-mode optical fibers that provide input information, a polarizing prism in combination with quarter-wave and half-wave retarders for residue arithmetic implementation in the adder, and a holographic array for spatial stability in the storage unit. Author

**N84-22421\*#** National Aeronautics and Space Administration. Lewis Research Center, Cleveland, Ohio.

**METHOD OF REDUCING TEMPERATURE IN HIGH-SPEED PHOTOGRAPHY**

E. D. WALKER and H. A. SLATER (Rochester Inst. of Tech.) Mar. 1984 9 p refs

(NASA-TM-83620; E-2021; NAS 1.15:83620) Avail: NTIS HC A02/MF A01 CSCL 20F

A continuing problem in high-speed motion picture photography is adequate lighting and the associated temperature rise. Large temperature rises can damage subject matter and make recording of the desired images impossible. The problem is more severe in macrophotography because of bellows extension and the necessary increase in light. This report covers one approach to reducing the initial temperature rise: the use of filters and heat-absorbing materials. The accompanying figures provide the starting point for selecting distance as a function of light intensity and determining the associated temperature rise. Using these figures will allow the photographer greater freedom in meeting different photographic situations. Author

**N84-32169\*#** National Aeronautics and Space Administration. Lewis Research Center, Cleveland, Ohio.  
**PRELIMINARY EXPERIMENTS ON PHASE CONJUGATION FOR FLOW VISUALIZATION**  
 D. WEIMER (Ohio Northern Univ.) and W. L. HOWES Aug. 1984 19 p refs  
 (NASA-TM-83766; E-2089; NAS 1.15:83766) Avail: NTIS HC A02/MF A01 CSCL 20F

Barium titanate single crystals are discussed in the context of: the procedure for polarizing a crystal; a test for phase conjugation; transients in the production of phase conjugation; real time readout by a separate laser of a hologram induced within the crystal, including conjugation response times to on-off switching of each beam; and a demonstration of a Twyman-Green interferometer utilizing phase conjugation. Author

## 75

## PLASMA PHYSICS

Includes magnetohydrodynamics and plasma fusion.

**A84-23390\*** Michigan State Univ., East Lansing.  
**CHARACTERISTICS OF A MICROWAVE PLASMA DISK ION SOURCE**  
 J. ASMUSSEN and J. ROOT (Michigan State University, East Lansing, MI) Applied Physics Letters (ISSN 0003-6951), vol. 44, Feb. 15, 1984, p. 396-398 refs  
 (Contract NSG-3299)

This letter describes an ion source using a cylindrical microwave cavity operating in a hybrid mode associated with the TE<sub>211</sub> empty cavity mode. The design principles and associated electrical systems are also discussed. Extracted beam current versus accelerating voltage, and specific energy versus extracted beam current are displayed over the range of flow rates 20-80 sccm and absorbed powers 80-150 W. The results show the feasibility of this concept. The ion source has many potential uses such as space propulsion, material processing, and neutral beam ion sources. Author

**A84-24049\*#** Texas Univ., Arlington.  
**TRANSIENT FLOW ANALYSIS OF THE AEDC/HPDE MHD GENERATOR**  
 D. R. WILSON, Y. M. LEE (Texas, University, Arlington, TX), and C. S. STEWART (General Dynamics Corp., Fort Worth, TX) Journal of Energy (ISSN 0146-0412), vol. 7, Nov.-Dec. 1983, p. 644-651. refs  
 (Contract NSG-3255)

Previously cited in issue 05, p. 686, Accession no. A83-16691

**A84-24058\*#** National Aeronautics and Space Administration. Lewis Research Center, Cleveland, Ohio.  
**OXIDANT SYSTEM IMPROVEMENTS FOR MHD ENERGY CONVERSION AND INDUSTRIAL PROCESSES**  
 A. J. JUHASZ (NASA, Lewis Research Center, Cleveland, OH) Journal of Energy (ISSN 0146-0412), vol. 7, Nov.-Dec. 1983, p. 716-723. refs  
 (Contract DE-AI01-77ET-10769; DEN3-165)  
 Previously cited in issue 05, p. 686, Accession no. A83-16735

**A84-46108\*#** Michigan State Univ., East Lansing.  
**ELECTROMAGNETIC PLASMA MODELS FOR MICROWAVE PLASMA CAVITY REACTORS**  
 L. FRASCH and J. ASMUSSEN (Michigan State University, East Lansing, MI) American Institute of Aeronautics and Astronautics, Fluid Dynamics, Plasma Dynamics, and Lasers Conference, 17th, Snowmass, CO, June 25-27, 1984. 10 p. refs  
 (Contract NAG3-305)  
 (AIAA PAPER 84-1521)

A procedure used to design cavity applicators that efficiently produce cylindrical and disk microwave discharges is reviewed. In contrast to most microwave applicators these cavities utilize single mode excitation of the plasma. This method of excitation has the advantage of providing efficient coupling (zero reflected power) to the plasma over a wide range of discharge loading conditions while also allowing, if desired, electric feedback control of the heating process. The design procedure is generalized to any lossy dielectric. Experimental and theoretical research required to further understand microwave discharges is also discussed. Author

**A84-46109\*#** Michigan State Univ., East Lansing.  
**SPATIAL ELECTRON DENSITY AND ELECTRIC FIELD STRENGTH MEASUREMENTS IN MICROWAVE CAVITY EXPERIMENTS**  
 M. PETERS, S. WHITEHAIR, J. ASMUSSEN, H. KERBER (Michigan State University, East Lansing, MI), and J. ROGERS (Michigan State University, East Lansing, MI; MIT, Lincoln Laboratory, Lexington, MA) American Institute of Aeronautics and Astronautics, Fluid Dynamics, Plasma Dynamics, and Lasers Conference, 17th, Snowmass, CO, June 25-27, 1984. 6 p. refs  
 (Contract NAG3-305)  
 (AIAA PAPER 84-1522)

Measurements of electron density and electric field strength have been made in an argon plasma contained in a resonant microwave cavity at 2.45 GHz. Spatial measurements of electron density,  $n_{sub e}$ , are correlated with fluorescence observations of the discharge. Measurements of  $n_{sub e}$  were made with Stark broadening and compared with  $n_{sub e}$  calculated from measured plasma conductivity. Additional measurements of  $n_{sub e}$  as a function of pressure and in mixtures of argon and oxygen are presented for pressures from 10 Torr to 1 atm. Measurements in flowing gases and in static systems are presented. In addition, limitations of these measurements are identified. Author

**N84-16991\*#** Iowa Univ., Iowa City. Dept. of Physics and Astronomy.  
**INTERPRETATION OF STS-3/PLASMA DIAGNOSTICS PACKAGE RESULTS IN TERMS OF LARGE SPACE STRUCTURE PLASMA INTERACTIONS** Semiannual Technical Progress Report, 10 Jul. 1983 - 25 Jan. 1984  
 W. S. KURTH 27 Jan. 1984 19 p  
 (Contract NAG3-449)  
 (NASA-CR-173266; NAS 1.26:173266) Avail: NTIS HC A02/MF A01 CSCL 20I

The Plasma Diagnostics Package, which was flown aboard STS-3 recorded various chemical releases from the Orbiter. Changes in the plasma environment were observed to occur during Flash Evaporator System (FES) releases, water dumps and maneuvering thruster operations. During flash evaporator operations, broadband Orbiter-generated electro-static noise is enhanced and plasma density irregularity ( $\delta n/n$ ) is observed to increase by as much as 4 times and is strongly peaked below 6 Hz. In the case of water dumps, background electrostatic noise is enhanced or suppressed depending on frequency and  $\Delta n/n$  is also seen to increase by as much as 4 times. Various changes in the plasma environment are effected by primary and vernier thruster operations. In addition, thruster activity stimulates electrostatic noise with a spectrum which is most intense at frequencies below 10 kHz. Author

C-3

**N84-21329\*#** National Aeronautics and Space Administration. Lewis Research Center, Cleveland, Ohio.

**RADICAL AND ION MOLECULE MECHANISMS IN THE POLYMERIZATION OF HYDROCARBONS AND CHLOROSILANES IN RF PLASMAS AT LOW PRESSURES (1:0 TORR)**

R. AVNI, U. CARMI (Ben Gurion Univ. of the Negev, Beer Sheva, Israel), A. INSPEKTOR (Nuclear Research Center Negev, Beer Sheva, Israel), and I. ROSENTHAL (Nuclear Research Center Negev, Beer Sheva, Israel) 13 Apr. 1984 24 p refs Presented at 11th Conf. Met. Coatings, San Diego, Calif., 9-13 Apr. 1984; sponsored by American Vacuum Society (NASA-TM-83602; E-2019; NAS 1.15:83602) Avail: NTIS HC A02/MF A01 CSCL 201

The ion-molecule and the radical-molecule mechanisms are responsible for the dissociation of hydrocarbons, and chlorosilane monomers and the formation of polymerized species, respectively, in the plasma state of a RF discharge. In the plasma, of a mixture of monomer with Ar, the rate determining step for both dissociation and polymerization is governed by an ion-molecular type interaction. Additions of H<sub>2</sub> or NH<sub>3</sub> to the monomer Ar(+) mixture transforms the rate determining step from an ion-molecular interaction to a radical-molecule type interaction for both monomer dissociation and polymerization processes. Author

**N84-21330\*#** National Aeronautics and Space Administration. Lewis Research Center, Cleveland, Ohio.

**CORRELATIONS BETWEEN PLASMA VARIABLES AND THE DEPOSITION PROCESS OF SI FILMS FROM CHLOROSILANES IN LOW PRESSURE RF PLASMA OF ARGON AND HYDROGEN**

R. AVNI, U. CARMI (Nuclear Research Center Negev, Beer Sheva, Israel), A. GRILL (Ben Gurion University of the Negev, Beer Sheva, Israel), R. MANORY (Ben Gurion University of the Negev, Beer Sheva, Israel), and E. GROSSMAN (Ben Gurion University of the Negev, Beer Sheva, Israel) 13 Apr. 1984 18 p refs Presented at 11th Intern. on Met. Coatings, San Diego, Calif., 24-28 Jul. 1983; sponsored by American Vacuum Society (NASA-TM-83603; E-2020; NAS 1.15:83603) Avail: NTIS HC A02/MF A01 CSCL 201

The dissociation of chlorosilanes to silicon and its deposition on a solid substrate in a RF plasma of mixtures of argon and hydrogen were investigated as a function of the macrovariables of the plasma. The dissociation mechanism of chlorosilanes and HCl as well as the formation of Si in the plasma state were studied by sampling the plasma with a quadrupole mass spectrometer. Macrovariables such as pressure, net RF power input and locations in the plasma reactor strongly influence the kinetics of dissociation. The deposition process of microcrystalline silicon films and its chlorine contamination were correlated to the dissociation mechanism of chlorosilanes and HCl. Author

**N84-25058\*#** National Aeronautics and Space Administration. Lewis Research Center, Cleveland, Ohio.

**STATUS OF PLASMA PHYSICS TECHNIQUES FOR THE DEPOSITION OF TRIBOLOGICAL COATINGS**

T. SPALVINS *In its Tribology in the 80's*, vol. 2 p 729-750 Apr. 1984 refs Avail: NTIS HC A17/MF A01 CSCL 201

The plasma physics deposition techniques of sputtering and ion-plating are reviewed. Their characteristics and potentials are discussed in terms of synthesis or deposition of tribological coatings. Since the glow discharge or plasma generated in the conventional sputtering and ion-plating techniques has a low ionization efficiency, rapid advances have been made in equipment design to further increase the ionization efficiency. The enhanced ionization favorably affects the nucleation and growth sequence of the coating. This leads to improved adherence and coherence, higher density, favorable morphological growth, and reduced internal stresses in the coatings. As a result, desirable coating characteristics can be precision tailored. Tribological coating characteristics of sputtered solid film lubricants such as MoS<sub>2</sub>, ion-plated soft gold and lead metallic films, and sputtered and

ion-plated wear-resistant refractory compound films such as nitrides and carbides are discussed. M.G.

## 76

## SOLID-STATE PHYSICS

Includes superconductivity.

**A84-17823\*#** National Aeronautics and Space Administration. Lewis Research Center, Cleveland, Ohio.

**SILICON CARBIDE, A HIGH TEMPERATURE SEMICONDUCTOR**

J. A. POWELL (NASA, Lewis Research Center, Cleveland, OH) Cleveland Electrical and Electronics Conference and Exposition, 28th, Cleveland, OH, Oct. 4-6, 1983, Paper. 5 p. refs

Electronic applications are described that would benefit from the availability of high temperature semiconductor devices. Comparisons are made among potential materials for these devices and the problems of each are discussed. Recent progress in developing silicon carbide as a high temperature semiconductor is described. Author

**A84-33918\*** Rockwell International Corp., Thousand Oaks, Calif. **INTERACTION BETWEEN BORON AND INTRINSIC DEFECTS IN GAAS**

K. R. ELLIOTT (Rockwell International Microelectronics Research and Development Center, Thousand Oaks, CA) *Journal of Applied Physics* (ISSN 0021-8979), vol. 55, May 15, 1984, p. 3856-3858. refs

(Contract NAS3-22235; NAS3-2224)

A model has been developed to describe the interaction between boron and antisite defects in bulk grown undoped liquid uncapsulated Czochralski GaAs. This model helps explain the observed experimental behavior. The model indicates that the residual double acceptor can most likely be associated with either Ga(As) or B(As). Author

**A84-40600\*** National Aeronautics and Space Administration. Lewis Research Center, Cleveland, Ohio.

**STUDY OF THE AUGER LINE SHAPE OF POLYETHYLENE AND DIAMOND**

M. DAYAN and S. V. PEPPER (NASA, Lewis Research Center, Cleveland, OH) *Surface Science* (ISSN 0039-6028), vol. 138, no. 2-3, March 1984, p. 549-560. refs

The KVV Auger electron line shapes of carbon in polyethylene and diamond have been studied. The spectra were obtained in derivative form by electron beam excitation. They were treated by background subtraction, integration and deconvolution to produce the intrinsic Auger line shape. Electron energy loss spectra provided the response function in the deconvolution procedure. The line shape from polyethylene is compared with spectra from linear alkanes and with a previous spectrum of Kelber et al. Both spectra are compared with the self-convolution of their full valence band densities of states and of their p-projected densities. The experimental spectra could not be understood in terms of existing theories. This is so even when correlation effects are qualitatively taken into account account to the theories of Cini and Sawatzky and Lenselink. Author

**A84-42829\*** Rensselaer Polytechnic Inst., Troy, N. Y.

**FREE DENDRITIC GROWTH**

M. E. GLICKSMAN (Rensselaer Polytechnic Institute, Troy, NY) *Materials Science and Engineering* (ISSN 0025-5416), vol. 65, July 1984, p. 45-55. refs

(Contract NSF DMR-83-08052; NAG3-333)

Free dendritic growth refers to the unconstrained development of crystals within a supercooled melt, which is the classical 'dendrite problem'. Great strides have been taken in recent years in both the theoretical understanding of dendritic growth and its

experimental status. The development of this field will be sketched, showing that transport theory and interfacial thermodynamics (capillarity theory) were sufficient ingredients to develop a truly predictive model of dendrite formation. The convenient, but incorrect, notion of 'maximum velocity' was used for many years to estimate the behavior of dendritic transformations until supplanted by modern dynamic stability theory. The proper combinations of transport theory and morphological stability seem to be able to predict the salient aspects of dendritic growth, especially in the neighborhood of the tip. The overall development of cast microstructures, such as equiaxed zone formation, rapidly solidified microstructures, etc., also seems to contain additional non-deterministic features which lie outside the current theories discussed here. Author

**A84-49620\*** Case Western Reserve Univ., Cleveland, Ohio.  
**THERMAL OXIDATION OF 3C SILICON CARBIDE SINGLE-CRYSTAL LAYERS ON SILICON**

C. D. FUNG and J. J. KOPANSKI (Case Western Reserve University, Cleveland, OH) Applied Physics Letters (ISSN 0003-6951), vol. 45, Oct. 1, 1984, p. 757-759. refs (Contract NAG3-490)

Thermal oxidation of thick single-crystal 3C SiC layers on silicon substrates was studied. The oxidations were conducted in a wet O<sub>2</sub> atmosphere at temperatures from 1000 to 1250 C for times from 0.1 to 50 h. Ellipsometry was used to determine the thickness and index of refraction of the oxide films. Auger analysis showed them to be homogeneous with near stoichiometric composition. The oxide growth followed a linear parabolic relationship with time. Activation energy of the parabolic rate constant was found to be 50 kcal/mole, while the linear rate constant was 74 kcal/mole. The latter value corresponds approximately to the energy required to break a Si-C bond. Electrical measurements show an effective density of  $4.6 \times 10$  to the 11th per sq cm for fixed oxide charges at the oxide-carbide interface, and the dielectric strength of the oxide film is approximately  $6 \times 10$  to the 6th V/cm. Author

**N84-14932\*** National Aeronautics and Space Administration. Lewis Research Center, Cleveland, Ohio.

**SILICON CARBIDE, A HIGH TEMPERATURE SEMICONDUCTOR**

J. A. POWELL 1983 7 p refs Presented at Cleveland Electron. Conf. (CECON '83), Cleveland, 4-6 Oct. 1983; sponsored by IEEE (NASA-TM-83514; E-1861; NAS 1.15:83514) Avail: NTIS HC A02/MF A01 CSCL 20L

Electronic applications are described that would benefit from the availability of high temperature semiconductor devices. Potential materials for these devices are compared and the problems of each are discussed. Recent progress in developing silicon carbide as a high temperature semiconductor is described. Author

**N84-17014\*** Rockwell International Corp., Thousand Oaks, Calif.

**LEC GAAS FOR INTEGRATED CIRCUIT APPLICATIONS**

C. G. KIRKPATRICK, R. T. CHEN, D. E. HOMES, P. M. ASBECK, K. R. ELLIOTT, R. D. FAIRMAN, and J. D. OLIVER 1984 131 p refs (Contract NAS3-22224)

(NASA-CR-173267; NAS 1.26:173267) Avail: NTIS HC A06/MF A01 CSCL 20L

Recent developments in liquid encapsulated Czochralski techniques for the growth of seminsulating GaAs for integrated circuit applications have resulted in significant improvements in the quality and quantity of GaAs material suitable for device processing. The emergence of high performance GaAs integrated circuit technologies has accelerated the demand for high quality, large diameter seminsulating GaAs substrates. The new device technologies, including digital integrated circuits, monolithic microwave integrated circuits and charge coupled devices have largely adopted direct ion implantation for the formation of doped layers. Ion implantation lends itself to good uniformity and reproducibility, high yield and low cost; however, this technique

also places stringent demands on the quality of the semiinsulating GaAs substrates. Although significant progress was made in developing a viable planar ion implantation technology, the variability and poor quality of GaAs substrates have hindered progress in process development. Author

**N84-20404\*** National Aeronautics and Space Administration. Lewis Research Center, Cleveland, Ohio.

**COAXIAL CARBON PLASMA GUN DEPOSITION OF AMORPHOUS CARBON FILMS**

D. M. SATER (Cincinnati Univ.), D. A. GULINO, and S. K. RUTLEDGE (Cleveland State Univ.) Mar. 1984 20 p refs (NASA-TM-83600, E-2012; NAS 1.15:83600) Avail: NTIS HC A02/MF A01 CSCL 20L

A unique plasma gun employing coaxial carbon electrodes was used in an attempt to deposit thin films of amorphous diamond-like carbon. A number of different structural, compositional, and electrical characterization techniques were used to characterize these films. These included scanning electron microscopy, scanning transmission electron microscopy, X ray diffraction and absorption, spectrographic analysis, energy dispersive spectroscopy, and selected area electron diffraction. Optical absorption and electrical resistivity measurements were also performed. The films were determined to be primarily amorphous, with poor adhesion to fused silica substrates. Many inclusions of particulates were found to be present as well. Analysis of these particulates revealed the presence of trace impurities, such as Fe and Cu, which were also found in the graphite electrode material. The electrodes were the source of these impurities. No evidence of diamond-like crystallite structure was found in any of the film samples. Details of the apparatus, experimental procedure, and film characteristics are presented. Author

**N84-28621\*** Rensselaer Polytechnic Inst., Troy, N. Y. Dept. of Materials Engineering.

**TRANSPORT PROCESSES IN DENDRITIC CRYSTALLIZATION**

M. E. GLICKSMAN In JPL Proc. of the Flat-Plate Solar Array Proj. Res. Forum on the High-Speed Growth and Characterization of Crystals for Solar Cells p 107-136 15 Apr. 1984 refs (Contract NAG3-333; NSF DMR-83-08052) Avail: NTIS HC A99/MF A01 CSCL 20B

Free dendritic growth refers to the unconstrained development of crystals within a supercooled melt, which is the classical dendrite problem. The development of theoretical understanding of dendritic growth and its experimental status is sketched showing that transport theory and interfacial thermodynamics (capillarity theory) are insufficient ingredients to develop a truly predictive model of dendrite formation. The convenient, but incorrect, notion of maximum velocity was used for many years to estimate the behavior of dendritic transformations until supplanted by modern dynamic stability theory. The proper combinations of transport theory and morphological stability seem to be able to predict the salient aspects of dendritic growth, especially in the neighborhood of the tip. A.R.H.

**N84-33210\*** Case Western Reserve Univ., Cleveland, Ohio. Dept. of Physics.

**PARTICLE ENVIRONMENT Final Report, 5 Nov. 1981 - 4 Nov. 1982**

W. L. GORDON and R. W. HOFFMAN Sep. 1984 24 p refs (Contract NSG-3235) (NASA-CR-173888; NAS 1.26:173888) Avail: NTIS HC A02/MF A01 CSCL 20L

The charging and discharging characteristics of an electrically isolated solar array segment were studied in order to simulate discharges seen during geomagnetic substorms. A solar array segment was floated while bombarded with monoenergetic electrons at various angles of incidence. The potentials of the array surface and of the interconnects were monitored using Trek voltage probes to maintain electrical isolation. A back plate was capacitively coupled to the array to provide information on the characteristics of the transients accompanying the discharges. Several modes of discharging of the array were observed at



relatively low differential and absolute potentials (a few kilovolts). A relatively slow discharge response in the array was observed, discharging over one second with currents of nanoamps. Two types of faster discharges were also seen which lasted a few hundredths of a millisecond and with currents on the order of microamps. Some results indicate an electron emission process associated with the arcs. Author

77

## THERMODYNAMICS AND STATISTICAL PHYSICS

Includes quantum mechanics; and Bose and Fermi statistics.

**A84-19359\*** California Univ., Santa Barbara.

### SCALING RELATIONS IN THE EQUATION OF STATE, THERMAL EXPANSION, AND MELTING OF METALS

F. GUINEA (California, University, Santa Barbara, CA), J. H. ROSE (U.S. Department of Energy, Ames Laboratory, Ames, IA; California, University, Santa Barbara, CA), J. R. SMITH (California, University, Santa Barbara, CA; GM Research Laboratories, Warren, MI), and J. FERRANTE (NASA, Lewis Research Center, Cleveland, OH) Applied Physics Letters (ISSN 0003-6951), vol. 44, Jan. 1, 1984, p. 53-55. refs

(Contract W-7405-ENG-82; NSF PHY-77-27084)

A simple and yet quite accurate prediction of volume as a function of pressure for metals and alloys is presented. Thermal expansion coefficients and melting temperatures are predicted by simple, analytic expressions and results compare favorably with experiment for a broad range of metals. All of these predictions are made possible by the discovery of universality in binding energy relations for metals. Author

**A84-20315\*** National Bureau of Standards, Washington, D.C.

### CAPILLARY RISE, WETTING LAYERS, AND CRITICAL PHENOMENA IN CONFINED GEOMETRY

M. R. MOLDOVER (National Bureau of Standards, Thermophysics Div., Washington, DC) and R. W. GAMMON (Maryland, University, College Park, MD) Journal of Chemical Physics (ISSN 0021-9606), vol. 80, Jan. 1, 1984, p. 528-535. refs

(Contract NASA ORDER C-62861-C; NASA ORDER M-27954-B)

Interferometric procedures have been used to measure the thickness of the wetting layers of liquid SF<sub>6</sub> which intrude between SF<sub>6</sub> vapor and the walls of an interferometer. Close to the critical temperature the measurements show that the layers become thicker as the height at which they are observed approaches the height of the bulk liquid-vapor meniscus. The functional form of the thickness increase agrees with the dependence expected from models in which the layers' thicknesses are governed by a competition between gravitational and van der Waals forces. The layers are a factor of three thicker than a simple estimate based on such models. No evidence is found of a transition from three-dimensional critical behavior towards two-dimensional critical behavior in the available temperature and size ranges. This contrasts with the interpretation of experiments in binary liquid mixtures carried out with comparable size and temperature resolution. C.D.

**A84-30391\*** Maryland Univ., College Park

### TURBIDITY VERY NEAR THE CRITICAL POINT OF METHANOL-CYCLOHEXANE MIXTURES

R. B. KOPELMAN, R. W. GAMMON (Maryland, University, College Park, MD), and M. R. MOLDOVER (National Bureau of Standards, Washington, DC) Physical Review A - General Physics, 3rd Series (ISSN 0556-2791), vol. 29, April 1984, p. 2048-2053. refs (Contract NASA ORDER C-62861-C; NASA ORDER H-27954-B)

The turbidity of a critical mixture of methanol and cyclohexane has been measured extremely close to the consolute point. The data span the reduced-temperature range between 10 to the -7th and 10 to the -3d, which is two decades closer to T<sub>c</sub> than previous

measurements. In this temperature range, the turbidity varies approximately as 1/t, as expected from the integrated form for Ornstein-Zernike scattering. A thin cell (200-micron optical path) with a very small volume (0.08 ml) was used to avoid multiple scattering. A carefully controlled temperature history was used to mix the sample and to minimize the effects of critical wetting layers. The data are consistent with a correlation-length amplitude of 3.9 plus or minus 1.0 Å, in agreement with the value 3.5 Å calculated from two-scale-factor universality and heat-capacity data from the literature. Author

80

## SOCIAL SCIENCES (GENERAL)

Includes educational matters.

**N84-16020\*#** National Aeronautics and Space Administration. Lewis Research Center, Cleveland, Ohio.

### CLEVELAND SPACE ODYSSEY

23 Mar. 1980 136 p refs Symp. held at Cleveland, 16-23 Mar. 1980 Sponsored in part by Cuyahoga Community College and Cleveland Public Schools (NASA-TM-85493; NAS 1.15:85493) Avail: NTIS HC A07/MF A01 CSCL 05I

The symposium included personal appearances by NASA astronauts, NASA exhibits, aerospace science lecture demonstrations (Spacemobile Lectures), souvenir photos for each student attending the symposium, and talks on job opportunities in aerospace and on the benefits of the Space Program. The program was directed mainly at (public, parochial and private) student groups, each of which spend three hours on the CCC campus to participate in the symposium activities. The symposium was open to the general public and consisted of the NASA exhibits, aerospace science lecture demonstrations, films, talks on the benefits of the space program, additional lectures by members of the American Institute of Aeronautics and Astronautics (AIAA), and a special tasting demonstration of space food meal systems. Author

**N84-16021\*#** National Aeronautics and Space Administration. Lewis Research Center, Cleveland, Ohio.

### CHICAGO MEETS OUTER SPACE PROGRAM Summary Report

H. ALLEN, JR. 8 Oct. 1978 112 p refs Symp. held at Chicago, 1-8 Oct. 1978 (NASA-TM-85492; NAS 1.15:85492) Avail: NTIS HC A06/MF A01 CSCL 05I

The symposium included personal appearances by NASA astronauts, NASA exhibits, souvenir photos for each student attending the symposium, live demonstrations of how the Communication Technology Satellite links the U. S. with people around the world, and talks on job opportunities in aerospace and on the benefits of space. Monday through Friday, the program was directed mainly at (public, parochial and private) student groups, each of which spent a half day on the CSU campus to participate in the symposium activities. On Saturday and Sunday, the symposium was open to the general public and consisted of the NASA exhibits, films, a shorter version of the lectures and a special demonstration and tasting opportunity of space food meal systems. These quick meal systems that were designed for senior citizens. Author

**N84-22488\*#** National Aeronautics and Space Administration. Lewis Research Center, Cleveland, Ohio.  
**SIMULTANEOUS CABIN AND AMBIENT OZONE MEASUREMENTS ON TWO BOEING 747 AIRPLANES. VOLUME 2: JANUARY TO OCTOBER 1978**

J. D. HOLDEMAN, L. C. PAPATHAKOS, G. J. HIGGINS (Control Data Corp., Minneapolis), and G. D. NASTROM (Control Data Corp., Minneapolis) Mar. 1984 47 p refs 2 Vol.  
 (Contract DOT-FA78WAI-893)

(NASA-TM-81733; E-789; NAS 1.15:81733; FAA-EE-83-7-VOL-2)  
 Avail: NTIS HC E05/MF A01 CSCL 01C

Measurements of ozone concentrations at cruise altitudes both outside and in the cabin of a Boeing 747SP and Boeing 747-100 airliners in routine commercial service are presented in this series of reports. Plotted and tabulated data are identified by route and are arranged chronologically for each airplane. These data were taken at 5- or 10-minute intervals by automated instrumentation used in the NASA Global Atmospheric Sampling Program (GASP). All GASP cabin ozone data obtained from January to early October 1978 are presented in this volume. Author

## 81

## ADMINISTRATION AND MANAGEMENT

Includes management planning and research.

**N84-14061\*#** National Aeronautics and Space Administration. Lewis Research Center, Cleveland, Ohio.

**RESEARCH AND TECHNOLOGY, 1983 Annual Report**

1983 60 p

(NASA-TM-83540; NAS 1.15:83540) Avail: NTIS HC A04/MF A01 CSCL 05A

Highlights of the research accomplishments of the Lewis Research Center covering aeronautics, spaceflight, space technology, and materials and structures are presented. Author

**N84-23315\*#** National Aeronautics and Space Administration. Lewis Research Center, Cleveland, Ohio.

**GOVERNMENT - CONTRACTOR INTERACTION Final Report**

D. M. THOMAS. In: AF Business Research Management Center Proc. of the Fed. Acquisition Res. Symp. with Theme p 118-121 1983

(AD-P002768) Avail: NTIS HC A24/MF A01 CSCL 15E

The development of the Administrative Contracting Officer represents an advance in the Government system of contract management because it provides an individual with knowledge, time, and a specialized function to insure performance of Government contracts. However, the development has created a dichotomy between the award and the post-award function which increases the adversary relationship with Government contractors. This paper advocates that this adversary relationship can be decreased if PCOs and ACOs are provided with opportunities to serve in the assignments of the other. Author (GRA)

## 83

## ECONOMICS AND COST ANALYSIS

Includes cost effectiveness studies

**A84-23119\*** National Aeronautics and Space Administration. Lewis Research Center, Cleveland, Ohio.

**ECONOMIC VIABILITY OF PHOTOVOLTAIC POWER FOR DEVELOPMENT ASSISTANCE APPLICATIONS**

W. J. BIFANO (NASA, Lewis Research Center, Cleveland, OH) IN: Photovoltaic Specialists Conference, 16th, San Diego, CA, September 27-30, 1982, Conference Record. New York, Institute of Electrical and Electronics Engineers, 1982, p. 1183-1188. refs

This paper briefly discusses the development assistance market and examines a number of specific photovoltaic (PV) development assistance field tests, including water pumping/grain grinding (Tangaye, Upper Volta), vaccine refrigerators slated for deployment in 24 countries, rural medical centers to be installed in Ecuador, Guyana, Kenya and Zimbabwe, and remote earth stations to be deployed in the near future. A comparison of levelized energy cost for diesel generators and PV systems covering a range of annual energy consumptions is also included. The analysis does not consider potential societal, environmental or political benefits associated with PV power. PV systems are shown to be competitive with diesel generators, based on life cycle cost considerations, assuming a system price of \$20/W(peak), for applications having an annual energy demand of up to 6000 kilowatt-hours per year.

Author

## 85

## URBAN TECHNOLOGY AND TRANSPORTATION

Includes applications of space technology to urban problems; technology transfer; technology assessment; and surface and mass transportation.

**N84-14071\*#** Dayton Univ., Ohio. Dept. of Electrical Engineering.

**STUDY AND REVIEW OF PERMANENT MAGNETS FOR ELECTRIC VEHICLE PROPULSION MOTORS Final Report**

K. J. STRNAT Sep. 1983 183 p refs

(Contract DEN3-189; DE-AI01-77CS-51044)

(NASA-CR-168178; DOE/NASA/0189-83/2; NAS 1.26:168178)

Avail: NTIS HC A09/MF A01 CSCL 13F

A study of permanent magnets (PM) was performed in support of the DOE/NASA electric and hybrid vehicle program. PM requirements for electric propulsion motors are analyzed, design principles and relevant properties of magnets are discussed. Available PM types are reviewed. For the needed high-grade magnets, design data, commercial varieties and sources are tabulated, based on a survey of vendors. Economic factors such as raw material availability, production capability and cost are analyzed, especially for cobalt and the rare earths. Extruded Mn-Al-C magnets from Japan were experimentally characterized. Dynamic magnetic data for the range -50 deg to +150 deg C and some mechanical properties are reported. The state of development of the important PM material families is reviewed. Feasible improvements or new developments of magnets for electric vehicle motors are identified. Author

**N84-14989\*#** National Aeronautics and Space Administration. Lewis Research Center, Cleveland, Ohio.

**DOWNSIZING ASSESSMENT OF AUTOMOTIVE STIRLING ENGINES Final Report**

R. H. KNOLL, R. C. TEW, JR., and J. L. KLANN Sep. 1983 42 p refs

(Contract DE-AI01-77CS-51040)

(NASA-TM-83468; E-1783; NAS 1.15:83468;

NASA/DOE/51040-49) Avail: NTIS HC A03/MF A01 CSCL 13F

A 67 kW (90 hp) Stirling engine design, sized for use in a 1984 1440 kg (3170 lb) automobile was the focal point for developing automotive Stirling engine technology. Since recent trends are towards lighter vehicles, an assessment was made of the applicability of the Stirling technology being developed for smaller, lower power engines. Using both the Philips scaling laws and a Lewis Research Center (Lewis) Stirling engine performance code, dimensional and performance characteristics were determined for a 26 kW (35 hp) and a 37 kW (50 hp) engine for use in a nominal 907 kg (2000 lb) vehicle. Key engine elements were sized and stressed and mechanical layouts were made to ensure mechanical fit and integrity of the engines. Fuel economy estimates indicated that the Stirling engine would maintain a 30 to 45 percent fuel economy advantage comparable spark ignition and diesel powered vehicles in the 1984 period. Author

**N84-14991\*#** Little (Arthur D.), Inc., Cambridge, Mass.

**CATALOG OF SELECTED HEAVY DUTY TRANSPORT ENERGY MANAGEMENT MODELS Contractor Report, Dec. 1982 - Nov. 1983**

R. G. COLELLO, A. B. BOGHANI, N. C. GARDELLA, P. G. GOTT, W. D. LEE, E. C. POLLAK, W. P. TEAGAN, R. G. THOMAS, C. M. SNYDER, and R. P. WILSON, JR. Nov. 1983 277 p (Contract DEN3-301)

(NASA-CR-168299; DOE/NASA/0301-1; NAS 1.26:168299; ADL-88683) Avail: NTIS HC A17/MF A01 CSCL 13F

A catalog of energy management models for heavy duty transport systems powered by diesel engines is presented. The catalog results from a literature survey, supplemented by telephone interviews and mailed questionnaires to discover the major computer models currently used in the transportation industry in the following categories: heavy duty transport systems, which consist of highway (vehicle simulation), marine (ship simulation), rail (locomotive simulation), and pipeline (pumping station simulation), and heavy duty diesel engines, which involve models that match the intake/exhaust system to the engine, fuel efficiency, emissions, combustion chamber shape, fuel injection system, heat transfer, intake/exhaust system, operating performance, and waste heat utilization devices, i.e., turbocharger, bottoming cycle. Author

**N84-17073\*#** Gould, Inc., Rolling Meadows, Ill. Electrical and Electronics Research: Electrical and Electronics Research

**INTEGRAL INVERTER/BATTERY CHARGER FOR USE IN ELECTRIC VEHICLES Final Report**

D. THIMMESCH Sep. 1983 136 p refs

(Contract DEN3-249; DE-AI01-77CS-51044)

(NASA-CR-168177; DOE/NASA/0249-81/1; NAS 1.26:168177)

Avail: NTIS HC A07/MF A01 CSCL 13F

The design and test results of a thyristor based inverter/charger are discussed. A battery charger is included integral to the inverter by using a subset of the inverter power circuit components. The resulting charger provides electrical isolation between the vehicle propulsion battery and ac line and is capable of charging a 25 kWh propulsion battery in 8 hours from a 220 volt ac line. The integral charger employs the inverter commutation components at a resonant ac/dc isolated converter rated at 3.6 kW. Charger efficiency and power factor at an output power of 3.6 kW are 86% and 95% respectively. The inverter, when operated with a matching polyphase ac induction motor and nominal 132 volt propulsion battery, can provide a peak shaft power of 34 kW (45 hp) during motoring operation and 45 kW (60 hp) during regeneration. Thyristors are employed for the inverter power

switching devices and are arranged in an input-commutated topology. This configuration requires only two thyristors to commutate the six main inverter thyristors. Inverter efficiency during motoring operation at motor shaft speeds above 450 rad/sec (4300 rpm) is 92-94% for output power levels above 11 kW (15 hp). The combined ac inverter/charger package weighs 47 kg (103 lbs). Author

**N84-18117\*#** Mechanical Technology, Inc., Latham, N. Y.

**AUTOMOTIVE STIRLING ENGINE DEVELOPMENT PROGRAM Semiannual Technical Progress Report, 1 Jan. - 30 Jun. 1983**

N. NIGHTINGALE, W. ERNST, A. RICHEY, M. SIMETKOSKY, G. SMITH, C. ROHDENBURG, and M. ANTONELLI, ed. Aug. 1983 87 p

(Contract DEN3-32; DE-AI01-77CS-51040)

(NASA-CR-168205; DOE/NASA/0032-21; NAS 1.26:168205;

MTI-83ASE334SA4) Avail: NTIS HC A05/MF A01 CSCL 13F

Program status and plans are discussed for component and technology development; reference engine system design, the upgraded Mod 1 engine; industry test and evaluation; and product assurance. Four current Mod 1 engines reached a total of 2523 operational hours, while two upgraded engines accumulated 166 hours. A R.H.

**N84-19185\*#** Cleveland State Univ., Ohio. Dept. of Electrical Engineering.

**OPTIMIZATION METHODS APPLIED TO HYBRID VEHICLE DESIGN Final Report**

J. F. DONOGHUE and J. H. BURGHART Jun. 1983 180 p refs

(Contract NAG3-84; DE-AI01-77CS-51044)

(NASA-CR-168292; DOE/NASA/0084-1; NAS 1.26:168292)

Avail: NTIS HC A09/MF A01 CSCL 13F

The use of optimization methods as an effective design tool in the design of hybrid vehicle propulsion systems is demonstrated. Optimization techniques were used to select values for three design parameters (battery weight, heat engine power rating and power split between the two on-board energy sources) such that various measures of vehicle performance (acquisition cost, life cycle cost and petroleum consumption) were optimized. The approach produced designs which were often significant improvements over hybrid designs already reported on in the literature. The principal conclusions are as follows. First, it was found that the strategy used to split the required power between the two on-board energy sources can have a significant effect on life cycle cost and petroleum consumption. Second, the optimization program should be constructed so that performance measures and design variables can be easily changed. Third, the vehicle simulation program has a significant effect on the computer run time of the overall optimization program; run time can be significantly reduced by proper design of the types of trips the vehicle takes in a one year period. Fourth, care must be taken in designing the cost and constraint expressions which are used in the optimization so that they are relatively smooth functions of the design variables. Fifth, proper handling of constraints on battery weight and heat engine rating, variables which must be large enough to meet power demands, is particularly important for the success of an optimization study. Finally, the principal conclusion is that optimization methods provide a practical tool for carrying out the design of a hybrid vehicle propulsion system. Author

**N84-21445\*#** United Technologies Research Center, East Hartford, Conn.

**EXTENSION TO AN ANALYSIS OF TURBULENT SWIRLING COMPRESSIBLE FLOW FOR APPLICATION TO AXISYMMETRIC SMALL GAS TURBINE DUCTS** Final Report, Nov. 1980 - Nov. 1981

O. L. ANDERSON, G. B. HANKINS, and D. E. EDWARDS Dec. 1981 69 p refs

(Contract DEN3-235; DE-AI01-77CS-51040)

(NASA-CR-165597; NAS 1.26:165597; R81-915395-12;

DOE/NASA/0235-1) Avail: NTIS HC A04/MF A01 CSCL 13F

An existing computer program, the Axisymmetric Diffuser Duct Code (ADD code), which calculates compressible turbulent swirling flow through axisymmetric ducts was modified to permit calculation of flows through small gas turbine ducts with struts, guide vanes and large degrees of turning. The improvements include a coordinate generator, an end-wall loss model, and a generalized geometry capability to describe struts and guide vanes in ducts which turn more than 90 degrees. An improved output format was developed to provide the solution on any arbitrary plane in the duct and an extensive literature survey of calculation procedures used in gas turbine technology was completed which suggests improvements in the computer code. Calculations are presented for the flow through the AGT101 small gas turbine inlet duct and turbine exhaust diffuser which demonstrate the ADD code modifications implemented in the investigation. The computed results compare favorably with experimental results. S.L.

**N84-22512\*#** National Aeronautics and Space Administration. Lewis Research Center, Cleveland, Ohio.

**OVERVIEW OF NASA LEWIS RESEARCH CENTER FREE-PISTON STIRLING ENGINE ACTIVITIES**

J. G. SLABY 1984 22 p refs Proposed for presentation at the 19th Intersociety Energy Conversion Eng. Conf., 19-24 Aug. 1984; sponsored by ANS, ASME, SAE, AIAA, IEEE, ACS and AIChE

(Contract DE-AI05-82OR-1005)

(NASA-TM-83649; DOE/NASA/1005-2; E-2094; NAS 1.15:83649) Avail: NTIS HC A02/MF A01 CSCL 13I

A generic free-piston Stirling technology project is being conducted to develop technologies generic to both space power and terrestrial heat pump applications in a cooperative, cost-shared effort. The generic technology effort includes extensive parametric testing of a 1 kW free-piston Stirling engine (RE-1000), development of a free-piston Stirling performance computer code, design and fabrication under contract of a hydraulic output modification for RE-1000 engine tests, and a 1000-hour endurance test, under contract, of a 3 kWe free-piston Stirling/alternator engine. A newly initiated space power technology feasibility demonstration effort addresses the capability of scaling a free-piston Stirling/alternator system to about 25 kWe; developing thermodynamic cycle efficiency or equal to 70 percent of Carnot at temperature ratios in the order of 1.5 to 2.0; achieving a power conversion unit specific weight of 6 kg/kWe; operating with noncontacting gas bearings; and dynamically balancing the system. Planned engine and component design and test efforts are described. A.R.H.

**N84-24509\*#** National Aeronautics and Space Administration. Lewis Research Center, Cleveland, Ohio.

**COMPARISON OF FREE-PISTON STIRLING ENGINE MODEL PREDICTIONS WITH RE1000 ENGINE TEST DATA**

R. C. TEW, JR. 1984 21 p refs Proposed for presentation at the 19th Intersoc. Energy Conversion Eng. Conf., San Francisco, 19-24 Aug. 1984; sponsored by American Nuclear Society, ASME, SAE, IEEE, AIAA, ACS, and AIChE

(Contract DE-AI05-82OR-1005)

(NASA-TM-83650; E-2095; DOE/NASA/1005-3; NAS 1.15:83650)

Avail: NTIS HC A02/MF A01 CSCL 13F

Predictions of a free-piston Stirling engine model are compared with RE1000 engine test data taken at NASA-Lewis Research Center. The model validation and the engine testing are being done under a joint interagency agreement between the Department of Energy's Oak Ridge National Laboratory and NASA-Lewis. A

kinematic code developed at Lewis was upgraded to permit simulation of free-piston engine performance; it was further upgraded and modified at Lewis and is currently being validated. The model predicts engine performance by numerical integration of equations for each control volume in the working space. Piston motions are determined by numerical integration of the force balance on each piston or can be specified as Fourier series. In addition, the model Fourier analyzes the various piston forces to permit the construction of phasor force diagrams. The paper compares predicted and experimental values of power and efficiency and shows phasor force diagrams for the RE1000 engine displacer and piston. Further development plans for the model are also discussed. Author

**N84-26484\*#** National Aeronautics and Space Administration. Lewis Research Center, Cleveland, Ohio.

**REAL-TIME SIMULATION OF AN AUTOMOTIVE GAS TURBINE USING THE HYBRID COMPUTER** Final Report

W. COSTAKIS and W. C. MERRILL May 1984 26 p

(Contract DE-AI01-77CS-51040)

(NASA-TM-83593; E-1994; DOE/NASA/51040-52; NAS 1.15:83593) Avail: NTIS HC A03/MF A01 CSCL 13F

A hybrid computer simulation of an Advanced Automotive Gas Turbine Powertrain System is reported. The system consists of a gas turbine engine, an automotive drivetrain with four speed automatic transmission, and a control system. Generally, dynamic performance is simulated on the analog portion of the hybrid computer while most of the steady state performance characteristics are calculated to run faster than real time and makes this simulation a useful tool for a variety of analytical studies. Author

**N84-29805\*#** Garrett Turbine Engine Co., Phoenix, Ariz.

**ADVANCED GAS TURBINE (AGT) Semiannual Progress Report, Jan. - Jun. 1983**

Dec. 1983 78 p refs

(Contract DEN3-167)

(NASA-CR-174694; DOE/NASA/0167-7; NAS 1.26:174694; GARRETT-31-3725(7); SAPR-7) Avail: NTIS HC A05/MF A01 CSCL 13F

The development and progress of the Advanced Gas Turbine engine program is examined. An analysis of the role of ceramics in the design and major engine components is included. Projected fuel economy, emissions and performance standards, and versatility in fuel use are also discussed. M.A.C.

**N84-32305\*#** Mechanical Technology, Inc., Latham, N. Y. Engine Systems Div.

**AUTOMOTIVE STIRLING ENGINE DEVELOPMENT PROGRAM Semiannual Technical Progress Report, 1 Jul. - 31 Dec. 1983**

N. NIGHTINGALE, W. ERNST, A. RICHEY, M. SIMETKOSKY, G. SMITH, C. ROHDENBURG, A. VATSKY, and M. ANTONELLI, ed. Mar. 1983 85 p

(Contract DEN3-32; DE-AI01-77CS-51040)

(NASA-CR-174622; DOE/NASA/0032-80/7; NAS 1.26:174622; REPT-84ASE369SA5) Avail: NTIS HC A05/MF A01 CSCL 13F

Activities performed on Mod I engine testing and test results, testing of the Mod I engine in the United States, Mod I engine characterization and analyses, Mod I Transient Test Bed fuel economy, upgraded Mod I performance and testing, Stirling engine reference engine manufacturing and reduced size studied, components and subsystems, and the study and test of low cost casting alloys are summarized. The overall program philosophy is outlined, and data and results are presented. Author

**N84-32306\*# Thermo Electron Corp., Waltham, Mass.  
AN RC-1 ORGANIC RANKINE BOTTOMING CYCLE FOR AN  
ADIABATIC DIESEL ENGINE**

L. R. DINANNO, F. A. DIBELLA, and M. D. KOPIOW Dec. 1983  
125 p refs  
(Contract DEN3-302; DE-AI01-80CS-50194)  
(NASA-CR-168256; DOE/NASA/0302-1; NAS 1.26:168256;  
TE4322-251-83) Avail: NTIS HC A06/MF A01 CSCL 10B

A system analysis and preliminary design were conducted for an organic Rankine-cycle system to bottom the high-temperature waste heat of an adiabatic diesel engine. The bottoming cycle is a compact package that includes a cylindrical air cooled condenser regenerator module and other unique features. The bottoming cycle output is 56 horsepower at design point conditions when compounding the reference 317 horsepower turbocharged diesel engine with a resulting brake specific fuel consumption of 0.268 lb/hp-hr for the compound engine. The bottoming cycle when applied to a turbocompound diesel delivers a compound engine brake specific fuel consumption of 0.258 lb/hp-hr. This system for heavy duty transport applications uses the organic working fluid RC-1, which is a mixture of 60 mole percent pentafluorobenzene and 40 mole percent hexafluorobenzene. The thermal stability of the RC-1 organic fluid was tested in a dynamic fluid test loop that simulates the operation of Rankine-cycle. More than 1600 hours of operation were completed with results showing that the RC-1 is thermally stable up to 900 F. A.R.H.

**N84-32307\*# United Technologies Research Center, East  
Hartford, Conn.  
WASTE HEAT RECOVERY FROM ADIABATIC DIESEL ENGINES  
BY EXHAUST-DRIVEN BRAYTON CYCLES**

H. E. KHALIFA Dec. 1983 109 p refs  
(Contract DEN3-304)  
(NASA-CR-168257; DOE/NASA/0304-1; NAS 1.26:168257)  
Avail: NTIS HC A06/MF A01 CSCL 10B

An evaluation of Bryton Bottoming Systems (BBS) as waste heat recovery devices for future adiabatic diesel engines in heavy duty trucks is presented. Parametric studies were performed to evaluate the influence of external and internal design parameters on BBS performance. Conceptual design and trade-off studies were undertaken to estimate the optimum configuration, size, and cost of major hardware components. The potential annual fuel savings of long-haul trucks equipped with BBS were estimated. The addition of a BBS to a turbocharged, nonaftercooled adiabatic engine would improve fuel economy by as much as 12%. In comparison with an aftercooled, turbocompound engine, the BBS-equipped turbocharged engine would offer a 4.4% fuel economy advantage. If installed in tandem with an aftercooled turbocompound engine, the BBS could effect a 7.2% fuel economy improvement. The cost of a mass-produced 38 Bhp BBS is estimated at about \$6460 or 170/Bhp. Technical and economic barriers that hinder the commercial introduction of bottoming systems were identified. Related studies in the area of waste heat recovery from adiabatic diesel engines and NASA-CR-168255 (Steam Rankine) and CR-168256 (Organic Rankine). Author

**N84-33304\*# Foster-Miller Associates, Inc., Waltham, Mass.  
STEAM BOTTOMING CYCLE FOR AN ADIABATIC DIESEL  
ENGINE Final Report**

E. POULIN, R. DEMIER, I. KREPCIN, and D. WALKER Mar. 1984 129 p refs  
(Contract DEN3-300; DE-AI01-80CS-50194)  
(NASA-CR-168255; DOE/NASA/0300-1; NAS 1.26:168255;  
FMI-NAS-8273) Avail: NTIS HC A07/MF A01 CSCL 13F

Steam bottoming cycles using adiabatic diesel engine exhaust heat which projected substantial performance and economic benefits for long haul trucks were studied. Steam cycle and system component variables, system cost, size and performance were analyzed. An 811 K/6.90 MPa state of the art reciprocating expander steam system with a monotube boiler and radiator core condenser was selected for preliminary design. The costs of the diesel with bottoming system (TC/B) and a NASA specified turbocompound adiabatic diesel with aftercooling with the same

total output were compared, the annual fuel savings less the added maintenance cost was determined to cover the increase initial cost of the TC/B system in a payback period of 2.3 years. Steam bottoming system freeze protection strategies were developed, technological advances required for improved system reliability are considered and the cost and performance of advanced systems are evaluated. E.A.K.

**N84-33306\*# Massachusetts Inst. of Tech., Cambridge.  
Automotive Lab.**

**COMPUTER SIMULATION OF THE HEAVY-DUTY  
TURBO-COMPOUNDED DIESEL CYCLE FOR STUDIES OF  
ENGINE EFFICIENCY AND PERFORMANCE Interim Report**

D. N. ASSANIS, J. A. EKCHIAN, J. B. HEYWOOD, and K. K. REPLOGLE May 1984 71 p refs  
(Contract NAG3-394; DE-AI01-80CS-50294)  
(NASA-CR-174755; DOE/NASA/0394-1; NAS 1.26:174755)  
Avail: NTIS HC A04/MF A01 CSCL 13F

Reductions in heat loss at appropriate points in the diesel engine which result in substantially increased exhaust enthalpy were shown. The concepts for this increased enthalpy are the turbocharged, turbocompounded diesel engine cycle. A computer simulation of the heavy duty turbocharged turbo-compounded diesel engine system was undertaken. This allows the definition of the tradeoffs which are associated with the introduction of ceramic materials in various parts of the total engine system, and the study of system optimization. The basic assumptions and the mathematical relationships used in the simulation of the model engine are described. E.A.K.

**N84-33307\*# Mechanical Technology, Inc., Latham, N. Y.  
AUTOMOTIVE STIRLING ENGINE DEVELOPMENT PROGRAM.  
RES D SUMMARY REPORT Final Report**

May 1984 217 p  
(Contract DEN3-32; DE-AI01-77CS-51040)  
(NASA-CR-174674; DOE/NASA/0032-23; NAS 1.26:174674;  
MTI-84ASE356DR3) Avail: NTIS HC A10/MF A01 CSCL 13F

The design of reference Stirling engine system as well as the engine auxiliaries and controls is described. Manufacturing costs in production quantity are also presented. Engine system performance predictions are discussed and vehicle integration is developed, along with projected fuel economy levels. A.R.H.

**N84-33309\*# SKF Industries, Inc., King of Prussia, Pa.**

**SOLID LUBRICATION DESIGN METHODOLOGY**

B. B. AGGARWAL, T. M. YONUSHONIS, and R. L. BOVENKERK May 1984 112 p refs  
(Contract DEN3-323; DE-AI01-80CS-50194)  
(NASA-CR-174690; DOE/NASA/0323-1; NAS 1.26:174690)  
Avail: NTIS HC A06/MF A01 CSCL 13I

A single element traction rig was used to measure the traction forces at the contact of a ball against a flat disc at room temperature under combined rolling and sliding. The load and speed conditions were selected to match those anticipated for bearing applications in adiabatic diesel engines. The test program showed that the magnitude of traction forces were almost the same for all the lubricants tested; a lubricant should, therefore, be selected on the basis of its ability to prevent wear of the contact surfaces. Traction vs. slide/roll ratio curves were similar to those for liquid lubricants but the traction forces were an order of magnitude higher. The test data was used to derive equations to predict traction force as a function of contact stress and rolling speed. Qualitative design guidelines for solid lubricated concentrated contacts are proposed. Author

**N84-34330\*#** National Aeronautics and Space Administration.  
Lewis Research Center, Cleveland, Ohio.

**BASELINE PERFORMANCE AND EMISSIONS DATA FOR A SINGLE-CYLINDER, DIRECT-INJECTED DIESEL ENGINE Final Report**

R. A. DEZELICK, J. J. MCFADDEN, L. W. REAM, and R. F. BARROWS Sep. 1983 67 p refs  
(Contract DE-AI01-80CS-50194)

(NASA-TM-86873; DOE/NASA/50194-38; E-2079; NAS 1.15:86873) Avail: NTIS HC A04/MF A01 CSCL 13F

Comprehensive fuel consumption, mean effective cylinder pressure, and emission test results for a supercharged, single-cylinder, direct-injected, four-stroke-cycle, diesel test engine are documented. Inlet air-to-exhaust pressure ratios were varied from 1.25 to 3.35 in order to establish the potential effects of turbocharging techniques on engine performance. Inlet air temperatures and pressures were adjusted from 34 to 107 C and from 193 to 414 kPa to determine the effects on engine performance and emissions. Engine output ranged from 300 to 2100 kPa (brake mean effective pressure) in the speed range of 1000 to 3000 rpm. Gaseous and particulate emission rates were measured. Real-time values of engine friction and pumping loop losses were measured independently and compared with motored engine values.

Author

**N84-34331\*#** Garrett Turbine Engine Co., Phoenix, Ariz.

**HIGH TEMPERATURE CERAMIC INTERFACE STUDY Final Report**

L. J. LINDBERG Aug. 1984 112 p refs

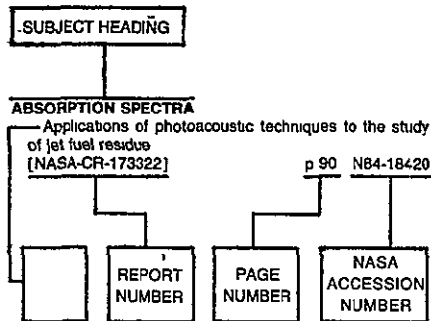
(Contract DEN3-324; DE-AI01-80CS-50194)

(NASA-CR-174728; NAS 1.26:174728; GTEC-31-5738) Avail: NTIS HC A06/MF A01 CSCL 11B

Monolithic SiC and Si<sub>3</sub>N<sub>4</sub> are susceptible to contact stress damage at static and sliding interfaces. Transformation-toughened zirconia (TTZ) was evaluated under sliding contact conditions to determine if the higher material fracture toughness would reduce the susceptibility to contact stress damage. Contact stress tests were conducted on four commercially available TTZ materials at normal loads ranging from 0.455 to 22.7 kg (1 to 50 pounds) at temperatures ranging from room temperature to 1204C (2200 F). Static and dynamic friction were measured as a function of temperature. Flexural strength measurements after these tests determined that the contact stress exposure did not reduce the strength of TTZ at contact loads of 0.455, 4.55, and 11.3 kg (1, 10, and 25 pounds). Prior testing with the lower toughness SiC and Si<sub>3</sub>N<sub>4</sub> materials resulted in a substantial strength reduction at loads of only 4.55 and 11.3 kg (10 and 25 pounds). An increase in material toughness appears to improve ceramic material resistance to contact stress damage. Baseline material flexure strength was established and the stress rupture capability of TTZ was evaluated. Stress rupture tests determined that TTZ materials are susceptible to deformation due to creep and that aging of TTZ materials at elevated temperatures results in a reduction of material strength.

R.J.F.

## Typical Subject Index Listing



The subject heading is a key to the subject content of the document. The title is used to provide a description of the subject matter. When the title is insufficiently descriptive of the document content, the title extension is added, separated from the title by three hyphens. The (NASA or AIAA) accession number and the page number are included in each entry to assist the user in locating the abstract in the abstract section (of this supplement). If applicable, a report number is also included as an aid in identifying the document. Under any one subject heading, the accession numbers are arranged in sequence with the AIAA accession numbers appearing first.

## A

### ABERRATION

Window aberration correction in laser velocimetry using multifaceted holographic optical elements p 134 N84-24663

### ABRASIVES

Abrasive tip treatment for use on compressor blades [NASA-CR-174666] p 145 N84-25065

### ABSORPTION SPECTRA

Applications of photoacoustic techniques to the study of jet fuel residue [NASA-CR-173322] p 90 N84-18420

### ABSORPTIVITY

Improved heat exchanger for electrothermal devices [NASA-CASE-LEW-14037-1] p 49 N84-32425

### AC GENERATORS

Three-phase, high-voltage, high-frequency distributed bus system for advanced aircraft p 105 N84-10058

### ACCELERATED LIFE TESTS

Long life nickel electrodes for a nickel-hydrogen cell I Initial performance p 162 N84-30186

### ACCELERATION (PHYSICS)

Self-similar blast waves incorporating deflagrations of variable speed p 116 N84-28379

### ACCEPTOR MATERIALS

Interaction between boron and intrinsic defects in GaAs p 190 N84-33918

### ACCUMULATORS

A multistage spent particle collector and a method for making same [NASA-CASE-LEW-13914-1] p 131 N84-12447

Performance of computer-designed small-size multistage depressed collectors for a high-perveance traveling wave tube [NASA-TP-2249] p 106 N84-15394

Secondary electron emission characteristics of ion-textured copper and high-purity isotropic graphite surfaces [NASA-TP-2342] p 86 N84-28989

### ACCURACY

Assessment of three-dimensional inviscid codes and loss calculations for turbine aerodynamic computations [NASA-TM-83571] p 8 N84-16142  
Error reduction program. A progress report p 27 N84-20536

### ACEE PROGRAM

Comparison of full-scale engine and subscale model performance of a mixed flow exhaust system for an energy efficient engine (E3) propulsion system [AIAA PAPER 84-0283] p 16 N84-17997  
The aerodynamic design and performance of the NASA/GE E3 low pressure turbine [AIAA PAPER 84-1162] p 21 N84-44186  
Energy efficient engine program contributions to aircraft fuel conservation [NASA-TM-83741] p 34 N84-29876

### ACID BASE EQUILIBRIUM

Moderate temperature rechargeable NaNiS<sub>2</sub> cells p 108 N84-21376

### ACOUSTIC ATTENUATION

Preliminary investigation of an electrical network model for ultrasonic scattering [NASA-CR-3770] p 149 N84-17606

### ACOUSTIC DUCTS

A numerical model of acoustic choking. I - Shock free solutions p 180 N84-21250  
Acoustic power dissipation on radiation through duct terminations - Experiments p 180 N84-21272

### ACOUSTIC EMISSION

Acoustic emission evaluation of plasma-sprayed thermal barrier coatings [ASME PAPER 84-GT-292] p 140 N84-47046

### ACOUSTIC EXCITATION

Tone generation by rotor-downstream strut interaction p 16 N84-22174  
Correlation of flight effects on centerline velocity decay for cold-flow acoustically excited jets [NASA-TM-83502] p 182 N84-11883  
Acoustic excitation. A promising new means of controlling shear layers [NASA-TM-83772] p 10 N84-31096

### ACOUSTIC IMPEDANCE

A finite element approach for predicting nozzle admittances p 180 N84-21184  
A numerical model of acoustic choking. I - Shock free solutions p 180 N84-21250

### ACOUSTIC MEASUREMENT

Experimental investigation of shock-cell noise reduction for dual-stream nozzles in simulated flight comprehensive data report. Volume 1: Test nozzles and acoustic data [NASA-CR-168336-VOL-1] p 184 N84-24323  
Studies of acoustical properties of bulk porous flexible materials [NASA-CR-173622] p 185 N84-27544

### ACOUSTIC NOZZLES

Jet noise modification by the 'whistler nozzle' p 181 N84-23355

### ACOUSTIC PROPAGATION

Acoustic power dissipation on radiation through duct terminations - Experiments p 180 N84-21272  
Recovery of burner acoustic source structure from far-field sound spectra [AIAA PAPER 83-0763] p 181 N84-32609  
Time dependent wave envelope finite difference analysis of sound propagation [NASA-TM-83744] p 185 N84-32118

### ACOUSTIC PROPERTIES

Studies of acoustical properties of bulk porous flexible materials [NASA-CR-173622] p 185 N84-27544

### ACUSTO-OPTICS

Advanced acousto-optic signal processors p 187 N84-28485  
Acoustooptic linear algebra processors - Architectures, algorithms, and applications p 175 N84-40266

### ACRYLIC RESINS

Kinetics of chromium ion absorption by cross-linked polyacrylate films [NASA-TM-83661] p 50 N84-23693

### ACTIVATION ENERGY

The energy dependence and surface morphology of Kapton (trademark) degradation under atomic oxygen bombardment p 187 N84-34484

### ACTUATORS

Fiberoptics for propulsion control system [NASA-TM-83542] p 1 N84-14111

### ADA (PROGRAMMING LANGUAGE)

ADA and multi-microprocessor real-time simulation p 176 N84-10905

### ADAPTIVE CONTROL

Adaptive arrays for satellite communications [NASA-CR-173548] p 99 N84-24924

### ADDITIVES

Grain-boundary phases in hot-pressed silicon nitride containing Y<sub>2</sub>O<sub>3</sub> and CeO<sub>2</sub> additives p 79 N84-19793  
\*Evaluation of CO<sub>2</sub> and CO dopants in hydrogen to reduce hydrogen permeation in the Stirling engine heater head tube alloy CG-27 [NASA-TM-83535] p 68 N84-15246  
Consolidation of Si<sub>3</sub>N<sub>4</sub> without additives (by hot isostatic pressing) [NASA-CR-173279] p 82 N84-17389  
Radiation damage and defect behavior in ion-implanted, lithium counterdoped silicon solar cells [NASA-TM-83646] p 109 N84-22890  
The effects of lithium counterdoping on radiation damage and annealing in n(+)-p silicon solar cells [NASA-TM-83755] p 110 N84-31513

### ADHESION

Characterization and measurement of polymer wear [NASA-TM-83628] p 83 N84-21739  
Considerations in friction and wear p 144 N84-23903  
Tribology in the 80's Volume 2: Sessions 5 - 8 [NASA-CP-2300-VOL-2] p 144 N84-25047  
Adhesion between polymers and evaporated gold and nickel films [NASA-TP-2360] p 87 N84-31379  
The role of material properties in adhesion [NASA-TM-83792] p 88 N84-34619

### ADHESION TESTS

Adhesion between polymers and evaporated gold and nickel films [NASA-TP-2360] p 87 N84-31379

### ADHESIVE BONDING

Surfaces --- characterization of surface properties for predicting bond quality p 50 N84-10680  
Ceramic-to-metal bonding for pressure transducers [NASA-CR-173500] p 84 N84-22753  
Tribology in the 80's Volume 1: Sessions 1 to 4 [NASA-CP-2300-VOL-1] p 144 N84-23891  
Metallic adhesion and bonding p 72 N84-23897  
The role of material properties in adhesion [NASA-TM-83792] p 88 N84-34619

### ADIABATIC CONDITIONS

An RC-1 organic Rankine bottoming cycle for an adiabatic diesel engine [NASA-CR-168256] p 196 N84-32306  
Steam bottoming cycle for an adiabatic diesel engine [NASA-CR-168255] p 196 N84-33304

### ADIABATIC FLOW

Dynamics of two-phase face seals p 137 N84-28792

### AEROACOUSTICS

A parametric study of the effect of inlet lip shape upon the radiated sound field [AIAA PAPER 84-0498] p 180 N84-18131  
Tone generation by rotor-downstream strut interaction p 16 N84-22174

Aeroacoustics of turbulent shear flows p 181 N84-22534

Generation of sound in turbulent shear flows p 183 N84-15031

A theoretical prediction of the acoustic pressure generated by turbulence-flame front interactions [NASA-TM-83587] p 184 N84-26393

A critical review of noise production models for turbulent, gas-fueled burners [NASA-CR-38803] p 184 N84-26394



- Acoustic pressures emanating from a turbomachine stage  
[NASA-TM-83734] p 129 N84-30224
- AERODYNAMIC CHARACTERISTICS**
- Hybrid C-H grids for turbomachinery cascades -- parabolic and Cartesian coordinates p 3 A84-11591
- Experimental and analytical investigations into airfoil icing p 12 A84-45054
- Free jet feasibility study of a thermal acoustic shield concept for AST/VCE application: Single stream nozzles  
[NASA-CR-3758] p 185 N84-29661
- Experimental investigation of shock-cell noise reduction for single-stream nozzles in simulated flight, comprehensive data report, Volume 2. Laser velocimeter data  
[NASA-CR-168234-VOL-2] p 186 N84-33149
- AERODYNAMIC CONFIGURATIONS**
- Tandem fan applications in advanced STOVL fighter configurations  
[AIAA PAPER 84-1402] p 19 A84-40245
- Application of an optimization method to high performance propeller designs  
[AIAA PAPER 84-1203] p 20 A84-44181
- Tandem fan applications in advanced STOVL fighter configurations  
[NASA-TM-83689] p 30 N84-24579
- Application of an optimization method to high performance propeller designs  
[NASA-TM-83710] p 2 N84-25607
- Energy efficient engine. Turbine intermediate case and low-pressure turbine component test hardware detailed design report  
[NASA-CR-167973] p 33 N84-28789
- AERODYNAMIC DRAG**
- Solar array Plasma interactions p 171 N84-29343
- AERODYNAMIC FORCES**
- The coupled response of turbomachinery blading to aerodynamic excitations p 17 A84-26959
- Aerodynamic effects of moveable sidewall nozzle geometry and rotor exit restriction on the performance of a radial turbine  
[SAE PAPER 831517] p 17 A84-29460
- AERODYNAMIC LOADS**
- Steady state stresses in nylon parachute canopies  
[AIAA PAPER 84-0816] p 11 A84-26580
- Effects of structural coupling on mistuned cascade flutter and response  
[ASME PAPER 83-GT-117] p 151 A84-33701
- Energy efficient engine Low-pressure turbine subsonic cascade component development and integration program  
[NASA-CR-165592] p 33 N84-27738
- AERODYNAMIC NOISE**
- Supersonic jet screech tone cancellation p 179 A84-10136
- High frequency green function for aerodynamic noise in moving media. I - General theory. II - Noise from a spreading jet p 180 A84-21273
- Low flight speed fan noise from a supersonic inlet p 182 A84-44508
- Fan noise reduction achieved by removing tip flow irregularities behind the rotor - forward arc test configurations  
[NASA-TM-83616] p 184 N84-23235
- An experimental investigation of the effect of boundary layer refraction on the noise from a high-speed propeller  
[NASA-TM-83764] p 186 N84-34230
- AERODYNAMIC STABILITY**
- Measurements of self-excited rotor-blade vibrations using optical displacements  
[ASME PAPER 83-GT-132] p 151 A84-33702
- Optimization and mechanisms of mistuning in cascades  
[ASME PAPER 84-GT-196] p 21 A84-46993
- AERODYNAMIC STALLING**
- Performance degradation of a typical twin engine commuter type aircraft in measured natural icing conditions  
[AIAA PAPER 84-0179] p 13 A84-21289
- Inlet boundary layer effects in an axial compressor rotor II - Throughflow effects  
[ASME PAPER 84-GT-85] p 7 A84-46927
- Performance degradation of a typical twin engine commuter type aircraft in measured natural icing conditions  
[NASA-TM-83564] p 14 N84-13173
- Subsonic/transonic stall flutter investigation of a rotating wing  
[NASA-CR-174625] p 36 N84-33417
- Identification of quasi-steady compressor characteristics from transient data  
[NASA-CR-174685] p 36 N84-34444

- AERODYNAMICS**
- Energy efficient engine fan component detailed design report  
[NASA-CR-165466] p 33 N84-27737
- AEROELASTICITY**
- The coupled response of turbomachinery blading to aerodynamic excitations p 17 A84-26959
- Effects of structural coupling on mistuned cascade flutter and response  
[ASME PAPER 83-GT-117] p 151 A84-33701
- Measurements of self-excited rotor-blade vibrations using optical displacements  
[ASME PAPER 83-GT-132] p 151 A84-33702
- Flutter analysis of advanced turbopropellers p 152 A84-36492
- Optimization and mechanisms of mistuning in cascades  
[ASME PAPER 84-GT-196] p 21 A84-46993
- Aeroelastic analysis for propellers - mathematical formulations and program user's manual  
[NASA-CR-3729] p 153 N84-12530
- Bladed-shrouded-disc aeroelastic analyses Computer program updates in NASTRAN level 17.7  
[NASA-CR-165428] p 25 N84-15154
- Flutter of swept fan blades  
[NASA-TM-83547] p 154 N84-16587
- Formulation of blade-flutter spectral analyses in stationary reference frame  
[NASA-TP-2296] p 27 N84-20562
- Flutter and forced response of mistuned rotors using standing wave analysis  
[NASA-CR-173555] p 32 N84-24586
- Summary of recent NASA propeller research  
[NASA-TM-83733] p 2 N84-32344
- AERONAUTICAL ENGINEERING**
- Research and technology, 1983  
[NASA-TM-83540] p 193 N84-14061
- Aeronautics and Space Engineering Board Aeronautics Assessment Committee  
[NASA-TM-85594] p 93 N84-22771
- AEROSPACE ENGINEERING**
- Detroit space odyssey p 37 N84-15164
- Cleveland Space Odyssey  
[NASA-TM-85493] p 192 N84-16020
- AEROSPACE ENVIRONMENTS**
- Ion-beam-textured and coated surfaces experiment (S1003) p 84 N84-24650
- Solar-array-materials passive LDEF experiment (A0171) p 168 N84-24656
- Advanced photovoltaic experiment (S0014) p 168 N84-24657
- Radiation tolerance of low resistivity, high voltage silicon solar cells p 170 N84-29318
- AEROSPACE SYSTEMS**
- Solar array Plasma interactions p 171 N84-29343
- AEROSPACE TECHNOLOGY TRANSFER**
- NASA priority technologies  
[IAF PAPER 83-345] p 37 A84-11793
- AEROTHERMOCHEMISTRY**
- Executive summary, aerothermal modeling program, phase 1  
[NASA-CR-174602] p 60 N84-12263
- Aerothermal modeling program, phase 1  
[NASA-CR-168243-VOL-2] p 60 N84-12265
- AEROTHERMODYNAMICS**
- Aerothermal modeling, phase 1. Volume 1: Model assessment  
[NASA-CR-168296-VOL-1] p 25 N84-15155
- Aerothermal modeling, phase 1. Volume 2: Experimental data  
[NASA-CR-168296-VOL-2] p 25 N84-15156
- Digital computer program for generating dynamic turbofan engine models (DIGTEM)  
[NASA-TM-83446] p 26 N84-16185
- AGING (MATERIALS)**
- Aging results for PRD 49 III/epoxy and Kevlar 49/epoxy composite pressure vessels p 52 A84-21847
- Characterization of PMR polyimide resin and prepreg  
[NASA-CR-168217] p 83 N84-20695
- Improved high temperature resistant matrix resins  
[NASA-CR-168210] p 87 N84-28995
- AIR**
- Forced convection heat transfer to air/water vapor mixtures  
[NASA-CR-3769] p 123 N84-16488
- AIR BREATHING ENGINES**
- Operating system for a real-time multiprocessor propulsion system simulator  
[NASA-TM-83605] p 177 N84-20258
- AIR CONDITIONING**
- Heat recovery subsystem and overall system integration of fuel cell on-site integrated energy systems  
[NASA-CR-168309] p 166 N84-20915
- Air modulation apparatus  
[NASA-CASE-LEW-13524-1] p 35 N84-33410

- AIR COOLING**
- Use of cooling air heat exchangers as replacements for hot section strategic materials  
[AIAA PAPER 83-2540] p 15 A84-15205
- Review and status of heat-transfer technology for internal passages of air-cooled turbine blades  
[NASA-TP-2232] p 126 N84-21828
- AIR FLOW**
- Calculation of a hollow-cone liquid spray in a uniform air stream  
[AIAA PAPER 84-1322] p 118 A84-35171
- A review of internal combustion engine combustion chamber process studies at NASA Lewis Research Center  
[AIAA PAPER 84-1316] p 121 A84-40242
- Multicomponent velocity measurement in a piston-cylinder configuration using laser velocimetry  
[NASA-TM-83534] p 8 N84-14121
- Review and status of heat-transfer technology for internal passages of air-cooled turbine blades  
[NASA-TP-2232] p 126 N84-21828
- Contingency power concepts for helicopter turboshaft engine  
[NASA-TM-83679] p 30 N84-23648
- A review of internal combustion engine combustion chamber process studies at NASA Lewis Research Center  
[NASA-TM-83666] p 127 N84-24999
- Atomization of liquid sheets in high pressure airflow  
[NASA-TM-83731] p 128 N84-30223
- AIR INTAKES**
- Formation and destruction of vortices in a motored four-stroke piston-cylinder configuration p 139 A84-38838
- AIR POLLUTION**
- Comparison of steady-state and transient CVS cycle emission of an automotive Stirling engine p 173 A84-41044
- AIR SAMPLING**
- Simultaneous cabin and ambient ozone measurements on two Boeing 747 airplanes Volume 2 January to October 1978  
[NASA-TM-81733] p 193 N84-22488
- AIRBORNE/SPACEBORNE COMPUTERS**
- Graphics enhanced computer emulation for improved timing-race and fault tolerance control system analysis -- of Centaur liquid-fuel booster  
[AIAA PAPER 83-2328] p 177 A84-10010
- Baseband processor development for the Advanced Communications Satellite Program p 93 A84-15828
- AIRCRAFT CONSTRUCTION MATERIALS**
- Nonlinear analysis for high-temperature composites: Turbine blades/vanes p 158 N84-31699
- AIRCRAFT DESIGN**
- Measurement of fluid properties using rapid-double-exposure and time-average holographic interferometry  
[AIAA PAPER 84-1461] p 130 A84-35223
- Improved design of subcritical and supercritical cascades using complex characteristics and boundary-layer correction p 5 A84-38839
- Tandem fan applications in advanced STOVL fighter configurations  
[AIAA PAPER 84-1402] p 19 A84-40245
- An advanced pitch change mechanism incorporating a hybrid traction drive  
[AIAA PAPER 84-1383] p 20 A84-44182
- Measurement of fluid properties using rapid-double-exposure and time-average holographic interferometry  
[NASA-TM-83630] p 132 N84-21849
- Tandem fan applications in advanced STOVL fighter configurations  
[NASA-TM-83689] p 30 N84-24579
- An advanced pitch change mechanism incorporating a hybrid traction drive  
[NASA-TM-83709] p 2 N84-25605
- Unsteady flow in turbomachinery: An overview p 128 N84-25961
- Energy efficient engine Turbine intermediate case and low-pressure turbine component test hardware detailed design report  
[NASA-CR-167973] p 33 N84-28789
- Improved methods of vibration analysis of pretwisted, airfoil blades  
[NASA-TM-83735] p 157 N84-30329
- Turbine blade and vane heat flux sensor development, phase 1  
[NASA-CR-168297] p 134 N84-32790
- AIRCRAFT ENGINES**
- Supersonic fan engines for military aircraft  
[AIAA PAPER 83-2541] p 15 A84-15206
- Study of a LH2-fueled topping cycle engine for aircraft propulsion  
[AIAA PAPER 83-2543] p 15 A84-15207

- Advanced electrical power system technology for the all electric aircraft p 15 A84-16528
- Comparison of full-scale engine and subscale model performance of a mixed flow exhaust system for an energy efficient engine (E3) propulsion system
- [AIAA PAPER 84-0283] p 16 A84-17997
- Three-dimensional viscous design methodology for advanced technology aircraft supersonic inlet systems
- [AIAA PAPER 84-0194] p 4 A84-21290
- NASA advanced low emissions combustor program
- [ASME PAPER 83-JPGC-GT-10] p 17 A84-28982
- Design of a high-performance rotary stratified-charge research aircraft engine
- [AIAA PAPER 84-1395] p 17 A84-35204
- Detonation wave augmentation of gas turbines
- [AIAA PAPER 84-1266] p 18 A84-37639
- Heat pipe applications in aircraft propulsion
- [AIAA PAPER 84-1269] p 18 A84-37640
- An overview of NASA intermittent combustion engine research
- [AIAA PAPER 84-1393] p 19 A84-40244
- The aerodynamic design and performance of the NASA/GE E3 low pressure turbine
- [AIAA PAPER 84-1162] p 21 A84-44186
- An assessment of the use of antimisting fuel in turbofan engines
- [NASA-CR-168081] p 89 N84-10332
- Overview of liquid lubricants for advanced aircraft
- [NASA-TM-83529] p 81 N84-11296
- Three-dimensional viscous design methodology for advanced technology aircraft supersonic inlet systems
- [NASA-TM-83559] p 23 N84-13190
- Aerothermal modeling Executive summary
- [NASA-CR-168330] p 25 N84-15152
- Broad specification fuels combustion technology program
- [NASA-CR-168179] p 89 N84-15283
- Design concepts for low-cost composite engine frames
- [NASA-TM-83544] p 26 N84-16186
- Analysis of a topping-cycle, aircraft, gas-turbine-engine system which uses cryogenic fuel
- [NASA-TM-2294] p 28 N84-21549
- Vortex generating flow passage design for increased film-cooling effectiveness and surface coverage — aircraft engine blade cooling
- [NASA-TM-83617] p 126 N84-22909
- An overview of NASA intermittent combustion engine research
- [NASA-TM-83668] p 31 N84-24583
- Unsteady flow in turbomachinery: An overview
- p 128 N84-25961
- Energy efficient engine high-pressure turbine detailed design report
- [NASA-CR-165608] p 33 N84-28788
- Energy efficient engine. Turbine intermediate case and low-pressure turbine component test hardware detailed design report
- [NASA-CR-167973] p 33 N84-28789
- An overview of the NASA rotary engine research program
- [NASA-TM-83699] p 34 N84-28791
- Improved high temperature resistant matrix resins
- [NASA-CR-168210] p 87 N84-28995
- Mode 2 fatigue crack growth specimen development
- [NASA-TM-83722] p 156 N84-29248
- Nonlinear analysis for high-temperature composites. Turbine blades/vanes
- p 158 N84-31699
- Diesel engine catalytic combustor system — aircraft engines
- [NASA-CASE-LEW-12995-1] p 148 N84-33808
- AIRCRAFT EQUIPMENT**
- Three-phase, high-voltage, high-frequency distributed bus system for advanced aircraft
- p 105 N84-10058
- Piezoelectric deicing device
- [NASA-CASE-LEW-13773-2] p 133 N84-32702
- AIRCRAFT FUEL SYSTEMS**
- Fuel system research and technology: An overview of the NASA program
- p 14 N84-23641
- In-flight atmospheric and fuel tank temperature measurements
- p 90 N84-23643
- AIRCRAFT FUELS**
- Temperature histories of commercial flights at severe conditions from GASP data
- [NASA-CR-168247] p 12 N84-11152
- Investigation of sources, properties and preparation of distillate test fuels
- [NASA-CR-168227] p 89 N84-13332
- Emission FTIR analyses of thin microscopic patches of jet fuel residue deposited on heated metal surface
- [NASA-CR-168331] p 90 N84-17410
- Analysis of a topping-cycle, aircraft, gas-turbine-engine system which uses cryogenic fuel
- [NASA-TP-2294] p 28 N84-21549
- Research on aviation fuel instability
- p 91 N84-24734
- Study of effects of fuel properties in turbine-powered business aircraft
- [NASA-CR-174627] p 91 N84-25854
- Summary of recent NASA propeller research
- [NASA-TM-83733] p 2 N84-32344
- AIRCRAFT LANDING**
- Tandem fan applications in advanced STOVL fighter configurations
- [AIAA PAPER 84-1402] p 19 A84-40245
- Tandem fan applications in advanced STOVL fighter configurations
- [NASA-TM-83689] p 30 N84-24579
- AIRCRAFT MODELS**
- Performance degradation of a model helicopter main rotor in hover and forward flight with a generic ice shape
- [AIAA PAPER 84-0609] p 13 A84-24195
- AIRCRAFT NOISE**
- Why credible propeller noise measurements are possible in the acoustically untreated NASA Lewis 8 ft by 6 ft wind tunnel
- p 181 A84-38091
- Noise of the SR-6 propeller model at 2 deg and 4 deg angles of attack
- [NASA-TM-83515] p 183 N84-16946
- Analysis of the effect on combustor noise measurements of acoustic waves reflected by the turbine and combustor inlet
- [NASA-TM-83760] p 185 N84-32122
- An experimental investigation of the effect of boundary layer refraction on the noise from a high-speed propeller
- [NASA-TM-83764] p 186 N84-34230
- AIRCRAFT PERFORMANCE**
- Performance degradation of propeller systems due to rime ice accretion
- [AIAA PAPER 82-0286] p 12 A84-17406
- Performance degradation of a typical twin engine commuter type aircraft in measured natural icing conditions
- [AIAA PAPER 84-0179] p 13 A84-21289
- Performance degradation of a typical twin engine commuter type aircraft in measured natural icing conditions
- [NASA-TM-83564] p 14 N84-13173
- AIRCRAFT SAFETY**
- Performance degradation of a typical twin engine commuter type aircraft in measured natural icing conditions
- [AIAA PAPER 84-0179] p 13 A84-21289
- Flight and wind tunnel tests of an electro-impulse de-icing system
- [AIAA PAPER 84-2234] p 12 A84-39280
- Performance degradation of a typical twin engine commuter type aircraft in measured natural icing conditions
- [NASA-TM-83564] p 14 N84-13173
- AIRCRAFT STRUCTURES**
- Numerical simulation of two-dimensional heat transfer in composite bodies with application to de-icing of aircraft components
- [NASA-CR-168283] p 122 N84-13490
- AIRFOIL PROFILES**
- The coupled response of turbomachinery blading to aerodynamic excitations
- p 17 A84-26959
- Effect of geometry on airfoil icing characteristics
- p 12 A84-37935
- Improved design of subcritical and supercritical cascades using complex characteristics and boundary-layer correction
- p 5 A84-38839
- Viscous-inviscid interactive procedure for rotational flow in cascades of airfoils
- p 6 A84-44639
- Experimental and analytical investigations into airfoil icing
- p 12 A84-45054
- AIRFOILS**
- Calculation of transonic flow in a linear cascade
- [AIAA PAPER 84-1301] p 6 A84-40241
- A viscous-inviscid interactive procedure for rotational flow in cascades of two dimensional airfoils of arbitrary shape
- [NASA-CR-174609] p 7 N84-13149
- Aerothermal modeling Executive summary
- [NASA-CR-168330] p 25 N84-15152
- Results of an experimental program investigating the effects of simulated ice on the performance of the NACA 63A15 airfoil with flap
- [NASA-CR-168288] p 8 N84-16145
- Potential flow analysis of glaze ice accretions on an airfoil
- [NASA-CR-168282] p 8 N84-16146
- Formulation of blade-flutter spectral analyses in stationary reference frame
- [NASA-TP-2296] p 27 N84-20562
- Effect of a rotor wake on heat transfer from a circular cylinder
- [NASA-TM-83613] p 126 N84-21832
- Calculation of transonic flow in a linear cascade
- [NASA-TM-83697] p 10 N84-24539
- Energy efficient engine Low-pressure turbine subsonic cascade component development and integration program
- [NASA-CR-165592] p 33 N84-27738
- Energy efficient engine high-pressure turbine detailed design report
- [NASA-CR-165608] p 33 N84-28788
- Feedback in separated flows over symmetric airfoils
- [NASA-TM-83758] p 10 N84-31091
- ALGEBRA**
- Optical systolic solutions of linear algebraic equations
- p 188 N84-22405
- ALGORITHMS**
- Analysis of inviscid and viscous flows in cascades with an explicit multiple-grid algorithm
- [AIAA PAPER 84-1663] p 5 A84-38043
- Acceleration of convergence of vector sequences
- [NASA-TP-2193] p 178 N84-13885
- Application of improved numerical schemes
- p 178 N84-20537
- Fast algorithms for combustion kinetics calculations: A companion
- p 61 N84-20554
- Application of advanced control techniques to aircraft propulsion systems
- p 28 N84-20590
- Analysis of inviscid and viscous flows in cascades with an explicit multiple-grid algorithm
- [NASA-TM-83636] p 1 N84-22527
- Development of Great Lakes algorithms for the Nimbus-G coastal zone color scanner
- [NASA-CR-173511] p 159 N84-27258
- Exponential-fitted methods for integrating stiff systems of ordinary differential equations. Applications to homogeneous gas-phase chemical kinetics
- p 179 N84-31279
- A comparison of the efficiency of numerical methods for integrating chemical kinetic rate equations
- p 49 N84-31280
- Slave finite elements: The temporal element approach to nonlinear analysis
- p 157 N84-31689
- Self-adaptive solution strategies
- p 158 N84-31693
- ALIGNMENT**
- Characteristics and capacities of the NASA Lewis Research Center high precision 67- by 67-m planar near-field scanner
- [NASA-TM-83785] p 133 N84-32789
- ALKALINE BATTERIES**
- Alkaline fuel cells for the regenerative fuel cell energy storage system
- p 162 A84-30183
- Pore size engineering applied to the design of separators for nickel-hydrogen cells and batteries
- p 162 A84-30187
- Additive for zinc electrodes — electric automobiles
- [NASA-CASE-LEW-13286-1] p 106 N84-14422
- ALKYL COMPOUNDS**
- Thermal oxidative degradation reactions of linear perfluoroalkyl ethers
- p 80 A84-30000
- ALLOYS**
- Hostile environmental conditions facing candidate alloys for the automotive Stirling engine
- p 136 A84-23522
- Thermal oxidative degradation reactions of perfluoroalkylethers
- [NASA-CR-168224] p 60 N84-11229
- Importance and definition of materials in inology
- Status of understanding
- p 84 N84-23893
- ALTERNATING CURRENT**
- AC propulsion system for an electric vehicle, phase 2
- [NASA-CR-168244] p 111 N84-31514
- ALUMINATES**
- Effects of surface chemistry on hot corrosion life
- [NASA-CR-174683] p 72 N84-24774
- ALUMINUM**
- Factors influencing the thermally-induced strength degradation of B/Al composites
- p 52 A84-28227
- Matrix effects in ion-induced emission as observed in Ne collisions with Cu-Mg and Cu-Al alloys
- [NASA-TM-83061] p 187 N84-10923
- Overlay coating degradation by simultaneous oxidation and coating/substrate interdiffusion
- [NASA-TM-83738] p 75 N84-31344
- ALUMINUM ALLOYS**
- Morphology of an aluminum alloy eroded by a normally incident jet of angular erodent particles
- p 64 A84-18244
- A simple application of the Bailey-Crowan creep model to Fe-39.8 at. pct Al and gamma/gamma prime - alpha
- p 64 A84-22012
- The structure of extruded NiAl
- p 65 A84-36047
- Solute transport and the prediction of breakaway oxidation in gamma + beta Ni-Cr-Al alloys
- p 65 A84-42658
- Investigation into the role of sodium chloride deposited on oxide and metal substrates in the initiation of hot corrosion
- [NASA-CR-173377] p 71 N84-20676

- Microstructure and orientation effects on properties of discontinuous silicon carbide/aluminum composites [NASA-TP-2302] p 51 N84-26749
- Modeling degradation and failure of Ni-Cr-Al overlay coatings [NASA-TM-83672] p 74 N84-27858
- ALUMINUM GRAPHITE COMPOSITES**
- Select fiber composites for space applications: A mechanistic assessment [NASA-TM-83631] p 55 N84-22702
- ALUMINUM OXIDES**
- Analysis of grain boundary phase devitrification of Y<sub>2</sub>O<sub>3</sub>- and Al<sub>2</sub>O<sub>3</sub>-doped Si<sub>3</sub>N<sub>4</sub> p 79 A84-19792
- Thermal degradation of the tensile properties of undirectionally-reinforced FP-Al<sub>2</sub>O<sub>3</sub>/EZ 33 magnesium composites p 52 A84-28229
- Solute transport and the prediction of breakaway oxidation in gamma + beta Ni-Cr-Al alloys p 65 A84-42658
- The strength of the metal. Aluminum oxide interface p 72 N84-23898
- Sputtered coatings for protection of spacecraft polymers [NASA-TM-83706] p 85 N84-26803
- Interaction of sulfuric acid corrosion and mechanical wear of iron [NASA-TM-83717] p 73 N84-27857
- Oxygen diffusion in alpha-Al<sub>2</sub>O<sub>3</sub> [NASA-TM-83622] p 86 N84-28990
- AMBIENCE**
- Tabulations of ozonesonde data, 1963 - 1980 [NASA-CR-174631] p 174 N84-27375
- AMORPHOUS MATERIALS**
- Shrinkage of amorphous silica fibers p 77 A84-13504
- Mechanical contact induced transformation from the amorphous to the crystalline state in metallic glass [NASA-TM-83583] p 71 N84-20673
- AMPLIFIER DESIGN**
- 0.5 W 2-21 GHz monolithic GaAs distributed amplifier p 103 A84-30857
- A K-band GaAs FET amplifier with 8.2-W output power p 104 A84-32290
- NASA seeking high-power 60-GHz IMPATT diodes p 104 A84-44912
- The 20 GHz spacecraft FET solid state transmitter [NASA-CR-168240] p 107 N84-17477
- ANALOG COMPUTERS**
- Development of dynamic simulation of TF34-GE-100 turbofan engine with post-stall capability [AIAA PAPER 84-1184] p 20 A84-44178
- Development of dynamic simulation of TF34-GE-100 turbofan engine with post-stall capability [NASA-TM-83660] p 32 N84-25712
- ANALOG SIMULATION**
- Circuit equivalent to the elastic spherical shell p 104 A84-39197
- ANEOCHIC CHAMBERS**
- Experimental investigation of shock-cell noise reduction for single-stream nozzles in simulated flight, comprehensive data report. Volume 3. Shadowgraph photos and facility description [NASA-CR-168234-VOL-3] p 186 N84-33150
- ANGLE OF ATTACK**
- Investigation of tangential blowing applied to a subsonic V/STOL inlet p 3 A84-11042
- Effect of an oscillating flow direction on leading edge heat transfer p 117 A84-33705
- Three-dimensional flow simulations for supersonic mixed-compression inlets at incidence p 5 A84-38828
- Experimental investigation of tangential blowing applied to a subsonic V/STOL inlet [NASA-TP-2297] p 9 N84-20493
- ANGULAR VELOCITY**
- Proving and slip in an angular contact bearing p 139 A84-40595
- Spin analysis of concentrated traction contacts [NASA-TM-83713] p 145 N84-27042
- ANIONS**
- Simulation of lubricating behavior of a thioether liquid lubricant by an electrochemical method [NASA-TP-2316] p 84 N84-23764
- ANNEALING**
- The effect of annealing on the creep of plasma-sprayed ceramics p 79 A84-19785
- The effects of lithium counterdoping on radiation damage and annealing in n(+)-p silicon solar cells [NASA-TM-83755] p 110 N84-31513
- ANNUAL VARIATIONS**
- Tabulations of ozonesonde data, 1963 - 1980 [NASA-CR-174631] p 174 N84-27375
- ANNULAR FLOW**
- Annulus wall boundary layer development in a compressor stage, including the effects of tip clearance p 26 N84-16207
- Supersonic jet shock noise reduction [NASA-TM-83799] p 186 N84-35085
- ANNULAR NOZZLES**
- Inverted velocity profile semi-annular nozzle jet exhaust noise experiments [NASA-TM-83525] p 182 N84-13924
- ANOMALIES**
- Anomalous high potentials observed on ISEE [NASA-CR-172791] p 41 N84-17252
- ANTENNA ARRAYS**
- The 30-GHz monolithic receive module [NASA-CR-168326] p 99 N84-20737
- The study of microstrip antenna arrays and related problems [NASA-CR-173534] p 99 N84-23807
- Adaptive arrays for satellite communications [NASA-CR-173548] p 99 N84-24924
- The 20 and 30 GHz MMIC technology for future space communication antenna system [NASA-TM-83745] p 100 N84-31460
- Monolithic microwave integrated circuit devices for active array antennas [NASA-CR-173981] p 112 N84-34675
- ANTENNA DESIGN**
- Multibeam antenna for 30/20 GHz advanced communications satellite using offset shaped, dual reflector surfaces p 93 A84-15627
- Advanced 30/20 GHz multiple-beam antennas for communications satellites p 40 A84-49250
- Phased-array-fed antenna configuration study Volume 1: Technology assessment [NASA-CR-168231] p 98 N84-16423
- Phased-array-fed antenna configuration study, volume 2 [NASA-CR-168232] p 98 N84-16424
- Reflector antennas with low sidelobes, low cross polarization, and high aperture efficiency [NASA-CR-174670] p 100 N84-31464
- Structural design of a vertical antenna boresight 18.3 by 18.3-m planar near-field antenna measurement system [NASA-TM-83781] p 133 N84-32783
- Characteristics and capacities of the NASA Lewis Research Center high precision 6.7- by 6.7-m planar near-field scanner [NASA-TM-83785] p 133 N84-32789
- ANTENNA RADIATION PATTERNS**
- Geometric models, antenna gains, and protection ratios as developed for EC SAT-R2 conference software [NASA-TM-83381] p 96 N84-11358
- Secondary pattern computation of an arbitrarily shaped main reflector [NASA-TM-85527] p 100 N84-25909
- Reflector antennas with low sidelobes, low cross polarization, and high aperture efficiency [NASA-CR-174670] p 100 N84-31464
- Structural design of a vertical antenna boresight 18.3 by 18.3-m planar near-field antenna measurement system [NASA-TM-83781] p 133 N84-32783
- ANTENNAS**
- Microwave monolithic integrated circuit development for future spaceborne phased array antennas [AIAA PAPER 84-0656] p 94 A84-25257
- Microwave monolithic integrated circuit development for future spaceborne phased array antennas [NASA-TM-83518] p 97 N84-13399
- The study of microstrip antenna arrays and related problems [NASA-CR-173534] p 99 N84-23807
- ANTI-FRICTION BEARINGS**
- Spin analysis of concentrated traction contacts [NASA-TM-83713] p 145 N84-27042
- ANTIMISTING FUELS**
- An assessment of the use of antimisting fuel in turbofan engines [NASA-CR-168081] p 89 N84-10332
- ANTIREFLECTION COATINGS**
- Solar-array-materials passive LDEF experiment (A0171) p 168 N84-24656
- APEXES**
- Development of partially fluorinated resin apex seals [NASA-CR-174706] p 148 N84-32828
- APPROACH**
- Tandem fan applications in advanced STOVL fighter configurations [AIAA PAPER 84-1402] p 19 A84-40245
- Tandem fan applications in advanced STOVL fighter configurations [NASA-TM-83689] p 30 N84-24579
- ARC DISCHARGES**
- Cathode degradation and erosion in high pressure arc discharges [NASA-TM-83638] p 47 N84-22631
- Characteristics of arc currents on a negatively biased solar cell array in a plasma [NASA-TM-83728] p 48 N84-27824
- ARC JET ENGINES**
- Demonstration of a new electrothermal thruster concept p 43 A84-34037
- Cathode degradation and erosion in high pressure arc discharges [NASA-TM-83638] p 47 N84-22631
- ARC SPRAYING**
- Arc spray fabrication of metal matrix composite monolayer — high temperature fiber-reinforced superalloy composites [NASA-CASE-LEW-13828-1] p 54 N84-15203
- Diamondlike flakes [NASA-CASE-LEW-13837-2] p 54 N84-22696
- ARCHITECTURE (COMPUTERS)**
- A scheme for handling arrays in data-flow systems p 175 A84-39972
- Acousto-optic linear algebra processors - Architectures, algorithms, and applications p 175 A84-40266
- ARGON**
- Development of advanced inert-gas ion thrusters [NASA-CR-168206] p 44 N84-10180
- ARGON PLASMA**
- Spatial electron density and electric field strength measurements in microwave cavity experiments [NASA-CR-173907] p 111 N84-32682
- ARITHMETIC AND LOGIC UNITS**
- Optical residue addition and storage units using a Hughes liquid crystal light valve p 188 N84-22417
- ASBESTOS**
- Separator development and testing of nickel-hydrogen cells [NASA-TM-83653] p 62 N84-22712
- ASPECT RATIO**
- Nonlinear finite element analysis of shells with large aspect ratio p 158 N84-31692
- ASTROLOGY (TRADEMARK)**
- The effect of microstructure on 650 C fatigue crack growth in P/M Astroloy p 63 A84-12395
- Fatigue crack growth and low cycle fatigue of two nickel base superalloys [NASA-CR-174534] p 66 N84-10267
- ASYMPTOTIC METHODS**
- Asymptotic analysis of numerical wave propagation in finite difference equations [NASA-CR-175323] p 98 N84-15360
- ATMOSPHERIC CIRCULATION**
- Tropical response to lateral forcing with a latitudinally and zonally nonuniform basic state p 174 A84-40399
- ATMOSPHERIC COMPOSITION**
- Simultaneous cabin and ambient ozone measurements on two Boeing 747 airplanes. Volume 2 January to October 1978 [NASA-TM-81733] p 193 N84-22488
- ATMOSPHERIC CORRECTION**
- Development of Great Lakes algorithms for the Nimbus-G coastal zone color scanner [NASA-CR-173511] p 159 N84-27258
- ATMOSPHERIC PRESSURE**
- Evaluation of gas-cooled pressurized phosphoric acid fuel cells for electric utility power generation [NASA-CR-168298] p 169 N84-25169
- ATMOSPHERIC TEMPERATURE**
- Temperature histories of commercial flights at severe conditions from GASP data [NASA-CR-168247] p 12 N84-11152
- In-flight atmosphere and fuel tank temperature measurements p 90 N84-23643
- ATOMIZING**
- Role of fuel chemical properties on combustor radiative heat load [AIAA PAPER 84-1493] p 89 A84-35236
- AUDIOMETRY**
- Input filter compensation for switching regulators [NASA-CR-173557] p 110 N84-24975
- AUGER SPECTROSCOPY**
- Study of the Auger line shape of polyethylene and diamond p 190 A84-40600
- Matrix effects in ion-induced emission as observed in Ne collisions with Cu-Mg and Cu-Al alloys [NASA-TM-83061] p 187 N84-10923
- AUTOMOBILE ENGINES**
- Combustor development for automotive gas turbines p 135 A84-10499
- Hostile environmental conditions facing candidate alloys for the automotive Stirling engine p 136 A84-23522
- New perspectives for advanced automobile diesel engines p 138 A84-30062
- DOE/NASA Automotive Stirling Engine Project Overview 83 p 138 A84-30069
- Automotive Stirling Engine Development Program Mod I Stirling engine development p 138 A84-30091
- Automotive Stirling engine development program - Overview and status report p 138 A84-30092

- Comparison of steady-state and transient CVS cycle emission of an automotive Stirling engine  
p 173 A84-41044  
Advanced Gas Turbine (AGT) technology development  
[NASA-CR-168235] p 141 N84-15554  
Automotive Stirling engine development program  
[NASA-CR-168205] p 194 N84-18117  
Real-time simulation of an automotive gas turbine using the hybrid computer  
[NASA-TM-83593] p 195 N84-26484  
Advanced Gas Turbine (AGT) Technology Project  
[NASA-CR-174629] p 146 N84-28089  
Automotive Stirling engine development program  
[NASA-CR-174622] p 195 N84-32305  
Automotive Stirling Engine Development Program  
RESD summary report  
[NASA-CR-174674] p 196 N84-33307
- AUTOMOBILE FUELS**  
Evaluation of dissociated and steam-reformed methanol as automotive engine fuels  
[NASA-CR-168242] p 91 N84-27909
- AUTOMOBILES**  
Downsizing assessment of automotive Stirling engines  
[NASA-TM-83468] p 194 N84-14989
- AUXILIARY POWER SOURCES**  
Aircraft Electric Secondary Power  
[NASA-CR-2282] p 22 N84-10055  
Application of advanced materials to rotating machines  
p 22 N84-10063  
New developments in power semiconductors  
p 105 N84-10065  
Lightweight, high-frequency transformers  
p 105 N84-10066
- AUXILIARY PROPULSION**  
Study of auxiliary propulsion requirements for large space systems, volume 2  
[NASA-CR-168193-VOL-2] p 45 N84-13218  
Radiative resistojel performance characterization tests  
[NASA-CR-174763] p 50 N84-33462
- AVALANCHE DIODES**  
High efficiency IMPATT diodes for 60 GHz intersatellite link applications  
[AIAA PAPER 84-0787] p 103 A84-25333  
NASA seeking high-power 60-GHz IMPATT diodes  
p 104 A84-44912  
A 20-GHz IMPATT transmitter  
[NASA-CR-168076] p 106 N84-11385  
High efficiency IMPATT diodes for 60 GHz intersatellite link applications  
[NASA-TM-83584] p 108 N84-19708  
The 20 GHz solid state transmitter design, impatt diode development and reliability assessment  
[NASA-CR-174716] p 112 N84-33715
- AXIAL FLOW**  
Performance of a high-work low aspect ratio turbine tested with a realistic inlet radial temperature profile  
[AIAA PAPER 84-1161] p 19 A84-40239  
Velocity and temperature characteristics of two-stream, coplanar jet exhaust plumes  
[AIAA PAPER 84-2205] p 21 A84-46106  
Performance of a high-work low aspect ratio turbine tested with a realistic inlet radial temperature profile  
[NASA-TM-83655] p 32 N84-24589  
The boundary layer on compressor cascade blades  
[NASA-CR-173514] p 127 N84-25001  
Velocity and temperature characteristics of two-stream, coplanar jet exhaust plumes  
[NASA-TM-83730] p 34 N84-28790
- AXIAL FLOW TURBINES**  
Aerodynamic effects of moveable sidewall nozzle geometry and rotor exit restriction on the performance of a radial turbine  
[SAE PAPER 831517] p 17 A84-29460  
Loss reduction in axial-flow compressors through low-speed model testing  
[ASME PAPER 84-GT-184] p 7 A84-46985  
Analytical and experimental investigation of stator endwall contouring in a small axial-flow turbine  
[NASA-TP-2309] p 35 N84-32338
- AXISYMMETRIC BODIES**  
Extension to an analysis of turbulent swirling compressible flow for application to axisymmetric small gas turbine ducts  
[NASA-CR-165597] p 195 N84-21445
- AXISYMMETRIC FLOW**  
Turbulence measurements in confined jets using a rotating single-wire probe technique  
p 113 A84-13584  
Computation of viscous flow in planar and axisymmetric ducts by an implicit marching procedure  
[AIAA PAPER 84-0256] p 114 A84-17979  
A finite element approach for predicting nozzle admittances  
p 180 A84-21184
- A review of internal combustion engine combustion chamber process studies at NASA Lewis Research Center  
[AIAA PAPER 84-1316] p 121 A84-40242  
A review of internal combustion engine combustion chamber process studies at NASA Lewis Research Center  
[NASA-TM-83668] p 127 N84-24999
- ## B
- BACKSCATTERING**  
Three component velocity measurements using Fabry-Perot interferometer  
[NASA-TM-83692] p 133 N84-26010
- BACKWARD FACING STEPS**  
Combustion in a turbulent mixing layer formed at a rearward-facing step  
p 58 A84-10140
- BACKWARD WAVES**  
Ladder supported ring bar circuit  
[NASA-CASE-LEW-13570-1] p 106 N84-16452  
Dielectric based submillimeter backward wave oscillator circuit  
[NASA-CASE-LEW-13736-1] p 110 N84-27974
- BALL BEARINGS**  
Pivoting and slip in an angular contact bearing  
p 139 A84-40595  
Topological reaction rate measurements related to scuffing  
[NASA-TM-83486] p 68 N84-14288  
The ball bearing as a rheological test device  
[NASA-TM-83570] p 142 N84-17591  
Comparison of predicted and experimental thermal performance of angular-contact ball bearings  
[NASA-TP-2275] p 142 N84-18654  
First order ball bearing kinematics  
[NASA-TM-83592] p 142 N84-19818  
Solid lubrication design methodology  
[NASA-CR-174690] p 196 N84-33309  
Optical and other property changes of M-50 bearing steel surfaces for different lubricants and additive prior to scuffing  
[NASA-TM-83746] p 88 N84-34620
- BANDWIDTH**  
The 20 x 20 high speed microwave switches  
[NASA-TM-83775] p 101 N84-32644
- BARIUM**  
Correlation of electron emission with changes in the surface concentration of barium and oxygen on a tungsten surface  
p 60 A84-45917
- BARIUM TITANATES**  
Preliminary experiments on phase conjugation for flow visualization — barium titanate single crystals  
[NASA-TM-83768] p 189 N84-32169
- BARRIER LAYERS**  
The role of potential barrier formation in spacecraft charging  
p 41 N84-17269
- BATCH PROCESSING**  
GCKP84-general chemical kinetics code for gas-phase flow and batch processes including heat transfer effects  
[NASA-TP-2320] p 63 N84-32446
- BATTERY CHARGERS**  
An SCR inverter with an integral battery charger for electric vehicles  
p 103 A84-24850  
Integral inverter/battery charger for use in electric vehicles  
[NASA-CR-168177] p 194 N84-17073
- BAUSCHINGER EFFECT**  
Finite elastic-plastic deformation of polycrystalline metals  
p 66 A84-43872
- BEADS**  
A study of the effect of solid particle impact and particle shape on the erosion morphology of ductile metals  
p 66 A84-45570  
Solid impingement erosion mechanisms and characterization of erosion resistance of ductile metals  
[NASA-TM-83492] p 67 N84-12287  
Erosion of iron-chromium alloys by glass particles  
[NASA-TP-2354] p 75 N84-28965
- BEAM CURRENTS**  
Improved ion containment using a ring-cusp ion thruster  
p 44 A84-49511
- BEAM SWITCHING**  
Approaches to optimization of SS/TDMA time slot assignment — satellite switched time division multiple access  
[NASA-CR-168328] p 40 N84-16243
- BEAMS (SUPPORTS)**  
Improved finite-difference vibration analysis of pretwisted, tapered beams  
[NASA-TM-83549] p 154 N84-16588
- BEARINGS**  
Nonlinear transient finite element analysis of rotor-bearing-stator systems  
p 136 A84-20580
- A blade loss response spectrum for flexible rotor systems  
[ASME PAPER 84-GT-29] p 139 A84-46893  
Special cases of friction and applications  
[NASA-TM-83523] p 141 N84-11500  
Surface topographical changes measured by phase-locked interferometry  
[NASA-CR-3757] p 188 N84-16984  
Mode 2 fatigue crack growth specimen development  
[NASA-TM-83722] p 156 N84-29248  
Summary of drive-train component technology in helicopters  
[NASA-TM-83726] p 147 N84-30294  
Research study for effects of case flexibility on bearing loads and rotor stability  
[NASA-CR-171147] p 148 N84-33811
- BENDING FATIGUE**  
Bending fatigue of electron-beam-welded foils. Application to a hydrodynamic air bearing in the Chrysler/DOE upgraded automotive gas turbine engine  
[NASA-TM-83539] p 155 N84-16589
- BENDING MOMENTS**  
Improved compliant hydrodynamic fluid journal bearing  
[NASA-CASE-LEW-13670-1] p 143 N84-22959
- BENDING VIBRATION**  
Vibrations of twisted cantilevered plates - Experimental investigation  
[ASME PAPER 84-GT-96] p 152 A84-46937
- BENZENE**  
Investigation of sources, properties and preparation of distillate test fuels  
[NASA-CR-168227] p 89 N84-13332
- BINARY FLUIDS**  
Turbidity very near the critical point of methanol-cyclohexane mixtures  
p 192 A84-30391
- BIODEGRADATION**  
Bacterial degradation of polychlorinated biphenyls in sludge from an industrial sewer lagoon  
[NASA-TM-83543] p 173 N84-11594
- BIPOLAR TRANSISTORS**  
A new FET-bipolar combinational power semiconductor switch  
p 104 A84-32293  
Development and fabrication of an augmented power transistor  
[NASA-CR-168262] p 106 N84-11388  
Hybrid power semiconductor switch  
[NASA-CASE-LEW-13922-1] p 106 N84-11389  
High voltage-high power components for large space power distribution systems  
[NASA-TM-83648] p 42 N84-22615
- BIPOLARITY**  
Test results of a ten cell bipolar nickel-hydrogen battery  
p 162 A84-30188  
Development of a large scale bipolar NiH2 battery  
p 162 A84-30189  
Teardown analysis of a ten cell bipolar nickel-hydrogen battery  
[NASA-TM-83618] p 168 N84-23026
- BIRDS**  
A laser system to remotely sense bird movements  
p 159 A84-31608
- BIT ERROR RATE**  
NTSC composite video at 1.6 bits/pel  
p 95 A84-49259
- BLADE SLAP NOISE**  
Low flight speed fan noise from a supersonic inlet  
p 182 A84-44508
- BLADE TIPS**  
Material removal considerations for metal-ceramic abradable turbine seal systems  
p 135 A84-15575  
Residual stress in plasma-sprayed ceramic turbine tip and gas-path seal specimens  
p 78 A84-19783  
Laser Doppler velocimeter measurement in the tip region of a compressor rotor  
[AIAA PAPER 84-1602] p 6 A84-39304  
A possible explanation for the present difference between linear noise theory and experimental data for supersonic helical tip speed propellers  
[NASA-TM-83467] p 183 N84-14874  
Annulus wall boundary layer development in a compressor stage, including the effects of tip clearance  
p 26 N84-16207  
Noise of the SR-6 propeller model at 2 deg and 4 deg angles of attack  
[NASA-TM-83515] p 183 N84-16946  
Tip cap for a rotor blade  
[NASA-CASE-LEW-13654-1] p 28 N84-22560  
Abrasive tip treatment for use on compressor blades  
[NASA-CR-174666] p 145 N84-25065
- BLOCKING**  
Swirl, expansion ratio and blockage effects on confined turbulent flow  
[NASA-CR-175391] p 125 N84-19746
- BLOWING**  
Investigation of tangential blowing applied to a subsonic V/STOL inlet  
p 3 A84-11042

- Analytical study of blowing boundary-layer control for subsonic V/STOL inlets  
[NASA-TM-83576] p 8 N84-16141
- BLUFF BODIES**  
Secondary effects in combustion instabilities leading to flashback p 58 A84-17436  
Calculations of turbulent mass transport in a bluff-body diffusion-flame combustor  
[AIAA PAPER 84-0372] p 114 A84-18048
- BOEING 747 AIRCRAFT**  
Simultaneous cabin and ambient ozone measurements on two Boeing 747 airplanes Volume 2. January to October 1978  
[NASA-TM-81733] p 193 N84-22488
- BOILERS**  
Cogeneration Technology Alternatives Study (CTAS). Volume 2: Comparison and evaluation of results  
[NASA-TM-81401] p 173 N84-34038
- BORIDES**  
Method of making a light weight battery plaque  
[NASA-CASE-LEW-13349-1] p 72 N84-22734
- BORON**  
Interaction between boron and intrinsic defects in GaAs p 190 A84-33918
- BORON FIBERS**  
Durability/life of fiber composites in hydrothermomechanical environments p 52 A84-27359  
Factors influencing the thermally-induced strength degradation of B/Al composites p 52 A84-28227  
Method for strengthening boron fibers  
[NASA-CASE-LEW-13826-2] p 55 N84-24711
- BORON REINFORCED MATERIALS**  
Durability/life of fiber composites in hydrothermomechanical environments p 52 A84-27359
- BOUNDARY ELEMENT METHOD**  
Nonlinear Structural Analysis  
[NASA-CP-2297] p 157 N84-31688  
Three-dimensional stress analysis using the boundary element method p 159 N84-31700
- BOUNDARY LAYER CONTROL**  
Investigation of tangential blowing applied to a subsonic V/STOL inlet p 3 A84-11042  
Analytical study of suction boundary layer control for subsonic V/STOL inlets  
[AIAA PAPER 84-1399] p 6 A84-44187  
Analytical study of blowing boundary-layer control for subsonic V/STOL inlets  
[NASA-TM-83576] p 8 N84-16141  
Experimental investigation of tangential blowing applied to a subsonic V/STOL inlet  
[NASA-TP-2297] p 9 N84-20493
- BOUNDARY LAYER FLOW**  
Turbulent boundary-layer flow and structure on a convex wall and its redevelopment on a flat wall p 115 A84-21378  
Convective heat transfer studies at high temperatures with pressure gradient for inlet flow Mach number of 0.45  
[AIAA PAPER 84-1487] p 119 A84-35233  
Inlet boundary layer effects in an axial compressor rotor I Blade-to-blade effects  
[ASME PAPER 84-GT-84] p 6 A84-46926  
Inlet boundary layer effects in an axial compressor rotor. II - Throughflow effects  
[ASME PAPER 84-GT-85] p 7 A84-46927  
The boundary layer on compressor cascade blades  
[NASA-CR-173514] p 127 N84-25001  
Turbulence and surface heat transfer near the stagnation point of a circular cylinder in turbulent flow  
[NASA-TM-83732] p 128 N84-29157
- BOUNDARY LAYER SEPARATION**  
Potential flow analysis of glaze ice accretions on an airfoil  
[NASA-CR-168282] p 8 N84-16146
- BOUNDARY LAYER TRANSITION**  
Boundary layer transition effects on flow separation around V/STOL engine inlets at high incidence  
[AIAA PAPER 84-0432] p 4 A84-18090  
Flat plate heat transfer for laminar transition and turbulent boundary layers using a shock tube  
[AIAA PAPER 84-1726] p 120 A84-37467
- BOUNDARY LAYERS**  
Application of a quasi-3D inviscid flow and boundary layer analysis to the hub-shroud contouring of a radial turbine  
[AIAA PAPER 84-1297] p 6 A84-44177  
Annulus wall boundary layer development in a compressor stage, including the effects of tip clearance p 26 N84-16207  
End-wall boundary layer measurements in a two-stage fan p 26 N84-16208

- Application of a quasi-3D inviscid flow and boundary layer analysis to the hub-shroud contouring of a radial turbine  
[NASA-TM-83669] p 10 N84-25647  
An experimental investigation of the effect of boundary layer refraction on the noise from a high-speed propeller  
[NASA-TM-83764] p 166 N84-34230
- BOUNDARY LUBRICATION**  
A thermomechanical model for energy propagation in a solid-fluid-solid system with one boundary in relative motion  
[ASME PAPER 83-HT-97] p 137 A84-29092  
Hydrodynamic lubrication of rigid nonconformal contacts in combined rolling and normal motion  
[NASA-TM-83578] p 142 N84-17592  
Lubrication of machine elements  
[NASA-RP-1126] p 147 N84-31640  
Solid lubrication design methodology  
[NASA-CR-174690] p 196 N84-33309
- BOUNDARY VALUE PROBLEMS**  
Eigenmode analysis of unsteady one-dimensional Euler equations  
[NASA-CR-172217] p 7 N84-10022  
Numerical methods and computers used in elastohydrodynamic lubrication  
[NASA-TM-83524] p 141 N84-11498
- BRANCHING (MATHEMATICS)**  
A numerical analysis of contact and limit-point behavior in a class of problems of finite elastic deformation p 150 A84-27370
- BRAYTON CYCLE**  
Overview of advanced Stirling and gas turbine engine development programs and implications for solar thermal electrical applications p 146 N84-28231  
Waste heat recovery from adiabatic diesel engines by exhaust-driven Brayton cycles  
[NASA-CR-168257] p 196 N84-32307
- BRAZING**  
Materials for Advanced Turbine Engines (MATE) Project 3: Design, fabrication and evaluation of an oxide dispersion strengthened sheet alloy combustor liner, volume 1  
[NASA-CR-174691] p 76 N84-32504
- BRISTOL-SIDDELEY BS 53 ENGINE**  
Real-time Pegasus propulsion system model  
V/STOL-piloted simulation evaluation p 15 A84-17362
- BROADBAND**  
Parallel-processing with surface plasmons, a new strategy for converting the broad solar spectrum p 160 A84-23006
- BROADBAND AMPLIFIERS**  
Jet noise modification by the 'whistler nozzle' p 181 A84-23355
- BROADCASTING**  
Geometric models, antenna gains, and protection ratios as developed for BC SAT-R2 conference software  
[NASA-TM-83381] p 96 N84-11358  
Broadcasting satellites at 12 GHz for Region 2. Technical characteristics  
[NASA-TM-83522] p 98 N84-19640  
Engineering calculations for communications satellite systems planning  
[NASA-CR-173532] p 38 N84-23662
- BRUSHES (ELECTRICAL CONTACTS)**  
Improved transistor-controlled and commutated brushless DC motors for electric vehicle propulsion  
[NASA-CR-168053] p 105 N84-10450
- BUBBLES**  
Bubble formation in oxide scales on SiC p 79 A84-23689  
Experimental study of bubble cavities attached to a rotating shaft in a reservoir  
[NASA-TM-83586] p 124 N84-17533
- BUCKLING**  
Tensile buckling of advanced turboprops p 149 A84-11039  
The effect of annealing on the creep of plasma-sprayed ceramics p 79 A84-19785
- BURGER EQUATION**  
Stability and structure of stretched vortices  
[AD-A142913] p 117 A84-29798
- BURNERS**  
Recovery of burner acoustic source structure from far-field sound spectra  
[AIAA PAPER 83-0763] p 181 A84-32609  
Micronized coal burner facility  
[NASA-CASE-LEW-13426-1] p 60 N84-16276  
A critical review of noise production models for turbulent, gas-fueled burners  
[NASA-CR-3803] p 184 N84-26384  
The structure of evaporating and combusting sprays  
Measurements and predictions  
[NASA-CR-173778] p 128 N84-29155

## BUS CONDUCTORS

- Three-phase, high-voltage, high-frequency distributed bus system for advanced aircraft p 105 N84-10058

## BUSHINGS

- Evaluation of two polyimides and of an improved liner retention design for self-lubricating bushings  
[NASA-TM-83719] p 86 N84-27887

## BYPASS RATIO

- HYTSS A hypothetical turbofan engine simplified simulation  
[NASA-TM-83561] p 26 N84-16184

## BYPASSES

- Method of making an ion beam sputter-etched ventricular catheter for hydrocephalus shunt  
[NASA-CASE-LEW-13107-2] p 174 N84-23095

## C

## CABIN ATMOSPHERES

- Simultaneous cabin and ambient ozone measurements on two Boeing 747 airplanes Volume 2. January to October 1978  
[NASA-TM-81733] p 193 N84-22488

## CALIBRATING

- Calibration of the Malvern particle sizer p 131 A84-40736  
Advanced high temperature heat flux sensors  
[NASA-TM-83526] p 123 N84-16493  
Advanced photovoltaic experiment (S0014) p 168 N84-24657

## CAMERAS

- In-situ measurements of alloy oxidation/corrosion/erosion using a video camera and proximity sensor with microcomputer control  
[NASA-TM-83673] p 74 N84-27859

## CANOPIES

- Steady state stresses in ribbon parachute canopies  
[AIAA PAPER 84-0816] p 11 A84-26580

## CANS

- Flame radiation and linear heat transfer in a tubular can combustor  
[AIAA PAPER 84-0443] p 16 A84-21300  
Flame radiation and liner heat transfer in a tubular-can combustor  
[NASA-TM-83538] p 23 N84-13188

## CANTILEVER BEAMS

- Forced response of a cantilever beam with a dry friction damper attached. I - Theory II - Experiment p 150 A84-21267  
An improved finite-difference analysis of uncoupled vibrations of tapered cantilever beams  
[NASA-TM-83495] p 154 N84-13610

## CANTILEVER MEMBERS

- The influence of gyroscopic forces on the dynamic behavior and flutter of rotating blades  
[NASA-CR-175444] p 27 N84-20524

## CANTILEVER PLATES

- Vibrations of twisted cantilevered plates - Experimental investigation  
[ASME PAPER 84-GT-56] p 152 A84-46937

## CAPACITANCE

- Parametric analysis of hollow conductor parallel and coaxial transmission lines for high frequency space power distribution  
[NASA-TM-83601] p 46 N84-20639  
Characteristics of arc currents on a negatively biased solar cell array in a plasma  
[NASA-TM-83728] p 48 N84-27824

## CAPACITORS

- Material considerations for high frequency, high power capacitors p 102 A84-22874  
High-current, high-frequency capacitors p 105 N84-10067

- Plasma polymerized high energy density dielectric films for capacitors  
[NASA-CR-168233] p 81 N84-13310

- Electromagnetic propulsion test facility  
[NASA-TM-83568] p 37 N84-16229

- High voltage-high power components for large space power distribution systems  
[NASA-TM-83648] p 42 N84-22615

## CAPILLARIES

- Capillary rise, wetting layers, and critical phenomena in confined geometry p 192 A84-20315

## CAPILLARY FLOW

- Vapor flow into a capillary propellant-acquisition device p 43 A84-36559

## CARBIDES

- Carbides in iron-nickel Fe-Mn-Cr-Mo-Al-Si-C systems p 64 A84-26815

## CARBON

- Study of the Auger line shape of polyethylene and diamond p 190 A84-40600

- Oxidation resistant slurry coating for carbon-based materials  
[NASA-CASE-LEW-13923-1] p 54 N84-16266
- Coaxial carbon plasma gun deposition of amorphous carbon films  
[NASA-TM-83600] p 191 N84-20404
- Diamondlike flakes  
[NASA-CASE-LEW-13837-2] p 54 N84-22696
- Chromium electrodes for REDOX cells  
[NASA-CASE-LEW-13653-1] p 170 N84-28205
- Dual ion beam deposition of carbon films with diamondlike properties  
[NASA-TM-83743] p 110 N84-31512
- CARBON COMPOUNDS**  
Diamondlike flake composites  
[NASA-CASE-LEW-13837-1] p 54 N84-22695
- CARBON DIOXIDE**  
Evaluation of CO<sub>2</sub> and CO dopants in hydrogen to reduce hydrogen permeation in the Stirling engine heater head tube alloy CG-27  
[NASA-TM-83535] p 68 N84-15246
- Carbon-13 and proton nuclear magnetic resonance analysis of shale-derived refinery products and jet fuels and of experimental referee broadened-specification jet fuels  
[NASA-CR-174761] p 92 N84-32552
- CARBON DIOXIDE LASERS**  
Measurement of heat pump processes induced by laser radiation  
[NASA-CR-168324] p 134 N84-18620
- CARBON FIBERS**  
Electronic properties of carbon fibers intercalated with copper chloride  
[NASA-TM-834521] p 104 N84-34521
- CARBON MONOXIDE**  
Evaluation of CO<sub>2</sub> and CO dopants in hydrogen to reduce hydrogen permeation in the Stirling engine heater head tube alloy CG-27  
[NASA-TM-83535] p 68 N84-15246
- CARBON-CARBON COMPOSITES**  
Mechanical behavior of carbon-carbon composites  
[NASA-CR-174767] p 57 N84-34575
- CARRIER FREQUENCIES**  
Carrier recovery methods for a dual-mode modem A design approach  
[NASA-CR-173355] p 36 N84-19360
- CARRIER TO NOISE RATIOS**  
The effect of variable S/N on the subjective evaluation of protection ratios for direct-TV satellite services  
p 95 N84-48452
- CASCADE FLOW**  
Hybrid C-H grids for turbomachinery cascades — parabolic and Cartesian coordinates p 3 N84-11591
- An implicit LU scheme for the Euler equations applied to arbitrary cascades — new method of factoring  
[AIAA PAPER 84-0467] p 4 N84-17925
- A rapid blade-to-blade solution for use in turbomachinery design  
[ASME PAPER 83-GT-67] p 4 N84-31289
- Effects of structural coupling on mistuned cascade flutter and response  
[ASME PAPER 83-GT-117] p 151 N84-33701
- Comparison of visualized turbine endwall secondary flows and measured heat transfer patterns  
[ASME PAPER 83-GT-83] p 117 N84-33703
- Redesign and cascade tests of a supercritical controlled diffusion stator blade-section  
[AIAA PAPER 84-1207] p 5 N84-36960
- Analysis of inviscid and viscous flows in cascades with an explicit multiple-grid algorithm  
[AIAA PAPER 84-1663] p 5 N84-38043
- Improved design of subcritical and supercritical cascades using complex characteristics and boundary-layer correction  
p 5 N84-38839
- Calculation of transonic flow in a linear cascade  
[AIAA PAPER 84-1301] p 6 N84-40241
- Viscous-inviscid interactive procedure for rotational flow in cascades of airfoils  
p 6 N84-44639
- Transonic cascade flow analysis using viscous/inviscid coupling concepts  
[AIAA PAPER 84-2159] p 6 N84-46103
- Design and performance of a fixed, nonaccelerating, guide vane cascade that operates over an inlet flow angle range of 60 deg  
[NASA-TM-83519] p 8 N84-14120
- Analysis of inviscid and viscous flows in cascades with an explicit multiple-grid algorithm  
[NASA-TM-83636] p 1 N84-22527
- Redesign and cascade tests of a supercritical controlled diffusion stator blade-section  
[NASA-TM-83635] p 10 N84-22533
- Calculation of transonic flow in a linear cascade  
[NASA-TM-83697] p 10 N84-24539
- Energy efficient engine, Low-pressure turbine subsonic, cascade component development and integration program  
[NASA-CR-165592] p 33 N84-27738
- Energy efficient engine high-pressure turbine supersonic cascade technology report  
[NASA-CR-165567] p 33 N84-27739
- Unsteady transonic flow in cascades  
[NASA-TM-83780] p 11 N84-32351
- A linear aerodynamic analysis for unsteady transonic cascades  
[NASA-CR-83833] p 11 N84-32355
- CASCADES**  
Optimization and mechanisms of mistuning in cascades  
[ASME PAPER 84-GT-196] p 21 N84-46993
- CASES (CONTAINERS)**  
Research study for effects of case flexibility on bearing loads and rotor stability  
[NASA-CR-171147] p 148 N84-33811
- CASING**  
Effects of volute geometry and impeller orbit on the hydraulic performance of a centrifugal pump  
p 136 N84-22316
- Dual clearance squeeze film damper  
[NASA-CASE-LEW-13506-1] p 29 N84-22562
- CASSEGRAIN ANTENNAS**  
Advanced 30/20 GHz multiple-beam antennas for communications satellites  
p 40 N84-49250
- CAST ALLOYS**  
The effects of Cr, Al, Ti, Mo, W, Ta, and Nb on the cyclic oxidation behavior of cast Ni-base superalloys at 1100 and 1150 C  
p 65 N84-27485
- CASTING**  
Two-region analysis of interface shape in continuous casting with superheated liquid  
p 139 N84-44918
- Low cycle fatigue behavior of conventionally cast MAR-M 200 AT 1000 deg C  
[NASA-TM-83769] p 77 N84-33564
- CATALYSTS**  
Full scale phosphoric acid fuel cell stack technology development  
[NASA-CR-174660] p 169 N84-26165
- Negative electrode catalyst for the iron-chromium REDOX energy storage system  
[NASA-CASE-LEW-14028-1] p 172 N84-32909
- CATALYTIC ACTIVITY**  
Importance of interatomic spacing in catalytic reduction of oxygen in phosphoric acid  
p 58 N84-12644
- Clean catalytic combustor program  
[NASA-CR-168323] p 24 N84-15151
- The role of surface generated radicals in catalytic combustion  
p 61 N84-20555
- Diesel engine catalytic combustor system — aircraft engines  
[NASA-CASE-LEW-12995-1] p 148 N84-33808
- CATHETERIZATION**  
Method of making an ion beam sputter-etched ventricular catheter for hydrocephalus shunt  
[NASA-CASE-LEW-13107-2] p 174 N84-23095
- CATHODES**  
Cathode degradation and erosion in high pressure arc discharges  
[NASA-TM-83638] p 47 N84-22631
- CATHODIC COATINGS**  
Cathode degradation and erosion in high pressure arc discharges  
[NASA-TM-83638] p 47 N84-22631
- CAVITATION CORROSION**  
Predictive capability of long-term cavitation and liquid impingement erosion models  
p 50 N84-32646
- Size scale effect in cavitation erosion  
[NASA-TM-83533] p 67 N84-11254
- Empirical relations for cavitation and liquid impingement erosion processes  
[NASA-TP-2339] p 76 N84-31349
- Characterization of erosion of metallic materials under cavitation attack in a mineral oil  
[NASA-TP-2368] p 147 N84-32825
- CAVITATION FLOW**  
Application of signal analysis to cavitation  
p 122 N84-49192
- CAVITIES**  
Experimental study of bubble cavities attached to a rotating shaft in a reservoir  
[NASA-TM-83586] p 124 N84-17533
- CAVITY RESONATORS**  
Spatial electron density and electric field strength measurements in microwave cavity experiments  
[AIAA PAPER 84-1522] p 169 N84-46109
- CENTAUR LAUNCH VEHICLE**  
Shuttle/Centaur - More capability for the 1980's  
[IAF PAPER 83-18] p 38 N84-11718
- Centaur D-1A guidance/software system  
[AAS PAPER 84-043] p 39 N84-49176
- Centaur D-1A guidance/software system  
[NASA-TM-83552] p 38 N84-16234
- A high energy stage for the National Space Transportation System  
[NASA-TM-83795] p 38 N84-32411
- CENTRIFUGAL PUMPS**  
Effects of volute geometry and impeller orbit on the hydraulic performance of a centrifugal pump  
p 136 N84-22316
- CENTRIPETAL FORCE**  
Forced vibration analysis of rotating cyclic structures in NASTRAN  
[NASA-CR-165429] p 153 N84-11514
- CERAMIC BONDING**  
The effect of annealing on the creep of plasma-sprayed ceramics  
p 79 N84-19785
- CERAMIC COATINGS**  
Ceramic composite liner material for gas turbine combustors  
[AIAA PAPER 84-0363] p 78 N84-18044
- Phase analysis of plasma-sprayed zirconia-yttria coatings  
p 78 N84-19781
- Anisotropic thermal expansion effects in plasma-sprayed ZrO<sub>2</sub>-8 percent Y<sub>2</sub>O<sub>3</sub> coatings  
p 78 N84-19782
- Mechanical and physical properties of plasma-sprayed stabilized zirconia  
p 79 N84-19786
- Thermal stress fracture of ceramic coatings  
p 80 N84-24553
- Degradation mechanisms of ceramic thermal barrier coatings in corrosive environments  
p 81 N84-42668
- Ceramic-coated metals can survive contact with hot working fluid  
p 81 N84-44482
- Heat transfer in thermal barrier coated rods with circumferential and radial temperature gradients  
[ASME PAPER 84-GT-181] p 121 N84-46982
- High temperature thermomechanical analysis of ceramic coatings  
p 152 N84-48565
- Development of strain tolerant thermal barrier coating systems, tasks 1 - 3  
[NASA-CR-168251] p 81 N84-12312
- Some inelastic effects of thermal cycling on yttria-stabilized zirconia  
[NASA-TM-83488] p 123 N84-16492
- Performance of thermal barrier coatings in high heat flux environments  
[NASA-TM-83663] p 72 N84-24772
- Sputtered coatings for protection of spacecraft polymers  
[NASA-TM-83706] p 85 N84-26803
- CERAMICS**  
Development of plane strain fracture toughness test for ceramics using Chevron notched specimens  
p 77 N84-11676
- Shrinkage of amorphous silica fibers  
p 77 N84-13504
- Material removal considerations for metal-ceramic abradable turbine seal systems  
p 135 N84-15575
- Residual stress in plasma-sprayed ceramic turbine tip and gas-path seal specimens  
p 78 N84-19783
- Correlation of compressive and shear stress with spalling of plasma-sprayed ceramic materials  
p 79 N84-19784
- Compositional effects on Si<sub>3</sub>N<sub>4</sub> fracture surfaces  
p 79 N84-19794
- Ceramic components for the AGT 100 engine  
p 136 N84-22878
- Microstructure, strength, and oxidation of a 10 wt pct zirconia-Si<sub>3</sub>N<sub>4</sub> ceramic  
p 80 N84-25402
- Advanced Gas Turbine (AGT). Power-train system development  
[NASA-CR-168056] p 140 N84-10581
- Ceramic composite liner material for gas turbine combustors  
[NASA-TM-83490] p 24 N84-14145
- Advanced Gas Turbine (AGT) technology development  
[NASA-CR-168235] p 141 N84-15554
- Some inelastic effects of thermal cycling on yttria-stabilized zirconia  
[NASA-TM-83488] p 123 N84-16492
- Ceramic wear in indentation and sliding  
[NASA-TM-83585] p 82 N84-19566
- Proceedings of the 20th Automotive Technology Development Contractors' Coordination Meeting.  
[NASA-CR-173412] p 143 N84-21877
- Ceramic-to-metal bonding for pressure transducers  
[NASA-CR-173500] p 84 N84-22753
- Method of fabricating an abradable gas path seal  
[NASA-CASE-LEW-13269-2] p 143 N84-22957
- Considerations in friction and wear  
p 144 N84-23903
- The impact resistance of SiC and other mechanical properties of SiC and Si<sub>3</sub>N<sub>4</sub>  
[NASA-CR-165325] p 84 N84-24809
- Deposition stress effects on thermal barrier coating burner life  
[NASA-TM-83670] p 85 N84-25830
- Advanced Gas Turbine (AGT) Technology Project  
[NASA-CR-174629] p 146 N84-28089
- High temperature ceramic interface study  
[NASA-CR-174728] p 197 N84-34331



## CEREBROSPINAL FLUID

Method of making an ion beam sputter-etched ventricular catheter for hydrocephalus shunt  
[NASA-CASE-LEW-13107-2] p 174 N84-23095

## CERMETS

Coating with overlay metallic-cermet alloy systems  
[NASA-CASE-LEW-13639-2] p 73 N84-27855  
Overlay metallic-cermet alloy coating systems  
[NASA-CASE-LEW-13639-1] p 77 N84-33555

## CHANNEL FLOW

Limitations and empirical extensions of the k-epsilon model as applied to turbulent confined swirling flows  
[AIAA PAPER 84-0441] p 114 A84-18096  
Multicolor printing plate joining  
[NASA-CASE-LEW-13598-1] p 132 N84-22930

## CHARACTERISTICS

Energy efficient engine fan component detailed design report  
[NASA-CR-165466] p 33 N84-27737

## CHARGE COUPLED DEVICES

LEC GaAs for integrated circuit applications  
[NASA-CR-173267] p 191 N84-17014

## CHARGED PARTICLES

Discharges on a negatively biased solar array in a charged particle environment  
[NASA-TM-83644] p 47 N84-23690

## CHARPY IMPACT TEST

The impact resistance of SiC and other mechanical properties of SiC and Si<sub>3</sub>N<sub>4</sub>  
[NASA-CR-165325] p 84 N84-24809

## CHEMICAL BONDS

Scaling relations in the equation of state, thermal expansion, and melting of metals p 192 A84-19359  
Chemical approach for controlling nadimide cure temperature and rate p 55 N84-22698  
Chemical approach for controlling nadimide cure temperature and rate p 55 N84-22699  
Chemical approach for controlling nadimide cure temperature and rate p 55 N84-22700  
Chemical approach for controlling nadimide cure temperature and rate p 55 N84-22701  
Considerations in friction and wear p 144 N84-23903

## CHEMICAL CLOUDS

Effects of chemical releases by the STS-3 Orbiter on the ionosphere  
[NASA-CR-171032] p 173 N84-25204

## CHEMICAL COMPOSITION

Compositional effects on Si<sub>3</sub>N<sub>4</sub> fracture surfaces p 79 A84-19794  
Effects of alloy composition on cyclic flame hot-corrosion attack of cast nickel-base superalloys at 900 deg C  
[NASA-TP-2338] p 73 N84-26783  
Erosion of iron-chromium alloys by glass particles  
[NASA-TP-2354] p 75 N84-28965

## CHEMICAL PROPERTIES

Surface chemistry, friction, and wear of Ni-Zn and Mn-Zn ferrites in contact with metals p 78 A84-13516  
Role of fuel chemical properties on combustor radiative heat load  
[AIAA PAPER 84-1493] p 89 A84-35236  
Aviation-fuel property effects on combustion  
[NASA-CR-168334] p 89 N84-17407  
Overview of zirconia with respect to gas turbine applications  
[NASA-TP-2286] p 83 N84-21740  
Effect of substrate chemical pretreatment on the tribological properties of graphite films  
[NASA-TM-83574] p 85 N84-25831

Lubrication of machine elements  
[NASA-RP-1128] p 147 N84-31640

## CHEMICAL PROPULSION

Evaluation of propellant tank insulation concepts for low-thrust chemical propulsion systems: Executive summary  
[NASA-CR-168321] p 83 N84-20699

## CHEMICAL REACTIONS

Thermal oxidative degradation reactions of perfluoroalkethers  
[NASA-CR-168224] p 60 N84-11229  
The ball bearing as a rheological test device  
[NASA-TM-83570] p 142 N84-17591  
Simulation of lubricating behavior of a thioether liquid lubricant by an electrochemical method  
[NASA-TP-2316] p 84 N84-29764  
Flame propagation in heterogeneous mixtures of fuel drops and air  
[NASA-CR-174644] p 91 N84-23775  
Direct simulations of chemically reacting turbulent mixing layers  
[NASA-CR-174640] p 32 N84-25710

Chemical mechanisms and reaction rates for the initiation of hot corrosion of IN-738  
[NASA-TP-2319] p 74 N84-28958

Calculation of vaporization rates assuming various rate determining steps: Application to the resistojet  
[NASA-TM-83757] p 51 N84-31283

Friction behavior of silicon in contact with titanium, nickel, silver and copper  
[NASA-TP-2362] p 88 N84-33590

## CHEMISTRY

Effects of surface chemistry on hot corrosion life  
[NASA-CR-174683] p 72 N84-24774

## CHIPS (ELECTRONICS)

Design considerations for FET-gated power transistors  
p 102 A84-18414

## CHLOROPHYLLS

Development of Great Lakes algorithms for the Nimbus-G coastal zone color scanner  
[NASA-CR-173511] p 159 N84-27258

## CHLOROSILANES

Radical and ion molecule mechanisms in the polymerization of hydrocarbons and chlorosilanes in RF plasmas at low pressures (1.0 torr)  
[NASA-TM-83602] p 190 N84-21329  
Correlations between plasma variables and the deposition process of Si films from chlorosilanes in low pressure RF plasma of argon and hydrogen  
[NASA-TM-83603] p 190 N84-21330

## CHOKES (RESTRICTIONS)

A numerical model of acoustic choking 1 - Shock free solutions p 180 A84-21250

## CHROMATOGRAPHY

Carbon-13 and proton nuclear magnetic resonance analysis of shale-derived refinery products and jet fuels and of experimental referee broadened-specification jet fuels  
[NASA-CR-174761] p 92 N84-32552

## CHROMIUM

Kinetics of chromium ion absorption by cross-linked polyacrylate films  
[NASA-TM-83661] p 50 N84-23693  
Erosion of iron-chromium alloys by glass particles  
[NASA-TP-2354] p 75 N84-28965  
Overlay coating degradation by simultaneous oxidation and coating/substrate interdiffusion  
[NASA-TM-83738] p 75 N84-31344  
Negative electrode catalyst for the iron-chromium REDOX energy storage system  
[NASA-CASE-LEW-14028-1] p 172 N84-32909

## CHROMIUM ALLOYS

Modeling degradation and failure of Ni-Cr-Al overlay coatings  
[NASA-TM-83672] p 74 N84-27858

## CHROMIUM COMPOUNDS

Chromium electrodes for REDOX cells  
[NASA-CASE-LEW-13653-1] p 170 N84-28205

## CIRCUIT PROTECTION

Inherent overload protection for the series resonant converter  
p 102 A84-23255

## CIRCUITS

Ladder supported ring bar circuit  
[NASA-CASE-LEW-13570-1] p 106 N84-16452  
Dielectric based submillimeter backward wave oscillator circuit  
[NASA-CASE-LEW-13738-1] p 110 N84-27974

## CIRCULAR CYLINDERS

Effect of location in an array on heat transfer to a short cylinder in crossflow p 119 A84-36150  
Heat transfer distributions around nominal ice accretion shapes formed on a cylinder in the NASA Lewis icing research tunnel  
[NASA-TM-83557] p 123 N84-14463  
Effect of a rotor wake on heat transfer from a circular cylinder  
[NASA-TM-83613] p 126 N84-21832  
Investigation of the effects of pressure gradient, temperature and wall temperature ratio on the stagnation point heat transfer for circular cylinders and gas turbine vanes  
[NASA-CR-174667] p 30 N84-23649  
Turbulence and surface heat transfer near the stagnation point of a circular cylinder in turbulent flow  
[NASA-TM-83732] p 128 N84-29157  
Mass transfer from a circular cylinder: Effects of flow unsteadiness and slight nonuniformities  
[NASA-TP-174759] p 129 N84-32751

## CIRCULAR PLATES

Vibration and flutter of mistuned bladed-disk assemblies  
[NASA-TM-83634] p 156 N84-23923

## CIVIL AVIATION

Sixth Annual Workshop on Meteorological and Environmental Inputs to Aviation Systems, 26-28 October 1982, Tullahoma, Tenn p 174 A84-23424

## CLEARANCES

Annulus wall boundary layer development in a compressor stage, including the effects of tip clearance p 26 N84-16207

Oxidizing seal for a turbine tip gas path  
[NASA-CASE-LEW-14053-1] p 29 N84-22563  
Dual clearance squeeze film damper for high load conditions  
[NASA-TM-83619] p 144 N84-25064

## CLIMATOLOGY

Climatology of ozone at altitudes from 19,000 to 59,000 feet based on combined GASP and ozonesonde data  
[NASA-TP-2303] p 174 N84-31865

## CLOUDS (METEOROLOGY)

Comparison of icing cloud instruments for 1982-1983 icing season flight program  
[NASA-TM-83569] p 14 N84-29870

## COAL

Cogeneration Technology Alternatives Study (CTAS) Volume 2: Comparison and evaluation of results  
[NASA-TM-81401] p 173 N84-34038

## COAL GASIFICATION

Micronized coal burner facility  
[NASA-CASE-LEW-13426-1] p 60 N84-16276

## COASTAL ZONE COLOR SCANNER

Development of Great Lakes algorithms for the Nimbus-G coastal zone color scanner  
[NASA-CR-173511] p 159 N84-27258

## COATING

Development of strain tolerant thermal barrier coating systems, tasks 1 - 3  
[NASA-CR-168251] p 81 N84-12312  
Oxidation resistant slurry coating for carbon-based materials  
[NASA-CASE-LEW-13923-1] p 54 N84-16266  
Status of plasma physics techniques for the deposition of tribological coatings p 190 N84-25058  
Abrasive tip treatment for use on compressor blades  
[NASA-CR-174666] p 145 N84-25065

## COATINGS

Durable solid lubricant coatings for foil gas bearings to 315 deg C  
[NASA-TM-83596] p 83 N84-19567  
Diamondlike flake composites  
[NASA-CASE-LEW-13837-1] p 54 N84-22695  
Effects of surface chemistry on hot corrosion life  
[NASA-CR-174683] p 72 N84-24774  
Status and new directions for solid lubricant coatings and composite materials p 85 N84-25055  
Status of plasma physics techniques for the deposition of tribological coatings p 190 N84-25058  
Overlay coating degradation by simultaneous oxidation and coating/substrate interdiffusion  
[NASA-TM-83738] p 75 N84-31344  
Dual ion beam deposition of carbon films with diamondlike properties  
[NASA-TM-83743] p 110 N84-31512  
RF sputtered silicon and hafnium nitrides as applied to 440C steel  
[NASA-TM-86862] p 87 N84-32536

## COAXIAL FLOW

Mass and momentum turbulent transport experiments with confined swirling coaxial jets I  
[AIAA PAPER 84-1380] p 119 A84-35664  
Mass and momentum turbulent transport experiments with confined swirling coaxial jets  
[NASA-CR-168252] p 124 N84-17530  
The influence of large-scale motion on turbulent transport for confined coaxial jets p 125 N84-20542

## COAXIAL PLASMA ACCELERATORS

Coaxial carbon plasma gun deposition of amorphous carbon films  
[NASA-TM-83600] p 191 N84-20404

## COBALT

Reaction of cobalt in SO<sub>2</sub> atmospheres at elevated temperatures p 65 A84-33440  
The role of cobalt on the creep of Waspalloy  
[NASA-CR-174628] p 70 N84-19523  
Effects of long-time elevated temperature exposures on hot-isostatically-pressed power-metallurgy Udmet 700 alloys with reduced cobalt contents  
[NASA-TM-83632] p 57 N84-28917  
Evaluation of candidate Stirling engine heater tube alloys after 3500 hours exposure to high pressure doped hydrogen or helium  
[NASA-TM-83782] p 77 N84-34603

## COBALT ALLOYS

Creep fatigue of low-cobalt superalloys Waspalloy, PM U 700 and wrought U 700  
[NASA-CR-168260] p 67 N84-13265  
Effects of cobalt in nickel-base superalloys  
[NASA-CR-168308] p 67 N84-14287  
Preliminary study of thermomechanical fatigue of polycrystalline MAR-M 200  
[NASA-TP-2280] p 69 N84-17350



- Influence of cobalt, tantalum and tungsten on the high temperature mechanical properties of single crystal nickel-base superalloys [NASA-TM-83479] p 70 N84-17355
- Analysis of thermoelectric properties of high-temperature complex alloys of nickel-base, iron-base and cobalt-base groups [NASA-TP-2278] p 70 N84-18370
- Effects of alloy composition on cyclic flame hot-corrosion attack of cast nickel-base superalloys at 900 deg C [NASA-TP-2338] p 73 N84-26783
- Creep-rupture behavior of candidate Stirling engine iron superalloys in high-pressure hydrogen. Volume 2: Hydrogen creep-rupture behavior [NASA-CR-174705] p 74 N84-28961
- High-temperature cyclic oxidation data, volume 1 [NASA-TM-83665] p 75 N84-31345
- Understanding the roles of the strategic element cobalt in nickel base superalloys p 76 N84-33471
- CODING**
- PURDU-WINCOF A computer code for establishing the performance of a fan-compressor unit with water ingestion [NASA-CR-168005] p 34 N84-29875
- COEFFICIENT OF FRICTION**
- Tribological and microstructural characteristics of iron-nitrided steels p 64 A84-19225
- An analytical method to predict efficiency of aircraft gearboxes [AIAA PAPER 84-1500] p 20 A84-44180
- Friction and morphology of magnetic tapes in sliding contact with nickel-zinc ferrite [NASA-TP-2267] p 82 N84-16334
- Mechanism of lubrication by tricresylphosphate (TCP) [NASA-TP-2274] p 142 N84-18653
- An analytical method to predict efficiency of aircraft gearboxes [NASA-TM-83716] p 2 N84-25606
- COGENERATION**
- An assessment of advanced technology for industrial cogeneration [NASA-CR-173456] p 167 N84-22001
- AFB/open cycle gas turbine conceptual design study [NASA-CR-168135] p 172 N84-31784
- COLD CATHODES**
- Evaluation of the emission capabilities of Spindt-type field emitting cathodes p 101 A84-12424
- COLD FLOW TESTS**
- On some flow characteristics of conventional and excited jets [AIAA PAPER 84-0532] p 181 A84-21304
- Alcohol cold starting - A theoretical study p 138 A84-30061
- On some flow characteristics of conventional and excited jets [NASA-TM-83503] p 182 N84-13922
- COLD WEATHER TESTS**
- Heating experiments for flowability improvement of near-freezing aviation fuel p 89 A84-26955
- COLOR TELEVISION**
- NTSC composite video at 16 bits/pel p 95 A84-49259
- COMBINED STRESS**
- Analyses of large quasistatic deformations of inelastic bodies by a new hybrid-stress finite element algorithm - Applications p 150 A84-16884
- COMBUSTIBLE FLOW**
- Evaporation and combustion of sprays p 58 A84-11636
- Turbulent flow field calculations in an internal combustion engine equipped with two valves p 112 A84-13311
- Formation and inflammation of a turbulent jet [AIAA PAPER 84-0572] p 114 A84-18171
- Extinction of premixed flames by stretch and radiative loss p 58 A84-23593
- Dynamic effects of combustion p 59 A84-29128
- Time-resolved density measurements in premixed turbulent flames p 59 A84-32612
- Analytic modeling of a spray diffusion flame [AIAA PAPER 84-1317] p 118 A84-35168
- COMBUSTION**
- Symposium (International) on Combustion, 19th, Technion Israel Institute of Technology, Haifa, Israel, August 8-13, 1982, Proceedings p 59 A84-35401
- Measurement of spray combustion processes p 61 N84-20530
- Turbulent swirling combustion p 61 N84-20535
- Free stream turbulence and density ratio effects on the interaction region of a jet in a cross flow p 125 N84-20546
- Assessment of Alternative Aircraft Fuels [NASA-CP-2307] p 30 N84-23630
- NASA broad-specification fuels combustion technology program p 62 N84-23637
- Flame propagation in heterogeneous mixtures of fuel drops and air [NASA-CR-174644] p 91 N84-23775
- Advanced high temperature materials for the energy efficient automotive Stirling engine [NASA-TM-83659] p 75 N84-28963
- The structure of evaporating and combusting sprays. Measurements and predictions [NASA-CR-173778] p 128 N84-29155
- A comparison of the efficiency of numerical methods for integrating chemical kinetic rate equations p 49 N84-31280
- An experimental investigation of gas jets in confined swirling air flow [NASA-CR-3832] p 36 N84-33412
- A theoretical model for the cross spectra between pressure and temperature downstream of a combustor [NASA-TM-83671] p 186 N84-34231
- COMBUSTION CHAMBERS**
- Combustor development for automotive gas turbines p 135 A84-10499
- Turbulence measurements in confined jets using a rotating single-wire probe technique p 113 A84-13564
- Ceramic composite liner material for gas turbine combustors [AIAA PAPER 84-0363] p 78 A84-18044
- Calculations of turbulent mass transport in a bluff-body diffusion-flame combustor [AIAA PAPER 84-0372] p 114 A84-18048
- Flame radiation and linear heat transfer in a tubular can combustor [AIAA PAPER 84-0443] p 16 A84-21300
- NASA advanced low emissions combustor program [ASME PAPER 83-JPGC-GT-10] p 17 A84-28982
- A temperature correlation for the radiation resistance of a thick-walled circular duct exhausting a hot gas p 101 A84-31103
- Role of fuel chemical properties on combustor radiative heat load [AIAA PAPER 84-1493] p 89 A84-35236
- Preliminary investigation of a two-zone swirl flow combustor [AIAA PAPER 84-1169] p 17 A84-36951
- Experimental investigation of the low NOx vortex airblast annular combustor [AIAA PAPER 84-1170] p 18 A84-36952
- Aerodynamic effect of combustor inlet-air pressure on fuel jet atomization [AIAA PAPER 84-1320] p 120 A84-36973
- Five-hole pitot probe measurements of swirl, confinement and nozzle effects on confined turbulent flow [AIAA PAPER 84-1605] p 120 A84-38000
- A review of internal combustion engine combustion chamber process studies at NASA Lewis Research Center [AIAA PAPER 84-1316] p 121 A84-40242
- Experiments in dilution jet mixing p 122 A84-48140
- Cross spectra between pressure and temperature in a constant-area duct downstream of a hydrogen-fueled combustor [NASA-TM-83463] p 182 N84-11885
- Executive summary, aerothermal modeling program, phase 1 [NASA-CR-174602] p 60 N84-12253
- Aerothermal modeling program, phase 1 [NASA-CR-168243-VOL-2] p 60 N84-12255
- A theoretical and experimental study of turbulent particle-laden jets [NASA-CR-168293] p 23 N84-13197
- Flame radiation and liner heat transfer in a tubular-can combustor [NASA-TM-83538] p 23 N84-13188
- Ceramic composite liner material for gas turbine combustors [NASA-TM-83490] p 24 N84-14145
- A review of NASA combustor and turbine heat transfer research [NASA-TM-83541] p 24 N84-14146
- Clean catalytic combustor program [NASA-CR-168323] p 24 N84-15151
- Aerothermal modeling Executive summary [NASA-CR-168330] p 25 N84-15152
- Aerothermal modeling, phase 1. Volume 1: Model assessment [NASA-CR-168296-VOL-1] p 25 N84-15155
- Micronized coal burner facility [NASA-CASE-LEW-13426-1] p 60 N84-16276
- Effects of broadened property fuels on radiant heat flux to gas turbine combustor liners [NASA-TM-83537] p 123 N84-16494
- Dynamic gas temperature measurement system, volume 1 [NASA-CR-168267-VOL-1] p 132 N84-16529
- Turbulence characteristics of swirling flowfields [NASA-CR-175392] p 124 N84-19744
- Error reduction program A progress report p 27 N84-20536
- Numerical modeling of turbulent flow p 125 N84-20538
- Modeling of dilution jet flowfields p 126 N84-20547
- Transient flow combustion p 62 N84-20560
- Combustor flame flashback p 62 N84-20561
- Preliminary investigation of a two-zone swirl flow combustor [NASA-TM-83637] p 29 N84-22565
- Aerodynamic effect of combustor inlet-air pressure on fuel jet atomization [NASA-TM-83611] p 126 N84-22910
- Heat pipes to reduce engine exhaust emissions [NASA-CASE-LEW-12590-1] p 143 N84-22958
- Combustor liner construction [NASA-CASE-LEW-14035-1] p 30 N84-24577
- Detailed fuel spray analysis techniques p 127 N84-24747
- A review of internal combustion engine combustion chamber process studies at NASA Lewis Research Center [NASA-TM-83666] p 127 N84-24999
- A critical review of noise production models for turbulent, gas-fueled burners [NASA-CR-3803] p 184 N84-26384
- Dilution jet mixing program [NASA-CR-174624] p 33 N84-26702
- Dilution jets in accelerated cross flows [NASA-CR-174717] p 34 N84-28794
- Helicopter engine core noise p 185 N84-29676
- Atomization of liquid sheets in high pressure airflow [NASA-TM-83731] p 128 N84-30223
- Analysis of the effect on combustor noise measurements of acoustic waves reflected by the turbine and combustor inlet [NASA-TM-83760] p 185 N84-32122
- A theoretical and experimental study of turbulent evaporating sprays [NASA-CR-174760] p 35 N84-32390
- Rocket injector anomalies study. Volume 1: Description of the mathematical model and solution procedure [NASA-CR-174702] p 49 N84-32428
- Rocket injector anomalies study Volume 2: Results of parametric studies [NASA-CR-174703] p 49 N84-32429
- Diesel engine catalytic combustor system - aircraft engines [NASA-CASE-LEW-12995-1] p 148 N84-33808
- COMBUSTION CONTROL**
- Extinction of premixed flames by stretch and radiative loss p 58 A84-23593
- COMBUSTION EFFICIENCY**
- Aerodynamic effect of combustor inlet-air pressure on fuel jet atomization [AIAA PAPER 84-1320] p 120 A84-36973
- Aerodynamic effect of combustor inlet-air pressure on fuel jet atomization [NASA-TM-83611] p 126 N84-22910
- Heat pipes to reduce engine exhaust emissions [NASA-CASE-LEW-12590-1] p 143 N84-22958
- Utilization of alternative fuels in diesel engines [NASA-CR-174669] p 91 N84-26813
- Development of carbon slurry fuels for transportation (hybrid fuels, phase 2) [NASA-CR-174659] p 74 N84-28960
- COMBUSTION PHYSICS**
- Combustion in a turbulent mixing layer formed at a reanward-facing step p 58 A84-10140
- Dynamic effects of combustion p 59 A84-29128
- Simplified combustion noise theory yielding a prediction of fluctuating pressure level [NASA-TP-2237] p 183 N84-19049
- Combustion characteristics in the transition region of liquid fuel sprays [NASA-CR-175396] p 61 N84-19495
- Combustion Fundamentals Research [NASA-CP-2309] p 27 N84-20525
- Transient flow combustion p 62 N84-20560
- Shock tube study of the fuel structure effects on the chemical kinetic mechanisms responsible for soot formation [NASA-CR-174661] p 62 N84-21677
- COMBUSTION PRODUCTS**
- Degradation mechanisms of ceramic thermal barrier coatings in corrosive environments p 81 A84-42668
- Experimental and theoretical study of combustion jet ignition [NASA-CR-168139] p 21 N84-10054
- Effects of broadened property fuels on radiant heat flux to gas turbine combustor liners [NASA-TM-83537] p 123 N84-16494
- Combustion gas properties of various fuels of interest to gas turbine engineers [NASA-TM-83682] p 31 N84-24584

- Deposition of Na<sub>2</sub>SO<sub>4</sub> from salt-seeded combustion gases of a high velocity burner  
[NASA-TM-83751] p 129 N84-31558
- COMBUSTION STABILITY**  
Secondary effects in combustion instabilities leading to flashback p 58 A84-17436  
Transient flow combustion p 62 N84-20560  
A theoretical prediction of the acoustic pressure generated by turbulence-flame front interactions  
[NASA-TM-83587] p 184 N84-26383
- COMMERCIAL AIRCRAFT**  
Temperature histories of commercial flights at severe conditions from GASP data  
[NASA-CR-168247] p 12 N84-11152  
Economic impact of fuel properties on turbine powered business aircraft p 14 N84-23646  
Fuel savings potential of the NASA Advanced Turboprop Program  
[NASA-TM-83736] p 35 N84-29878
- COMMERCIAL ENERGY**  
The worldwide market for photovoltaics in the rural sector p 161 A84-23135  
Heat recovery subsystem and overall system integration of fuel cell on-site integrated energy systems  
[NASA-CR-168309] p 166 N84-20915
- COMMUNICATION EQUIPMENT**  
NASA's multibeam communications technology program p 39 A84-21397  
30/20 GHz communications systems baseband processor development p 95 A84-38251
- COMMUNICATION NETWORKS**  
Concept for advanced satellite communications and required technologies p 93 A84-15626  
A system for the simulation and evaluation of satellite communication networks  
[AIAA PAPER 84-0680] p 94 A84-25272  
A study of 60 GHz intersatellite link applications p 40 A84-49288  
Mobile radio alternative systems study, Volume 1. Traffic model  
[NASA-CR-168062] p 95 N84-10402  
A system for the simulation and evaluation of satellite communication networks  
[NASA-TM-83531] p 97 N84-13400  
Communications network design and costing model technical manual  
[NASA-CR-168236] p 97 N84-14376  
Communications network design and costing model programmers manual  
[NASA-CR-168237] p 97 N84-14377  
Communications network design and costing model users manual  
[NASA-CR-168238] p 97 N84-14378
- COMMUNICATION SATELLITES**  
Baseband processor development for the Advanced Communications Satellite Program p 93 A84-15628  
Serial MSK modem for the Advanced Communications Satellite Program p 93 A84-15629  
A new multiple beam satellite antenna for 30/20 GHz communications coverage of CONUS-experimental evaluation  
[AIAA PAPER 84-0655] p 94 A84-25256  
A system for the simulation and evaluation of satellite communication networks  
[AIAA PAPER 84-0680] p 94 A84-25272  
Economic comparison of FDMA and TDMA options for communications by Ka-band multiple beam satellites  
[AIAA PAPER 84-0740] p 94 A84-25299  
NASA's geostationary communications platform program  
[AIAA PAPER 84-0702] p 95 A84-25326  
High efficiency IMPATT diodes for 60 GHz intersatellite link applications  
[AIAA PAPER 84-0767] p 103 A84-25333  
30/20 GHz communications systems baseband processor development p 95 A84-38251  
The effect of variable S/N on the subjective evaluation of protection ratios for direct-TV satellite services p 95 A84-48452  
Advanced 30/20 GHz multiple-beam antennas for communications satellites p 40 A84-49250  
High-speed wide band 20 x 20 microwave switch matrix p 105 A84-49253  
Interference performance analysis of M-ary CPSK and M-ary CAPK digital transmission systems and the computation of 'required isolation' for efficient utilization of geostationary satellite orbit/spectrum p 95 A84-49303  
A comparison of the domestic satellite communications forecast to the year 2000  
[NASA-TM-83516] p 96 N84-10405  
A system for the simulation and evaluation of satellite communication networks  
[NASA-TM-83531] p 97 N84-13400
- Broadcasting satellites at 12 GHz for Region 2. Technical characteristics  
[NASA-TM-83522] p 98 N84-19640  
Advanced technology satellites in the commercial environment. Volume 1. Executive summary  
[NASA-CR-174635-VOL-1] p 38 N84-20611  
Advanced technology satellites in the commercial environment, volume 2  
[NASA-CR-174635-VOL-2] p 38 N84-20612  
Determination of the key parameters affecting historic communications satellite trends  
[NASA-TM-83633] p 99 N84-25908  
Secondary pattern computation of an arbitrarily shaped main reflector  
[NASA-TM-85527] p 100 N84-25909  
Spectrum/orbit utilization program for geostationary satellites  
[NASA-TM-83759] p 100 N84-30146  
The 20 and 30 GHz MMIC technology for future space communication antenna system  
[NASA-TM-83745] p 100 N84-31460  
The 20 x 20 high speed microwave switches  
[NASA-TM-83775] p 101 N84-32644  
The 20 GHz solid state transmitter design, impact diode development and reliability assessment  
[NASA-CR-174716] p 112 N84-33715
- COMMUNICATIONS TECHNOLOGY SATELLITE**  
ACTS TDMA network control -- Advanced Communication Technology Satellite  
[AIAA PAPER 84-0682] p 94 A84-25274
- COMUTATION**  
New propulsion components for electric vehicles p 103 A84-30209
- COMPARISON**  
Comparison between measured turbine stage performance and the predicted performance using quasi-3D flow and boundary layer analyses  
[AIAA PAPER 84-1299] p 18 A84-36972  
Application of an optimization method to high performance propeller designs  
[AIAA PAPER 84-1203] p 20 A84-44181  
The influence of large-scale motion on turbulent transport for confined coaxial jets p 125 N84-20542  
Comparison between measured turbine stage performance and the predicted performance using quasi-3D flow and boundary layer analyses  
[NASA-TM-83640] p 29 N84-22564  
Application of an optimization method to high performance propeller designs  
[NASA-TM-83710] p 2 N84-25607  
Cogeneration Technology Alternatives Study (CTAS). Volume 2: Comparison and evaluation of results  
[NASA-TM-81401] p 173 N84-34038
- COMPONENT RELIABILITY**  
Engine cyclic durability by analysis and material testing  
[NASA-TM-83577] p 155 N84-18683  
Creep-rupture reliability analysis  
[NASA-CR-3790] p 155 N84-19925  
NASA Orbit Transfer Rocket Engine Technology Program  
[NASA-CR-168156] p 48 N84-28901  
Advanced Gas Turbine (AGT)  
[NASA-CR-174694] p 195 N84-29805
- COMPOSITE MATERIALS**  
Environmental and high strain rate effects on composites for engine applications p 51 A84-17444  
Ceramic composite liner material for gas turbine combustors  
[AIAA PAPER 84-0363] p 78 A84-18044  
Indentation law for composite laminates p 52 A84-27356  
Examination, evaluation and repair of laminated wood blades after service on the Mod-OA wind turbine  
[NASA-TM-83493] p 163 N84-10684  
INHYP. Computer code for intraply hybrid composite design. A users manual  
[NASA-TP-2239] p 54 N84-13224  
Diamondlike flake composites  
[NASA-CASE-LEW-13837-1] p 54 N84-22695  
Full scale phosphoric acid fuel cell stack technology development  
[NASA-CR-174660] p 169 N84-26165
- COMPOSITE STRUCTURES**  
Characterization of composite materials by means of the ultrasonic stress wave factor p 51 A84-10430  
Aging results for PRD 49 III/epoxy and Kevlar 49/epoxy composite pressure vessels p 52 A84-21847  
Numerical simulation of two-dimensional heat transfer in composite bodies with application to de-icing of aircraft components  
[NASA-CR-168283] p 122 N84-13490  
Design concepts for low-cost composite engine frames  
[NASA-TM-83544] p 26 N84-16186
- Improved high temperature resistant matrix resins  
[NASA-CR-168210] p 87 N84-28995
- COMPRESSED GAS**  
Assessment of institutional barriers to the use of natural gas fuel in automotive vehicle fleets  
[NASA-CR-168183] p 165 N84-14587
- COMPRESSIBLE FLOW**  
Boundary conditions for the solution of compressible Navier-Stokes equations by an implicit factored method p 113 A84-13495  
Comparison of experimental and computational compressible flow in a S-duct  
[AIAA PAPER 84-0033] p 4 A84-19226  
Extension to an analysis of turbulent swirling compressible flow for application to axisymmetric small gas turbine ducts  
[NASA-CR-165597] p 195 N84-21445  
Acoustic pressures emanating from a turbomachine stage  
[NASA-TM-83734] p 129 N84-30224
- COMPRESSION RATIO**  
Formation and destruction of vortices in a motored four-stroke piston-cylinder configuration p 139 A84-33838
- COMPRESSION TESTS**  
Compressive behavior of unidirectional fibrous composites p 53 A84-29894
- COMPRESSIVE STRENGTH**  
Elevated temperature compressive steady state deformation and failure in the oxide dispersion strengthened alloy MA 6000E p 66 A84-45785
- COMPRESSOR BLADES**  
Annulus wall boundary layer development in a compressor stage, including the effects of tip clearance p 26 N84-16207  
Secondary flow spanwise deviation model for the stators of NASA middle compressor stages  
[NASA-CR-173380] p 27 N84-18202  
The boundary layer on compressor cascade blades  
[NASA-CR-173514] p 127 N84-25001  
Abrasive tip treatment for use on compressor blades  
[NASA-CR-174666] p 145 N84-25065
- COMPRESSOR ROTORS**  
Three-dimensional flowfield inside a low-speed axial flow compressor rotor p 3 A84-13574  
Laser Doppler velocimeter measurement in the tip region of a compressor rotor  
[AIAA PAPER 84-1602] p 6 A84-39304  
Inlet boundary layer effects in an axial compressor rotor. I Blade-to-blade effects  
[ASME PAPER 84-GT-84] p 6 A84-46926  
Inlet boundary layer effects in an axial compressor rotor II - Throughflow effects  
[ASME PAPER 84-GT-85] p 7 A84-46927  
Loss reduction in axial-flow compressors through low-speed model testing  
[ASME PAPER 84-GT-184] p 7 A84-46985  
An experimental study of the compressor rotor blade boundary layer  
[ASME PAPER 84-GT-193] p 7 A84-46991  
Annulus wall boundary layer development in a compressor stage, including the effects of tip clearance p 26 N84-16207  
End-wall boundary layer measurements in a two-stage fan p 26 N84-16208  
Compressor rotor aerodynamics p 26 N84-16210  
Lewis Research Center spinning and its use in vibration analysis of rotating systems  
[NASA-TP-2304] p 30 N84-24578  
Investigation of the three-dimensional flow field within a transonic fan rotor: Experiment and analysis  
[NASA-TM-83739] p 11 N84-32357
- COMPRESSORS**  
Determination of compressor in-stall characteristics from engine surge transients  
[AIAA PAPER 84-1206] p 18 A84-36959  
Bladed-shrouded-disc aeroelastic analyses. Computer program updates in NASTRAN level 17.7  
[NASA-CR-165428] p 25 N84-15154  
Determination of compressor in-stall characteristics from engine surge transients  
[NASA-TM-83639] p 29 N84-22566  
Aeronautics and Space Engineering Board. Aeronautics Assessment Committee  
[NASA-TM-85594] p 93 N84-22771  
Solar photovoltaic powered refrigerators/freezers for medical use in remote geographic locations  
[NASA-CR-168268] p 169 N84-25163  
Identification of quasi-steady compressor characteristics from transient data  
[NASA-CR-174685] p 36 N84-34444
- COMPUTATION**  
Multiple-grid convergence acceleration of viscous and inviscid flow computations p 116 A84-23950

- Reflector antennas with low sidelobes, low cross polarization, and high aperture efficiency  
[NASA-CR-174670] p 100 N84-31464
- COMPUTATIONAL FLUID DYNAMICS**
- A direct method for the solution of unsteady two-dimensional incompressible Navier-Stokes equations p 2 A84-10078
- Application of a finite element algorithm to the solution of steady transonic Euler equations p 3 A84-10133
- Hybrid C-H grids for turbomachinery cascades — parabolic and Cartesian coordinates p 3 A84-11591
- Modeling of transient two-component flow using a four-point implicit method p 112 A84-13237
- Turbulent flow field calculations in an internal combustion engine equipped with two valves p 112 A84-13311
- Boundary conditions for the solution of compressible Navier-Stokes equations by an implicit fractional method p 113 A84-13495
- Streamwise computation of three-dimensional parabolic flows p 113 A84-16828
- The application of vortex theory to the optimum swept propeller [AIAA PAPER 84-0036] p 3 A84-17841
- An implicit LU scheme for the Euler equations applied to arbitrary cascades — new method of factoring [AIAA PAPER 84-0167] p 4 A84-17925
- Computation of viscous flow in planar and axisymmetric ducts by an implicit marching procedure [AIAA PAPER 84-0258] p 114 A84-17979
- Boundary layer transition effects on flow separation around V-STOL engine inlets at high incidence [AIAA PAPER 84-0432] p 4 A84-18090
- One-dimensional unsteady modeling of supersonic inlet unstart/restart [AIAA PAPER 84-0439] p 4 A84-18094
- Formation and inflammation of a turbulent jet [AIAA PAPER 84-0572] p 114 A84-18171
- Comparison of experimental and computational compressible flow in a S-duct [AIAA PAPER 84-0033] p 4 A84-19228
- A finite element approach for predicting nozzle admittances p 180 A84-21184
- Computation of viscous flow in curved ducts and comparison with experimental data [AIAA PAPER 84-0531] p 115 A84-21303
- Turbulent boundary-layer flow and structure on a convex wall and its redevelopment on a flat wall p 115 A84-21378
- Transient flow analysis of the AEDC/HPDE MHD generator p 189 A84-24049
- Finite-analytic numerical method for unsteady two-dimensional Navier-Stokes equations p 116 A84-25807
- Finite element formulation of transonic flow problems p 116 A84-25859
- Investigation of mixing in a turbofan exhaust duct. II Computer code application and verification p 17 A84-27140
- A rapid blade-to-blade solution for use in turbomachinery design [ASME PAPER 83-GT-67] p 4 A84-31289
- Calculation of a hollow-cone liquid spray in a uniform air stream [AIAA PAPER 84-1322] p 118 A84-35171
- Random element method for numerical modeling of diffusional processes p 119 A84-35318
- Application of a polynomial spline in higher-order accurate viscous-flow computations p 119 A84-35349
- Computation of three-dimensional viscous flows using a space-marching method [AIAA PAPER 84-1298] p 5 A84-36971
- Conservative streamtube solution of steady-state Euler equations [AIAA PAPER 84-1643] p 120 A84-38030
- Three-dimensional stability of an elliptical vortex in a straining field [AD-A146317] p 120 A84-38557
- Three-dimensional flow simulations for supersonic mixed-compression inlets at incidence p 5 A84-38828
- Computational modeling of jet induced mixing of cryogenic propellants in low-G [AIAA PAPER 84-1344] p 121 A84-40243
- Turbulent solutions of the equations of fluid motion p 121 A84-41156
- Viscous-inviscid interactive procedure for rotational flow in cascades of airfoils p 6 A84-44639
- Transonic cascade flow analysis using viscous/inviscid coupling concepts [AIAA PAPER 84-2159] p 6 A84-46103
- Investigation of the three-dimensional flow field within a transonic fan rotor - Experiment and analysis [ASME PAPER 84-GT-200] p 7 A84-46995
- On numerical simulation of viscous flows p 122 A84-49112
- Computation of viscous flow in curved ducts and comparison with experimental data [NASA-TM-83548] p 122 N84-13494
- Further development of a method for computing three-dimensional subsonic viscous flows in turbofan lobe mixers [NASA-CR-168304] p 122 N84-14462
- Programs for calculating quasi-three-dimensional flow in a turbomachine blade row [NASA-TM-83588] p 9 N84-17138
- Combustion Fundamentals Research [NASA-CP-2309] p 27 N84-20525
- Turbulent swirling combustion p 61 N84-20535
- Application of improved numerical schemes p 178 N84-20537
- Fast algorithms for combustion kinetics calculations: A comparison p 61 N84-20554
- Random vortex method for combustor flows p 62 N84-20558
- Computational modeling of jet induced mixing of cryogenic propellants in low-G [NASA-TM-83703] p 127 N84-25000
- Numerical aspects of unsteady flow calculations p 128 N84-25968
- Lubricant jet flow phenomena in spur and helical gears with modified center distances and/or addendums for out-of-mesh conditions [NASA-TM-83723] p 146 N84-29224
- Unsteady transonic flow in cascades [NASA-TM-83780] p 11 N84-32351
- COMPUTATIONAL GRIDS**
- Hybrid C-H grids for turbomachinery cascades — parabolic and Cartesian coordinates p 3 A84-11591
- Multiple-grid convergence acceleration of viscous and inviscid flow computations p 116 A84-23950
- Dynamic response of shock waves in transonic diffuser and supersonic inlet - An analysis with the Navier-Stokes equations and adaptive grid [AIAA PAPER 84-1609] p 5 A84-38004
- Parameter studies of gear cooling using an automatic finite element mesh generator [NASA-TM-83721] p 146 N84-28087
- Characteristics and capacities of the NASA Lewis Research Center high precision 67- by 67-m planar near-field scanner [NASA-TM-83785] p 133 N84-32789
- COMPUTER AIDED DESIGN**
- Parametric study of minimum converter loss in an energy-storage dc-to-dc converter p 101 A84-18403
- A rapid blade-to-blade solution for use in turbomachinery design [ASME PAPER 83-GT-67] p 4 A84-31289
- Improved design of subcritical and supercritical cascades using complex characteristics and boundary-layer correction p 5 A84-38839
- AESOP, An interactive computer program for the design of linear quadratic regulators and Kalman filters [NASA-TP-2221] p 178 N84-16843
- Design considerations for a 10-kW integrated hydrogen-oxygen regenerative fuel cell system [NASA-TM-83684] p 167 N84-23023
- Users' manual for computer program for three-dimensional analysis of coupler-cavity traveling wave tubes [NASA-CR-168269] p 109 N84-23841
- COMPUTER AIDED MAPPING**
- Development of Great Lakes algorithms for the Nimbus-G coastal zone color scanner [NASA-CR-173511] p 159 N84-27258
- COMPUTER DESIGN**
- Optical flip-flops and sequential logic circuits using a liquid crystal light valve p 188 A84-40332
- COMPUTER GRAPHICS**
- Graphics enhanced computer emulation for improved timing-race and fault tolerance control system analysis — of Centaur liquid-fuel booster [AIAA PAPER 83-2328] p 177 A84-10010
- COMPUTER NETWORKS**
- Parallelism and pipelining in high-speed digital simulators p 175 A84-11876
- COMPUTER PROGRAMMING**
- RTMPL: A structured programming and documentation utility for real-time multiprocessor simulations [NASA-TM-83606] p 177 N84-20259
- COMPUTER PROGRAMS**
- Software simulator for multiple computer simulation system p 176 A84-11892
- Test results and description of a 1 kW free-piston Stirling engine with a dashpot load p 138 A84-30095
- Comparison between measured turbine stage performance and the predicted performance using quasi-3D flow and boundary layer analyses [AIAA PAPER 84-1299] p 18 A84-36972
- Analysis of inviscid and viscous flows in cascades with an explicit multiple-grid algorithm [AIAA PAPER 84-1663] p 5 A84-38043
- Calculation of transonic flow in a linear cascade [AIAA PAPER 84-1301] p 6 A84-40241
- Finite element-integral acoustic simulation of JT15D turbofan engine p 182 A84-41132
- An analytical method to predict efficiency of aircraft gearboxes [AIAA PAPER 84-1500] p 20 A84-44180
- On modeling dilution jet flowfields [AIAA PAPER 84-1379] p 121 A84-44183
- Centaur D-1A guidance/software system [AAS PAPER 84-043] p 39 A84-49176
- Geometric models, antenna gains, and protection ratios as developed for BC SAT-R2 conference software [NASA-TM-83381] p 96 N84-11358
- A generalized computer code for developing dynamic gas turbine engine models (DIGTEM) [NASA-TM-83508] p 22 N84-12166
- PREWATE: An interactive preprocessing computer code to the Weight Analysis of Turbine Engines (WATE) computer code [NASA-TM-83545] p 176 N84-13812
- Design and performance of a fixed, nonaccelerating, guide vane cascade that operates over an inlet flow angle range of 60 deg [NASA-TM-83519] p 8 N84-14120
- Communications network design and costing model programmers manual [NASA-CR-168237] p 97 N84-14377
- A simplified method for elastic-plastic-creep structural analysis [NASA-TM-83509] p 154 N84-14542
- Aerothermal modeling Executive summary [NASA-CR-168330] p 25 N84-15152
- Assessment of three-dimensional inviscid codes and loss calculations for turbine aerodynamic computations [NASA-TM-83571] p 8 N84-16142
- Digital computer program for generating dynamic turbofan engine models (DIGTEM) [NASA-TM-83446] p 26 N84-16185
- Centaur D-1A guidance/software system [NASA-TM-83552] p 38 N84-16234
- Progress toward the development of an aircraft icing analysis capability [NASA-TM-83562] p 9 N84-20490
- Development of a simplified procedure for cyclic structural analysis [NASA-TP-2243] p 155 N84-20878
- Analysis of inviscid and viscous flows in cascades with an explicit multiple-grid algorithm [NASA-TM-83636] p 1 N84-22527
- Comparison between measured turbine stage performance and the predicted performance using quasi-3D flow and boundary layer analyses [NASA-TM-83640] p 29 N84-22564
- Engineering calculations for communications satellite systems planning [NASA-CR-173532] p 38 N84-23662
- Users' manual for computer program for three-dimensional analysis of coupler-cavity traveling wave tubes [NASA-CR-168269] p 109 N84-23841
- Calculation of transonic flow in a linear cascade [NASA-TM-83697] p 10 N84-24539
- An analytical method to predict efficiency of aircraft gearboxes [NASA-TM-83716] p 2 N84-25605
- Direct simulations of chemically reacting turbulent mixing layers [NASA-CR-174640] p 32 N84-25710
- On modeling dilution jet flowfields [NASA-TM-83708] p 32 N84-25713
- Dynamic stress analysis of smooth and notched fiber composite flexural specimens [NASA-TM-83694] p 56 N84-25770
- High voltage solar array models and Shuttle tie charging [AD-P002123] p 177 N84-26209
- ICAN Integrated composites analyzer [NASA-TM-83700] p 56 N84-26755
- Development of Great Lakes algorithms for the Nimbus-G coastal zone color scanner [NASA-CR-173511] p 159 N84-27258
- Progressive fracture of fiber composites [NASA-TM-83701] p 56 N84-27831
- Computer analysis of effects of altering jet fuel properties on refinery costs and yields [NASA-CR-174642] p 91 N84-27908
- An investigation of the transient thermal analysis of spur gears [NASA-TM-83724] p 146 N84-28088
- A computer program for predicting nonlinear uniaxial material responses using viscoplastic models [NASA-TM-83675] p 156 N84-29247

- PURDU-WINCOF. A computer code for establishing the performance of a fan-compressor unit with water ingestion  
[NASA-CR-168005] p 34 N84-29875
- Spectrum/orbit utilization program for geostationary satellites  
[NASA-TM-83759] p 100 N84-30146
- Application of finite element substructuring to composite micromechanics  
[NASA-TM-83729] p 57 N84-31288
- Analytical and experimental investigation of stator endwall countouring in a small axial-flow turbine  
[NASA-TP-2309] p 35 N84-32388
- GCKP84-general chemical kinetics code for gas-phase flow and batch processes including heat transfer effects  
[NASA-TP-2320] p 63 N84-32446
- Manual of phosphoric acid fuel cell power plant cost model and computer program  
[NASA-CR-174720] p 173 N84-34037
- Fracture modes in notched angleply composite laminates  
[NASA-TM-83802] p 58 N84-34576
- COMPUTER STORAGE DEVICES**  
Properties of ferrites important to their friction and wear behavior  
[NASA-TM-83718] p 87 N84-28994
- COMPUTER SYSTEMS DESIGN**  
A scheme for handling arrays in data-flow systems  
[NASA-TM-83972] p 175 N84-39972
- Operating system for a real-time multiprocessor propulsion system simulator  
[NASA-TM-83605] p 177 N84-20258
- COMPUTER SYSTEMS PERFORMANCE**  
Operating system for a real-time multiprocessor propulsion system simulator  
[NASA-TM-83605] p 177 N84-20258
- COMPUTER SYSTEMS PROGRAMS**  
Automatic finite element generators  
[NASA-TM-83695] p 158 N84-31695
- COMPUTERIZED SIMULATION**  
ADA and multi-microprocessor real-time simulation  
[NASA-TM-84-10905] p 176 N84-10905
- Software simulator for multiple computer simulation system  
[NASA-TM-84-11892] p 176 N84-11892
- Comments on some problems in computational penetration mechanics  
[NASA-TM-84-13545] p 150 N84-13545
- Real-time Pegasus propulsion system model V-STOL-piloted simulation evaluation  
[NASA-TM-84-17362] p 15 N84-17362
- Potentials in a plasma over a biased pinhole  
[NASA-TM-84-20711] p 102 N84-20711
- A large-signal dynamic simulation for the series resonant converter  
[NASA-TM-84-23258] p 103 N84-23258
- Transient flow analysis of the AEDC/HPDE MHD generator  
[NASA-TM-84-24049] p 189 N84-24049
- A system for the simulation and evaluation of satellite communication networks  
[AIAA PAPER 84-0680] p 94 N84-25272
- Diffused junction p(+)-n solar cells in bulk GaAs. II - Device characterization and modeling  
[NASA-TM-84-26028] p 161 N84-26028
- New perspectives for advanced automobile diesel engines  
[NASA-TM-84-30062] p 138 N84-30062
- Determination of compressor in-stall characteristics from engine surge transients  
[AIAA PAPER 84-1206] p 18 N84-36959
- Finite element-integral acoustic simulation of JT15D turbofan engine  
[NASA-TM-84-11132] p 182 N84-41132
- Development of dynamic simulation of TF34-GE-100 turbofan engine with post-stall capability  
[AIAA PAPER 84-1184] p 20 N84-44178
- On numerical simulation of viscous flows  
[NASA-TM-84-49112] p 122 N84-49112
- Computer simulator for a mobile telephone system  
[NASA-CR-174533] p 95 N84-10401
- Aeroelastic analysis for propellers - mathematical formulations and program user's manual  
[NASA-CR-3729] p 153 N84-12530
- A system for the simulation and evaluation of satellite communication networks  
[NASA-TM-83531] p 97 N84-13400
- HYTESS A hypothetical turbofan engine simplified simulation  
[NASA-TM-83561] p 26 N84-16184
- A real-time, portable, microcomputer-based jet engine simulator  
[NASA-TM-83550] p 176 N84-16812
- A study of nucleation and growth of thin films by means of computer simulation. General features  
[NASA-TM-83559] p 179 N84-17982
- Parallel processor engine model program  
[NASA-CR-174641] p 27 N84-19353
- Operating system for a real-time multiprocessor propulsion system simulator  
[NASA-TM-83605] p 177 N84-20258
- Determination of compressor in-stall characteristics from engine surge transients  
[NASA-TM-83639] p 29 N84-22566
- Engineering calculations for communications satellite systems planning  
[NASA-CR-173532] p 38 N84-23662
- Users' manual for computer program for three-dimensional analysis of coupler-cavity traveling wave tubes  
[NASA-CR-168269] p 109 N84-23841
- Comparison of free-piston Stirling engine model predictions with RE1000 engine test data  
[NASA-TM-83650] p 195 N84-24509
- Direct simulations of chemically reacting turbulent mixing layers  
[NASA-CR-174640] p 32 N84-25710
- Development of dynamic simulation of TF34-GE-100 turbofan engine with post-stall capability  
[NASA-TM-83660] p 32 N84-25712
- High voltage solar array models and Shuttle tile charging  
[AD-P002123] p 177 N84-26209
- Real-time simulation of an automotive gas turbine using the hybrid computer  
[NASA-TM-83593] p 195 N84-26484
- Evaluation of the effect of crack closure on fatigue crack growth of simulated short cracks  
[NASA-TM-83778] p 75 N84-31348
- Computer simulation of the heavy-duty turbo-compounded diesel cycle for studies of engine efficiency and performance  
[NASA-CR-174755] p 196 N84-33306
- Advanced onboard storage concepts for natural gas-fueled automotive vehicles  
[NASA-CR-174655] p 172 N84-34036
- CONCENTRATORS**  
Optimal design of GaAs-based concentrator space solar cells for 100 AMO, 80 deg C operation  
[NASA-TM-84-29312] p 170 N84-29312
- Development of a 30 percent efficient 3-junction monolithic cascade solar cell  
[NASA-TM-84-29328] p 171 N84-29328
- CONDUCTIVE HEAT TRANSFER**  
Two-region analysis of interface shape in continuous casting with superheated liquid  
[NASA-TM-84-44918] p 139 N84-44918
- Numerical simulation of two-dimensional heat transfer in composite bodies with application to de-icing of aircraft components  
[NASA-CR-168283] p 122 N84-13490
- Thermal stress analysis for a wood composite blade - wind turbines  
[NASA-CR-173994] p 156 N84-21903
- Modeling of zero gravity venting  
[NASA-CR-173503] p 127 N84-23854
- CONFERENCES**  
Symposium (International) on Combustion, 19th, Technion Israel Institute of Technology, Haifa, Israel, August 8-13, 1982, Proceedings  
[NASA-CP-2282] p 59 N84-35401
- Aircraft Electric Secondary Power  
[NASA-CP-2282] p 22 N84-10055
- Detroit space odyssey  
[NASA-TM-85487] p 37 N84-15164
- Cleveland Space Odyssey  
[NASA-TM-85493] p 192 N84-16020
- Chicago Meets Outer Space program  
[NASA-TM-85492] p 192 N84-16021
- Combustion Fundamentals Research  
[NASA-CP-2309] p 27 N84-20525
- Proceedings of the 20th Automotive Technology Development Contractors' Coordination Meeting  
[NASA-CR-173412] p 143 N84-21677
- Assessment of Alternative Aircraft Fuels  
[NASA-CP-2307] p 30 N84-23630
- Technology in the 80's Volume 2. Sessions 5 - 8  
[NASA-CP-2300-VOL-2] p 144 N84-25047
- Space Photovoltaic Research and Technology 1983  
[NASA-CR-173412] p 143 N84-21677
- High Efficiency, Radiation Damage, and Blanket Technology  
[NASA-CP-2314] p 170 N84-29307
- Nonlinear Structural Analysis  
[NASA-CP-2297] p 157 N84-31688
- Fundamentals of Alloy Solidification Applied to Industrial Processes  
[NASA-CP-2337] p 77 N84-34589
- CONFINEMENT**  
Swirl, confinement and nozzle effects on confined turbulent flow  
[AIAA PAPER 84-1377] p 118 N84-35197
- An experimental investigation of gas jets in confined swirling air flow  
[NASA-CR-3832] p 35 N84-33412
- CONICAL NOZZLES**  
Inverted velocity profile semi-annular nozzle jet exhaust noise experiments  
[NASA-TM-83525] p 182 N84-13924
- CONSTITUTIVE EQUATIONS**  
Research and development program for the development of advanced time-temperature dependent constitutive relationships. Volume 1: Theoretical discussion  
[NASA-CR-168191-VOL-1] p 153 N84-10613
- Research and development program for the development of advanced time-temperature dependent constitutive relationships. Volume 2. Programming manual  
[NASA-CR-168191-VOL-2] p 153 N84-10614
- CONTAINERLESS MELTS**  
Gravitational effects in dendritic growth  
[NASA-TM-84-22346] p 37 N84-22346
- CONTAINERS**  
Flame radiation and linear heat transfer in a tubular can combustor  
[AIAA PAPER 84-0443] p 16 N84-21300
- Flame radiation and liner heat transfer in a tubular-can combustor  
[NASA-TM-83538] p 23 N84-13188
- CONTAMINANTS**  
Importance and definition of materials in tribology. Status of understanding  
[NASA-TM-84-23893] p 84 N84-23893
- CONTINUUM MECHANICS**  
Comments on some problems in computational penetration mechanics  
[NASA-TM-84-13545] p 150 N84-13545
- CONTOURS**  
Analytical and experimental investigation of stator endwall countouring in a small axial-flow turbine  
[NASA-TP-2309] p 35 N84-32388
- CONTRACT MANAGEMENT**  
Government - contractor interaction  
[AD-P002768] p 193 N84-23315
- CONTRACTION**  
On the design of contractions and settling chambers for optimal turbulence manipulations in wind tunnels  
[AIAA PAPER 84-0536] p 115 N84-22922
- CONTRACTORS**  
Government - contractor interaction  
[AD-P002768] p 193 N84-23315
- CONTROL SYSTEMS DESIGN**  
The application of LQR synthesis techniques to the turboshaft engine control problem  
[AIAA PAPER 84-1455] p 21 N84-44185
- CONTROL THEORY**  
An application of tensor ideas to nonlinear modeling of a turbofan jet engine  
[NASA-TM-84-42382] p 20 N84-42382
- F100 multivariable control synthesis program. Computer implementation of the F100 multivariable control algorithm  
[NASA-TP-2231] p 22 N84-11171
- Application of advanced control techniques to aircraft propulsion systems  
[NASA-TM-84-20590] p 28 N84-20590
- Acoustic excitation. A promising new means of controlling shear layers  
[NASA-TM-83772] p 10 N84-31096
- CONTROLLERS**  
New propulsion components for electric vehicles  
[NASA-TM-84-30209] p 103 N84-30209
- CONVECTION**  
Preliminary design of two Space Shuttle fluid physics experiments  
[NASA-CR-174649] p 39 N84-23667
- CONVECTIVE HEAT TRANSFER**  
Measurements of local convective heat transfer coefficients on ice accretion shapes  
[AIAA PAPER 84-0018] p 113 N84-17835
- Deposit formation and heat transfer in hydrocarbon rocket fuels  
[AIAA PAPER 84-0512] p 88 N84-18142
- Convective heat transfer studies at high temperatures with pressure gradient for inlet flow Mach number of 0.45  
[AIAA PAPER 84-1487] p 119 N84-35233
- Thermoacoustic convection heat-transfer phenomenon  
[NASA-TM-84-38857] p 120 N84-38857
- Forced convection heat transfer to air/water vapor mixtures  
[NASA-CR-3769] p 123 N84-16488
- Measurement of local convective heat transfer coefficients of four ice accretion shapes  
[NASA-CR-174680] p 10 N84-25646
- CONVERGENCE**  
Acceleration of convergence of vector sequences  
[NASA-TP-2193] p 178 N84-13885
- CONVERGENT-DIVERGENT NOZZLES**  
Experimental investigation of shock-cell noise reduction for dual-stream nozzles in simulated flight comprehensive data report. Volume 1: Test nozzles and acoustic data  
[NASA-CR-168336-VOL-1] p 184 N84-24323
- Experimental investigation of shock-cell noise reduction for dual-stream nozzles in simulated flight comprehensive data report. Volume 2. Laser velocimeter data, static pressures and shadowgraph photos  
[NASA-CR-168336-VOL-2] p 184 N84-24324

- Experimental investigation of shock-cell noise reduction for single-stream nozzles in simulated flight, comprehensive data report. Volume 1: Test nozzles and acoustic data  
[NASA-CR-168234-VOL-1] p 185 N84-33148
- Experimental investigation of shock-cell noise reduction for single-stream nozzles in simulated flight, comprehensive data report. Volume 3: Shadowgraph photos and facility description  
[NASA-CR-168234-VOL-3] p 186 N84-33150
- Supersonic jet shock noise reduction  
[NASA-TM-83799] p 186 N84-35085
- COOLING**
- Shape of porous region to control cooling along curved exit boundary p 115 A84-23591
- Correlation of thermophoretically-modified small particle diffusional deposition rates in forced convection systems with variable properties, transpiration cooling and/or viscous dissipation p 117 A84-32323
- Aerothermal modeling Executive summary  
[NASA-CR-168330] p 25 N84-15152
- Measurement of heat pump processes induced by laser radiation  
[NASA-CR-168324] p 134 N84-18620
- Tip cap for a rotor blade  
[NASA-CASE-LEW-13654-1] p 28 N84-22560
- Combustor liner construction  
[NASA-CASE-LEW-14035-1] p 30 N84-24577
- Qualification testing of solar photovoltaic powered refrigerator freezers for medical use in remote geographic locations  
[NASA-CR-168181] p 169 N84-25162
- Parameter studies of gear cooling using an automatic finites element mesh generator  
[NASA-TM-83721] p 146 N84-28087
- Air modulation apparatus  
[NASA-CASE-LEW-13524-1] p 35 N84-33410
- COOLING SYSTEMS**
- Heat pipe applications in aircraft propulsion  
[AIAA PAPER 84-1269] p 18 A84-37640
- Deposit formation and heat transfer in hydrocarbon rocket fuels  
[NASA-CR-168277] p 45 N84-12225
- Develop and test fuel cell powered on-site integrated total energy systems. Phase 3 Full-scale power plant development  
[NASA-CR-168294] p 164 N84-13672
- Vortex generating flow passage design for increased film cooling effectiveness  
[NASA-CASE-LEW-14039-1] p 126 N84-20782
- Vortex generating flow passage design for increased film-cooling effectiveness and surface coverage -- aircraft engine blade cooling  
[NASA-TM-83617] p 126 N84-22909
- Combustor liner construction  
[NASA-CASE-LEW-14035-1] p 30 N84-24577
- COPOLYMERIZATION**
- Chemical approach for controlling nadimide cure temperature and rate  
[NASA-CASE-LEW-13770-3] p 55 N84-22698
- Chemical approach for controlling nadimide cure temperature and rate  
[NASA-CASE-LEW-13770-4] p 55 N84-22699
- Chemical approach for controlling nadimide cure temperature and rate  
[NASA-CASE-LEW-13770-5] p 55 N84-22700
- Chemical approach for controlling nadimide cure temperature and rate  
[NASA-CASE-LEW-13770-6] p 55 N84-22701
- Chemical approach for controlling nadimide cure temperature and rate  
[NASA-CASE-LEW-13770-1] p 86 N84-27885
- COPPER**
- Matrix effects in ion-induced emission as observed in Ne collisions with Cu-Mg and Cu-Al alloys  
[NASA-TM-83061] p 187 N84-10923
- Secondary electron emission characteristics of ion-textured copper and high-purity isotropic graphite surfaces  
[NASA-TP-2342] p 86 N84-28989
- COPPER ALLOYS**
- Status of understanding for gear materials p 144 N84-25061
- COPPER CHLORIDES**
- Electronic properties of carbon fibers intercalated with copper chloride p 104 A84-34521
- COROLLIS EFFECT**
- Forced vibration analysis of rotating cyclic structures in NASTRAN  
[NASA-CR-165429] p 153 N84-11514
- CORRELATION**
- Ground correlation investigation of thruster spacecraft interactions to be measured on the IAPS flight test  
[NASA-TM-83598] p 47 N84-23691
- CORROSION**
- Reaction of cobalt in SO<sub>2</sub> atmospheres at elevated temperatures p 65 A84-33440
- Thermal oxidative degradation reactions of perfluoroalkethers  
[NASA-CR-168224] p 60 N84-11229
- Mechanism of corrosion of Ni base superalloys by molten Na<sub>2</sub>MoO<sub>4</sub> at elevated temperatures  
[NASA-TM-83580] p 70 N84-20672
- Friction and wear of iron in sulfuric acid  
[NASA-TP-2289] p 71 N84-21716
- Friction and wear of nickel in sulfuric acid  
[NASA-TP-2290] p 72 N84-21721
- Interaction of sulfuric acid corrosion and mechanical wear of iron  
[NASA-TM-83717] p 73 N84-27857
- Advanced high temperature materials for the energy efficient automotive Stirling engine  
[NASA-TM-83659] p 75 N84-28963
- CORROSION PREVENTION**
- Overlay coating degradation by simultaneous oxidation and coating/substrate interdiffusion  
[NASA-TM-83738] p 75 N84-31344
- CORROSION RESISTANCE**
- Hostile environmental conditions facing candidate alloys for the automotive Stirling engine p 136 A84-23522
- Oxidation and corrosion resistance of candidate Stirling engine heater-head-tube alloys  
[NASA-TM-83609] p 74 N84-28962
- CORROSION TESTS**
- Effects of alloy composition on cyclic flame hot-corrosion attack of cast nickel-base superalloys at 900 deg C  
[NASA-TP-2338] p 73 N84-26783
- COST ANALYSIS**
- Study to establish cost projections for production of Redox chemicals  
[NASA-CR-167881] p 164 N84-11580
- Communications network design and costing model technical manual  
[NASA-CR-168236] p 97 N84-14376
- Communications network design and costing model programmers manual  
[NASA-CR-168237] p 97 N84-14377
- Communications network design and costing model users manual  
[NASA-CR-168238] p 97 N84-14378
- Status of understanding for gear materials p 144 N84-25061
- Energy efficient engine component development and integration program  
[NASA-CR-173884] p 35 N84-32389
- COST EFFECTIVENESS**
- High speed, low cost, LEO-thermal-cycling facility p 171 N84-29340
- COST ESTIMATES**
- Trends of jet fuel demand and properties p 90 N84-23631
- Computer analysis of effects of altering jet fuel properties on refinery costs and yields  
[NASA-CR-174642] p 91 N84-27908
- Manual of phosphoric acid fuel cell power plant cost model and computer program  
[NASA-CR-174720] p 173 N84-34037
- Cogeneration Technology Alternatives Study (CTAS) Volume 2: Comparison and evaluation of results  
[NASA-TM-81401] p 173 N84-34038
- COST REDUCTION**
- Determination of the key parameters affecting historic communications satellite trends  
[NASA-TM-83633] p 99 N84-25908
- Wind turbine generator interaction with conventional diesel generators on Block Island, Rhode Island. Volume 2: Data analysis  
[NASA-CR-168319] p 172 N84-31783
- COUNTER ROTATION**
- Feasibility analysis of a spiral groove ring seal for counter-rotating shafts p 139 A84-45965
- Technology and benefits of aircraft counter rotation propellers  
[NASA-CR-168258] p 22 N84-13186
- COUNTER-ROTATING WHEELS**
- Precision of spiral-bevel gears  
[ASME PAPER 82-WA/DE-33] p 135 A84-15950
- COUPLED MODES**
- Vibration and flutter of mistuned bladed-disk assemblies  
[NASA-TM-83634] p 156 N84-23923
- COUPLING**
- Effects of structural coupling on mistuned cascade flutter and response  
[ASME PAPER 83-GT-117] p 151 A84-33701
- Radiating dipole model of interference induced in spacecraft circuitry by surface discharges  
[NASA-TP-2240] p 40 N84-16247
- Basic experimental study of the coupling between flow instabilities and incident sound  
[NASA-CR-3789] p 163 N84-21275
- Dilute plasma coupling currents to a high voltage solar array in weak magnetic fields  
[NASA-TM-83687] p 47 N84-24708
- COVERINGS**
- Solar-array-materials passive LDEF experiment (A0171) p 168 N84-24656
- CRACK GEOMETRY**
- Effect of crack curvature on stress intensity factors for ASTM standard compact tension specimens  
[NASA-CR-168280] p 153 N84-11513
- Crack layer theory  
[NASA-CR-174634] p 156 N84-22980
- CRACK INITIATION**
- Creep fatigue of low-cobalt superalloys. Waspalloy, PM U 700 and wrought U 700  
[NASA-CR-168260] p 67 N84-13265
- Literature survey on oxidations and fatigue lives at elevated temperatures  
[NASA-CR-174639] p 71 N84-20674
- Crack layer theory  
[NASA-CR-174634] p 156 N84-22980
- Crack tip field and fatigue crack growth in general yielding and low cycle fatigue  
[NASA-CR-174686] p 76 N84-32503
- CRACK PROPAGATION**
- The effect of microstructure on 650 C fatigue crack growth in P/M Astroloy p 63 A84-12395
- The effects of frequency and hold times on fatigue crack propagation rates in a nickel base superalloy p 64 A84-18733
- Elevated temperature compressive steady state deformation and failure in the oxide dispersion strengthened alloy MA 6000E p 66 A84-46785
- Fatigue crack growth and low cycle fatigue of two nickel base superalloys  
[NASA-CR-174634] p 66 N84-10267
- A total life prediction model for stress concentration sites  
[NASA-CR-168225] p 152 N84-10612
- Crack layer theory  
[NASA-CR-174634] p 156 N84-22980
- Mode 2 fatigue crack growth specimen development  
[NASA-TM-83722] p 156 N84-29248
- Failure analysis of plasma-sprayed thermal barrier coatings  
[NASA-TM-83777] p 75 N84-31347
- Evaluation of the effect of crack closure on fatigue crack growth of simulated short cracks  
[NASA-TM-83778] p 75 N84-31348
- Inelastic and dynamic fracture and stress analyses p 158 N84-31697
- Crack tip field and fatigue crack growth in general yielding and low cycle fatigue  
[NASA-CR-174686] p 76 N84-32503
- On stress analysis of a crack-layer  
[NASA-CR-174774] p 159 N84-34774
- CRACK TIPS**
- Crack tip field and fatigue crack growth in general yielding and low cycle fatigue  
[NASA-CR-174686] p 76 N84-32503
- CRACKING (FRACTURING)**
- Crack layer theory  
[NASA-CR-174634] p 156 N84-22980
- Materials for Advanced Turbine Engines (MATE) Project 3: Design, fabrication and evaluation of an oxide dispersion strengthened sheet alloy combustor liner, volume 1  
[NASA-CR-174691] p 76 N84-32504
- CRACKS**
- Analysis of an internally radially cracked ring segment subject to three-point radial loading p 150 A84-18691
- Wide range weight functions for the strip with a single edge crack  
[NASA-TM-83478] p 153 N84-11512
- On stress analysis of a crack-layer  
[NASA-CR-174774] p 159 N84-34774
- CREEP ANALYSIS**
- Tensile and compressive constitutive response of 316 stainless steel at elevated temperatures  
[NASA-TM-83506] p 68 N84-15249
- The role of cobalt on the creep of Waspalloy  
[NASA-CR-174628] p 70 N84-19523
- CREEP BUCKLING**
- Algorithms for elasto-plastic-creep postbuckling p 152 A84-38480
- CREEP PROPERTIES**
- The effect of annealing on the creep of plasma-sprayed ceramics p 79 A84-19785
- A simple application of the Bailey-Orowan creep model to Fe-39.8 at pct Al and gamma/gamma prime - alpha p 64 A84-22012

Fatigue crack growth and low cycle fatigue of two nickel base superalloys  
[NASA-CR-174534] p 66 N84-10267

Low strain, long life creep fatigue of AF2-1DA and INCO 718  
[NASA-CR-167989] p 66 N84-10268

Research and development program for the development of advanced time-temperature dependent constitutive relationships. Volume 2 Programming manual  
[NASA-CR-166191-VOL-2] p 153 N84-10614

Creep fatigue of low-cobalt superalloys Waspalloy, PM U 700 and wrought U 700  
[NASA-CR-168260] p 67 N84-13265

Tensile and compressive constitutive response of 316 stainless steel at elevated temperatures  
[NASA-TM-83506] p 68 N84-15249

Factors which influence directional coarsening of Gamma prime during creep in nickel-base superalloy single crystals  
[NASA-TM-83595] p 69 N84-17353

Influence of composition on the microstructure and mechanical properties of a nickel-base superalloy single crystal  
[NASA-TM-83563] p 70 N84-17354

Development of a simplified procedure for rocket engine thrust chamber life prediction with creep  
[NASA-CR-168261] p 46 N84-19472

Creep-rupture behavior of candidate Stirling engine iron superalloys in high-pressure hydrogen Volume 2 Hydrogen creep-rupture behavior  
[NASA-CR-174705] p 74 N84-28961

Advanced high temperature materials for the energy efficient automotive Stirling engine  
[NASA-TM-83659] p 75 N84-28963

Oxygen diffusion in alpha-Al<sub>2</sub>O<sub>3</sub>  
[NASA-TM-83622] p 86 N84-28990

**CREEP RUPTURE STRENGTH**

Hostile environmental conditions facing candidate alloys for the automotive Stirling engine p 136 A84-23522

Creep-rupture behavior of six candidate Stirling engine superalloys tested in air p 65 A84-36173

Creep-rupture reliability analysis  
[NASA-CR-3790] p 155 N84-19925

Creep-rupture behavior of candidate Stirling engine alloys after long-term aging at 760 deg C in low-pressure hydrogen  
[NASA-TM-83676] p 73 N84-25793

**CRITICAL TEMPERATURE**

Turbidity very near the critical point of methanol-cyclohexane mixtures p 192 A84-30391

**CROSS CORRELATION**

Ultrasonic velocity measurement using phase-slope cross-correlation methods  
[NASA-TM-83794] p 149 N84-34769

**CROSS FLOW**

Heat transfer distributions around nominal ice accretion shapes formed on a cylinder in the NASA Lewis icing research tunnel  
[NASA-TM-83557] p 123 N84-14463

Free stream turbulence and density ratio effects on the interaction region of a jet in a cross flow p 125 N84-20546

**CROSSLINKING**

Plasma polymerized high energy density dielectric films for capacitors  
[NASA-CR-168233] p 81 N84-13310

Chemical approach for controlling nadimide cure temperature and rate  
[NASA-CASE-LEW-13770-3] p 55 N84-22698

Chemical approach for controlling nadimide cure temperature and rate  
[NASA-CASE-LEW-13770-4] p 55 N84-22699

Chemical approach for controlling nadimide cure temperature and rate  
[NASA-CASE-LEW-13770-5] p 55 N84-22700

Chemical approach for controlling nadimide cure temperature and rate  
[NASA-CASE-LEW-13770-6] p 55 N84-22701

Kinetics of chromium ion absorption by cross-linked polyacrylate films  
[NASA-TM-83661] p 50 N84-23693

**CRUDE OIL**

Assessment of Alternative Aircraft Fuels  
[NASA-CP-2307] p 30 N84-23630

**CRUISE MISSILES**

Application of in-flight thrust determination uncertainty  
[SAE PAPER 831439] p 13 A84-29453

**CRYOGENIC EQUIPMENT**

Design study of magnetic eddy-current vibration suppression dampers for application to cryogenic turbomachinery  
[NASA-CR-173273] p 141 N84-16562

**CRYOGENIC FLUID STORAGE**

Cryogenic Fluid Management Facility  
[AIAA PAPER 84-1340] p 44 A84-44184

Cryogenic Fluid Management Experiment (CFME) trunnion verification testing  
[NASA-CR-168310] p 92 N84-16381

Evaluation of propellant tank insulation concepts for low-thrust chemical propulsion systems: Executive summary  
[NASA-CR-168321] p 83 N84-20699

**CRYOGENIC FLUIDS**

On-orbit cryogenic fluid transfer  
[AIAA PAPER 84-1343] p 44 A84-44176

On-orbit cryogenic fluid transfer  
[NASA-TM-83688] p 39 N84-25753

**CRYOGENIC ROCKET PROPELLANTS**

Vapor flow into a capillary propellant-acquisition device  
[AIAA PAPER 84-1344] p 121 A84-40243

Computational modeling of jet induced mixing of cryogenic propellants in low-G  
[NASA-TM-83703] p 127 N84-25000

**CRYOGENICS**

Study of a LH<sub>2</sub>-fueled topping cycle engine for aircraft propulsion  
[AIAA PAPER 83-2543] p 15 A84-15207

Select fiber composites for space applications. A mechanistic assessment  
[NASA-TM-83631] p 55 N84-22702

**CRYSTAL DEFECTS**

Interaction between boron and intrinsic defects in GaAs p 190 A84-33918

Cell and defect behavior in lithium-counterdoped solar cells p 170 N84-29322

**CRYSTAL DISLOCATIONS**

The structure of extruded NiAl p 65 A84-36047

**CRYSTAL GROWTH**

Gravitational effects in dendritic growth  
[NASA-CR-174634] p 37 A84-22346

Free dendritic growth p 190 A84-42829

Thermal oxidation of 3C silicon carbide single-crystal layers on silicon p 191 A84-49620

Characteristic morphological and functional changes in sputtered MoS<sub>2</sub>/sub 2 films  
[NASA-TM-83565] p 92 N84-16380

Fundamentals of Alloy Solidification Applied to Industrial Processes  
[NASA-CP-2337] p 77 N84-34589

**CRYSTAL LATTICES**

Development of a 30 percent efficient 3-junction monolithic cascade solar cell p 171 N84-29328

**CRYSTAL STRUCTURE**

Surfaces — characterization of surface properties for predicting bond quality p 50 A84-10680

Frictional and morphological properties of Au-MoS<sub>2</sub> films sputtered from a compact target  
[NASA-TM-83604] p 143 N84-20858

Effect of substrate chemical pretreatment on the tribological properties of graphite films  
[NASA-TM-83574] p 85 N84-25831

Characterization of erosion of metallic materials under cavitation attack in a mineral oil  
[NASA-TP-2368] p 147 N84-32825

**CRYSTALLIZATION**

Mechanical contact induced transformation from the amorphous to the crystalline state in metallic glass  
[NASA-TM-83583] p 71 N84-20673

Transport processes in dendritic crystallization p 191 N84-28621

**CRYSTALLOGRAPHY**

Considerations in friction and wear p 144 N84-23903

**CURING**

Chemical approach for controlling nadimide cure temperature and rate  
[NASA-CASE-LEW-13770-3] p 55 N84-22698

Chemical approach for controlling nadimide cure temperature and rate  
[NASA-CASE-LEW-13770-4] p 55 N84-22699

Chemical approach for controlling nadimide cure temperature and rate  
[NASA-CASE-LEW-13770-5] p 55 N84-22700

Chemical approach for controlling nadimide cure temperature and rate  
[NASA-CASE-LEW-13770-6] p 55 N84-22701

Kinetics of chromium ion absorption by cross-linked polyacrylate films  
[NASA-TM-83661] p 50 N84-23693

**CURRENT REGULATORS**

Input filter compensation for switching regulators  
[NASA-CR-173557] p 110 N84-24975

**CURVES (GEOMETRY)**

Precision of spiral-bevel gears  
[ASME PAPER 82-WA/DE-33] p 135 A84-15950

**CUTTERS**

A review of the use of wear-resistant coatings in the cutting-tool industry  
[NASA-TM-83512] p 81 N84-11295

**CYCLIC LOADS**

Benchmark cyclic plastic notch strain measurements  
[NASA-TM-83722] p 63 A84-11194

Development of a simplified procedure for cyclic structural analysis  
[NASA-TP-2243] p 155 N84-20878

Mode 2 fatigue crack growth specimen development  
[NASA-TM-83756] p 156 N84-29248

Cyclic torsion testing  
[NASA-TM-83756] p 157 N84-31687

**CYCLOHEXANE**

Turbidity very near the critical point of methanol-cyclohexane mixtures p 192 A84-30391

**CYLINDERS**

Heat transfer distributions around nominal ice accretion shapes formed on a cylinder in the NASA Lewis Icing Research Tunnel  
[AIAA PAPER 84-0017] p 113 A84-17834

**CYLINDRICAL BODIES**

Heat transfer distributions around nominal ice accretion shapes formed on a cylinder in the NASA Lewis icing research tunnel  
[NASA-TM-83557] p 123 N84-14463

Effects of unsteady free stream velocity and free stream turbulence on stagnation point heat transfer  
[NASA-CR-3804] p 127 N84-25943

**CZOCHRALSKI METHOD**

Interaction between boron and intrinsic defects in GaAs p 190 A84-33918

LEC GaAs for integrated circuit applications  
[NASA-CR-173267] p 191 N84-17014

**D**

**DAMAGE ASSESSMENT**

Crack layer theory  
[NASA-CR-174634] p 156 N84-22980

**DAMPERS (VALVES)**

Experimental study of uncentralized squeeze film dampers  
[NASA-CR-168317] p 155 N84-19927

**DAMPING**

Dual clearance squeeze film damper  
[NASA-CASE-LEW-13506-1] p 29 N84-22562

**DATA ACQUISITION**

Free stream turbulence and density ratio effects on the interaction region of a jet in a cross flow p 125 N84-20546

Climatology of ozone at altitudes from 19,000 at 59,000 feet based on combined GASP and ozonesonde data  
[NASA-TP-2303] p 174 N84-31865

**DATA COMPRESSION**

NTSC composite video at 1.6 bits/pel p 95 A84-49259

**DATA CORRELATION**

Creep-rupture reliability analysis  
[NASA-CR-3790] p 155 N84-19925

Climatology of ozone at altitudes from 19,000 at 59,000 feet based on combined GASP and ozonesonde data  
[NASA-TP-2303] p 174 N84-31865

**DATA FLOW ANALYSIS**

A scheme for handling arrays in data-flow systems p 175 A84-39972

Dataflow computing approach in high-speed digital simulation  
[NASA-CR-173552] p 176 N84-25336

**DATA PROCESSING**

Review of the DOE/NASA wind turbine engineering information system p 163 A84-33766

Determination of the key parameters affecting historic communications satellite trends  
[NASA-TM-83633] p 99 N84-25908

**DATA SAMPLING**

Output statistics of laser anemometers in sparsely seeded flows p 117 A84-28738

**DATA STRUCTURES**

A scheme for handling arrays in data-flow systems p 175 A84-39972

**DATA SYSTEMS**

Dataflow computing approach in high-speed digital simulation  
[NASA-CR-173552] p 176 N84-25336

**DATA TRANSMISSION**

A comparison of the domestic satellite communications forecast to the year 2000  
[NASA-TM-83516] p 96 N84-10405

**DEBRIS**

Particulate erosion mechanisms  
[NASA-TM-83551] p 68 N84-14289



- DEFECTS**  
Radiation damage and defect behavior in ion-implanted, lithium counterdoped silicon solar cells  
[NASA-TM-83646] p 109 N84-22890  
The impact resistance of SiC and other mechanical properties of SiC and Si3N4  
[NASA-CR-185925] p 84 N84-24809
- DEFLAGRATION**  
Self-similar blast waves incorporating deflagrations of variable speed p 116 A84-28379
- DEFLECTION**  
A linear aerodynamic analysis for unsteady transonic cascades  
[NASA-CR-3833] p 11 N84-32355
- DEFORMATION**  
On the suppression of zero energy deformation modes p 150 A84-21541  
Friction and morphology of magnetic tapes in sliding contact with nickel-zinc ferrite  
[NASA-TP-2267] p 82 N84-16334  
Inelastic and dynamic fracture and stress analyses p 158 N84-31697
- DEGRADATION**  
Thermal oxidative degradation reactions of perfluoroketones  
[NASA-CR-168224] p 60 N84-11229  
Results of an experimental program investigating the effects of simulated ice on the performance of the NACA 63A415 airfoil with flap  
[NASA-CR-168288] p 8 N84-16145  
Laboratory degradation of Kapton in a low energy oxygen ion beam  
[NASA-TM-83530] p 41 N84-18310  
Cathode degradation and erosion in high pressure arc discharges  
[NASA-TM-83638] p 47 N84-22631  
Ion-beam-textured and coated surfaces experiment (S1003) p 84 N84-24650  
Interply layer degradation effects on composite structural response  
[NASA-TM-83702] p 56 N84-26756  
Radiation tolerance of low resistivity, high voltage silicon solar cells p 170 N84-29318  
Effects of water-vapor on friction and deformation of polymeric magnetic media in contact with a ceramic oxide  
[NASA-TM-83727] p 87 N84-30072  
The energy dependence and surface morphology of Kapton (trademark) degradation under atomic oxygen bombardment p 187 N84-34484
- DEICERS**  
Flight and wind tunnel tests of an electro-impulse de-icing system  
[AIAA PAPER 84-2234] p 12 A84-39280  
Piezoelectric deicing device  
[NASA-CASE-LEW-13773-2] p 133 N84-32782
- DEICING**  
Numerical simulation of two-dimensional heat transfer in composite bodies with application to de-icing of aircraft components  
[NASA-CR-168283] p 122 N84-13490
- DELAMINATING**  
Edge delamination in angle-ply composite laminates p 52 A84-21515  
Interply layer degradation effects on composite structural response  
[NASA-TM-83702] p 56 N84-26756
- DEMAND (ECONOMICS)**  
Trends of jet fuel demand and properties p 90 N84-23631
- DENDRITIC CRYSTALS**  
Gravitational effects in dendritic growth p 37 A84-22346  
Free dendritic growth p 190 A84-42829  
Some fundamental aspects of solidification in a supercooled melt p 73 N84-26787  
Transport processes in dendritic crystallization p 191 N84-28621
- DENSITY (MASS/VOLUME)**  
Consolidation of Si3N4 without additives (by hot isostatic pressing)  
[NASA-CR-173279] p 82 N84-17389
- DENSITY MEASUREMENT**  
Time-resolved density measurements in premixed turbulent flames p 59 A84-32612
- DEPOSITION**  
Experimental and theoretical deposition rates from salt-seeded combustion gases of a Mach 0.3 burner rig  
[NASA-TP-2225] p 124 N84-19741  
Diamondlike flake composites  
[NASA-CASE-LEW-13837-1] p 54 N84-22695  
Status of plasma physics techniques for the deposition of tribological coatings p 190 N84-25058  
Deposition of diamondlike carbon films  
[NASA-CASE-LEW-14080-1] p 86 N84-28986
- Dual ion beam deposition of carbon films with diamondlike properties  
[NASA-TM-83743] p 110 N84-31512
- DEPOSITS**  
Deposit formation and heat transfer in hydrocarbon rocket fuels  
[NASA-CR-168277] p 45 N84-12225  
Emission FTIR analyses of thin microscopic patches of jet fuel residue deposited on heated metal surface  
[NASA-CR-168331] p 90 N84-17410  
FTIR analysis of aviation fuel deposits  
[NASA-TM-83773] p 92 N84-33608
- DEPTH MEASUREMENT**  
The X-ray photoelectron spectroscopy depth profiling and tribological characterization of ion-plated gold on various metals p 50 A84-20465
- DESIGN**  
AFB/open cycle gas turbine conceptual design study  
[NASA-CR-168135] p 172 N84-31784
- DESIGN ANALYSIS**  
Design analysis of Rayleigh-step floating-ring seals  
[ASLE PREPRINT 83-LC-3B-2] p 137 A84-28989  
Development of a large scale bipolar NiH2 battery p 162 A84-30189  
Energy efficient engine. Flight propulsion system, preliminary analysis and design update  
[NASA-CR-167980] p 22 N84-11170  
Size scale effect in cavitation erosion  
[NASA-TM-83533] p 87 N84-11254  
Design and performance of a fixed, nonaccelerating, guide vane cascade that operates over an inlet flow angle range of 60 deg  
[NASA-TM-83519] p 8 N84-14120  
Double-injection, deep-impunity switch development  
[NASA-CR-168335] p 108 N84-18536  
A 37.5-kW point design comparison of the nickel-cadmium battery, bipolar nickel-hydrogen battery, and regenerative hydrogen-oxygen fuel cell energy storage subsystems for low Earth orbit  
[NASA-TM-83651] p 167 N84-23022  
Advanced designs for IPV nickel-hydrogen cells  
[NASA-TM-83643] p 168 N84-23025  
Contingency power concepts for helicopter turboshaft engine  
[NASA-TM-83679] p 30 N84-23648  
Design considerations for a monolithic, GaAs, dual-mode, QPSK/QASK, high-throughput rate transceiver  
[NASA-CR-173560] p 110 N84-24974  
Factors that affect the fatigue strength of power transmission shafting  
[NASA-TM-83608] p 145 N84-26029  
Optimal design of GaAs-based concentrator space solar cells for 100 AMO, 80 deg C operation p 170 N84-29312  
Plasmon device design: Conversion from surface to junction plasmons with grating-couplers p 171 N84-29330  
Reflector antennas with low sidelobes, low cross polarization, and high aperture efficiency  
[NASA-CR-174670] p 100 N84-31464  
Energy efficient engine component development and integration program  
[NASA-CR-173884] p 35 N84-32389  
A high energy stage for the National Space Transportation System  
[NASA-TM-83795] p 38 N84-32411  
Preliminary design of a 10-kW thermophotovoltaic system for space applications p 49 N84-32427  
Characteristics and capacities of the NASA Lewis Research Center high precision 6.7- by 6.7-m planar near-field scanner  
[NASA-TM-83785] p 133 N84-32789
- DESORPTION**  
Correlation of electron emission with changes in the surface concentration of barium and oxygen on a tungsten surface p 60 A84-45917
- DETECTION**  
Sensor failure detection for jet engines using analytical redundancy  
[NASA-TM-83695] p 31 N84-24585
- DETONATION WAVES**  
Self-similar blast waves incorporating deflagrations of variable speed p 116 A84-28379  
Detonation wave augmentation of gas turbines  
[AIAA PAPER 84-1266] p 18 A84-37639
- DEVELOPING NATIONS**  
The worldwide market for photovoltaics in the rural sector p 161 A84-23185
- DEVIATION**  
Secondary flow spanwise deviation model for the stators of NASA middle compressor stages  
[NASA-CR-173360] p 27 N84-18202
- DIAMINES**  
Polyimides formulated from a partially fluorinated diamine for aerospace tribological applications p 80 A84-40594
- DIAMONDS**  
Study of the Auger line shape of polyethylene and diamond p 190 A84-40600
- DIELECTRIC PROPERTIES**  
K-band latching switches  
[NASA-CR-168253] p 109 N84-24973
- DIELECTRICS**  
Material considerations for high frequency, high power capacitors p 102 A84-22874  
Interference phenomena in the refraction of a surface plasmon by vertical dielectric barriers p 179 A84-24410  
Deposition of diamondlike carbon films  
[NASA-CASE-LEW-14080-1] p 86 N84-28986  
Wave attenuation and mode dispersion in a waveguide coated with lossy dielectric material  
[NASA-CR-173820] p 100 N84-30145
- DIESEL ENGINES**  
New perspectives for advanced automobile diesel engines p 138 A84-30082  
An overview of NASA intermittent combustion engine research  
[AIAA PAPER 84-1393] p 19 A84-40244  
Catalog of selected heavy duty transport energy management models  
[NASA-CR-168299] p 194 N84-14991  
An overview of NASA intermittent combustion engine research  
[NASA-TM-83668] p 31 N84-24583  
Utilization of alternative fuels in diesel engines  
[NASA-CR-174669] p 91 N84-26813  
Development of carbon slurry fuels for transportation (hybrid fuels, phase 2)  
[NASA-CR-174659] p 74 N84-28960  
Wind turbine generator interaction with conventional diesel generators on Block Island, Rhode Island Volume 1: Executive summary  
[NASA-CR-168318] p 171 N84-29357  
An RC-1 organic Rankine bottoming cycle for an adiabatic diesel engine  
[NASA-CR-168256] p 196 N84-32306  
Waste heat recovery from adiabatic diesel engines by exhaust-driven Brayton cycles  
[NASA-CR-168257] p 196 N84-32307  
Steam bottoming cycle for an adiabatic diesel engine  
[NASA-CR-168255] p 196 N84-33304  
Computer simulation of the heavy-duty turbo-compounded diesel cycle for studies of engine efficiency and performance  
[NASA-CR-174755] p 196 N84-33306  
Diesel engine catalytic combustor system — aircraft engines  
[NASA-CASE-LEW-12395-1] p 148 N84-33808  
Baseline performance and emissions data for a single-cylinder, direct-injected diesel engine  
[NASA-TM-86873] p 197 N84-34330  
Evaluation of candidate Stirling engine heater tube alloys after 3500 hours exposure to high pressure doped hydrogen or helium  
[NASA-TM-83782] p 77 N84-34603
- DIESEL FUELS**  
Utilization of alternative fuels in diesel engines  
[NASA-CR-174669] p 91 N84-26813
- DIFFERENTIAL EQUATIONS**  
Exponential-fitted methods for integrating stiff systems of ordinary differential equations. Applications to homogeneous gas-phase chemical kinetics p 179 N84-31279  
A comparison of the efficiency of numerical methods for integrating chemical kinetic rate equations p 49 N84-31280
- DIFFRACTION PATTERNS**  
Optimization of fringe-type laser anemometers for turbine engine component testing  
[AIAA PAPER 84-1459] p 131 A84-40248  
Ion-beam nitriding of steels  
[NASA-TM-83599] p 71 N84-21719  
Optimization of fringe-type laser anemometers for turbine engine component testing  
[NASA-TM-83658] p 133 N84-25019
- DIFFUSION**  
Double-injection, deep-impunity switch development  
[NASA-CR-168335] p 108 N84-18536  
The effect of diffusion induced lattice stress on the open-circuit voltage in silicon solar cells  
[NASA-TM-83667] p 168 N84-23027  
Oxygen diffusion in alpha-Al2O3  
[NASA-TM-83622] p 86 N84-28990  
Overlay coating degradation by simultaneous oxidation and coating/substrate interdiffusion  
[NASA-TM-83798] p 75 N84-31344



**DIFFUSION FLAMES**

- Calculations of turbulent mass transport in a bluff-body diffusion-flame combustor [AIAA PAPER 84-0372] p 114 A84-18048
- Analytic modeling of a spray diffusion flame [AIAA PAPER 84-1317] p 118 A84-35168
- Numerical solution for the problem of flame propagation by the random element method p 60 A84-48139
- Combustor flame flashback p 62 N84-20561

**DIFFUSION THEORY**

- Random element method for numerical modeling of diffusional processes p 119 A84-35318

**DIGITAL COMPUTERS**

- Digital computer program for generating dynamic turbofan engine models (DIGTEM) [NASA-TM-83446] p 26 N84-16185

**DIGITAL FILTERS**

- Input filter compensation for switching regulators [NASA-CR-173247] p 107 N84-16459

**DIGITAL SIMULATION**

- Parallelism and pipelining in high-speed digital simulators p 175 A84-11876
- NASCAP simulations of spacecraft charging of the SCATHA satellite — NASA (spacecraft) charging analyzer program (NASCAP) p 41 N84-17268
- Dataflow computing approach in high-speed digital simulation [NASA-CR-173552] p 176 N84-25336

**DIGITAL SYSTEMS**

- Interference performance analysis of M-ary CPSK and M-ary CAPK digital transmission systems and the computation of 'required isolation' for efficient utilization of geostationary satellite orbit/spectrum p 95 A84-49303
- Fiberoptics for propulsion control system [NASA-TM-83542] p 1 N84-14111

**DIGITAL TECHNIQUES**

- Input-output characterization of an ultrasonic testing system by digital signal analysis [NASA-CR-3756] p 149 N84-15565
- Digital computer program for generating dynamic turbofan engine models (DIGTEM) [NASA-TM-83446] p 26 N84-16185
- Lewis Research Center spin ring and its use in vibration analysis of rotating systems [NASA-TP-2304] p 30 N84-24578

**DILUTION**

- On modeling dilution jet flowfields [AIAA PAPER 84-1379] p 121 A84-44183
- Modeling of dilution jet flowfields p 126 N84-20547
- On modeling dilution jet flowfields [NASA-TM-83708] p 32 N84-25713
- Dilution jet mixing program [NASA-CR-174624] p 33 N84-26702

**DIMENSIONS**

- Length to diameter ratio and row number effects in short pin fin heat transfer [ASME PAPER 83-GT-54] p 118 A84-33706

**DIODES**

- High voltage-high power components for large space power distribution systems [NASA-TM-83648] p 42 N84-22615

**DIRECT CURRENT**

- Improved transistor-controlled and commutated brushless DC motors for electric vehicle propulsion [NASA-CR-168053] p 105 N84-10450
- Development of a DC propulsion system for an electric vehicle [NASA-CR-168306] p 166 N84-20014
- Solar photovoltaic powered refrigerators/freezers for medical use in remote geographic locations [NASA-CR-168268] p 169 N84-25163

**DIRECTIONAL SOLIDIFICATION (CRYSTALS)**

- Two-region analysis of interface shape in continuous casting with superheated liquid p 139 A84-44918

**DISCONTINUITY**

- Monolithic microwave integrated circuit devices for active array antennas [NASA-CR-173981] p 112 N84-34675

**DISKS (SHAPES)**

- Low strain, long life creep fatigue of AF2-1DA and INCO 718 [NASA-CR-167889] p 66 N84-10268
- NASTRAN documentation for flutter analysis of advanced turbopropellers [NASA-CR-167927] p 25 N84-15153

**DISPERSING**

- A theoretical and experimental study of turbulent evaporating sprays [NASA-CR-174760] p 35 N84-32390

**DISPLACEMENT**

- Analysis of an internally radially cracked ring segment subject to three-point radial loading p 150 A84-18691
- Measurements of self-excited rotor-blade vibrations using optical displacements [ASME PAPER 83-GT-132] p 151 A84-33702

- A blade loss response spectrum for flexible rotor systems [ASME PAPER 84-GT-29] p 139 A84-46893

- Theoretical and software considerations for nonlinear dynamic analysis [NASA-CR-174504] p 154 N84-15589

- Nonlinear displacement analysis of advanced propeller structures using NASTRAN [NASA-TM-83737] p 157 N84-31683

**DISSIPATION**

- Correlation of thermophoretically-modified small particle diffusional deposition rates in forced convection systems with variable properties, transpiration-cooling and/or viscous dissipation p 117 A84-32323

**DISSOCIATION**

- Homogeneous reactions of hydrocarbons, silane, and chlorosilanes in radiofrequency plasmas at low pressures [NASA-TP-2301] p 50 N84-20643

**DISTORTION**

- Response of a small-turboshaft-engine compression system to inlet temperature distortion [NASA-TM-83765] p 36 N84-33414

**DISTRIBUTED AMPLIFIERS**

- 0.5 W 2-21 GHz monolithic GaAs distributed amplifier p 103 A84-30857

**DOMESTIC SATELLITE COMMUNICATIONS SYSTEMS**

- Multibeam antenna for 30/20 GHz advanced communications satellite using offset shaped, dual reflector surfaces p 93 A84-15627
- A frequency-division multiple-access system concept for 30/20 GHz high-capacity domestic satellite service p 94 A84-22141
- ACTS TDMA network control — Advanced Communication Technology Satellite [AIAA PAPER 84-0682] p 94 A84-25274

**DOPED CRYSTALS**

- Analysis of grain boundary phase devitrification of Y2O3- and Al2O3-doped Si3N4 p 79 A84-19782
- Increased radiation resistance in lithium-counterdoped silicon solar cells p 163 A84-34846
- Development and fabrication of a high current, fast recovery power diode [NASA-CR-168196] p 106 N84-13443
- Cell and defect behavior in lithium-counterdoped solar cells p 170 N84-29322

**DOPPLER EFFECT**

- Optimization of fringe-type laser anemometers for turbine engine component testing [AIAA PAPER 84-1459] p 131 A84-40248
- Optimization of fringe-type laser anemometers for turbine engine component testing [NASA-TM-83658] p 133 N84-25019

**DROP SIZE**

- A technique combining the visibility of a Doppler signal with the peak intensity of the pedestal to measure the size and velocity of droplets in a spray [AIAA PAPER 84-0203] p 129 A84-17946
- Development of the phase/Doppler spray analyzer for liquid drop size and velocity characterizations [AIAA PAPER 84-1199] p 131 A84-36958
- Aerodynamic effect of combustor inlet-air pressure on fuel jet atomization [AIAA PAPER 84-1320] p 120 A84-36973
- Calibration of the Malvern particle sizer p 131 A84-40736
- Fuel spray diagnostics p 125 N84-20527
- Development and implementation of advanced diagnostic techniques p 132 N84-20528
- Measurement of spray combustion processes p 61 N84-20530

- Automatic holographic droplet analysis for liquid fuel sprays p 125 N84-20531

- Predictions of spray combustion interactions p 61 N84-20532

- Aerodynamic effect of combustor inlet-air pressure on fuel jet atomization [NASA-TM-83611] p 126 N84-22910

- The structure of evaporating and combusting sprays: Measurements and predictions [NASA-CR-173778] p 128 N84-29155

- Analysis and testing of a new method for drop size measurement using laser scatter interferometry [NASA-CR-174636] p 133 N84-31595

**DROPS (LIQUIDS)**

- Detailed fuel spray analysis techniques p 127 N84-24747
- Comparison of icing cloud instruments for 1982-1983 icing season flight program [NASA-TM-83569] p 14 N84-29870

**DRY FRICTION**

- Forced response of a cantilever beam with a dry friction damper attached I - Theory II - Experiment p 150 A84-21267

**DUCTED FLOW**

- Computation of viscous flow in planar and axisymmetric ducts by an implicit marching procedure [AIAA PAPER 84-0256] p 114 A84-17979
- Comparison of experimental and computational compressible flow in a S-duct [AIAA PAPER 84-0033] p 4 A84-19228
- Developing flow in S-shaped ducts p 116 A84-28709

- On modeling dilution jet flowfields [AIAA PAPER 84-1379] p 121 A84-44183
- Extension to an analysis of turbulent, swirling compressible flow for application to axisymmetric small gas turbine ducts [NASA-CR-165597] p 195 N84-21445

- On modeling dilution jet flowfields [NASA-TM-83708] p 32 N84-25713

**DUCTILITY**

- Failure analysis of a tool steel torque shaft p 148 A84-17546
- A study of the effect of solid particle impact and particle shape on the erosion morphology of ductile metals p 66 A84-45570

- Solid impingement erosion mechanisms and characterization of erosion resistance of ductile metals [NASA-TM-83492] p 67 N84-12287
- Particulate erosion mechanisms [NASA-TM-83551] p 68 N84-14289

**DURABILITY**

- Free-piston string engine endurance test program p 136 A84-22864
- Durability/life of fiber composites in hydrothermomechanical environments p 52 A84-27359
- Some comments on longevity by a technologist p 45 N84-12247

**DYNAMIC CHARACTERISTICS**

- Wind turbine generator interaction with conventional diesel generators on Block Island, Rhode Island Volume 1 Executive summary [NASA-CR-168318] p 171 N84-29357

**DYNAMIC LOADS**

- Dynamics of early planetary gear trains [NASA-CR-37893] p 145 N84-26027
- Evaluation of two polyimides and of an improved liner retention design for self-lubricating bushings [NASA-TM-83719] p 86 N84-27887
- Effect of vortex generators on the power conversion performance and structural dynamic loads of the Mod-2 wind turbine [NASA-TM-83680] p 171 N84-29347

**DYNAMIC MODELS**

- A large-signal dynamic simulation for the series resonant converter p 103 A84-23258
- Scaling and modeling of three-dimensional, end-wall, turbulent boundary layers [NASA-CR-3792] p 127 N84-25941

- A theoretical and experimental study of turbulent evaporating sprays [NASA-CR-174760] p 35 N84-32390

**DYNAMIC PRESSURE**

- The infinite line pressure probe [NASA-TM-83582] p 132 N84-19787

**DYNAMIC PROGRAMMING**

- Theoretical and software considerations for nonlinear dynamic analysis [NASA-CR-174504] p 154 N84-15589

**DYNAMIC RESPONSE**

- Dynamic response of shock waves in transonic diffuser and supersonic inlet - An analysis with the Navier-Stokes equations and adaptive grid [AIAA PAPER 84-1609] p 5 A84-38004
- Dynamic behavior of spiral-groove and Rayleigh-Step self-acting face seals [NASA-TP-2286] p 25 N84-16181
- Flutter and forced response of mistuned rotors using standing wave analysis [NASA-CR-173555] p 32 N84-24586

**DYNAMIC STRUCTURAL ANALYSIS**

- The coupled response of turbomachinery blading to aerodynamic excitations p 17 A84-26959
- NASTRAN forced vibration analysis of rotating cyclic structures [ASME PAPER 83-DET-20] p 151 A84-29103
- Structural dynamics of rotating bladed-disk assemblies coupled with flexible shaft motions p 21 A84-44645
- Resin selection criteria for tough composite structures [NASA-TM-83449] p 81 N84-10310
- Blade loss transient dynamics analysis with flexible bladed disk [NASA-CR-168176] p 23 N84-13193
- The influence of gyroscopic forces on the dynamic behavior and flutter of rotating blades [NASA-CR-175444] p 27 N84-20524

- Lewis Research Center spin rig and its use in vibration analysis of rotating systems  
[NASA-TP-2304] p 30 N84-24576
- Effect of vortex generators on the power conversion performance and structural dynamic loads of the Mod-2 wind turbine  
[NASA-TM-83680] p 171 N84-29347

## E

## EARTH ORBITS

- Test results of a ten cell bipolar nickel-hydrogen battery  
p 162 A84-30188
- Laboratory degradation of Kapton in a low energy oxygen ion beam  
[NASA-TM-83530] p 41 N84-18310
- A 37.5-kW point design comparison of the nickel-cadmium battery, bipolar nickel-hydrogen battery, and regenerative hydrogen-oxygen fuel cell energy storage subsystems for low Earth orbit  
[NASA-TM-83651] p 167 N84-23022
- Advanced designs for IPV nickel-hydrogen cells  
[NASA-TM-83643] p 168 N84-23025
- Teardown: analysis of a ten cell bipolar nickel-hydrogen battery  
[NASA-TM-83618] p 168 N84-23026

## ECONOMIC ANALYSIS

- Economic comparison of FDMA and TDMA options for communications by Ka-band multiple beam satellites  
[AIAA PAPER 84-0740] p 94 A84-25299
- Energy efficient engine: Flight propulsion system, preliminary analysis and design update  
[NASA-CR-167980] p 22 N84-11170
- P/M superalloys A troubled adolescent?  
[NASA-TM-83623] p 73 N84-26785

## ECONOMIC DEVELOPMENT

- Economic viability of photovoltaic power for development assistance applications  
p 193 A84-23119

## ECONOMIC FACTORS

- Economic competitiveness of fuel cell onsite integrated energy systems  
[NASA-TM-83403] p 164 N84-10685

## ECONOMIC IMPACT

- Economic impact of fuel properties on turbine powered business aircraft  
p 14 N84-23646

## EDDY CURRENTS

- Design study of magnetic eddy-current vibration suppression dampers for application to cryogenic turbomachinery  
[NASA-CR-173273] p 141 N84-16562

## EDGE DISLOCATIONS

- Finite elastic-plastic deformation of polycrystalline metals  
p 66 A84-43872

## EDGES

- Edge delamination in angle-ply composite laminates  
p 52 A84-21515
- Wide range weight functions for the strip with a single edge crack  
[NASA-TM-83478] p 153 N84-11512

## EFFICIENCY

- Comparison between measured turbine stage performance and the predicted performance using quasi-3D flow and boundary layer analyses  
[AIAA PAPER 84-1299] p 18 A84-36972
- An overview of NASA intermittent combustion engine research  
[AIAA PAPER 84-1393] p 19 A84-40244
- An analytical method to predict efficiency of aircraft gearboxes  
[AIAA PAPER 84-1500] p 20 A84-44180
- Application of an optimization method to high performance propeller designs  
[AIAA PAPER 84-1203] p 20 A84-44181
- Comparison between measured turbine stage performance and the predicted performance using quasi-3D flow and boundary layer analyses  
[NASA-TM-83640] p 29 N84-22564
- An overview of NASA intermittent combustion engine research  
[NASA-TM-83668] p 31 N84-24583
- An analytical method to predict efficiency of aircraft gearboxes  
[NASA-TM-83716] p 2 N84-25606
- Application of an optimization method to high performance propeller designs  
[NASA-TM-83710] p 2 N84-25607
- Energy efficient engine high-pressure turbine supersonic cascade technology report  
[NASA-CR-165567] p 33 N84-27739
- Efficiency of nonstandard and high contact ratio involute spur gears  
[NASA-TM-83725] p 146 N84-29223
- High speed, low cost, LEO-thermal-cycling facility  
p 171 N84-29340

## Fuel savings potential of the NASA Advanced Turboprop Program

- [NASA-TM-83736] p 35 N84-29876
- Improved heat exchanger for electrothermal devices  
[NASA-CASE-LEW-14037-1] p 49 N84-32425

## EIGENVALUES

- Eigenmode analysis of unsteady one-dimensional Euler equations  
[NASA-CR-172217] p 7 N84-10022

## EJECTORS

- Supersonic STOVL ejector aircraft from a propulsion point of view  
[AIAA PAPER 84-1401] p 19 A84-40246
- Supersonic STOVL ejector aircraft from a propulsion point of view  
[NASA-TM-83641] p 31 N84-24581

## ELASTIC BODIES

- A numerical analysis of contact and limit-point behavior in a class of problems of finite elastic deformation  
p 150 A84-27370

## ELASTIC DEFORMATION

- A numerical analysis of contact and limit-point behavior in a class of problems of finite elastic deformation  
p 150 A84-27370

## ELASTIC PROPERTIES

- Elasticity solutions for a class of composite laminate problems with stress singularities  
p 53 A84-33389
- A total life prediction model for stress concentration sites  
[NASA-CR-168225] p 152 N84-10612

## ELASTIC SHELLS

- Circuit equivalent to the elastic spherical shell  
p 104 A84-39197

## ELASTIC WAVES

- Thermoacoustic convection heat-transfer phenomenon  
p 120 A84-38857

## ELASTODYNAMICS

- An analysis of traction drive torsional stiffness  
[NASA-TM-83712] p 145 N84-27043
- Optical and other property changes of M-50 bearing steel surfaces for different lubricants and additive prior to scuffing  
[NASA-TM-83746] p 88 N84-34620

## ELASTOHYDRODYNAMICS

- Nonlinear transient finite element analysis of rotor-bearing-stator systems  
p 136 A84-20580
- Assessment of two neglected effects in the analysis of an oil pumping ring seal  
[ASME PAPER 83-LUB-16] p 137 A84-23097
- Thermal and elastohydrodynamic analysis of reciprocating rod seals in the Stirling engine  
p 138 A84-30085
- Non-Newtonian fluid model incorporated into elastohydrodynamic lubrication of rectangular contacts  
[ASME PAPER 83-LUB-15] p 139 A84-44300
- Numerical methods and computers used in elastohydrodynamic lubrication  
[NASA-TM-83524] p 141 N84-11498
- Topological reaction rate measurements related to scuffing  
[NASA-TM-83485] p 68 N84-14288
- The ball bearing as a rheological test device  
[NASA-TM-83570] p 142 N84-17591
- Elastohydrodynamic lubrication of smooth surfaces  
p 144 N84-24895
- Elastohydrodynamic lubrication Status of understanding  
p 144 N84-25048
- Lubrication of machine elements  
[NASA-RP-1126] p 147 N84-31640

## ELASTOPLASTICITY

- Algorithms for elasto-plastic-creep postbuckling  
p 152 A84-38480
- Finite elastic-plastic deformation of polycrystalline metals  
p 66 A84-43872

## ELECTRIC ARCS

- Metal vapor vacuum arc switching - Applications and results -- for launchers  
p 103 A84-32029

## ELECTRIC AUTOMOBILES

- Additive for zinc electrodes -- electric automobiles  
[NASA-CASE-LEW-13286-1] p 103 N84-14422

## ELECTRIC BATTERIES

- Cycle life test and failure model of nickel-hydrogen cells  
p 162 A84-30185
- Space power technology into the 21st Century  
[NASA-TM-83690] p 49 N84-26746
- AC propulsion system for an electric vehicle, phase 2  
[NASA-CR-168244] p 111 N84-31514

## ELECTRIC BRIDGES

- Inherent overload protection for the series resonant converter  
p 102 A84-23255
- The 25 kW resonant dc/dc power converter  
[NASA-CR-168273] p 108 N84-17481
- A study of the high frequency limitations of series resonant converters  
[NASA-CR-173868] p 111 N84-32678

## ELECTRIC CONDUCTORS

- Intercalated graphite electrical conductors  
p 105 N84-10064

## ELECTRIC CURRENT

- Development and fabrication of an augmented power transistor  
[NASA-CR-168262] p 106 N84-11388
- Hybrid power semiconductor switch  
[NASA-CASE-LEW-13922-1] p 106 N84-11389

## ELECTRIC DIPOLES

- Radiating dipole model of interference induced in spacecraft circuitry by surface discharges  
[NASA-TP-2240] p 40 N84-16247

## ELECTRIC DISCHARGES

- Particle environment -- solar arrays and electric discharges  
[NASA-CR-173888] p 191 N84-33210

## ELECTRIC ENERGY STORAGE

- Parametric study of minimum converter loss in an energy-storage dc-to-dc converter  
p 101 A84-18403
- Alkaline fuel cells for the regenerative fuel cell energy storage system  
p 162 A84-30183
- Single cell performance studies on the FE/CR Redox Energy Storage System using mixed reactant solutions at elevated temperature  
p 163 A84-30194

## ELECTRIC FIELD STRENGTH

- Spatial electron density and electric field strength measurements in microwave cavity experiments  
[AIAA PAPER 84-1522] p 189 A84-46109

## ELECTRIC FIELDS

- Radiating dipole model of interference induced in spacecraft circuitry by surface discharges  
[NASA-TP-2240] p 40 N84-16247
- Spatial electron density and electric field strength measurements in microwave cavity experiments  
[NASA-CR-173907] p 111 N84-32682

## ELECTRIC FILTERS

- Stability analysis of a buck regulator employing input filter compensation  
p 102 A84-18412

## ELECTRIC GENERATORS

- Advanced electrical power system technology for the all electric aircraft  
p 15 A84-16528
- Aircraft Electric Secondary Power  
[NASA-CP-2282] p 22 N84-10055
- MOD-2 wind turbine development  
[NASA-TM-83460] p 164 N84-13670
- A mathematical model for the doubly-fed wound rotor generator, part 2  
[NASA-TM-83581] p 107 N84-17479
- Wind turbine generator interaction with conventional diesel generators on Block Island, Rhode Island Volume 1 Executive summary  
[NASA-CR-168318] p 171 N84-29357

## ELECTRIC MOTOR VEHICLES

- An SCR inverter with an integral battery charger for electric vehicles  
p 103 A84-24850
- New propulsion components for electric vehicles  
p 103 A84-30209
- Improved transistor-controlled and commutated brushless DC motors for electric vehicle propulsion  
[NASA-CR-168053] p 105 N84-10450
- Study and review of permanent magnets for electric vehicle propulsion motors  
[NASA-CR-168178] p 193 N84-14071
- Integral inverter/battery charger for use in electric vehicles  
[NASA-CR-168177] p 194 N84-17079
- Optimization methods applied to hybrid vehicle design  
[NASA-CR-168292] p 194 N84-19185
- Development of a DC propulsion system for an electric vehicle  
[NASA-CR-168306] p 166 N84-20014
- Road load simulator tests of the Gould phase 1 functional model silicon controlled rectifier ac motor controller for electric vehicles  
[NASA-TM-83497] p 166 N84-20016
- Electric vehicle propulsion alternatives  
[NASA-TM-83504] p 166 N84-20017
- Results of electric-vehicle propulsion system performance on three lead-acid battery systems  
[NASA-TM-83657] p 169 N84-25166
- AC propulsion system for an electric vehicle, phase 2  
[NASA-CR-168244] p 111 N84-31514

## ELECTRIC MOTORS

- New propulsion components for electric vehicles  
p 103 A84-30209
- Application of advanced materials to rotating machines  
p 22 N84-10063

## ELECTRIC NETWORKS

- Investigation of the residue in an electric rail gun employing a plasma armature  
p 103 A84-32046
- Preliminary investigation of an electrical network model for ultrasonic scattering  
[NASA-CR-3770] p 149 N84-17606

## ELECTRIC POTENTIAL

- New developments in power semiconductors p 105 N84-10065
- Lightweight, high-frequency transformers p 105 N84-10066
- Hybrid power semiconductor switch [NASA-CASE-LEW-13922-1] p 106 N84-11389
- Electromagnetic propulsion test facility [NASA-TM-83568] p 37 N84-16229
- Anomalous high potentials observed on ISEE [NASA-CR-172791] p 41 N84-17252
- Double-injection, deep-impurity switch development [NASA-CR-168335] p 108 N84-18536
- Voltage controlling mechanisms in low resistivity silicon solar cells: A unified approach [NASA-TM-83612] p 167 N84-20916
- Tear-down analysis of a ten cell bipolar nickel-hydrogen battery [NASA-TM-83618] p 168 N84-23026
- The effect of diffusion induced lattice stress on the open-circuit voltage in silicon solar cells [NASA-TM-83667] p 168 N84-23027
- Discharges on a negatively biased solar array in a charged particle environment [NASA-TM-83644] p 47 N84-23690
- Particle environment — solar arrays and electric discharges [NASA-CR-173888] p 191 N84-33210
- Simplified dc to dc converter [NASA-CASE-LEW-13495-1] p 111 N84-33663
- ELECTRIC POWER**
- Investigation of energy management strategies for photovoltaic systems - An analysis technique p 160 A84-22993
- ELECTRIC POWER PLANTS**
- Oxidant system improvements for MHD energy conversion and industrial processes p 189 A84-24058
- Develop and test fuel cell powered on-site integrated total energy system [NASA-CR-168159] p 164 N84-11591
- Cogeneration Technology Alternatives Study (CTAS) Volume 2 Comparison and evaluation of results [NASA-TM-81401] p 173 N84-34038
- ELECTRIC POWER SUPPLIES**
- Aircraft Electric Secondary Power [NASA-CP-2282] p 22 N84-10055
- Three-phase, high-voltage, high-frequency distributed bus system for advanced aircraft p 105 N84-10058
- Application of advanced materials to rotating machines p 22 N84-10063
- New developments in power semiconductors p 105 N84-10065
- All-purpose bidirectional four-quadrant controller p 22 N84-10070
- High voltage-high power components for large space power distribution systems [NASA-TM-83648] p 42 N84-22615
- ELECTRIC POWER TRANSMISSION**
- New developments in power semiconductors p 105 N84-10065
- Preliminary investigation of an electrical network model for ultrasonic scattering [NASA-CR-3770] p 149 N84-17606
- Factors that affect the fatigue strength of power transmission shafting [NASA-TM-83608] p 145 N84-26029
- ELECTRIC PROPULSION**
- Investigation of a pulsed electrothermal thruster [NASA-CR-168266] p 45 N84-12227
- Experimental investigation of a Hall-current thruster [NASA-CR-168133] p 46 N84-18321
- Sputtering phenomena in ion thrusters [NASA-CR-168172] p 46 N84-18322
- Performance capabilities of the 12-centimeter Xenon ion thruster [NASA-TM-83674] p 48 N84-27825
- Radiative resistor performance characterization tests [NASA-CR-174763] p 50 N84-33462
- ELECTRIC PULSES**
- Flight and wind tunnel tests of an electro-impulse de-icing system [AIAA PAPER 84-2234] p 12 A84-39280
- ELECTRIC SWITCHES**
- A new FET-bipolar combinational power semiconductor switch p 104 A84-32293
- ELECTRICAL MEASUREMENT**
- Potentials in a plasma over a biased pinhole p 102 A84-20711
- ELECTRICAL PROPERTIES**
- Ion-beam-textured and coated surfaces experiment (S1003) p 84 N84-24650
- ELECTRICAL RESISTIVITY**
- Electronic properties of carbon fibers intercalated with copper chloride p 104 A84-34521
- Intercalated graphite electrical conductors p 105 N84-10064

- Voltage controlling mechanisms in low resistivity silicon solar cells: A unified approach [NASA-TM-83612] p 167 N84-20916
- The effect of diffusion induced lattice stress on the open-circuit voltage in silicon solar cells [NASA-TM-83667] p 168 N84-23027
- Deposition of diamondlike carbon films [NASA-CASE-LEW-14080-1] p 86 N84-28986
- Radiation tolerance of low resistivity, high voltage silicon solar cells p 170 N84-29318
- Anion permselective membrane [NASA-CR-174725] p 172 N84-29358
- ELECTRICITY**
- An assessment of advanced technology for industrial cogeneration [NASA-CR-173456] p 167 N84-22001
- Improved heat exchanger for electrothermal devices [NASA-CASE-LEW-14037-1] p 49 N84-32425
- ELECTROCATALYSTS**
- Importance of interatomic spacing in catalytic reduction of oxygen in phosphoric acid p 58 A84-12644
- ELECTROCHEMICAL CELLS**
- Simulation of lubricating behavior of a thioether liquid lubricant by an electrochemical method [NASA-TP-2316] p 84 N84-23764
- Electrochemical storage p 171 N84-29342
- ELECTROCHEMISTRY**
- NASA redox storage system development project, calendar year 1982 [NASA-TM-83469] p 164 N84-11579
- Electrochemical studies of redox systems for energy storage [NASA-CR-174503] p 165 N84-15681
- ELECTRODES**
- Electrode kinetics of oxygen reduction - A theoretical and experimental analysis of the rotating ring-disc electrode method p 59 A84-29999
- Development of a large scale bipolar NiH<sub>2</sub> battery p 162 A84-30189
- Hybrid power semiconductor switch [NASA-CASE-LEW-13922-1] p 106 N84-11389
- A multistage spent particle collector and a method for making same [NASA-CASE-LEW-13914-1] p 131 N84-12447
- Performance of computer-designed small-size multistage depressed collectors for a high-perveance traveling wave tube [NASA-TP-2249] p 106 N84-15394
- Method of making a light weight battery plaque [NASA-CASE-LEW-13349-1] p 72 N84-22734
- Advanced designs for IPV nickel-hydrogen cells [NASA-TM-83643] p 168 N84-23025
- Full scale phosphoric acid fuel cell stack technology development [NASA-CR-174660] p 169 N84-26165
- Chromium electrodes for REDOX cells [NASA-CASE-LEW-13653-1] p 170 N84-28205
- Ion sputter textured graphite electrode plates [NASA-CASE-LEW-12919-2] p 179 N84-28565
- Secondary electron emission characteristics of ion-textured copper and high-purity isotropic graphite surfaces [NASA-TP-2342] p 86 N84-28989
- Development of a lightweight nickel electrode [NASA-TM-86861] p 172 N84-30528
- Negative electrode catalyst for the iron-chromium REDOX energy storage system [NASA-CASE-LEW-14028-1] p 172 N84-32909
- ELECTROLESS DEPOSITION**
- Development of a lightweight nickel electrode [NASA-TM-86861] p 172 N84-30528
- ELECTROLYTES**
- Develop and test fuel cell powered on-site integrated total energy systems [NASA-CR-174714] p 170 N84-27329
- Chromium electrodes for REDOX cells [NASA-CASE-LEW-13653-1] p 170 N84-28205
- ELECTROMAGNETIC ACCELERATION**
- Energy partitioning in an inductively driven rail gun p 104 A84-33325
- ELECTROMAGNETIC COMPATIBILITY**
- Design guidelines for assessing and controlling spacecraft charging effects [NASA-TP-2361] p 42 N84-33452
- ELECTROMAGNETIC FIELDS**
- Solar array: Plasma interactions p 171 N84-29343
- ELECTROMAGNETIC INTERFERENCE**
- Interference phenomena in the refraction of a surface plasmon by vertical dielectric barriers p 179 A84-24410
- The effect of variable S/N on the subjective evaluation of protection ratios for direct-TV satellite services p 95 A84-48452

- Interference performance analysis of M-ary CPSK and M-ary CAPK digital transmission systems and the computation of 'required isolation' for efficient utilization of geostationary satellite orbit/spectrum p 95 A84-49303
- ELECTROMAGNETIC NOISE**
- Fiberoptics for propulsion control system [NASA-TM-83542] p 1 N84-14111
- ELECTROMAGNETIC PROPULSION**
- Metal vapor vacuum arc switching - Applications and results — for launchers p 103 A84-32029
- LeRC rail accelerators — Test designs and diagnostic techniques p 42 A84-32031
- Electromagnetic propulsion test facility [NASA-TM-83568] p 37 N84-16229
- ELECTROMAGNETIC PULSES**
- Fiberoptics for propulsion control system [NASA-TM-83542] p 1 N84-14111
- Design guidelines for assessing and controlling spacecraft charging effects [NASA-TP-2361] p 42 N84-33452
- ELECTROMAGNETIC SCATTERING**
- Numerical methods for analyzing electromagnetic scattering [NASA-CR-175423] p 98 N84-19620
- Numerical methods for analyzing electromagnetic scattering [NASA-CR-173916] p 101 N84-32645
- ELECTROMAGNETIC SURFACE WAVES**
- Harnessing surface plasmons for solar energy conversion p 159 A84-16395
- Coupling of radiation into thin film modes by means of localized plasma resonances p 187 A84-16397
- ELECTRON BEAM WELDING**
- Bending fatigue of electron-beam-welded foils Application to a hydrodynamic air bearing in the Chrysler/DOE upgraded automotive gas turbine engine [NASA-TM-83539] p 155 N84-16589
- ELECTRON BEAMS**
- Particle environment — solar arrays and electric discharges [NASA-CR-173888] p 191 N84-33210
- ELECTRON BOMBARDMENT**
- Diamondlike flake composites [NASA-CASE-LEW-13837-1] p 54 N84-22695
- Ground correlation investigation of thruster spacecraft interactions to be measured on the IAPS flight test [NASA-TM-83598] p 47 N84-23691
- Performance capabilities of the 12-centimeter Xenon ion thruster [NASA-TM-83674] p 48 N84-27825
- Ion sputter textured graphite electrode plates [NASA-CASE-LEW-12919-2] p 179 N84-28565
- ELECTRON DENSITY (CONCENTRATION)**
- Spatial electron density and electric field strength measurements in microwave cavity experiments [AIAA PAPER 84-1522] p 189 A84-46109
- Spatial electron density and electric field strength measurements in microwave cavity experiments [NASA-CR-173907] p 111 N84-32682
- ELECTRON EMISSION**
- Correlation of electron emission with changes in the surface concentration of barium and oxygen on a tungsten surface p 60 A84-45917
- Beam impingement angle effects on secondary electron emission characteristics of textured pyrolytic graphite [NASA-TP-2285] p 82 N84-18400
- ELECTRON IRRADIATION**
- Increased radiation resistance in lithium-counterdoped silicon solar cells p 163 A84-34846
- Double-injection, deep-impurity switch development [NASA-CR-168335] p 108 N84-18536
- The effects of lithium counterdoping on radiation damage and annealing in n(+)-p silicon solar cells [NASA-TM-83755] p 110 N84-31513
- ELECTRON TRAJECTORIES**
- Orbital stability in combined uniform axial and three-dimensional wiggler magnetic fields for free-electron lasers [NASA-TM-83753] p 134 N84-30273
- ELECTRON TRANSITIONS**
- Matrix effects in ion-induced emission as observed in Ne collisions with Cu-Mg and Cu-Al alloys [NASA-TM-83061] p 187 N84-10923
- ELECTRON TUBES**
- Evaluation of the emission capabilities of Spindt-type field emitting cathodes p 101 A84-12424
- ELECTRONIC EQUIPMENT**
- Simplification of power electronics for ion thruster neutralizers p 44 A84-49509
- Development of an instrument for real-time computation of indicated mean effective pressure [NASA-TP-2238] p 107 N84-16461
- ELECTRONIC FILTERS**
- Input filter compensation for switching regulators [NASA-CR-173557] p 110 N84-24975

**ELECTRONIC MODULES**

30/20 GHz spacecraft GaAs FET solid state transmitter for trunking and customer-premise-service application [NASA-CR-168276] p 107 N84-16463  
MMIC technology for advanced space communications systems [NASA-TM-83749] p 100 N84-30147

The 20 and 30 GHz MMIC technology for future space communication antenna system [NASA-TM-83745] p 100 N84-31460

**ELECTRONIC PACKAGING**

High-speed wide band 20 x 20 microwave switch matrix p 105 A84-49253  
Monolithic microwave integrated circuits Interconnections and packaging considerations [NASA-TM-83774] p 100 N84-31461

**ELECTRONICS**

Monolithic microwave integrated circuits Interconnections and packaging considerations [NASA-TM-83774] p 100 N84-31461

**ELECTRONS**

A multistage spent particle collector and a method for making same [NASA-CASE-LEW-13914-1] p 131 N84-12447  
Interpretation of STS-3/plasma diagnostics package results in terms of large space structure plasma interactions [NASA-CR-173266] p 189 N84-16991

**ELECTROSTATICS**

Correlations between plasma variables and the deposition process of Si films from chlorosilanes in low pressure RF plasma of argon and hydrogen [NASA-TM-83603] p 190 N84-21330

**ELECTROTHERMAL ENGINES**

Demonstration of a new electrothermal thruster concept p 43 A84-34037  
Experimental investigation of the pulsed electrothermal (PET) thruster [AIAA PAPER 84-1366] p 43 A84-35201  
Proposed system design for a 20 kW pulsed electrothermal thruster [AIAA PAPER 84-1367] p 43 A84-35202  
Investigation of a pulsed electrothermal thruster [NASA-CR-168266] p 45 N84-12227  
Improved heat exchanger for electrothermal devices [NASA-CASE-LEW-14037-1] p 49 N84-32425

**ELONGATION**

Effects of long-time elevated temperature exposures on hot-isostatically-pressed power-metallurgy Udmet 700 alloys with reduced cobalt contents [NASA-TM-83632] p 57 N84-28917

**EMBEDDING**

Embedding methods for the steady Euler equations [NASA-TM-83481] p 178 N84-11631

**EMITTERS**

Voltage controlling mechanisms in low resistivity silicon solar cells: A unified approach [NASA-TM-83612] p 167 N84-20916  
Preliminary design of a 10-kW thermophotovoltaic system for space applications [NASA-TM-83768] p 49 N84-32427

**ENERGY ABSORPTION**

Solid impingement erosion mechanisms and characterization of erosion resistance of ductile metals [NASA-TM-83492] p 67 N84-12287  
Impact resistance of fiber composites Energy absorbing mechanisms and environmental effects [NASA-TM-83594] p 55 N84-24712

**ENERGY ABSORPTION FILMS**

Photovoltaic power system for satellite Earth stations in remote areas Project status and design description [NASA-TM-83789] p 101 N84-33642

**ENERGY CONSERVATION**

Energy efficient engine Flight propulsion system, preliminary analysis and design update [NASA-CR-167980] p 22 N84-11170  
Energy efficient engine fan component detailed design report [NASA-CR-165466] p 33 N84-27737

**ENERGY CONSUMPTION**

Oxidant system improvements for MHD energy conversion and industrial processes p 189 A84-24058

**ENERGY CONVERSION**

Single cell performance studies on the FE/CR Redox Energy Storage System using mixed reactant solutions at elevated temperature p 163 A84-30194  
Pyroelectric conversion in space: A conceptual design study [NASA-CR-168272] p 165 N84-14585  
An assessment of advanced technology for industrial cogeneration [NASA-CR-173456] p 167 N84-22001  
Study of solar array switching power management technology for space power system [NASA-CR-167890-EXEC-SUM] p 167 N84-23021

Basic and applied research related to the technology of space energy conversion systems, 1982 - 1983 [NASA-CR-173554] p 169 N84-25168  
Wind turbine generator interaction with conventional diesel generators on Block Island, Rhode Island Volume 1. Executive summary [NASA-CR-168318] p 171 N84-29357

**ENERGY CONVERSION EFFICIENCY**

Harnessing surface plasmons for solar energy conversion p 159 A84-16395  
Effects of indirect bandgap top cells in a monolithic cascade cell structure p 160 A84-22987  
New implantation techniques for improved solar cell junctions p 161 A84-23059  
Investigation of energy management strategies for photovoltaic systems - A predictive control algorithm p 161 A84-25468  
Ion implanted junctions for silicon space solar cells p 42 A84-30143  
Multibandgap photovoltaic receiver using back surface reflectors p 161 A84-30162  
Energy partitioning in an inductively driven rail gun p 104 A84-33325

Basic and applied research related to the technology of space energy conversion systems, 1982 - 1983 [NASA-CR-173554] p 169 N84-25168  
Effect of vortex generators on the power conversion performance and structural dynamic loads of the Mcd-2 wind turbine [NASA-TM-83680] p 171 N84-29347  
Wind turbine generator interaction with conventional diesel generators on Block Island, Rhode Island Volume 2: Data analysis [NASA-CR-168319] p 172 N84-31783

**ENERGY DISSIPATION**

Parametric study of minimum converter loss in an energy-storage dc-to-dc converter p 101 A84-18403  
Acoustic power dissipation on radiation through duct terminations - Experiments p 180 A84-21272  
Application of advanced materials to rotating machines p 22 N84-10063  
Lightweight, high-frequency transformers p 105 N84-10066

**ENERGY GAPS (SOLID STATE)**

Multibandgap photovoltaic receiver using back surface reflectors p 161 A84-30162

**ENERGY POLICY**

Economic viability of photovoltaic power for development assistance applications p 193 A84-23119  
Evaluation of dissociated and steam-reformed methanol as automotive engine fuels [NASA-CR-168242] p 91 N84-27909  
AFB/open cycle gas turbine conceptual design study [NASA-CR-168135] p 172 N84-31784

**ENERGY STORAGE**

Cycle life test and failure model of nickel-hydrogen cells p 162 A84-30185  
Some comments on longevity by a technologist p 45 N84-12247  
Electrochemical studies of redox systems for energy storage [NASA-CR-174503] p 165 N84-15681  
Energy stores and switches for rail-launcher systems [NASA-CR-173249] p 107 N84-16458  
Advanced nickel-hydrogen cell configuration study [NASA-CR-173417] p 108 N84-22889  
Design considerations for a 10-kW integrated hydrogen-oxygen regenerative fuel cell system [NASA-TM-83664] p 167 N84-23023  
Design of a 1-kWh bipolar nickel hydrogen battery [NASA-TM-83647] p 168 N84-23024  
The potential impact of new power system technology on the design of a manned space station [NASA-TM-83770] p 49 N84-31272  
Negative electrode catalyst for the iron-chromium REDOX energy storage system [NASA-CASE-LEW-14028-1] p 172 N84-32909  
Regenerative hydrogen-oxygen fuel cell-electrolyzer systems for orbital energy storage p 111 N84-33670

**ENERGY TECHNOLOGY**

Recent advances in thin silicon solar cells p 160 A84-22981  
Investigation of energy management strategies for photovoltaic systems - An analysis technique p 160 A84-22993  
An SCR inverter with an integral battery charger for electric vehicles p 103 A84-24850  
Space power technology into the 21st century [AIAA PAPER 84-1136] p 43 A84-34013  
Basic and applied research related to the technology of space energy conversion systems, 1982 - 1983 [NASA-CR-173554] p 169 N84-25168

**ENERGY TRANSFER**

A thermomechanical model for energy propagation in a solid-fluid-solid system with one boundary in relative motion [ASME PAPER 83-HT-97] p 137 A84-29092  
Plasmon device design. Conversion from surface to junction plasmons with grating-couplers p 171 N84-29330

**ENGINE CONTROL**

An application of tensor ideas to nonlinear modeling of a turbofan jet engine p 20 A84-42382  
The application of LQR synthesis techniques to the turboshaft engine control problem [AIAA PAPER 84-1455] p 21 A84-44185

**ENGINE COOLANTS**

Shape of porous region to control cooling along curved exit boundary p 115 A84-23591  
Vortex generating flow passage design for increased film-cooling effectiveness and surface coverage — aircraft engine blade cooling [NASA-TM-83617] p 126 N84-22909

**ENGINE DESIGN**

Combustor development for automotive gas turbines p 135 A84-10499  
Turbulent flow field calculations in an internal combustion engine equipped with two valves p 112 A84-19311  
NASA advanced low emissions combustor program [ASME PAPER 83-JPGC-GT-10] p 17 A84-28982  
New perspectives for advanced automobile diesel engines p 138 A84-30062  
Automotive Stirling Engine Development Program Mod I Stirling engine development p 138 A84-30091  
Automotive Stirling engine development program - Overview and status report p 138 A84-30092  
Design of a high-performance rotary stratified-charge research aircraft engine [AIAA PAPER 84-1395] p 17 A84-35204  
Creep-rupture behavior of six candidate Stirling engine superalloys tested in air p 65 A84-36173  
Preliminary investigation of a two-zone swirl flow combustor [AIAA PAPER 84-1169] p 17 A84-36951  
Advanced propan drive system characteristics and technology needs [AIAA PAPER 84-1194] p 18 A84-36957  
Detonation wave augmentation of gas turbines [AIAA PAPER 84-1266] p 18 A84-37639  
Heat pipe applications in aircraft propulsion [AIAA PAPER 84-1269] p 18 A84-37640  
Powerplant design for one-engine-inoperative operation p 19 A84-40787  
Comparison of steady-state and transient CVS cycle emission of an automotive Stirling engine p 173 A84-41044  
Integration becomes the name of the OTV game p 44 A84-44045  
The aerodynamic design and performance of the NASA/GE E3 low pressure turbine [AIAA PAPER 84-1162] p 21 A84-44186  
Analytical study of suction boundary layer control for subsonic V/STOL inlets [AIAA PAPER 84-1399] p 6 A84-44187  
Ceramic-coated metals can survive contact with hot working fluid p 81 A84-44482  
Processing of sintered alpha SiC [ASME PAPER 84-GT-127] p 140 A84-46954  
F100 multivariable control synthesis program Computer implementation of the F100 multivariable control algorithm [NASA-TP-2231] p 22 N84-11171  
Executive summary, aerothermal modeling program, phase 1 [NASA-CR-174602] p 60 N84-12263  
Aerothermal modeling program, phase 1 [NASA-CR-168243-VOL-2] p 60 N84-12265  
Design concepts for low-cost composite engine frames [NASA-TM-83544] p 26 N84-16186  
Automotive Stirling engine development program [NASA-CR-168205] p 194 N84-18117  
Identification of multivariable high-performance turbofan engine dynamics from closed loop data p 28 N84-20580  
Application of advanced control techniques to aircraft propulsion systems p 28 N84-20590  
Advanced turbocharger design study program [NASA-CR-174633] p 143 N84-21879  
Overview of NASA Lewis Research Center free-piston Stirling engine activities [NASA-TM-83649] p 195 N84-22512  
Oxidizing seal for a turbine tip gas path [NASA-CASE-LEW-14053-1] p 29 N84-22563  
Preliminary investigation of a two-zone swirl flow combustor [NASA-TM-83637] p 29 N84-22565

- Energy efficient engine fan component detailed design report  
[NASA-CR-165466] p 33 N84-27737
- Advanced Gas Turbine (AGT) Technology Project  
[NASA-CR-174629] p 146 N84-28089
- Energy efficient engine high-pressure turbine detailed design report  
[NASA-CR-165608] p 33 N84-28788
- Energy efficient engine Turbine intermediate case and low-pressure turbine component test hardware detailed design report  
[NASA-CR-167973] p 33 N84-28789
- NASA Orbit Transfer Rocket Engine Technology Program  
[NASA-CR-168156] p 48 N84-28901
- Development of carbon slurry fuels for transportation (hybrid fuels, phase 2)  
[NASA-CR-174659] p 74 N84-28960
- Oxidation and corrosion resistance of candidate Stirling engine heater-head-tube alloys  
[NASA-TM-83609] p 74 N84-28962
- Advanced Gas Turbine (AGT)  
[NASA-CR-174694] p 195 N84-29805
- Nonlinear analysis for high-temperature composites: Turbine blades/vanes p 158 N84-31699
- Energy efficient engine component development and integration program  
[NASA-CR-173884] p 35 N84-32389
- Automotive Stirling Engine Development Program RESD summary report  
[NASA-CR-174674] p 196 N84-33307
- ENGINE FAILURE**
- Ferrographic and spectrometer oil analysis from a failed gas turbine engine p 135 A84-11273
- Powerplant design for one-engine-inoperative operation p 19 A84-40787
- Development of dynamic simulation of TF34-GE-100 turbofan engine with post-stall capability  
[AIAA PAPER 84-1184] p 20 A84-44178
- Contingency power concepts for helicopter turboshaft engine  
[NASA-TM-83679] p 30 N84-23648
- Development of dynamic simulation of TF34-GE-100 turbofan engine with post-stall capability  
[NASA-TM-83660] p 32 N84-25712
- ENGINE INLETS**
- Boundary layer transition effects on flow separation around V/STOL engine inlets at high incidence  
[AIAA PAPER 84-0432] p 4 A84-18090
- A parametric study of the effect of inlet lip shape upon the radiated sound field  
[AIAA PAPER 84-0498] p 180 A84-18131
- Analytical study of suction boundary layer control for subsonic V/STOL inlets  
[AIAA PAPER 84-1399] p 6 A84-44187
- Low flight speed fan noise from a supersonic inlet p 182 A84-44508
- Experimental investigation of tangential blowing applied to a subsonic V/STOL inlet  
[NASA-TP-2297] p 9 N84-20493
- ENGINE MONITORING INSTRUMENTS**
- Application of laser anemometry in turbine engine research p 130 A84-22872
- Development of an instrument for real-time computation of indicated mean effective pressure  
[NASA-TP-2238] p 107 N84-16461
- ENGINE NOISE**
- Tone generation by rotor-downstream strut interaction p 16 A84-22174
- Finite element-integral acoustic simulation of JT15D turbofan engine p 182 A84-41132
- Helicopter engine core noise p 185 N84-29676
- Analysis of the effect on combustor noise measurements of acoustic waves reflected by the turbine and combustor inlet  
[NASA-TM-83760] p 185 N84-32122
- A theoretical model for the cross spectra between pressure and temperature downstream of a combustor  
[NASA-TM-83671] p 186 N84-34231
- ENGINE PARTS**
- High-temperature fatigue in metals - A brief review of life prediction methods developed at the Lewis Research Center of NASA p 64 A84-14286
- Ceramic components for the AGT 100 engine p 136 A84-22878
- Hostile environmental conditions facing candidate alloys for the automotive Stirling engine p 136 A84-23522
- Test results and description of a 1 kW free-piston Stirling engine with a dashpot load p 138 A84-30095
- Progress in net shape fabrication of alpha sic turbine components  
[ASME PAPER 84-GT-273] p 140 A84-47036
- Development of strain tolerant thermal barrier coating systems, tasks 1 - 3  
[NASA-CR-168251] p 81 N84-12312
- Advanced Gas Turbine (AGT) Technology Project  
[NASA-CR-174629] p 146 N84-28089
- Energy efficient engine: Turbine intermediate case and low-pressure turbine component test hardware detailed design report  
[NASA-CR-167973] p 33 N84-28789
- NASA Orbit Transfer Rocket Engine Technology Program  
[NASA-CR-168156] p 48 N84-28901
- Oxidation and corrosion resistance of candidate Stirling engine heater-head-tube alloys  
[NASA-TM-83609] p 74 N84-28962
- Three-dimensional stress analysis using the boundary element method p 159 N84-31700
- ENGINE TESTS**
- Combustor development for automotive gas turbines p 135 A84-10499
- Effects of wind on turbofan engines in outdoor static test stands  
[AIAA PAPER 83-2766] p 15 A84-15204
- Comparison of full-scale engine and subscale model performance of a mixed flow exhaust system for an energy efficient engine (E3) propulsion system  
[AIAA PAPER 84-0283] p 16 A84-17997
- Free-piston Stirling engine endurance test program p 136 A84-22864
- Liquid chromatographic analysis of a formulated ester from a gas-turbine engine test  
[ASLE PREPRINT 83-LC-1A-1] p 80 A84-28995
- Experimental investigation of the pulsed electrothermal (PET) thruster  
[AIAA PAPER 84-1386] p 43 A84-35201
- Preliminary investigation of a two-zone swirl flow combustor  
[AIAA PAPER 84-1169] p 17 A84-36951
- The aerodynamic design and performance of the NASA/GE E3 low pressure turbine  
[AIAA PAPER 84-1162] p 21 A84-44186
- Automotive Stirling engine development program  
[NASA-CR-168205] p 194 N84-18117
- Preliminary investigation of a two-zone swirl flow combustor p 29 N84-22565
- Unsteady flow in turbomachinery: An overview p 128 N84-25961
- Advanced Gas Turbine (AGT)  
[NASA-CR-174694] p 195 N84-29805
- Energy efficient engine component development and integration program  
[NASA-CR-173884] p 35 N84-32389
- Response of a small-turboshaft-engine compression system to inlet temperature distortion p 36 N84-33414
- Baseline performance and emissions data for a single-cylinder, direct-injected diesel engine  
[NASA-TM-86873] p 197 N84-34330
- Identification of quasi-steady compressor characteristics from transient data  
[NASA-CR-174685] p 36 N84-34444
- ENGINES**
- Creep-rupture behavior of candidate Stirling engine alloys after long-term aging at 760 deg C in low-pressure hydrogen  
[NASA-TM-83676] p 73 N84-25793
- Overview of advanced Stirling and gas turbine engine development programs and implications for solar thermal electrical applications p 146 N84-28231
- Inelastic and dynamic fracture and stress analyses p 158 N84-31697
- ENTHALPY**
- Computer simulation of the heavy-duty turbo-compounded diesel cycle for studies of engine efficiency and performance  
[NASA-CR-174755] p 196 N84-33306
- ENTRAINMENT**
- Experimental study of bubble cavities attached to a rotating shaft in a reservoir  
[NASA-TM-83586] p 124 N84-17533
- The influence of large-scale motion on turbulent transport for confined coaxial jets p 125 N84-20542
- ENVIRONMENT EFFECTS**
- Impact resistance of fiber composites: Energy absorbing mechanisms and environmental effects  
[NASA-TM-83594] p 55 N84-24712
- ENVIRONMENTAL TESTS**
- Solute transport and the prediction of breakaway oxidation in gamma + beta Ni-Cr-Al alloys' p 65 A84-42658
- The effect of variable S/N on the subjective evaluation of protection ratios for direct-TV satellite services p 95 A84-48452
- Fatigue crack growth and low cycle fatigue of two nickel base superalloys  
[NASA-CR-174534] p 66 N84-10267
- EPOXY MATRIX COMPOSITES**
- Prediction of composite hygral behavior made simple p 51 A84-14285
- Aging results for PRD 49 III/epoxy and Kevlar 49/epoxy composite pressure vessels p 52 A84-21847
- Durability/life of fiber composites in hygrothermomechanical environments p 52 A84-27359
- EQUATIONS OF STATE**
- Scaling relations in the equation of state, thermal expansion, and melting of metals p 192 A84-19359
- EQUATORIAL ATMOSPHERE**
- Tropical response to lateral forcing with a latitudinally and zonally nonuniform basic state p 174 A84-40399
- EQUIPMENT SPECIFICATIONS**
- Advanced 30/20 GHz multiple-beam antennas for communications satellites p 40 A84-49250
- EQUIVALENT CIRCUITS**
- GaAs dual-gate FET for operation up to K-band p 104 A84-32281
- Circuit equivalent to the elastic spherical shell p 104 A84-39197
- EROSION**
- Morphology of an aluminum alloy eroded by a normally incident jet of angular erodent particles p 64 A84-18244
- Predictive capability of long-term cavitation and liquid impingement erosion models p 50 A84-32646
- A study of the effect of solid particle impact and particle shape on the erosion morphology of ductile metals p 66 A84-45570
- Application of signal analysis to cavitation p 122 A84-49192
- Solid impingement erosion mechanisms and characterization of erosion resistance of ductile metals  
[NASA-TM-83492] p 67 N84-12287
- Particulate erosion mechanisms  
[NASA-TM-83551] p 68 N84-14289
- Cathode degradation and erosion in high pressure arc discharges  
[NASA-TM-83638] p 47 N84-22631
- In-situ measurements of alloy oxidation/corrosion/erosion using a video camera and proximity sensor with microcomputer control  
[NASA-TM-83673] p 74 N84-27859
- Erosion of iron-chromium alloys by glass particles  
[NASA-TP-2354] p 75 N84-28965
- Empirical relations for cavitation and liquid impingement erosion processes p 76 N84-31349
- Characterization of erosion of metallic materials under cavitation attack in a mineral oil  
[NASA-TP-2368] p 147 N84-32825
- The energy dependence and surface morphology of Kapton (trademark) degradation under atomic oxygen bombardment p 187 N84-34484
- ERROR ANALYSIS**
- Optimizing and comparing laser anemometers p 130 A84-28739
- Uncertainty methodology for in-flight thrust determination  
[SAE PAPER 831438] p 13 A84-29452
- Application of in-flight thrust determination uncertainty  
[SAE PAPER 831439] p 13 A84-29453
- ESTERS**
- Liquid chromatographic analysis of a formulated ester from a gas-turbine engine test  
[ASLE PREPRINT 83-LC-1A-1] p 80 A84-28995
- ETCHING**
- Method of making an ion beam sputter-etched ventricular catheter for hydrocephalus shunt  
[NASA-CASE-LEW-13107-2] p 174 N84-23095
- ETHERS**
- Thermal oxidative degradation reactions of linear perfluoroalkyl ethers p 80 A84-30000
- Thermal oxidative degradation reactions of perfluoroalkyl ethers p 60 N84-11229
- ETHYL ALCOHOL**
- Utilization of alternative fuels in diesel engines  
[NASA-CR-174669] p 91 N84-26813
- EULER EQUATIONS OF MOTION**
- Application of a finite element algorithm to the solution of steady transonic Euler equations p 3 A84-10133
- An implicit LU scheme for the Euler equations applied to arbitrary cascades - new method of factoring  
[AIAA PAPER 84-0167] p 4 A84-17925
- Relaxation solution of the full Euler equations p 119 A84-35323
- Conservative streamtube solution of steady-state Euler equations  
[AIAA PAPER 84-1643] p 120 A84-38030
- Eigenmode analysis of unsteady one-dimensional Euler equations  
[NASA-CR-172217] p 7 N84-10022

- Embedding methods for the steady Euler equations  
[NASA-TM-83481] p 178 N84-11831
- EVAPORATION**  
Evaluation of single crystal LaB<sub>6</sub> cathodes for use in a high frequency backward wave oscillator tube  
[NASA-CR-173343] p 108 N84-19709  
A theoretical and experimental study of turbulent evaporating sprays  
[NASA-CR-174760] p 35 N84-32390
- EXHAUST EMISSION**  
Combustor development for automotive gas turbines  
p 135 A84-10499  
NASA advanced low emissions combustor program  
[ASME PAPER 83-JFGC-GT-10] p 17 A84-28982  
Experimental investigation of the low NO<sub>x</sub> vortex airblast annular combustor  
[AIAA PAPER 84-1170] p 18 A84-36952  
Clean catalytic combustor program  
[NASA-CR-168323] p 24 N84-15151  
Evaluation of dissociated and steam-reformed methanol as automotive engine fuels  
[NASA-CR-168242] p 91 N84-27909  
Computer simulation of the heavy-duty turbo-compounded diesel cycle for studies of engine efficiency and performance  
[NASA-CR-174755] p 196 N84-33306  
Baseline performance and emissions data for a single-cylinder, direct-injected diesel engine  
[NASA-TM-86873] p 197 N84-34330
- EXHAUST FLOW SIMULATION**  
Comparison of full-scale engine and subscale model performance of a mixed flow exhaust system for an energy efficient engine (E3) propulsion system  
[AIAA PAPER 84-0283] p 16 A84-17997
- EXHAUST GASES**  
A temperature correlation for the radiation resistance of a thick-walled circular duct exhausting a hot gas  
p 181 A84-31103  
Comparison of steady-state and transient CVS cycle emission of an automotive Stirling engine  
p 173 A84-41044  
Dynamic gas temperature measurement system, volume 1  
[NASA-CR-168267-VOL-1] p 132 N84-16529  
Deposition of Na<sub>2</sub>SO<sub>4</sub> from salt-seeded combustion gases of a high velocity burner rig  
[NASA-TM-83751] p 129 N84-31558
- EXHAUST NOZZLES**  
Velocity and temperature characteristics of two-stream, coplanar jet exhaust plumes  
[AIAA PAPER 84-2205] p 21 A84-46106  
Inverted velocity profile semi-annular nozzle jet exhaust noise experiments  
[NASA-TM-83525] p 182 N84-13924  
Fluid shielding of high-velocity jet noise  
[NASA-TP-2259] p 183 N84-15894  
Low frequency noise in a quiet, clean, general aviation turbofan engine  
[NASA-TM-83520] p 183 N84-20320  
Velocity and temperature characteristics of two-stream, coplanar jet exhaust plumes  
[NASA-TM-83730] p 34 N84-28790
- EXHAUST VELOCITY**  
Investigation of a pulsed electrothermal thruster  
[NASA-CR-168266] p 45 N84-12227
- EXOTHERMIC REACTIONS**  
Low-cost single-crystal turbine blades, volume 1  
[NASA-CR-168218] p 68 N84-15247
- EXPANSION**  
Swirl, expansion ratio and blockage effects on confined turbulent flow  
[NASA-CR-175391] p 125 N84-19746
- EXPERIMENT DESIGN**  
Measurement of spray combustion processes  
p 61 N84-20530  
Preliminary design of two Space Shuttle fluid physics experiments  
[NASA-CR-174649] p 39 N84-23667
- EXPERIMENTATION**  
Effect of location in an array on heat transfer to a short cylinder in crossflow  
p 119 A84-36150
- EXPONENTIAL FUNCTIONS**  
Exponential-fitted methods for integrating stiff systems of ordinary differential equations Applications to homogeneous gas-phase chemical kinetics  
p 179 N84-31279
- EXTINCTION**  
Extinction of premixed flames by stretch and radiative loss  
p 58 A84-23593  
An experimental study on extinction and stability of stretched premixed flames  
p 59 A84-35425
- EXTRAPOLATION**  
Cogeneration Technology Alternatives Study (CTAS) Volume 2 Comparison and evaluation of results  
[NASA-TM-81401] p 173 N84-34038
- EXTREMELY HIGH FREQUENCIES**  
Concept for advanced satellite communications and required technologies  
p 93 A84-15626  
Economic comparison of FDMA and TDMA options for communications by Ka-band multiple beam satellites  
[AIAA PAPER 84-0740] p 94 A84-25299  
GaAs dual-gate FET for operation up to K-band  
p 104 A84-32281  
A K-band GaAs FET amplifier with 8.2-W output power  
p 104 A84-32290  
Recent developments in EHF Satcom technology  
p 39 A84-46620  
The 30 GHz communications satellite low noise receiver  
[NASA-CR-168254] p 97 N84-13398  
The 30-GHz monolithic receive module  
[NASA-CR-168326] p 99 N84-20737  
K-band latching switches  
[NASA-CR-168253] p 109 N84-24973
- EXTRUDING**  
The structure of extruded NiAl  
p 65 A84-36047
- F**
- FABRICATION**  
Large area space solar cell assemblies  
p 42 A84-22980  
Diffused junction p(+)-n solar cells in bulk GaAs. I Fabrication and cell performance  
p 161 A84-26027  
Arc spray fabrication of metal matrix composite monolayer — high temperature fiber-reinforced superalloy composites  
[NASA-CASE-LEW-13828-1] p 54 N84-15203  
Method of making a light weight battery plaque  
[NASA-CASE-LEW-13349-1] p 72 N84-22734  
Fabrication development for ODS-superalloy, air-cooled turbine blades  
[NASA-CR-174650] p 32 N84-25711
- FABRY-PEROT INTERFEROMETERS**  
Application of laser anemometry in turbine engine research  
[NASA-TM-83513] p 131 N84-11456
- FACE CENTERED CUBIC LATTICES**  
The development of directional coarsening of the gamma-prime precipitate in superalloy single crystals  
p 63 A84-10597
- FACTORIZATION**  
An implicit LU scheme for the Euler equations applied to arbitrary cascades — new method of factoring  
[AIAA PAPER 84-0167] p 4 A84-17925  
Element-by-element solution procedures for nonlinear structural analysis  
p 158 N84-31694
- FAILURE ANALYSIS**  
Ferographic and spectrometer oil analysis from a failed gas turbine engine  
p 135 A84-11273  
Failure analysis of a tool steel torque shaft  
p 148 A84-17546  
A real-time implementation of an advanced sensor failure detection, isolation, and accommodation algorithm  
[AIAA PAPER 84-0569] p 176 A84-21305  
Cycle life test and failure model of nickel-hydrogen cells  
p 162 A84-30185  
Advanced Gas Turbine (AGT) Power-train system development  
[NASA-CR-168056] p 140 N84-10581  
A real-time implementation of an advanced sensor failure detection, isolation, and accommodation algorithm  
[NASA-TM-83553] p 1 N84-13140  
Sputtering phenomena in ion thrusters  
[NASA-CR-168172] p 46 N84-18322  
Ceramic-to-metal bonding for pressure transducers  
[NASA-CR-173500] p 84 N84-22753  
Teardown analysis of a ten cell bipolar nickel-hydrogen battery  
[NASA-TM-83618] p 168 N84-23026  
Contingency power concepts for helicopter turboshaft engine  
[NASA-TM-83679] p 30 N84-23648  
Sensor failure detection for jet engines using analytical redundancy  
[NASA-TM-83695] p 31 N84-24585  
Deposition stress effects on thermal barrier coating burner life  
[NASA-TM-83670] p 85 N84-25830  
Hygrothermomechanical fracture stress criteria for fiber composites with sense-panty  
[NASA-TM-83691] p 57 N84-28918  
Mode 2 fatigue crack growth specimen development  
[NASA-TM-83722] p 156 N84-29248  
Failure analysis of plasma-sprayed thermal barrier coatings  
[NASA-TM-83777] p 75 N84-31347
- FAILURE MODES**  
Compressive behavior of unidirectional fibrous composites  
p 53 A84-29894
- Mode 2 fatigue crack growth specimen development  
[NASA-TM-83722] p 156 N84-29248
- FAN BLADES**  
Three-dimensional turbulent boundary-layer development on a fan rotor blade  
p 3 A84-17437  
Optimization and mechanisms of mistuning in cascades  
[ASME PAPER 84-GT-196] p 21 A84-46993  
Flutter of swept fan blades  
[NASA-TM-83547] p 154 N84-16587  
V/STOL model fan stage rig design report  
[NASA-CR-174688] p 29 N84-23629  
Detailed flow measurements in casing boundary layer of 429-meter-per-second tip-speed two-stage fan  
[NASA-TP-2052] p 34 N84-28795  
Subsonic/transonic stall flutter investigation of a rotating fan  
[NASA-CR-174625] p 36 N84-33417
- FAN IN WING AIRCRAFT**  
Tandem fan applications in advanced STOVL fighter configurations  
[AIAA PAPER 84-1402] p 19 A84-40245  
Tandem fan applications in advanced STOVL fighter configurations  
[NASA-TM-83689] p 30 N84-24579
- FANS**  
Investigation of the three-dimensional flow field within a transonic fan rotor - Experiment and analysis  
[ASME PAPER 84-GT-200] p 7 A84-46995  
End-wall boundary layer measurements in a two-stage fan  
p 26 N84-16208
- FAR FIELDS**  
Jet noise modification by the 'whistler nozzle'  
p 181 A84-23355
- FAST FOURIER TRANSFORMATIONS**  
Secondary pattern computation of an arbitrarily shaped main reflector  
[NASA-TM-85527] p 100 N84-25909
- FATIGUE (MATERIALS)**  
Creep fatigue of low-cobalt superalloys Waspalloy, PM U 700 and wrought U 700  
[NASA-CR-168260] p 67 N84-13265  
Complexities of high temperature metal fatigue: Some steps toward understanding  
[NASA-TM-83507] p 154 N84-14541  
Use of the WEST-1 wind turbine simulator to predict blade fatigue load distribution  
[NASA-TM-83532] p 165 N84-14586  
Theoretical and software considerations for nonlinear dynamic analysis  
[NASA-CR-174504] p 154 N84-15589  
Cryogenic Fluid Management Experiment (CFME) trunnion verification testing  
[NASA-CR-168310] p 92 N84-16381  
Elevated temperature biaxial fatigue  
[NASA-CR-173473] p 156 N84-21905  
Crack layer theory  
[NASA-CR-174634] p 156 N84-22980  
Factors that affect the fatigue strength of power transmission shafting  
[NASA-TM-83608] p 145 N84-26029  
Design of power-transmitting shafts  
[NASA-RP-1123] p 145 N84-27041  
Evaluation of the effect of crack closure on fatigue crack growth of simulated short cracks  
[NASA-TM-83778] p 75 N84-31348  
Crack tip field and fatigue crack growth in general yielding and low cycle fatigue  
[NASA-CR-174686] p 76 N84-32503
- FATIGUE LIFE**  
High-temperature fatigue in metals - A brief review of life prediction methods developed at the Lewis Research Center of NASA  
p 64 A84-14286  
Simplified analytical procedures for representing material cyclic response — for high temperature gas turbine engine analysis  
p 151 A84-31596  
Advanced reliability method for fatigue analysis  
p 151 A84-31596  
Low strain, long life creep fatigue of AF2-1DA and INCO 718  
[NASA-CR-167939] p 66 N84-10268  
Bending fatigue of electron-beam-welded foils  
Application to a hydrodynamic air bearing in the Chrysler/DOE upgraded automotive gas turbine engine  
[NASA-TM-83539] p 155 N84-16589  
Crack tip field and fatigue crack growth in general yielding and low cycle fatigue  
[NASA-CR-174686] p 76 N84-32503  
Low cycle fatigue behavior of conventionally cast MAR-M 200 AT 1000 deg C  
[NASA-TM-83769] p 77 N84-33564
- FATIGUE TESTS**  
The effects of frequency and hold times on fatigue crack propagation rates in a nickel base superalloy  
p 64 A84-18733



- Effects of processing and microstructure on the fatigue behaviour of the nickel-base superalloy Rene95 p 66 A84-48715
- Fatigue crack growth and low cycle fatigue of two nickel base superalloys [NASA-CR-174534] p 66 N84-10267
- Preliminary study of thermomechanical fatigue of polycrystalline MAR-M 200 [NASA-TP-2280] p 69 N84-17350
- Engine cyclic durability by analysis and material testing [NASA-TM-83577] p 155 N84-18683
- Cyclic torsion testing [NASA-TM-83756] p 157 N84-31687
- FAULT TOLERANCE**
- Graphics enhanced computer emulation for improved timing-race and fault tolerance control system analysis — of Centaur liquid-fuel booster [AIAA PAPER 83-2328] p 177 A84-10010
- FEASIBILITY ANALYSIS**
- A frequency-division multiple-access system concept for 30/20 GHz high-capacity domestic satellite service p 94 A84-22141
- Feasibility analysis of a spiral groove ring seal for counter-rotating shafts p 139 A84-45965
- FEEDBACK**
- Feedback in separated flows over symmetric airfoils [NASA-TM-83758] p 10 N84-31091
- FEEDBACK CONTROL**
- Extensions of the discrete-average models for converter power stages p 102 A84-18411
- Identification of multivariable high performance turbofan engine dynamics from closed loop data p 16 A84-18582
- Inherent overload protection for the series resonant converter p 102 A84-23255
- FEEDFORWARD CONTROL**
- Input filter compensation for switching regulators [NASA-CR-173247] p 107 N84-16459
- Input filter compensation for switching regulators [NASA-CR-173557] p 110 N84-24975
- FERRITES**
- Properties of ferrites important to their friction and wear behavior [NASA-TM-83718] p 87 N84-28994
- FERROGRAPHY**
- Ferrographic and spectrometer oil analysis from a failed gas turbine engine p 135 A84-11273
- FIBER COMPOSITES**
- Prediction of composite hygral behavior made simple p 51 A84-14285
- Durability/life of fiber composites in hygrothermomechanical environments p 52 A84-27359
- Compressive behavior of unidirectional fibrous composites p 53 A84-29894
- Simplified composite micromechanics equations for strength, fracture toughness and environmental effects p 53 A84-41858
- Simplified composite micromechanics equations of hygral, thermal, and mechanical properties p 53 A84-49377
- Select fiber composites for space applications: A mechanistic assessment [NASA-TM-83631] p 55 N84-22702
- Impact resistance of fiber composites: Energy absorbing mechanisms and environmental effects [NASA-TM-83594] p 55 N84-24712
- Dynamic stress analysis of smooth and notched fiber composite flexural specimens [NASA-TM-83694] p 56 N84-25770
- ICAN Integrated composites analyzer [NASA-TM-83700] p 56 N84-26755
- Interply layer degradation effects on composite structural response [NASA-TM-83702] p 56 N84-26756
- Studies of acoustical properties of bulk porous flexible materials [NASA-CR-173622] p 185 N84-27544
- Method and apparatus for gripping uniaxial fibrous composite materials [NASA-CASE-LEW-13758-1] p 56 N84-27829
- Progressive fracture of fiber composites [NASA-TM-83701] p 56 N84-27831
- Simplified composite micromechanics equations for strength, fracture toughness and environmental effects [NASA-TM-83696] p 56 N84-27832
- Application of finite element substructuring to composite micromechanics [NASA-TM-83729] p 57 N84-31288
- FIBER OPTICS**
- Fiberoptics for propulsion control system [NASA-TM-83542] p 1 N84-14111
- Optical residue addition and storage units using a Hughes liquid crystal light valve p 188 N84-22417

- FIBER ORIENTATION**
- Off-axis tensile properties and fracture in a unidirectional graphite/polyimide composite (Celon 6000/PMR 15) p 53 A84-43553
- FIBER REINFORCED COMPOSITES**
- Thermal degradation of the tensile properties of unidirectionally reinforced FP-AI2O3/EZ 33 magnesium composites p 52 A84-28229
- Tungsten-fiber-reinforced superalloy composite, high-temperature component design considerations p 53 A84-28241
- Elasticity solutions for a class of composite laminate problems with stress singularities p 53 A84-33389
- Evaluation of two polyimides and of an improved liner retention design for self-lubricating bushings [NASA-TM-83719] p 86 N84-27887
- Nonlinear analysis for high-temperature composites: Turbine blades/vanes p 158 N84-31699
- FIBER STRENGTH**
- Indentation law for composite laminates p 52 A84-27356
- Method for strengthening boron fibers [NASA-CASE-LEW-13826-2] p 55 N84-24711
- FIELD EFFECT TRANSISTORS**
- A Ka-band GaAs monolithic phase shifter p 101 A84-18371
- Design considerations for FET-gated power transistors p 102 A84-18414
- GaAs dual-gate FET for operation up to K-band p 104 A84-32281
- A K-band GaAs FET amplifier with 8.2-W output power p 104 A84-32290
- A new FET-bipolar combinational power semiconductor switch p 104 A84-32293
- Hybrid power semiconductor switch [NASA-CASE-LEW-13922-1] p 106 N84-11389
- 30/20 GHz spacecraft GaAs FET solid state transmitter for trunking and customer-premise service application [NASA-CR-168276] p 107 N84-16463
- The 20 GHz spacecraft FET solid state transmitter [NASA-CR-168240] p 107 N84-17477
- A study of the high frequency limitations of series resonant converters [NASA-CR-173868] p 111 N84-32678
- FIELD EMISSION**
- Evaluation of the emission capabilities of Spindt-type field emitting cathodes p 101 A84-12424
- FIGHTER AIRCRAFT**
- Aircraft Electric Secondary Power [NASA-CP-2282] p 22 N84-10055
- FILM COOLING**
- Vortex generating flow passage design for increased film cooling effectiveness [NASA-CASE-LEW-14039-1] p 126 N84-20782
- Vortex generating flow passage design for increased film-cooling effectiveness and surface coverage — aircraft engine blade cooling [NASA-TM-83617] p 126 N84-22909
- FILM THICKNESS**
- Dynamics of two-phase face seals p 137 A84-26792
- Dynamic behavior of spiral-groove and Rayleigh-Step self-acting face seals [NASA-TP-2266] p 25 N84-16181
- Characteristic morphological and frictional changes in sputtered MoS<sub>2</sub>/sub 2 films [NASA-TM-83565] p 92 N84-16380
- Elastohydrodynamic lubrication of smooth surfaces p 144 N84-24895
- FINITE DIFFERENCE THEORY**
- Boundary conditions for the solution of compressible Navier-Stokes equations by an implicit factored method p 113 A84-13495
- Streamwise computation of three-dimensional parabolic flows p 113 A84-16828
- Aerothermal modeling Executive summary [NASA-CR-168330] p 25 N84-15152
- Asymptotic analysis of numerical wave propagation in finite difference equations [NASA-CR-175323] p 98 N84-15360
- Improved finite-difference vibration analysis of pretwisted, tapered beams [NASA-TM-83549] p 154 N84-16588
- Error reduction program: A progress report p 27 N84-20536
- Improved methods of vibration analysis of pretwisted, airfoil blades [NASA-TM-83735] p 157 N84-30329
- Time dependent wave envelope finite difference analysis of sound propagation [NASA-TM-83744] p 185 N84-32118
- Turbine blade and vane heat flux sensor development, phase 1 [NASA-CR-168297] p 134 N84-32790

- FINITE ELEMENT METHOD**
- Application of a finite element algorithm to the solution of steady transonic Euler equations p 3 A84-10133
- Inelastic stress analyses at finite deformation through complementary energy approaches p 149 A84-13248
- Analyses of large quasistatic deformations of inelastic bodies by a new hybrid-stress finite element algorithm p 150 A84-16874
- Analyses of large quasistatic deformations of inelastic bodies by a new hybrid-stress finite element algorithm - Applications p 150 A84-16884
- Nonlinear transient finite element analysis of rotor-bearing-stator systems p 136 A84-20580
- A finite element approach for predicting nozzle admittances p 180 A84-21184
- On the suppression of zero energy deformation modes p 150 A84-21541
- Finite-analytic numerical method for unsteady two-dimensional Navier-Stokes equations p 116 A84-25807
- Finite element formulation of transonic flow problems p 116 A84-25859
- A numerical analysis of contact and limit-point behavior in a class of problems of finite elastic deformation p 150 A84-27370
- The structural response of a rail acceleration p 151 A84-32039
- Finite element-integral acoustic simulation of JT15D turbofan engine p 182 A84-41132
- A mixed shear flexible finite element for the analysis of laminated plates p 152 A84-45894
- Penalty function finite element analysis of steady viscous incompressible flow in rotating coordinates [ASME PAPER 84-GT-36] p 121 A84-46900
- Numerical solution for the problem of flame propagation by the random element method p 60 A84-48139
- Finite element forced vibration analysis of rotating cyclic structures [NASA-CR-165430] p 153 N84-11515
- A simplified method for elastic-plastic-creep structural analysis [NASA-TM-83509] p 154 N84-14542
- Bladed-shrouded-disc aeroelastic analyses Computer program updates in NASTRAN level 17 [NASA-CR-165428] p 25 N84-15154
- Theoretical and software considerations for nonlinear dynamic analysis [NASA-CR-174504] p 154 N84-16589
- Impact resistance of fiber composites: Energy absorbing mechanisms and environmental effects [NASA-TM-83594] p 55 N84-24712
- Parameter studies of gear cooling using an automatic finites element mesh generator [NASA-TM-83721] p 146 N84-28087
- An investigation of the transient thermal analysis of spur gears [NASA-TM-83724] p 146 N84-28088
- Application of finite element substructuring to composite micromechanics [NASA-TM-83729] p 57 N84-31288
- Nonlinear Structural Analysis [NASA-CP-2297] p 157 N84-31688
- Slave finite elements: The temporal element approach to nonlinear analysis p 157 N84-31689
- New variational formulations of hybrid stress elements p 158 N84-31690
- Nonlinear finite element analysis of shells with large aspect ratio p 158 N84-31692
- Self-adaptive solution strategies p 158 N84-31693
- Element-by-element solution procedures for nonlinear structural analysis p 158 N84-31694
- Automatic finite element generators p 158 N84-31695
- Stability and convergence of underintegrated finite element approximations p 158 N84-31696
- FINS**
- Length to diameter ratio and row number effects in short pin fin heat transfer [ASME PAPER 83-GT-54] p 118 A84-33706
- FLAKES**
- Diamondlike flakes [NASA-CASE-LEW-13837-2] p 54 N84-22696
- FLAME PROPAGATION**
- Secondary effects in combustion instabilities leading to flashback p 58 A84-17436
- Formation and inflammation of a turbulent jet [AIAA PAPER 84-0572] p 114 A84-18171
- An invariant derivation of flame stretch p 58 A84-18925
- Flame radiation and linear heat transfer in a tubular can combustor [AIAA PAPER 84-0443] p 16 A84-21300
- Self-similar blast waves incorporating deflagrations of variable speed p 116 A84-28379
- Dynamic effects of combustion p 59. A84-29128



- Analytic modeling of a spray diffusion flame  
[AIAA PAPER 84-1317] p 118 A84-35168
- An experimental study on extinction and stability of stretched premixed flames p 59 A84-35425
- Numerical solution for the problem of flame propagation by the random element method p 60 A84-48139
- Flame radiation and liner heat transfer in a tubular-can combustor  
[NASA-TM-83536] p 23 N84-13188
- Combustor flame flashback p 62 N84-20561
- FLAME SPECTROSCOPY**  
The chemical kinetics and thermodynamics of sodium species in oxygen-rich hydrogen flames p 59 A84-27724
- FLAME STABILITY**  
An experimental study on extinction and stability of stretched premixed flames p 59 A84-35425
- FLAMES**  
A theoretical prediction of the acoustic pressure generated by turbulence-flame front interactions  
[NASA-TM-83587] p 184 A84-26383
- FLAMMABILITY**  
Effect of gravity on halogenated hydrocarbon flame retardant effectiveness  
[NASA-TM-83761] p 63 N84-33536
- FLASHBACK**  
Secondary effects in combustion instabilities leading to flashback p 58 A84-17436
- Combustor flame flashback p 62 N84-20561
- FLAT PLATES**  
Experimental studies on two dimensional shock boundary layer interactions  
[AIAA PAPER 84-0039] p 3 A84-17881
- Convective heat transfer studies at high temperatures with pressure gradient for inlet flow Mach number of 0.45  
[AIAA PAPER 84-1487] p 119 A84-35233
- Flat plate heat transfer for laminar transition and turbulent boundary layers using a shock tube  
[AIAA PAPER 84-1726] p 120 A84-37467
- Engineering correlations of variable-property effects on laminar forced convection mass transfer for dilute vapor species and small particles in air  
[NASA-CR-169322] p 124 N84-18578
- FLEXIBILITY**  
Vibration and flutter of mistuned bladed-disk assemblies  
[NASA-TM-83634] p 156 N84-23923
- Research study for effects of case flexibility on bearing loads and rotor stability  
[NASA-CR-171147] p 148 N84-33811
- FLEXIBLE BODIES**  
Structural dynamics of rotating bladed-disk assemblies coupled with flexible shaft motions p 21 A84-44645
- A blade loss response spectrum for flexible rotor systems  
[ASME PAPER 84-GT-29] p 139 A84-46893
- FLEXING**  
Characteristics of Si<sub>3</sub>N<sub>4</sub>-SiO<sub>2</sub>-Ce<sub>2</sub>O<sub>3</sub> compositions sintered in high-pressure nitrogen p 79 A84-19913
- Thermal degradation of the tensile properties of unidirectionally reinforced FP-Al<sub>2</sub>O<sub>3</sub>/EZ 33 magnesium composites p 52 A84-28229
- FLIGHT CHARACTERISTICS**  
Correlation of flight effects on centerline velocity decay for cold-flow acoustically excited jets  
[NASA-TM-83502] p 182 N84-11883
- FLIGHT CONDITIONS**  
Sixth Annual Workshop on Meteorological and Environmental Inputs to Aviation Systems, 26-28 October 1982, Tullahoma, Tenn p 174 A84-23424
- Identification of multivariable high-performance turbofan engine dynamics from closed loop data p 28 N84-20580
- FLIGHT CONTROL**  
Graphics enhanced computer emulation for improved timing-race and fault tolerance control system analysis --- of Centaur liquid-fuel booster  
[AIAA PAPER 83-2326] p 177 A84-10010
- Rotorcraft flight-propulsion control integration p 36 A84-46524
- FLIGHT HAZARDS**  
Performance degradation of propeller systems due to rime ice accretion  
[AIAA PAPER 82-0286] p 12 A84-17406
- Experimental study of performance degradation of a model helicopter main rotor with simulated ice shapes  
[AIAA PAPER 84-0184] p 13 A84-17937
- Experimental and analytical investigations into airfoil icing p 12 A84-45054
- Performance degradation of a model helicopter rotor with a generic ice shape p 14 A84-49096
- FLIGHT SIMULATION**  
Real-time Pegasus propulsion system model V/STOL-piloted simulation evaluation p 15 A84-17382
- Experimental investigation of shock-cell noise reduction for dual-stream nozzles in simulated flight comprehensive data report. Volume 1. Test nozzles and acoustic data  
[NASA-CR-168336-VOL-1] p 184 N84-24323
- Experimental investigation of shock-cell noise reduction for dual-stream nozzles in simulated flight comprehensive data report. Volume 2. Laser velocimeter data, static pressures and shadowgraph photos  
[NASA-CR-168336-VOL-2] p 184 N84-24324
- Experimental investigation of shock-cell noise reduction for single-stream nozzles in simulated flight, comprehensive data report. Volume 1. Test nozzles and acoustic data  
[NASA-CR-169234-VOL-1] p 185 N84-33148
- FLIGHT TESTS**  
Supersonic fan engines for military aircraft  
[AIAA PAPER 83-2541] p 15 A84-15206
- Flight and wind tunnel tests of an electro-impulse de-icing system  
[AIAA PAPER 84-2234] p 12 A84-39280
- Aeronautical propulsion Present status and future directions  
[NASA-TM-83589] p 1 N84-16119
- Ground correlation investigation of thruster spacecraft interactions to be measured on the IAPS flight test  
[NASA-TM-83598] p 47 N84-23691
- Fuel savings potential of the NASA Advanced Turboprop Program  
[NASA-TM-83736] p 35 N84-29878
- FLIP-FLOPS**  
Optical flip-flops and sequential logic circuits using a liquid crystal light valve p 158 A84-40332
- FLOW CHARACTERISTICS**  
On some flow characteristics of conventional and excited jets  
[AIAA PAPER 84-0532] p 181 A84-21304
- Investigation of mixing in a turbofan exhaust duct II Computer code application and verification p 17 A84-27140
- Application of a quasi-3D inviscid flow and boundary layer analysis to the hub-shroud contouring of a radial turbine  
[AIAA PAPER 84-1297] p 6 A84-44177
- Executive summary, aerothermal modeling program, phase 1  
[NASA-CR-174602] p 60 N84-12263
- Aerothermal modeling program, phase 1  
[NASA-CR-168243-VOL-2] p 60 N84-12265
- On some flow characteristics of conventional and excited jets  
[NASA-TM-83503] p 182 N84-13922
- Vortex generating flow passage design for increased film-cooling effectiveness and surface coverage --- aircraft engine blade cooling  
[NASA-TM-83617] p 126 N84-22909
- Application of a quasi-3D inviscid flow and boundary layer analysis to the hub-shroud contouring of a radial turbine  
[NASA-TM-83669] p 10 N84-25647
- FLOW DISTORTION**  
Inlet flow distortion in turbomachinery - Companion of theory and experiment in a transonic fan stage p 3 A84-13592
- Companion of experimental and computational compressible flow in a S-duct  
[AIAA PAPER 84-0033] p 4 A84-19228
- The production of turbulent stress in a shear flow by irrotational fluctuations p 115 A84-21390
- FLOW DISTRIBUTION**  
Turbulent flow field calculations in an internal combustion engine equipped with two valves p 112 A84-13311
- Turbulence measurements in confined jets using a rotating single-wire probe technique p 113 A84-13564
- Computation of viscous flow in curved ducts and companion with experimental data  
[AIAA PAPER 84-0531] p 115 A84-21303
- Flow visualization and interpretation of visualization data for deflected thrust V/STOL nozzles  
[AIAA PAPER 84-0102] p 16 A84-21852
- Calculation of a hollow-cone liquid spray in a uniform air stream  
[AIAA PAPER 84-1322] p 118 A84-35171
- Analysis of inviscid and viscous flows in cascades with an explicit multiple-grid algorithm  
[AIAA PAPER 84-1663] p 5 A84-38043
- On modeling dilution jet flowfields  
[AIAA PAPER 84-1379] p 121 A84-44183
- Application of laser anemometry in turbine engine research  
[NASA-TM-83513] p 131 N84-11456
- Computation of viscous flow in curved ducts and comparison with experimental data  
[NASA-TM-83548] p 122 N84-13494
- Flow visualization and interpretation of visualization data for deflected thrust V/STOL nozzles  
[NASA-TM-83554] p 24 N84-14147
- Assessment of three-dimensional inviscid codes and loss calculations for turbine aerodynamic computations  
[NASA-TM-83571] p 8 N84-16142
- Turbulence characteristics of swirling flowfields  
[NASA-CR-175392] p 124 N84-19744
- Numerical modeling of turbulent flow p 125 N84-20538
- Random vortex method for combustor flows p 62 N84-20558
- Vortex generating flow passage design for increased film cooling effectiveness  
[NASA-CASE-LEW-14039-1] p 126 N84-20782
- Analysis of inviscid and viscous flows in cascades with an explicit multiple-grid algorithm  
[NASA-TM-83636] p 1 N84-22527
- The boundary layer on compressor cascade blades  
[NASA-CR-173514] p 127 N84-25001
- Holographic aids for internal combustion engine flow studies  
[NASA-TM-83681] p 132 N84-25017
- On modeling dilution jet flowfields p 32 N84-25713
- Acoustic excitation: A promising new means of controlling shear layers  
[NASA-TM-83772] p 10 N84-31096
- Summary of recent NASA propeller research  
[NASA-TM-83733] p 2 N84-32344
- Investigation of the three-dimensional flow field within a transonic fan rotor Experiment and analysis  
[NASA-TM-83739] p 11 N84-32357
- FLOW EQUATIONS**  
A direct method for the solution of unsteady two-dimensional incompressible Navier-Stokes equations p 2 A84-10078
- An implicit LU scheme for the Euler equations applied to arbitrary cascades --- new method of factoring  
[AIAA PAPER 84-0167] p 4 A84-17925
- Multiple-grid convergence acceleration of viscous and inviscid flow computations p 116 A84-23950
- Aerodynamic effect of combustor inlet-air pressure on fuel jet atomization  
[AIAA PAPER 84-1320] p 120 A84-36973
- Aerodynamic effect of combustor inlet-air pressure on fuel jet atomization  
[NASA-TM-83611] p 126 N84-22910
- Numerical aspects of unsteady flow calculations p 128 N84-25968
- FLOW GEOMETRY**  
Turbulent boundary-layer flow and structure on a convex wall and its redevelopment on a flat wall p 115 A84-21378
- On the design of contractions and settling chambers for optimal turbulence manipulations in wind tunnels  
[AIAA PAPER 84-0535] p 115 A84-22922
- Developing flow in S-shaped ducts p 116 A84-28709
- Stability and structure of stretched vortices  
[AD-A142913] p 117 A84-29798
- Turbulence modeling for three-dimensional shear flows over curved rotating bodies p 122 A84-48138
- FLOW MEASUREMENT**  
Turbulence measurements in confined jets using a rotating single-wire probe technique p 113 A84-13564
- Three-dimensional flowfield inside a low-speed axial flow compressor rotor p 3 A84-13574
- Three-dimensional turbulent boundary-layer development on a fan rotor blade p 3 A84-17437
- Structure of nonevaporating sprays - Measurements and predictions  
[AIAA PAPER 84-0125] p 114 A84-17897
- Accuracy and directional sensitivity of the single-wire technique p 130 A84-18047
- Acoustic power dissipation on radiation through duct terminations - Experiments p 180 A84-21272
- Developing flow in S-shaped ducts p 116 A84-28709
- Output statistics of laser anemometers in sparsely seeded flows p 117 A84-28738
- Turbulence measurements in a complex flowfield using a crossed hot-wire  
[AIAA PAPER 84-1604] p 131 A84-37999
- An experimental study of the compressor rotor blade boundary layer  
[ASME PAPER 84-GT-193] p 7 A84-46991
- Investigation of the three-dimensional flow field within a transonic fan rotor - Experiment and analysis  
[ASME PAPER 84-GT-200] p 7 A84-46995
- End-wall boundary layer measurements in a two-stage fan p 26 N84-16208
- Random vortex method for combustor flows p 62 N84-20558

- Detailed flow measurements in casing boundary layer of 429-meter-per-second-tip-speed two-stage fan [NASA-TP-2052] p 34 N84-28795
- The structure of evaporating and combusting sprays Measurements and predictions [NASA-CR-173778] p 128 N84-29155
- Free jet feasibility study of a thermal acoustic shield concept for AST/VCE application: Single stream nozzles [NASA-CR-3758] p 185 N84-29661
- FLOW STABILITY**
- Sound generated by instability waves of supersonic flows. I - Two-dimensional mixing layers II - Axisymmetric jets p-181 A84-24597
- Stability and structure of stretched vortices [AD-A142913] p 117 A84-29798
- Three-dimensional stability of an elliptical vortex in a straining field [AD-A146317] p 120 A84-38557
- Basic experimental study of the coupling between flow instabilities and incident sound [NASA-CR-3789] p 183 N84-21275
- FLOW THEORY**
- The application of vortex theory to the optimum swept propeller [AIAA PAPER 84-0036] p 3 A84-17841
- Gas flow across a wet screen - Analogy to a relief valve with hysteresis p 121 A84-43548
- Inlet boundary layer effects in an axial compressor rotor. II - Throughflow effects [ASME PAPER 84-GT-85] p 7 A84-46927
- FLOW VELOCITY**
- Streamwise computation of three-dimensional parabolic flows p 113 A84-16828
- Secondary effects in combustion instabilities leading to flashback p 58 A84-17436
- Structure of particle-laden jets - Measurements and predictions [AIAA PAPER 84-0038] p 113 A84-17842
- A technique combining the visibility of a Doppler signal with the peak intensity of the pedestal to measure the size and velocity of droplets in a spray [AIAA PAPER 84-0203] p 129 A84-17946
- An invariant derivation of flame stretch p 58 A84-18925
- Application of laser anemometry in turbine engine research p 130 A84-22872
- Further time-mean measurements in confined swirling flows p 116 A84-27138
- Swirl flow turbulence modeling [AIAA PAPER 84-1376] p 118 A84-35196
- Velocity and temperature characteristics of two-stream, coplanar jet exhaust plumes [AIAA PAPER 84-2205] p 21 A84-46108
- Correlation of flight effects on centerline velocity decay for cold-flow acoustically excited jets [NASA-TM-83502] p 182 N84-11883
- Experimental investigation of shock-cell noise reduction for dual-stream nozzles in simulated flight comprehensive data report. Volume 2 Laser velocimeter data, static pressures and shadowgraph photos [NASA-CR-168336-VOL-2] p 184 N84-24324
- The boundary layer on compressor cascade blades [NASA-CR-173514] p 127 N84-25001
- Three component velocity measurements using Fabry-Perot interferometer [NASA-TM-83692] p 133 N84-26010
- Velocity and temperature characteristics of two-stream, coplanar jet exhaust plumes [NASA-TM-83730] p 34 N84-28790
- Analysis and testing of a new method for drop size measurement using laser scatter interferometry [NASA-CR-174636] p 133 N84-31595
- Experimental investigation of shock-cell noise reduction for single-stream nozzles in simulated flight, comprehensive data report. Volume 2 Laser velocimeter data [NASA-CR-168234-VOL-2] p 186 N84-33149
- FLOW VISUALIZATION**
- Secondary effects in combustion instabilities leading to flashback p 58 A84-17436
- Flow visualization and interpretation of visualization data for deflected thrust V/STOL nozzles [AIAA PAPER 84-0102] p 16 A84-21852
- Comparison of visualized turbine endwall secondary flows and measured heat transfer patterns [ASME PAPER 83-GT-83] p 117 A84-33703
- Measurement of fluid properties using rapid-double-exposure and time-average holographic interferometry [AIAA PAPER 84-1461] p 130 A84-35223
- Flow visualization and interpretation of visualization data for deflected thrust V/STOL nozzles [NASA-TM-83554] p 24 N84-14147
- Measurement of fluid properties using rapid-double-exposure and time-average holographic interferometry [NASA-TM-83630] p 132 N84-21849
- Holographic aids for internal combustion engine flow studies [NASA-TM-83681] p 132 N84-25017
- Dilution jets in accelerated cross flows [NASA-CR-174717] p 34 N84-28794
- Preliminary experiments on phase conjugation for flow visualization — barium titanate single crystals [NASA-TM-83766] p 189 N84-32169
- Experimental investigation of shock-cell noise reduction for single-stream nozzles in simulated flight, comprehensive data report. Volume 3: Shadowgraph photos and facility description [NASA-CR-168234-VOL-3] p 186 N84-33150
- FLUID DYNAMICS**
- Effect of location in an array on heat transfer to a short cylinder in crossflow p 119 A84-36150
- On-orbit cryogenic fluid transfer [AIAA PAPER 84-1343] p 44 A84-44176
- Design and performance of a fixed, nonaccelerating, guide vane cascade that operates over an inlet flow angle range of 60 deg [NASA-TM-83519] p 8 N84-14120
- Measurement of spray combustion processes p 61 N84-20530
- Preliminary design of two Space Shuttle fluid physics experiments [NASA-CR-174649] p 39 N84-23567
- Elastohydrodynamic lubrication Status of understanding p 144 N84-25048
- On-orbit cryogenic fluid transfer [NASA-TM-83688] p 39 N84-25753
- Mass transfer from a circular cylinder Effects of flow unsteadiness and slight nonuniformities [NASA-CR-174759] p 129 N84-32751
- An experimental investigation of gas jets in confined swirling air flow [NASA-CR-3832] p 36 N84-33412
- FLUID FILMS**
- Dynamics of two-phase face seals p 137 A84-28792
- A thermomechanical model for energy propagation in a solid-fluid-solid system with one boundary in relative motion [ASME PAPER 83-HT-97] p 137 A84-29092
- Assessment of two neglected effects in the analysis of an oil pumping ring seal [ASME PAPER 83-LUB-16] p 137 A84-29097
- FLUID FLOW**
- Heating experiments for flowability improvement of near-freezing aviation fuel p 89 A84-26955
- On numerical simulation of viscous flows p 122 A84-49112
- A viscous-inviscid interactive procedure for rotational flow in cascades of two-dimensional airfoils of arbitrary shape [NASA-CR-174609] p 7 N84-13149
- Combustion Fundamentals Research [NASA-CR-2309] p 27 N84-20525
- Application of improved numerical schemes p 178 N84-20537
- FLUID INJECTION**
- Structure of nonevaporating sprays - Measurements and predictions [AIAA PAPER 84-0125] p 114 A84-17897
- Experiments in dilution jet mixing p 122 A84-48140
- FLUID MANAGEMENT**
- On-orbit cryogenic fluid transfer [AIAA PAPER 84-1343] p 44 A84-44176
- Cryogenic Fluid Management Facility [AIAA PAPER 84-1340] p 44 A84-44184
- On-orbit cryogenic fluid transfer [NASA-TM-83688] p 39 N84-25753
- FLUID MECHANICS**
- Basic experimental study of the coupling between flow instabilities and incident sound [NASA-CR-3789] p 183 N84-21275
- Vortex generating flow passage design for increased film-cooling effectiveness and surface coverage — aircraft engine blade cooling [NASA-TM-83617] p 126 N84-22909
- Effects of unsteady free stream velocity and free stream turbulence on stagnation point heat transfer [NASA-CR-3804] p 127 N84-25943
- A semi-direct procedure using a local relaxation factor and its application to an internal flow problem [NASA-TM-83704] p 128 N84-25946
- Three component velocity measurements using Fabry-Perot interferometer [NASA-TM-83692] p 133 N84-26010
- Investigation of the three-dimensional flow field within a transonic fan rotor Experiment and analysis [NASA-TM-83739] p 11 N84-32357
- FLUID PRESSURE**
- Dynamics of two-phase face seals p 137 A84-28792
- FLUID-SOLID INTERACTIONS**
- A thermomechanical model for energy propagation in a solid-fluid-solid system with one boundary in relative motion [ASME PAPER 83-HT-97] p 137 A84-29092
- Gas flow across a wet screen - Analogy to a relief valve with hysteresis p 121 A84-43548
- FLUIDIZED BED PROCESSORS**
- AFB/open cycle gas-turbine-conceptual design study [NASA-CR-168135] p 172 N84-31784
- FLUORO COMPOUNDS**
- Synthesis of perfluoroalkylene dianilines [NASA-CR-168004] p 60 N84-11228
- FLUOROAMINES**
- Low wear partially fluorinated polyimides [NASA-TM-83629] p 84 N84-24808
- FLUTTER**
- Measurements of self-excited rotor-blade vibrations using optical displacements [ASME PAPER 83-GT-132] p 151 A84-33702
- NASTRAN flutter analysis of advanced turbopropellers [NASA-CR-167926] p 24 N84-14148
- Flutter of swept fan blades [NASA-TM-83547] p 154 N84-16587
- Formulation of blade-flutter spectral analyses in stationary reference frame [NASA-TP-2296] p 27 N84-20562
- Vibration and flutter of mistuned bladed-disk assemblies [NASA-TM-83634] p 156 N84-23923
- FLUTTER ANALYSIS**
- Flutter analysis of advanced turbopropellers p 152 A84-36492
- Aeroelastic analysis for propellers - mathematical formulations and program user's manual [NASA-CR-3729] p 153 N84-12530
- NASTRAN documentation for flutter analysis of advanced turbopropellers [NASA-CR-167927] p 25 N84-15153
- Flutter of swept fan blades [NASA-TM-83547] p 154 N84-16587
- Flutter and forced response of mistuned rotors using standing wave analysis [NASA-CR-173555] p 32 N84-24586
- FLUX DENSITY**
- Application of advanced materials to rotating machines p 22 N84-10063
- Some comments on longevity by a technologist p 45 N84-12247
- Development of a lightweight nickel electrode [NASA-TM-86861] p 172 N84-30528
- FLYWHEELS**
- Some comments on longevity by a technologist p 45 N84-12247
- FOAMS**
- Evaluation of propellant tank insulation concepts for low-thrust chemical propulsion systems: Executive summary [NASA-CR-168321] p 83 N84-20699
- FOIL BEARINGS**
- Bending fatigue of electron-beam-welded foils Application to a hydrodynamic air bearing in the Chrysler/DOE upgraded automotive gas turbine engine [NASA-TM-83539] p 155 N84-16589
- Durable solid lubricant coatings for foil gas bearings to 315 deg C [NASA-TM-83596] p 83 N84-19567
- FORCED CONVECTION**
- Correlation of thermophoretically-modified small particle diffusional deposition rates in forced convection systems with variable properties, transpiration cooling and/or viscous dissipation p 117 A84-32323
- Forced convection heat transfer to air/water vapor mixtures [NASA-CR-3769] p 123 N84-16488
- Engineering correlations of variable-property effects on laminar forced convection mass transfer for dilute vapor species and small particles in air [NASA-CR-168322] p 124 N84-18578
- FORCED VIBRATION**
- Forced response of a cantilever beam with a dry friction damper attached I - Theory. II - Experiment p 150 A84-21267
- NASTRAN forced vibration analysis of rotating cyclic structures [ASME PAPER 83-DET-20] p 151 A84-29103
- The interaction between mistuning and friction in the forced response of bladed disk assemblies [ASME PAPER 84-GT-139] p 152 A84-46957
- Forced vibration analysis of rotating cyclic structures in NASTRAN [NASA-CR-165429] p 153 N84-11514

- Finite element forced vibration analysis of rotating cyclic structures  
[NASA-CR-165430] p 153 N84-11515
- Vibration and flutter of mistuned bladed-disk assemblies  
[NASA-TM-83634] p 156 N84-23923
- Flutter and forced response of mistuned rotors using standing wave analysis  
[NASA-CR-173555] p 32 N84-24586
- NASTRAN forced vibration analysis of rotating cyclic structures  
[NASA-CR-173821] p 157 N84-29252
- FORECASTING**  
Trends of jet fuel demand and properties p 90 N84-23631
- FORGING**  
Fabrication development for ODS-superalloy, air-cooled turbine blades  
[NASA-CR-174650] p 32 N84-25711
- FORTTRAN**  
A generalized computer code for developing dynamic gas turbine engine models (DIGTEM)  
[NASA-TM-83508] p 22 N84-12166
- FOURIER TRANSFORMATION**  
FTIR analysis of aviation fuel deposits  
[NASA-TM-83773] p 92 N84-33608
- FRACTOGRAPHY**  
Fracture surface characteristics of notched angleplied graphite/epoxy composites  
[NASA-TM-83786] p 57 N84-33522
- FRACTURE MECHANICS**  
Compositional effects on Si<sub>3</sub>N<sub>4</sub> fracture surfaces p 79 A84-19794
- Edge delamination in angle-ply composite laminates p 52 A84-21515
- Elasticity solutions for a class of composite laminate problems with stress singularities p 53 A84-33389
- Wide range weight functions for the strip with a single edge crack  
[NASA-TM-83478] p 153 N84-11512
- Aeronautics and Space Engineering Board Aeronautics Assessment Committee  
[NASA-TM-85594] p 93 N84-22771
- The impact resistance of SiC and other mechanical properties of SiC and Si<sub>3</sub>N<sub>4</sub>  
[NASA-CR-165325] p 84 N84-24809
- Creep-rupture behavior of candidate Stirling engine alloys after long-term aging at 760 deg C in low-pressure hydrogen  
[NASA-TM-83676] p 73 N84-25793
- Progressive fracture of fiber composites  
[NASA-TM-83701] p 56 N84-27831
- Simplified composite micromechanics equations for strength, fracture toughness and environmental effects  
[NASA-TM-83696] p 56 N84-27832
- Hygrothermomechanical fracture stress criteria for fiber composites with sense-parity  
[NASA-TM-83691] p 57 N84-28918
- Failure analysis of plasma-sprayed thermal barrier coatings  
[NASA-TM-83777] p 75 N84-31347
- FRACTURE STRENGTH**  
Development of plane strain fracture toughness test for ceramics using Chevron notched specimens p 77 A84-11676
- Thermal stress fracture of ceramic coatings p 80 A84-24553
- Microstructure, strength, and oxidation of a 10 wt pct zirconia-Si<sub>3</sub>N<sub>4</sub> ceramic p 80 A84-25402
- Factors influencing the thermally-induced strength degradation of B/Al composites p 52 A84-28227
- Sinterability, strength and oxidation of alpha silicon carbide powders p 80 A84-32306
- Simplified composite micromechanics equations for strength, fracture toughness and environmental effects p 53 A84-11858
- Off-axis tensile properties and fracture in a unidirectional graphite/polymide composite (Celion 6000/PMR 15) p 53 A84-43553
- Dynamic stress analysis of smooth and notched fiber composite flexural specimens  
[NASA-TM-83694] p 56 N84-25770
- Progressive fracture of fiber composites  
[NASA-TM-83701] p 56 N84-27831
- Simplified composite micromechanics equations for strength, fracture toughness and environmental effects  
[NASA-TM-83696] p 56 N84-27832
- High temperature ceramic interface study  
[NASA-CR-174728] p 197 N84-34331
- FRACTURES (MATERIALS)**  
Nonlinear Structural Analysis  
[NASA-CR-2297] p 157 N84-31688
- Inelastic and dynamic fracture and stress analyses p 158 N84-31697
- Fracture modes in notched angleplied composite laminates  
[NASA-TM-83802] p 58 N84-34576
- FRAMES**  
Design concepts for low-cost composite engine frames  
[NASA-TM-83544] p 25 N84-16186
- FREE CONVECTION**  
Thermacoustic convection heat-transfer phenomenon p 120 A84-38857
- FREE ELECTRON LASERS**  
Orbital stability in combined uniform axial and three-dimensional wiggler magnetic fields for free-electron lasers  
[NASA-TM-83753] p 134 N84-30273
- FREE FLOW**  
Effect of geometry on airfoil icing characteristics p 12 A84-37935
- FREE JETS**  
Three component velocity measurements using Fabry-Perot interferometer  
[NASA-TM-83692] p 133 N84-26010
- FREEZING**  
Qualification testing of solar photovoltaic powered refrigerator freezers for medical use in remote geographic locations  
[NASA-CR-168181] p 169 N84-25162
- FREQUENCIES**  
Engineering calculations for communications satellite systems planning  
[NASA-CR-173532] p 38 N84-23662
- Vibration and flutter of mistuned bladed-disk assemblies  
[NASA-TM-83634] p 156 N84-23923
- Test results for 27.5- to 30-GHz communications satellite receivers  
[NASA-TM-83662] p 100 N84-27954
- FREQUENCY ASSIGNMENT**  
The subjective effect of multiple co-channel frequency modulated television interference  
[NASA-TM-83415] p 97 N84-11360
- Test results for 27.5- to 30-GHz communications satellite receivers  
[NASA-TM-83662] p 100 N84-27954
- FREQUENCY DIVISION MULTIPLE ACCESS**  
A frequency-division multiple-access system concept for 30/20 GHz high-capacity domestic satellite service p 94 A84-22141
- Economic comparison of FDMA and TDMA options for communications by Ka-band multiple beam satellites  
[AIAA PAPER 84-0740] p 94 A84-25299
- FREQUENCY REUSE**  
Concept for advanced satellite communications and required technologies p 93 A84-15626
- Phased-array-fed antenna configuration study, volume 2 p 98 N84-16424
- FREQUENCY SHIFT KEYING**  
Serial MSK modem for the Advanced Communications Satellite Program p 93 A84-15629
- FRICION**  
Surface chemistry, friction, and wear of Ni-Zn and Mn-Zn ferrites in contact with metals p 78 A84-13516
- Surface roughness effects with solid lubricants dispersed in mineral oils  
[ASLE PREPRINT 83-LC-4C-1] p 137 A84-28987
- Tribological characteristics of gold films deposited on metals by ion plating and vapor deposition  
[NASA-TM-83572] p 69 N84-17352
- Water-vapor effects on friction of magnetic tape in contact with nickel-zinc ferrite  
[NASA-TP-2279] p 82 N84-18399
- Fictional and morphological properties of Au-MoS<sub>2</sub> films sputtered from a compact target  
[NASA-TM-83604] p 143 N84-20858
- Characterization and measurement of polymer wear  
[NASA-TM-83628] p 83 N84-21739
- Tribology in the 80's. Volume 1: Sessions 1 to 4  
[NASA-CR-2300-VOL-1] p 144 N84-23891
- Metallic adhesion and bonding p 72 N84-23897
- The strength of the metal Aluminum oxide interface p 72 N84-23898
- Considerations in friction and wear p 144 N84-23903
- Tribology in the 80's. Volume 2: Sessions 5 - 8  
[NASA-CR-2300-VOL-2] p 144 N84-25047
- Tribological applications of surface analysis  
[NASA-TM-83707] p 51 N84-25766
- Effect of substrate chemical pretreatment on the tribological properties of graphite films  
[NASA-TM-83574] p 85 N84-25831
- Evaluation of two polyimides and of an improved liner retention design for self-lubricating bushings  
[NASA-TM-83719] p 86 N84-27887
- Erosion of iron-chromium alloys by glass particles  
[NASA-TP-2354] p 75 N84-28965
- Properties of ferrites important to their friction and wear behavior  
[NASA-TM-83718] p 87 N84-28994
- Automotive Stirling engine development program  
[NASA-CR-174622] p 195 N84-32305
- Microstructure and surface chemistry of amorphous alloys important to their friction and wear behavior  
[NASA-TM-83762] p 76 N84-32508
- The friction behavior of semiconductors Si and GaAs in contact with pure metals  
[NASA-TM-83779] p 87 N84-32531
- Optical and other property changes of M-50 bearing steel surfaces for different lubricants and additive prior to scuffing  
[NASA-TM-83746] p 88 N84-34620
- FRICION MEASUREMENT**  
Selection of burn-resistant materials for oxygen-driven turbopumps  
[AIAA PAPER 84-1287] p 43 A84-35157
- Measurement of rolling friction by a damped oscillator  
[NASA-TP-2257] p 141 N84-13577
- Friction behavior of silicon in contact with titanium, nickel, silver and copper  
[NASA-TP-2362] p 88 N84-33590
- FRICION REDUCTION**  
Forced response of a cantilever beam with a dry friction damper attached I - Theory. II - Experiment p 150 A84-21267
- Special cases of friction and applications  
[NASA-TM-83523] p 141 N84-11500
- Lubrication of machine elements  
[NASA-RP-1126] p 147 N84-31640
- Friction behavior of silicon in contact with titanium, nickel, silver and copper  
[NASA-TP-2362] p 88 N84-33590
- FUEL CELLS**  
Pore size engineering applied to the design of separators for nickel-hydrogen cells and batteries p 162 A84-30187
- Economic competitiveness of fuel cell on-site integrated energy systems  
[NASA-TM-83403] p 164 N84-10665
- Develop and test fuel cell powered on-site integrated total energy systems Phase 3. Full-scale power plant development  
[NASA-CR-168294] p 164 N84-13672
- Heat recovery subsystem and overall system integration of fuel cell on-site integrated energy systems  
[NASA-CR-168309] p 166 N84-20915
- Method of making a light weight battery plaque  
[NASA-CASE-LEW-13349-1] p 72 N84-22734
- Develop and test fuel cell powered on-site integrated total energy systems  
[NASA-CR-174714] p 170 N84-27329
- Electrochemical storage p 171 N84-29342
- FUEL COMBUSTION**  
Combustion in a turbulent mixing layer formed at a rearward-facing step p 58 A84-10140
- Evaporation and combustion of sprays p 58 A84-11636
- NASA/General Electric Broad-Specification Fuels Combustion Technology Program - Phase I p 16 A84-24033
- NASA advanced low emissions combustor program  
[ASME PAPER 83-JPGC-GT-10] p 17 A84-28982
- Recovery of burner acoustic source structure from far-field sound spectra  
[AIAA PAPER 83-0763] p 181 A84-32609
- Role of fuel chemical properties on combustor radiative heat load  
[AIAA PAPER 84-1493] p 89 A84-35236
- A review of internal combustion engine combustion chamber process studies at NASA Lewis Research Center  
[AIAA PAPER 84-1316] p 121 A84-40242
- Investigation of sources, properties and preparation of distillate test fuels  
[NASA-CR-168227] p 89 N84-13332
- Broad specification fuels combustion technology program  
[NASA-CR-168179] p 89 N84-15283
- Advanced Gas Turbine (AGT) technology development  
[NASA-CR-168235] p 141 N84-15554
- Aviation-fuel property effects on combustion  
[NASA-CR-168334] p 89 N84-17407
- The role of surface generated radicals in catalytic combustion p 61 N84-20555
- Transient flow combustion p 62 N84-20560
- Heat pipes to reduce engine exhaust emissions  
[NASA-CASE-LEW-12590-1] p 143 N84-22958
- A review of internal combustion engine combustion chamber process studies at NASA Lewis Research Center  
[NASA-TM-83666] p 127 N84-24999

- A critical review of noise production models for turbulent, gas-fueled burners  
[NASA-CR-3803] p 184 N84-26384
- Development of carbon slurry fuels for transportation (hybrid fuels, phase 2)  
[NASA-CR-174659] p 74 N84-28960
- ### FUEL CONSUMPTION
- New perspectives for advanced automobile diesel engines  
p 138 A84-30062
- DOE/NASA Automotive Stirling Engine Project Overview  
p 138 A84-30069
- Catalog of selected heavy duty transport energy management models  
[NASA-CR-168299] p 194 N84-14991
- Trends of jet fuel demand and properties  
p 90 N84-23631
- Study of effects of fuel properties in turbine-powered business aircraft  
[NASA-CR-174627] p 91 N84-25854
- Develop and test fuel cell powered on-site integrated total energy systems  
[NASA-CR-174714] p 170 N84-27329
- Wind turbine generator interaction with conventional diesel generators on Block Island, Rhode Island' Volume 1: Executive summary  
[NASA-CR-168318] p 171 N84-29357
- Energy efficient engine program contributions to aircraft fuel conservation  
[NASA-TM-83741] p 34 N84-29876
- Baseline performance and emissions data for a single-cylinder, direct-injected diesel engine  
[NASA-TM-66873] p 197 N84-34330
- ### FUEL CONTROL
- Heat pipes to reduce engine exhaust emissions  
[NASA-CASE-LEW-12590-1] p 143 N84-22958
- ### FUEL FLOW
- Vapor flow into a capillary propellant-acquisition device  
p 43 A84-36559
- ### FUEL INJECTION
- Role of fuel chemical properties on combustor radiative heat load  
[AIAA PAPER 84-1493] p 89 A84-35236
- Aerodynamic effect of combustor inlet-air pressure on fuel jet atomization  
[AIAA PAPER 84-1320] p 120 A84-36973
- Experimental study of the operating characteristics of premixing-prevaporizing fuel/air mixing passages  
[NASA-CR-168279] p 23 N84-14143
- Aerodynamic effect of combustor inlet-air pressure on fuel jet atomization  
[NASA-TM-83611] p 126 N84-22910
- Heat pipes to reduce engine exhaust emissions  
[NASA-CASE-LEW-12590-1] p 143 N84-22958
- Flame propagation in heterogeneous mixtures of fuel drops and air  
[NASA-CR-174644] p 91 N84-23775
- ### FUEL OILS
- Flame propagation in heterogeneous mixtures of fuel drops and air  
[NASA-CR-174644] p 91 N84-23775
- ### FUEL PRODUCTION
- Assessment of Alternative Aircraft Fuels  
[NASA-CP-2307] p 30 N84-23630
- Trends of jet fuel demand and properties  
p 90 N84-23631
- ### FUEL SPRAYS
- Evaporation and combustion of sprays  
p 58 A84-11636
- A technique combining the visibility of a Doppler signal with the peak intensity of the pedestal to measure the size and velocity of droplets in a spray  
[AIAA PAPER 84-0203] p 129 A84-17946
- Alcohol cold starting - A theoretical study  
p 138 A84-30061
- Analytic modeling of a spray diffusion flame  
[AIAA PAPER 84-1317] p 118 A84-35168
- Calculation of a hollow-cone liquid spray in a uniform air stream  
[AIAA PAPER 84-1322] p 118 A84-35171
- Development of the phase/Doppler spray analyzer for liquid drop size and velocity characterizations  
[AIAA PAPER 84-1199] p 131 A84-36958
- Experimental study of the operating characteristics of premixing-prevaporizing fuel/air mixing passages  
[NASA-CR-168279] p 23 N84-14143
- Combustion characteristics in the transition region of liquid fuel sprays  
[NASA-CR-175396] p 61 N84-19495
- Combustion Fundamentals Research  
[NASA-CP-2309] p 27 N84-20525
- Fuel spray diagnostics  
p 125 N84-20527
- Development and implementation of advanced diagnostic techniques  
p 132 N84-20528
- Measurement of spray combustion processes  
p 61 N84-20530
- Automatic holographic droplet analysis for liquid fuel sprays  
p 125 N84-20531
- Predictions of spray combustion interactions  
p 61 N84-20532
- Detailed fuel spray analysis techniques  
p 127 N84-24747
- ### FUEL SYSTEMS
- Study of a LH2-fueled topping cycle engine for aircraft propulsion  
[AIAA PAPER 83-2543] p 15 A84-15207
- Emission FTIR analyses of thin microscopic patches of jet fuel residue deposited on heated metal surface  
[NASA-CR-168331] p 90 N84-17410
- Assessment of Alternative Aircraft Fuels  
[NASA-CP-2307] p 30 N84-23630
- ### FUEL TANKS
- In-flight atmospheric and fuel tank temperature measurements  
p 90 N84-23643
- Advanced onboard storage concepts for natural gas-fueled automotive vehicles  
[NASA-CR-174655] p 172 N84-34036
- ### FUEL TESTS
- Deposit formation and heat transfer in hydrocarbon rocket fuels  
[AIAA PAPER 84-0512] p 88 A84-18142
- Development of carbon slurry fuels for transportation (hybrid fuels, phase 2)  
[NASA-CR-174659] p 74 N84-28960
- ### FUEL-AIR RATIO
- Experimental study of the operating characteristics of premixing-prevaporizing fuel/air mixing passages  
[NASA-CR-168279] p 23 N84-14143
- Detailed fuel spray analysis techniques  
p 127 N84-24747
- ### FUELS
- Group-type hydrocarbon standards for high-performance liquid chromatographic analysis of middistillate fuels  
[NASA-TP-2317] p 90 N84-23774
- ### FUNCTIONAL DESIGN SPECIFICATIONS
- Status of understanding for gear materials  
p 144 N84-25061
- Qualification testing of solar photovoltaic powered refrigerator freezers for medical use in remote geographic locations  
[NASA-CR-168181] p 169 N84-25162
- Propulsion issues for advanced orbit transfer vehicles  
[NASA-TM-83624] p 47 N84-25762
- Evaluation of two polyimides and of an improved liner retention design for self-lubricating bushings  
[NASA-TM-83719] p 86 N84-27887
- Propulsion issues for advanced orbit transfer vehicles  
p 48 N84-29937
- ### FUSION (MELTING)
- Multicolor printing plate joining  
[NASA-CASE-LEW-13598-1] p 132 N84-22930
- ## G
- ### GALILEO PROJECT
- A high energy stage for the National Space Transportation System  
[NASA-TM-83795] p 38 N84-32411
- ### GALLIUM ARSENIDES
- A Ka-band GaAs monolithic phase shifter  
p 101 A84-18371
- Effect of electron flux on radiation damage in GaAs solar cells  
p 160 A84-22998
- Photovoltaic characteristics of diffused P+/N bulk GaAs solar cells  
p 161 A84-23115
- Microwave monolithic integrated circuit development for future spaceborne phased array antennas  
[AIAA PAPER 84-0656] p 94 A84-25257
- Diffused junction p(-)-n solar cells in bulk GaAs I  
Fabrication and cell performance p 161 A84-26027
- Diffused junction p(+)-n solar cells in bulk GaAs. II - Device characterization and modelling  
p 161 A84-26028
- 0.5 W 2-21 GHz monolithic GaAs distributed amplifier  
p 103 A84-30857
- GaAs dual-gate FET for operation up to K-band  
p 104 A84-32281
- A K-band GaAs FET amplifier with 8.2-W output power  
p 104 A84-32290
- Interaction between boron and intrinsic defects in GaAs  
p 190 A84-33918
- NASA seeking high-power 60-GHz IMPATT diodes  
p 104 A84-44912
- A 20-GHz IMPATT transmitter  
[NASA-CR-168076] p 106 N84-11385
- Microwave monolithic integrated circuit development for future spaceborne phased array antennas  
[NASA-TM-83518] p 97 N84-13399
- 30/20 GHz spacecraft GaAs FET solid state transmitter for trunking and customer-premise-service application  
[NASA-CR-168276] p 107 N84-16463
- LEC GaAs for integrated circuit applications  
[NASA-CR-173287] p 191 N84-17014
- Design considerations for a monolithic, GaAs, dual-mode, GPSK/QASK, high-throughput rate transceiver  
[NASA-CR-173550] p 110 N84-24974
- Optimal design of GaAs-based concentrator space solar cells for 100 AMO, 80 deg C operation  
p 170 N84-29312
- The friction behavior of semiconductors Si and GaAs in contact with pure metals  
[NASA-TM-83779] p 87 N84-32531
- ### GAS BEARINGS
- Feasibility analysis of a spiral groove ring seal for counter-rotating shafts  
p 139 A84-45966
- Dynamic behavior of spiral-groove and Rayleigh-Step self-acting face seals  
[NASA-TP-2266] p 25 N84-16181
- Durable solid lubricant coatings for foil gas bearings to 315 deg C  
[NASA-TM-83596] p 83 N84-19567
- Improved compliant hydrodynamic fluid journal bearing  
[NASA-CASE-LEW-13670-1] p 143 N84-22958
- ### GAS COMPOSITION
- Combustion gas properties of various fuels of interest to gas turbine engines  
[NASA-TM-83682] p 31 N84-24584
- ### GAS COOLING
- Evaluation of gas cooling for pressurized phosphoric acid fuel cell stacks  
p 163 A84-30199
- Evaluation of gas-cooled pressurized phosphoric acid fuel cells for electric utility power generation  
[NASA-CR-168298] p 169 N84-25165
- ### GAS DYNAMICS
- A numerical model of acoustic choking. I - Shock free solutions  
p 180 A84-21251
- Transient flow analysis of the AEDC/HPDE MHI generator  
p 189 A84-24041
- Time dependent wave envelope finite difference analysis of sound propagation  
[NASA-TM-83744] p 185 N84-32111
- ### GAS EXCHANGE
- Oxygen diffusion in alpha-Al2O3  
[NASA-TM-83622] p 86 N84-28991
- ### GAS FLOW
- Vapor flow into a capillary propellant-acquisition device  
p 43 A84-36559
- Gas flow across a wet screen - Analogy to a relief valve with hysteresis  
p 121 A84-43541
- GCKP84-general chemical kinetics code for gas-phase flow and batch processes including heat transfer effect  
[NASA-TP-2320] p 63 N84-32441
- ### GAS IONIZATION
- Radical and ion molecule mechanisms in the polymerization of hydrocarbons and chlorosilanes in RF plasmas at low pressures (1.0 torr)  
[NASA-TM-83602] p 190 N84-2132
- ### GAS JETS
- An experimental investigation of gas jets in confine swirling air flow  
[NASA-CR-3832] p 36 N84-3341
- ### GAS MIXTURES
- Forced convection heat transfer to air/water vapor mixtures  
[NASA-CR-3769] p 123 N84-1648
- ### GAS SPECTROSCOPY
- Acoustically-induced modulation spectroscopy for ultra-sensitive gas analysis  
[AIAA PAPER 84-1460] p 131 A84-3698
- ### GAS TEMPERATURE
- Dynamic gas temperature measurement system, volume 1  
[NASA-CR-168267-VOL-1] p 132 N84-1652
- ### GAS TURBINE ENGINES
- Combustor development for automotive gas turbines  
p 135 A84-1049
- Ferrographic and spectrometer oil analysis from a failed gas turbine engine  
p 135 A84-1127
- High-temperature fatigue in metals - A brief review of life prediction methods developed at the Lewis Research Center of NASA  
p 64 A84-1428
- Ceramic composite liner material for gas turbine combustors  
[AIAA PAPER 84-0363] p 78 A84-1804
- Calculations of turbulent mass transport in a bluff-body diffusion-flame combustor  
[AIAA PAPER 84-0372] p 114 A84-1804
- Simplified analytical procedures for representative material cyclic response - for high temperature gas turbine engine analysis  
p 16 A84-2287
- Ceramic components for the AGT 100 engine  
p 136 A84-2287

- NASA/General Electric Broad-Specification Fuels Combustion Technology Program - Phase I p 16 A84-24033
- Liquid chromatographic analysis of a formulated ester from a gas-turbine engine test [ASLE PREPRINT 83-LC-1A-1] p 80 A84-28895
- Aerodynamic effects of moveable sidewall nozzle geometry and rotor exit restriction on the performance of a radial turbine [SAE PAPER 831517] p 17 A84-29460
- Detonation wave augmentation of gas turbines [AIAA PAPER 84-1266] p 18 A84-37639
- Heat pipe applications in aircraft propulsion [AIAA PAPER 84-1269] p 18 A84-37640
- Degradation mechanisms of ceramic thermal barrier coatings in corrosive environments p 81 A84-42668
- The application of LQR synthesis techniques to the turbohaft engine control problem [AIAA PAPER 84-1455] p 21 A84-44185
- The interaction between mistuning and friction in the forced response of bladed disk assemblies [ASME PAPER 84-GT-139] p 152 A84-46957
- Experiments in dilution jet mixing p 122 A84-48140
- Low strain, long life creep fatigue of AF2-IDA and INCO 718 [NASA-CR-167989] p 66 N84-10268
- Research and development program for the development of advanced time-temperature dependent constitutive relationships Volume 2 Programming manual [NASA-CR-168191-VOL-2] p 153 N84-10614
- Executive summary, aerothermal modeling program, phase 1 [NASA-CR-174602] p 60 N84-12263
- Aerothermal modeling program, phase 1 [NASA-CR-168243-VOL-2] p 60 N84-12265
- A review of NASA combustor and turbine heat transfer research [NASA-TM-83541] p 24 N84-14146
- Broad specification fuels combustion technology program [NASA-CR-168179] p 89 N84-15283
- Digital computer program for generating dynamic turbofan engine models (DIGTEM) [NASA-TM-83446] p 26 N84-16185
- Program for development of strain tolerant thermal barrier coating system [NASA-CR-173214] p 82 N84-16337
- Dynamic gas temperature measurement system, volume 1 [NASA-CR-168267-VOL-1] p 132 N84-16529
- Bending fatigue of electron-beam-welded foils Application to a hydrodynamic air bearing in the Chrysler/DOE upgraded automotive gas turbine engine [NASA-TM-83539] p 155 N84-16589
- Aviation-fuel property effects on combustion [NASA-CR-168334] p 89 N84-17407
- Engine cyclic durability by analysis and material testing [NASA-TM-83577] p 155 N84-18683
- Combustion Fundamentals Research [NASA-CP-2309] p 27 N84-20525
- Error reduction program A progress report p 27 N84-20536
- Numerical modeling of turbulent flow p 125 N84-20538
- Analysis of a topping-cycle, aircraft, gas-turbine-engine system which uses cryogenic fuel [NASA-TP-2294] p 28 N84-21549
- Overview of zirconia with respect to gas turbine applications [NASA-TP-2286] p 83 N84-21740
- Proceedings of the 20th Automotive Technology Development Contractors' Coordination Meeting [NASA-CR-173412] p 143 N84-21877
- Elevated temperature biaxial fatigue [NASA-CR-173473] p 156 N84-21905
- Tip cap for a rotor blade [NASA-CASE-LEW-13654-1] p 28 N84-22560
- Oxidizing seal for a turbine tip gas path [NASA-CASE-LEW-14053-1] p 29 N84-22563
- Improved compliant hydrodynamic fluid journal bearing [NASA-CASE-LEW-13670-1] p 143 N84-22959
- Assessment of Alternative Aircraft Fuels [NASA-CP-2307] p 30 N84-23630
- Combustor liner construction [NASA-CASE-LEW-14035-1] p 30 N84-24577
- Sensor failure detection for jet engines using analytical redundancy [NASA-TM-83695] p 31 N84-24585
- Detailed fuel spray analysis techniques p 127 N84-24747
- Real-time simulation of an automotive gas turbine using the hybrid computer [NASA-TM-83593] p 195 N84-26484
- Dilution jet mixing program [NASA-CR-174624] p 33 N84-26702
- Advanced Gas Turbine (AGT) Technology Project [NASA-CR-174629] p 146 N84-28089
- Overview of advanced Stirling and gas turbine engine development programs and implications for solar thermal electrical applications p 146 N84-28231
- Energy efficient engine Turbine intermediate case and low-pressure turbine component test hardware detailed design report [NASA-CR-167973] p 33 N84-28789
- Advanced Gas Turbine (AGT) [NASA-CR-174694] p 195 N84-29805
- PURDU-WINCOF: A computer code for establishing the performance of a fan-compressor unit with water ingestion [NASA-CR-168005] p 34 N84-29875
- Atomization of liquid sheets in high pressure airflow [NASA-TM-83731] p 128 N84-30223
- Nonlinear Structural Analysis [NASA-CP-2297] p 157 N84-31688
- Nonlinear analysis for high-temperature composites: Turbine blades/vanes p 158 N84-31699
- Three-dimensional stress analysis using the boundary element method p 159 N84-31700
- Turbine blade and vane heat flux sensor development, phase 1 [NASA-CR-168297] p 134 N84-32790
- Air modulation apparatus [NASA-CASE-LEW-13524-1] p 35 N84-33410
- Understanding the roles of the strategic element cobalt in nickel base superalloys p 76 N84-33471
- GAS TURBINES**
- Residual stress in plasma-sprayed ceramic turbine tip and gas-path seal specimens p 78 A84-19783
- Comparison between measured turbine stage performance and the predicted performance using quasi-3D flow and boundary layer analyses [AIAA PAPER 84-1299] p 18 A84-36972
- Application of a quasi-3D inviscid flow and boundary layer analysis to the hub-shroud contouring of a radial turbine [AIAA PAPER 84-1297] p 6 A84-44177
- Comparisons of rational engineering correlations of thermophoretically-augmented particle mass transfer with STANS-predictions for developing boundary layers [ASME PAPER 84-GT-158] p 92 A84-46965
- Advanced Gas Turbine (AGT) Power-train system development [NASA-CR-168056] p 140 N84-10581
- Aerothermal modeling, phase 1 Volume 1 Model assessment [NASA-CR-168296-VOL-1] p 25 N84-15155
- Advanced Gas Turbine (AGT) technology development [NASA-CR-168235] p 141 N84-15554
- Aeronautical propulsion. Present status and future directions [NASA-TM-83589] p 1 N84-16119
- Comparisons of rational engineering correlations of thermophoretically-augmented particle mass transfer with STANS-predictions for developing boundary layers [NASA-CR-168221] p 93 N84-19606
- Modeling of dilution jet flowfields p 126 N84-20547
- Extension to an analysis of turbulent swirling compressible flow for application to axisymmetric small gas turbine ducts [NASA-CR-165597] p 195 N84-21445
- Dual clearance squeeze film damper [NASA-CASE-LEW-13506-1] p 29 N84-22562
- Comparison between measured turbine stage performance and the predicted performance using quasi-3D flow and boundary layer analyses [NASA-TM-83640] p 29 N84-22584
- Investigation of the effects of pressure gradient, temperature and wall temperature ratio on the stagnation point heat transfer for circular cylinders and gas turbine vanes [NASA-CR-174687] p 30 N84-23649
- Combustion gas properties of various fuels of interest to gas turbine engineers [NASA-TM-83682] p 31 N84-24584
- Application of a quasi-3D inviscid flow and boundary layer analysis to the hub-shroud contouring of a radial turbine [NASA-TM-83669] p 10 N84-25647
- Unsteady flow in turbomachinery: An overview p 128 N84-25961
- AFB/open cycle gas turbine conceptual design study [NASA-CR-168135] p 172 N84-31784
- Mass transfer from a circular cylinder: Effects of flow unsteadiness and slight nonuniformities [NASA-CR-174769] p 129 N84-32751
- GAS-LIQUID INTERACTIONS**
- Modeling of zero gravity venting [NASA-CR-173503] p 127 N84-23854
- GAS-METAL INTERACTIONS**
- Reaction of cobalt in SO<sub>2</sub> atmospheres at elevated temperatures p 65 A84-33440
- GASOLIN (FUEL)**
- Alcohol cold starting - A theoretical study p 138 A84-30061
- GATES (CIRCUITS)**
- GaAs dual-gate FET for operation up to K-band p 104 A84-32281
- The 30-GHz monolithic receive module [NASA-CR-168326] p 99 N84-20737
- GEAR TEETH**
- Precision of spiral-bevel gears [ASME PAPER 82-WA/DE-33] p 135 A84-15950
- Efficiency of nonstandard and high contact ratio involute spur gears [NASA-TM-83725] p 146 N84-29223
- Lubricant jet flow phenomena in spur and helical gears with modified center distances and/or addendums for out-of-mesh conditions [NASA-TM-83723] p 146 N84-29224
- GEARS**
- Precision of spiral-bevel gears [ASME PAPER 82-WA/DE-33] p 135 A84-15950
- Kinematic precision of gear trains [ASME PAPER 82-WA/DE-34] p 135 A84-15951
- Advanced propfan drive system characteristics and technology needs [AIAA PAPER 84-1194] p 18 A84-36957
- An analytical method to predict efficiency of aircraft gearboxes [AIAA PAPER 84-1500] p 20 A84-44180
- Development of large rotorcraft transmissions p 21 A84-46354
- Status of understanding for gear materials p 144 N84-25061
- An analytical method to predict efficiency of aircraft gearboxes [NASA-TM-83716] p 2 N84-25606
- Dynamics of early planetary gear trains [NASA-CR-3793] p 145 N84-26027
- Parameter studies of gear cooling using an automatic finites element mesh generator [NASA-TM-83721] p 146 N84-28087
- An investigation of the transient thermal analysis of spur gears [NASA-TM-83724] p 146 N84-28088
- Efficiency of nonstandard and high contact ratio involute spur gears [NASA-TM-83725] p 146 N84-29223
- Lubricant jet flow phenomena in spur and helical gears with modified center distances and/or addendums for out-of-mesh conditions [NASA-TM-83723] p 146 N84-29224
- Summary of drive-train component technology in helicopters [NASA-TM-83726] p 147 N84-30294
- GENERAL AVIATION AIRCRAFT**
- Design of a high-performance rotary stratified-charge research aircraft engine [AIAA PAPER 84-1395] p 17 A84-35204
- GEOMETRIC RECTIFICATION (IMAGERY)**
- Development of Great Lakes algorithms for the Nimbus-G coastal zone color scanner [NASA-CR-173511] p 159 N84-27258
- GEOMETRICAL OPTICS**
- Stress measurement in thin films by geometrical optics p 130 A84-28797
- GEOMETRY**
- First order ball bearing kinematics [NASA-TM-83592] p 142 N84-19816
- GEOS 2 SATELLITE**
- Comparison of thermal plasma observations on SCATHA and GEOS p 41 N84-17262
- GEOSYNCHRONOUS ORBITS**
- NASA's geostationary communications platform program [AIAA PAPER 84-0702] p 95 A84-25326
- The role of potential barrier formation in spacecraft charging p 41 N84-17269
- Spectrum/orbit utilization program for geostationary satellites [NASA-TM-83759] p 100 N84-30146
- Design guidelines for assessing and controlling spacecraft charging effects [NASA-TP-2361] p 42 N84-33452
- GLAZES**
- Results of an experimental program investigating the effects of simulated ice on the performance of the NACA 63A15 airfoil with flap [NASA-CR-168288] p 8 N84-16145
- GLOBAL AIR SAMPLING PROGRAM**
- Simultaneous cabin and ambient ozone measurements on two Boeing 747 airplanes. Volume 2. January to October 1978 [NASA-TM-81733] p 193 N84-22488

- Tabulations of ozonesonde data, 1963 - 1980  
[NASA-CR-174631] p 174 N84-27375  
Climatology of ozone at altitudes from 19,000 to 59,000 feet based on combined GASP and ozonesonde data  
[NASA-TP-2303] p 174 N84-31865
- GOLD COATINGS**  
The X-ray photoelectron spectroscopy depth profiling and in biological characterization of ion-plated gold on various metals p 50 A84-20465  
Tribological characteristics of gold films deposited on metals by ion plating and vapor deposition  
[NASA-TM-83572] p 69 N84-17352  
Functional and morphological properties of Au-MoS<sub>2</sub> films sputtered from a compact target  
[NASA-TM-83604] p 143 N84-20858  
Chromium electrodes for REDOX cells  
[NASA-CASE-LEW-13653-1] p 170 N84-28205  
Adhesion between polymers and evaporated gold and nickel films  
[NASA-TP-2360] p 87 N84-31379
- GOVERNMENT PROCUREMENT**  
Government - contractor interaction  
[AD-P002768] p 193 N84-23315
- GOVERNMENT/INDUSTRY RELATIONS**  
Government - contractor interaction  
[AD-P002768] p 193 N84-23315
- GRAIN BOUNDARIES**  
Grain-boundary phases in hot-pressed silicon nitride containing Y<sub>2</sub>O<sub>3</sub> and CeO<sub>2</sub> additives p 79 A84-19793  
Literature survey on oxidations and fatigue lives at elevated temperatures  
[NASA-CR-174639] p 71 N84-20674
- GRAPHITE**  
Processing of fused silicide coatings for carbon-based materials p 51 A84-19780  
Intercalated graphite electrical conductors p 105 N84-10064  
Beam impingement angle effects on secondary electron emission characteristics of textured pyrolytic graphite  
[NASA-TP-2285] p 82 N84-18400  
Effect of substrate chemical pretreatment on the tribological properties of graphite films  
[NASA-TM-83574] p 85 N84-25831
- GRAPHITE-EPOXY COMPOSITES**  
Select fiber composites for space applications: A mechanistic assessment p 55 N84-22702  
Fracture surface characteristics of notched angle-plyed graphite/epoxy composites  
[NASA-TM-83786] p 57 N84-33522
- GRAPHITE-POLYIMIDE COMPOSITES**  
The effect of a coating on the thermo-oxidative stability of Celion 6000 graphite fiber/PMR 15 polyimide composites p 52 A84-21844  
Off-axis tensile properties and fracture in a unidirectional graphite/polyimide composite (Celion 6000/PMR 15) p 53 A84-43553  
Evaluation of two polyimides and of an improved liner retention design for self-lubricating bushings  
[NASA-TM-83719] p 86 N84-27887
- GRAVITATIONAL EFFECTS**  
Gravitational effects in dendritic growth p 37 A84-22346  
Thermoacoustic convection heat-transfer phenomenon p 120 A84-38857  
Effect of gravity on halogenated hydrocarbon flame retardant effectiveness  
[NASA-TM-83761] p 63 N84-33536
- GREAT LAKES (NORTH AMERICA)**  
Development of Great Lakes algorithms for the Nimbus-G coastal zone color scanner  
[NASA-CR-173511] p 159 N84-27258
- GREEN'S FUNCTIONS**  
High frequency green function for aerodynamic noise in moving media. I - General theory II - Noise from a spreading jet p 180 A84-21273
- GRIT**  
Abrasive tip treatment for use on compressor blades  
[NASA-CR-174666] p 145 N84-25065
- GROOVES**  
Feasibility analysis of a spiral groove ring seal for counter-rotating shafts p 139 A84-45865
- GROUND STATIONS**  
Modular approach for satellite communication ground terminals  
[NASA-CR-168327] p 98 N84-16425  
Photovoltaic power system for satellite Earth stations in remote areas: Project status and design description  
[NASA-TM-83789] p 101 N84-33642
- GUIDE VANES**  
Design and performance of a fixed, nonaccelerating, guide vane cascade that operates over an inlet flow angle range of 60 deg  
[NASA-TM-83519] p 8 N84-14120  
V/STOL model fan stage ng design report  
[NASA-CR-174688] p 29 N84-23629
- Energy efficient engine: Turbine intermediate case and low-pressure turbine component test hardware detailed design report  
[NASA-CR-167973] p 33 N84-28789
- GUN LAUNCHERS**  
Investigation of the residue in an electric rail gun employing a plasma armature p 103 A84-32046
- H**
- HAFNIUM COMPOUNDS**  
RF sputtered silicon and hafnium nitrides as applied to 440C steel  
[NASA-TM-86662] p 87 N84-32536
- HALL EFFECT**  
Experimental investigation of a Hall-current thruster  
[NASA-CR-168133] p 46 N84-18321
- HARDNESS**  
Erosion of iron-chromium alloys by glass particles  
[NASA-TP-2354] p 75 N84-28965  
Deposition of diamondlike carbon films  
[NASA-CASE-LEW-14080-1] p 86 N84-28986
- HEART VALVES**  
Prediction of turbulent flow past a prosthetic heart valve p 175 A84-49108
- HEAT**  
An assessment of advanced technology for industrial cogeneration  
[NASA-CR-173456] p 167 N84-22001
- HEAT EXCHANGERS**  
High effectiveness liquid droplet/gas heat exchanger for space power applications  
[IAF PAPER 83-433] p 42 A84-11819  
Use of cooling air heat exchangers as replacements for hot section strategic materials  
[AIAA PAPER 83-2540] p 15 A84-15205
- HEAT FLUX**  
A review of NASA combustor and turbine heat transfer research  
[NASA-TM-83541] p 24 N84-14146  
Advanced high temperature heat flux sensors  
[NASA-TM-83526] p 123 N84-18493  
Effects of broadened property fuels on radiant heat flux to gas turbine combustor liners  
[NASA-TM-83537] p 123 N84-18494  
Investigation of the effects of pressure gradient, temperature and wall temperature ratio on the stagnation point heat transfer for circular cylinders and gas turbine vanes  
[NASA-CR-174667] p 30 N84-23649  
Performance of thermal barrier coatings in high heat flux environments  
[NASA-TM-83663] p 72 N84-24772  
Turbine blade and vane heat flux sensor development, phase 1  
[NASA-CR-168297] p 134 N84-32790
- HEAT PIPES**  
Heat pipe applications in aircraft propulsion  
[AIAA PAPER 84-1269] p 18 A84-37640
- HEAT PUMPS**  
Measurement of heat pump processes induced by laser radiation  
[NASA-CR-168324] p 134 N84-18620  
Overview of NASA Lewis Research Center free-piston Stirling engine activities  
[NASA-TM-83649] p 195 N84-22512
- HEAT RESISTANT ALLOYS**  
The development of directional coarsening of the gamma-prime precipitate in superalloy single crystals p 63 A84-10597  
The effect of microstructure on 650 C fatigue crack growth in P/M Astroloy p 63 A84-12395  
The effects of frequency and hold times on fatigue crack propagation rates in a nickel base superalloy p 64 A84-18733  
A simple application of the Bailey-Orowan creep model to Fe-39.8 at. pct Al and gamma/gamma prime - alpha p 64 A84-22012  
Carbides in iron-rich Fe-Mn-Cr-Mo-Al-Si-C systems p 64 A84-25815  
The effects of Cr, Al, Ti, Mo, W, Ta, and Nb on the cyclic oxidation behavior of cast Ni-base superalloys at 1100 and 1150 C p 65 A84-27485  
Creep-rupture behavior of six candidate Stirling engine superalloys tested in air p 65 A84-36173  
Effects of processing and microstructure on the fatigue behaviour of the nickel-base superalloy Rene95 p 66 A84-48715  
Fatigue crack growth and low cycle fatigue of two nickel base superalloys  
[NASA-CR-174534] p 68 N84-10267  
Replacing critical and strategic refractory metal elements in nickel-base superalloys - NASA's COSAM program  
[NASA-TM-83528] p 67 N84-13264
- Creep fatigue of low-cobalt superalloys Waspalloy, PM U 700 and wrought U 700 p 67 N84-13265  
Effects of cobalt in nickel-base superalloys  
[NASA-CR-168308] p 67 N84-14287  
Complexities of high temperature metal fatigue. Some steps toward understanding p 154 N84-14541  
Arc spray fabrication of metal matrix composite monolayer - high temperature fiber-reinforced superalloy composites p 54 N84-15203  
Evaluation of CO<sub>2</sub> and CO dopants in hydrogen to reduce hydrogen permeation in the Stirling engine heater head tube alloy CG-27 p 68 N84-15246  
[NASA-TM-83535] p 68 N84-15246  
Preliminary study of thermomechanical fatigue of polycrystalline MAR-M 200 p 69 N84-17350  
[NASA-TP-2280] p 69 N84-17350  
Factors which influence directional coarsening of Gamma prime during creep in nickel-base superalloy single crystals p 69 N84-17353  
Influence of composition on the microstructure and mechanical properties of a nickel-base superalloy single crystal p 70 N84-17354  
[NASA-TM-83563] p 70 N84-17354  
Influence of cobalt, tantalum and tungsten on the high temperature mechanical properties of single crystal nickel-base superalloys p 70 N84-17355  
[NASA-TM-83479] p 70 N84-17355  
Analysis of thermoelectric properties of high-temperature complex alloys of nickel-base, iron-base and cobalt-base groups p 70 N84-18370  
[NASA-TP-2278] p 70 N84-18370  
Mechanism of corrosion of Ni base superalloys by molten Na<sub>2</sub>MoO<sub>4</sub> at elevated temperatures p 70 N84-20672  
[NASA-TM-83580] p 70 N84-20672  
Literature survey on oxidations and fatigue lives at elevated temperatures p 71 N84-20674  
[NASA-CR-174639] p 71 N84-20674  
Fabrication development for ODS-superalloy, air-cooled turbine blades p 32 N84-25711  
[NASA-CR-174650] p 32 N84-25711  
Effects of alloy composition on cyclic flame hot-corrosion attack of cast nickel-base superalloys at 900 deg C p 73 N84-26783  
[NASA-TP-2338] p 73 N84-26783  
P/M superalloys: A troubled adolescent? p 73 N84-26785  
[NASA-TM-83623] p 73 N84-26785  
Coating with overlay metallic-cermet alloy systems  
[NASA-CASE-LEW-13639-2] p 73 N84-27855  
Chemical mechanisms and reaction rates for the initiation of hot corrosion of IN-738 p 74 N84-28958  
[NASA-TP-2319] p 74 N84-28958  
Oxidation and corrosion resistance of candidate Stirling engine heater-head-tube alloys p 74 N84-28962  
[NASA-TM-83509] p 74 N84-28962  
Nonlinear analysis for high-temperature composites p 158 N84-31699  
Turbine blades/vanes p 158 N84-31699  
Understanding the roles of the strategic element cobalt in nickel base superalloys p 76 N84-33471  
Low cycle fatigue behavior of conventionally cast MAR-M 200 AT 1000 deg C p 77 N84-33564  
[NASA-TM-83769] p 77 N84-33564  
Evaluation of candidate Stirling engine heater tube alloys after 3500 hours exposure to high pressure doped hydrogen or helium p 77 N84-34803  
[NASA-TM-83782] p 77 N84-34803
- HEAT SHIELDING**  
Free jet feasibility study of a thermal acoustic shield concept for AST/VCE application: Single stream nozzles p 185 N84-29661  
[NASA-CR-3758] p 185 N84-29661
- HEAT STORAGE**  
High-temperature molten salt thermal energy storage systems for solar applications p 185 N84-15879  
[NASA-CR-167916] p 185 N84-15879
- HEAT TRANSFER**  
Residual stress in plasma-sprayed ceramic turbine tip and gas-path seal specimens p 78 A84-19783  
Flame radiation and linear heat transfer in a tubular can combustor p 16 A84-21300  
[AIAA PAPER 84-0443] p 16 A84-21300  
Comparison of visualized turbine endwall secondary flows and measured heat transfer patterns p 117 A84-33703  
[ASME PAPER 83-GT-83] p 117 A84-33703  
Length to diameter ratio and row number effects in short pin fin heat transfer p 118 A84-33706  
[ASME PAPER 83-GT-54] p 118 A84-33706  
Effect of location in an array on heat transfer to a short cylinder in crossflow p 119 A84-36150  
Flat plate heat transfer for laminar transition and turbulent boundary layers using a shock tube p 120 A84-37467  
[AIAA PAPER 84-1726] p 120 A84-37467



- Heat transfer in thermal barrier coated rods with circumferential and radial temperature gradients  
[ASME PAPER 84-GT-181] p 121 A84-46982
- Deposit formation and heat transfer in hydrocarbon rocket fuels  
[NASA-CR-168277] p 45 N84-12225
- Flame radiation and liner heat transfer in a tubular-can combustor  
[NASA-TM-83538] p 23 N84-13188
- A review of NASA combustor and turbine heat transfer research  
[NASA-TM-83541] p 24 N84-14146
- Experimental and theoretical deposition rates from salt-seeded combustion gases of a Mach 0.3 burner  
[NASA-TP-2225] p 124 N84-19741
- Evaluation of propellant tank insulation concepts for low-thrust chemical propulsion systems  
[NASA-CR-168320] p 46 N84-20634
- Review and status of heat-transfer technology for internal passages of air-cooled turbine blades  
[NASA-TP-2232] p 126 N84-21826
- Effect of a rotor wake on heat transfer from a circular cylinder  
[NASA-TM-83613] p 126 N84-21832
- Tip cap for a rotor blade  
[NASA-CASE-LEW-13654-1] p 28 N84-22560
- Heat pipes to reduce engine exhaust emissions  
[NASA-CASE-LEW-12590-1] p 143 N84-22558
- Investigation of the effects of pressure gradient, temperature and wall temperature ratio on the stagnation point heat transfer for circular cylinders and gas turbine vanes  
[NASA-CR-174667] p 30 N84-23649
- Evaluation of gas-cooled pressurized phosphoric acid fuel cells for electric utility power generation  
[NASA-CR-168298] p 169 N84-25169
- Effects of unsteady free stream velocity and free stream turbulence on stagnation point heat transfer  
[NASA-CR-3804] p 127 N84-25943
- Turbulence and surface heat transfer near the stagnation point of a circular cylinder in turbulent flow  
[NASA-TM-83732] p 128 N84-29157
- GCKP84-general chemical kinetics code for gas-phase flow and batch processes including heat transfer effects  
[NASA-TP-2320] p 63 N84-32446
- Mass transfer from a circular cylinder: Effects of flow unsteadiness and slight nonuniformities  
[NASA-CR-174759] p 129 N84-32751
- HEAT TRANSFER COEFFICIENTS**  
Internal heat transfer coefficients of porous metals  
p 112 A84-13239
- Heat transfer distributions around nominal ice accretion shapes formed on a cylinder in the NASA Lewis long Research Tunnel  
[AIAA PAPER 84-0017] p 113 A84-17834
- Measurements of local convective heat transfer coefficients on ice accretion shapes  
[AIAA PAPER 84-0018] p 113 A84-17835
- Effect of an oscillating flow direction on leading edge heat transfer  
p 117 A84-33705
- Heat transfer distributions around nominal ice accretion shapes formed on a cylinder in the NASA Lewis icing research tunnel  
[NASA-TM-83557] p 123 N84-14463
- Measurement of local convective heat transfer coefficients of four ice accretion shapes  
[NASA-CR-174680] p 10 N84-25646
- HEAT TREATMENT**  
Method for strengthening boron fibers  
[NASA-CASE-LEW-13826-2] p 55 N84-24711
- HEATING**  
Heating experiments for flowability improvement of near-freezing aviation fuel  
p 89 A84-26955
- Heat recovery subsystem and overall system integration of fuel cell on-site integrated energy systems  
[NASA-CR-168309] p 166 N84-20915
- Evaluation of candidate Stirling engine heater tube alloys after 3500 hours exposure to high pressure doped hydrogen or helium  
[NASA-TM-83782] p 77 N84-34603
- HEATING EQUIPMENT**  
Heat pipe applications in aircraft propulsion  
[AIAA PAPER 84-1269] p 18 A84-37640
- HELICOPTER CONTROL**  
The application of LQR synthesis techniques to the turboshaft engine control problem  
[AIAA PAPER 84-1455] p 21 A84-44185
- Rotorcraft flight-propulsion control integration  
p 36 A84-46524
- HELICOPTER DESIGN**  
Development of large rotorcraft transmissions  
p 21 A84-46354
- Transmission efficiency measurements and correlations with physical characteristics of the lubricant  
[NASA-TM-83740] p 147 N84-30293
- Summary of drive-train component technology in helicopters  
[NASA-TM-83726] p 147 N84-30294
- HELICOPTER ENGINES**  
Powerplant design for one-engine-inoperative operation  
p 19 A84-40787
- The application of LQR synthesis techniques to the turboshaft engine control problem  
[AIAA PAPER 84-1455] p 21 A84-44185
- NASA transmission research and its probable effects on helicopter transmission design  
p 139 A84-46355
- HELICOPTER PERFORMANCE**  
Experimental study of performance degradation of a model helicopter main rotor with simulated ice shapes  
[AIAA PAPER 84-0184] p 13 A84-17937
- Performance degradation of a model helicopter main rotor in hover and forward flight with a generic ice shape  
[AIAA PAPER 84-0609] p 13 A84-24195
- Performance degradation of a model helicopter rotor with a generic ice shape  
p 14 A84-49096
- HELICOPTER PROPELLER DRIVE**  
Summary of drive-train component technology in helicopters  
[NASA-TM-83726] p 147 N84-30294
- HELICOPTERS**  
Helicopter rotor performance degradation in natural icing encounter  
p 12 A84-17412
- Contingency power concepts for helicopter turboshaft engine  
[NASA-TM-83679] p 30 N84-23648
- Rotorcraft contingency power study  
[NASA-CR-174675] p 31 N84-24580
- Helicopter engine core noise  
p 185 N84-29676
- HELIUM**  
Evaluation of candidate Stirling engine heater tube alloys after 3500 hours exposure to high pressure doped hydrogen or helium  
[NASA-TM-83782] p 77 N84-34603
- HELMHOLTZ EQUATIONS**  
Volume integrals associated with the inhomogeneous Helmholtz equation Part 1: Ellipsoidal region  
[NASA-CR-3749] p 148 N84-14525
- Volume integrals associated with the inhomogeneous Helmholtz equation Part 2: Cylindrical region, rectangular region  
[NASA-CR-3750] p 148 N84-14526
- HEURISTIC METHODS**  
Communications network design and costing model technical manual  
[NASA-CR-168236] p 97 N84-14376
- HIGH FREQUENCIES**  
High frequency green function for aerodynamic noise in moving media. I - General theory II - Noise from a spreading jet  
p 180 A84-21273
- Lightweight, high-frequency transformers  
p 105 N84-10066
- High-current, high-frequency capacitors  
p 105 N84-10067
- Parametric analysis of hollow conductor parallel and coaxial transmission lines for high frequency space power distribution  
[NASA-TM-83601] p 46 N84-20639
- Development of high frequency low weight power magnetics for aerospace power systems  
[NASA-TM-83656] p 109 N84-22892
- HIGH PRESSURE**  
Characteristics of Si<sub>3</sub>N<sub>4</sub>-SiO<sub>2</sub>-Ce<sub>2</sub>O<sub>3</sub> compositions sintered in high-pressure nitrogen  
p 79 A84-19913
- Test verification of LOX/RP-1 high-pressure fuel/oxidizer-nch preburner designs  
p 42 A84-22134
- Emission FTIR analyses of thin microscopic patches of jet fuel residue deposited on heated metal surface  
[NASA-CR-168331] p 90 N84-17410
- Cathode degradation and erosion in high pressure arc discharges  
[NASA-TM-83638] p 47 N84-22631
- Investigation of the effects of pressure gradient, temperature and wall temperature ratio on the stagnation point heat transfer for circular cylinders and gas turbine vanes  
[NASA-CR-174667] p 30 N84-23649
- Energy efficient engine high-pressure turbine supersonic cascade technology report  
[NASA-CR-165567] p 33 N84-27739
- Energy efficient engine high-pressure turbine detailed design report  
[NASA-CR-165608] p 33 N84-28788
- Creep-rupture behavior of candidate Stirling engine iron superalloys in high-pressure hydrogen. Volume 2. Hydrogen creep-rupture behavior  
[NASA-CR-174705] p 74 N84-28861
- Evaluation of candidate Stirling engine heater tube alloys after 3500 hours exposure to high pressure doped hydrogen or helium  
[NASA-TM-83782] p 77 N84-34603
- HIGH REYNOLDS NUMBER**  
The boundary layer on compressor cascade blades  
[NASA-CR-173514] p 127 N84-25001
- HIGH SPEED**  
A possible explanation for the present difference between linear noise theory and experimental data for supersonic helical tip speed propellers  
[NASA-TM-83467] p 183 N84-14874
- Dataflow computing approach in high-speed digital simulation  
[NASA-CR-173552] p 176 N84-25336
- HIGH STRENGTH ALLOYS**  
Carbides in iron-nickel-Fe-Mn-Cr-Mo-Al-Si-C systems  
p 84 A84-26815
- HIGH TEMPERATURE**  
Correlation of compressive and shear stress with spalling of plasma-sprayed ceramic materials  
p 79 A84-19784
- Application of laser anemometry in turbine engine research  
[NASA-TM-83513] p 131 N84-11456
- Emission FTIR analyses of thin microscopic patches of jet fuel residue deposited on heated metal surface  
[NASA-CR-168331] p 90 N84-17410
- Elevated temperature biaxial fatigue  
[NASA-CR-173473] p 155 N84-21905
- Effects of long-time elevated temperature exposures on hot-isostatically-pressed power-metallurgy Udimet 700 alloys with reduced cobalt contents  
[NASA-TM-83632] p 57 N84-28917
- Advanced high temperature materials for the energy efficient automotive Stirling engine  
[NASA-TM-83659] p 75 N84-28963
- Improved high temperature resistant matrix resins  
[NASA-CR-168210] p 87 N84-28995
- Negative electrode catalyst for the iron-chromium REDOX energy storage system  
[NASA-CASE-LEW-14028-1] p 172 N84-32909
- Overlay metallic-cermet alloy coating systems  
[NASA-CASE-LEW-13639-1] p 77 N84-33555
- Low cycle fatigue behavior of conventionally cast MAR-M 200 AT 1000 deg C  
[NASA-TM-83769] p 77 N84-33564
- HIGH TEMPERATURE ENVIRONMENTS**  
Silicon carbide, a high temperature semiconductor  
p 190 A84-17823
- Algorithms for elasto-plastic-creep postbuckling  
p 152 A84-38480
- Thermal oxidation of 3C silicon carbide single-crystal layers on silicon  
p 191 A84-48620
- Silicon carbide, a high temperature semiconductor  
[NASA-TM-83514] p 191 N84-14932
- Performance of thermal barrier coatings in high heat flux environments  
[NASA-TM-83663] p 72 N84-24772
- HIGH TEMPERATURE GASES**  
A temperature correlation for the radiation resistance of a thick-walled circular duct exhausting a hot gas  
p 181 A84-31103
- Fluid shielding of high-velocity jet noise  
[NASA-TP-2259] p 183 N84-15894
- HIGH TEMPERATURE LUBRICANTS**  
Overview of liquid lubricants for advanced aircraft  
[NASA-TM-83529] p 81 N84-11296
- Status and new directions for solid lubricant coatings and composite materials  
p 85 N84-25055
- HIGH TEMPERATURE RESEARCH**  
Reaction of cobalt in SO<sub>2</sub> atmospheres at elevated temperatures  
p 65 A84-33440
- Analysis of thermoelectric properties of high-temperature complex alloys of nickel-base, iron-base and cobalt-base groups  
[NASA-TP-2278] p 70 N84-18370
- HIGH TEMPERATURE TESTS**  
The effects of frequency and hold times on fatigue crack propagation rates in a nickel base superalloy  
p 64 A84-18733
- The effects of Cr, Al, Ti, Mo, W, Ta, and Nb on the cyclic oxidation behavior of cast Ni-base superalloys at 1100 and 1150 C  
p 65 A84-27485
- Convective heat transfer studies at high temperatures with pressure gradient for inlet flow Mach number of 0.45  
[AIAA PAPER 84-1487] p 118 A84-35233
- Oxidation behavior of a thermal barrier coating  
p 65 A84-42667
- High temperature thermomechanical analysis of ceramic coatings  
p 152 A84-48565
- High-temperature cyclic oxidation data, volume 1  
[NASA-TM-83665] p 75 N84-31345
- HIGH VOLTAGES**  
Potentials in a plasma over a biased pinhole  
p 102 A84-20711
- Surface effects in high voltage silicon solar cells  
p 160 A84-23002
- Three-phase, high-voltage, high-frequency distributed bus system for advanced aircraft  
p 105 N84-10058



- Radiating dipole model of interference induced in spacecraft circuitry by surface discharges  
[NASA-TP-2240] p 40 N84-16247
- Dilute plasma coupling currents to a high voltage solar array in weak magnetic fields  
[NASA-TM-83687] p 47 N84-24708
- High voltage solar array models and Shuttle tile charging  
[AD-P002123] p 177 N84-26209
- Radiation tolerance of low resistivity, high voltage silicon solar cells p 170 N84-29318
- HISTORIES**
- Determination of the key parameters affecting historic communications satellite trends  
[NASA-TM-83633] p 99- N84-25908
- HOLDERS**
- Method and apparatus for gripping uniaxial fibrous composite materials  
[NASA-CASE-LEW-13758-1] p 56 N84-27829
- HOLOGRAPHIC INTERFEROMETRY**
- The use of heterodyne speckle photogrammetry to measure high-temperature strain distributions p 130 A84-28623
- HOLOGRAPHY**
- Window aberration correction in laser velocimetry using multifaceted holographic optical elements p 134 A84-24663
- Measurement of fluid properties using rapid-double-exposure and time-average holographic interferometry  
[AIAA PAPER 84-1461] p 130<sup>\*</sup> A84-35223
- Automatic holographic droplet analysis for liquid fuel sprays p 125 N84-20531
- Measurement of fluid properties using rapid-double-exposure and time-average holographic interferometry  
[NASA-TM-83630] p 132 N84-21849
- Holographic aids for internal combustion engine flow studies  
[NASA-TM-83681] p 132 N84-25017
- HOT CORROSION**
- Degradation mechanisms of ceramic thermal barrier coatings in corrosive environments p 81 A84-42668
- Application of induction coil measurements to the study of superalloy hot corrosion and oxidation  
[NASA-TM-83560] p 69 N84-16311
- Investigation into the role of sodium chloride deposited on oxide and metal substrates in the initiation of hot corrosion  
[NASA-CR-173377] p 71 N84-20676
- Effects of surface chemistry on hot corrosion life  
[NASA-CR-174683] p 72 N84-24774
- Effects of alloy composition on cyclic flame hot-corrosion attack of cast nickel-base superalloys at 900 deg C  
[NASA-TP-29398] p 73 N84-26783
- Chemical mechanisms and reaction rates for the initiation of hot corrosion of IN-738  
[NASA-TP-2319] p 74 N84-28958
- High-temperature cyclic oxidation data, volume 1  
[NASA-TM-83665] p 75 N84-31345
- Deposition of Na<sub>2</sub>SO<sub>4</sub> from salt-seeded combustion gases of a high velocity burner rig  
[NASA-TM-83751] p 129 N84-31558
- HOT PRESSING**
- Grain-boundary phases in hot-pressed silicon nitride containing Y<sub>2</sub>O<sub>3</sub> and CeO<sub>2</sub> additives p 79 A84-19793
- Effects of processing and microstructure on the fatigue behaviour of the nickel-base superalloy Rene95 p 66 A84-48715
- Consolidation of Si<sub>3</sub>N<sub>4</sub> without additives (by hot isostatic pressing)  
[NASA-CR-173279] p 82 N84-17389
- HOT-WIRE ANEMOMETERS**
- Accuracy and directional sensitivity of the single-wire technique  
[AIAA PAPER 84-0367] p 130 A84-18047
- Turbulence measurements in a complex flowfield using a crossed hot-wire  
[AIAA PAPER 84-1604] p 131 A84-37999
- HOT-WIRE FLOWMETERS**
- Turbulence measurements in confined jets using a rotating single-wire probe technique p 113 A84-13564
- HOVERING**
- Documentation of ice shapes on the main rotor of a UH-1H helicopter in hover  
[NASA-CR-168332] p 9 N84-17139
- HUBS**
- Application of a quasi-3D inviscid flow and boundary layer analysis to the hub-shroud contouring of a radial turbine  
[AIAA PAPER 84-1297] p 6 A84-44177
- Application of a quasi-3D inviscid flow and boundary layer analysis to the hub-shroud contouring of a radial turbine  
[NASA-TM-83669] p 10 N84-25647

**HUMIDITY**

- Water-vapor effects on friction of magnetic tape in contact with nickel-zinc ferrite  
[NASA-TP-2279] p 82 N84-18399
- HYBRID CIRCUITS**
- Design considerations for FET-gated power transistors p 102 A84-18414
- Hybrid power semiconductor switch  
[NASA-CASE-LEW-13922-1] p 106 N84-11389
- HYBRID COMPUTERS**
- Real-time hybrid computer simulation of a small turboshaft engine and control system  
[NASA-TM-83579] p 28 N84-21548
- HYBRID PROPULSION**
- Optimization methods applied to hybrid vehicle design  
[NASA-CR-168292] p 194 N84-19185
- HYDRAULIC EQUIPMENT**
- Effects of volute geometry and impeller orbit on the hydraulic performance of a centrifugal pump p 136 A84-22316
- HYDROCARBON FUELS**
- Deposit formation and heat transfer in hydrocarbon rocket fuels  
[AIAA PAPER 84-0512] p 88 A84-18142
- Deposit formation and heat transfer in hydrocarbon rocket fuels  
[NASA-CR-168277] p 45 N84-12225
- HYDROCARBONS**
- Homogeneous reactions of hydrocarbons, silane, and chlorosilanes in radiofrequency plasmas at low pressures  
[NASA-TP-2301] p 50 N84-20643
- Radical and ion molecule mechanisms in the polymerization of hydrocarbons and chlorosilanes in RF plasmas at low pressures (1.0 torr)  
[NASA-TM-83602] p 190 N84-21329
- Group-type hydrocarbon standards for high-performance liquid chromatographic analysis of middistillate fuels  
[NASA-TP-2317] p 90 N84-23774
- Thermal and oxidative stabilities of liquid lubricants p 84 N84-23907
- Effect of gravity on halogenated hydrocarbon flame retardant effectiveness  
[NASA-TM-83761] p 63 N84-33536
- HYDRODYNAMICS**
- Design analysis of Rayleigh-step floating-ring seals [ASLE PREPRINT 83-LC-3B-2] p 137 A84-26989
- Dynamic behavior of spiral-groove and Rayleigh-Step self-acting face seals  
[NASA-TP-2266] p 25 N84-16181
- Hydrodynamic lubrication of rigid nonconformal contacts in combined rolling and normal motion  
[NASA-TM-83578] p 142 N84-17592
- Atomization of liquid sheets in high pressure airflow  
[NASA-TM-83731] p 128 N84-30223
- HYDROGEN**
- Evaluation of CO<sub>2</sub> and CO dopants in hydrogen to reduce hydrogen permeation in the Stirling engine heater head tube alloy CG-27  
[NASA-TM-83535] p 68 N84-15246
- Creep-rupture behavior of candidate Stirling engine iron superalloys in high-pressure hydrogen Volume 2. Hydrogen creep-rupture behavior  
[NASA-CR-174705] p 74 N84-28961
- Evaluation of candidate Stirling engine heater tube alloys after 3500 hours exposure to high-pressure doped hydrogen or helium  
[NASA-TM-83782] p 77 N84-34603
- HYDROGEN FUELS**
- Analysis of a topping-cycle, aircraft, gas-turbine-engine system which uses cryogenic fuel  
[NASA-TP-2294] p 28 N84-21549
- HYDROGEN OXYGEN ENGINES**
- The chemical kinetics and thermodynamics of sodium species in oxygen-rich hydrogen flames p 59 A84-27724
- NASA Orbit Transfer Rocket Engine Technology Program  
[NASA-CR-168156] p 48 N84-28901
- HYDROGEN OXYGEN FUEL CELLS**
- Design considerations for a 10-kW integrated hydrogen-oxygen regenerative fuel cell system  
[NASA-TM-83664] p 167 N84-23023
- Regenerative hydrogen-oxygen fuel cell-electrolyzer systems for orbital energy storage p 111 N84-33670
- HYDROXYL RADICALS**
- The role of surface generated radicals in catalytic combustion p 61 N84-20555
- HYGRAL PROPERTIES**
- Prediction of composite hygral behavior made simple p 51 A84-14285
- ICAN: Integrated composites analyzer  
[NASA-TM-83700] p 56 N84-26755

**HYGROSCOPICITY**

- Environmental and high strain rate effects on composites for engine applications p 51 A84-17444
- ICE**
- Potential flow analysis of glaze ice accretions on an airfoil  
[NASA-CR-168282] p 8 N84-16146
- Comparison of icing cloud instruments for 1982-1983 icing season flight program.  
[NASA-TM-83569] p 14 N84-29870
- ICE FORMATION**
- Performance degradation of propeller systems due to rime ice accretion  
[AIAA PAPER 82-0286] p 12 A84-17406
- Helicopter rotor performance degradation in natural icing encounter p 12 A84-17412
- Heat transfer distributions around nominal ice accretion shapes formed on a cylinder in the NASA Lewis Icing Research Tunnel  
[AIAA PAPER 84-0017] p 113 A84-17834
- Measurements of local convective heat transfer coefficients on ice accretion shapes  
[AIAA PAPER 84-0018] p 113 A84-17835
- Experimental study of performance degradation of a model helicopter main rotor with simulated ice shapes  
[AIAA PAPER 84-0184] p 13 A84-17937
- Performance degradation of a typical twin engine commuter type aircraft in measured natural icing conditions p 13 A84-21289
- Performance degradation of a model helicopter main rotor in hover and forward flight with a generic ice shape  
[AIAA PAPER 84-0609] p 13 A84-24195
- Effect of geometry on airfoil icing characteristics p 12 A84-37935
- Experimental and analytical investigations into airfoil icing p 12 A84-45054
- Performance degradation of a model helicopter rotor with a generic ice shape p 14 A84-49096
- Performance degradation of a typical twin engine commuter type aircraft in measured natural icing conditions p 14 N84-13173
- Heat transfer distributions around nominal ice accretion shapes formed on a cylinder in the NASA Lewis icing research tunnel  
[NASA-TM-83557] p 123 N84-14463
- Results of an experimental program investigating the effects of simulated ice on the performance of the NACA 63A15 airfoil with flap  
[NASA-CR-168288] p 8 N84-16145
- Documentation of ice shapes on the main rotor of a UH-1H helicopter in hover  
[NASA-CR-168332] p 9 N84-17139
- Progress toward the development of an aircraft icing analysis capability  
[NASA-TM-83562] p 9 N84-20490
- Measurement of local convective heat transfer coefficients of four ice accretion shapes  
[NASA-CR-174680] p 10 N84-25646
- ICE PREVENTION**
- Progress toward the development of an aircraft icing analysis capability  
[NASA-TM-83562] p 9 N84-20490
- Measurement of local convective heat transfer coefficients of four ice accretion shapes  
[NASA-CR-174680] p 10 N84-25646
- IDEAL GAS**
- A numerical model of acoustic choking. I - Shock free solutions p 180 A84-21250
- GCKP84-general chemical kinetics code for gas-phase flow and batch processes including heat transfer effects  
[NASA-TP-2320] p 63 N84-32446
- IGNITION**
- The role of surface generated radicals in catalytic combustion p 61 N84-20555
- IGNITION LIMITS**
- Effect of gravity on halogenated hydrocarbon flame retardant effectiveness  
[NASA-TM-83761] p 63 N84-33536
- IGNITION SYSTEMS**
- Experimental and theoretical study of combustion jet ignition  
[NASA-CR-168139] p 21 N84-10054
- IGNITION TEMPERATURE**
- Alcohol cold starting - A theoretical study p 138 A84-30061
- ILLUMINATING**
- Method of reducing temperature in high-speed photography  
[NASA-TM-83620] p 188 N84-22421

IMAGE FILTERS

Rainbow schlieren and its applications p 131 A84-40738

IMAGE RECONSTRUCTION

Automatic holographic droplet analysis for liquid fuel sprays p 125 N84-20531

IMPACT DAMAGE

A study of the effect of solid particle impact and particle shape on the erosion morphology of ductile metals p 66 A84-45570

Particulate erosion mechanisms [NASA-TM-83551] p 68 N84-14289

IMPACT RESISTANCE

Simplified composite micromechanics equations for strength, fracture toughness and environmental effects p 53 A84-41858

Impact resistance of fiber composites Energy absorbing mechanisms and environmental effects [NASA-TM-83594] p 55 N84-24712

Simplified composite micromechanics equations for strength, fracture toughness and environmental effects [NASA-TM-83696] p 56 N84-27832

IMPACT TESTS

Indentation law for composite laminates p 52 A84-27356

IMPEDANCE

Input filter compensation for switching regulators [NASA-CR-173557] p 110 N84-24975

IMPINGEMENT

Predictive capability of long-term cavitation and liquid impingement erosion models p 50 A84-32646  
A study of the effect of solid particle impact and particle shape on the erosion morphology of ductile metals p 66 A84-45570

Solid impingement erosion mechanisms and characterization of erosion resistance of ductile metals [NASA-TM-83492] p 67 N84-12287  
Lubricant jet flow phenomena in spur and helical gears with modified center distances and/or addendums for out-of-mesh conditions [NASA-TM-83723] p 146 N84-29224

IMPURITIES

Interaction between boron and intrinsic defects in GaAs p 190 A84-33518  
Double-injection, deep-impurity switch development [NASA-CR-168335] p 108 N84-18536

IN-FLIGHT MONITORING

Uncertainty methodology for in-flight thrust determination [SAE PAPER 831438] p 13 A84-29452  
Application of in-flight thrust determination uncertainty [SAE PAPER 831439] p 13 A84-29453

INCOMPRESSIBLE FLOW

A direct method for the solution of unsteady two-dimensional incompressible Navier-Stokes equations p 2 A84-10078  
Turbulent solutions of the equations of fluid motion p 121 A84-41156

Penalty function finite element analysis of steady viscous incompressible flow in rotating coordinates [ASME PAPER 84-GT-36] p 121 A84-46900  
Numerical modeling of turbulent flow in a channel [NASA-CR-168278] p 23 N84-13189

INCONEL (TRADEMARK)

Benchmark cyclic plastic notch strain measurements p 63 A84-11194  
Ceramic-to-metal bonding for pressure transducers [NASA-CR-173500] p 84 N84-22753

INDENTATION

Indentation law for composite laminates p 52 A84-27356  
Ceramic wear in indentation and sliding [NASA-TM-83585] p 82 N84-18566

INDONESIA

Photovoltaic power system for satellite Earth stations in remote areas Project status and design description [NASA-TM-83789] p 101 N84-33642

INDUSTRIAL ENERGY

AFB/open cycle gas turbine conceptual design study [NASA-CR-168135] p 172 N84-31784

INDUSTRIAL PLANTS

Cogeneration Technology Alternatives Study (CTAS) Volume 2. Comparison and evaluation of results [NASA-TM-81401] p 173 N84-34038

INELASTIC STRESS

Inelastic stress analyses at finite deformation through complementary energy approaches p 149 A84-13248  
Analyses of large quasistatic deformations of inelastic bodies by a new hybrid-stress finite element algorithm p 150 A84-16874

Development of a simplified procedure for cyclic structural analysis [NASA-TP-2243] p 155 N84-20878

Nonlinear Structural Analysis [NASA-CP-2297] p 157 N84-31688

Inelastic and dynamic fracture and stress analyses

p 158 N84-31697

INERTIAL GUIDANCE

Centaur D-1A guidance/software system [AAS PAPER 84-043] p 39 A84-49176

Centaur D-1A guidance/software system [NASA-TM-83552] p 38 N84-16234

INFORMATION DISSEMINATION

Sixth Annual Workshop on Meteorological and Environmental Inputs to Aviation Systems, 26-28 October 1982, Tulsa, Oklahoma, Tenn p 174 A84-23424  
Combustion gas properties of various fuels of interest to gas turbine engines [NASA-TM-83682] p 31 N84-24584

INFORMATION MANAGEMENT

Review of the DOE/NASA wind turbine engineering information system p 163 A84-33766

INFRARED SPECTRA

Synthesis of perfluoroalkylene dianilines [NASA-CR-168004] p 60 N84-11228

INFRARED SPECTROPHOTOMETERS

FTIR analysis of aviation fuel deposits [NASA-TM-83773] p 92 N84-33608

INGOTS

Two-region analysis of interface shape in continuous casting with superheated liquid p 139 A84-44918

INHOMOGENEITY

Volume integrals associated with the inhomogeneous Helmholtz equation Part 1: Ellipsoidal region [NASA-CR-3749] p 148 N84-14525

Volume integrals associated with the inhomogeneous Helmholtz equation Part 2: Cylindrical region, rectangular region [NASA-CR-3750] p 148 N84-14526

An experimental investigation of gas jets in confined swirling air flow [NASA-CR-3832] p 36 N84-33412

INJECTION MOLDING

Progress in net shape fabrication of alpha sic turbine components [ASME PAPER 84-GT-273] p 140 A84-47036  
An investigation into the injection molding of PMR-15 polyimide [NASA-CR-173550] p 85 N84-24810

INJECTORS

Test verification of LOX/RP-1 high-pressure fuel/oxidizer-rich preburner designs p 42 A84-22134

INKS

Multicolor printing plate joining [NASA-CASE-LEW-13598-1] p 132 N84-22930

INLET FLOW

Investigation of tangential blowing applied to a subsonic V/STOL inlet p 3 A84-11042  
Inlet flow distortion in turbomachinery - Comparison of theory and experiment in a transonic fan stage p 3 A84-13592

One-dimensional unsteady modeling of supersonic inlet unstart/restart [AIAA PAPER 84-0439] p 4 A84-18094

Three-dimensional viscous design methodology for advanced technology aircraft supersonic inlet systems [AIAA PAPER 84-0194] p 4 A84-21290

Convective heat transfer studies at high temperatures with pressure gradient for inlet flow Mach number of 0.45 [AIAA PAPER 84-1487] p 119 A84-35233

Dynamic response of shock waves in transonic diffuser and supersonic inlet - An analysis with the Navier-Stokes equations and adaptive grid [AIAA PAPER 84-1609] p 5 A84-38004

Three-dimensional flow simulations for supersonic mixed-compression inlets at incidence p 5 A84-38828  
Inlet boundary layer effects in an axial compressor rotor. I Blade-to-blade effects [ASME PAPER 84-GT-84] p 6 A84-46926

Inlet boundary layer effects in an axial compressor rotor. II - Throughflow effects [ASME PAPER 84-GT-85] p 7 A84-46927

Three-dimensional viscous design methodology for advanced technology aircraft supersonic inlet systems [NASA-TM-83558] p 23 N84-13190

Broad specification fuels combustion technology program [NASA-CR-168179] p 89 N84-15283

V/STOL model fan stage ng design report [NASA-CR-174688] p 29 N84-23629

INLET PRESSURE

V/STOL model fan stage ng design report [NASA-CR-174688] p 29 N84-23629

INPUT/OUTPUT ROUTINES

Input-output characterization of an ultrasonic testing system by digital signal analysis [NASA-CR-3756] p 149 N84-15555

INSTRUMENT ERRORS

Optimizing and comparing laser anemometers p 130 A84-28739

INSTRUMENT ORIENTATION

Accuracy and directional sensitivity of the single-wire technique [AIAA PAPER 84-0367] p 130 A84-18047

INSULATION

Evaluation of propellant tank insulation concepts for low-thrust chemical propulsion systems [NASA-CR-168320] p 46 N84-20634

INTAKE SYSTEMS

Analytical study of blowing boundary-layer control for subsonic V/STOL inlets [NASA-TM-83576] p 8 N84-16141

INTEGRAL EQUATIONS

Volume integrals associated with the inhomogeneous Helmholtz equation Part 1: Ellipsoidal region [NASA-CR-3749] p 148 N84-14525

Volume integrals associated with the inhomogeneous Helmholtz equation Part 2: Cylindrical region, rectangular region [NASA-CR-3750] p 148 N84-14526

INTEGRALS

Volume integrals associated with the inhomogeneous Helmholtz equation. Part 1: Ellipsoidal region [NASA-CR-3749] p 148 N84-14525

Volume integrals associated with the inhomogeneous Helmholtz equation Part 2: Cylindrical region, rectangular region [NASA-CR-3750] p 148 N84-14526

INTEGRATED CIRCUITS

A Ka-band GaAs monolithic phase shifter p 101 A84-18371

A three-stage power amplifier for a 20 GHz monolithic transmit module p 102 A84-22873

Microwave monolithic integrated circuit development for future spaceborne phased array antennas [AIAA PAPER 84-0656] p 94 A84-25257

A new FET-bipolar combinational power semiconductor switch p 104 A84-32293

Microwave monolithic integrated circuit development for future spaceborne phased array antennas [NASA-TM-83518] p 97 N84-13399

LEC GaAs for integrated circuit applications [NASA-CR-173267] p 191 N84-17014

The 30-GHz monolithic receive module [NASA-CR-168326] p 99 N84-20737

Design considerations for a monolithic, GaAs, dual-mode, QPSK/QASK, high-throughput rate transceiver [NASA-CR-173560] p 110 N84-24874

MMIC technology for advanced space communications systems [NASA-TM-83749] p 100 N84-30147

The 20 and 30 GHz MMIC technology for future space communication antenna system [NASA-TM-83745] p 100 N84-31460

Monolithic microwave integrated circuits: Interconnections and packaging considerations [NASA-TM-83774] p 100 N84-31461

Monolithic microwave integrated circuit devices for active array antennas [NASA-CR-173981] p 112 N84-34675

INTEGRATED ENERGY SYSTEMS

Economic competitiveness of fuel cell onsite integrated energy systems [NASA-TM-83403] p 164 N84-10665

INTEGRATED OPTICS

Coupling of radiation into thin film modes by means of localized plasma resonances p 187 A84-16397

INTERACTIONAL AERODYNAMICS

Viscous-inviscid interactive procedure for rotational flow in cascades of airfoils p 6 A84-44639

Rotorcraft flight-propulsion control integration p 36 A84-46524

INTERACTIVE CONTROL

AESOP. An interactive computer program for the design of linear quadratic regulators and Kalman filters [NASA-TP-2221] p 178 N84-16843

INTERATOMIC FORCES

Scaling relations in the equation of state, thermal expansion, and melting of metals p 192 A84-19359

INTERCALATION

Intercalated graphite electrical conductors p 105 N84-10984

INTERFACES

Tribological characteristics of gold films deposited on metals by ion plating and vapor deposition [NASA-TM-83572] p 69 N84-17352

INTERFACIAL TENSION

Factors influencing the thermally-induced strength degradation of B/AI composites p 52 A84-28227  
The strength of the metal Aluminum oxide interface p 72 N84-23898

Tribological applications of surface analysis [NASA-TM-83707] p 51 N84-25766

## INTERFERENCE

- Adaptive arrays for satellite communications  
[NASA-CR-173548] p 99 N84-24924
- INTERFEROMETERS**  
Large-aperture interferometer with local reference beam p 130 A84-34528
- INTERFEROMETRY**  
Measurement of fluid properties using rapid-double-exposure and time-average holographic interferometry  
[AIAA PAPER 84-1461] p 130 A84-35223  
Measurement of fluid properties using rapid-double-exposure and time-average holographic interferometry  
[NASA-TM-83630] p 132 N84-21849  
Preliminary experiments on phase conjugation for flow visualization — barium titanate single crystals  
[NASA-TM-83766] p 189 N84-32169
- INTERMODULATION**  
The 20 x 20 high speed microwave switches  
[NASA-TM-83775] p 101 N84-32644
- INTERNAL COMBUSTION ENGINES**  
Turbulent flow field calculations in an internal combustion engine equipped with two valves p 112 A84-13311  
A review of internal combustion engine combustion chamber process studies at NASA Lewis Research Center  
[AIAA PAPER 84-1316] p 121 A84-40242  
An overview of NASA intermittent combustion engine research  
[AIAA PAPER 84-1393] p 19 A84-40244  
Multicomponent velocity measurement in a piston-cylinder configuration using laser velocimetry  
[NASA-TM-83534] p 8 N84-14121  
A dynamic analysis of rotary combustion engine seals  
[NASA-TM-83536] p 141 N84-14519  
Development of an instrument for real-time computation of indicated mean effective pressure  
[NASA-TP-2238] p 107 N84-16461  
Proceedings of the 20th Automotive Technology Development Contractors' Coordination Meeting  
[NASA-CR-173412] p 143 N84-21877  
Real time pressure signal system for a rotary engine  
[NASA-CASE-LEW-13622-1] p 28 N84-22559  
An overview of NASA intermittent combustion engine research  
[NASA-TM-83668] p 31 N84-24583  
A review of internal combustion engine combustion chamber process studies at NASA Lewis Research Center  
[NASA-TM-83666] p 127 N84-24999  
Holographic aids for internal combustion engine flow studies  
[NASA-TM-83681] p 132 N84-25017
- INTERNAL COMPRESSION INLETS**  
Three-dimensional flow simulations for supersonic mixed-compression inlets at incidence p 5 A84-38828
- INTERNATIONAL COOPERATION**  
Economic viability of photovoltaic power for development assistance applications p 193 A84-23119
- INTERNATIONAL SUN EARTH EXPLORER 1**  
Anomalous high potentials observed on ISEE p 41 N84-17258
- INTERNATIONAL SUN EARTH EXPLORERS**  
Anomalous high potentials observed on ISEE  
[NASA-CR-172791] p 41 N84-17252
- INTERPOLATION**  
Slave finite elements The temporal element approach to nonlinear analysis p 157 N84-31689
- INVARIANCE**  
An invariant derivation of flame stretch p 58 A84-18925
- INVERTED CONVERTERS (DC TO AC)**  
A study of the high frequency limitations of series resonant converters  
[NASA-CR-173868] p 111 N84-32678
- INVERTERS**  
Integral inverter/battery charger for use in electric vehicles  
[NASA-CR-168177] p 194 N84-17073  
AC propulsion system for an electric vehicle, phase 2  
[NASA-CR-168244] p 111 N84-31514
- INVESTMENT CASTING**  
Low-cost single-crystal turbine blades, volume 1  
[NASA-CR-168218] p 68 N84-15247
- INVISCID FLOW**  
Multiple-grid convergence acceleration of viscous and inviscid flow computations p 116 A84-23950  
Analysis of inviscid and viscous flows in cascades with an explicit multiple-grid algorithm  
[AIAA PAPER 84-1663] p 5 A84-38043

- Application of a quasi-3D inviscid flow and boundary layer analysis to the hub-shroud contouring of a radial turbine  
[AIAA PAPER 84-1297] p 6 A84-44177
- A viscous-inviscid interactive procedure for rotational flow in cascades of two dimensional airfoils of arbitrary shape  
[NASA-CR-174609] p 7 N84-13149  
Assessment of three-dimensional inviscid codes and loss calculations for turbine aerodynamic computations  
[NASA-TM-83571] p 8 N84-16142  
Companion of secondary flows predicted by a viscous code and an inviscid code with experimental data for a turning duct  
[NASA-TM-83575] p 9 N84-17142  
Progress toward the development of an aircraft icing analysis capability  
[NASA-TM-83582] p 9 N84-20480  
Analysis of inviscid and viscous flows in cascades with an explicit multiple-grid algorithm  
[NASA-TM-83636] p 1 N84-22527  
Application of a quasi-3D inviscid flow and boundary layer analysis to the hub-shroud contouring of a radial turbine  
[NASA-TM-83669] p 10 N84-25647
- ION BEAMS**  
Laboratory degradation of Kapton in a low energy oxygen ion beam  
[NASA-TM-83530] p 41 N84-18310  
Ion-beam nitriding of steels  
[NASA-TM-83599] p 71 N84-21719  
Method of making an ion beam sputter-etched ventricular catheter for hydrocephalus shunt  
[NASA-CASE-LEW-13107-2] p 174 N84-23095  
Ion sputter textured graphite electrode plates  
[NASA-CASE-LEW-12919-2] p 179 N84-28565  
Dual ion beam deposition of carbon films with diamondlike properties  
[NASA-TM-83743] p 110 N84-31512  
Improved heat exchanger for electrothermal devices  
[NASA-CASE-LEW-14037-1] p 49 N84-32425
- ION ENGINES**  
Simplification of power electronics for ion thruster neutralizers p 44 A84-49509  
Sputtering phenomena in ion thrusters  
[NASA-CR-168172] p 46 N84-18322  
Cathode degradation and erosion in high pressure arc discharges p 47 N84-22631  
Performance capabilities of the 12-centimeter Xenon ion thruster  
[NASA-TM-83674] p 48 N84-27825
- ION EXCHANGING**  
Kinetics of chromium ion absorption by cross-linked polyacrylate films  
[NASA-TM-83661] p 50 N84-23693  
Anion permselective membrane  
[NASA-CR-174725] p 172 N84-29358
- ION IMPLANTATION**  
Large area space solar cell assemblies p 42 A84-22980  
New implantation techniques for improved solar cell junctions p 161 A84-23059  
Ion implanted junctions for silicon space solar cells p 42 A84-30143  
The 30-GHz monolithic receive module  
[NASA-CR-168326] p 99 N84-20737  
Radiation damage and defect behavior in ion-implanted, lithium counterdoped silicon solar cells  
[NASA-TM-83646] p 109 N84-22890  
Cell and defect behavior in lithium-counterdoped solar cells p 170 N84-29322
- ION IRRADIATION**  
The energy dependence and surface morphology of Kapton (trademark) degradation under atomic oxygen bombardment p 187 N84-34484
- ION PLATING**  
The X-ray photoelectron spectroscopy depth profiling and tribological characterization of ion-plated gold on various metals p 50 A84-20465  
Metallic glass as a temperature sensor during ion plating  
[NASA-TM-83566] p 69 N84-17351  
Tribological characteristics of gold films deposited on metals by ion plating and vapor deposition  
[NASA-TM-83572] p 69 N84-17352  
Diamondlike flake composites  
[NASA-CASE-LEW-13837-1] p 54 N84-22695  
Status of plasma physics techniques for the deposition of tribological coatings p 190 N84-25058
- ION PROPULSION**  
Improved ion containment using a ring-cusp ion thruster p 44 A84-49511  
Development of advanced inert-gas ion thrusters  
[NASA-CR-168206] p 44 N84-10180

- Ground correlation investigation of thruster spacecraft interactions to be measured on the IAPS flight test  
[NASA-TM-83598] p 47 N84-23691
- ION SOURCES**  
Characteristics of a microwave plasma disk ion source p 189 A84-23390
- IONOSONDES**  
Tabulations of ozonesonde data, 1963 - 1980  
[NASA-CR-174631] p 174 N84-27375
- IONS**  
Interpretation of STS-3/plasma diagnostics package results in terms of large space structure plasma interactions  
[NASA-CR-173266] p 189 N84-16991
- IRON**  
Friction and wear of iron in sulfuric acid  
[NASA-TP-2239] p 71 N84-21716  
Interaction of sulfuric acid corrosion and mechanical wear of iron  
[NASA-TM-83717] p 73 N84-27857  
Negative electrode catalyst for the iron-chromium REDOX energy storage system  
[NASA-CASE-LEW-14028-1] p 172 N84-32909
- IRON ALLOYS**  
A simple application of the Bailey-Crowan creep model to Fe-39.8 at. pct Al and gamma/gamma prime - alpha p 64 A84-22012  
Carbides in iron-nickel Fe-Mn-Cr-Mo-Al-Si-C systems p 64 A84-26815  
Creep-rupture behavior of six candidate Stirling engine superalloys tested in air p 65 A84-36173  
Analysis of thermoelectric properties of high-temperature complex alloys of nickel-base, iron-base and cobalt-base groups  
[NASA-TP-2278] p 70 N84-18370  
Status of understanding for gear materials p 144 N84-25061  
Creep-rupture behavior of candidate Stirling engine alloys after long-term aging at 760 deg C in low-pressure hydrogen  
[NASA-TM-83676] p 73 N84-25793  
Creep-rupture behavior of candidate Stirling engine iron superalloys in high-pressure hydrogen Volume 2  
Hydrogen creep-rupture behavior  
[NASA-CR-174705] p 74 N84-28961  
Erosion of iron-chromium alloys by glass particles  
[NASA-TP-2354] p 75 N84-28965
- IRON CHLORIDES**  
Chromium electrodes for REDOX cells  
[NASA-CASE-LEW-13653-1] p 170 N84-28205
- ISOPARAMETRIC FINITE ELEMENTS**  
Stability and convergence of undenintegrated finite element approximations p 158 N84-31696
- ISOSTATIC PRESSURE**  
Consolidation of Si3N4 without additives (by hot isostatic pressing)  
[NASA-CR-173279] p 82 N84-17389
- ITERATION**  
Turbulence and surface heat transfer near the stagnation point of a circular cylinder in turbulent flow  
[NASA-TM-83732] p 128 N84-29157
- ITERATIVE SOLUTION**  
A companion of the efficiency of numerical methods for integrating chemical kinetic rate equations p 49 N84-31280
- J**
- J INTEGRAL**  
Crack tip field and fatigue crack growth in general yielding and low cycle fatigue  
[NASA-CR-174686] p 76 N84-32503
- JET AIRCRAFT NOISE**  
A parametric study of the effect of inlet lip shape upon the radiated sound field  
[AIAA PAPER 84-0498] p 180 A84-18131  
Tone generation by rotor-downstream strut interaction p 16 A84-22174  
Jet noise modification by the 'whistler nozzle' p 181 A84-23355  
Inverted velocity profile semi-annular nozzle jet exhaust noise experiments  
[NASA-TM-83525] p 182 N84-13924  
Fluid shielding of high-velocity jet noise  
[NASA-TP-2259] p 183 N84-15894  
Low frequency noise in a quiet, clean, general aviation turbofan engine  
[NASA-TM-83520] p 183 N84-20320  
Experimental investigation of shock-cell noise reduction for dual-stream nozzles in simulated flight comprehensive data report. Volume 1: Test nozzles and acoustic data  
[NASA-CR-168336-VOL-1] p 184 N84-24323

- Experimental investigation of shock-cell noise reduction for dual-stream nozzles in simulated flight comprehensive data report. Volume 2. Laser velocimeter data, static pressures and shadowgraph photos  
[NASA-CR-168336-VOL-2] p 184 N84-24324
- Supersonic jet shock noise reduction  
[NASA-TM-83799] p 186 N84-35085
- JET ENGINE FUELS**  
NASA/General Electric Broad-Specification Fuels Combustion Technology Program - Phase I  
p 16 A84-24033
- Heating experiments for flowability improvement of near-freezing aviation fuel  
p 89 A84-26955
- Effects of broadened property fuels on radiant heat flux to gas turbine combustor liners  
[NASA-TM-83537] p 123 N84-16494
- Aviation-fuel property effects on combustion  
[NASA-CR-168334] p 89 N84-17407
- Applications of photoacoustic techniques to the study of jet fuel residue  
[NASA-CR-173322] p 90 N84-18420
- Assessment of Alternative Aircraft Fuels  
[NASA-CP-2307] p 30 N84-23630
- Trends of jet fuel demand and properties  
p 90 N84-23631
- NASA broad-specification fuels combustion technology program  
p 62 N84-23637
- Fuel system research and technology: An overview of the NASA program  
p 14 N84-23541
- Research on aviation fuel instability  
p 90 N84-23642
- Economic impact of fuel properties on turbine powered business aircraft  
p 14 N84-23646
- Computer analysis of effects of altering jet fuel properties on refinery costs and yields  
[NASA-CR-174642] p 91 N84-27908
- Carbon-13 and proton nuclear magnetic resonance analysis of shale-derived refinery products and jet fuels and of experimental referee broadened-specification jet fuels  
[NASA-CR-174761] p 92 N84-32552
- FTIR analysis of aviation fuel deposits  
[NASA-TM-83773] p 92 N84-33608
- JET ENGINES**  
Preliminary investigation of a two-zone swirl flow combustor  
[AIAA PAPER 84-1169] p 17 A84-36951
- Aircraft Electric Secondary Power  
[NASA-CP-2282] p 22 N84-10055
- A real-time, portable, microcomputer-based jet engine simulator  
[NASA-TM-83550] p 176 N84-16812
- Preliminary investigation of a two-zone swirl-flow combustor  
[NASA-TM-83637] p 29 N84-22585
- Research on aviation fuel instability  
p 90 N84-23642
- JET EXHAUST**  
Velocity and temperature characteristics of two-stream, coplanar jet exhaust plumes  
[AIAA PAPER 84-2205] p 21 A84-48106
- Fluid shielding of high-velocity jet noise  
[NASA-TP-2259] p 183 N84-15894
- Velocity and temperature characteristics of two-stream, coplanar jet exhaust plumes  
[NASA-TM-83730] p 34 N84-23790
- JET FLOW**  
Structure of nonevaporating sprays - Measurements and predictions  
[AIAA PAPER 84-0125] p 114 A84-17897
- Mass and momentum turbulent transport experiments with confined swirling coaxial jets. I  
[AIAA PAPER 84-1380] p 119 A84-35664
- On modeling dilution jet flowfields  
[AIAA PAPER 84-1379] p 121 A84-44183
- Correlation of flight effects on centerline velocity decay for cold-flow acoustically excited jets  
[NASA-TM-83502] p 182 N84-11883
- Free stream turbulence and density ratio effects on the interaction region of a jet in a cross flow  
p 125 N84-20546
- On modeling dilution jet flowfields  
[NASA-TM-83708] p 32 N84-25713
- Dilution jets in accelerated cross flows  
[NASA-CR-174717] p 34 N84-28794
- Lubricant jet flow phenomena in spur and helical gears with modified center distances and/or addendums for out-of-mesh conditions  
[NASA-TM-83723] p 146 N84-29224
- A theoretical and experimental study of turbulent nonevaporating sprays  
[NASA-CR-174668] p 35 N84-29877
- JET IMPIINGEMENT**  
Morphology of an aluminum alloy eroded by a normally incident jet of angular erodent particles  
p 64 A84-18244
- Empirical relations for cavitation and liquid impingement erosion processes  
[NASA-TP-2339] p 76 N84-31349
- JET MIXING FLOW**  
Sound generated by instability waves of supersonic flows I Two-dimensional mixing layers II - Axisymmetric jets  
p 181 A84-24597
- Investigation of mixing in a turbofan exhaust duct. II Computer code application and verification  
p 17 A84-27140
- Preliminary investigation of a two-zone swirl flow combustor  
[AIAA PAPER 84-1169] p 17 A84-36951
- Computational modeling of jet induced mixing of cryogenic propellants in low-G  
[AIAA PAPER 84-1344] p 121 A84-40243
- Experiments in dilution jet mixing  
p 122 A84-48140
- Preliminary investigation of a two-zone swirl flow combustor  
[NASA-TM-83637] p 29 N84-22565
- Computational modeling of jet induced mixing of cryogenic propellants in low-G  
[NASA-TM-83703] p 127 N84-25000
- Dilution jet mixing program  
[NASA-CR-174624] p 33 N84-26702
- Dilution jets in accelerated cross flows  
[NASA-CR-174717] p 34 N84-28794
- JET NOZZLES**  
Supersonic jet screech tone cancellation  
p 179 A84-10136
- Turbulence measurements in a complex flowfield using a crossed hot-wire  
[AIAA PAPER 84-1604] p 131 A84-37999
- Lubricant jet flow phenomena in spur and helical gears with modified center distances and/or addendums for out-of-mesh conditions  
[NASA-TM-83723] p 146 N84-29224
- JET PROPULSION**  
Application of advanced control techniques to aircraft propulsion systems  
p 28 N84-20590
- JOINING**  
Monolithic microwave integrated circuits Interconnections and packaging considerations  
[NASA-TM-83774] p 100 N84-31481
- JOURNAL BEARINGS**  
Improved compliant hydrodynamic fluid journal bearing  
[NASA-CASE-LEW-13670-1] p 143 N84-22959
- K**
- KALMAN FILTERS**  
State estimation Kalman filter using optical processors  
Noise statistics known  
p 178 A84-23602
- Optical Kalman filtering for missile guidance  
p 178 A84-38596
- AESOP: An interactive computer program for the design of linear quadratic regulators and Kalman filters  
[NASA-TP-2221] p 178 N84-16843
- KAPTON (TRADEMARK)**  
Sputtered coatings for protection of spacecraft polymers  
[NASA-TM-83706] p 85 N84-26603
- The energy dependence and surface morphology of Kapton (trademark) degradation under atomic oxygen bombardment  
p 187 N84-34484
- KELVIN-HELMHOLTZ INSTABILITY**  
Feedback in separated flows over symmetric airfoils  
[NASA-TM-83758] p 10 N84-31091
- KEROSENE**  
An assessment of the use of antimisting fuel in turbofan engines  
[NASA-CR-168081] p 89 N84-10332
- KEVLAR (TRADEMARK)**  
Aging results for PRD 49 III/epoxy and Kevlar 49/epoxy composite pressure vessels  
p 52 A84-21647
- KINEMATICS**  
Kinematic precision of gear trains  
[ASME PAPER 82-WA/DE-34] p 135 A84-15951
- Pivoting and slip in an angular contact bearing  
p 139 A84-40595
- Special cases of friction and applications  
[NASA-TM-83523] p 141 N84-11500
- First order ball bearing kinematics  
[NASA-TM-83592] p 142 N84-19816
- Spin analysis of concentrated traction contacts  
[NASA-TM-83713] p 145 N84-27042
- L**
- LABYRINTH SEALS**  
Labyrinth seal forces on a whirling rotor  
p 135 A84-13228
- LADDERS**  
Dielectric based submillimeter backward wave oscillator circuit  
[NASA-CASE-LEW-13736-1] p 110 N84-27974
- LAMINAR BOUNDARY LAYER**  
Flat plate heat transfer for laminar transition and turbulent boundary layers using a shock tube  
[AIAA PAPER 84-1726] p 120 A84-37467
- Engineering correlations of variable-property effects on laminar forced convection mass transfer for dilute vapor species and small particles in air  
[NASA-CR-168322] p 124 N84-18578
- LAMINAR FLOW**  
Streamwise computation of three-dimensional parabolic flows  
p 113 A84-16828
- Developing flow in S-shaped ducts  
p 116 A84-28709
- Numerical solution for the problem of flame propagation by the random element method  
p 60 A84-48139
- On numerical simulation of viscous flows  
p 122 A84-49112
- LAMINATES**  
Edge delamination in angle-ply composite laminates  
p 52 A84-21515
- Indentation law for composite laminates  
p 52 A84-27356
- Compressive behavior of unidirectional fibrous composites  
p 53 A84-29894
- Elasticity solutions for a class of composite laminate problems with stress singularities  
p 53 A84-33389
- A mixed shear flexible finite element for the analysis of laminated plates  
p 152 A84-45994
- Examination, evaluation and repair of laminated wood blades after service on the Mod-OA wind turbine  
[NASA-TM-83483] p 163 N84-10664
- Interply layer degradation effects on composite structural response  
[NASA-TM-83702] p 56 N84-26756
- Thermal-stress analysis for wood composite blade - horizontal axis wind turbines  
[NASA-CR-173830] p 157 N84-31685
- Nonlinear Structural Analysis  
[NASA-CP-2297] p 157 N84-31068
- Nonlinear analysis for high-temperature composites: Turbine blades/vanes  
p 158 N84-31699
- Fracture modes in notched angle-ply composite laminates  
[NASA-TM-83802] p 58 N84-34576
- LAND MOBILE SATELLITE SERVICE**  
Rural land mobile radio market assessment and satellite and terrestrial system concepts  
[AIAA PAPER 84-0754] p 95 A84-25324
- Computer simulator for a mobile telephone system  
[NASA-CR-174593] p 95 N84-10401
- Mobile radio alternative systems study satellite/terrestrial (hybrid) systems concepts  
[NASA-SP-168064] p 96 N84-10404
- Rural land mobile radio market assessment and satellite and terrestrial system concepts  
[NASA-TM-83591] p 99 N84-19541
- LARGE SPACE STRUCTURES**  
Resistojet propulsion for large spacecraft systems  
[NASA-TM-83489] p 45 N84-11206
- Study of auxiliary propulsion requirements for large space systems Volume 1 Executive summary  
[NASA-CR-168193-VOL-1] p 45 N84-12226
- Study of auxiliary propulsion requirements for large space systems, volume 2  
[NASA-CR-168193-VOL-2] p 45 N84-13218
- Interpretation of STS-3/plasma diagnostics package results in terms of large space structure plasma interactions  
[NASA-CR-173266] p 189 N84-16991
- LASER ANEMOMETERS**  
Estimating time and time-lag in time-of-flight velocimetry  
p 129 A84-13192
- Application of laser anemometry in turbine engine research  
p 130 A84-22872
- Output statistics of laser anemometers in sparsely seeded flows  
p 117 A84-28738
- Optimizing and comparing laser anemometers  
p 130 A84-28739
- Optimization of fringe-type laser anemometers for turbine engine component testing  
[AIAA PAPER 84-1459] p 131 A84-40248
- Application of laser anemometry in turbine engine research  
[NASA-TM-83513] p 131 N84-11458
- Investigation of flow phenomena in a transonic fan rotor using laser anemometry  
[NASA-TM-83555] p 9 N84-17143
- Optimization of fringe-type laser anemometers for turbine engine component testing  
[NASA-TM-83658] p 133 N84-25019

- Investigation of the three-dimensional flow field within a transonic fan rotor Experiment and analysis  
[NASA-TM-83739] p 11 N84-32357
- LASER APPLICATIONS**  
A laser system to remotely sense bird movements  
p 159 A84-31608  
Measurement of heat pump processes induced by laser radiation  
[NASA-CR-168324] p 134 N84-18620  
Photodeposition of nitride insulators on 3-5 substrates  
[NASA-CR-173393] p 71 N84-21720
- LASER DOPPLER VELOCIMETERS**  
Application of laser anemometry in turbine engine research  
p 130 A84-22872  
Window aberration correction in laser velocimetry using multifaceted holographic optical elements  
p 134 A84-24683  
Development of the phase/Doppler spray analyzer for liquid drop size and velocity characterizations  
[AIAA PAPER 84-1199] p 131 A84-36958  
Laser Doppler velocimeter measurement in the tip region of a compressor rotor  
[AIAA PAPER 84-1602] p 6 A84-39304  
A review of internal combustion engine combustion chamber process studies at NASA Lewis Research Center  
[AIAA PAPER 84-1316] p 121 A84-40242  
Multicomponent velocity measurement in a piston-cylinder configuration using laser velocimetry  
[NASA-TM-83534] p 8 N84-14121  
A review of internal combustion engine combustion chamber process studies at NASA Lewis Research Center  
[NASA-TM-83666] p 127 N84-24999  
Experimental investigation of shock-cell noise reduction for single-stream nozzles in simulated flight, comprehensive data report. Volume 2: Laser velocimeter data  
[NASA-CR-168234-VOL-2] p 186 N84-33149
- LASER INTERFEROMETRY**  
Surface topographical changes measured by phase-locked interferometry  
[NASA-CR-3757] p 188 N84-16984  
Fuel spray diagnostics  
p 125 N84-20527  
Measurement of spray combustion processes  
p 61 N84-20530  
Analysis and testing of a new method for drop size measurement using laser scatter interferometry  
[NASA-CR-174636] p 133 N84-31595
- LASER OUTPUTS**  
Development of the phase/Doppler spray analyzer for liquid drop size and velocity characterizations  
[AIAA PAPER 84-1199] p 131 A84-36958  
Method and apparatus for coating substrates using a laser  
[NASA-CASE-LEW-13526-1] p 134 N84-22944
- LASER WINDOWS**  
Window aberration correction in laser velocimetry using multifaceted holographic optical elements  
p 134 A84-24683
- LASERS**  
Method and apparatus for coating substrates using a laser  
[NASA-CASE-LEW-13526-1] p 134 N84-22944
- LAUNCHERS**  
Metal vapor vacuum arc switching - Applications and results - for launchers  
p 103 A84-32029  
Energy stores and switches for rail-launcher systems  
[NASA-CR-173249] p 107 N84-16458
- LAYERS**  
On stress analysis of a crack-layer  
[NASA-CR-174774] p 159 N84-34774
- LEAD ACID BATTERIES**  
Results of electric-vehicle propulsion system performance on three lead-acid battery systems  
[NASA-TM-83657] p 169 N84-25166
- LEADING EDGES**  
Effect of an oscillating flow direction on leading edge heat transfer  
p 117 A84-33705  
Potential flow analysis of glaze ice accretions on an airfoil  
[NASA-CR-168282] p 8 N84-16146
- LEAKAGE**  
Analysis for leakage and rotordynamic coefficients of surface-roughened tapered annular gas seals  
[ASME PAPER 84-GT-32] p 140 A84-46896
- LENSES**  
Large-aperture interferometer with local reference beam  
p 130 A84-34528
- LIFE (DURABILITY)**  
Durability/life of fiber composites in hygrothermomechanical environments  
p 52 A84-27359  
Cycle life test and failure model of nickel-hydrogen cells  
p 162 A84-30185
- Complexes of high temperature metal fatigue Some steps toward understanding  
[NASA-TM-83507] p 154 N84-14541  
Engine cyclic durability by analysis and material testing  
[NASA-TM-83577] p 155 N84-18683  
Elevated temperature biaxial fatigue  
[NASA-CR-173473] p 156 N84-21905  
Status of understanding for gear materials  
p 144 N84-25061  
Improved heat exchanger for electrothermal devices  
[NASA-CASE-LEW-14037-1] p 49 N84-32425
- LIFE CYCLE COSTS**  
Rotorcraft contingency power study  
[NASA-CR-174675] p 31 N84-24580
- LIGHT AIRCRAFT**  
An overview of the NASA rotary engine research program  
[NASA-TM-83699] p 34 N84-28791
- LIGHT BEAMS**  
Optical residue addition and storage units using a Hughes liquid crystal light valve  
p 188 N84-22417
- LIGHT MODULATION**  
Advanced acousto-optic signal processors  
p 187 A84-28485  
Acoustically-induced modulation spectroscopy for ultra-sensitive gas analysis  
[AIAA PAPER 84-1460] p 131 A84-35981
- LIGHT SCATTERING**  
Analysis and testing of a new method for drop size measurement using laser scatter interferometry  
[NASA-CR-174636] p 133 N84-31595
- LIGHT VALVES**  
Optical flip-flops and sequential logic circuits using a liquid crystal light valve  
p 188 A84-40332  
Optical pulse generator using liquid crystal light valve  
p 188 N84-22414
- LIGHTNING**  
How to protect a wind turbine from lightning  
[NASA-CR-168229] p 163 N84-10661
- LINE SHAPE**  
Study of the Auger line shape of polyethylene and diamond  
p 190 A84-40600
- LINE SPECTRA**  
Study of the Auger line shape of polyethylene and diamond  
p 190 A84-40600
- LINEAR ARRAYS**  
Optical systolic solutions of linear algebraic equations  
p 188 N84-22405
- LINEAR EQUATIONS**  
Optical systolic solutions of linear algebraic equations  
p 188 N84-22405
- LINEARITY**  
Theoretical and software considerations for nonlinear dynamic analysis  
[NASA-CR-174504] p 154 N84-15589
- LINEARIZATION**  
A TWT amplifier with a linear power transfer characteristic and improved efficiency  
[AIAA PAPER 84-0782] p 104 A84-41035  
A TWT amplifier with a linear power transfer characteristic and improved efficiency  
[NASA-TM-83590] p 108 N84-21803
- LININGS**  
Ceramic composite liner material for gas turbine combustors  
[AIAA PAPER 84-0363] p 78 A84-18044  
Ceramic composite liner material for gas turbine combustors  
[NASA-TM-83490] p 24 N84-14145  
Effects of broadened property fuels on radiant heat flux to gas turbine combustor liners  
[NASA-TM-83537] p 123 N84-16454  
Combustor liner construction  
[NASA-CASE-LEW-14035-1] p 30 N84-24577  
Evaluation of two polyimides and of an improved liner retention design for self-lubricating bushings  
[NASA-TM-83719] p 65 N84-27867
- LINKAGES**  
Special cases of friction and applications  
[NASA-TM-83523] p 141 N84-11500
- LIQUEFIED NATURAL GAS**  
Assessment of institutional barriers to the use of natural gas fuel in automotive vehicle fleets  
[NASA-CR-168183] p 165 N84-14587
- LIQUID ATOMIZATION**  
Atomization of liquid sheets in high pressure airflow  
[NASA-TM-83731] p 128 N84-30223
- LIQUID CHROMATOGRAPHY**  
Liquid chromatographic analysis of a formulated ester from a gas-turbine engine test  
[ASLE PREPRINT 83-LC-1A-1] p 80 A84-28895  
Group-type hydrocarbon standards for high-performance liquid chromatographic analysis of middle distillate fuels  
[NASA-TP-2317] p 90 N84-23774
- LIQUID CRYSTALS**  
Optical flip-flops and sequential logic circuits using a liquid crystal light valve  
p 188 A84-40332  
Optical pulse generator using liquid crystal light valve  
p 188 N84-22414
- LIQUID FLOW**  
Multicolor printing plate joining  
[NASA-CASE-LEW-13598-1] p 132 N84-22930
- LIQUID FUELS**  
Calculation of a hollow-cone liquid spray in a uniform air stream  
[AIAA PAPER 84-1322] p 118 A84-35171  
Combustion characteristics in the transition region of liquid fuel sprays  
[NASA-CR-175396] p 61 N84-19495  
Automatic holographic droplet analysis for liquid fuel sprays  
p 125 N84-20531  
Utilization of alternative fuels in diesel engines  
[NASA-CR-174669] p 91 N84-26813
- LIQUID HYDROGEN**  
Cryogenic Fluid Management Experiment (CFME) transient verification testing  
[NASA-CR-168310] p 92 N84-16381  
Analysis of a topping-cycle, aircraft, gas-turbine-engine system which uses cryogenic fuel  
[NASA-TP-2294] p 28 N84-21549
- LIQUID OXYGEN**  
Test verification of LOX/RP-1 high-pressure fuel/oxidizer-rich preburner designs  
p 42 A84-22134  
Selection of burn-resistant materials for oxygen-driven turbopumps  
[AIAA PAPER 84-1287] p 43 A84-35157
- LIQUID PROPELLANT ROCKET ENGINES**  
Rocket injector anomalies study Volume 2 Results of parametric studies  
[NASA-CR-174703] p 49 N84-32429
- LIQUID ROCKET PROPELLANTS**  
Deposit formation and heat transfer in hydrocarbon rocket fuels  
[AIAA PAPER 84-0512] p 88 A84-18142  
Test verification of LOX/RP-1 high-pressure fuel/oxidizer-rich preburner designs  
p 42 A84-22134
- LIQUID-SOLID INTERFACES**  
Two-region analysis of interface shape in continuous casting with superheated liquid  
p 139 A84-44918  
Dual clearance squeeze film damper  
[NASA-CASE-LEW-13508-1] p 29 N84-22562
- LIQUID-VAPOR INTERFACES**  
Capillary rise, wetting layers, and critical phenomena in confined geometry  
p 192 A84-20315
- LIQUIDS**  
Thermal and oxidative stabilities of liquid lubricants  
p 84 N84-23907  
Carbon-13 and proton nuclear magnetic resonance analysis of shale-derived refinery products and jet fuels and of experimental referee broadened-specification jet fuels  
[NASA-CR-174761] p 92 N84-32552
- LITHIUM**  
Increased radiation resistance in lithium-counterdoped silicon solar cells  
p 163 A84-34846  
Radiation damage and defect behavior in ion-implanted, lithium counterdoped silicon solar cells  
[NASA-TM-83546] p 109 N84-22890  
Cell and defect behavior in lithium-counterdoped solar cells  
p 170 N84-29322  
The effects of lithium counterdoping on radiation damage and annealing in n(+)-p silicon solar cells  
[NASA-TM-83755] p 110 N84-31513
- LOAD TESTS**  
Indentation law for composite laminates  
p 52 A84-27356  
Qualification testing of solar photovoltaic powered refrigerator freezers for medical use in remote geographic locations  
[NASA-CR-168181] p 169 N84-25162  
Mechanical behavior of carbon-carbon composites  
[NASA-CR-174767] p 57 N84-34575
- LOADS (FORCES)**  
NASTRAN flutter analysis of advanced turbopropellers  
[NASA-CR-167926] p 24 N84-14148  
Dual clearance squeeze film damper for high load conditions  
[NASA-TM-93619] p 144 N84-25064  
Dynamics of early planetary gear trains  
[NASA-CR-3793] p 145 N84-26027  
Evaluation of the effect of crack closure on fatigue crack growth of simulated short cracks  
[NASA-TM-83778] p 75 N84-31348  
Research study for effects of case flexibility on bearing loads and rotor stability  
[NASA-CR-171147] p 148 N84-33811
- LOCOMOTIVES**  
New applications for phosphoric acid fuel cells  
[NASA-CR-168203] p 166 N84-18757

## LOGIC CIRCUITS

- Optical flip-flops and sequential logic circuits using a liquid crystal light valve p 188 A84-40332

## LONG TERM EFFECTS

- Predictive capability of long-term cavitation and liquid impingement erosion models p 50 A84-32646  
Photochemical deposition of nitride insulators on 3-5 substrates [NASA-CR-173393] p 71 N84-21720  
Effects of surface chemistry on hot corrosion life [NASA-TM-174683] p 72 N84-24774  
Effects of long-time elevated temperature exposures on hot-isostatically-pressed power-metallurgy Udmet 700 alloys with reduced cobalt contents [NASA-TM-83632] p 57 N84-28917

## LONGITUDINAL CONTROL

- An advanced pitch change mechanism incorporating a hybrid traction drive [AIAA PAPER 84-1383] p 20 A84-44182  
An advanced pitch change mechanism incorporating a hybrid traction drive [NASA-TM-83709] p 2 N84-25605

## LOSSES

- A study of the high frequency limitations of series resonant converters [NASA-CR-173868] p 111 N84-32678  
Thermal analysis of a planetary transmission with spherical roller bearings operating after complete loss of oil [NASA-TP-2367] p 147 N84-32824

## LOSSY MEDIA

- Wave attenuation and mode dispersion in a waveguide coated with lossy dielectric material [NASA-CR-173820] p 100 N84-30145

## LOUVERS

- Materials for Advanced Turbine Engines (MATE) Project 3: Design, fabrication and evaluation of an oxide dispersion strengthened sheet alloy combustor liner, volume 1 [NASA-CR-174691] p 76 N84-32504

## LOW ASPECT RATIO

- Performance of a high-work low aspect ratio turbine tested with a realistic inlet radial temperature profile [AIAA PAPER 84-1161] p 19 A84-40239  
Performance of a high-work low aspect ratio turbine tested with a realistic inlet radial temperature profile [NASA-TM-83655] p 32 N84-24589

## LOW FREQUENCIES

- Low-frequency switching voltage regulators for terrestrial photovoltaic systems [NASA-TM-83625] p 110 N84-25926

## LOW GRAVITY MANUFACTURING

- Gravitational effects in dendritic growth p 37 A84-22346  
Fundamentals of Alloy Solidification Applied to Industrial Processes [NASA-CP-2337] p 77 N84-34589

## LOW LEVEL TURBULENCE

- On the design of contractions and settling chambers for optimal turbulence manipulations in wind tunnels [AIAA PAPER 84-0536] p 115 A84-22922

## LOW PRESSURE

- Energy efficient engine Low-pressure turbine subsonic cascade component development and integration program [NASA-CR-165592] p 33 N84-27738

## LOW SPEED WIND TUNNELS

- Low light speed fan noise from a supersonic inlet p 182 A84-44508

## LOW TEMPERATURE

- Free stream turbulence and density ratio effects on the interaction region of a jet in a cross flow p 125 N84-20546

## LUBRICANT TESTS

- Liquid chromatographic analysis of a formulated ester from a gas-turbine engine test [ASLE PREPRINT 83-LC-1A-1] p 80 A84-28995  
Solid lubrication design methodology [NASA-CR-174690] p 195 N84-33309

## LUBRICANTS

- Elastic model of the traction behavior of two traction lubricants p 136 A84-28791  
Characteristic morphological and frictional changes in sputtered MoS<sub>2</sub>/sub 2 films [NASA-TM-83565] p 92 N84-16380  
The ball bearing as a rheological test device [NASA-TM-83570] p 142 N84-17591  
Comparison of predicted and experimental thermal performance of angular-contact ball bearings [NASA-TP-2275] p 142 N84-18654  
Simulation of lubricating behavior of a thioether liquid lubricant by an electrochemical method [NASA-TP-2316] p 84 N84-23764  
Importance and definition of materials in tribology. Status of understanding p 84 N84-23893  
Thermal and oxidative stabilities of liquid lubricants p 84 N84-23907

- Operating characteristics of a three-piece-inner-ring large-bore roller bearing to speeds of 3 million DN [NASA-TP-2355] p 146 N84-29226  
Transmission efficiency measurements and correlations with physical characteristics of the lubricant [NASA-TM-83740] p 147 N84-30293

## LUBRICATING OILS

- Ferrographic and spectrometer oil analysis from a failed gas turbine engine p 135 A84-11273  
Tribology in the 80's Volume 2 Sessions 5 - 8 [NASA-CP-2300-VOL-2] p 144 N84-25047  
Optical and other property changes of M-50 bearing steel surfaces for different lubricants and additive prior to scuffing [NASA-TM-83746] p 88 N84-34520

## LUBRICATION

- Non-Newtonian fluid model incorporated into elastohydrodynamic lubrication of rectangular contacts [ASME PAPER 83-LUB-15] p 138 A84-44300  
Numerical methods and computers used in elastohydrodynamic lubrication [NASA-TM-83524] p 141 N84-11498  
Mechanism of lubrication by trisylphosphate (TCP) [NASA-TP-2274] p 142 N84-18553  
Elastohydrodynamic lubrication of smooth surfaces p 144 N84-24895  
Surface topography-connections between lubrication and failure initiation p 144 N84-24898  
Elastohydrodynamic lubrication Status of understanding p 144 N84-25048  
Effect of substrate chemical pretreatment on the tribological properties of graphite films [NASA-TM-83574] p 85 N84-25831  
Lubricant jet flow phenomena in spur and helical gears with modified center distances and/or addendums for out-of-mesh conditions [NASA-TM-83723] p 146 N84-28224

## LUMINOUS INTENSITY

- Method of reducing temperature in high-speed photography [NASA-TM-83620] p 188 N84-22421

## M

## MACH NUMBER

- Investigation of mixing in a turbofan exhaust duct. II Computer code application and verification p 17 A84-27140

## MACHINERY

- Precision of spiral-bevel gears [ASME PAPER 82-WA/DE-33] p 135 A84-15950

## MACHINING

- Determination of near-surface plastic deformation in sliding contacts p 140 A84-48996

## MAGNESIUM

- Matrix effects in ion-induced emission as observed in Ne collisions with Cu-Mg and Cu-Al alloys [NASA-TM-83061] p 187 N84-10923  
Select fiber composites for space applications. A mechanistic assessment [NASA-TM-83631] p 55 N84-22702

## MAGNESIUM ALLOYS

- Thermal degradation of the tensile properties of unidirectionally reinforced FP-AI2O3/EZ 33 magnesium composites p 52 A84-28229

## MAGNETIC FIELD CONFIGURATIONS

- Orbital stability in combined uniform axial and three-dimensional wiggler magnetic fields for free-electron lasers [NASA-TM-83753] p 134 N84-30273

## MAGNETIC FLUX

- Dilute plasma coupling currents to a high voltage solar array in weak magnetic fields [NASA-TM-83687] p 47 N84-24708

## MAGNETIC PROPERTIES

- New propulsion components for electric vehicles p 103 A84-30209

## K-band latching switches

- [NASA-CR-168253] p 109 N84-24973

## MAGNETIC STORMS

- Particle environment --- solar arrays and electric discharges [NASA-CR-173888] p 191 N84-33210

## MAGNETIC TAPES

- Friction and morphology of magnetic tapes in sliding contact with nickel-zinc ferrite [NASA-TP-2267] p 82 N84-16334  
Water-vapor effects on friction of magnetic tape in contact with nickel-zinc ferrite [NASA-TP-2279] p 82 N84-18399  
Properties of ferrites important to their friction and wear behavior [NASA-TM-83718] p 87 N84-28994

- Effects of water-vapor on friction and deformation of polymers magnetic media in contact with a ceramic oxide [NASA-TM-83727] p 87 N84-30072

## MAGNETIZATION

- Development of high frequency low weight power magnets for aerospace power systems [NASA-TM-83656] p 109 N84-22892

## MAGNETOHYDRODYNAMIC GENERATORS

- Transient flow analysis of the AEDC/HPDE MHD generator p 189 A84-24049  
Oxidant system improvements for MHD energy conversion and industrial processes p 189 A84-24058

## MAGNETOHYDRODYNAMIC STABILITY

- Discharges on a negatively biased solar array in a charged particle environment [NASA-TM-83644] p 47 N84-23690

## MAGNETORESISTIVITY

- Electronic properties of carbon fibers intercalated with copper chloride p 104 A84-34521

## MAGNETS

- Improved transistor-controlled and commutated brushless DC motors for electric vehicle propulsion [NASA-CR-168053] p 105 N84-10450  
Study and review of permanent magnets for electric vehicle propulsion motors [NASA-CR-168178] p 193 N84-14071

## MANGANESE

- Surface chemistry, friction, and wear of Ni-Zn and Mn-Zn ferrites in contact with metals p 78 A84-13516

## MANNED SPACECRAFT

- Space Station propulsion analysis study [AIAA PAPER 84-1326] p 44 A84-44179  
Space station propulsion analysis study [NASA-TM-83715] p 47 N84-25764  
The potential impact of new power system technology on the design of a manned space station [NASA-TM-83770] p 49 N84-31272

## MANUALS

- Manual of phosphoric acid fuel cell power plant cost model and computer program [NASA-CR-174720] p 173 N84-34037

## MANUFACTURING

- Study to establish cost projections for production of Redox chemicals [NASA-CR-167881] p 164 N84-11580

## MARKET RESEARCH

- Rural land mobile radio market assessment and satellite and terrestrial system concepts [AIAA PAPER 84-0754] p 95 A84-25324  
Mobile radio alternative systems study Volume 1 Traffic model [NASA-CR-168062] p 96 N84-10402  
Mobile radio alternative systems study satellite/terrestrial (hybrid) systems concepts [NASA-CR-168064] p 96 N84-10404

## MARKETING

- The worldwide market for photovoltaics in the rural sector p 161 A84-23135

## MASS TRANSFER

- Calculations of turbulent mass transport in a bluff-body diffusion-flame combustor [AIAA PAPER 84-0372] p 114 A84-18048  
Mass and momentum turbulent transport experiments with confined swirling coaxial jets I [AIAA PAPER 84-1380] p 119 A84-35664  
Comparisons of rational engineering correlations of thermophoretically-augmented particle mass transfer with STAN5-predictions for developing boundary layers [ASME PAPER 84-GT-158] p 92 A84-46965  
Mass and momentum turbulent transport experiments with confined swirling coaxial jets [NASA-CR-168252] p 124 N84-17530  
Engineering correlations of variable-property effects on laminar forced convection mass transfer for dilute vapor species and small particles in air [NASA-CR-168322] p 124 N84-18578  
Comparisons of rational engineering correlations of thermophoretically-augmented particle mass transfer with STAN5-predictions for developing boundary layers [NASA-CR-168221] p 93 N84-19606  
Experimental and theoretical deposition rates from salt-seeded combustion gases of a Mach 0.3 burner rig [NASA-TP-2225] p 124 N84-19741  
Modeling of zero gravity venting [NASA-CR-173503] p 127 N84-23854  
Mass transfer from a circular cylinder: Effects of flow unsteadiness and slight nonuniformities [NASA-CR-174759] p 129 N84-32751

## MATERIALS HANDLING

- Characterization and measurement of polymer wear [NASA-TM-83628] p 83 N84-21739

## MATERIALS SCIENCE

- Tribology in the 80's. Volume 2. Sessions 5 - 8 [NASA-CP-2300-VOL-2] p 144 N84-25047



**MATERIALS TESTS**

Material removal considerations for metal-ceramic  
 abradable turbine seal systems p 135 A84-15575  
 Characterization and measurement of polymer wear  
 [NASA-TM-83628] p 83 N84-21739

**MATHEMATICAL MODELS**

Identification of multivariable high performance turbofan  
 engine dynamics from closed loop data p 16 A84-18582  
 A thermomechanical model for energy propagation in  
 a solid-fluid-solid system with one boundary in relative  
 motion [ASME PAPER 83-HT-97] p 137 A84-29092  
 Predictive capability of long-term cavitation and liquid  
 impingement erosion models p 50 A84-32646  
 Analytic modeling of a spray diffusion flame  
 [AIAA PAPER 84-1317] p 118 A84-35168  
 Secondary flow spanwise deviation model for the stators  
 of NASA middle compressor stages [NASA-CR-173360] p 27 N84-18202  
 Turbulent swirling combustion p 61 N84-20535  
 Error reduction program. A progress report p 27 N84-20536  
 Identification of multivariable high-performance turbofan  
 engine dynamics from closed loop data p 28 N84-20580

Modeling of zero gravity venting  
 [NASA-CR-173503] p 127 N84-23854  
 Comparison of free-piston Stirling engine model  
 predictions with RE1000 engine test data [NASA-TM-83650] p 195 N84-24509  
 Study of effects of fuel properties in turbine-powered  
 business aircraft [NASA-CR-174627] p 91 N84-25854  
 Three component velocity measurements using  
 Fabry-Perot interferometer [NASA-TM-83692] p 133 N84-26010  
 Modeling degradation and failure of Ni-Cr-Al overlay  
 coatings [NASA-TM-83672] p 74 N84-27858  
 Dilution jets in accelerated cross flows  
 [NASA-CR-174717] p 34 N84-28794  
 The structure of evaporating and combusting sprays  
 Measurements and predictions [NASA-CR-173778] p 128 N84-29155  
 A theoretical and experimental study of turbulent  
 nonevaporating sprays [NASA-CR-174668] p 35 N84-29877  
 Atomization of liquid sheets in high pressure airflow  
 [NASA-TM-83731] p 128 N84-30223  
 Empirical relations for cavitation and liquid impingement  
 erosion processes [NASA-TP-2339] p 76 N84-31349  
 Unsteady transonic flow in cascades  
 [NASA-TM-83780] p 11 N84-32351  
 Rocket injector anomalies study. Volume 1: Description  
 of the mathematical model and solution procedure  
 [NASA-CR-174702] p 49 N84-32428  
 A theoretical model for the cross spectra between  
 pressure and temperature downstream of a combustor  
 [NASA-TM-83671] p 186 N84-34231

**MATRICES (MATHEMATICS)**

Direct and implicit optical matrix-vector algorithms  
 p 187 A84-13184  
 Acoustooptic linear algebra processors - Architectures,  
 algorithms, and applications p 175 A84-40266  
 Element-by-element solution procedures for nonlinear  
 structural analysis p 158 N84-31694  
 Automatic finite element generators p 158 N84-31695

**MATRIX MATERIALS**

Improved high temperature resistant matrix resins  
 [NASA-CR-168210] p 87 N84-28995

**MATRIX METHODS**

Resin selection criteria for tough composite structures  
 [NASA-TM-83449] p 81 N84-10310

**MEASURING INSTRUMENTS**

Advanced high temperature heat flux sensors  
 [NASA-TM-83526] p 123 N84-16493  
 Comparison of icing cloud instruments for 1982-1983  
 icing season flight program [NASA-TM-83569] p 14 N84-29870

**MECHANICAL DEVICES**

Precision of spiral-bevel gears  
 [ASME PAPER 82-WA/DE-33] p 135 A84-15950  
 Method and apparatus for gripping uniaxial fibrous  
 composite materials [NASA-CASE-LEW-13758-1] p 56 N84-27829  
 Lubrication of machine elements  
 [NASA-RP-1126] p 147 N84-31640

**MECHANICAL DRIVES**

Kinematic precision of gear trains  
 [ASME PAPER 82-WA/DE-34] p 135 A84-15951  
 Elastic model of the traction behavior of two traction  
 lubricants p 136 A84-28791

An advanced pitch change mechanism incorporating a  
 hybrid traction drive [AIAA PAPER 84-1383] p 20 A84-44182  
 An advanced pitch change mechanism incorporating a  
 hybrid traction drive [NASA-TM-83709] p 2 N84-25605  
 Dynamics of early planetary gear trains  
 [NASA-CR-3793] p 145 N84-26027  
 An analysis of traction drive torsional stiffness  
 [NASA-TM-83712] p 145 N84-27043  
 Automotive Stirling engine development program  
 [NASA-CR-174622] p 195 N84-32305

**MECHANICAL MEASUREMENT**

Mechanical behavior of carbon-carbon composites  
 [NASA-CR-174767] p 57 N84-34575

**MECHANICAL PROPERTIES**

Environmental and high strain rate effects on composites  
 for engine applications p 51 A84-17444  
 Residual stress in plasma-sprayed ceramic turbine tip  
 and gas-path seal specimens p 78 A84-19783  
 Mechanical and physical properties of plasma-sprayed  
 stabilized zirconia p 79 A84-19786  
 Carbides in iron-rich Fe-Mn-Cr-Mo-Al-Si-C systems  
 p 64 A84-26815  
 Simplified composite micromechanics equations of  
 hygral, thermal, and mechanical properties p 53 A84-49377  
 Effects of cobalt in nickel-base superalloys  
 [NASA-CR-168308] p 67 N84-14287  
 Influence of cobalt, tantalum and tungsten on the high  
 temperature mechanical properties of single crystal  
 nickel-base superalloys [NASA-TM-83479] p 70 N84-17355  
 Overview of zirconia with respect to gas turbine  
 applications [NASA-TP-2286] p 83 N84-21740  
 The impact resistance of SiC and other mechanical  
 properties of SiC and Si3N4 [NASA-CR-165925] p 84 N84-24809  
 An investigation into the injection molding of PMR-15  
 polyimide [NASA-CR-173550] p 85 N84-24810  
 Status of understanding for gear materials p 144 N84-25061  
 Fabrication development for ODS-superalloy, air-cooled  
 turbine blades [NASA-CR-174650] p 32 N84-25711  
 Microstructure and orientation effects on properties of  
 discontinuous silicon carbide/aluminum composites  
 [NASA-TP-2302] p 51 N84-26749  
 ICAN: Integrated composites analyzer [NASA-TM-83700] p 56 N84-26755  
 Development of partially fluorinated resin apex seals  
 [NASA-CR-174706] p 148 N84-32828  
 The role of material properties in adhesion  
 [NASA-TP-83792] p 88 N84-34619

**MEDICAL EQUIPMENT**

Qualification testing of solar photovoltaic powered  
 refrigerator freezers for medical use in remote geographic  
 locations [NASA-CR-168181] p 169 N84-25162  
 Solar photovoltaic powered refrigerators/freezers for  
 medical use in remote geographic locations  
 [NASA-CR-168268] p 169 N84-25163

**MELT SPINNING**

Rapid solidification via melt spinning - Equipment and  
 techniques p 65 A84-31915

**MELTING POINTS**

Scaling relations in the equation of state, thermal  
 expansion, and melting of metals p 192 A84-19359

**MELTS (CRYSTAL GROWTH)**

Free dendritic growth p 190 A84-42829  
 Some fundamental aspects of solidification in a  
 supercooled melt [NASA-TM-83714] p 73 N84-26787  
 Transport processes in dendritic crystallization  
 p 191 N84-28621

**MEMBRANES**

Anion permselective membrane  
 [NASA-CR-174725] p 172 N84-29358

**MERIDIONAL FLOW**

Programs for calculating quasi-three-dimensional flow  
 in a turbomachine blade row [NASA-TM-83588] p 9 N84-17138

**MESSAGE PROCESSING**

30/20 GHz communications systems baseband  
 processor development p 95 A84-38251

**METAL COATINGS**

Oxidation behavior of a thermal barrier coating  
 p 65 A84-42667  
 Modeling degradation and failure of Ni-Cr-Al overlay  
 coatings [NASA-TM-83672] p 74 N84-27858

**METAL CRYSTALS**

The development of directional coarsening of the  
 gamma-prime precipitate in superalloy single crystals  
 p 63 A84-10597  
 Some fundamental aspects of solidification in a  
 supercooled melt [NASA-TM-83714] p 73 N84-26787  
 Characterization of erosion of metallic materials under  
 cavitation attack in a mineral oil [NASA-TP-2368] p 147 N84-32825

**METAL FATIGUE**

High-temperature fatigue in metals - A brief review of  
 life prediction methods developed at the Lewis Research  
 Center of NASA p 64 A84-14286  
 The effects of frequency and hold times on fatigue crack  
 propagation rates in a nickel base superalloy p 64 A84-18733  
 Fatigue crack growth and low cycle fatigue of two nickel  
 base superalloys [NASA-CR-174534] p 66 N84-10267  
 Effect of crack curvature on stress intensity factors for  
 ASTM standard compact tension specimens  
 [NASA-CR-168280] p 153 N84-11513  
 Preliminary study of thermomechanical fatigue of  
 polycrystalline MAR-M 200 [NASA-TP-2280] p 69 N84-17350  
 Literature survey on oxidations and fatigue lives at  
 elevated temperatures [NASA-CR-174639] p 71 N84-20674  
 Optical and other property changes of M-50 bearing steel  
 surfaces for different lubricants and additive prior to  
 scuffing [NASA-TM-83746] p 88 N84-34620

**METAL FILMS**

Parallel-processing with surface plasmons, a new  
 strategy for converting the broad solar spectrum p 160 A84-23006

Adhesion between polymers and evaporated gold and  
 nickel films [NASA-TP-2360] p 87 N84-31379

**METAL MATRIX COMPOSITES**

Factors influencing the thermally-induced strength  
 degradation of B/Al composites p 52 A84-28227  
 Tungsten-fiber-reinforced superalloy composite,  
 high-temperature component design considerations p 53 A84-28241  
 Arc spray fabrication of metal matrix composite  
 monolayer - high temperature fiber-reinforced superalloy  
 composites [NASA-CASE-LEW-13828-1] p 54 N84-15203  
 Analysis of stress-strain, fracture and ductility behavior  
 of aluminum matrix composites containing discontinuous  
 silicon carbide reinforcement [NASA-TM-83610] p 54 N84-21666  
 The strength of the metal. Aluminum oxide interface  
 p 72 N84-23898  
 Microstructure and orientation effects on properties of  
 discontinuous silicon carbide/aluminum composites  
 [NASA-TP-2302] p 51 N84-26749  
 Nonlinear analysis for high-temperature composites  
 Turbine blades/vanes p 158 N84-31699

**METAL OXIDES**

Structure of transient oxides formed on NiCrAl alloys  
 p 63 A84-12385  
 Improved thermal barrier coating system  
 [NASA-CASE-LEW-14057-1] p 88 N84-33595

**METAL PLATES**

Multicolor printing plate joining  
 [NASA-CASE-LEW-13598-1] p 132 N84-22930  
 Optical and other property changes of M-50 bearing steel  
 surfaces for different lubricants and additive prior to  
 scuffing [NASA-TM-83746] p 88 N84-34620

**METAL POWDER**

Internal heat transfer coefficients of porous metals  
 p 112 A84-13239  
 Diamondlike flakes [NASA-CASE-LEW-13837-2] p 54 N84-22696  
 Status of understanding for gear materials p 144 N84-25061

**METAL SPRAYING**

Arc spray fabrication of metal matrix composite  
 monolayer - high temperature fiber-reinforced superalloy  
 composites [NASA-CASE-LEW-13828-1] p 54 N84-15203

**METAL SURFACES**

Surfaces - characterization of surface properties for  
 predicting bond quality p 50 A84-10680  
 A study of the effect of solid particle impact and particle  
 shape on the erosion morphology of ductile metals  
 p 66 A84-45570  
 Correlation of electron emission with changes in the  
 surface concentration of barium and oxygen on a tungsten  
 surface p 60 A84-45917  
 Determination of near-surface plastic deformation in  
 sliding contacts p 140 A84-48996



- Friction and wear of nickel in sulfonic acid  
[NASA-TP-2280] p 72 N84-21721
- Coating with overlay metallic-cermet alloy systems  
[NASA-CASE-LEW-13639-2] p 73 N84-27855
- Empirical relations for cavitation and liquid impingement erosion processes  
[NASA-TP-2339] p 76 N84-31349
- METAL VAPOURS**
- Metal vapor vacuum arc switching - Applications and results --- for launchers p 103 A84-32029
- METAL-METAL BONDING**
- Tribology in the 80's Volume 1. Sessions 1 to 4  
[NASA-CP-2300-VOL-1] p 144 N84-23891
- Metallic adhesion and bonding p 72 N84-23897
- Materials for Advanced Turbine Engines (MATE) Project 3: Design, fabrication and evaluation of an oxide dispersion strengthened sheet alloy combustor liner, volume 1  
[NASA-CR-174691] p 76 N84-32504
- METALLIC GLASSES**
- Metallic glass as a temperature sensor during ion plating  
[NASA-TM-83566] p 69 N84-17351
- Mechanical contact induced transformation from the amorphous to the crystalline state in metallic glass  
[NASA-TM-83583] p 71 N84-20673
- Microstructure and surface chemistry of amorphous alloys important to their friction and wear behavior  
[NASA-TM-83762] p 76 N84-32508
- METALLIZING**
- Overlay metallic-cermet alloy coating systems  
[NASA-CASE-LEW-13639-1] p 77 N84-33555
- METALLOGRAPHY**
- Morphology of an aluminum alloy eroded by a normally incident jet of angular erodent particles p 64 A84-18244
- METALS**
- Scaling relations in the equation of state, thermal expansion, and melting of metals p 192 A84-19359
- Ceramic composite liner material for gas turbine combustors  
[NASA-TM-83490] p 24 N84-14145
- Particulate erosion mechanisms  
[NASA-TM-83551] p 68 N84-14289
- Importance and definition of materials in tribology  
Status of understanding p 84 N84-23893
- The strength of the metal. Aluminum oxide interface p 72 N84-23898
- Fundamentals of Alloy Solidification Applied to Industrial Processes  
[NASA-CP-2337] p 77 N84-34589
- METEOROLOGICAL SERVICES**
- Sixth Annual Workshop on Meteorological and Environmental Inputs to Aviation Systems, 26-28 October 1982, Tullahoma, Tenn p 174 A84-23424
- METHANE**
- Effect of gravity on halogenated hydrocarbon flame retardant effectiveness  
[NASA-TM-83761] p 63 N84-33536
- METHYL ALCOHOLS**
- Turbidity very near the critical point of methanol-cyclohexane mixtures p 192 A84-30391
- Develop and test fuel cell powered on-site integrated total energy system  
[NASA-CR-168159] p 164 N84-11581
- Utilization of alternative fuels in diesel engines  
[NASA-CR-174669] p 91 N84-26813
- Evaluation of dissociated and steam-reformed methanol as automotive engine fuels  
[NASA-CR-168242] p 91 N84-27909
- MICROCOMPUTERS**
- A real-time, portable, microcomputer-based jet engine simulator  
[NASA-TM-83550] p 176 N84-16012
- MICROMECHANICS**
- Simplified composite micromechanics equations for strength, fracture toughness and environmental effects p 53 A84-41858
- Simplified composite micromechanics equations for strength, fracture toughness and environmental effects  
[NASA-TM-83696] p 56 N84-27832
- Application of finite element substructuring to composite micromechanics  
[NASA-TM-83729] p 57 N84-31288
- MICROPROCESSORS**
- ADA and multi-microprocessor real-time simulation p 176 A84-10905
- A generalized computer code for developing dynamic gas turbine engine models (DIGTEM)  
[NASA-TM-83508] p 22 N84-12166
- MICROSTRIP TRANSMISSION LINES**
- The study of microstrip antenna arrays and related problems  
[NASA-CR-173534] p 99 N84-23807
- Monolithic microwave integrated circuits  
Interconnections and packaging considerations  
[NASA-TM-83774] p 100 N84-31461
- Monolithic microwave integrated circuit devices for active array antennas  
[NASA-CR-173981] p 112 N84-34675
- MICROSTRUCTURE**
- Structure of transient oxides formed on NiCrAl alloys p 63 A84-12385
- The effect of microstructure on 650 C fatigue crack growth in P/M Astroloy p 63 A84-12395
- Compositional effects on Si3N4 fracture surfaces p 79 A84-19794
- Free dendritic growth p 190 A84-42829
- Effects of processing and microstructure on the fatigue behaviour of the nickel-base superalloy Rene95 p 66 A84-48715
- Simplified composite micromechanics equations of hygral, thermal, and mechanical properties p 53 A84-49377
- Effects of cobalt in nickel-base superalloys  
[NASA-CR-168308] p 67 N84-14287
- Characteristic morphological and frictional changes in sputtered MoS/sub 2 films  
[NASA-TM-83565] p 92 N84-16380
- Influence of composition on the microstructure and mechanical properties of a nickel-base superalloy single crystal  
[NASA-TM-83563] p 70 N84-17354
- Functional and morphological properties of Au-MoS2 films sputtered from a compact target p 143 N84-20658
- Method of making an ion beam sputter-etched ventricular catheter for hydrocephalus shunt  
[NASA-CASE-LEW-13107-2] p 174 N84-23095
- The impact resistance of SiC and other mechanical properties of SiC and Si3N4  
[NASA-CR-165325] p 84 N84-24809
- Microstructure and orientation effects on properties of discontinuous silicon carbide/aluminum composites  
[NASA-TP-2302] p 51 N84-26749
- Effects of long-time elevated temperature exposures on hot-isostatically-pressed power-metallurgy Udmet 700 alloys with reduced cobalt contents  
[NASA-TM-83632] p 57 N84-28917
- Microstructure and surface chemistry of amorphous alloys important to their friction and wear behavior  
[NASA-TM-83762] p 76 N84-32508
- RF sputtered silicon and hafnium nitrides as applied to 440C steel  
[NASA-TM-85862] p 87 N84-32536
- The role of the reflection coefficient in precision measurement of ultrasonic attenuation  
[NASA-TM-83788] p 149 N84-32849
- Fracture surface characteristics of notched angleplyed graphite/epoxy composites  
[NASA-TM-83786] p 57 N84-33522
- MICROWAVE AMPLIFIERS**
- A three-stage power amplifier for a 20 GHz monolithic transmit module p 102 A84-22873
- 0.5 W 2-21 GHz monolithic GaAs distributed amplifier p 103 A84-30857
- A K-band GaAs FET amplifier with 8.2-W output power p 104 A84-32280
- NASA seeking high-power 60-GHz IMPATT diodes p 104 A84-44912
- Beam impingement angle effects on secondary electron emission characteristics of textured pyrolytic graphite  
[NASA-TP-2285] p 82 N84-18400
- Secondary electron emission characteristics of ion-textured copper and high-purity isotropic graphite surfaces  
[NASA-TP-2342] p 86 N84-28989
- MICROWAVE ANTENNAS**
- Multibeam antenna for 30/20 GHz advanced communications satellite using offset shaped, dual reflector surfaces p 93 A84-15627
- MICROWAVE CIRCUITS**
- A Ka-band GaAs monolithic phase shifter p 101 A84-18371
- GaAs dual-gate FET for operation up to K-band p 104 A84-32281
- MMIC technology for advanced space communications systems  
[NASA-TM-83749] p 100 N84-30147
- Monolithic microwave integrated circuit devices for active array antennas  
[NASA-CR-173981] p 112 N84-34675
- MICROWAVE EQUIPMENT**
- Electromagnetic plasma models for microwave plasma cavity reactors  
[AIAA PAPER 84-1521] p 189 A84-46108
- MICROWAVE OSCILLATORS**
- High efficiency IMPATT diodes for 60 GHz intersatellite link applications  
[AIAA PAPER 84-0767] p 103 A84-25333
- MICROWAVE PLASMA PROBES**
- Spatial electron density and electric field strength measurements in microwave cavity experiments  
[AIAA PAPER 84-1522] p 189 A84-46109
- MICROWAVE SWITCHING**
- Serial MSK modem for the Advanced Communications Satellite Program p 93 A84-15629
- 30/20 GHz communications systems baseband processor development p 95 A84-38251
- High-speed wide band 20 x 20 microwave switch matrix p 105 A84-49253
- The 20 x 20 high speed microwave switches  
[NASA-TM-83775] p 101 N84-32644
- MICROWAVE TRANSMISSION**
- A three-stage power amplifier for a 20 GHz monolithic transmit module p 102 A84-22873
- Recent developments in EHF Satcom technology p 39 A84-46620
- Millimeter wave transmission systems and related devices  
[NASA-CR-173515] p 99 N84-24918
- MICROWAVES**
- Characteristics of a microwave plasma disk ion source p 189 A84-23390
- Microwave monolithic integrated circuit development for future spaceborne phased array antennas  
[AIAA PAPER 84-0656] p 94 A84-25257
- Microwave monolithic integrated circuit development for future spaceborne phased array antennas  
[NASA-TM-83518] p 97 N84-13399
- Laboratory degradation of Kapton in a low energy oxygen ion beam  
[NASA-TM-83530] p 41 N84-18310
- MIGRATION**
- A laser system to remotely sense bird movements p 159 A84-31608
- MILLIMETER WAVES**
- A Ka-band GaAs monolithic phase shifter p 101 A84-18371
- Recent developments in EHF Satcom technology p 39 A84-46620
- The 30 GHz communications satellite low noise receiver  
[NASA-CR-168254] p 97 N84-13398
- Millimeter wave transmission systems and related devices  
[NASA-CR-173515] p 99 N84-24918
- MMIC technology for advanced space communications systems  
[NASA-TM-83749] p 100 N84-30147
- MINERAL OILS**
- Surface roughness effects with solid lubricants dispersed in mineral oils  
[ASLE PREPRINT 83-LC-4C-1] p 137 A84-28987
- Characterization of erosion of metallic materials under cavitation attack in a mineral oil  
[NASA-TP-2368] p 147 N84-32825
- MISMATCH (ELECTRICAL)**
- Development of a 30 percent efficient 3-junction monolithic cascade solar cell p 171 N84-29328
- MISSILE CONTROL**
- Optical Kalman filtering for missile guidance p 178 A84-38596
- MIXERS**
- Further development of a method for computing three-dimensional subsonic viscous flows in turbofan lobe mixers  
[NASA-CR-168304] p 122 N84-14462
- MIXING LENGTH FLOW THEORY**
- Hot-flow tests of a series of 10-percent-scale turbofan forced mixing nozzles  
[NASA-TP-2268] p 123 N84-17525
- MIXTURES**
- Investigation of sources, properties and preparation of distillate test fuels  
[NASA-CR-168227] p 89 N84-13332
- Flame propagation in heterogeneous mixtures of fuel drops and air  
[NASA-CR-174644] p 91 N84-29775
- MODAL RESPONSE**
- Stagger angle dependence of inertial and elastic coupling in bladed disks p 151 A84-31903
- MODEMS**
- Serial MSK modem for the Advanced Communications Satellite Program p 93 A84-15629
- Carrier recovery methods for a dual-mode modem. A design approach  
[NASA-CR-173355] p 36 N84-19360
- Design considerations for a monolithic, GaAs, dual-mode, QPSK/QASK, high-throughput rate transceiver  
[NASA-CR-173560] p 110 N84-24974
- MODULATION**
- Air modulation apparatus  
[NASA-CASE-LEW-13524-1] p 35 N84-33410

## MODULATORS

- Design considerations for a monolithic, GaAs, dual-mode, QPSK/QASK, high-throughput rate transceiver  
[NASA-CR-173560] p 110 N84-24974
- MODULUS OF ELASTICITY**  
Elastic model of the traction behavior of two traction lubricants p 136 A84-28791  
Finite elastic-plastic deformation of polycrystalline metals p 66 A84-43372
- MOISTURE**  
Application of finite element substructuring to composite micromechanics  
[NASA-TM-83729] p 57 N84-31288
- MOLECULAR BEAM EPITAXY**  
High efficiency IMPATT diodes for 60 GHz intersatellite link applications  
[NASA-TM-83584] p 108 N84-19708
- MOLECULAR ROTATION**  
Measurement of heat pump processes induced by laser radiation  
[NASA-CR-168324] p 134 N84-18320
- MOLYBDENUM DISULFIDES**  
Fractional and morphological properties of Au-MoS<sub>2</sub> films sputtered from a compact target  
[NASA-TM-83604] p 143 N84-20958
- MOLYBDENUM SULFIDES**  
Characteristic morphological and fractional changes in sputtered MoS<sub>2</sub>/sub 2 films  
[NASA-TM-83565] p 92 N84-16380
- MOMENTUM**  
Determination of compressor in-stall characteristics from engine surge transients  
[AIAA PAPER 84-1206] p 18 A84-36959  
The influence of large-scale motion on turbulent transport for confined coaxial jets p 125 N84-20542  
Determination of compressor in-stall characteristics from engine surge transients  
[NASA-TM-83639] p 29 N84-22566
- MOMENTUM TRANSFER**  
Mass and momentum turbulent transport experiments with confined swirling coaxial jets I  
[AIAA PAPER 84-1380] p 119 A84-35564  
Mass and momentum turbulent transport experiments with confined swirling coaxial jets  
[NASA-CR-168252] p 124 N84-17530
- MONOMERS**  
Characterization of PMR polyimide resin and prepreg  
[NASA-CR-168217] p 83 N84-20595  
Chemical approach for controlling nadimide cure temperature and rate  
[NASA-CASE-LEW-13770-1] p 86 N84-27885
- MORPHOLOGY**  
Fractional and morphological properties of Au-MoS<sub>2</sub> films sputtered from a compact target  
[NASA-TM-83604] p 143 N84-20958
- MOTION PICTURES**  
Method of reducing temperature in high-speed photography  
[NASA-TM-83620] p 188 N84-22421
- MOTOR VEHICLES**  
Assessment of institutional barriers to the use of natural gas fuel in automotive vehicle fleets  
[NASA-CR-168183] p 165 N84-14587
- MULTIBEAM ANTENNAS**  
Concept for advanced satellite communications and required technologies p 93 A84-15626  
Multibeam antenna for 30/20 GHz advanced communications satellite using offset shaped, dual reflector surfaces p 93 A84-15627  
A new multiple beam satellite antenna for 30/20 GHz communications coverage of CONUS-experimental evaluation  
[AIAA PAPER 84-0655] p 94 A84-25256  
Economic comparison of FDMA and TDMA options for communications by Ka-band multiple beam satellites  
[AIAA PAPER 84-0740] p 94 A84-25299  
Advanced 30/20 GHz multiple-beam antennas for communications satellites p 40 A84-49250
- MULTILAYER INSULATION**  
Evaluation of propellant tank insulation concepts for low-thrust chemical propulsion systems' Executive summary  
[NASA-CR-168321] p 83 N84-20699
- MULTIPLE ACCESS**  
High-speed wide band 20 x 20 microwave switch matrix p 105 A84-49253
- MULTIPLIERS**  
The pressure multiplier revisited p 129 A84-13125
- MULTIPROCESSING (COMPUTERS)**  
ADA and multi-microprocessor real-time simulation p 176 A84-10905  
Operating system for a real-time multiprocessor propulsion system simulator  
[NASA-TM-83605] p 177 N84-20258

- RTMPL. A structured programming and documentation utility for real-time multiprocessor simulations  
[NASA-TM-83606] p 177 N84-20259
- MULTIVARIATE STATISTICAL ANALYSIS**  
Identification of multivariable high performance turbofan engine dynamics from closed loop data p 16 A84-18582

## N

## NACELLES

- Large, horizontal-axis wind turbines  
[NASA-TM-83546] p 169 N84-27327

## NAPHTHENES

- Investigation of sources, properties and preparation of distillate test fuels  
[NASA-CR-168227] p 89 N84-13332

## NASA PROGRAMS

- NASA priority technologies  
[IAF PAPER 83-345] p 37 A84-11793  
Concept for advanced satellite communications and required technologies p 93 A84-15626  
NASA's multibeam communications technology program p 39 A84-21397  
NASA's geostationary communications platform program  
[AIAA PAPER 84-0702] p 95 A84-25326  
NASA advanced low emissions combustor program  
[ASME PAPER 83-JPGG-GT-10] p 17 A84-28982  
Replacing critical and strategic refractory metal elements in nickel-base superalloys — NASA's COSAM program  
[NASA-TM-83528] p 67 N84-13264  
Detroit space odyssey  
[NASA-TM-85487] p 37 N84-15164  
Cleveland Space Odyssey  
[NASA-TM-85493] p 192 N84-16020  
Overview of NASA Lewis Research Center free-piston Stirling engine activities  
[NASA-TM-83649] p 195 N84-22512

## NASTRAN

- NASTRAN forced vibration analysis of rotating cyclic structures  
[ASME PAPER 83-DET-20] p 151 A84-29103  
Finite element forced vibration analysis of rotating cyclic structures  
[NASA-CR-165430] p 153 N84-11515  
NASTRAN flutter analysis of advanced turbopropellers  
[NASA-CR-167926] p 24 N84-14148  
NASTRAN documentation for flutter analysis of advanced turbopropellers  
[NASA-CR-167927] p 25 N84-15153  
NASTRAN forced vibration analysis of rotating cyclic structures  
[NASA-CR-173821] p 157 N84-29252  
Nonlinear displacement analysis of advanced propeller structures using NASTRAN  
[NASA-TM-83737] p 157 N84-31683

## NATURAL GAS

- Assessment of institutional barriers to the use of natural gas fuel in automotive vehicle fleets  
[NASA-CR-168183] p 165 N84-14587  
Advanced onboard storage concepts for natural gas-fueled automotive vehicles  
[NASA-CR-174655] p 172 N84-34036

## NAVIER-STOKES EQUATION

- A direct method for the solution of unsteady two-dimensional incompressible Navier-Stokes equations p 2 A84-10078  
Boundary conditions for the solution of compressible Navier-Stokes equations by an implicit factored method p 113 A84-13495  
Computation of viscous flow in curved ducts and comparison with experimental data  
[AIAA PAPER 84-0531] p 115 A84-21303  
Finite-analytic numerical method for unsteady two-dimensional Navier-Stokes equations p 116 A84-25807  
Dynamic response of shock waves in transonic diffuser and supersonic inlet - An analysis with the Navier-Stokes equations and adaptive grid  
[AIAA PAPER 84-1609] p 5 A84-38004  
Turbulent solutions of the equations of fluid motion p 121 A84-41155  
Computation of viscous flow in curved ducts and comparison with experimental data  
[NASA-TM-83548] p 122 N84-13494  
Application of improved numerical schemes p 178 N84-20537

## NEAR FIELDS

- Characteristics and capacities of the NASA Lewis Research Center high precision 6.7- by 6.7-m planar near-field scanner  
[NASA-TM-83785] p 133 N84-32789

## NETWORK ANALYSIS

- Parametric study of minimum converter loss in an energy-storage dc-to-dc converter p 101 A84-18403  
Communications network design and costing model technical manual  
[NASA-CR-168236] p 97 N84-14376  
Communications network design and costing model programmers manual  
[NASA-CR-168237] p 97 N84-14377  
Communications network design and costing model users manual  
[NASA-CR-168238] p 97 N84-14378
- NETWORK CONTROL**  
ACTS TDMA network control — Advanced Communication Technology Satellite  
[AIAA PAPER 84-0682] p 94 A84-25274
- NETWORK SYNTHESIS**  
Extensions of the discrete-average models for converter power stages p 102 A84-18411  
Stability analysis of a buck regulator employing input filter compensation p 102 A84-18412  
Design considerations for FET-gated power transistors p 102 A84-18414  
Inherent overload protection for the series resonant converter p 102 A84-23255
- NEUTRALIZERS**  
Simplification of power electronics for ion thruster neutralizers p 44 A84-49509
- NEUTRON IRRADIATION**  
Development and fabrication of a high current, fast recovery power diode  
[NASA-CR-168196] p 106 N84-13443
- NEWTON-RAPHSON METHOD**  
Algorithms for elasto-plastic-creep postbuckling p 152 A84-38480  
Self-adaptive solution strategies p 158 N84-31693
- NEWTONIAN FLUIDS**  
Prediction of turbulent flow past a prosthetic heart valve p 175 A84-49108  
Elastohydrodynamic lubrication. Status of understanding p 144 N84-25048
- NICKEL**  
Surface chemistry, fraction, and wear of Ni-Zn and Mn-Zn ferrites in contact with metals p 78 A84-13516  
Fraction and wear of nickel in sulfuric acid  
[NASA-TP-2290] p 72 N84-21721  
Method of making a light weight battery plaque  
[NASA-CASE-LEW-13349-1] p 72 N84-22734  
Development of a lightweight nickel electrode  
[NASA-TM-86861] p 172 N84-30528  
Overlay coating degradation by simultaneous oxidation and coating/substrate interdiffusion  
[NASA-TM-83738] p 75 N84-31344  
Low cycle fatigue behavior of conventionally cast MAR-M 200 AT 1000 deg C  
[NASA-TM-83769] p 77 N84-33564
- NICKEL ALLOYS**  
The development of directional coarsening of the gamma-prime precipitate in superalloy single crystals p 63 A84-10597  
Structure of transient oxides formed on NiCrAl alloys p 63 A84-12385  
The effects of frequency and hold times on fatigue crack propagation rates in a nickel base superalloy p 64 A84-18793  
The effects of Cr, Al, Ti, Mo, W, Ta, and Co on the cyclic oxidation behavior of cast Ni-base superalloys at 1100 and 1150 C p 65 A84-27485  
The structure of extruded NiAl p 65 A84-36047  
Solute transport and the prediction of breakaway oxidation in gamma + beta Ni-Cr-Al alloys p 65 A84-42658  
Elevated temperature compressive steady state deformation and failure in the oxide dispersion strengthened alloy MA 6000E p 66 A84-46785  
Low strain, long life creep fatigue of AF2-1DA and INCO 718  
[NASA-CR-167989] p 66 N84-10268  
Replacing critical and strategic refractory metal elements in nickel-base superalloys — NASA's COSAM program  
[NASA-TM-83528] p 67 N84-13264  
Effects of cobalt in nickel-base superalloys  
[NASA-CR-168308] p 67 N84-14287  
Low-cost single-crystal turbine blades, volume 1  
[NASA-CR-168218] p 68 N84-15247  
Application of induction coil measurements to the study of superalloy hot corrosion and oxidation  
[NASA-TM-83560] p 69 N84-16311  
Fraction and morphology of magnetic tapes in sliding contact with nickel-zinc ferrite  
[NASA-TP-2267] p 82 N84-16334  
Factors which influence directional coarsening of Gamma prime during creep in nickel-base superalloy single crystals  
[NASA-TM-83595] p 69 N84-17353

- Influence of cobalt, tantalum and tungsten on the high temperature mechanical properties of single crystal nickel-base superalloys  
[NASA-TM-83479] p 70 N84-17355
- Analysis of thermoelectric properties of high-temperature complex alloys of nickel-base, iron-base and cobalt-base groups  
[NASA-TP-2278] p 70 N84-18370
- Water-vapor effects on friction of magnetic tape in contact with nickel-zinc ferrite  
[NASA-TP-2279] p 82 N84-18399
- Mechanism of corrosion of Ni base superalloys by molten Na<sub>2</sub>MoO<sub>4</sub> at elevated temperatures  
[NASA-TM-83580] p 70 N84-20672
- Literature survey on oxidations and fatigue lives at elevated temperatures  
[NASA-CR-174639] p 71 N84-20674
- Effects of alloy composition on cyclic flame hot-corrosion attack of cast nickel-base superalloys at 900 deg C  
[NASA-TP-2338] p 73 N84-26783
- Modeling degradation and failure of Ni-Cr-Al overlay coatings  
[NASA-TM-83672] p 74 N84-27858
- Chemical mechanisms and reaction rates for the initiation of hot corrosion of IN-738  
[NASA-TP-2319] p 74 N84-28958
- High-temperature cyclic oxidation data, volume 1  
[NASA-TM-83665] p 75 N84-31345
- Understanding the roles of the strategic element cobalt in nickel base superalloys p 76 N84-33471
- NICKEL CADMIUM BATTERIES**
- A 37.5-kW point design comparison of the nickel-cadmium battery, bipolar nickel-hydrogen battery, and regenerative hydrogen-oxygen fuel cell energy storage subsystems for low Earth orbit  
[NASA-TM-83651] p 167 N84-23022
- NICKEL COATINGS**
- Adhesion between polymers and evaporated gold and nickel films  
[NASA-TP-2360] p 37 N84-31379
- NICKEL HYDROGEN BATTERIES**
- Cycle life test and failure model of nickel-hydrogen cells p 162 N84-30185
- Long life nickel electrodes for a nickel-hydrogen cell. I  
Initial performance p 162 N84-30186
- Pore size engineering applied to the design of separators for nickel-hydrogen cells and batteries p 162 N84-30187
- Test results of a ten cell bipolar nickel-hydrogen battery p 162 N84-30188
- Development of a large scale bipolar NiH<sub>2</sub> battery p 162 N84-30189
- Separator development and testing of nickel-hydrogen cells  
[NASA-TM-83653] p 62 N84-22712
- Advanced nickel-hydrogen cell configuration study  
[NASA-CR-173417] p 108 N84-22889
- A 37.5-kW point design comparison of the nickel-cadmium battery, bipolar nickel-hydrogen battery, and regenerative hydrogen-oxygen fuel cell energy storage subsystems for low Earth orbit  
[NASA-TM-83651] p 167 N84-23022
- Design of a 1-kWh bipolar nickel hydrogen battery  
[NASA-TM-83647] p 168 N84-23024
- Advanced designs for IPV nickel-hydrogen cells  
[NASA-TM-83643] p 168 N84-23025
- Teardown analysis of a ten cell bipolar nickel-hydrogen battery  
[NASA-TM-83618] p 168 N84-23026
- Oxygen recombination in individual pressure vessel nickel-hydrogen batteries  
[NASA-CASE-LEW-13822-1] p 110 N84-29084
- Test results of a ten cell bipolar nickel-hydrogen battery p 112 N84-33702
- NICKEL ZINC BATTERIES**
- Additive for zinc electrodes --- electric automobiles  
[NASA-CASE-LEW-13286-1] p 106 N84-14422
- NIMBUS 7 SATELLITE**
- Development of Great Lakes algorithms for the Nimbus-G coastal zone color scanner  
[NASA-CR-173511] p 159 N84-27258
- NITRIDING**
- Metallurgical and microstructural characteristics of ion-nitrided steels p 64 N84-19225
- Ion-beam nitriding of steels  
[NASA-TM-83599] p 71 N84-21719
- NITROGEN**
- Characteristics of Si<sub>3</sub>N<sub>4</sub>-SiO<sub>2</sub>-Ce<sub>2</sub>O<sub>3</sub> compositions sintered in high-pressure nitrogen p 79 N84-19913
- NITROGEN OXIDES**
- Experimental investigation of the low NO<sub>x</sub> vortex airblast annular combustor  
[AIAA PAPER 84-1170] p 18 N84-36952
- NOISE GENERATORS**
- A critical review of noise production models for turbulent, gas-fueled burners  
[NASA-CR-3803] p 184 N84-26384
- NOISE INTENSITY**
- Helicopter engine core noise p 185 N84-29676
- Acoustic pressures emanating from a turbomachine stage  
[NASA-TM-83734] p 129 N84-30224
- NOISE MEASUREMENT**
- Why credible propeller noise measurements are possible in the acoustically untreated NASA Lewis 8 ft by 6 ft wind tunnel p 181 N84-38091
- Simplified combustion noise theory yielding a prediction of fluctuating pressure level  
[NASA-TP-2237] p 183 N84-19049
- Analysis of the effect on combustor noise measurements of acoustic waves reflected by the turbine and combustor inlet  
[NASA-TM-83760] p 185 N84-32122
- An experimental investigation of the effect of boundary layer refraction on the noise from a high-speed propeller  
[NASA-TM-83764] p 186 N84-34230
- NOISE POLLUTION**
- Helicopter engine core noise p 185 N84-29676
- NOISE PREDICTION**
- A theoretical prediction of the acoustic pressure generated by turbulence-flame front interactions  
[NASA-TM-83587] p 184 N84-26383
- NOISE PREDICTION (AIRCRAFT)**
- A parametric study of the effect of inlet lip shape upon the radiated sound field  
[AIAA PAPER 84-0498] p 180 N84-18131
- NOISE PROPAGATION**
- Jet noise modification by the 'whistler nozzle' p 181 N84-23355
- Cross spectra between pressure and temperature in a constant-area duct downstream of a hydrogen-fueled combustor  
[NASA-TM-83463] p 182 N84-11885
- NOISE REDUCTION**
- Supersonic jet screech tone cancellation p 179 N84-10136
- Inverted velocity profile semi-annular nozzle jet exhaust noise experiments  
[NASA-TM-83525] p 182 N84-13924
- A possible explanation for the present difference between linear noise theory and experimental data for supersonic helical tip speed propellers  
[NASA-TM-83467] p 183 N84-14874
- Fluid shielding of high-velocity jet noise  
[NASA-TP-2259] p 183 N84-15894
- Fan noise reduction achieved by removing tip flow irregularities behind the rotor - forward arc test configurations  
[NASA-TM-83616] p 184 N84-23235
- Experimental investigation of shock-cell noise reduction for dual-stream nozzles in simulated flight comprehensive data report. Volume 1: Test nozzles and acoustic data  
[NASA-CR-168336-VOL-1] p 184 N84-24323
- Experimental investigation of shock-cell noise reduction for dual-stream nozzles in simulated flight comprehensive data report. Volume 2: Laser velocimeter data, static pressures and shadowgraph photos  
[NASA-CR-168336-VOL-2] p 184 N84-24324
- Helicopter engine core noise p 185 N84-29676
- Experimental investigation of shock-cell noise reduction for single-stream nozzles in simulated flight, comprehensive data report Volume 1: Test nozzles and acoustic data  
[NASA-CR-168234-VOL-1] p 185 N84-33148
- Supersonic jet shock noise reduction  
[NASA-TM-83799] p 186 N84-35085
- NOISE SPECTRA**
- State estimation Kalman filter using optical processings  
Noise statistics known p 178 N84-23602
- Recovery of burner acoustic source structure from far-field sound spectra  
[AIAA PAPER 83-0763] p 181 N84-32609
- Inverted velocity profile semi-annular nozzle jet exhaust noise experiments  
[NASA-TM-83525] p 182 N84-13924
- An experimental study of the properties of surface pressure fluctuations in strong adverse pressure gradient turbulent boundary layers  
[NASA-CR-175410] p 9 N84-20488
- NONDESTRUCTIVE TESTS**
- Characterization of composite materials by means of the ultrasonic stress wave factor p 51 N84-10430
- The use of heterodyne speckle photogrammetry to measure high-temperature strain distributions p 130 N84-28623
- Application of induction coil measurements to the study of superalloy hot corrosion and oxidation  
[NASA-TM-83560] p 69 N84-16311
- In-situ measurements of alloy oxidation/corrosion/erosion using a video camera and proximity sensor with microcomputer control  
[NASA-TM-83673] p 74 N84-27859
- Mechanical behavior of carbon-carbon composites  
[NASA-CR-174767] p 57 N84-34575
- Ultrasonic velocity measurement using phase-slope cross-correlation methods  
[NASA-TM-83794] p 149 N84-34769
- NONFERROUS METALS**
- Status of understanding for gear materials p 144 N84-25061
- NONFLAMMABLE MATERIALS**
- Selection of burn-resistant materials for oxygen-driven turbopumps  
[AIAA PAPER 84-1287] p 43 N84-35157
- NONLINEAR EQUATIONS**
- Self-adaptive solution strategies p 158 N84-31693
- NONLINEAR PROGRAMMING**
- Engineering calculations for communications satellite systems planning  
[NASA-CR-173532] p 38 N84-23662
- NONLINEAR SYSTEMS**
- A large-signal dynamic simulation for the series resonant converter p 103 N84-23258
- Nonlinear displacement analysis of advanced propeller structures using NASTRAN  
[NASA-TM-83737] p 157 N84-31683
- Nonlinear Structural Analysis  
[NASA-CP-2297] p 157 N84-31688
- Slave finite elements The temporal element approach to nonlinear analysis p 157 N84-31689
- Nonlinear finite element analysis of shells with large aspect ratio p 158 N84-31692
- Element-by-element solution procedures for nonlinear structural analysis p 158 N84-31694
- Nonlinear analysis for high-temperature composites: Turbine blades/vanes p 158 N84-31699
- NONLINEARITY**
- A simplified method for elastic-plastic-creep structural analysis  
[NASA-TM-83509] p 154 N84-14542
- Theoretical and software considerations for nonlinear dynamic analysis  
[NASA-CR-174504] p 154 N84-15589
- Development of a simplified procedure for cyclic structural analysis  
[NASA-TP-2243] p 155 N84-20878
- A computer program for predicting nonlinear uniaxial material responses using viscoplastic models  
[NASA-TM-83675] p 156 N84-29247
- NONNEWTONIAN FLUIDS**
- Non-Newtonian fluid model incorporated into elastohydrodynamic lubrication of rectangular contacts  
[ASME PAPER 83-LUB-15] p 139 N84-44300
- NOTCH TESTS**
- Benchmark cyclic plastic notch strain measurements p 63 N84-11194
- Development of plane strain fracture toughness test for ceramics using Chevron notched specimens p 77 N84-11676
- Mode 2 fatigue crack growth specimen development  
[NASA-TM-83722] p 155 N84-29248
- Fracture surface characteristics of notched angleplied graphite/epoxy composites  
[NASA-TM-83786] p 57 N84-33522
- NOTCHES**
- Fracture modes in notched angleplied composite laminates  
[NASA-TM-83802] p 53 N84-34576
- NOZZLE DESIGN**
- Flow visualization and interpretation of visualization data for deflected thrust V/STOL nozzles  
[AIAA PAPER 84-0102] p 16 N84-21852
- Flow visualization and interpretation of visualization data for deflected thrust V/STOL nozzles  
[NASA-TM-83554] p 24 N84-14147
- Experimental investigation of shock-cell noise reduction for dual-stream nozzles in simulated flight comprehensive data report Volume 1: Test nozzles and acoustic data  
[NASA-CR-168336-VOL-1] p 184 N84-24323
- Supersonic jet shock noise reduction  
[NASA-TM-83799] p 186 N84-35085
- NOZZLE FLOW**
- A finite element approach for predicting nozzle admittances p 180 N84-21184
- Swirl flow turbulence modeling  
[AIAA PAPER 84-1376] p 118 N84-35196
- Swirl, confinement and nozzle effects on confined turbulent flow  
[AIAA PAPER 84-1377] p 118 N84-35197
- Turbulence measurements in a complex flowfield using a crossed hot-wire  
[AIAA PAPER 84-1604] p 131 N84-37999

- Five-hole pitot probe measurements of swirl, confinement and nozzle effects on confined turbulent flow  
[AIAA PAPER 84-1605] p 120 A84-38000  
[NASA-TM-83520] p 183 N84-20320  
Experimental investigation of shock-cell noise reduction for dual-stream nozzles in simulated flight comprehensive data report. Volume 1: Test nozzles and acoustic data [NASA-CR-168336-VOL-1] p 184 N84-24323  
Experimental investigation of shock-cell noise reduction for dual-stream nozzles in simulated flight comprehensive data report. Volume 2: Laser velocimeter data, static pressures and shadowgraph photos [NASA-CR-168336-VOL-2] p 184 N84-24324  
Velocity and temperature characteristics of two-stream, coplanar jet exhaust plumes [NASA-TM-83730] p 34 N84-28790
- NOZZLE GEOMETRY**  
Flow visualization and interpretation of visualization data for deflected thrust V/STOL nozzles [AIAA PAPER 84-0102] p 16 A84-21652  
Aerodynamic effects of moveable sidewall nozzle geometry and rotor exit restriction on the performance of a radial turbine [SAE PAPER 831517] p 17 A84-29460  
Flow visualization and interpretation of visualization data for deflected thrust V/STOL nozzles [NASA-TM-83554] p 24 N84-14147  
Experimental investigation of shock-cell noise reduction for dual-stream nozzles in simulated flight comprehensive data report. Volume 1: Test nozzles and acoustic data [NASA-CR-168336-VOL-1] p 184 N84-24323  
Experimental investigation of shock-cell noise reduction for dual-stream nozzles in simulated flight comprehensive data report. Volume 2: Laser velocimeter data, static pressures and shadowgraph photos [NASA-CR-168336-VOL-2] p 184 N84-24324  
Free jet feasibility study of a thermal acoustic shield concept for AST/VCE application: Single stream nozzles [NASA-CR-3758] p 185 N84-29661  
Experimental investigation of shock-cell noise reduction for single-stream nozzles in simulated flight, comprehensive data report. Volume 1: Test nozzles and acoustic data [NASA-CR-168234-VOL-1] p 185 N84-33148  
Supersonic jet shock noise reduction [NASA-TM-83799] p 186 N84-35085
- NOZZLE WALLS**  
Aerodynamic effects of moveable sidewall nozzle geometry and rotor exit restriction on the performance of a radial turbine [SAE PAPER 831517] p 17 A84-29460
- NUCLEAR ELECTRIC POWER GENERATION**  
The potential impact of new power system technology on the design of a manned space station [NASA-TM-83770] p 49 N84-31272
- NUCLEAR MAGNETIC RESONANCE**  
Carbon-13 and proton nuclear magnetic resonance analysis of shale-derived refinery products and jet fuels and of experimental referee broadened-specification jet fuels [NASA-CR-174761] p 92 N84-32552
- NUCLEATION**  
A study of nucleation and growth of thin films by means of computer simulation: General features [NASA-TM-83559] p 179 N84-17982
- NUMERICAL ANALYSIS**  
Random element method for numerical modeling of diffusional processes p 119 A84-35318  
Numerical methods for analyzing electromagnetic scattering [NASA-CR-173916] p 101 N84-32645
- NUMERICAL CONTROL**  
Real-time hybrid computer simulation of a small turboshaft engine and control system [NASA-TM-83579] p 28 N84-21548
- NUMERICAL FLOW VISUALIZATION**  
Limitations and empirical extensions of the k-epsilon model as applied to turbulent confined swirling flows [AIAA PAPER 84-0441] p 114 A84-18096  
Formation and destruction of vortices in a motored four-stroke piston-cylinder configuration p 139 A84-38838  
A review of internal combustion engine combustion chamber process studies at NASA Lewis Research Center [AIAA PAPER 84-1316] p 121 A84-40242  
On numerical simulation of viscous flows p 122 A84-49112

- A review of internal combustion engine combustion chamber process studies at NASA Lewis Research Center [NASA-TM-83666] p 127 N84-24999
- NUMERICAL INTEGRATION**  
Fast algorithms for combustion kinetics calculations: A comparison p 61 N84-20554
- NUMERICAL STABILITY**  
Comments on some problems in computational penetration mechanics p 150 A84-13545  
Algorithms for elasto-plastic-creep postbuckling p 152 A84-38480
- NUSSELT NUMBER**  
Internal heat transfer coefficients of porous metals p 112 A84-13239

## O

## O RING SEALS

- Dynamics of two-phase face seals p 137 A84-28792  
Design analysis of Rayleigh-step floating-ring seals [ASLE PREPRINT 83-LC-3B-2] p 137 A84-28989  
Assessment of two neglected effects in the analysis of an oil pumping ring seal [ASME PAPER 83-LUB-16] p 137 A84-29097  
Feasibility analysis of a spiral groove ring seal for counter-rotating shafts p 139 A84-45965

## OBLIQUE SHOCK WAVES

- Experimental studies on two dimensional shock boundary layer interactions [AIAA PAPER 84-0099] p 3 A84-17881

## OFF-ON CONTROL

- Extensions of the discrete-average models for converter power stages p 102 A84-18411  
Stability analysis of a buck regulator employing input filter compensation p 102 A84-18412  
A new FET-bipolar combinational power semiconductor switch p 104 A84-32293

## OILS

- Experimental study of bubble cavities attached to a rotating shaft in a reservoir [NASA-TM-83586] p 124 N84-17533  
Thermal analysis of a planetary transmission with spherical roller bearings operating after complete loss of oil [NASA-TP-2367] p 147 N84-32824

## ONBOARD DATA PROCESSING

- Baseband processor development for the Advanced Communications Satellite Program p 93 A84-15628  
30/20 GHz communications systems baseband processor development p 95 A84-38251

## ONE DIMENSIONAL FLOW

- One-dimensional unsteady modeling of supersonic inlet unstart/restart [AIAA PAPER 84-0439] p 4 A84-18094

## OPERATING SYSTEMS (COMPUTERS)

- Operating system for a real-time multiprocessor propulsion system simulator [NASA-TM-83605] p 177 N84-20258

## OPTICAL COMPUTERS

- Acoustooptic linear algebra processors - Architectures, algorithms, and applications p 175 A84-40266  
Optical flip-flops and sequential logic circuits using a liquid crystal light valve p 188 A84-40332

## OPTICAL CORRECTION PROCEDURE

- Window aberration correction in laser velocimetry using multifaceted holographic optical elements p 134 A84-24663

## OPTICAL DATA PROCESSING

- Direct and implicit optical matrix-vector algorithms p 187 A84-13184  
State estimation Kalman filter using optical processings Noise statistics known p 178 A84-23602  
Advanced acousto-optic signal processors p 187 A84-28485

- Optical Kalman filtering for missile guidance p 178 A84-38596

- Acoustooptic linear algebra processors - Architectures, algorithms, and applications p 175 A84-40266  
Optical systolic solutions of linear algebraic equations p 188 N84-22405  
Optical pulse generator using liquid crystal light valve p 188 N84-22414

- Optical residue addition and storage units using a Hughes liquid crystal light valve p 188 N84-22417

## OPTICAL FILTERS

- Optical Kalman filtering for missile guidance p 178 A84-38596

## OPTICAL HETERODYNING

- The use of heterodyne speckle photogrammetry to measure high-temperature strain distributions p 130 A84-28623

## OPTICAL MEASURING INSTRUMENTS

- Application of laser anemometry in turbine engine research p 130 A84-22872  
Acoustically-induced modulation spectroscopy for ultra-sensitive gas analysis [AIAA PAPER 84-1480] p 131 A84-36981  
Calibration of the Malvern particle sizer p 131 A84-40736

## OPTICAL PROPERTIES

- Measurements of self-excited rotor-blade vibrations using optical displacements [ASME PAPER 83-GT-132] p 151 A84-33702  
Application of laser anemometry in turbine engine research [NASA-TM-83513] p 131 N84-11456  
Laboratory degradation of Kapton in a low energy oxygen ion beam [NASA-TM-83530] p 41 N84-18310  
Ion-beam-textured and coated surfaces experiment (S1003) p 84 N84-24650  
Optical and other property changes of M-50 bearing steel surfaces for different lubricants and additive prior to scuffing [NASA-TM-83746] p 88 N84-34620

## OPTICAL WAVEGUIDES

- Coupling of radiation into thin film modes by means of localized plasma resonances p 187 A84-16397

## OPTIMIZATION

- Optimizing and comparing laser anemometers p 130 A84-28739  
A review of internal combustion engine combustion chamber process studies at NASA Lewis Research Center [AIAA PAPER 84-1316] p 121 A84-40242  
Optimization of fringe-type laser anemometers for turbine engine component testing [AIAA PAPER 84-1459] p 131 A84-40248  
Application of an optimization method to high performance propeller designs [AIAA PAPER 84-1203] p 20 A84-44181  
Approaches to optimization of SS/TDMA time slot assignment - satellite switched time division multiple access [NASA-CR-168328] p 40 N84-16243  
Optimization methods applied to hybrid vehicle design [NASA-CR-168292] p 194 N84-19185  
A review of internal combustion engine combustion chamber process studies at NASA Lewis Research Center [NASA-TM-83666] p 127 N84-24999  
Optimization of fringe-type laser anemometers for turbine engine component testing [NASA-TM-83658] p 133 N84-25019  
Application of an optimization method to high performance propeller designs [NASA-TM-83710] p 2 N84-25607

## ORBIT SPECTRUM UTILIZATION

- Interference performance analysis of M-ary CPSK and M-ary CAPK digital transmission systems and the computation of 'required isolation' for efficient utilization of geostationary satellite orbit/spectrum p 95 A84-49303

- Geometric models, antenna gains, and protection ratios as developed for BC SAT-R2 conference software [NASA-TM-83381] p 96 N84-11358

## ORBIT TRANSFER VEHICLES

- Selection of burn-resistant materials for oxygen-driven turbopumps [AIAA PAPER 84-1287] p 43 A84-35157  
Integration becomes the name of the OTV game p 44 A84-44045

- Propulsion issues for advanced orbit transfer vehicles [NASA-TM-83624] p 47 N84-25762

- NASA Orbit Transfer Rocket Engine Technology Program [NASA-CR-168156] p 48 N84-28901

- Propulsion issues for advanced orbit transfer vehicles p 48 N84-29937

## ORBITAL MANEUVERS

- Centaur D-1A guidance/software system [AAS PAPER 84-043] p 39 A84-49176  
Centaur D-1A guidance/software system [NASA-TM-83552] p 38 N84-16234

## ORBITAL POSITION ESTIMATION

- Engineering calculations for communications satellite systems planning [NASA-CR-173532] p 38 N84-23662

## ORBITS

- Solar array: Plasma interactions p 171 N84-29343

## ORGANIC CHEMISTRY

- Chemical approach for controlling nadimide cure temperature and rate [NASA-CASE-LEW-13770-3] p 55 N84-22698  
Chemical approach for controlling nadimide cure temperature and rate [NASA-CASE-LEW-13770-4] p 55 N84-22699

- Chemical approach for controlling nadimide cure temperature and rate p 55 N84-22700  
[NASA-CASE-LEW-13770-5]
- Chemical approach for controlling nadimide cure temperature and rate p 55 N84-22701  
[NASA-CASE-LEW-13770-6]
- ORGANIC COMPOUNDS**  
Synthesis of perfluoroalkylene dianilines p 60 N84-11228  
[NASA-CR-168004]
- ORTHOTROPIC PLATES**  
A mixed shear flexible finite element for the analysis of laminated plates p 152 A84-45994
- OSCILLATING FLOW**  
The production of turbulent stress in a shear flow by rotational fluctuations p 115 A84-21390  
Effect of an oscillating flow direction on leading edge heat transfer p 117 A84-33705
- OSCILLATION DAMPERS**  
Measurement of rolling friction by a damped oscillator [NASA-TP-2257] p 141 N84-13577
- OSCILLATORS**  
Ladder supported ring bar circuit p 106 N84-16452  
[NASA-CASE-LEW-13570-1]  
Dielectric based submillimeter backward wave oscillator circuit p 110 N84-27974  
[NASA-CASE-LEW-13736-1]
- OUTGASSING**  
Solar-array-materials passive LDEF experiment (A0171) p 168 N84-24656
- OXIDATION**  
The effects of Cr, Al, Ti, Mo, W, Ta, and Nb on the cyclic oxidation behavior of cast Ni-base superalloys at 1100 and 1150 C p 65 A84-27485  
Thermal oxidative degradation reactions of linear perfluoroalkyl ethers p 80 A84-30000  
Oxidation behavior of a thermal barrier coating p 55 A84-42667  
Thermal oxidation of 3C silicon carbide single-crystal layers on silicon p 191 A84-49620  
Thermal oxidative degradation reactions of perfluoroalkyl ethers p 60 N84-11229  
[NASA-CR-168224]  
Literature survey on oxidations and fatigue lives at elevated temperatures p 71 N84-20674  
[NASA-CR-174639]  
Investigation into the role of sodium chloride deposited on oxide and metal substrates in the initiation of hot corrosion p 71 N84-20676  
[NASA-CR-173377]  
Method for strengthening boron fibers p 55 N84-24711  
[NASA-CASE-LEW-13826-2]  
Performance of thermal barrier coatings in high heat flux environments p 72 N84-24772  
[NASA-TM-83663]  
Modeling degradation and failure of Ni-Cr-Al overlay coatings p 74 N84-27858  
[NASA-TM-83672]  
In-situ measurements of alloy oxidation/corrosion/erosion using a video camera and proximity sensor with microcomputer control p 74 N84-27859  
[NASA-TM-83673]  
Advanced high temperature materials for the energy efficient automotive Stirling engine p 75 N84-28963  
[NASA-TM-83659]  
Overlay coating degradation by simultaneous oxidation and coating/substrate interdiffusion p 75 N84-31344  
[NASA-TM-83738]  
High-temperature cyclic oxidation data, volume I p 75 N84-31345  
[NASA-TM-83665]  
Overlay metallic-cermet alloy coating systems p 77 N84-33555  
[NASA-CASE-LEW-13639-1]
- OXIDATION RESISTANCE**  
Processing of fused silicide coatings for carbon-based materials p 51 A84-19780  
Characteristics of Si<sub>3</sub>N<sub>4</sub>-SiO<sub>2</sub>-Ce<sub>2</sub>O<sub>3</sub> compositions sintered in high-pressure nitrogen p 79 A84-19913  
The effect of a coating on the thermo-oxidative stability of Celcon 6000 graphite fiber/PMR 15 polyimide composites p 52 A84-21844  
Microstructure, strength, and oxidation of a 10 wt pct zirconia-Si<sub>3</sub>N<sub>4</sub> ceramic p 80 A84-25402  
The effects of Cr, Al, Ti, Mo, W, Ta, and Nb on the cyclic oxidation behavior of cast Ni-base superalloys at 1100 and 1150 C p 65 A84-27485  
Sinterability, strength and oxidation of alpha silicon carbide powders p 80 A84-32305  
Solute transport and the prediction of breakaway oxidation in gamma + beta Ni-Cr-Al alloys p 65 A84-42658  
Oxidation resistant slurry coating for carbon-based materials p 54 N84-16266  
[NASA-CASE-LEW-13923-1]  
Thermal and oxidative stabilities of liquid lubricants p 84 N84-23907
- OXIDE FILMS**  
Structure of transient oxides formed on NiCrAl alloys p 63 A84-12385  
Bubble formation in oxide scales on SiC p 79 A84-23689  
Thermal oxidation of 3C silicon carbide single-crystal layers on silicon p 191 A84-49620  
Ion-beam-textured and coated surfaces experiment (S1003) p 84 N84-24650  
Improved thermal barrier coating system [NASA-CASE-LEW-14057-1] p 88 N84-33595
- OXYGEN**  
Importance of interatomic spacing in catalytic reduction of oxygen in phosphoric acid p 58 A84-12644  
Electrode kinetics of oxygen reduction - A theoretical and experimental analysis of the rotating ring-disc electrode method p 59 A84-29999  
Correlation of electron emission with changes in the surface concentration of barium and oxygen on a tungsten surface p 60 A84-45917  
Separator development and testing of nickel-hydrogen cells p 62 N84-22712  
[NASA-TM-83653]  
Oxygen diffusion in alpha-Al<sub>2</sub>O<sub>3</sub> p 86 N84-28990  
[NASA-TM-83622]
- OXYGEN ATOMS**  
The energy dependence and surface morphology of Kapton (trademark) degradation under atomic oxygen bombardment p 187 N84-34484
- OXYGEN RECOMBINATION**  
Oxygen recombination in individual pressure vessel nickel-hydrogen batteries p 110 N84-29084  
[NASA-CASE-LEW-13822-1]
- OXYGEN SUPPLY EQUIPMENT**  
Oxidant system improvements for MHD energy conversion and industrial processes p 189 A84-24058
- OXYNITRIDES**  
Analysis of grain boundary phase devitrification of Y<sub>2</sub>O<sub>3</sub>- and Al<sub>2</sub>O<sub>3</sub>-doped Si<sub>3</sub>N<sub>4</sub> p 79 A84-19792  
Grain-boundary phases in hot-pressed silicon nitride containing Y<sub>2</sub>O<sub>3</sub> and CeO<sub>2</sub> additives p 79 A84-19793
- OZONE**  
Tabulations of ambient ozone data obtained by GASP (Global Air Sampling Program) airliners, March 1975 to July 1979 p 174 N84-18806  
[NASA-TM-82742]  
Tabulations of ozonesonde data, 1963 - 1980 p 174 N84-27375  
[NASA-CR-174631]  
Climatology of ozone at altitudes from 19,000 to 59,000 feet based on combined GASP and ozonesonde data p 174 N84-31865  
[NASA-TP-2303]
- OZONOMETRY**  
Simultaneous cabin and ambient ozone measurements on two Boeing 747 airplanes Volume 2 January to October 1978 p 193 N84-22488  
[NASA-TM-81733]
- P**
- P-I-N JUNCTIONS**  
Development and fabrication of a high current, fast recovery power diode p 106 N84-13443  
[NASA-CR-168196]
- P-N JUNCTIONS**  
New implantation techniques for improved solar cell junctions p 161 A84-23059  
Photovoltaic characteristics of diffused P+/N bulk GaAs solar cells p 161 A84-23115  
Diffused junction p(+)-n solar cells in bulk GaAs I p 161 A84-26027  
Fabrication and cell performance p 161 A84-26027  
Diffused junction p(+)-n solar cells in bulk GaAs. II - Device characterization and modelling p 161 A84-26028
- PANEL METHOD (FLUID DYNAMICS)**  
A rapid blade-to-blade solution for use in turbomachinery design p 4 A84-31289  
[ASME PAPER 83-GT-67]
- PANELS**  
Combustor liner construction p 30 N84-24577  
[NASA-CASE-LEW-14035-1]
- PARABOLOID MIRRORS**  
Large-aperture interferometer with local reference beam p 130 A84-34528
- PARAFFINS**  
Investigation of sources, properties and preparation of distillate test fuels p 89 N84-13332  
[NASA-CR-168227]
- PARALLEL FLOW**  
High frequency green function for aerodynamic noise in moving media. I - General theory. II - Noise from a spreading jet p 180 A84-21273
- PARALLEL PLATES**  
Capillary rise, wetting layers, and critical phenomena in confined geometry p 192 A84-20315
- PARALLEL PROCESSING (COMPUTERS)**  
Parallelism and pipelining in high-speed digital simulators p 175 A84-11876  
Software simulator for multiple computer simulation system p 176 A84-11892  
A scheme for handling arrays in data-flow systems p 175 A84-39972  
Acoustooptic linear algebra processors - Architectures, algorithms, and applications p 175 A84-40266  
Parallel processor engine model program [NASA-CR-174641] p 27 N84-19353
- PARAMETER IDENTIFICATION**  
Identification of multivariable high performance turbofan engine dynamics from closed loop data p 16 A84-18582  
State estimation Kalman filter using optical processings Noise statistics known p 178 A84-23602  
Identification of quasi-steady compressor characteristics from transient data p 36 N84-34444  
[NASA-CR-174685]
- PARTIAL DIFFERENTIAL EQUATIONS**  
Asymptotic analysis of numerical wave propagation in finite difference equations p 98 N84-15360  
[NASA-CR-175323]  
A semi-direct procedure using a local relaxation factor and its application to an internal flow problem p 128 N84-25946  
[NASA-TM-83704]
- PARTICLE ACCELERATORS**  
Experimental investigation of a Hall-current thruster [NASA-CR-168133] p 46 N84-18321
- PARTICLE DIFFUSION**  
Correlation of thermophoretically-modified small particle diffusional deposition rates in forced convection systems with variable properties, transpiration cooling and/or viscous dissipation p 117 A84-32323
- PARTICLE LADEN JETS**  
Structure of particle-laden jets - Measurements and predictions p 113 A84-17842  
[AIAA PAPER 84-0038]  
Morphology of an aluminum alloy eroded by a normally incident jet of angular erodent particles p 64 A84-18244  
A theoretical and experimental study of turbulent particle-laden jets p 23 N84-13187  
[NASA-CR-168293]  
Predictions of spray combustion interactions p 61 N84-20532
- PARTICLE MASS**  
Comparisons of rational engineering correlations of thermophoretically-augmented particle mass transfer with STANS-predictions for developing boundary layers p 92 A84-46965  
[ASME PAPER 84-GT-158]  
Comparisons of rational engineering correlations of thermophoretically-augmented particle mass transfer with STANS-predictions for developing boundary layers p 93 N84-19606  
[NASA-CR-168221]
- PARTICLE SIZE DISTRIBUTION**  
Calibration of the Malvern particle sizer p 131 A84-40736  
Predictions of spray combustion interactions p 61 N84-20532  
Flame propagation in heterogeneous mixtures of fuel drops and air p 91 N84-23775  
[NASA-CR-174644]  
A theoretical and experimental study of turbulent nonevaporating sprays p 35 N84-29877  
[NASA-CR-174688]  
Analysis and testing of a new method for drop size measurement using laser scatter interferometry p 133 N84-31595  
[NASA-CR-174636]
- PASSAGEWAYS**  
Vortex generating flow passage design for increased film cooling effectiveness p 126 N84-20782  
[NASA-CASE-LEW-14039-1]  
Review and status of heat-transfer technology for internal passages of air-cooled turbine blades p 126 N84-21828  
[NASA-TP-2232]
- PENALTY FUNCTION**  
Penalty function finite element analysis of steady viscous incompressible flow in rotating coordinates p 121 A84-46900  
[ASME PAPER 84-GT-36]
- PERFLUORO COMPOUNDS**  
Thermal oxidative degradation reactions of linear perfluoroalkyl ethers p 80 A84-30000
- PERFLUOROALKANE**  
Thermal oxidative degradation reactions of perfluoroalkyl ethers p 60 N84-11229  
[NASA-CR-168224]
- PERFORMANCE PREDICTION**  
Helicopter rotor performance degradation in natural icing encounter p 12 A84-17412  
Structure of nonevaporating sprays - Measurements and predictions p 114 A84-17897  
[AIAA PAPER 84-0125]  
Elastic model of the traction behavior of two traction lubricants p 136 A84-28791

A thermomechanical model for energy propagation in a solid-fluid-solid system with one boundary in relative motion  
[ASME PAPER 83-HT-97] p 137 A84-29092

Long life nickel electrodes for a nickel-hydrogen cell  
Initial performance p 162 A84-30186

Evaluation of gas cooling for pressurized phosphoric acid fuel cell stacks p 163 A84-30191

Comparison between measured turbine stage performance and the predicted performance using quasi-3D flow and boundary layer analyses  
[AIAA PAPER 84-1299] p 18 A84-36972

The aerodynamic design and performance of the NASA/GE E3 low pressure turbine  
[AIAA PAPER 84-1162] p 21 A84-44186

Interference performance analysis of M-ary CPSK and M-ary CAPK digital transmission systems and the computation of 'required isolation' for efficient utilization of geostationary satellite orbit/spectrum  
p 95 A84-49303

Progress toward the development of an aircraft icing analysis capability  
[NASA-TM-83562] p 9 N84-20490

Comparison between measured turbine stage performance and the predicted performance using quasi-3D flow and boundary layer analyses  
[NASA-TM-83640] p 29 N84-22564

Comparison of free-piston Stirling engine model predictions with RE1000 engine test data  
[NASA-TM-83650] p 195 N84-24509

An investigation of the transient thermal analysis of spur gears  
[NASA-TM-83724] p 146 N84-28088

Operating characteristics of a three-piece-inner-ring large-bore roller bearing to speeds of 3 million DN  
[NASA-TP-2355] p 146 N84-29226

PURDU-WINCOF: A computer code for establishing the performance of a fan-compressor unit with water ingestion  
[NASA-CR-168005] p 34 N84-29875

Automotive Stirling Engine Development Program RESD summary report  
[NASA-CR-174674] p 196 N84-33307

**PERFORMANCE TESTS**

Test verification of LOX/JP-1 high-pressure fuel/oxidizer-rich preburner designs p 42 A84-22134

Effects of volute geometry and impeller orbit on the hydraulic performance of a centrifugal pump  
p 136 A84-22316

Single cell performance studies on the FE/CR Redox Energy Storage System using mixed reactant solutions at elevated temperature p 163 A84-30194

Preliminary investigation of a two-zone swirl flow combustor  
[AIAA PAPER 84-1169] p 17 A84-36951

Acoustic emission evaluation of plasma-sprayed thermal barrier coatings  
[ASME PAPER 84-GT-292] p 140 A84-47046

Investigation of sources, properties and preparation of distillate test fuels  
[NASA-CR-168227] p 89 N84-13332

Preliminary investigation of a two-zone swirl flow combustor  
[NASA-TM-83637] p 29 N84-22565

Group-type hydrocarbon standards for high-performance liquid chromatographic analysis of middistillate fuels  
[NASA-TP-2317] p 90 N84-23774

Performance capabilities of the 12-centimeter Xenon ion thruster  
[NASA-TM-83674] p 48 N84-27825

Test results for 27.5- to 30-GHz communications satellite receivers  
[NASA-TM-83662] p 100 N84-27954

Reflector antennas with low sidelobes, low cross polarization, and high aperture efficiency  
[NASA-CR-174670] p 100 N84-31484

**PERIODIC VARIATIONS**

Mass transfer from a circular cylinder: Effects of flow unsteadiness and slight nonuniformities  
[NASA-CR-174759] p 129 N84-32751

**PERMEABILITY**

Anion permselective membrane  
[NASA-CR-174725] p 172 N84-29358

**PERMEATING**

Evaluation of CO<sub>2</sub> and CO dopants in hydrogen to reduce hydrogen permeation in the Stirling engine heater head tube alloy CG-27  
[NASA-TM-83535] p 68 N84-15246

**PERSONNEL DEVELOPMENT**

Government - contractor interaction  
[AD-P002768] p 193 N84-23315

**PERTURBATION THEORY**

Orbital stability in combined uniform axial and three-dimensional wiggler magnetic fields for free-electron lasers  
[NASA-TM-83753] p 134 N84-30273

**PETROLEUM PRODUCTS**

Assessment of Alternative Aircraft Fuels  
[NASA-CP-2307] p 30 N84-23630

**PHASE CONJUGATION**

Preliminary experiments on phase conjugation for flow visualization — barium titanate single crystals  
[NASA-TM-83768] p 189 N84-32169

**PHASE DIAGRAMS**

Carbides in iron-rich Fe-Mn-Cr-Mo-Al-Si-C systems  
p 64 A84-26815

**PHASE ERROR**

Carrier recovery methods for a dual-mode modem: A design approach  
[NASA-CR-173355] p 36 N84-19360

**PHASE LOCKED SYSTEMS**

Surface topographical changes measured by phase-locked interferometry  
[NASA-CR-3757] p 188 N84-16984

**PHASE SHIFT CIRCUITS**

A Ka-band GaAs monolithic phase shifter  
p 101 A84-18371

**PHASE SHIFT KEYING**

Serial MSK modem for the Advanced Communications Satellite Program p 93 A84-15629

Interference performance analysis of M-ary CPSK and M-ary CAPK digital transmission systems and the computation of 'required isolation' for efficient utilization of geostationary satellite orbit/spectrum  
p 95 A84-49303

**PHASE TRANSFORMATIONS**

Phase distributions in plasma-sprayed zirconia-yttria  
p 78 A84-18948

Consolidation of Si<sub>3</sub>N<sub>4</sub> without additives (by hot isostatic pressing)  
[NASA-CR-173279] p 82 N84-17389

Overview of zirconia with respect to gas turbine applications  
[NASA-TP-2286] p 83 N84-21740

Transport processes in dendritic crystallization  
p 191 N84-28621

**PHASE VELOCITY**

A TWT amplifier with a linear power transfer characteristic and improved efficiency  
[AIAA PAPER 84-0762] p 104 A84-41035

A TWT amplifier with a linear power transfer characteristic and improved efficiency  
[NASA-TM-83590] p 108 N84-21803

**PHASED ARRAYS**

Microwave monolithic integrated circuit development for future spaceborne phased array antennas  
[AIAA PAPER 84-0656] p 94 A84-25257

Microwave monolithic integrated circuit development for future spaceborne phased array antennas  
[NASA-TM-83518] p 97 N84-13399

Phased-array-fed antenna configuration study. Volume 1: Technology assessment  
[NASA-CR-168231] p 98 N84-16423

Phased-array-fed antenna configuration study, volume 2  
[NASA-CR-168232] p 98 N84-16424

**PHOSPHATES**

Mechanism of lubrication by trisylphosphate (TCP)  
[NASA-TP-2274] p 142 N84-18653

**PHOSPHORIC ACID**

Importance of interatomic spacing in catalytic reduction of oxygen in phosphoric acid  
p 58 A84-12644

**PHOSPHORIC ACID FUEL CELLS**

Evaluation of gas cooling for pressurized phosphoric acid fuel cell stacks p 163 A84-30191

Develop and test fuel cell powered on-site integrated total energy system  
[NASA-CR-168239] p 164 N84-13673

New applications for phosphoric acid fuel cells  
[NASA-CR-168203] p 166 N84-18757

Evaluation of gas-cooled pressurized phosphoric acid fuel cells for electric utility power generation  
[NASA-CR-168298] p 169 N84-25169

Full scale phosphoric acid fuel cell stack technology development  
[NASA-CR-174660] p 169 N84-26165

Manual of phosphoric acid fuel cell power plant cost model and computer program  
[NASA-CR-174720] p 173 N84-34037

**PHOSPHORUS**

New implantation techniques for improved solar cell junctions p 161 A84-23059

**PHOTOACOUSTIC SPECTROSCOPY**

Acoustically-induced modulation spectroscopy for ultra-sensitive gas analysis  
[AIAA PAPER 84-1460] p 131 A84-36981

**PHOTOELECTRICITY**

Photovoltaic power system for satellite Earth stations in remote areas: Project status and design description  
[NASA-TM-83789] p 101 N84-33642

**PHOTOELECTRON SPECTROSCOPY**

The X-ray photoelectron spectroscopy depth profiling and tribological characterization of ion-plated gold on various metals p 50 A84-20465

**PHOTOGRAMMETRY**

The use of heterodyne speckle photogrammetry to measure high-temperature strain distributions p 130 A84-28623

**PHOTONS**

Preliminary design of a 10-kW thermophotovoltaic system for space applications  
[NASA-TM-83768] p 49 N84-32427

**PHOTOVOLTAGES**

Photovoltaic power system for satellite Earth stations in remote areas: Project status and design description  
[NASA-TM-83789] p 101 N84-33642

**PHOTOVOLTAIC CELLS**

Photovoltaic characteristics of diffused P/ $\alpha$ -N bulk GaAs solar cells p 161 A84-23115

Thermionic-photovoltaic energy converter  
[NASA-CASE-LEW-14077-1] p 167 N84-20918

Advanced photovoltaic experiment (S0014)  
p 168 N84-24657

Qualification testing of solar photovoltaic powered refrigerator freezers for medical use in remote geographic locations  
[NASA-CR-168181] p 169 N84-25162

Solar photovoltaic powered refrigerators/freezers for medical use in remote geographic locations  
[NASA-CR-168268] p 169 N84-25163

Photovoltaics: The endless spring  
[NASA-TM-83684] p 172 N84-31782

Preliminary design of a 10-kW thermophotovoltaic system for space applications  
[NASA-TM-83768] p 49 N84-32427

**PHOTOVOLTAIC CONVERSION**

Investigation of energy management strategies for photovoltaic systems - An analysis technique  
p 160 A84-22993

Economic viability of photovoltaic power for development assistance applications  
p 193 A84-23119

The worldwide market for photovoltaics in the rural sector p 161 A84-23135

Investigation of energy management strategies for photovoltaic systems - A predictive control algorithm  
p 161 A84-25468

Multibandgap photovoltaic receiver using back surface reflectors p 161 A84-30162

Thermionic-photovoltaic energy converter  
[NASA-CASE-LEW-14077-1] p 167 N84-20918

**PHOTOVOLTAIC EFFECT**

Low-frequency switching voltage regulators for terrestrial photovoltaic systems  
[NASA-TM-83625] p 110 N84-25926

Space power technology into the 21st Century  
[NASA-TM-83690] p 48 N84-26746

Preliminary design of a 10-kW thermophotovoltaic system for space applications  
[NASA-TM-83768] p 49 N84-32427

**PIEZOELECTRIC TRANSDUCERS**

Application of signal analysis to cavitation  
p 122 A84-49192

Piezoelectric deicing device  
[NASA-CASE-LEW-13773-2] p 133 N84-32782

**PINHOLES**

Potentials in a plasma over a biased pinhole  
p 102 A84-20711

**PINS**

Length to diameter ratio and row number effects in short pin fin heat transfer  
[ASME PAPER 83-GT-54] p 118 A84-33706

Water-vapor effects on friction of magnetic tape in contact with nickel-zinc ferrite  
[NASA-TP-2279] p 82 N84-18399

Effects of water-vapor on friction and deformation of polymers magnetic media in contact with a ceramic oxide  
[NASA-TM-83727] p 87 N84-30072

**PIPE FLOW**

Modeling of transient two-component flow using a four-point implicit method p 112 A84-13237

**PIPELINING (COMPUTERS)**

Parallelism and pipelining in high-speed digital simulators p 175 A84-11876

**PIPES (TUBES)**

Evaluation of CO<sub>2</sub> and CO dopants in hydrogen to reduce hydrogen permeation in the Stirling engine heater head tube alloy CG-27  
[NASA-TM-83535] p 68 N84-15246



- Method of making an ion beam sputter-etched ventricular catheter for hydrocephalus shunt [NASA-CASE-LEW-13107-2] p 174 N84-23095
- PISTON ENGINES**  
Free-piston Stirling engine endurance test program p 136 A84-22864  
Comparison of seal materials for use in Stirling engines p 64 A84-22879  
Formation and destruction of vortices in a motored four-stroke piston-cylinder configuration p 139 A84-38838  
Overview of NASA Lewis Research Center free-piston Stirling engine activities [NASA-TM-83649] p 195 N84-22512  
Creep-rupture behavior of candidate Stirling engine iron superalloys in high-pressure hydrogen Volume 2 Hydrogen creep-rupture behavior [NASA-CR-174705] p 74 N84-28961
- PISTONS**  
Test results and description of a 1 kW free-piston Stirling engine with a dashpot load p 138 A84-30095  
Comparison of free-piston Stirling engine model predictions with RE1000 engine test data [NASA-TM-83650] p 195 N84-24509
- PITOT TUBES**  
Further time-mean measurements in confined swirling flows p 116 A84-27138
- PIVOTS**  
Pivoting and slip in an angular contact bearing p 139 A84-40595
- PLANE STRAIN**  
Development of plane strain fracture toughness test for ceramics using Chevron notched specimens p 77 A84-11676
- PLANETARY WAVES**  
Tropical response to lateral forcing with a latitudinally and zonally nonuniform basic state p 174 A84-40399
- PLASMA CURRENTS**  
Dilute plasma coupling currents to a high voltage solar array in weak magnetic fields [NASA-TM-83687] p 47 N84-24708
- PLASMA DENSITY**  
Interpretation of STS-3/plasma diagnostics package results in terms of large space structure plasma interactions [NASA-CR-173266] p 189 N84-16991
- PLASMA DIAGNOSTICS**  
Spatial electron density and electric field strength measurements in microwave cavity experiments [AIAA PAPER 84-1522] p 189 A84-46109  
Interpretation of STS-3/plasma diagnostics package results in terms of large space structure plasma interactions [NASA-CR-173266] p 189 N84-16991  
Comparison of thermal plasma observations on SCATHA and GEOS p 41 N84-17262  
Effects of chemical releases by the STS-3 Orbiter on the ionosphere [NASA-CR-171032] p 173 N84-25204
- PLASMA GENERATORS**  
Characteristics of a microwave plasma disk ion source p 189 A84-23390  
Electromagnetic plasma models for microwave plasma cavity reactors [AIAA PAPER 84-1521] p 189 A84-46108
- PLASMA GUNS**  
Coaxial carbon plasma gun deposition of amorphous carbon films [NASA-TM-83600] p 191 N84-20404
- PLASMA HEATING**  
Correlations between plasma variables and the deposition process of Si films from chlorosilanes in low pressure RF plasma of argon and hydrogen [NASA-TM-83603] p 190 N84-21330
- PLASMA INTERACTIONS**  
Plasma sheath structure surrounding a large powered spacecraft [AIAA PAPER 84-0329] p 40 A84-18025  
Interpretation of STS-3/plasma diagnostics package results in terms of large space structure plasma interactions [NASA-CR-173266] p 189 N84-16991  
Discharges on a negatively biased solar array in a charged particle environment [NASA-TM-83644] p 47 N84-23690  
Charged particle effects on space systems [AD-P002103] p 187 N84-26189  
High voltage solar array models and Shuttle tile charging [AD-P002123] p 177 N84-26209  
Characteristics of arc currents on a negatively biased solar cell array in a plasma [NASA-TM-83728] p 48 N84-27824  
Solar array: Plasma interactions p 171 N84-29343
- PLASMA JETS**  
Electromagnetic plasma models for microwave plasma cavity reactors [AIAA PAPER 84-1521] p 189 A84-46108  
Homogeneous reactions of hydrocarbons, silane, and chlorosilanes in radiofrequency plasmas at low pressures [NASA-TP-2301] p 50 N84-20643  
Deposition stress effects on thermal barrier coating burner tile life [NASA-TM-83670] p 85 N84-25830
- PLASMA PHYSICS**  
Status of plasma physics techniques for the deposition of tribological coatings p 190 N84-25058
- PLASMA POTENTIALS**  
Potentials in a plasma over a biased pinhole p 102 A84-20711  
Anomalous, high potentials observed on ISEE p 41 N84-17258  
The role of potential barrier formation in spacecraft charging p 41 N84-17269
- PLASMA RESONANCE**  
Coupling of radiation into thin film modes by means of localized plasma resonances p 187 A84-16397
- PLASMA SHEATHS**  
Plasma sheath structure surrounding a large powered spacecraft [AIAA PAPER 84-0329] p 40 A84-18025  
High voltage solar array models and Shuttle tile charging [AD-P002123] p 177 N84-26209
- PLASMA SPRAYING**  
Phase distributions in plasma-sprayed zirconia-yttria p 78 A84-18948  
Phase analysis of plasma-sprayed zirconia-yttria coatings p 78 A84-19781  
Residual stress in plasma-sprayed ceramic turbine tip and gas-path seal specimens p 78 A84-19783  
Correlation of compressive and shear stress with spalling of plasma-sprayed ceramic materials p 79 A84-19784  
The effect of annealing on the creep of plasma-sprayed ceramics p 79 A84-19785  
Mechanical and physical properties of plasma-sprayed stabilized zirconia p 79 A84-19786  
Acoustic emission evaluation of plasma-sprayed thermal barrier coatings [ASME PAPER 84-GT-292] p 140 A84-47046  
Ceramic composite liner material for gas turbine combustors [NASA-TM-83490] p 24 N84-14145  
Abrasive tip treatment for use on compressor blades [NASA-CR-174666] p 145 N84-25065  
Deposition stress effects on thermal barrier coating burner tile life [NASA-TM-83670] p 85 N84-25830  
Failure analysis of plasma-sprayed thermal barrier coatings [NASA-TM-83777] p 75 N84-31347  
Improved thermal barrier coating system [NASA-CASE-LEW-14057-1] p 88 N84-33595
- PLASMAS (PHYSICS)**  
Plasma polymerized high energy density dielectric films for capacitors [NASA-CR-168233] p 81 N84-13910  
Radical and ion molecule mechanisms in the polymerization of hydrocarbons and chlorosilanes in RF plasmas at low pressures (10 torr) [NASA-TM-83602] p 190 N84-21329
- PLASMONS**  
Harnessing surface plasmons for solar energy conversion p 159 A84-16395  
Parallel-processing with surface plasmons, a new strategy for converting the broad solar spectrum p 160 A84-23006  
Plasmon device design Conversion from surface to junction plasmons with grating-couplers p 171 N84-29330
- PLASTIC DEFORMATION**  
Benchmark cyclic plastic notch strain measurements p 63 A84-11194  
Analyses of large quasistatic deformations of inelastic bodies by a new hybrid-stress finite element algorithm p 150 A84-16874  
Analyses of large quasistatic deformations of inelastic bodies by a new hybrid-stress finite element algorithm - Applications p 150 A84-16884  
Determination of near-surface plastic deformation in sliding contacts p 140 A84-48996  
Effects of water-vapor on friction and deformation of polymeric magnetic media in contact with a ceramic oxide [NASA-TM-83727] p 87 N84-30072
- PLASTIC FLOW**  
The effect of annealing on the creep of plasma-sprayed ceramics p 79 A84-19785
- PLASTIC PROPERTIES**  
Research and development program for the development of advanced time-temperature dependent constitutive relationships Volume 2 Programming manual [NASA-CR-168191-VOL-2] p 153 N84-10614  
Some inelastic effects of thermal cycling on yttria-stabilized zirconia [NASA-TM-83483] p 123 N84-16492
- PLASTICS**  
Status of understanding for gear materials p 144 N84-25061
- PLATE THEORY**  
A mixed shear flexible finite element for the analysis of laminated plates p 152 A84-45994
- PLATES**  
Nonlinear finite element analysis of shells with large aspect ratio p 158 N84-31692
- PLUG NOZZLES**  
Experimental investigation of shock-cell noise reduction for dual-stream nozzles in simulated flight comprehensive data report. Volume 1: Test nozzles and acoustic data [NASA-CR-168336-VOL-1] p 184 N84-24323  
Experimental investigation of shock-cell noise reduction for dual-stream nozzles in simulated flight comprehensive data report. Volume 2: Laser velocimeter data, static pressures and shadowgraph photos [NASA-CR-168336-VOL-2] p 184 N84-24324
- PLUMES**  
On some flow characteristics of conventional and excited jets [AIAA PAPER 84-0532] p 181 A84-21304  
On some flow characteristics of conventional and excited jets [NASA-TM-83503] p 182 N84-13922
- PLY ORIENTATION**  
INHVD Computer code for intraply hybrid composite design A users manual [NASA-TP-2239] p 54 N84-13224  
Hygrothermomechanical fracture stress criteria for fiber composites with sense-ply [NASA-TM-83691] p 57 N84-28918
- PLYWOOD**  
Thermal stress analysis for a wood composite blade --- wind turbines [NASA-CR-173394] p 156 N84-21903
- POISSON RATIO**  
Indentation law for composite laminates p 52 A84-27356
- POLARIZED LIGHT**  
Interference phenomena in the refraction of a surface polarized by vertical dielectric barriers p 179 A84-24410
- POLARONS**  
Interference phenomena in the refraction of a surface polarized by vertical dielectric barriers p 179 A84-24410
- POLYCHLORINATED BIPHENYLS**  
Bacterial degradation of polychlorinated biphenyls in sludge from an industrial sewer lagoon [NASA-TM-83543] p 173 N84-11594
- POLYCRYSTALS**  
Bubble formation in oxide scales on SiC p 79 A84-23689  
Finite elastic-plastic deformation of polycrystalline metals p 66 A84-43872
- POLYETHYLENES**  
Study of the Auger line shape of polyethylene and diamond p 190 A84-40600  
Adhesion between polymers and evaporated gold and nickel films [NASA-TP-2360] p 87 N84-31379
- POLYIMIDE RESINS**  
Characterization of PMR polyimide resin and prepreg [NASA-CR-168217] p 83 N84-20695  
Chemical approach for controlling nadimide cure temperature and rate [NASA-CASE-LEW-13770-3] p 55 N84-22698  
Chemical approach for controlling nadimide cure temperature and rate [NASA-CASE-LEW-13770-4] p 55 N84-22699  
Chemical approach for controlling nadimide cure temperature and rate [NASA-CASE-LEW-13770-5] p 55 N84-22700  
Chemical approach for controlling nadimide cure temperature and rate [NASA-CASE-LEW-13770-6] p 55 N84-22701  
Chemical approach for controlling nadimide cure temperature and rate [NASA-CASE-LEW-13770-1] p 86 N84-27885  
Development of partially fluonated resin apex seals [NASA-CR-174706] p 148 N84-32828
- POLYIMIDES**  
Polyimides formulated from a partially fluonated diamine for aerospace tribological applications p 80 A84-40594



- Low wear partially fluorinated polyimides  
[NASA-TM-83629] p 84 N84-24808
- An investigation into the injection molding of PMR-15 polyimide  
[NASA-CR-173550] p 85 N84-24310
- POLYMER CHEMISTRY**
- Characterization of PMR polyimide resin and prepreg  
[NASA-CR-168217] p 83 N84-20695
- Characterization and measurement of polymer wear  
[NASA-TM-83628] p 83 N84-21739
- Development of partially fluorinated resin apex seals  
[NASA-CR-174706] p 148 N84-32828
- POLYMERIC FILMS**
- Material considerations for high frequency, high power capacitors p 102 A84-22874
- Ion-beam-textured and coated surfaces experiment (S1003) p 84 N84-24650
- POLYMERIZATION**
- Plasma polymerized high energy density dielectric films for capacitors p 81 N84-13310
- Radical and ion molecule mechanisms in the polymerization of hydrocarbons and chlorosilanes in RF plasmas at low pressures (1.0 torr)  
[NASA-CR-83602] p 190 N84-21329
- POLYMERS**
- High-current, high-frequency capacitors p 105 N84-10067
- Synthesis of perfluoroalkylene dianilines  
[NASA-CR-168004] p 60 N84-11228
- Characterization and measurement of polymer wear  
[NASA-TM-83628] p 83 N84-21739
- POLYNOMIALS**
- Slate finite elements The temporal element approach to nonlinear analysis p 157 N84-31689
- POLYPROPYLENE**
- Material considerations for high frequency, high power capacitors p 102 A84-22874
- High-current, high-frequency capacitors p 105 N84-10067
- POLYTETRAFLUOROETHYLENE**
- Surfaces — characterization of surface properties for predicting bond quality p 50 A84-10680
- Comparison of seal materials for use in Stirling engines p 64 A84-22879
- POROUS BOUNDARY LAYER CONTROL**
- Shape of porous region to control cooling along curved exit boundary p 115 A84-23591
- POROUS MATERIALS**
- Internal heat transfer coefficients of porous metals p 112 A84-13239
- Apparatus analysis and preliminary design of low gravity porous solids experiment for STS Orbiter mid-deck  
[NASA-CR-168248] p 37 N84-10109
- Studies of acoustical properties of bulk porous flexible materials  
[NASA-CR-173622] p 185 N84-27544
- POTENTIAL FLOW**
- The production of turbulent stress in a shear flow by irrotational fluctuations p 115 A84-18357
- Small-amplitude viscous motion on arbitrary potential flows p 116 A84-24892
- Potential flow analysis of glaze ice accretions on an airfoil  
[NASA-CR-168282] p 8 N84-16146
- POWDER METALLURGY**
- The effect of microstructure on 650 C fatigue crack growth in P/M Astroloy p 63 A84-12395
- Sinterability, strength and oxidation of alpha silicon carbide powders p 80 A84-32306
- Effects of processing and microstructure on the fatigue behaviour of the nickel-base superalloy Rene95 p 66 A84-48715
- P/M superalloys: A troubled adolescent?  
[NASA-TM-83623] p 73 N84-26785
- POWER**
- Development of high frequency low weight power magnetics for aerospace power systems  
[NASA-TM-83656] p 109 N84-22892
- POWER AMPLIFIERS**
- A three-stage power amplifier for a 20 GHz monolithic transmit module p 102 A84-22873
- 0.5 W 2-21 GHz monolithic GaAs distributed amplifier p 103 A84-30857
- A K-band GaAs FET amplifier with 8.2-W output power p 104 A84-32290
- NASA seeking high-power 60-GHz IMPATT diodes p 104 A84-44912
- 30/20 GHz spacecraft GaAs FET solid state transmitter for trunking and customer-premise-service application  
[NASA-CR-168276] p 107 N84-16463
- POWER CONDITIONING**
- A new FET-bipolar combination power semiconductor switch p 104 A84-32293

**POWER CONVERTERS**

- Extensions of the discrete-average models for converter power stages p 102 A84-18411
- Stability analysis of a buck regulator employing input filter compensation p 102 A84-18412
- Design considerations for FET-gated power transistors p 102 A84-18414
- Inherent overload protection for the series resonant converter p 102 A84-23255
- A large-signal dynamic simulation for the series resonant converter p 103 A84-23258
- POWER EFFICIENCY**
- High efficiency IMPATT diodes for 60 GHz intersatellite link applications  
[AIAA PAPER 84-0767] p 103 A84-25333
- Evaluation of gas cooling for pressurized phosphoric acid fuel cell stacks p 163 A84-30191
- Powerplant design for one-engine-inoperative operation p 19 A84-40787
- Development of high frequency low weight power magnetics for aerospace power systems  
[NASA-TM-83656] p 109 N84-22892
- POWER FACTOR CONTROLLERS**
- All-purpose bidirectional four-quadrant controller p 22 N84-10070
- Advances in solid state switchgear technology for large space power systems  
[NASA-TM-83652] p 109 N84-22891
- POWER LINES**
- Parametric analysis of hollow conductor parallel and coaxial transmission lines for high frequency space power distribution  
[NASA-TM-83601] p 46 N84-20639
- POWER SPECTRA**
- Application of signal analysis to cavitation p 122 A84-49192
- POWER SUPPLIES**
- Development of high frequency low weight power magnetics for aerospace power systems  
[NASA-TM-83656] p 109 N84-22892
- Computer analysis of effects of altering jet fuel properties on refinery costs and yields  
[NASA-CR-174642] p 91 N84-27908
- POWER SUPPLY CIRCUITS**
- Development of high frequency low weight power magnetics for aerospace power systems  
[NASA-TM-83656] p 109 N84-22892
- POWER TRANSMISSION**
- Design of power-transmitting shafts  
[NASA-RP-1123] p 145 N84-27041
- PREBURNERS**
- Test verification of LOX/RP-1 high-pressure fuel/oxidizer-rich preburner designs p 42 A84-22134
- PRECESSION**
- The influence of gyroscopic forces on the dynamic behavior and flutter of rotating blades  
[NASA-CR-175444] p 27 N84-20524
- PRECIPITATION (CHEMISTRY)**
- Correlations between plasma variables and the deposition process of Si films from chlorosilanes in low pressure RF plasma of argon and hydrogen  
[NASA-TM-83603] p 190 N84-21330
- PRECIPITATION HARDENING**
- Elevated temperature compressive steady state deformation and failure in the oxide dispersion strengthened alloy MA 6000E p 66 A84-46785
- PREDICTION ANALYSIS TECHNIQUES**
- Prediction of composite hygral behavior made simple p 51 A84-14285
- A finite element approach for predicting nozzle admittances p 160 A84-21184
- Investigation of energy management strategies for photovoltaic systems - A predictive control algorithm p 161 A84-25468
- A review of NASA combustor and turbine heat transfer research  
[NASA-TM-83541] p 24 N84-14146
- Development of a simplified procedure for rocket engine thrust chamber life prediction with creep  
[NASA-CR-168261] p 46 N84-19472
- Predictions of spray combustion interactions p 61 N84-20532
- Tbology in the 80's Volume 1. Sessions 1 to 4  
[NASA-CP-2300-VOL-1] p 144 N84-23891
- A theoretical prediction of the acoustic pressure generated by turbulence-flame front interactions  
[NASA-TM-83587] p 184 N84-26383
- Progressive fracture of fiber composites  
[NASA-TM-83701] p 66 N84-27831
- Simplified composite micromechanics equations for strength, fracture toughness and environmental effects  
[NASA-TM-83696] p 66 N84-27832
- Efficiency of nonstandard and high contact ratio involute spur gears  
[NASA-TM-83725] p 146 N84-29223

- A computer program for predicting nonlinear uniaxial material responses using viscoplastic models  
[NASA-TM-83675] p 156 N84-29247
- PREDICTIONS**
- Predictive capability of long-term cavitation and liquid impingement erosion models p 50 A84-32646
- PREWATE** An interactive preprocessing computer code to the Weight Analysis of Turbine Engines (WATE) computer code p 176 N84-13812
- A theoretical and experimental study of turbulent nonevaporating sprays  
[NASA-CR-174668] p 35 N84-29877
- PREMIXED FLAMES**
- Combustion in a turbulent mixing layer formed at a rearward-facing step p 58 A84-10140
- Extinction of premixed flames by stretch and radiative loss p 58 A84-23593
- Time-resolved density measurements in premixed turbulent flames p 59 A84-32612
- An experimental study on extinction and stability of stretched premixed flames p 59 A84-35425
- Numerical solution for the problem of flame propagation by the random element method p 60 A84-48139
- Combustor flame flashback p 62 N84-20561
- PREMIXING**
- Experimental study of the operating characteristics of premixing-prevapourizing fuel/air mixing passages  
[NASA-CR-168279] p 23 N84-14143
- Combustor flame flashback p 62 N84-20561
- PREPREGS**
- Characterization of PMR polyimide resin and prepreg  
[NASA-CR-163217] p 83 N84-20695
- PRESSURE DEPENDENCE**
- Cross spectra between pressure and temperature in a constant-area duct downstream of a hydrogen-fueled combustor  
[NASA-TM-83463] p 182 N84-11885
- PRESSURE DISTRIBUTION**
- Potential flow analysis of glaze ice accretions on an airfoil  
[NASA-CR-168282] p 8 N84-16146
- A theoretical model for the cross spectra between pressure and temperature downstream of a combustor  
[NASA-TM-83671] p 188 N84-34231
- PRESSURE EFFECTS**
- Real time pressure signal system for a rotary engine  
[NASA-CASE-LEW-13622-1] p 28 N84-22559
- PRESSURE GRADIENTS**
- An experimental study of the properties of surface pressure fluctuations in strong adverse pressure gradient turbulent boundary layers  
[NASA-CR-175410] p 9 N84-20488
- Investigation of the effects of pressure gradient, temperature and wall temperature ratio on the stagnation point heat transfer for circular cylinders and gas turbine vanes  
[NASA-CR-174667] p 30 N84-23649
- Modeling of zero gravity venting  
[NASA-CR-173503] p 127 N84-23854
- Analytical and experimental investigation of stator endwall countouring in a small axial-flow turbine  
[NASA-TP-2309] p 35 N84-32388
- PRESSURE MEASUREMENT**
- The pressure multiplier revisited p 129 A84-13125
- Acoustic power dissipation on radiation through duct terminations - Experiments p 180 A84-21272
- Hot-flow tests of a series of 10-percent-scale turbofan forced mixing nozzles  
[NASA-TP-2268] p 123 N84-17525
- Simplified combustion noise theory yielding a prediction of fluctuating pressure level  
[NASA-TP-2237] p 183 N84-19049
- The infinite line pressure probe  
[NASA-TM-83582] p 132 N84-19787
- Lubrication of machine elements  
[NASA-RP-1126] p 147 N84-31640
- PRESSURE REDUCTION**
- Method of making an ion beam sputter-etched ventricular catheter for hydrocephalus shunt  
[NASA-CASE-LEW-13107-2] p 174 N84-23095
- Modeling of zero gravity venting  
[NASA-CR-173503] p 127 N84-23854
- PRESSURE SENSORS**
- The infinite line pressure probe  
[NASA-TM-83582] p 132 N84-19787
- Ceramic-to-metal bonding for pressure transducers  
[NASA-CR-173500] p 84 N84-22753
- PRESSURE VESSELS**
- Aging results for PRD 49 III/epoxy and Kevlar 49/epoxy composite pressure vessels p 62 A84-21847
- Cycle life test and failure model of nickel-hydrogen cells p 162 A84-30185
- Oxygen recombination in individual pressure vessel nickel-hydrogen batteries  
[NASA-CASE-LEW-13822-1] p 110 N84-29084

**PRESSURIZING**

Evaluation of gas cooling for pressurized phosphoric acid fuel cell stacks p 163 A84-30191

**PREVAPORIZATION**

Experimental study of the operating characteristics of premixing-prevaporizing fuel/air mixing passages [NASA-CR-168279] p 23 N84-14143

**PRINTING**

Multicolor printing plate joining [NASA-CASE-LEW-13598-1] p 132 N84-22930

**PROBABILITY DENSITY FUNCTIONS**

Mass and momentum turbulent transport experiments with confined swirling coaxial jets [NASA-CR-168252] p 124 N84-17530

**PROBABILITY THEORY**

Creep-rupture reliability analysis [NASA-CR-3780] p 155 N84-19925

**PROBLEM SOLVING**

Multiple-grid convergence acceleration of viscous and inviscid flow computations p 116 A84-23950

Embedding methods for the steady Euler equations [NASA-TM-83481] p 178 N84-11831

Asymptotic analysis of numerical wave propagation in finite difference equations [NASA-CR-175323] p 98 N84-15360

**PROCESS CONTROL (INDUSTRY)**

Investigation of energy management strategies for photovoltaic systems - A predictive control algorithm p 161 A84-25468

**PRODUCT DEVELOPMENT**

Ceramic components for the AGT 100 engine p 136 A84-22878

Automotive Stirling engine development program - Overview and status report p 138 A84-30092

**PRODUCTION ENGINEERING**

Processing of sintered alpha SiC [ASME PAPER 84-GT-127] p 140 A84-46954

**PROGRAM VERIFICATION (COMPUTERS)**

Comparison of free-piston Stirling engine model predictions with RE1000 engine test data [NASA-TM-83650] p 195 N84-24509

**PROGRAMMING LANGUAGES**

Dataflow computing approach in high-speed digital simulation [NASA-CR-173552] p 176 N84-25336

**PROJECTILES**

LeRC rail accelerators - Test designs and diagnostic techniques p 42 A84-32031

**PROP-FAN TECHNOLOGY**

Advanced propfan drive system characteristics and technology needs [AIAA PAPER 84-1194] p 18 A84-36957

Technology and benefits of aircraft counter rotation propellers [NASA-CR-168258] p 22 N84-13186

**PROPAGATION MODES**

Wave attenuation and mode dispersion in a waveguide coated with lossy dielectric material [NASA-CR-173820] p 100 N84-30145

**PROPAGATION VELOCITY**

Self-similar blast waves incorporating deflagrations of variable speed p 116 A84-28379

**PROPANE**

Synthesis of perfluoroalkylene dianilines [NASA-CR-168004] p 60 N84-11228

The role of surface generated radicals in catalytic combustion p 61 N84-20555

**PROPELLANT COMBUSTION**

Test verification of LOX/RP-1 high-pressure fuel/oxidizer-rich preburner designs p 42 A84-22134

**PROPELLANT EVAPORATION**

Evaporation and combustion of sprays p 58 A84-11636

**PROPELLANT PROPERTIES**

NASA/General Electric Broad-Specification Fuels Combustion Technology Program - Phase I p 16 A84-24033

**PROPELLANT STORAGE**

Vapor flow into a capillary propellant-acquisition device p 43 A84-36559

Space Station propulsion analysis study [AIAA PAPER 84-1326] p 44 A84-44179

Space station propulsion analysis study [NASA-TM-83715] p 47 N84-25764

Advanced onboard storage concepts for natural gas-fueled automotive vehicles [NASA-CR-174655] p 172 N84-34036

**PROPELLANT TANKS**

Evaluation of propellant tank insulation concepts for low-thrust chemical propulsion systems Executive summary [NASA-CR-168321] p 83 N84-20699

Modeling of zero gravity venting [NASA-CR-173503] p 127 N84-23854

**PROPELLER BLADES**

Tensile buckling of advanced turboprops p 149 A84-11039

The application of vortex theory to the optimum swept propeller [AIAA PAPER 84-0036] p 3 A84-17841

Flutter analysis of advanced turbopropellers p 152 A84-36492

Why credible propeller noise measurements are possible in the acoustically untreated NASA Lewis 8 ft by 6 ft wind tunnel p 181 A84-38091

Application of an optimization method to high performance propeller designs [AIAA PAPER 84-1203] p 20 A84-44181

Noise of the SR-6 propeller model at 2 deg and 4 deg angles of attack [NASA-TM-83515] p 183 N84-16946

Application of an optimization method to high performance propeller designs [NASA-TM-83710] p 2 N84-25607

Nonlinear displacement analysis of advanced propeller structures using NASTRAN [NASA-TM-83737] p 157 N84-31683

**PROPELLER DRIVE**

Advanced propfan drive system characteristics and technology needs [AIAA PAPER 84-1194] p 18 A84-36957

**PROPELLER EFFICIENCY**

Performance degradation of propeller systems due to rim ice accretion [AIAA PAPER 82-0286] p 12 A84-17406

**PROPELLER FANS**

Advanced propfan drive system characteristics and technology needs [AIAA PAPER 84-1194] p 18 A84-36957

**PROPELLERS**

Application of an optimization method to high performance propeller designs [AIAA PAPER 84-1203] p 20 A84-44181

An advanced pitch change mechanism incorporating a hybrid traction drive [AIAA PAPER 84-1383] p 20 A84-44182

Forced vibration analysis of rotating cyclic structures in NASTRAN [NASA-CR-165429] p 153 N84-11514

Aeroelastic analysis for propellers - mathematical formulations and program user's manual [NASA-CR-3729] p 153 N84-12530

Technology and benefits of aircraft counter rotation propellers [NASA-CR-168258] p 22 N84-13186

A possible explanation for the present difference between linear noise theory and experimental data for supersonic helical tip speed propellers [NASA-TM-83467] p 183 N84-14874

NASTRAN documentation for flutter analysis of advanced turbopropellers [NASA-CR-167927] p 25 N84-15153

An advanced pitch change mechanism incorporating a hybrid traction drive [NASA-TM-83709] p 2 N84-25605

Application of an optimization method to high performance propeller designs [NASA-TM-83710] p 2 N84-25607

Summary of recent NASA propeller research [NASA-TM-83733] p 2 N84-32344

An experimental investigation of the effect of boundary layer refraction on the noise from a high-speed propeller [NASA-TM-83764] p 186 N84-34230

**PROPULSION**

The structural response of a rail acceleration p 151 A84-32039

A piecewise linear state variable technique for real time propulsion system simulation p 20 A84-42378

**PROPULSION SYSTEM CONFIGURATIONS**

Aerodynamic effect of combustor inlet-air pressure on fuel jet atomization [AIAA PAPER 84-1320] p 120 A84-36973

Study and review of permanent magnets for electric vehicle propulsion motors [NASA-CR-168178] p 193 N84-14071

Downsizing assessment of automotive Stirling engines [NASA-TM-83468] p 194 N84-14989

Development of a DC propulsion system for an electric vehicle [NASA-CR-168306] p 166 N84-20014

Electric vehicle propulsion alternatives [NASA-TM-83504] p 166 N84-20017

Evaluation of propellant tank insulation concepts for low-thrust chemical propulsion systems [NASA-CR-168320] p 46 N84-20634

Aerodynamic effect of combustor inlet-air pressure on fuel jet atomization [NASA-TM-83611] p 126 N84-22910

Propulsion issues for advanced orbit transfer vehicles [NASA-TM-83624] p 47 N84-25762

**PROPULSION SYSTEM PERFORMANCE**

Development of carbon slurry fuels for transportation (hybrid fuels, phase 2) [NASA-CR-174659] p 74 N84-28960

Propulsion issues for advanced orbit transfer vehicles p 48 N84-29937

AC propulsion system for an electric vehicle, phase 2 [NASA-CR-168244] p 111 N84-31514

Energy efficient engine component development and integration program [NASA-CR-173884] p 35 N84-32389

Rocket injector anomalies study. Volume 1: Description of the mathematical model and solution procedure [NASA-CR-174702] p 49 N84-32428

Rocket injector anomalies study. Volume 2: Results of parametric studies [NASA-CR-174703] p 49 N84-32429

**PROPULSION SYSTEM PERFORMANCE**

Shuttle/Centaur - More capability for the 1980's [IAF PAPER 83-18] p 38 A84-11718

Real-time Pegasus propulsion system model V-STOL-piloted simulation evaluation p 15 A84-17362

Comparison of full-scale engine and subscale model performance of a mixed flow exhaust system for an energy efficient engine (E3) propulsion system [AIAA PAPER 84-0283] p 16 A84-17997

Investigation of the residue in an electric rail gun employing a plasma armature p 103 A84-32046

Measurement of fluid properties using rapid-double-exposure and time-average holographic interferometry [AIAA PAPER 84-1461] p 130 A84-35223

Preliminary investigation of a two-zone swirl flow combustor [AIAA PAPER 84-1169] p 17 A84-36951

Aerodynamic effect of combustor inlet-air pressure on fuel jet atomization [AIAA PAPER 84-1320] p 120 A84-36973

An overview of NASA intermittent combustion engine research [AIAA PAPER 84-1393] p 19 A84-40244

Supersonic STOVL ejector aircraft from a propulsion point of view [AIAA PAPER 84-1401] p 19 A84-40246

Supersonic STOVL aircraft with turbine bypass/turbo-compressor engines [AIAA PAPER 84-1403] p 19 A84-40247

A piecewise linear state variable technique for real time propulsion system simulation p 20 A84-42378

Space Station propulsion analysis study [AIAA PAPER 84-1326] p 44 A84-44179

Rotorcraft flight-propulsion control integration p 36 A84-46524

Energy efficient engine: Flight propulsion system, preliminary analysis and design update [NASA-CR-167980] p 22 N84-11170

Fiberoptics for propulsion control system [NASA-TM-83542] p 1 N84-14111

Aeronautical propulsion. Present status and future directions [NASA-TM-83589] p 1 N84-16119

Measurement of fluid properties using rapid-double-exposure and time-average holographic interferometry [NASA-TM-83630] p 132 N84-21849

Preliminary investigation of a two-zone swirl flow combustor [NASA-TM-83637] p 29 N84-22565

Aerodynamic effect of combustor inlet-air pressure on fuel jet atomization [NASA-TM-83611] p 126 N84-22910

Rotorcraft contingency power study [NASA-CR-174675] p 31 N84-24580

Supersonic STOVL ejector aircraft from a propulsion point of view [NASA-TM-83641] p 31 N84-24581

Supersonic STOVL aircraft with turbine bypass/turbo-compressor engines [NASA-TM-83686] p 31 N84-24582

An overview of NASA intermittent combustion engine research [NASA-TM-83668] p 31 N84-24583

Results of electric-vehicle propulsion system performance on three lead-acid battery systems [NASA-TM-83657] p 169 N84-25166

Space station propulsion analysis study [NASA-TM-83715] p 47 N84-25764

Unsteady flow in turbomachinery: An overview p 128 N84-25961

Utilization of alternative fuels in diesel engines [NASA-CR-174669] p 91 N84-26813

Energy efficient engine component development and integration program [NASA-CR-173884] p 35 N84-32389

## PROPULSIVE EFFICIENCY

- Experimental investigation of the pulsed electrothermal (PET) thruster  
[AIAA PAPER 84-1386] p 43 A84-35201  
Improved ion containment using a ring-cusp ion thruster p 44 A84-49511

## PROSTHETIC DEVICES

- Prediction of turbulent flow past a prosthetic heart valve p 175 A84-49108

## PROTECTION

- How to protect a wind turbine from lightning  
[NASA-CR-168229] p 163 N84-10661

## PROTECTIVE COATINGS

- Processing of fused silicide coatings for carbon-based materials p 51 A84-19780  
The effect of a coating on the thermo-oxidative stability of Celcon 6000 graphite fiber/PMR 15 polyimide composites p 52 A84-21844  
Solute transport and the prediction of breakthrough oxidation in gamma + beta Ni-Cr-Al alloys p 65 A84-42658  
A review of the use of wear-resistant coatings in the cutting-tool industry  
[NASA-TM-83512] p 81 N84-11295  
Oxidation resistant slurry coating for carbon-based materials  
[NASA-CASE-LEW-13923-1] p 54 N84-16266  
Method and apparatus for coating substrates using a laser  
[NASA-CASE-LEW-13526-1] p 134 N84-22944  
Performance of thermal barrier coatings in high heat flux environments  
[NASA-TM-83663] p 72 N84-24772  
Coating with overlay metallic-cermet alloy systems  
[NASA-CASE-LEW-13639-2] p 73 N84-27855  
Deposition of diamondlike carbon films  
[NASA-CASE-LEW-14080-1] p 86 N84-28986  
Overlay metallic-cermet alloy coating systems  
[NASA-CASE-LEW-13639-1] p 77 N84-33555  
Improved thermal barrier coating system  
[NASA-CASE-LEW-14057-1] p 88 N84-33595
- PULSE COMMUNICATION**  
Interference performance analysis of M-ary CPSK and M-ary CAPK digital transmission systems and the computation of 'required isolation' for efficient utilization of geostationary satellite orbit/spectrum p 95 A84-49303

## PULSE GENERATORS

- Optical pulse generator using liquid crystal light valve p 188 N84-22414

## PULSE HEATING

- Fight and wind tunnel tests of an electro-impulse deicing system  
[AIAA PAPER 84-2234] p 12 A84-39280

## PULSE MODULATION

- All-purpose bidirectional four-quadrant controller p 22 N84-10070

## PULSED JET ENGINES

- Investigation of a pulsed electrothermal thruster  
[NASA-CR-168266] p 45 N84-12227

## PUMP IMPELLERS

- Effects of volute geometry and impeller orbit on the hydraulic performance of a centrifugal pump p 136 A84-22316

## PUMPING

- Determination of compressor in-stall characteristics from engine surge transients  
[AIAA PAPER 84-1206] p 18 A84-36959  
Determination of compressor in-stall characteristics from engine surge transients  
[NASA-TM-83639] p 29 N84-22566

## PUMPS

- Assessment of two neglected effects in the analysis of an oil pumping ring seal  
[ASME PAPER 83-LUB-16] p 137 A84-29097

## PYROELECTRICITY

- Pyroelectric conversion in space. A conceptual design study  
[NASA-CR-168272] p 165 N84-14585

## PYROLYTIC GRAPHITE

- A multistage spent particle collector and a method for making same  
[NASA-CASE-LEW-13914-1] p 131 N84-12447  
Ion sputter textured graphite electrode plates  
[NASA-CASE-LEW-12919-2] p 179 N84-28565  
Secondary electron emission characteristics of ion-textured copper and high-purity isotropic graphite surfaces  
[NASA-TP-2342] p 86 N84-28989

## Q

## QUALITY CONTROL

- Automotive Stirling engine development program  
[NASA-CR-168205] p 194 N84-18117

## QUANTUM EFFICIENCY

- Photovoltaic characteristics of diffused P+/N bulk GaAs solar cells p 161 A84-23115  
Diffused junction p(+)-n solar cells in bulk GaAs II - Device characterization and modelling p 161 A84-26028

## R

## RADIAL DISTRIBUTION

- Analysis of an internally radially cracked ring segment subject to three-point radial loading p 150 A84-18691

## RADIAL FLOW

- Aerodynamic effects of moveable sidewall nozzle geometry and rotor exit restriction on the performance of a radial turbine  
[SAE PAPER 831517] p 17 A84-29460  
Application of a quasi-3D inviscid flow and boundary layer analysis to the hub-shroud contouring of a radial turbine  
[AIAA PAPER 84-1297] p 6 A84-44177  
Velocity and temperature characteristics of two-stream, coplanar jet exhaust plumes  
[AIAA PAPER 84-2205] p 21 A84-46106  
Variable stator radial turbine  
[NASA-CR-174663] p 29 N84-22568  
Application of a quasi-3D inviscid flow and boundary layer analysis to the hub-shroud contouring of a radial turbine  
[NASA-TM-83669] p 10 N84-25647  
Velocity and temperature characteristics of two-stream, coplanar jet exhaust plumes  
[NASA-TM-83730] p 34 N84-28790

## RADIATION DAMAGE

- Effect of electron flux on radiation damage in GaAs solar cells p 160 A84-22998  
Radiation damage and defect behavior in ion-implanted, lithium counterdoped silicon solar cells  
[NASA-TM-83646] p 109 N84-22890  
Space Photovoltaic Research and Technology 1983 High Efficiency, Radiation Damage, and Blanket Technology  
[NASA-CP-2314] p 170 N84-29307  
The effects of lithium counterdoping on radiation damage and annealing in n(+)-p silicon solar cells  
[NASA-TM-83755] p 110 N84-31513

## RADIATION EFFECTS

- The energy dependence and surface morphology of Kapton (trademark) degradation under atomic oxygen bombardment p 187 N84-34484

## RADIATION HARDENING

- Increased radiation resistance in lithium-counterdoped silicon solar cells p 163 A84-34846  
Thin N-P-P radiation resistant solar cells  
[NASA-CR-168284] p 166 N84-15682

## RADIATION MEASUREMENT

- Flame radiation and linear heat transfer in a tubular can combustor  
[AIAA PAPER 84-0443] p 16 A84-21300  
Flame radiation and linear heat transfer in a tubular can combustor  
[NASA-TM-83538] p 23 N84-13188

## RADIATION TOLERANCE

- A temperature correlation for the radiation resistance of a thick-walled circular duct exhausting a hot gas p 181 A84-31103  
Radiation tolerance of low resistivity, high voltage silicon solar cells p 170 N84-29318  
Cell and defect behavior in lithium-counterdoped solar cells p 170 N84-29322  
The effects of lithium counterdoping on radiation damage and annealing in n(+)-p silicon solar cells  
[NASA-TM-83755] p 110 N84-31513

## RADIATIVE HEAT TRANSFER

- Extinction of premixed flames by stretch and radiative loss p 58 A84-23593  
Role of fuel chemical properties on combustor radiative heat load  
[AIAA PAPER 84-1493] p 89 A84-35236

## RADIO ANTENNAS

- A new multiple beam satellite antenna for 30/20 GHz communications coverage of CONUS-experimental evaluation  
[AIAA PAPER 84-0655] p 94 A84-25256

## RADIO COMMUNICATION

- Rural land mobile radio market assessment and satellite and terrestrial system concepts  
[AIAA PAPER 84-0754] p 95 A84-25324  
Mobile radio alternative systems study Volume 1: Traffic model  
[NASA-CR-168062] p 96 N84-10402  
Mobile radio alternative systems study Volume 2: Terrestrial - rural areas  
[NASA-CR-168063] p 96 N84-10403

- Mobile radio alternative systems study  
satellite/terrestrial (hybrid) systems concepts  
[NASA-CR-168064] p 96 N84-10404  
Rural land mobile radio market assessment and satellite and terrestrial system concepts  
[NASA-TM-83591] p 99 N84-19641

## RADIO FREQUENCIES

- Correlations between plasma variables and the deposition process of Si films from chlorosilanes in low pressure RF plasma of argon and hydrogen  
[NASA-TM-83603] p 190 N84-21330

## RADIO FREQUENCY INTERFERENCE

- Spectrum/orbit utilization program for geostationary satellites

## [NASA-TM-83759]

- p 100 N84-30146

## RADIO RECEIVERS

- The 30 GHz communications satellite low noise receiver  
[NASA-CR-168254] p 97 N84-13398  
Test results for 27.5- to 30-GHz communications satellite receivers  
[NASA-TM-83662] p 100 N84-27954

## RADIO RELAY SYSTEMS

- High efficiency IMPATT diodes for 60 GHz intersatellite link applications  
[AIAA PAPER 84-0767] p 103 A84-25333

## RAILGUN ACCELERATORS

- LeRC rail accelerators - Test designs and diagnostic techniques p 42 A84-32031  
The structural response of a rail acceleration p 151 A84-32039  
Investigation of the residue in an electric rail gun employing a plasma armature p 103 A84-32046  
Energy partitioning in an inductively driven rail gun p 104 A84-33325  
Electromagnetic propulsion test facility  
[NASA-TM-83568] p 37 N84-16229

## RAILS

- Characteristics and capacities of the NASA Lewis Research Center high precision 6.7- by 6.7-m planar near-field scanner  
[NASA-TM-83785] p 133 N84-32789

## RAINDROPS

- Effect of geometry on airfoil icing characteristics p 12 A84-37935  
Experimental and analytical investigations into airfoil icing p 12 A84-45054

## RANDOM VARIABLES

- Advanced reliability method for fatigue analysis p 151 A84-31596

## RANDOM WALK

- Random element method for numerical modeling of diffusional processes p 119 A84-35318  
Numerical solution for the problem of flame propagation by the random element method p 60 A84-48139

## RANKINE CYCLE

- An RC-1 organic Rankine bottoming cycle for an adiabatic diesel engine p 196 N84-32306  
[NASA-CR-168256] p 196 N84-32306  
Steam bottoming cycle for an adiabatic diesel engine  
[NASA-CR-168255] p 196 N84-32304

## RAPID QUENCHING (METALLURGY)

- Rapid solidification via melt spinning - Equipment and techniques p 65 A84-31915

## RAYLEIGH SCATTERING

- Time-resolved density measurements in premixed turbulent flames p 59 A84-32612

## RCA SATCOM SATELLITES

- Recent developments in EHF Satcom technology p 39 A84-46620

## REACTION KINETICS

- The chemical kinetics and thermodynamics of sodium species in oxygen-rich hydrogen flames p 59 A84-27724  
Electrode kinetics of oxygen reduction - A theoretical and experimental analysis of the rotating ring-disc electrode method p 59 A84-29999  
Reaction of cobalt in SO<sub>2</sub> atmospheres at elevated temperatures p 65 A84-33440  
Synthesis of perfluoroalkylene dianilines  
[NASA-CR-168004] p 60 N84-11228  
NASA redox storage system development project, calendar year 1982  
[NASA-TM-83468] p 164 N84-11579  
Fast algorithms for combustion kinetics calculations. A companion p 61 N84-20554  
Shock tube study of the fuel structure effects on the chemical kinetic mechanisms responsible for soot formation  
[NASA-CR-174661] p 62 N84-21677  
Kinetics of chromium ion absorption by cross-linked polyacrylate films  
[NASA-TM-83661] p 50 N84-23693  
Direct simulations of chemically reacting turbulent mixing layers  
[NASA-CR-174640] p 32 N84-25710

- Chemical mechanisms and reaction rates for the initiation of hot corrosion of IN-738 [NASA-TP-2319] p 74 N84-28958
- Exponential-fitted methods for integrating stiff systems of ordinary differential equations Applications to homogeneous gas-phase chemical kinetics p 179 N84-31279
- A comparison of the efficiency of numerical methods for integrating chemical kinetic rate equations p 49 N84-31280
- GCKP84-general chemical kinetics code for gas-phase flow and batch processes including heat transfer effects [NASA-TP-2320] p 63 N84-32446
- REAL TIME OPERATION**
- ADA and multi-microprocessor real-time simulation p 176 A84-10905
- Real-time Pogasus propulsion system model V/STOL-piloted simulation evaluation p 15 A84-17362
- A real-time implementation of an advanced sensor failure detection, isolation, and accommodation algorithm [AIAA PAPER 84-0569] p 176 A84-21305
- A piecewise linear state variable technique for real time propulsion system simulation p 20 A84-42378
- A generalized computer code for developing dynamic gas turbine engine models (DIGTEM) [NASA-TM-83508] p 22 N84-12166
- A real-time implementation of an advanced sensor failure detection, isolation, and accommodation algorithm [NASA-TM-83553] p 1 N84-13140
- Development of an instrument for real-time computation of indicated mean effective pressure [NASA-TP-2238] p 107 N84-16461
- Operating system for a real-time multiprocessor propulsion system simulator [NASA-TM-83605] p 177 N84-20258
- RTMPL: A structured programming and documentation utility for real-time multiprocessor simulations [NASA-TM-83608] p 177 N84-20259
- Real-time hybrid computer simulation of a small turboshaft engine and control system [NASA-TM-83579] p 28 N84-21548
- RECEIVERS**
- The 30-GHz monolithic receive module [NASA-CR-168326] p 99 N84-20737
- RECIRCULATIVE FLUID FLOW**
- Limitations and empirical extensions of the k-epsilon model as applied to turbulent confined swirling flows [AIAA PAPER 84-0441] p 114 A84-18096
- Turbulence characteristics of swirling flowfields [NASA-CR-175392] p 124 N84-19744
- Confined turbulent swirling recirculating flow predictions [NASA-CR-175397] p 125 N84-19745
- RECOVERY**
- An assessment of advanced technology for industrial cogeneration [NASA-CR-173456] p 167 N84-22001
- RECTANGULAR WAVEGUIDES**
- Monolithic microwave integrated circuit devices for active array antennas [NASA-CR-173981] p 112 N84-34675
- REDOX CELLS**
- Single cell performance studies on the FE/CR Redox Energy Storage System using mixed reactant solutions at elevated temperature p 163 A84-30194
- NASA redox storage system development project, calendar year 1982 [NASA-TM-83469] p 164 N84-11579
- Study to establish cost projections for production of Redox chemicals [NASA-CR-167881] p 164 N84-11580
- Electrochemical studies of redox systems for energy storage [NASA-CR-174503] p 165 N84-15681
- Chromium electrodes for REDOX cells [NASA-CASE-LEW-13653-1] p 170 N84-28205
- Anion permselective membrane [NASA-CR-174725] p 172 N84-29358
- Negative electrode catalyst for the iron-chromium REDOX energy storage system [NASA-CASE-LEW-14028-1] p 172 N84-32909
- REDUCED GRAVITY**
- Computational modeling of jet induced mixing of cryogenic propellants in low-G [AIAA PAPER 84-1344] p 121 A84-40243
- Apparatus analysis and preliminary design of low gravity porous solids experiment for STS Orbiter mid-deck [NASA-CR-168248] p 37 N84-10109
- Computational modeling of jet induced mixing of cryogenic propellants in low-G [NASA-TM-83703] p 127 N84-25000
- REDUCTION (CHEMISTRY)**
- Importance of interatomic spacing in catalytic reduction of oxygen in phosphoric acid p 58 A84-12644
- Electrode kinetics of oxygen reduction - A theoretical and experimental analysis of the rotating ring-disc electrode method p 59 A84-29999
- REDUNDANCY**
- Sensor failure detection for jet engines using analytical redundancy [NASA-TM-83695] p 31 N84-24585
- REDUNDANCY ENCODING**
- A real-time implementation of an advanced sensor failure detection, isolation, and accommodation algorithm [AIAA PAPER 84-0569] p 176 A84-21305
- A real-time implementation of an advanced sensor failure detection, isolation, and accommodation algorithm [NASA-TM-83553] p 1 N84-13140
- REFINING**
- NASA broad-specification fuels combustion technology program p 62 N84-23637
- Computer analysis of effects of alternate jet fuel properties on refinery costs and yields [NASA-CR-174642] p 91 N84-27908
- REFLECTION**
- Preliminary design of a 10-kW thermophotovoltaic system for space applications [NASA-TM-83768] p 49 N84-32427
- REFLECTORS**
- Phased-array-fed antenna configuration study. Volume 1: Technology assessment [NASA-CR-168231] p 98 N84-16423
- Secondary pattern computation of an arbitrarily shaped main reflector [NASA-TM-85527] p 100 N84-25909
- REFRACTED WAVES**
- Interference phenomena in the refraction of a surface polariton by vertical dielectric barriers p 179 A84-24410
- REFRACTION**
- An experimental investigation of the effect of boundary layer refraction on the noise from a high-speed propeller [NASA-TM-83764] p 186 N84-34230
- REFRACTIVITY**
- Rainbow schlieren and its applications p 131 A84-40738
- Group-type hydrocarbon standards for high-performance liquid chromatographic analysis of middistillate fuels [NASA-TP-2317] p 90 N84-23774
- REFRACTORY METALS**
- Replacing critical and strategic refractory metal elements in nickel-base superalloys - NASA's COSAM program [NASA-TM-83528] p 67 N84-13264
- REFRIGERATORS**
- Qualification testing of solar photovoltaic powered refrigerator freezers for medical use in remote geographic locations [NASA-CR-168181] p 169 N84-25162
- Solar photovoltaic powered refrigerators/freezers for medical use in remote geographic locations [NASA-CR-168268] p 169 N84-25163
- REGENERATIVE FUEL CELLS**
- Alkaline fuel cells for the regenerative fuel cell energy storage system p 162 A84-30183
- Design considerations for a 10-kW integrated hydrogen-oxygen regenerative fuel cell system [NASA-TM-83664] p 167 N84-23023
- Regenerative hydrogen-oxygen fuel cell-electrolyzer systems for orbital energy storage p 111 N84-33670
- REGRESSION COEFFICIENTS**
- Elastic model of the traction behavior of two traction lubricants p 136 A84-28791
- REGULATORS**
- AESOP: An interactive computer program for the design of linear quadratic regulators and Kalman filters [NASA-TP-2221] p 178 N84-16843
- REISSNER THEORY**
- On the suppression of zero energy deformation modes p 150 A84-21541
- RELAXATION METHOD (MATHEMATICS)**
- Relaxation solution of the full Euler equations p 119 A84-35323
- A semi-direct procedure using a local relaxation factor and its application to an internal flow problem [NASA-TM-83704] p 128 N84-25946
- RELIABILITY ANALYSIS**
- Advanced reliability method for fatigue analysis p 151 A84-31596
- REMOTE CONTROL**
- Advances in solid state switchgear technology for large space power systems [NASA-TM-83652] p 109 N84-22391
- REMOTE SENSING**
- A laser system to remotely sense bird movements p 159 A84-31608
- Development of Great Lakes algorithms for the Nimbus-G coastal zone color scanner [NASA-CR-173511] p 159 N84-27258
- RENE 95**
- Effects of processing and microstructure on the fatigue behaviour of the nickel-base superalloy Rene95 p 66 A84-48715
- Fatigue crack growth and low cycle fatigue of two nickel base superalloys [NASA-CR-174534] p 66 N84-10267
- REPEATERS**
- Mobile radio alternative systems study. Volume 2 Terrestrial - rural areas [NASA-CR-168063] p 96 N84-10403
- RESEARCH AIRCRAFT**
- Design of a high-performance rotary stratified-charge research aircraft engine [AIAA PAPER 84-1395] p 17 A84-35204
- RESEARCH AND DEVELOPMENT**
- NASA priority technologies [IAF PAPER 83-345] p 37 A84-11793
- NASA/General Electric Broad-Specification Fuels Combustion Technology Program - Phase I p 16 A84-24033
- Automotive Stirling Engine Development Program Model Stirling engine development p 138 A84-30091
- Alkaline fuel cells for the regenerative fuel cell energy storage system p 162 A84-30183
- An overview of NASA intermittent combustion engine research [AIAA PAPER 84-1393] p 19 A84-40244
- NASA transmission research and its probable effects on helicopter transmission design p 139 A84-46355
- Aeronautical propulsion Present status and future directions [NASA-TM-83589] p 1 N84-16119
- An overview of NASA intermittent combustion engine research [NASA-TM-83668] p 31 N84-24583
- Advanced Gas Turbine (AGT) [NASA-CR-174694] p 195 N84-29805
- RESEARCH VEHICLES**
- Advanced onboard storage concepts for natural gas-fueled automotive vehicles [NASA-CR-174655] p 172 N84-34036
- RESIDUES**
- Applications of photoacoustic techniques to the study of jet fuel residue [NASA-CR-173322] p 90 N84-18420
- RESIN MATRIX COMPOSITES**
- Resin selection criteria for tough composite structures [NASA-TM-83449] p 81 N84-10310
- RESISTOJET ENGINES**
- Demonstration of a new electrothermal thruster concept p 43 A84-34037
- Resistojet propulsion for large spacecraft systems [NASA-TM-83489] p 45 N84-11206
- Calculation of vaporization rates assuming various rate determining steps Application to the resistojet [NASA-TM-83757] p 51 N84-31283
- RESONANT FREQUENCIES**
- All-purpose bidirectional four-quadrant controller p 22 N84-10070
- Blade loss transient dynamics analysis with flexible bladed disk [NASA-CR-168176] p 23 N84-13193
- An improved finite-difference analysis of uncoupled vibrations of tapered cantilever beams [NASA-TM-83495] p 154 N84-13610
- The 25 kW resonant dc/dc power converter [NASA-CR-168273] p 108 N84-17481
- A study of the high frequency limitations of series resonant converters [NASA-CR-173868] p 111 N84-32678
- RESONANT VIBRATION**
- Vibrations of twisted cantilevered plates - Experimental investigation [ASME PAPER 84-GT-96] p 152 A84-46937
- Improved finite-difference vibration analysis of pretwisted, tapered beams [NASA-TM-83549] p 154 N84-16588
- RETROFITTING**
- A graphics subsystem retrofit design for the bladed-disk data acquisition system [NASA-TM-83510] p 175 N84-12730
- REYNOLDS NUMBER**
- Internal heat transfer coefficients of porous metals p 112 A84-13239
- Investigation of mixing in a turbofan exhaust duct II Computer code application and verification p 17 A84-27140
- REYNOLDS STRESS**
- Turbulence modeling for three-dimensional shear flows over curved rotating bodies p 122 A84-48138
- RHENIUM**
- Calculation of vaporization rates assuming various rate determining steps Application to the resistojet [NASA-TM-83757] p 51 N84-31283

## RHEOLOGY

- The ball bearing as a rheological test device  
[NASA-TM-83570] p 142 N84-17591
- Tribology in the 80's Volume 1: Sessions 1 to 4  
[NASA-CP-2300-VOL-1] p 144 N84-23891
- An investigation into the injection molding of PMR-15 polyimide  
[NASA-CR-173550] p 85 N84-24810
- Elastohydrodynamic lubrication of smooth surfaces  
p 144 N84-24695

## RHODE ISLAND

- Wind turbine generator interaction with conventional diesel generators on Block Island, Rhode Island Volume 2. Data analysis  
[NASA-CR-168319] p 172 N84-31783

## RIBBON PARACHUTES

- Steady state stresses in ribbon parachute canopies  
[AIAA PAPER 84-0816] p 11 A84-26580

## RIBBONS

- Arc spray fabrication of metal matrix composite monolayers — high temperature fiber-reinforced superalloy composites  
[NASA-CASE-LEW-13828-1] p 54 N84-15203

## RIGID ROTORS

- Progress in net shape fabrication of alpha sic turbine components  
[ASME PAPER 84-GT-273] p 140 A84-47036

## RIGID STRUCTURES

- Analyses of large quasistatic deformations of inelastic bodies by a new hybrid-stress finite element algorithm  
p 150 A84-16874

## RING STRUCTURES

- Analysis of an internally radially cracked ring segment subject to three-point radial loading p 150 A84-18691
- A multistage spent particle collector and a method for making same  
[NASA-CASE-LEW-13914-1] p 131 N84-12447

## ROCKET ENGINE DESIGN

- Shuttle/Centaur - More capability for the 1980's  
[IAF PAPER 83-18] p 38 A84-11718
- Test verification of LOX/RP-1 high-pressure fuel/oxidizer-rich preburner designs p 42 A84-22134
- Proposed system design for a 20 kW pulsed electrothermal thruster  
[AIAA PAPER 84-1387] p 43 A84-35202
- Simplification of power electronics for ion thruster neutralizers p 44 A84-49509
- Improved ion containment using a ring-cusp ion thruster p 44 A84-49511

## ROCKET ENGINES

- Development of a simplified procedure for rocket engine thrust chamber life prediction with creep  
[NASA-CR-168261] p 46 N84-19472
- Rocket injector anomalies study. Volume 1: Description of the mathematical model and solution procedure  
[NASA-CR-174702] p 49 N84-32428

## ROCKET EXHAUST

- Correlation of flight effects on centerline velocity decay for cold-flow acoustically excited jets  
[NASA-TM-83502] p 182 N84-11883
- Effects of chemical releases by the STS-3 Orbiter on the ionosphere  
[NASA-CR-171032] p 173 N84-25204

## ROCKET PROPELLANTS

- Development of advanced inert-gas ion thrusters  
[NASA-CR-168206] p 44 N84-10180

## ROCKET THRUST

- Investigation of a pulsed electrothermal thruster  
[NASA-CR-168266] p 45 N84-12227

## RODS

- Heat transfer in thermal barrier coated rods with circumferential and radial temperature gradients  
[ASME PAPER 84-GT-181] p 121 A84-46982

## ROLLER BEARINGS

- Operating characteristics of a three-piece-inner-ring large-bore roller bearing to speeds of 3 million DN  
[NASA-TP-2355] p 146 N84-29226
- Thermal analysis of a planetary transmission with spherical roller bearings operating after complete loss of oil  
[NASA-TP-2367] p 147 N84-32824

## ROLLING

- Hydrodynamic lubrication of rigid nonconformal contacts in combined rolling and normal motion  
[NASA-TM-83578] p 142 N84-17592

## ROLLING CONTACT LOADS

- Subsurface stress evaluations under rolling/sliding contacts  
[ASME PAPER 83-LUB-18] p 137 A84-29099
- Measurement of rolling friction by a damped oscillator  
[NASA-TP-2257] p 141 N84-13577
- Hydrodynamic lubrication of rigid nonconformal contacts in combined rolling and normal motion  
[NASA-TM-83578] p 142 N84-17592

## ROTARY ENGINES

- Design of a high-performance rotary stratified-charge research aircraft engine  
[AIAA PAPER 84-1395] p 17 A84-35204
- A review of internal combustion engine combustion chamber process studies at NASA Lewis Research Center  
[AIAA PAPER 84-1316] p 121 A84-40242
- A review of internal combustion engine combustion chamber process studies at NASA Lewis Research Center  
[NASA-TM-83666] p 127 N84-24999
- An overview of the NASA rotary engine research program  
[NASA-TM-83699] p 34 N84-28791
- Development of partially fluorinated resin apex seals  
[NASA-CR-174706] p 148 N84-32828

## ROTARY STABILITY

- Labyrinth seal forces on a whirling rotor p 135 A84-13228
- Effects of different rub models on simulated rotor dynamics  
[NASA-TP-2220] p 142 N84-17590

## ROTARY WING AIRCRAFT

- Variable stator radial turbine  
[NASA-CR-174663] p 29 N84-22568

## ROTARY WINGS

- Performance degradation of propeller systems due to rime ice accretion  
[AIAA PAPER 82-0286] p 12 A84-17406
- Helicopter rotor performance degradation in natural icing encounter p 12 A84-17412
- Experimental study of performance degradation of a model helicopter main rotor with simulated ice shapes  
[AIAA PAPER 84-0184] p 13 A84-17937
- Performance degradation of a model helicopter main rotor in hover and forward flight with a generic ice shape  
[AIAA PAPER 84-0609] p 13 A84-24195
- Performance degradation of a model helicopter rotor with a generic ice shape p 14 A84-49096
- Documentation of ice shapes on the main rotor of a UH-1H helicopter in hover  
[NASA-CR-168332] p 9 N84-17139
- Subsonic/transonic stall flutter investigation of a rotating wing  
[NASA-CR-174625] p 36 N84-33417

## ROTATING BODIES

- Turbulence modeling for three-dimensional shear flows over curved rotating bodies p 122 A84-48138
- Forced vibration analysis of rotating cyclic structures in NASTRAN  
[NASA-CR-165429] p 153 N84-11514
- NASTRAN forced vibration analysis of rotating cyclic structures  
[NASA-CR-173821] p 157 N84-29252

## ROTATING DISKS

- Stagger angle dependence of inertial and elastic coupling in bladed disks p 151 A84-31903
- Structural dynamics of rotating bladed-disk assemblies coupled with flexible shaft motions p 21 A84-44645
- Finite element forced vibration analysis of rotating cyclic structures  
[NASA-CR-165430] p 153 N84-11515
- Vibration and flutter of mistuned bladed-disk assemblies  
[NASA-TM-83634] p 156 N84-23923

## ROTATING FLUIDS

- Viscous-inviscid interactive procedure for rotational flow in cascades of airfoils p 6 A84-44639
- Penalty function finite element analysis of steady viscous incompressible flow in rotating coordinates  
[ASME PAPER 84-GT-38] p 121 A84-46900
- Unsteady flow in turbomachinery: An overview  
p 128 N84-25961

## ROTATING SHAFTS

- Experimental study of bubble cavities attached to a rotating shaft in a reservoir  
[NASA-TM-83586] p 124 N84-17533
- Design of power-transmitting shafts  
[NASA-RP-1123] p 145 N84-27041

## ROTATING STALLS

- Numerical aspects of unsteady flow calculations  
p 128 N84-25968

## ROTOR AERODYNAMICS

- Labyrinth seal forces on a whirling rotor p 135 A84-13228
- Three-dimensional turbulent boundary-layer development on a fan rotor blade p 3 A84-17437
- Review of the DOE/NASA wind turbine engineering information system p 163 A84-33766
- Application of a quasi-3D inviscid flow- and boundary layer analysis to the hub-shroud contouring of a radial turbine  
[AIAA PAPER 84-1297] p 6 A84-44177

Investigation of the three-dimensional flow field within a transonic fan rotor - Experiment and analysis

- [ASME PAPER 84-GT-200] p 7 A84-46995
- Performance degradation of a model helicopter rotor with a generic ice shape p 14 A84-49096
- Aeroelastic analysis for propellers - mathematical formulations and program user's manual  
[NASA-CR-3729] p 153 N84-12530
- Compressor rotor aerodynamics p 26 N84-16210
- Investigation of flow phenomena in a transonic fan rotor using laser anemometry  
[NASA-TM-83555] p 9 N84-17143
- Effects of different rub models on simulated rotor dynamics  
[NASA-TP-2220] p 142 N84-17590
- Flutter and forced response of mistuned rotors using standing wave analysis  
[NASA-CR-173555] p 32 N84-24586
- Application of a quasi-3D inviscid flow and boundary layer analysis to the hub-shroud contouring of a radial turbine  
[NASA-TM-83669] p 10 N84-25647

## ROTOR BLADES

- Stagger angle dependence of inertial and elastic coupling in bladed disks p 151 A84-31903
- A blade loss response spectrum for flexible rotor systems  
[ASME PAPER 84-GT-29] p 139 A84-46893
- An experimental study of the compressor rotor blade boundary layer  
[ASME PAPER 84-GT-193] p 7 A84-46991

## ROTOR BLADES (TURBOMACHINERY)

- Residual stress in plasma-sprayed ceramic turbine tip and gas-path seal specimens p 78 A84-19783
- NASTRAN forced vibration analysis of rotating cyclic structures  
[ASME PAPER 83-DET-20] p 151 A84-29103
- Measurements of self-excited rotor-blade vibrations using optical displacements  
[ASME PAPER 83-GT-132] p 151 A84-33702
- NASTRAN flutter analysis of advanced turbopropellers  
[NASA-CR-167926] p 24 N84-14148
- Effects of different rub models on simulated rotor dynamics  
[NASA-TP-2220] p 142 N84-17590
- Effect of a rotor wake on heat transfer from a circular cylinder  
[NASA-TM-83613] p 126 N84-21832
- Tip cap for a rotor blade  
[NASA-CASE-LEW-13654-1] p 28 N84-22560
- Oxidizing seal for a turbine tip gas path  
[NASA-CASE-LEW-14053-1] p 29 N84-22563
- Heat transfer in serpentine passages with turbulence promoters  
[NASA-TM-83614] p 126 N84-22911
- Fan noise reduction achieved by removing tip flow irregularities behind the rotor - forward arc test configurations  
[NASA-TM-83616] p 184 N84-23235
- Effects of unsteady free stream velocity and free stream turbulence on stagnation point heat transfer  
[NASA-CR-3804] p 127 N84-25943
- Effect of vortex generators on the power conversion performance and structural dynamic loads of the Mod-2 wind turbine  
[NASA-TM-83680] p 171 N84-29347
- Acoustic pressures emanating from a turbomachine stage  
[NASA-TM-83734] p 129 N84-30224
- Improved methods of vibration analysis of pretwisted, airfoil blades  
[NASA-TM-83735] p 157 N84-30329
- Deposition of Na<sub>2</sub>SO<sub>4</sub> from salt-seeded combustion gases of a high velocity burner  
[NASA-TM-83751] p 129 N84-31558
- Research study for effects of case flexibility on bearing loads and rotor stability  
[NASA-CR-171147] p 148 N84-33811

## ROTOR BODY INTERACTIONS

- Tone generation by rotor-downstream strut interaction  
p 16 A84-22174
- Rotorcraft flight-propulsion control integration  
p 36 A84-46524

## ROTOR SPEED

- Analysis for leakage and rotordynamic coefficients of surface-roughened tapered annular gas seals  
[ASME PAPER 84-GT-32] p 140 A84-46896

## ROTORCRAFT AIRCRAFT

- Development of large rotorcraft transmissions  
p 21 A84-46354
- Rotorcraft flight-propulsion control integration  
p 36 A84-46524

## ROTORS

- Nonlinear transient finite element analysis of rotor-bearing-stator systems p 136 A84-20580

- A blade loss response spectrum for flexible rotor systems  
[ASME PAPER 84-GT-29] p 139 A84-46893
- A mathematical model for the doubly-fed wound rotor generator, part 2  
[NASA-TM-83581] p 107 N84-17479
- An experimental study of the properties of surface pressure fluctuations in strong adverse pressure gradient turbulent boundary layers  
[NASA-CR-175410] p 9 N84-20488
- The influence of gyroscopic forces on the dynamic behavior and flutter of rotating blades  
[NASA-CR-175444] p 27 N84-20524
- Dual clearance squeeze film damper  
[NASA-CASE-LEW-13506-1] p 29 N84-22562
- Effect of vortex generators on the power conversion performance and structural dynamic loads of the Mod-2 wind turbine  
[NASA-TM-83680] p 171 N84-29347
- RUN TIME (COMPUTERS)**
- Parallelism and pipelining in high-speed digital simulators p 175 A84-11876
- RUPTURING**
- Creep-rupture behavior of candidate Stirling engine iron superalloys in high-pressure hydrogen. Volume 2  
Hydrogen creep-rupture behavior  
[NASA-CR-174705] p 74 N84-28961
- RURAL AREAS**
- The worldwide market for photovoltaics in the rural sector p 161 A84-23135
- Rural land mobile radio market assessment and satellite and terrestrial system concepts  
[AIAA PAPER 84-0754] p 95 A84-25324
- Mobile radio alternative systems study. Volume 1 Traffic model  
[NASA-CR-168062] p 96 N84-10402
- Mobile radio alternative systems study. Volume 2 Terrestrial — rural areas  
[NASA-CR-168063] p 96 N84-10403
- Rural land mobile radio market assessment and satellite and terrestrial system concepts  
[NASA-TM-83591] p 99 N84-19641
- S**
- SAFETY**
- Electromagnetic propulsion test facility  
[NASA-TM-83568] p 37 N84-16229
- SATELLITE ANTENNAS**
- Multibeam antenna for 30/20 GHz advanced communications satellite using offset shaped, dual reflector surfaces p 93 A84-15627
- A new multiple beam satellite antenna for 30/20 GHz communications coverage of CONUS-experimental evaluation  
[AIAA PAPER 84-0655] p 94 A84-25256
- Advanced 30/20 GHz multiple-beam antennas for communications satellites p 40 A84-49250
- Broadcasting satellites at 12 GHz for Region 2 Technical characteristics  
[NASA-TM-83522] p 98 N84-19640
- The 20 and 30 GHz MMIC technology for future space communication antenna system  
[NASA-TM-83745] p 100 N84-31480
- SATELLITE ATTITUDE CONTROL**
- Study of auxiliary propulsion requirements for large space systems, volume 2  
[NASA-CR-168193-VOL-2] p 45 N84-13218
- SATELLITE GROUND SUPPORT**
- Graphics enhanced computer emulation for improved timing-race and fault tolerance control system analysis — of Centaur liquid-fuel booster  
[AIAA PAPER 83-2328] p 177 A84-10010
- SATELLITE NETWORKS**
- ACTS TDMA network control — Advanced Communication Technology Satellite  
[AIAA PAPER 84-0682] p 94 A84-25274
- High efficiency IMPATT diodes for 60 GHz intersatellite link applications  
[AIAA PAPER 84-0767] p 103 A84-25333
- A study of 60 GHz intersatellite link applications p 40 A84-49268
- SATELLITE TELEVISION**
- The effect of variable S/N on the subjective evaluation of protection ratios for direct-TV satellite services p 95 A84-48452
- SATELLITE TRANSMISSION**
- Baseband processor development for the Advanced Communications Satellite Program p 93 A84-15628
- NASA seeking high-power 60-GHz IMPATT diodes p 104 A84-44912
- A study of 60 GHz intersatellite link applications p 40 A84-49268
- Mobile radio alternative systems study  
satellite/terrestrial (hybrid) systems concepts  
[NASA-CR-168064] p 96 N84-10404
- Photovoltaic power system for satellite Earth stations in remote areas: Project status and design description  
[NASA-TM-83789] p 101 N84-33642
- SCALE (CORROSION)**
- Structure of transient oxides formed on NiCrAl alloys p 63 A84-12385
- Bubble formation in oxide scales on SiC p 79 A84-23689
- SCALING LAWS**
- Size scale effect in cavitation erosion  
[NASA-TM-83533] p 67 N84-11254
- Scaling and modeling of three-dimensional, end-wall, turbulent boundary layers  
[NASA-CR-3792] p 127 N84-25941
- SCANNERS**
- Characteristics and capacities of the NASA Lewis Research Center high precision 6.7- by 6.7-m planar near-field scanner  
[NASA-TM-83785] p 133 N84-32789
- SCATHA SATELLITE**
- Comparison of thermal plasma observations on SCATHA and GEOS p 41 N84-17262
- NASCAP simulations of spacecraft charging of the SCATHA satellite — NASA (spacecraft) charging analyzer program (NASCAP) p 41 N84-17268
- SCATTERING CROSS SECTIONS**
- Preliminary investigation of an electrical network model for ultrasonic scattering  
[NASA-CR-3770] p 149 N84-17605
- SCHLIEREN PHOTOGRAPHY**
- Rainbow schlieren and its applications p 131 A84-40738
- SCHOTTKY DIODES**
- The 20 GHz solid state transmitter design, impatt diode development and reliability assessment  
[NASA-CR-174716] p 112 N84-33715
- SCREENS**
- Gas flow across a wet screen - Analogy to a relief valve with hysteresis p 121 A84-43546
- SEALS (STOPPERS)**
- Material removal considerations for metal-ceramic abradable turbine seal systems p 135 A84-15575
- Correlation of compressive and shear stress with spalling of plasma-sprayed ceramic materials p 79 A84-19784
- Comparison of seal materials for use in Stirling engines p 64 A84-22879
- Thermal and elastohydrodynamic analysis of reciprocating rod seals in the Stirling engine p 138 A84-30085
- Analysis for leakage and rotordynamic coefficients of surface-roughened tapered annular gas seals  
[ASME PAPER 84-GT-32] p 140 A84-46896
- A dynamic analysis of rotary combustion engine seals  
[NASA-TM-83536] p 141 N84-14519
- Dynamic behavior of spiral-groove and Rayleigh-Step self-acting face seals  
[NASA-TP-2266] p 25 N84-16181
- Method of fabricating an abradable gas path seal  
[NASA-CASE-LEW-13269-2] p 143 N84-22957
- Development of partially fluorinated resin apex seals  
[NASA-CR-174706] p 148 N84-32828
- SECONDARY EMISSION**
- Beam impingement angle effects on secondary electron emission characteristics of textured pyrolytic graphite  
[NASA-TP-2285] p 82 N84-18400
- Secondary electron emission characteristics of ion-textured copper and high-purity isotropic graphite surfaces  
[NASA-TP-2342] p 86 N84-28989
- SECONDARY FLOW**
- Comparison of experimental and computational compressible flow in a S-duct  
[AIAA PAPER 84-0033] p 4 A84-19228
- Developing flow in S-shaped ducts p 116 A84-28709
- Comparison of visualized turbine endwall secondary flows and measured heat transfer patterns  
[ASME PAPER 83-GT-83] p 117 A84-33703
- Comparison of secondary flows predicted by a viscous code and an inviscid code with experimental data for a turning duct  
[NASA-TM-83575] p 9 N84-17142
- Secondary flow spanwise deviation model for the stators of NASA middle compressor stages  
[NASA-CR-173360] p 27 N84-18202
- SELF INDUCED VIBRATION**
- The coupled response of turbomachinery blading to aerodynamic excitations p 17 A84-26959
- SELF SEALING**
- Oxidizing seal for a turbine tip gas path  
[NASA-CASE-LEW-14053-1] p 29 N84-22563
- SEMICONDUCTOR DEVICES**
- Effects of indirect bandgap top cells in a monolithic cascade cell structure p 160 A84-22987
- Surface effects in high voltage silicon solar cells p 160 A84-23002
- New developments in power semiconductors p 105 N84-10065
- Silicon carbide, a high temperature semiconductor  
[NASA-TM-83514] p 191 N84-14932
- SEMICONDUCTORS (MATERIALS)**
- Silicon carbide, a high temperature semiconductor p 190 A84-17823
- Advances in solid state switchgear technology for large space power systems  
[NASA-TM-83652] p 109 N84-22891
- The friction behavior of semiconductors Si and GaAs in contact with pure metals  
[NASA-TM-83779] p 87 N84-32531
- Friction behavior of silicon in contact with titanium, nickel, silver and copper  
[NASA-TP-2362] p 88 N84-33590
- SENSORS**
- Fiberoptics for propulsion control system  
[NASA-TM-83542] p 1 N84-14111
- Sensor failure detection for jet engines using analytical redundancy  
[NASA-TM-83695] p 31 N84-24585
- SEPARATED FLOW**
- Boundary layer transition effects on flow separation around V/STOL engine inlets at high incidence  
[AIAA PAPER 84-0432] p 4 A84-18090
- Feedback in separated flows over symmetric airfoils  
[NASA-TM-83758] p 10 N84-31091
- SEPARATORS**
- Separator development and testing of nickel-hydrogen cells  
[NASA-TM-83653] p 62 N84-22712
- Full scale phosphoric acid fuel cell stack technology development  
[NASA-CR-174660] p 169 N84-26165
- Oxygen recombination in individual pressure vessel nickel-hydrogen batteries  
[NASA-CASE-LEW-13822-1] p 110 N84-29084
- Anion permselective membrane  
[NASA-CR-174725] p 172 N84-29358
- SEQUENTIAL COMPUTERS**
- Optical flip-flops and sequential logic circuits using a liquid crystal light valve p 188 A84-40332
- SERVICE LIFE**
- Long life nickel electrodes for a nickel-hydrogen cell. I Initial performance p 162 A84-30186
- Tip cap for a rotor blade  
[NASA-CASE-LEW-13654-1] p 28 N84-22560
- Materials for Advanced Turbine Engines (MATE) Project 3 Design, fabrication and evaluation of an oxide dispersion strengthened sheet alloy combustor liner, volume 1  
[NASA-CR-174691] p 76 N84-32504
- SERVOMECHANISMS**
- An analysis of traction drive torsional stiffness  
[NASA-TM-83712] p 145 N84-27043
- SHADOWGRAPH PHOTOGRAPHY**
- Experimental investigation of shock-cell noise reduction for single-stream nozzles in simulated flight, comprehensive data report Volume 3. Shadowgraph photos and facility description  
[NASA-CR-168234-VOL-3] p 186 N84-33150
- SHAFTS (MACHINE ELEMENTS)**
- Failure analysis of a tool steel torque shaft p 148 A84-17546
- Cryogenic Fluid Management Experiment (CFME) trunnion verification testing  
[NASA-CR-168310] p 92 N84-16381
- Factors that affect the fatigue strength of power transmission shafting  
[NASA-TM-83608] p 145 N84-26029
- Design of power-transmitting shafts  
[NASA-RP-1123] p 145 N84-27041
- SHAKERS**
- Lewis Research Center spin rig and its use in vibration analysis of rotating systems  
[NASA-TP-2304] p 30 N84-24578
- SHALE OIL**
- Utilization of alternative fuels in diesel engines  
[NASA-CR-174669] p 91 N84-26813
- SHEAR FLOW**
- The production of turbulent stress in a shear flow by rotational fluctuations p 115 A84-18357
- The production of turbulent stress in a shear flow by rotational fluctuations p 115 A84-21390
- Aeroacoustics of turbulent shear flows p 181 A84-22584
- Turbulence modeling for three-dimensional shear flows over curved rotating bodies p 122 A84-48138
- Generation of sound in turbulent shear flows p 183 N84-15031



## SHEAR LAYERS

- Basic experimental study of the coupling between flow instabilities and incident sound  
[NASA-CR-8789] p 183 N84-21275
- Acoustic excitation A promising new means of controlling shear layers  
[NASA-TM-83772] p 10 N84-31096
- SHEAR STRAIN**  
A mixed shear flexible finite element for the analysis of laminated plates p 152 A84-45994
- SHEAR STRESS**  
The production of turbulent stress in a shear flow by irrotational fluctuations p 115 A84-18357  
Correlation of compressive and shear stress with spalling of plasma-sprayed ceramic materials p 79 A84-19784  
The production of turbulent stress in a shear flow by irrotational fluctuations p 115 A84-21390  
Elastic model of the traction behavior of two traction lubricants p 136 A84-28791  
Surface topography-connections between lubrication and failure initiation p 144 N84-24898  
Cyclic torsion testing  
[NASA-TM-83756] p 157 N84-31687
- SHELL THEORY**  
New variational formulations of hybrid stress elements p 158 N84-31690
- SHELLS (STRUCTURAL FORMS)**  
Nonlinear Structural Analysis  
[NASA-CP-2297] p 157 N84-31688  
New variational formulations of hybrid stress elements p 158 N84-31690  
Nonlinear finite element analysis of shells with large aspect ratio p 158 N84-31692
- SHIELDING**  
Fluid shielding of high-velocity jet noise  
[NASA-TP-2259] p 183 N84-15894
- SHOCK FRONTS**  
Self-similar blast waves incorporating deflagrations of variable speed p 116 A84-28379
- SHOCK RESISTANCE**  
Method of fabricating an abradable gas path seal  
[NASA-CASE-LEW-13269-2] p 143 N84-22957
- SHOCK SPECTRA**  
A blade loss response spectrum for flexible rotor systems  
[ASME PAPER 84-GT-29] p 139 A84-46893
- SHOCK TUBES**  
Flat plate heat transfer for laminar transition and turbulent boundary layers using a shock tube  
[AIAA PAPER 84-1726] p 120 A84-37467  
Shock tube study of the fuel structure effects on the chemical kinetic mechanisms responsible for soot formation  
[NASA-CR-174661] p 62 N84-21677  
Investigation of the effects of pressure gradient, temperature and wall temperature ratio on the stagnation point heat transfer for circular cylinders and gas turbine vanes  
[NASA-CR-174667] p 30 N84-23649
- SHOCK WAVE INTERACTION**  
Experimental studies on two dimensional shock boundary layer interactions  
[AIAA PAPER 84-0099] p 3 A84-17881
- SHOCK WAVES**  
Dynamic response of shock waves in transonic diffuser and supersonic inlet - An analysis with the Navier-Stokes equations and adaptive grid  
[AIAA PAPER 84-1609] p 5 A84-38004  
Experimental investigation of shock-cell noise reduction for dual-stream nozzles in simulated flight comprehensive data report. Volume 1 Test nozzles and acoustic data  
[NASA-CR-168336-VOL-1] p 184 N84-24323  
Experimental investigation of shock-cell noise reduction for dual-stream nozzles in simulated flight comprehensive data report. Volume 2 Laser velocimeter data, static pressures and shadowgraph photos  
[NASA-CR-168336-VOL-2] p 184 N84-24324
- SHORT TAKEOFF AIRCRAFT**  
Supersonic STOVL ejector aircraft from a propulsion point of view  
[AIAA PAPER 84-1401] p 19 A84-40246  
Supersonic STOVL aircraft with turbine bypass/turbo-compressor engines  
[AIAA PAPER 84-1403] p 19 A84-40247  
Supersonic STOVL ejector aircraft from a propulsion point of view  
[NASA-TM-83641] p 31 N84-24581  
Supersonic STOVL aircraft with turbine bypass/turbo-compressor engines  
[NASA-TM-83686] p 31 N84-24582
- SHRINKAGE**  
Shrinkage of amorphous silica fibers p 77 A84-13504

## SHROUDED PROPELLERS

- Energy efficient engine fan component detailed design report  
[NASA-CR-165466] p 33 N84-27737
- SHROUDED TURBINES**  
The interaction between mistuning and friction in the forced response of bladed disk assemblies  
[ASME PAPER 84-GT-139] p 152 A84-46957
- SHROUDS**  
Application of a quasi-3D inviscid flow and boundary layer analysis to the hub-shroud contouring of a radial turbine  
[AIAA PAPER 84-1297] p 6 A84-44177  
Method of fabricating an abradable gas path seal  
[NASA-CASE-LEW-13269-2] p 143 N84-22957  
Application of a quasi-3D inviscid flow and boundary layer analysis to the hub-shroud contouring of a radial turbine  
[NASA-TM-83669] p 10 N84-25647
- SIGNAL ANALYSIS**  
Input-output characterization of an ultrasonic testing system by digital signal analysis  
[NASA-CR-3756] p 149 N84-15565  
The role of the reflection coefficient in precision measurement of ultrasonic attenuation  
[NASA-TM-83788] p 149 N84-32849
- SIGNAL ENCODING**  
NTSC composite video at 1.6 bits/pel p 95 A84-49259
- SIGNAL PROCESSING**  
Advanced acousto-optic signal processors p 187 A84-28485  
Output statistics of laser anemometers in sparsely seeded flows p 117 A84-28738  
Optical Kalman filtering for missile guidance p 178 A84-38596  
Real time pressure signal system for a rotary engine  
[NASA-CASE-LEW-13622-1] p 28 N84-22559
- SIGNAL TO NOISE RATIOS**  
The effect of variable S/N on the subjective evaluation of protection ratios for direct-TV satellite services p 95 A84-48452
- SILANES**  
Homogeneous reactions of hydrocarbons, silane, and chlorosilanes in radiofrequency plasmas at low pressures  
[NASA-TP-2301] p 50 N84-20643
- SILICIDES**  
Processing of fused silicide coatings for carbon-based materials p 51 A84-19780
- SILICON**  
Recent advances in thin silicon solar cells p 160 A84-22991  
Development and fabrication of a high current, fast recovery power diode  
[NASA-CR-168196] p 106 N84-13443  
Thin N-I-P radiation resistant solar cells  
[NASA-CR-168284] p 166 N84-15682  
Double-injection, deep-impurity switch development  
[NASA-CR-168335] p 108 N84-18536  
Voltage controlling mechanisms in low resistivity silicon solar cells: A unified approach p 167 N84-20916  
The effect of diffusion induced lattice stress on the open-circuit voltage in silicon solar cells  
[NASA-TM-83667] p 168 N84-23027  
The friction behavior of semiconductors Si and GaAs in contact with pure metals  
[NASA-TM-83779] p 87 N84-32531
- SILICON CARBIDES**  
Silicon carbide, a high temperature semiconductor p 190 A84-17823  
Bubble formation in oxide scales on SiC p 79 A84-23689  
Sinterability, strength and oxidation of alpha silicon carbide powders p 80 A84-32306  
Processing of sintered alpha SiC  
[ASME PAPER 84-GT-127] p 140 A84-46954  
Progress in net shape fabrication of alpha SiC turbine components  
[ASME PAPER 84-GT-273] p 140 A84-47036  
Thermal oxidation of 3C silicon carbide single-crystal layers on silicon p 191 A84-49620  
Silicon carbide, a high temperature semiconductor  
[NASA-TM-83514] p 191 N84-14932  
Analysis of stress-strain, fracture and ductility behavior of aluminum matrix composites containing discontinuous silicon carbide reinforcement  
[NASA-TM-83610] p 54 N84-21666  
The impact resistance of SiC and other mechanical properties of SiC and Si<sub>3</sub>N<sub>4</sub>  
[NASA-CR-165325] p 84 N84-24809  
Microstructure and orientation effects on properties of discontinuous silicon carbide/aluminum composites  
[NASA-TP-2302] p 51 N84-26749

## SILICON CONTROLLED RECTIFIERS

- Road load simulator tests of the Gould phase 1 functional model silicon controlled rectifier ac motor controller for electric vehicles  
[NASA-TM-83497] p 166 N84-20016
- SILICON DIOXIDE**  
Shrinkage of amorphous silica fibers p 77 A84-13504  
Sputtered coatings for protection of spacecraft polymers  
[NASA-TM-83706] p 85 N84-26803
- SILICON JUNCTIONS**  
Ion implanted junctions for silicon space solar cells p 42 A84-30143  
Increased radiation resistance in lithium-counterdoped silicon solar cells p 163 A84-34846
- SILICON NITRIDES**  
Analysis of grain boundary phase devitification of Y<sub>2</sub>O<sub>3</sub>- and Al<sub>2</sub>O<sub>3</sub>-doped Si<sub>3</sub>N<sub>4</sub> p 79 A84-19792  
Grain-boundary phases in hot-pressed silicon nitride containing Y<sub>2</sub>O<sub>3</sub> and CeO<sub>2</sub> additives p 79 A84-19793  
Compositional effects on Si<sub>3</sub>N<sub>4</sub> fracture surfaces p 79 A84-19794  
Characteristics of Si<sub>3</sub>N<sub>4</sub>-SiO<sub>2</sub>-CeO<sub>2</sub> compositions sintered in high-pressure nitrogen p 79 A84-19913  
Microstructure, strength, and oxidation of a 10 wt pct zirconia-Si<sub>3</sub>N<sub>4</sub> ceramic p 80 A84-25402  
RF sputtered silicon and hafnium nitrides as applied to 440C steel  
[NASA-TM-86862] p 87 N84-32536
- SILVER ZINC BATTERIES**  
Additive for zinc electrodes — electric automobiles  
[NASA-CASE-LEW-13286-1] p 106 N84-14422
- SIMULATION**  
A piecewise linear state variable technique for real time propulsion system simulation p 20 A84-42378  
RTMPL: A structured programming and documentation utility for real-time multiprocessor simulations  
[NASA-TM-83606] p 177 N84-20259  
Identification of multivariable high-performance turbofan engine dynamics from closed loop data p 28 N84-20580  
Simulation of lubricating behavior of a thioether liquid lubricant by an electrochemical method  
[NASA-TP-2316] p 84 N84-23764
- SIMULATORS**  
Software simulator for multiple computer simulation system p 176 A84-11892  
Road load simulator tests of the Gould phase 1 functional model silicon controlled rectifier ac motor controller for electric vehicles  
[NASA-TM-83497] p 166 N84-20016
- SINGLE CRYSTALS**  
Bubble formation in oxide scales on SiC p 79 A84-23689  
Low-cost single-crystal turbine blades, volume 1  
[NASA-CR-168218] p 68 N84-15247  
Factors which influence directional coarsening of Gamma prime during creep in nickel-base superalloy single crystals p 69 N84-17353  
Influence of composition on the microstructure and mechanical properties of a nickel-base superalloy single crystal  
[NASA-TM-83563] p 70 N84-17354  
Evaluation of single crystal LaB<sub>6</sub> cathodes for use in a high frequency backward wave oscillator tube  
[NASA-CR-173343] p 108 N84-19709  
Energy efficient engine high-pressure turbine detailed design report  
[NASA-CR-165608] p 33 N84-28788  
Preliminary experiments on phase conjugation for flow visualization — barium titanate single crystals  
[NASA-TM-83766] p 189 N84-32169
- SINGULARITY (MATHEMATICS)**  
Elasticity solutions for a class of composite laminate problems with stress singularities p 53 A84-33389
- SINTERING**  
Characteristics of Si<sub>3</sub>N<sub>4</sub>-SiO<sub>2</sub>-CeO<sub>2</sub> compositions sintered in high-pressure nitrogen p 79 A84-19913  
Sinterability, strength and oxidation of alpha silicon carbide powders p 80 A84-32306  
Processing of sintered alpha SiC  
[ASME PAPER 84-GT-127] p 140 A84-46954  
Method of making a light weight battery plaque  
[NASA-CASE-LEW-13349-1] p 72 N84-22734  
Development of a lightweight nickel electrode  
[NASA-TM-86861] p 172 N84-30528
- SIZE DETERMINATION**  
A technique combining the visibility of a Doppler signal with the peak intensity of the pedestal to measure the size and velocity of droplets in a spray  
[AIAA PAPER 84-0203] p 129 A84-17946  
Calibration of the Malvern particle sizer p 131 A84-40736  
Fuel spray diagnostics p 125 N84-20527

- Development and implementation of advanced diagnostic techniques p 132 N84-20528
- SIZE DISTRIBUTION**
- Pore size engineering applied to the design of separators for nickel-hydrogen cells and batteries p 162 A84-30187
- SLIDING**
- Pivoting and slip in an angular contact bearing p 139 A84-40595
- Hydrodynamic lubrication of rigid nonconformal contacts in combined rolling and normal motion [NASA-TM-83578] p 142 N84-17592
- SLIDING CONTACT**
- Determination of near-surface plastic deformation in sliding contacts p 140 A84-48996
- Hydrodynamic lubrication of rigid nonconformal contacts in combined rolling and normal motion [NASA-TM-83578] p 142 N84-17592
- SLIDING FRICTION**
- Companson of seal materials for use in Stirling engines p 64 A84-22879
- Subsurface stress evaluations under rolling/sliding contacts [ASME PAPER 83-LUB-18] p 137 A84-29099
- Polyimides formulated from a partially fluorinated diamine for aerospace tribological applications p 80 A84-40594
- Friction and morphology of magnetic tapes in sliding contact with nickel-zinc ferrite [NASA-TP-2267] p 82 N84-16334
- Ceramic wear in indentation and sliding [NASA-TM-83585] p 82 N84-19566
- Mechanical contact induced transformation from the amorphous to the crystalline state in metallic glass [NASA-TM-83583] p 71 N84-20573
- Friction and wear of iron in sulfuric acid [NASA-TP-2289] p 71 N84-21716
- Friction and wear of nickel in sulfuric acid [NASA-TP-2290] p 72 N84-21721
- Interaction of sulfuric acid corrosion and mechanical wear of iron [NASA-TM-83717] p 73 N84-27857
- Friction behavior of silicon in contact with titanium, nickel, silver and copper [NASA-TP-2362] p 88 N84-33590
- SLIP CASTING**
- Progress in net shape fabrication of alpha sic turbine components [ASME PAPER 84-GT-273] p 140 A84-47036
- SLUDGE**
- Bacterial degradation of polychlorinated biphenyls in sludge from an industrial sewer lagoon [NASA-TM-83543] p 173 N84-11594
- SLURRIES**
- Processing of fused silicide coatings for carbon-based materials p 51 A84-19780
- Oxidation resistant slurry coating for carbon-based materials [NASA-CASE-LEW-13923-1] p 54 N84-16266
- SMALL PERTURBATION FLOW**
- Small-amplitude viscous motion on arbitrary potential flows p 116 A84-24892
- SODIUM CHLORIDES**
- Investigation into the role of sodium chloride deposited on oxide and metal substrates in the initiation of hot corrosion [NASA-CR-173377] p 71 N84-20676
- SODIUM COMPOUNDS**
- The chemical kinetics and thermodynamics of sodium species in oxygen-rich hydrogen flames p 59 A84-27724
- SODIUM SULFATES**
- Mechanism of corrosion of Ni-base superalloys by molten Na<sub>2</sub>MoO<sub>4</sub> at elevated temperatures [NASA-TM-83580] p 70 N84-20672
- Deposition of Na<sub>2</sub>SO<sub>4</sub> from salt-seeded combustion gases of a high velocity burner ng [NASA-TM-83751] p 129 N84-31558
- SODIUM SULFUR BATTERIES**
- Moderate temperature rechargeable NaNiS<sub>2</sub> cells p 108 N84-21376
- SOFTWARE TOOLS**
- Software simulator for multiple computer simulation system p 176 A84-11892
- Computer simulator for a mobile telephone system [NASA-CR-174533] p 95 N84-10401
- SOLAR ARRAYS**
- Study of solar array switching power management technology for space power system [NASA-CR-167890-EXEC-SUM] p 167 N84-23021
- A 37.5-kW point design companson of the nickel-cadmium battery, bipolar nickel-hydrogen battery, and regenerative hydrogen-oxygen fuel cell energy storage subsystems for low Earth orbit [NASA-TM-83651] p 167 N84-23022
- Discharges on a negatively biased solar array in a charged particle environment [NASA-TM-83644] p 47 N84-23690
- Solar-array-materials passive LDEF experiment (A0171) p 168 N84-24656
- Dilute plasma coupling currents to a high voltage solar array in weak magnetic fields [NASA-TM-83687] p 47 N84-24708
- Qualification testing of solar photovoltaic powered refrigerator freezers for medical use in remote geographic locations [NASA-CR-168181] p 169 N84-25162
- Solar photovoltaic powered refrigerators/freezers for medical use in remote geographic locations [NASA-CR-168268] p 169 N84-25163
- Charged particle effects on space systems [AD-P002103] p 187 N84-26189
- High voltage solar array models and Shuttle tile charging [AD-P002123] p 177 N84-26209
- Characteristics of arc currents on a negatively biased solar cell array in a plasma [NASA-TM-83728] p 48 N84-27824
- High speed, low cost, LEO-thermal-cycling facility [NASA-CR-173888] p 191 N84-33210
- SOLAR BLANKETS**
- Space Photovoltaic Research and Technology 1983 High Efficiency, Radiation Damage, and Blanket Technology [NASA-CR-2314] p 170 N84-29307
- SOLAR CELLS**
- Harnessing surface plasmons for solar energy conversion p 159 A84-16395
- Large area space solar cell assemblies p 42 A84-22980
- Recent advances in thin silicon solar cells p 160 A84-22981
- Effects of indirect bandgap top cells in a monolithic cascade cell structure p 160 A84-22987
- Effect of electron flux on radiation damage in GaAs solar cells p 160 A84-22998
- Surface effects in high voltage silicon solar cells p 160 A84-23002
- New implantation techniques for improved solar cell junctions p 161 A84-23059
- Photovoltaic characteristics of diffused P+/N bulk GaAs solar cells p 161 A84-23115
- Diffused junction p(+)-n solar cells in bulk GaAs. I Fabrication and cell performance p 161 A84-26027
- Diffused junction p(+)-n solar cells in bulk GaAs II - Device characterization and modelling p 161 A84-26028
- Ion implanted junctions for silicon space solar cells p 42 A84-30143
- Multibandgap photovoltaic receiver using back surface reflectors p 161 A84-30162
- Increased radiation resistance in lithium-counterdoped silicon solar cells p 163 A84-34846
- Thin N+-P radiation resistant solar cells [NASA-CR-168284] p 166 N84-15682
- Voltage controlling mechanisms in low resistivity silicon solar cells A unified approach [NASA-TM-83612] p 167 N84-20916
- Radiation damage and defect behavior in ion-implanted, lithium counterdoped silicon solar cells [NASA-TM-83646] p 109 N84-22890
- The effect of diffusion induced lattice stress on the open-circuit voltage in silicon solar cells [NASA-TM-83667] p 168 N84-23027
- Discharges on a negatively biased solar array in a charged particle environment [NASA-TM-83644] p 47 N84-23690
- Solar-array-materials passive LDEF experiment (A0171) p 168 N84-24656
- Advanced photovoltaic experiment (S0014) p 168 N84-24657
- Characteristics of arc currents on a negatively biased solar cell array in a plasma [NASA-TM-83728] p 48 N84-27824
- Optimal design of GaAs-based concentrator space solar cells for 100 AMO, 80 deg C operation p 173 N84-29312
- Radiation tolerance of low resistivity, high voltage silicon solar cells p 170 N84-29318
- Cell and defect behavior in lithium-counterdoped solar cells p 170 N84-29322
- Development of a 30 percent efficient 3-junction monolithic cascade solar cell p 171 N84-29328
- High speed, low cost, LEO-thermal-cycling facility p 171 N84-29340
- The potential impact of new power system technology on the design of a manned space station [NASA-TM-83770] p 49 N84-31272
- The effects of lithium counterdoping on radiation damage and annealing in n(+)-p silicon solar cells [NASA-TM-83755] p 110 N84-31513
- SOLAR ENERGY**
- The worldwide market for photovoltaics in the rural sector p 161 A84-23135
- High-temperature molten salt thermal energy storage systems for solar applications [NASA-CR-167916] p 165 N84-15679
- Study of solar array switching power management technology for space power system [NASA-CR-167890-EXEC-SUM] p 167 N84-23021
- Basic and applied research related to the technology of space energy conversion systems, 1982 - 1983 [NASA-CR-173554] p 169 N84-25168
- SOLAR ENERGY CONVERSION**
- Harnessing surface plasmons for solar energy conversion p 159 A84-16395
- Parallel-processing with surface plasmons, a new strategy for converting the broad solar spectrum p 160 A84-23006
- Qualification testing of solar photovoltaic powered refrigerator freezers for medical use in remote geographic locations [NASA-CR-168181] p 169 N84-25162
- Solar photovoltaic powered refrigerators/freezers for medical use in remote geographic locations [NASA-CR-168268] p 169 N84-25163
- Plasmon device design Conversion from surface to junction plasmons with grating-couplers p 171 N84-29330
- SOLAR REFLECTORS**
- Ion implanted junctions for silicon space solar cells p 42 A84-30143
- Multibandgap photovoltaic receiver using back surface reflectors p 161 A84-30162
- SOLAR SIMULATORS**
- High speed, low cost, LEO-thermal-cycling facility p 171 N84-29340
- SOLAR SPECTRA**
- Advanced photovoltaic experiment (S0014) p 168 N84-24657
- SOLAR THERMAL ELECTRIC POWER PLANTS**
- Space power technology into the 21st Century [NASA-TM-83690] p 48 N84-26746
- SOLAR TOTAL ENERGY SYSTEMS**
- Investigation of energy management strategies for photovoltaic systems - A predictive control algorithm p 161 A84-25468
- SOLENOIDS**
- Application of induction coil measurements to the study of superalloy hot corrosion and oxidation [NASA-TM-83560] p 69 N84-16311
- SOLID ELECTRODES**
- Long life nickel electrodes for a nickel-hydrogen cell I Initial performance p 162 A84-30186
- Additive for zinc electrodes --- electric automobiles [NASA-CASE-LEW-13286-1] p 106 N84-14422
- SOLID ELECTROLYTES**
- Moderate temperature rechargeable NaNiS<sub>2</sub> cells p 108 N84-21376
- SOLID LUBRICANTS**
- Surface roughness effects with solid lubricants dispersed in mineral oils [ASLE PREPRINT 83-LC-4C-1] p 137 A84-28937
- Durable solid lubricant coatings for foil gas bearings to 315 deg C [NASA-TM-83596] p 83 N84-19567
- Low wear partially fluorinated polyimides [NASA-TM-83629] p 84 N84-24808
- Tribology in the 80's Volume 2 Sessions 5 - 8 [NASA-CP-2300-VOL-2] p 144 N84-25047
- Status and new directions for solid lubricant coatings and composite materials p 85 N84-25055
- Status of plasma physics techniques for the deposition of tribological coatings p 190 N84-25058
- Solid lubrication design methodology [NASA-CR-174690] p 196 N84-33309
- SOLID PHASES**
- Grain-boundary phases in hot-pressed silicon nitride containing Y<sub>2</sub>O<sub>3</sub> and CeO<sub>2</sub> additives p 79 A84-19793
- SOLID STATE**
- The 20 GHz spacecraft FET solid state transmitter [NASA-CR-168240] p 107 N84-17477
- SOLID STATE DEVICES**
- Advances in solid state switchgear technology for large space power systems [NASA-TM-83652] p 109 N84-22891
- SOLID SURFACES**
- The role of material properties in adhesion [NASA-TM-83792] p 88 N84-34619

## SOLID-SOLID INTERFACES

- A numerical analysis of contact and limit-point behavior in a class of problems of finite elastic deformation p 150 A84-27370
- Tribological applications of surface analysis [NASA-TM-83707] p 51 N84-25766
- SOLIDIFICATION**
- Rapid solidification via melt spinning - Equipment and techniques p 65 A84-31915
- Some fundamental aspects of solidification in a supercooled melt [NASA-TM-83714] p 73 N84-26787
- Fundamentals of Alloy Solidification Applied to Industrial Processes [NASA-CP-2337] p 77 N84-34589
- SOLIDS**
- Apparatus analysis and preliminary design of low gravity porous solids experiment for STS Orbiter mid-deck [NASA-CR-168248] p 37 N84-10109
- Preliminary investigation of an electrical network model for ultrasonic scattering [NASA-CR-3770] p 149 N84-17606
- Ultrasonic velocity measurement using phase-slope cross-correlation methods [NASA-TM-83794] p 149 N84-34769
- SOOT**
- Effects of broadened property fuels on radiant heat flux to gas turbine combustor liners [NASA-TM-83537] p 123 N84-16494
- Shock tube study of the fuel structure effects on the chemical kinetic mechanisms responsible for soot formation [NASA-CR-174661] p 62 N84-21677
- SOUND FIELDS**
- A parametric study of the effect of inlet lip shape upon the radiated sound field [AIAA PAPER 84-0498] p 180 A84-18131
- Recovery of burner acoustic source structure from far-field sound spectra [AIAA PAPER 83-0763] p 181 A84-32609
- SOUND GENERATORS**
- Sound generated by instability waves of supersonic flows. I - Two-dimensional mixing layers. II - Axisymmetric jets p 181 A84-24597
- Generation of sound in turbulent shear flows p 183 N84-15031
- A theoretical prediction of the acoustic pressure generated by turbulence-flame front interactions [NASA-TM-83587] p 184 N84-26383
- SOUND PRESSURE**
- Recovery of burner acoustic source structure from far-field sound spectra [AIAA PAPER 83-0763] p 181 A84-32609
- Application of signal analysis to cavitation p 122 A84-49192
- SOUND PROPAGATION**
- Studies of acoustical properties of bulk porous flexible materials [NASA-CR-173622] p 185 N84-27544
- Analysis of the effect on combustor noise measurements of acoustic waves reflected by the turbine and combustor inlet [NASA-TM-83760] p 185 N84-32122
- SOUND WAVES**
- Basic experimental study of the coupling between flow instabilities and incident sound [NASA-CR-3789] p 183 N84-21275
- Analysis of the effect on combustor noise measurements of acoustic waves reflected by the turbine and combustor inlet [NASA-TM-83760] p 185 N84-32122
- SPACE COMMUNICATION**
- Beam impingement angle effects on secondary electron emission characteristics of textured pyrolytic graphite [NASA-TP-2285] p 82 N84-18400
- MMIC technology for advanced space communications systems [NASA-TM-83749] p 100 N84-30147
- The 20 and 30 GHz MMIC technology for future space communication antenna system [NASA-TM-83745] p 100 N84-31460
- SPACE FLIGHT**
- Research and technology, 1983 [NASA-TM-83540] p 193 N84-14061
- SPACE PLASMAS**
- Radiating dipole model of interference induced in spacecraft circuitry by surface discharges [NASA-TP-2240] p 40 N84-16247
- Dilute plasma coupling currents to a high voltage solar array in weak magnetic fields [NASA-TM-83687] p 47 N84-24708
- High voltage solar array models and Shuttle tile charging [AD-P002123] p 177 N84-26209

## SPACE PLATFORMS

- NASA's geostationary communications platform program [AIAA PAPER 84-0702] p 95 A84-25326
- SPACE POWER REACTORS**
- Advanced nickel-hydrogen cell configuration study [NASA-CR-173417] p 108 N84-22889
- Design of a 1-kWh bipolar nickel hydrogen battery [NASA-TM-83647] p 168 N84-23024
- Charged particle effects on space systems [AD-P002103] p 187 N84-26189
- Space power technology into the 21st Century [NASA-TM-83690] p 48 N84-26746
- SPACE PROCESSING**
- Gravitational effects in dendritic growth p 37 A84-22346
- SPACE PROGRAMS**
- Chicago Meets Outer Space program [NASA-TM-85492] p 192 N84-16021
- SPACE SHUTTLE BOOSTERS**
- Graphics enhanced computer emulation for improved timing-race and fault tolerance control system analysis --- of Centaur liquid-fuel booster [AIAA PAPER 83-2328] p 177 A84-10010
- SPACE SHUTTLE MAIN ENGINE**
- Design study of magnetic eddy-current vibration suppression dampers for application to cryogenic turbomachinery [NASA-CR-173273] p 141 N84-16562
- SPACE SHUTTLE ORBITERS**
- Shuttle/Centaur - More capability for the 1980's [IAF PAPER 83-18] p 38 A84-11718
- Apparatus analysis and preliminary design of low gravity porous solids experiment for STS Orbiter mid-deck [NASA-CR-168248] p 37 N84-10109
- SPACE SHUTTLE PAYLOADS**
- Cryogenic Fluid Management Facility [AIAA PAPER 84-1340] p 44 A84-44184
- Preliminary design of two Space Shuttle fluid physics experiments [NASA-CR-174649] p 39 N84-23667
- Effects of chemical releases by the STS-3 Orbiter on the ionosphere [NASA-CR-171032] p 173 N84-25204
- Fundamentals of Alloy Solidification Applied to Industrial Processes [NASA-CP-2337] p 77 N84-34589
- SPACE SHUTTLES**
- Study of auxiliary propulsion requirements for large space systems Volume 1: Executive summary [NASA-CR-168193-VOL-1] p 45 N84-12226
- Laboratory degradation of Kapton in a low energy oxygen ion beam [NASA-TM-83530] p 41 N84-18310
- A high energy stage for the National Space Transportation System [NASA-TM-83795] p 38 N84-32411
- Regenerative hydrogen-oxygen fuel cell-electrolyzer systems for orbital energy storage p 111 N84-33670
- SPACE STATIONS**
- Space Station propulsion analysis study [AIAA PAPER 84-1326] p 44 A84-44179
- Space station propulsion analysis study [NASA-TM-83715] p 47 N84-25764
- Factors that influence space station propulsion requirements p 48 N84-29931
- Radiative resistor performance characterization tests [NASA-CR-174763] p 50 N84-33462
- SPACE TRANSPORTATION SYSTEM**
- Evaluation of propellant tank insulation concepts for low-thrust chemical propulsion systems: Executive summary [NASA-CR-168321] p 83 N84-20699
- A high energy stage for the National Space Transportation System [NASA-TM-83795] p 38 N84-32411
- SPACEBORNE EXPERIMENTS**
- Preliminary design of two Space Shuttle fluid physics experiments [NASA-CR-174649] p 39 N84-23667
- Ion-beam-textured and coated surfaces experiment (S1003) p 84 N84-24650
- Solar-array-materials passive LDEF experiment (AO171) p 168 N84-24656
- Advanced photovoltaic experiment (S0014) p 168 N84-24657
- SPACECRAFT ANTENNAS**
- Structural design of a vertical antenna boresight 18.3 by 18.3-m planar near-field antenna measurement system [NASA-TM-83781] p 133 N84-32783
- SPACECRAFT CHARGING**
- Radiating dipole model of interference induced in spacecraft circuitry by surface discharges [NASA-TP-2240] p 40 N84-16247

- Anomalous high potentials observed on ISEE p 41 N84-17258
- NASCAP simulations of spacecraft charging of the SCATHA satellite --- NASA (spacecraft) charging analyzer program (NASCAP) p 41 N84-17268
- The role of potential barrier formation in spacecraft charging p 41 N84-17269
- Charged particle effects on space systems [AD-P002103] p 187 N84-26189
- High voltage solar array models and Shuttle tile charging [AD-P002123] p 177 N84-26209
- Design guidelines for assessing and controlling spacecraft charging effects [NASA-TP-2361] p 42 N84-33452
- SPACECRAFT COMMUNICATION**
- Concept for advanced satellite communications and required technologies p 93 A84-15626
- NASA's multibeam communications technology program p 39 A84-21397
- Geometric models, antenna gains, and protection ratios as developed for BC SAT-R2 conference software [NASA-TM-83361] p 96 N84-11358
- The 30 GHz communications satellite low noise receiver [NASA-CR-168254] p 97 N84-13398
- Phased-array-fed antenna configuration study, volume 2 [NASA-CR-168232] p 98 N84-16424
- Modular approach for satellite communication ground terminals [NASA-CR-168327] p 98 N84-16425
- The 20 GHz spacecraft FET solid state transmitter [NASA-CR-168240] p 107 N84-17477
- High efficiency IMPATT diodes for 60 GHz intersatellite link applications [NASA-TM-83584] p 108 N84-19708
- Users' manual for computer program for three-dimensional analysis of coupler-cavity traveling wave tubes [NASA-CR-168269] p 109 N84-23841
- Adaptive arrays for satellite communications [NASA-CR-173548] p 99 N84-24924
- Test results for 27 5- to 30-GHz communications satellite receivers [NASA-TM-83662] p 100 N84-27954
- Reflector antennas with low sidelobes, low cross polarization, and high aperture efficiency [NASA-CR-174670] p 100 N84-31464
- Characteristics and capacities of the NASA Lewis Research Center high precision 6.7- by 6.7-m planar near-field scanner [NASA-TM-83765] p 133 N84-32789
- SPACECRAFT COMPONENTS**
- High voltage-high power components for large space power distribution systems [NASA-TM-83648] p 42 N84-22615
- SPACECRAFT CONFIGURATIONS**
- Factors that influence space station propulsion requirements p 48 N84-29931
- SPACECRAFT CONSTRUCTION MATERIALS**
- Sputtered coatings for protection of spacecraft polymers [NASA-TM-83706] p 85 N84-26803
- The energy dependence and surface morphology of Kapton (trademark) degradation under atomic oxygen bombardment p 187 N84-34484
- SPACECRAFT DESIGN**
- Plasma sheath structure surrounding a large powered spacecraft [AIAA PAPER 84-0329] p 40 A84-18025
- Integration becomes the name of the OTV game p 44 A84-44045
- Research and technology, 1983 [NASA-TM-83540] p 193 N84-14061
- Factors that influence space station propulsion requirements p 48 N84-29931
- Propulsion issues for advanced orbit transfer vehicles p 48 N84-29937
- The potential impact of new power system technology on the design of a manned space station [NASA-TM-83770] p 49 N84-31272
- Design guidelines for assessing and controlling spacecraft charging effects [NASA-TP-2361] p 42 N84-33452
- SPACECRAFT ELECTRONIC EQUIPMENT**
- 30/20 GHz spacecraft GaAs FET solid state transmitter for trunking and customer-premise-service application [NASA-CR-168276] p 107 N84-16463
- MMIC technology for advanced space communications systems [NASA-TM-83749] p 100 N84-30147
- SPACECRAFT ENVIRONMENTS**
- Plasma sheath structure surrounding a large powered spacecraft [AIAA PAPER 84-0329] p 40 A84-18025

## SPACECRAFT GUIDANCE

- Centaur D-1A guidance/software system  
[AAS PAPER 84-043] p 39 A84-49176
- Centaur D-1A guidance/software system  
[NASA-TM-83552] p 38 N84-16234

## SPACECRAFT LAUNCHING

- Study of auxiliary propulsion requirements for large space systems. Volume 1. Executive summary  
[NASA-CR-168193-VOL-1] p 45 N84-12226

## SPACECRAFT POWER SUPPLIES

- High effectiveness liquid droplet/gas heat exchanger for space power applications  
[IAF PAPER 83-433] p 42 A84-11819
- Harnessing surface plasmons for solar energy conversion  
p 159 A84-16395
- Plasma sheath structure surrounding a large powered spacecraft  
[AIAA PAPER 84-0329] p 40 A84-18025

- Large area space solar cell assemblies  
p 42 A84-22080
- Effects of indirect bandgap top cells in a monolithic cascade cell structure  
p 160 A84-22987
- Characteristics of a microwave plasma disk ion source  
p 189 A84-23390

- Ion implanted junctions for silicon space solar cells  
p 42 A84-30143
- Alkaline fuel cells for the regenerative fuel cell energy storage system  
p 182 A84-30183
- Development of a large scale bipolar NiH<sub>2</sub> battery  
p 162 A84-30189

- Space power technology into the 21st century  
[AIAA PAPER 84-1136] p 43 A84-34013
- High-current, high-frequency capacitors  
p 105 N84-10067

- Pyroelectric conversion in space: A conceptual design study  
[NASA-CR-168272] p 165 N84-14585
- Overview of NASA Lewis Research Center free-piston Stirling engine activities  
[NASA-TM-83649] p 195 N84-22512

- Advances in solid state switchgear technology for large space power systems  
[NASA-TM-83652] p 109 N84-22681
- Study of solar array switching power management technology for space power system  
[NASA-CR-167890-EXEC-SUM] p 167 N84-23021

- Basic and applied research related to the technology of space energy conversion systems, 1982 - 1983  
[NASA-CR-173554] p 169 N84-25168
- Space Photovoltaic Research and Technology 1983  
High Efficiency, Radiation Damage, and Blanket Technology  
[NASA-CP-2314] p 170 N84-29307

- Regenerative hydrogen-oxygen fuel cell-electrolyzer systems for orbital energy storage  
p 111 N84-33670
- Test results of a ten cell bipolar nickel-hydrogen battery  
p 112 N84-33702

## SPACECRAFT PROPULSION

- Demonstration of a new electrothermal thruster concept  
p 43 A84-34037
- Proposed system design for a 20 kW pulsed electrothermal thruster  
[AIAA PAPER 84-1387] p 43 A84-35202
- Resistojet propulsion for large spacecraft systems  
[NASA-TM-83489] p 45 N84-11206

- Study of auxiliary propulsion requirements for large space systems. Volume 1. Executive summary  
[NASA-CR-168193-VOL-1] p 45 N84-12226
- Ground correlation investigation of thruster spacecraft interactions to be measured on the IAPS flight test  
[NASA-TM-83598] p 47 N84-23691

- Propulsion issues for advanced orbit transfer vehicles  
[NASA-TM-83624] p 47 N84-25762
- Factors that influence space station propulsion requirements  
p 48 N84-29931
- Propulsion issues for advanced orbit transfer vehicles  
p 48 N84-29937

- Radiative resistojet performance characterization tests  
[NASA-CR-174763] p 50 N84-33482

## SPACECRAFT STRUCTURES

- Microwave monolithic integrated circuit development for future spaceborne phased array antennas  
[AIAA PAPER 84-0656] p 94 A84-25257
- Microwave monolithic integrated circuit development for future spaceborne phased array antennas  
[NASA-TM-83518] p 97 N84-13399

- Program for development of strain tolerant thermal barrier coating system  
[NASA-CR-173214] p 82 N84-16337

## SPALLING

- The effect of annealing on the creep of plasma-sprayed ceramics  
p 79 A84-19785
- Thermal stress fracture of ceramic coatings  
p 80 A84-24553

- Diamondlike flakes  
[NASA-CASE-LEW-13837-2] p 54 N84-22696

- SPANWISE BLOWING  
Experimental investigation of tangential blowing applied to a subsonic V/STOL inlet  
[NASA-TP-2297] p 9 N84-20493

## SPATIAL FILTERING

- Advanced acousto-optic signal processors  
p 187 A84-28485

## SPATIAL MARCHING

- Computation of three-dimensional viscous flows using a space-marching method  
[AIAA PAPER 84-1298] p 5 A84-36971

## SPATIAL RESOLUTION

- Tabulations of ambient ozone data obtained by GASP (Global Air Sampling Program) airliners, March 1975 to July 1979  
[NASA-TM-82742] p 174 N84-18806

## SPECIFIC IMPULSE

- Experimental investigation of the pulsed electrothermal (PET) thruster  
[AIAA PAPER 84-1386] p 43 A84-35201
- Experimental investigation of a Hall-current thruster  
[NASA-CR-168133] p 46 N84-18321

## SPECIFICATIONS

- NASA broad-specification fuels combustion technology program  
p 62 N84-23637
- Computer analysis of effects of altimeter fuel properties on refinery costs and yields  
[NASA-CR-174642] p 91 N84-27908

## SPECIMEN GEOMETRY

- Mode 2 fatigue crack growth specimen development  
[NASA-TM-83722] p 156 N84-29248

## SPECKLE PATTERNS

- The use of heterodyne speckle photogrammetry to measure high-temperature strain distributions  
p 130 A84-28623

## SPECTRA

- A theoretical model for the cross spectra between pressure and temperature downstream of a combustor  
[NASA-TM-83871] p 186 N84-34231

## SPECTRAL SENSITIVITY

- Diffused junction p(+)-n solar cells in bulk GaAs. II - Device characterization and modelling  
p 161 A84-26028

## SPECTRUM ANALYSIS

- Ferrographic and spectrometer oil analysis from a failed gas turbine engine  
p 135 A84-11273
- Formulation of blade-flutter spectral analyses in stationary reference frame  
[NASA-TP-2296] p 27 N84-20562

## SPHERICAL SHELLS

- A numerical analysis of contact and limit-point behavior in a class of problems of finite elastic deformation  
p 150 A84-27370
- Circuit equivalent to the elastic spherical shell  
p 104 A84-39197

## SPIN

- Spin analysis of concentrated traction contacts  
[NASA-TM-83713] p 145 N84-27042

## SPIN TESTS

- Lewis Research Center spin rig and its use in vibration analysis of rotating systems  
[NASA-TP-2304] p 30 N84-24578

## SPLINE FUNCTIONS

- Application of a polynomial spline in higher-order accurate viscous-flow computations  
p 119 A84-35349

## SPOOLS

- Energy efficient engine fan component detailed design report  
[NASA-CR-165466] p 33 N84-27737

## SPRAY CHARACTERISTICS

- A technique combining the visibility of a Doppler signal with the peak intensity of the pedestal to measure the size and velocity of droplets in a spray  
[AIAA PAPER 84-0203] p 129 A84-17946

- Analytic modeling of a spray diffusion flame  
[AIAA PAPER 84-1317] p 118 A84-35168

- A theoretical and experimental study of turbulent particle-laden jets  
[NASA-CR-168293] p 23 N84-13187

- A theoretical and experimental study of turbulent nonevaporating sprays  
[NASA-CR-174658] p 35 N84-29877

## SPRAY NOZZLES

- A theoretical and experimental study of turbulent particle-laden jets  
[NASA-CR-168293] p 23 N84-13187

## SPRAYED COATINGS

- Phase distributions in plasma-sprayed zirconia-yttria  
p 78 A84-18948

- Phase analysis of plasma-sprayed zirconia-yttria coatings  
p 78 A84-19781

- Anisotropic thermal expansion effects in plasma-sprayed ZrO<sub>2</sub>-9 percent Y<sub>2</sub>O<sub>3</sub> coatings  
p 78 A84-19782

- Mechanical and physical properties of plasma-sprayed stabilized zirconia  
p 79 A84-19786

- Oxidation behavior of a thermal barrier coating  
p 85 A84-42667

- Acoustic emission evaluation of plasma-sprayed thermal barrier coatings  
[ASME PAPER 84-GT-292] p 140 A84-47046

- Development of strain tolerant thermal barrier coating systems, tasks 1 - 3  
[NASA-CR-168251] p 81 N84-12312

- Oxidation resistant slurry coating for carbon-based materials  
[NASA-CASE-LEW-13923-1] p 54 N84-16266

- Improved thermal barrier coating system  
[NASA-CASE-LEW-14057-1] p 88 N84-33595

## SPRAYERS

- Structure of nonevaporating sprays - Measurements and predictions  
[AIAA PAPER 84-0125] p 114 A84-17897

- The structure of evaporating and combusting sprays  
Measurements and predictions  
[NASA-CR-173778] p 128 N84-29155

- A theoretical and experimental study of turbulent evaporating sprays  
[NASA-CR-174760] p 35 N84-32390

## SPRAYING

- The structure of evaporating and combusting sprays  
Measurements and predictions  
[NASA-CR-173778] p 128 N84-29155

## SPUTTERING

- Characteristic morphological and frictional changes in sputtered MoS<sub>2</sub>/sub 2 films  
[NASA-TM-83565] p 92 N84-16380

- Sputtering phenomena in ion thrusters  
[NASA-CR-168172] p 46 N84-18322

- Frictional and morphological properties of Au-MoS<sub>2</sub> films sputtered from a compact target  
[NASA-TM-83304] p 143 N84-20858

- Diamondlike flake composites  
[NASA-CASE-LEW-13837-1] p 54 N84-22695

- Method of making an ion beam sputter-etched ventricular catheter for hydrocephalus shunt  
[NASA-CASE-LEW-13107-2] p 174 N84-23095

- Status of plasma physics techniques for the deposition of tribological coatings  
p 190 N84-25058

- Sputtered coatings for protection of spacecraft polymers  
[NASA-TM-83706] p 85 N84-26803

- Ion sputter textured graphite electrode plates  
[NASA-CASE-LEW-12919-2] p 179 N84-28565

- Dual ion beam deposition of carbon films with diamondlike properties  
[NASA-TM-83743] p 110 N84-31512

- RF sputtered silicon and hafnium nitrides as applied to 440C steel  
[NASA-TM-86852] p 87 N84-32536

## SQUEEZE FILMS

- Nonlinear transient finite element analysis of rotor-bearing-stator systems  
p 136 A84-20580

- Experimental study of uncentralized squeeze film dampers  
[NASA-CR-168317] p 155 N84-19927

- Dual clearance squeeze film damper  
[NASA-CASE-LEW-13506-1] p 29 N84-22562

- Dual clearance squeeze film damper for high load conditions  
[NASA-TM-83619] p 144 N84-25064

## STABILITY

- Stability and convergence of underintegrated finite element approximations  
p 158 N84-31696

## STABILITY DERIVATIVES

- Optimization and mechanisms of mistuning in cascades  
[ASME PAPER 84-GT-196] p 21 A84-46993

## STABLE OSCILLATIONS

- Orbital stability in combined uniform axial and three-dimensional wiggler magnetic fields for free-electron lasers  
[NASA-TM-83753] p 134 N84-30273

## STACKS

- Develop and test fuel cell powered on-site integrated total energy system  
[NASA-CR-168239] p 164 N84-13673

- Evaluation of gas-cooled pressurized phosphoric acid fuel cells for electric utility power generation  
[NASA-CR-168298] p 169 N84-25169

## STAGNATION POINT

- Engineering correlations of variable-property effects on laminar forced convection mass transfer for dilute vapor species and small particles in air  
[NASA-CR-168322] p 124 N84-18578

- Turbulence and surface heat transfer near the stagnation point of a circular cylinder in turbulent flow  
[NASA-TM-83732] p 128 N84-29157

## STAINLESS STEELS

- Tribological and microstructural characteristics of ion-nitrided steels p 64 A84-19225
- Topological reaction rate measurements related to scuffing [NASA-TM-83486] p 68 N84-14288
- Tensile and compressive constitutive response of 316 stainless steel at elevated temperatures [NASA-TM-83506] p 68 N84-15249
- RF sputtered silicon and hafnium nitrides as applied to 440C steel [NASA-TM-86862] p 87 N84-32536
- STANDARD DEVIATION**
- Tabulations of ambient ozone data obtained by GASP (Global-Air-Sampling-Program) airliners, March 1975 to July 1979 [NASA-TM-82742] p 174 N84-18806
- STANDARDS**
- Group-type hydrocarbon standards for high-performance liquid chromatographic analysis of middisillate fuels [NASA-TM-2317] p 90 N84-23774
- STANDING WAVES**
- Supersonic jet screech tone cancellation p 179 A84-10136
- Vibration and flutter of mistuned bladed-disk assemblies [NASA-TM-83634] p 156 N84-23923
- Flutter and forced response of mistuned rotors using standing wave analysis [NASA-CR-173555] p 32 N84-24586
- STARTING**
- Alcohol cold starting - A theoretical study p 138 A84-30061
- STATE VECTORS**
- State estimation Kalman filter using optical processings Noise statistics known p 178 A84-23602
- STATIC LOADS**
- Steady state stresses in ribbon parachute canopies [AIAA PAPER 84-0816] p 11 A84-26580
- STATIC PRESSURE**
- Hot-flow tests of a series of 10-percent-scale turbofan forced mixing nozzles [NASA-TM-2268] p 123 N84-17525
- Experimental investigation of shock-cell noise reduction for dual-stream nozzles in simulated flight comprehensive data report, Volume 2 Laser velocimeter data, static pressures and shadowgraph photos [NASA-CR-168336-VOL-2] p 184 N84-24324
- The boundary layer on compressor cascade blades [NASA-CR-173514] p 127 N84-25001
- STATISTICAL ANALYSIS**
- Durability/life of fiber composites in hydrothermomechanical environments p 52 A84-27359
- Output statistics of laser anemometers in sparsely seeded flows p 117 A84-28738
- Model development and statistical investigation of turbine blade mistuning p 17 A84-31905
- Review of the DOE/NASA wind turbine engineering information system p 163 A84-33766
- Determination of the key parameters affecting historic communications satellite trends [NASA-TM-83633] p 99 N84-25908
- STATISTICAL DISTRIBUTIONS**
- State estimation Kalman filter using optical processings Noise statistics known p 178 A84-23602
- Creep-rupture reliability analysis [NASA-CR-3790] p 155 N84-19925
- STATOR BLADES**
- Redesign and cascade tests of a supercritical controlled diffusion stator blade-section [AIAA PAPER 84-1207] p 5 A84-36960
- Redesign and cascade tests of a supercritical controlled diffusion stator blade-section [NASA-TM-83635] p 10 N84-22533
- STATORS**
- Nonlinear transient finite element analysis of rotor-bearing-stator systems p 136 A84-20580
- A mathematical model for the doubly-fed wound rotor generator, part 2 [NASA-TM-83581] p 107 N84-17479
- Secondary flow spanwise deviation model for the stators of NASA middle compressor stages [NASA-CR-173360] p 27 N84-18202
- Analytical and experimental investigation of stator endwall countouring in a small axial-flow turbine [NASA-TP-2309] p 35 N84-32388
- STEADY FLOW**
- Application of a finite element algorithm to the solution of steady transonic Euler equations p 3 A84-10133
- Small-amplitude viscous motion on arbitrary potential flows p 116 A84-24892
- Conservative streamtube solution of steady-state Euler equations [AIAA PAPER 84-1643] p 120 A84-38030

- Penalty function finite element analysis of steady viscous incompressible flow in rotating coordinates [ASME PAPER 84-GT-36] p 121 A84-46900
- STEADY STATE**
- Digital computer program for generating dynamic turbofan engine models (DIGTEM) [NASA-TM-83448] p 26 N84-16185
- Response of a small-turboshaft-engine compression system to inlet temperature distortion [NASA-TM-83765] p 36 N84-33414
- STEAM**
- Forced convection heat transfer to air/water vapor mixtures [NASA-CR-3769] p 123 N84-16488
- Steam bottoming cycle for an adiabatic diesel engine [NASA-CR-168255] p 195 N84-33304
- STEAM TURBINES**
- AFB/open cycle gas turbine conceptual design study [NASA-CR-168135] p 172 N84-31784
- STEELS**
- Failure analysis of a tool steel torque shaft p 148 A84-17546
- Mechanism of lubrication by tetracyclicphosphate (TCP) [NASA-TP-2274] p 142 N84-18653
- Ion-beam nitriding of steels [NASA-TM-83599] p 71 N84-21719
- Status of understanding for gear materials p 144 N84-25061
- Optical and other property changes of M-50 bearing steel surfaces for different lubricants and additive prior to scuffing [NASA-TM-83746] p 88 N84-34620
- STIFFNESS MATRIX**
- On the suppression of zero energy deformation modes p 150 A84-21541
- Automatic finite element generators p 158 N84-31695
- Stability and convergence of underintegrated finite element approximations p 158 N84-31696
- STIRLING CYCLE**
- Free-piston Stirling engine endurance test program p 136 A84-22864
- Comparison of seal materials for use in Stirling engines p 64 A84-22879
- Hostile environmental conditions facing candidate alloys for the automotive Stirling engine p 136 A84-23522
- DOE/NASA Automotive Stirling Engine Project Overview p 138 A84-30069
- Thermal and elastohydrodynamic analysis of reciprocating rod seals in the Stirling engine p 138 A84-30085
- Automotive Stirling Engine Development Program Mod I Stirling engine development p 138 A84-30091
- Automotive Stirling engine development program - Overview and status report p 138 A84-30092
- Test results and description of a 1 kW free-piston Stirling engine with a dashpot load p 138 A84-30095
- Creep-rupture behavior of six candidate Stirling engine superalloys tested in air p 65 A84-36173
- Comparison of steady-state and transient CVS cycle emission of an automotive Stirling engine p 173 A84-41044
- Downsizing assessment of automotive Stirling engines [NASA-TM-83468] p 194 N84-14989
- Evaluation of CO<sub>2</sub> and CO dopants in hydrogen to reduce hydrogen permeation in the Stirling engine heater head tube alloy CG-27 [NASA-TM-83535] p 68 N84-15246
- Automotive Stirling engine development program [NASA-CR-168205] p 194 N84-18117
- Overview of NASA Lewis Research Center free-piston Stirling engine activities [NASA-TM-83649] p 195 N84-22512
- Comparison of free-piston Stirling engine model predictions with RE1000 engine test data [NASA-TM-83650] p 195 N84-24509
- Creep-rupture behavior of candidate Stirling engine alloys after long-term aging at 760 deg C in low-pressure hydrogen [NASA-TM-83676] p 73 N84-25793
- Overview of advanced Stirling and gas turbine engine development programs and implications for solar thermal electrical applications p 146 N84-28231
- Creep-rupture behavior of candidate Stirling engine iron superalloys in high-pressure hydrogen Volume 2: Hydrogen creep-rupture behavior [NASA-CR-174705] p 74 N84-28961
- Oxidation and corrosion resistance of candidate Stirling engine heater-head-tube alloys [NASA-TM-83609] p 74 N84-28962
- Advanced high temperature materials for the energy efficient automotive Stirling engine [NASA-TM-83659] p 75 N84-28963
- Automotive Stirling engine development program [NASA-CR-174622] p 195 N84-32305

- Automotive Stirling Engine Development Program RESD summary report [NASA-CR-174674] p 196 N84-33307
- Evaluation of candidate Stirling engine heater tube alloys after 3500 hours exposure to high-pressure doped hydrogen or helium [NASA-TM-83782] p 77 N84-34603
- STOICHIOMETRY**
- Flame propagation in heterogeneous mixtures of fuel drops and air [NASA-CR-174644] p 91 N84-23775
- STORAGE BATTERIES**
- An SCR inverter with an integral battery charger for electric vehicles p 103 A84-24850
- Solar photovoltaic powered refrigerators/freezers for medical use in remote geographic locations [NASA-CR-168268] p 169 N84-25163
- Electrochemical storage p 171 N84-29342
- STORAGE RINGS (PARTICLE ACCELERATORS)**
- Improved ion containment using a ring-cusp ion thruster p 44 A84-49511
- STORAGE STABILITY**
- Photodeposition of nitride insulators on 3-5 substrates [NASA-CR-173393] p 71 N84-21720
- Research on aviation fuel instability p 90 N84-23642
- STORAGE TANKS**
- Cryogenic Fluid Management Experiment (CFME) trunnion verification testing [NASA-CR-168310] p 92 N84-16381
- STRAIN ENERGY METHODS**
- On the suppression of zero energy deformation modes p 150 A84-21541
- STRAIN GAGES**
- Benchmark cyclic plastic notch strain measurements p 63 A84-11194
- STRAIN HARDENING**
- Finite elastic-plastic deformation of polycrystalline metals p 66 A84-43872
- STRAIN RATE**
- Environmental and high strain rate effects on composites for engine applications p 51 A84-17444
- Indentation law for composite laminates p 52 A84-27356
- Elevated temperature compressive steady state deformation and failure in the oxide dispersion strengthened alloy MA 6000E p 66 A84-46785
- STRATEGIC MATERIALS**
- Replacing critical and strategic refractory metal elements in nickel-base superalloys — NASA's COSAM program [NASA-TM-83628] p 67 N84-13264
- STREAMLINED BODIES**
- Conservative streamtube solution of steady-state Euler equations [AIAA PAPER 84-1643] p 120 A84-38030
- STRESS ANALYSIS**
- Inelastic stress analyses at finite deformation through complementary energy approaches p 149 A84-13248
- Analyses of large quasistatic deformations of inelastic bodies by a new hybrid-stress finite element algorithm p 150 A84-16874
- Analyses of large quasistatic deformations of inelastic bodies by a new hybrid-stress finite element algorithm - Applications p 150 A84-16884
- Correlation of compressive and shear stress with spalling of plasma-sprayed ceramic materials p 79 A84-19784
- Edge delamination in angle-ply composite laminates p 52 A84-21515
- Steady state stresses in ribbon parachute canopies [AIAA PAPER 84-0816] p 11 A84-26580
- Subsurface stress evaluations under rolling/sliding contacts [ASME PAPER 83-LUB-18] p 137 A84-29099
- Advanced reliability method for fatigue analysis p 151 A84-31596
- High temperature thermomechanical analysis of ceramic coatings p 152 A84-48565
- Thermal stress analysis for a wood composite blade — wind turbines [NASA-CR-173394] p 156 N84-21903
- Dynamic stress analysis of smooth and notched fiber composite flexural specimens [NASA-TM-83694] p 56 N84-25770
- Interply layer degradation effects on composite structural response [NASA-TM-83702] p 56 N84-26756
- Thermal-stress analysis for wood composite blade — horizontal axis wind turbines [NASA-CR-173830] p 157 N84-31685
- Nonlinear Structural Analysis [NASA-CP-2297] p 157 N84-31688
- New variational formulations of hybrid stress elements p 158 N84-31690
- Inelastic and dynamic fracture and stress analyses p 158 N84-31697

- Nonlinear analysis for high-temperature composites—  
Turbine blades/vanes p 158 N84-31699
- On stress analysis of a crack-layer  
[NASA-CR-174774] p 159 N84-34774
- STRESS CONCENTRATION**  
A total life prediction model for stress concentration sites  
[NASA-CR-168225] p 152 N84-10612
- Analysis of stress-strain, fracture and ductility behavior of aluminum matrix composites containing discontinuous silicon carbide reinforcement  
[NASA-TM-83610] p 54 N84-21666
- Crack tip field and fatigue crack growth in general yielding and low cycle fatigue  
[NASA-CR-174686] p 76 N84-32503
- STRESS INTENSITY FACTORS**  
Development of plane strain fracture toughness test for ceramics using Chevron notched specimens p 77 A84-11676
- Analysis of an internally radially cracked ring segment subject to three-point radial loading p 150 A84-18691
- Elasticity solutions for a class of composite laminate problems with stress singularities p 53 A84-33389
- Resin selection criteria for tough composite structures [NASA-TM-83449] p 81 N84-10310
- Effect of crack curvature on stress intensity factors for ASTM standard compact tension specimens  
[NASA-CR-168280] p 153 N84-11513
- On stress analysis of a crack-layer  
[NASA-CR-174774] p 159 N84-34774
- STRESS MEASUREMENT**  
Benchmark cyclic plastic notch strain measurements p 63 A84-11194
- The use of heterodyne speckle photogrammetry to measure high-temperature strain distributions p 130 A84-28623
- Stress measurement in thin films by geometrical optics p 130 A84-28797
- Deposition stress effects on thermal barrier coating burner rig life  
[NASA-TM-83670] p 85 N84-25830
- STRESS PROPAGATION**  
Circuit equivalent to the elastic spherical shell p 104 A84-39197
- STRESS WAVES**  
Characterization of composite materials by means of the ultrasonic stress wave factor p 51 A84-10430
- Input-output characterization of an ultrasonic testing system by digital signal analysis  
[NASA-CR-3755] p 149 N84-15565
- STRESS-STRAIN DIAGRAMS**  
Simplified analytical procedures for representing material cyclic response— for high temperature gas turbine engine analysis p 16 A84-22877
- STRESS-STRAIN RELATIONSHIPS**  
On the suppression of zero energy deformation modes p 150 A84-21541
- Particulate erosion mechanisms  
[NASA-TM-83551] p 68 N84-14289
- A simplified method for elasto-plastic-creep structural analysis  
[NASA-TM-83509] p 154 N84-14542
- Tensile and compressive constitutive response of 316 stainless steel at elevated temperatures  
[NASA-TM-83506] p 68 N84-15249
- Development of a simplified procedure for cyclic structural analysis  
[NASA-TP-2243] p 155 N84-20878
- A computer program for predicting nonlinear uniaxial material responses using viscoplastic models  
[NASA-TM-83675] p 156 N84-29247
- STRESSES**  
Theoretical and software considerations for nonlinear dynamic analysis  
[NASA-CR-174504] p 154 N84-15589
- New variational formulations of hybrid stress elements p 158 N84-31690
- STRUCTURAL ANALYSIS**  
Comments on some problems in computational penetration mechanics p 150 A84-13545
- Analyses of large quasistatic deformations of inelastic bodies by a new hybrid-stress finite element algorithm p 150 A84-16874
- Analyses of large quasistatic deformations of inelastic bodies by a new hybrid-stress finite element algorithm - Applications p 150 A84-16884
- The structural response of a rail acceleration p 151 A84-32039
- Effects of structural coupling on mistuned cascade flutter and response  
[ASME PAPER 83-GT-117] p 151 A84-33701
- Algorithms for elasto-plastic-creep postbuckling p 152 A84-38480
- Engine cyclic durability by analysis and material testing  
[NASA-TM-83577] p 155 N84-18683
- Development of a simplified procedure for cyclic structural analysis  
[NASA-TP-2243] p 155 N84-20878
- Crack layer theory  
[NASA-CR-174534] p 156 N84-22980
- ICAN Integrated composites analyzer p 56 N84-26755
- Interply layer degradation effects on composite structural response  
[NASA-TM-83702] p 56 N84-26756
- Nonlinear Structural Analysis  
[NASA-CP-2297] p 157 N84-31688
- New variational formulations of hybrid stress elements p 158 N84-31690
- Nonlinear finite element analysis of shells with large aspect ratio p 158 N84-31692
- Self-adaptive solution strategies p 158 N84-31693
- Element-by-element solution procedures for nonlinear structural analysis p 158 N84-31694
- Inelastic and dynamic fracture and stress analyses p 158 N84-31697
- Nonlinear analysis for high-temperature composites  
Turbine blades/vanes p 158 N84-31699
- Three-dimensional stress analysis using the boundary element method p 159 N84-31700
- Fracture modes in notched angleply composite laminates  
[NASA-TM-83602] p 58 N84-34576
- STRUCTURAL DESIGN**  
MOD-2 wind turbine development  
[NASA-TM-83460] p 164 N84-13670
- STRUCTURAL DESIGN CRITERIA**  
Advanced Gas Turbine (AGT) Power-train system development  
[NASA-CR-168056] p 140 N84-10581
- Improved compliant hydrodynamic fluid journal bearing  
[NASA-CASE-LEW-13670-1] p 143 N84-22959
- Creep-rupture behavior of candidate Stirling engine alloys after long-term aging at 760 deg C in low-pressure hydrogen  
[NASA-TM-83676] p 73 N84-25793
- Dynamics of early planetary gear trains  
[NASA-CR-3793] p 145 N84-26027
- Large, horizontal-axis wind turbines  
[NASA-TM-83546] p 169 N84-27327
- Structural design of a vertical antenna boresight 18.3 by 18.3-m planar near-field antenna measurement system  
[NASA-TM-83781] p 133 N84-32783
- STRUCTURAL RELIABILITY**  
Advanced reliability method for fatigue analysis p 151 A84-31596
- STRUCTURAL VIBRATION**  
NASTRAN forced vibration analysis of rotating cyclic structures  
[ASME PAPER 83-DET-20] p 151 A84-29103
- Stagger angle dependence of inertial and elastic coupling in bladed disks p 151 A84-31903
- Model development and statistical investigation of turbine-blade mistuning p 17 A84-31905
- An improved finite-difference analysis of uncoupled vibrations of tapered cantilever beams  
[NASA-TM-83495] p 154 N84-13610
- Improved finite-difference vibration analysis of prewisted, tapered beams  
[NASA-TM-83549] p 154 N84-16588
- Vibration and flutter of mistuned bladed-disk assemblies  
[NASA-TM-83634] p 156 N84-23923
- NASTRAN forced vibration analysis of rotating cyclic structures  
[NASA-CR-173821] p 157 N84-29252
- STRUCTURAL WEIGHT**  
Advanced electrical power system technology for the all electric aircraft p 15 A84-16528
- SUBMILLIMETER WAVES**  
Ladder supported ring bar circuit  
[NASA-CASE-LEW-13570-1] p 106 N84-16452
- SUBSONIC FLOW**  
Three-dimensional flowfield inside a low-speed axial flow compressor rotor p 3 A84-13574
- High frequency green function for aerodynamic noise in moving media. I - General theory II - Noise from a spreading jet p 180 A84-21273
- Conservative streamtube solution of steady-state Euler equations  
[AIAA PAPER 84-1643] p 120 A84-38030
- Why credible propeller noise measurements are possible in the acoustically untreated NASA Lewis 8 ft by 6 ft wind tunnel p 181 A84-38091
- Analytical study of suction boundary layer control for subsonic V/STOL inlets  
[AIAA PAPER 84-1399] p 6 A84-44187
- Velocity and temperature characteristics of two-stream, coplanar jet exhaust plumes  
[AIAA PAPER 84-2205] p 21 A84-46106
- Further development of a method for computing three-dimensional subsonic viscous flows in turbofan lobe mixers  
[NASA-CR-168304] p 122 N84-14462
- Energy efficient engine Low-pressure turbine subsonic cascade component development and integration program  
[NASA-CR-165592] p 33 N84-27738
- Velocity and temperature characteristics of two-stream, coplanar jet exhaust plumes  
[NASA-TM-83730] p 34 N84-28790
- SUBSONIC FLUTTER**  
Subsonic/transonic stall flutter investigation of a rotating wing  
[NASA-CR-174625] p 36 N84-33417
- SUBSONIC SPEED**  
Flow visualization and interpretation of visualization data for deflected thrust V/STOL nozzles  
[AIAA PAPER 84-0102] p 16 A84-21852
- Flow visualization and interpretation of visualization data for deflected thrust V/STOL nozzles  
[NASA-TM-83554] p 24 N84-14147
- SUBSONIC WIND TUNNELS**  
Performance degradation of a model helicopter rotor with a generic ice shape p 14 A84-49096
- SUBSTITUTES**  
Replacing critical and strategic refractory metal elements in nickel-base superalloys — NASA's COSAM program  
[NASA-TM-83528] p 67 N84-13264
- Effects of cobalt in nickel-base superalloys  
[NASA-CR-168308] p 67 N84-14287
- Understanding the roles of the strategic element cobalt in nickel base superalloys p 76 N84-33471
- SUBSTRATES**  
Correlation of compressive and shear stress with spalling of plasma-sprayed ceramic materials p 79 A84-19784
- Ceramic composite liner material for gas turbine combustors  
[NASA-TM-83490] p 24 N84-14145
- Metallic glass as a temperature sensor during ion plating  
[NASA-TM-83586] p 69 N84-17351
- Tribological characteristics of gold films deposited on metals by ion plating and vapor deposition  
[NASA-TM-83572] p 69 N84-17352
- Laboratory degradation of Kapton in a low energy oxygen ion beam  
[NASA-TM-83530] p 41 N84-18310
- Investigation into the role of sodium chloride deposited on oxide and metal substrates in the initiation of hot corrosion  
[NASA-CR-173377] p 71 N84-20576
- Method and apparatus for coating substrates using a laser  
[NASA-CASE-LEW-13526-1] p 134 N84-22944
- Deposition stress effects on thermal barrier coating burner rig life  
[NASA-TM-83670] p 85 N84-25830
- Coating with overlay metallic-cermet alloy systems  
[NASA-CASE-LEW-13639-2] p 73 N84-27855
- Overlay coating degradation by simultaneous oxidation and coating/substrate interdiffusion  
[NASA-TM-83738] p 75 N84-31344
- Overlay metallic-cermet alloy coating systems  
[NASA-CASE-LEW-13639-1] p 77 N84-33555
- SUCTION**  
Analytical study of suction boundary layer control for subsonic V/STOL inlets  
[AIAA PAPER 84-1399] p 6 A84-44187
- SULFUR FLUORIDES**  
Capillary rise, wetting layers, and critical phenomena in confined geometry p 192 A84-20315
- SULFURIC ACID**  
Friction and wear of iron in sulfuric acid  
[NASA-TP-2289] p 71 N84-21716
- Friction and wear of nickel in sulfuric acid  
[NASA-TP-2290] p 72 N84-21721
- Interaction of sulfuric acid corrosion and mechanical wear of iron  
[NASA-TM-83717] p 73 N84-27857
- SUPERCHARGERS**  
Advanced turbocharger design study program  
[NASA-CR-174633] p 143 N84-21879
- An overview of the NASA rotary engine research program  
[NASA-TM-83699] p 34 N84-28791
- Diesel engine catalytic combustor system — aircraft engines  
[NASA-CASE-LEW-12895-1] p 148 N84-33808
- SUPERCOOLING**  
Some fundamental aspects of solidification in a supercooled melt  
[NASA-TM-83714] p 73 N84-26787



**SUPERCritical AIRFOILS**

- Redesign and cascade tests of a supercritical controlled diffusion stator blade-section  
[AIAA PAPER 84-1207] p 5 A84-36960
- Redesign and cascade tests of a supercritical controlled diffusion stator blade-section  
[NASA-TM-83635] p 10 N84-22533

**SUPERCritical WINGS**

- Improved design of subcritical and supercritical cascades using complex characteristics and boundary-layer correction p 5 A84-38839

**SUPERHEATING**

- Two-region analysis of interface shape in continuous casting with superheated liquid p.139 A84-44918

**SUPERSONIC AIRCRAFT**

- Supersonic STOVL ejector aircraft from a propulsion point of view  
[AIAA PAPER 84-1401] p 19 A84-40246
- Supersonic STOVL ejector aircraft from a propulsion point of view  
[NASA-TM-83641] p 31 N84-24581
- Supersonic jet shock noise reduction  
[NASA-TM-83799] p 186 N84-35085

**SUPERSONIC FLOW**

- One-dimensional unsteady modeling of supersonic inlet unstart/restart  
[AIAA PAPER 84-0439] p 4 A84-18094
- Sound generated by instability waves of supersonic flows I Two-dimensional mixing layers II - Axisymmetric jets p 181 A84-24597
- Conservative streamtube solution of steady-state Euler equations  
[AIAA PAPER 84-1643] p 120 A84-38030

**SUPERSONIC FLUTTER**

- Subsonic/transonic stall flutter investigation of a rotating rig  
[NASA-CR-174625] p 36 N84-33417

**SUPERSONIC INLETS**

- Three-dimensional viscous design methodology for advanced technology aircraft supersonic inlet systems  
[AIAA PAPER 84-0194] p 4 A84-21290
- Dynamic response of shock waves in transonic diffuser and supersonic inlet - An analysis with the Navier-Stokes equations and adaptive grid  
[AIAA PAPER 84-1609] p 5 A84-38004
- Three-dimensional flow simulations for supersonic mixed-compression inlets at incidence p 5 A84-98828
- Low flight speed fan noise from a supersonic inlet p 182 A84-44508
- Three-dimensional viscous design methodology for advanced technology aircraft supersonic inlet systems  
[NASA-TM-83558] p 23 N84-13190

**SUPERSONIC JET FLOW**

- Supersonic jet screech tone cancellation p 179 A84-10136

**SUPERSONIC NOZZLES**

- Experimental investigation of shock-cell noise reduction for dual-stream nozzles in simulated flight comprehensive data report. Volume 1: Test nozzles and acoustic data  
[NASA-CR-168336-VOL-1] p 184 N84-24323
- Experimental investigation of shock-cell noise reduction for dual-stream nozzles in simulated flight comprehensive data report. Volume 2: Laser velocimeter data, static pressures and shadowgraph photos  
[NASA-CR-168336-VOL-2] p 184 N84-24324

**SUPERSONIC SPEEDS**

- Noise of the SR-6 propeller model at 2 deg and 4 deg angles of attack  
[NASA-TM-83515] p 183 N84-16946

**SUPERSONIC WIND TUNNELS**

- Experimental studies on two dimensional shock boundary layer interactions  
[AIAA PAPER 84-0099] p 3 A84-17881

**SURFACE CRACKS**

- Compositional effects on Si3N4 fracture surfaces p 79 A84-19794
- Evaluation of the effect of crack closure on fatigue crack growth of simulated short cracks  
[NASA-TM-83778] p 75 N84-31348

**SURFACE DISTORTION**

- Determination of near-surface plastic deformation in sliding contacts p 140 A84-48996

**SURFACE PROPERTIES**

- Surface chemistry, friction, and wear of Ni-Zn and Mn-Zn ferrites in contact with metals p 78 A84-13516
- Surface effects in high voltage silicon solar cells p 160 A84-23002
- Topological reaction rate measurements related to sintering  
[NASA-TM-83486] p 68 N84-14288
- Tribology in the 80's Volume 1: Sessions 1 to 4  
[NASA-CP-2300-VOL-1] p 144 N84-23891
- Importance and definition of materials in tribology. Status of understanding p 84 N84-23893
- Effects of surface chemistry on hot corrosion life  
[NASA-CR-174683] p 72 N84-24774

**Elastohydrodynamic lubrication of smooth surfaces**

- p 144 N84-24895

**Surface topography-connections between lubrication and failure initiation**

- p 144 N84-24898

**Secondary electron emission characteristics of ion-textured copper and high-purity isotropic graphite surfaces**

- [NASA-TP-2342] p 86 N84-28989

**Properties of ferrites important to their friction and wear behavior**

- [NASA-TM-83716] p 87 N84-28994

**Plasmon device design. Conversion from surface-to-junction plasmons with grating-couplers**

- p 171 N84-29330

**Fracture surface characteristics of notched angle-ply graphite/epoxy composites**

- [NASA-TM-83786] p 57 N84-33522

**SURFACE REACTIONS**

- Correlation of electron emission with changes in the surface concentration of barium and oxygen on a tungsten surface p 60 A84-45917

**Surface topographical changes measured by phase-locked interferometry**

- [NASA-CR-3757] p 188 N84-16984

**The role of surface generated radicals in catalytic combustion**

- p 61 N84-20555

**Mechanical contact induced transformation from the amorphous to the crystalline state in metallic glass**

- [NASA-TM-83583] p 71 N84-20673

**Cathode degradation and erosion in high pressure arc discharges**

- [NASA-TM-83638] p 47 N84-22631

**Effects of water-vapor on friction and deformation of polymeric magnetic media in contact with a ceramic oxide**

- [NASA-TM-83727] p 87 N84-30072

**The energy dependence and surface morphology of Kapton (trademark) degradation under atomic oxygen bombardment**

- p 187 N84-34484

**SURFACE ROUGHNESS**

- Surfaces — characterization of surface properties for predicting bond quality p 50 A84-10680
- The effect of annealing on the creep of plasma-sprayed ceramics p 79 A84-19785
- Surface roughness effects with solid lubricants dispersed in mineral oils p 137 A84-28987

**ASLE PREPRINT 83-LC-4C-1 Ion sputter textured graphite electrode plates**

- [NASA-CASE-LEW-12919-2] p 179 N84-28565

**The role of the reflection coefficient in precision measurement of ultrasonic attenuation**

- [NASA-TM-83788] p 149 N84-32849

**SURFACE ROUGHNESS EFFECTS**

- Measurements of local convective heat transfer coefficients on ice accretion shapes  
[AIAA PAPER 84-0018] p 113 A84-17835
- Analysis for leakage and rotordynamic coefficients of surface-roughened tapered annular gas seals  
[ASME PAPER 84-GT-32] p 140 A84-46896

**SURFACE TEMPERATURE**

- Shape of porous region to control cooling along curved exit boundary p 115 A84-23591

**Metallic glass as a temperature sensor during ion plating**

- [NASA-TM-83566] p 69 N84-17351

**An investigation of the transient thermal analysis of spur gears**

- [NASA-TM-83724] p 146 N84-28088

**SURGES**

- Numerical aspects of unsteady flow calculations p 128 N84-25968

**SWEEP ANGLE**

- The application of vortex theory to the optimum swept propeller  
[AIAA PAPER 84-0036] p 3 A84-17841

**SWEEP EFFECT**

- Flutter of swept fan blades  
[NASA-TM-83547] p 154 N84-16587

**SWELLING**

- Prediction of composite hygral behavior made simple p 51 A84-14285

**SWIRLING**

- Limitations and empirical extensions of the k-epsilon model as applied to turbulent confined swirling flows  
[AIAA PAPER 84-0441] p 114 A84-18096

**Further time-mean measurements in confined swirling flows**

- p 116 A84-27138

**Swirl flow turbulence modeling**

- [AIAA PAPER 84-1376] p 118 A84-35196

**Swirl, confinement and nozzle effects on confined turbulent flow**

- [AIAA PAPER 84-1377] p 118 A84-35197

**Mass and momentum turbulent transport experiments with confined swirling coaxial jets I**

- [AIAA PAPER 84-1380] p 119 A84-35664

**Five-hole pitot probe measurements of swirl, confinement and nozzle effects on confined turbulent flow**

- [AIAA PAPER 84-1605] p 120 A84-38000

**Confined turbulent swirling recirculating flow predictions**

- [NASA-CR-175397] p 125 N84-19745

**Swirl, expansion ratio and blockage effects on confined turbulent flow**

- [NASA-CR-175391] p 125 N84-19746

**Turbulent swirling combustion**

- p 61 N84-20535

**Extension to an analysis of turbulent swirling compressible flow for application to axisymmetric small gas turbine ducts**

- [NASA-CR-165597] p 195 N84-21445

**An experimental investigation of gas jets in confined swirling air flow**

- [NASA-CR-3832] p 36 N84-33412

**SWITCHES**

- Energy stores and switches for rail-launcher systems  
[NASA-CR-173249] p 107 N84-16458

**Double-injection, deep-impurity switch development**

- [NASA-CR-168335] p 108 N84-18535

**Advances in solid state switchgear technology for large space power systems**

- [NASA-TM-83652] p 109 N84-22891

**K-band latching switches**

- [NASA-CR-168253] p 109 N84-24973

**The 20 x 20 high speed microwave switches**

- [NASA-TM-83775] p 101 N84-32644

**SWITCHING**

- Development and fabrication of an augmented power transistor  
[NASA-CR-168262] p 106 N84-11388

**High voltage-high power components for large space power distribution systems**

- [NASA-TM-83648] p 42 N84-22615

**SWITCHING CIRCUITS**

- Metal vapor vacuum arc switching - Applications and results — for launchers p 103 A84-32029

**High-speed wide band 20 x 20 microwave switch matrix**

- Input filter compensation for switching regulators  
[NASA-CR-173247] p 107 N84-16459

**Study of solar array switching power management technology for space power system**

- [NASA-CR-167890-EXEC-SUM] p 167 N84-23021

**Input filter compensation for switching regulators**

- [NASA-CR-173557] p 110 N84-24975

**Low-frequency switching voltage regulators for terrestrial photovoltaic systems**

- [NASA-TM-83625] p 110 N84-25926

**Simplified dc to dc converter**

- [NASA-CASE-LEW-13495-1] p 111 N84-33663

**SYNCHRONOUS PLATFORMS**

- NASA's geostationary communications platform program  
[AIAA PAPER 84-0702] p 95 A84-25326

**SYNCHRONOUS SATELLITES**

- Integration becomes the name of the OTV game p 44 A84-44045

**SYNTHESIS (CHEMISTRY)**

- Shock tube study of the fuel structure effects on the chemical kinetic mechanisms responsible for soot formation  
[NASA-CR-174661] p 62 N84-21677

**SYSTEM EFFECTIVENESS**

- Transmission efficiency measurements and correlations with physical characteristics of the lubricant  
[NASA-TM-83740] p 147 N84-30293

**SYSTEMS ANALYSIS**

- Mobile radio alternative systems study. Volume 2 Terrestrial — rural areas  
[NASA-CR-168063] p 96 N84-10403

**An RC-1 organic Rankine bottoming cycle for an adiabatic diesel engine**

- [NASA-CR-168256] p 196 N84-32306

**SYSTEMS COMPATIBILITY**

- Large, horizontal-axis wind turbines  
[NASA-TM-83546] p 169 N84-27327

**SYSTEMS ENGINEERING**

- A frequency-division multiple-access system concept for 30/20 GHz high-capacity domestic satellite service p 94 A84-22141

**Advanced acousto-optic signal processors**

- p 187 A84-28485

**Pore size engineering applied to the design of separators for nickel-hydrogen cells and batteries**

- p 162 A84-30187

**Recent developments in EHF Satcom technology**

- p 39 A84-46620

**Automotive Stirling engine development program**

- [NASA-CR-168205] p 194 N84-18117

**SYSTEMS INTEGRATION**

- Rotorcraft flight-propulsion control integration p 36 A84-46524

- Develop and test fuel cell powered on-site integrated total energy systems  
[NASA-CR-174714] p 170 N84-27329
- SYSTEMS SIMULATION**  
Software simulator for multiple computer simulation system p 176 N84-11892  
Geometric models, antenna gains, and protection ratios as developed for BC SAT-R2 conference software [NASA-TM-83381] p 96 N84-11358
- SYSTEMS STABILITY**  
Stability analysis of a buck regulator employing input filter compensation p 102 N84-18412
- SYSTOLE**  
Optical systolic solutions of linear algebraic equations p 188 N84-22405
- T**
- TANGENTS**  
Investigation of tangential blowing applied to a subsonic V/STOL inlet p 3 N84-11042
- TANTALUM ALLOYS**  
Influence of cobalt, tantalum and tungsten on the high temperature mechanical properties of single crystal nickel-base superalloys [NASA-TM-83479] p 70 N84-17355
- TANTALUM CARBIDES**  
Calculation of vaporization rates assuming various rate determining steps: Application to the resistor jet [NASA-TM-83757] p 51 N84-31283
- TAPERED COLUMNS**  
An improved finite-difference analysis of uncoupled vibrations of tapered cantilever beams [NASA-TM-83495] p 154 N84-13610
- TAPERING**  
Analysis for leakage and rotor dynamic coefficients of surface-roughened tapered annular gas seals [ASME PAPER 84-GT-32] p 140 N84-46896
- TECHNOLOGICAL FORECASTING**  
Space power technology into the 21st century [AIAA PAPER 84-1136] p 43 N84-34013  
P/M superalloys A troubled adolescent? [NASA-TM-83623] p 73 N84-26785
- TECHNOLOGY ASSESSMENT**  
NASA priority technologies [IAF PAPER 83-345] p 37 N84-11793  
NASA's multibeam communications technology program p 39 N84-21397  
Recent advances in thin silicon solar cells p 160 N84-22981  
Rural land mobile radio market assessment and satellite and terrestrial system concepts [AIAA PAPER 84-0754] p 95 N84-25324  
Recent developments in EHF Satcom technology p 39 N84-46620  
Some comments on longevity by a technologist p 45 N84-12247
- Aeronautical propulsion Present status and future directions**  
[NASA-TM-83589] p 1 N84-16119  
Phased-array-fed antenna configuration study. Volume 1: Technology assessment [NASA-CR-168231] p 98 N84-16423  
An assessment of advanced technology for industrial cogeneration [NASA-CR-173456] p 167 N84-22001  
NASA broad-specification fuels combustion technology program p 62 N84-23637  
Status and new directions for solid lubricant coatings and composite materials p 85 N84-25055  
Basic and applied research related to the technology of space energy conversion systems, 1982 - 1983 [NASA-CR-173554] p 169 N84-25168  
P/M superalloys A troubled adolescent? [NASA-TM-83623] p 73 N84-26785
- TECHNOLOGY TRANSFER**  
Advanced turbocharger design study program [NASA-CR-174633] p 143 N84-21879
- TECHNOLOGY UTILIZATION**  
Chicago Meets Outer Space program [NASA-TM-85492] p 192 N84-16021  
Status and new directions for solid lubricant coatings and composite materials p 85 N84-25055
- TELECOMMUNICATION**  
The subjective effect of multiple co-channel frequency modulated television interference [NASA-TM-83415] p 97 N84-11360  
Communications network design and costing model technical manual [NASA-CR-168236] p 97 N84-14376
- TELECONFERENCING**  
Photovoltaic power system for satellite Earth stations in remote areas. Project status and design description [NASA-TM-83789] p 101 N84-33642

- TELEVISION TRANSMISSION**  
NTSC composite video at 1.6 bits/pel p 95 N84-49259  
The subjective effect of multiple co-channel frequency modulated television interference [NASA-TM-83415] p 97 N84-11360
- TEMPERATURE**  
Velocity and temperature characteristics of two-stream, coplanar jet exhaust plumes [AIAA PAPER 84-2205] p 21 N84-46106  
Velocity and temperature characteristics of two-stream, coplanar jet exhaust plumes [NASA-TM-83730] p 34 N84-28790
- TEMPERATURE CONTROL**  
High effectiveness liquid droplet/gas heat exchanger for space power applications [IAF PAPER 83-433] p 42 N84-11819
- TEMPERATURE DEPENDENCE**  
Turbidity very near the critical point of methanol-cyclohexane mixtures p 192 N84-30391  
A temperature correlation for the radiation resistance of a thick-walled circular duct exhausting a hot gas p 181 N84-31103  
Electronic properties of carbon fibers intercalated with copper chloride p 104 N84-34521  
Research and development program for the development of advanced time-temperature dependent constitutive relationships. Volume 1. Theoretical discussion [NASA-CR-168191-VOL-1] p 153 N84-10613  
Cross spectra between pressure and temperature in a constant-area duct downstream of a hydrogen-fueled combustor [NASA-TM-83463] p 182 N84-11885  
Mechanism of lubrication by tricesylphosphate (TCP) [NASA-TP-2274] p 142 N84-18653  
A 37.5-kW point design comparison of the nickel-cadmium battery, bipolar nickel-hydrogen battery, and regenerative hydrogen-oxygen fuel cell energy storage subsystems for low Earth orbit [NASA-TM-83C51] p 167 N84-23022
- TEMPERATURE DISTRIBUTION**  
Modeling of dilution jet flowfields p 126 N84-20547  
A theoretical model for the cross spectra between pressure and temperature downstream of a combustor [NASA-TM-83671] p 186 N84-34231
- TEMPERATURE EFFECTS**  
Some inelastic effects of thermal cycling on yttria-stabilized zirconia [NASA-TM-83488] p 123 N84-16492  
Method of reducing temperature in high-speed photography [NASA-TM-83620] p 188 N84-22421  
Elastohydrodynamic lubrication. Status of understanding p 144 N84-25048  
Effects of long-time elevated temperature exposures on hot-isostatically-pressed power-metallurgy Udmet 700 alloys with reduced cobalt contents [NASA-TM-83632] p 57 N84-28917  
Operating characteristics of a three-piece-inner-ring large-bore roller bearing to speeds of 3 million DN [NASA-TP-2355] p 146 N84-29226  
Mechanical behavior of carbon-carbon composites [NASA-CR-174767] p 57 N84-34575
- TEMPERATURE GRADIENTS**  
Heat transfer in thermal barrier coated rods with circumferential and radial temperature gradients [ASME PAPER 84-GT-181] p 121 N84-46982  
Aerothermal modeling, phase 1 Volume 2 Experimental data [NASA-CR-168296-VOL-2] p 25 N84-15156  
Tensile and compressive constitutive response of 316 stainless steel at elevated temperatures [NASA-TM-83506] p 68 N84-15249
- TEMPERATURE MEASUREMENT**  
Internal heat transfer coefficients of porous metals p 112 N84-13239  
Aerothermal modeling Executive summary [NASA-CR-168330] p 25 N84-15152  
Dynamic gas temperature measurement system, volume 1 [NASA-CR-168267-VOL-1] p 132 N84-16529  
Parametric analysis of hollow conductor parallel and coaxial transmission lines for high frequency space power distribution [NASA-TM-83601] p 46 N84-20639  
In-flight atmospheric and fuel tank temperature measurements p 90 N84-23643  
Dilution jets in accelerated cross flows [NASA-CR-174717] p 34 N84-28794
- TEMPERATURE PROFILES**  
Performance of a high-work low aspect ratio turbine tested with a realistic inlet radial temperature profile [AIAA PAPER 84-1101] p 19 N84-40239
- Performance of a high-work low aspect ratio turbine tested with a realistic inlet radial temperature profile [NASA-TM-83655] p 32 N84-24589
- TEMPERATURE SENSORS**  
Metallic glass as a temperature sensor during ion plating [NASA-TM-83566] p 69 N84-17351
- TENSILE DEFORMATION**  
Tensile buckling of advanced turboprops p 149 N84-11039
- TENSILE PROPERTIES**  
Off-axis tensile properties and fracture in a unidirectional graphite/polyimide composite (Celon 6000/PMR 15) p 53 N84-43553
- TENSILE STRENGTH**  
Thermal degradation of the tensile properties of unidirectionally reinforced FP-AI2O3/EZ 33 magnesium composites p 52 N84-28229  
Simplified composite micromechanics equations for strength, fracture toughness and environmental effects p 53 N84-41856  
Method for strengthening boron fibers [NASA-CASE-LEW-13826-2] p 55 N84-24711  
Effects of long-time elevated temperature exposures on hot-isostatically-pressed power-metallurgy Udmet 700 alloys with reduced cobalt contents [NASA-TM-83632] p 57 N84-28917  
Materials for Advanced Turbine Engines (MATE) Project 3. Design, fabrication and evaluation of an oxide dispersion strengthened sheet alloy combustor liner, volume 1 [NASA-CR-174691] p 76 N84-32504
- TENSILE TESTS**  
Method and apparatus for gripping uniaxial fibrous composite materials [NASA-CASE-LEW-13758-1] p 56 N84-27829
- TENSORS**  
An application of tensor ideas to nonlinear modeling of a turbofan jet engine p 20 N84-42382
- TEST FACILITIES**  
Test results and description of a 1 kW free-piston Stirling engine with a dashpot load p 138 N84-30095  
Electromagnetic propulsion test facility [NASA-TM-83568] p 37 N84-16229  
Progressive fracture of fiber composites [NASA-TM-83701] p 56 N84-27831
- THERMAL ANALYSIS**  
Thermal and elastohydrodynamic analysis of reciprocating rod seals in the Stirling engine p 138 N84-30095  
High temperature thermomechanical analysis of ceramic coatings p 152 N84-48555  
Parameter studies of gear cooling using an automatic finites element mesh generator [NASA-TM-83721] p 146 N84-28087  
An investigation of the transient thermal analysis of spur gears [NASA-TM-83724] p 146 N84-28088  
Thermal analysis of a planetary transmission with spherical roller bearings operating after complete loss of oil [NASA-TP-2367] p 147 N84-32824
- THERMAL CONDUCTIVITY**  
Program for development of strain tolerant thermal barrier coating system [NASA-CR-173214] p 82 N84-16337  
Applications of photoacoustic techniques to the study of jet fuel residue [NASA-CR-173322] p 90 N84-18420  
Overview of zirconia with respect to gas turbine applications [NASA-TP-2286] p 83 N84-21740
- THERMAL CONTROL COATINGS**  
Phase distributions in plasma-sprayed zirconia-yttria p 78 N84-18948  
Phase analysis of plasma-sprayed zirconia-yttria coatings p 78 N84-19781  
Anisotropic thermal expansion effects in plasma-sprayed ZrO2-8 percent Y2O3 coatings p 78 N84-19782  
Mechanical and physical properties of plasma-sprayed stabilized zirconia p 79 N84-19786  
Thermal stress fracture of ceramic coatings p 80 N84-24553  
Oxidation behavior of a thermal barrier coating p 65 N84-42667  
Degradation mechanisms of ceramic thermal barrier coatings in corrosive environments p 81 N84-42668  
Ceramic-coated metals can survive contact with hot working fluid p 81 N84-44482  
Heat transfer in thermal barrier coated rods with circumferential and radial temperature gradients [ASME PAPER 84-GT-181] p 121 N84-46982  
Acoustic emission evaluation of plasma-sprayed thermal barrier coatings [ASME PAPER 84-GT-292] p 140 N84-47046

Development of strain tolerant thermal barrier coating systems, tasks 1 - 3 [NASA-CR-168251] p 81 N84-12312  
 Program for development of strain tolerant thermal barrier coating system [NASA-CR-173214] p 82 N84-16337  
 Ion-beam-textured and coated surfaces experiment (S1003) p 84 N84-24650  
 Failure analysis of plasma-sprayed thermal barrier coatings [NASA-TM-83777] p 75 N84-31347

**THERMAL CYCLING TESTS**  
 Simplified analytical procedures for representing material cyclic response—for high temperature gas turbine engine analysis p 16 A84-22877  
 Thermal stress fracture of ceramic coatings p 80 A84-24553  
 Some inelastic effects of thermal cycling on yttria-stabilized zirconia [NASA-TM-83488] p 123 N84-16492  
 Preliminary study of thermomechanical fatigue of polycrystalline MAR-M 200 [NASA-TP-2280] p 69 N84-17350  
 Oxidation and corrosion resistance of candidate Stirling engine heater-head-tube alloys [NASA-TM-83609] p 74 N84-28962  
 High speed, low cost, LEO-thermal-cycling facility p 171 N84-29340  
 High-temperature cyclic oxidation data, volume 1 [NASA-TM-83665] p 75 N84-31345

**THERMAL DEGRADATION**  
 Thermal degradation of the tensile properties of unidirectionally reinforced FP-Al<sub>2</sub>O<sub>3</sub>/EZ 33 magnesium composites p 52 A84-28229  
 Thermal oxidative degradation reactions of linear perfluoroalkyl ethers p 80 A84-30000  
 Degradation mechanisms of ceramic thermal barrier coatings in corrosive environments p 81 A84-42668  
 Research on aviation fuel instability p 91 N84-24734  
 Modeling degradation and failure of Ni-Cr-Al overlay coatings [NASA-TM-83672] p 74 N84-27858

**THERMAL DIFFUSION**  
 Diffused junction p(+)-n solar cells in bulk GaAs I Fabrication and cell performance p 161 A84-26027

**THERMAL ENERGY**  
 High-temperature molten salt thermal energy storage systems for solar applications [NASA-CR-167916] p 165 N84-15679

**THERMAL EXPANSION**  
 Scaling relations in the equation of state, thermal expansion, and melting of metals p 192 A84-19359  
 Anisotropic thermal expansion effects in plasma-sprayed ZrO<sub>2</sub>-8 percent Y<sub>2</sub>O<sub>3</sub> coatings p 78 A84-19782  
 The effect of annealing on the creep of plasma-sprayed ceramics p 79 A84-19785  
 Program for development of strain tolerant thermal barrier coating system [NASA-CR-173214] p 82 N84-16337

**THERMAL FATIGUE**  
 The effect of microstructure on 650 C fatigue crack growth in P/M Astroloy p 63 A84-12395  
 High-temperature fatigue in metals - A brief review of life prediction methods developed at the Lewis Research Center of NASA p 64 A84-14286  
 Simplified analytical procedures for representing material cyclic response—for high temperature gas turbine engine analysis p 16 A84-22877  
 Thermal stress fracture of ceramic coatings p 80 A84-24553  
 Preliminary study of thermomechanical fatigue of polycrystalline MAR-M 200 [NASA-TP-2280] p 69 N84-17350  
 Engine cyclic durability by analysis and material testing [NASA-TM-83577] p 155 N84-18683

**THERMAL PLASMAS**  
 Comparison of thermal plasma observations on SCATHA and GEOS p 41 N84-17262

**THERMAL PROTECTION**  
 Ceramic-coated metals can survive contact with hot working fluid p 81 A84-44482  
 Acoustic emission evaluation of plasma-sprayed thermal barrier coatings [ASME PAPER 84-GT-292] p 140 A84-47046  
 Improved thermal barrier coating system [NASA-CASE-LEW-14057-1] p 88 N84-33595

**THERMAL RESISTANCE**  
 Performance of thermal barrier coatings in high heat flux environments [NASA-TM-83663] p 72 N84-24772

**THERMAL STABILITY**  
 The effect of a coating on the thermo-oxidative stability of Celcon 6000 graphite fiber/PMR 15 polyimide composites p 52 A84-21844

Electronic properties of carbon fibers intercalated with copper chloride p 104 A84-34521  
 An assessment of the use of atomizing fuel in turbofan engines [NASA-CR-168081] p 89 N84-10332  
 A review of the use of wear-resistant coatings in the cutting-tool industry [NASA-TM-83512] p 81 N84-11295  
 Moderate temperature rechargeable NaHS<sub>2</sub> cells p 108 N84-21376  
 Research on aviation fuel instability p 90 N84-23642  
 Thermal and oxidative stabilities of liquid lubricants p 84 N84-23907  
 Research on aviation fuel instability p 91 N84-24734  
 FTIR analysis of aviation fuel deposits [NASA-TM-83773] p 92 N84-33608

**THERMAL STRESSES**  
 Factors influencing the thermally-induced strength degradation of B/AI composites p 52 A84-28227  
 Degradation mechanisms of ceramic thermal barrier coatings in corrosive environments p 81 A84-42668  
 High temperature thermomechanical analysis of ceramic coatings p 152 A84-48565  
 Comparison of predicted and experimental thermal performance of angular-contact ball bearings [NASA-TP-2275] p 142 N84-18654  
 Thermal stress analysis for a wood composite blade—wind turbines [NASA-CR-173394] p 156 N84-21903  
 Hydrothermomechanical fracture stress criteria for fiber composites with sense-parity [NASA-TM-83691] p 57 N84-28918  
 Thermal-stress analysis for wood composite blade—horizontal axis wind turbines [NASA-CR-173830] p 157 N84-31685

**THERMIONIC CONVERTERS**  
 Thermionic-photovoltaic energy converter [NASA-CASE-LEW-14077-1] p 167 N84-20918

**THERMIONIC EMISSION**  
 Correlation of electron emission with changes in the surface concentration of barium and oxygen on a tungsten surface p 60 A84-45917  
 Evaluation of single crystal LaB<sub>6</sub> cathodes for use in a high frequency backward wave oscillator tube [NASA-CR-173343] p 108 N84-19709

**THERMODYNAMIC CYCLES**  
 Analysis of a topping-cycle, aircraft, gas-turbine-engine system which uses cryogenic fuel [NASA-TP-2294] p 28 N84-21549

**THERMODYNAMIC EFFICIENCY**  
 Overview of NASA Lewis Research Center free-piston Stirling engine activities [NASA-TM-83649] p 195 N84-22512

**THERMODYNAMIC PROPERTIES**  
 The chemical kinetics and thermodynamics of sodium species in oxygen-rich hydrogen flames p 59 A84-27724  
 Simplified composite micromechanics equations of hygral, thermal, and mechanical properties p 53 A84-49377  
 Combustion gas properties of various fuels of interest to gas turbine engines [NASA-TM-83682] p 31 N84-24584  
 ICAN Integrated composites analyzer [NASA-TM-83700] p 56 N84-26755

**THERMODYNAMICS**  
 Effect of location in an array on heat transfer to a short cylinder in crossflow p 119 A84-36150  
 INHYD Computer code for intraply hybrid composite design A users manual [NASA-TP-2239] p 54 N84-13224  
 Crack layer theory [NASA-CR-174634] p 156 N84-22980  
 Oxygen diffusion in alpha-Al<sub>2</sub>O<sub>3</sub> [NASA-TM-83622] p 86 N84-28990

**THERMOELASTICITY**  
 Assessment of two neglected effects in the analysis of an oil pumping ring seal [ASME PAPER 83-LUB-16] p 137 A84-23097

**THERMOELECTRIC GENERATORS**  
 Thermionic-photovoltaic energy converter [NASA-CASE-LEW-14077-1] p 167 N84-20918

**THERMOELECTRICITY**  
 Analysis of thermoelectric properties of high-temperature complex alloys of nickel-base, iron-base and cobalt-base groups [NASA-TP-2278] p 70 N84-18370

**THERMOMECHANICAL TREATMENT**  
 Effects of processing and microstructure on the fatigue behaviour of the nickel-base superalloy René95 p 68 A84-48715  
 Select fiber composites for space applications: A mechanistic assessment [NASA-TM-83631] p 55 N84-22702

**THERMOPLASTICITY**  
 Simplified analytical procedures for representing material cyclic response—for high temperature gas turbine engine analysis p 16 A84-22877

**THERMOSETTING RESINS**  
 An investigation into the injection molding of PMR-15 polyimide [NASA-CR-173550] p 85 N84-24810

**THERMOVISCOELASTICITY**  
 Research and development program for the development of advanced time-temperature dependent constitutive relationships. Volume 2 Programming manual [NASA-CR-168191-VOL-2] p 153 N84-10614

**THIN FILMS**  
 Coupling of radiation into thin film modes by means of localized plasma resonances p 187 A84-16397  
 Stress measurement in thin films by geometrical optics p 130 A84-28797  
 Plasma polymerized high energy density dielectric films for capacitors [NASA-CR-168233] p 81 N84-13310  
 The ball bearing as a rheological test device [NASA-TM-83570] p 142 N84-17591  
 A study of nucleation and growth of thin films by means of computer simulation General features [NASA-TM-83558] p 179 N84-17982  
 Coaxial carbon plasma gun deposition of amorphous carbon films [NASA-TM-83600] p 191 N84-20404  
 Fractional and morphological properties of Au-MoS<sub>2</sub> films sputtered from a compact target [NASA-TM-83604] p 143 N84-20858  
 Photodeposition of nitride insulators on 3-5 substrates [NASA-CR-173393] p 71 N84-21720  
 Sputtered coatings for protection of spacecraft polymers [NASA-TM-83706] p 85 N84-26803  
 Deposition of diamondlike carbon films [NASA-CASE-LEW-14080-1] p 86 N84-28986  
 Dual ion beam deposition of carbon films with diamondlike properties [NASA-TM-83743] p 110 N84-31512

**THIN PLATES**  
 A mixed shear flexible finite element for the analysis of laminated plates p 152 A84-45994

**THREE DIMENSIONAL BOUNDARY LAYER**  
 Three-dimensional turbulent boundary-layer development on a fan rotor blade p 3 A84-17437  
 Scaling and modeling of three-dimensional, end-wall, turbulent boundary layers [NASA-CR-17392] p 127 N84-25941

**THREE DIMENSIONAL FLOW**  
 Three-dimensional flowfield inside a low-speed axial flow compressor rotor p 3 A84-13574  
 Streamwise computation of three-dimensional parabolic flows p 113 A84-16828  
 Three-dimensional viscous design methodology for advanced technology aircraft supersonic inlet systems [AIAA PAPER 84-0194] p 4 A84-21290  
 Computation of viscous flow in curved ducts and comparison with experimental data [AIAA PAPER 84-0531] p 115 A84-21303  
 Computation of three-dimensional viscous flows using a space-marching method [AIAA PAPER 84-1298] p 5 A84-36971  
 Three-dimensional stability of an elliptical vortex in a straining field [AD-A146317] p 120 A84-38557  
 Three-dimensional flow simulations for supersonic mixed-compression inlets at incidence p 5 A84-38828  
 Application of a quasi-3D inviscid flow and boundary layer analysis to the hub-shroud contouring of a radial turbine [AIAA PAPER 84-1297] p 6 A84-44177  
 Investigation of the three-dimensional flow field within a transonic fan rotor - Experiment and analysis [ASME PAPER 84-GT-200] p 7 A84-46995  
 Turbulence modeling for three-dimensional shear flows over curved rotating bodies p 122 A84-48138  
 Three-dimensional viscous design methodology for advanced technology aircraft supersonic inlet systems [NASA-TM-83558] p 23 N84-13180  
 Computation of viscous flow in curved ducts and comparison with experimental data [NASA-TM-83548] p 122 N84-13494  
 Further development of a method for computing three-dimensional subsonic viscous flows in turbofan lobe mixers [NASA-CR-168304] p 122 N84-14462  
 Programs for calculating quasi-three-dimensional flow in a turbomachine blade row [NASA-TM-83588] p 9 N84-17138  
 Modeling of dilution jet flowfields p 126 N84-20547

- Application of a quasi-3D inviscid flow and boundary layer analysis to the hub-shroud contouring of a radial turbine  
[NASA-TM-83669] p 10 N84-25647
- THRUST**  
Centaur D-1A guidance/software system  
[AAS PAPER 84-043] p 39 A84-49176  
Centaur D-1A guidance/software system  
[NASA-TM-83552] p 38 N84-16234
- THRUST CHAMBERS**  
Development of a simplified procedure for rocket engine thrust chamber life prediction with creep  
[NASA-CR-168261] p 46 N84-19472
- THRUST CONTROL**  
Identification of multivariable high-performance turbofan engine dynamics from closed loop data  
p 28 N84-20580
- THRUST LOADS**  
Review of the DOE/NASA wind turbine engineering information system  
p 163 A84-33766
- THRUST MEASUREMENT**  
Uncertainty methodology for in-flight thrust determination  
[SAE PAPER 831438] p 13 A84-29452  
Application of in-flight thrust determination uncertainty  
[SAE PAPER 831439] p 13 A84-29453
- THRUSTERS**  
Demonstration of a new electrothermal thruster concept  
p 43 A84-34037
- TIME DEPENDENCE**  
Research and development program for the development of advanced time-temperature dependent constitutive relationships. Volume 1 Theoretical discussion  
[NASA-CR-168191-VOL-1] p 153 N84-10613  
Time dependent wave envelope finite difference analysis of sound propagation  
[NASA-TM-83744] p 185 N84-32118
- TIME DIVISION MULTIPLE ACCESS**  
Baseband processor development for the Advanced Communications Satellite Program  
p 93 A84-15628  
Serial MSK modem for the Advanced Communications Satellite Program  
p 93 A84-15629  
ACTS TDMA network control — Advanced Communication Technology Satellite  
[AIAA PAPER 84-0682] p 94 A84-25274  
Economic comparison of FDMA and TDMA options for communications by Ka-band multiple beam satellites  
[AIAA PAPER 84-0740] p 94 A84-25299  
30/20 GHz communications systems baseband processor development  
p 95 A84-38251  
Approaches to optimization of SS/TDMA time slot assignment — satellite switched time division multiple access  
[NASA-CR-168328] p 40 N84-16243  
Modular approach for satellite communication ground terminals  
[NASA-CR-168327] p 98 N84-16425
- TIME LAG**  
Estimating time and time-lag in time-of-flight velocimetry  
p 129 A84-13192
- TIME MARCHING**  
Computation of viscous flow in planar and axisymmetric ducts by an implicit marching procedure  
[AIAA PAPER 84-0256] p 114 A84-17979
- TIME MEASUREMENT**  
Estimating time and time-lag in time-of-flight velocimetry  
p 129 A84-13192
- TIME SERIES ANALYSIS**  
Identification of multivariable high performance turbofan engine dynamics from closed loop data  
p 16 A84-18582
- TIP DRIVEN ROTORS**  
Analytical and experimental investigation of stator endwall contouring in a small axial-flow turbine  
[NASA-TP-2309] p 35 N84-32388
- TITANIUM**  
Method and apparatus for coating substrates using a laser  
[NASA-CASE-LEW-13526-1] p 134 N84-22944
- TITANIUM ALLOYS**  
Method and apparatus for coating substrates using a laser  
[NASA-CASE-LEW-13526-1] p 134 N84-22944
- TOPOGRAPHY**  
Surface topographical changes measured by phase-locked interferometry  
[NASA-CR-3757] p 188 N84-16984  
Surface topography-connections between lubrication and failure initiation  
p 144 N84-24898
- TOPOLOGY**  
Flow visualization and interpretation of visualization data for deflected thrust V/STOL nozzles  
[AIAA PAPER 84-0102] p 16 A84-21852
- Flow visualization and interpretation of visualization data for deflected thrust V/STOL nozzles  
[NASA-TM-83554] p 24 N84-14147
- TORQUE**  
Application of advanced materials to rotating machines  
p 22 N84-10063  
Dynamics of early planetary gear trains  
[NASA-CR-3793] p 145 N84-26027
- TORQUE CONVERTERS**  
All-purpose bidirectional four-quadrant controller  
p 22 N84-10070
- TORSION**  
Cyclic torsion testing  
[NASA-TM-83756] p 157 N84-31687
- TORSIONAL STRESS**  
Failure analysis of a tool steel torque shaft  
p 148 A84-17546  
An analysis of traction drive torsional stiffness  
[NASA-TM-83712] p 145 N84-27043
- TORSIONAL VIBRATION**  
Dynamics of early planetary gear trains  
[NASA-CR-3793] p 145 N84-26027
- TOTAL ENERGY SYSTEMS**  
Develop and test fuel cell powered on-site integrated total energy system  
[NASA-CR-168159] p 164 N84-11581  
Develop and test fuel cell powered on-site integrated total energy systems Phase 3 Full-scale power plant development  
[NASA-CR-168294] p 164 N84-13672
- TOUGHNESS**  
Resin selection criteria for tough composite structures  
[NASA-TM-83449] p 81 N84-10310  
Effect of crack curvature on stress intensity factors for ASTM standard compact tension specimens  
[NASA-CR-168280] p 153 N84-11513
- TOWERS**  
Large, horizontal-axis wind turbines  
[NASA-TM-83546] p 169 N84-27327
- TRACTION**  
Elastic model of the traction behavior of two traction lubricants  
p 136 A84-28791  
Spin analysis of concentrated traction contacts  
[NASA-TM-83713] p 145 N84-27042  
An analysis of traction drive torsional stiffness  
[NASA-TM-83712] p 145 N84-27043  
Solid lubrication design methodology  
[NASA-CR-174690] p 196 N84-33309
- TRADEOFFS**  
Broad specification fuels combustion technology program  
[NASA-CR-168179] p 89 N84-15283
- TRAILING EDGES**  
Calculation of transonic flow in a linear cascade  
[AIAA PAPER 84-1301] p 6 A84-40241  
Calculation of transonic flow in a linear cascade  
[NASA-TM-83697] p 10 N84-24539
- TRAJECTORY ANALYSIS**  
Effect of geometry on airfoil icing characteristics  
p 12 A84-37935
- TRANSFER FUNCTIONS**  
A TWT amplifier with a linear power transfer characteristic and improved efficiency  
[AIAA PAPER 84-0762] p 104 A84-41035  
Identification of multivariable high-performance turbofan engine dynamics from closed loop data  
p 28 N84-20580  
A TWT amplifier with a linear power transfer characteristic and improved efficiency  
[NASA-TM-83590] p 108 N84-21803
- TRANSFORMERS**  
Lightweight, high-frequency transformers  
p 105 N84-10066  
Development of high frequency low weight power magnetics for aerospace power systems  
[NASA-TM-83656] p 109 N84-22892
- TRANSIENT PRESSURES**  
Transient flow combustion  
p 62 N84-20560
- TRANSIENT RESPONSE**  
A large-signal dynamic simulation for the series resonant converter  
p 103 A84-23258  
Transient flow analysis of the AEDC/JHPDE MHD generator  
p 189 A84-24049  
Blade loss transient dynamics analysis with flexible bladed disk  
[NASA-CR-168176] p 23 N84-13193  
Effects of different rub models on simulated rotor dynamics  
[NASA-TP-2220] p 142 N84-17590  
Monolithic microwave integrated circuit devices for active array antennas  
[NASA-CR-173981] p 112 N84-34675
- TRANSISTOR AMPLIFIERS**  
A three-stage power amplifier for a 20 GHz monolithic transmit module  
p 102 A84-22673
- TRANSISTOR CIRCUITS**  
Design considerations for FET-gated power transistors  
p 102 A84-18414
- TRANSISTORS**  
Improved transistor-controlled and commutated brushless DC motors for electric vehicle propulsion  
[NASA-CR-168053] p 105 N84-10450  
The 25 kW resonant dc/dc power converter  
[NASA-CR-168273] p 108 N84-17481
- TRANSMISSION**  
Precision of spiral-bevel gears  
[ASME PAPER 82-WA/DE-33] p 135 A84-15950
- TRANSMISSION CIRCUITS**  
A three-stage power amplifier for a 20 GHz monolithic transmit module  
p 102 A84-22673
- TRANSMISSION EFFICIENCY**  
Test results for 27 5-to-30-GHz communications satellite receivers  
[NASA-TM-83662] p 100 N84-27954
- TRANSMISSION LINES**  
Preliminary investigation of an electrical network model for ultrasonic scattering  
[NASA-CR-3770] p 149 N84-17606  
Parametric analysis of hollow conductor parallel and coaxial transmission lines for high frequency space power distribution  
[NASA-TM-83601] p 46 N84-20639  
Millimeter wave transmission systems and related devices  
[NASA-CR-179515] p 99 N84-24918
- TRANSMISSIONS (MACHINE ELEMENTS)**  
Kinematic precision of gear trains  
[ASME PAPER 82-WA/DE-34] p 135 A84-15951  
New propulsion components for electric vehicles  
p 103 A84-30209  
Development of large rotorcraft transmissions  
p 21 A84-46354  
NASA transmission research and its probable effects on helicopter transmission design  
p 139 A84-46355  
Electric vehicle propulsion alternatives  
[NASA-TM-83504] p 166 N84-20017  
Transmission efficiency measurements and correlations with physical characteristics of the lubricant  
[NASA-TM-83740] p 147 N84-30293  
Summary of drive-train component technology in helicopters  
[NASA-TM-83726] p 147 N84-30294  
Thermal analysis of a planetary transmission with spherical roller bearings operating after complete loss of oil  
[NASA-TP-2367] p 147 N84-32824
- TRANSMITTER RECEIVERS**  
Design considerations for a monolithic, GaAs, dual-mode, QPSK/QASK, high-throughput rate transceiver  
[NASA-CR-173560] p 110 N84-24974
- TRANSMITTERS**  
A 20-GHz IMPATT transmitter  
[NASA-CR-168076] p 106 N84-11385  
30/20 GHz spacecraft GaAs FET solid state transmitter for trunking and customer-premise-service application  
[NASA-CR-168276] p 107 N84-16463  
The 20 GHz spacecraft FET solid state transmitter  
[NASA-CR-168240] p 107 N84-17477  
The 20 GHz solid state transmitter design, impact diode development and reliability assessment  
[NASA-CR-174716] p 112 N84-33715
- TRANSMUTATION**  
Development and fabrication of a 'high current, fast recovery power diode  
[NASA-CR-168193] p 106 N84-13443
- TRANSONIC FLOW**  
Application of a finite element algorithm to the solution of steady transonic Euler equations  
p 3 A84-10133  
Inlet flow distortion in turbomachinery - Comparison of theory and experiment in a transonic fan stage  
p 3 A84-13592  
A numerical model of acoustic choking I - Shock free solutions  
p 180 A84-21250  
Finite element formulation of transonic flow problems  
p 116 A84-25859  
Redesign and cascade tests of a supercritical controlled diffusion stator blade-section  
[AIAA PAPER 84-1207] p 5 A84-36960  
Calculation of transonic flow in a linear cascade  
[AIAA PAPER 84-1301] p 6 A84-40241  
Transonic cascade flow analysis using viscous/inviscid coupling concepts  
[AIAA PAPER 84-2159] p 6 A84-46103  
Investigation of the three-dimensional flow field within a transonic fan rotor - Experiment and analysis  
[ASME PAPER 84-GT-200] p 7 A84-46995  
Investigation of flow phenomena in a transonic fan rotor using laser anemometry  
[NASA-TM-83555] p 9 N84-17143

- Redesign and cascade tests of a supercritical controlled diffusion stator blade-section  
[NASA-TM-83635] p 10 N84-22533
- Calculation of transonic flow in a linear cascade  
[NASA-TM-83697] p 10 N84-24539
- Unsteady transonic flow in cascades  
[NASA-TM-83780] p 11 N84-32351
- A linear aerodynamic analysis for unsteady transonic cascades  
[NASA-CR-3833] p 11 N84-32355
- TRANSONIC FLUTTER**
- Subsonic/transonic stall flutter investigation of a rotating wing  
[NASA-CR-174625] p 36 N84-33417
- TRANSONIC SPEED**
- Unsteady transonic flow in cascades  
[NASA-TM-83780] p 11 N84-32351
- TRANSPARATION**
- Correlation of thermophoretically-modified small particle diffusional deposition rates in forced convection systems with variable properties, transpiration cooling and/or viscous dissipation p 117 A84-32323
- TRANSPONDERS**
- A companion of the domestic satellite communications forecast to the year 2000  
[NASA-TM-83516] p 96 N84-10405
- Advanced technology satellites in the commercial environment. Volume 1: Executive summary  
[NASA-CR-174635-VOL-1] p 38 N84-20611
- Advanced technology satellites in the commercial environment, volume 2  
[NASA-CR-174635-VOL-2] p 38 N84-20612
- TRANSPORT AIRCRAFT**
- Energy efficient engine program contributions to aircraft fuel conservation  
[NASA-TM-83741] p 34 N84-29876
- TRANSPORT PROPERTIES**
- Transport processes in dendritic crystallization p 191 N84-28621
- TRANSPORT THEORY**
- Mass and momentum turbulent transport experiments with confined swirling coaxial jets  
[NASA-CR-168252] p 124 N84-17530
- TRANSPORTATION**
- Catalog of selected heavy duty transport energy management models  
[NASA-CR-168299] p 194 N84-14991
- TRAVELING WAVE AMPLIFIERS**
- A TWT amplifier with a linear power transfer characteristic and improved efficiency  
[AIAA PAPER 84-0762] p 104 A84-41035
- Ladder supported ring bar circuit  
[NASA-CASE-LEW-13570-1] p 106 N84-16452
- A TWT amplifier with a linear power transfer characteristic and improved efficiency  
[NASA-TM-83590] p 108 N84-21803
- TRAVELING WAVE TUBES**
- A TWT amplifier with a linear power transfer characteristic and improved efficiency  
[AIAA PAPER 84-0762] p 104 A84-41035
- Performance of computer-designed small-size multistage depressed collectors for a high-perveance traveling wave tube  
[NASA-TP-2248] p 106 N84-15394
- Beam impingement angle effects on secondary electron emission characteristics of textured pyrolytic graphite  
[NASA-TP-2285] p 82 N84-18400
- A TWT amplifier with a linear power transfer characteristic and improved efficiency  
[NASA-TM-83590] p 108 N84-21803
- Users' manual for computer program for three-dimensional analysis of coupler-cavity traveling wave tubes  
[NASA-CR-168269] p 109 N84-23841
- Secondary electron emission characteristics of ion-textured copper and high-purity isotropic graphite surfaces  
[NASA-TP-2342] p 86 N84-28989
- TRAVELING WAVES**
- Vibration and flutter of mistuned bladed-disk assemblies  
[NASA-TM-83634] p 156 N84-23923
- TRIBOLOGY**
- The X-ray photoelectron spectroscopy depth profiling and tribological characterization of ion-plated gold on various metals p 50 A84-20465
- Polyimides formulated from a partially fluorinated diamine for aerospace tribological applications p 80 A84-40594
- Numerical methods and computers used in elastohydrodynamic lubrication  
[NASA-TM-83524] p 141 N84-11498
- Surface topographical changes measured by phase-locked interferometry  
[NASA-CR-3757] p 188 N84-16984
- Tribological characteristics of gold films deposited on metals by ion plating and vapor deposition  
[NASA-TM-83572] p 69 N84-17352
- Friction and wear of iron in sulfuric acid  
[NASA-TP-2289] p 71 N84-21716
- Friction and wear of nickel in sulfuric acid  
[NASA-TP-2290] p 72 N84-21721
- Tribology in the 80's Volume 1: Sessions 1 to 4  
[NASA-CP-2300-VOL-1] p 144 N84-23891
- Importance and definition of materials in tribology  
Status of understanding p 84 N84-23893
- Metallic adhesion and bonding p 72 N84-23897
- Considerations in friction and wear p 144 N84-23903
- Low wear partially fluorinated polyimides  
[NASA-TM-83629] p 84 N84-24808
- Tribology in the 80's Volume 2: Sessions 5 - 8  
[NASA-CP-2300-VOL-2] p 144 N84-25047
- Status of understanding for gear materials p 144 N84-25061
- Tribological applications of surface analysis  
[NASA-TM-83707] p 51 N84-25766
- Microstructure and surface chemistry of amorphous alloys important to their friction and wear behavior  
[NASA-TM-83762] p 76 N84-32508
- The friction behavior of semiconductors Si and GaAs in contact with pure metals  
[NASA-TM-83779] p 87 N84-32531
- TROPICAL METEOROLOGY**
- Tropical response to lateral forcing with a latitudinally and zonally nonuniform basic state p 174 A84-40399
- TUBES**
- Flame radiation and linear heat transfer in a tubular can combustor  
[AIAA PAPER 84-0443] p 16 A84-21300
- Flame radiation and linear heat transfer in a tubular-can combustor  
[NASA-TM-83538] p 23 N84-13188
- TUNGSTEN**
- Tungsten-fiber-reinforced superalloy composite, high-temperature component design considerations p 53 A84-28241
- Correlation of electron emission with changes in the surface concentration of barium and oxygen on a tungsten surface p 60 A84-45917
- TUNGSTEN ALLOYS**
- Influence of cobalt, tantalum and tungsten on the high temperature mechanical properties of single crystal nickel-base superalloys  
[NASA-TM-83479] p 70 N84-17355
- TUNING**
- Model development and statistical investigation of turbine blade mistuning p 17 A84-31905
- Effects of structural coupling on mistuned cascade flutter and response  
[ASME PAPER 83-GT-117] p 151 A84-33701
- Vibration and flutter of mistuned bladed-disk assemblies  
[NASA-TM-83634] p 156 N84-23923
- TUNNEL DIODES**
- Parallel-processing with surface plasmons, a new strategy for converting the broad solar spectrum p 160 A84-23006
- Plasmon device design Conversion from surface to junction plasmons with grating-couplers p 171 N84-29330
- TURBIDITY**
- Turbidity very near the critical point of methanol-cyclohexane mixtures p 192 A84-30391
- TURBINE BLADES**
- Material removal considerations for metal-ceramic abradable turbine seal systems p 135 A84-15575
- Tungsten-fiber-reinforced superalloy composite, high-temperature component design considerations p 53 A84-28241
- Model development and statistical investigation of turbine blade mistuning p 17 A84-31905
- Effects of structural coupling on mistuned cascade flutter and response  
[ASME PAPER 83-GT-117] p 151 A84-33701
- Effect of an oscillating flow direction on leading edge heat transfer p 117 A84-33705
- Improved design of subcritical and supercritical cascades using complex characteristics and boundary-layer correction p 5 A84-38839
- Performance of a high-work low aspect ratio turbine tested with a realistic inlet radial temperature profile  
[AIAA PAPER 84-1161] p 19 A84-40239
- Structural dynamics of rotating bladed-disk assemblies coupled with flexible shaft motions p 21 A84-44645
- Vibrations of twisted cantilevered plates - Experimental investigation  
[ASME PAPER 84-GT-96] p 152 A84-46937
- The interaction between mistuning and friction in the forced response of bladed disk assemblies  
[ASME PAPER 84-GT-139] p 152 A84-46957
- Examination, evaluation and repair of laminated wood blades after service on the Mod-OA wind turbine  
[NASA-TM-83483] p 163 N84-10664
- Development of strain tolerant thermal barrier coating systems, tasks 1 - 3  
[NASA-CR-168251] p 81 N84-12312
- A graphics subsystem retrofit design for the bladed-disk data acquisition system  
[NASA-TM-83510] p 175 N84-12730
- Blade loss transient dynamics analysis with flexible bladed disk  
[NASA-CR-168176] p 23 N84-13193
- Use of the WEST-1 wind turbine simulator to predict blade fatigue load distribution  
[NASA-TM-83532] p 165 N84-14586
- Low-cost single-crystal turbine blades, volume 1  
[NASA-CR-168218] p 68 N84-15247
- Review and status of heat-transfer technology for internal passages of air-cooled turbine blades  
[NASA-TP-2232] p 126 N84-21828
- Thermal stress analysis for a wood composite blade --- wind turbines  
[NASA-CR-173394] p 156 N84-21903
- Performance of a high-work low aspect ratio turbine tested with a realistic inlet radial temperature profile  
[NASA-TM-83655] p 32 N84-24589
- Fabrication development for ODS-superalloy, air-cooled turbine blades  
[NASA-CR-174650] p 32 N84-25711
- Energy efficient engine high-pressure turbine supersonic cascade technology report  
[NASA-CR-165567] p 33 N84-27739
- Energy efficient engine high-pressure turbine detailed design report  
[NASA-CR-165608] p 33 N84-28788
- Detailed flow measurements in casing boundary layer of 429-meter-per-second tip-speed two-stage fan  
[NASA-TP-2052] p 34 N84-28795
- Thermal-stress analysis for wood composite blade --- horizontal axis wind turbines  
[NASA-CR-173830] p 157 N84-31685
- Nonlinear analysis for high-temperature composites  
Turbine blades/vanes p 158 N84-31699
- Turbine blade and vane heat flux sensor development, phase 1  
[NASA-CR-168297] p 134 N84-32790
- TURBINE ENGINES**
- Application of laser anemometry in turbine engine research p 130 A84-22872
- Performance of a high-work low aspect ratio turbine tested with a realistic inlet radial temperature profile  
[AIAA PAPER 84-1161] p 19 A84-40239
- Supersonic STOVL aircraft with turbine bypass/turbo-compressor engines  
[AIAA PAPER 84-1403] p 19 A84-40247
- Optimization of fringe-type laser anemometers for turbine engine component testing  
[AIAA PAPER 84-1459] p 131 A84-40248
- The aerodynamic design and performance of the NASA/GE E3 low pressure turbine  
[AIAA PAPER 84-1162] p 21 A84-44186
- Energy efficient engine: Flight propulsion system, preliminary analysis and design update  
[NASA-CR-167980] p 22 N84-11170
- Size scale effect in cavitation erosion  
[NASA-TM-83533] p 67 N84-11254
- Application of laser anemometry in turbine engine research  
[NASA-TM-83513] p 131 N84-11456
- A generalized computer code for developing dynamic gas turbine engine models (DIGTEM)  
[NASA-TM-83508] p 22 N84-12166
- Blade loss transient dynamics analysis with flexible bladed disk  
[NASA-CR-168176] p 23 N84-13193
- PREWATE: An interactive preprocessing computer code to the Weight Analysis of Turbine Engines (WATE) computer code  
[NASA-TM-83545] p 176 N84-13812
- Aerothermal modeling Executive summary  
[NASA-CR-168330] p 25 N84-15152
- Variable stator radial turbine  
[NASA-CR-174663] p 29 N84-22568
- Lewis Research Center spin up and its use in vibration analysis of rotating systems  
[NASA-TP-2304] p 30 N84-24578
- Rotorcraft contingency power study  
[NASA-CR-174675] p 31 N84-24580
- Supersonic STOVL aircraft with turbine bypass/turbo-compressor engines  
[NASA-TM-83686] p 31 N84-24582
- Performance of a high-work low aspect ratio turbine tested with a realistic inlet radial temperature profile  
[NASA-TM-83655] p 32 N84-24589

- Optimization of fringe-type laser anemometers for turbine engine component testing  
[NASA-TM-83658] p 133 N84-25019
- Study of effects of fuel properties in turbine-powered business aircraft  
[NASA-CR-174627] p 91 N84-25854
- Energy efficient engine high-pressure turbine supersonic cascade technology report  
[NASA-CR-165567] p 33 N84-27739
- Energy efficient engine high-pressure turbine detailed design report  
[NASA-CR-165608] p 33 N84-28788
- Response of a small-turboshaft-engine compression system to inlet temperature distortion  
[NASA-TM-83765] p 36 N84-33414
- TURBINE PUMPS**  
Selection of burn-resistant materials for oxygen-driven turbopumps  
[AIAA PAPER 84-1267] p 43 A84-35157
- TURBINE WHEELS**  
Labyrinth seal forces on a whirling rotor  
p 135 A84-13228
- NASTRAN forced vibration analysis of rotating cyclic structures  
[ASME PAPER 83-DET-20] p 151 A84-29103
- Stagger angle dependence of inertial and elastic coupling in bladed disks  
p 151 A84-31903
- Model development and statistical investigation of turbine blade mistuning  
p 17 A84-31905
- TURBINES**  
Assessment of three-dimensional inviscid codes and loss calculations for turbine aerodynamic computations  
[NASA-TM-83571] p 8 N84-16142
- Aeronautics and Space Engineering Board Aeronautics Assessment Committee  
[NASA-TM-85594] p 93 N84-22771
- Energy efficient engine Low-pressure turbine subsonic cascade component development and integration program  
[NASA-CR-165592] p 33 N84-27739
- Energy efficient engine Turbine intermediate case and low-pressure turbine component test hardware detailed design report  
[NASA-CR-167973] p 33 N84-28789
- TURBOCOMPRESSORS**  
Three-dimensional flowfield inside a low-speed axial flow compressor rotor  
p 3 A84-13574
- Supersonic STOVL aircraft with turbine bypass/turbo-compressor engines  
[AIAA PAPER 84-1403] p 19 A84-40247
- Inlet boundary layer effects in an axial compressor rotor. I Blade-to-blade effects  
[ASME PAPER 84-GT-84] p 6 A84-46926
- Inlet boundary layer effects in an axial compressor rotor II - Throughflow effects  
[ASME PAPER 84-GT-85] p 7 A84-46927
- Loss reduction in axial-flow compressors through low-speed model testing  
[ASME PAPER 84-GT-184] p 7 A84-46985
- Secondary flow spanwise deviation model for the stators of NASA middle compressor stages  
[NASA-CR-173360] p 27 N84-18202
- Advanced turbocharger design study program  
[NASA-CR-174633] p 143 N84-21879
- Combustor liner construction  
[NASA-CASE-LEW-14035-1] p 30 N84-24577
- Supersonic STOVL aircraft with turbine bypass/turbo-compressor engines  
[NASA-TM-83686] p 31 N84-24582
- Numerical aspects of unsteady flow calculations  
p 128 N84-25968
- PURDU-WINCOF. A computer code for establishing the performance of a fan-compressor unit with water ingestion  
[NASA-CR-168005] p 34 N84-29875
- Investigation of the three-dimensional flow field within a transonic fan rotor Experiment and analysis  
[NASA-TM-83739] p 11 N84-32357
- Diesel engine catalytic combustor system --- aircraft engines  
[NASA-CASE-LEW-12995-1] p 148 N84-33808
- TURBOPROP ENGINES**  
Effects of wind on turboprop engines in outdoor static test stands  
[AIAA PAPER 83-2766] p 15 A84-15204
- Use of cooling air heat exchangers as replacements for hot section strategic materials  
[AIAA PAPER 83-2540] p 15 A84-15205
- Supersonic fan engines for military aircraft  
[AIAA PAPER 83-2541] p 15 A84-15206
- Identification of multivariable high performance turboprop engine dynamics from closed loop data  
p 16 A84-18582
- Tone generation by rotor-downstream strut interaction  
p 16 A84-22174
- Investigation of mixing in a turboprop exhaust duct. II Computer code application and verification  
p 17 A84-27140
- Finite element-integral acoustic simulation of JT15D turboprop engine  
p 182 A84-41132
- An application of tensor ideas to nonlinear modeling of a turboprop jet engine  
p 20 A84-42382
- Development of dynamic simulation of TF34-GE-100 turboprop engine with post-stall capability  
[AIAA PAPER 84-1184] p 20 A84-44178
- Low flight speed fan noise from a supersonic inlet  
p 182 A84-44508
- Structural dynamics of rotating bladed-disk assemblies coupled with flexible shaft motions  
p 21 A84-44645
- F100 multivariable control synthesis program Computer implementation of the F100 multivariable control algorithm  
[NASA-TP-2231] p 22 N84-11171
- PREWATE. An interactive preprocessing computer code to the Weight Analysis of Turbine Engines (WATE) computer code  
[NASA-TM-83545] p 176 N84-13812
- HYTESS. A hypothetical turboprop engine simplified simulation  
[NASA-TM-83561] p 26 N84-16184
- Hot-flow tests of a series of 10-percent-scale turboprop forced mixing nozzles  
[NASA-TP-2268] p 123 N84-17525
- Parallel processor engine model program  
[NASA-CR-174641] p 27 N84-19353
- Low frequency noise in a quiet, clean, general aviation turboprop engine  
[NASA-TM-83520] p 183 N84-20320
- Fan noise reduction achieved by removing tip flow irregularities behind the rotor - forward arc test configurations  
[NASA-TM-83616] p 184 N84-23235
- NASA broad-specification fuels combustion technology program  
p 62 N84-23637
- Development of dynamic simulation of TF34-GE-100 turboprop engine with post-stall capability  
[NASA-TM-83560] p 32 N84-25712
- Energy efficient engine program contributions to aircraft fuel conservation  
[NASA-TM-83741] p 34 N84-29876
- Energy efficient engine component development and integration program  
[NASA-CR-173884] p 35 N84-32389
- TURBOPROPS**  
Inlet flow distortion in turboprop machinery - Comparison of theory and experiment in a transonic fan stage  
p 3 A84-13592
- Vibration and flutter of mistuned bladed-disk assemblies  
[NASA-TM-83634] p 156 N84-23923
- Identification of quasi-steady compressor characteristics from transient data  
[NASA-CR-174685] p 36 N84-34444
- TURBOGENERATORS**  
Wind turbine generator interaction with conventional diesel generators on Block Island, Rhode Island. Volume 2: Data analysis  
[NASA-CR-168319] p 172 N84-31783
- Computer simulation of the heavy-duty turbo-compounded diesel cycle for studies of engine efficiency and performance  
[NASA-CR-174755] p 196 N84-33306
- TURBOJET ENGINE CONTROL**  
Application of advanced control techniques to aircraft propulsion systems  
p 28 N84-20590
- TURBOJET ENGINES**  
Environmental and high strain rate effects on composites for engine applications  
p 51 A84-17444
- Overview of liquid lubricants for advanced aircraft  
[NASA-TM-83529] p 81 N84-11296
- A graphics subsystem retrofit design for the bladed-disk data acquisition system  
[NASA-TM-83510] p 175 N84-12730
- TURBOMACHINE BLADES**  
The coupled response of turbomachinery blading to aerodynamic excitations  
p 17 A84-26959
- Calculation of transonic flow in a linear cascade  
[AIAA PAPER 84-1301] p 6 A84-40241
- Inlet boundary layer effects in an axial compressor rotor. I Blade-to-blade effects  
[ASME PAPER 84-GT-84] p 6 A84-46926
- Improved finite-difference vibration analysis of pretwisted, tapered beams  
[NASA-TM-83549] p 154 N84-16568
- Programs for calculating quasi-three-dimensional flow in a turbomachine blade row  
[NASA-TM-83588] p 9 N84-17138
- The influence of gyroscopic forces on the dynamic behavior and flutter of rotating blades  
[NASA-CR-175444] p 27 N84-20524
- Vibration and flutter of mistuned bladed-disk assemblies  
[NASA-TM-83634] p 156 N84-23923
- Calculation of transonic flow in a linear cascade  
[NASA-TM-83697] p 10 N84-24539
- The boundary layer on compressor cascade blades  
[NASA-CR-173514] p 127 N84-25001
- Unsteady transonic flow in cascades  
[NASA-TM-83780] p 11 N84-32351
- TURBOMACHINERY**  
Hybrid C-H grids for turbomachinery cascades --- parabolic and Cartesian coordinates  
p 3 A84-11591
- A rapid blade-to-blade solution for use in turbomachinery design  
[ASME PAPER 83-GT-67] p 4 A84-31289
- Determination of compressor in-stall characteristics from engine surge transients  
[AIAA PAPER 84-1206] p 18 A84-36959
- Analysis of inviscid and viscous flows in cascades with an explicit multiple-grid algorithm  
[AIAA PAPER 84-1663] p 5 A84-38043
- Calculation of transonic flow in a linear cascade  
[AIAA PAPER 84-1301] p 6 A84-40241
- Forced vibration analysis of rotating cyclic structures in NASTRAN  
[NASA-CR-165429] p 153 N84-11514
- Design study of magnetic eddy-current vibration suppression dampers for application to cryogenic turbomachinery  
[NASA-CR-173273] p 141 N84-16562
- Analysis of inviscid and viscous flows in cascades with an explicit multiple-grid algorithm  
[NASA-TM-83636] p 1 N84-22527
- Oxidizing seal for a turbine tip gas path  
[NASA-CASE-LEW-14053-1] p 29 N84-22563
- Determination of compressor in-stall characteristics from engine surge transients  
[NASA-TM-83639] p 29 N84-22566
- Method of fabricating an abradable gas path seal  
[NASA-CASE-LEW-13269-2] p 143 N84-22957
- Improved compliant hydrodynamic fluid journal bearing  
[NASA-CASE-LEW-13670-1] p 143 N84-22959
- Calculation of transonic flow in a linear cascade  
[NASA-TM-83697] p 10 N84-24539
- Lewis Research Center spin rig and its use in vibration analysis of rotating systems  
[NASA-TP-2304] p 30 N84-24578
- Unsteady flow in turbomachinery. An overview  
p 128 N84-25961
- Numerical aspects of unsteady flow calculations  
p 128 N84-25968
- Detailed flow measurements in casing boundary layer of 429-meter-per-second-tip-speed two-stage fan  
[NASA-TP-2052] p 34 N84-28795
- Advanced Gas Turbine (AGT)  
[NASA-CR-174694] p 195 N84-29805
- TURBOPROP AIRCRAFT**  
An analytical method to predict efficiency of aircraft gearboxes  
[AIAA PAPER 84-1500] p 20 A84-44180
- A possible explanation for the present difference between linear noise theory and experimental data for supersonic helical tip speed propellers  
[NASA-TM-83467] p 183 N84-14874
- An analytical method to predict efficiency of aircraft gearboxes  
[NASA-TM-83716] p 2 N84-25806
- Summary of recent NASA propeller research  
[NASA-TM-83733] p 2 N84-32344
- TURBOPROP ENGINES**  
Flutter analysis of advanced turbopropellers  
p 152 A84-36492
- Advanced propfan drive system characteristics and technology needs  
[AIAA PAPER 84-1194] p 18 A84-36957
- Fuel savings potential of the NASA Advanced Turboprop Program  
[NASA-TM-83736] p 35 N84-29878
- TURBOSHAPTS**  
The application of LQR synthesis techniques to the turboshaft engine control problem  
[AIAA PAPER 84-1455] p 21 A84-44185
- Structural dynamics of rotating bladed-disk assemblies coupled with flexible shaft motions  
p 21 A84-44645
- A real-time, portable, microcomputer-based jet engine simulator  
[NASA-TM-83550] p 176 N84-16812
- Real-time hybrid computer simulation of a small turboshaft engine and control system  
[NASA-TM-83579] p 28 N84-21548
- Rotorcraft contingency power study  
[NASA-CR-174675] p 31 N84-24580
- Dual clearance squeeze film damper for high load conditions  
[NASA-TM-83619] p 144 N84-25064



- Response of a small-turboshaft-engine compression system to inlet temperature distortion  
[NASA-TM-83765] p 36 N84-33414
- TURBULENCE**
- Effect of location in an array, on heat transfer to a short cylinder in crossflow p 119 A84-36150
- Executive summary, aerothermal modeling program, phase 1  
[NASA-CR-174602] p 60 N84-12263
- Free stream turbulence and density ratio effects on the interaction region of a jet in a cross flow p 125 N84-20546
- TURBULENCE EFFECTS**
- Turbulence characteristics of swirling flowfields  
[NASA-CR-175392] p 124 N84-19744
- TURBULENCE BOUNDARY LAYER**
- Three-dimensional turbulent boundary-layer development on a fan rotor blade p 3 A84-17437
- Experimental studies on two dimensional shock boundary layer interactions  
[AIAA PAPER 84-0099] p 3 A84-17881
- Turbulent boundary-layer flow and structure on a convex wall and its redevelopment on a flat wall p 115 A84-21378
- Flat plate heat transfer for laminar transition and turbulent boundary layers using a shock tube  
[AIAA PAPER 84-1726] p 120 A84-37467
- An experimental study of the compressor rotor blade boundary layer  
[ASME PAPER 84-GT-193] p 7 A84-46991
- An experimental study of the properties of surface pressure fluctuations in strong adverse pressure gradient turbulent boundary layers  
[NASA-CR-175410] p 9 N84-20488
- Scaling and modeling of three-dimensional, end-wall, turbulent boundary layers  
[NASA-CR-3792] p 127 N84-25941
- Turbulence and surface heat transfer near the stagnation point of a circular cylinder in turbulent flow  
[NASA-TM-83732] p 128 N84-29157
- TURBULENT FLOW**
- Evaporation and combustion of sprays p 58 A84-11636
- Turbulent flow field calculations in an internal combustion engine equipped with two valves p 112 A84-13311
- Secondary effects in combustion instabilities leading to flashback p 58 A84-17436
- Computation of viscous flow in planar and axisymmetric ducts by an implicit marching procedure  
[AIAA PAPER 84-0256] p 114 A84-17979
- Accuracy and directional sensitivity of the single-wire technique  
[AIAA PAPER 84-0367] p 130 A84-18047
- Calculations of turbulent mass transport in a bluff-body diffusion-flame combustor  
[AIAA PAPER 84-0372] p 114 A84-18048
- Limitations and empirical extensions of the k-epsilon model as applied to turbulent confined swirling flows  
[AIAA PAPER 84-0441] p 114 A84-18096
- The production of turbulent stress in a shear flow by irrotational fluctuations p 115 A84-18357
- An invariant derivation of flame stretch p 58 A84-18925
- High frequency green function for aerodynamic noise in moving media. I - General theory. II - Noise from a spreading jet p 180 A84-21273
- The production of turbulent stress in a shear flow by irrotational fluctuations p 115 A84-21390
- Aeroacoustics of turbulent shear flows p 181 A84-22584
- On the design of contractions and settling chambers for optimal turbulence manipulations in wind tunnels  
[AIAA PAPER 84-0536] p 115 A84-22922
- Small-amplitude viscous motion on arbitrary potential flows p 116 A84-24892
- Developing flow in S-shaped ducts p 116 A84-28709
- Stability and structure of stretched vortices  
[AD-A142913] p 117 A84-29798
- Time-resolved density measurements in premixed turbulent flames p 59 A84-32612
- Swirl flow turbulence modeling  
[AIAA PAPER 84-1376] p 118 A84-35196
- Swirl, confinement and nozzle effects on confined turbulent flow  
[AIAA PAPER 84-1377] p 118 A84-35197
- Preliminary investigation of a two-zone swirl flow combustor  
[AIAA PAPER 84-1169] p 17 A84-36951
- Five-hole pitot probe measurements of swirl, confinement and nozzle effects on confined turbulent flow  
[AIAA PAPER 84-1605] p 120 A84-38000

- Formation and destruction of vortices in a motored four-stroke piston-cylinder configuration p 139 A84-38838
- A review of internal combustion engine combustion chamber process studies at NASA Lewis Research Center  
[AIAA PAPER 84-1316] p 121 A84-40242
- Computational modeling of jet induced mixing of cryogenic propellants in low-G  
[AIAA PAPER 84-1344] p 121 A84-40243
- Turbulent solutions of the equations of fluid motion p 121 A84-41156
- Turbulence modeling for three-dimensional shear flows over curved rotating bodies p 122 A84-48138
- Prediction of turbulent flow past a prosthetic heart valve p 175 A84-49108
- A theoretical and experimental study of turbulent particle-laden jets  
[NASA-CR-168293] p 23 N84-13187
- Numerical modeling of turbulent flow in a channel  
[NASA-CR-168278] p 23 N84-13189
- Generation of sound in turbulent shear flows p 183 A84-15031
- Confined turbulent swirling recirculating flow predictions  
[NASA-CR-175397] p 125 N84-19745
- Swirl, expansion ratio and blockage effects on confined turbulent flow  
[NASA-CR-175391] p 125 N84-19746
- Turbulent swirling combustion p 61 N84-20535
- Numerical modeling of turbulent flow p 125 N84-20538
- The influence of large-scale motion on turbulent transport for confined coaxial jets p 125 N84-20542
- Random vortex method for combustor flows p 62 N84-20558
- Extension to an analysis of turbulent swirling compressible flow for application to axisymmetric small gas turbine ducts  
[NASA-CR-165597] p 195 N84-21445
- Review and status of heat-transfer technology for internal passages of air-cooled turbine blades  
[NASA-TP-2232] p 126 N84-21828
- Effect of a rotor wake on heat transfer from a circular cylinder  
[NASA-TM-83613] p 126 N84-21832
- Preliminary investigation of a two-zone swirl flow combustor  
[NASA-TM-83637] p 29 N84-22565
- A review of internal combustion engine combustion chamber process studies at NASA Lewis Research Center  
[NASA-TM-83666] p 127 N84-24999
- Computational modeling of jet induced mixing of cryogenic propellants in low-G  
[NASA-CR-83703] p 127 N84-25000
- The boundary layer on compressor cascade blades  
[NASA-CR-173514] p 127 N84-25001
- Acoustic excitation A promising new means of controlling shear layers  
[NASA-TM-83772] p 10 N84-31096
- A theoretical and experimental study of turbulent evaporating sprays  
[NASA-CR-174760] p 35 N84-32390
- Experimental investigation of shock-cell noise reduction for single-stream nozzles in simulated flight, comprehensive data report. Volume 2. Laser velocimeter data  
[NASA-CR-168234-VOL-2] p 186 N84-33149
- TURBULENCE HEAT TRANSFER**
- Heat transfer in serpentine passages with turbulence promoters  
[NASA-TM-83614] p 126 N84-22911
- TURBULENCE JETS**
- Turbulence measurements in confined jets using a rotating single-wire probe technique p 113 A84-13564
- Structure of particle-laden jets - Measurements and predictions  
[AIAA PAPER 84-0038] p 113 A84-17842
- Formation and inflammation of a turbulent jet  
[AIAA PAPER 84-0572] p 114 A84-18171
- Turbulence measurements in a complex flowfield using a crossed hot-wire  
[AIAA PAPER 84-1604] p 131 A84-37999
- Experimental and theoretical study of combustion jet ignition  
[NASA-CR-168139] p 21 N84-10054
- Mass and momentum turbulent transport experiments with confined swirling coaxial jets  
[NASA-CR-168252] p 124 N84-17530
- TURBULENCE MIXING**
- Combustion in a turbulent mixing layer formed at a rearward-facing step p 58 A84-10140
- Mass and momentum turbulent transport experiments with confined swirling coaxial jets. I  
[AIAA PAPER 84-1380] p 119 A84-35664

- Further development of a method for computing three-dimensional subsonic viscous flows in turbofan lobe mixers  
[NASA-CR-168304] p 122 N84-14462
- A theoretical prediction of the acoustic pressure generated by turbulence-flame front interactions  
[NASA-TM-83587] p 184 N84-26383
- An experimental investigation of gas jets in confined swirling air flow  
[NASA-CR-3832] p 36 N84-33412
- TWISTING**
- Vibrations of twisted cantilevered plates - Experimental investigation  
[ASME PAPER 84-GT-96] p 152 A84-46937
- TWO DIMENSIONAL BOUNDARY LAYER**
- The boundary layer on compressor cascade blades  
[NASA-CR-173514] p 127 N84-25001
- TWO DIMENSIONAL FLOW**
- A direct method for the solution of unsteady two-dimensional incompressible Navier-Stokes equations p 2 A84-10078
- Experimental studies on two dimensional shock boundary layer interactions  
[AIAA PAPER 84-0099] p 3 A84-17881
- Sound generated by instability waves of supersonic flows I Two-dimensional mixing layers II - Axisymmetric jets p 181 A84-24597
- Finite-analytic numerical method for unsteady two-dimensional Navier-Stokes equations p 116 A84-25807
- Transonic cascade flow analysis using viscous/inviscid coupling concepts  
[AIAA PAPER 84-2159] p 6 A84-46103
- Numerical modeling of turbulent flow in a channel  
[NASA-CR-168278] p 23 N84-13189
- Compressor rotor aerodynamics p 26 N84-16210
- Application of improved numerical schemes p 178 N84-20537
- A linear aerodynamic analysis for unsteady transonic cascades  
[NASA-CR-3833] p 11 N84-32355
- TWO PHASE FLOW**
- Modeling of transient two-component flow using a four-point implicit method p 112 A84-13237
- Structure of particle-laden jets - Measurements and predictions  
[AIAA PAPER 84-0038] p 113 A84-17842
- Structure of nonevaporating sprays - Measurements and predictions  
[AIAA PAPER 84-0125] p 114 A84-17897
- Dynamics of two-phase face seals p 137 A84-28792
- Experimental study of bubble cavities attached to a rotating shaft in a reservoir  
[NASA-TM-83586] p 124 N84-17533
- TWO REFLECTOR ANTENNAS**
- Multibeam antenna for 30/20 GHz advanced communications satellite using offset shaped, dual reflector surfaces p 93 A84-15627

## U

- UDIMET ALLOYS**
- Effects of long-time elevated temperature exposures on hot-isostatically-pressed power-metallurgy Udimet 700 alloys with reduced cobalt contents  
[NASA-TM-83332] p 57 N84-28917
- UH-1 HELICOPTER**
- Documentation of ice shapes on the main rotor of a UH-1H helicopter in hover  
[NASA-CR-168332] p 9 N84-17139
- ULTRAHIGH FREQUENCIES**
- A 20-GHz IMPATT transmitter  
[NASA-CR-168076] p 106 N84-11385
- ULTRASONIC TESTS**
- Characterization of composite materials by means of the ultrasonic stress wave factor. p 51 A84-10430
- ULTRASONICS**
- Input-output characterization of an ultrasonic testing system by digital signal analysis  
[NASA-CR-3756] p 149 N84-15565
- The role of the reflection coefficient in precision measurement of ultrasonic attenuation  
[NASA-TM-83788] p 149 N84-32849
- Ultrasonic velocity measurement using phase-slope cross-correlation methods  
[NASA-TM-83794] p 149 N84-34769
- UNIFORM FLOW**
- Calculation of a hollow-cone liquid spray in a uniform air stream  
[AIAA PAPER 84-1322] p 118 A84-35171
- UNLOADING WAVES**
- Indentation law for composite laminates p 52 A84-27356

# UNSTEADY FLOW

- A direct method for the solution of unsteady two-dimensional incompressible Navier-Stokes equations p 2 A84-10078
- Modeling of transient two-component flow using a four-point implicit method p 112 A84-13237
- One-dimensional unsteady modeling of supersonic inlet unstart/restart [AIAA PAPER 84-0439] p 4 A84-18094
- Transient flow analysis of the AEDC/HPDE MHD generator p 189 A84-24049
- Finite-analytic numerical method for unsteady two-dimensional Navier-Stokes equations p 116 A84-25807
- Effects of unsteady free stream velocity and free stream turbulence on stagnation point heat transfer [NASA-CR-3804] p 127 N84-25943
- Unsteady flow in turbomachinery An overview p 128 N84-25961
- Numerical aspects of unsteady flow calculations p 128 N84-25968
- Unsteady transonic flow in cascades [NASA-TM-83780] p 11 N84-32351
- A linear aerodynamic analysis for unsteady transonic cascades [NASA-CR-3833] p 11 N84-32355
- UPPER STAGE ROCKET ENGINES
- Shuttle/Centaur - More capability for the 1980's [IAF PAPER 83-18] p 38 A84-11718
- USER MANUALS (COMPUTER PROGRAMS)
- Aeroelastic analysis for propellers - mathematical formulations and program user's manual [NASA-CR-3729] p 153 N84-12530
- Communications network design and costing model programmers manual [NASA-CR-168237] p 97 N84-14377
- Communications network design and costing model users manual [NASA-CR-168238] p 97 N84-14378
- Users' manual for computer program for three-dimensional analysis of coupler-cavity traveling wave tubes [NASA-CR-168259] p 109 N84-23841
- USER REQUIREMENTS
- Advanced technology satellites in the commercial environment. Volume 1- Executive summary [NASA-CR-174835-VOL-1] p 38 N84-20611
- Advanced technology satellites in the commercial environment, volume 2 [NASA-CR-174835-VOL-2] p 38 N84-20612
- UTILITIES
- Investigation of energy management strategies for photovoltaic systems - An analysis technique p 160 A84-22993

# V

## V/STOL AIRCRAFT

- Investigation of tangential blowing applied to a subsonic V/STOL inlet p 3 A84-11042
- Real-time Pegasus propulsion system model V/STOL-piloted simulation evaluation p 15 A84-17362
- Boundary layer transition effects on flow separation around V/STOL engine inlets at high incidence [AIAA PAPER 84-0432] p 4 A84-18090
- Flow visualization and interpretation of visualization data for deflected thrust V/STOL nozzles [AIAA PAPER 84-0102] p 16 A84-21852
- Tandem fan applications in advanced STOVL fighter configurations [AIAA PAPER 84-1402] p 19 A84-40245
- Supersonic STOVL aircraft with turbine bypass/turbo-compressor engines [AIAA PAPER 84-1403] p 19 A84-40247
- Analytical study of suction boundary layer control for subsonic V/STOL inlets [AIAA PAPER 84-1399] p 6 A84-44187
- Flow visualization and interpretation of visualization data for deflected thrust V/STOL nozzles [NASA-TM-83554] p 24 N84-14147
- Analytical study of blowing boundary-layer control for subsonic V/STOL inlets [NASA-TM-83576] p 8 N84-16141
- V/STOL model fan stage ng design report [NASA-CR-174688] p 29 N84-23629
- Tandem fan applications in advanced STOVL fighter configurations [NASA-TM-83689] p 30 N84-24579
- Supersonic STOVL aircraft with turbine bypass/turbo-compressor engines [NASA-TM-83686] p 31 N84-24582
- VACUUM DEPOSITION
- Diamondlike flakes [NASA-CASE-LEW-13837-2] p 54 N84-22696

## VACUUM EFFECTS

- Metal vapor vacuum arc switching - Applications and results - for launchers p 103 A84-32029
- VANES
- Investigation of the effects of pressure gradient, temperature and wall temperature ratio on the stagnation point heat transfer for circular cylinders and gas turbine vanes [NASA-CR-174667] p 30 N84-23649
- Deposition of Na2SO4 from salt-seeded combustion gases of a high velocity burner ng [NASA-TM-83751] p 129 N84-31558
- Nonlinear analysis for high-temperature composites - Turbine blades/vanes p 158 N84-31699
- VAPOR DEPOSITION
- Photodeposition of nitride insulators on 3-5 substrates [NASA-CR-173393] p 71 N84-21720
- Deposition of Na2SO4 from salt-seeded combustion gases of a high velocity burner ng [NASA-TM-83751] p 129 N84-31558
- VAPORIZING
- Alcohol cold starting - A theoretical study p 138 A84-30061
- Calculation of vaporization rates assuming various rate determining steps Application to the resistojet [NASA-TM-83757] p 51 N84-31283
- VARIABILITY
- V/STOL model fan stage ng design report [NASA-CR-174688] p 29 N84-23629
- VARIABLE GEOMETRY STRUCTURES
- Variable stator radial turbine [NASA-CR-174669] p 29 N84-22668
- VARIANCE (STATISTICS)
- Optimizing and comparing laser anemometers p 130 A84-28739
- VECTORS (MATHEMATICS)
- Direct and implicit optical matrix-vector algorithms p 187 A84-13184
- Acceleration of convergence of vector sequences [NASA-TP-2193] p 178 N84-13885
- VEGETABLES
- Utilization of alternative fuels in diesel engines [NASA-CR-174669] p 91 N84-26813
- VELOCITY
- First order ball bearing kinematics [NASA-TM-83592] p 142 N84-19816
- VELOCITY DISTRIBUTION
- Three-dimensional turbulent boundary-layer development on a fan rotor blade p 3 A84-17437
- VELOCITY MEASUREMENT
- Estimating time and time-lag in time-of-flight velocimetry p 129 A84-13192
- Structure of particle-laden jets - Measurements and predictions [AIAA PAPER 84-0038] p 113 A84-17842
- A technique combining the visibility of a Doppler signal with the peak intensity of the pedestal to measure the size and velocity of droplets in a spray [AIAA PAPER 84-0203] p 129 A84-17946
- Further time-mean measurements in confined swirling flows p 116 A84-27138
- Output statistics of laser anemometers in sparsely seeded flows p 117 A84-28738
- Optimizing and comparing laser anemometers p 130 A84-28739
- LeRC rail accelerators - Test designs and diagnostic techniques p 42 A84-32031
- Development of the phase/Doppler spray analyzer for liquid drop size and velocity characterizations [AIAA PAPER 84-1109] p 131 A84-36958
- Turbulence measurements in a complex flowfield using a crossed hot-wire [AIAA PAPER 84-1604] p 131 A84-37999
- Laser Doppler velocimeter measurement in the tip region of a compressor rotor [AIAA PAPER 84-1602] p 6 A84-39304
- Multicomponent velocity measurement in a piston-cylinder configuration using laser velocimetry [NASA-TM-83534] p 8 N84-14121
- Fuel spray diagnostics p 125 N84-20527
- Development and implementation of advanced diagnostic techniques p 132 N84-20528
- Automatic holographic droplet analysis for liquid fuel sprays p 125 N84-20531
- Experimental investigation of shock-cell noise reduction for dual-stream nozzles in simulated flight comprehensive data report. Volume 2. Laser velocimeter data, static pressures and shadowgraph photos [NASA-CR-168336-VOL-2] p 184 N84-24324
- Ultrasonic velocity measurement using phase-slope cross-correlation methods [NASA-TM-83794] p 149 N84-34769
- VENTILATION
- Heat recovery subsystem and overall system integration of fuel cell on-site integrated energy systems [NASA-CR-168309] p 166 N84-20915

## VENTING

- Modeling of zero gravity venting [NASA-TP-173503] p 127 N84-23854
- VIBRATION
- Dynamic behavior of spiral-groove and Rayleigh-Step self-acting face seals [NASA-TP-2266] p 25 N84-16181
- Lewis Research Center spin ng and its use in vibration analysis of rotating systems [NASA-TP-2304] p 30 N84-24578
- Improved methods of vibration analysis of pretwisted, airfoil blades [NASA-TM-83735] p 157 N84-30329
- VIBRATION DAMPING
- The interaction between mistuning and friction in the forced response of bladed disk assemblies [ASME PAPER 84-GT-139] p 152 A84-46957
- Optimization and mechanisms of mistuning in cascades [ASME PAPER 84-GT-196] p 21 A84-46993
- Design study of magnetic eddy-current vibration suppression dampers for application to cryogenic turbomachinery [NASA-CR-173273] p 141 N84-16562
- Dual clearance squeeze film damper for high load conditions [NASA-TM-83619] p 144 N84-25064
- VIBRATION EFFECTS
- Experimental study of uncanceled squeeze film dampers [NASA-CR-168317] p 155 N84-19927
- Advanced turbocharger design study program [NASA-TP-174633] p 143 N84-21879
- VIBRATION ISOLATORS
- Dual clearance squeeze film damper [NASA-CASE-LEW-13506-1] p 29 N84-22562
- VIBRATION MEASUREMENT
- Forced vibration analysis of rotating cyclic structures in NASTRAN [NASA-CR-165429] p 153 N84-11514
- VIBRATION MODE
- Blade loss transient dynamics analysis with flexible bladed disk [NASA-CR-168176] p 23 N84-13193
- VIBRATION SIMULATORS
- Lewis Research Center spin ng and its use in vibration analysis of rotating systems [NASA-TP-2304] p 30 N84-24578
- VIBRATION TESTS
- Measurements of self-excited rotor-blade vibrations using optical displacements [ASME PAPER 83-GT-132] p 151 A84-33702
- Vibrations of twisted cantilevered plates - Experimental investigation [ASME PAPER 84-GT-96] p 152 A84-46937
- VIDEO COMMUNICATION
- A companion of the domestic satellite communications forecast to the year 2000 [NASA-TM-83516] p 96 N84-10405
- VIDEO EQUIPMENT
- In-situ measurements of alloy oxidation/corrosion/erosion using a video camera and proximity sensor with microcomputer control [NASA-TM-83673] p 74 N84-27859
- VIDEO SIGNALS
- NTSC composite video at 1.6 bits/pel p 95 A84-49259
- VISCOPLASTICITY
- Determination of near-surface plastic deformation in sliding contacts p 140 A84-48906
- Research and development program for the development of advanced time-temperature dependent constitutive relationships. Volume 2 Programming manual [NASA-CR-168191-VOL-2] p 153 N84-10614
- VISCOSITY
- Shrinkage of amorphous silica fibers p 77 A84-13504
- An investigation into the injection molding of PMR-15 polyimide [NASA-CR-173550] p 85 N84-24810
- Lubrication of machine elements [NASA-RP-1126] p 147 N84-31640
- VISCOUS FLOW
- Computation of viscous flow in planar and axisymmetric ducts by an implicit marching procedure [AIAA PAPER 84-0256] p 114 A84-17979
- Three-dimensional viscous design methodology for advanced technology aircraft supersonic inlet systems [AIAA PAPER 84-0194] p 4 A84-21290
- Multiple-grid convergence acceleration of viscous and inviscid flow computations p 116 A84-23950
- Small-amplitude viscous motion on arbitrary potential flows p 116 A84-24892
- Application of a polynomial spline in higher-order accurate viscous-flow computations p 119 A84-35349

- Computation of three-dimensional viscous flows using a space-marching method  
[AIAA PAPER 84-1298] p 5 A84-36971
- Analysis of inviscid and viscous flows in cascades with an explicit multiple-grid algorithm  
[AIAA PAPER 84-1663] p 5 A84-38043
- Penalty function finite element analysis of steady viscous incompressible flow in rotating coordinates  
[ASME PAPER 84-GT-38] p 121 A84-46900
- On numerical simulation of viscous flows  
p 122 A84-49112
- A viscous-inviscid interactive procedure for rotational flow in cascades of two dimensional airfoils of arbitrary shape  
[NASA-CR-174609] p 7 N84-13149
- Three-dimensional viscous design methodology for advanced technology aircraft supersonic inlet systems  
[NASA-TM-83558] p 23 N84-13190
- Further development of a method for computing three-dimensional subsonic viscous flows in turbofan lobe mixers  
[NASA-CR-168304] p 122 N84-14462
- Comparison of secondary flows predicted by a viscous code and an inviscid code with experimental data for a turning duct  
[NASA-TM-83575] p 9 N84-17142
- Analysis of inviscid and viscous flows in cascades with an explicit multiple-grid algorithm  
[NASA-TM-83636] p 1 N84-22527

**VITRIFICATION**

- Analysis of grain boundary phase devitrification of Y2O3- and Al2O3-doped Si3N4  
p 79 A84-19792

**VOICE COMMUNICATION**

- A comparison of the domestic satellite communications forecast to the year 2000  
[NASA-TM-83516] p 96 N84-10405

**VOLT-AMPERE CHARACTERISTICS**

- Photovoltaic characteristics of diffused P+/N bulk GaAs solar cells  
p 161 A84-23115
- Diffused junction p(+)-n solar cells in bulk GaAs I  
Fabrication and cell performance p 161 A84-25027

**VOLTAGE CONTROLLED OSCILLATORS**

- Inherent overload protection for the series resonant converter  
p 102 A84-23255

**VOLTAGE CONVERTERS (DC TO DC)**

- Parametric study of minimum converter loss in an energy-storage dc-to-dc converter  
p 101 A84-18403
- Extensions of the discrete-average models for converter power stages  
p 102 A84-18411
- A large-signal dynamic simulation for the series resonant converter  
p 103 A84-23258
- The 25 kW resonant dc/dc power converter  
[NASA-CR-168273] p 108 N84-17481
- Input filter compensation for switching regulators  
[NASA-CR-173557] p 110 N84-24975
- Simplified dc to dc converter  
[NASA-CASE-LEW-13495-1] p 111 N84-33663

**VOLTAGE REGULATORS**

- Extensions of the discrete-average models for converter power stages  
p 102 A84-18411
- Stability analysis of a buck regulator employing input filter compensation  
p 102 A84-18412
- Low-frequency switching voltage regulators for terrestrial photovoltaic systems  
[NASA-TM-83625] p 110 N84-25926

**VOLUME**

- Volume integrals associated with the inhomogeneous Helmholtz equation. Part 1. Ellipsoidal region  
[NASA-CR-3749] p 148 N84-14525
- Volume integrals associated with the inhomogeneous Helmholtz equation Part 2 Cylindrical region, rectangular region  
[NASA-CR-3750] p 148 N84-14526

**VORTEX BREAKDOWN**

- Formation and destruction of vortices in a motored four-stroke piston-cylinder configuration  
p 139 A84-38838

**VORTEX GENERATORS**

- Vortex generating flow passage design for increased film cooling effectiveness  
[NASA-CASE-LEW-14039-1] p 126 N84-20782
- Effect of vortex generators on the power conversion performance and structural dynamic loads of the Mod-2 wind turbine  
[NASA-TM-83680] p 171 N84-29347

**VORTEX SHEDDING**

- Finite-analytic numerical method for unsteady two-dimensional Navier-Stokes equations  
p 116 A84-25807

**VORTEX SHEETS**

- The application of vortex theory to the optimum swept propeller  
[AIAA PAPER 84-0036] p 3 A84-17841

**VORTICES**

- Application of a finite element algorithm to the solution of steady transonic Euler equations  
p 3 A84-10133

- Formation and inflammation of a turbulent jet  
[AIAA PAPER 84-0572] p 114 A84-18171
- The production of turbulent stress in a shear flow by irrotational fluctuations  
p 115 A84-21390
- Stability and structure of stretched vortices  
[AD-A142913] p 117 A84-29798
- Experimental investigation of the low NOx vortex airblast annular combustor  
[AIAA PAPER 84-1170] p 18 A84-36952
- Three-dimensional stability of an elliptical vortex in a straining field  
[AD-A146317] p 120 A84-38557
- A viscous-inviscid interactive procedure for rotational flow in cascades of two dimensional airfoils of arbitrary shape  
[NASA-CR-174609] p 7 N84-13149
- Vortex generating flow passage design for increased film-cooling effectiveness and surface coverage — aircraft engine blade cooling  
[NASA-TM-83617] p 126 N84-22909
- Fan noise reduction achieved by removing tip flow irregularities behind the rotor - forward arc test configurations  
[NASA-TM-83616] p 184 N84-23235
- Direct simulations of chemically reacting turbulent mixing layers  
[NASA-CR-174640] p 32 N84-25710

**W****WALL FLOW**

- Turbulent boundary-layer flow and structure on a convex wall and its redevelopment on a flat wall  
p 115 A84-21378
- Annulus wall boundary layer development in a compressor stage, including the effects of tip clearance  
p 26 N84-16207
- Scaling and modeling of three-dimensional, end-wall, turbulent boundary layers  
[NASA-CR-3792] p 127 N84-25941

**WALL PRESSURE**

- Comparison of experimental and computational compressible flow in a S-duct  
[AIAA PAPER 84-0033] p 4 A84-19228

**WASPALOY**

- The role of cobalt on the creep of Waspaloy  
[NASA-CR-174628] p 70 N84-19523

**WASTE ENERGY UTILIZATION**

- Develop and test fuel cell powered on-site integrated total energy systems  
[NASA-CR-174714] p 170 N84-27329
- Waste heat recovery from adiabatic diesel engines by exhaust-driven Brayton cycles  
[NASA-CR-168257] p 196 N84-32307
- Steam bottoming cycle for an adiabatic diesel engine  
[NASA-CR-168255] p 196 N84-33304

**WASTE HEAT**

- Waste heat recovery from adiabatic diesel engines by exhaust-driven Brayton cycles  
[NASA-CR-168257] p 196 N84-32307
- Steam bottoming cycle for an adiabatic diesel engine  
[NASA-CR-168255] p 196 N84-33304

**WATER INJECTION**

- Rotorcraft contingency power study  
[NASA-CR-174675] p 31 N84-24580

**WATER VAPOR**

- Forced convection heat transfer to air/water vapor mixtures  
[NASA-CR-3769] p 123 N84-16488
- Effects of water-vapor on friction and deformation of polymers magnetic media in contact with a ceramic oxide  
[NASA-TM-83727] p 87 N84-30072

**WAVE ATTENUATION**

- Wave attenuation and mode dispersion in a waveguide coated with lossy dielectric material  
[NASA-CR-173820] p 100 N84-30145
- Numerical methods for analyzing electromagnetic scattering  
[NASA-CR-173916] p 101 N84-32645
- The role of the reflection coefficient in precision measurement of ultrasonic attenuation  
[NASA-TM-83788] p 149 N84-32849

**WAVE DISPERSION**

- Wave attenuation and mode dispersion in a waveguide coated with lossy dielectric material  
[NASA-CR-173820] p 100 N84-30145

**WAVE INTERACTION**

- Basic experimental study of the coupling between flow instabilities and incident sound  
[NASA-CR-3789] p 183 N84-21275

**WAVE PROPAGATION**

- Volume integrals associated with the inhomogeneous Helmholtz equation Part 1: Ellipsoidal region  
[NASA-CR-3749] p 148 N84-14525

- Volume integrals associated with the inhomogeneous Helmholtz equation Part 2 Cylindrical region, rectangular region  
[NASA-CR-3750] p 148 N84-14526
- Asymptotic analysis of numerical wave propagation in finite difference equations  
[NASA-CR-175323] p 98 N84-15360
- Numerical methods for analyzing electromagnetic scattering  
[NASA-CR-175423] p 98 N84-19620
- Dynamic stress analysis of smooth and notched fiber composite flexural specimens  
[NASA-TM-83594] p 56 N84-25770
- Studies of acoustic properties of bulk porous flexible materials  
[NASA-CR-173622] p 185 N84-27544
- Feedback in separated flows over symmetric airfoils  
[NASA-TM-83758] p 10 N84-31091
- Ultrasonic velocity measurement using phase-slope cross-correlation methods  
[NASA-TM-83794] p 149 N84-34769

**WAVE REFLECTION**

- Supersonic jet screech tone cancellation  
p 179 A84-10136
- Interference phenomena in the refraction of a surface polariton by vertical dielectric barriers  
p 179 A84-24410

**WAVEGUIDES**

- Millimeter wave transmission systems and related devices  
[NASA-CR-173515] p 99 N84-24918
- K-band latching switches  
[NASA-CR-168253] p 109 N84-24973
- Wave attenuation and mode dispersion in a waveguide coated with lossy dielectric material  
[NASA-CR-173820] p 100 N84-30145
- Numerical methods for analyzing electromagnetic scattering  
[NASA-CR-173916] p 101 N84-32645

**WEAR**

- Tribological and microstructural characteristics of ion-nitrided steels  
p 64 A84-19225
- Surface roughness effects with solid lubricants dispersed in mineral oils  
[ASLE PREPRINT 83-LC-4C-1] p 137 A84-28987
- Tribological characteristics of gold films deposited on metals by ion plating and vapor deposition  
[NASA-TM-83572] p 69 N84-17352
- Ceramic wear in indentation and sliding  
[NASA-TM-83585] p 82 N84-19566
- Mechanical contact induced transformation from the amorphous to the crystalline state in metallic glass  
[NASA-TM-83583] p 71 N84-20673
- Frictional and morphological properties of Au-MoS2 films sputtered from a compact target  
[NASA-TM-83604] p 143 N84-20858
- Characterization and measurement of polymer wear  
[NASA-TM-83628] p 83 N84-21739
- Tribology in the 80's Volume 1 Sessions 1 to 4  
[NASA-CP-2300-VOL-1] p 144 N84-23891
- Metallic adhesion and bonding  
p 72 N84-23897
- The strength of the metal Aluminum oxide interface  
p 72 N84-23898

- Low wear partially fluorinated polyimides  
[NASA-TM-83629] p 84 N84-24808
- Effect of substrate chemical pretreatment on the tribological properties of graphite films  
[NASA-TM-83574] p 85 N84-25831
- Interaction of sulfuric acid corrosion and mechanical wear of iron  
[NASA-TM-83717] p 73 N84-27857
- Evaluation of two polyimides and of an improved liner retention design for self-lubricating bushings  
[NASA-TM-83719] p 86 N84-27887
- Properties of ferrites important to their friction and wear behavior  
[NASA-TM-83718] p 87 N84-28994
- Microstructure and surface chemistry of amorphous alloys important to their friction and wear behavior  
[NASA-TM-83762] p 76 N84-32508

**WEAR INHIBITORS**

- A review of the use of wear-resistant coatings in the cutting-tool industry  
[NASA-TM-83512] p 81 N84-11295

**WEAR TESTS**

- Comparison of seal materials for use in Stirling engines  
p 64 A84-22879
- Polyimides formulated from a partially fluorinated diamine for aerospace tribological applications  
p 80 A84-40594
- Friction and wear of iron in sulfuric acid  
[NASA-TP-2289] p 71 N84-21716
- Friction and wear of nickel in sulfuric acid  
[NASA-TP-2290] p 72 N84-21721
- Tribology in the 80's Volume 2. Sessions 5 - 8  
[NASA-CP-2300-VOL-2] p 144 N84-25047

**WEIGHT (MASS)**

Lightweight, high-frequency transformers  
p 105 N84-10086

**PREWATE** An interactive preprocessing computer code to the Weight Analysis of Turbine Engines (WATE) computer code  
[NASA-TM-83545] p 176 N84-13812

**WEIGHT REDUCTION**

Advanced electrical power system technology for the all electric aircraft  
p 15 A84-16528

**WEIGHTING FUNCTIONS**

Wide range weight functions for the strip with a single edge crack  
[NASA-TM-83478] p 153 N84-11512

**WEIGHTLESSNESS**

Thermoacoustic convection heat-transfer phenomenon  
p 120 A84-38857

On-orbit cryogenic fluid transfer.  
[AIAA PAPER 84-1343] p 44 A84-44176

Modeling of zero gravity venting  
[NASA-CR-173503] p 127 N84-23854

On-orbit cryogenic fluid transfer  
[NASA-TM-83688] p 39 N84-25753

**WETTABILITY**

Pore size engineering applied to the design of separators for nickel-hydrogen cells and batteries  
p 162 A84-30187

**WETTING**

Capillary rise, wetting layers, and critical phenomena in confined geometry  
p 192 A84-20315

**WHISKER COMPOSITES**

Analysis of stress-strain, fracture and ductility behavior of aluminum matrix composites containing discontinuous silicon carbide reinforcement  
[NASA-TM-83610] p 54 N84-21666

Microstructure and orientation effects on properties of discontinuous silicon carbide/aluminum composites  
[NASA-TP-2302] p 51 N84-26749

**WIGGLER MAGNETS**

Orbital stability in combined uniform axial and three-dimensional wiggler magnetic fields for free-electron lasers  
[NASA-TM-83753] p 134 N84-30273

**WIND EFFECTS**

Effects of wind on turbofan engines in outdoor static test stands  
[AIAA PAPER 83-2766] p 15 A84-15204

**WIND TUNNEL APPARATUS**

On the design of contractions and settling chambers for optimal turbulence manipulations in wind tunnels  
[AIAA PAPER 84-0536] p 115 A84-22922

**WIND TUNNEL TESTS**

Heat transfer distributions around nominal ice accretion shapes formed on a cylinder in the NASA Lewis Icing Research Tunnel  
[AIAA PAPER 84-0017] p 113 A84-17834

Performance degradation of a model helicopter main rotor in hover and forward flight with a generic ice shape  
[AIAA PAPER 84-0609] p 13 A84-24195

Effect of an oscillating flow direction on leading edge heat transfer  
p 117 A84-33705

Why credible propeller noise measurements are possible in the acoustically untreated NASA Lewis 8 ft by 6 ft wind tunnel  
p 181 A84-38091

Flight and wind tunnel tests of an electro-impulse de-icing system  
[AIAA PAPER 84-2234] p 12 A84-39280

Design and performance of a fixed, nonaccelerating, guide vane cascade that operates over an inlet flow angle range of 60 deg  
[NASA-TM-83519] p 8 N84-14120

Noise of the SR-6 propeller model at 2 deg and 4 deg angles of attack  
[NASA-TM-83515] p 183 N84-16946

An experimental study of the properties of surface pressure fluctuations in strong adverse pressure gradient turbulent boundary layers  
[NASA-CR-175410] p 9 N84-20488

Fuel savings potential of the NASA Advanced Turboprop Program  
[NASA-TM-83736] p 35 N84-29878

An experimental investigation of the effect of boundary layer retraction on the noise from a high-speed propeller  
[NASA-TM-83764] p 186 N84-34230

**WIND TURBINES**

Review of the DOE/NASA wind turbine engineering information system  
p 163 A84-33766

How to protect a wind turbine from lightning  
[NASA-CR-168229] p 163 N84-10661

Examination, evaluation and repair of laminated wood blades after service on the Mod-OA wind turbine  
[NASA-TM-83483] p 163 N84-10664

MOD-2 wind turbine development  
[NASA-TM-83460] p 164 N84-13670

Use of the WEST-1 wind turbine simulator to predict blade fatigue load distribution  
[NASA-TM-83532] p 165 N84-14586

Thermal stress analysis for a wood composite blade --- wind turbines  
[NASA-CR-173394] p 156 N84-21803

Large, horizontal-axis wind turbines  
[NASA-TM-83546] p 169 N84-27327

Effect of vortex generators on the power conversion performance and structural dynamic loads of the Mod-2 wind turbine  
[NASA-TM-83680] p 171 N84-29347

Wind turbine generator interaction with conventional diesel generators on Block Island, Rhode Island. Volume 1: Executive summary  
[NASA-CR-168318] p 171 N84-29357

Thermal-stress analysis for wood composite blade --- horizontal axis wind turbines  
[NASA-CR-173830] p 157 N84-31685

Wind turbine generator interaction with conventional diesel generators on Block Island, Rhode Island. Volume 2: Data analysis  
[NASA-CR-168319] p 172 N84-31783

**WINDING**  
A mathematical model for the doubly-fed wound rotor generator, part 2  
[NASA-TM-83581] p 107 N84-17479

**WINDPOWER UTILIZATION**  
MOD-2 wind turbine development  
[NASA-TM-83460] p 164 N84-13670

**WINGS**  
Piezoelectric deicing device  
[NASA-CASE-LEW-13773-2] p 133 N84-32782

**WINTER**  
Wind turbine generator interaction with conventional diesel generators on Block Island, Rhode Island. Volume 2 Data analysis  
[NASA-CR-168319] p 172 N84-31783

**WOOD**  
Examination, evaluation and repair of laminated wood blades after service on the Mod-OA wind turbine  
[NASA-TM-83483] p 163 N84-10664

Thermal-stress analysis for wood composite blade --- horizontal axis wind turbines  
[NASA-CR-173830] p 157 N84-31685

**WORK HARDENING**  
A simple application of the Bailey-Crowan creep model to Fe-39.8 at. pct Al and gamma/gamma prime - alpha  
p 64 A84-22012

**WORKING FLUIDS**  
High effectiveness liquid droplet/gas heat exchanger for space power applications  
[IAF PAPER 83-433] p 42 A84-11819

An RC-1 organic Rankine bottoming cycle for an adiabatic diesel engine  
[NASA-CR-168256] p 196 N84-32306

**X****X RAY ANALYSIS**

The X-ray photoelectron spectroscopy depth profiling and tribological characterization of ion-plated gold on various metals  
p 50 A84-20485

Laboratory degradation of Kapton in a low energy oxygen ion beam  
[NASA-TM-83530] p 41 N84-18310

**XENON**  
Development of advanced inert-gas ion thrusters  
[NASA-CR-168206] p 44 N84-10180

Performance capabilities of the 12-centimeter Xenon ion thruster  
[NASA-TM-83674] p 48 N84-27825

**Y****YIELD STRENGTH**

Effects of long-time elevated temperature exposures on hot-isostatically-pressed power-metallurgy Udimet 700 alloys with reduced cobalt contents  
[NASA-TM-83632] p 57 N84-28917

**YTTERBIUM COMPOUNDS**  
Improved thermal barrier coating system  
[NASA-CASE-LEW-14057-1] p 88 N84-33595

**YTTRIUM OXIDES**  
Phase distributions in plasma-sprayed zirconia-yttria  
p 78 A84-18948

Phase analysis of plasma-sprayed zirconia-yttria coatings  
p 78 A84-19781

Anisotropic thermal expansion effects in plasma-sprayed ZrO<sub>2</sub>-8 percent Y<sub>2</sub>O<sub>3</sub> coatings  
p 78 A84-19782

Analysis of grain boundary phase identification of Y<sub>2</sub>O<sub>3</sub>- and Al<sub>2</sub>O<sub>3</sub>-doped Si<sub>3</sub>N<sub>4</sub>  
p 79 A84-19792

Elevated temperature compressive steady state deformation and failure in the oxide dispersion strengthened alloy MA 6000E  
p 86 A84-46785

**Materials for Advanced Turbine Engines (MATE).**  
Project 3 Design, fabrication and evaluation of an oxide dispersion strengthened sheet alloy combustor liner, volume 1  
[NASA-CR-174691] p 76 N84-32504

**Z****ZINC**

Surface chemistry, friction, and wear of Ni-Zn and Mn-Zn ferrites in contact with metals  
p 78 A84-13516

**ZINC ALLOYS**

Friction and morphology of magnetic tapes in sliding contact with nickel-zinc ferrite  
[NASA-TP-2267] p 82 N84-16334

Water-vapor effects on friction of magnetic tape in contact with nickel-zinc ferrite  
[NASA-TP-2279] p 82 N84-18399

**ZIRCONIUM**  
High temperature ceramic interface study  
[NASA-CR-174728] p 197 N84-34331

**ZIRCONIUM OXIDES**  
Phase distributions in plasma-sprayed zirconia-yttria  
p 78 A84-18948

Phase analysis of plasma-sprayed zirconia-yttria coatings  
p 78 A84-19781

Anisotropic thermal expansion effects in plasma-sprayed ZrO<sub>2</sub>-8 percent Y<sub>2</sub>O<sub>3</sub> coatings  
p 78 A84-19782

Mechanical and physical properties of plasma-sprayed stabilized zirconia  
p 79 A84-19786

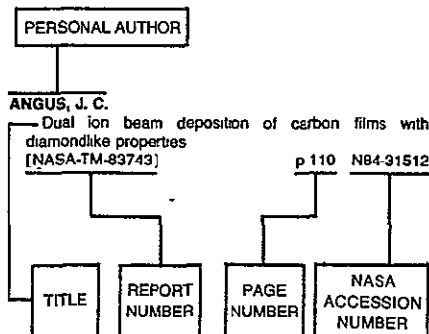
Some inelastic effects of thermal cycling on yttria-stabilized zirconia  
[NASA-TM-83488] p 123 N84-16492

Overview of zirconia with respect to gas turbine applications  
[NASA-TP-2286] p 83 N84-21740

Separator development and testing of nickel-hydrogen cells  
[NASA-TM-83653] p 62 N84-22712

Improved thermal barrier coating system  
[NASA-CASE-LEW-14057-1] p 88 N84-33595

## Typical Personal Author Index Listing



Listings in this index are arranged alphabetically by personal author. The title of the document provides the user with a brief description of the subject matter. The report number helps to indicate the type of document listed (e.g., NASA report, translation, NASA contractor report). The page and accession numbers are located beneath and to the right of the title. Under any one author's name the accession numbers are arranged in sequence with the AIAA accession numbers appearing first

## A

- ABBEY, K. M.**  
Pore size engineering applied to the design of separators for nickel-hydrogen cells and batteries  
p 162 A84-30187
- ABERNETHY, R. B.**  
Uncertainty methodology for in-flight thrust determination  
[SAE PAPER 831438] p 13 A84-29452  
Application of in-flight thrust determination uncertainty  
[SAE PAPER 831439] p 13 A84-29453
- ABRAHAM, K. M.**  
Moderate temperature rechargeable NaNiS<sub>2</sub> cells  
p 108 N84-21376
- ABUJELALA, M. T.**  
Limitations and empirical extensions of the k-epsilon model as applied to turbulent confined swirling flows  
[AIAA PAPER 84-0441] p 114 A84-18096  
Swirl flow turbulence modeling  
[AIAA PAPER 84-1376] p 118 A84-35196  
Swirl, confinement and nozzle effects on confined turbulent flow  
[AIAA PAPER 84-1377] p 118 A84-35197  
Confined turbulent swirling recirculating flow predictions  
[NASA-CR-175397] p 125 N84-19745
- ACOSTA, R.**  
Secondary pattern computation of an arbitrarily shaped main reflector  
[NASA-TM-85527] p 100 N84-25909
- ADAMCZYK, J. J.**  
Numerical aspects of unsteady flow calculations  
p 128 N84-25968  
Unsteady transonic flow in cascades  
[NASA-TM-83780] p 11 N84-32351
- ADAMS, G. R.**  
Uncertainty methodology for in-flight thrust determination  
[SAE PAPER 831438] p 13 A84-29452  
Application of in-flight thrust determination uncertainty  
[SAE PAPER 831439] p 13 A84-29453
- ADAMS, J. C., JR.**  
One-dimensional unsteady modeling of supersonic inlet unstart/restart  
[AIAA PAPER 84-0439] p 4 A84-18094

- ADAMS, M.**  
Nonlinear transient finite element analysis of rotor-bearing-stator systems  
p 136 A84-20580
- ADLER, E.**  
Development of a large scale bipolar NiH<sub>2</sub> battery  
p 162 A84-30189
- AGGARWAL, B. B.**  
Solid lubrication design methodology  
[NASA-CR-174690] p 196 N84-33309
- AHMED, S. A.**  
An experimental investigation of gas jets in confined swirling air flow  
[NASA-CR-3832] p 36 N84-33412
- AHUJA, K. K.**  
Acoustic power dissipation on radiation through duct terminations - Experiments  
p 180 A84-21272  
Basic experimental study of the coupling between flow instabilities and incident sound  
[NASA-CR-3789] p 183 N84-21275
- AIELLO, R. A.**  
Tensile buckling of advanced turboprops  
p 149 A84-11039
- AKAY, H. U.**  
Application of a finite element algorithm to the solution of steady transonic Euler equations  
p 3 A84-10133  
Finite element formulation of transonic flow problems  
p 116 A84-25859
- AKHTER, M. M.**  
HYTESS A hypothetical turbofan engine simplified simulation  
[NASA-TM-83561] p 26 N84-16184
- AKIN, L. S.**  
Parameter studies of gear cooling using an automatic finite element mesh generator  
[NASA-TM-83721] p 146 N84-28087  
An investigation of the transient thermal analysis of spur gears  
[NASA-TM-83724] p 146 N84-28088  
Lubricant jet flow phenomena in spur and helical gears with modified center distances and/or addendums for out-of-mesh conditions  
[NASA-TM-83723] p 146 N84-29224
- ALAM, J.**  
Effect of crack curvature on stress intensity factors for ASTM standard compact tension specimens  
[NASA-CR-168280] p 153 N84-11513
- ALAM, M.**  
A blade loss response spectrum for flexible rotor systems  
[ASME PAPER 84-GT-29] p 139 A84-46893
- ALEXANDER, S. S.**  
Anion permselective membrane  
[NASA-CR-174725] p 172 N84-29358
- ALEXOVICH, R. E.**  
Characteristics and capacities of the NASA Lewis Research Center high precision 6.7- by 6.7-m planar near-field scanner  
[NASA-TM-83785] p 133 N84-32789
- ALGER, D.**  
Overview of advanced Stirling and gas turbine engine development programs and implications for solar thermal electrical applications  
p 146 N84-28231
- ALKASAB, K. A.**  
Manual of phosphoric acid fuel cell power plant cost model and computer program  
[NASA-CR-174720] p 173 N84-34037
- ALLAIRE, P. E.**  
Penalty function finite element analysis of steady viscous incompressible flow in rotating coordinates  
[ASME PAPER 84-GT-36] p 121 A84-46900
- ALLEN, H., JR.**  
Detroit space odyssey  
[NASA-TM-85487] p 37 N84-15164  
Chicago Meets Outer Space program  
[NASA-TM-85492] p 192 N84-16021
- ANDERSON, B. H.**  
Three-dimensional viscous design methodology for advanced technology aircraft supersonic inlet systems  
[AIAA PAPER 84-0194] p 4 A84-21290  
Investigation of mixing in a turbofan exhaust duct II  
Computer code application and verification  
p 17 A84-27140

- Developing flow in S-shaped ducts  
p 116 A84-28709
- Three-dimensional viscous design methodology for advanced technology aircraft supersonic inlet systems  
[NASA-TM-83558] p 23 N84-13190
- ANDERSON, D. L.**  
Heat pipe applications in aircraft propulsion  
[AIAA PAPER 84-1269] p 18 A84-37640
- ANDERSON, D. N.**  
Combustor development for automotive gas turbines  
p 135 A84-10499  
Combustor flame flashback  
p 62 N84-20561
- ANDERSON, L. M.**  
Harnessing surface plasmons for solar energy conversion  
p 159 A84-16395  
Parallel-processing with surface plasmons, a new strategy for converting the broad solar spectrum  
p 160 A84-23006  
Plasmon device design Conversion from surface to junction plasmons with grating-couplers  
p 171 N84-29330
- ANDERSON, N. E.**  
An analytical method to predict efficiency of aircraft gearboxes  
[AIAA PAPER 84-1500] p 20 A84-44180  
An analytical method to predict efficiency of aircraft gearboxes  
[NASA-TM-83716] p 2 N84-25606  
Efficiency of nonstandard and high contact ratio involute spur gears  
[NASA-TM-83725] p 146 N84-29223
- ANDERSON, N. P.**  
Development of strain tolerant thermal barrier coating systems, tasks 1 - 3  
[NASA-CR-168251] p 81 N84-12312  
Program for development of strain tolerant thermal barrier coating system  
[NASA-CR-173214] p 82 N84-16337
- ANDERSON, O. L.**  
Extension to an analysis of turbulent swirling compressible flow for application to axisymmetric small gas turbine ducts  
[NASA-CR-165597] p 195 N84-21445
- ANDERSON, R. D.**  
Advanced propan drive system characteristics and technology needs  
[AIAA PAPER 84-1194] p 18 A84-36957
- ANDERSON, R. E.**  
Mobile radio alternative systems study Volume 1: Traffic model  
[NASA-CR-168062] p 96 N84-10402  
Mobile radio alternative systems study. Volume 2  
Terrestrial  
[NASA-CR-168063] p 96 N84-10403  
Mobile radio alternative systems study  
satellite/terrestrial (hybrid) systems concepts  
[NASA-CR-168064] p 96 N84-10404
- ANDERSSON, C. A.**  
Thermal stress fracture of ceramic coatings  
p 80 A84-24553
- ANDREWS, J. S.**  
MOD-2 wind turbine development  
[NASA-TM-83460] p 164 N84-13670
- ANGUS, J. C.**  
Dual ion beam deposition of carbon films with diamondlike properties  
[NASA-TM-83743] p 110 N84-31512
- ANTONELLI, G.**  
Free-piston Stirling engine endurance test program  
p 136 A84-22864
- ANTONELLI, M.**  
Automotive Stirling engine development program  
[NASA-CR-168205] p 194 N84-18117  
Automotive Stirling engine development program  
[NASA-CR-174622] p 195 N84-32305
- ANZIC, G.**  
Microwave monolithic integrated circuit development for future spaceborne phased array antennas  
[AIAA PAPER 84-0656] p 94 A84-25257  
A study of 80 GHz intersatellite link applications  
p 40 A84-49268

- Microwave monolithic integrated circuit development for future spaceborne phased array antennas  
[NASA-TM-83518] p 97 N84-13399
- MMIC technology for advanced space communications systems  
[NASA-TM-83749] p 100 N84-30147
- The 20 and 30 GHz MMIC technology for future space communication antenna system  
[NASA-TM-83745] p 100 N84-31460
- Monolithic microwave integrated circuits  
Interconnections and packaging considerations  
[NASA-TM-83774] p 100 N84-31461
- ARIMILLI, R. V.**  
Measurements of local convective heat-transfer coefficients on ice accretion shapes  
[AIAA PAPER 84-0018] p 113 A84-17835
- ARMAN, E. F.**  
Measurement of spray combustion processes  
p 61 N84-20530
- ARMILLI, R. V.**  
Measurement of local convective heat transfer coefficients of four ice accretion shapes  
[NASA-CR-174680] p 10 N84-25646
- ARNDT, R. A.**  
Surface effects in high voltage silicon solar cells  
p 160 A84-23002
- ARON, P. R.**  
Characterization and measurement of polymer wear  
[NASA-TM-83628] p 83 N84-21739
- RF sputtered silicon and hafnium nitrides as applied to 440C steel  
[NASA-TM-86862] p 87 N84-32536
- ARPASI, D. J.**  
RTMPL: A structured programming and documentation utility for real-time multiprocessor simulations  
[NASA-TM-83606] p 177 N84-20259
- ARTILES, A.**  
Design analysis of Rayleigh-step floating-ring seals  
[ASLE PREPRINT 83-LC-3B-2] p 137 A84-28989
- ASBECK, P. M.**  
LEC GaAs for integrated circuit applications  
[NASA-CR-173267] p 191 N84-17014
- ASCOUGH, J. C.**  
Uncertainty methodology for in-flight thrust determination  
[SAE PAPER 831438] p 13 A84-29452
- Application of in-flight thrust determination uncertainty  
[SAE PAPER 831439] p 13 A84-29453
- ASMUS, J. R.**  
The 20 GHz solid state transmitter design, impatt diode development and reliability assessment  
[NASA-CR-174716] p 112 N84-33715
- ASMUSSEN, J.**  
Characteristics of a microwave plasma disk ion source  
p 189 A84-23390
- Demonstration of a new electrothermal thruster concept  
p 43 A84-34037
- Electromagnetic plasma models for microwave plasma cavity reactors  
[AIAA PAPER 84-1521] p 189 A84-46108
- Spatial electron density and electric field strength measurements in microwave cavity experiments  
[AIAA PAPER 84-1522] p 189 A84-46109
- Spatial electron density and electric field strength measurements in microwave cavity experiments  
[NASA-CR-173907] p 111 N84-32682
- ASSANIS, D. N.**  
Computer simulation of the heavy-duty turbo-compounded diesel cycle for studies of engine efficiency and performance  
[NASA-CR-174755] p 196 N84-33306
- ATASSI, H. M.**  
Feedback in separated flows over symmetric airfoils  
[NASA-TM-83758] p 10 N84-31091
- ATKINSON, W.**  
Advanced high temperature heat flux sensors  
[NASA-TM-83526] p 123 N84-16493
- ATKINSON, W. H.**  
Turbine blade and vane heat flux sensor development, phase 1  
[NASA-CR-168297] p 134 N84-32790
- ATLURI, S. N.**  
Inelastic stress analyses at finite deformation through complementary energy approaches  
p 149 A84-13248
- Analyses of large quasistatic deformations of inelastic bodies by a new hybrid-stress finite element algorithm  
p 150 A84-16874
- Analyses of large quasistatic deformations of inelastic bodies by a new hybrid-stress finite element algorithm - Applications  
p 150 A84-16884
- Inelastic and dynamic fracture and stress analyses  
p 158 N84-31697
- AUGUST, R.**  
Dynamics of early planetary gear trains  
[NASA-CR-3793] p 145 N84-26027

- AVNI, R.**  
Homogeneous reactions of hydrocarbons, silane, and chlorosilanes in radiofrequency plasmas at low pressures  
[NASA-TP-2301] p 50 N84-20643
- Radical and ion molecule mechanisms in the polymerization of hydrocarbons and chlorosilanes in RF plasmas at low pressures (1.0 torr)  
[NASA-TM-83602] p 190 N84-21329
- Correlations between plasma variables and the deposition process of Si films from chlorosilanes in low pressure RF plasma of argon and hydrogen  
[NASA-TM-83603] p 190 N84-21330
- AYDELOTT, J. C.**  
Computational modeling of jet induced mixing of cryogenic propellants in low-G  
[NASA-TM-83703] p 127 N84-25000
- AYDELOTT, J. C.**  
Computational modeling of jet induced mixing of cryogenic propellants in low-G  
[AIAA PAPER 84-1344] p 121 A84-40243
- On-orbit cryogenic fluid transfer  
[AIAA PAPER 84-1343] p 44 A84-44176
- On-orbit cryogenic fluid transfer  
[NASA-TM-83688] p 39 N84-25753

## B

- BACH, L.**  
Blade loss transient dynamics analysis with flexible bladed disk  
[NASA-CR-168176] p 23 N84-13193
- BACHALO, W. D.**  
Development of the phase/Doppler spray analyzer for liquid drop size and velocity characterizations  
[AIAA PAPER 84-1199] p 131 A84-36958
- Analysis and testing of a new method for drop size measurement using laser scatter interferometry  
[NASA-CR-174636] p 133 N84-31595
- BADLANI, M. L.**  
Development of a simplified procedure for rocket engine thrust chamber life prediction with creep  
[NASA-CR-168261] p 46 N84-19472
- BAGWELL, J.**  
NASA's multibeam communications technology program  
p 39 A84-21397
- BAGWELL, J. W.**  
A system for the simulation and evaluation of satellite communication networks  
[AIAA PAPER 84-0680] p 94 A84-25272
- A system for the simulation and evaluation of satellite communication networks  
[NASA-TM-83531] p 97 N84-13400
- BAHR, D. W.**  
NASA/General Electric Broad-Specification Fuels Combustion Technology Program - Phase I  
p 16 A84-24033
- BAIL, I.**  
Executive summary, aerothermal modeling program, phase 1  
[NASA-CR-174602] p 60 N84-12263
- BAILEY, B. K.**  
Carbon-13 and proton nuclear magnetic resonance analysis of shale-derived refinery products and jet fuels and of experimental referee broadened-specification jet fuels  
[NASA-CR-174761] p 92 N84-32552
- BAILEY, W. J.**  
Cryogenic Fluid Management Facility  
[AIAA PAPER 84-1340] p 44 A84-44184
- Cryogenic Fluid Management Experiment (CFME) trunnion verification testing  
[NASA-CR-168310] p 92 N84-16381
- BAKER, C. E.**  
Research on aviation fuel instability  
p 90 N84-23642
- Research on aviation fuel instability  
p 91 N84-24734
- BAKER, I.**  
The structure of extruded NiAl  
p 65 A84-36047
- BALDERRAMA, E.**  
High-speed wide band 20 x 20 microwave switch matrix  
p 105 A84-49253
- BALL, C. L.**  
End-wall boundary layer measurements in a two-stage fan  
p 26 N84-16208
- BALL, I.**  
Aerothermal modeling program, phase 1  
[NASA-CR-168243-VOL-2] p 60 N84-12265
- BALODIS, V.**  
Development and fabrication of a high current, fast recovery power diode  
[NASA-CR-168196] p 106 N84-13443
- BALOMBIN, J. R.**  
Tone generation by rotor-downstream strut interaction  
p 16 A84-22174
- BALSA, T. F.**  
Free jet feasibility study of a thermal acoustic shield concept for AST/VCE application Single stream nozzles  
[NASA-CR-3758] p 185 N84-29861
- BANERJEE, P. K.**  
Three-dimensional stress analysis using the boundary element method  
p 159 N84-31700
- BANKS, B.**  
Piezoelectric sensing device  
[NASA-CASE-LEW-13773-2] p 133 N84-32782
- BANKS, B. A.**  
Intercalated graphite electrical conductors  
p 105 N84-10064
- Diamondlike flake composites  
[NASA-CASE-LEW-13837-1] p 54 N84-22695
- Diamondlike flakes  
[NASA-CASE-LEW-13837-2] p 54 N84-22696
- Method of making an ion beam sputter-etched ventricular catheter for hydrocephalus shunt  
[NASA-CASE-LEW-13107-2] p 174 N84-23095
- Sputtered coatings for protection of spacecraft polymers  
[NASA-TM-83706] p 85 N84-26803
- Deposition of diamondlike carbon films  
[NASA-CASE-LEW-14080-1] p 86 N84-28986
- BARAONA, C.**  
Recent advances in thin silicon solar cells  
p 160 A84-22981
- BARBER, J. P.**  
Investigation of the residue in an electric rail gun employing a plasma armature  
p 103 A84-32046
- BARRETT, C. A.**  
The effects of Cr, Al, Ti, Mo, W, Ta, and Cb on the cyclic oxidation behavior of cast Ni-base superalloys at 1100 and 1150 C  
p 65 A84-27485
- Oxidation and corrosion resistance of candidate Stirling engine heater-head-tube alloys  
[NASA-TM-83609] p 74 N84-28962
- High-temperature cyclic oxidation data, volume 1  
[NASA-TM-83665] p 75 N84-31345
- BARROWS, R. F.**  
Baseline performance and emissions data for a single-cylinder, direct-injected diesel engine  
[NASA-TM-86873] p 197 N84-34330
- BASS, J. A.**  
Solar-array-materials passive LDEF experiment (A0171)  
p 168 N84-24656
- BATTERTON, P. G.**  
Energy efficient engine program contributions to aircraft fuel conservation  
[NASA-TM-83741] p 34 N84-29876
- BAUER, D. P.**  
Investigation of the residue in an electric rail gun employing a plasma armature  
p 103 A84-32046
- BAUHAHN, P.**  
The 30-GHz monolithic receive module  
[NASA-CR-168326] p 99 N84-20737
- BAUHAHN, P. E.**  
A Ka-band GaAs monolithic phase shifter  
p 101 A84-18371
- BAUMBICK, R. J.**  
Fiberoptics for propulsion control system  
[NASA-TM-83542] p 1 N84-14111
- BAUMEISTER, K. J.**  
Finite element-integral acoustic simulation of JT15D turbofan engine  
p 182 A84-41132
- Time dependent wave envelope finite difference analysis of sound propagation  
[NASA-TM-83744] p 185 N84-32118
- BEACH, R. F.**  
Electric vehicle propulsion alternatives  
[NASA-TM-83504] p 166 N84-20017
- BEACHER, B. F.**  
Subsonic/transonic stall flutter investigation of a rotating wing  
[NASA-CR-174625] p 36 N84-33417
- BEATTIE, E. C.**  
HYTESS A hypothetical turbofan engine simplified simulation  
[NASA-TM-83561] p 26 N84-16184
- BECKER, E. B.**  
A numerical analysis of contact and limit-point behavior in a class of problems of finite elastic deformation  
p 150 A84-27370
- BEECHAN, C. M.**  
Synthesis of perfluoroalkylene dianilines  
[NASA-CR-168004] p 60 N84-11228
- BEELER, R. M.**  
Dynamics of two-phase face seals  
p 137 A84-28792



- BEHNING, F. P.**  
Effect of a rotor wake on heat transfer from a circular cylinder  
[NASA-TM-83613] p 126 N84-21832
- BELTRAN, M. R.**  
Heat pipe applications in aircraft propulsion  
[AIAA PAPER 84-1289] p 18 A84-37640
- BENNETT, J. C.**  
The influence of large-scale motion on turbulent transport for confined coaxial jets p 125 N84-20542
- BEREMAND, D. G.**  
DOE/NASA Automotive Stirling Engine Project Overview  
83 p 138 A84-30069
- BERENFELD, A.**  
Experiments in dilution jet mixing p 122 A84-48140
- BERK, G.**  
A frequency-division multiple-access system concept for 30/20 GHz high-capacity domestic satellite service  
p 94 A84-22141
- BERMAN, A. H.**  
Development and fabrication of a high current, fast recovery power diode  
[NASA-CR-168195] p 106 N84-13443
- BERNDT, C. C.**  
Phase analysis of plasma-sprayed zirconia-yttria coatings p 78 A84-19781  
Anisotropic thermal expansion effects in plasma-sprayed ZrO<sub>2</sub>-8 percent Y<sub>2</sub>O<sub>3</sub> coatings p 78 A84-19782  
Acoustic emission evaluation of plasma-sprayed thermal barrier coatings  
[ASME PAPER 84-GT-292] p 140 A84-47046  
Performance of thermal barrier coatings in high heat flux environments  
[NASA-TM-83683] p 72 N84-24772  
Failure analysis of plasma-sprayed thermal barrier coatings  
[NASA-TM-83777] p 75 N84-31347
- BERRY, R.**  
Executive summary, aerothermal modeling program, phase 1  
[NASA-CR-174602] p 60 N84-12263  
Aerothermal modeling program, phase 1  
[NASA-CR-168243-VOL-2] p 60 N84-12265
- BHASIN, K. B.**  
Monolithic microwave integrated circuits: Interconnections and packaging considerations  
[NASA-TM-83774] p 100 N84-31461
- BHAT, I.**  
Diffused junction p(+)-n solar cells in bulk GaAs I  
Fabrication and cell performance p 161 A84-26027  
Diffused junction p(+)-n solar cells in bulk GaAs II - Device characterization and modelling p 161 A84-26028
- BHAT, I. B.**  
Photovoltaic characteristics of diffused P/+N bulk GaAs solar cells p 161 A84-23115
- BHAT, K. N.**  
Photovoltaic characteristics of diffused P/+N bulk GaAs solar cells p 161 A84-23115  
Diffused junction p(+)-n solar cells in bulk GaAs I  
Fabrication and cell performance p 161 A84-26027
- BHATT, R. T.**  
Thermal degradation of the tensile properties of undirectionally reinforced FP-AI<sub>2</sub>O<sub>3</sub>/EZ 33 magnesium composites p 52 A84-28229
- BHATTACHARYYA, S.**  
Creep-rupture behavior of six candidate Stirling engine superalloys tested in air p 65 A84-36173  
Creep-rupture behavior of candidate Stirling engine iron superalloys in high-pressure hydrogen Volume 2  
Hydrogen creep-rupture behavior  
[NASA-CR-174705] p 74 N84-28961
- BHUSHAN, B.**  
Friction and morphology of magnetic tapes in sliding contact with nickel-zinc ferrite  
[NASA-TP-2267] p 82 N84-16334
- BIAGLOW, J. A.**  
Preliminary investigation of a two-zone swirl flow combustor  
[AIAA PAPER 84-1169] p 17 A84-36951  
Experimental investigation of the low NO<sub>x</sub> vortex airblast annular combustor  
[AIAA PAPER 84-1170] p 18 A84-36952  
Preliminary investigation of a two-zone swirl flow combustor  
[NASA-TM-83637] p 29 N84-22565
- BIEGEN, R. J.**  
Study of effects of fuel properties in turbine-powered business aircraft  
[NASA-CR-174627] p 91 N84-25854
- BIELAWA, R. L.**  
Aeroelastic analysis for propellers - mathematical formulations and program user's manual  
[NASA-CR-3729] p 153 N84-12530
- BIESIADNY, T.**  
Uncertainty methodology for in-flight thrust determination  
[SAE PAPER 831438] p 13 A84-28452  
Application of in-flight thrust determination uncertainty  
[SAE PAPER 831439] p 13 A84-28453
- BIESIADNY, T. J.**  
Response of a small-turboshaft-engine compression system to inlet temperature distortion  
[NASA-TM-83765] p 36 N84-33414
- BIFANO, W. J.**  
Economic viability of photovoltaic power for development assistance applications p 193 A84-23119
- BILL, R. C.**  
Some inelastic effects of thermal cycling on yttria-stabilized zirconia  
[NASA-TM-83488] p 123 N84-16492  
Preliminary study of thermomechanical fatigue of polycrystalline MAR-M 200  
[NASA-TP-2280] p 69 N84-17350  
Method of fabricating an abradable gas path seal  
[NASA-CASE-LEW-13269-2] p 143 N84-22957  
Low cycle fatigue behavior of conventionally cast MAR-M 200 AT 1000 deg C  
[NASA-TM-83769] p 77 N84-33564
- BIRKS, N.**  
Investigation into the role of sodium chloride deposited on oxide and metal substrates in the initiation of hot corrosion  
[NASA-CR-173377] p 71 N84-20676
- BISHOP, A. R.**  
Three-dimensional flow simulations for supersonic mixed-compression inlets at incidence p 5 A84-38828
- BITTKER, D. A.**  
Research on aviation fuel instability p 90 N84-23642  
Research on aviation fuel instability p 91 N84-24734  
GCKP84-general chemical kinetics code for gas-phase flow and batch processes including heat transfer effects  
[NASA-TP-2320] p 63 N84-32446
- BLACK, G.**  
Blade loss transient dynamics analysis with flexible bladed disk  
[NASA-CR-168176] p 23 N84-13193
- BLACK, J. D.**  
An analytical method to predict efficiency of aircraft gearboxes  
[AIAA PAPER 84-1500] p 20 A84-44180  
An analytical method to predict efficiency of aircraft gearboxes  
[NASA-TM-83716] p 2 N84-25806
- BLASER, C.**  
Long life nickel electrodes for a nickel-hydrogen cell. I  
Initial performance p 162 A84-30186
- BLECH, R. A.**  
A real-time, portable, microcomputer-based jet engine simulator  
[NASA-TM-83550] p 176 N84-16812
- BOBER, L. J.**  
Summary of recent NASA propeller research  
[NASA-TM-83733] p 2 N84-32344
- BOBULA, G. A.**  
The application of LQR synthesis techniques to the turboshaft engine control problem  
[AIAA PAPER 84-1455] p 21 A84-44185
- BOGHANI, A. B.**  
Catalog of selected heavy duty transport energy management models  
[NASA-CR-168299] p 194 N84-14991
- BOLES, M. A.**  
Analytical study of suction boundary layer control for subsonic V/STOL inlets  
[AIAA PAPER 84-1399] p 6 A84-44187
- BOLLENBACHER, G.**  
Economic competitiveness of fuel cell onsite integrated energy systems  
[NASA-TM-83403] p 164 N84-10665
- BOLTON, R. J.**  
Comparison of steady-state and transient CVS cycle emission of an automotive Stirling engine p 173 A84-41044
- BOROTA, M.**  
Baseband processor development for the Advanced Communications Satellite Program p 93 A84-15628  
30/20 GHz communications systems baseband processor development p 95 A84-38251
- BORREGO, J. M.**  
Photovoltaic characteristics of diffused P/+N bulk GaAs solar cells p 161 A84-23115  
Diffused junction p(+)-n solar cells in bulk GaAs I  
Fabrication and cell performance p 161 A84-26027  
Diffused junction p(+)-n solar cells in bulk GaAs II - Device characterization and modelling p 161 A84-26028
- BOSQUE, M. A.**  
Fuel spray diagnostics p 125 N84-20527  
Detailed fuel spray analysis techniques p 127 N84-24747
- BOVENKERK, R. L.**  
Solid lubrication design methodology  
[NASA-CR-174690] p 196 N84-33309
- BOWDEN, J. N.**  
Investigation of sources, properties and preparation of distillate test fuels  
[NASA-CR-168227] p 89 N84-13332
- BOWLES, E. B.**  
Vapor flow into a capillary propellant-acquisition device p 43 A84-36559
- BOYLE, R. J.**  
Comparison between measured turbine stage performance and the predicted performance using quasi-3D flow and boundary layer analyses  
[AIAA PAPER 84-1299] p 18 A84-36972  
Comparison between measured turbine stage performance and the predicted performance using quasi-3D flow and boundary layer analyses  
[NASA-TM-83640] p 29 N84-22564  
Heat transfer in serpentine passages with turbulence promoters  
[NASA-TM-83614] p 126 N84-22911  
Analytical and experimental investigation of stator endwall countouring in a small axial-flow turbine  
[NASA-TP-2309] p 35 N84-32388
- BRADHORST, H. W., JR.**  
Advanced photovoltaic experiment (S0014) p 168 N84-24657
- BRADLEY, E.**  
Technology and benefits of aircraft counter rotation propellers  
[NASA-CR-168258] p 22 N84-13186
- BRADT, R. C.**  
The impact resistance of SiC and other mechanical properties of SiC and Si<sub>3</sub>N<sub>4</sub>  
[NASA-CR-165325] p 84 N84-24809
- BRADY, F. J.**  
A mathematical model for the doubly-fed wound rotor generator, part 2  
[NASA-TM-83581] p 107 N84-17479
- BRAAG, M. B.**  
Effect of geometry on airfoil icing characteristics p 12 A84-37935  
Experimental and analytical investigations into airfoil icing p 12 A84-45054  
Results of an experimental program investigating the effects of simulated ice on the performance of the NACA 63A15 airfoil with flap  
[NASA-CR-168288] p 8 N84-16145
- BRAINARD, W. A.**  
The worldwide market for photovoltaics in the rural sector p 161 A84-23135
- BRANDHORST, H. W., JR.**  
Solar-array-materials passive LDEF experiment (A0171) p 168 N84-24656  
The effects of lithium counterdoping on radiation damage and annealing in n(+)-p silicon solar cells  
[NASA-TM-83755] p 110 N84-31513  
Photovoltaics: The endless spring  
[NASA-TM-83584] p 172 N84-31782
- BRATTON, R. J.**  
Degradation mechanisms of ceramic thermal barrier coatings in corrosive environments p 81 A84-42668
- BRAUN, M. J.**  
A thermomechanical model for energy propagation in a solid-fluid-solid system with one boundary in relative motion  
[ASME PAPER 83-HT-97] p 137 A84-29092  
Heat transfer in thermal barrier coated rods with circumferential and radial temperature gradients  
[ASME PAPER 84-GT-181] p 121 A84-46982  
High temperature thermomechanical analysis of ceramic coatings p 152 A84-48565  
Experimental study of bubble cavities attached to a rotating shaft in a reservoir  
[NASA-TM-83586] p 124 N84-17533
- BRAUSCH, J. F.**  
Experimental investigation of shock-cell noise reduction for dual-stream nozzles in simulated flight comprehensive data report. Volume 1: Test nozzles and acoustic data  
[NASA-CR-168336-VOL-1] p 184 N84-24323  
Experimental investigation of shock-cell noise reduction for dual-stream nozzles in simulated flight comprehensive data report. Volume 2. Laser velocimeter data, static pressures and shadowgraph photos  
[NASA-CR-168336-VOL-2] p 184 N84-24324  
Free jet feasibility study of a thermal acoustic shield concept for AST/VCE application: Single stream nozzles  
[NASA-CR-3758] p 185 N84-29661

- Experimental investigation of shock-cell noise reduction for single-stream nozzles in simulated flight, comprehensive data report. Volume 1: Test nozzles and acoustic data  
[NASA-CR-168234-VOL-1] p 185 N84-33148
- Experimental investigation of shock-cell noise reduction for single-stream nozzles in simulated flight, comprehensive data report. Volume 2: Laser velocimeter data  
[NASA-CR-168234-VOL-2] p 186 N84-33149
- Experimental investigation of shock-cell noise reduction for single-stream nozzles in simulated flight, comprehensive data report. Volume 3: Shadowgraph photos and facility description  
[NASA-CR-168234-VOL-3] p 186 N84-33150
- BRETON, T.**  
Computer analysis of effects of altering jet fuel properties on refinery costs and yields  
[NASA-CR-174642] p 91 N84-27908
- BREUER, C. T.**  
New applications for phosphoric acid fuel cells  
[NASA-CR-168203] p 166 N84-18757
- BREWE, D. E.**  
Hydrodynamic lubrication of rigid nonconformal contacts in combined rolling and normal motion  
[NASA-TM-83578] p 142 N84-17592
- BRIGHAM, B. A.**  
Length to diameter ratio and row number effects in short pin fin heat transfer  
[ASME PAPER 83-GT-54] p 118 A84-33706
- BRILEY, W. R.**  
Further development of a method for computing three-dimensional subsonic viscous flows in turbulent lobe mixers  
[NASA-CR-168304] p 122 N84-14462
- BRITTON, D. L.**  
Pore size engineering applied to the design of separators for nickel-hydrogen cells and batteries  
p 162 A84-30187  
[NASA-TM-86861] p 172 N84-30528
- BROGREN, E.**  
Evaluation of propellant tank insulation concepts for low-thrust chemical propulsion systems  
[NASA-CR-168320] p 46 N84-20634  
Evaluation of propellant tank insulation concepts for low-thrust chemical propulsion systems. Executive summary  
[NASA-CR-168321] p 83 N84-20699
- BRONDUM, D. C.**  
The influence of large-scale motion on turbulent transport for confined coaxial jets  
p 125 N84-20542
- BROSTMEYER, J. D.**  
Flat plate heat transfer for laminar transition and turbulent boundary layers using a shock tube  
[AIAA PAPER 84-1726] p 120 A84-37467
- BROWN, G. V.**  
Lewis Research Center spin rig and its use in vibration analysis of rotating systems  
[NASA-TP-2304] p 30 N84-24678
- BROWN, L.**  
30/20 GHz communications systems baseband processor development  
p 95 A84-38251
- BROWNING, L. H.**  
Alcohol cold starting - A theoretical study  
p 138 A84-30061
- BRUCKNER, A. P.**  
High effectiveness liquid droplet/gas heat exchanger for space power applications  
[IAF PAPER 83-433] p 42 A84-11819
- BUBSEY, R. T.**  
Development of plane strain fracture toughness test for ceramics using Chevron notched specimens  
p 77 A84-11676
- BUCKLEY, D. H.**  
Surfaces  
p 50 A84-10680  
Surface chemistry, friction, and wear of Ni-Zn and Mn-Zn ferrites in contact with metals  
p 78 A84-13516  
Morphology of an aluminum alloy eroded by a normally incident jet of angular erodent particles  
p 64 A84-18244  
The X-ray photoelectron spectroscopy depth profiling and tribological characterization of ion-plated gold on various metals  
p 50 A84-20465  
Predictive capability of long-term cavitation and liquid impingement erosion models  
p 50 A84-32646  
A study of the effect of solid particle impact and particle shape on the erosion morphology of ductile metals  
p 66 A84-45570  
Size scale effect in cavitation erosion  
[NASA-TM-83533] p 67 N84-11254  
Solid impingement erosion mechanisms and characterization of erosion resistance of ductile metals  
[NASA-TM-83492] p 67 N84-12287  
Measurement of rolling friction by a damped oscillator  
[NASA-TP-2257] p 141 N84-13577
- Particulate erosion mechanisms  
[NASA-TM-83551] p 68 N84-14289  
Friction and morphology of magnetic tapes in sliding contact with nickel-zinc ferrite  
[NASA-TP-2267] p 82 N84-16334  
Metallic glass as a temperature sensor during ion plating  
[NASA-TM-83566] p 69 N84-17351  
Tribological characteristics of gold films deposited on metals by ion plating and vapor deposition  
[NASA-TM-83572] p 69 N84-17352  
Water-vapor effects on friction of magnetic tape in contact with nickel-zinc ferrite  
[NASA-TP-2279] p 82 N84-18399  
Mechanism of lubrication by tricresylphosphate (TCP)  
[NASA-TP-2274] p 142 N84-18653  
Ceramic wear in indentation and sliding  
[NASA-TM-83585] p 82 N84-19566  
Mechanical contact induced transformation from the amorphous to the crystalline state in metallic glass  
[NASA-TM-83583] p 71 N84-20673  
Friction and wear of iron in sulfonic acid  
[NASA-TP-2289] p 71 N84-21716  
Friction and wear of nickel in sulfonic acid  
[NASA-TP-2290] p 72 N84-21721  
Characterization and measurement of polymer wear  
[NASA-TM-83628] p 83 N84-21739  
Importance and definition of materials in tribology. Status of understanding  
p 84 N84-23893  
Considerations in friction and wear  
p 144 N84-23903  
Interaction of sulfonic acid corrosion and mechanical wear of iron  
[NASA-TM-83717] p 73 N84-27857  
Erosion of iron-chromium alloys by glass particles  
[NASA-TP-2354] p 75 N84-28965  
Properties of ferrites important to their friction and wear behavior  
[NASA-TM-83718] p 87 N84-28994  
Effects of water-vapor on friction and deformation of polymeric magnetic media in contact with a ceramic oxide  
[NASA-TM-83727] p 87 N84-30072  
Empirical relations for cavitation and liquid impingement erosion processes  
[NASA-TP-2339] p 76 N84-31349  
Adhesion between polymers and evaporated gold and nickel films  
[NASA-TP-2360] p 87 N84-31379  
Microstructure and surface chemistry of amorphous alloys important to their friction and wear behavior  
[NASA-TM-83762] p 76 N84-32508  
Characterization of erosion of metallic materials under cavitation attack in a mineral oil  
[NASA-TP-2368] p 147 N84-32825  
Friction behavior of silicon in contact with titanium, nickel, silver and copper  
[NASA-TP-2362] p 88 N84-33590  
The role of material properties in adhesion  
[NASA-TM-83792] p 88 N84-34619
- BULICZ, T.**  
Advanced onboard storage concepts for natural gas-fueled automotive vehicles  
[NASA-CR-174655] p 172 N84-34036
- BUNDAS, D. J.**  
Flutter and forced response of mistuned rotors using standing wave analysis  
[NASA-CR-173555] p 32 N84-24586
- BUNKER, S. N.**  
New implantation techniques for improved solar cell junctions  
p 161 A84-23059
- BURATYNSKI, E. K.**  
An implicit LU scheme for the Euler equations applied to arbitrary cascades  
[AIAA PAPER 84-0167] p 4 A84-17925
- BURGHART, J. H.**  
Optimization methods applied to hybrid vehicle design  
[NASA-CR-168292] p 194 N84-19185
- BURLEY, R. R.**  
Investigation of tangential blowing applied to a subsonic V/STOL inlet  
p 3 A84-11042  
Experimental investigation of tangential blowing applied to a subsonic V/STOL inlet  
[NASA-TP-2297] p 9 N84-20493
- BURNS, R. J.**  
An experimental investigation of the effect of boundary layer refraction on the noise from a high-speed propeller  
[NASA-TM-83764] p 186 N84-34230
- BURRUS, D. L.**  
Aerothermal modeling. Executive summary  
[NASA-CR-168330] p 25 N84-15152  
Aerothermal modeling, phase 1. Volume 1: Model assessment  
[NASA-CR-168296-VOL-1] p 25 N84-15155
- Aerothermal modeling, phase 1. Volume 2: Experimental data  
[NASA-CR-168296-VOL-2] p 25 N84-15155
- BURSTADT, P. L.**  
Flow visualization and interpretation of visualization data for deflected thrust V/STOL nozzles  
[AIAA PAPER 84-0102] p 16 A84-21852  
Flow visualization and interpretation of visualization data for deflected thrust V/STOL nozzles  
[NASA-TM-83554] p 24 N84-14147
- BURTON, D. E.**  
Sound generated by instability waves of supersonic flows. I Two-dimensional mixing layers II - Axisymmetric jets  
p 181 A84-24597
- BURTON, R. L.**  
Experimental investigation of the pulsed electrothermal (PET) thruster  
[AIAA PAPER 84-1386] p 43 A84-35201  
Proposed system design for a 20 kW pulsed electrothermal thruster  
[AIAA PAPER 84-1387] p 43 A84-35202  
Investigation of a pulsed electrothermal thruster  
[NASA-CR-168266] p 45 N84-12227
- BUZEK, B.**  
Microstructure, strength, and oxidation of a 10 wt pct zirconium-Si3N4 ceramic  
p 80 A84-25402
- BUZZARD, R. J.**  
Mode 2 fatigue crack growth specimen development  
[NASA-TM-83722] p 156 N84-29248

## C

- CALFO, F. D.**  
Micronized coal burner facility  
[NASA-CASE-LEW-13426-1] p 60 N84-16276
- CALVO, E. J.**  
Electrochemical studies of redox systems for energy storage  
[NASA-CR-174503] p 165 N84-15681
- CAMARA, E. H.**  
Advanced onboard storage concepts for natural gas-fueled automotive vehicles  
[NASA-CR-174655] p 172 N84-34036
- CAMP, D. W.**  
Sixth Annual Workshop on Meteorological and Environmental Inputs to Aviation Systems, 26-28 October 1982, Tallahassee, Tenn  
p 174 A84-23424
- CAMPANELLA, S. J.**  
ACTS TDMA network control  
[AIAA PAPER 84-0682] p 94 A84-25274
- CARMU, U.**  
Homogeneous reactions of hydrocarbons, silane, and chlorosilanes in radiofrequency plasmas at low pressures  
[NASA-TP-2301] p 50 N84-20643  
Radical and ion molecule mechanisms in the polymerization of hydrocarbons and chlorosilanes in RF plasmas at low pressures (1.0 torr)  
[NASA-TM-83802] p 190 N84-21329  
Correlations between plasma variables and the deposition process of Si films from chlorosilanes in low pressure RF plasma of argon and hydrogen  
[NASA-TM-83803] p 190 N84-21330
- CARNEY, R. R.**  
A graphics subsystem retrofit design for the bladed-disk data acquisition system  
[NASA-TM-83510] p 175 N84-12730
- CARPENTER, M. H.**  
Turbulent flow field calculations in an internal combustion engine equipped with two valves  
p 112 A84-13311
- CARUSO, J. J.**  
Application of finite element substructuring to composite micromechanics  
[NASA-TM-83729] p 57 N84-31288
- CASASANT, D.**  
Direct and implicit optical matrix-vector algorithms  
p 187 A84-13184  
State estimation Kalman filter using optical processings  
Noise statistics known  
p 178 A84-23602  
Advanced acousto-optic signal processors  
p 187 A84-28485  
Optical Kalman filtering for missile guidance  
p 178 A84-38596  
Acoustooptic linear algebra processors - Architectures, algorithms, and applications  
p 175 A84-40266  
Optical systolic solutions of linear algebraic equations  
p 188 N84-22405
- CASE, S.**  
Window aberration correction in laser velocimetry using multifaceted holographic optical elements  
p 134 A84-24663

- CASPAR, J. R.**  
A linear aerodynamic analysis for unsteady transonic cascades  
[NASA-CR-3833] p 11 N84-32355
- CASSENTI, B. N.**  
Research and development program for the development of advanced time-temperature dependent constitutive relationships Volume 1 Theoretical discussion  
[NASA-CR-168191-VOL-1] p 153 N84-10613  
Research and development program for the development of advanced time-temperature dependent constitutive relationships Volume 2 Programming manual  
[NASA-CR-168191-VOL-2] p 153 N84-10614
- CASSINELLI, J. E.**  
Study of solar array switching power management technology for space power system  
[NASA-CR-167890-EXEC-SUM] p 167 N84-23021
- CATALDO, R. L.**  
Test results of a ten cell bipolar nickel-hydrogen battery p 162 A84-30188  
Design of a 1-kWh bipolar nickel hydrogen battery  
[NASA-TM-83647] p 168 N84-23024  
Test results of a ten cell bipolar nickel-hydrogen battery p 112 N84-33702
- CAUGHEY, D. A.**  
An implicit LU scheme for the Euler equations applied to arbitrary cascades  
[AIAA PAPER 84-0167] p 4 A84-17925
- CAULEY, M. A.**  
The subjective effect of multiple co-channel frequency modulated television interference  
[NASA-TM-83415] p 97 N84-11360
- CAULFIELD, H. J.**  
Automatic holographic droplet analysis for liquid fuel sprays p 125 N84-20531
- CAVANAGH, J. R.**  
Material removal considerations for metal-ceramic abradable turbine seal systems p 135 A84-15575
- CAVICCHI, R. H.**  
Design and performance of a fixed, nonaccelerating, guide vane cascade that operates over an inlet flow angle range of 60 deg  
[NASA-TM-83519] p 8 N84-14120
- CAWLEY, J. D.**  
Overview of zirconia with respect to gas turbine applications  
[NASA-TP-2286] p 83 N84-21740  
Oxidizing seal for a turbine tip gas path  
[NASA-CASE-LEW-14053-1] p 29 N84-22563  
Oxygen diffusion in alpha-Al<sub>2</sub>O<sub>3</sub>  
[NASA-TM-83622] p 86 N84-28990
- CERNANSKY, N. P.**  
Combustion characteristics in the transition region of liquid fuel sprays  
[NASA-CR-175396] p 61 N84-19495
- CHAMBERLIN, R.**  
Comparison of full-scale engine and subscale model performance of a mixed flow exhaust system for an energy efficient engine (E3) propulsion system  
[AIAA PAPER 84-0283] p 16 A84-17997
- CHAMIS, C. C.**  
Tensile buckling of advanced turboprops p 149 A84-11039  
Prediction of composite hygral behavior made simple p 51 A84-14285  
Environmental and high strain rate effects on composites for engine applications p 51 A84-17444  
Durability/life of fiber composites in hygrothermomechanical environments p 52 A84-27359  
Compressive behavior of unidirectional fibrous composites p 53 A84-29894  
Simplified composite micromechanics equations for strength, fracture toughness and environmental effects p 53 A84-41858  
Simplified composite micromechanics equations of hygral, thermal, and mechanical properties p 53 A84-49377  
Resin selection criteria for tough composite structures  
[NASA-TM-83449] p 81 N84-10310  
INHVD Computer code for intraply hybrid composite design A users manual  
[NASA-TP-2239] p 54 N84-13224  
Design concepts for low-cost composite engine frames  
[NASA-TM-83544] p 26 N84-16186  
Select fiber composites for space applications: A mechanistic assessment  
[NASA-TM-83631] p 55 N84-22702  
Impact resistance of fiber composites Energy absorbing mechanisms and environmental effects  
[NASA-TM-83594] p 55 N84-24712
- Dynamic stress analysis of smooth and notched fiber composite flexural specimens  
[NASA-TM-83694] p 56 N84-25770  
ICAN Integrated composites analyzer p 56 N84-26755  
Interply layer degradation effects on composite structural response  
[NASA-TM-83702] p 56 N84-26756  
Simplified composite micromechanics equations for strength, fracture toughness and environmental effects  
[NASA-TM-83686] p 56 N84-27832  
Hygrothermomechanical fracture stress criteria for fiber composites with sense-panty  
[NASA-TM-83691] p 57 N84-28918  
Nonlinear analysis for high-temperature composites  
Turbine blades/vanes p 158 N84-31690
- CHAN, J. L.**  
A 20-GHz IMPATT transmitter  
[NASA-CR-168076] p 106 N84-11385
- CHANDRAN, K. B.**  
Prediction of turbulent flow past a prosthetic heart valve p 175 A84-49108
- CHANDRASEKARAN, S.**  
A new FET-bipolar combinational power semiconductor switch p 104 A84-32293
- CHANG, A. T.**  
The influence of gyroscopic forces on the dynamic behavior and flutter of rotating blades  
[NASA-CR-175444] p 27 N84-20524
- CHANG, G. E.**  
Improved high temperature resistant matrix resins  
[NASA-CR-168210] p 87 N84-28995
- CHANG, G. E. C.**  
Development of partially fluorinated resin apex seals  
[NASA-CR-174706] p 148 N84-32828
- CHANG, S. C.**  
A semi-direct procedure using a local relaxation factor and its application to an internal flow problem  
[NASA-TM-83704] p 128 N84-25946
- CHANG, S. H.**  
Embedding methods for the steady Euler equations  
[NASA-TM-83431] p 178 N84-11831
- CHANG, T. Y.**  
A computer program for predicting nonlinear uniaxial material responses using viscoplastic models  
[NASA-TM-83675] p 156 N84-29247  
Nonlinear finite element analysis of shells with large aspect ratio p 158 N84-31692
- CHAO, C.**  
A Ka-band GaAs monolithic phase shifter p 101 A84-18371
- CHAO, D. F. K.**  
Numerical simulation of two-dimensional heat transfer in composite bodies with application to de-icing of aircraft components  
[NASA-CR-168283] p 122 N84-13490
- CHARLESTON, A.**  
Chromium electrodes for REDOX cells  
[NASA-CASE-LEW-13653-1] p 170 N84-28205
- CHEATHAM, J. G.**  
V/STOL model fan stage design report  
[NASA-CR-174688] p 29 N84-23629
- CHEN, A. G.**  
Variable stator radial turbine  
[NASA-CR-174663] p 29 N84-22568
- CHEN, C. J.**  
Prediction of turbulent flow past a prosthetic heart valve p 175 A84-49108
- CHEN, C.-J.**  
Finite-analytic numerical method for unsteady two-dimensional Navier-Stokes equations p 116 A84-25807
- CHEN, D.**  
On the suppression of zero energy deformation modes p 150 A84-21541
- CHEN, D. Y.**  
Formation and inflammation of a turbulent jet  
[AIAA PAPER 84-0572] p 114 A84-18171  
Design considerations for FET-gated power transistors p 102 A84-18414  
A new FET-bipolar combinational power semiconductor switch p 104 A84-32293  
Experimental and theoretical study of combustion jet ignition  
[NASA-CR-168139] p 21 N84-10054  
Hybrid power semiconductor switch  
[NASA-CASE-LEW-13922-1] p 106 N84-11389
- CHEN, H.-C.**  
Finite-analytic numerical method for unsteady two-dimensional Navier-Stokes equations p 116 A84-25807
- CHEN, R.**  
Interference performance analysis of M-ary CPSK and M-ary CAPK digital transmission systems and the computation of 'required isolation' for efficient utilization of geostationary satellite orbit/spectrum p 95 A84-49303
- CHEN, R. T.**  
LEC GaAs for integrated circuit applications  
[NASA-CR-173267] p 191 N84-17014
- CHEN, R. T. N.**  
Rotorcraft flight-propulsion control integration p 36 A84-46524
- CHERRY, D. G.**  
The aerodynamic design and performance of the NASA/GE E3 low pressure turbine  
[AIAA PAPER 84-1162] p 21 A84-44186
- CHI, R. M.**  
Aeroelastic analysis for propellers - mathematical formulations and program user's manual  
[NASA-CR-3729] p 153 N84-12530  
Subsonic/transonic stall flutter investigation of a rotating ng  
[NASA-CR-174625] p 36 N84-33417
- CHIANG, N.**  
High-speed wide band 20 x 20 microwave switch matrix p 105 A84-49253
- CHIARAMONTE, F. P.**  
Determination of compressor in-stall characteristics from engine surge transients  
[AIAA PAPER 84-1206] p 18 A84-36959  
Determination of compressor in-stall characteristics from engine surge transients  
[NASA-TM-83639] p 29 N84-22566
- CHIMA, R. V.**  
Analysis of inviscid and viscous flows in cascades with an explicit multiple-grid algorithm  
[AIAA PAPER 84-1663] p 5 A84-38043  
Analysis of inviscid and viscous flows in cascades with an explicit multiple-grid algorithm  
[NASA-TM-83636] p 1 N84-22527
- CHIN, D.-T.**  
Electrode kinetics of oxygen reduction - A theoretical and experimental analysis of the rotating ring-disc electrode method p 59 A84-23999
- CHIN, L.**  
The role of cobalt on the creep of Waspaloy  
[NASA-CR-174628] p 70 N84-19523
- CHIN, S. A.**  
Design considerations for FET-gated power transistors p 102 A84-18414  
A new FET-bipolar combinational power semiconductor switch p 104 A84-32293
- CHITWOOD, J. S.**  
A study of 60 GHz intersatellite link applications p 40 A84-49288
- CHLEBECEK, R. A.**  
Multicomponent velocity measurement in a piston-cylinder configuration using laser velocimetry  
[NASA-TM-83534] p 8 N84-14121
- CHO, Y.**  
The 20 GHz solid state transmitter design, impatt diode development and reliability assessment  
[NASA-CR-174716] p 112 N84-33715
- CHOE, S. J.**  
Fatigue crack growth and low cycle fatigue of two nickel base superalloys  
[NASA-CR-174534] p 66 N84-10267
- CHOPRA, M.**  
Gravitational effects in dendritic growth p 37 A84-22346
- CHOU, D. C.**  
Boundary layer transition effects on flow separation around V/STOL engine inlets at high incidence  
[AIAA PAPER 84-0432] p 4 A84-18090
- CHRISTNER, L.**  
Full scale phosphoric acid fuel cell stack technology development  
[NASA-CR-174660] p 169 N84-26165
- CHUANG, S. L.**  
Wave attenuation and mode dispersion in a waveguide coated with lossy dielectric material  
[NASA-CR-173820] p 100 N84-30145  
Numerical methods for analyzing electromagnetic scattering  
[NASA-CR-173916] p 101 N84-32645
- CHUBB, D. L.**  
Thermionic-photovoltaic energy converter  
[NASA-CASE-LEW-14077-1] p 167 N84-20918
- CHUDNOVSKY, A.**  
Crack layer theory  
[NASA-CR-174634] p 156 N84-22980  
On stress analysis of a crack-layer  
[NASA-CR-174774] p 159 N84-34774

- CHUNG, B. T. F.**  
Heat transfer in thermal barrier coated rods with circumferential and radial temperature gradients [ASME PAPER 84-GT-181] p 121 A84-46982  
High temperature thermomechanical analysis of ceramic coatings p 152 A84-48565
- CHUNG, S. H.**  
An invariant derivation of flame stretch p 58 A84-18925
- CIVINSKAS, K.**  
Application of a quasi-3D inviscid flow and boundary layer analysis to the hub-shroud contouring of a radial turbine [AIAA PAPER 84-1297] p 6 A84-44177
- CIVINSKAS, K. C.**  
Application of a quasi-3D inviscid flow and boundary layer analysis to the hub-shroud contouring of a radial turbine [NASA-TM-83669] p 10 N84-25647
- CLAAR, T. D.**  
High-temperature molten salt thermal energy storage systems for solar applications [NASA-CR-167916] p 165 N84-15679
- CLARK, C. A.**  
Communications network design and costing model technical manual [NASA-CR-168236] p 97 N84-14376  
Communications network design and costing model programmers manual [NASA-CR-168237] p 97 N84-14377  
Communications network design and costing model users manual [NASA-CR-168238] p 97 N84-14378
- CLASPY, P. C.**  
Applications of photoacoustic techniques to the study of jet fuel residue [NASA-CR-173322] p 90 N84-18420
- CLAUS, R. W.**  
Flame radiation and linear heat transfer in a tubular can combustor [AIAA PAPER 84-0443] p 16 A84-21300  
Flame radiation and linear heat transfer in a tubular-can combustor [NASA-TM-83538] p 23 N84-13188  
Numerical modeling of turbulent flow p 125 N84-20538
- CLINE, J. G.**  
A temperature correlation for the radiation resistance of a thick-walled circular duct exhausting a hot gas p 181 A84-31103
- CLINE, S.**  
Blade loss transient dynamics analysis with flexible bladed disk [NASA-CR-168176] p 23 N84-13193
- CLINGMAN, D. L.**  
Material removal considerations for metal-ceramic abradable turbine seal systems p 135 A84-15575
- COBAN, E.**  
High-speed wide band 20 x 20 microwave switch matrix p 105 A84-49253
- COE, H. H.**  
Thermal analysis of a planetary transmission with spherical roller bearings operating after complete loss of oil [NASA-TP-2367] p 147 N84-32824
- COHEN, S. M.**  
Research on aviation fuel instability p 90 N84-23642  
Research on aviation fuel instability p 91 N84-24734
- COLALUCA, M. A.**  
An investigation into the injection molding of PMR-15 polyimide [NASA-CR-173550] p 85 N84-24810
- COLE, G. L.**  
Operating system for a real-time multiprocessor propulsion system simulator [NASA-TM-83605] p 177 N84-20258
- COLELLO, R. G.**  
Catalog of selected heavy duty transport energy management models [NASA-CR-168299] p 194 N84-14991
- COLEMAN, E.**  
Dilution jet mixing program [NASA-CR-174524] p 33 N84-26702
- COLLINS, G. J.**  
Photodeposition of nitride insulators on 3-5 substrates [NASA-CR-173393] p 71 N84-21720
- COLLINS, S. A., JR.**  
Optical flip-flops and sequential logic circuits using a liquid crystal light valve p 188 A84-40332  
Optical pulse generator using liquid crystal light valve p 188 N84-22414  
Optical residue addition and storage units using a Hughes liquid crystal light valve p 188 N84-22417
- COLLINS, W. R.**  
ADA and multi-microprocessor real-time simulation p 176 A84-10905
- CONNOLLY, D. J.**  
Microwave monolithic integrated circuit development for future spaceborne phased array antennas [AIAA PAPER 84-0656] p 94 A84-25257  
A study of 60 GHz intersatellite link applications p 40 A84-49288  
Microwave monolithic integrated circuit development for future spaceborne phased array antennas [NASA-TM-83516] p 97 N84-13399  
MMIC technology for advanced space communications systems [NASA-TM-83749] p 100 N84-30147  
The 20 and 30 GHz MMIC technology for future space communication antenna system [NASA-TM-83745] p 100 N84-31460  
Monolithic microwave integrated circuits Interconnections and packaging considerations [NASA-TM-83774] p 100 N84-31461
- CONROY, M. J.**  
Test results for 27.5- to 30-GHz communications satellite receivers [NASA-TM-83662] p 100 N84-27954
- CONTOLATIS, A.**  
A Ka-band GaAs monolithic phase shifter p 101 A84-18371
- COONS, F.**  
Sixth Annual Workshop on Meteorological and Environmental Inputs to Aviation Systems, 26-28 October 1982, Tullahoma, Tenn p 174 A84-23424
- COOPER, A. R.**  
Oxygen diffusion in alpha-Al<sub>2</sub>O<sub>3</sub> [NASA-TM-83622] p 86 N84-28990
- COOPER, L. P.**  
Propulsion issues for advanced orbit transfer vehicles [NASA-TM-83624] p 47 N84-25762  
Propulsion issues for advanced orbit transfer vehicles p 48 N84-29937
- COPE, D.**  
Metal vapor vacuum arc switching - Applications and results p 103 A84-32029
- CORNELL, C. C.**  
Experimental study of performance degradation of a model helicopter main rotor with simulated ice shapes [AIAA PAPER 84-0184] p 13 A84-17937
- CORREA, S. M.**  
Aerothermal modeling Executive summary [NASA-CR-168330] p 25 N84-15152  
Aerothermal modeling, phase 1. Volume 1. Model assessment [NASA-CR-168296-VOL-1] p 25 N84-15155  
Aerothermal modeling, phase 1. Volume 2. Experimental data [NASA-CR-168296-VOL-2] p 25 N84-15156
- CORSMEIER, R. J.**  
Air modulation apparatus [NASA-CASE-LEW-13524-1] p 35 N84-33410
- COSTAKIS, W.**  
Real-time simulation of an automotive gas turbine using the hybrid computer [NASA-TM-83593] p 195 N84-26484
- COWLES, B. A.**  
Low strain, long life creep fatigue of AF2-1DA and INCO 718 [NASA-CR-167989] p 66 N84-10268
- COY, J. J.**  
Precision of spiral-bevel gears [ASME PAPER 82-WA/DE-33] p 135 A84-15950  
Kinematic precision of gear trains [ASME PAPER 82-WA/DE-34] p 135 A84-15951  
NASA transmission research and its probable effects on helicopter transmission design p 139 A84-46355  
Special cases of friction and applications [NASA-TM-83523] p 141 N84-11500  
Transmission efficiency measurements and correlations with physical characteristics of the lubricant [NASA-TM-83740] p 147 N84-30293  
Summary of drive-train component technology in helicopters [NASA-TM-83726] p 147 N84-30294
- CRAIG, H. M.**  
Combustor liner construction [NASA-CASE-LEW-14035-1] p 30 N84-24577
- CRAWLEY, E. F.**  
Stagger angle dependence of inertial and elastic coupling in bladed disks p 151 A84-31903  
Optimization and mechanisms of mistuning in cascades [ASME PAPER 84-GT-196] p 21 A84-46993
- CREASON, T. L.**  
V/STOL model fan stage ng design report [NASA-CR-174688] p 29 N84-23629
- CREEKMORE, R.**  
Real-time Pegasus propulsion system model V/STOL-piloted simulation evaluation p 15 A84-17362
- CROMWELL, N.**  
Mobile radio alternative systems study. Volume 2 Terrestrial [NASA-CR-168063] p 96 N84-10403
- CROSS, E. J., JR.**  
Experimental study of performance degradation of a model helicopter-main rotor with simulated ice shapes [AIAA PAPER 84-0184] p 13 A84-17937  
Performance degradation of a model helicopter main rotor in hover and forward flight with a generic ice shape [AIAA PAPER 84-0609] p 13 A84-24195  
Performance degradation of a model helicopter rotor with a generic ice shape p 14 A84-49096
- CROSS, K. R.**  
Material removal considerations for metal-ceramic abradable turbine seal systems p 135 A84-15575
- CULL, R. C.**  
Investigation of energy management strategies for photovoltaic systems - An analysis technique p 160 A84-22993  
Investigation of energy management strategies for photovoltaic systems - A predictive control algorithm p 161 A84-25468
- CULY, D. G.**  
Advanced turbocharger design study program [NASA-CR-174633] p 143 N84-21879
- CURREN, A. N.**  
Beam impingement angle effects on secondary electron emission characteristics of textured pyrolytic graphite [NASA-TP-2285] p 82 N84-18400  
Ion sputter textured graphite electrode plates [NASA-CASE-LEW-12919-2] p 179 N84-28565  
Secondary electron emission characteristics of ion-textured copper and high-purity isotropic graphite surfaces [NASA-TP-2342] p 86 N84-28969
- CURTIS, H.**  
Recent advances in thin silicon solar cells p 160 A84-22981  
Optimal design of GaAs-based concentrator space solar cells for 100 AMO, 60 deg C operation p 170 N84-29312
- CURTIS, H. B.**  
Effects of indirect bandgap top cells in a monolithic cascade cell structure p 160 A84-22987
- CUSANO, C.**  
Surface roughness effects with solid lubricants dispersed in mineral oils [ASLE PREPRINT 83-LC-4C-1] p 137 A84-28987
- CYR, M. A.**  
Turbine blade and vane heat flux sensor development, phase 1 [NASA-CR-168297] p 134 N84-32790

## D

- DADONE, L.**  
Performance degradation of propeller systems due to rime ice accretion [AIAA PAPER 82-0286] p 12 A84-17406  
Helicopter rotor performance degradation in natural icing encounter p 12 A84-17412
- DAI, Y. W.**  
Numerical modeling of turbulent flow in a channel [NASA-CR-168278] p 23 N84-13189
- DAILY, J. W.**  
Combustion in a turbulent mixing layer formed at a rearward-facing step p 58 A84-10140
- DALLING, D. K.**  
Carbon-13 and proton nuclear magnetic resonance analysis of shale-derived refinery products and jet fuels and of experimental referee broadened-specification jet fuels [NASA-CR-174761] p 92 N84-32552
- DANDEKAR, K. V.**  
Time-resolved density measurements in premixed turbulent flames p 59 A84-32612
- DANIELE, C. J.**  
A generalized computer code for developing dynamic gas turbine engine models (DIGTEM) [NASA-TM-83508] p 22 N84-12166  
Digital computer program for generating dynamic turbofan engine models (DIGTEM) [NASA-TM-83446] p 26 N84-16185
- DARKAZALLI, G.**  
Solar photovoltaic powered refrigerators/freezers for medical use in remote geographic locations [NASA-CR-168268] p 169 N84-25163

- DAVIS, P. R.**  
Evaluation of single crystal LaB<sub>6</sub> cathodes for use in a high frequency backward wave oscillator tube  
[NASA-CR-173343] p 108 N84-19709
- DAVIS, R. H.**  
Contingency power concepts for helicopter turboshaft engine  
[NASA-TM-83679] p 30 N84-23648  
Rotorcraft contingency power study  
[NASA-CR-174675] p 31 N84-24580
- DAVIS, R. L.**  
Energy efficient engine high-pressure turbine supersonic cascade technology report  
[NASA-CR-165567] p 33 N84-27739
- DAWICKE, D. S.**  
A total life prediction model for stress concentration sites  
[NASA-CR-168225] p 152 N84-10612
- DAYAN, M.**  
Study of the Auger line shape of polyethylene and diamond  
Measurement of rolling friction by a damped oscillator  
[NASA-TP-2257] p 141 N84-13577
- DE LOS REYES, G.**  
The application of LQR synthesis techniques to the turboshaft engine control problem  
[AIAA PAPER 84-1455] p 21 A84-44185
- DEADMORE, D. L.**  
Application of induction coil measurements to the study of superalloy hot corrosion and oxidation  
[NASA-TM-83560] p 69 N84-16311  
Effects of alloy composition on cyclic flame hot-corrosion attack of cast nickel-base superalloys at 900 deg C  
[NASA-TP-2338] p 73 N84-26783  
In-situ measurements of alloy oxidation/corrosion/erosion using a video camera and proximity sensor with microcomputer control  
[NASA-TM-83673] p 74 N84-27859
- DECKER, A. J.**  
Measurement of fluid properties using rapid-double-exposure and time-average holographic interferometry  
[AIAA PAPER 84-1461] p 130 A84-35223  
Measurement of fluid properties using rapid-double-exposure and time-average holographic interferometry  
[NASA-TM-83630] p 132 N84-21849
- DECREAU, P.**  
Comparison of thermal plasma observations on SCATHA and GEOS  
p 41 N84-17262
- DESSLER, R. G.**  
Turbulent solutions of the equations of fluid motion  
p 121 A84-41156
- DELAAT, J. C.**  
Areal-time implementation of an advanced sensor failure detection, isolation, and accommodation algorithm  
[AIAA PAPER 84-0569] p 176 A84-21305  
Areal-time implementation of an advanced sensor failure detection, isolation, and accommodation algorithm  
[NASA-TM-83553] p 1 N84-13140
- DELOMBARD, R.**  
Low-frequency switching voltage regulators for terrestrial photovoltaic systems  
[NASA-TM-83625] p 110 N84-25926  
Photovoltaic power system for satellite Earth stations in remote areas Project status and design description  
[NASA-TM-83789] p 101 N84-33642
- DEMERDASH, N. A.**  
Improved transistor-controlled and commutated brushless DC motors for electric vehicle propulsion  
[NASA-CR-168053] p 105 N84-10450
- DEMIER, R.**  
Steam bottoming cycle for an adiabatic diesel engine  
[NASA-CR-168255] p 196 N84-33304
- DENGLER, R. P.**  
The aerodynamic design and performance of the NASA/GE E3 low pressure turbine  
[AIAA PAPER 84-1162] p 21 A84-44186
- DENHAM, J. W.**  
Supersonic jet screech tone cancellation  
p 179 A84-10136
- DENNETT, J. T.**  
Large, horizontal-axis wind turbines  
[NASA-TM-83546] p 169 N84-27327
- DEUTSCH, S.**  
The boundary layer on compressor cascade blades  
[NASA-CR-173514] p 127 N84-25001
- DEVANCE, D. C.**  
Development and fabrication of a high current, fast recovery power diode  
[NASA-CR-168196] p 106 N84-13443
- DEVLIN, R. E.**  
Advanced propfan drive system characteristics and technology needs  
[AIAA PAPER 84-1194] p 18 A84-36957
- DEZELICK, R. A.**  
Baseline performance and emissions data for a single-cylinder, direct-injected diesel engine  
[NASA-TM-86873] p 197 N84-34330
- DIBELLA, F. A.**  
An RC-1 organic Rankine bottoming cycle for an adiabatic diesel engine  
[NASA-CR-168258] p 196 N84-32306
- DICARLO, J. A.**  
Factors influencing the thermally-induced strength degradation of B/AI composites  
p 52 A84-28227  
Method for strengthening boron fibers  
[NASA-CASE-LEW-13826-2] p 55 N84-24711
- DICKINSON, T. W.**  
AFB/open cycle gas turbine conceptual design study  
[NASA-CR-168135] p 172 N84-31784
- DIETZE, W. T.**  
Development of a 30 percent efficient 3-junction monolithic cascade solar cell  
p 171 N84-29328
- DIMITRIADIS, B. D.**  
The effect of variable S/N on the subjective evaluation of protection ratios for direct-TV satellite services  
p 95 A84-48452
- DINANNO, L. R.**  
An RC-1 organic Rankine bottoming cycle for an adiabatic diesel engine  
[NASA-CR-168256] p 196 N84-32306
- DIRUSSO, E.**  
Feasibility analysis of a spiral groove ring seal for counter-rotating shafts  
p 139 A84-45965  
Dynamic behavior of spiral-groove and Rayleigh-Step self-acting face seals  
[NASA-TP-2266] p 25 N84-16181
- DITTMAR, J. H.**  
Why credible propeller noise measurements are possible in the acoustically untreated NASA Lewis 8 ft by 6 ft wind tunnel  
p 181 A84-38091  
A possible explanation for the present difference between linear noise theory and experimental data for supersonic helical tip speed propellers  
[NASA-TM-83467] p 183 N84-14874  
Noise of the SR-6 propeller model at 2 deg and 4 deg angles of attack  
[NASA-TM-83515] p 183 N84-16946  
Fan noise reduction achieved by removing tip flow irregularities behind the rotor - forward arc test configurations  
[NASA-TM-83616] p 184 N84-23235  
An experimental investigation of the effect of boundary layer refraction on the noise from a high-speed propeller  
[NASA-TM-83764] p 186 N84-34230
- DOCHAT, G.**  
Free-piston stirling engine endurance test program  
p 136 A84-22864
- DODD, C. W.**  
How to protect a wind turbine from lightning  
[NASA-CR-168229] p 163 N84-10661
- DODDS, R. H., JR.**  
Theoretical and software considerations for nonlinear dynamic analysis  
[NASA-CR-174504] p 154 N84-15589
- DODDS, W. J.**  
NASA/General Electric Broad-Specification Fuels Combustion Technology Program - Phase I  
p 16 A84-24033  
Clean catalytic combustor program  
[NASA-CR-168323] p 24 N84-15151  
Broad specification fuels combustion technology program  
[NASA-CR-168179] p 89 N84-15283
- DODGE, F. T.**  
Vapor flow into a capillary propellant-acquisition device  
p 43 A84-36559  
Gas flow across a wet screen - Analogy to a relief valve with hysteresis  
p 121 A84-43546
- DODGE, L. G.**  
Calibration of the Malvern particle sizer  
p 131 A84-40736  
Development of carbon slurry fuels for transportation (hybrid fuels, phase 2)  
[NASA-CR-174659] p 74 N84-28960
- DOLGOPOLSKY, A.**  
On stress analysis of a crack-layer  
[NASA-CR-174774] p 159 N84-34774
- DONOGHUE, J. F.**  
Optimization methods applied to hybrid vehicle design  
[NASA-CR-168292] p 194 N84-19185
- DONOVAN, L. F.**  
Redesign and cascade tests of a supercritical controlled diffusion stator blade-section  
[AIAA PAPER 84-1207] p 5 A84-36960  
Calculation of transonic flow in a linear cascade  
[AIAA PAPER 84-1301] p 6 A84-40241  
Redesign and cascade tests of a supercritical controlled diffusion stator blade-section  
[NASA-TM-83635] p 10 N84-22533
- Calculation of transonic flow in a linear cascade  
[NASA-TM-83697] p 10 N84-24539
- DONOVAN, R. M.**  
Space Station propulsion analysis study  
[AIAA PAPER 84-1326] p 44 A84-44179  
Space station propulsion analysis study  
[NASA-TM-83715] p 47 N84-25764
- DOUGHERTY, D.**  
High temperature thermomechanical analysis of ceramic coatings  
p 152 A84-48565
- DOWELL, E. H.**  
Forced response of a cantilever beam with a dry friction damper attached I - Theory II - Experiment  
p 150 A84-21267
- DOWNEY, A. N.**  
Microwave monolithic integrated circuit development for future spaceborne phased array antennas  
[AIAA PAPER 84-0656] p 94 A84-25257  
Microwave monolithic integrated circuit development for future spaceborne phased array antennas  
[NASA-TM-83518] p 97 N84-13399  
MMIC technology for advanced space communications systems  
[NASA-TM-83749] p 100 N84-30147  
Monolithic microwave integrated circuits Interconnections and packaging considerations  
[NASA-TM-83774] p 100 N84-31461
- DRAGO, R. J.**  
Development of large rotorcraft transmissions  
p 21 A84-46354
- DRELA, M.**  
Conservative streamtube solution of steady-state Euler equations  
[AIAA PAPER 84-1643] p 120 A84-38030
- DRESHFIELD, R. L.**  
Replacing critical and strategic refractory metal elements in nickel-base superalloys  
[NASA-TM-83528] p 67 N84-13264  
P/M superalloys A troubled adolescent?  
[NASA-TM-83623] p 73 N84-26785  
Understanding the roles of the strategic element cobalt in nickel base superalloys  
p 76 N84-33471
- DRING, R. P.**  
Inlet boundary layer effects in an axial compressor rotor I Blade-to-blade effects  
[ASME PAPER 84-GT-84] p 6 A84-46926  
Inlet boundary layer effects in an axial compressor rotor II - Throughflow effects  
[ASME PAPER 84-GT-85] p 7 A84-46927  
Compressor rotor aerodynamics  
p 26 N84-16210  
Energy efficient engine high-pressure turbine supersonic cascade technology report  
[NASA-CR-165567] p 33 N84-27739
- DUFFY, R. E.**  
Investigation of the effects of pressure gradient, temperature and wall temperature ratio on the stagnation point heat transfer for circular cylinders and gas turbine vanes  
[NASA-CR-174667] p 30 N84-23649
- DUKE, A. M.**  
Study of effects of fuel properties in turbine-powered business aircraft  
[NASA-CR-174627] p 91 N84-25854
- DUKE, J. C., JR.**  
Characterization of composite materials by means of the ultrasonic stress wave factor  
p 51 A84-10430
- DULIKRACH, G. S.**  
Transonic cascade flow analysis using viscous/inviscid coupling concepts  
[AIAA PAPER 84-2159] p 6 A84-46103
- DUNBAR, D.**  
Computer analysis of effects of altering jet fuel properties on refinery costs and yields  
[NASA-CR-174642] p 91 N84-27908
- DUNGUNDJI, J.**  
Flutter and forced response of mistuned rotors using standing wave analysis  
[NASA-CR-173555] p 32 N84-24586
- DUQUETTE, D. J.**  
The effects of frequency and hold times on fatigue crack propagation rates in a nickel base superalloy  
p 64 A84-18733  
Fatigue crack growth and low cycle fatigue of two nickel base superalloys  
[NASA-CR-174534] p 66 N84-10267
- DURBIN, P. A.**  
The production of turbulent stress in a shear flow by irrotational fluctuations  
p 115 A84-18357  
High frequency green function for aerodynamic noise in moving media I - General theory II - Noise from a spreading jet  
p 180 A84-21273  
The production of turbulent stress in a shear flow by irrotational fluctuations  
p 115 A84-21390

- DURRETT, R.**  
NASA's geostationary communications platform program  
[AIAA PAPER 84-0702] p 95 A84-25326
- DUTTA, S.**  
Compositional effects on Si3N4 fracture surfaces p 79 A84-19794  
Microstructure, strength, and oxidation of a 10 wt pct zirconia-Si3N4 ceramic p 80 A84-25402  
Sinterability, strength and oxidation of alpha silicon carbide powders p 80 A84-32306
- DYBBS, A.**  
Internal heat transfer coefficients of porous metals p 112 A84-13239

## E

- EBERHARDT, R. N.**  
On-orbit cryogenic fluid transfer  
[AIAA PAPER 84-1343] p 44 A84-44176  
Cryogenic Fluid Management Facility  
[AIAA PAPER 84-1340] p 44 A84-44184  
On-orbit cryogenic fluid transfer  
[NASA-TM-83688] p 39 A84-25753
- EBERT, L. J.**  
The development of directional coarsening of the gamma-prime precipitate in superalloy single crystals p 63 A84-10597  
Factors which influence directional coarsening of Gamma prime during creep in nickel-base superalloy single crystals  
[NASA-TM-83595] p 69 A84-17353  
Influence of composition on the microstructure and mechanical properties of a nickel-base superalloy single crystal  
[NASA-TM-83563] p 70 A84-17354
- EBIHARA, B. T.**  
A multistage spent particle collector and a method for making same  
[NASA-CASE-LEW-13914-1] p 131 A84-12447
- ECER, A.**  
Application of a finite element algorithm to the solution of steady transonic Euler equations p 3 A84-10133  
Finite element formulation of transonic flow problems p 116 A84-25859
- EDELMAN, R. B.**  
Analytic modeling of a spray diffusion flame  
[AIAA PAPER 84-1317] p 118 A84-35168
- EDWARDS, D. E.**  
Extension to an analysis of turbulent swirling compressible flow for application to axisymmetric small gas turbine ducts  
[NASA-CR-165597] p 195 A84-21445
- EDWARDS, R. V.**  
Output statistics of laser anemometers in sparsely seeded flows p 117 A84-28738  
Optimizing and comparing laser anemometers p 130 A84-28739
- EKCHIAN, J. A.**  
Computer simulation of the heavy-duty turbo-compounded diesel cycle for studies of engine efficiency and performance  
[NASA-CR-174755] p 196 A84-33306
- EKSTEDT, E. E.**  
NASA/General Electric Broad-Specification Fuels Combustion Technology Program - Phase I p 16 A84-24033  
NASA advanced low emissions combustor program  
[ASME PAPER 83-JPGC-GT-10] p 17 A84-28982  
Clean catalytic combustor program  
[NASA-CR-168323] p 24 A84-15151  
Broad specification fuels combustion technology program  
[NASA-CR-168179] p 89 A84-15283
- EL-BAYOUMY, L. E.**  
Parameter studies of gear cooling using an automatic finite element mesh generator  
[NASA-TM-83721] p 146 A84-28087  
An investigation of the transient thermal analysis of spur gears  
[NASA-TM-83724] p 146 A84-28088
- ELCHURI, V.**  
NASTRAN forced-vibration analysis of rotating cyclic structures  
[ASME PAPER 83-DET-20] p 151 A84-29103  
Flutter analysis of advanced turbopropellers p 152 A84-36492  
Forced vibration analysis of rotating cyclic structures in NASTRAN  
[NASA-CR-165429] p 153 A84-11514  
Finite element forced vibration analysis of rotating cyclic structures  
[NASA-CR-165430] p 153 A84-11515  
NASTRAN flutter analysis of advanced turbopropellers  
[NASA-CR-167926] p 24 A84-14148

- NASTRAN documentation for flutter analysis of advanced turbopropellers  
[NASA-CR-167927] p 25 A84-15153  
Bladed-shrouded-disc aeroelastic analyses: Computer program updates in NASTRAN level 17.7  
[NASA-CR-165428] p 25 A84-15154  
NASTRAN forced vibration analysis of rotating cyclic structures  
[NASA-CR-173821] p 157 A84-29252
- ELKINS, R. H.**  
Advanced onboard storage concepts for natural gas-fueled automotive vehicles  
[NASA-CR-174655] p 172 A84-34036
- ELLIOTT, K. R.**  
Interaction between boron and intrinsic defects in GaAs p 190 A84-33918  
LEC GaAs for integrated circuit applications  
[NASA-CR-173267] p 191 A84-17014
- ELMORE, D. L.**  
Dynamic gas temperature measurement system, volume 1  
[NASA-CR-168267-VOL-1] p 132 A84-16529
- ELTIMSAHY, A. H.**  
Investigation of energy management strategies for photovoltaic systems - An analysis technique p 160 A84-22993  
Investigation of energy management strategies for photovoltaic systems - A predictive control algorithm p 161 A84-25468
- ENDO, T.**  
A numerical analysis of contact and limit-point behavior in a class of problems of finite elastic deformation p 150 A84-27370
- ENGLUND, D. R.**  
The infinite line pressure probe p 132 A84-19787
- ERCEGOVIC, M. D.**  
A scheme for handling arrays in data-flow systems p 175 A84-39972  
Dataflow computing approach in high-speed digital simulation  
[NASA-CR-173552] p 176 A84-25336
- ERCEGOVIC, D. B.**  
Ceramic composite liner material for gas turbine combustors  
[AIAA PAPER 84-0363] p 78 A84-18044  
Ceramic composite liner material for gas turbine combustors  
[NASA-TM-83490] p 24 A84-14145
- ERNST, W.**  
Automotive Stirling engine development program  
[NASA-CR-168205] p 194 A84-18117  
Automotive Stirling engine development program  
[NASA-CR-174622] p 195 A84-32305
- ERWIN, J.**  
Investigation of sources, properties and preparation of distillate test fuels  
[NASA-CR-168227] p 89 A84-13332
- ESKEY, M. A.**  
Tandem fan applications in advanced STOVL fighter configurations  
[AIAA PAPER 84-1402] p 19 A84-40245  
Tandem fan applications in advanced STOVL fighter configurations  
[NASA-TM-83689] p 30 A84-24579
- EVANICH, P.**  
Sixth Annual Workshop on Meteorological and Environmental Inputs to Aviation Systems, 26-28 October 1982, Tullahoma, Tenn p 174 A84-23424
- EVERSMAN, W.**  
A numerical model of acoustic choking I - Shock free solutions p 180 A84-21250
- EWASHINKA, J. G.**  
Results of electric-vehicle propulsion system performance on three lead-acid battery systems  
[NASA-TM-83657] p 169 A84-25166

## F

- FADDOUL, J. R.**  
Examination, evaluation and repair of laminated wood blades after service on the Mod-OA wind turbine  
[NASA-TM-83483] p 183 A84-10664
- FAETH, G. M.**  
Evaporation and combustion of sprays p 58 A84-11636  
Structure of particle-laden jets - Measurements and predictions  
[AIAA PAPER 84-0038] p 113 A84-17842  
Structure of nonevaporating sprays - Measurements and predictions  
[AIAA PAPER 84-0125] p 114 A84-17897  
A theoretical and experimental study of turbulent particle-laden jets  
[NASA-CR-168293] p 23 A84-13187

- Predictions of spray combustion interactions p 61 A84-20532  
The structure of evaporating and combusting sprays  
Measurements and predictions  
[NASA-CR-173778] p 128 A84-29155  
A theoretical and experimental study of turbulent nonevaporating sprays  
[NASA-CR-174668] p 36 A84-29877  
A theoretical and experimental study of turbulent evaporating sprays  
[NASA-CR-174760] p 35 A84-32390
- FAIGEN, I. M.**  
Reflector-antennas with low sidelobes, low cross polarization, and high aperture efficiency  
[NASA-CR-174670] p 100 A84-31464
- FAIRMAN, R. D.**  
LEC GaAs for integrated circuit applications  
[NASA-CR-173267] p 191 A84-17014
- FARMER, W. M.**  
Measurement of spray combustion processes p 61 A84-20530
- FAROOQUE, M.**  
Evaluation of gas cooling for pressurized phosphoric acid fuel cell stacks p 163 A84-30191
- FAROOQUE, M.**  
Evaluation of gas-cooled pressurized phosphoric acid fuel cells for electric utility power generation  
[NASA-CR-168298] p 169 A84-25169  
Full scale phosphoric acid fuel cell stack technology development  
[NASA-CR-174660] p 169 A84-26165
- FARRELL, R. A.**  
Comparison of steady-state and transient CVS cycle emission of an automotive Stirling engine p 173 A84-41044
- FATEHI, M. T.**  
Optical flip-flops and sequential logic circuits using a liquid crystal light valve p 188 A84-40332
- FATMI, H.**  
NTSC composite video at 1.6 bits/pel p 95 A84-49259
- FAUT, O. D.**  
Mechanism of lubrication by trisylphosphate (TCP)  
[NASA-TP-2274] p 142 A84-18653
- FAYMON, K. A.**  
Space power technology into the 21st century  
[AIAA PAPER 84-1136] p 43 A84-34013  
Space power technology into the 21st Century  
[NASA-TM-83690] p 48 A84-26746
- FEAR, J. S.**  
NASA/General Electric Broad-Specification Fuels Combustion Technology Program - Phase I p 16 A84-24033  
NASA broad-specification fuels combustion technology program p 62 A84-23637
- FEIGENBAUM, H.**  
Develop and test fuel cell powered on-site integrated total energy systems. Phase 3 Full-scale power plant development  
[NASA-CR-168294] p 164 A84-13672  
Develop and test fuel cell powered on-site integrated total energy system  
[NASA-CR-168239] p 164 A84-13673
- FENWICK, J. R.**  
Research study for effects of case flexibility on bearing loads and rotor stability  
[NASA-CR-171147] p 148 A84-33811
- FERGUSON, D. C.**  
Laboratory degradation of Kapton in a low energy oxygen ion beam  
[NASA-TM-83530] p 41 A84-18311  
The energy dependence and surface morphology of Kapton (trademark) degradation under atomic oxygen bombardment p 187 A84-34484
- FERRANTE, J.**  
Scaling relations in the equation of state, thermal expansion, and melting of metals p 192 A84-19355  
Matrix effects in ion-induced emission as observed in Ne collisions with Cu-Mg and Cu-Al alloys  
[NASA-TM-83061] p 187 A84-10923  
Metallic adhesion and bonding p 72 A84-23897
- FERTIS, D.**  
Nonlinear transient finite element analysis of rotor-bearing-stator systems p 136 A84-20581
- FESTER, D. A.**  
Cryogenic Fluid Management Experiment (CFME) trunnion verification testing  
[NASA-CR-168310] p 92 A84-16381
- FEYOCK, S.**  
ADA and multi-microprocessor real-time simulation p 176 A84-10905
- FINKE, R.**  
Piezoelectric deicing device  
[NASA-CASE-LEW-13773-2] p 133 A84-32782



- FINKE, R. C.**  
Advanced electrical power system technology for the all electric aircraft p 15 A84-16528  
Three-phase, high-voltage, high-frequency distributed bus system for advanced aircraft p 105 N84-10058
- FIORENTINO, A. J.**  
An assessment of the use of antimisting fuel in turbofan engines [NASA-CR-168081] p 89 N84-10332
- FISHBACH, L. H.**  
Study of a LH<sub>2</sub>-fueled topping cycle engine for aircraft propulsion [AIAA PAPER 83-2543] p 15 A84-15207  
PREWATE .An interactive preprocessing computer code to the Weight Analysis of Turbine Engines (WATE) computer code [NASA-TM-83545] p 176 N84-13812  
Analysis of a topping-cycle, aircraft, gas-turbine-engine system which uses cryogenic fuel [NASA-TP-2294] p 28 N84-21549
- FISHER, D. M.**  
Evaluation of the effect of crack closure on fatigue crack growth of simulated short cracks [NASA-TM-83778] p 75 N84-31348
- FLACK, R. D.**  
Effects of volute geometry and impeller orbit on the hydraulic performance of a centrifugal pump p 136 A84-22316
- FLEETER, R. D.**  
Apparatus analysis and preliminary design of low gravity porous solids experiment for STS Orbiter mid-deck [NASA-CR-168248] p 37 N84-10109
- FLEETER, S.**  
The coupled response of turbomachinery blading to aerodynamic excitations p 17 A84-26959
- FLEMING, D. P.**  
Dual clearance squeeze film damper [NASA-CASE-LEW-13506-1] p 29 N84-22562  
Dual clearance squeeze film damper for high load conditions [NASA-TM-83619] p 144 N84-25064
- FLORSCHUETZ, L. W.**  
Forced convection heat transfer to air/water vapor mixtures [NASA-CR-3769] p 123 N84-16488
- FORD, W. F.**  
Acceleration of convergence of vector sequences [NASA-TP-2193] p 178 N84-13885
- FORDYCE, J. S.**  
Space power technology into the 21st century [AIAA PAPER 84-1136] p 43 A84-34013  
Space power technology into the 21st Century [NASA-TM-83690] p 48 N84-26746  
The potential impact of new power system technology on the design of a manned space station [NASA-TM-83770] p 49 N84-31272
- FORESTIERI, A. F.**  
Solar-array-materials passive LDEF experiment (A0171) p 168 N84-24656  
Advanced photovoltaic experiment (S0014) p 168 N84-24657
- FORMAN, R.**  
Evaluation of the emission capabilities of Spindt-type field emitting cathodes p 101 A84-12424  
Correlation of electron emission with changes in the surface concentration of barium and oxygen on a tungsten surface p 60 A84-45917  
Ion sputter textured graphite electrode plates [NASA-CASE-LEW-12919-2] p 179 N84-28565
- FOSS, J. F.**  
Free stream turbulence and density ratio effects on the interaction region of a jet in a cross flow p 125 N84-20546
- FOST, R. B.**  
Subsonic/transonic stall flutter investigation of a rotating ng [NASA-CR-174625] p 36 N84-33417
- FRANCISCUS, L. C.**  
Supersonic fan engines for military aircraft [AIAA PAPER 83-2541] p 15 A84-15206  
Supersonic STOVL aircraft with turbine bypass/turbo-compressor engines [AIAA PAPER 84-1403] p 19 A84-40247  
Supersonic STOVL aircraft with turbine bypass/turbo-compressor engines [NASA-TM-83686] p 31 N84-24582
- FRASCH, L.**  
Electromagnetic plasma models for microwave plasma cavity reactors [AIAA PAPER 84-1521] p 189 A84-46108
- FRATER, J. L.**  
Dynamics of early planetary gear trains [NASA-CR-3793] p 145 N84-28027
- FRECHETTE, F. J.**  
Progress in net shape fabrication of alpha sic turbine components [ASME PAPER 84-GT-273] p 140 A84-47036
- FRENKLACH, M.**  
Shock tube study of the fuel structure effects on the chemical kinetic mechanisms responsible for soot formation [NASA-CR-174661] p 62 N84-21677
- FRIEDMAN, R.**  
Heating experiments for flowability improvement of near-freezing aviation fuel p 89 A84-26955  
Trends of jet fuel demand and properties p 90 N84-23631
- FROST, W.**  
Sixth Annual Workshop on Meteorological and Environmental Inputs to Aviation Systems, 26-28 October 1982, Tullahoma, Tenn p 174 A84-23424
- FRYBURG, G. C.**  
Chemical mechanisms and reaction rates for the initiation of hot corrosion of IN-738 [NASA-TP-2319] p 74 N84-28958
- FRYXELL, R. E.**  
Effects of surface chemistry on hot corrosion life [NASA-CR-174683] p 72 N84-24774
- FU, K. C.**  
Thermal stress analysis for a wood composite blade [NASA-CR-173394] p 156 N84-21903  
Thermal-stress analysis for wood composite blade [NASA-CR-173830] p 157 N84-31685
- FU, L. S.**  
Volume integrals associated with the inhomogeneous Helmholtz equation Part 1: Ellipsoidal region [NASA-CR-3749] p 148 N84-14525  
Volume integrals associated with the inhomogeneous Helmholtz equation Part 2: Cylindrical region, rectangular region [NASA-CR-3750] p 148 N84-14526
- FUJII, M.**  
Low-cost single-crystal turbine blades, volume 1 [NASA-CR-168218] p 68 N84-15247
- FUNG, C. D.**  
Thermal oxidation of 3C silicon carbide single-crystal layers on silicon p 191 A84-49620
- FUNG, S. S.**  
Topological reaction rate measurements related to sootting [NASA-TM-83486] p 68 N84-14288  
Surface topographical changes measured by phase-locked interferometry [NASA-CR-3757] p 188 N84-16984
- FUSARO, R. L.**  
Polyimides formulated from a partially fluorinated diamine for aerospace tribological applications p 80 A84-40594  
Low wear partially fluorinated polyimides [NASA-TM-83629] p 84 N84-24808  
Effect of substrate chemical pretreatment on the tribological properties of graphite films [NASA-TM-83574] p 85 N84-25831
- G**
- GADDY, E. M.**  
Solar-array-materials passive LDEF experiment (A0171) p 168 N84-24656
- GAHN, R. F.**  
Single cell performance studies on the FE/CR Redox Energy Storage System using mixed reactant solutions at elevated temperature p 163 A84-30194  
Negative electrode catalyst for the iron-chromium REDOX energy storage system [NASA-CASE-LEW-14028-1] p 172 N84-32909
- GALLARDO, V. C.**  
Blade loss transient dynamics analysis with flexible bladed disk [NASA-CR-168176] p 23 N84-13193
- GALLO, A. M.**  
NASTRAN forced vibration analysis of rotating cyclic structures [ASME PAPER 83-DET-20] p 151 A84-29103  
Forced vibration analysis of rotating cyclic structures in NASTRAN [NASA-CR-165429] p 153 N84-11514  
NASTRAN documentation for flutter analysis of advanced turbopropellers [NASA-CR-167927] p 25 N84-15153  
Bladed-shrouded-disc aeroelastic analyses. Computer program updates in NASTRAN level 17.7 [NASA-CR-165428] p 25 N84-15154  
NASTRAN forced vibration analysis of rotating cyclic structures [NASA-CR-173821] p 157 N84-29252
- GALMES, J. M.**  
An experimental study of the compressor rotor blade boundary layer [ASME PAPER 84-GT-193] p 7 A84-46991  
Turbulence modeling for three-dimensional shear flows over curved rotating bodies p 122 A84-48138
- GALPERIN, I.**  
Material considerations for high frequency, high power capacitors p 102 A84-22874
- GAMMON, R. W.**  
Capillary rise, wetting layers, and critical phenomena in confined geometry p 192 A84-20315  
Turbidity very near the critical point of methanol-cyclohexane mixtures p 192 A84-30391
- GANGWANI, S. T.**  
Aeroelastic analysis for propellers - mathematical formulations and program user's manual [NASA-CR-3729] p 163 N84-12530
- GARBUNY, M.**  
Measurement of heat pump processes induced by laser radiation [NASA-CR-168324] p 134 N84-18620
- GARDELLA, N. C.**  
Catalog of selected heavy duty transport energy management models [NASA-CR-168299] p 194 N84-14991
- GARLAND, S.**  
Integration becomes the name of the OTV game p 44 A84-44045
- GARLICK, R. G.**  
Phase distributions in plasma-sprayed zirconia-yttria p 78 A84-18948  
High-temperature cyclic oxidation data, volume 1 [NASA-TM-83665] p 75 N84-31345
- GARRARD, W. L.**  
Steady state stresses in ribbon parachute canopies [AIAA PAPER 84-0816] p 11 A84-26580
- GARRETT, H. B.**  
Design guidelines for assessing and controlling spacecraft charging effects [NASA-TP-2361] p 42 N84-33452
- GARTSHORE, I. S.**  
The production of turbulent stress in a shear flow by irrotational fluctuations p 115 A84-18357  
The production of turbulent stress in a shear flow by irrotational fluctuations p 115 A84-21390
- GAT, N.**  
Preliminary design of two Space Shuttle fluid physics experiments [NASA-CR-174649] p 39 N84-23667
- GAUDIOT, J.-L.**  
A scheme for handling arrays in data-flow systems p 175 A84-39972
- GAUGH, C. E.**  
Development and fabrication of a high current, fast recovery power diode [NASA-CR-168196] p 106 N84-13443
- GAUGLER, R. E.**  
Comparison of visualized turbine endwall secondary flows and measured heat transfer patterns [ASME PAPER 83-GT-83] p 117 A84-33703
- GAUNTNER, J. W.**  
Use of cooling air heat exchangers as replacements for hot section strategic materials [AIAA PAPER 83-2540] p 15 A84-15205  
Contingency power concepts for helicopter turboshaft engine [NASA-TM-83679] p 30 N84-23648
- GAY, C. H., JR.**  
Tip cap for a rotor blade [NASA-CASE-LEW-13654-1] p 28 N84-22560
- GAYDA, J.**  
The effect of microstructure on 650 C fatigue crack growth in P/M Astroloy p 63 A84-12395  
Effects of processing and microstructure on the fatigue behaviour of the nickel-base superalloy Rene95 p 66 A84-48715
- GEDDES, J.**  
The 30-GHz monolithic receive module [NASA-CR-168326] p 99 N84-20737
- GEDDES, J. J.**  
A Ka-band GaAs monolithic phase shifter p 101 A84-18371
- GEDEON, L.**  
NASCAP simulations of spacecraft charging of the SCATHA satellite p 41 N84-17268
- GEDWILL, M. A.**  
Coating with overlay metallic-cermet alloy systems [NASA-CASE-LEW-13639-2] p 73 N84-27855  
Overlay metallic-cermet alloy coating systems [NASA-CASE-LEW-13639-1] p 77 N84-33555
- GEISLER, M. J.**  
Development and fabrication of an augmented power transistor [NASA-CR-168262] p 106 N84-11388

- GELDER, T. F.**  
Redesign and cascade tests of a supercritical controlled diffusion stator blade-section  
[AIAA PAPER 84-1207] p 5 A84-36960  
Design and performance of a fixed, nonaccelerating, guide vane cascade that operates over an inlet flow angle range of 60 deg  
[NASA-TM-83519] p 8 N84-14120  
Redesign and cascade tests of a supercritical controlled diffusion stator blade-section  
[NASA-TM-83635] p 10 N84-22533
- GELLER, B. D.**  
Phased-array-fed antenna configuration study. Volume 1: Technology assessment  
[NASA-CR-168231] p 98 N84-16423  
Phased-array-fed antenna configuration study, volume 2  
[NASA-CR-168232] p 98 N84-16424
- GELLIN, S.**  
Slave finite elements: The temporal element approach to nonlinear analysis p 157 N84-31689
- GENERAZIO, E. R.**  
The role of the reflection coefficient in precision measurement of ultrasonic attenuation  
[NASA-TM-83788] p 149 N84-32849
- GERHART, P. M.**  
Computational modeling of jet induced mixing of cryogenic propellants in low-G  
[AIAA PAPER 84-1344] p 121 A84-40243  
Computational modeling of jet induced mixing of cryogenic propellants in low-G  
[NASA-TM-83703] p 127 N84-25000
- GERSON, H. I.**  
Phased-array-fed antenna configuration study. Volume 1: Technology assessment  
[NASA-CR-168231] p 98 N84-16423
- GERSTENMAIER, W. H.**  
Hot-flow tests of a series of 10-percent-scale turbofan forced mixing nozzles  
[NASA-TP-2268] p 123 N84-17525
- GEYSER, L. C.**  
AESOP. An interactive computer program for the design of linear quadratic regulators and Kalman filters  
[NASA-TP-2221] p 178 N84-16843
- GHALLA-GORADIA, M.**  
Optimal design of GaAs-based concentrator space solar cells for 100 AMO, 80 deg C operation p 170 N84-29312  
Preliminary design of a 10-kW thermophotovoltaic system for space applications  
[NASA-TM-83768] p 49 N84-32427
- GHANDHI, S. K.**  
Photovoltaic characteristics of diffused P(+)-N bulk GaAs solar cells p 161 A84-23115  
Diffused junction p(+)-n solar cells in bulk GaAs I. Fabrication and cell performance p 161 A84-26027  
Diffused junction p(+)-n solar cells in bulk GaAs II. Device characterization and modelling p 161 A84-26028
- GHIA, K. N.**  
A direct method for the solution of unsteady two-dimensional incompressible Navier-Stokes equations p 2 A84-10078  
Hybrid C-H grids for turbomachinery cascades p 3 A84-11591  
Application of a polynomial spline in higher-order accurate viscous-flow computations p 119 A84-35349  
On numerical simulation of viscous flows p 122 A84-49112
- GHIA, U.**  
A direct method for the solution of unsteady two-dimensional incompressible Navier-Stokes equations p 2 A84-10078  
Hybrid C-H grids for turbomachinery cascades p 3 A84-11591  
Application of a polynomial spline in higher-order accurate viscous-flow computations p 119 A84-35349  
On numerical simulation of viscous flows p 122 A84-49112
- GHONIEM, A. F.**  
Formation and inflammation of a turbulent jet  
[AIAA PAPER 84-0572] p 114 A84-18171  
Random element method for numerical modeling of diffusional processes p 119 A84-35318  
Numerical solution for the problem of flame propagation by the random element method p 60 A84-48139  
Experimental and theoretical study of combustion jet ignition  
[NASA-CR-168139] p 21 N84-10054  
Numerical modeling of turbulent flow in a channel  
[NASA-CR-168278] p 23 N84-13189
- GHOSH, A.**  
Direct and implicit optical matrix-vector algorithms p 187 A84-13184
- GHOSH, M. K.**  
Hydrodynamic lubrication of rigid nonconformal contacts in combined rolling and normal motion  
[NASA-TM-83578] p 142 N84-17592
- GIBALA, R.**  
Structure of transient oxides formed on NiCrAl alloys p 63 A84-12385
- GIBSON, R. K.**  
Advanced Gas Turbine (AGT) Power-train system development  
[NASA-CR-168056] p 140 N84-10581
- GILES, M.**  
Conservative streamtube solution of steady-state Euler equations  
[AIAA PAPER 84-1643] p 120 A84-38030  
Eigenmode analysis of unsteady one-dimensional Euler equations  
[NASA-CR-172217] p 7 N84-10022  
Asymptotic analysis of numerical wave propagation in finite difference equations  
[NASA-CR-175323] p 98 N84-15360
- GILLES, J. P.**  
On-orbit cryogenic fluid transfer  
[AIAA PAPER 84-1343] p 44 A84-44176  
On-orbit cryogenic fluid transfer  
[NASA-TM-83688] p 39 N84-25753
- GILLIS, J. C.**  
Turbulent boundary-layer flow and structure on a convex wall and its redevelopment on a flat wall p 115 A84-21378
- GILSTRAP, P.**  
Stress measurement in thin films by geometrical optics p 130 A84-28797
- GINTY, C. A.**  
Select fiber composites for space applications. A mechanistic assessment  
[NASA-TM-83631] p 55 N84-22702  
Progressive fracture of fiber composites  
[NASA-TM-83701] p 56 N84-27831  
Hygrothermomechanical fracture stress criteria for fiber composites with sense-parity  
[NASA-TM-83691] p 57 N84-28918  
Fracture surface characteristics of notched angle-ply graphite/epoxy composites  
[NASA-TM-83786] p 57 N84-33522  
Fracture modes in notched angle-ply composite laminates  
[NASA-TM-83802] p 58 N84-34576
- GIOVANNETTI, A. J.**  
Deposit formation and heat transfer in hydrocarbon rocket fuels  
[AIAA PAPER 84-0512] p 88 A84-18142  
Deposit formation and heat transfer in hydrocarbon rocket fuels  
[NASA-CR-168277] p 45 N84-12225
- GLASER, F. W.**  
Low flight speed fan noise from a supersonic inlet p 182 A84-44508
- GLASGOW, T. K.**  
Rapid solidification via melt spinning - Equipment and techniques p 65 A84-31915  
Coating with overlay metallic-cermet alloy systems  
[NASA-CASE-LEW-13639-2] p 73 N84-27855  
Overlay metallic-cermet alloy coating systems  
[NASA-CASE-LEW-13639-1] p 77 N84-33555
- GLASSMAN, A.**  
Supersonic STOVL ejector aircraft from a propulsion point of view  
[AIAA PAPER 84-1401] p 19 A84-40246  
Supersonic STOVL ejector aircraft from a propulsion point of view  
[NASA-TM-83641] p 31 N84-24581
- GLICKSMAN, M. E.**  
Gravitational effects in dendritic growth p 37 A84-22346  
Free dendritic growth p 190 A84-42829  
Transport processes in dendritic crystallization p 191 N84-28621
- GODLEWSKI, M. P.**  
Effects of indirect bandgap top cells in a monolithic cascade cell structure p 160 A84-22987  
Voltage controlling mechanisms in low resistivity silicon solar cells. A unified approach p 167 N84-20916  
The effect of diffusion induced lattice stress on the open-circuit voltage in silicon solar cells  
[NASA-TM-83667] p 168 N84-23027
- GODSTON, J.**  
Technology and benefits of aircraft counter rotation propellers  
[NASA-CR-168258] p 22 N84-13186
- GOEKOGLU, S. A.**  
Engineering correlations of variable-property effects on laminar forced convection mass transfer for dilute vapor species and small particles in air  
[NASA-CR-168322] p 124 N84-18578
- Comparisons of rational engineering correlations of thermophoretically-augmented particle mass transfer with STANS-predictions for developing boundary layers  
[NASA-CR-168221] p 93 N84-19606  
Experimental and theoretical deposition rates from salt-seeded combustion gases of a Mach 0.3 burner rig  
[NASA-TP-2225] p 124 N84-19741  
Deposition of Na<sub>2</sub>SO<sub>4</sub> from salt-seeded combustion gases of a high velocity burner rig  
[NASA-TM-83751] p 129 N84-31558
- GOEL, J.**  
A K-band GaAs FET amplifier with 8.2-W output power p 104 A84-32290
- GOERTZ, C. K.**  
Effects of chemical releases by the STS-3 Orbiter on the ionosphere  
[NASA-CR-171032] p 173 N84-25204
- GOGLIA, P. R.**  
Surface roughness effects with solid lubricants dispersed in mineral oils  
[ASLE PREPRINT 83-LC-4C-1] p 137 A84-28987
- GOKOGLU, S. A.**  
Correlation of thermophoretically-modified small particle diffusional deposition rates in forced convection systems with variable properties, transpiration cooling and/or viscous dissipation p 117 A84-32323  
Comparisons of rational engineering correlations of thermophoretically-augmented particle mass transfer with STANS-predictions for developing boundary layers  
[ASME PAPER 84-GT-158] p 92 A84-46985
- GOLDBERG, U. C.**  
Scaling and modeling of three-dimensional, end-wall, turbulent boundary layers  
[NASA-CR-3792] p 127 N84-25941
- GOLDMAN, L. J.**  
Three component velocity measurements using Fabry-Perot interferometer  
[NASA-TM-83692] p 133 N84-26010
- GOLDRICH, R. N.**  
Precision of spiral-bevel gears  
[ASME PAPER 82-WA/DE-33] p 135 A84-15950  
Kinematic precision of gear trains  
[ASME PAPER 82-WA/DE-34] p 135 A84-15951
- GOLDSTEIN, D. N.**  
Contingency power concepts for helicopter turboshaft engine  
[NASA-TM-83679] p 30 N84-23648  
Rotorcraft contingency power study  
[NASA-CR-174675] p 31 N84-24580
- GOLDSTEIN, M. E.**  
Aeroacoustics of turbulent shear flows p 181 A84-22584  
Small-amplitude viscous motion on arbitrary potential flows p 116 A84-24892  
Generation of sound in turbulent shear flows p 183 N84-15031
- GOLDSTEIN, S. A.**  
Experimental investigation of the pulsed electrothermal (PET) thruster  
[AIAA PAPER 84-1386] p 43 A84-35201  
Proposed system design for a 20 kW pulsed electrothermal thruster  
[AIAA PAPER 84-1387] p 43 A84-35202  
Investigation of a pulsed electrothermal thruster  
[NASA-CR-168266] p 45 N84-12227
- GOLWALKER, S.**  
The effects of frequency and hold times on fatigue crack propagation rates in a nickel base superalloy p 64 A84-18733  
Fatigue crack growth and low cycle fatigue of two nickel base superalloys  
[NASA-CR-174534] p 66 N84-10267
- GONSALVEZ, D. J.**  
Engineering calculations for communications satellite systems planning  
[NASA-CR-173532] p 38 N84-23662
- GONZALEZ-SANABRIA, O. D.**  
Separator development and testing of nickel-hydrogen cells  
[NASA-TM-83653] p 62 N84-22712  
Design considerations for a 10-kW integrated hydrogen-oxygen regenerative fuel cell system  
[NASA-TM-83664] p 167 N84-23023  
Advanced designs for IPV nickel-hydrogen cells  
[NASA-TM-83643] p 168 N84-23025  
Teardown analysis of a ten cell bipolar nickel-hydrogen battery  
[NASA-TM-83618] p 168 N84-23026
- GOODER, S. T.**  
Electromagnetic propulsion test facility  
[NASA-TM-83568] p 37 N84-16229
- GOODYKOONTZ, J.**  
Velocity and temperature characteristics of two-stream, coplanar jet exhaust plumes  
[AIAA PAPER 84-2205] p 21 A84-46106

- GOODYKOONTZ, J. H.**  
Inverted velocity profile semi-annular nozzle jet exhaust noise experiments [NASA-TM-83525] p 182 N84-13924  
Fluid shielding of high-velocity jet noise [NASA-TP-2259] p 183 N84-15894  
Low frequency noise in a quiet, clean, general aviation turbofan engine [NASA-TM-83520] p 183 N84-20320  
Velocity and temperature characteristics of two-stream, coplanar jet exhaust plumes [NASA-TM-83730] p 34 N84-28790
- GORDADIA, C.**  
Optimal design of GaAs-based concentrator space solar cells for 100 AMO, 80 deg C operation p 170 N84-29312
- GORDAN, A. L.**  
Centaur D-1A guidance/software system [AAS PAPER 84-043] p 39 A84-49176  
Centaur D-1A guidance/software system [NASA-TM-83552] p 38 N84-16234
- GORDON, L. H.**  
MOD-2 wind turbine development [NASA-TM-83460] p 164 N84-13670
- GORDON, W. L.**  
Particle environment [NASA-CR-173888] p 191 N84-33210
- GORLA, R. S. R.**  
Effects of unsteady free stream velocity and free stream turbulence on stagnation point heat transfer [NASA-CR-3804] p 127 N84-25843
- GORRELL, W. T.**  
Detailed flow measurements in casing boundary layer of 429-meter-per-second-tip-speed two-stage fan [NASA-TP-2052] p 34 N84-28795
- GOTT, P. G.**  
Catalog of selected heavy duty transport energy management models [NASA-CR-168299] p 194 N84-14991
- GOULD, G. R.**  
Modular approach for satellite communication ground terminals [NASA-CR-168327] p 98 N84-16425
- GOULDIN, F. C.**  
Time-resolved density measurements in premixed turbulent flames p 59 A84-32612
- GOURASH, F.**  
Road load simulator tests of the Gould phase 1 functional model silicon controlled rectifier ac motor controller for electric vehicles [NASA-TM-83497] p 166 N84-20016
- GOVINDAN, T. R.**  
Three-dimensional turbulent boundary-layer development on a fan rotor blade p 3 A84-17437  
Annulus wall boundary layer development in a compressor stage, including the effects of tip clearance p 26 N84-16207
- GOYAL, A.**  
NASA advanced low emissions combustor program [ASME PAPER 83-JPGG-GT-10] p 17 A84-28982
- GRAHAM, R. W.**  
A review of NASA combustor and turbine heat transfer research [NASA-TM-83541] p 24 N84-14146
- GRAY, H. R.**  
P/M superalloys A troubled adolescent? [NASA-TM-83623] p 73 N84-26785
- GREBER, I.**  
Experimental studies on two dimensional shock boundary layer interactions [AIAA PAPER 84-0099] p 3 A84-17861  
Dilution jets in accelerated cross flows [NASA-CR-174717] p 34 N84-28794
- GRECO, C. C.**  
Study to establish cost projections for production of Redox chemicals [NASA-CR-167891] p 164 N84-11580
- GREEN, H. E.**  
Development of partially fluorinated resin apex seals [NASA-CR-174706] p 148 N84-32828
- GREEN, W. L.**  
A laser system to remotely sense bird movements p 159 A84-31608
- GREGOREK, G. M.**  
Experimental and analytical investigations into airfoil icing p 12 A84-45054  
Results of an experimental program investigating the effects of simulated ice on the performance of the NACA 63A415 airfoil with flap [NASA-CR-168288] p 8 N84-16145
- GREYWALL, M. S.**  
Streamwise computation of three-dimensional parabolic flows p 113 A84-16828
- GRIER, N. T.**  
Dilute plasma coupling currents to a high voltage solar array in weak magnetic fields [NASA-TM-83687] p 47 N84-24708
- GRIFFIN, J. H.**  
Model development and statistical investigation of turbine blade mistuning p 17 A84-31905  
The interaction between mistuning and friction in the forced response of bladed disk assemblies [ASME PAPER 84-GT-139] p 152 A84-46957
- GRILL, A.**  
Correlations between plasma variables and the deposition process of Si films from chlorosilanes in low pressure RF plasma of argon and hydrogen [NASA-TM-83603] p 190 N84-21330  
RF sputtered silicon and hafnium nitrides as applied to 440C steel [NASA-TM-86862] p 87 N84-32536
- GRIMES, H. H.**  
Thermal degradation of the tensile properties of unidirectionally reinforced FP-Al<sub>2</sub>O<sub>3</sub>/EZ 33 magnesium composites p 52 A84-28229
- GROESBECK, D. E.**  
Low frequency noise in a quiet, clean, general aviation turbofan engine [NASA-TM-83520] p 183 N84-20320
- GROSS, B.**  
Analysis of an internally radially cracked ring segment subject to three-point radial loading p 150 A84-18591  
Mode 2 fatigue crack growth specimen development [NASA-TM-83722] p 156 N84-29248
- GROSSMAN, E.**  
Correlations between plasma variables and the deposition process of Si films from chlorosilanes in low pressure RF plasma of argon and hydrogen [NASA-TM-83603] p 190 N84-21330
- GROTELUESCHEN, L. P.**  
Determination of near-surface plastic deformation in sliding contacts p 140 A84-48996
- GROUMPOS, P. P.**  
The effect of variable S/N on the subjective evaluation of protection ratios for direct-TV satellite services p 95 A84-48452  
The subjective effect of multiple co-channel frequency modulated television interference [NASA-TM-83415] p 97 N84-11360
- GRUBER, R. P.**  
Simplification of power electronics for ion thruster neutralizers p 44 A84-49509  
Simplified dc to dc converter [NASA-CASE-LEW-13495-1] p 111 N84-33663
- GUHA, J. P.**  
Grain-boundary phases in hot-pressed silicon nitride containing Y<sub>2</sub>O<sub>3</sub> and CeO<sub>2</sub> additives p 79 A84-19793
- GUINEA, F.**  
Scaling relations in the equation of state, thermal expansion, and melting of metals p 192 A84-19359
- GUIRGUIS, R. H.**  
Self-similar blast waves incorporating deflagrations of variable speed p 116 A84-28379
- GULINO, D. A.**  
Coaxial carbon plasma gun deposition of amorphous carbon films [NASA-TM-83600] p 191 N84-20404
- GUNTER, E. J.**  
Design study of magnetic eddy-current vibration suppression dampers for application to cryogenic turbomachinery [NASA-CR-173273] p 141 N84-16562
- GUPTA, A. K.**  
A three-stage power amplifier for a 20 GHz monolithic transmit module p 102 A84-22873
- GUPTA, H.**  
Carbides in iron-rich Fe-Mn-Cr-Mo-Al-Si-C systems p 64 A84-26815
- GUPTA, I. J.**  
Adaptive arrays for satellite communications [NASA-CR-173548] p 99 N84-24924
- HABIBY, S. F.**  
Optical residue addition and storage units using a Hughes liquid crystal light valve p 188 N84-22417
- HADY, W. F.**  
Low wear partially fluorinated polyimides [NASA-TM-83629] p 84 N84-24808  
An overview of the NASA rotary engine research program [NASA-TM-83699] p 34 N84-28791
- HAGEDORN, N. H.**  
Single cell performance studies on the FE/CR Redox Energy Storage System using mixed reactant solutions at elevated temperature p 163 A84-30194  
Negative electrode catalyst for the iron-chromium REDOX energy storage system [NASA-CASE-LEW-14028-1] p 172 N84-32909
- HAGGARD, J. B., JR.**  
Effects of broadened property fuels on radiant heat flux to gas turbine combustor liners [NASA-TM-83537] p 123 N84-16494
- HAH, C.**  
Three-dimensional turbulent boundary-layer development on a fan rotor blade p 3 A84-17437
- HAJEK, T.**  
Aerodynamic effects of moveable sidewall nozzle geometry and rotor exit restriction on the performance of a radial turbine [SAE PAPER 831517] p 17 A84-29460  
Variable stator radial turbine [NASA-CR-174663] p 29 N84-22568
- HALES, C.**  
Creep-rupture behavior of candidate Stirling engine iron superalloys in high-pressure hydrogen Volume 2 Hydrogen creep-rupture behavior [NASA-CR-174705] p 74 N84-28961
- HALFORD, G. R.**  
High-temperature fatigue in metals - A brief review of life prediction methods developed at the Lewis Research Center of NASA p 64 A84-14286  
Complexities of high temperature metal fatigue Some steps toward understanding [NASA-TM-83507] p 154 N84-14541  
Tensile and compressive constitutive response of 316 stainless steel at elevated temperatures [NASA-TM-83506] p 68 N84-15249  
Bending fatigue of electron-beam-welded foils Application to a hydrodynamic air bearing in the Chrysler/DOE upgraded automotive gas turbine engine [NASA-TM-83539] p 155 N84-16589  
Preliminary study of thermomechanical fatigue of polycrystalline MAR-M 200 [NASA-TP-2280] p 69 N84-17350  
Engine cyclic durability by analysis and material testing [NASA-TM-83577] p 155 N84-18683
- HALL, D. G.**  
Coupling of radiation into thin film modes by means of localized plasma resonances p 187 A84-16397
- HALL, K. C.**  
Optimization and mechanisms of mistuning in cascades [ASME PAPER 84-GT-196] p 21 A84-46993
- HALL, W. N.**  
Charged particle effects on space systems [AD-P002103] p 187 N84-26189
- HALLE, J. E.**  
Energy efficient engine fan component detailed design report [NASA-CR-165466] p 33 N84-27737
- HALLER, W.**  
Supersonic STOVL ejector aircraft from a propulsion point of view [AIAA PAPER 84-1401] p 19 A84-40246  
Supersonic STOVL ejector aircraft from a propulsion point of view [NASA-TM-83641] p 31 N84-24581
- HALLORAN, J. W.**  
Oxygen diffusion in alpha-Al<sub>2</sub>O<sub>3</sub> [NASA-TM-83622] p 86 N84-28990
- HAMROCK, B. J.**  
Non-Newtonian fluid model incorporated into elastohydrodynamic lubrication of rectangular contacts [ASME PAPER 83-LUB-15] p 139 A84-44300  
Numerical methods and computers used in elastohydrodynamic lubrication [NASA-TM-83524] p 141 N84-11499  
Hydrodynamic lubrication of rigid nonconformal contacts in combined rolling and normal motion [NASA-TM-83578] p 142 N84-17592  
Elastohydrodynamic lubrication of smooth surfaces p 144 N84-24895  
Elastohydrodynamic lubrication Status of understanding p 144 N84-25048  
Transmission efficiency measurements and correlations with physical characteristics of the lubricant [NASA-TM-83740] p 147 N84-30293

## H

- HAAS, J. E.**  
Comparison between measured turbine stage performance and the predicted performance using quasi-3D flow and boundary layer analyses [AIAA PAPER 84-1299] p 18 A84-36972  
Comparison between measured turbine stage performance and the predicted performance using quasi-3D flow and boundary layer analyses [NASA-TM-83640] p 29 N84-22564  
Analytical and experimental investigation of stator endwall contouring in a small axial-flow turbine [NASA-TP-2309] p 35 N84-32388

- Lubrication of machine elements  
[NASA-RP-1126] p 147 N84-31640
- HAMSTAD, M. A.**  
Aging results for PRD 49 ill/epoxy and Kevlar 49/epoxy composite pressure vessels p 52 A84-21847
- HAN, C. C.**  
A new multiple beam satellite antenna for 30/20 GHz communications coverage of CONUS-experimental evaluation  
[AIAA PAPER 84-0655] p 94 A84-25256
- HANKINS, G. B.**  
Extension to an analysis of turbulent swirling compressible flow for application to axisymmetric small gas turbine ducts  
[NASA-CR-165597] p 195 N84-21445
- HANNUM, N. B.**  
Space Station propulsion analysis study  
[AIAA PAPER 84-1326] p 44 A84-44179  
Space station propulsion analysis study  
[NASA-TM-83715] p 47 N84-25764
- HANSEN, I. G.**  
All-purpose bidirectional four-quadrant controller p 22 N84-10070
- HARB, A.**  
Thermal stress analysis for a wood composite blade  
[NASA-CR-173394] p 156 N84-21903  
Thermal-stress analysis for wood composite blade  
[NASA-CR-173330] p 157 N84-31685
- HARDING, R.**  
Documentation of ice shapes on the main rotor of a UH-1H helicopter in hover  
[NASA-CR-168332] p 9 N84-17139
- HARDY, T. L.**  
Cathode degradation and erosion in high pressure arc discharges  
[NASA-TM-83638] p 47 N84-22631
- HARPER, J.**  
Off-axis tensile properties and fracture in a unidirectional graphite/polyimide composite (Celcon 6000/PMR 15)  
p 53 A84-43553
- HARRIS, D. H.**  
Synthesis of perfluoroalkylene dianilines  
[NASA-CR-168004] p 60 N84-11228  
Thermal oxidative degradation reactions of perfluoroalkethers  
[NASA-CR-168224] p 60 N84-11229
- HARRY, R. W.**  
Evaluation of gas cooling for pressurized phosphoric acid fuel cell stacks p 163 A84-30191
- HARSHA, P. T.**  
Analytic modeling of a spray diffusion flame  
[AIAA PAPER 84-1317] p 118 A84-35168
- HART, C. E.**  
Real-time hybrid computer simulation of a small turboshaft engine and control system  
[NASA-TM-83579] p 28 N84-21548
- HART, F. H.**  
Effects of long-time elevated temperature exposures on hot-isostatically-pressed power-metallurgy Udimet 700 alloys with reduced cobalt contents  
[NASA-TM-83632] p 57 N84-28917
- HART, R. E.**  
Voltage controlling mechanisms in low resistivity silicon solar cells: A unified approach  
[NASA-TM-83612] p 167 N84-20916
- HART, R. E., JR.**  
High speed, low cost, LEO-thermal-cycling facility p 171 N84-29340
- HARTMAN, G. A.**  
A total life prediction model for stress concentration sites  
[NASA-CR-168225] p 152 N84-10612
- HARTMANN, M. J.**  
Aeronautical propulsion Present status and future directions  
[NASA-TM-83589] p 1 N84-16119
- HASAN, M. A. Z.**  
Jet noise modification by the 'whistler nozzle' p 181 A84-28355
- HAUGLAND, E. J.**  
High efficiency IMPATT diodes for 60 GHz intersatellite link applications  
[AIAA PAPER 84-0767] p 103 A84-25333  
Electronic properties of carbon fibers intercalated with copper chloride p 104 A84-34521  
NASA seeking high-power 60-GHz IMPATT diodes p 104 A84-44912  
A study of 60 GHz intersatellite link applications p 40 A84-49288  
High efficiency IMPATT diodes for 60 GHz intersatellite link applications  
[NASA-TM-83584] p 108 N84-18708
- HAVEY, C. T.**  
Uncertainty methodology for in-flight thrust determination  
[SAE PAPER 831438] p 13 A84-29452
- Application of in-flight thrust determination uncertainty  
[SAE PAPER 831439] p 13 A84-29453
- HAYNES, J. F.**  
Contingency power concepts for helicopter turboshaft engine  
[NASA-TM-83679] p 30 N84-23648  
Rotorcraft contingency power study  
[NASA-CR-174675] p 31 N84-24580
- HAZONY, D.**  
Circuit equivalent to the elastic spherical shell p 104 A84-39197
- HEAD, V. L.**  
Hot-flow tests of a series of 10-percent-scale turbofan forced mixing nozzles  
[NASA-TP-2268] p 123 N84-17525
- HEATH, B.**  
Low-cost single-crystal turbine blades, volume 1  
[NASA-CR-168218] p 68 N84-15247
- HEBERT, L. M.**  
Millimeter wave transmission systems and related devices  
[NASA-CR-173515] p 99 N84-24918
- HECKEL, R. W.**  
Solute transport and the prediction of breakaway oxidation in gamma + beta Ni-Cr-Al alloys p 65 A84-42658  
Modeling degradation and failure of Ni-Cr-Al overlay coatings  
[NASA-TM-83672] p 74 N84-27858
- HEIN, G. F.**  
Solar photovoltaic powered refrigerators/freezers for medical use in remote geographic locations  
[NASA-CR-168268] p 169 N84-25163
- HEITMAN, P. W.**  
Ceramic components for the AGT 100 engine p 136 A84-22878
- HELDENBRAND, R. W.**  
Advanced turbocharger design study program  
[NASA-CR-174633] p 143 N84-21879
- HELMICK, L. S.**  
FTIR analysis of aviation fuel deposits  
[NASA-TM-83773] p 92 N84-33608
- HELMES, H. E.**  
Ceramic components for the AGT 100 engine p 136 A84-22878  
Advanced Gas Turbine (AGT) Power-train system development  
[NASA-CR-168056] p 140 N84-10581
- HENCH, L. L.**  
Analysis of grain boundary phase devitrification of Y2O3- and Al2O3-doped Si3N4 p 79 A84-19792  
Grain-boundary phases in hot-pressed silicon nitride containing Y2O3 and CeO2 additives p 79 A84-19793  
Compositional effects on Si3N4 fracture surfaces p 79 A84-19794
- HENDRICKS, R.**  
Heat transfer in thermal barrier coated rods with circumferential and radial temperature gradients  
[ASME PAPER 84-GT-181] p 121 A84-46982  
High temperature thermomechanical analysis of ceramic coatings p 152 A84-48565
- HENDRICKS, R. C.**  
Residual stress in plasma-sprayed ceramic turbine tip and gas-path seal specimens p 78 A84-19783  
Correlation of compressive and shear stress with spalling of plasma-sprayed ceramic materials p 79 A84-19784  
The effect of annealing on the creep of plasma-sprayed ceramics p 79 A84-19785  
A thermomechanical model for energy propagation in a solid-fluid-solid system with one boundary in relative motion  
[ASME PAPER 83-HT-97] p 137 A84-29092  
Some inelastic effects of thermal cycling on yttria-stabilized zirconia  
[NASA-TM-83488] p 123 N84-16492  
Experimental study of bubble cavities attached to a rotating shaft in a reservoir  
[NASA-TM-83586] p 124 N84-17533
- HENNEKE, E. G.**  
Characterization of composite materials by means of the ultrasonic stress wave factor p 51 A84-10430
- HENNINGSEN, T.**  
Measurement of heat pump processes induced by laser radiation  
[NASA-CR-168324] p 134 N84-18620
- HENRICKS, R. J.**  
Materials for Advanced Turbine Engines (MATE): Project 3. Design, fabrication and evaluation of an oxide dispersion strengthened sheet alloy combustor liner, volume 1  
[NASA-CR-174691] p 76 N84-32504
- HERBELL, T. P.**  
Characteristics of Si3N4-SiO2-Ce2O3 compositions sintered in high-pressure nitrogen p 79 A84-19913
- HERMAN, H.**  
Phase analysis of plasma-sprayed zirconia-yttria coatings p 78 A84-19781  
Anisotropic thermal expansion effects in plasma-sprayed ZrO2-8 percent Y2O3 coatings p 78 A84-19782
- HERTZBERG, A.**  
Basic and applied research related to the technology of space energy conversion systems, 1982 - 1983  
[NASA-CR-173554] p 169 N84-25168
- HERZAU, J. S.**  
Teardown analysis of a ten cell bipolar nickel-hydrogen battery  
[NASA-TM-83618] p 168 N84-23026
- HESS, C. F.**  
A technique combining the visibility of a Doppler signal with the peak intensity of the pedestal to measure the size and velocity of droplets in a spray  
[AIAA PAPER 84-0203] p 129 A84-17946  
Development and implementation of advanced diagnostic techniques p 132 N84-20528
- HEUER, A. H.**  
Bubble formation in oxide scales on SiC p 79 A84-23689
- HEYWOOD, J. B.**  
Computer simulation of the heavy-duty turbo-compounded diesel cycle for studies of engine efficiency and performance  
[NASA-CR-174755] p 196 N84-33306
- HIGGINS, G. J.**  
Simultaneous cabin and ambient ozone measurements on two Boeing 747 airplanes Volume 2 January to October 1978  
[NASA-TM-81733] p 193 N84-22488
- HIKO, B. K.**  
Experimental investigation of the pulsed electrothermal (PET) thruster  
[AIAA PAPER 84-1386] p 43 A84-35201
- HILKO, B. K.**  
Proposed system design for a 20 kW pulsed electrothermal thruster  
[AIAA PAPER 84-1387] p 43 A84-35202  
Investigation of a pulsed electrothermal thruster  
[NASA-CR-168266] p 45 N84-12227
- HILL, F. E.**  
Development and fabrication of an augmented power transistor  
[NASA-CR-168262] p 106 N84-11388
- HINCKEL, J. A.**  
Convective heat transfer studies at high temperatures with pressure gradient for inlet flow Mach number of 0.45  
[AIAA PAPER 84-1487] p 119 A84-35233
- HINGST, W. R.**  
Experimental studies on two dimensional shock boundary layer interactions  
[AIAA PAPER 84-0099] p 3 A84-17881  
Companion of experimental and computational compressible flow in a S-duct  
[AIAA PAPER 84-0033] p 4 A84-19228
- HIRSCHKRON, R.**  
Powerplant design for one-engine-inoperative operation p 19 A84-40787  
Contingency power concepts for helicopter turboshaft engine  
[NASA-TM-83679] p 30 N84-23648  
Rotorcraft contingency power study  
[NASA-CR-174675] p 31 N84-24580
- HO, F.**  
Recent advances in thin silicon solar cells p 160 A84-22881
- HO, P.**  
High-speed wide band 20 x 20 microwave switch matrix p 105 A84-49253
- HOBART, H. F.**  
Advanced high temperature heat flux sensors  
[NASA-TM-83526] p 123 N84-16493
- HOBERECHT, M. A.**  
A 37.5-kW point design companion of the nickel-cadmium battery, bipolar nickel-hydrogen battery, and regenerative hydrogen-oxygen fuel cell energy storage subsystems for low Earth orbit  
[NASA-TM-83651] p 167 N84-23022  
Design considerations for a 10-kW integrated hydrogen-oxygen regenerative fuel cell system  
[NASA-TM-83664] p 167 N84-23023
- HOCHSTEIN, J. I.**  
Computational modeling of jet induced mixing of cryogenic propellants in low-G  
[AIAA PAPER 84-1344] p 121 A84-40243  
Computational modeling of jet induced mixing of cryogenic propellants in low-G  
[NASA-TM-83703] p 127 N84-25000
- HODGDON, R. B.**  
Anion permselective membrane  
[NASA-CR-174725] p 172 N84-29358

- HOERST, D. J.**  
Experimental investigation of shock-cell noise reduction for dual-stream nozzles in simulated flight comprehensive data report. Volume 1: Test nozzles and acoustic data [NASA-CR-168335-VOL-1] p 184 N84-24323  
Experimental investigation of shock-cell noise reduction for dual-stream nozzles in simulated flight comprehensive data report. Volume 2: Laser velocimeter data, static pressures and shadowgraph photos [NASA-CR-168335-VOL-2] p 184 N84-24324  
Experimental investigation of shock-cell noise reduction for single-stream nozzles in simulated flight, comprehensive data report. Volume 1: Test nozzles and acoustic data [NASA-CR-168234-VOL-1] p 185 N84-33148  
Experimental investigation of shock-cell noise reduction for single-stream nozzles in simulated flight, comprehensive data report. Volume 2: Laser velocimeter data [NASA-CR-168234-VOL-2] p 186 N84-33149  
Experimental investigation of shock-cell noise reduction for single-stream nozzles in simulated flight, comprehensive data report. Volume 3: Shadowgraph photos and facility description [NASA-CR-168234-VOL-3] p 186 N84-33150
- HOFFMAN, C. A.**  
Microstructure and orientation effects on properties of discontinuous silicon carbide/aluminum composites [NASA-TP-2302] p 51 N84-26749
- HOFFMAN, J. D.**  
Computation of viscous flow in planar and axisymmetric ducts by an implicit marching procedure [AIAA PAPER 84-0256] p 114 A84-17979  
Three-dimensional flow simulations for supersonic mixed-compression inlets at incidence p 5 A84-38828
- HOFFMAN, R. W.**  
Particle environment [NASA-CR-173888] p 191 N84-33210
- HOFLE, M. M.**  
Correlation of compressive and shear stress with spalling of plasma-sprayed ceramic materials p 79 A84-19784
- HOLLADA, R.**  
Analysis of thermoelectric properties of high-temperature complex alloys of nickel-base, iron-base and cobalt-base groups [NASA-TP-2278] p 70 N84-18370
- HOLDEMAN, J. D.**  
On modeling dilution jet flowfields [AIAA PAPER 84-1379] p 121 A84-44183  
Experiments in dilution jet mixing p 122 A84-48140  
Tabulations of ambient ozone data obtained by GASP (Global Air Sampling Program) airplanes, March 1975 to July 1979 [NASA-TM-82742] p 174 N84-18806  
Modeling of dilution jet flowfields p 126 N84-20547  
Simultaneous cabin and ambient ozone measurements on two Boeing 747 airplanes. Volume 2. January to October 1978 [NASA-TM-81733] p 193 N84-22488  
On modeling dilution jet flowfields [NASA-TM-83708] p 32 N84-25713  
Climatology of ozone at altitudes from 19,000 to 59,000 feet based on combined GASP and ozonesonde data [NASA-TP-2303] p 174 N84-31865
- HOLLAND, W. R.**  
Coupling of radiation into thin film modes by means of localized plasma resonances p 187 A84-16397
- HOM, K.**  
Secondary effects in combustion instabilities leading to flashback p 58 A84-17436
- HOMES, D. E.**  
LEC GaAs for integrated circuit applications [NASA-CR-173267] p 191 N84-17014
- HOOSAC, T. M.**  
Model development and statistical investigation of turbine blade mistuning p 17 A84-31905
- HOPKINS, D. A.**  
Nonlinear analysis for high-temperature composites. Turbine blades/vanes p 158 N84-31699
- HOPPER, A. T.**  
Creep fatigue of low-cobalt superalloys: Waspalloy, PM U 700 and wrought U 700 [NASA-CR-168260] p 67 N84-13265
- HORNKOHL, J. O.**  
Measurement of spray combustion processes p 61 N84-20530
- HOROWITZ, S. J.**  
Finite element-integral acoustic simulation of JT15D turbofan engine p 182 A84-41132
- HOUSER, M. J.**  
Development of the phase/Doppler spray analyzer for liquid drop size and velocity characterizations [AIAA PAPER 84-1199] p 131 A84-36958  
Analysis and testing of a new method for drop size measurement using laser scatter interferometry [NASA-CR-174636] p 133 N84-31595
- HOWE, D. C.**  
Energy efficient engine high-pressure turbine detailed design report [NASA-CR-165608] p 33 N84-28788  
Energy efficient engine. Turbine intermediate case and low-pressure turbine component test hardware detailed design report [NASA-CR-167973] p 33 N84-28789
- HOWES, W. L.**  
Large-aperture interferometer with local reference beam p 130 A84-34628  
Rainbow schlieren and its applications p 131 A84-40738  
Preliminary experiments on phase conjugation for flow visualization [NASA-TM-83766] p 189 N84-32169
- HOYNIAK, D.**  
The coupled response of turbomachinery blading to aerodynamic excitations p 17 A84-26959
- HSUEH, K.-L.**  
Electrode kinetics of oxygen reduction - A theoretical and experimental analysis of the rotating ring-disk electrode method p 59 A84-29999
- HUFF, R. G.**  
Simplified combustion noise theory yielding a prediction of fluctuating pressure level [NASA-TP-2237] p 183 N84-19049  
Low frequency noise in a quiet, clean, general aviation turbofan engine [NASA-TM-83520] p 183 N84-20320  
A theoretical prediction of the acoustic pressure generated by turbulence-flame front interactions [NASA-TM-83587] p 184 N84-26383  
Analysis of the effect on combustor noise measurements of acoustic waves reflected by the turbine and combustor inlet [NASA-TM-83760] p 185 N84-32122
- HUGHES, T. J. R.**  
Element-by-element solution procedures for nonlinear structural analysis p 158 N84-31694
- HUGHES, W. F.**  
Dynamics of two-phase face seals p 137 A84-28792  
Thermal and elastohydrodynamic analysis of reciprocating rod seals in the Stirling engine p 138 A84-30085
- HULL, D. R.**  
The effects of Cr, Al, Ti, Mo, W, Ta, and Nb on the cyclic oxidation behavior of cast Ni-base superalloys at 1100 and 1150 C p 65 A84-27485  
Ultrasonic velocity measurement using phase-slope cross-correlation methods [NASA-TM-83794] p 149 N84-34769
- HUMENIK, F. M.**  
Flame radiation and linear heat transfer in a tubular can combustor [AIAA PAPER 84-0443] p 16 A84-21300  
Flame radiation and linear heat transfer in a tubular-can combustor [NASA-TM-83536] p 23 N84-13188  
Detailed fuel spray analysis techniques p 127 N84-24747
- HUMPHRIES, R. R.**  
Design study of magnetic eddy-current vibration suppression dampers for application to cryogenic turbomachinery [NASA-CR-173273] p 141 N84-16562
- HUNT, J. C. R.**  
The production of turbulent stress in a shear flow by irrotational fluctuations p 115 A84-18357  
The production of turbulent stress in a shear flow by irrotational fluctuations p 115 A84-21390
- HURWITZ, F. I.**  
The effect of a coating on the thermo-oxidative stability of Celcon 6000 graphite fiber/PMR 15 polyimide composites p 52 A84-21844  
Off-axis tensile properties and fracture in a unidirectional graphite/polyimide composite (Celcon 6000/PMR 15) p 53 A84-43553  
Method and apparatus for gripping uniaxial fibrous composite materials [NASA-CASE-LEW-13758-1] p 56 N84-27829
- HUSSAIN, A. K. M. F.**  
Jet noise modification by the 'whistler nozzle' p 181 A84-23355
- HWANG, D. P.**  
Investigation of tangential blowing applied to a subsonic V/STOL inlet p 3 A84-11042  
Boundary layer transition effects on flow separation around V/STOL engine inlets at high incidence [AIAA PAPER 84-0432] p 4 A84-18090  
Analytical study of suction boundary layer control for subsonic V/STOL inlets [AIAA PAPER 84-1399] p 6 A84-44187
- Analytical study of blowing boundary-layer control for subsonic V/STOL inlets [NASA-TM-83576] p 8 N84-16141
- HYNES, A. J.**  
The chemical kinetics and thermodynamics of sodium species in oxygen-rich hydrogen flames p 59 A84-27724
- IDE, R. F.**  
Comparison of icing cloud instruments for 1982-1983 icing season flight program [NASA-TM-83569] p 14 N84-29870
- ILES, P. A.**  
Recent advances in thin silicon solar cells p 160 A84-22981
- INGEBO, R. D.**  
Aerodynamic effect of combustor inlet-air pressure on fuel jet atomization [AIAA PAPER 84-1320] p 120 A84-36973  
Aerodynamic effect of combustor inlet-air pressure on fuel jet atomization [NASA-TM-83611] p 126 N84-22910  
Atomization of liquid sheets in high pressure airflow [NASA-TM-83731] p 128 N84-30223
- INSPEKTOR, A.**  
Homogeneous reactions of hydrocarbons, silane, and chlorosilanes in radiofrequency plasmas at low pressures [NASA-TP-2301] p 50 N84-20643  
Radical and ion molecule mechanisms in the polymerization of hydrocarbons and chlorosilanes in RF plasmas at low pressures (1.0 torr) [NASA-TM-83602] p 190 N84-21329
- INUKAI, T.**  
ACTS TDMA network control [AIAA PAPER 84-0682] p 94 A84-25274
- IRVIN, T. B.**  
Progressive fracture of fiber composites [NASA-TM-83701] p 56 N84-27831
- IRVINE, T. B.**  
Fracture surface characteristics of notched angle-plyed graphite/epoxy composites [NASA-TM-83786] p 57 N84-33522  
Fracture modes in notched angle-plyed composite laminates [NASA-TM-83802] p 58 N84-34576
- ISHIZUKA, S.**  
An experimental study on extinction and stability of stretched premixed flames p 59 A84-35425
- ISLAM, O.**  
Jet noise modification by the 'whistler nozzle' p 181 A84-23355
- ITO, T. I.**  
Thermal oxidative degradation reactions of linear perfluoroalkyl ethers p 60 A84-30000  
Synthesis of perfluoroalkylene dianilines [NASA-CR-168004] p 60 N84-11228
- IWAKUMA, T.**  
Finite elastic-plastic deformation of polycrystalline metals p 66 A84-43872

## J

- JABLONSKI, J.**  
Assessment of institutional barriers to the use of natural gas fuel in automotive vehicle fleets [NASA-CR-168183] p 165 N84-14587
- JACKSON, J.**  
State estimation Kalman filter using optical processings. Noise statistics known p 178 A84-23602
- JACKSON, T. W.**  
Turbulence measurements in confined jets using a rotating single-wire probe technique p 113 A84-13564  
Accuracy and directional sensitivity of the single-wire technique [AIAA PAPER 84-0367] p 130 A84-18047  
Swirl flow turbulence modeling [AIAA PAPER 84-1376] p 118 A84-35186  
Turbulence characteristics of swirling flowfields [NASA-CR-175392] p 124 N84-19744
- JACOBSON, B. O.**  
Non-Newtonian fluid model incorporated into elastohydrodynamic lubrication of rectangular contacts [ASME PAPER 83-LUB-15] p 139 A84-44300
- JACOBSON, N. S.**  
Reaction of cobalt in SO<sub>2</sub> atmospheres at elevated temperatures p 65 A84-33440
- JALAN, V.**  
Importance of interatomic spacing in catalytic reduction of oxygen in phosphoric acid p 58 A84-12644  
Chromium electrodes for REDOX cells [NASA-CASE-LEW-13653-1] p 170 N84-28205

## JANARDAN, B. A.

- Experimental investigation of shock-cell noise reduction for dual-stream nozzles in simulated flight comprehensive data report. Volume 1: Test nozzles and acoustic data [NASA-CR-168336-VOL-1] p 184 N84-24323
- Experimental investigation of shock-cell noise reduction for dual-stream nozzles in simulated flight comprehensive data report. Volume 2: Laser velocimeter data, static pressures and shadowgraph photos [NASA-CR-168336-VOL-2] p 184 N84-24324
- Free jet feasibility study of a thermal acoustic shield concept for AST/VCE application. Single stream nozzles [NASA-CR-3758] p 185 N84-29661
- Experimental investigation of shock-cell noise reduction for single-stream nozzles in simulated flight, comprehensive data report. Volume 1: Test nozzles and acoustic data [NASA-CR-168234-VOL-1] p 185 N84-33148
- Experimental investigation of shock-cell noise reduction for single-stream nozzles in simulated flight, comprehensive data report. Volume 2: Laser velocimeter data [NASA-CR-168234-VOL-2] p 186 N84-33149
- Experimental investigation of shock-cell noise reduction for single-stream nozzles in simulated flight, comprehensive data report. Volume 3: Shadowgraph photos and facility description [NASA-CR-168234-VOL-3] p 186 N84-33150
- JANETZKE, D. C.  
Use of the WEST-1 wind turbine simulator to predict blade fatigue load distribution [NASA-TM-83532] p 165 N84-14586
- JANJUA, S. I.  
Turbulence measurements in confined jets using a rotating single-wire probe technique p 113 A84-13584
- JARRETT, R. N.  
Effects of cobalt in nickel-base superalloys [NASA-CR-168308] p 67 N84-14287
- The role of cobalt on the creep of Waspaloy [NASA-CR-174628] p 70 N84-19523
- JASPERSON, W. H.  
Temperature histories of commercial flights at severe conditions from GASP data [NASA-CR-168247] p 12 N84-11152
- Tabulations of ambient ozone data obtained by GASP (Global Air Sampling Program) airliners, March 1975 to July 1979 [NASA-TM-82742] p 174 N84-18806
- Tabulations of ozonesonde data, 1963 - 1980 [NASA-CR-174631] p 174 N84-27375
- Climatology of ozone at altitudes from 19,000 to 59,000 feet based on combined GASP and ozonesonde data [NASA-TP-2303] p 174 N84-31865
- JEAN, P. N.  
A frequency-division multiple-access system concept for 30/20 GHz high-capacity domestic satellite service p 94 A84-22141
- JECH, R. W.  
Rapid solidification via melt spinning - Equipment and techniques p 65 A84-31915
- JEFFRIES, K. S.  
Parametric analysis of hollow conductor parallel and coaxial transmission lines for high frequency space power distribution [NASA-TM-83601] p 46 N84-20639
- JENSEN, A. S.  
Output statistics of laser anemometers in sparsely seeded flows p 117 A84-28738
- Optimizing and comparing laser anemometers p 130 A84-28739
- JENSEN, K. A.  
Beam impingement angle effects on secondary electron emission characteristics of textured pyrolytic graphite [NASA-TP-2285] p 82 N84-18400
- Secondary electron emission characteristics of ion-textured copper and high-purity isotropic graphite surfaces [NASA-TP-2342] p 86 N84-28989
- JOHNS, A. L.  
Flow visualization and interpretation of visualization data for deflected thrust V/STOL nozzles [AIAA PAPER 84-0102] p 16 A84-21852
- Flow visualization and interpretation of visualization data for deflected thrust V/STOL nozzles [NASA-TM-83554] p 24 N84-14147
- JOHNSON, B. V.  
Mass and momentum turbulent transport experiments with confined swirling coaxial jets I [AIAA PAPER 84-1380] p 119 A84-35664
- Mass and momentum turbulent transport experiments with confined swirling coaxial jets [NASA-CR-168252] p 124 N84-17530
- JOHNSON, G. M.  
Multiple-grid convergence acceleration of viscous and inviscid flow computations p 116 A84-23950

- Relaxation solution of the full Euler equations p 119 A84-35323
- Embedding methods for the steady Euler equations [NASA-TM-83481] p 178 N84-11831
- JOHNSON, J. F. E.  
Comparison of thermal plasma observations on SCATHA and GEOS p 41 N84-17262
- JOHNSON, K.  
Executive summary, aerothermal modeling program, phase 1 [NASA-CR-174602] p 60 N84-12263
- Aerothermal modeling program, phase 1 [NASA-CR-168243-VOL-2] p 60 N84-12265
- Dilution jet mixing program [NASA-CR-174624] p 33 N84-26702
- JOHNSON, R. A.  
Advanced Gas Turbine (AGT). Power-train system development [NASA-CR-168056] p 140 N84-10581
- JOHNSON, S. A.  
Aeroelastic analysis for propellers - mathematical formulations and program user's manual [NASA-CR-3729] p 153 N84-12530
- JOHNSON, S. M.  
Preliminary investigation of a two-zone swirl flow combustor [AIAA PAPER 84-1169] p 17 A84-36951
- Experimental investigation of the low NOx vortex airblast annular combustor [AIAA PAPER 84-1170] p 18 A84-36952
- Preliminary investigation of a two-zone swirl flow combustor [NASA-TM-83637] p 29 N84-22565
- JOHNSTON, J. P.  
Turbulent boundary-layer flow and structure on a convex wall and its redevelopment on a flat wall p 115 A84-21378
- JOHNSTON, S.  
Orbital stability in combined uniform axial and three-dimensional wiggler magnetic fields for free-electron lasers [NASA-TM-83753] p 134 N84-30273
- JOHNSTON, W.  
Viscous-inviscid interactive procedure for rotational flow in cascades of airfoils p 6 A84-44639
- JOHNSTON, W. A.  
A viscous-inviscid interactive procedure for rotational flow in cascades of two dimensional airfoils of arbitrary shape [NASA-CR-174609] p 7 N84-13149
- JONES, C.  
Design of a high-performance rotary stratified-charge research aircraft engine [AIAA PAPER 84-1395] p 17 A84-35204
- JONES, H. F.  
Design analysis of Rayleigh-step floating-ring seals [ASLE PREPRINT 83-LC-3B-2] p 137 A84-28989
- JONES, J. D.  
A temperature correlation for the radiation resistance of a thick-walled circular duct exhausting a hot gas p 181 A84-31103
- Recovery of burner acoustic source structure from far-field sound spectra [AIAA PAPER 83-0763] p 181 A84-32609
- JONES, R. E.  
Combustion gas properties of various fuels of interest to gas turbine engines [NASA-TM-83682] p 31 N84-24584
- JONES, R. J.  
Improved high temperature resistant matrix resins [NASA-CR-168210] p 87 N84-28995
- JONES, W. R., JR.  
Ferographic and spectrometer oil analysis from a failed gas turbine engine p 135 A84-11273
- Liquid chromatographic analysis of a formulated ester from a gas-turbine engine test [ASLE PREPRINT 83-LC-1A-1] p 80 A84-28995
- Thermal oxidative degradation reactions of linear perfluoroalkyl ethers p 80 A84-30000
- Topological reaction rate measurements related to scuffing [NASA-TM-83486] p 68 N84-14288
- Thermal and oxidative stabilities of liquid lubricants p 84 N84-23907
- JONGEWARD, G. A.  
Plasma sheath structure surrounding a large powered spacecraft [AIAA PAPER 84-0329] p 40 A84-18025
- JORDAN, E. H.  
Elevated temperature biaxial fatigue [NASA-CR-173473] p 156 N84-21905
- JOSLYN, H. D.  
Inlet boundary layer effects in an axial compressor rotor. I Blade-to-blade effects [ASME PAPER 84-GT-84] p 6 A84-46926

- Inlet boundary layer effects in an axial compressor rotor II - Throughflow effects [ASME PAPER 84-GT-85] p 7 A84-46927
- Compressor rotor aerodynamics p 26 N84-16210
- JUHASZ, A. J.  
Oxidant system improvements for MHD energy conversion and industrial processes p 189 A84-24058
- JUTRAS, R. R.  
Subsonic/transonic stall flutter investigation of a rotating ng [NASA-CR-174625] p 36 N84-33417

## K

- KACHANOV, M.  
On stress analysis of a crack-layer [NASA-CR-174774] p 159 N84-34774
- KAMATH, G. S.  
Effect of electron flux on radiation damage in GaAs solar cells p 160 A84-22998
- KAMEL, M. M.  
Self-similar blast waves incorporating deflagrations of variable speed p 116 A84-28379
- KAMO, R.  
New perspectives for advanced automobile diesel engines p 138 A84-30062
- KANG, D.  
New variational formulations of hybrid stress elements p 158 N84-31690
- KANNEL, J. W.  
Subsurface stress evaluations under rolling/sliding contacts [ASME PAPER 83-LUB-18] p 137 A84-29099
- KAO, H. C.  
Flow visualization and interpretation of visualization data for deflected thrust V/STOL nozzles [AIAA PAPER 84-0102] p 16 A84-21852
- Flow visualization and interpretation of visualization data for deflected thrust V/STOL nozzles [NASA-TM-83554] p 24 N84-14147
- KAR, K. K.  
Internal heat transfer coefficients of porous metals p 112 A84-13239
- KARAGUELLE, H.  
Input-output characterization of an ultrasonic testing system by digital signal analysis [NASA-CR-3756] p 149 N84-15565
- KARLSSON, E. A.  
Development and fabrication of a high current, fast recovery power diode [NASA-CR-168196] p 106 N84-13443
- KARPLUS, W. J.  
Parallelism and pipelining in high-speed digital simulators p 175 A84-11876
- Dataflow computing approach in high-speed digital simulation [NASA-CR-173552] p 176 N84-25336
- KASCAK, A. F.  
Effects of different rub models on simulated rotor dynamics [NASA-TP-2220] p 142 N84-17590
- KASCAK, T. J.  
Microwave monolithic integrated circuit development for future spaceborne phased array antennas [AIAA PAPER 84-0656] p 94 A84-25257
- Microwave monolithic integrated circuit development for future spaceborne phased array antennas [NASA-TM-83518] p 97 N84-13399
- KASUBA, R.  
Dynamics of early planetary gear trains [NASA-CR-3793] p 145 N84-26027
- KASZETA, W. J.  
Qualification testing of solar photovoltaic powered refrigerator freezers for medical use in remote geographic locations [NASA-CR-168181] p 169 N84-25162
- KATSANIS, T.  
Comparison between measured turbine stage performance and the predicted performance using quasi-3D flow and boundary layer analyses [AIAA PAPER 84-1299] p 18 A84-36972
- Programs for calculating quasi-three-dimensional flow in a turbomachine blade row [NASA-TM-83588] p 9 N84-17138
- Comparison between measured turbine stage performance and the predicted performance using quasi-3D flow and boundary layer analyses [NASA-TM-83640] p 29 N84-22564
- KATZ, I.  
Plasma sheath structure surrounding a large powered spacecraft [AIAA PAPER 84-0329] p 40 A84-18025
- Potentials in a plasma over a biased pinhole p 102 A84-20711



- NASCAP simulations of spacecraft charging of the SCATHA satellite p 41 N84-17268
- KAUFMAN, A.**  
Simplified analytical procedures for representing material cyclic response p 16 A84-22877  
Develop and test fuel cell powered on-site integrated total energy systems Phase 3. Full-scale power plant development [NASA-CR-168294] p 164 N84-13672  
Develop and test fuel cell powered on-site integrated total energy system [NASA-CR-168239] p 164 N84-13673  
A simplified method for elastic-plastic-creep structural analysis [NASA-TM-83509] p 154 N84-14542  
Engine cyclic durability by analysis and material testing [NASA-TM-83577] p 155 N84-18683  
Development of a simplified procedure for cyclic structural analysis [NASA-TP-2243] p 155 N84-20878  
Develop and test fuel cell powered on-site integrated total energy systems [NASA-CR-174714] p 170 N84-27329
- KAUTZ, H. E.**  
Ultrasonic velocity measurement using phase-slope cross-correlation methods [NASA-TM-83794] p 149 N84-34769
- KAZA, K. R. V.**  
Effects of structural coupling on mistuned cascade flutter and response [ASME PAPER 83-GT-117] p 151 A84-33701  
An improved finite-difference analysis of uncoupled vibrations of tapered cantilever beams [NASA-TM-83495] p 154 N84-13610  
Flutter of swept fan blades [NASA-TM-83547] p 154 N84-16587  
Improved finite-difference vibration analysis of pretwisted, tapered beams [NASA-TM-83549] p 154 N84-16588  
Vibration and flutter of mistuned bladed-disk assemblies [NASA-TM-83634] p 156 N84-23923  
Improved methods of vibration analysis of pretwisted, airfoil blades [NASA-TM-83735] p 157 N84-30329
- KEENER, K. M.**  
Long life nickel electrodes for a nickel-hydrogen cell. I Initial performance p 162 A84-30186
- KEENEY, R.**  
Diffused junction p(+)-n solar cells in bulk GaAs. II - Device characterization and modelling p 161 A84-26028
- KEENEY, R. P.**  
Photovoltaic characteristics of diffused P/+N bulk GaAs solar cells p 161 A84-23115
- KEITH, J. S.**  
Application of a polynomial spline in higher-order accurate viscous-flow computations p 119 A84-35349
- KEITH, T. G.**  
Assessment of two neglected effects in the analysis of an oil pumping ring seal [ASME PAPER 83-LUB-16] p 137 A84-29097
- KELKAR, S. S.**  
Stability analysis of a buck regulator employing input filter compensation p 102 A84-18412  
Input filter compensation for switching regulators [NASA-CR-173247] p 107 N84-16459
- KELLEDES, W. L.**  
Development of a DC propulsion system for an electric vehicle [NASA-CR-168306] p 166 N84-20014
- KENDALL, B. R. F.**  
The pressure multiplier revisited p 129 A84-13125
- KENNEDY, F. E., JR.**  
Determination of near-surface plastic deformation in sliding contacts p 140 A84-48995
- KENWORTHY, M. J.**  
Aerothermal modeling, phase 1. Volume 1 Model assessment [NASA-CR-168296-VOL-1] p 25 N84-15155  
Aerothermal modeling, phase 1. Volume 2. Experimental data [NASA-CR-168296-VOL-2] p 25 N84-15156
- KENWORTHY, M. K.**  
Aerothermal modeling Executive summary [NASA-CR-168330] p 25 N84-15152
- KERBER, H.**  
Spatial electron density and electric field strength measurements in microwave cavity experiments [AIAA PAPER 84-1522] p 189 A84-46109
- KERBER, R.**  
Spatial electron density and electric field strength measurements in microwave cavity experiments [NASA-CR-173907] p 111 N84-32682
- KERMANI, M. M.**  
Heat transfer in thermal barrier coated rods with circumferential and radial temperature gradients [ASME PAPER 84-GT-181] p 121 A84-46982
- KERSLAKE, W. R.**  
LERC rail accelerators - Test designs and diagnostic techniques p 42 A84-32031
- KESHOCK, E. G.**  
Measurements of local convective heat transfer coefficients on ice accretion shapes [AIAA PAPER 84-0018] p 113 A84-17835  
Measurement of local convective heat transfer coefficients of four ice accretion shapes [NASA-CR-174680] p 10 N84-25646
- KHADER, N.**  
Structural dynamics of rotating bladed-disk assemblies coupled with flexible shaft motions p 21 A84-44645
- KHALIFA, H. E.**  
Waste heat recovery from adiabatic diesel engines by exhaust-driven Brayton cycles [NASA-CR-168257] p 196 N84-32307
- KIELB, R. E.**  
Effects of structural coupling on mistuned cascade flutter and response [ASME PAPER 83-GT-117] p 151 A84-33701  
Vibrations of twisted cantilevered plates - Experimental investigation [ASME PAPER 84-GT-96] p 152 A84-46937  
Flutter of swept fan blades [NASA-TM-83547] p 154 N84-16587  
Vibration and flutter of mistuned bladed-disk assemblies [NASA-TM-83634] p 156 N84-23923  
Lewis Research Center spin rig and its use in vibration analysis of rotating systems [NASA-TP-2304] p 30 N84-24578  
Nonlinear displacement analysis of advanced propeller structures using NASTRAN [NASA-TM-83737] p 157 N84-31683
- KIESLING, J. D.**  
Mobile radio alternative systems study satellite/terrestrial (hybrid) systems concepts [NASA-CR-168064] p 95 N84-10404
- KIM, B.**  
0.5 W 2-21 GHz monolithic GaAs distributed amplifier p 103 A84-30857  
GaAs dual-gate FET for operation up to K-band p 104 A84-32281
- KIM, W. S.**  
Bacterial degradation of polychlorinated biphenyls in sludge from an industrial sewer lagoon [NASA-TM-83543] p 173 N84-11594
- KING, R. J.**  
Inherent overload protection for the series resonant converter p 102 A84-23255  
A large-signal dynamic simulation for the series resonant converter p 103 A84-23258  
A study of the high frequency limitations of series resonant converters [NASA-CR-173868] p 111 N84-32678
- KINGBURY, E.**  
First order ball bearing kinematics [NASA-TM-83592] p 142 N84-19816
- KINGSBURY, E.**  
Pivoting and slip in an angular contact bearing p 139 A84-40585  
The ball bearing as a rheological test device [NASA-TM-83570] p 142 N84-17591
- KIRKPATRICK, C. G.**  
LEC GaAs for integrated circuit applications [NASA-CR-173267] p 191 N84-17014
- KLANN, G. A.**  
Response of a small-turboshaft-engine compression system to inlet temperature distortion [NASA-TM-83765] p 35 N84-33414
- KLANN, J. L.**  
Downsizing assessment of automotive Stirling engines [NASA-TM-83468] p 194 N84-14989
- KLINGLER, T. A.**  
An application of tensor ideas to nonlinear modeling of a turbfan jet engine p 20 A84-42382
- KNECHTL, R. C.**  
Effect of electron flux on radiation damage in GaAs solar cells p 160 A84-22998
- KNOLL, J.**  
A dynamic analysis of rotary combustion engine seals [NASA-TM-83536] p 141 N84-14519
- KNOLL, R. H.**  
Downsizing assessment of automotive Stirling engines [NASA-TM-83468] p 194 N84-14989
- KNOTT, K.**  
Comparison of thermal plasma observations on SCATHA and GEOS p 41 N84-17262
- KNOTT, P. R.**  
Free jet feasibility study of a thermal acoustic shield concept for AST/VCE application Single stream nozzles [NASA-CR-3758] p 185 N84-29861  
Experimental investigation of shock-cell noise reduction for single-stream nozzles in simulated flight, comprehensive data report. Volume 1: Test nozzles and acoustic data [NASA-CR-168234-VOL-1] p 185 N84-33148  
Experimental investigation of shock-cell noise reduction for single-stream nozzles in simulated flight, comprehensive data report. Volume 2 Laser velocimeter data [NASA-CR-168234-VOL-2] p 186 N84-33149  
Experimental investigation of shock-cell noise reduction for single-stream nozzles in simulated flight, comprehensive data report Volume 3 Shadowgraph photos and facility description [NASA-CR-168234-VOL-3] p 186 N84-33150
- KNUDSEN, L. K.**  
Energy efficient engine. Low-pressure turbine subsonic cascade component development and integration program [NASA-CR-165592] p 33 N84-27738
- KOFEL, W. K.**  
Tip cap for a rotor blade [NASA-CASE-LEW-13654-1] p 28 N84-22560
- KOHL, F. J.**  
Experimental and theoretical deposition rates from salt-seeded combustion gases of a Mach 0.3 burner rig [NASA-TP-2225] p 124 N84-19741  
Chemical mechanisms and reaction rates for the initiation of hot corrosion of IN-738 [NASA-TP-2319] p 74 N84-28958  
Deposition of Na<sub>2</sub>SO<sub>4</sub> from salt-seeded combustion gases of a high velocity burner rig [NASA-TM-83751] p 129 N84-31558
- KONICEK, L.**  
Window aberration correction in laser velocimetry using multifaceted holographic optical elements p 134 A84-24663
- KOPANSKI, J. J.**  
Thermal oxidation of 3C silicon carbide single-crystal layers on silicon p 191 A84-49620
- KOPELMAN, R. B.**  
Turbidity very near the critical point of methanol-cyclohexane mixtures p 192 A84-30391
- KOPLOW, M. D.**  
An RC-1 organic Rankine bottoming cycle for an adiabatic diesel engine [NASA-CR-168256] p 196 N84-32306
- KOPPER, F. C.**  
Energy efficient engine Low-pressure turbine subsonic cascade component development and integration program [NASA-CR-165592] p 33 N84-27738  
Energy efficient engine high-pressure turbine supersonic cascade technology report [NASA-CR-165567] p 33 N84-27739
- KORKAN, K. D.**  
Performance degradation of propeller systems due to nme ice accretion [AIAA PAPER 82-0286] p 12 A84-17406  
Helicopter rotor performance degradation in natural icing encounter p 12 A84-17412  
Experimental study of performance degradation of a model helicopter main rotor with simulated ice shapes [AIAA PAPER 84-0184] p 13 A84-17937  
Performance degradation of a model helicopter main rotor in hover and forward flight with a generic ice shape [AIAA PAPER 84-0609] p 13 A84-24195  
Performance degradation of a model helicopter rotor with a generic ice shape p 14 A84-49096
- KORSCHGEN, C. E.**  
A laser system to remotely sense bird movements p 159 A84-31608
- KOSMAHL, H. G.**  
A TWT amplifier with a linear power transfer characteristic and improved efficiency [AIAA PAPER 84-0762] p 104 A84-41035  
A study of 60 GHz intersatellite link applications p 40 A84-49288  
Ladder supported ring bar circuit [NASA-CASE-LEW-13570-1] p 106 N84-16452  
A TWT amplifier with a linear power transfer characteristic and improved efficiency [NASA-TM-83590] p 108 N84-21803  
Dielectric based submillimeter backward wave oscillator circuit [NASA-CASE-LEW-13736-1] p 110 N84-27974
- KOT, R. A.**  
Design considerations for a monolithic, GaAs, dual-mode, QPSK/QASK, high-throughput rate transceiver [NASA-CR-173560] p 110 N84-24974

- KOTHMANN, R. E.**  
Evaluation of gas cooling for pressurized phosphoric acid fuel cell stacks p 163 N84-30191
- KRAMER, T.**  
Evaluation of propellant tank insulation concepts for low-thrust chemical propulsion systems [NASA-CR-168320] p 46 N84-20634  
Evaluation of propellant tank insulation concepts for low-thrust chemical propulsion systems. Executive summary [NASA-CR-168321] p 83 N84-20699
- KRATZER, R. H.**  
Thermal oxidative degradation reactions of linear perfluoroalkyl ethers p 80 N84-30000  
Synthesis of perfluoroalkylene dianilines [NASA-CR-168004] p 60 N84-11228  
Thermal oxidative degradation reactions of perfluoroalkyl ethers [NASA-CR-168224] p 60 N84-11229
- KREJSA, E. A.**  
Cross spectra between pressure and temperature in a constant-area duct downstream of a hydrogen-fueled combustor [NASA-TM-83463] p 182 N84-11885  
A theoretical model for the cross spectra between pressure and temperature downstream of a combustor [NASA-TM-83671] p 186 N84-34231
- KREPINCH, I.**  
Steam bottoming cycle for an adiabatic diesel engine [NASA-CR-168255] p 196 N84-33304
- KRESKOVSKY, J. P.**  
Further development of a method for computing three-dimensional subsonic viscous flows in turbofan lobe mixers [NASA-CR-168304] p 122 N84-14462
- KRINSKY, I. S.**  
Anomalous high potentials observed on ISEE [NASA-CR-172791] p 41 N84-17252  
Anomalous high potentials observed on ISEE p 41 N84-17258
- KRISHNAN, R. V.**  
A simple application of the Bailey-Orowan creep model to Fe-39 B at pct Al and gamma/gamma prime - alpha p 64 N84-22012
- KROEGER, E. W.**  
Cryogenic Fluid Management Facility [AIAA PAPER 84-1340] p 44 N84-44184
- KROPP, J. L.**  
Apparatus analysis and preliminary design of low gravity porous solids experiment for STS Orbiter mid-deck [NASA-CR-168248] p 37 N84-10109  
Preliminary design of two Space Shuttle fluid physics experiments [NASA-CR-174649] p 39 N84-23667
- KROSEL, S. M.**  
Development of dynamic simulation of TF34-GE-100 turbofan engine with post-stall capability [AIAA PAPER 84-1184] p 20 N84-44178  
Digital computer program for generating dynamic turbofan engine models (DIGTEM) [NASA-TM-83446] p 26 N84-16185  
Development of dynamic simulation of TF34-GE-100 turbofan engine with post-stall capability [NASA-TM-83660] p 32 N84-25712
- KRUSE, V. J.**  
Wind turbine generator interaction with conventional diesel generators on Block Island, Rhode Island Volume 1: Executive summary [NASA-CR-168318] p 171 N84-29357  
Wind turbine generator interaction with conventional diesel generators on Block Island, Rhode Island Volume 2: Data analysis [NASA-CR-168319] p 172 N84-31783
- KSIENSKI, A. A.**  
Adaptive arrays for satellite communications [NASA-CR-173548] p 99 N84-24924
- KUCHAR, A. P.**  
Comparison of full-scale engine and subscale model performance of a mixed flow exhaust system for an energy efficient engine (E3) propulsion system [AIAA PAPER 84-0283] p 16 N84-17997
- KUUVINEN, D. E.**  
Bacterial degradation of polychlorinated biphenyls in sludge from an industrial sewer lagoon [NASA-TM-83543] p 173 N84-11594
- KUNATH, R. R.**  
Characteristics and capacities of the NASA Lewis Research Center high precision 6.7- by 6.7-m planar near-field scanner [NASA-TM-83785] p 133 N84-32789
- KURKOV, A. P.**  
Measurements of self-excited rotor-blade vibrations using optical displacements [ASME PAPER 83-GT-132] p 151 N84-33702
- Formulation of blade-flutter spectral analyses in stationary reference frame [NASA-TP-2296] p 27 N84-20562
- KURTH, W. S.**  
Interpretation of STS-3/plasma diagnostics package results in terms of large space structure plasma-interactions [NASA-CR-173266] p 189 N84-16991  
Effects of chemical releases by the STS-3 Orbiter on the ionosphere [NASA-CR-171032] p 173 N84-25204
- KWATRA, S. C.**  
NTSC composite video at 1.6 bits/pel p 95 N84-49259
- L**
- LADING, L.**  
Estimating time and time-lag in time-of-flight velocimetry p 129 N84-13192  
Optimizing and comparing laser anemometers p 130 N84-28739
- LAKSHMINARAYANA, B.**  
Three-dimensional flowfield inside a low-speed axial flow compressor rotor p 3 N84-13574  
Three-dimensional turbulent boundary-layer development on a fan rotor blade p 3 N84-17437  
Computation of three-dimensional viscous flows using a space-marching method [AIAA PAPER 84-1298] p 5 N84-36971  
Laser Doppler velocimeter measurement in the tip region of a compressor rotor [AIAA PAPER 84-1602] p 6 N84-39304  
An experimental study of the compressor rotor blade boundary layer [ASME PAPER 84-GT-193] p 7 N84-46991  
Turbulence modeling for three-dimensional shear flows over curved rotating bodies p 122 N84-48138  
Annulus wall boundary layer development in a compressor stage, including the effects of tip clearance p 26 N84-16207
- LALK, T. R.**  
Evaluation of dissociated and steam-reformed methanol as automotive engine fuels [NASA-CR-168242] p 91 N84-27909
- LAM, P.**  
Nonlinear transient finite element analysis of rotor-bearing-stator systems p 136 N84-20580
- LAM, P. T. C.**  
Secondary pattern computation of an arbitrarily shaped main reflector [NASA-TM-85527] p 100 N84-25909
- LAMBERT, R. F.**  
Studies of acoustical properties of bulk porous flexible materials [NASA-CR-173622] p 185 N84-27544
- LANES, R. F.**  
Effects of volute geometry and impeller-orbit on the hydraulic performance of a centrifugal pump p 136 N84-22316
- LAPP, M.**  
Acoustically-induced modulation spectroscopy for ultra-sensitive gas analysis [AIAA PAPER 84-1460] p 131 N84-36981
- LAPRAD, R. F.**  
HYTESS: A hypothetical turbofan engine simplified simulation [NASA-TM-83581] p 26 N84-16184
- LAU, S. K.**  
Degradation mechanisms of ceramic thermal-barrier coatings in corrosive environments p 81 N84-42668
- LAUER, J. L.**  
Topological reaction rate measurements related to scuffing [NASA-TM-83486] p 68 N84-14268  
Surface topographical changes measured by phase-locked interferometry [NASA-CR-3757] p 188 N84-16984  
Emission FTIR analyses of thin microscopic patches of jet fuel residue deposited on heated metal surface [NASA-CR-168331] p 90 N84-17410  
Optical and other property changes of M-50 bearing steel surfaces for different lubricants and additive prior to scuffing [NASA-TM-83746] p 88 N84-34620
- LAUVER, R. W.**  
Chemical approach for controlling nadimide cure temperature and rate [NASA-CASE-LEW-13770-3] p 55 N84-22698  
Chemical approach for controlling nadimide cure temperature and rate [NASA-CASE-LEW-13770-4] p 55 N84-22699  
Chemical approach for controlling nadimide cure temperature and rate [NASA-CASE-LEW-13770-5] p 55 N84-22700
- Chemical approach for controlling nadimide cure temperature and rate [NASA-CASE-LEW-13770-6] p 55 N84-22701  
Chemical approach for controlling nadimide cure temperature and rate [NASA-CASE-LEW-13770-1] p 86 N84-27885
- LAW, C. K.**  
An invariant derivation of flame stretch p 58 N84-18925  
Extinction of premixed flames by stretch and radiative loss p 58 N84-23593  
An experimental study on extinction and stability of stretched premixed flames p 59 N84-35425
- LAWRENCE, C.**  
Nonlinear displacement analysis of advanced propeller structures using NASTRAN [NASA-TM-83737] p 157 N84-31683
- LAWRENCE, M.**  
Assessment of institutional barriers to the use of natural gas fuel in automotive vehicle fleets [NASA-CR-168183] p 165 N84-14587
- LAWVER, B. R.**  
Test verification of LOX/RP-1 high-pressure fuel/oxidizer-rich preburner designs p 42 N84-22134
- LAXMANAN, V.**  
Some fundamental aspects of solidification in a supercooled melt [NASA-TM-83714] p 73 N84-26787
- LEACH, K.**  
Energy efficient engine. Turbine intermediate case and low-pressure turbine component test hardware detailed design report [NASA-CR-167973] p 33 N84-28789
- LECIEJEWSKI, D. J.**  
An experimental investigation of the effect of boundary layer refraction on the noise from a high-speed propeller [NASA-TM-83764] p 186 N84-34230
- LEE, B. S.**  
Phased-array-fed antenna configuration study. Volume 1: Technology assessment [NASA-CR-168231] p 98 N84-16423  
Phased-array-fed antenna configuration study, volume 2 [NASA-CR-168232] p 98 N84-16424
- LEE, C. S.**  
Wave attenuation and mode dispersion in a waveguide coated with lossy dielectric material [NASA-CR-173820] p 100 N84-30145
- LEE, E. A.**  
A new multiple beam satellite antenna for 30/20 GHz communications coverage of CONUS-experimental evaluation [AIAA PAPER 84-0655] p 94 N84-25256
- LEE, F. C.**  
Extensions of the discrete-average models for converter power stages p 102 N84-18411  
Stability analysis of a buck regulator employing input filter compensation p 102 N84-18412  
Input filter compensation for switching regulators [NASA-CR-173247] p 107 N84-16459  
Input filter compensation for switching regulators [NASA-CR-173557] p 110 N84-24975
- LEE, J. D.**  
Experimental and analytical investigations into airfoil icing Documentation of ice shapes on the main rotor of a UH-1H helicopter in hover [NASA-CR-168332] p 9 N84-17139
- LEE, S. S.**  
Input-output characterization of an ultrasonic testing system by digital signal analysis [NASA-CR-3756] p 149 N84-15565
- LEE, S. W.**  
Numerical methods for analyzing electromagnetic scattering [NASA-CR-175423] p 98 N84-19620  
Secondary pattern computation of an arbitrarily shaped main reflector [NASA-TM-85527] p 100 N84-25909  
Wave attenuation and mode dispersion in a waveguide coated with lossy dielectric material [NASA-CR-173820] p 100 N84-30145  
Numerical methods for analyzing electromagnetic scattering [NASA-CR-173916] p 101 N84-32645
- LEE, W. D.**  
Catalog of selected heavy duty transport energy management models [NASA-CR-168299] p 194 N84-14991
- LEE, Y. M.**  
Transient flow analysis of the AEDC/HPDE MHD generator p 189 N84-24049
- LEESE, G. E.**  
Cyclic torsion testing [NASA-TM-83756] p 157 N84-31687

- LEFEBVRE, A. H.**  
Flame propagation in heterogeneous mixtures of fuel drops and air  
[NASA-CR-174644] p 91 N84-23775
- LEHTINEN, B.**  
AESOP. An interactive computer program for the design of linear quadratic regulators and Kalman filters  
[NASA-TP-2221] p 178 N84-16843  
Application of advanced control techniques to aircraft propulsion systems p 28 N84-20590
- LEIS, B. N.**  
Creep fatigue of low-cobalt superalloys Waspalloy, PM U 700 and wrought U 700  
[NASA-CR-168260] p 67 N84-13265
- LEISSA, A. W.**  
Vibrations of twisted cantilevered plates - Experimental investigation  
[ASME PAPER 84-GT-96] p 152 A84-46937
- LEKAN, J. F.**  
A comparison of the domestic satellite communications forecast to the year 2000  
[NASA-TM-83516] p 96 N84-10405
- LEMKEY, F. D.**  
Carbides in iron-nickel Fe-Mn-Cr-Mo-Al-Si-C systems  
p 64 A84-26815
- LENAHAN, D. T.**  
Air modulation apparatus  
[NASA-CASE-LEW-13524-1] p 35 N84-33410
- LENT, L.**  
Assessment of institutional barriers to the use of natural gas fuel in automotive vehicle fleets  
[NASA-CR-168183] p 165 N84-14587
- LEONARDO, M.**  
PURDU-WINCOF A computer code for establishing the performance of a fan-compressor unit with water ingestion  
[NASA-CR-168005] p 34 N84-29875
- LESTER, H. L.**  
Mobile radio alternative systems study. Volume 2. Terrestrial  
[NASA-CR-168063] p 96 N84-10403
- LESTZ, S. A.**  
Utilization of alternative fuels in diesel engines  
[NASA-CR-174669] p 91 N84-26813
- LEVINE, S. R.**  
Ceramic-coated metals can survive contact with hot working fluid p 81 A84-44482  
Deposition stress effects on thermal barrier coating burner rig life  
[NASA-TM-83670] p 85 N84-25830  
Coating with overlay metallic-cermet alloy systems  
[NASA-CASE-LEW-13639-2] p 73 N84-27855  
Overlay metallic-cermet alloy coating systems  
[NASA-CASE-LEW-13639-1] p 77 N84-33555
- LEVIS, C. A.**  
Engineering calculations for communications satellite systems planning  
[NASA-CR-173532] p 38 N84-23662
- LEVIT, I.**  
Element-by-element solution procedures for nonlinear structural analysis p 158 N84-31694
- LEWIS, C. R.**  
Development of a 30 percent efficient 3-junction monolithic cascade solar cell p 171 N84-29328
- LI, K. C.**  
Application of an optimization method to high performance propeller designs  
[AIAA PAPER 84-1203] p 20 A84-44181  
Application of an optimization method to high performance propeller designs  
[NASA-TM-83710] p 2 N84-25607
- LILLEY, D. G.**  
Turbulence measurements in confined jets using a rotating single-wire probe technique p 113 A84-13564  
Accuracy and directional sensitivity of the single-wire technique  
[AIAA PAPER 84-0367] p 130 A84-18047  
Limitations and empirical extensions of the k-epsilon model as applied to turbulent confined swirling flows  
[AIAA PAPER 84-0441] p 114 A84-18096  
Further time-mean measurements in confined swirling flows p 116 A84-27138  
Swirl flow turbulence modeling  
[AIAA PAPER 84-1376] p 118 A84-35196  
Swirl, confinement and nozzle effects on confined turbulent flow  
[AIAA PAPER 84-1377] p 118 A84-35197  
Turbulence measurements in a complex flowfield using a crossed hot-wire  
[AIAA PAPER 84-1604] p 131 A84-37999  
Five-hole pitot probe measurements of swirl, confinement and nozzle effects on confined turbulent flow  
[AIAA PAPER 84-1605] p 120 A84-38000
- LIM, H. S.**  
Long life nickel electrodes for a nickel-hydrogen cell I Initial performance p 162 A84-30186
- LIN, S. J.**  
Further development of a method for computing three-dimensional subsonic viscous flows in turbofan lobe mixers  
[NASA-CR-168304] p 122 N84-14462
- LINDBERG, L. J.**  
High temperature ceramic interface study  
[NASA-CR-174728] p 197 N84-34331
- LINDENMEYER, P. H.**  
Characterization of PMR polyimide resin and prepreg  
[NASA-CR-168217] p 83 N84-20695
- LING, J. S.**  
Single cell performance studies on the FE/CR Redox Energy Storage System using mixed reactant solutions at elevated temperature p 163 A84-30194
- LINSCOTT, B. S.**  
Large, horizontal-axis wind turbines  
[NASA-TM-83546] p 169 N84-27327
- LIPSHITZ, A.**  
Dilution jets in accelerated cross flows  
[NASA-CR-174717] p 34 N84-28794
- LITTLE, J. K.**  
Response of a small-turboshaft-engine compression system to inlet temperature distortion  
[NASA-TM-83765] p 36 N84-33414
- LITVIN, F. L.**  
Precision of spiral-bevel gears  
[ASME PAPER 82-WA/DE-33] p 135 A84-15950  
Kinematic precision of gear trains  
[ASME PAPER 82-WA/DE-34] p 135 A84-15951  
Special cases of friction and applications  
[NASA-TM-83523] p 141 N84-11500
- LIU, D. C.**  
Microwave monolithic integrated circuit development for future spaceborne phased array antennas  
[AIAA PAPER 84-0656] p 94 A84-25257  
Microwave monolithic integrated circuit development for future spaceborne phased array antennas  
[NASA-TM-83518] p 97 N84-13399
- LIU, H. W.**  
Literature survey on oxidations and fatigue lives at elevated temperatures  
[NASA-CR-174639] p 71 N84-20674  
Crack tip field and fatigue crack growth in general yielding and low cycle fatigue  
[NASA-CR-174686] p 76 N84-32503
- LIU, N.-S.**  
Dynamic response of shock waves in transonic diffuser and supersonic inlet - An analysis with the Navier-Stokes equations and adaptive grid  
[AIAA PAPER 84-1609] p 5 A84-38004
- LO, R. Q.**  
The study of microstrip antenna arrays and related problems  
[NASA-CR-173534] p 99 N84-23807
- LO, Y. T.**  
Numerical methods for analyzing electromagnetic scattering  
[NASA-CR-175423] p 98 N84-19620  
Wave attenuation and mode dispersion in a waveguide coated with lossy dielectric material  
[NASA-CR-173820] p 100 N84-30145  
Numerical methods for analyzing electromagnetic scattering  
[NASA-CR-173916] p 101 N84-32645
- LOEWENTHAL, S. H.**  
Elastic model of the traction behavior of two traction lubricants p 136 A84-28791  
An analytical method to predict efficiency of aircraft gearboxes  
[AIAA PAPER 84-1500] p 20 A84-44180  
An advanced pitch change mechanism incorporating a hybrid traction drive  
[AIAA PAPER 84-1383] p 20 A84-44182  
An advanced pitch change mechanism incorporating a hybrid traction drive  
[NASA-TM-83709] p 2 N84-25805  
An analytical method to predict efficiency of aircraft gearboxes  
[NASA-TM-83716] p 2 N84-25606  
Factors that affect the fatigue strength of power transmission shafting  
[NASA-TM-83608] p 145 N84-26029  
Design of power-transmitting shafts  
[NASA-RP-1123] p 145 N84-27041  
Spin analysis of concentrated traction contacts  
[NASA-TM-83713] p 145 N84-27042  
An analysis of traction drive torsional stiffness  
[NASA-TM-83712] p 145 N84-27043  
Efficiency of nonstandard and high contact ratio involute spur gears  
[NASA-TM-83725] p 146 N84-29223
- LOEWY, R. G.**  
Structural dynamics of rotating bladed-disk assemblies coupled with flexible shaft motions p 21 A84-44645
- LOGAN, K. P.**  
Communications network design and costing model technical manual  
[NASA-CR-168236] p 97 N84-14376  
Communications network design and costing model programmers manual  
[NASA-CR-168237] p 97 N84-14377  
Communications network design and costing model users manual  
[NASA-CR-168238] p 97 N84-14378
- LOO, R. Y.**  
Effect of electron flux on radiation damage in GaAs solar cells p 160 A84-22998
- LOOMIS, W. R.**  
Overview of liquid lubricants for advanced aircraft  
[NASA-TM-83529] p 81 N84-11296
- LORENZO, C. F.**  
Determination of compressor in-stall characteristics from engine surge transients  
[AIAA PAPER 84-1206] p 18 A84-36959  
Determination of compressor in-stall characteristics from engine surge transients  
[NASA-TM-83639] p 29 N84-22566
- LOWELL, C. E.**  
High-temperature cyclic oxidation data, volume 1  
[NASA-TM-83665] p 75 N84-31345
- LU, C. Y.**  
Manual of phosphoric acid fuel cell power plant cost model and computer program  
[NASA-CR-174720] p 173 N84-34037
- LUCAS, J. G.**  
Low flight speed fan noise from a supersonic inlet p 182 A84-44508
- LUDOWISE, M. J.**  
Development of a 30 percent efficient 3-junction monolithic cascade solar cell p 171 N84-29328
- LUH, H. S.**  
Multibeam antenna for 30/20 GHz advanced communications satellite using offset shaped, dual reflector surfaces p 93 A84-15627
- LUIDENS, R.**  
Supersonic STOVL ejector aircraft from a propulsion point of view  
[AIAA PAPER 84-1401] p 19 A84-40246
- LUIDENS, R. W.**  
Supersonic STOVL aircraft with turbine bypass/turbo-compressor engines  
[AIAA PAPER 84-1403] p 19 A84-40247  
Supersonic STOVL ejector aircraft from a propulsion point of view  
[NASA-TM-83641] p 31 N84-24581  
Supersonic STOVL aircraft with turbine bypass/turbo-compressor engines  
[NASA-TM-83686] p 31 N84-24582
- LUNDHOLM, G.**  
Comparison of seal materials for use in Stirling engines p 64 A84-22879
- LUPTON, M. W.**  
Micronized coal burner facility  
[NASA-CASE-LEW-13426-1] p 60 N84-16276
- LUSIGNAN, B. B.**  
Interference performance analysis of M-ary CPSK and M-ary CAPK digital transmission systems and the computation of 'required isolation' for efficient utilization, of geostationary satellite orbit/spectrum p 95 A84-49303
- LYCAS, J.**  
Optical Kalman filtering for missile guidance p 178 A84-38596
- LYON, T. F.**  
Clean catalytic combustor program  
[NASA-CR-168323] p 24 N84-15151
- LYZENGA, D. R.**  
Development of Great Lakes algorithms for the Nimbus-G coastal zone color scanner  
[NASA-CR-173511] p 159 N84-27258

## M

- MACBAIN, J. C.**  
Vibrations of twisted cantilevered plates - Experimental investigation  
[ASME PAPER 84-GT-96] p 152 A84-46937
- MACBETH, J. W.**  
Progress in net shape fabrication of alpha sic turbine components  
[ASME PAPER 84-GT-273] p 140 A84-47036
- MACHLES, G. W.**  
Study of auxiliary propulsion requirements for large space systems Volume 1: Executive summary  
[NASA-CR-168193-VOL-1] p 45 N84-12226

- Study of auxiliary propulsion requirements for large space systems, volume 2  
[NASA-CR-168193-VOL-2] p 45 N84-13218
- MACK, J. C.**  
Development of large rotorcraft transmissions  
p 21 A84-46354
- MACKAY, R. A.**  
The development of directional coarsening of the gamma-prime precipitate in superalloy single crystals  
p 63 A84-10597  
Factors which influence directional coarsening of Gamma prime during creep in nickel-base superalloy single crystals  
[NASA-TM-83595] p 69 N84-17353
- MACKENZIE, J. D.**  
Ceramic-to-metal bonding for pressure transducers  
[NASA-CR-173500] p 84 N84-22753
- MACKLIN, M. J.**  
Fan noise reduction achieved by removing tip flow irregularities behind the rotor forward arc test configurations  
[NASA-TM-83616] p 184 N84-23235
- MAHAN, J. R.**  
A temperature correlation for the radiation resistance of a thick-walled circular duct exhausting a hot gas  
p 181 A84-31103  
Recovery of burner acoustic source structure from far-field sound spectra  
[AIAA PAPER 83-0763] p 181 A84-32609  
A critical review of noise production models for turbulent, gas-fueled burners  
[NASA-CR-3803] p 184 N84-26384
- MAISEL, J. E.**  
Preliminary investigation of an electrical network model for ultrasonic scattering  
[NASA-CR-3770] p 149 N84-17606
- MAJJIGI, R. K.**  
Free jet feasibility study of a thermal acoustic shield concept for AST/VCE application Single stream nozzles  
[NASA-CR-3758] p 185 N84-26661
- MAK, M.**  
Tropical response to lateral forcing with a latitudinally and zonally nonuniform basic state p 174 A84-40399
- MANDELL, M. J.**  
Plasma sheath structure surrounding a large powered spacecraft  
[AIAA PAPER 84-0329] p 40 A84-18025  
Potentials in a plasma over a biased pinhole  
p 102 A84-20711
- MANORY, R.**  
Correlations between plasma variables and the deposition process of Si films from chlorosilanes in low pressure RF plasma of argon and hydrogen  
[NASA-TM-83603] p 190 N84-21330
- MANSON, S. S.**  
Complexities of high temperature metal fatigue Some steps toward understanding  
[NASA-TM-83507] p 154 N84-14541  
Tensile and compressive constitutive response of 316 stainless steel at elevated temperatures  
[NASA-TM-83506] p 68 N84-15249
- MANTENIEKS, M.**  
Performance capabilities of the 12-centimeter Xenon ion thruster  
[NASA-TM-83674] p 48 N84-27825
- MANZO, M. A.**  
Separator development and testing of nickel-hydrogen cells  
[NASA-TM-83653] p 62 N84-22712  
A 37.5-kW point design companion of the nickel-cadmium battery, bipolar nickel-hydrogen battery, and regenerative hydrogen-oxygen fuel cell energy storage subsystems for low Earth orbit  
[NASA-TM-83651] p 167 N84-23022  
Advanced designs for IPV nickel-hydrogen cells  
[NASA-TM-83643] p 168 N84-23025  
Tear-down analysis of a ten cell bipolar nickel-hydrogen battery  
[NASA-TM-83618] p 168 N84-23026
- MARADUDIN, A. A.**  
Interference phenomena in the refraction of a surface polariton by vertical dielectric barriers  
p 179 A84-24410
- MAREK, C. J.**  
Random vortex method for combustor flows  
p 62 N84-20558
- MARINOS, C.**  
Improved heat exchanger for electrothermal devices  
[NASA-CASE-LEW-14037-1] p 49 N84-32425
- MARION, A.**  
On the design of contractions and settling chambers for optimal turbulence manipulations in wind tunnels  
[AIAA PAPER 84-0536] p 115 A84-22922
- MARSHALL, R. A.**  
Energy stores and switches for rail-launcher systems  
[NASA-CR-173249] p 107 N84-16458
- MARTIN, C. H.**  
Engineering calculations for communications satellite systems planning  
[NASA-CR-173532] p 38 N84-23662
- MARTIN, C. S.**  
Modeling of transient two-component flow using a four-point implicit method p 112 A84-13237  
Application of signal analysis to cavitation  
p 122 A84-49192
- MARTIN, E.**  
Powerplant design for one-engine-inoperative operation  
p 19 A84-40787
- MARTIN, R. E.**  
Alkaline fuel cells for the regenerative fuel cell energy storage system p 162 A84-30183
- MARTINDALE, W. R.**  
One-dimensional unsteady modeling of supersonic inlet unstart/restart  
[AIAA PAPER 84-0439] p 4 A84-18094
- MARTO, P. J.**  
Heat pipe applications in aircraft propulsion  
[AIAA PAPER 84-1269] p 18 A84-37640
- MARU, H. C.**  
Evaluation of gas cooling for pressurized phosphoric acid fuel cell stacks p 163 A84-30191
- MARXER, N.**  
Optical and other property changes of M-50 bearing steel surfaces for different lubricants and additive prior to scuffing  
[NASA-TM-83746] p 88 N84-34620
- MARZIALE, M. L.**  
Effect of an oscillating flow direction on leading edge heat transfer p 117 A84-33705  
Mass transfer from a circular cylinder Effects of flow unsteadiness and slight nonuniformities  
[NASA-CR-174759] p 129 N84-32751
- MATHUR, G.**  
Diffused junction p(+)-n solar cells in bulk GaAs I Fabrication and cell performance p 161 A84-26027
- MATTHEWS, E. W.**  
A new multiple beam satellite antenna for 30/20 GHz communications coverage of CONUS-experimental evaluation  
[AIAA PAPER 84-0655] p 94 A84-25256
- MATTICK, A. T.**  
High effectiveness liquid droplet/gas heat exchanger for space power applications  
[IAF PAPER 83-433] p 42 A84-11819
- MATWEY, M. D.**  
Inlet flow distortion in turbomachinery - Companion of theory and experiment in a transonic fan stage  
p 3 A84-13592
- MAY, C. E.**  
Kinetics of chromium ion absorption by cross-linked polyacrylate films  
[NASA-TM-83661] p 50 N84-23693  
Calculation of vaporization rates assuming various rate determining steps Application to the resistor jet  
[NASA-TM-83757] p 51 N84-31283
- MAYLE, R. E.**  
Effect of an oscillating flow direction on leading edge heat transfer p 117 A84-33705  
Mass transfer from a circular cylinder Effects of flow unsteadiness and slight nonuniformities  
[NASA-CR-174759] p 129 N84-32751
- MCCARDLE, J. G.**  
Effects of wind on turbofan engines in outdoor static test stands  
[AIAA PAPER 83-2766] p 15 A84-15204
- MCCALL, D. M.**  
Evaluation of dissociated and steam-reformed methanol as automotive engine fuels  
[NASA-CR-168242] p 91 N84-27909
- MCCALLA, T., JR.**  
How to protect a wind turbine from lightning  
[NASA-CR-168229] p 163 N84-10661
- MCCALLISTER, R.**  
Baseband processor development for the Advanced Communications Satellite Program p 93 A84-15628  
30/20 GHz communications systems baseband processor development p 95 A84-38251
- MCCANLIES, J. M.**  
Evaluation of dissociated and steam-reformed methanol as automotive engine fuels  
[NASA-CR-168242] p 91 N84-27909
- MCCORMICK, B. W.**  
The application of vortex theory to the optimum swept propeller  
[AIAA PAPER 84-0036] p 3 A84-17841
- MCDANIELS, D. L.**  
Analysis of stress-strain, fracture and ductility behavior of aluminum matrix composites containing discontinuous silicon carbide reinforcement  
[NASA-TM-33610] p 54 N84-21665  
Microstructure and orientation effects on properties of discontinuous silicon carbide/aluminum composites  
[NASA-TP-2302] p 51 N84-26749
- MCDONALD, G.**  
Residual stress in plasma-sprayed ceramic turbine tip and gas-path seal specimens p 78 A84-19783  
Correlation of compressive and shear stress with spalling of plasma-sprayed ceramic materials p 79 A84-19784  
The effect of annealing on the creep of plasma-sprayed ceramics p 79 A84-19785  
Some inelastic effects of thermal cycling on yttria-stabilized zirconia  
[NASA-TM-83488] p 123 N84-16492
- MCDONALD, H.**  
Dynamic response of shock waves in transonic diffuser and supersonic inlet - An analysis with the Navier-Stokes equations and adaptive grid  
[AIAA PAPER 84-1609] p 5 A84-38004  
Further development of a method for computing three-dimensional subsonic viscous flows in turbofan lobe mixers  
[NASA-CR-168304] p 122 N84-14462
- MCFADDEN, J. J.**  
Baseline performance and emissions data for a single-cylinder, direct-injected diesel engine  
[NASA-TM-86873] p 197 N84-34330
- MCFARLAND, E. R.**  
A rapid blade-to-blade solution for use in turbomachinery design  
[ASME PAPER 83-GT-67] p 4 A84-31289  
Design and performance of a fixed, nonaccelerating, guide vane cascade that operates over an inlet flow angle range of 60 deg  
[NASA-TM-83519] p 8 N84-14120
- MCGAW, M. A.**  
Preliminary study of thermomechanical fatigue of polycrystalline MAR-M 200  
[NASA-TP-2280] p 69 N84-17350
- MCKILLOP, B. E.**  
Turbulence measurements in a complex flowfield using a crossed hot-wire  
[AIAA PAPER 84-1604] p 131 A84-37999
- MCKINZIE, D. J., JR.**  
Acoustic excitation A promising new means of controlling shear layers  
[NASA-TM-83772] p 10 N84-31096
- MCKNIGHT, R. C.**  
Performance degradation of a typical twin engine commuter type aircraft in measured natural icing conditions  
[AIAA PAPER 84-0179] p 13 A84-21289  
Performance degradation of a typical twin engine commuter type aircraft in measured natural icing conditions  
[NASA-TM-83564] p 14 N84-13173
- MCLAUGHLIN, D. K.**  
Turbulence measurements in confined jets using a rotating single-wire probe technique p 113 A84-13564
- MCLAUGHLIN, P.**  
Parallel processor engine model program  
[NASA-CR-174641] p 27 N84-19353
- MCMANUS, K. R.**  
Calculations of turbulent mass transport in a bluff-body diffusion-flame combustor  
[AIAA PAPER 84-0372] p 114 A84-18048  
Calculation of a hollow-cone liquid spray in a uniform air stream  
[AIAA PAPER 84-1322] p 118 A84-35171
- MEHALIC, C. M.**  
Determination of compressor in-stall characteristics from engine surge transients  
[AIAA PAPER 84-1206] p 18 A84-36959  
Determination of compressor in-stall characteristics from engine surge transients  
[NASA-TM-83639] p 29 N84-22566
- MEHAN, R. L.**  
Mechanical and physical properties of plasma-sprayed stabilized zirconia p 79 A84-19786
- MEHTA, S.**  
Increased radiation resistance in lithium-counterdoped silicon solar cells p 163 A84-34846  
Radiation damage and defect behavior in ion-implanted, lithium counterdoped silicon solar cells  
[NASA-TM-83646] p 109 N84-22890  
Cell and defect behavior in lithium-counterdoped solar cells p 170 N84-29322  
The effects of lithium counterdoping on radiation damage and annealing in n(+)-p silicon solar cells  
[NASA-TM-83755] p 110 N84-31513

- MEIER, J. G.**  
Experimental study of the operating characteristics of premixing-prevaporizing fuel/air mixing passages [NASA-CR-168279] p 23 N84-14143
- MENDELSON, A.**  
Effect of crack curvature on stress intensity factors for ASTM standard compact tension specimens [NASA-CR-168280] p 153 N84-11513
- MENG, P. R.**  
An overview of the NASA rotary engine research program [NASA-TM-83699] p 34 N84-28791
- MERRILL, W.**  
Identification of multivariable high performance turbofan engine dynamics from closed loop data p 16 A84-18582
- MERRILL, W. C.**  
A real-time implementation of an advanced sensor failure detection, isolation, and accommodation algorithm [AIAA PAPER 84-0569] p 176 A84-21305  
A real-time implementation of an advanced sensor failure detection, isolation, and accommodation algorithm [NASA-TM-83553] p 1 N84-13140  
HYTES: A hypothetical turbofan engine simplified simulation [NASA-TM-83561] p 26 N84-16184  
Identification of multivariable high-performance turbofan engine dynamics from closed loop data p 28 N84-20580  
Sensor failure detection for jet engines using analytical redundancy [NASA-TM-83695] p 31 N84-24585  
Real-time simulation of an automotive gas turbine using the hybrid computer [NASA-TM-83593] p 195 N84-26484
- MERTE, H. JR.**  
Modeling of zero gravity venting [NASA-CR-173503] p 127 N84-23854
- METCALFE, R. W.**  
Direct simulations of chemically reacting turbulent mixing layers [NASA-CR-174640] p 32 N84-25710
- METZ, R. N.**  
Radiating dipole model of interference induced in spacecraft circuitry by surface discharges [NASA-TP-2240] p 40 N84-16247
- MEULENBERG, A.**  
Surface effects in high voltage silicon solar cells p 160 A84-23002  
Thin N-IP radiation resistant solar cells [NASA-CR-168284] p 166 N84-15682
- MEYER, W. L.**  
A parametric study of the effect of inlet lip shape upon the radiated sound field [AIAA PAPER 84-0498] p 180 A84-18131
- MEYN, E. H.**  
Lewis Research Center spin ng and its use in vibration analysis of rotating systems [NASA-TP-2304] p 30 N84-24578
- MICHAEL, C. J.**  
Energy efficient engine fan component detailed design report [NASA-CR-165466] p 33 N84-27737
- MIESKOWSKI, D. M.**  
Bubble formation in oxide scales on SiC p 79 A84-23689
- MIHALOE, J. R.**  
Real-time Pegasus propulsion system model V/STOL-piloted simulation evaluation p 15 A84-17362  
A piecewise linear state variable technique for real time propulsion system simulation p 20 A84-42378  
Rotorcraft flight-propulsion control integration p 36 A84-46524  
A real-time, portable, microcomputer-based jet engine simulator [NASA-TM-83550] p 176 N84-16812
- MIKKELSEN, K. L.**  
Performance degradation of a typical twin engine commuter type aircraft in measured natural icing conditions [AIAA PAPER 84-0179] p 13 A84-21289  
Performance degradation of a typical twin engine commuter type aircraft in measured natural icing conditions [NASA-TM-83564] p 14 N84-13173
- MIKKELSON, D. C.**  
Summary of recent NASA propeller research [NASA-TM-83733] p 2 N84-32344
- MILANO, R.**  
Energy efficient engine high-pressure turbine supersonic cascade technology report [NASA-CR-165567] p 33 N84-27739
- MILES, J. H.**  
Cross spectra between pressure and temperature in a constant-area duct downstream of a hydrogen-fueled combustor [NASA-TM-83463] p 182 N84-11885  
A theoretical model for the cross spectra between pressure and temperature downstream of a combustor [NASA-TM-83671] p 186 N84-34231
- MILLER, E. F.**  
Geometric models, antenna gains, and protection ratios as developed for BC SAT-R2 conference software [NASA-TM-83381] p 96 N84-11358  
Broadcasting satellites at 12 GHz for Region 2. Technical characteristics [NASA-TM-83522] p 98 N84-19640  
Spectrum/orbit utilization program for geostationary satellites [NASA-TM-83759] p 100 N84-30146
- MILLER, R. A.**  
Phase distributions in plasma-sprayed zirconia-yttria p 78 A84-18948  
Oxidation behavior of a thermal barrier coating p 65 A84-42667  
Ceramic-coated metals can survive contact with hot working fluid p 81 A84-44482  
Performance of thermal barrier coatings in high heat flux environments [NASA-TM-83663] p 72 N84-24772  
Failure analysis of plasma-sprayed thermal barrier coatings [NASA-TM-83777] p 75 N84-31347
- MILLER, R. H.**  
Improved transistor-controlled and commutated brushless DC motors for electric vehicle propulsion [NASA-CR-168053] p 105 N84-10450
- MILLER, T.**  
A numerical analysis of contact and limit-point behavior in a class of problems of finite elastic deformation p 150 A84-27370
- MILLER, T. B.**  
Design considerations for a 10-kW integrated hydrogen-oxygen regenerative fuel cell system [NASA-TM-83664] p 167 N84-23023
- MILLER, T. L.**  
Performance degradation of a model helicopter main rotor in hover and forward flight with a generic ice shape [AIAA PAPER 84-0609] p 13 A84-24195  
Performance degradation of a model helicopter rotor with a generic ice shape p 14 A84-49096
- MILLIGAN, W. W.**  
Low cycle fatigue behavior of conventionally cast MAR-M 200 AT 1000 deg C [NASA-TM-83769] p 77 N84-33564
- MINER, R. V.**  
The effect of microstructure on 650 C fatigue crack growth in P/M Astroloy p 63 A84-12395  
The effects of Cr, Al, Ti, Mo, W, Ta, and Nb on the cyclic oxidation behavior of cast Ni-base superalloys at 1100 and 1150 C p 65 A84-27485  
Effects of processing and microstructure on the fatigue behaviour of the nickel-base superalloy Rene95 p 66 A84-48715
- MINZHONG, Z.**  
Crack tip field and fatigue crack growth in general yielding and low cycle fatigue [NASA-CR-174686] p 76 N84-32503
- MIRTICH, M. J.**  
Resistojet propulsion for large spacecraft systems [NASA-TM-83489] p 45 N84-11206  
Sputtered coatings for protection of spacecraft polymers [NASA-TM-83706] p 65 N84-26803  
Deposition of diamondlike carbon films [NASA-CASE-LEW-14080-1] p 66 N84-28986  
Dual ion beam deposition of carbon films with diamondlike properties [NASA-TM-83743] p 110 N84-31512  
Improved heat exchanger for electrothermal devices [NASA-CASE-LEW-14037-1] p 49 N84-32425
- MIRTICH, M. J., JR.**  
Ion-beam-textured and coated surfaces experiment (S1003) p 84 N84-24650
- MISENICK, J. A.**  
Evaluation of CO<sub>2</sub> and CO dopants in hydrogen to reduce hydrogen permeation in the Stirling engine heater head tube alloy CG-27 [NASA-TM-83535] p 68 N84-15246  
Evaluation of candidate Stirling engine heater tube alloys after 3500 hours exposure to high pressure doped hydrogen or helium [NASA-TM-83782] p 77 N84-34603
- MISHINA, H.**  
The friction behavior of semiconductor's Si and GaAs in contact with pure metals [NASA-TM-83779] p 87 N84-32531
- Friction behavior of silicon in contact with titanium, nickel, silver and copper [NASA-TP-2362] p 88 N84-33590
- MISRA, A. K.**  
Mechanism of corrosion of Ni-base superalloys by molten Na<sub>2</sub>MoO<sub>4</sub> at elevated temperatures [NASA-TM-83580] p 70 N84-20672
- MITCHELL, A. M.**  
Transmission efficiency measurements and correlations with physical characteristics of the lubricant [NASA-TM-83740] p 147 N84-30293
- MITCHELL, G. A.**  
Summary of recent NASA propeller research [NASA-TM-83733] p 2 N84-32344
- MITCHELL, T. E.**  
Bubble formation in oxide scales on SiC p 79 A84-23689
- MITTRA, R.**  
Monolithic microwave integrated circuit devices for active array antennas [NASA-CR-173981] p 112 N84-34675
- MIYAKE, C. I.**  
Radiative resistojet performance characterization tests [NASA-CR-174763] p 50 N84-33462
- MIYOSHI, K.**  
Surface chemistry, friction, and wear of Ni-Zn and Mn-Zn ferrites in contact with metals p 78 A84-13516  
The X-ray photoelectron spectroscopy depth profiling and tribological characterization of ion-plated gold on various metals p 50 A84-20465  
Friction and morphology of magnetic tapes in sliding contact with nickel-zinc ferrite [NASA-TP-2267] p 82 N84-16334  
Metallic glass as a temperature sensor during ion plating [NASA-TM-83566] p 69 N84-17351  
Tribological characteristics of gold films deposited on metals by ion plating and vapor deposition [NASA-TM-83572] p 69 N84-17352  
Water-vapor effects on friction of magnetic tape in contact with nickel-zinc ferrite [NASA-TP-2279] p 82 N84-18399  
Ceramic wear in indentation and sliding [NASA-TM-83585] p 82 N84-19566  
Mechanical contact induced transformation from the amorphous to the crystalline state in metallic glass [NASA-TM-83583] p 71 N84-20673  
Friction and wear of iron in sulfuric acid [NASA-TP-2289] p 71 N84-21716  
Friction and wear of nickel in sulfuric acid [NASA-TP-2290] p 72 N84-21721  
Considerations in friction and wear p 144 N84-23903  
Interaction of sulfuric acid corrosion and mechanical wear of iron [NASA-TM-83717] p 73 N84-27857  
Properties of ferrites important to their friction and wear behavior [NASA-TM-83718] p 87 N84-28994  
Effects of water-vapor on friction and deformation of polymeric magnetic media in contact with a ceramic oxide [NASA-TM-83727] p 87 N84-30072  
Microstructure and surface chemistry of amorphous alloys important to their friction and wear behavior [NASA-TM-83762] p 76 N84-32508
- MOAT, D.**  
Baseband processor development for the Advanced Communications Satellite Program p 93 A84-15628
- MOFFITT, T. P.**  
Performance of a high-work low aspect ratio turbine tested with a realistic inlet radial temperature profile [AIAA PAPER 84-1161] p 19 A84-40239  
Performance of a high-work low aspect ratio turbine tested with a realistic inlet radial temperature profile [NASA-TM-83655] p 32 N84-24589
- MOKADAM, D. R.**  
Stagger angle dependence of inertial and elastic coupling in bladed disks p 151 A84-31903
- MOLDOVER, M. R.**  
Capillary rise, wetting layers, and critical phenomena in confined geometry p 192 A84-20315  
Turbidity very near the critical point of methanol-cyclohexane mixtures p 192 A84-30391
- MONGEAU, P.**  
Metal vapor vacuum arc switching - Applications and results p 103 A84-32029
- MONGIA, H.**  
Executive summary, aerothermal modeling program, phase 1 [NASA-CR-174602] p 60 N84-12263  
Aerothermal modeling program, phase 1 [NASA-CR-168243-VOL-2] p 60 N84-12265  
An experimental investigation of gas jets in confined swirling air flow [NASA-CR-3832] p 36 N84-33412

- MONGIA, H. C.**  
An experimental investigation of gas jets in confined swirling air flow  
[NASA-CR-3832] p 36 N84-33412
- MOORE, A. S.**  
Effects of wind on turbofan engines in outdoor static test stands  
[AIAA PAPER 83-2766] p 15 A84-15204
- MOORE, N.**  
An assessment of advanced technology for industrial cogeneration  
[NASA-CR-173456] p 167 N84-22001
- MOORE, T. J.**  
Rapid solidification via melt spinning - Equipment and techniques  
p 65 A84-31915
- MORACZ, D. J.**  
Fabrication development for ODS-superalloy, air-cooled turbine blades  
[NASA-CR-174650] p 32 N84-25711
- MORALES, W.**  
Liquid chromatographic analysis of a formulated ester from a gas-turbine engine test  
[ASLE PREPRINT 83-LC-1A-1] p 80 A84-28995
- Simulation of lubricating behavior of a thioether liquid lubricant by an electrochemical method  
[NASA-TP-2316] p 84 N84-23764
- MOREHOUSE, K. A.**  
Effect of a rotor wake on heat transfer from a circular cylinder  
[NASA-TM-83613] p 126 N84-21832
- MORENO, V.**  
Simplified analytical procedures for representing material cyclic response  
p 16 A84-22877
- MORRIS, R. E.**  
Lewis Research Center spin ring and its use in vibration analysis of rotating systems  
[NASA-TP-2304] p 30 N84-24578
- MOSULA, R. J.**  
Turbulent swirling combustion  
p 61 N84-20535
- MOUGIN, L. J.**  
Heat recovery subsystem and overall system integration of fuel cell on-site integrated energy systems  
[NASA-CR-168309] p 166 N84-20915
- MOUNT, R. E.**  
Design of a high-performance rotary stratified-charge research aircraft engine  
[AIAA PAPER 84-1395] p 17 A84-35204
- MUELLER, A. A.**  
Flight and wind tunnel tests of an electro-impulse de-icing system  
[AIAA PAPER 84-2234] p 12 A84-39280
- MULARZ, E. J.**  
Detailed fuel spray analysis techniques  
p 127 N84-24747
- MULLEN, R. L.**  
Residual stress in plasma-sprayed ceramic turbine tip and gas-path seal specimens  
p 78 A84-19783
- Correlation of compressive and shear stress with spalling of plasma-sprayed ceramic materials  
p 79 A84-19784
- The effect of annealing on the creep of plasma-sprayed ceramics  
p 79 A84-19785
- A thermomechanical model for energy propagation in a solid-fluid-solid system with one boundary in relative motion  
[ASME PAPER 83-HT-97] p 137 A84-29092
- Experimental study of bubble cavities attached to a rotating shaft in a reservoir  
[NASA-TM-83586] p 124 N84-17533
- MUNZ, D.**  
Development of plane strain fracture toughness test for ceramics using Chevron notched specimens  
p 77 A84-11676
- MURA, T.**  
Volume integrals associated with the inhomogeneous Helmholtz equation Part 1: Ellipsoidal region  
[NASA-CR-3749] p 148 N84-14525
- MURALIDHARAN, U.**  
Tensile and compressive constitutive response of 316 stainless steel at elevated temperatures  
[NASA-TM-83506] p 68 N84-15249
- MURAMOTO, K. K.**  
Steady state stresses in ribbon parachute canopies  
[AIAA PAPER 84-0816] p 11 A84-26580
- MURPHY, G. B.**  
Effects of chemical releases by the STS-3 Orbiter on the ionosphere  
[NASA-CR-171032] p 173 N84-25204
- MURTHY, K. N. S.**  
Three-dimensional flowfield inside a low-speed axial flow compressor rotor  
p 3 A84-13574
- Computation of three-dimensional viscous flows using a space-marching method  
[AIAA PAPER 84-1298] p 5 A84-36971
- Laser Doppler velocimeter measurement in the tip region of a compressor rotor  
[AIAA PAPER 84-1602] p 6 A84-39304
- Annulus wall boundary layer development in a compressor stage, including the effects of tip clearance  
p 26 N84-16207
- MURTHY, P. L. N.**  
Dynamic stress analysis of smooth and notched fiber composite flexural specimens  
[NASA-TM-83694] p 56 N84-25770
- ICAN: Integrated composites analyzer  
[NASA-TM-83700] p 56 N84-26755
- MURTHY, S. N. B.**  
PURDU-WINCOF: A computer code for establishing the performance of a fan-compressor unit with water ingestion  
[NASA-CR-168005] p 34 N84-29875
- MYERS, G. D.**  
Flame propagation in heterogeneous mixtures of fuel drops and air  
[NASA-CR-174644] p 91 N84-23775
- MYHRE, R. W.**  
Advanced 30/20 GHz multiple-beam antennas for communications satellites  
p 40 A84-49250
- ## N
- NACHMAN, A.**  
Gas flow across a wet screen - Analogy to a relief valve with hysteresis  
p 121 A84-43546
- NAGAMATSU, H. T.**  
Convective heat transfer studies at high temperatures with pressure gradient for inlet flow Mach number of 0.45  
[AIAA PAPER 84-1487] p 119 A84-35233
- Flat plate heat transfer for laminar transition and turbulent boundary layers using a shock tube  
[AIAA PAPER 84-1726] p 120 A84-37467
- Investigation of the effects of pressure gradient, temperature and wall temperature ratio on the stagnation point heat transfer for circular cylinders and gas turbine vanes  
[NASA-CR-174667] p 30 N84-23649
- NAGEL, R. T.**  
Supersonic jet screech tone cancellation  
p 179 A84-10136
- NAGHASH, M.**  
Modeling of transient two-component flow using a four-point implicit method  
p 112 A84-13237
- NAGIB, H. M.**  
On the design of contractions and settling chambers for optimal turbulence manipulations in wind tunnels  
[AIAA PAPER 84-0536] p 115 A84-22922
- NAGLE, W. J.**  
Additive for zinc electrodes  
[NASA-CASE-LEW-13286-1] p 106 N84-14422
- NAKAHAM, J. H.**  
Synthesis of perfluoroalkylene dianilines  
[NASA-CR-168004] p 60 N84-11228
- NAKANISHI, S.**  
Demonstration of a new electrothermal thruster concept  
p 43 A84-34037
- Cathode degradation and erosion in high pressure arc discharges  
[NASA-TM-83638] p 47 N84-22631
- NAMER, I.**  
Combustion characteristics in the transition region of liquid fuel sprays  
[NASA-CR-175396] p 61 N84-19495
- NAMKOONG, D.**  
Determination of the key parameters affecting historic communications satellite trends  
[NASA-TM-83633] p 99 N84-25908
- NASTROM, G. D.**  
Temperature histories of commercial flights at severe conditions from GASP data  
[NASA-CR-168247] p 12 N84-11152
- Simultaneous cabin and ambient ozone measurements on two Boeing 747 airplanes Volume 2. January to October 1978  
[NASA-TM-81733] p 193 N84-22488
- Climatology of ozone at altitudes from 19,000 to 59,000 feet based on combined GASP and ozonesonde data  
[NASA-TP-2303] p 174 N84-31865
- NATARAJAN, V.**  
Electronic properties of carbon fibers intercalated with copper chloride  
p 104 A84-34521
- NATHAL, M. V.**  
Replacing critical and strategic refractory metal elements in nickel-base superalloys  
[NASA-TM-83528] p 67 N84-13264
- Influence of composition on the microstructure and mechanical properties of a nickel-base superalloy single crystal  
[NASA-TM-83563] p 70 N84-17354
- Influence of cobalt, tantalum and tungsten on the high temperature mechanical properties of single crystal nickel-base superalloys  
[NASA-TM-83479] p 70 N84-17355
- NEELY, G. H.**  
Application of improved numerical schemes  
p 178 N84-20537
- NEELY, G. M.**  
Flame radiation and linear heat transfer in a tubular can combustor  
[AIAA PAPER 84-0443] p 16 A84-21300
- Flame radiation and linear heat transfer in a tubular-can combustor  
[NASA-TM-83538] p 23 N84-13188
- NEHL, T. W.**  
Improved transistor-controlled and commutated brushless DC motors for electric vehicle propulsion  
[NASA-CR-168053] p 105 N84-10450
- NELSON, C. C.**  
Analysis for leakage and rotordynamic coefficients of surface-roughened tapered annular gas seals  
[ASME PAPER 84-GT-32] p 140 A84-46896
- NELSON, H. D.**  
A blade loss response spectrum for flexible rotor systems  
[ASME PAPER 84-GT-29] p 139 A84-46893
- NELSON, S.**  
30/20 GHz spacecraft GaAs FET solid state transmitter for trunking and customer-premise-service application  
[NASA-CR-168276] p 107 N84-16463
- NEMAT-NASSER, S.**  
Finite elastic-plastic deformation of polycrystalline metals  
p 66 A84-43872
- NESBITT, J. A.**  
Solute transport and the prediction of breakaway oxidation in gamma + beta Ni-Cr-Al alloys  
p 65 A84-42658
- Modeling degradation and failure of Ni-Cr-Al overlay coatings  
[NASA-TM-83672] p 74 N84-27858
- Overlay coating degradation by simultaneous oxidation and coating/substrate interdiffusion  
[NASA-TM-83738] p 75 N84-31344
- NEUMAN, C. P.**  
Optical Kalman filtering for missile guidance  
p 178 A84-38596
- Optical systolic solutions of linear algebraic equations  
p 188 N84-22405
- NEUSTADTER, H. E.**  
Review of the DOE/NASA wind turbine engineering information system  
p 163 A84-33766
- NIGHTINGALE, N.**  
Automotive Stirling engine development program  
[NASA-CR-168205] p 194 N84-18117
- Automotive Stirling engine development program  
[NASA-CR-174622] p 195 N84-32305
- NIGHTINGALE, N. P.**  
Automotive Stirling engine development program - Overview and status report  
p 138 A84-30092
- NORGREN, C. T.**  
Ceramic composite liner material for gas turbine combustors  
[AIAA PAPER 84-0363] p 78 A84-18044
- Ceramic composite liner material for gas turbine combustors  
[NASA-TM-83490] p 24 N84-14145
- NOVICK, A. S.**  
Advanced propfan drive system characteristics and technology needs  
[AIAA PAPER 84-1194] p 18 A84-36957
- NOWLAN, M. J.**  
Large area space solar cell assemblies  
p 42 A84-22980
- NOWOTNY, H.**  
Carbides in iron-rich Fe-Mn-Cr-Mo-Al-Si-C systems  
p 64 A84-26815
- NUNES, K. B.**  
Identification of quasi-steady compressor characteristics from transient data  
[NASA-CR-174685] p 36 N84-34444
- NYAMUSA, T. A.**  
Improved transistor-controlled and commutated brushless DC motors for electric vehicle propulsion  
[NASA-CR-168053] p 105 N84-10450
- ## O
- OBERLE, L. G.**  
Optimization of fringe-type laser anemometers for turbine engine component testing  
[AIAA PAPER 84-1459] p 131 A84-40248
- Optimization of fringe-type laser anemometers for turbine engine component testing  
[NASA-TM-83658] p 133 N84-25019



- ODEN, J. T.**  
Comments on some problems in computational penetration mechanics p 150 A84-13545  
A numerical analysis of contact and limit-point behavior in a class of problems of finite elastic deformation p 150 A84-27370  
Stability and convergence of underintegrated finite element approximations p 158 A84-31696
- ODONNELL, W. J.**  
Development of a simplified procedure for rocket engine thrust chamber life prediction with creep [NASA-CR-168261] p 46 A84-19472
- OGRADY, E. P.**  
Software simulator for multiple computer simulation system p 176 A84-11892
- OHUCHI, F.**  
Compositional effects on Si<sub>3</sub>N<sub>4</sub> fracture surfaces p 79 A84-19794
- OKEAN, H. C.**  
Recent developments in EHF Satcom technology p 39 A84-46620
- OLIVER, J. D.**  
LEC GaAs for integrated circuit applications [NASA-CR-173267] p 191 A84-17014  
Design considerations for a monolithic, GaAs, dual-mode, QPSK/QASK, high-throughput rate transceiver [NASA-CR-173560] p 110 A84-24974
- OLLING, C. R.**  
Transonic cascade flow analysis using viscous/inviscid coupling concepts [AIAA PAPER 84-2159] p 6 A84-46103
- OLSEN, R. B.**  
Pyroelectric conversion in space. A conceptual design study [NASA-CR-168272] p 165 A84-14585
- OLSEN, R. C.**  
Anomalously high potentials observed on ISEE [NASA-CR-172791] p 41 A84-17252  
Anomalously high potentials observed on ISEE p 41 A84-17258  
Comparison of thermal plasma observations on SCATHA and GEOS p 41 A84-17262
- OLSEN, W. A.**  
Heat transfer distributions around nominal ice accretion shapes formed on a cylinder in the NASA Lewis icing Research Tunnel [AIAA PAPER 84-0017] p 113 A84-17834  
Heat transfer distributions around nominal ice accretion shapes formed on a cylinder in the NASA Lewis icing research tunnel [NASA-TM-83557] p 123 A84-14463
- OMALLEY, T. A.**  
Users' manual for computer program for three-dimensional analysis of coupler-cavity traveling wave tubes [NASA-CR-168269] p 109 A84-23841
- ONG, E.**  
High-temperature molten salt thermal energy storage systems for solar applications [NASA-CR-167916] p 165 A84-15679
- OPPENHEIM, A. K.**  
Secondary effects in combustion instabilities leading to flashback p 58 A84-17436  
Formation and inflammation of a turbulent jet [AIAA PAPER 84-0572] p 114 A84-18171  
Self-similar blast waves incorporating deflagrations of variable speed p 116 A84-28379  
Dynamic effects of combustion p 59 A84-29123  
Random element method for numerical modeling of diffusional processes p 119 A84-35313  
Numerical solution for the problem of flame propagation by the random element method p 60 A84-48139  
Experimental and theoretical study of combustion jet ignition [NASA-CR-168139] p 21 A84-10054  
Numerical modeling of turbulent flow in a channel [NASA-CR-168278] p 23 A84-13189
- ORANGE, T. W.**  
Wide range weight functions for the strip with a single edge crack [NASA-TM-83478] p 153 A84-11512
- ORTH, N. W.**  
Rapid solidification via melt spinning - Equipment and techniques p 65 A84-31915
- OSHIDA, Y.**  
Literature survey on oxidations and fatigue lives at elevated temperatures [NASA-CR-174639] p 71 A84-20674
- OSHIMA, H.**  
Electronic properties of carbon fibers intercalated with copper chloride p 104 A84-34521
- OSSWALD, G. A.**  
A direct method for the solution of unsteady two-dimensional incompressible Navier-Stokes equations p 2 A84-10078
- OSTOP, J. A.**  
Development and fabrication of an augmented power transistor [NASA-CR-168262] p 106 A84-11388
- OTTERSON, D. A.**  
Group-type hydrocarbon standards for high-performance liquid chromatographic analysis of middle distillate fuels [NASA-TP-2317] p 90 A84-23774
- OWEN, H. A., JR.**  
Parametric study of minimum converter loss in an energy-storage dc-to-dc converter p 101 A84-18403
- ## P
- PACIOREK, K. L.**  
Synthesis of perfluoroalkylene dianilines [NASA-CR-168004] p 60 A84-11228  
Thermal oxidative degradation reactions of perfluoroalkylethers [NASA-CR-168224] p 60 A84-11229
- PACLOREK, K. J. L.**  
Thermal oxidative degradation reactions of linear perfluoroalkyl ethers p 80 A84-30000
- PADOVAN, J.**  
Nonlinear transient finite element analysis of rotor-bearing-stator systems p 136 A84-20580  
Algorithms for elasto-plastic-creep postbuckling p 152 A84-38480  
Heat transfer in thermal barrier coated rods with circumferential and radial temperature gradients [ASME PAPER 84-GT-181] p 121 A84-46982  
High temperature thermomechanical analysis of ceramic coatings p 152 A84-48565  
Self-adaptive solution strategies p 158 A84-31693
- PALCO, R. L.**  
Documentation of ice shapes on the main rotor of a UH-1H helicopter in hover [NASA-CR-168332] p 9 A84-17139
- PAPATHAKOS, L. C.**  
Simultaneous cabin and ambient ozone measurements on two Boeing 747 airplanes Volume 2: January to October 1978 [NASA-TM-81733] p 193 A84-22488
- PAPATHANASIOU, A. G.**  
Supersonic jet screech tone cancellation p 179 A84-10136
- PAPELL, S. S.**  
Vortex generating flow passage design for increased film cooling effectiveness [NASA-CASE-LEW-14039-1] p 126 A84-20782  
Vortex generating flow passage design for increased film-cooling effectiveness and surface coverage [NASA-TM-83517] p 126 A84-22909
- PARANG, M.**  
Thermoacoustic convection heat-transfer phenomenon p 120 A84-38857
- PARKER, R. J.**  
Comparison of predicted and experimental thermal performance of angular-contact ball bearings [NASA-TP-2275] p 142 A84-18654
- PEDERSEN, A.**  
Comparison of thermal plasma observations on SCATHA and GEOS p 41 A84-17262
- PEDERSEN, H. C.**  
Abrasive tip treatment for use on compressor blades [NASA-CR-174666] p 145 A84-25065
- PEDROSA, A. C. F.**  
Convective heat transfer studies at high temperatures with pressure gradient for inlet flow Mach number of 0.45 [AIAA PAPER 84-1487] p 119 A84-35233
- PELOSE, J.**  
High-speed wide band 20 x 20 microwave switch matrix p 105 A84-49253
- PENKO, P. F.**  
Improved heat exchanger for electrothermal devices [NASA-CASE-LEW-14037-1] p 49 A84-32425
- PENNEY, C. M.**  
Acoustically-induced modulation spectroscopy for ultra-sensitive gas analysis [AIAA PAPER 84-1460] p 131 A84-36981
- PEPPER, S. V.**  
Study of the Auger line shape of polyethylene and diamond p 190 A84-40600  
Matrix effects in ion-induced emission as observed in Ne collisions with Cu-Mg and Cu-Al alloys [NASA-TM-83061] p 187 A84-10923  
The strength of the metal. Aluminum oxide interface p 72 A84-23898
- PERALTA-DURAN, A.**  
Creep-rupture reliability analysis [NASA-CR-3790] p 155 A84-19925
- PEREZ, F.**  
Development of a large scale bipolar NiH<sub>2</sub> battery p 162 A84-30189
- PERKINS, P.**  
Large, horizontal-axis wind turbines [NASA-TM-83546] p 169 A84-27327
- PERKINS, P. J., JR.**  
Performance degradation of a typical twin engine commuter type aircraft in measured natural icing conditions [AIAA PAPER 84-0179] p 13 A84-21289  
Performance degradation of a typical twin engine commuter type aircraft in measured natural icing conditions [NASA-TM-83564] p 14 A84-13173
- PETERMAN, W.**  
Creep-rupture behavior of candidate Stirling engine iron superalloys in high-pressure hydrogen. Volume 2. Hydrogen creep-rupture behavior [NASA-CR-174705] p 74 A84-28961
- PETERS, C. E.**  
Measurement of spray combustion processes p 61 A84-20530
- PETERS, M.**  
Spatial electron density and electric field strength measurements in microwave cavity experiments [AIAA PAPER 84-1522] p 189 A84-46109  
Spatial electron density and electric field strength measurements in microwave cavity experiments [NASA-CR-173907] p 111 A84-32582
- PETERSEN, W. C.**  
A three-stage power amplifier for a 20 GHz monolithic transmit module p 102 A84-22873
- PETERSON, D. B.**  
Development of a simplified procedure for rocket engine thrust chamber life prediction with creep [NASA-CR-168261] p 46 A84-19472
- PETERSON, J. C.**  
A TWT amplifier with a linear power transfer characteristic and improved efficiency [AIAA PAPER 84-0762] p 104 A84-41035  
A TWT amplifier with a linear power transfer characteristic and improved efficiency [NASA-TM-83590] p 108 A84-21803
- PETRI, R. J.**  
High-temperature molten salt thermal energy storage systems for solar applications [NASA-CR-167916] p 165 A84-15679
- PFEIL, W. H.**  
The application of LQR synthesis techniques to the turboshaft engine control problem [AIAA PAPER 84-1455] p 21 A84-44185
- PHILLIPS, B. R.**  
Fuel system research and technology: An overview of the NASA program p 14 A84-23641
- PIAN, T. H. H.**  
On the suppression of zero energy deformation modes p 150 A84-21541  
New variational formulations of hybrid stress elements p 158 A84-31690
- PICKETT, J. S.**  
Effects of chemical releases by the STS-3 Orbiter on the ionosphere [NASA-CR-171032] p 173 A84-25204
- PICKUP, N.**  
Free jet feasibility study of a thermal acoustic shield concept for AST/VCE application. Single stream nozzles [NASA-CR-3758] p 185 A84-29661
- PICONE, S.**  
The 20 GHz solid state transmitter design, impatt diode development and reliability assessment [NASA-CR-174716] p 112 A84-33715
- PIERZGA, M. J.**  
Investigation of the three-dimensional flow field within a transonic fan rotor - Experiment and analysis [ASME PAPER 84-GT-200] p 7 A84-46995  
Investigation of the three-dimensional flow field within a transonic fan rotor: Experiment and analysis [NASA-TM-83739] p 11 A84-32357
- PINTZ, A.**  
Dynamics of early planetary gear trains [NASA-CR-3793] p 145 A84-26027
- PIOTROWSKI, W. S.**  
K-band latching switches [NASA-CR-168253] p 109 A84-24973
- PISZCZOR, M. F., JR.**  
Preliminary design of a 10-kW thermophotovoltaic system for space applications [NASA-TM-83768] p 49 A84-32427
- PITZ, R. W.**  
Combustion in a turbulent mixing layer formed at a rearward-facing step p 58 A84-10140  
Acoustically-induced modulation spectroscopy for ultra-sensitive gas analysis [AIAA PAPER 84-1460] p 131 A84-36981

- PLANELL, J. R.**  
An assessment of the use of antimisting fuel in turbofan engines  
[NASA-CR-168081] p 89 N84-10332
- PLANK, G. M.**  
Experimental investigation of a half-current thruster  
[NASA-CR-168133] p 46 N84-18321
- PLENCNER, R.**  
Supersonic STOVL ejector aircraft from a propulsion point of view  
[AIAA PAPER 84-1401] p 19 A84-40246  
Supersonic STOVL ejector aircraft from a propulsion point of view  
[NASA-TM-83641] p 31 N84-24581
- POESCHEL, R. L.**  
Development of advanced inert-gas ion thrusters  
[NASA-CR-168206] p 44 N84-10180
- POLEY, W. A.**  
A companion of the domestic satellite communications forecast to the year 2000  
[NASA-TM-83516] p 96 N84-10405
- POLLAK, E. C.**  
Catalog of selected heavy duty transport energy management models  
[NASA-CR-168299] p 194 N84-14991
- PONCHAK, G. E.**  
Monolithic microwave integrated circuits interconnections and packaging considerations  
[NASA-TM-83774] p 100 N84-31461
- POROWSKI, J. S.**  
Development of a simplified procedure for rocket engine thrust chamber life prediction with creep  
[NASA-CR-168261] p 46 N84-19472
- POST, R. E.**  
Method of making a light weight battery plaque  
[NASA-CASE-LEW-13349-1] p 72 N84-22734
- POSTA, S. J.**  
Lewis Research Center spin ng and its use in vibration analysis of rotating systems  
[NASA-TP-2304] p 30 N84-24578
- POUGARE, M.**  
Three-dimensional flowfield inside a low-speed axial flow compressor rotor p 3 A84-13574  
An experimental study of the compressor rotor blade boundary layer  
[ASME PAPER 84-GT-193] p 7 A84-46991  
Annulus wall boundary layer development in a compressor stage, including the effects of tip clearance p 26 N84-16207
- POULIN, E.**  
Steam bottoming cycle for an adiabatic diesel engine  
[NASA-CR-168255] p 196 N84-33304
- POVINELLI, L. A.**  
Investigation of mixing in a turbofan exhaust duct. II  
Computer code application and verification p 17 A84-27140  
Application of a quasi-3D inviscid flow and boundary layer analysis to the hub-shroud contouring of a radial turbine  
[AIAA PAPER 84-1297] p 6 A84-44177  
Assessment of three-dimensional inviscid codes and loss calculations for turbine aerodynamic computations  
[NASA-TM-83571] p 8 N84-16142  
Comparison of secondary flows predicted by a viscous code and an inviscid code with experimental data for a turning duct  
[NASA-TM-83575] p 9 N84-17142  
Hot-flow tests of a series of 10-percent-scale turbofan forced mixing nozzles  
[NASA-TP-2268] p 123 N84-17525  
Application of a quasi-3D inviscid flow and boundary layer analysis to the hub-shroud contouring of a radial turbine  
[NASA-TM-83669] p 10 N84-25647
- POWELL, F. D.**  
Economic impact of fuel properties on turbine powered business aircraft p 14 N84-23646  
Study of effects of fuel properties in turbine-powered business aircraft  
[NASA-CR-174627] p 91 N84-25854
- POWELL, J. A.**  
Silicon carbide, a high temperature semiconductor p 190 N84-17823  
Silicon carbide, a high temperature semiconductor  
[NASA-TM-83514] p 191 N84-14932
- POWELL, S. H.**  
Improved high temperature resistant matrix resins  
[NASA-CR-168210] p 87 N84-28995  
Development of partially fluorinated resin apex seals  
[NASA-CR-174706] p 148 N84-32828
- POWER, J. L.**  
Ground correlation investigation of thruster spacecraft interactions to be measured on the IAPS flight test  
[NASA-TM-83598] p 47 N84-23691
- PRATT, D. T.**  
Exponential-fitted methods for integrating stiff systems of ordinary differential equations Applications to homogeneous gas-phase chemical kinetics p 179 N84-31279
- PRICE, A. O.**  
Experimental investigation of shock-cell noise reduction for dual-stream nozzles in simulated flight comprehensive data report. Volume 1 Test nozzles and acoustic data  
[NASA-CR-168336-VOL-1] p 184 N84-24323  
Experimental investigation of shock-cell noise reduction for dual-stream nozzles in simulated flight comprehensive data report. Volume 2. Laser velocimeter data, static pressures and shadowgraph photos  
[NASA-CR-168336-VOL-2] p 184 N84-24324  
Experimental investigation of shock-cell noise reduction for single-stream nozzles in simulated flight, comprehensive data report. Volume 1. Test nozzles and acoustic data  
[NASA-CR-168234-VOL-1] p 185 N84-33148  
Experimental investigation of shock-cell noise reduction for single-stream nozzles in simulated flight, comprehensive data report. Volume 2 Laser velocimeter data  
[NASA-CR-168234-VOL-2] p 186 N84-33149  
Experimental investigation of shock-cell noise reduction for single-stream nozzles in simulated flight, comprehensive data report. Volume 3 Shadowgraph photos and facility description  
[NASA-CR-168234-VOL-3] p 186 N84-33150
- PROCTOR, M. P.**  
Combustor flame flashback p 62 N84-20561
- PROVENCER, C.**  
Rural land mobile radio market assessment and satellite and terrestrial system concepts  
[AIAA PAPER 84-0754] p 95 A84-25324
- PROVENCER, C. E.**  
Rural land mobile radio market assessment and satellite and terrestrial system concepts  
[NASA-TM-83591] p 99 N84-19641
- PRZEKAS, A. J.**  
Rocket injector anomalies study Volume 1: Description of the mathematical model and solution procedure  
[NASA-CR-174702] p 49 N84-32428  
Rocket injector anomalies study Volume 2: Results of parametric studies  
[NASA-CR-174703] p 49 N84-32429
- PUDICK, S.**  
Develop and test fuel cell powered on-site integrated total energy systems  
[NASA-CR-174714] p 170 N84-27329
- PUGMIRE, R. J.**  
Carbon-13 and proton nuclear magnetic resonance analysis of shale-derived refinery products and jet fuels and of experimental referee broadened-specification jet fuels  
[NASA-CR-174761] p 92 N84-32552
- PURVIS, C. K.**  
The role of potential barrier formation in spacecraft charging p 41 N84-17269  
Solar array Plasma interactions p 171 N84-29343  
Design guidelines for assessing and controlling spacecraft charging effects  
[NASA-TP-2361] p 42 N84-33452
- PUTCHA, N. S.**  
A mixed shear flexible finite element for the analysis of laminated plates p 152 A84-45994
- Q**
- QUINN, R. D.**  
Experimental study of uncentralized squeeze film dampers  
[NASA-CR-168317] p 155 N84-19927
- R**
- RADHAKRISHNAN, K.**  
Fast algorithms for combustion kinetics calculations A companion p 61 N84-20554  
A companion of the efficiency of numerical methods for integrating chemical kinetic rate equations p 49 N84-31280
- RAMACHANDRA, S. M.**  
Acoustic pressures emanating from a turbomachine stage  
[NASA-TM-83734] p 129 N84-30224
- RAMAMURTI, R.**  
Hybrid C-H gnds for turbomachinery cascades p 3 A84-11591
- RAMESH, K.**  
Analytical study of suction boundary layer control for subsonic V/STOL inlets  
[AIAA PAPER 84-1399] p 6 A84-44187
- RAMINS, P.**  
Performance of computer-designed small-size multistage depressed collectors for a high-perveance traveling wave tube  
[NASA-TP-2248] p 106 N84-15394
- RAMLER, J.**  
NASA's geostationary communications platform program  
[AIAA PAPER 84-0702] p 95 A84-25326
- RAMLER, J. R.**  
Concept-for-advanced satellite communications and required technologies p 93 A84-15626
- RAMOS, J. I.**  
Turbulent flow field calculations in an internal combustion engine equipped with two valves p 112 A84-13311  
Formation and destruction of vortices in a motored four-stroke piston-cylinder configuration p 139 A84-38838
- RANAUDO, R. J.**  
Performance degradation of a typical twin engine commuter type aircraft in measured natural icing conditions  
[AIAA PAPER 84-0179] p 13 A84-21289  
Performance degradation of a typical twin engine commuter type aircraft in measured natural icing conditions  
[NASA-TM-83564] p 14 N84-13173
- RAO, B. C.**  
Size scale effect in cavitation erosion  
[NASA-TM-83533] p 67 N84-11254
- RAO, B. C. S.**  
Characterization of erosion of metallic materials under cavitation attack in a mineral oil  
[NASA-TP-2368] p 147 N84-32825
- RAO, P. V.**  
Modeling of transient two-component flow using a four-point implicit method p 112 A84-13237  
Morphology of an aluminum alloy eroded by a normally incident jet of angular erodent particles p 64 A84-18244  
Predictive capability of long-term cavitation and liquid impingement erosion models p 50 A84-32646  
A study of the effect of solid particle impact and particle shape on the erosion morphology of ductile metals p 66 A84-45570  
Size scale effect in cavitation erosion  
[NASA-TM-83533] p 67 N84-11254  
Empirical relations for cavitation and liquid impingement erosion processes  
[NASA-TP-2339] p 76 N84-31349
- RAO, V. P.**  
Solid impingement erosion mechanisms and characterization of erosion resistance of ductile metals  
[NASA-TM-83492] p 67 N84-12287
- RAQUET, C. A.**  
Characteristics and capacities of the NASA Lewis Research Center high precision 6.7- by 6.7-m planar near-field scanner  
[NASA-TM-83785] p 133 N84-32789
- RAUCH, J.**  
Free-piston stirling engine endurance test program p 136 A84-22864
- RAUE, J. E.**  
K-band latching switches  
[NASA-CR-168253] p 109 N84-24973
- RAY, P. K.**  
Energy partitioning in an inductively driven rail gun p 104 A84-33325
- REAGAN, J. R.**  
Failure analysis of a tool steel torque shaft p 148 A84-17546
- REAM, L. W.**  
Diesel engine catalytic combustor system  
[NASA-CASE-LEW-12995-1] p 148 N84-33808  
Baseline performance and emissions data for a single-cylinder, direct-injected diesel engine  
[NASA-TM-86873] p 197 N84-34330
- REDDY, J. N.**  
A mixed shear flexible finite element for the analysis of laminated plates p 152 A84-45994
- REED, K. W.**  
Inelastic stress analyses at finite deformation through complementary energy approaches p 149 A84-13248  
Analyses of large quasistatic deformations of inelastic bodies by a new hybrid-stress finite element algorithm p 150 A84-16874  
Analyses of large quasistatic deformations of inelastic bodies by a new hybrid-stress finite element algorithm - Applications p 150 A84-16884
- REGAN, C.**  
Holographic aids for internal combustion engine flow studies  
[NASA-TM-83681] p 132 N84-25017

- REGAN, C. A.**  
Multicomponent velocity measurement in a piston-cylinder configuration using laser velocimetry [NASA-TM-83534] p 8 N84-14121
- REICHERT, C. F.**  
Reflector antennas with low sidelobes, low cross polarization, and high aperture efficiency [NASA-CR-174670] p 100 N84-31464
- REID, L.**  
End-wall boundary layer measurements in a two-stage fan p 26 N84-16208
- REID, M. A.**  
Method of making a light weight battery plaque [NASA-CASE-LEW-13349-1] p 72 N84-22734  
Chromium electrodes for REDOX cells [NASA-CASE-LEW-13653-1] p 170 N84-28205  
Development of a lightweight nickel electrode [NASA-TM-86861] p 172 N84-30528
- REIFSNIDER, K. L.**  
Characterization of composite materials by means of the ultrasonic stress wave factor p 51 A84-10430
- REMICK, R. J.**  
Advanced onboard storage concepts for natural gas-fueled automotive vehicles [NASA-CR-174655] p 172 N84-34036
- RENGSTORFF, G. W. P.**  
Friction and wear of iron in sulfuric acid [NASA-TP-2289] p 71 N84-21716  
Friction and wear of nickel in sulfuric acid [NASA-TP-2290] p 72 N84-21721  
Interaction of sulfuric acid corrosion and mechanical wear of iron [NASA-TM-83717] p 73 N84-27857
- RENZ, D. D.**  
High-current, high-frequency capacitors p 105 N84-10067  
Parametric analysis of hollow conductor parallel and coaxial transmission lines for high frequency space power distribution [NASA-TM-83601] p 46 N84-20639  
High voltage-high power components for large space power distribution systems [NASA-TM-83648] p 42 N84-22615
- REPLIGLE, K. K.**  
Computer simulation of the heavy-duty turbo-compounded diesel cycle for studies of engine efficiency and performance [NASA-CR-174755] p 196 N84-33306
- RESHOTKO, E.**  
Scaling and modeling of three-dimensional, end-wall, turbulent boundary layers [NASA-CR-3792] p 127 N84-25941
- REYNOLDS, R.**  
Executive summary, aerothermal modeling program, phase 1 [NASA-CR-174602] p 60 N84-12263  
Aerothermal modeling program, phase 1 [NASA-CR-168243-VOL-2] p 60 N84-12265
- RICE, J. G.**  
Penalty function finite element analysis of steady viscous incompressible flow in rotating coordinates [ASME PAPER 84-GT-36] p 121 A84-46900
- RICE, W. J.**  
Multicomponent velocity measurement in a piston-cylinder configuration using laser velocimetry [NASA-TM-83534] p 8 N84-14121  
Development of an instrument for real-time computation of indicated mean effective pressure [NASA-TP-2238] p 107 N84-16461  
Real time pressure signal system for a rotary engine [NASA-CASE-LEW-13622-1] p 28 N84-22559
- RICHARDS, C. W.**  
Carrier recovery methods for a dual-mode modem A design approach [NASA-CR-173355] p 36 N84-19360
- RICHARDS, D. R.**  
Forced convection heat transfer to air/water vapor mixtures [NASA-CR-3769] p 123 N84-16488
- RICHARDS, W. B.**  
The infinite line pressure probe [NASA-TM-83582] p 132 N84-19787
- RICHARDSON, N. R.**  
Advanced turbocharger design study program [NASA-CR-174633] p 143 N84-21879
- RICHEY, A.**  
Automotive Stirling engine development program [NASA-CR-168205] p 194 N84-18117  
Automotive Stirling engine development program [NASA-CR-174622] p 195 N84-32305
- RICHTER, G. P.**  
Comparison of icing cloud instruments for 1982-1983 icing season flight program [NASA-TM-83569] p 14 N84-29870
- RIEKER, L. L.**  
Design considerations for a 10-kW integrated hydrogen-oxygen regenerative fuel cell system [NASA-TM-83664] p 167 N84-23023
- RILEY, J. J.**  
Direct simulations of chemically reacting turbulent mixing layers [NASA-CR-174640] p 32 N84-25710
- RIMON, Y.**  
Boundary conditions for the solution of compressible Navier-Stokes equations by an implicit factored method p 113 A84-13455
- ROBACK, R.**  
Mass and momentum turbulent transport experiments with confined swirling coaxial jets I [AIAA PAPER 84-1380] p 119 A84-35664  
Mass and momentum turbulent transport experiments with confined swirling coaxial jets [NASA-CR-168252] p 124 N84-17530
- ROBERTS, T. E.**  
A new multiple beam satellite antenna for 30/20 GHz communications coverage of CONUS-experimental evaluation [AIAA PAPER 84-0855] p 94 A84-25256
- ROBERTS, W. B.**  
Secondary flow spanwise deviation model for the stators of NASA middle compressor stages [NASA-CR-173350] p 27 N84-18202
- ROBINSON, A. C.**  
Stability and structure of stretched vortices [AD-A142913] p 117 A84-29798  
Three-dimensional stability of an elliptical vortex in a straining field [AD-A146317] p 120 A84-38557
- ROBINSON, R. S.**  
Sputtering phenomena in ion thrusters [NASA-CR-168172] p 46 N84-18322
- ROBINSON, W. W.**  
Dynamic gas temperature measurement system, volume 1 [NASA-CR-168267-VOL-1] p 132 N84-16529
- ROBSON, R. R.**  
The 25 kW resonant dc/dc power converter [NASA-CR-168273] p 108 N84-17481
- ROCHE, J. C.**  
NASCAP simulations of spacecraft charging of the SCATHA satellite p 41 N84-17258
- ROCK, S. M.**  
HYTESS. A hypothetical turbofan engine simplified simulation [NASA-TM-83561] p 26 N84-16184  
Identification of quasi-steady compressor characteristics from transient data [NASA-CR-174685] p 36 N84-34444
- RODE, H.**  
Diffused junction p(+)-n solar cells in bulk GaAs II - Device characterization and modeling p 161 A84-26028
- ROELKE, R.**  
Aerodynamic effects of moveable sidewall nozzle geometry and rotor exit restriction on the performance of a radial turbine [SAE PAPER 831517] p 17 A84-29450
- ROGERS, J.**  
Spatial electron density and electric field strength measurements in microwave cavity experiments [AIAA PAPER 84-1522] p 189 A84-46109  
Spatial electron density and electric field strength measurements in microwave cavity experiments [NASA-CR-173907] p 111 N84-32682
- ROGO, C.**  
Aerodynamic effects of moveable sidewall nozzle geometry and rotor exit restriction on the performance of a radial turbine [SAE PAPER 831517] p 17 A84-29460  
Variable stator radial turbine [NASA-CR-174663] p 29 N84-22568
- ROHDENBURG, C.**  
Automotive Stirling engine development program [NASA-CR-168205] p 194 N84-18117  
Automotive Stirling engine development program [NASA-CR-174622] p 195 N84-32305
- ROHN, D. A.**  
Elastic model of the traction behavior of two traction lubricants p 136 A84-28791  
An analysis of traction drive torsional stiffness [NASA-TM-83712] p 145 N84-27043
- ROHY, D. A.**  
Experimental study of the operating characteristics of premixing-prevaporizing fuel/air mixing passages [NASA-CR-168279] p 23 N84-14143
- ROMANOFFSKY, R. R.**  
Monolithic microwave integrated circuits Interconnections and packaging considerations [NASA-TM-83774] p 100 N84-31461
- RONNEY, P. D.**  
Effect of gravity on halogenated hydrocarbon flame retardant effectiveness [NASA-TM-83761] p 63 N84-33536
- ROOT, J.**  
Characteristics of a microwave plasma disk ion source p 189 A84-23390
- ROSE, J. H.**  
Scaling relations in the equation of state, thermal expansion, and melting of metals p 192 A84-19359  
Metallic adhesion and bonding p 72 N84-23897
- ROSEN, M. C.**  
Penalty function finite element analysis of steady viscous incompressible flow in rotating coordinates [ASME PAPER 84-GT-36] p 121 A84-46900
- ROSENTHAL, I.**  
Homogeneous reactions of hydrocarbons, silane, and chlorosilanes in radiofrequency plasmas at low pressures [NASA-TP-2301] p 50 N84-20643  
Radical and ion molecule mechanisms in the polymerization of hydrocarbons and chlorosilanes in RF plasmas at low pressures (1.0 torr) [NASA-TM-83602] p 190 N84-21329
- ROSFJORD, T. J.**  
Role of fuel chemical properties on combustor radiative heat load [AIAA PAPER 84-1493] p 89 A84-35236  
Aviation-fuel property effects on combustion [NASA-CR-168334] p 89 N84-17407
- ROSNER, D. E.**  
Correlation of thermophoretically-modified small particle diffusional deposition rates in forced convection systems with variable properties, transpiration cooling and/or viscous dissipation p 117 A84-32323  
Comparisons of rational engineering correlations of thermophoretically-augmented particle mass transfer with STANS-predictions for developing boundary layers [ASME PAPER 84-GT-158] p 92 A84-46965  
Engineering correlations of variable-property effects on laminar forced convection mass transfer for dilute vapor species and small particles in air [NASA-CR-168322] p 124 N84-18578  
Comparisons of rational engineering correlations of thermophoretically-augmented particle mass transfer with STANS-predictions for developing boundary layers [NASA-CR-168221] p 93 N84-19606  
Experimental and theoretical deposition rates from salt-seeded combustion gases of a Mach 0.3 burner ng [NASA-TP-2225] p 124 N84-19741  
Deposition of Na<sub>2</sub>SO<sub>4</sub> from salt-seeded combustion gases of a high velocity burner ng [NASA-TM-83751] p 129 N84-31558
- ROSS, P. T.**  
Combustor development for automotive gas turbines p 135 A84-10499
- ROSSNAGEL, S. M.**  
Stress measurement in thin films by geometrical optics p 130 A84-28797  
Sputtering phenomena in ion thrusters [NASA-CR-168172] p 46 N84-18322
- ROTH, S. P.**  
Real-time Pegasus propulsion system model V/STOL-piloted simulation evaluation p 15 A84-17362  
A piecewise linear state variable technique for real time propulsion system simulation p 20 A84-42378
- ROTHOLZ, E.**  
A frequency-division multiple-access system concept for 30/20 GHz high-capacity domestic satellite service p 94 A84-22141
- ROYCE, B. S. H.**  
The role of surface generated radicals in catalytic combustion p 61 N84-20555
- ROZAK, G. A.**  
Mechanical behavior of carbon-carbon composites [NASA-CR-174767] p 57 N84-34575
- RUBIN, A. G.**  
NASCAP simulations of spacecraft charging of the SCATHA satellite p 41 N84-17268  
High voltage solar array models and Shuttle tile charging [AD-P002123] p 177 N84-26209
- RUDEY, R. A.**  
A review of NASA combustor and turbine heat transfer research [NASA-TM-83541] p 24 N84-14146
- RUJKORAKARN, R.**  
Stress measurement in thin films by geometrical optics p 130 A84-28797
- RUNGTA, R.**  
Creep fatigue of low-cobalt superalloys. Waspalloy, PM U 700 and wrought U 700 [NASA-CR-168260] p 67 N84-13265

## RUSINKO, R. N.

Study to establish cost projections for production of Redox chemicals  
[NASA-CR-167881] p 164 N84-11580

## RUSSELL, L. M.

Comparison of visualized turbine endwall secondary flows and measured heat transfer patterns  
[ASME PAPER 83-GT-83] p 117 A84-33703

## RUTLEDGE, S. K.

Coaxial carbon plasma gun deposition of amorphous carbon films  
[NASA-TM-83600] p 191 N84-20404

Sputtered coatings for protection of spacecraft polymers  
[NASA-TM-83706] p 85 N84-26803

## RYAN, T. W., III

Development of carbon slurry fuels for transportation (hybrid fuels, phase 2)  
[NASA-CR-174659] p 74 N84-28960

## RYBICKI, G.

Oxidation resistant slurry coating for carbon-based materials  
[NASA-CASE-LEW-13923-1] p 54 N84-16266

## S

## SABLA, P. E.

Clean catalytic combustor program  
[NASA-CR-168323] p 24 N84-15151

## SABOURIN, D.

Baseband processor development for the Advanced Communications Satellite Program  
30/20 GHz communications systems baseband processor development p 93 A84-15628 p 95 A84-38251

## SADIN, S. R.

NASA priority technologies  
[IAF PAPER 83-345] p 37 A84-11793

## SAFFMAN, P. G.

Stability and structure of stretched vortices  
[AD-A142913] p 117 A84-29798  
Three-dimensional stability of an elliptical vortex in a straining field  
[AD-A146317] p 120 A84-38557

## SAIN, M. K.

An application of tensor ideas to nonlinear modeling of a turbofan jet engine p 20 A84-42382

## SALAH-EDDINE, A.

Thermoacoustic convection heat-transfer phenomenon p 120 A84-38857

## SALARI, K.

Boundary layer transition effects on flow separation around V-STOL engine inlets at high incidence  
[AIAA PAPER 84-0432] p 4 A84-18090

## SALIK, J.

A review of the use of wear-resistant coatings in the cutting-tool industry  
[NASA-TM-83512] p 81 N84-11295

A study of nucleation and growth of thin films by means of computer simulation General features  
[NASA-TM-83559] p 179 N84-17982

Ion-beam nitriding of steels  
[NASA-TM-83599] p 71 N84-21719

Erosion of iron-chromium alloys by glass particles  
[NASA-TM-2354] p 75 N84-28965

## SALIKUDDIN, M.

Acoustic power dissipation on radiation through duct terminations - Experiments p 180 A84-21272

## SALTSMAN, J. F.

Bending fatigue of electron-beam-welded foils Application to a hydrodynamic air bearing in the Chrysler/DOE upgraded automotive gas turbine engine  
[NASA-TM-83539] p 155 N84-16589

## SALZMAN, J. A.

Concept for advanced satellite communications and required technologies p 93 A84-15626

A comparison of the domestic satellite communications forecast to the year 2000  
[NASA-TM-83516] p 96 N84-10405

## SAMANICH, N.

Powerplant design for one-engine-inoperative operation p 19 A84-40787

## SAMANICH, N. E.

Development of large rotorcraft transmissions p 21 A84-46354

## SANDERCOCK, D. M.

Secondary flow spanwise deviation model for the stators of NASA middle compressor stages  
[NASA-CR-173360] p 27 N84-18202

## SANDERS, W. A.

Characteristics of Si3N4-SiO2-Ce2O3 compositions sintered in high-pressure nitrogen p 79 A84-19913

## SANFACON, M. M.

Ion implanted junctions for silicon space solar cells p 42 A84-30143

## SANGER, N. L.

Design and performance of a fixed, nonaccelerating, guide vane cascade that operates over an inlet flow angle range of 60 deg  
[NASA-TM-83519] p 8 N84-14120

## SANTARPIA, D.

NASA's multibeam communications technology program p 39 A84-21397

## SANTAVICCA, D. A.

The role of surface generated radicals in catalytic combustion p 61 N84-20555

## SANTORO, G. J.

Experimental and theoretical deposition rates from salt-seeded combustion gases of a Mach 0.3 burner  
[NASA-TP-2225] p 124 N84-19741

Deposition of Na2SO4 from salt-seeded combustion gases of a high velocity burner  
[NASA-TM-83751] p 129 N84-31558

## SANZ, J. M.

Improved design of subcritical and supercritical cascades using complex characteristics and boundary-layer correction p 5 A84-38839

Design and performance of a fixed, nonaccelerating, guide vane cascade that operates over an inlet flow angle range of 60 deg  
[NASA-TM-83519] p 8 N84-14120

## SARGISSON, D. F.

An advanced pitch change mechanism incorporating a hybrid traction drive  
[AIAA PAPER 84-1383] p 20 A84-44182

An advanced pitch change mechanism incorporating a hybrid traction drive  
[NASA-TM-83709] p 2 N84-25605

## SATER, D. M.

Coaxial carbon plasma gun deposition of amorphous carbon films  
[NASA-TM-83600] p 191 N84-20404

## SAUNDERS, A.

The 20 x 20 high speed microwave switches  
[NASA-TM-83775] p 101 N84-32644

## SAUNIER, P.

GaAs dual-gate FET for operation up to K-band  
30/20 GHz spacecraft GaAs FET solid state transmitter for trunking and customer-premise-service application  
[NASA-CR-168276] p 107 N84-16463

## SAWAMPHAKDI, K.

Nonlinear finite element analysis of shells with large aspect ratio p 158 N84-31692

## SCAGLIONE, L. J.

Teardown analysis of a ten cell bipolar nickel-hydrogen battery  
[NASA-TM-83618] p 168 N84-23026

## SCHARRER, G. L.

Five-hole pitot probe measurements of swirl, confinement and nozzle effects on confined turbulent flow  
[AIAA PAPER 84-1605] p 120 A84-38000

Swirl, expansion ratio and blockage effects on confined turbulent flow  
[NASA-CR-175391] p 125 N84-19746

## SCHATZ, M.

Performance capabilities of the 12-centimeter Xenon ion thruster  
[NASA-TM-83674] p 48 N84-27825

## SCHECHTER, B.

Material removal considerations for metal-ceramic abradable turbine seal systems p 135 A84-15575

## SCHILLING, D. L.

Computer simulator for a mobile telephone system  
[NASA-CR-174533] p 95 N84-10401

## SCHMIDT, J. F.

Redesign and cascade tests of a supercritical controlled diffusion stator blade-section  
[AIAA PAPER 84-1207] p 5 A84-36960

End-wall boundary layer measurements in a two-stage fan p 26 N84-16208

Redesign and cascade tests of a supercritical controlled diffusion stator blade-section  
[NASA-TM-83635] p 10 N84-22533

## SCHMIDT, R. J.

Theoretical and software considerations for nonlinear dynamic analysis  
[NASA-CR-174504] p 154 N84-15589

## SCHOCK, H. J.

Window aberration correction in laser velocimetry using multifaceted holographic optical elements p 134 A84-24663

Formation and destruction of vortices in a motored four-stroke piston-cylinder configuration p 139 A84-38838

A review of internal combustion engine combustion chamber process studies at NASA Lewis Research Center  
[AIAA PAPER 84-1316] p 121 A84-40242

Multicomponent velocity measurement in a piston-cylinder configuration using laser velocimetry  
[NASA-TM-83534] p 8 N84-14121

A dynamic analysis of rotary combustion engine seals  
[NASA-TM-83536] p 141 N84-14519

A review of internal combustion engine combustion chamber process studies at NASA Lewis Research Center  
[NASA-TM-83666] p 127 N84-24999

## SCHOENMAN, L.

Selection of burn-resistant materials for oxygen-driven turbopumps  
[AIAA PAPER 84-1287] p 43 A84-35157

## SCHOFIELD, K.

The chemical kinetics and thermodynamics of sodium species in oxygen-rich hydrogen flames p 59 A84-27724

## SCHREIBER, J.

Test results and description of a 1 kW free-piston Stirling engine with a dashpot load p 138 A84-30095

## SCHUH, R. M.

Electric vehicle propulsion alternatives  
[NASA-TM-83504] p 166 N84-20017

## SCHULLER, F. T.

Operating characteristics of a three-piece-inner-ring large-bore roller bearing to speeds of 3 million DN  
[NASA-TP-2355] p 146 N84-29226

## SCHULSON, E. M.

The structure of extruded NiAl p 65 A84-36047

## SCHULTZ, D. F.

Heat pipes to reduce engine exhaust emissions  
[NASA-CASE-LEW-12590-1] p 143 N84-22958

## SCHWAB, J. R.

Comparison of secondary flows predicted by a viscous code and an inviscid code with experimental data for a turning duct  
[NASA-TM-83575] p 9 N84-17142

## SCHWARTZ, H. B.

Forced response of a cantilever beam with a dry friction damper attached I - Theory II - Experiment p 150 A84-21267

## SCHWARTZ, H. J.

The potential impact of new power system technology on the design of a manned space station  
[NASA-TM-83770] p 49 N84-31272

## SCHWARZE, G. E.

Lightweight, high-frequency transformers p 105 N84-10066

Development of high frequency low weight power magnetics for aerospace power systems  
[NASA-TM-83656] p 109 N84-22992

## SCHWIND, G. A.

Evaluation of single crystal LaB6 cathodes for use in a high frequency backward wave oscillator tube  
[NASA-CR-173343] p 108 N84-19709

## SCOTT, G. W.

Wind turbine generator interaction with conventional diesel generators on Block Island, Rhode Island Volume 1 - Executive summary  
[NASA-CR-168318] p 171 N84-29357

Wind turbine generator interaction with conventional diesel generators on Block Island, Rhode Island Volume 2. Data analysis  
[NASA-CR-168319] p 172 N84-31783

## SCULLIN, V. J.

GCKP84-general chemical kinetics code for gas-phase flow and batch processes including heat transfer effects  
[NASA-TP-2320] p 63 N84-32446

## SEASHOLTZ, R. G.

Application of laser anemometry in turbine engine research p 130 A84-22872

A laser system to remotely sense bird movements p 159 A84-31608

Optimization of fringe-type laser anemometers for turbine engine component testing  
[AIAA PAPER 84-1459] p 131 A84-40248

Application of laser anemometry in turbine engine research  
[NASA-TM-83513] p 131 N84-11456

Optimization of fringe-type laser anemometers for turbine engine component testing  
[NASA-TM-83658] p 133 N84-25019

Three component velocity measurements using Fabry-Perot interferometer  
[NASA-TM-83692] p 133 N84-26010

## SECUNDE, R. R.

New propulsion components for electric vehicles p 103 A84-30209

Electric vehicle propulsion alternatives  
[NASA-TM-83504] p 166 N84-20017

## SEIDEL, B. S.

Inlet flow distortion in turbomachinery - Comparison of theory and experiment in a transonic fan stage p 3 A84-13592

## SEIDEN, E.

Turbulent swirling combustion p 61 N84-20535

- SEIGEL, B.**  
Evaluation of propellant tank insulation concepts for low-thrust chemical propulsion systems [NASA-CR-168320] p 46 N84-20634
- SEKAR, R.**  
New perspectives for advanced automobile diesel engines p 138 A84-30062
- SELIM, F. A.**  
Double-injection, deep-purity switch development [NASA-CR-168335] p 108 N84-18536
- SEN, K. K.**  
Energy partitioning in an inductively driven rail gun p 104 A84-33325
- SENG, G. T.**  
Research on aviation fuel instability p 90 N84-23642  
Group-type hydrocarbon standards for high-performance liquid chromatographic analysis of middlestage fuels [NASA-TP-2317] p 90 N84-23774  
Research on aviation fuel instability p 91 N84-24734  
FTIR analysis of aviation fuel deposits [NASA-TM-83773] p 92 N84-33608
- SEVERSON, S. J.**  
Design study of magnetic eddy-current vibration suppression dampers for application to cryogenic turbomachinery [NASA-CR-173273] p 141 N84-16562
- SHAMROTH, S. J.**  
Dynamic response of shock waves in transonic diffuser and supersonic inlet - An analysis with the Navier-Stokes equations and adaptive grid [AIAA PAPER 84-1609] p 5 A84-38004
- SHANKAR, N. R.**  
Phase analysis of plasma-sprayed zirconia-yttria coatings p 78 A84-19781
- SHANNON, J. L., JR.**  
Development of plane strain fracture toughness test for ceramics using Chevron notched specimens p 77 A84-11676
- SHAPIRO, W.**  
Design analysis of Rayleigh-step floating-ring seals [ASLE PREPRINT 83-LC-3B-2] p 137 A84-28989
- SHARMA, O. P.**  
Energy efficient engine Low-pressure turbine subsonic cascade component development and integration program [NASA-CR-165592] p 33 N84-27738
- SHARP, G. R.**  
Structural design of a vertical antenna boresight 18.3 by 18.3-m planar near-field antenna measurement system [NASA-TM-83781] p 133 N84-32783  
Characteristics and capacities of the NASA Lewis Research Center high precision 6.7- by 6.7-m planar near-field scanner [NASA-TM-83785] p 133 N84-32789
- SHARPE, W. N., JR.**  
Benchmark cyclic plastic notch strain measurements p 63 A84-11194
- SHAW, R. J.**  
Performance degradation of propeller systems due to rime ice accretion [AIAA PAPER 82-0286] p 12 A84-17406  
Helicopter rotor performance degradation in natural icing encounter p 12 A84-17412  
Heat transfer distributions around nominal ice accretion shapes formed on a cylinder in the NASA Lewis Icing Research Tunnel [AIAA PAPER 84-0017] p 113 A84-17834  
Heat transfer distributions around nominal ice accretion shapes formed on a cylinder in the NASA Lewis icing research tunnel [NASA-TM-83557] p 123 N84-14463  
Progress toward the development of an aircraft icing analysis capability [NASA-TM-83562] p 9 N84-20490
- SHAWHAN, S. D.**  
Effects of chemical releases by the STS-3 Orbiter on the ionosphere [NASA-CR-171032] p 173 N84-25204
- SHEFFLER, K. D.**  
Development of strain tolerant thermal barrier coating systems, tasks 1 - 3 [NASA-CR-168251] p 81 N84-12312  
Materials for Advanced Turbine Engines (MATE) Project 3: Design, fabrication and evaluation of an oxide dispersion strengthened sheet alloy combustor liner, volume 1 [NASA-CR-174691] p 76 N84-32504
- SHEIBLEY, D. W.**  
Additive for zinc electrodes [NASA-CASE-LEW-13288-1] p 106 N84-14422  
Regenerative hydrogen-oxygen fuel cell-electrolyzer systems for orbital energy storage p 111 N84-33670
- SHEN, T. P.**  
Interference phenomena in the refraction of a surface polariton by vertical dielectric barriers p 179 A84-24410
- SHEPPARD, C. H.**  
Characterization of PMR polyimide resin and prepreg [NASA-CR-168217] p 63 N84-20695
- SHERMAN, F. S.**  
Numerical modeling of turbulent flow in a channel [NASA-CR-168278] p 23 N84-13189
- SHIH, T. I.-P.**  
Boundary conditions for the solution of compressible Navier-Stokes equations by an implicit factored method p 113 A84-13495
- SHORE, R. A.**  
Reflector antennas with low sidelobes, low cross polarization, and high aperture efficiency [NASA-CR-174670] p 100 N84-31464
- SHORTT, D. J.**  
Extensions of the discrete-average models for converter power stages p 102 A84-16411
- SHUEN, J. S.**  
A theoretical and experimental study of turbulent particle-laden jets [NASA-CR-168293] p 23 N84-13187  
Predictions of spray combustion interactions p 61 N84-20532  
The structure of evaporating and combusting sprays Measurements and predictions [NASA-CR-173778] p 128 N84-29155  
A theoretical and experimental study of turbulent nonevaporating sprays [NASA-CR-174668] p 35 N84-29877  
A theoretical and experimental study of turbulent evaporating sprays [NASA-CR-174760] p 35 N84-32390
- SHUEN, J.-S.**  
Structure of particle-laden jets - Measurements and predictions [AIAA PAPER 84-0038] p 113 A84-17842  
Structure of nonevaporating sprays - Measurements and predictions [AIAA PAPER 84-0125] p 114 A84-17397
- SIDDIQI, S.**  
Phased-array-fed antenna configuration study. Volume 1: Technology assessment [NASA-CR-168231] p 98 N84-16423  
Phased-array-fed antenna configuration study, volume 2 [NASA-CR-168232] p 98 N84-16424
- SIDI, A.**  
Acceleration of convergence of vector sequences [NASA-TP-2193] p 178 N84-13885
- SIDORAK, L. G.**  
High speed, low cost, LEO-thermal-cycling facility p 171 N84-29340
- SIEGEL, B.**  
Evaluation of propellant tank insulation concepts for low-thrust chemical propulsion systems Executive summary [NASA-CR-168321] p 63 N84-20699
- SIEGEL, R.**  
Shape of porous region to control cooling along curved exit boundary p 115 A84-23591  
Two-region analysis of interface shape in continuous casting with superheated liquid p 139 A84-44918
- SIEMERS, P. A.**  
Mechanical and physical properties of plasma-sprayed stabilized zirconia p 79 A84-19786
- SIEVERS, G. K.**  
Fuel savings potential of the NASA Advanced Turboprop Program [NASA-TM-83736] p 35 N84-28878
- SIGMAN, R. K.**  
A finite element approach for predicting nozzle admittances p 180 A84-21184
- SIMETKOSKY, M.**  
Automotive Stirling engine development program [NASA-CR-168205] p 194 N84-18117  
Automotive Stirling engine development program [NASA-CR-174622] p 195 N84-32305
- SIMETKOSKY, M. A.**  
Automotive Stirling Engine Development Program Mod 1 Stirling engine development p 138 A84-30091
- SIMONEAU, R. J.**  
Heat transfer distributions around nominal ice accretion shapes formed on a cylinder in the NASA Lewis Icing Research Tunnel [AIAA PAPER 84-0017] p 113 A84-17834  
Effect of location in an array on heat transfer to a short cylinder in crossflow p 119 A84-36150  
Heat transfer distributions around nominal ice accretion shapes formed on a cylinder in the NASA Lewis icing research tunnel [NASA-TM-83557] p 123 N84-14463
- Effect of a rotor wake on heat transfer from a circular cylinder [NASA-TM-83613] p 126 N84-21832
- SIMPSON, R. L.**  
An experimental study of the properties of surface pressure fluctuations in strong adverse pressure gradient turbulent boundary layers [NASA-CR-175410] p 9 N84-20488
- SINCLAIR, J. H.**  
Prediction of composite hygral behavior made simple p 51 A84-14285  
Durability/life of fiber composites in hygrothermomechanical environments p 52 A84-27359  
Compressive behavior of unidirectional fibrous composites p 53 A84-29894  
INHYD Computer code for intraply hybrid composite design A users manual [NASA-TP-2239] p 54 N84-13224  
Impact resistance of fiber composites Energy absorbing mechanisms and environmental effects [NASA-TM-83594] p 55 N84-24712
- SINGER, I. D.**  
Energy efficient engine high-pressure turbine detailed design report [NASA-CR-165608] p 33 N84-28788
- SINGH, N. B.**  
Gravitational effects in dendritic growth p 37 A84-22346
- SINGHAL, A. K.**  
Rocket injector anomalies study Volume 1 Description of the mathematical model and solution procedure [NASA-CR-174702] p 49 N84-32428  
Rocket injector anomalies study Volume 2. Results of parametric studies [NASA-CR-174703] p 49 N84-32429
- SINHA, A.**  
The interaction between mistuning and friction in the forced response of bladed disk assemblies [ASME PAPER 84-GT-139] p 152 A84-46957
- SISTO, F.**  
The influence of gyroscopic forces on the dynamic behavior and flutter of rotating blades [NASA-CR-175444] p 27 N84-20524
- SKALSKI, S. C.**  
Forced vibration analysis of rotating cyclic structures in NASTRAN [NASA-CR-165429] p 153 N84-11514  
NASTRAN documentation for flutter analysis of advanced turbopropellers [NASA-CR-167927] p 25 N84-15153  
Bladed-shrouded-disc aeroelastic analyses Computer program updates in NASTRAN level 17.7 [NASA-CR-165428] p 25 N84-15154
- SKEBE, S. A.**  
Experimental studies on two dimensional shock boundary layer interactions [AIAA PAPER 84-0099] p 3 A84-17881
- SKOK, A. J.**  
Evaluation of gas cooling for pressurized phosphoric acid fuel cell stacks p 163 A84-30191
- SLABY, J. G.**  
Overview of NASA Lewis Research Center free-piston Stirling engine activities [NASA-TM-83649] p 195 N84-22512
- SLATER, H. A.**  
Method of reducing temperature in high-speed photography [NASA-TM-83620] p 188 N84-22421
- SLETTEN, C. J.**  
Reflector antennas with low sidelobes, low cross polarization, and high aperture efficiency [NASA-CR-174670] p 100 N84-31464
- SLICKER, J. M.**  
AC propulsion system for an electric vehicle, phase 2 [NASA-CR-168244] p 111 N84-31514
- SLINEY, H. E.**  
Surface roughness effects with solid lubricants dispersed in mineral oils [ASLE PREPRINT 83-LC-4C-1] p 137 A84-28987  
Durable solid lubricant coatings for foil gas bearings to 315 deg C [NASA-TM-83596] p 83 N84-19567  
Status and new directions for solid lubricant coatings and composite materials p 85 N84-25055  
Evaluation of two polyimides and of an improved liner retention design for self-lubricating bushings [NASA-TM-83719] p 86 N84-27887
- SLONE, H. O.**  
NASA priority technologies [IAF PAPER 83-345] p 37 A84-11793
- SMIALEK, J. L.**  
Structure of transient oxides formed on NiCrAl alloys p 63 A84-12385  
Phase distributions in plasma-sprayed zirconia-yttria p 78 A84-18948

- Processing of fused silicide coatings for carbon-based materials p 51 A84-19780  
Oxidation resistant slurry coating for carbon-based materials [NASA-CASE-LEW-13923-1] p 54 N84-16266
- SMITH, C. F., JR.**  
Solar-array-materials passive LDEF experiment (A0171) p 168 N84-24656
- SMITH, D. A.**  
Acceleration of convergence of vector sequences [NASA-TP-2193] p 178 N84-13885
- SMITH, D. W.**  
The 30 GHz communications satellite low noise receiver [NASA-CR-168254] p 97 N84-13398
- SMITH, G.**  
Automotive Stirling engine development program [NASA-CR-168205] p 194 N84-18117  
Automotive Stirling engine development program [NASA-CR-174622] p 195 N84-32305
- SMITH, G. C. C.**  
NASTRAN forced vibration analysis of rotating cyclic structures [ASME PAPER 83-DET-20] p 151 A84-29103  
Flutter analysis of advanced turbopropellers p 152 A84-36492  
Finite element forced vibration analysis of rotating cyclic structures [NASA-CR-165430] p 153 N84-11515  
NASTRAN flutter analysis of advanced turbopropellers [NASA-CR-167926] p 24 N84-14148  
NASTRAN forced vibration analysis of rotating cyclic structures [NASA-CR-173821] p 157 N84-29252
- SMITH, G. E.**  
Boundary conditions for the solution of compressible Navier-Stokes equations by an implicit factored method p 113 A84-13495
- SMITH, G. T.**  
Environmental and high strain rate effects on composites for engine applications p 51 A84-17444  
Resin selection criteria for tough composite structures [NASA-TM-83449] p 81 N84-10310
- SMITH, J. M.**  
Preliminary investigation of a two-zone swirl flow combustor [AIAA PAPER 84-1169] p 17 A84-36951  
Experimental investigation of the low NOx vortex airblast annular combustor [AIAA PAPER 84-1170] p 18 A84-36952  
Preliminary investigation of a two-zone swirl flow combustor [NASA-TM-83637] p 29 N84-22595
- SMITH, J. R.**  
Scaling relations in the equation of state, thermal expansion, and melting of metals p 192 A84-19359  
Metallic adhesion and bonding p 72 N84-23897
- SMITH, L. B.**  
Advanced Gas Turbine (AGT): Power-train system development [NASA-CR-168056] p 140 N84-10531
- SMITH, M. E.**  
Measurements of local convective heat transfer coefficients on ice accretion shapes [AIAA PAPER 84-0018] p 113 A84-17835  
Measurement of local convective heat transfer coefficients of four ice accretion shapes [NASA-CR-174680] p 10 N84-25646
- SMITH, P. J.**  
Assessment of two neglected effects in the analysis of an oil pumping ring seal [ASME PAPER 83-LUB-16] p 137 A84-29097
- SMITH, R. F.**  
Wind turbine generator interaction with conventional diesel generators on Block Island, Rhode Island Volume 1: Executive summary [NASA-CR-168318] p 171 N84-29357  
Wind turbine generator interaction with conventional diesel generators on Block Island, Rhode Island Volume 2: Data analysis [NASA-CR-168319] p 172 N84-31783
- SMITH, W. W.**  
Study of auxiliary propulsion requirements for large space systems Volume 1. Executive summary [NASA-CR-168193-VOL-1] p 45 N84-12226  
Study of auxiliary propulsion requirements for large space systems, volume 2 [NASA-CR-168193-VOL-2] p 45 N84-13218  
Factors that influence space station propulsion requirements p 48 N84-29931
- SMITHRICK, J. J.**  
Cycle life test and failure model of nickel-hydrogen cells p 162 A84-30185  
Advanced designs for IPV nickel-hydrogen cells [NASA-TM-83643] p 168 N84-23025
- Oxygen recombination in individual pressure vessel nickel-hydrogen batteries [NASA-CASE-LEW-13822-1] p 110 N84-29084
- SMOLL, A. E.**  
Multibeam antenna for 30/20 GHz advanced communications satellite using offset shaped, dual reflector surfaces p 93 A84-15627  
A new multiple beam satellite antenna for 30/20 GHz communications coverage of CONUS-experimental evaluation [AIAA PAPER 84-0655] p 94 A84-25256
- SMYTHE, M. E.**  
Thermal oxidative degradation reactions of perfluoroalkethers [NASA-CR-168224] p 60 N84-11229
- SNYDER, A.**  
Shape of porous region to control cooling along curved exit boundary p 115 A84-23591
- SNYDER, C. M.**  
Catalog of selected heavy duty transport energy management models [NASA-CR-168299] p 194 N84-14991
- SNYDER, D. B.**  
Discharges on a negatively biased solar array in a charged particle environment [NASA-TM-83644] p 47 N84-23690  
Characteristics of arc currents on a negatively biased solar cell array in a plasma [NASA-TM-83728] p 48 N84-27824
- SOCKOL, P.**  
Viscous-inviscid interactive procedure for rotational flow in cascades of airfoils p 6 A84-44639
- SOEDER, J. F.**  
F100 multivariable control synthesis program. Computer implementation of the F100 multivariable control algorithm [NASA-TP-2231] p 22 N84-11171  
A real-time, portable, microcomputer-based jet engine simulator [NASA-TM-83550] p 176 N84-16812
- SOHRAB, S. H.**  
Extinction of premixed flames by stretch and radiative loss p 58 A84-23593
- SOKOLOV, V.**  
A Ka-band GaAs monolithic phase shifter p 101 A84-18371  
The 30-GHz monolithic receive module [NASA-CR-168326] p 99 N84-20737
- SOLOMON, A. S. P.**  
Structure of particle-laden jets - Measurements and predictions [AIAA PAPER 84-0038] p 113 A84-17842  
Structure of nonevaporating sprays - Measurements and predictions [AIAA PAPER 84-0125] p 114 A84-17897  
A theoretical and experimental study of turbulent particle-laden jets [NASA-CR-168293] p 23 N84-13187  
Predictions of spray combustion interactions p 61 N84-20532  
The structure of evaporating and combusting sprays. Measurements and predictions [NASA-CR-173778] p 128 N84-29155  
A theoretical and experimental study of turbulent nonevaporating sprays [NASA-CR-174668] p 35 N84-29877  
A theoretical and experimental study of turbulent evaporating sprays [NASA-CR-174760] p 35 N84-32390
- SOLTIS, D. G.**  
Additive for zinc electrodes [NASA-CASE-LEW-13286-1] p 106 N84-14422  
Method of making a light weight battery plaque [NASA-CASE-LEW-13349-1] p 72 N84-22734
- SOMES, S. S.**  
Communications network design and costing model technical manual [NASA-CR-168236] p 97 N84-14376  
Communications network design and costing model programmers manual [NASA-CR-168237] p 97 N84-14377  
Communications network design and costing model users manual [NASA-CR-168238] p 97 N84-14378
- SOMMER, H. T.**  
Turbulent swirling combustion p 61 N84-20535
- SORBELLO, R. M.**  
Phased-array-fed antenna configuration study Volume 1: Technology assessment [NASA-CR-168231] p 98 N84-16423  
Phased-array-fed antenna configuration study, volume 2 [NASA-CR-168232] p 98 N84-16424
- SOSOKA, D. J.**  
Formation and destruction of vortices in a motored four-stroke piston-cylinder configuration p 139 A84-38838
- SOVEY, J. S.**  
Space Station propulsion analysis study [AIAA PAPER 84-1326] p 44 A84-44179  
Improved ion containment using a ring-cusp ion thruster p 44 A84-49511  
Space station propulsion analysis study [NASA-TM-83715] p 47 N84-25764  
Ion sputter textured graphite electrode plates [NASA-CASE-LEW-12919-2] p 179 N84-28565  
Deposition of diamondlike carbon films [NASA-CASE-LEW-14080-1] p 86 N84-28986  
Improved heat exchanger for electrothermal devices [NASA-CASE-LEW-14037-1] p 49 N84-32425
- SPADACCINI, L. J.**  
Deposit formation and heat transfer in hydrocarbon rocket fuels [AIAA PAPER 84-0512] p 88 A84-18142  
Deposit formation and heat transfer in hydrocarbon rocket fuels [NASA-CR-168277] p 45 N84-12225
- SALVINS, T.**  
Tribological and microstructural characteristics of ion-nitrided steels p 64 A84-19225  
The X-ray photoelectron spectroscopy depth profiling and tribological characterization of ion-plated gold on various metals p 50 A84-20465  
Characteristic morphological and frictional changes in sputtered MoS<sub>2</sub>/sub 2 films [NASA-TM-83565] p 92 N84-16380  
Metallic glass as a temperature sensor during ion plating [NASA-TM-83566] p 69 N84-17351  
Tribological characteristics of gold films deposited on metals by ion plating and vapor deposition [NASA-TM-83572] p 69 N84-17352  
Functional and morphological properties of Au-MoS<sub>2</sub> films sputtered from a compact target [NASA-TM-83604] p 143 N84-20858  
Status of plasma physics techniques for the deposition of tribological coatings p 190 N84-25058
- SPERA, D. A.**  
Review of the DOE/NASA wind turbine engineering information system p 163 A84-33766
- SPITZER, M. B.**  
Large area space solar cell assemblies p 42 A84-22980  
New implantation techniques for improved solar cell junctions p 161 A84-23059  
Ion implanted junctions for silicon space solar cells p 42 A84-30143
- SPRINGER, G. S.**  
Boundary conditions for the solution of compressible Navier-Stokes equations by an implicit factored method p 113 A84-13495
- SPRINKLE, C. H.**  
Sixth Annual Workshop on Meteorological and Environmental Inputs to Aviation Systems, 26-28 October 1982, Tullahoma, Tenn p 174 A84-23424
- SPURLOCK, O. F.**  
Shuttle/Centaur - More capability for the 1980's [IAF PAPER 83-18] p 38 A84-11718
- STRAWLEY, J. E.**  
Analysis of an internally radially cracked ring segment subject to three-point radial loading p 150 A84-18691  
Mode 2 fatigue crack growth specimen development [NASA-TM-83722] p 156 N84-29248
- SRINIVAS, D. N.**  
Phased-array-fed antenna configuration study. Volume 1 Technology assessment [NASA-CR-168231] p 98 N84-16423
- SRINIVASAN, R.**  
On modeling dilution jet flowfields [AIAA PAPER 84-1379] p 121 A84-44183  
Experiments in dilution jet mixing p 122 A84-48140  
Executive summary, aerothermal modeling program, phase 1 [NASA-CR-174602] p 60 N84-12263  
Aerothermal modeling program, phase 1 [NASA-CR-168243-VOL-2] p 60 N84-12265  
Modeling of dilution jet flowfields p 126 N84-20547  
On modeling dilution jet flowfields [NASA-TM-83708] p 32 N84-25713  
Dilution jet mixing program [NASA-CR-174624] p 33 N84-26702
- SRINIVASAN, S.**  
Electrode kinetics of oxygen reduction - A theoretical and experimental analysis of the rotating ring-disc electrode method p 59 A84-29999
- STABE, R. G.**  
Performance of a high-work low aspect ratio turbine tested with a realistic inlet radial temperature profile [AIAA PAPER 84-1161] p 19 A84-40239



- Performance of a high-work low aspect ratio turbine tested with a realistic inlet radial temperature profile [NASA-TM-83655] p 32 N84-24589
- STANNARD, P. R.**  
NASCAP simulations of spacecraft charging of the SCATHA satellite p 41 N84-17268
- STANTON, A. C.**  
Automatic holographic droplet analysis for liquid fuel sprays p 125 N84-20531
- STEARNS, C. A.**  
Experimental and theoretical deposition rates from salt-seeded combustion gases of a Mach 0.3 burner rig [NASA-TP-2225] p 124 N84-19741  
Mechanism of corrosion of Ni base superalloys by molten Na<sub>2</sub>MoO<sub>4</sub> at elevated temperatures [NASA-TM-83580] p 70 N84-20672  
Chemical mechanisms and reaction rates for the initiation of hot corrosion of IN-738 [NASA-TP-2319] p 74 N84-28958  
Deposition of Na<sub>2</sub>SO<sub>4</sub> from salt-seeded combustion gases of a high velocity burner rig [NASA-TM-83751] p 129 N84-31558
- STEARNS, E. M.**  
Energy efficient engine: Flight propulsion system, preliminary analysis and design update [NASA-CR-167980] p 22 N84-11170
- STECURA, S.**  
Improved thermal barrier coating system [NASA-CASE-LEW-14057-1] p 88 N84-33595
- STEFFEK, L. J.**  
The 30 GHz communications satellite low noise receiver [NASA-CR-168254] p 97 N84-13398
- STEFKO, G. L.**  
Application of an optimization method to high performance propeller designs [AIAA PAPER 84-1203] p 20 A84-44181  
Noise of the SR-6 propeller model at 2 deg and 4 deg angles of attack [NASA-TM-83515] p 183 N84-16946  
Application of an optimization method to high performance propeller designs [NASA-TM-83710] p 2 N84-25607
- STEGEMAN, G. I.**  
Interference phenomena in the refraction of a surface polaron by vertical dielectric barriers p 179 A84-24410
- STEIN, Y.**  
The role of surface generated radicals in catalytic combustion p 61 N84-20555
- STEINBERG, M.**  
The chemical kinetics and thermodynamics of sodium species in oxygen-rich hydrogen flames p 59 A84-27724
- STEINETZ, B. M.**  
An advanced pitch change mechanism incorporating a hybrid traction drive [AIAA PAPER 84-1383] p 20 A84-44182  
An advanced pitch change mechanism incorporating a hybrid traction drive [NASA-TM-83709] p 2 N84-25605
- STELLA, P. M.**  
Solar-array-materials passive LDEF experiment (A0171) p 168 N84-24656
- STEPHENS, J. B.**  
Understanding the roles of the strategic element cobalt in nickel base superalloys p 76 N84-33471
- STEPHENS, J. R.**  
Hostile environmental conditions facing candidate alloys for the automotive Stirling engine p 136 A84-23522  
Replacing critical and strategic refractory metal elements in nickel-base superalloys p 67 N84-13264  
Oxidation and corrosion resistance of candidate Stirling engine heater-head-tube alloys [NASA-TM-83609] p 74 N84-28962  
Advanced high temperature materials for the energy efficient automotive Stirling engine [NASA-TM-83659] p 75 N84-28963
- STEPKA, F. S.**  
Review and status of heat-transfer technology for internal passages of air-cooled turbine blades [NASA-TP-2232] p 126 N84-21828
- STERMAN, A. P.**  
Tip cap for a rotor blade [NASA-CASE-LEW-13654-1] p 28 N84-22560  
Air modulation apparatus [NASA-CASE-LEW-13524-1] p 35 N84-33410
- STERN, T. G.**  
Multibandgap photovoltaic receiver using back surface reflectors p 161 A84-30162
- STETSON, K. A.**  
The use of heterodyne speckle photogrammetry to measure high-temperature strain distributions p 130 A84-28623
- STEURER, J. W.**  
Uncertainty methodology for in-flight thrust determination [SAE PAPER 831438] p 13 A84-29452  
Application of in-flight thrust determination uncertainty [SAE PAPER 831439] p 13 A84-29453
- STEVENS, G. H.**  
Economic comparison of FDMA and TDMA options for communications by Ka-band multiple beam satellites [AIAA PAPER 84-0740] p 94 A84-25299
- STEVENSON, M. J.**  
Charged particle effects on space systems [AD-P002103] p 187 N84-26189  
High voltage solar array models and Shuttle tile charging [AD-P002123] p 177 N84-26209  
Design guidelines for assessing and controlling spacecraft charging effects [NASA-TP-2361] p 42 N84-33452
- STEVENSON, S.**  
Rural land mobile radio market assessment and satellite and terrestrial system concepts [AIAA PAPER 84-0754] p 95 A84-25324
- STEVENSON, S. M.**  
A comparison of the domestic satellite communications forecast to the year 2000 [NASA-TM-83516] p 96 N84-10405  
Rural land mobile radio market assessment and satellite and terrestrial system concepts [NASA-TM-83591] p 99 N84-19641
- STEWART, C. S.**  
Transient flow analysis of the AEDC/HPDE MHD generator p 189 A84-24049
- STEWART, G. W.**  
Automatic holographic droplet analysis for liquid fuel sprays p 125 N84-20531
- STICKLES, R. P.**  
New applications for phosphoric acid fuel cells [NASA-CR-168203] p 166 N84-18757
- STILLER, P. H.**  
Wind turbine generator interaction with conventional diesel generators on Block Island, Rhode Island. Volume 1: Executive summary [NASA-CR-168318] p 171 N84-29357  
Wind turbine generator interaction with conventional diesel generators on Block Island, Rhode Island. Volume 2: Data analysis [NASA-CR-168319] p 172 N84-31783
- STILWELL, J.**  
Baseband processor development for the Advanced Communications Satellite Program p 93 A84-15628  
30/20 GHz communications systems baseband processor development p 95 A84-38251
- STILWELL, J. H.**  
Serial MSK modem for the Advanced Communications Satellite Program p 93 A84-15629
- STINCHCOMB, W. W.**  
Characterization of composite materials by means of the ultrasonic stress wave factor p 51 A84-10430
- STOCKEMER, F. J.**  
Heating experiments for flowability improvement of near-freezing aviation fuel p 89 A84-26955
- STOEFFLER, R. C.**  
Energy efficient engine high-pressure turbine supersonic cascade technology report [NASA-CR-165567] p 33 N84-27739
- STOFAN, A. J.**  
A high energy stage for the National Space Transportation System [NASA-TM-83795] p 38 N84-32411
- STOLOFF, N. S.**  
The effects of frequency and hold times on fatigue crack propagation rates in a nickel base superalloy p 64 A84-18733  
Fatigue crack growth and low cycle fatigue of two nickel base superalloys [NASA-CR-174534] p 66 N84-10267
- STONE, J. R.**  
Acoustic excitation A promising new means of controlling shear layers [NASA-TM-83772] p 10 N84-31096  
Supersonic jet shock noise reduction [NASA-TM-83799] p 186 N84-35085
- STORACE, A.**  
Blade loss transient dynamics analysis with flexible bladed disk [NASA-CR-168176] p 23 N84-13193
- STORM, R. S.**  
Processing of sintered alpha SiC [ASME PAPER 84-GT-127] p 140 A84-46954
- STRANGE, R. R.**  
Advanced high temperature heat flux sensors [NASA-TM-83526] p 123 N84-16493  
Turbine blade and vane heat flux sensor development, phase 1 [NASA-CR-168297] p 134 N84-32790
- STRANGMAN, T. E.**  
Low-cost single-crystal turbine blades, volume 1 [NASA-CR-168218] p 68 N84-15247
- STRAZISAR, A. J.**  
Investigation of flow phenomena in a transonic fan rotor using laser anemometry [NASA-TM-83555] p 9 N84-17143
- STRNAT, K. J.**  
Study and review of permanent magnets for electric vehicle propulsion motors [NASA-CR-168178] p 193 N84-14071
- STROCK, W. J.**  
Combustor liner construction [NASA-CASE-LEW-14035-1] p 30 N84-24577
- STUART, T. A.**  
Inherent overload protection for the series resonant converter p 102 A84-23255  
A large-signal dynamic simulation for the series resonant converter p 103 A84-23258  
A study of the high frequency limitations of series resonant converters [NASA-CR-173868] p 111 N84-32673
- STUMPF, R. P.**  
A dynamic analysis of rotary combustion engine seals [NASA-TM-83536] p 141 N84-14519
- STURGEON, G. J.**  
Calculations of turbulent mass transport in a bluff-body diffusion-flame combustor [AIAA PAPER 84-0372] p 114 A84-18048  
Calculation of a hollow-cone liquid spray in a uniform air stream [AIAA PAPER 84-1322] p 118 A84-35171
- STURMAN, J. C.**  
LeRC rail accelerators - Test designs and diagnostic techniques p 42 A84-32031
- SUBRAHMANYAM, K. B.**  
An improved finite-difference analysis of uncoupled vibrations of tapered cantilever beams [NASA-TM-83495] p 154 N84-13610  
Improved finite-difference vibration analysis of pretwisted, tapered beams [NASA-TM-83549] p 154 N84-16588  
Improved methods of vibration analysis of pretwisted, airfoil blades [NASA-TM-83735] p 157 N84-30329
- SULLIVAN, T. L.**  
Effect of vortex generators on the power conversion performance and structural dynamic loads of the Mod-2 wind turbine [NASA-TM-83680] p 171 N84-29347
- SUMIHARA, K.**  
New variational formulations of hybrid stress elements p 158 N84-31690
- SUN, C.**  
A 20-GHz IMPATT transmitter [NASA-CR-168076] p 106 N84-11385
- SUN, C. T.**  
Indentation law for composite laminates p 52 A84-27356
- SUNDARAM, L. G.**  
Photovoltaic characteristics of diffused P<sup>+</sup>-N bulk GaAs solar cells p 161 A84-23115
- SUNDARAM, L. M. G.**  
Diffused junction p<sup>+</sup>-n solar cells in bulk GaAs. II - Device characterization and modelling p 161 A84-26028
- SUNDBERG, G. R.**  
Advanced electrical power system technology for the all electric aircraft p 15 A84-16528  
New developments in power semiconductors p 105 N84-10065  
Advances in solid state switchgear technology for large space power systems [NASA-TM-83652] p 109 N84-22891
- SURAMPUDI, S. P.**  
Unsteady transonic flow in cascades [NASA-TM-83780] p 11 N84-32351
- SVEHLA, R.**  
In-flight atmospheric and fuel tank temperature measurements p 90 N84-23643
- SWANSON, L. W.**  
Evaluation of single crystal LaB<sub>6</sub> cathodes for use in a high frequency backward wave oscillator tube [NASA-CR-173343] p 108 N84-19709
- SWARTZ, C. K.**  
Increased radiation resistance in lithium-counterdoped silicon solar cells p 163 A84-34846  
Voltage controlling mechanisms in low resistivity silicon solar cells A unified approach [NASA-TM-83612] p 167 N84-20916  
Radiation damage and defect behavior in ion-implanted, lithium counterdoped silicon solar cells [NASA-TM-83646] p 109 N84-22890  
Radiation tolerance of low resistivity, high voltage silicon solar cells p 170 N84-29318

- Cell and defect behavior in lithium-counterdoped solar cells p 170 N84-29322
- The effects of lithium counterdoping on radiation damage and annealing in n(+)-p silicon solar cells [NASA-TM-83755] p 110 N84-31513
- SWEC, D. M.**
- Sputtered coatings for protection of spacecraft polymers [NASA-TM-83706] p 85 N84-26803
- Dual ion beam deposition of carbon films with diamondlike properties [NASA-TM-83743] p 110 N84-31512
- SWEETING, T. B.**
- Progress in net shape fabrication of alpha sic turbine components [ASME PAPER 84-GT-273] p 140 A84-47036
- SYED, S. A.**
- Calculation of a hollow-cone liquid spray in a uniform air stream [AIAA PAPER 84-1322] p 118 A84-35171
- Error reduction program A progress report p 27 N84-20536
- SYMONS, E. P.**
- Cryogenic Fluid Management Facility [AIAA PAPER 84-1340] p 44 A84-44184
- SZANISZLO, A. J.**
- NASA advanced low emissions combustor program [ASME PAPER 83-JPGC-GT-10] p 17 A84-28982
- SZATKOWSKI, G. P.**
- Graphics enhanced computer emulation for improved timing-race and fault tolerance control system analysis [AIAA PAPER 83-2328] p 177 A84-10010
- SZETELA, E. J.**
- Deposit formation and heat transfer in hydrocarbon rocket fuels [AIAA PAPER 84-0512] p 88 A84-18142
- Deposit formation and heat transfer in hydrocarbon rocket fuels [NASA-CR-168277] p 45 N84-12225
- SZUCH, J. R.**
- Digital computer program for generating dynamic turbofan engine models (DIGTEM) [NASA-TM-83446] p 26 N84-16185

## T

- TACINA, R. R.**
- Transient flow combustion p 62 N84-20560
- TAKACS, A. M.**
- Bacterial degradation of polychlorinated biphenyls in sludge from an industrial sewer lagoon [NASA-TM-83543] p 173 N84-11594
- TAM, C. K. W.**
- Sound generated by instability waves of supersonic flows. I Two-dimensional mixing layers. II - Axisymmetric jets p 181 A84-24597
- TAM, L. T.**
- Rocket injector anomalies study. Volume 1: Description of the mathematical model and solution procedure [NASA-CR-174702] p 49 N84-32428
- Rocket injector anomalies study Volume 2 Results of parametric studies [NASA-CR-174703] p 49 N84-32429
- TAN-ATICHAT, J.**
- On the design of contractions and settling chambers for optimal turbulence manipulations in wind tunnels [AIAA PAPER 84-0536] p 115 A84-22922
- TANIS, F. J.**
- Development of Great Lakes algorithms for the Nimbus-G coastal zone color scanner [NASA-CR-173511] p 159 N84-27258
- TARN, R. B.**
- Research study for effects of case flexibility on bearing loads and rotor stability [NASA-CR-171147] p 148 N84-33811
- TASHJIAN, R.**
- AFB/open cycle gas turbine conceptual design study [NASA-CR-168135] p 172 N84-31784
- TAUTZ, M. F.**
- NASCAP simulations of spacecraft charging of the SCATHA satellite p 41 N84-17268
- TAYLOR, A. M. K. P.**
- Developing flow in S-shaped ducts p 116 A84-28709
- TAYLOR, E. J.**
- Importance of interatomic spacing in catalytic reduction of oxygen in phosphoric acid p 58 A84-12644
- TEAGAN, W. P.**
- Catalog of selected heavy duty transport energy management models [NASA-CR-168299] p 194 N84-14991
- TELESMA, J.**
- Evaluation of the effect of crack closure on fatigue crack growth of simulated short cracks [NASA-TM-83778] p 75 N84-31348

- TERDAN, F. F.**
- LERC rail accelerators - Test designs and diagnostic techniques p 42 A84-32031
- TEVAARWERK, J. L.**
- Subsurface stress evaluations under rolling/sliding contacts [ASME PAPER 83-LUB-18] p 137 A84-29099
- TEW, R. C., JR.**
- Downsizing assessment of automotive Stirling engines [NASA-TM-83468] p 194 N84-14989
- Comparison of free-piston Stirling engine model predictions with RE1000 engine test data [NASA-TM-83650] p 195 N84-24509
- THAKKER, A. B.**
- Low strain, long life creep fatigue of AF2-1DA and INCO 718 [NASA-CR-167989] p 66 N84-10268
- THALLER, L. H.**
- Some comments on longevity by a technologist p 45 N84-12247
- Electrochemical storage p 171 N84-29342
- THIMMEACH, D.**
- An SCR inverter with an integral battery charger for electric vehicles p 103 A84-24850
- THIMMESCH, D.**
- Integral inverter/battery charger for use in electric vehicles [NASA-CR-168177] p 194 N84-17073
- THOMAS, D. M.**
- Government - contractor interaction [AD-P002768] p 193 N84-23315
- THOMAS, R. G.**
- Catalog of selected heavy duty transport energy management models [NASA-CR-168299] p 194 N84-14991
- THOMPSON, W. T., JR.**
- Conservative streamtube solution of steady-state Euler equations [AIAA PAPER 84-1643] p 120 A84-38030
- Asymptotic analysis of numerical wave propagation in finite difference equations [NASA-CR-175323] p 98 N84-15360
- THOMPSON, J. W., JR.**
- Uncertainty methodology for in-flight thrust determination [SAE PAPER 831438] p 13 A84-29452
- Application of in-flight thrust determination uncertainty [SAE PAPER 831439] p 13 A84-29453
- THOMPSON, R. L.**
- A computer program for predicting nonlinear uniaxial material responses using viscoplastic models [NASA-TM-83675] p 156 N84-29247
- THULIN, R. D.**
- Energy efficient engine, high-pressure turbine detailed design report [NASA-CR-165608] p 33 N84-28788
- Energy efficient engine, turbine intermediate case and low-pressure turbine component test hardware detailed design report [NASA-CR-167973] p 33 N84-28789
- TIDMAN, D. A.**
- Experimental investigation of the pulsed electrothermal (PET) thruster [AIAA PAPER 84-1386] p 43 A84-35201
- Proposed system design for a 20 kW pulsed electrothermal thruster [AIAA PAPER 84-1387] p 43 A84-35202
- Investigation of a pulsed electrothermal thruster [NASA-CR-168266] p 45 N84-12227
- TIDONA, R. J.**
- Combustion characteristics in the transition region of liquid fuel sprays [NASA-CR-175396] p 61 N84-19495
- TIEN, J. K.**
- Effects of cobalt in nickel-base superalloys [NASA-CR-168308] p 67 N84-14287
- The role of cobalt on the creep of Waspaloy [NASA-CR-174628] p 70 N84-19523
- TIEN, J. S.**
- Combustor flame flashback p 62 N84-20561
- TITRAN, R. H.**
- Creep-rupture behavior of candidate Stirling engine alloys after long-term aging at 760 deg C in low-pressure hydrogen [NASA-TM-83676] p 73 N84-25793
- Advanced high temperature materials for the energy efficient automotive Stirling engine [NASA-TM-83659] p 75 N84-28963
- Evaluation of candidate Stirling engine heater tube alloys after 3500 hours exposure to high pressure doped hydrogen or helium [NASA-TM-83782] p 77 N84-34603
- TOMKO, J. J.**
- Effects of different rub models on simulated rotor dynamics [NASA-TP-2220] p 142 N84-17590

- TORBERT, R. B.**
- Anomalous high potentials observed on ISEE [NASA-CR-172791] p 41 N84-17252
- Anomalous high potentials observed on ISEE p 41 N84-17258
- TOVICHAKCHAIKUL, S.**
- Algorithms for elasto-plastic-creep postbuckling p 152 A84-38480
- TOWNE, C. E.**
- Computation of viscous flow in planar and axisymmetric ducts by an implicit marching procedure [AIAA PAPER 84-0256] p 114 A84-17979
- Comparison of experimental and computational compressible flow in a S-duct [AIAA PAPER 84-0033] p 4 A84-19228
- Computation of viscous flow in curved ducts and comparison with experimental data [AIAA PAPER 84-0531] p 115 A84-21303
- Computation of viscous flow in curved ducts and comparison with experimental data [NASA-TM-83548] p 122 N84-13494
- TOWNSEND, D. P.**
- NASA transmission research and its probable effects on helicopter transmission design p 139 A84-46355
- Status of understanding for gear materials p 144 N84-25061
- Parameter studies of gear cooling using an automatic finite element mesh generator [NASA-TM-83721] p 146 N84-28087
- An investigation of the transient thermal analysis of spur gears [NASA-TM-83724] p 146 N84-28088
- Lubricant jet flow phenomena in spur and helical gears with modified center distances and/or addendums for out-of-mesh conditions [NASA-TM-83723] p 146 N84-29224
- TOZZI, L.**
- New perspectives for advanced automobile diesel engines p 138 A84-30062
- TRIMARCHI, P. A.**
- Structural design of a vertical antenna boresight 18.3 by 18.3-m planar near-field antenna measurement system [NASA-TM-83781] p 133 N84-32783
- TRINER, J. E.**
- Application of advanced materials to rotating machines p 22 N84-10063
- TRIPP, J. H.**
- Numerical methods and computers used in elastohydrodynamic lubrication [NASA-TM-83524] p 141 N84-11498
- TROEGER, R. E.**
- Tip cap for a rotor blade [NASA-CASE-LEW-13654-1] p 28 N84-22560
- TROUT, A. M.**
- Combustion gas properties of various fuels of interest to gas turbine engines [NASA-TM-83682] p 31 N84-24584
- TSENG, H. Q.**
- 0.5 W 2-21 GHz monolithic GaAs distributed amplifier p 103 A84-30857
- GaAs dual-gate FET for operation up to K-band p 104 A84-32281
- TSUCHIYA, T.**
- PURDUE-WINCOF: A computer code for establishing the performance of a fan-compressor unit with water ingestion [NASA-CR-168005] p 34 N84-29875
- TSUZUKU, T.**
- Electronic properties of carbon fibers intercalated with copper chloride p 104 A84-34521
- TUCKER, W. T.**
- Mobile radio alternative systems study. Volume 1: Traffic model [NASA-CR-168062] p 96 N84-10402
- TULEY, E. N.**
- Tip cap for a rotor blade [NASA-CASE-LEW-13654-1] p 28 N84-22560
- TURNER, M. G.**
- Application of a polynomial spline in higher-order accurate viscous-flow computations p 119 A84-35349
- TURNER, G. E.**
- Study of a LH2-fueled topping cycle engine for aircraft propulsion [AIAA PAPER 83-2543] p 15 A84-15207
- Analysis of a topping-cycle, aircraft, gas-turbine-engine system which uses cryogenic fuel [NASA-TP-2294] p 28 N84-21549

## V

- VADYAK, J.**
- Three-dimensional flow simulations for supersonic mixed-compression inlets at incidence p 5 A84-38828

- VAIDYANATHAN, P. N.**  
Analysis of grain boundary phase devitrification of Y2O3- and Al2O3-doped Si3N4 p 79 N84-19792  
Compositional effects on Si3N4 fracture surfaces p 79 N84-19794
- VAKILJ, A.**  
Comparison of experimental and computational compressible flow in a S-duct [AIAA PAPER 84-0033] p 4 N84-19228
- VALGORA, M. E.**  
Factors that influence space station propulsion requirements p 48 N84-29931
- VAN FOSSEN, G. J.**  
Heat transfer distributions around nominal ice accretion shapes formed on a cylinder in the NASA Lewis Long Research Tunnel [AIAA PAPER 84-0017] p 113 N84-17834
- VANEVELD, L.**  
Secondary effects in combustion instabilities leading to flashback p 58 N84-17436
- VANFOSSEN, G. J.**  
Length to diameter ratio and row number effects in short pin fin heat transfer [ASME PAPER 83-GT-54] p 118 N84-33706  
Heat transfer distributions around nominal ice accretion shapes formed on a cylinder in the NASA Lewis long research tunnel [NASA-TM-83557] p 123 N84-14463  
Effect of a rotor wake on heat transfer from a circular cylinder [NASA-TM-83613] p 126 N84-21832
- VANFOSSEN, G. J., JR.**  
Effect of location in an array on heat transfer to a short cylinder in crossflow p 119 N84-36150
- VARNER, M. O.**  
One-dimensional unsteady modeling of supersonic inlet unstart/restart [AIAA PAPER 84-0439] p 4 N84-18094
- VARY, A.**  
Ultrasonic velocity measurement using phase-slope cross-correlation methods [NASA-TM-83794] p 149 N84-34769
- VATSKY, A.**  
Automotive Stirling engine development program [NASA-CR-174622] p 195 N84-32305
- VEERABHADRA RAO, P.**  
Application of signal analysis to cavitation p 122 N84-49192
- VEERABHADRARAO, P.**  
Particulate erosion mechanisms [NASA-TM-83551] p 68 N84-14289
- VERDON, J. M.**  
A linear aerodynamic analysis for unsteady transonic cascades [NASA-CR-3833] p 11 N84-32355
- VERRILLI, M. J.**  
Preliminary study of thermomechanical fatigue of polycrystalline MAR-M 200 [NASA-TP-2280] p 69 N84-17350
- VERZWYVELT, S. A.**  
Long life nickel electrodes for a nickel-hydrogen cell I Initial performance p 162 N84-30186
- VILMANN, C. R.**  
A dynamic analysis of rotary combustion engine seals [NASA-TM-83536] p 141 N84-14519
- VOGEL, P.**  
Emission FTIR analyses of thin microscopic patches of jet fuel residue deposited on heated metal surface [NASA-CR-168331] p 90 N84-17410
- VON GLAHN, U.**  
Velocity and temperature characteristics of two-stream, coplanar jet exhaust plumes [AIAA PAPER 84-2205] p 21 N84-46106
- VON GLAHN, U. H.**  
On some flow characteristics of conventional and excited jets [AIAA PAPER 84-0532] p 181 N84-21304
- VONGLAHN, U. H.**  
Correlation of flight effects on centerline velocity decay for cold-flow acoustically excited jets [NASA-TM-83502] p 182 N84-11883  
On some flow characteristics of conventional and excited jets [NASA-TM-83503] p 182 N84-13922  
Velocity and temperature characteristics of two-stream, coplanar jet exhaust plumes [NASA-TM-83730] p 34 N84-28790  
Helicopter engine core noise p 185 N84-29676
- W**
- WADE, T. O.**  
Approaches to optimization of SS/TDMA time slot assignment [NASA-CR-168328] p 40 N84-16243
- WADSWORTH, A. L., III**  
Study to establish cost projections for production of Redox chemicals [NASA-CR-167881] p 164 N84-11580
- WAGNER, D. A.**  
Advanced propfan drive system characteristics and technology needs [AIAA PAPER 84-1194] p 18 N84-36957
- WAGNER, J. H.**  
Inlet boundary layer effects in an axial compressor rotor. I Blade-to-blade effects [ASME PAPER 84-GT-84] p 6 N84-46926  
Inlet boundary layer effects in an axial compressor rotor II - Throughflow effects [ASME PAPER 84-GT-85] p 7 N84-46927  
Compressor rotor aerodynamics p 26 N84-16210
- WAGNER, R. C.**  
Durable solid lubricant coatings for foil gas bearings to 315 deg C [NASA-TM-83596] p 83 N84-19567
- WAGNER, W. B.**  
Combustor liner construction [NASA-CASE-LEW-14035-1] p 30 N84-24577
- WAITE, W. A.**  
Anion permselective membrane [NASA-TM-174725] p 172 N84-29358
- WALKER, C. L.**  
Ceramic composite liner material for gas turbine combustors [AIAA PAPER 84-0363] p 78 N84-18044  
Ceramic composite liner material for gas turbine combustors [NASA-TM-83490] p 24 N84-14145
- WALKER, D.**  
Steam bottoming cycle for an adiabatic diesel engine [NASA-CR-168255] p 196 N84-33304
- WALKER, E. D.**  
Method of reducing temperature in high-speed photography [NASA-TM-83620] p 188 N84-22421
- WALKINGTON, N. J.**  
A numerical model of acoustic choking I - Shock free solutions p 180 N84-21250
- WALLIS, R. F.**  
Interference phenomena in the refraction of a surface polariton by vertical dielectric barriers p 179 N84-24410
- WALTHER, J. F.**  
Study to establish cost projections for production of Redox chemicals [NASA-CR-167881] p 164 N84-11580
- WANG, C. L.**  
Develop and test fuel cell powered on-site integrated total energy systems Phase 3 Full-scale power plant development [NASA-CR-168294] p 164 N84-13672  
Develop and test fuel cell powered on-site integrated total energy system [NASA-CR-168239] p 164 N84-13673  
Develop and test fuel cell powered on-site integrated total energy systems [NASA-CR-174714] p 170 N84-27329
- WANG, C. R.**  
Turbulence and surface heat transfer near the stagnation point of a circular cylinder in turbulent flow [NASA-TM-83732] p 128 N84-29157
- WANG, C. W.**  
Engineering calculations for communications satellite systems planning [NASA-CR-173532] p 38 N84-23662
- WANG, P. S.**  
Automatic finite element generators p 158 N84-31695
- WANG, S. S.**  
Edge delamination in angle-ply composite laminates p 52 N84-21515  
Elasticity solutions for a class of composite laminate problems with stress singularities p 53 N84-33389
- WANG, S. Y.**  
LeRC rail accelerators - Test designs and diagnostic techniques p 42 N84-32031  
The structural response of a rail acceleration p 151 N84-32039
- WANHAINEN, J. S.**  
Structural design of a vertical antenna boresight 18.3 by 18.3-m planar near-field antenna measurement system [NASA-TM-83781] p 133 N84-32783
- WARD, M.**  
Benchmark cyclic plastic notch strain measurements p 63 N84-11194
- WARK, C. E.**  
Free stream turbulence and density ratio effects on the interaction region of a jet in a cross flow p 125 N84-20546
- WARREN, E. L.**  
Improved compliant hydrodynamic fluid journal bearing [NASA-CASE-LEW-13670-1] p 143 N84-22959
- WASMUNDT, K. C.**  
Optical flip-flops and sequential logic circuits using a liquid crystal light valve p 198 N84-40332
- WASSERBAUER, C.**  
Velocity and temperature characteristics of two-stream, coplanar jet exhaust plumes [AIAA PAPER 84-2205] p 21 N84-46106  
Velocity and temperature characteristics of two-stream, coplanar jet exhaust plumes [NASA-TM-83730] p 34 N84-28790
- WASSERBAUER, C. A.**  
Cross spectra between pressure and temperature in a constant-area duct downstream of a hydrogen-fueled combustor [NASA-TM-83463] p 182 N84-11885
- WATERS, W. J.**  
Multicolor printing plate joining [NASA-CASE-LEW-13598-1] p 132 N84-22930
- WATKINS, W. B.**  
Dynamic gas temperature measurement system, volume 1 [NASA-CR-168267-VOL-1] p 132 N84-16529
- WATSON, J. W.**  
Deposition stress effects on thermal barrier coating burner ng life [NASA-TM-83670] p 85 N84-25830
- WAYNE, S. F.**  
Carbides in iron-rich Fe-Mn-Cr-Mo-Al-Si-C systems p 64 N84-26815
- WEAR, J. D.**  
Combustion gas properties of various fuels of interest to gas turbine engines [NASA-TM-83682] p 31 N84-24584
- WEDEN, G. J.**  
Summary of drive-train component technology in helicopters [NASA-TM-83726] p 147 N84-30294
- WEDEVEN, L. D.**  
Surface topography-connections between lubrication and failure initiation p 144 N84-24898
- WEIKLE, D. H.**  
Optimization of fringe-type laser anemometers for turbine engine component testing [AIAA PAPER 84-1459] p 131 N84-40248  
Optimization of fringe-type laser anemometers for turbine engine component testing [NASA-TM-83658] p 133 N84-25019
- WEIMER, D.**  
Preliminary experiments on phase conjugation for flow visualization [NASA-TM-83766] p 189 N84-32169
- WEINBERG, I.**  
Increased radiation resistance in lithium-counterdoped silicon solar cells p 163 N84-34846  
Radiation damage and defect behavior in ion-implanted, lithium counterdoped silicon solar cells [NASA-TM-83646] p 109 N84-22890  
Radiation tolerance of low resistivity, high voltage silicon solar cells p 170 N84-29318  
Cell and defect behavior in lithium-counterdoped solar cells p 170 N84-29322  
The effects of lithium counterdoping on radiation damage and annealing in n(+)-p silicon solar cells [NASA-TM-83755] p 110 N84-31513
- WEISBRICH, A. L.**  
Technology and benefits of aircraft counter rotation propellers [NASA-CR-168258] p 22 N84-13188
- WEITZ, P. G., JR.**  
Study of effects of fuel properties in turbine-powered business aircraft [NASA-CR-174627] p 91 N84-25854
- WEIZER, V. G.**  
Voltage controlling mechanisms in low resistivity silicon solar cells: A unified approach [NASA-TM-83612] p 167 N84-20916  
The effect of diffusion induced lattice stress on the open-circuit voltage in silicon solar cells [NASA-TM-83667] p 168 N84-23027  
Radiation tolerance of low resistivity, high voltage silicon solar cells p 170 N84-29318
- WELDON, W. F.**  
Energy stores and switches for rail-launcher systems [NASA-CR-173249] p 107 N84-16458
- WENZEL, L. M.**  
Real-time hybrid computer simulation of a small turboshaft engine and control system [NASA-TM-83579] p 28 N84-21548
- WERTH, J.**  
Develop and test fuel cell powered on-site integrated total energy systems. Phase 3: Full-scale power plant development [NASA-CR-168294] p 164 N84-13672

- Develop and test fuel cell powered on-site integrated total energy system  
[NASA-CR-168239] p 164 N84-13673
- Develop and test fuel cell powered on-site integrated total energy systems  
[NASA-CR-174714] p 170 N84-27329
- WESTERKAMP, E. J.**  
Digital computer program for generating dynamic turbofan engine models (DIGTEM)  
[NASA-TM-83446] p 26 N84-16185
- WESTFALL, L. J.**  
Arc spray fabrication of metal matrix composite monolayer  
[NASA-CASE-LEW-13828-1] p 54 N84-15203
- WHEELER, D. R.**  
Tribological applications of surface analysis  
[NASA-TM-83707] p 51 N84-25766
- Adhesion between polymers and evaporated gold and nickel films  
[NASA-TP-2360] p 87 N84-31379
- WHELAN, J. A.**  
Develop and test fuel cell powered on-site integrated total energy systems Phase 3: Full-scale power plant development  
[NASA-CR-168294] p 164 N84-13672
- Develop and test fuel cell powered on-site integrated total energy system  
[NASA-CR-168239] p 164 N84-13673
- Develop and test fuel cell powered on-site integrated total energy systems  
[NASA-CR-174714] p 170 N84-27329
- WHIPPLE, E. C.**  
Anomalous high potentials observed on ISEE  
[NASA-CR-172791] p 41 N84-17252
- Anomalous high potentials observed on ISEE  
p 41 N84-17258
- WHITAKER, A. F.**  
Solar-array-materials passive LDEF experiment (A0171) p 168 N84-24656
- WHITE, B. E.**  
A frequency-division multiple-access system concept for 30/20 GHz high-capacity domestic satellite service  
p 94 A84-22141
- WHITE, G.**  
An advanced pitch change mechanism incorporating a hybrid traction drive  
[AIAA PAPER 84-1383] p 20 A84-44182
- An advanced pitch change mechanism incorporating a hybrid traction drive  
[NASA-TM-83709] p 2 N84-25605
- WHITE, L.**  
Assessment of institutional barriers to the use of natural gas fuel in automotive vehicle fleets  
[NASA-CR-168183] p 165 N84-14587
- WHITE, W.**  
Material considerations for high frequency, high power capacitors  
p 102 A84-22874
- WHITEHAIR, S.**  
Demonstration of a new electrothermal thruster concept  
p 43 A84-34037
- Spatial electron density and electric field strength measurements in microwave cavity experiments  
[AIAA PAPER 84-1522] p 189 A84-46109
- Spatial electron density and electric field strength measurements in microwave cavity experiments  
[NASA-CR-173907] p 111 N84-32682
- WHITELAW, J. H.**  
Developing flow in S-shaped ducts  
p 116 A84-28709
- WHITLOW, J. B., JR.**  
Fuel savings potential of the NASA Advanced Turboprop Program  
[NASA-TM-83736] p 35 N84-29878
- WHITNEY, W. J.**  
Performance of a high-work low aspect ratio turbine tested with a realistic inlet radial temperature profile  
[AIAA PAPER 84-1161] p 19 A84-40239
- Performance of a high-work low aspect ratio turbine tested with a realistic inlet radial temperature profile  
[NASA-TM-83655] p 32 N84-24589
- WHITSON, D. W.**  
Double-injection, deep-impurity switch development  
[NASA-CR-168335] p 108 N84-18536
- WHITTENBERGER, J. D.**  
The effect of a coating on the thermo-oxidative stability of Celcon 6000 graphite fiber/PMR 15 polyimide composites  
p 52 A84-21844
- A simple application of the Bailey-Orowan creep model to Fe-39 B at pct Al and gamma/gamma prime - alpha  
p 64 A84-22012
- Off-axis tensile properties and fracture in a unidirectional graphite/polyimide composite (Celcon 6000/PMR 15)  
p 53 A84-43553
- Elevated temperature compressive steady state deformation and failure in the oxide dispersion strengthened alloy MA 6000E  
p 66 A84-46785
- Method and apparatus for gripping uniaxial fibrous composite materials  
[NASA-CASE-LEW-13758-1] p 56 N84-27829
- WHITTLESEY, A. C.**  
Design guidelines for assessing and controlling spacecraft charging effects  
[NASA-TP-2361] p 42 N84-33452
- WHYTE, W.**  
The effect of variable S/N on the subjective evaluation of protection ratios for direct-TV satellite services  
p 95 A84-48452
- WHYTE, W. A., JR.**  
The subjective effect of multiple co-channel frequency modulated television interference  
[NASA-TM-83415] p 97 N84-11360
- WIGGERT, D. C.**  
Modeling of transient two-component flow using a four-point implicit method  
p 112 A84-13237
- WILCOX, R. W.**  
Tabulations of ozonesonde data, 1963 - 1980  
[NASA-CR-174631] p 174 N84-27375
- WILKINSON, C. L.**  
Factors that influence space station propulsion requirements  
p 48 N84-29931
- WILLIAMS, D. D.**  
Uncertainty methodology for in-flight thrust determination  
[SAE PAPER 831438] p 13 A84-29452
- Application of in-flight thrust determination uncertainty  
[SAE PAPER 831439] p 13 A84-29453
- WILLIAMS, G. C.**  
Interply layer degradation effects on composite structural response  
[NASA-TM-83702] p 56 N84-26756
- WILLIAMS, J. R.**  
Combustor development for automotive gas turbines  
p 135 A84-10499
- WILLIAMS, J., JR.**  
Input-output characterization of an ultrasonic testing system by digital signal analysis  
[NASA-CR-3756] p 149 N84-15585
- WILLIS, E. A.**  
An overview of NASA intermittent combustion engine research  
[AIAA PAPER 84-1393] p 19 A84-40244
- An overview of NASA intermittent combustion engine research  
[NASA-TM-83688] p 31 N84-24583
- WILREKER, V. F.**  
Wind turbine generator interaction with conventional diesel generators on Block Island, Rhode Island Volume 1. Executive summary  
[NASA-CR-168318] p 171 N84-29357
- Wind turbine generator interaction with conventional diesel generators on Block Island, Rhode Island Volume 2: Data analysis  
[NASA-CR-168319] p 172 N84-31783
- WILSON, D. R.**  
Transient flow analysis of the AEDC/HPDE MHD generator  
p 189 A84-24049
- WILSON, J. D.**  
Tropical response to lateral forcing with a latitudinally and zonally nonuniform basic state  
p 174 A84-40399
- WILSON, R. B.**  
Three-dimensional stress analysis using the boundary element method  
p 159 N84-31700
- WILSON, R. P., JR.**  
Catalog of selected heavy duty transport energy management models  
[NASA-CR-168299] p 194 N84-14991
- WILSON, S. B., III**  
Tandem fan applications in advanced STOVL fighter configurations  
[AIAA PAPER 84-1402] p 19 A84-40245
- Tandem fan applications in advanced STOVL fighter configurations  
[NASA-TM-83689] p 30 N84-24579
- WILSON, S. G.**  
Camer recovery methods for a dual-mode modem A design approach  
[NASA-CR-173355] p 36 N84-19360
- Design considerations for a monolithic, GaAs, dual-mode, QPSK/QASK, high-throughput rate transceiver  
[NASA-CR-173560] p 110 N84-24974
- WILSON, T. G.**  
Parametric study of minimum converter loss in an energy-storage dc-to-dc converter  
p 101 A84-18403
- WINGET, J. M.**  
Element-by-element solution procedures for nonlinear structural analysis  
p 158 N84-31694
- WINSER, E. A.**  
Tungsten-fiber-reinforced superalloy composite, high-temperature component design considerations  
p 53 A84-28241
- WINSOR, N. K.**  
Experimental investigation of the pulsed electrothermal (PET) thruster  
[AIAA PAPER 84-1386] p 43 A84-35201
- Proposed system design for a 20 kW pulsed electrothermal thruster  
[AIAA PAPER 84-1387] p 43 A84-35202
- Investigation of a pulsed electrothermal thruster  
[NASA-CR-168266] p 45 N84-12227
- WINTUCKY, E. G.**  
Ion sputter textured graphite electrode plates  
[NASA-CASE-LEW-12919-2] p 179 N84-28565
- WINTUCKY, W. T.**  
An overview of NASA intermittent combustion engine research  
[AIAA PAPER 84-1393] p 19 A84-40244
- An overview of NASA intermittent combustion engine research  
[NASA-TM-83688] p 31 N84-24583
- WIRSCHING, P. H.**  
Advanced reliability method for fatigue analysis  
p 151 A84-31596
- Creep-rupture reliability analysis  
[NASA-CR-3790] p 155 N84-19925
- WISANDER, D. W.**  
Method of fabricating an abradable gas path seal  
[NASA-CASE-LEW-13269-2] p 143 N84-22957
- WISLER, D. C.**  
Loss reduction in axial-flow compressors through low-speed model testing  
[ASME PAPER 84-GT-184] p 7 A84-46985
- WISNIEWSKI, J.**  
High-speed wide band 20 x 20 microwave switch matrix  
p 105 A84-49253
- WOLFSON, R. G.**  
Ion implanted junctions for silicon space solar cells  
p 42 A84-30143
- WONG, C. P.**  
Boundary layer transition effects on flow separation around V/STOL engine inlets at high incidence  
[AIAA PAPER 84-0432] p 4 A84-18090
- WONG, R. C.**  
Parametric study of minimum converter loss in an energy-storage dc-to-dc converter  
p 101 A84-18403
- WOOD, J. C.**  
New perspectives for advanced automobile diesel engines  
p 138 A84-30062
- WOOD, J. G.**  
How to protect a wind turbine from lightning  
[NASA-CR-168229] p 163 N84-10661
- WOOD, J. R.**  
Investigation of the three-dimensional flow field within a transonic fan rotor - Experiment and analysis  
[ASME PAPER 84-GT-200] p 7 A84-46995
- Investigation of the three-dimensional flow field within a transonic fan rotor: Experiment and analysis  
[NASA-TM-83739] p 11 N84-32357
- WOODWARD, R. P.**  
Tone generation by rotor-downstream strut interaction  
p 16 A84-22174
- Low flight speed fan noise from a supersonic inlet  
p 182 A84-44508
- Fan noise reduction achieved by removing tip flow irregularities behind the rotor - forward arc test configurations  
[NASA-TM-83616] p 184 N84-23235
- WOOLLAM, J. A.**  
Electronic properties of carbon fibers intercalated with copper chloride  
p 104 A84-34521
- WORRELL, W. L.**  
Reaction of cobalt in SO<sub>2</sub> atmospheres at elevated temperatures  
p 65 A84-33440
- WORTMAN, A.**  
Detonation wave augmentation of gas turbines  
[AIAA PAPER 84-1266] p 18 A84-37639
- WRENN, G.**  
Comparison of thermal plasma observations on SCATHA and GEOS  
p 41 N84-17262
- WRIGHT, D. V.**  
Labyrinth seal forces on a whirling rotor  
p 135 A84-13228
- WU, C. D.**  
Electrochemical studies of redox systems for energy storage  
[NASA-CR-174503] p 165 N84-15681
- WU, J. M.**  
Comparison of experimental and computational compressible flow in a S-duct  
[AIAA PAPER 84-0033] p 4 A84-19228
- WU, K. Y.**  
Steady state stresses in nylon parachute canopies  
[AIAA PAPER 84-0816] p 11 A84-26580
- WU, Y.-T.**  
Advanced reliability method for fatigue analysis  
p 151 A84-31596

## Y

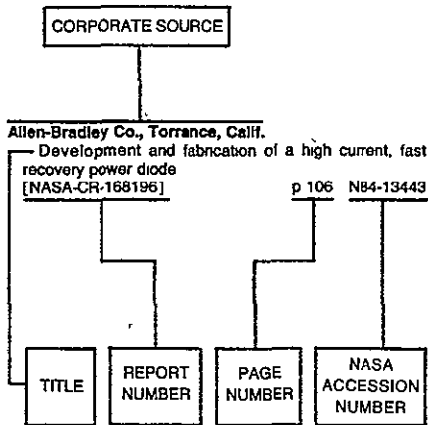
- YAMADA, Y.**  
Adhesion between polymers and evaporated gold and nickel films  
[NASA-TP-2360] p 87 N84-31379
- YAMAGISHI, F. G.**  
Plasma polymerized high energy density dielectric films for capacitors  
[NASA-CR-168233] p 81 N84-13310
- YAMAMOTO, K.**  
Experimental investigation of shock-cell noise reduction for dual-stream nozzles in simulated flight comprehensive data report. Volume 1: Test nozzles and acoustic data [NASA-CR-168336-VOL-1] p 184 N84-24323  
Experimental investigation of shock-cell noise reduction for dual-stream nozzles in simulated flight comprehensive data report. Volume 2: Laser velocimeter data, static pressures and shadowgraph photos [NASA-CR-168336-VOL-2] p 184 N84-24324  
Experimental investigation of shock-cell noise reduction for single-stream nozzles in simulated flight, comprehensive data report. Volume 1: Test nozzles and acoustic data [NASA-CR-168234-VOL-1] p 185 N84-33148  
Experimental investigation of shock-cell noise reduction for single-stream nozzles in simulated flight, comprehensive data report. Volume 2: Laser velocimeter data [NASA-CR-168234-VOL-2] p 186 N84-33149  
Experimental investigation of shock-cell noise reduction for single-stream nozzles in simulated flight, comprehensive data report. Volume 3: Shadowgraph photos and facility description [NASA-CR-168234-VOL-3] p 186 N84-33150
- YANG, S. H.**  
Indentation law for composite laminates  
p 52 A84-27356
- YANG, Y.**  
Thermal and elastohydrodynamic analysis of reciprocating rod seals in the Stirling engine  
p 138 A84-30085
- YATES, K.**  
Development of partially fluorinated resin apex seals  
[NASA-CR-174706] p 148 N84-32328
- YAVROUJIAN, A.**  
Electronic properties of carbon fibers intercalated with copper chloride  
p 104 A84-34521
- YEAGER, E.**  
Electrochemical studies of redox systems for energy storage  
[NASA-CR-174503] p 165 N84-15581
- YEH, F. C.**  
Review and status of heat-transfer technology for internal passages of air-cooled turbine blades  
[NASA-TP-2232] p 126 N84-21828
- YEH, H. C.**  
Consolidation of Si<sub>3</sub>N<sub>4</sub> without additives (by hot isostatic pressing)  
[NASA-CR-173279] p 82 N84-17389
- YIANNESKIS, M.**  
Developing flow in S-shaped ducts  
p 116 A84-28709
- YONUSHONIS, T. M.**  
Solid lubrication design methodology  
[NASA-CR-174690] p 196 N84-33309
- YOON, H. K.**  
Further time-mean measurements in confined swirling flows  
p 116 A84-27138
- YOUNG, L. E.**  
Solar-array-materials passive LDEF experiment (A0171)  
p 168 N84-24656
- YOUNG, S. G.**  
Morphology of an aluminum alloy eroded by a normally incident jet of angular erodent particles  
p 64 A84-18244  
A study of the effect of solid particle impact and particle shape on the erosion morphology of ductile metals  
p 68 A84-45570
- YU, C. H.**  
Prediction of turbulent flow past a prosthetic heart valve  
p 175 A84-49108
- YURKOVICH, S.**  
An application of tensor ideas to nonlinear modeling of a turbofan jet engine  
p 20 A84-42382
- YUSTINICH, J. B.**  
Energy efficient engine Low-pressure turbine subsonic cascade component development and integration program  
[NASA-CR-165502] p 33 N84-27738

## Z

- ZAGHILOUL, A. I.**  
Phased-array-fed antenna configuration study. Volume 1: Technology assessment  
[NASA-CR-168231] p 98 N84-16423  
Phased-array-fed antenna configuration study, volume 2  
[NASA-CR-168232] p 98 N84-16424
- ZAGULI, R. J.**  
Results of an experimental program investigating the effects of simulated ice on the performance of the NACA 63A415 airfoil with flap  
[NASA-CR-168288] p 8 N84-16145  
Potential flow analysis of glaze ice accretions on an airfoil  
[NASA-CR-168282] p 8 N84-16146
- ZAKRAJSEK, R. J.**  
Characteristics and capacities of the NASA Lewis Research Center high precision 6.7- by 6.7-m planar near-field scanner  
[NASA-TM-83785] p 133 N84-32789
- ZANA, L. M.**  
LeRC rail accelerators - Test designs and diagnostic techniques  
p 42 A84-32031
- ZAPLATYNSKY, I.**  
Shrinkage of amorphous silica fibers  
p 77 A84-13504  
Method and apparatus for coating substrates using a laser  
[NASA-CASE-LEW-13525-1] p 134 N84-22944
- ZARETSKY, E. V.**  
Precision of spiral-bevel gears  
[ASME PAPER 82-WA/DE-33] p 135 A84-15950  
Kinematic precision of gear trains  
[ASME PAPER 82-WA/DE-34] p 135 A84-15951  
NASA transmission research and its probable effects on helicopter transmission design  
p 139 A84-46355
- ZAVESKY, R. J.**  
Improved heat exchanger for electrothermal devices  
[NASA-CASE-LEW-14037-1] p 49 N84-32425
- ZEID, I.**  
Nonlinear transient finite element analysis of rotor-bearing-stator systems  
p 136 A84-20580
- ZHANG, Q. F.**  
A theoretical and experimental study of turbulent particle-laden jets  
[NASA-CR-168293] p 23 N84-13187  
A theoretical and experimental study of turbulent nonevaporating sprays  
[NASA-CR-174668] p 35 N84-29877  
A theoretical and experimental study of turbulent evaporating sprays  
[NASA-CR-174760] p 35 N84-32390
- ZHANG, Q.-F.**  
Structure of particle-laden jets - Measurements and predictions  
[AIAA PAPER 84-0038] p 113 A84-17842  
Structure of nonevaporating sprays - Measurements and predictions  
[AIAA PAPER 84-0125] p 114 A84-17897
- ZHONG, W. F.**  
Volume integrals associated with the inhomogeneous Helmholtz equation. Part 2: Cylindrical region, rectangular region  
[NASA-CR-3750] p 148 N84-14526
- ZIEGLER, C.**  
Computer simulator for a mobile telephone system  
[NASA-CR-174533] p 95 N84-10401
- ZIERKE, W. C.**  
The boundary layer on compressor cascade blades  
[NASA-CR-173514] p 127 N84-25001
- ZIMMERMAN, D. K.**  
MOD-2 wind turbine development  
[NASA-TM-83460] p 164 N84-13670
- ZINN, B. T.**  
A parametric study of the effect of inlet lip shape upon the radiated sound field  
[AIAA PAPER 84-0498] p 180 A84-18131  
A finite element approach for predicting nozzle admittances  
p 180 A84-21184
- ZOLA, C. L.**  
Tandem fan applications in advanced STOVL fighter configurations  
[AIAA PAPER 84-1402] p 19 A84-40245  
Tandem fan applications in advanced STOVL fighter configurations  
[NASA-TM-83689] p 30 N84-24579
- ZOWARKA, R. C.**  
Energy stores and switches for rail-launcher systems  
[NASA-CR-173249] p 107 N84-16458
- ZUMWALT, G. W.**  
Flight and wind tunnel tests of an electro-impulse de-icing system  
[AIAA PAPER 84-2234] p 12 A84-39280

# CORPORATE SOURCE INDEX

## Typical Corporate Source Index Listing



Listings in this index are arranged alphabetically by corporate source. The title of the document is used to provide a brief description of the subject matter. The page number and the accession number are included in each entry to assist the user in locating the abstract in the abstract section. If applicable, a report number is also included as an aid in identifying the document.

## A

- Aerodyne Research, Inc., Bedford, Mass.**  
Automatic holographic droplet analysis for liquid fuel sprays p 125 N84-20531
- Aerojet Liquid Rocket Co., Sacramento, Calif.**  
Test verification of LOX/RP-1 high-pressure fuel/oxidizer-rich preburner designs p 42 N84-22134
- Aerojet Techsystems Co., Sacramento, Calif.**  
Selection of burn-resistant materials for oxygen-driven turbopumps [AIAA PAPER 84-1287] p 43 A84-35157
- Aerometrics, Inc., Mountain View, Calif.**  
Development of the phase/Doppler spray analyzer for liquid drop size and velocity characterizations [AIAA PAPER 84-1199] p 131 A84-36958  
Analysis and testing of a new method for drop size measurement using laser scatter interferometry [NASA-CR-174636] p 133 N84-31595
- Air Force Aero Propulsion Lab., Wright-Patterson AFB, Ohio.**  
Vibrations of twisted cantilevered plates - Experimental investigation [ASME PAPER 84-GT-96] p 152 A84-46937
- Air Force Geophysics Lab., Hanscom AFB, Mass.**  
Charged particle effects on space systems [AD-P002103] p 187 N84-26189  
High voltage solar array models and Shuttle tile charging [AD-P002123] p 177 N84-26209
- Air Force Systems Command, Wright-Patterson AFB, Ohio.**  
Uncertainty methodology for in-flight thrust determination [SAE PAPER 831438] p 13 A84-29452  
Application of in-flight thrust determination uncertainty [SAE PAPER 831439] p 13 A84-29453
- Akron Univ., Ohio.**  
Nonlinear transient finite element analysis of rotor-bearing-stator systems p 136 A84-20560

- A thermomechanical model for energy propagation in a solid-fluid-solid system with one boundary in relative motion [ASME PAPER 83-HT-97] p 137 A84-29092  
Algorithms for elasto-plastic-creep postbuckling p 152 A84-38480  
Heat transfer in thermal barrier coated rods with circumferential and radial temperature gradients [ASME PAPER 84-GT-181] p 121 A84-46982  
High temperature thermomechanical analysis of ceramic coatings p 152 A84-48565  
Experimental study of uncentralized squeeze film dampers [NASA-CR-168317] p 155 N84-19927  
Nonlinear finite element analysis of shells with large aspect ratio p 158 N84-31692  
Self-adaptive solution strategies p 158 N84-31693
- Alabama Univ., Huntsville.**  
Comparison of thermal plasma observations on SCATHA and GEOS p 41 N84-17262
- Allen-Bradley Co., Torrance, Calif.**  
Development and fabrication of a high current, fast recovery power diode [NASA-CR-168196] p 106 N84-13443
- Allied Chemical Corp., Solvay, N. Y.**  
Study to establish cost projections for production of Redox chemicals [NASA-CR-167861] p 164 N84-11580
- Ames Lab., Iowa.**  
Scaling relations in the equation of state, thermal expansion, and melting of metals p 192 A84-19359
- Analex Corp., Cleveland, Ohio.**  
Approaches to optimization of SS/TDMA time slot assignment [NASA-CR-168328] p 40 N84-16243  
Modular approach for satellite communication ground terminals [NASA-CR-168327] p 98 N84-16425  
Engineering correlations of variable-property effects on laminar forced convection mass transfer for dilute vapor species and small particles in air [NASA-CR-166922] p 124 N84-18578  
Users' manual for computer program for three-dimensional analysis of coupler-cavity traveling wave tubes [NASA-CR-168269] p 109 N84-23841
- Applied Solar Energy Corp., City of Industry, Calif.**  
Recent advances in thin silicon solar cells p 160 A84-22981
- Arizona State Univ., Tempe.**  
Software simulator for multiple computer simulation system p 176 A84-11892  
A blade loss response spectrum for flexible rotor systems [ASME PAPER 84-GT-29] p 139 A84-46893  
Forced convection heat transfer to air/water vapor mixtures [NASA-CR-3769] p 123 N84-16468  
An experimental investigation of gas jets in confined swirling air flow [NASA-CR-3832] p 36 N84-33412
- Arizona Univ., Tucson.**  
Interference phenomena in the refraction of a surface polariton by vertical dielectric barriers p 179 A84-24410  
Advanced reliability method for fatigue analysis p 151 A84-31596  
Creep-rupture reliability analysis [NASA-CR-3790] p 155 N84-19925
- Army Aviation Research and Development Command, Cleveland, Ohio.**  
Ceramic composite liner material for gas turbine combustors [AIAA PAPER 84-0363] p 78 A84-18044  
Ceramic composite liner material for gas turbine combustors [NASA-TM-83490] p 24 N84-14145  
Detailed flow measurements in casing boundary layer of 429-meter-per-second-tip-speed two-stage fan [NASA-TP-2052] p 34 N84-28795

- Army Propulsion Lab., Cleveland, Ohio.**  
Precision of spiral-bevel gears - [ASME PAPER 82-WA/DE-33] p 135 A84-15950  
Kinematic precision of gear trains [ASME PAPER 82-WA/DE-34] p 135 A84-15951  
Thermal degradation of the tensile properties of unidirectionally reinforced FP-Al<sub>2</sub>O<sub>3</sub>/E2 33 magnesium composites p 52 A84-28229  
Application of a quasi-3D inviscid flow and boundary layer analysis to the hub-shroud contouring of a radial turbine [AIAA PAPER 84-1297] p 6 A84-44177  
An analytical method to predict efficiency of aircraft gearboxes [AIAA PAPER 84-1500] p 20 A84-44180  
The application of LQR synthesis techniques to the turboshaft engine control problem [AIAA PAPER 84-1455] p 21 A84-44185  
Investigation of the three-dimensional flow field within a transonic fan rotor - Experiment and analysis [ASME PAPER 84-GT-200] p 7 A84-46995
- Army Research and Technology Labs., Cleveland, Ohio.**  
Comparison between measured turbine stage performance and the predicted performance using quasi-3D flow and boundary layer analyses [AIAA PAPER 84-1299] p 18 A84-36972  
Effects of different rub models on simulated rotor dynamics [NASA-TP-2220] p 142 N84-17590  
Hydrodynamic lubrication of rigid nonconformal contacts in combined rolling and normal motion [NASA-TM-83578] p 142 N84-17592  
Efficiency of nonstandard and high contact ratio involute spur gears [NASA-TM-83725] p 146 N84-29223  
Comparison of icing cloud instruments for 1982-1983 icing season flight program [NASA-TM-83569] p 14 N84-29870  
Transmission efficiency measurements and correlations with physical characteristics of the lubricant [NASA-TM-83740] p 147 N84-30293  
Summary of drive-train component technology in helicopters [NASA-TM-83726] p 147 N84-30294  
Investigation of the three-dimensional flow field within a transonic fan rotor: Experiment and analysis [NASA-TM-83739] p 11 N84-32357  
Analytical and experimental investigation of stator endwall contouring in a small axial-flow turbine [NASA-TP-2309] p 35 N84-32388
- Arnold Engineering Development Center, Arnold Air Force Station, Tenn.**  
Measurements of local convective heat transfer coefficients on ice accretion shapes [AIAA PAPER 84-0018] p 113 A84-17835

## B

- Battelle Columbus Labs., Ohio.**  
Subsurface stress evaluations under rolling/sliding contacts [ASME PAPER 83-LUB-18] p 137 A84-29099  
Creep fatigue of low-cobalt superalloys. Waspalloy, PM U 700 and wrought U 700 [NASA-CR-168260] p 67 N84-13265
- Bell Aerospace Co., Buffalo, N. Y.**  
Flutter analysis of advanced turbopropellers p 152 A84-36492
- Bell Telephone Labs., Inc., Whippany, N. J.**  
Stability analysis of a buck regulator employing input filter compensation p 102 A84-18412
- Beltran Associates, Inc., Syosset, N.Y.**  
Heat pipe applications in aircraft propulsion [AIAA PAPER 84-1269] p 18 A84-37640
- Boeing Aerospace Co., Seattle, Wash.**  
Study of auxiliary propulsion requirements for large space systems Volume 1. Executive summary [NASA-CR-168193-VOL-1] p 45 N84-12226



- Study of auxiliary propulsion requirements for large space systems, volume 2 p 45 N84-13218  
[NASA-CR-168193-VOL-2]
- Evaluation of propellant tank insulation concepts for low-thrust chemical propulsion systems p 46 N84-20634  
[NASA-CR-168320]
- Characterization of PMR polyimide resin and prepreg [NASA-CR-168217] p 83 N84-20695
- Evaluation of propellant tank insulation concepts for low-thrust chemical propulsion systems: Executive summary p 83 N84-20699  
[NASA-CR-168321]
- Boeing Military Airplane Development, Wichita, Kans.**
- Uncertainty methodology for in-flight thrust determination [SAE PAPER 831438] p 13 A84-29452
- Application of in-flight thrust determination uncertainty [SAE PAPER 831439] p 13 A84-29453
- Boeing Vertol Co., Philadelphia, Pa.**
- Performance degradation of propeller systems due to rime ice accretion p 12 A84-17406  
[AIAA PAPER 82-0286]
- Helicopter rotor performance degradation in natural icing encounter p 12 A84-17412
- Development of large rotorcraft transmissions p 21 A84-46354
- British Columbia Univ., Vancouver.**
- The production of turbulent stress in a shear flow by irrotational fluctuations p 115 A84-18357
- The production of turbulent stress in a shear flow by irrotational fluctuations p 115 A84-21390
- California Inst. of Tech., Pasadena**
- Stability and structure of stretched vortices [AD-A142913] p 117 A84-29798
- Three-dimensional stability of an elliptical vortex in a straining field [AD-A146317] p 120 A84-38557
- California State Univ., Fullerton.**
- Detonation wave augmentation of gas turbines [AIAA PAPER 84-1266] p 18 A84-37639
- California Univ., Berkeley.**
- Combustion in a turbulent mixing layer formed at a rearward-facing step p 58 A84-10140
- Secondary effects in combustion instabilities leading to flashback p 58 A84-17436
- Formation and inflammation of a turbulent jet [AIAA PAPER 84-0572] p 114 A84-18171
- Self-similar blast waves incorporating deflagrations of variable speed p 116 A84-28379
- Dynamic effects of combustion p 59 A84-29128
- Random element method for numerical modeling of diffusional processes p 119 A84-35318
- Numerical solution for the problem of flame propagation by the random element method p 60 A84-48139
- Experimental and theoretical study of combustion jet ignition [NASA-CR-168139] p 21 N84-10054
- Numerical modeling of turbulent flow in a channel [NASA-CR-168278] p 23 N84-13189
- California Univ., Irvine.**
- Interference phenomena in the refraction of a surface polariton by vertical dielectric barriers p 179 A84-24410
- California Univ., La Jolla.**
- Anomalous high potentials observed on ISEE p 41 N84-17258
- California Univ., Livermore.**
- Aging results for PRD 49 III/epoxy and Kevlar 49/epoxy composite pressure vessels p 52 A84-21847
- California Univ., Los Angeles.**
- Parallelism and pipelining in high-speed digital simulators p 175 A84-11876
- A scheme for handling arrays in data-flow systems p 175 A84-39972
- Ceramic-to-metal bonding for pressure transducers [NASA-CR-173500] p 84 N84-22753
- Dataflow computing approach in high-speed digital simulation [NASA-CR-173552] p 176 N84-25336
- California Univ., San Diego, La Jolla.**
- Anomalous high potentials observed on ISEE [NASA-CR-172791] p 41 N84-17252
- California Univ., Santa Barbara.**
- Scaling relations in the equation of state, thermal expansion, and melting of metals p 192 A84-19359
- The chemical kinetics and thermodynamics of sodium species in oxygen-rich hydrogen flames p 59 A84-27724
- Cambridge Univ. (England).**
- The production of turbulent stress in a shear flow by irrotational fluctuations p 115 A84-18357
- The production of turbulent stress in a shear flow by irrotational fluctuations p 115 A84-21390
- Carborundum Co., Niagara Falls, N. Y.**
- Processing of sintered alpha SiC [ASME PAPER 84-GT-127] p 140 A84-46954
- Progress in net shape fabrication of alpha sic turbine components [ASME PAPER 84-GT-273] p 140 A84-47036
- Carnegie-Mellon Univ., Pittsburgh, Pa.**
- Direct and implicit optical matrix-vector algorithms p 187 A84-13184
- Turbulent flow field calculations in an internal combustion engine equipped with two valves p 112 A84-13311
- State estimation Kalman filter using optical processings Noise statistics known p 178 A84-23602
- Advanced acousto-optic signal processors p 187 A84-28485
- Dynamics of two-phase face seals p 137 A84-28792
- Thermal and elastohydrodynamic analysis of reciprocating rod seals in the Stirling engine p 138 A84-30085
- Model development and statistical investigation of turbine blade mistuning p 17 A84-31905
- Optical Kalman filtering for missile guidance p 178 A84-38596
- Formation and destruction of vortices in a motored four-stroke piston-cylinder configuration p 139 A84-38838
- Acoustooptic linear algebra processors - Architectures, algorithms, and applications p 175 A84-40266
- The interaction between mistuning and friction in the forced response of bladed disk assemblies [ASME PAPER 84-GT-139] p 152 A84-46957
- Turbulent swirling combustion p 61 N84-20535
- Optical systolic solutions of linear algebraic equations p 188 N84-22405
- Case Western Reserve Univ., Cleveland, Ohio.**
- The development of directional coarsening of the gamma-prime precipitate in superalloy single crystals p 63 A84-10597
- Structure of transient oxides formed on NiCrAl alloys p 63 A84-12385
- Internal heat transfer coefficients of porous metals p 112 A84-13239
- Experimental studies on two dimensional shock boundary layer interactions [AIAA PAPER 84-0099] p 3 A84-17881
- Residual stress in plasma-sprayed ceramic turbine tip and gas-path seal specimens p 78 A84-19763
- Correlation of compressive and shear stress with spalling of plasma-sprayed ceramic materials p 79 A84-19784
- The effect of annealing on the creep of plasma-sprayed ceramics p 79 A84-19785
- Bubble formation in oxide scales on SiC p 79 A84-23689
- Output statistics of laser anemometers in sparsely seeded flows p 117 A84-28738
- Optimizing and comparing laser anemometers p 130 A84-28739
- A thermomechanical model for energy propagation in a solid-fluid-solid system with one boundary in relative motion [ASME PAPER 83-HT-97] p 137 A84-29092
- Circuit equivalent to the elastic spherical shell p 104 A84-39197
- Thermal oxidation of 3C silicon carbide single-crystal layers on silicon p 191 A84-49620
- Effect of crack curvature on stress intensity factors for ASTM standard compact tension specimens [NASA-CR-168280] p 153 N84-11513
- Electrochemical studies of redox systems for energy storage [NASA-CR-174503] p 165 N84-15681
- Applications of photoacoustic techniques to the study of jet fuel residue [NASA-CR-173322] p 90 N84-18420
- Crack layer theory [NASA-CR-174634] p 156 N84-22980
- Millimeter wave transmission systems and related devices [NASA-CR-173515] p 99 N84-24918
- Scaling and modeling of three-dimensional, end-wall, turbulent boundary layers [NASA-CR-3792] p 127 N84-25941
- Dilution jets in accelerated cross flows [NASA-CR-174717] p 34 N84-28794
- Particle environment [NASA-CR-173888] p 191 N84-33210
- Mechanical behavior of carbon-carbon composites [NASA-CR-174767] p 57 N84-34575
- On stress analysis of a crack-layer [NASA-CR-174774] p 159 N84-34774
- Catalytic, Inc., Philadelphia, Pa.**
- AFB/open cycle gas turbine conceptual design study [NASA-CR-168135] p 172 N84-31784
- Centro Tecnico Aeroespacial, San Jose dos Campos (Brazil).**
- Convective heat transfer studies at high temperatures with pressure gradient for inlet flow Mach number of 0.45 [AIAA PAPER 84-1487] p 119 A84-35233
- Cessna Aircraft Co., Wichita, Kans.**
- Flight and wind tunnel tests of an electro-impulse de-icing system [AIAA PAPER 84-2234] p 12 A84-39280
- CHAM of North America, Inc., Huntsville, Ala.**
- Rocket injector anomalies study. Volume 1: Description of the mathematical model and solution procedure [NASA-CR-174702] p 49 N84-32428
- Rocket injector anomalies study. Volume 2: Results of parametric studies [NASA-CR-174703] p 49 N84-32429
- Chronos Research Labs., Inc., Olivehain, Calif.**
- Pyroelectric conversion in space A conceptual design study [NASA-CR-168272] p 165 N84-14585
- Chu Associates, Inc., Littleton, Mass.**
- Reflector antennas with low sidelobes, low cross polarization, and high aperture efficiency [NASA-CR-174670] p 100 N84-31464
- Cincinnati Univ., Ohio.**
- A direct method for the solution of unsteady two-dimensional incompressible Navier-Stokes equations p 2 A84-10078
- Hybrid C-H grids for turbomachinery cascades p 3 A84-11591
- Application of a polynomial spline in higher-order accurate viscous-flow computations p 119 A84-35349
- On numerical simulation of viscous flows p 122 A84-49112
- City Coll. of the City Univ. of New York.**
- Computer simulator for a mobile telephone system [NASA-CR-174533] p 95 N84-10401
- Clarkson Coll. of Technology, Potsdam, N.Y.**
- Electrode kinetics of oxygen reduction - A theoretical and experimental analysis of the rotating ring-disc electrode method p 59 A84-29999
- Cleveland State Univ., Ohio.**
- The effect of variable S/N on the subjective evaluation of protection ratios for direct-TV satellite services p 95 A84-48452
- Consolidation of Si3N4 without additives (by hot isostatic pressing) [NASA-CR-173279] p 82 N84-17389
- Preliminary investigation of an electrical network model for ultrasonic scattering [NASA-CR-3770] p 149 N84-17606
- Optimization methods applied to hybrid vehicle design [NASA-CR-168292] p 194 N84-19185
- Effects of unsteady free stream velocity and free stream turbulence on stagnation point heat transfer [NASA-CR-3804] p 127 N84-25943
- Dynamics of early planetary gear trains [NASA-CR-3793] p 145 N84-26027
- Manual of phosphoric acid fuel cell power plant cost model and computer program [NASA-CR-174720] p 173 N84-34037
- College of William and Mary, Williamsburg, Va.**
- ADA and multi-microprocessor real-time simulation p 176 A84-10905
- Colorado State Univ., Fort Collins.**
- Stress measurement in thin films by geometrical optics p 130 A84-28797
- Experimental investigation of a Hall-current thruster [NASA-CR-168133] p 46 N84-18321
- Sputtering phenomena in ion thrusters [NASA-CR-168172] p 46 N84-18322
- Colorado Univ., Denver.**
- Optical flip-flops and sequential logic circuits using a liquid crystal light valve p 188 A84-40332
- Columbia Univ., New York.**
- Effects of cobalt in nickel-base superalloys [NASA-CR-168308] p 67 N84-14287
- The role of cobalt on the creep of Waspaloy [NASA-CR-174628] p 70 N84-19523
- Communications Satellite Corp., Clarksburg, Md.**
- Surface effects in high voltage silicon solar cells p 160 A84-23002
- ACTS TDMA network control [AIAA PAPER 84-0682] p 94 A84-25274
- Thin N-I-P radiation resistant solar cells [NASA-CR-168284] p 166 N84-15682
- Phased-array-fed antenna configuration study Volume 1. Technology assessment [NASA-CR-158231] p 98 N84-16423
- Phased-array-fed antenna configuration study, volume 2 [NASA-CR-168232] p 98 N84-16424

**Connecticut Univ., Storrs.**

- Carbides in iron-rich Fe-Mn-Cr-Mo-Al-Si-C systems  
p 64 A84-26815
- The influence of large-scale motion on turbulent transport for confined coaxial jets p 125 N84-20542
- Elevated temperature biaxial fatigue  
[NASA-CR-173473] p 156 N84-21905
- Control Data Corp., Minneapolis, Minn.**  
Temperature histories of commercial flights at severe conditions from GASP data  
[NASA-CR-168247] p 12 N84-11152
- Tabulations of ozonesonde data, 1963 - 1980  
[NASA-CR-174631] p 174 N84-27375
- Cornell Univ., Ithaca, N.Y.**  
An implicit LU scheme for the Euler equations applied to arbitrary cascades  
[AIAA PAPER 84-0167] p 4 A84-17925
- Time-resolved density measurements in premixed turbulent flames p 59 A84-32612
- Cummins Engine Co., Inc., Columbus, Ind.**  
New perspectives for advanced automobile diesel engines p 138 A84-30062

**D**

- Dartmouth Coll., Hanover, N.H.**  
The structure of extruded NiAl p 65 A84-36047
- Determination of near-surface plastic deformation in sliding contacts p 140 A84-48996
- Dayton Univ., Ohio.**  
A total life prediction model for stress concentration sites  
[NASA-CR-168225] p 152 N84-10612
- Study and review of permanent magnets for electric vehicle propulsion motors  
[NASA-CR-168178] p 193 N84-14071
- Delaware Univ., Newark.**  
Inlet flow distortion in turbomachinery - Comparison of theory and experiment in a transonic fan stage  
p 3 A84-13592
- Department of Energy, Washington, D.C.**  
Proceedings of the 20th Automotive Technology Development Contractors' Coordination Meeting  
[NASA-CR-173412] p 143 N84-21877
- Department of the Air Force, Washington, D.C.**  
Finite element-integral acoustic simulation of JT15D turbofan engine p 182 A84-41132
- Detroit Diesel Allison, Indianapolis, Ind.**  
Material removal considerations for metal-ceramic abrasible turbine seal systems p 135 A84-15575
- Ceramic components for the AGT 100 engine p 136 A84-22878
- Advanced Gas Turbine (AGT) Power-train system development  
[NASA-CR-168056] p 140 N84-10581
- Deutsche Forschungs- und Versuchsanstalt fuer Luft- und Raumfahrt, Cologne (West Germany).**  
Development of plane strain fracture toughness test for ceramics using Chevron notched specimens p 77 A84-11676
- Draper (Charles Stark) Lab., Inc., Cambridge, Mass.**  
Pivoting and slip in an angular contact bearing p 139 A84-40595
- Drexel Univ., Philadelphia, Pa.**  
Combustion characteristics in the transition region of liquid fuel sprays  
[NASA-CR-175396] p 61 N84-19495
- Du Pont de Nemours (E. I.) and Co., Wilmington, Del.**  
Compositional effects on Si3N4 fracture surfaces p 79 A84-19794
- Duke Univ., Durham, N.C.**  
Parametric study of minimum converter loss in an energy-storage dc-to-dc converter p 101 A84-18403
- Dynamics Technology, Inc., Torrance, Calif.**  
Turbulence measurements in confined jets using a rotating single-wire probe technique p 113 A84-13564

**E**

- Eagle-Picher Industries, Inc., Colorado Springs, Colo.**  
Long life nickel electrodes for a nickel-hydrogen cell. I Initial performance p 162 A84-30186
- Eaton Corp., Southfield, Mich.**  
Development of a DC propulsion system for an electric vehicle  
[NASA-CR-168306] p 166 N84-20014
- AC propulsion system for an electric vehicle, phase 2  
[NASA-CR-168244] p 111 N84-31514
- EIC, Inc., Newton, Mass.**  
Moderate temperature rechargeable NaHS2 cells p 108 N84-21376
- Energy Research Corp., Danbury, Conn.**  
Evaluation of gas cooling for pressurized phosphoric acid fuel cell stacks p 163 A84-30191

- Evaluation of gas-cooled pressurized phosphoric acid fuel cells for electric utility power generation  
[NASA-CR-168298] p 169 N84-25169
- Full scale phosphoric acid fuel cell stack technology development  
[NASA-CR-174660] p 169 N84-26165
- Engelhard Corp., Menlo Park, Calif.**  
Develop and test fuel cell powered on-site integrated total energy systems Phase 3 Full-scale power plant development  
[NASA-CR-169294] p 164 N84-13672
- Engelhard Industries, Inc., Edison, N.J.**  
Develop and test fuel cell powered on-site integrated total energy system  
[NASA-CR-169159] p 164 N84-11581
- Develop and test fuel cell powered on-site integrated total energy system  
[NASA-CR-168239] p 164 N84-13673
- Engelhard Minerals and Chemicals Corp., Edison, N.J.**  
Develop and test fuel cell powered on-site integrated total energy systems  
[NASA-CR-174714] p 170 N84-27329
- Environmental Research Inst. of Michigan, Ann Arbor.**  
Development of Great Lakes algorithms for the Nimbus-G coastal zone color scanner  
[NASA-CR-173511] p 159 N84-27258

**F**

- Faucett (Jack) Associates, Inc., Chevy Chase, Md.**  
Assessment of institutional barriers to the use of natural gas fuel in automotive vehicle fleets  
[NASA-CR-168183] p 165 N84-14587
- Federal Aviation Administration, Washington, D.C.**  
Sixth Annual Workshop on Meteorological and Environmental Inputs to Aviation Systems, 26-28 October 1982, Tallahassee, Tenn. p 174 A84-23424
- Florida State Dept. of Education, Tallahassee.**  
Sound generated by instability waves of supersonic flows I Two-dimensional mixing layers. II - Axisymmetric jets p 181 A84-24597
- Florida Univ., Gainesville.**  
Analysis of grain boundary phase devitrification of Y2O3- and Al2O3-doped Si3N4 p 79 A84-19792
- Grain-boundary phases in hot-pressed silicon nitride containing Y2O3 and CeO2 additives p 79 A84-19793
- Compositional effects on Si3N4 fracture surfaces p 79 A84-19794
- Flow Research, Inc., Kent, Wash.**  
Direct simulations of chemically reacting turbulent mixing layers  
[NASA-CR-174640] p 32 N84-25710
- Ford Aerospace and Communications Corp., Palo Alto, Calif.**  
Multibeam antenna for 30/20 GHz advanced communications satellite using offset shaped, dual reflector surfaces p 93 A84-15827
- A new multiple beam satellite antenna for 30/20 GHz communications coverage of CONUS-experimental evaluation  
[AIAA PAPER 84-0655] p 94 A84-25256
- High-speed wide band 20 x 20 microwave switch matrix p 105 A84-49253
- Foster-Miller Associates, Inc., Waltham, Mass.**  
Steam bottoming cycle for an adiabatic diesel engine  
[NASA-CR-168255] p 196 N84-33304
- Future Systems, Inc., Gaithersburg, Md.**  
Advanced technology satellites in the commercial environment Volume 1: Executive summary  
[NASA-CR-174635-VOL-1] p 38 N84-20611
- Advanced technology satellites in the commercial environment, volume 2  
[NASA-CR-174635-VOL-2] p 38 N84-20612
- Garrett Turbine Engine Co., Phoenix, Ariz.**  
Experiments in dilution jet mixing p 122 A84-48140
- Executive summary, aerothermal modeling program, phase 1  
[NASA-CR-174602] p 60 N84-12263
- Aerothermal modeling program, phase 1  
[NASA-CR-168243-VOL-2] p 60 N84-12265
- Low-cost single-crystal turbine blades, volume 1  
[NASA-CR-168218] p 68 N84-15247
- Advanced turbocharger design study program  
[NASA-CR-174633] p 143 N84-21879
- Dilution jet mixing program  
[NASA-CR-174624] p 33 N84-26702
- Advanced Gas Turbine (AGT)  
[NASA-CR-174694] p 195 N84-29805
- High temperature ceramic interface study  
[NASA-CR-174728] p 197 N84-34331

**G**

- General Dynamics/Convair, San Diego, Calif.**  
Graphics enhanced computer emulation for improved timing-race and fault tolerance control system analysis  
[AIAA PAPER 83-2328] p 177 A84-10010
- General Dynamics Corp., Fort Worth, Tex.**  
Transient flow analysis of the AEDC/HPDE MHD generator p 189 A84-24049
- General Dynamics Corp., San Diego, Calif.**  
Multibandgap photovoltaic receiver using back surface reflectors p 161 A84-30162
- General Dynamics Corp., St. Louis, Mo.**  
Effects of volute geometry and impeller orbit on the hydraulic performance of a centrifugal pump p 136 A84-22316
- General Electric Co., Cincinnati, Ohio.**  
Comparison of full-scale engine and subscale model performance of a mixed flow exhaust system for an energy efficient engine (E3) propulsion system  
[AIAA PAPER 84-0283] p 16 A84-17997
- NASA/General Electric Broad-Specification Fuels Combustion Technology Program - Phase I p 16 A84-24033
- NASA advanced low emissions combustor program  
[ASME PAPER 83-JPGC-GT-10] p 17 A84-28982
- Application of a polynomial spline in higher-order accurate viscous-flow computations p 119 A84-35349
- The aerodynamic design and performance of the NASA/GE E3 low pressure turbine p 21 A84-44186
- Loss reduction in axial-flow compressors through low-speed model testing  
[ASME PAPER 84-GT-164] p 7 A84-46985
- Blade loss transient dynamics analysis with flexible bladed disk  
[NASA-CR-168176] p 23 N84-13193
- Clean catalytic combustor program  
[NASA-CR-168323] p 24 N84-15151
- Aerothermal modeling Executive summary  
[NASA-CR-168330] p 25 N84-15152
- Aerothermal modeling, phase 1. Volume 1: Model assessment  
[NASA-CR-168296-VOL-1] p 25 N84-15155
- Aerothermal modeling, phase 1. Volume 2  
[NASA-CR-168296-VOL-2] p 25 N84-15156
- Broad specification fuels combustion technology program  
[NASA-CR-168179] p 89 N84-15283
- Tip cap for a rotor blade  
[NASA-CASE-LEW-13654-1] p 28 N84-22560
- Experimental investigation of shock-cell noise reduction for dual-stream nozzles in simulated flight comprehensive data report. Volume 1: Test nozzles and acoustic data  
[NASA-CR-168336-VOL-1] p 184 N84-24323
- Experimental investigation of shock-cell noise reduction for dual-stream nozzles in simulated flight comprehensive data report. Volume 2: Laser velocimeter data, static pressures and shadowgraph photos  
[NASA-CR-168336-VOL-2] p 184 N84-24324
- Free jet feasibility study of a thermal acoustic shield concept for AST/VCE application: Single stream nozzles  
[NASA-CR-3758] p 185 N84-29661
- Experimental investigation of shock-cell noise reduction for single-stream nozzles in simulated flight, comprehensive data report. Volume 1: Test nozzles and acoustic data  
[NASA-CR-168234-VOL-1] p 185 N84-33148
- Experimental investigation of shock-cell noise reduction for single-stream nozzles in simulated flight, comprehensive data report. Volume 2: Laser velocimeter data  
[NASA-CR-168234-VOL-2] p 186 N84-33149
- Experimental investigation of shock-cell noise reduction for single-stream nozzles in simulated flight, comprehensive data report. Volume 3: Shadowgraph photos and facility description  
[NASA-CR-168234-VOL-3] p 186 N84-33150
- Air modulation apparatus  
[NASA-CASE-LEW-13524-1] p 35 N84-33410
- Subsonic/transonic stall flutter investigation of a rotating wing  
[NASA-CR-174625] p 36 N84-33417
- General Electric Co., Evendale, Ohio.**  
An advanced pitch change mechanism incorporating a hybrid traction drive  
[AIAA PAPER 84-1383] p 20 A84-44182
- Energy efficient engine. Flight propulsion system, preliminary analysis and design update  
[NASA-CR-167980] p 22 N84-11170
- Effects of surface chemistry on hot corrosion life  
[NASA-CR-174683] p 72 N84-24774
- General Electric Co., Lynn, Mass.**  
Powerplant design for one-engine-inoperative operation p 19 A84-40787

- The application of LQR synthesis techniques to the turbohaft engine control problem  
[AIAA PAPER 84-1455] p 21 A84-44185
- Rotorcraft contingency power study  
[NASA-CR-174675] p 31 N84-24580
- General Electric Co., Schenectady, N. Y.**
- Mechanical and physical properties of plasma-sprayed stabilized zirconia p 79 A84-19786
- Acoustically-induced modulation spectroscopy for ultra-sensitive gas analysis  
[AIAA PAPER 84-1460] p 131 A84-36981
- Mobile radio alternative systems study. Volume 1: Traffic model  
[NASA-CR-168062] p 96 N84-10402
- Mobile radio alternative systems study. Volume 2: Terrestrial  
[NASA-CR-168063] p 96 N84-10403
- Mobile radio alternative systems study satellite/terrestrial (hybrid) systems concepts  
[NASA-CR-168064] p 96 N84-10404
- General Motors Corp., Indianapolis, Ind.**
- Combustor development for automotive gas turbines p 135 A84-10499
- Advanced propfan drive system characteristics and technology needs  
[AIAA PAPER 84-1194] p 18 A84-36957
- An analytical method to predict efficiency of aircraft gearboxes  
[AIAA PAPER 84-1500] p 20 A84-44180
- Advanced Gas Turbine (AGT) technology development  
[NASA-CR-168235] p 141 N84-15554
- Advanced Gas Turbine (AGT) Technology Project  
[NASA-CR-174629] p 146 N84-28089
- General Motors Research Labs., Warren, Mich.**
- Scaling relations in the equation of state, thermal expansion, and melting of metals p 192 A84-19359
- General Tire and Rubber Co., Akron, Ohio.**
- High temperature thermomechanical analysis of ceramic coatings p 152 A84-48565
- Georgia Inst. of Tech., Atlanta.**
- Modeling of transient two-component flow using a four-point implicit method p 112 A84-13237
- Inelastic stress analyses at finite deformation through complementary energy approaches p 149 A84-13248
- Analyses of large quasistatic deformations of inelastic bodies by a new hybrid-stress finite element algorithm p 150 A84-16874
- Analyses of large quasistatic deformations of inelastic bodies by a new hybrid-stress finite element algorithm - Applications p 150 A84-16884
- A parametric study of the effect of inlet lip shape upon the radiated sound field  
[AIAA PAPER 84-0498] p 180 A84-18131
- A finite element approach for predicting nozzle admittances p 180 A84-21184
- Viscous-inviscid interactive procedure for rotational flow in cascades of airfoils p 6 A84-44639
- Application of signal analysis to cavitation p 122 A84-49192
- A viscous-inviscid interactive procedure for rotational flow in cascades of two dimensional airfoils of arbitrary shape  
[NASA-CR-174609] p 7 N84-13149
- Inelastic and dynamic fracture and stress analyses p 158 N84-31697
- Giner, Inc., Waltham, Mass.**
- Importance of interatomic spacing in catalytic reduction of oxygen in phosphoric acid p 58 A84-12644
- Gould, Inc., Rolling Meadows, Ill.**
- An SCR inverter with an integral battery charger for electric vehicles p 103 A84-24850
- Integral inverter/battery charger for use in electric vehicles  
[NASA-CR-168177] p 194 N84-17073
- GT-Devices, Alexandria, Va.**
- Experimental investigation of the pulsed electrothermal (PET) thruster  
[AIAA PAPER 84-1386] p 43 A84-35201
- Proposed system design for a 20 kW pulsed electrothermal thruster  
[AIAA PAPER 84-1387] p 43 A84-35202
- Investigation of a pulsed electrothermal thruster  
[NASA-CR-168266] p 45 N84-12227

## H

- Hamilton Standard, Windsor Locks, Conn.**
- Technology and benefits of aircraft counter rotation propellers  
[NASA-CR-168258] p 22 N84-13186
- Honeywell Corporate Research Center, Bloomington, Minn.**
- A Ka-band GaAs monolithic phase shifter p 101 A84-18371

- Honeywell, Inc., Bloomington, Minn.**
- The 30-GHz monolithic receive module  
[NASA-CR-168326] p 99 N84-20737
- Houston Univ., Tex.**
- Jet noise modification by the 'whistler nozzle' p 181 A84-23355
- Hughes Aircraft Co., El Segundo, Calif.**
- Development of a large scale bipolar NiH<sub>2</sub> battery  
Advanced nickel-hydrogen cell configuration study  
[NASA-CR-173417] p 108 N84-22889
- Hughes Aircraft Co., Torrance, Calif.**
- A TWT amplifier with a linear power transfer characteristic and improved efficiency  
[AIAA PAPER 84-0762] p 104 A84-41035
- Hughes Research Labs., Malibu, Calif.**
- Effect of electron flux on radiation damage in GaAs solar cells p 160 A84-22998
- Long life nickel electrodes for a nickel-hydrogen cell. I Initial performance p 162 A84-30186
- Development of advanced inert-gas ion thrusters  
[NASA-CR-168206] p 44 N84-10160
- Plasma polymerized high energy density dielectric films for capacitors  
[NASA-CR-168233] p 81 N84-13310
- The 25 kW resonant dc/dc power converter  
[NASA-CR-168273] p 108 N84-17481

## I

- IAP Research, Inc., Dayton, Ohio.**
- Investigation of the residue in an electric rail gun employing a plasma armature p 103 A84-32046
- ICF, Inc., Washington, D. C.**
- Computer analysis of effects of altering jet fuel properties on refinery costs and yields  
[NASA-CR-174642] p 91 N84-27908
- IIT Research Inst., Chicago, Ill.**
- Creep-rupture behavior of candidate Stirling engine iron superalloys in high-pressure hydrogen Volume 2: Hydrogen creep-rupture behavior  
[NASA-CR-174705] p 74 N84-28961
- Illinois Inst. of Tech., Chicago**
- On the design of contractions and settling chambers for optimal turbulence manipulations in wind tunnels  
[AIAA PAPER 84-0536] p 115 A84-22922
- Creep-rupture behavior of six candidate Stirling engine superalloys tested in air p 65 A84-36173
- Illinois Univ., Chicago.**
- Precision of spiral-bevel gears  
[ASME PAPER 82-WA/DE-33] p 135 A84-15950
- Kinematic precision of gear trains  
[ASME PAPER 82-WA/DE-34] p 135 A84-15951
- Time-resolved density measurements in premixed turbulent flames p 59 A84-32612
- Illinois Univ., Urbana.**
- Edge delamination in angle-ply composite laminates p 52 A84-21515
- Surface roughness effects with solid lubricants dispersed in mineral oils  
[ASLE PREPRINT 83-LC-4C-1] p 137 A84-28987
- Elasticity solutions for a class of composite laminate problems with stress singularities p 53 A84-33389
- Numerical methods for analyzing electromagnetic scattering  
[NASA-CR-175423] p 98 N84-19620
- Numerical methods for analyzing electromagnetic scattering  
[NASA-CR-173916] p 101 N84-32645
- Monolithic microwave integrated circuit devices for active array antennas  
[NASA-CR-173981] p 112 N84-34675
- Illinois Univ., Urbana-Champaign.**
- Tropical response to lateral forcing with a latitudinally and zonally nonuniform basic state p 174 A84-40399
- The study of microstrip antenna arrays and related problems  
[NASA-CR-173534] p 99 N84-23807
- Wave attenuation and mode dispersion in a waveguide coated with lossy dielectric material  
[NASA-CR-173820] p 100 N84-30145
- Imperial Coll. of Science and Technology, London (England).**
- Developing flow in S-shaped ducts p 116 A84-28709

- Institute of Gas Technology, Chicago, Ill.**
- High-temperature molten salt thermal energy storage systems for solar applications  
[NASA-CR-167916] p 165 N84-15679
- Advanced onboard storage concepts for natural gas-fueled automotive vehicles  
[NASA-CR-174655] p 172 N84-34036
- Ionics, Inc., Watertown, Mass.**
- Anion permselective membrane  
[NASA-CR-174725] p 172 N84-29358

- Iowa Univ., Iowa City.**
- Finite-analytic numerical method for unsteady two-dimensional Navier-Stokes equations p 116 A84-25807
- Prediction of turbulent flow past a prosthetic heart valve p 175 A84-49108
- Interpretation of STS-3/plasma diagnostics package results in terms of large space structure plasma interactions  
[NASA-CR-173266] p 189 N84-16991
- ISTAR, Inc., Santa Monica, Calif.**
- Detonation wave augmentation of gas turbines  
[AIAA PAPER 84-1266] p 18 A84-37639

## J

- Jet Propulsion Lab., California Inst. of Tech., Pasadena.**
- Electronic properties of carbon fibers intercalated with copper chloride p 104 A84-34521
- An assessment of advanced technology for industrial cogeneration  
[NASA-CR-173456] p 167 N84-22001
- Solar-array-materials passive LDEF experiment (A0171) p 168 N84-24656

## K

- Kansas Univ., Lawrence.**
- Theoretical and software considerations for nonlinear dynamic analysis  
[NASA-CR-174504] p 154 N84-15589
- Kent State Univ., Ohio.**
- Automatic finite element generators p 158 N84-31695

## L

- Levy (Salomon), Inc., Campbell, Calif.**
- Turbulent boundary-layer flow and structure on a convex wall and its redevelopment on a flat wall p 115 A84-21378
- Lincoln Lab., Mass. Inst. of Tech., Lexington.**
- Spatial electron density and electric field strength measurements in microwave cavity experiments  
[AIAA PAPER 84-1522] p 189 A84-46109
- Little (Arthur D.), Inc., Cambridge, Mass.**
- Catalog of selected heavy duty transport energy management models  
[NASA-CR-168299] p 194 N84-14991
- New applications for phosphoric acid fuel cells  
[NASA-CR-168203] p 166 N84-18757
- LNR Communications, Inc., Hauppauge, N. Y.**
- Recent developments in EHF Satcom technology p 39 A84-46620
- The 30 GHz communications satellite low noise receiver  
[NASA-CR-168254] p 97 N84-13398
- The 20 GHz solid state transmitter design, impact diode development and reliability assessment  
[NASA-CR-174716] p 112 N84-33715
- Lockheed-Georgia Co., Marietta.**
- Acoustic power dissipation on radiation through duct terminations - Experiments p 180 A84-21272
- Basic experimental study of the coupling between flow instabilities and incident sound p 183 N84-21275
- Los Alamos Scientific Lab., N. Mex.**
- Electrode kinetics of oxygen reduction - A theoretical and experimental analysis of the rotating ring-disc electrode method p 59 A84-29999
- Louisiana State Univ., Baton Rouge.**
- Benchmark cyclic plastic notch strain measurements p 63 A84-11194
- Shock tube study of the fuel structure effects on the chemical kinetic mechanisms responsible for soot formation  
[NASA-CR-174661] p 62 N84-21677
- Lulea Univ. (Sweden).**
- Non-Newtonian fluid model incorporated into elastohydrodynamic lubrication of rectangular contacts  
[ASME PAPER 83-LUB-15] p 139 A84-44300

## M

- Martin Marietta Aerospace, Denver, Colo.**
- On-orbit cryogenic fluid transfer  
[AIAA PAPER 84-1343] p 44 A84-44176
- Cryogenic Fluid Management Facility  
[AIAA PAPER 84-1340] p 44 A84-44184
- Cryogenic Fluid Management Experiment (CFME) trunnion verification testing  
[NASA-CR-168310] p 92 N84-16381

**Maryland Univ., College Park.**

- Capillary rise, wetting layers, and critical phenomena in confined geometry p 192 A84-20315  
 Turbidity very near the critical point of methanol-cyclohexane mixtures p 192 A84-30391

**Massachusetts Inst. of Tech., Cambridge.**

- Formation and inflammation of a turbulent jet [AIAA PAPER 84-0572] p 114 A84-18171  
 On the suppression of zero energy deformation modes p 150 A84-21541  
 Stagger angle dependence of inertial and elastic coupling in bladed disks p 151 A84-31903  
 Metal vapor vacuum arc switching - Applications and results p 103 A84-32029  
 Conservative streamtube solution of steady-state Euler equations [AIAA PAPER 84-1643] p 120 A84-38030  
 Optimization and mechanisms of mistuning in cascades [ASME PAPER 84-GT-196] p 21 A84-46993  
 Numerical solution for the problem of flame propagation by the random element method p 60 A84-48139  
 Eigenmode analysis of unsteady one-dimensional Euler equations [NASA-CR-172217] p 7 A84-10022  
 Asymptotic analysis of numerical wave propagation in finite difference equations p 98 A84-15360  
 Input-output characterization of an ultrasonic testing system by digital signal analysis [NASA-CR-3758] p 149 A84-15565  
 Flutter and forced response of mistuned rotors using standing wave analysis [NASA-CR-173555] p 32 A84-24586  
 New variational formulations of hybrid stress elements p 158 A84-31690  
 Computer simulation of the heavy-duty turbo-compounded diesel cycle for studies of engine efficiency and performance [NASA-CR-174755] p 195 A84-33306

**Maxwell Labs., Inc., San Diego, Calif.**

- Material considerations for high frequency, high power capacitors p 102 A84-22874

**McDonnell Aircraft Co., St. Louis, Mo.**

- Uncertainty methodology for in-flight thrust determination [SAE PAPER 831438] p 13 A84-29452  
 Application of in-flight thrust determination uncertainty [SAE PAPER 831439] p 13 A84-29453

**Mechanical Technology, Inc., Latham, N. Y.**

- Free-piston Stirling engine endurance test program p 136 A84-22864  
 Design analysis of Rayleigh-stop floating-ring seals [ASLE PREPRINT 83-LC-3B-2] p 137 A84-28989  
 Automotive Stirling Engine Development Program Model Stirling engine development p 138 A84-30091  
 Automotive Stirling engine development program - Overview and status report p 138 A84-30092  
 Comparison of steady-state and transient CVS cycle emission of an automotive Stirling engine p 173 A84-41044  
 Automotive Stirling engine development program [NASA-CR-168205] p 194 A84-18117  
 Automotive Stirling engine development program [NASA-CR-174622] p 195 A84-32305  
 Automotive Stirling Engine Development Program. RESD summary report [NASA-CR-174674] p 196 A84-33307

**Michigan State Univ., East Lansing.**

- Modeling of transient two-component flow using a four-point implicit method p 112 A84-13237  
 Characteristics of a microwave plasma disk ion source p 189 A84-23390  
 Demonstration of a new electrothermal thruster concept p 43 A84-34037  
 Electromagnetic plasma models for microwave plasma cavity reactors [AIAA PAPER 84-1521] p 189 A84-46108  
 Spatial electron density and electric field strength measurements in microwave cavity experiments [AIAA PAPER 84-1522] p 189 A84-46109  
 Free stream turbulence and density ratio effects on the interaction region of a jet in a cross flow p 125 A84-20546  
 Spatial electron density and electric field strength measurements in microwave cavity experiments [NASA-CR-173907] p 111 A84-32682

**Michigan Technological Univ., Houghton.**

- Solute transport and the prediction of breakaway oxidation in gamma + beta Ni-Cr-Al alloys p 65 A84-42658

**Michigan Univ., Ann Arbor.**

- Boundary conditions for the solution of compressible Navier-Stokes equations by an implicit factored method p 113 A84-13495

- Modeling of zero gravity venting [NASA-CR-173503] p 127 A84-23854  
**Ministry of Defence, Haifa (Israel).**  
 Boundary conditions for the solution of compressible Navier-Stokes equations by an implicit factored method p 113 A84-13495

**Minnesota Univ., Minneapolis.**

- Steady state stresses in ribbon parachute canopies [AIAA PAPER 84-0816] p 11 A84-26580  
 Studies of acoustical properties of bulk porous flexible materials [NASA-CR-173622] p 185 A84-27544

**Missouri Univ., Rolla.**

- Grain-boundary phases in hot-pressed silicon nitride containing Y<sub>2</sub>O<sub>3</sub> and CeO<sub>2</sub> additives p 79 A84-19793  
 A numerical model of acoustic choking I - Shock free solutions p 180 A84-21250

**Mitre Corp., Bedford, Mass.**

- A frequency-division multiple-access system concept for 30/20 GHz high-capacity domestic satellite service p 94 A84-22141

**Motorola, Inc., Phoenix, Ariz.**

- Qualification testing of solar photovoltaic powered refrigerator freezers for medical use in remote geographic locations [NASA-CR-168181] p 169 A84-25162

**Motorola, Inc., Scottsdale, Ariz.**

- Baseband processor development for the Advanced Communications Satellite Program p 93 A84-15628  
 30/20 GHz communications systems baseband processor development p 95 A84-38251

**N****National Aeronautical Lab., Bangalore (India).**

- A simple application of the Bailey-Crowan creep model to Fe-39 S at pct Al and gamma/gamma prime - alpha p 64 A84-22012

**National Aeronautics and Space Administration,****Washington, D. C.**

- NASA priority technologies [IAF PAPER 83-345] p 37 A84-11793  
 NASA's multibeam communications technology program p 39 A84-21397  
 Effects of chemical releases by the STS-3 Orbiter on the ionosphere [NASA-CR-171032] p 173 A84-25204

**National Aeronautics and Space Administration. Ames Research Center, Moffett Field, Calif.**

- Tandem fan applications in advanced STOVL fighter configurations [AIAA PAPER 84-1402] p 19 A84-40245  
 Rotorcraft flight-propulsion control integration p 36 A84-46524

**National Aeronautics and Space Administration. Goddard Space Flight Center, Greenbelt, Md.**

- A study of 60 GHz intersatellite link applications p 40 A84-49288  
 Solar-array-materials passive LDEF experiment (A0171) p 168 A84-24656

**National Aeronautics and Space Administration.****Langley Research Center, Hampton, Va.**

- Experimental and theoretical deposition rates from salt-seeded combustion gases of a Mach 0.3 burner rig [NASA-TP-2225] p 124 A84-19741

**National Aeronautics and Space Administration.****Marshall Space Flight Center, Huntsville, Ala.**

- Sixth Annual Workshop on Meteorological and Environmental Inputs to Aviation Systems, 26-28 October 1982, Tullahoma, Tenn. p 174 A84-23424  
 NASA's geostationary communications platform program [AIAA PAPER 84-0702] p 95 A84-25326  
 Solar-array-materials passive LDEF experiment (A0171) p 168 A84-24656

**National Bureau of Standards, Washington, D. C.**

- Capillary rise, wetting layers, and critical phenomena in confined geometry p 192 A84-20315  
 Turbidity very near the critical point of methanol-cyclohexane mixtures p 192 A84-30391

**National Weather Service, Silver Spring, Md.**

- Sixth Annual Workshop on Meteorological and Environmental Inputs to Aviation Systems, 26-28 October 1982, Tullahoma, Tenn. p 174 A84-23424

**Nebraska Univ., Lincoln.**

- Electronic properties of carbon fibers intercalated with copper chloride p 104 A84-34521

**New Mexico Univ., Albuquerque.**

- Boundary layer transition effects on flow separation around V/STOL engine inlets at high incidence [AIAA PAPER 84-0432] p 4 A84-18090

**Nihon Univ., Tokyo (Japan).**

- Electronic properties of carbon fibers intercalated with copper chloride p 104 A84-34521

**North Carolina State Univ., Raleigh.**

- Supersonic jet screech tone cancellation p 179 A84-10136  
 Analytical study of suction boundary layer control for subsonic V/STOL inlets [AIAA PAPER 84-1399] p 6 A84-44187

**Northwestern Univ., Evanston, Ill.**

- An invariant derivation of flame stretch p 58 A84-18925  
 Extinction of premixed flames by stretch and radiative loss p 58 A84-23593  
 An experimental study on extinction and stability of stretched premixed flames p 59 A84-35425  
 Finite elastic-plastic deformation of polycrystalline metals p 66 A84-43872

**Notre Dame Univ., Ind.**

- An application of tensor ideas to nonlinear modeling of a turbofan jet engine p 20 A84-42382

**O****O'Donnell and Associates, Inc., Pittsburgh, Pa.**

- Development of a simplified procedure for rocket engine thrust chamber life prediction with creep [NASA-CR-168261] p 46 A84-19472

**Ohio State Univ., Columbus.**

- Effect of geometry on airfoil icing characteristics p 12 A84-37935  
 Optical flip-flops and sequential logic circuits using a liquid crystal light valve p 188 A84-40332  
 Experimental and analytical investigations into airfoil icing p 12 A84-45054  
 Vibrations of twisted cantilevered plates - Experimental investigation [ASME PAPER 84-GT-96] p 152 A84-46937

- Volume integrals associated with the inhomogeneous Helmholtz equation Part 1 Ellipsoidal region [NASA-CR-3749] p 148 A84-14525  
 Volume integrals associated with the inhomogeneous Helmholtz equation Part 2 Cylindrical region, rectangular region [NASA-CR-3750] p 148 A84-14526

- Results of an experimental program investigating the effects of simulated ice on the performance of the NACA 63A415 airfoil with flap [NASA-CR-168288] p 8 A84-16145  
 Potential flow analysis of glaze ice accretions on an airfoil [NASA-CR-168282] p 8 A84-16146  
 Documentation of ice shapes on the main rotor of a UH-1H helicopter in hover [NASA-CR-168332] p 9 A84-17139

- Optical pulse generator using liquid crystal light valve p 188 A84-22414  
 Optical residue addition and storage units using a Hughes liquid crystal light valve p 188 A84-22417  
 Engineering calculations for communications satellite systems planning [NASA-CR-173532] p 38 A84-23662  
 Adaptive arrays for satellite communications [NASA-CR-173548] p 99 A84-24924

- Oklahoma State Univ., Stillwater.**  
 Turbulence measurements in confined jets using a rotating single-wire probe technique p 113 A84-13584  
 Accuracy and directional sensitivity of the single-wire technique [AIAA PAPER 84-0357] p 130 A84-18047

- Limitations and empirical extensions of the k-epsilon model as applied to turbulent confined swirling flows [AIAA PAPER 84-0441] p 114 A84-18096  
 Further time-mean measurements in confined swirling flows p 116 A84-27138

- Swirl flow turbulence modeling [AIAA PAPER 84-1376] p 118 A84-35196  
 Swirl, confinement and nozzle effects on confined turbulent flow [AIAA PAPER 84-1377] p 118 A84-35197

- Turbulence measurements in a complex flowfield using a crossed hot-wire [AIAA PAPER 84-1604] p 131 A84-37999

- Five-hole pitot probe measurements of swirl, confinement and nozzle effects on confined turbulent flow [AIAA PAPER 84-1605] p 120 A84-38000

- Turbulence characteristics of swirling flowfields [NASA-CR-175392] p 124 A84-19744  
 Confined turbulent swirling recirculating flow predictions [NASA-CR-175397] p 125 A84-19745

- Oregon Graduate Center for Study and Research, Beaverton.**  
 Evaluation of single crystal LaB<sub>6</sub> cathodes for use in a high frequency backward wave oscillator tube [NASA-CR-173343] p 108 A84-19709

# P

## Pennsylvania State Univ., State College.

- The boundary layer on compressor cascade blades  
[NASA-CR-173514] p 127 N84-25001
- Pennsylvania State Univ., University Park.  
Evaporation and combustion of sprays  
p 58 A84-11636
- Three-dimensional flowfield inside a low-speed axial flow compressor rotor  
p 3 A84-13574
- Three-dimensional turbulent boundary-layer development on a fan rotor blade  
p 3 A84-17437
- The application of vortex theory to the optimum swept propeller  
[AIAA PAPER 84-0036] p 3 A84-17841
- Structure of particle-laden jets - Measurements and predictions  
[AIAA PAPER 84-0038] p 113 A84-17842
- Structure of nonevaporating sprays - Measurements and predictions  
[AIAA PAPER 84-0125] p 114 A84-17897
- Computation of three-dimensional viscous flows using a space-marching method  
[AIAA PAPER 84-1298] p 5 A84-36971
- Laser Doppler velocimeter measurement in the tip region of a compressor rotor  
[AIAA PAPER 84-1602] p 6 A84-39304
- The interaction between mistuning and friction in the forced response of bladed disk assemblies  
[ASME PAPER 84-GT-139] p 152 A84-46957
- An experimental study of the compressor rotor blade boundary layer  
[ASME PAPER 84-GT-193] p 7 A84-46991
- Turbulence modeling for three-dimensional shear flows over curved rotating bodies  
p 122 A84-48138
- A theoretical and experimental study of turbulent particle-laden jets  
[NASA-CR-168293] p 23 N84-13167
- Annulus wall boundary layer development in a compressor stage, including the effects of tip clearance  
p 26 N84-16207
- Predictions of spray combustion interactions  
p 61 N84-20532
- The impact resistance of SiC and other mechanical properties of SiC and Si3N4  
[NASA-CR-165325] p 84 N84-24809
- Utilization of alternative fuels in diesel engines  
[NASA-CR-174669] p 91 N84-26313
- The structure of evaporating and combusting sprays - Measurements and predictions  
[NASA-CR-173778] p 128 N84-29155
- A theoretical and experimental study of turbulent nonevaporating sprays  
[NASA-CR-174668] p 35 N84-29877
- A theoretical and experimental study of turbulent evaporating sprays  
[NASA-CR-174760] p 35 N84-32390
- Pennsylvania Univ., Philadelphia.  
Reaction of cobalt in SO2 atmospheres at elevated temperatures  
p 65 A84-33440
- Pittsburgh Univ., Pa.  
Investigation into the role of sodium chloride deposited on oxide and metal substrates in the initiation of hot corrosion  
[NASA-CR-173377] p 71 N84-20676
- Pratt and Whitney Aircraft, East Hartford, Conn.  
Uncertainty methodology for in-flight thrust determination  
[SAE PAPER 831438] p 13 A84-29452
- Application of in-flight thrust determination uncertainty  
[SAE PAPER 831439] p 13 A84-29453
- Program for development of strain tolerant thermal barrier coating system  
[NASA-CR-173214] p 82 N84-16337
- Three-dimensional stress analysis using the boundary element method  
p 159 N84-31700
- Turbine blade and vane heat flux sensor development, phase 1  
[NASA-CR-168297] p 134 N84-32790
- Pratt and Whitney Aircraft, West Palm Beach, Fla.  
Dynamic gas temperature measurement system, volume 1  
[NASA-CR-168267-VOL-1] p 132 N84-16529
- Error reduction program: A progress report  
p 27 N84-20536
- V/STOL model fan stage rig design report  
[NASA-CR-174688] p 29 N84-23629
- NASA Orbit Transfer Rocket Engine Technology Program  
[NASA-CR-168156] p 48 N84-28901
- Pratt and Whitney Aircraft Group, East Hartford, Conn.  
Simplified analytical procedures for representing material cyclic response  
p 16 A84-22877
- Calculation of a hollow-cone liquid spray in a uniform air stream

- [AIAA PAPER 84-1322] p 118 A84-35171
- Development of strain tolerant thermal barrier coating systems, tasks 1 - 3  
[NASA-CR-168251] p 81 N84-12312
- Parallel processor engine model program  
[NASA-CR-174641] p 27 N84-19353
- Energy efficient engine fan component detailed design report  
[NASA-CR-165466] p 33 N84-27737
- Energy efficient engine: Low-pressure turbine subsonic cascade component development and integration program  
[NASA-CR-165592] p 33 N84-27738
- Energy efficient engine high-pressure turbine detailed design report  
[NASA-CR-165608] p 33 N84-28788
- Energy efficient engine Turbine intermediate case and low-pressure turbine component test hardware detailed design report  
[NASA-CR-167973] p 33 N84-28789
- Energy efficient engine component development and integration program  
[NASA-CR-173884] p 35 N84-32389
- Pratt and Whitney Aircraft Group, West Palm Beach, Fla.  
Real-time Pegasus propulsion system model V/STOL-piloted simulation evaluation  
p 15 A84-17362
- Low strain, long life creep fatigue of AF2-1DA and INCO 718  
[NASA-CR-167989] p 66 N84-10268
- Princeton Univ., N. J.  
Forced response of a cantilever beam with a dry friction damper attached. I - Theory. II - Experiment  
p 150 A84-21267
- The role of surface generated radicals in catalytic combustion  
p 61 N84-20555
- Purdue Univ., Lafayette, Ind.  
Computation of viscous flow in planar and axisymmetric ducts by an implicit marching procedure  
[AIAA PAPER 84-0256] p 114 A84-17979
- The coupled response of turbomachinery blading to aerodynamic excitations  
p 17 A84-26959
- Indentation law for composite laminates  
p 52 A84-27356
- Three-dimensional flow simulations for supersonic mixed-compression inlets at incidence  
p 5 A84-38828
- Application of an optimization method to high performance propeller designs  
[AIAA PAPER 84-1203] p 20 A84-44181
- Flame propagation in heterogeneous mixtures of fuel drops and air  
[NASA-CR-174644] p 91 N84-23775
- PURDU-WINCOF: A computer code for establishing the performance of a fan-compressor unit with water ingestion  
[NASA-CR-168005] p 34 N84-29875
- Purdue Univ. School of Science at Indianapolis, Ind.  
Application of a finite element algorithm to the solution of steady transonic Euler equations  
p 3 A84-10133
- Finite element formulation of transonic flow problems  
p 116 A84-25859
- Rensselaer Polytechnic Inst., Troy, N. Y.  
The effects of frequency and hold times on fatigue crack propagation rates in a nickel base superalloy  
p 64 A84-18733
- Correlation of compressive and shear stress with spalling of plasma-sprayed ceramic materials  
p 79 A84-19784
- Gravitational effects in dendritic growth  
p 37 A84-22346
- Photovoltaic characteristics of diffused P+/N bulk GaAs solar cells  
p 161 A84-23115
- Diffused junction p(+)-n solar cells in bulk GaAs I  
Fabrication and cell performance  
p 161 A84-26027
- Diffused junction p(+)-n solar cells in bulk GaAs II - Device characterization and modeling  
p 161 A84-26028
- Effect of an oscillating flow direction on leading edge heat transfer  
p 117 A84-33705
- Convective heat transfer studies at high temperatures with pressure gradient for inlet flow Mach number of 0.45  
[AIAA PAPER 84-1487] p 119 A84-35233
- Fiat plate heat transfer for laminar transition and turbulent boundary layers using a shock tube  
[AIAA PAPER 84-1726] p 120 A84-37467
- Free dendritic growth  
p 190 A84-42829
- Structural dynamics of rotating bladed-disk assemblies coupled with flexible shaft motions  
p 21 A84-44845
- Fatigue crack growth and low cycle fatigue of two nickel base superalloys

- [NASA-CR-174534] p 66 N84-10267
- Surface topographical changes measured by phase-locked interferometry  
[NASA-CR-3757] p 188 N84-16984
- Emission FTIR analyses of thin microscopic patches of jet fuel residue deposited on heated metal surface  
[NASA-CR-168331] p 90 N84-17410
- Investigation of the effects of pressure gradient, temperature and wall temperature ratio on the stagnation point heat transfer for circular cylinders and gas turbine vanes  
[NASA-CR-174667] p 30 N84-23649
- Transport processes in dendritic crystallization  
p 191 N84-28621
- Mass transfer from a circular cylinder: Effects of flow unsteadiness and slight nonuniformities  
[NASA-CR-174759] p 129 N84-32751
- Research Inst. of Colorado, Fort Collins.  
Photodeposition of nitride insulators on 3-5 substrates  
[NASA-CR-173393] p 71 N84-21720
- Riso National Lab., Roskilde (Denmark).  
Estimating time and time-lag in time-of-flight velocimetry  
p 129 A84-13192
- Output statistics of laser anemometers in sparsely seeded flows  
p 117 A84-28738
- Optimizing and comparing laser anemometers  
p 130 A84-28739
- Rochester Univ., N. Y.  
Coupling of radiation into thin film modes by means of localized plasma resonances  
p 187 A84-16397
- Rocket Research Corp., Redmond, Wash.  
Radiative resistojet performance characterization tests  
[NASA-CR-174763] p 50 N84-33462
- Rocketdyne, Canoga Park, Calif.  
Research study for effects of case flexibility on bearing loads and rotor stability  
[NASA-CR-171147] p 148 N84-33811
- Rockwell International Corp., Thousand Oaks, Calif.  
A three-stage power amplifier for a 20 GHz monolithic transmit module  
p 102 A84-22873
- Interaction between boron and intrinsic defects in GaAs  
p 190 A84-33918
- LEC GaAs for integrated circuit applications  
[NASA-CR-173267] p 191 N84-17014
- Rolls-Royce Ltd., London (England).  
Uncertainty methodology for in-flight thrust determination  
[SAE PAPER 831438] p 13 A84-29452
- Application of in-flight thrust determination uncertainty  
[SAE PAPER 831439] p 13 A84-29453
- Royal Aircraft Establishment, Farnborough (England).  
Uncertainty methodology for in-flight thrust determination  
[SAE PAPER 831438] p 13 A84-29452
- Application of in-flight thrust determination uncertainty  
[SAE PAPER 831439] p 13 A84-29453

# S

- Santa Clara Univ., Calif.  
Alcohol cold starting - A theoretical study  
p 138 A84-30061
- Secondary flow spanwise deviation model for the stators of NASA middle compressor stages  
[NASA-CR-173360] p 27 N84-18202
- Science Applications, Inc., Chatsworth, Calif.  
Analytic modeling of a spray diffusion flame  
[AIAA PAPER 84-1317] p 118 A84-35168
- Scientific Research Associates, Inc., Glastonbury, Conn.  
Dynamic response of shock waves in transonic diffuser and supersonic inlet - An analysis with the Navier-Stokes equations and adaptive grid  
[AIAA PAPER 84-1609] p 5 A84-38004
- Further development of a method for computing three-dimensional subsonic viscous flows in turbofan lobe mixers  
[NASA-CR-168304] p 122 N84-14462
- Seattle Univ., Wash.  
Exponential-fitted methods for integrating stiff systems of ordinary differential equations Applications to homogeneous gas-phase chemical kinetics  
p 179 N84-31279
- Simmonds Precision Products, Inc., Vergennes, Vermont.  
Economic impact of fuel properties on turbine powered business aircraft  
p 14 N84-23646
- Study of effects of fuel properties in turbine-powered business aircraft  
[NASA-CR-174627] p 91 N84-25854
- SKF Industries, Inc., King of Prussia, Pa.  
Solid lubrication design methodology  
[NASA-CR-174690] p 196 N84-33309
- Societe Europeenne de Propulsion, Vernon (France).  
An experimental study of the compressor rotor blade boundary layer

# R

- [ASME PAPER 84-GT-193] p 7 A84-46991  
**Solar Energy Technology, Inc., Bedford, Mass.**  
 Reflector antennas with low sidelobes, low cross polarization, and high aperture efficiency  
 [NASA-CR-174670] p 100 N84-31464
- Solar Power Corp., Woburn, Mass.**  
 Solar photovoltaic powered refrigerators/freezers for medical use in remote geographic locations  
 [NASA-CR-168268] p 169 N84-25163
- Solar Turbines International, San Diego, Calif.**  
 Experimental study of the operating characteristics of premixing-prevaporing fuel/air mixing passages  
 [NASA-CR-168279] p 23 N84-14143
- Sonalytix, Inc., Waterford, Conn.**  
 Communications network design and costing model technical manual  
 [NASA-CR-168236] p 97 N84-14376  
 Communications network design and costing model programmers manual  
 [NASA-CR-168237] p 97 N84-14377  
 Communications network design and costing model users manual  
 [NASA-CR-168238] p 97 N84-14378
- Southern Methodist Univ., Dallas, Tex.**  
 An experimental study of the properties of surface pressure fluctuations in strong adverse pressure gradient turbulent boundary layers  
 [NASA-CR-175410] p 9 N84-20468
- Southwest Research Inst., San Antonio, Tex.**  
 Vapor flow into a capillary propellant-acquisition device  
 [NASA-CR-175410] p 43 A84-36559  
 Calibration of the Malvern particle sizer  
 [NASA-CR-175410] p 131 A84-40736  
 Gas flow across a wet screen - Analogy to a relief valve with hysteresis  
 [NASA-CR-175410] p 121 A84-43545  
 Investigation of sources, properties and preparation of distillate test fuels  
 [NASA-CR-168227] p 89 N84-13332  
 Development of carbon slurry fuels for transportation (hybrid fuels, phase 2)  
 [NASA-CR-174659] p 74 N84-28960
- Spectron Development Labs., Inc., Costa Mesa, Calif.**  
 A technique combining the visibility of a Doppler signal with the peak intensity of the pedestal to measure the size and velocity of droplets in a spray  
 [AIAA PAPER 84-0203] p 129 A84-17946  
 Development and implementation of advanced diagnostic techniques  
 [NASA-CR-175410] p 132 N84-20528
- Spire Corp., Bedford, Mass.**  
 Large area space solar cell assemblies  
 [NASA-CR-175410] p 42 A84-22980  
 New implantation techniques for improved solar cell junctions  
 [NASA-CR-175410] p 161 A84-23059  
 Ion implanted junctions for silicon space solar cells  
 [NASA-CR-175410] p 42 A84-30143
- Stanford Univ., Calif.**  
 Turbulent boundary-layer flow and structure on a convex wall and its redevelopment on a flat wall  
 [NASA-CR-175410] p 115 A84-21378  
 Interference performance analysis of M-ary CPSK and M-ary CAPK digital transmission systems and the computation of "required isolation" for efficient utilization of geostationary satellite orbit/spectrum  
 [NASA-CR-175410] p 95 A84-49303  
 Element-by-element solution procedures for nonlinear structural analysis  
 [NASA-CR-175410] p 158 N84-31694
- State Univ. of New York, Stony Brook.**  
 Phase analysis of plasma-sprayed zirconia-yttria coatings  
 [NASA-CR-175410] p 78 A84-19781  
 Anisotropic thermal expansion effects in plasma-sprayed ZrO<sub>2</sub>-8 percent Y<sub>2</sub>O<sub>3</sub> coatings  
 [NASA-CR-175410] p 78 A84-19782
- Stevens Inst. of Tech., Hoboken, N. J.**  
 The influence of gyroscopic forces on the dynamic behavior and flutter of rotating blades  
 [NASA-CR-175444] p 27 N84-20524
- Sverdrup Technology, Inc., Arnold Air Force Station, Tenn.**  
 One-dimensional unsteady modeling of supersonic inlet unstart/restart  
 [AIAA PAPER 84-0439] p 4 A84-18094
- Syracuse Univ., N. Y.**  
 Literature survey on oxidations and fatigue lives at elevated temperatures  
 [NASA-CR-174639] p 71 N84-20674  
 Crack tip field and fatigue crack growth in general yielding and low cycle fatigue  
 [NASA-CR-174686] p 76 N84-32503
- Systems Science and Software, La Jolla, Calif.**  
 Plasma sheath structure surrounding a large powered spacecraft  
 [AIAA PAPER 84-0329] p 40 A84-18025  
 Potentials in a plasma over a biased pinhole  
 [NASA-CR-175410] p 102 A84-20711

## T

- Teledyne CAE, Toledo, Ohio.**  
 Aerodynamic effects of moveable sidewall nozzle geometry and rotor exit restriction on the performance of a radial turbine  
 [SAE PAPER 831517] p 17 A84-29460  
 Variable stator radial turbine  
 [NASA-CR-174663] p 29 N84-22568
- Tennessee Univ., Knoxville.**  
 Measurements of local convective heat transfer coefficients on ice accretion shapes  
 [AIAA PAPER 84-0018] p 113 A84-17835  
 Thermoacoustic convection heat-transfer phenomenon  
 [NASA-CR-174660] p 10 N84-25646  
 Measurement of local convective heat transfer coefficients of four ice accretion shapes  
 [NASA-CR-174660] p 10 N84-25646
- Tennessee Univ., Tullahoma.**  
 Comparison of experimental and computational compressible flow in a S-duct  
 [AIAA PAPER 84-0033] p 4 A84-19228  
 Sixth Annual Workshop on Meteorological and Environmental Inputs to Aviation Systems, 26-28 October 1982, Tullahoma, Tenn.  
 [NASA-CR-174660] p 174 A84-23424
- Tennessee Univ. Space Inst., Tullahoma.**  
 Measurement of spray combustion processes  
 [NASA-CR-174660] p 61 N84-20530
- Texas A&M Univ., College Station.**  
 Performance degradation of propeller systems due to rime ice accretion  
 [AIAA PAPER 82-0286] p 12 A84-17406  
 Helicopter rotor performance degradation in natural icing encounter  
 [AIAA PAPER 84-0184] p 12 A84-17412  
 Experimental study of performance degradation of a model helicopter main rotor with simulated ice shapes  
 [AIAA PAPER 84-0184] p 13 A84-17937  
 Performance degradation of a model helicopter main rotor in hover and forward flight with a generic ice shape  
 [AIAA PAPER 84-0609] p 13 A84-24195  
 Analysis for leakage and rotordynamic coefficients of surface-roughened tapered annular gas seals  
 [ASME PAPER 84-GT-32] p 140 A84-46896  
 Performance degradation of a model helicopter rotor with a generic ice shape  
 [NASA-CR-173550] p 85 N84-24810  
 Evaluation of dissociated and steam-reformed methanol as automotive engine fuels  
 [NASA-CR-168242] p 91 N84-27909
- Texas Instruments, Inc., Dallas.**  
 0.5 W 2-21 GHz monolithic GaAs distributed amplifier  
 [NASA-CR-168207] p 103 A84-30857  
 GaAs dual-gate FET for operation up to K-band  
 [NASA-CR-168240] p 104 A84-32281  
 30/20 GHz spacecraft GaAs FET solid state transmitter for trunking and customer-premise-service application  
 [NASA-CR-168276] p 107 N84-16463
- Texas Univ., Arlington.**  
 Transient flow analysis of the AEDC/HPDE MHD generator  
 [NASA-CR-168240] p 189 A84-24049
- Texas Univ., Austin.**  
 Comments on some problems in computational penetration mechanics  
 [NASA-CR-168240] p 150 A84-13545  
 A numerical analysis of contact and limit-point behavior in a class of problems of finite elastic deformation  
 [NASA-CR-168240] p 150 A84-27370  
 Transonic cascade flow analysis using viscous/inviscid coupling concepts  
 [AIAA PAPER 84-2159] p 6 A84-46103  
 Energy stores and switches for rail-launcher systems  
 [NASA-CR-173249] p 107 N84-16458  
 Stability and convergence of undenintegrated finite element approximations  
 [NASA-CR-173249] p 158 N84-31696
- Textron Bell Aerospace Co., Buffalo, N. Y.**  
 NASTRAN forced vibration analysis of rotating cyclic structures  
 [ASME PAPER 83-DET-20] p 151 A84-29103  
 Forced vibration analysis of rotating cyclic structures in NASTRAN  
 [NASA-CR-165429] p 153 N84-11514  
 Finite element forced vibration analysis of rotating cyclic structures  
 [NASA-CR-165430] p 153 N84-11515  
 NASTRAN flutter analysis of advanced turbopropellers  
 [NASA-CR-167926] p 24 N84-14148  
 NASTRAN documentation for flutter analysis of advanced turbopropellers  
 [NASA-CR-167927] p 25 N84-15153  
 Bladed-shrouded-disc aeroelastic analyses: Computer program updates in NASTRAN level 17  
 [NASA-CR-165428] p 25 N84-15154  
 NASTRAN forced vibration analysis of rotating cyclic structures

United Stirling<sup>7</sup>A.B. Malmö (Sweden).

- [NASA-CR-173821] p 157 N84-29252  
 Slave finite elements The temporal element approach to nonlinear analysis  
 [NASA-CR-173821] p 157 N84-31689
- Thermo Electron Corp., Waltham, Mass.**  
 An RC-1 organic Rankine bottoming cycle for an adiabatic diesel engine  
 [NASA-CR-168256] p 196 N84-32306
- Toledo Univ., Ohio.**  
 Investigation of energy management strategies for photovoltaic systems - An analysis technique  
 [NASA-CR-168256] p 160 A84-22993  
 Inherent overload protection for the series resonant converter  
 [NASA-CR-168256] p 102 A84-23255  
 A large-signal dynamic simulation for the series resonant converter  
 [NASA-CR-168256] p 103 A84-23258  
 Investigation of energy management strategies for photovoltaic systems - A predictive control algorithm  
 [NASA-CR-168256] p 161 A84-25468  
 Assessment of two neglected effects in the analysis of an oil pumping ring seal  
 [ASME PAPER 83-LUB-16] p 137 A84-29097  
 NTSC composite video at 1.6 bits/pel  
 [NASA-CR-168256] p 95 A84-49259  
 Numerical simulation of two-dimensional heat transfer in composite bodies with application to de-icing of aircraft components  
 [NASA-CR-168283] p 122 N84-13490  
 Thermal stress analysis for a wood composite blade  
 [NASA-CR-173394] p 156 N84-21803  
 Thermal-stress analysis for wood composite blade  
 [NASA-CR-173830] p 157 N84-31685
- Trane Co., LaCrosse, Wis.**  
 Heat recovery subsystem and overall system integration of fuel cell on-site integrated energy systems  
 [NASA-CR-168308] p 166 N84-20915
- Transmission Research, Inc., Cleveland, Ohio.**  
 An advanced pitch change mechanism incorporating a hybrid traction drive  
 [AIAA PAPER 84-1383] p 20 A84-44182
- TRW Electronic Systems Group, Redondo Beach, Calif.**  
 A K-band GaAs FET amplifier with 8.2-W output power  
 [NASA-CR-168240] p 104 A84-32290  
 A 20-GHz IMPATT transmitter  
 [NASA-CR-168076] p 106 N84-11385  
 The 20 GHz spacecraft FET solid state transmitter  
 [NASA-CR-168240] p 107 N84-17477  
 K-band latching switches  
 [NASA-CR-168253] p 109 N84-24973
- TRW, Inc., Cleveland, Ohio.**  
 Fabrication development for ODS-superalloy, air-cooled turbine blades  
 [NASA-CR-174650] p 32 N84-25711
- TRW, Inc., El Segundo, Calif.**  
 A scheme for handling arrays in data-flow systems  
 [NASA-CR-174650] p 175 A84-39972
- TRW, Inc., Redondo Beach, Calif.**  
 Apparatus analysis and preliminary design of low gravity porous solids experiment for STS Orbiter mid-deck  
 [NASA-CR-168248] p 37 N84-10109  
 Improved high temperature resistant matrix resins  
 [NASA-CR-168210] p 87 N84-28995  
 Development of partially fluorinated resin apex seals  
 [NASA-CR-174706] p 148 N84-32828
- TRW Space Technology Labs., Redondo Beach, Calif.**  
 Study of solar array switching power management technology for space power system  
 [NASA-CR-167890-EXEC-SUM] p 167 N84-23021  
 Preliminary design of two Space Shuttle fluid physics experiments  
 [NASA-CR-174649] p 39 N84-23667
- Tuskegee Inst., Ala.**  
 Energy partitioning in an inductively driven rail gun  
 [NASA-CR-174649] p 104 A84-33325

## U

- Ultrasystems, Inc., Irvine, Calif.**  
 Thermal oxidative degradation reactions of linear perfluoroalkyl ethers  
 [NASA-CR-168004] p 80 A84-30000  
 Synthesis of perfluoroalkylene dianilines  
 [NASA-CR-168004] p 60 N84-11228  
 Thermal oxidative degradation reactions of perfluoroalkylethers  
 [NASA-CR-168224] p 60 N84-11229  
 Union Carbide Corp., Indianapolis, Ind.  
 Determination of near-surface plastic deformation in sliding contacts  
 [NASA-CR-168224] p 140 A84-48995
- United Stirling A.B. Malmö (Sweden).**  
 Comparison of seal materials for use in Stirling engines  
 [NASA-CR-168224] p 64 A84-22879



**United Technologies Corp., East Hartford, Conn.**

- Calculations of turbulent mass transport in a bluff-body diffusion-flame combustor  
[AIAA PAPER 84-0372] p 114 A84-18048
- An assessment of the use of antimisting fuel in turbofan engines  
[NASA-CR-168081] p 89 N84-10332
- Deposit formation and heat transfer in hydrocarbon rocket fuels  
[NASA-CR-168277] p 45 N84-12225
- Combustor liner construction  
[NASA-CASE-LEW-14035-1] p 30 N84-24577
- Energy efficient engine high-pressure turbine supersonic cascade technology report  
[NASA-CR-165567] p 33 N84-27739
- Materials for Advanced Turbine Engines (MATE) Project 3. Design, fabrication and evaluation of an oxide dispersion strengthened sheet alloy combustor liner, volume 1  
[NASA-CR-174691] p 76 N84-32504
- United Technologies Corp., South Windsor, Conn.**
- Alkaline fuel cells for the regenerative fuel cell energy storage system  
p 162 A84-30183
- United Technologies Corp., West Palm Beach, Fla.**
- A piecewise linear state variable technique for real time propulsion system simulation  
p 20 A84-42378
- United Technologies Research Center, East Hartford, Conn.**
- Deposit formation and heat transfer in hydrocarbon rocket fuels  
[AIAA PAPER 84-0512] p 88 A84-18142
- Carbides in iron-rich Fe-Mn-Cr-Mo-Al-Si-C systems  
p 64 A84-26815
- The use of heterodyne speckle photogrammetry to measure high-temperature strain distributions  
p 130 A84-28623
- Role of fuel chemical properties on combustor radiative heat load  
[AIAA PAPER 84-1493] p 89 A84-35236
- Mass and momentum turbulent transport experiments with confined swirling coaxial jets I  
[AIAA PAPER 84-1380] p 119 A84-35664
- Inlet boundary layer effects in an axial compressor rotor I Blade-to-blade effects  
[ASME PAPER 84-GT-84] p 6 A84-46926
- Inlet boundary layer effects in an axial compressor rotor II - Throughflow effects  
[ASME PAPER 84-GT-85] p 7 A84-46927
- Research and development program for the development of advanced time-temperature dependent constitutive relationships. Volume 1: Theoretical discussion  
[NASA-CR-168191-VOL-1] p 153 N84-10613
- Research and development program for the development of advanced time-temperature dependent constitutive relationships Volume 2: Programming manual  
[NASA-CR-168191-VOL-2] p 153 N84-10614
- Aeroelastic analysis for propellers - mathematical formulations and program user's manual  
[NASA-CR-3729] p 153 N84-12530
- Compressor rotor aerodynamics  
p 26 N84-16210
- Aviation-fuel property effects on combustion  
[NASA-CR-168334] p 89 N84-17407
- Mass and momentum turbulent transport experiments with confined swirling coaxial jets  
[NASA-CR-168252] p 124 N84-17530
- Extension to an analysis of turbulent swirling compressible flow for application to axisymmetric small gas turbine ducts  
[NASA-CR-165597] p 195 N84-21445
- Abrasive tip treatment for use on compressor blades  
[NASA-CR-174666] p 145 N84-25065
- Waste heat recovery from adiabatic diesel engines by exhaust-driven Brayton cycles  
[NASA-CR-168257] p 196 N84-32307
- A linear aerodynamic analysis for unsteady transonic cascades  
[NASA-CR-3833] p 11 N84-32355
- Universities Space Research Association, Columbia, Md.**
- Improved design of subcritical and supercritical cascades using complex characteristics and boundary-layer correction  
p 5 A84-38839
- University of Northern Arizona, Flagstaff.**
- Swirl, expansion ratio and blockage effects on confined turbulent flow  
[NASA-CR-175391] p 125 N84-19746
- University of Southern Illinois, Carbondale.**
- How to protect a wind turbine from lightning  
[NASA-CR-168229] p 163 N84-10681
- Utah Univ., Salt Lake City.**
- Carbon-13 and proton nuclear magnetic resonance analysis of shale-derived refinery products and jet fuels and of experimental referee broadened-specification-jet fuels  
[NASA-CR-174761] p 92 N84-32552

**V**

- Varian Associates, Palo Alto, Calif.**
- Development of a 30 percent efficient 3-junction monolithic cascade solar cell  
p 171 N84-29328
- Virginia Polytechnic Inst., Blacksburg**
- A temperature correlation for the radiation resistance of a thick-walled circular duct exhausting a hot gas  
p 181 A84-31103
- Virginia Polytechnic Inst. and State Univ., Blacksburg.**
- Characterization of composite materials by means of the ultrasonic stress wave factor  
p 51 A84-10430
- Extensions of the discrete-average models for converter power stages  
p 102 A84-18411
- Stability analysis of a buck regulator employing input filter compensation  
p 102 A84-18412
- Design considerations for FET-gated power transistors  
p 102 A84-18414
- A new FET-bipolar combinational power semiconductor switch  
p 104 A84-32293
- Recovery of burner acoustic source structure from far-field sound spectra  
[AIAA PAPER 83-0763] p 181 A84-32609
- A mixed shear flexible finite element for the analysis of laminated plates  
p 152 A84-45994
- Improved transistor-controlled and commutated brushless DC motors for electric vehicle propulsion  
[NASA-CR-168053] p 105 N84-10450
- Input filter compensation for switching regulators  
[NASA-CR-173247] p 107 N84-16459
- Input filter compensation for switching regulators  
[NASA-CR-173557] p 110 N84-24975
- A critical review of noise production models for turbulent, gas-fueled burners  
[NASA-CR-3803] p 184 N84-26384
- Virginia Univ., Charlottesville.**
- Effects of volute geometry and impeller orbit on the hydraulic performance of a centrifugal pump  
p 136 A84-22316
- Penalty function finite element analysis of steady viscous incompressible flow in rotating coordinates  
[ASME PAPER 84-GT-36] p 121 A84-46900
- Design study of magnetic eddy-current vibration suppression dampers for application to cryogenic turbomachinery  
[NASA-CR-173273] p 141 N84-16562
- Carrier recovery methods for a dual-mode modem A design approach  
[NASA-CR-173355] p 36 N84-19360
- Design considerations for a monolithic, GaAs, dual-mode, QPSK/QASK, high-throughput rate transceiver  
[NASA-CR-173560] p 110 N84-24974

**W**

- Washington Univ., Seattle.**
- High effectiveness liquid droplet/gas heat exchanger for space power applications  
[IAF PAPER 83-433] p 42 A84-11819
- Basic and applied research related to the technology of space-energy conversion systems, 1982 - 1983  
[NASA-CR-173554] p 169 N84-25168
- Westinghouse Electric Corp., Pittsburgh, Pa.**
- Evaluation of gas cooling for pressurized phosphoric acid fuel cell stacks  
p 163 A84-30191
- Development and fabrication of an augmented power transistor  
[NASA-CR-168262] p 106 N84-11388
- Wind turbine generator interaction with conventional diesel generators on Block Island, Rhode Island. Volume 1: Executive summary  
[NASA-CR-168318] p 171 N84-29357
- Wind turbine generator interaction with conventional diesel generators on Block Island, Rhode Island. Volume 2: Data analysis  
[NASA-CR-168319] p 172 N84-31783
- Westinghouse Research and Development Center, Pittsburgh, Pa.**
- Labyrinth seal forces on a whirling rotor  
p 135 A84-13228
- Thermal stress fracture of ceramic coatings  
p 80 A84-24553
- Degradation mechanisms of ceramic thermal barrier coatings in corrosive environments  
p 81 A84-42668
- Double-injection, deep-impurity switch development  
[NASA-CR-168335] p 108 N84-18536
- Measurement of heat pump processes induced by laser radiation  
[NASA-CR-168324] p 134 N84-18620
- Wichita State Univ., Kans.**
- Streamwise computation of three-dimensional parabolic flows  
p 113 A84-16828

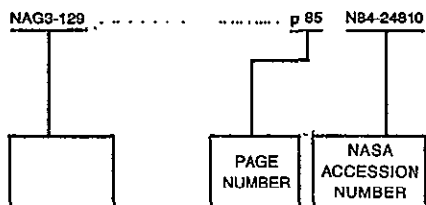
- Flight and wind tunnel tests of an electro-impulse de-icing system  
[AIAA PAPER 84-2234] p 12 A84-39280

**Y****Yale Univ., New Haven, Conn.**

- Correlation of thermophoretically-modified small particle diffusional deposition rates in forced convection systems with variable properties, transpiration cooling and/or viscous dissipation  
p 117 A84-32323
- Comparisons of rational engineering correlations of thermophoretically-augmented particle mass transfer with STANS-predictions for developing boundary layers  
[ASME PAPER 84-GT-158] p 92 A84-46965
- Comparisons of rational engineering correlations of thermophoretically-augmented particle mass transfer with STANS-predictions for developing boundary layers  
[NASA-CR-168221] p 93 N84-19608

# CONTRACT NUMBER INDEX

## Typical Contract Number Index Listing



Listings in this index are arranged alphanumerically by contract number. Under each contract number, the accession numbers denoting documents that have been produced as a result of research done under that contract are arranged in ascending order with the AIAA accession numbers appearing first. The accession number denotes the number by which the citation is identified in the abstract section. Preceding the accession number is the page number on which the citation may be found.

AF-AFOSR-0005-81 ... p 90 N84-17410  
 AF-AFOSR-0091-79 ... p 188 N84-22405  
 AF-AFOSR-6475 ... p 61 N84-20555  
 AF-AFOSR-79-0091 ... p 187 N84-13184  
 ... p 178 N84-23602  
 ... p 178 N84-38596  
 ... p 175 N84-40266  
 AF-AFOSR-80-0160 ... p 2 N84-10078  
 ... p 122 N84-49112  
 AF-AFOSR-81-0142 ... p 152 N84-45994  
 DA PROJ 1L1-61101-AH-45 ... p 147 N84-30294  
 DA PROJ 1L1-61102-AH-45 ... p 29 N84-22568  
 ... p 145 N84-25065  
 ... p 10 N84-25647  
 DAAG24-83-K-0058 ... p 90 N84-17410  
 DAAG29-81-K-0134 ... p 187 N84-16397  
 DAAG29-82-K-0018 ... p 179 N84-24410  
 DE-AC02-79ER-10515-A000 ... p 116 N84-25807  
 DE-AC22-81PC-40276 ... p 118 N84-35168  
 DE-AI01-76ET-20320 ... p 163 N84-10861  
 ... p 165 N84-14586  
 ... p 107 N84-17479  
 ... p 169 N84-27327  
 ... p 171 N84-29347  
 ... p 171 N84-29357  
 ... p 172 N84-31783  
 DE-AI01-77CS-1040 ... p 141 N84-15554  
 DE-AI01-77CS-51040 ... p 140 N84-10581  
 ... p 194 N84-14989  
 ... p 68 N84-15246  
 ... p 155 N84-16589  
 ... p 194 N84-18117  
 ... p 195 N84-21445  
 ... p 73 N84-25793  
 ... p 195 N84-26484  
 ... p 146 N84-28089  
 ... p 74 N84-28961  
 ... p 74 N84-28962  
 ... p 75 N84-28963  
 ... p 195 N84-32305  
 ... p 196 N84-33307  
 ... p 77 N84-34603  
 DE-AI01-77CS-51044 ... p 105 N84-10450  
 ... p 193 N84-14071  
 ... p 194 N84-17073  
 ... p 194 N84-19185  
 ... p 166 N84-20014  
 ... p 166 N84-20016  
 ... p 166 N84-20017  
 ... p 169 N84-25166  
 ... p 91 N84-27909

DE-AI01-77ET-10769 ... p 189 N84-24058  
 DE-AI01-77ET-13111 ... p 172 N84-31784  
 ... p 173 N84-34038  
 DE-AI01-79ET-20305 ... p 164 N84-13670  
 DE-AI01-79ET-20320 ... p 163 N84-10664  
 DE-AI01-79ET-20485 ... p 110 N84-25926  
 DE-AI01-80CS-50194 ... p 196 N84-32306  
 ... p 196 N84-33304  
 ... p 196 N84-33309  
 ... p 197 N84-34330  
 ... p 197 N84-34331  
 DE-AI01-80CS-50294 ... p 196 N84-33306  
 DE-AI01-80ET-17088 ... p 164 N84-10665  
 ... p 164 N84-11581  
 ... p 164 N84-13672  
 ... p 164 N84-13673  
 ... p 170 N84-27329  
 DE-AI01-81CS-50006 ... p 165 N84-14587  
 ... p 91 N84-23775  
 ... p 91 N84-26813  
 ... p 74 N84-28960  
 ... p 172 N84-34036  
 DE-AI04-80AL-12726 ... p 164 N84-11579  
 ... p 164 N84-11580  
 ... p 172 N84-29358  
 DE-AI05-82OR-1005 ... p 195 N84-22512  
 ... p 195 N84-24509  
 DE-AI05-82OR-21005 ... p 138 N84-30095  
 DE-AI21-80ET-17088 ... p 166 N84-18757  
 ... p 169 N84-25169  
 ... p 169 N84-26165  
 ... p 173 N84-34037  
 DE-AM03-76SF-00034-PA-372 ... p 59 N84-27724  
 DE-FG22-82PC-50259 ... p 59 N84-35401  
 DEN3-110 ... p 80 N84-24553  
 DEN3-156 ... p 165 N84-15679  
 DEN3-165 ... p 189 N84-24058  
 DEN3-167 ... p 140 N84-46954  
 ... p 140 N84-47036  
 ... p 195 N84-29805  
 DEN3-168 ... p 135 N84-10499  
 ... p 136 N84-22878  
 ... p 140 N84-46954  
 ... p 140 N84-47036  
 ... p 140 N84-10581  
 ... p 141 N84-15554  
 ... p 146 N84-28089  
 DEN3-17 ... p 140 N84-46954  
 ... p 140 N84-47036  
 DEN3-189 ... p 193 N84-14071  
 DEN3-201 ... p 163 N84-30191  
 ... p 169 N84-25169  
 DEN3-205 ... p 169 N84-26165  
 DEN3-211 ... p 111 N84-31514  
 DEN3-217 ... p 65 N84-36173  
 DEN3-235 ... p 195 N84-21445  
 DEN3-238 ... p 169 N84-25163  
 DEN3-240 ... p 169 N84-25162  
 DEN3-241 ... p 164 N84-11581  
 ... p 164 N84-13672  
 ... p 164 N84-13673  
 ... p 166 N84-20915  
 ... p 170 N84-27329  
 DEN3-249 ... p 103 N84-24850  
 ... p 194 N84-17073  
 DEN3-250 ... p 164 N84-11580  
 DEN3-257 ... p 172 N84-31784  
 DEN3-258 ... p 166 N84-20014  
 DEN3-261 ... p 138 N84-30062  
 DEN3-263 ... p 74 N84-28960  
 DEN3-264 ... p 172 N84-29358  
 DEN3-275 ... p 171 N84-29357  
 DEN3-287 ... p 143 N84-21877  
 DEN3-291 ... p 166 N84-18757  
 DEN3-294 ... p 58 N84-12644  
 DEN3-295 ... p 165 N84-14587  
 DEN3-300 ... p 196 N84-33304  
 DEN3-301 ... p 194 N84-14991  
 DEN3-302 ... p 196 N84-32306  
 DEN3-303 ... p 74 N84-28961  
 DEN3-304 ... p 196 N84-32307  
 DEN3-323 ... p 196 N84-33309  
 DEN3-324 ... p 197 N84-34331

DEN3-327 ... p 172 N84-34036  
 DEN3-32 ... p 64 N84-22879  
 ... p 138 N84-30091  
 ... p 138 N84-30092  
 ... p 173 N84-41044  
 ... p 194 N84-18117  
 ... p 195 N84-32305  
 ... p 196 N84-33307  
 DEN3-333 ... p 136 N84-22864  
 DEN3-354 ... p 171 N84-29357  
 DEN3-65 ... p 105 N84-10450  
 DEN3-954 ... p 172 N84-31783  
 DOT-FA78WAI-893 ... p 174 N84-18806  
 ... p 193 N84-22488  
 ... p 174 N84-27375  
 ... p 174 N84-31865  
 F04701-77-C-0062 ... p 41 N84-17262  
 F29601-82-K-0009 ... p 130 N84-28797  
 F33575-80-C-1182 ... p 39 N84-46620  
 F33615-77-C-2036 ... p 122 N84-49192  
 F33615-77-C-2083 ... p 6 N84-46926  
 ... p 7 N84-46927  
 ... p 26 N84-16210  
 F33615-81-K-2036 ... p 151 N84-31903  
 F49620-78-C-0053 ... p 79 N84-23689  
 F49620-78-C-0083 ... p 150 N84-13545  
 F49620-78-C-0084 ... p 120 N84-38030  
 F49620-80-C-0082 ... p 118 N84-35168  
 F49620-82-K-0020 ... p 117 N84-32323  
 F49620-83-C-0060 ... p 129 N84-17946  
 F49620-84-C-0023 ... p 131 N84-36958  
 NAG1-409 ... p 175 N84-40266  
 NAG1-74 ... p 115 N84-22922  
 NAG3-102 ... p 3 N84-17881  
 NAG3-109 ... p 12 N84-17406  
 ... p 12 N84-17412  
 NAG3-112 ... p 176 N84-11892  
 NAG3-124 ... p 181 N84-31103  
 ... p 181 N84-32609  
 ... p 184 N84-26384  
 NAG3-129 ... p 65 N84-24810  
 NAG3-131 ... p 114 N84-18171  
 ... p 116 N84-26379  
 ... p 59 N84-29128  
 ... p 119 N84-35318  
 ... p 60 N84-48139  
 ... p 21 N84-10054  
 ... p 23 N84-13189  
 NAG3-132 ... p 175 N84-11876  
 ... p 175 N84-39972  
 ... p 176 N84-25336  
 NAG3-134 ... p 66 N84-43872  
 NAG3-137 ... p 59 N84-29128  
 NAG3-13 ... p 65 N84-36047  
 NAG3-142 ... p 91 N84-27909  
 NAG3-143 ... p 138 N84-30061  
 NAG3-147 ... p 61 N84-20554  
 ... p 49 N84-31280  
 NAG3-153 ... p 137 N84-28987  
 NAG3-156 ... p 95 N84-48452  
 NAG3-159 ... p 38 N84-23662  
 NAG3-160 ... p 156 N84-21905  
 NAG3-161 ... p 185 N84-27544  
 NAG3-164 ... p 78 N84-19781  
 ... p 78 N84-19782  
 ... p 140 N84-47046  
 NAG3-166 ... p 137 N84-28792  
 NAG3-16 ... p 42 N84-11819  
 ... p 169 N84-25168  
 NAG3-172 ... p 51 N84-10430  
 NAG3-178 ... p 180 N84-21250  
 NAG3-179 ... p 117 N84-29798  
 ... p 120 N84-38557  
 NAG3-17 ... p 9 N84-20488  
 NAG3-180 ... p 136 N84-22316  
 ... p 121 N84-46900  
 NAG3-181 ... p 140 N84-46896  
 NAG3-182 ... p 181 N84-24597  
 NAG3-186 ... p 145 N84-26027  
 NAG3-188 ... p 161 N84-23115  
 ... p 161 N84-26027  
 ... p 161 N84-26028  
 NAG3-189 ... p 179 N84-10136

NAG3-190	p 58	A84-11636	NAG3-329	p 150	A84-13545	NAS1-17130	p 7	N84-10022
	p 113	A84-17842		p 150	A84-27370	NAS3-151	p 95	A84-49303
	p 114	A84-17897		p 158	N84-31696	NAS3-156	p 137	A84-29097
	p 23	N84-13187	NAG3-32	p 154	N84-15589	NAS3-20070	p 7	A84-46985
	p 61	N84-20532	NAG3-333	p 37	A84-22346	NAS3-20072	p 76	N84-32504
	p 128	N84-29155		p 190	A84-42829	NAS3-20073	p 68	N84-15247
	p 35	N84-29877		p 191	N84-28621	NAS3-20605	p 36	N84-33417
	p 35	N84-32390	NAG3-339	p 178	N84-11831	NAS3-20643	p 22	N84-11170
NAG3-194	p 3	A84-11591	NAG3-33	p 150	A84-21541	NAS3-20646	p 33	N84-27737
	p 122	A84-49112		p 158	N84-31690		p 33	N84-27738
NAG3-198	p 181	A84-23355	NAG3-340	p 104	A84-32293		p 33	N84-27739
NAG3-19	p 4	A84-17925		p 148	N84-14526		p 33	N84-28788
NAG3-200	p 151	A84-31803	NAG3-346	p 149	A84-13248		p 33	N84-28789
NAG3-201	p 117	A84-32323		p 158	N84-31697		p 35	N84-32389
	p 92	A84-46665	NAG3-348	p 71	N84-20674	NAS3-20662	p 23	N84-14143
	p 124	N84-18578		p 76	N84-32503	NAS3-20797	p 180	A84-21272
	p 93	N84-19606	NAG3-350	p 125	N84-20542	NAS3-20825	p 135	A84-13228
	p 124	N84-19741	NAG3-353	p 61	N84-20555	NAS3-21249	p 12	N84-11152
NAG3-204	p 34	N84-29875	NAG3-361	p 58	A84-18925		p 174	N84-27375
NAG3-205	p 90	N84-17410		p 58	A84-23593	NAS3-21377	p 81	A84-42668
NAG3-208	p 152	A84-45994	NAG3-362	p 149	N84-17606	NAS3-21726	p 108	N84-21376
NAG3-209	p 130	A84-28797	NAG3-370	p 61	N84-20530	NAS3-21727	p 79	A84-19786
	p 46	N84-18322	NAG3-373	p 156	N84-21903	NAS3-21977	p 89	A84-26955
	p 41	N84-17258		p 157	N84-31685	NAS3-22003	p 24	N84-15151
NAG3-20	p 27	N84-18202	NAG3-37	p 21	A84-44645	NAS3-22012	p 135	A84-15575
NAG3-212	p 32	N84-24586	NAG3-382	p 61	N84-19495	NAS3-22045	p 89	N84-10332
NAG3-214	p 165	N84-15681	NAG3-38	p 150	A84-16874	NAS3-22063	p 89	N84-15283
NAG3-219	p 112	A84-13311		p 150	A84-16884	NAS3-22110	p 33	N84-26702
NAG3-220	p 102	A84-18412	NAG3-392	p 179	A84-24410	NAS3-22126	p 130	A84-28623
	p 107	N84-16459	NAG3-394	p 196	N84-33306	NAS3-22137	p 185	N84-29661
	p 110	N84-24975	NAG3-3	p 115	A84-21378	NAS3-22143	p 21	A84-46354
NAG3-221	p 150	A84-21267	NAG3-401	p 61	N84-20535	NAS3-22224	p 191	N84-17014
NAG3-222	p 188	N84-16984	NAG3-40	p 102	A84-18414	NAS3-22227	p 160	A84-22998
NAG3-223	p 159	N84-34774	NAG3-414	p 187	A84-16397		p 160	A84-23002
NAG3-227	p 179	N84-31279	NAG3-418	p 99	N84-23807	NAS3-22228	p 160	A84-22981
NAG3-22	p 64	A84-18733	NAG3-419	p 100	N84-25909	NAS3-22229	p 160	A84-22981
	p 66	N84-10267	NAG3-41	p 151	A84-31596	NAS3-22232	p 171	N84-29328
NAG3-231	p 17	A84-31905		p 155	N84-19925	NAS3-22234	p 162	A84-30183
	p 152	A84-46957	NAG3-420	p 112	N84-34675	NAS3-22235	p 190	A84-33918
NAG3-232	p 176	A84-10905	NAG3-42	p 95	A84-49259	NAS3-22236	p 42	A84-22980
NAG3-233	p 4	A84-19228	NAG3-434	p 108	N84-19709		p 161	A84-23059
NAG3-238	p 59	A84-29999	NAG3-449	p 189	N84-16991		p 42	A84-30143
NAG3-239	p 120	A84-38857		p 173	N84-25204	NAS3-22238	p 162	A84-30186
NAG3-23	p 156	N84-22980	NAG3-44	p 71	N84-20676	NAS3-22245	p 166	N84-15682
NAG3-242	p 12	A84-17406	NAG3-464	p 57	N84-34575	NAS3-22247	p 108	N84-18536
	p 12	A84-17412	NAG3-475	p 98	N84-19620	NAS3-22249	p 162	A84-30189
	p 13	A84-17937		p 100	N84-30145		p 108	N84-22889
	p 13	A84-24195	NAG3-47	p 101	N84-32645	NAS3-2224	p 190	A84-33918
NAG3-244	p 14	A84-49096		p 27	N84-20524	NAS3-22251	p 3	A84-17841
NAG3-245	p 75	N84-31944	NAG3-490	p 191	A84-49620	NAS3-22252	p 161	A84-30162
NAG3-246	p 125	N84-20546	NAG3-50	p 155	N84-19927	NAS3-22324	p 177	A84-10010
NAG3-249	p 152	N84-10612	NAG3-536	p 99	N84-24924	NAS3-22336	p 109	N84-24973
NAG3-24	p 170	N84-29312	NAG3-53	p 58	A84-23593	NAS3-22343	p 100	N84-31464
NAG3-260	p 104	A84-39197		p 59	A84-35425	NAS3-22387	p 66	N84-10268
NAG3-263	p 36	N84-33412	NAG3-54	p 152	A84-38480	NAS3-22442	p 159	N84-27258
NAG3-263	p 141	N84-16562		p 158	N84-31693	NAS3-22474	p 44	N84-10180
NAG3-265	p 121	A84-46982	NAG3-57	p 67	N84-14287	NAS3-22491	p 39	A84-46620
	p 152	A84-48565		p 70	N84-19523		p 112	N84-33715
NAG3-266	p 91	N84-23775	NAG3-5	p 187	A84-13184	NAS3-22492	p 106	N84-11385
NAG3-270	p 127	N84-25341		p 178	A84-23602	NAS3-22494	p 39	A84-46620
NAG3-271	p 64	A84-26815		p 187	A84-28485		p 97	N84-13398
NAG3-273	p 9	N84-17139		p 175	A84-38596	NAS3-22498	p 93	A84-15627
NAG3-274	p 102	A84-18411		p 175	A84-40266		p 94	A84-25256
NAG3-276	p 71	N84-21716	NAG3-61	p 188	N84-22405	NAS3-22501	p 105	A84-49253
	p 72	N84-21721		p 3	A84-17861	NAS3-22502	p 93	A84-15628
NAG3-277	p 95	N84-10401	NAG3-67	p 180	A84-18131		p 93	A84-15629
NAG3-27	p 92	N84-32552	NAG3-6	p 139	A84-46893		p 95	A84-38251
NAG3-283	p 103	A84-32029	NAG3-72	p 122	N84-13490	NAS3-22503	p 104	A84-32290
NAG3-284	p 12	A84-39280	NAG3-74	p 113	A84-13564		p 107	N84-17477
NAG3-288	p 99	N84-24918		p 130	A84-18047	NAS3-22504	p 107	N84-16463
NAG3-28	p 12	A84-37935		p 114	A84-18096	NAS3-22507	p 32	N84-25711
	p 12	A84-45054		p 116	A84-27138	NAS3-22514	p 185	N84-33148
	p 8	N84-16145		p 118	A84-35196		p 186	N84-33149
	p 8	N84-16146		p 118	A84-35197		p 186	N84-33150
NAG3-292	p 119	A84-35233		p 131	A84-37999	NAS3-22517	p 60	N84-11229
	p 120	A84-37467		p 120	A84-39000	NAS3-22519	p 60	N84-11228
	p 30	N84-23649		p 124	N84-19744	NAS3-22522	p 63	A84-11194
NAG3-294	p 61	N84-20554		p 125	N84-19745	NAS3-22523	p 83	N84-20695
NAG3-295	p 84	N84-22753		p 125	N84-19746	NAS3-22533	p 151	A84-29103
NAG3-298	p 158	N84-31895	NAG3-76	p 104	A84-33325		p 152	A84-36492
NAG3-2	p 129	A84-13192	NAG3-83	p 113	A84-17835		p 153	N84-11514
	p 117	A84-28738		p 10	N84-25646		p 153	N84-11515
	p 130	A84-28739	NAG3-84	p 194	N84-19185		p 24	N84-14148
NAG3-303	p 107	N84-16458	NAG3-91	p 91	N84-26813		p 25	N84-15153
NAG3-305	p 189	A84-46108	NAG3-95	p 104	A84-34521		p 25	N84-15154
	p 189	A84-46109	NAG3-98	p 90	N84-18420		p 157	N84-29252
	p 111	N84-32682	NAG3-9	p 120	A84-38030	NAS3-22536	p 41	N84-17268
NAG3-3161	p 36	N84-19360		p 7	N84-10022	NAS3-22548	p 81	N84-12312
NAG3-316	p 110	N84-24974		p 98	N84-15360		p 82	N84-16337
NAG3-317	p 6	A84-46103	NASA ORDER C-13980-C	p 52	A84-21847	NAS3-22647	p 42	A84-22134
	p 158	N84-31692	NASA ORDER C-2742911	p 167	N84-22001	NAS3-22656	p 167	N84-23021
NAG3-318	p 127	N84-25000	NASA ORDER C-49029-D	p 94	A84-22141	NAS3-22664	p 43	A84-36559
NAG3-319	p 158	N84-31694	NASA ORDER C-62861-C	p 192	A84-20315		p 121	A84-43546
NAG3-320	p 41	N84-17252		p 192	A84-30391	NAS3-22668	p 102	A84-22874
NAG3-323	p 51	A84-10430	NASA ORDER H-27954-B	p 192	A84-30391	NAS3-2271	p 124	N84-17530
NAG3-328	p 149	N84-15565	NASA ORDER M-27954-B	p 192	A84-20315	NAS3-22750	p 143	N84-21879

NAS3-22753	p 153	N84-12530	NAS3-23684	p 131	A84-36958	NSG-3260	p 7	N84-13149
NAS3-22758	p 122	N84-14482		p 133	N84-31595	NSG-3262	p 117	A84-33705
NAS3-22763	p 21	A84-44185	NAS3-23686	p 27	N84-20536		p 129	N84-32751
NAS3-22771	p 119	A84-35664	NAS3-23696	p 11	N84-32355	NSG-3264	p 127	N84-25001
NAS3-22779	p 29	N84-23829	NAS3-23697	p 159	N84-31700	NSG-3266	p 3	A84-13574
NAS3-22780	p 91	N84-27908	NAS3-23705	p 31	N84-24580		p 3	A84-17437
NAS3-22782	p 106	N84-11388	NAS3-23772	p 43	A84-35157		p 5	A84-36971
NAS3-22783	p 89	N84-13332	NAS3-23774	p 39	N84-23667		p 7	A84-46991
NAS3-22808	p 137	A84-29099	NAS3-23779	p 43	A84-35201		p 122	A84-48138
NAS3-22813	p 145	N84-25065		p 45	N84-12227	NSG-3267	p 2	A84-10078
NAS3-22819	p 103	A84-32046	NAS3-23781	p 103	A84-30857		p 119	A84-35349
NAS3-22822	p 118	A84-35168	NAS3-23783	p 38	N84-20611	NSG-3269	p 148	N84-14525
NAS3-22824	p 46	N84-20634		p 38	N84-20612	NSG-3281	p 102	A84-23255
	p 83	N84-20699	NAS3-23866	p 43	A84-35201		p 103	A84-23253
NAS3-22827	p 14	N84-23646		p 43	A84-35202		p 111	N84-32678
	p 91	N84-25854	NAS3-23868	p 50	N84-33462	NSG-3283	p 136	A84-20580
NAS3-22828	p 81	N84-13310	NAS3-23923	p 98	N84-16425		p 155	N84-19927
NAS3-22877	p 134	N84-18620	NAS3-23926	p 72	N84-24774	NSG-3291	p 86	N84-28990
NAS3-22886	p 104	A84-32261	NAS3-24084	p 131	A84-36881	NSG-3294	p 3	A84-10193
NAS3-22905	p 94	A84-25274	NAS3-24090	p 131	A84-40736		p 116	A84-25859
NAS3-23043	p 22	N84-13186	NAS3-24094	p 125	N84-20531	NSG-3299	p 189	A84-23390
NAS3-23044	p 20	A84-44182	NAS3-24095	p 18	A84-37640	NSG-3301	p 129	N84-13125
	p 2	N84-25605	NAS3-24098	p 18	A84-37639	NSG-3302	p 188	A84-40332
NAS3-23046	p 18	A84-36957	NAS3-34964	p 148	N84-33811		p 188	N84-22414
NAS3-23052	p 165	N84-14585	NAS3-403	p 127	N84-23854	NSG-3305	p 116	A84-25807
NAS3-23053	p 5	A84-38004	NAS7-100	p 161	A84-23059		p 43	A84-34037
NAS3-23054	p 148	N84-32828	NAS7-918	p 167	N84-22001		p 175	A84-49108
NAS3-23056	p 17	A84-35204	NAS8-32807	p 173	N84-25204	NSG-3306	p 58	A84-11636
NAS3-23058	p 40	A84-18025	NAS8-33982	p 41	N84-17262	NSG-3311	p 5	A84-38828
	p 102	A84-20711	NAS8-35339	p 41	N84-17262	NSG-350	p 57	N84-31288
NAS3-23154	p 132	N84-16529	NCC3-17	p 173	N84-34037	NSG-388	p 6	A84-44187
NAS3-23157	p 6	A84-46926	NCC3-21	p 50	A84-32846	N00014-79-C-0579	p 53	A84-33389
	p 7	A84-46927		p 76	N84-31349	N00014-80-C-0588	p 59	A84-35425
	p 26	N84-16210	NCC3-27	p 140	A84-47046	N00014-80-K-0460	p 131	A84-40736
NAS3-23159	p 108	N84-17481	NCC3-28	p 71	N84-21720	N00123-79-C-1529	p 39	A84-46620
NAS3-23163	p 29	N84-22568	NCC3-3	p 127	N84-25843	PHS-HL-26269	p 175	A84-49108
NAS3-23166	p 184	N84-24323	NCC3-7	p 163	N84-10661	W-7405-ENG-48	p 58	A84-17436
	p 184	N84-24324	NGR-99-009-077	p 58	N84-11836		p 114	A84-18171
NAS3-23167	p 89	A84-35236	NIH-EY-03251	p 104	A84-39197		p 52	A84-21847
	p 89	N84-17407	NSF ATM-80-19423	p 174	A84-40399		p 116	A84-28379
NAS3-23171	p 48	N84-28901	NSF CME-78-05122-A01	p 181	A84-24597		p 59	A84-29128
NAS3-23244	p 96	N84-10402	NSF CPE-80-17868	p 117	A84-28738		p 119	A84-35318
	p 96	N84-10403	NSF CPE-81-15163	p 114	A84-18171		p 60	A84-48139
	p 96	N84-10404		p 59	A84-29128		p 21	N84-10054
NAS3-23245	p 92	N84-16381		p 60	A84-48139		p 23	N84-13189
NAS3-23247	p 102	A84-22873	NSF CPE-81-2019	p 21	N84-10054	W-7405-ENG-82	p 192	A84-19359
NAS3-23248	p 45	N84-12226	NSF CPE-81-20506	p 23	N84-13189	179-10-10	p 73	N84-26787
	p 45	N84-13218	NSF CPE-81-20506	p 59	A84-35401	179-80-51	p 63	N84-33536
NAS3-23250	p 98	N84-16423	NSF DMR-79-23647	p 59	A84-33440	307-03-01	p 123	N84-16488
	p 98	N84-16424	NSF DMR-83-06052	p 190	A84-42829	500-40-62	p 127	N84-24999
NAS3-23254	p 37	N84-10109		p 191	A84-28621	505-04-1A	p 129	N84-31558
NAS3-23260	p 137	A84-28888	NSF ECS-81-14344	p 187	A84-28485	505-08-22	p 193	N84-22488
NAS3-23273	p 153	N84-10613	NSF ENG-78-17782	p 112	A84-13239	505-31-0A	p 8	N84-14120
	p 153	N84-10614	NSF ENG-78-712372	p 41	N84-17262	505-31-0A	p 9	N84-17138
NAS3-23274	p 87	N84-28995	NSF MEA-80-06806	p 116	A84-28379		p 127	N84-25941
NAS3-23279	p 157	N84-31689	NSF MEA-81-11676	p 119	A84-35233	505-31-02B	p 122	N84-13494
NAS3-23280	p 106	N84-13443	NSF PHY-77-27084	p 181	A84-23355		p 122	N84-14462
NAS3-23281	p 23	N84-13193	NSF 80-06806	p 192	A84-19359	505-31-02	p 10	N84-24539
NAS3-23283	p 27	N84-19353	NSF ENG-77-02019	p 120	A84-37467	505-31-08	p 128	N84-25946
NAS3-23286	p 183	N84-21275	NSG-3011	p 58	A84-10140		p 11	N84-32351
NAS3-23289	p 67	N84-13265	NSG-3016	p 46	N84-18321	505-31-1B	p 88	N84-34619
NAS3-23293	p 92	A84-46965	NSG-3019	p 84	N84-24809	505-31-3A	p 10	N84-22533
	p 40	N84-16243	NSG-3036	p 59	A84-32612	505-31-3B	p 182	N84-13922
	p 124	N84-18578	NSG-3040	p 180	A84-21184		p 183	N84-21275
	p 93	N84-19606	NSG-3044	p 112	A84-13239		p 184	N84-23235
	p 124	N84-19741		p 52	A84-21515		p 34	N84-28790
	p 109	N84-23841	NSG-3048	p 53	A84-33389		p 10	N84-31096
NAS3-23343	p 46	N84-19472	NSG-3075	p 20	A84-42382		p 185	N84-32122
NAS3-23344	p 68	A84-18142	NSG-3079	p 123	N84-16488		p 186	N84-34231
	p 45	N84-12225	NSG-3124	p 21	A84-46993	505-31-31	p 185	N84-29661
NAS3-23348	p 97	N84-14376	NSG-3150	p 115	A84-21378	505-31-32	p 182	N84-11833
	p 97	N84-14377	NSG-3155	p 41	N84-17262		p 182	N84-11885
	p 97	N84-14378	NSG-3157	p 82	N84-17389		p 182	N84-13924
NAS3-23352	p 49	N84-32428	NSG-3160	p 101	A84-18403		p 183	N84-14874
	p 49	N84-32429	NSG-3185	p 178	N84-13883		p 183	N84-15894
NAS3-23353	p 48	N84-29931	NSG-3186	p 52	A84-27356		p 183	N84-16946
NAS3-23355	p 44	A84-44184	NSG-3189	p 113	A84-16828		p 183	N84-19049
NAS3-23356	p 101	A84-18371	NSG-3202	p 3	A84-13592		p 183	N84-20320
	p 99	N84-20737	NSG-3206	p 138	A84-30085	505-31-38	p 185	N84-32118
NAS3-23370	p 59	A84-35401	NSG-3212	p 34	N84-28794			
NAS3-23523	p 60	N84-12263	NSG-3215	p 6	A84-39304		p 21	N84-10054
	p 60	N84-12265	NSG-3220	p 26	N84-16207	505-31-42	p 23	N84-13187
NAS3-23524	p 114	A84-18048	NSG-3227	p 65	A84-42658		p 23	N84-13188
NAS3-23525	p 25	N84-15152		p 115	A84-22922		p 23	N84-13189
	p 25	N84-15155	NSG-3235	p 58	A84-10140		p 23	N84-14143
	p 25	N84-15156	NSG-3246	p 58	A84-17436		p 24	N84-14145
NAS3-23529	p 134	N84-32790		p 191	N84-33210		p 24	N84-14146
NAS3-23531	p 32	N84-25710	NSG-3251	p 63	A84-10597		p 8	N84-16142
NAS3-23532	p 131	A84-30981	NSG-3253	p 69	N84-17353		p 123	N84-16494
NAS3-23537	p 36	N84-34444	NSG-3254	p 153	N84-11513		p 9	N84-17142
NAS3-23538	p 129	A84-17946		p 140	A84-48996		p 90	N84-17410
	p 132	N84-20528		p 79	A84-19792		p 126	N84-21832
NAS3-23542	p 62	N84-21677		p 79	A84-19793		p 126	N84-22909
NAS3-235924	p 118	A84-35171		p 79	A84-19794		p 126	N84-22911
NAS3-23606	p 178	N84-13885	NSG-3255	p 189	A84-24049		p 30	N84-23649
NAS3-23682	p 4	A84-18094	NSG-3256	p 59	A84-27724		p 10	N84-25647

	p 91	N84-27908		p 30	N84-24578		p 73	N84-27857
	p 128	N84-29157	505-33-58 . . . . .	p 56	N84-26755		p 86	N84-27887
	p 35	N84-29877	505-34-01B . . . . .	p 23	N84-13190		p 87	N84-28994
	p 133	N84-31595	505-34-02 . . . . .	p 22	N84-11171		p 87	N84-30072
	p 63	N84-32446		p 28	N84-21548		p 76	N84-31349
	p 92	N84-32552		p 195	N84-26484		p 87	N84-31379
	p 36	N84-33412	505-34-06 . . . . .	p 178	N84-16843		p 147	N84-31640
	p 92	N84-33608	505-36-12 . . . . .	p 60	N84-11229		p 76	N84-32508
505-31-52 . . . . .	p 123	N84-16493		p 188	N84-16984		p 87	N84-32531
	p 132	N84-21849	505-36-22 . . . . .	p 127	N84-25943		p 87	N84-32536
	p 133	N84-26010		p 10	N84-31091		p 147	N84-32825
505-31-5352 . . . . .	p 189	N84-32169	505-40-02 . . . . .	p 24	N84-14147		p 88	N84-33590
505-32-01 . . . . .	p 1	N84-22527		p 123	N84-17525	506-53-113 . . . . .	p 69	N84-17351
505-32-02 . . . . .	p 184	N84-26384	505-40-1A . . . . .	p 9	N84-17143	506-53-12B . . . . .	p 72	N84-21721
505-32-2A . . . . .	p 34	N84-29875		p 11	N84-32357	506-53-12 . . . . .	p 142	N84-18653
505-32-2B . . . . .	p 126	N84-21828	505-40-1B . . . . .	p 132	N84-19787	506-53-18 . . . . .	p 68	N84-14289
505-32-22 . . . . .	p 154	N84-14542	505-40-12C . . . . .	p 34	N84-29976	506-54-1A . . . . .	p 134	N84-30273
	p 34	N84-28795	505-40-22 . . . . .	p 1	N84-16119	506-55-22 . . . . .	p 45	N84-11206
505-32-32 . . . . .	p 29	N84-22565		p 126	N84-22910		p 37	N84-16229
	p 32	N84-25710		p 31	N84-24584		p 48	N84-27825
505-32-4A . . . . .	p 91	N84-23775		p 32	N84-24589	506-55-24 . . . . .	p 51	N84-31283
505-32-42 . . . . .	p 68	N84-14288		p 128	N84-30223	506-55-28 . . . . .	p 50	N84-33462
505-32-52 . . . . .	p 124	N84-17533	505-40-32 . . . . .	p 174	N84-31865	506-55-42 . . . . .	p 167	N84-20916
	p 142	N84-17590		p 2	N84-32344		p 109	N84-22890
505-32-6A . . . . .	p 36	N84-33414	505-40-42 . . . . .	p 141	N84-11500		p 168	N84-23027
505-32-6B . . . . .	p 1	N84-13140		p 142	N84-18654		p 48	N84-26746
	p 26	N84-16184		p 2	N84-25605		p 170	N84-29307
	p 31	N84-24585		p 2	N84-25606		p 49	N84-31272
505-33-1A . . . . .	p 67	N84-13264		p 145	N84-26027		p 110	N84-31513
	p 67	N84-14287		p 145	N84-26029		p 49	N84-32427
	p 69	N84-16311		p 145	N84-27041	506-55-52 . . . . .	p 62	N84-22712
	p 69	N84-17353		p 145	N84-27042		p 167	N84-23022
	p 70	N84-17354		p 145	N84-27043		p 167	N84-23023
	p 70	N84-19523		p 146	N84-28087		p 168	N84-23024
	p 124	N84-19741		p 146	N84-28088		p 168	N84-23025
	p 50	N84-23693		p 146	N84-29223		p 168	N84-23026
	p 72	N84-24772		p 146	N84-29224		p 172	N84-30528
	p 85	N84-25830		p 146	N84-29226	506-55-62 . . . . .	p 195	N84-22512
	p 73	N84-26783		p 147	N84-30293	506-55-72 . . . . .	p 40	N84-16247
	p 74	N84-27858	505-40-5A . . . . .	p 191	N84-14932		p 41	N84-18310
	p 74	N84-27859		p 27	N84-20562		p 191	N84-20404
	p 57	N84-28917		p 29	N84-22566		p 46	N84-20639
	p 74	N84-28958		p 129	N84-30224		p 42	N84-22615
	p 75	N84-31345	505-40-5B . . . . .	p 22	N84-12166		p 109	N84-22891
	p 76	N84-32504		p 26	N84-16185		p 109	N84-22892
	p 57	N84-34575		p 176	N84-16812		p 47	N84-23690
505-33-1B . . . . .	p 81	N84-11296		p 177	N84-20258		p 47	N84-24708
	p 142	N84-17591		p 177	N84-20259		p 85	N84-26803
	p 142	N84-17592		p 32	N84-25712		p 110	N84-31512
	p 83	N84-19567	505-40-62B . . . . .	p 107	N84-16461		p 42	N84-33452
	p 142	N84-19816	505-40-62 . . . . .	p 8	N84-14121	506-58-22 . . . . .	p 106	N84-15394
	p 84	N84-23764		p 141	N84-14519		p 82	N84-18400
	p 84	N84-24808		p 31	N84-24583		p 108	N84-19708
	p 85	N84-25831		p 132	N84-25017		p 109	N84-23841
505-33-12 . . . . .	p 88	N84-34620	505-40-82 . . . . .	p 176	N84-13812		p 100	N84-30147
	p 155	N84-18683		p 31	N84-24581		p 100	N84-31460
	p 73	N84-26785		p 31	N84-24582		p 100	N84-31461
505-33-22 . . . . .	p 152	N84-10612	505-42-62 . . . . .	p 30	N84-23648		p 133	N84-32783
	p 153	N84-11512	505-424A . . . . .	p 91	N84-25813		p 133	N84-32789
	p 153	N84-11513	505-43-02 . . . . .	p 8	N84-16141		p 184	N84-26383
	p 154	N84-14541		p 9	N84-20493	506-60-12 . . . . .	p 47	N84-25762
	p 69	N84-17350		p 30	N84-24579	506-60-42 . . . . .	p 97	N84-13399
	p 155	N84-19925	505-43-12 . . . . .	p 9	N84-20490	506-62-52 . . . . .	p 108	N84-21803
	p 71	N84-20674	505-44-22 . . . . .	p 174	N84-18806		p 68	N84-15247
	p 155	N84-20878	505-45-02 . . . . .	p 122	N84-13490	510-55-12 . . . . .	p 11	N84-32355
	p 156	N84-22980		p 8	N84-16145	533-04-1A . . . . .	p 131	N84-11456
	p 156	N84-29248		p 8	N84-16146		p 70	N84-18370
	p 75	N84-31348		p 10	N84-25646		p 93	N84-19606
	p 157	N84-31687	505-45-1A . . . . .	p 9	N84-17139		p 133	N84-25019
	p 77	N84-33564		p 14	N84-29870		p 32	N84-25713
505-33-32 . . . . .	p 159	N84-34774	505-45-12 . . . . .	p 123	N84-14463		p 174	N84-27375
	p 60	N84-11228	505-53-1A . . . . .	p 149	N84-32849		p 156	N84-29247
	p 54	N84-21666	505-53-1B . . . . .	p 187	N84-10923		p 75	N84-31347
505-33-42 . . . . .	p 51	N84-26749	505-53-12 . . . . .	p 148	N84-14526	533-04-1C . . . . .	p 84	N84-24809
	p 154	N84-13610	505-55-42 . . . . .	p 172	N84-31782	533-04-1E . . . . .	p 70	N84-20672
	p 154	N84-16587	505-55-72 . . . . .	p 48	N84-27824		p 75	N84-31344
	p 154	N84-16588	506-52-42 . . . . .	p 46	N84-20634	533-042-1A . . . . .	p 25	N84-15156
	p 157	N84-30329	506-52-62 . . . . .	p 148	N84-14525	535-03-12 . . . . .	p 2	N84-25607
505-33-5A . . . . .	p 144	N84-25064	506-53-1A . . . . .	p 149	N84-15565		p 35	N84-29878
	p 145	N84-25065		p 149	N84-17606		p 157	N84-31683
	p 86	N84-28990		p 149	N84-34769		p 186	N84-34230
505-33-5B . . . . .	p 55	N84-22702	506-53-1B . . . . .	p 67	N84-11254	535-05-12 . . . . .	p 29	N84-22564
	p 55	N84-24712		p 81	N84-11295		p 35	N84-32388
	p 56	N84-25770		p 82	N84-16334	535-06-12 . . . . .	p 12	N84-11152
	p 56	N84-26756		p 92	N84-16380		p 89	N84-13332
	p 56	N84-27831		p 69	N84-17352	542-03-12 . . . . .	p 39	N84-25753
	p 56	N84-27832		p 179	N84-17982	542-05-12 . . . . .	p 47	N84-23691
	p 57	N84-31288		p 82	N84-18399	555-04-1E . . . . .	p 157	N84-31688
	p 58	N84-34576		p 82	N84-19566	605-55-22 . . . . .	p 47	N84-22631
505-33-52 . . . . .	p 81	N84-10310		p 71	N84-20673	643-10-01 . . . . .	p 97	N84-11360
	p 175	N84-12730		p 143	N84-20858		p 100	N84-30146
	p 54	N84-13224		p 190	N84-21329	643-10-02 . . . . .	p 99	N84-19641
	p 25	N84-16181		p 190	N84-21330	650-60-23 . . . . .	p 97	N84-13400
	p 26	N84-16186		p 71	N84-21719		p 101	N84-32844
	p 123	N84-16492		p 83	N84-21739	650-60-26 . . . . .	p 96	N84-10405
	p 83	N84-21740		p 51	N84-25766		p 99	N84-25908

CONTRACT NUMBER INDEX

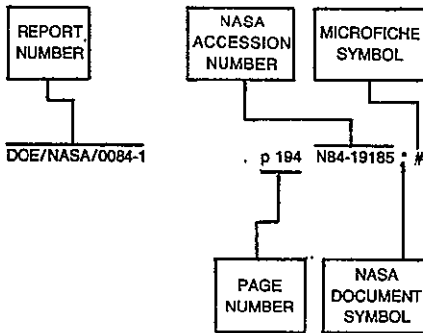
917-60-00

776-33-41	p 163	N84-10661
	p 163	N84-10664
	p 165	N84-14586
	p 107	N84-17479
	p 169	N84-27327
	p 171	N84-29347
776-54-01	p 110	N84-25926
	p 101	N84-33642
776-72-41	p 164	N84-11579
778-14-10	p 172	N84-31784
	p 173	N84-34038
778-16-12	p 195	N84-24509
778-17-01	p 164	N84-10665
	p 166	N84-18757
	p 169	N84-25169
778-32-001	p 155	N84-16589
778-35-03-00	p 73	N84-25793
778-35-03	p 194	N84-14989
	p 68	N84-15246
	p 74	N84-28962
	p 75	N84-28963
	p 77	N84-34603
778-36-06	p 193	N84-14071
	p 194	N84-19185
	p 166	N84-20016
	p 166	N84-20017
778-36-68	p 169	N84-25165
779-00-00	p 167	N84-22001
917-60-00	p 38	N84-16234



# REPORT NUMBER INDEX

## Typical Report Number Index Listing



Listings in this index are arranged alphanumerically by report number. The page number indicates the page on which the citation is located. The accession number denotes the number by which the citation is identified. An asterisk (\*) indicates that the item is a NASA report. A pound sign (#) indicates that the item is available on microfiche.

A-83-40-66-7000 . . . . . p 30 N84-23648 \* #  
AARL-TR-83-2 . . . . . p 8 N84-16145 \* #  
AAS PAPER 84-043 . . . . . p 39 A84-49176 \* #  
AD-A138495 . . . . . p 142 N84-17590 \* #  
AD-A142913 . . . . . p 117 A84-29798 \* #  
AD-A146317 . . . . . p 120 A84-38557 \* #  
AD-P002103 . . . . . p 187 N84-20189 \* #  
AD-P002123 . . . . . p 177 N84-26209 \* #  
AD-P002768 . . . . . p 193 N84-23315 \* #  
ADL-88036 . . . . . p 166 N84-18757 \* #  
ADL-88683 . . . . . p 194 N84-14991 \* #  
AFSCOM-TR-83-C-8 . . . . . p 142 N84-17590 \* #  
AIAA PAPER 82-0286 . . . . . p 12 A84-17406 \* #  
AIAA PAPER 83-0763 . . . . . p 181 A84-32609 \* #  
AIAA PAPER 83-2328 . . . . . p 177 A84-10010 \* #  
AIAA PAPER 83-2540 . . . . . p 15 A84-15205 \* #  
AIAA PAPER 83-2541 . . . . . p 15 A84-15206 \* #  
AIAA PAPER 83-2543 . . . . . p 15 A84-15207 \* #  
AIAA PAPER 83-2766 . . . . . p 15 A84-15204 \* #  
AIAA PAPER 84-0017 . . . . . p 113 A84-17834 \* #  
AIAA PAPER 84-0018 . . . . . p 113 A84-17835 \* #  
AIAA PAPER 84-0033 . . . . . p 4 A84-19228 \* #  
AIAA PAPER 84-0036 . . . . . p 3 A84-17841 \* #  
AIAA PAPER 84-0038 . . . . . p 113 A84-17842 \* #  
AIAA PAPER 84-0099 . . . . . p 3 A84-17881 \* #  
AIAA PAPER 84-0102 . . . . . p 16 A84-21852 \* #  
AIAA PAPER 84-0125 . . . . . p 114 A84-17897 \* #  
AIAA PAPER 84-0167 . . . . . p 4 A84-17925 \* #  
AIAA PAPER 84-0179 . . . . . p 13 A84-21289 \* #  
AIAA PAPER 84-0184 . . . . . p 13 A84-17937 \* #  
AIAA PAPER 84-0194 . . . . . p 4 A84-21290 \* #  
AIAA PAPER 84-0203 . . . . . p 129 A84-17946 \* #  
AIAA PAPER 84-0256 . . . . . p 114 A84-17979 \* #  
AIAA PAPER 84-0283 . . . . . p 16 A84-17997 \* #  
AIAA PAPER 84-0329 . . . . . p 40 A84-18025 \* #  
AIAA PAPER 84-0363 . . . . . p 78 A84-18044 \* #  
AIAA PAPER 84-0367 . . . . . p 130 A84-18047 \* #  
AIAA PAPER 84-0372 . . . . . p 114 A84-18048 \* #  
AIAA PAPER 84-0432 . . . . . p 4 A84-18090 \* #  
AIAA PAPER 84-0439 . . . . . p 4 A84-18094 \* #  
AIAA PAPER 84-0441 . . . . . p 114 A84-18096 \* #  
AIAA PAPER 84-0443 . . . . . p 16 A84-21300 \* #  
AIAA PAPER 84-0498 . . . . . p 180 A84-18131 \* #  
AIAA PAPER 84-0512 . . . . . p 88 A84-18142 \* #  
AIAA PAPER 84-0531 . . . . . p 115 A84-21303 \* #  
AIAA PAPER 84-0532 . . . . . p 181 A84-21304 \* #  
AIAA PAPER 84-0536 . . . . . p 115 A84-22922 \* #  
AIAA PAPER 84-0569 . . . . . p 176 A84-21305 \* #

AIAA PAPER 84-0572 . . . . . p 114 A84-18171 \* #  
AIAA PAPER 84-0609 . . . . . p 13 A84-24195 \* #  
AIAA PAPER 84-0655 . . . . . p 94 A84-25256 \* #  
AIAA PAPER 84-0656 . . . . . p 94 A84-25257 \* #  
AIAA PAPER 84-0680 . . . . . p 94 A84-25272 \* #  
AIAA PAPER 84-0682 . . . . . p 94 A84-25274 \* #  
AIAA PAPER 84-0702 . . . . . p 95 A84-25326 \* #  
AIAA PAPER 84-0740 . . . . . p 94 A84-25299 \* #  
AIAA PAPER 84-0754 . . . . . p 95 A84-25324 \* #  
AIAA PAPER 84-0762 . . . . . p 104 A84-41035 \* #  
AIAA PAPER 84-0767 . . . . . p 103 A84-25333 \* #  
AIAA PAPER 84-0816 . . . . . p 11 A84-26580 \* #  
AIAA PAPER 84-1136 . . . . . p 43 A84-34013 \* #  
AIAA PAPER 84-1161 . . . . . p 19 A84-40239 \* #  
AIAA PAPER 84-1162 . . . . . p 21 A84-44186 \* #  
AIAA PAPER 84-1169 . . . . . p 17 A84-36951 \* #  
AIAA PAPER 84-1170 . . . . . p 18 A84-36952 \* #  
AIAA PAPER 84-1184 . . . . . p 20 A84-44178 \* #  
AIAA PAPER 84-1194 . . . . . p 18 A84-36957 \* #  
AIAA PAPER 84-1199 . . . . . p 131 A84-36958 \* #  
AIAA PAPER 84-1203 . . . . . p 20 A84-44181 \* #  
AIAA PAPER 84-1206 . . . . . p 18 A84-36959 \* #  
AIAA PAPER 84-1207 . . . . . p 5 A84-36960 \* #  
AIAA PAPER 84-1256 . . . . . p 18 A84-37639 \* #  
AIAA PAPER 84-1259 . . . . . p 18 A84-37640 \* #  
AIAA PAPER 84-1237 . . . . . p 43 A84-35157 \* #  
AIAA PAPER 84-1237 . . . . . p 6 A84-44177 \* #  
AIAA PAPER 84-1298 . . . . . p 5 A84-36971 \* #  
AIAA PAPER 84-1299 . . . . . p 18 A84-36972 \* #  
AIAA PAPER 84-1301 . . . . . p 6 A84-40241 \* #  
AIAA PAPER 84-1316 . . . . . p 121 A84-40242 \* #  
AIAA PAPER 84-1317 . . . . . p 118 A84-35168 \* #  
AIAA PAPER 84-1320 . . . . . p 120 A84-36973 \* #  
AIAA PAPER 84-1322 . . . . . p 118 A84-35171 \* #  
AIAA PAPER 84-1326 . . . . . p 44 A84-44179 \* #  
AIAA PAPER 84-1340 . . . . . p 44 A84-44184 \* #  
AIAA PAPER 84-1343 . . . . . p 44 A84-44176 \* #  
AIAA PAPER 84-1344 . . . . . p 121 A84-40243 \* #  
AIAA PAPER 84-1376 . . . . . p 118 A84-35196 \* #  
AIAA PAPER 84-1377 . . . . . p 118 A84-35197 \* #  
AIAA PAPER 84-1379 . . . . . p 121 A84-44183 \* #  
AIAA PAPER 84-1380 . . . . . p 119 A84-35664 \* #  
AIAA PAPER 84-1383 . . . . . p 20 A84-44182 \* #  
AIAA PAPER 84-1386 . . . . . p 43 A84-35201 \* #  
AIAA PAPER 84-1387 . . . . . p 43 A84-35202 \* #  
AIAA PAPER 84-1393 . . . . . p 19 A84-40244 \* #  
AIAA PAPER 84-1395 . . . . . p 17 A84-35204 \* #  
AIAA PAPER 84-1399 . . . . . p 6 A84-44187 \* #  
AIAA PAPER 84-1401 . . . . . p 19 A84-40246 \* #  
AIAA PAPER 84-1402 . . . . . p 19 A84-40245 \* #  
AIAA PAPER 84-1403 . . . . . p 19 A84-40247 \* #  
AIAA PAPER 84-1455 . . . . . p 21 A84-44185 \* #  
AIAA PAPER 84-1459 . . . . . p 131 A84-40248 \* #  
AIAA PAPER 84-1460 . . . . . p 131 A84-36981 \* #  
AIAA PAPER 84-1461 . . . . . p 130 A84-35223 \* #  
AIAA PAPER 84-1487 . . . . . p 119 A84-35233 \* #  
AIAA PAPER 84-1493 . . . . . p 89 A84-35236 \* #  
AIAA PAPER 84-1500 . . . . . p 20 A84-44180 \* #  
AIAA PAPER 84-1521 . . . . . p 189 A84-46108 \* #  
AIAA PAPER 84-1522 . . . . . p 189 A84-46109 \* #  
AIAA PAPER 84-1602 . . . . . p 6 A84-39304 \* #  
AIAA PAPER 84-1604 . . . . . p 131 A84-37999 \* #  
AIAA PAPER 84-1605 . . . . . p 120 A84-38000 \* #  
AIAA PAPER 84-1609 . . . . . p 5 A84-39004 \* #  
AIAA PAPER 84-1643 . . . . . p 120 A84-38030 \* #  
AIAA PAPER 84-1663 . . . . . p 5 A84-38043 \* #  
AIAA PAPER 84-1726 . . . . . p 120 A84-37467 \* #  
AIAA PAPER 84-2159 . . . . . p 6 A84-46103 \* #  
AIAA PAPER 84-2205 . . . . . p 21 A84-46106 \* #  
AIAA PAPER 84-2234 . . . . . p 12 A84-39280 \* #  
AIAA-84-0192 . . . . . p 23 N84-13190 \* #  
AIAA-84-0531 . . . . . p 122 N84-13494 \* #  
AIAA-84-0991 . . . . . p 166 N84-23923 \* #  
AIAA-84-1161 . . . . . p 32 N84-24589 \* #  
AIAA-84-1184 . . . . . p 32 N84-25712 \* #  
AIAA-84-1203 . . . . . p 2 N84-25607 \* #  
AIAA-84-1297 . . . . . p 10 N84-25647 \* #  
AIAA-84-1326 . . . . . p 47 N84-25764 \* #  
AIAA-84-1343 . . . . . p 39 N84-25753 \* #  
AIAA-84-1344 . . . . . p 127 N84-25000 \* #  
AIAA-84-1379 . . . . . p 32 N84-25713 \* #  
AIAA-84-1383 . . . . . p 2 N84-25605 \* #

AIAA-84-1452 . . . . . p 31 N84-24585 \* #  
AIAA-84-1459 . . . . . p 133 N84-25019 \* #  
AIAA-84-1500 . . . . . p 2 N84-25606 \* #  
AIAA-84-2205 . . . . . p 34 N84-28790 \* #  
AR-1 . . . . . p 99 N84-20737 \* #  
AR-1 . . . . . p 72 N84-24774 \* #  
ASLE PREPRINT 83-LC-1A-1 . . . . . p 80 A84-28995 \* #  
ASLE PREPRINT 83-LC-3B-2 . . . . . p 137 A84-28989 \* #  
ASLE PREPRINT 83-LC-4C-1 . . . . . p 137 A84-28987 \* #  
ASME PAPER 82-WA/DE-33 . . . . . p 135 A84-15950 \* #  
ASME PAPER 82-WA/DE-34 . . . . . p 135 A84-15951 \* #  
ASME PAPER 83-DET-20 . . . . . p 151 A84-29103 \* #  
ASME PAPER 83-GT-117 . . . . . p 151 A84-33701 \* #  
ASME PAPER 83-GT-132 . . . . . p 151 A84-33702 \* #  
ASME PAPER 83-GT-136 . . . . . p 118 A84-33705 \* #  
ASME PAPER 83-GT-67 . . . . . p 4 A84-31289 \* #  
ASME PAPER 83-GT-83 . . . . . p 117 A84-33703 \* #  
ASME PAPER 83-HT-97 . . . . . p 137 A84-29082 \* #  
ASME PAPER 83-JPGC-GT-10 . . . . . p 17 A84-28982 \* #  
ASME PAPER 83-LUB-15 . . . . . p 139 A84-44300 \* #  
ASME PAPER 83-LUB-16 . . . . . p 137 A84-28097 \* #  
ASME PAPER 83-LUB-18 . . . . . p 137 A84-29099 \* #  
ASME PAPER 84-GT-127 . . . . . p 140 A84-46954 \* #  
ASME PAPER 84-GT-139 . . . . . p 152 A84-46957 \* #  
ASME PAPER 84-GT-158 . . . . . p 92 A84-46955 \* #  
ASME PAPER 84-GT-181 . . . . . p 121 A84-46982 \* #  
ASME PAPER 84-GT-184 . . . . . p 7 A84-46985 \* #  
ASME PAPER 84-GT-193 . . . . . p 7 A84-46991 \* #  
ASME PAPER 84-GT-196 . . . . . p 21 A84-46993 \* #  
ASME PAPER 84-GT-200 . . . . . p 7 A84-46995 \* #  
ASME PAPER 84-GT-273 . . . . . p 140 A84-47036 \* #  
ASME PAPER 84-GT-292 . . . . . p 140 A84-47046 \* #  
ASME PAPER 84-GT-29 . . . . . p 139 A84-46893 \* #  
ASME PAPER 84-GT-32 . . . . . p 140 A84-46896 \* #  
ASME PAPER 84-GT-36 . . . . . p 121 A84-46900 \* #  
ASME PAPER 84-GT-84 . . . . . p 6 A84-46926 \* #  
ASME PAPER 84-GT-85 . . . . . p 7 A84-46927 \* #  
ASME PAPER 84-GT-96 . . . . . p 152 A84-46937 \* #  
AST-84-1808-VOL-2 . . . . . p 172 N84-31783 \* #  
AST-84-1808 . . . . . p 171 N84-23937 \* #  
AVRADCOM-TR-81-C-28 . . . . . p 34 N84-28795 \* #  
AVRADCOM-TR-83-C-10 . . . . . p 123 N84-15492 \* #  
AVRADCOM-TR-83-C-11 . . . . . p 24 N84-14145 \* #  
AVRADCOM-TR-83-C-9 . . . . . p 141 N84-11500 \* #  
AVRADCOM-TR-84-C-2 . . . . . p 142 N84-17592 \* #  
AVRADCOM-TR-84-C-6 . . . . . p 29 N84-22564 \* #  
AVSCOM-TR-83-C-6 . . . . . p 69 N84-17350 \* #  
AVSCOM-TR-84-C-5 . . . . . p 35 N84-32388 \* #  
BAC-D180-28273-1 . . . . . p 46 N84-20634 \* #  
BAC-D180-28274-1 . . . . . p 83 N84-20699 \* #  
CAES-700-84 . . . . . p 91 N84-25813 \* #  
CATALYTIC-43790 . . . . . p 172 N84-31784 \* #  
CHAM-H3605/15-VOL-1 . . . . . p 49 N84-32428 \* #  
CHAM-H3605/16-VOL-2 . . . . . p 49 N84-32429 \* #  
CONF-821055 . . . . . p 143 N84-21877 \* #  
CR-R-83036 . . . . . p 123 N84-15488 \* #  
DDA-EDR-11185 . . . . . p 140 N84-10581 \* #  
DE83-015840 . . . . . p 143 N84-21877 \* #  
DOE/NASA/0007-1 . . . . . p 163 N84-10661 \* #  
DOE/NASA/0017-2 . . . . . p 173 N84-34037 \* #  
DOE/NASA/0032-21 . . . . . p 194 N84-18117 \* #  
DOE/NASA/0032-23 . . . . . p 196 N84-33307 \* #  
DOE/NASA/0032-80/7 . . . . . p 195 N84-32305 \* #  
DOE/NASA/0065-83/1 . . . . . p 105 N84-10450 \* #  
DOE/NASA/0084-1 . . . . . p 194 N84-19185 \* #  
DOE/NASA/0091-1 . . . . . p 91 N84-25813 \* #  
DOE/NASA/0131-1 . . . . . p 21 N84-10054 \* #  
DOE/NASA/0131-2 . . . . . p 23 N84-13189 \* #

DOE/NASA/0142-1	p 91	N84-27909 * #	E-1752	p 124	N84-19741 * #	E-1926	p 142	N84-17592 * #
DOE/NASA/0156-83/1	p 165	N84-15679 * #	E-1754	p 25	N84-16181 * #	E-1927	p 38	N84-16234 * #
DOE/NASA/0167-7	p 195	N84-29805 * #	E-1755	p 54	N84-13224 * #	E-1928	p 1	N84-13140 * #
DOE/NASA/0168-5	p 140	N84-10581 * #	E-1760	p 175	N84-12730 * #	E-1930	p 109	N84-23841 * #
DOE/NASA/0168-6	p 141	N84-15554 * #	E-1762	p 81	N84-10310 * #	E-1931	p 90	N84-23774 * #
DOE/NASA/0168-7	p 146	N84-28089 * #	E-1768	p 82	N84-18399 * #	E-1933	p 24	N84-14147 * #
DOE/NASA/0189-83/2	p 193	N84-14071 * #	E-1775	p 40	N84-16247 * #	E-1934	p 9	N84-17143 * #
DOE/NASA/0201-4	p 169	N84-25169 * #	E-1776	p 164	N84-13670 * #	E-1936	p 23	N84-13190 * #
DOE/NASA/0205-8	p 169	N84-26165 * #	E-1779	p 182	N84-11885 * #	E-1937	p 69	N84-16311 * #
DOE/NASA/0211-1	p 111	N84-31514 * #	E-1781	p 183	N84-14874 * #	E-1938	p 69	N84-17351 * #
DOE/NASA/0235-1	p 195	N84-21445 * #	E-1783	p 194	N84-14989 * #	E-1940	p 26	N84-16184 * #
DOE/NASA/0241-10	p 164	N84-13672 * #	E-1784	p 164	N84-11579 * #	E-1941	p 9	N84-20490 * #
DOE/NASA/0241-12	p 166	N84-20915 * #	E-1789	p 81	N84-11295 * #	E-1942	p 70	N84-17354 * #
DOE/NASA/0241-13	p 170	N84-27329 * #	E-1793	p 108	N84-21803 * #	E-1943	p 14	N84-13173 * #
DOE/NASA/0241-5	p 164	N84-13673 * #	E-1794	p 153	N84-11512 * #	E-1947	p 71	N84-20573 * #
DOE/NASA/0241-7	p 164	N84-11581 * #	E-1795	p 69	N84-17350 * #	E-1948	p 37	N84-16229 * #
DOE/NASA/0249-81/1	p 194	N84-17073 * #	E-1796	p 70	N84-17355 * #	E-1949	p 147	N84-31640 * #
DOE/NASA/0250-1	p 164	N84-11580 * #	E-1797	p 141	N84-11498 * #	E-1950	p 14	N84-29870 * #
DOE/NASA/0257-1	p 172	N84-31784 * #	E-1801	p 142	N84-17590 * #	E-1951	p 8	N84-16142 * #
DOE/NASA/0258-1	p 166	N84-20014 * #	E-1803	p 178	N84-11831 * #	E-1956	p 85	N84-25831 * #
DOE/NASA/0263-1	p 74	N84-28960 * #	E-1805	p 163	N84-10664 * #	E-1958	p 9	N84-17142 * #
DOE/NASA/0264-1	p 172	N84-29358 * #	E-1806	p 146	N84-29226 * #	E-1960	p 98	N84-16425 * #
DOE/NASA/0266-1	p 91	N84-23775 * #	E-1808	p 84	N84-23764 * #	E-1962	p 184	N84-26383 * #
DOE/NASA/0291-1	p 166	N84-18757 * #	E-1810	p 68	N84-14288 * #	E-1963	p 8	N84-16141 * #
DOE/NASA/0295-1	p 165	N84-14587 * #	E-1812	p 123	N84-16492 * #	E-1964	p 155	N84-18683 * #
DOE/NASA/0300-1	p 196	N84-33304 * #	E-1813	p 45	N84-11206 * #	E-1967	p 172	N84-30528 * #
DOE/NASA/0301-1	p 194	N84-14991 * #	E-1814	p 142	N84-17591 * #	E-1968	p 28	N84-21548 * #
DOE/NASA/0302-1	p 196	N84-32306 * #	E-1817	p 72	N84-21721 * #	E-1970	p 70	N84-20672 * #
DOE/NASA/0304-1	p 196	N84-32307 * #	E-1819	p 24	N84-14145 * #	E-1972-PT-2	p 107	N84-17479 * #
DOE/NASA/0323-1	p 196	N84-33309 * #	E-1823	p 67	N84-12287 * #	E-1973	p 132	N84-19787 * #
DOE/NASA/0327-1	p 172	N84-34036 * #	E-1828	p 154	N84-13610 * #	E-1974	p 108	N84-19708 * #
DOE/NASA/0354-1	p 171	N84-29357 * #	E-1829	p 30	N84-24578 * #	E-1975	p 124	N84-17533 * #
DOE/NASA/0354-2	p 172	N84-31783 * #	E-1831	p 168	N84-20016 * #	E-1977	p 51	N84-26749 * #
DOE/NASA/0394-1	p 196	N84-33306 * #	E-1834	p 98	N84-19640 * #	E-1982	p 155	N84-19925 * #
DOE/NASA/1005-2	p 195	N84-22512 * #	E-1835	p 8	N84-14121 * #	E-1983	p 9	N84-17138 * #
DOE/NASA/1005-3	p 195	N84-24509 * #	E-1841	p 41	N84-18310 * #	E-1984	p 145	N84-26029 * #
DOE/NASA/12726-23	p 164	N84-11579 * #	E-1842	p 182	N84-11883 * #	E-1985	p 73	N84-27857 * #
DOE/NASA/13111-14	p 173	N84-34038 * #	E-1843	p 182	N84-13922 * #	E-1986	p 87	N84-30072 * #
DOE/NASA/17088-4	p 164	N84-10665 * #	E-1845	p 166	N84-20017 * #	E-1987	p 1	N84-16119 * #
DOE/NASA/20305-9	p 164	N84-13670 * #	E-1846	p 142	N84-18653 * #	E-1990	p 99	N84-19641 * #
DOE/NASA/20320-53	p 163	N84-10664 * #	E-1847	p 74	N84-28958 * #	E-1991	p 93	N84-19606 * #
DOE/NASA/20320-57-PT-2	p 107	N84-17479 * #	E-1852	p 154	N84-14541 * #	E-1992	p 71	N84-21719 * #
DOE/NASA/20320-58	p 169	N84-27327 * #	E-1853	p 22	N84-12166 * #	E-1993	p 87	N84-32536 * #
DOE/NASA/20320-59	p 171	N84-29347 * #	E-1854	p 70	N84-18370 * #	E-1994	p 195	N84-26484 * #
DOE/NASA/20485-16	p 110	N84-25926 * #	E-1855-1	p 154	N84-14542 * #	E-1995	p 100	N84-27954 * #
DOE/NASA/50194-38	p 197	N84-34330 * #	E-1855	p 155	N84-20878 * #	E-1996	p 55	N84-24712 * #
DOE/NASA/51040-50	p 68	N84-15246 * #	E-1856	p 183	N84-19049 * #	E-1997	p 69	N84-17353 * #
DOE/NASA/51040-51	p 155	N84-16589 * #	E-1857	p 141	N84-11500 * #	E-2000	p 47	N84-22631 * #
DOE/NASA/51040-52	p 195	N84-26484 * #	E-1859	p 96	N84-10405 * #	E-2002	p 87	N84-28994 * #
DOE/NASA/51040-53	p 74	N84-28962 * #	E-1860	p 131	N84-11456 * #	E-2004	p 143	N84-20858 * #
DOE/NASA/51040-55	p 73	N84-25793 * #	E-1861	p 191	N84-14932 * #	E-2005	p 170	N84-29307 * #
DOE/NASA/51040-56	p 77	N84-34603 * #	E-1862	p 86	N84-28990 * #	E-2007	p 47	N84-23691 * #
DOE/NASA/51044-33	p 166	N84-20017 * #	E-1864	p 183	N84-16946 * #	E-2008	p 147	N84-32824 * #
DOE/NASA/51044-34	p 166	N84-20016 * #	E-1867	p 97	N84-13399 * #	E-2009	p 73	N84-26783 * #
DOE/NASA/51044-36	p 169	N84-25166 * #	E-1868	p 8	N84-14120 * #	E-2010	p 72	N84-24772 * #
DYD-10892-CE	p 106	N84-11388 * #	E-1869	p 179	N84-17982 * #	E-2012	p 191	N84-20404 * #
D180-26031-2	p 83	N84-20695 * #	E-1872	p 76	N84-31349 * #	E-2013	p 46	N84-20639 * #
D180-27728-1	p 45	N84-12226 * #	E-1873	p 149	N84-15565 * #	E-2015	p 169	N84-25166 * #
D180-27728-2	p 45	N84-13218 * #	E-1876	p 92	N84-16380 * #	E-2016	p 167	N84-23022 * #
D2536-941006	p 25	N84-15154 * #	E-1877	p 69	N84-17352 * #	E-2017	p 62	N84-22712 * #
D2536-941007	p 153	N84-11514 * #	E-1878	p 30	N84-23630 * #	E-2018	p 87	N84-31379 * #
D2536-941008	p 153	N84-11515 * #	E-1879	p 183	N84-20320 * #	E-2019	p 190	N84-21329 * #
D2536-941009	p 24	N84-14148 * #	E-1884	p 82	N84-19566 * #	E-2020	p 190	N84-21330 * #
D2536-941010	p 25	N84-15153 * #	E-1885	p 63	N84-32448 * #	E-2021	p 188	N84-22421 * #
E-1055	p 174	N84-18806 * #	E-1886	p 82	N84-18400 * #	E-2022	p 48	N84-27825 * #
E-1296	p 147	N84-30294 * #	E-1888	p 27	N84-20562 * #	E-2023	p 177	N84-20258 * #
E-1373	p 126	N84-21828 * #	E-1889	p 123	N84-16488 * #	E-2024	p 127	N84-25941 * #
E-1496	p 22	N84-11171 * #	E-1890	p 182	N84-13924 * #	E-2025	p 177	N84-20259 * #
E-1499	p 75	N84-31345 * #	E-1891	p 123	N84-16493 * #	E-2028	p 74	N84-28962 * #
E-1532	p 187	N84-10923 * #	E-1894	p 67	N84-13264 * #	E-2029	p 29	N84-22565 * #
E-1538-1	p 67	N84-11254 * #	E-1895	p 149	N84-17606 * #	E-2032	p 54	N84-21668 * #
E-1559	p 144	N84-23891 * #	E-1897	p 97	N84-13400 * #	E-2033	p 83	N84-21739 * #
E-1559	p 144	N84-25047 * #	E-1898	p 165	N84-14586 * #	E-2034	p 126	N84-22910 * #
E-1583	p 141	N84-13577 * #	E-1899	p 145	N84-27041 * #	E-2036	p 88	N84-33590 * #
E-1615	p 75	N84-28965 * #	E-1901	p 68	N84-15246 * #	E-2037	p 168	N84-23024 * #
E-1626	p 174	N84-31865 * #	E-1902	p 141	N84-14519 * #	E-2039	p 126	N84-21832 * #
E-1832	p 22	N84-10055 * #	E-1903	p 157	N84-31688 * #	E-2040	p 126	N84-22911 * #
E-1635	p 71	N84-21716 * #	E-1904	p 83	N84-19567 * #	E-2041	p 167	N84-23023 * #
E-1650	p 107	N84-16461 * #	E-1905	p 123	N84-14463 * #	E-2043	p 109	N84-22892 * #
E-1655	p 96	N84-11358 * #	E-1906	p 123	N84-16494 * #	E-2047	p 184	N84-23235 * #
E-1681	p 164	N84-10665 * #	E-1907	p 9	N84-20493 * #	E-2048	p 126	N84-22909 * #
E-1686	p 178	N84-16843 * #	E-1909	p 23	N84-13188 * #	E-2049	p 147	N84-32825 * #
E-1700	p 106	N84-15394 * #	E-1910	p 155	N84-16589 * #	E-2050	p 35	N84-32388 * #
E-1703	p 97	N84-11360 * #	E-1912	p 24	N84-14146 * #	E-2051	p 168	N84-23026 * #
E-1705	p 183	N84-15894 * #	E-1913	p 1	N84-14111 * #	E-2052	p 168	N84-23025 * #
E-1719	p 178	N84-13885 * #	E-1914	p 68	N84-14289 * #	E-2053	p 144	N84-25064 * #
E-1720	p 82	N84-16334 * #	E-1915	p 173	N84-11594 * #	E-2054	p 47	N84-24708 * #
E-1726	p 83	N84-21740 * #	E-1916	p 26	N84-16186 * #	E-2056	p 75	N84-28963 * #
E-1735	p 28	N84-21549 * #	E-1917	p 176	N84-13812 * #	E-2057	p 73	N84-26785 * #
E-1740	p 81	N84-11296 * #	E-1918	p 142	N84-19816 * #	E-2058	p 47	N84-25762 * #
E-1746	p 123	N84-17525 * #	E-1919	p 50	N84-20643 * #	E-2060	p 110	N84-25926 * #
E-1748	p 26	N84-16185 * #	E-1920	p 169	N84-27327 * #	E-2062	p 27	N84-20525 * #
E-1751	p 142	N84-18654 * #	E-1921	p 154	N84-16587 * #	E-2063	p 75	N84-31348 * #
			E-1922	p 122	N84-13494 * #	E-2064	p 86	N84-28989 * #
			E-1923	p 154	N84-16588 * #	E-2085	p 29	N84-22564 * #
			E-1925	p 176	N84-16812 * #	E-2066	p 84	N84-24808 * #

E-2067	p 132	N84-21849 *	#	E-2232	p 157	N84-31687 *	#	LG83ER0137	p 183	N84-21275 *	#
E-2069	p 55	N84-22702 *	#	E-2233	p 185	N84-32118 *	#				
E-2070	p 132	N84-25017 *	#	E-2234	p 88	N84-34620 *	#	LNR-300	p 112	N84-33715 *	#
E-2071	p 57	N84-28917 *	#	E-2235	p 77	N84-34589 *	#	LNR-400	p 97	N84-13398 *	#
E-2072	p 99	N84-25908 *	#	E-2236	p 100	N84-30147 *	#				
E-2073	p 42	N84-33452 *	#	E-2237	p 129	N84-31558 *	#	MCR-83-624	p 92	N84-16381 *	#
E-2074	p 156	N84-23923 *	#	E-2241	p 134	N84-30273 *	#				
E-2077	p 10	N84-22533 *	#	E-2243	p 110	N84-31513 *	#	ME-RT-82006	p 27	N84-20524 *	#
E-2078	p 1	N84-22527 *	#	E-2244	p 51	N84-31283 *	#	MTI-83ASE334SA4	p 194	N84-18117 *	#
E-2079	p 197	N84-34330 *	#	E-2246	p 10	N84-31091 *	#	MTI-84ASE356DR3	p 196	N84-33307 *	#
E-2080	p 110	N84-31512 *	#	E-2247	p 100	N84-30146 *	#				
E-2082	p 29	N84-22566 *	#	E-2250	p 185	N84-32122 *	#	NAS 1.15 81401	p 173	N84-34038 *	#
E-2083	p 86	N84-27887 *	#	E-2251	p 63	N84-33536 *	#	NAS 1.15 81733	p 193	N84-22468 *	#
E-2084	p 31	N84-24581 *	#	E-2257	p 186	N84-34230 *	#	NAS 1.15 82742	p 174	N84-18806 *	#
E-2085	p 127	N84-24999 *	#	E-2259	p 49	N84-32427 *	#	NAS 1.15 83061	p 187	N84-10923 *	#
E-2086	p 2	N84-25607 *	#	E-2260	p 77	N84-33564 *	#	NAS 1.15 83381	p 96	N84-11358 *	#
E-2089	p 189	N84-32169 *	#	E-2261	p 49	N84-31272 *	#	NAS 1.15 83403	p 164	N84-10665 *	#
E-2090	p 47	N84-23690 *	#	E-2263	p 10	N84-31096 *	#	NAS 1.15 83415	p 97	N84-11360 *	#
E-2091	p 109	N84-22890 *	#	E-2266	p 100	N84-31461 *	#	NAS 1.15 83446	p 26	N84-16185 *	#
E-2092	p 85	N84-26803 *	#	E-2269	p 75	N84-31347 *	#	NAS 1.15 83449	p 81	N84-10310 *	#
E-2093	p 42	N84-22615 *	#	E-2272	p 11	N84-32351 *	#	NAS 1.15 83460	p 164	N84-13670 *	#
E-2094	p 195	N84-22512 *	#	E-2274	p 133	N84-32793 *	#	NAS 1.15 83463	p 182	N84-11865 *	#
E-2095	p 195	N84-24509 *	#	E-2276	p 77	N84-34603 *	#	NAS 1.15 83467	p 183	N84-14874 *	#
E-2096	p 109	N84-22891 *	#	E-2281	p 133	N84-32789 *	#	NAS 1.15 83468	p 194	N84-14989 *	#
E-2098	p 332	N84-24589 *	#	E-2284	p 57	N84-33522 *	#	NAS 1.15 83469	p 164	N84-11579 *	#
E-2099	p 133	N84-25019 *	#	E-2285	p 101	N84-33562 *	#	NAS 1.15 83478	p 153	N84-11512 *	#
E-2100	p 127	N84-25943 *	#	E-2289	p 149	N84-34769 *	#	NAS 1.15 83479	p 70	N84-17355 *	#
E-2103	p 145	N84-27042 *	#	E-2292	p 38	N84-32411 *	#	NAS 1.15 83481	p 178	N84-11831 *	#
E-2104	p 32	N84-25712 *	#	E-2299	p 186	N84-35085 *	#	NAS 1.15 83483	p 163	N84-10664 *	#
E-2105	p 50	N84-23693 *	#	E-2307	p 58	N84-34576 *	#	NAS 1.15 83486	p 68	N84-14288 *	#
E-2108	p 156	N84-29248 *	#	E-2470	p 81	N84-25854 *	#	NAS 1.15 83488	p 123	N84-16492 *	#
E-2110	p 168	N84-23027 *	#	E-311	p 173	N84-34038 *	#	NAS 1.15 83489	p 45	N84-11206 *	#
E-2111	p 31	N84-24583 *	#	E-789	p 193	N84-22488 *	#	NAS 1.15 83490	p 24	N84-14145 *	#
E-2112	p 10	N84-25647 *	#					NAS 1.15 83492	p 67	N84-12287 *	#
E-2113	p 85	N84-25830 *	#	EDR-11443	p 141	N84-15554 *	#	NAS 1.15 83495	p 154	N84-13610 *	#
E-2114	p 186	N84-34231 *	#	EDR-11577	p 146	N84-26089 *	#	NAS 1.15 83497	p 166	N84-20016 *	#
E-2116	p 74	N84-27858 *	#					NAS 1.15 83502	p 182	N84-11883 *	#
E-2117	p 74	N84-27859 *	#	EL-TR-84-13	p 100	N84-30145 *	#	NAS 1.15 83503	p 182	N84-13922 *	#
E-2118	p 145	N84-27043 *	#	ELSR-84-7	p 100	N84-25909 *	#	NAS 1.15 83504	p 166	N84-20017 *	#
E-2120	p 156	N84-29247 *	#					NAS 1.15 83506	p 68	N84-15249 *	#
E-2121	p 172	N84-31782 *	#	ER-8162-F	p 32	N84-25711 *	#	NAS 1.15 83507	p 154	N84-14541 *	#
E-2123	p 31	N84-24585 *	#					NAS 1.15 83508	p 22	N84-12166 *	#
E-2124	p 73	N84-25793 *	#	ERC-TR-83020	p 166	N84-20014 *	#	NAS 1.15 83509	p 154	N84-14542 *	#
E-2128	p 30	N84-23648 *	#	ERC-TR-83024	p 111	N84-31514 *	#	NAS 1.15 83510	p 175	N84-12730 *	#
E-2131	p 171	N84-29347 *	#					NAS 1.15 83512	p 81	N84-11295 *	#
E-2132	p 185	N84-29661 *	#	ERIM-150000-11-F	p 159	N84-27258 *	#	NAS 1.15 83513	p 131	N84-11456 *	#
E-2133	p 31	N84-24584 *	#					NAS 1.15 83514	p 191	N84-14932 *	#
E-2137	p 2	N84-25605 *	#	ESL-719533-4	p 38	N84-23662 *	#	NAS 1.15 83515	p 183	N84-16946 *	#
E-2138	p 31	N84-24582 *	#	ESL-716111-1	p 99	N84-24924 *	#	NAS 1.15 83516	p 96	N84-10405 *	#
E-2139	p 39	N84-25753 *	#	FAA-EE-83-13	p 174	N84-27375 *	#	NAS 1.15 83518	p 97	N84-13399 *	#
E-2140	p 30	N84-24579 *	#	FAA-EE-83-7-VOL-2	p 193	N84-22488 *	#	NAS 1.15 83519	p 8	N84-14120 *	#
E-2144	p 48	N84-26746 *	#					NAS 1.15 83520	p 183	N84-20320 *	#
E-2146	p 57	N84-28918 *	#	FMI-NAS-8273	p 196	N84-33304 *	#	NAS 1.15 83522	p 98	N84-19640 *	#
E-2148	p 133	N84-26010 *	#					NAS 1.15 83523	p 141	N84-11500 *	#
E-2150	p 11	N84-32357 *	#	FR-15652	p 66	N84-10258 *	#	NAS 1.15 83524	p 141	N84-11498 *	#
E-2152	p 55	N84-25770 *	#	FR-6	p 71	N84-20676 *	#	NAS 1.15 83525	p 182	N84-13924 *	#
E-2153	p 73	N84-26787 *	#	GARRETT-21-4314-1	p 68	N84-15247 *	#	NAS 1.15 83526	p 123	N84-16493 *	#
E-2154	p 55	N84-27832 *	#	GARRETT-21-4742-2	p 60	N84-12265 *	#	NAS 1.15 83528	p 67	N84-13264 *	#
E-2155	p 10	N84-24539 *	#	GARRETT-21-4766	p 60	N84-12263 *	#	NAS 1.15 83529	p 81	N84-11296 *	#
E-2157	p 34	N84-28791 *	#	GARRETT-21-4804	p 33	N84-26702 *	#	NAS 1.15 83530	p 41	N84-18310 *	#
E-2158	p 55	N84-26755 *	#	GARRETT-31-3725(7)	p 195	N84-29805 *	#	NAS 1.15 83531	p 97	N84-13400 *	#
E-2159	p 55	N84-27831 *	#					NAS 1.15 83532	p 165	N84-14586 *	#
E-2160	p 55	N84-26756 *	#	GE-CRD-83-SRD-037	p 96	N84-10402 *	#	NAS 1.15 83533	p 67	N84-11254 *	#
E-2161	p 127	N84-25000 *	#	GE-CRD-83-SRD-038	p 96	N84-10403 *	#	NAS 1.15 83534	p 8	N84-14121 *	#
E-2162	p 128	N84-25946 *	#	GE-CRD-83-SRD-039	p 96	N84-10404 *	#	NAS 1.15 83535	p 68	N84-15246 *	#
E-2166	p 51	N84-25766 *	#					NAS 1.15 83536	p 141	N84-14519 *	#
E-2167	p 147	N84-30293 *	#	GT/PDL-170	p 32	N84-24586 *	#	NAS 1.15 83537	p 123	N84-16494 *	#
E-2168	p 32	N84-25713 *	#	GT/PDL-171	p 98	N84-15360 *	#	NAS 1.15 83538	p 23	N84-13188 *	#
E-2169	p 2	N84-25606 *	#					NAS 1.15 83539	p 155	N84-16589 *	#
E-2170	p 48	N84-27824 *	#	GTD-83-10	p 45	N84-12227 *	#	NAS 1.15 83540	p 193	N84-14061 *	#
E-2173	p 146	N84-29223 *	#					NAS 1.15 83541	p 24	N84-14146 *	#
E-2175	p 157	N84-30329 *	#	GTEC-21-4498	p 143	N84-21879 *	#	NAS 1.15 83542	p 1	N84-14111 *	#
E-2180	p 47	N84-25764 *	#	GTEC-31-5738	p 197	N84-34331 *	#	NAS 1.15 83543	p 173	N84-11594 *	#
E-2182	p 101	N84-32644 *	#					NAS 1.15 83544	p 26	N84-16186 *	#
E-2185	p 149	N84-32849 *	#	HSE-8856	p 22	N84-13186 *	#	NAS 1.15 83545	p 176	N84-13812 *	#
E-2187	p 146	N84-28087 *	#					NAS 1.15 83546	p 169	N84-27327 *	#
E-2190	p 146	N84-29224 *	#	IAF PAPER 83-18	p 38	A84-11718 *	#	NAS 1.15 83547	p 154	N84-16587 *	#
E-2192	p 146	N84-28088 *	#	IAF PAPER 83-345	p 37	A84-11793 *	#	NAS 1.15 83548	p 122	N84-13494 *	#
E-2198	p 36	N84-33414 *	#	IAF PAPER 83-433	p 42	A84-11819 *	#	NAS 1.15 83549	p 154	N84-16588 *	#
E-219	p 34	N84-28795 *	#					NAS 1.15 83550	p 176	N84-16812 *	#
E-2200	p 92	N84-33608 *	#	IAF-84-15	p 38	N84-32411 *	#	NAS 1.15 83551	p 68	N84-14289 *	#
E-2202	p 11	N84-32355 *	#					NAS 1.15 83552	p 38	N84-16234 *	#
E-2203	p 57	N84-31288 *	#	IITRI-M06116-15	p 74	N84-28961 *	#	NAS 1.15 83553	p 1	N84-13140 *	#
E-2205	p 34	N84-28790 *	#					NAS 1.15 83554	p 24	N84-14147 *	#
E-2207	p 128	N84-30223 *	#	ISBN-0-98883-081-8	p 143	N84-21877 *	#	NAS 1.15 83555	p 9	N84-17143 *	#
E-2210	p 128	N84-29157 *	#					NAS 1.15 83557	p 123	N84-14463 *	#
E-2213	p 76	N84-32508 *	#	JACKFAU-83-302	p 165	N84-14587 *	#	NAS 1.15 83558	p 23	N84-13190 *	#
E-2216	p 2	N84-32344 *	#					NAS 1.15 83559	p 179	N84-17982 *	#
E-2217	p 129	N84-30224 *	#	JPL-PUB-83-66	p 167	N84-22001 *	#	NAS 1.15 83560	p 69	N84-16311 *	#
E-2218	p 35	N84-29878 *	#					NAS 1.15 83561	p 26	N84-16164 *	#
E-2222	p 157	N84-31683 *	#	L-2178	p 36	N84-33412 *	#	NAS 1.15 83562	p 9	N84-20490 *	#
E-2223	p 75	N84-31344 *	#					NAS 1.15 83563	p 70	N84-17354 *	#
E-2226	p 34	N84-29876 *	#					NAS 1.15 83564	p 14	N84-13173 *	#
E-2227	p 100	N84-31460 *	#					NAS 1.15 83565	p 92	N84-16380 *	#
E-2228	p 87	N84-32531 *	#						p 69	N84-17351 *	#
E-2230	p 88	N84-34619 *	#								

NAS 1.15 83568	p 37	N84-16229	#	NAS 1.15 83674	p 48	N84-27825	#	NAS 1.15 83795	p 38	N84-32411	#
NAS 1.15 83569	p 14	N84-29870	#	NAS 1.15 83675	p 156	N84-29247	#	NAS 1.15 83799	p 186	N84-35085	#
NAS 1.15 83570	p 142	N84-17591	#	NAS 1.15 83676	p 73	N84-25793	#	NAS 1.15 83802	p 58	N84-34576	#
NAS 1.15 83571	p 8	N84-16142	#	NAS 1.15 83679	p 30	N84-23648	#	NAS 1.15 85487	p 37	N84-15164	#
NAS 1.15 83572	p 69	N84-17352	#	NAS 1.15 83680	p 171	N84-29347	#	NAS 1.15 85492	p 192	N84-16021	#
NAS 1.15 83574	p 85	N84-25831	#	NAS 1.15 83681	p 132	N84-25017	#	NAS 1.15 85493	p 192	N84-16020	#
NAS 1.15 83575	p 9	N84-17142	#	NAS 1.15 83682	p 31	N84-24584	#	NAS 1.15 85527	p 100	N84-25909	#
NAS 1.15 83576	p 8	N84-16141	#	NAS 1.15 83684	p 172	N84-31782	#	NAS 1.15 85594	p 93	N84-22771	#
NAS 1.15 83577	p 155	N84-18683	#	NAS 1.15 83686	p 31	N84-24582	#	NAS 1.15 86861	p 172	N84-30528	#
NAS 1.15 83578	p 142	N84-17592	#	NAS 1.15 83687	p 47	N84-24708	#	NAS 1.15 86862	p 87	N84-32536	#
NAS 1.15 83579	p 28	N84-21548	#	NAS 1.15 83688	p 39	N84-25753	#	NAS 1.15 86873	p 197	N84-34330	#
NAS 1.15 83580	p 70	N84-20672	#	NAS 1.15 83689	p 30	N84-24579	#	NAS 1.26 165325	p 84	N84-24809	#
NAS 1.15 83581	p 107	N84-17479	#	NAS 1.15 83690	p 48	N84-26746	#	NAS 1.26 165428	p 25	N84-15154	#
NAS 1.15 83582	p 132	N84-19787	#	NAS 1.15 83691	p 57	N84-28918	#	NAS 1.26 165429	p 153	N84-11514	#
NAS 1.15 83583	p 71	N84-20673	#	NAS 1.15 83692	p 133	N84-26010	#	NAS 1.26 165430	p 153	N84-11515	#
NAS 1.15 83584	p 108	N84-19708	#	NAS 1.15 83694	p 56	N84-25770	#	NAS 1.26 165466	p 33	N84-27737	#
NAS 1.15 83585	p 82	N84-19566	#	NAS 1.15 83695	p 31	N84-24585	#	NAS 1.26 165567	p 33	N84-27739	#
NAS 1.15 83586	p 124	N84-17593	#	NAS 1.15 83696	p 56	N84-27832	#	NAS 1.26 165592	p 33	N84-27738	#
NAS 1.15 83587	p 184	N84-26383	#	NAS 1.15 83697	p 10	N84-24539	#	NAS 1.26 165597	p 195	N84-21445	#
NAS 1.15 83588	p 9	N84-17138	#	NAS 1.15 83699	p 34	N84-28791	#	NAS 1.26 165608	p 33	N84-28788	#
NAS 1.15 83589	p 1	N84-16119	#	NAS 1.15 83700	p 56	N84-26755	#	NAS 1.26 167881	p 164	N84-11580	#
NAS 1.15 83590	p 108	N84-21803	#	NAS 1.15 83701	p 56	N84-27831	#	NAS 1.26 167890-EXEC-SUM	p 167	N84-23021	#
NAS 1.15 83591	p 99	N84-19641	#	NAS 1.15 83702	p 56	N84-26756	#	NAS 1.26 167916	p 165	N84-15679	#
NAS 1.15 83592	p 142	N84-19816	#	NAS 1.15 83703	p 127	N84-25000	#	NAS 1.26 167926	p 24	N84-14148	#
NAS 1.15 83593	p 195	N84-26484	#	NAS 1.15 83704	p 128	N84-25946	#	NAS 1.26 167927	p 25	N84-15153	#
NAS 1.15 83594	p 55	N84-24712	#	NAS 1.15 83706	p 85	N84-26803	#	NAS 1.26 167973	p 33	N84-28789	#
NAS 1.15 83595	p 69	N84-17353	#	NAS 1.15 83707	p 51	N84-25766	#	NAS 1.26 167980	p 22	N84-11170	#
NAS 1.15 83596	p 83	N84-19567	#	NAS 1.15 83708	p 32	N84-25713	#	NAS 1.26 167989	p 66	N84-10268	#
NAS 1.15 83598	p 47	N84-23691	#	NAS 1.15 83709	p 2	N84-25605	#	NAS 1.26 168004	p 60	N84-11228	#
NAS 1.15 83599	p 71	N84-21719	#	NAS 1.15 83710	p 2	N84-25607	#	NAS 1.26 168005	p 34	N84-29875	#
NAS 1.15 83600	p 191	N84-20404	#	NAS 1.15 83712	p 145	N84-27043	#	NAS 1.26 168053	p 105	N84-10450	#
NAS 1.15 83601	p 46	N84-20639	#	NAS 1.15 83713	p 145	N84-27042	#	NAS 1.26 168056	p 140	N84-10581	#
NAS 1.15 83602	p 190	N84-21329	#	NAS 1.15 83714	p 73	N84-26787	#	NAS 1.26 168062	p 96	N84-10402	#
NAS 1.15 83603	p 190	N84-21330	#	NAS 1.15 83715	p 47	N84-25764	#	NAS 1.26 168063	p 96	N84-10403	#
NAS 1.15 83604	p 143	N84-20858	#	NAS 1.15 83716	p 2	N84-25606	#	NAS 1.26 168064	p 96	N84-10404	#
NAS 1.15 83605	p 177	N84-20258	#	NAS 1.15 83717	p 73	N84-27857	#	NAS 1.26 168076	p 106	N84-11385	#
NAS 1.15 83606	p 177	N84-20259	#	NAS 1.15 83718	p 87	N84-28994	#	NAS 1.26 168081	p 89	N84-10332	#
NAS 1.15 83608	p 145	N84-26029	#	NAS 1.15 83719	p 86	N84-27887	#	NAS 1.26 168133	p 46	N84-18321	#
NAS 1.15 83609	p 74	N84-28962	#	NAS 1.15 83721	p 146	N84-28087	#	NAS 1.26 168135	p 172	N84-31784	#
NAS 1.15 83610	p 54	N84-21666	#	NAS 1.15 83722	p 156	N84-29248	#	NAS 1.26 168139	p 21	N84-10054	#
NAS 1.15 83611	p 126	N84-22910	#	NAS 1.15 83723	p 146	N84-29224	#	NAS 1.26 168156	p 48	N84-28901	#
NAS 1.15 83612	p 167	N84-20916	#	NAS 1.15 83724	p 146	N84-28088	#	NAS 1.26 168159	p 164	N84-11581	#
NAS 1.15 83613	p 126	N84-21832	#	NAS 1.15 83725	p 146	N84-29223	#	NAS 1.26 168172	p 46	N84-18322	#
NAS 1.15 83614	p 126	N84-22911	#	NAS 1.15 83726	p 147	N84-30294	#	NAS 1.26 168176	p 23	N84-13193	#
NAS 1.15 83616	p 184	N84-23235	#	NAS 1.15 83727	p 87	N84-30072	#	NAS 1.26 168177	p 194	N84-17073	#
NAS 1.15 83617	p 126	N84-22909	#	NAS 1.15 83728	p 48	N84-27824	#	NAS 1.26 168178	p 193	N84-14071	#
NAS 1.15 83618	p 168	N84-23026	#	NAS 1.15 83729	p 57	N84-31288	#	NAS 1.26 168179	p 89	N84-15283	#
NAS 1.15 83619	p 144	N84-25064	#	NAS 1.15 83730	p 34	N84-28790	#	NAS 1.26 168181	p 169	N84-25162	#
NAS 1.15 83620	p 188	N84-22421	#	NAS 1.15 83731	p 128	N84-30223	#	NAS 1.26 168183	p 165	N84-14587	#
NAS 1.15 83622	p 86	N84-28990	#	NAS 1.15 83732	p 128	N84-29157	#	NAS 1.26 168191-VOL-1	p 153	N84-10613	#
NAS 1.15 83623	p 73	N84-26785	#	NAS 1.15 83733	p 2	N84-32344	#	NAS 1.26 168191-VOL-2	p 153	N84-10614	#
NAS 1.15 83624	p 47	N84-25762	#	NAS 1.15 83734	p 129	N84-30224	#	NAS 1.26 168193-VOL-1	p 45	N84-12226	#
NAS 1.15 83625	p 110	N84-25926	#	NAS 1.15 83735	p 157	N84-30329	#	NAS 1.26 168193-VOL-2	p 45	N84-13218	#
NAS 1.15 83628	p 83	N84-21739	#	NAS 1.15 83736	p 35	N84-29878	#	NAS 1.26 168196	p 106	N84-13443	#
NAS 1.15 83629	p 84	N84-24808	#	NAS 1.15 83737	p 157	N84-31683	#	NAS 1.26 168203	p 166	N84-18757	#
NAS 1.15 83630	p 132	N84-21649	#	NAS 1.15 83738	p 75	N84-31344	#	NAS 1.26 168205	p 194	N84-18117	#
NAS 1.15 83631	p 55	N84-22702	#	NAS 1.15 83739	p 11	N84-32357	#	NAS 1.26 168206	p 44	N84-10180	#
NAS 1.15 83632	p 57	N84-28917	#	NAS 1.15 83740	p 147	N84-30293	#	NAS 1.26 168210	p 87	N84-28995	#
NAS 1.15 83633	p 99	N84-25908	#	NAS 1.15 83741	p 34	N84-29876	#	NAS 1.26 168217	p 83	N84-26095	#
NAS 1.15 83634	p 156	N84-23923	#	NAS 1.15 83743	p 110	N84-31512	#	NAS 1.26 168218	p 68	N84-15247	#
NAS 1.15 83635	p 10	N84-22533	#	NAS 1.15 83744	p 185	N84-32118	#	NAS 1.26 168221	p 93	N84-19606	#
NAS 1.15 83636	p 1	N84-22527	#	NAS 1.15 83745	p 100	N84-31460	#	NAS 1.26 168224	p 60	N84-11229	#
NAS 1.15 83637	p 29	N84-22565	#	NAS 1.15 83746	p 88	N84-34620	#	NAS 1.26 168225	p 152	N84-10612	#
NAS 1.15 83638	p 47	N84-22631	#	NAS 1.15 83749	p 100	N84-30147	#	NAS 1.26 168227	p 89	N84-13332	#
NAS 1.15 83639	p 29	N84-22566	#	NAS 1.15 83751	p 129	N84-31558	#	NAS 1.26 168229	p 163	N84-10661	#
NAS 1.15 83640	p 29	N84-22564	#	NAS 1.15 83753	p 134	N84-30273	#	NAS 1.26 168231	p 98	N84-16423	#
NAS 1.15 83641	p 31	N84-24581	#	NAS 1.15 83755	p 110	N84-31513	#	NAS 1.26 168232	p 98	N84-16424	#
NAS 1.15 83643	p 168	N84-23025	#	NAS 1.15 83756	p 157	N84-31687	#	NAS 1.26 168233	p 81	N84-13310	#
NAS 1.15 83644	p 47	N84-23690	#	NAS 1.15 83757	p 51	N84-31283	#	NAS 1.26 168234-VOL-1	p 185	N84-33148	#
NAS 1.15 83646	p 109	N84-22890	#	NAS 1.15 83758	p 10	N84-31091	#	NAS 1.26 168234-VOL-2	p 186	N84-33149	#
NAS 1.15 83647	p 168	N84-23024	#	NAS 1.15 83759	p 100	N84-30146	#	NAS 1.26 168234-VOL-3	p 186	N84-33150	#
NAS 1.15 83648	p 42	N84-22615	#	NAS 1.15 83760	p 185	N84-32122	#	NAS 1.26 168235	p 141	N84-15554	#
NAS 1.15 83649	p 195	N84-22512	#	NAS 1.15 83761	p 63	N84-33536	#	NAS 1.26 168236	p 97	N84-14376	#
NAS 1.15 83650	p 195	N84-24509	#	NAS 1.15 83762	p 76	N84-32508	#	NAS 1.26 168237	p 97	N84-14377	#
NAS 1.15 83651	p 167	N84-23022	#	NAS 1.15 83764	p 188	N84-34230	#	NAS 1.26 168238	p 97	N84-14378	#
NAS 1.15 83652	p 109	N84-22891	#	NAS 1.15 83765	p 36	N84-33414	#	NAS 1.26 168239	p 164	N84-13673	#
NAS 1.15 83653	p 62	N84-22712	#	NAS 1.15 83766	p 189	N84-32169	#	NAS 1.26 168240	p 107	N84-17477	#
NAS 1.15 83655	p 32	N84-24589	#	NAS 1.15 83768	p 49	N84-32427	#	NAS 1.26 168242	p 91	N84-27909	#
NAS 1.15 83656	p 109	N84-22892	#	NAS 1.15 83769	p 77	N84-33564	#	NAS 1.26 168243-VOL-2	p 60	N84-12265	#
NAS 1.15 83657	p 169	N84-25166	#	NAS 1.15 83770	p 49	N84-31272	#	NAS 1.26 168244	p 111	N84-31514	#
NAS 1.15 83658	p 133	N84-25019	#	NAS 1.15 83772	p 10	N84-31096	#	NAS 1.26 168247	p 12	N84-11152	#
NAS 1.15 83659	p 75	N84-28963	#	NAS 1.15 83773	p 92	N84-33608	#	NAS 1.26 168248	p 37	N84-10109	#
NAS 1.15 83660	p 32	N84-25712	#	NAS 1.15 83774	p 100	N84-31461	#	NAS 1.26 168251	p 81	N84-12312	#
NAS 1.15 83661	p 50	N84-23693	#	NAS 1.15 83775	p 101	N84-32644	#	NAS 1.26 168252	p 124	N84-17530	#
NAS 1.15 83662	p 100	N84-27954	#	NAS 1.15 83777	p 75	N84-31347	#	NAS 1.26 168253	p 109	N84-24973	#
NAS 1.15 83663	p 72	N84-24772	#	NAS 1.15 83778	p 75	N84-31348	#	NAS 1.26 168254	p 97	N84-13398	#
NAS 1.15 83664	p 167	N84-23023	#	NAS 1.15 83779	p 87	N84-32531	#	NAS 1.26 168255	p 196	N84-33304	#
NAS 1.15 83665	p 75	N84-31345	#	NAS 1.15 83780	p 11	N84-32351	#	NAS 1.26 168256	p 196	N84-32306	#
NAS 1.15 83666	p 127	N84-24999	#	NAS 1.15 83781	p 133	N84-32783	#	NAS 1.26 168257	p 196	N84-32307	#
NAS 1.15 83667	p 168	N84-23027	#	NAS 1.15 83782	p 77	N84-34603	#	NAS 1.26 168258	p 22	N84-13186	#
NAS 1.15 83668	p 31	N84-24583	#	NAS 1.15 83785	p 133	N84-32789	#	N			

NAS 1 26 168269	p 109	N84-23841 *	#	NAS 1.26.174622	p 185	N84-32305 *	#	NAS 1 60 2238	p 107	N84-16461 *	#
NAS 1 26 168272	p 165	N84-14585 *	#	NAS 1.26.174624	p 33	N84-26702 *	#	NAS 1 60 2239	p 54	N84-13224 *	#
NAS 1 26 168273	p 108	N84-17481 *	#	NAS 1.26.174625	p 36	N84-33417 *	#	NAS 1 60 2240	p 40	N84-16247 *	#
NAS 1.26.168276	p 107	N84-16463 *	#	NAS 1 26 174627	p 91	N84-25854 *	#	NAS 1 60 2243	p 155	N84-20878 *	#
NAS 1.26.168277	p 45	N84-12225 *	#	NAS 1 26 174628	p 70	N84-19523 *	#	NAS 1 60 2248	p 106	N84-15394 *	#
NAS 1 26 168278	p 23	N84-13189 *	#	NAS 1 26 174629	p 146	N84-28089 *	#	NAS 1.60.2257	p 141	N84-13577 *	#
NAS 1 26 168279	p 23	N84-14143 *	#	NAS 1 26 174631	p 174	N84-27375 *	#	NAS 1.60.2259	p 183	N84-15894 *	#
NAS 1 26 168280	p 153	N84-11513 *	#	NAS 1 26 174633	p 143	N84-21879 *	#	NAS 1.60.2266	p 25	N84-16181 *	#
NAS 1 26 168282	p 8	N84-16146 *	#	NAS 1 26 174634	p 156	N84-22980 *	#	NAS 1 60 2267	p 82	N84-16334 *	#
NAS 1 26 168283	p 122	N84-13490 *	#	NAS 1.26.174635-VOL-1	p 38	N84-20611 *	#	NAS 1 60 2268	p 123	N84-17525 *	#
NAS 1.26.168284	p 166	N84-15682 *	#	NAS 1 26 174635-VOL-2	p 38	N84-20612 *	#	NAS 1 60 2274	p 142	N84-18653 *	#
NAS 1 26 168288	p 8	N84-16145 *	#	NAS 1 26 174636	p 133	N84-31595 *	#	NAS 1 60 2275	p 142	N84-18654 *	#
NAS 1 26 168292	p 194	N84-19185 *	#	NAS 1 26 174639	p 71	N84-20674 *	#	NAS 1.60.2278	p 70	N84-18370 *	#
NAS 1 26 168293	p 23	N84-13187 *	#	NAS 1.26.174640	p 32	N84-25710 *	#	NAS 1.60.2279	p 82	N84-18399 *	#
NAS 1 26 168294	p 164	N84-13672 *	#	NAS 1.26.174641	p 27	N84-19353 *	#	NAS 1.60.2280	p 69	N84-17350 *	#
NAS 1 26 168296-VOL-1	p 25	N84-15155 *	#	NAS 1 26 174642	p 91	N84-27908 *	#	NAS 1 60 2285	p 82	N84-18400 *	#
NAS 1 26 168296-VOL-2	p 25	N84-15156 *	#	NAS 1.26.174644	p 91	N84-23775 *	#	NAS 1 60 2286	p 83	N84-21740 *	#
NAS 1 26 168297	p 134	N84-32790 *	#	NAS 1.26.174649	p 39	N84-23667 *	#	NAS 1 60 2289	p 71	N84-21716 *	#
NAS 1.26.168298	p 169	N84-25169 *	#	NAS 1 26 174650	p 32	N84-25711 *	#	NAS 1 60 2290	p 72	N84-21721 *	#
NAS 1 26 168299	p 184	N84-14991 *	#	NAS 1.26.174655	p 172	N84-34036 *	#	NAS 1 60 2294	p 28	N84-21549 *	#
NAS 1 26 168304	p 122	N84-14462 *	#	NAS 1 26 174659	p 74	N84-28960 *	#	NAS 1 60 2296	p 27	N84-20562 *	#
NAS 1 26 168306	p 166	N84-20014 *	#	NAS 1.26.174660	p 169	N84-26165 *	#	NAS 1 60 2297	p 9	N84-20493 *	#
NAS 1 26 168308	p 67	N84-14287 *	#	NAS 1 26 174661	p 62	N84-21677 *	#	NAS 1.60.2301	p 50	N84-20643 *	#
NAS 1 26 168309	p 166	N84-20915 *	#	NAS 1 26 174663	p 29	N84-22568 *	#	NAS 1 60 2302	p 51	N84-26749 *	#
NAS 1.26.168310	p 92	N84-16381 *	#	NAS 1 26 174666	p 145	N84-25065 *	#	NAS 1 60 2303	p 174	N84-31865 *	#
NAS 1.26.168317	p 155	N84-19927 *	#	NAS 1 26 174667	p 30	N84-23640 *	#	NAS 1 60 2304	p 30	N84-24578 *	#
NAS 1 26 168318	p 171	N84-29357 *	#	NAS 1 26 174668	p 35	N84-29877 *	#	NAS 1 60 2309	p 35	N84-32388 *	#
NAS 1 26 168319	p 172	N84-31783 *	#	NAS 1 26 174669	p 91	N84-26813 *	#	NAS 1 60 2316	p 84	N84-23764 *	#
NAS 1 26 168320	p 46	N84-20634 *	#	NAS 1.26.174670	p 100	N84-31464 *	#	NAS 1.60.2317	p 90	N84-23774 *	#
NAS 1.26.168321	p 83	N84-20699 *	#	NAS 1.26.174674	p 196	N84-33307 *	#	NAS 1.60.2319	p 74	N84-28958 *	#
NAS 1 26 168322	p 124	N84-18578 *	#	NAS 1.26.174675	p 31	N84-24580 *	#	NAS 1.60.2320	p 63	N84-32446 *	#
NAS 1.26.168323	p 24	N84-15151 *	#	NAS 1.26.174680	p 10	N84-25646 *	#	NAS 1.60.2338	p 73	N84-26783 *	#
NAS 1 26 168324	p 134	N84-18620 *	#	NAS 1.26.174683	p 72	N84-24774 *	#	NAS 1 60 2339	p 76	N84-31349 *	#
NAS 1 26 168326	p 99	N84-20737 *	#	NAS 1.26.174685	p 36	N84-34444 *	#	NAS 1 60 2342	p 86	N84-28989 *	#
NAS 1 26 168327	p 98	N84-16425 *	#	NAS 1.26.174686	p 76	N84-32503 *	#	NAS 1 60 2354	p 75	N84-28665 *	#
NAS 1 26 168328	p 40	N84-16243 *	#	NAS 1 26 174688	p 29	N84-23629 *	#	NAS 1 60 2355	p 146	N84-29226 *	#
NAS 1 26 168330	p 25	N84-15152 *	#	NAS 1.26.174690	p 186	N84-33309 *	#	NAS 1 60 2360	p 87	N84-31379 *	#
NAS 1 26 168331	p 90	N84-17410 *	#	NAS 1.26.174691	p 76	N84-32504 *	#	NAS 1 60 2361	p 42	N84-33452 *	#
NAS 1.26.168332	p 9	N84-17139 *	#	NAS 1.26.174694	p 195	N84-29805 *	#	NAS 1 60 2362	p 88	N84-33590 *	#
NAS 1.26.168334	p 89	N84-17407 *	#	NAS 1 26 174702	p 49	N84-32428 *	#	NAS 1 60 2367	p 147	N84-32824 *	#
NAS 1.26.168335	p 108	N84-18536 *	#	NAS 1 26 174703	p 49	N84-32429 *	#	NAS 1 60 2368	p 147	N84-32825 *	#
NAS 1.26.168336-VOL-1	p 184	N84-24323 *	#	NAS 1 26 174705	p 74	N84-28961 *	#	NAS 1 61 1123	p 145	N84-27041 *	#
NAS 1 26 168336-VOL-2	p 184	N84-24324 *	#	NAS 1 26 174706	p 148	N84-32828 *	#	NAS 1 61 1126	p 147	N84-31640 *	#
NAS 1.26.171032	p 173	N84-25204 *	#	NAS 1 26 174714	p 170	N84-27329 *	#	NAS 1.71 LEW-12995-1	p 148	N84-33808 *	#
NAS 1 26 171147	p 148	N84-39811 *	#	NAS 1 26 174716	p 112	N84-33715 *	#	NAS 1.71 LEW-13495-1	p 111	N84-33663 *	#
NAS 1.26.172217	p 7	N84-10022 *	#	NAS 1 26 174717	p 34	N84-28794 *	#	NAS 1.71 LEW-13524-1	p 35	N84-33410 *	#
NAS 1.26.172791	p 41	N84-17252 *	#	NAS 1 26 174720	p 173	N84-34037 *	#	NAS 1.71 LEW-13639-1	p 77	N84-33555 *	#
NAS 1 26 173214	p 82	N84-16337 *	#	NAS 1.26.174725	p 172	N84-29358 *	#	NAS 1 71 LEW-13773-2	p 133	N84-32782 *	#
NAS 1 26 173247	p 107	N84-16459 *	#	NAS 1.26.174728	p 197	N84-34331 *	#	NAS 1 71 LEW-14028-1	p 172	N84-32909 *	#
NAS 1 26 173249	p 107	N84-16458 *	#	NAS 1 26 174755	p 186	N84-33306 *	#	NAS 1 71 LEW-14037-1	p 49	N84-32425 *	#
NAS 1 26 173266	p 189	N84-16991 *	#	NAS 1 26 174759	p 129	N84-32751 *	#	NAS 1 71 LEW-14057-1	p 88	N84-33595 *	#
NAS 1 26 173267	p 191	N84-17014 *	#	NAS 1 26 174760	p 35	N84-32390 *	#	NASA-CASE-LEW-12590-1	p 143	N84-22958 *	#
NAS 1 26 173273	p 141	N84-16562 *	#	NAS 1 26 174761	p 92	N84-32552 *	#	NASA-CASE-LEW-12919-2	p 179	N84-28565 *	#
NAS 1 26 173279	p 82	N84-17389 *	#	NAS 1.26.174763	p 50	N84-33462 *	#	NASA-CASE-LEW-12995-1	p 148	N84-33808 *	#
NAS 1 26 173322	p 90	N84-18420 *	#	NAS 1 26 174767	p 57	N84-34575 *	#	NASA-CASE-LEW-13107-2	p 174	N84-23095 *	#
NAS 1 26 173343	p 108	N84-19709 *	#	NAS 1 26 174774	p 159	N84-34774 *	#	NASA-CASE-LEW-13269-2	p 143	N84-22957 *	#
NAS 1 26 173360	p 27	N84-18202 *	#	NAS 1 26 175323	p 93	N84-15360 *	#	NASA-CASE-LEW-13286-1	p 106	N84-14422 *	#
NAS 1 26 173377	p 71	N84-20675 *	#	NAS 1 26 175391	p 125	N84-19746 *	#	NASA-CASE-LEW-13349-1	p 72	N84-22734 *	#
NAS 1 26 173393	p 71	N84-21720 *	#	NAS 1 26 175392	p 124	N84-19744 *	#	NASA-CASE-LEW-13426-1	p 60	N84-16276 *	#
NAS 1 26 173394	p 156	N84-21903 *	#	NAS 1 26 175396	p 61	N84-19495 *	#	NASA-CASE-LEW-13495-1	p 111	N84-33663 *	#
NAS 1.26.173412	p 143	N84-21877 *	#	NAS 1 26 175397	p 125	N84-19745 *	#	NASA-CASE-LEW-13506-1	p 29	N84-22562 *	#
NAS 1.26.173417	p 108	N84-22889 *	#	NAS 1 26 175410	p 9	N84-20488 *	#	NASA-CASE-LEW-13524-1	p 35	N84-33410 *	#
NAS 1.26.173456	p 167	N84-22001 *	#	NAS 1 26 175423	p 93	N84-19620 *	#	NASA-CASE-LEW-13526-1	p 134	N84-22944 *	#
NAS 1 26 173473	p 156	N84-21905 *	#	NAS 1.26.175444	p 27	N84-20524 *	#	NASA-CASE-LEW-13570-1	p 106	N84-16452 *	#
NAS 1 26 173500	p 84	N84-22753 *	#	NAS 1.26.3729	p 153	N84-12530 *	#	NASA-CASE-LEW-13598-1	p 132	N84-22930 *	#
NAS 1 26 173503	p 127	N84-23854 *	#	NAS 1 26 3749	p 148	N84-14525 *	#	NASA-CASE-LEW-13622-1	p 28	N84-22559 *	#
NAS 1 26 173511	p 159	N84-27258 *	#	NAS 1 26 3750	p 148	N84-14526 *	#	NASA-CASE-LEW-13639-1	p 77	N84-33555 *	#
NAS 1 26 173514	p 127	N84-25001 *	#	NAS 1 26 3756	p 149	N84-15565 *	#	NASA-CASE-LEW-13639-2	p 73	N84-27855 *	#
NAS 1 26 173515	p 99	N84-24918 *	#	NAS 1 26 3757	p 188	N84-16984 *	#	NASA-CASE-LEW-13653-1	p 170	N84-28205 *	#
NAS 1 26 173532	p 38	N84-23662 *	#	NAS 1 26 3758	p 185	N84-29661 *	#	NASA-CASE-LEW-13654-1	p 28	N84-22560 *	#
NAS 1.26.173534	p 99	N84-23807 *	#	NAS 1 26 3769	p 123	N84-16488 *	#	NASA-CASE-LEW-13670-1	p 143	N84-22959 *	#
NAS 1 26 173548	p 99	N84-24924 *	#	NAS 1 26 3770	p 149	N84-17606 *	#	NASA-CASE-LEW-13736-1	p 110	N84-27974 *	#
NAS 1 26 173550	p 85	N84-24810 *	#	NAS 1.26.3789	p 193	N84-21275 *	#	NASA-CASE-LEW-13758-1	p 56	N84-27829 *	#
NAS 1 26 173552	p 176	N84-25336 *	#	NAS 1 26 3790	p 155	N84-19925 *	#	NASA-CASE-LEW-13770-1	p 86	N84-27885 *	#
NAS 1 26 173554	p 169	N84-25168 *	#	NAS 1 26 3792	p 127	N84-25941 *	#	NASA-CASE-LEW-13770-3	p 55	N84-22698 *	#
NAS 1 26 173555	p 32	N84-24586 *	#	NAS 1 26 3793	p 145	N84-26027 *	#	NASA-CASE-LEW-13770-4	p 55	N84-22699 *	#
NAS 1.26.173557	p 110	N84-24975 *	#	NAS 1 26 3803	p 184	N84-26384 *	#	NASA-CASE-LEW-13770-5	p 55	N84-22701 *	#
NAS 1.26.17355	p 36	N84-19360 *	#	NAS 1.26.3804	p 127	N84-25943 *	#	NASA-CASE-LEW-13773-2	p 133	N84-32782 *	#
NAS 1 26 173560	p 110	N84-24974 *	#	NAS 1 26 3832	p 36	N84-33412 *	#	NASA-CASE-LEW-13822-1	p 110	N84-29084 *	#
NAS 1.26.173622	p 185	N84-27544 *	#	NAS 1 26 3833	p 11	N84-32355 *	#	NASA-CASE-LEW-13826-2	p 55	N84-24711 *	#
NAS 1 26 173778	p 128	N84-29155 *	#	NAS 1.55.2282	p 22	N84-10055 *	#	NASA-CASE-LEW-13829-1	p 54	N84-15203 *	#
NAS 1 26 173820	p 100	N84-30145 *	#	NAS 1.55.2297	p 167	N84-31688 *	#	NASA-CASE-LEW-13837-1	p 54	N84-22695 *	#
NAS 1 26 173821	p 167	N84-29252 *	#	NAS 1 55 2300-VOL-1	p 144	N84-23681 *	#	NASA-CASE-LEW-13837-2	p 54	N84-22696 *	#
NAS 1.26.173830	p 157	N84-31685 *	#	NAS 1 55 2300-VOL-2	p 144	N84-25047 *	#	NASA-CASE-LEW-13914-1	p 131	N84-12447 *	#
NAS 1 26 173868	p 111	N84-32678 *	#	NAS 1 55 2307	p 30	N84-23630 *	#	NASA-CASE-LEW-13922-1	p 106	N84-11389 *	#
NAS 1 26 173884	p 35	N84-32389 *	#	NAS 1 55 2309	p 27	N84-20525 *	#	NASA-CASE-LEW-13923-1	p 54	N84-16266 *	#
NAS 1.26.173888	p 191	N84-33210 *	#	NAS 1 55 2314	p 170	N84-29307 *	#	NASA-CASE-LEW-14028-1	p 172	N84-32909 *	#
NAS 1 26 173907	p 111	N84-32682 *	#	NAS 1 55 2337	p 77	N84-34589 *	#	NASA-CASE-LEW-14035-1	p 30	N84-24577 *	#
NAS 1 26 173916	p 101	N84-32645 *	#	NAS 1							

NASA-CP-2282	....	p 22	N84-10055 *	NASA-CR-168273	.....	p 108	N84-17481 *	NASA-CR-174625	.....	p 36	N84-33417 *
NASA-CP-2297	.....	p 157	N84-31688 *	NASA-CR-168276	.....	p 107	N84-16463 *	NASA-CR-174627	.....	p 91	N84-25854 *
NASA-CP-2300-VOL-1	.....	p 144	N84-23891 *	NASA-CR-168277	.....	p 45	N84-12225 *	NASA-CR-174628	.....	p 70	N84-19523 *
NASA-CP-2300-VOL-2	.....	p 144	N84-25047 *	NASA-CR-168278	.....	p 23	N84-13189 *	NASA-CR-174629	.....	p 146	N84-28089 *
NASA-CP-2307	.....	p 30	N84-23630 *	NASA-CR-168279	.....	p 23	N84-14143 *	NASA-CR-174631	.....	p 174	N84-27375 *
NASA-CP-2309	.....	p 27	N84-20525 *	NASA-CR-168280	.....	p 153	N84-11513 *	NASA-CR-174633	.....	p 143	N84-21879 *
NASA-CP-2314	.....	p 170	N84-29307 *	NASA-CR-168282	.....	p 8	N84-16146 *	NASA-CR-174634	.....	p 156	N84-22980 *
NASA-CP-2337	.....	p 77	N84-34589 *	NASA-CR-168283	.....	p 122	N84-13490 *	NASA-CR-174635-VOL-1	.....	p 38	N84-20611 *
				NASA-CR-168284	.....	p 166	N84-15682 *	NASA-CR-174635-VOL-2	.....	p 38	N84-20612 *
NASA-CR-165325	.....	p 84	N84-24809 *	NASA-CR-168288	.....	p 8	N84-16145 *	NASA-CR-174636	.....	p 133	N84-31595 *
NASA-CR-165428	.....	p 25	N84-15154 *	NASA-CR-168292	.....	p 194	N84-19185 *	NASA-CR-174639	.....	p 71	N84-20674 *
NASA-CR-165429	.....	p 153	N84-11514 *	NASA-CR-168293	.....	p 23	N84-13187 *	NASA-CR-174640	.....	p 32	N84-25710 *
NASA-CR-165430	.....	p 153	N84-11515 *	NASA-CR-168294	.....	p 164	N84-13672 *	NASA-CR-174641	.....	p 27	N84-19353 *
NASA-CR-165466	.....	p 33	N84-27737 *	NASA-CR-168296-VOL-1	.....	p 25	N84-15155 *	NASA-CR-174642	.....	p 91	N84-27908 *
NASA-CR-165567	.....	p 33	N84-27739 *	NASA-CR-168297	.....	p 25	N84-15156 *	NASA-CR-174644	.....	p 91	N84-23775 *
NASA-CR-165592	.....	p 33	N84-27738 *	NASA-CR-168298	.....	p 134	N84-32790 *	NASA-CR-174649	.....	p 39	N84-23667 *
NASA-CR-165597	.....	p 195	N84-21445 *	NASA-CR-168299	.....	p 169	N84-25169 *	NASA-CR-174650	.....	p 32	N84-25711 *
NASA-CR-165608	.....	p 33	N84-28788 *	NASA-CR-168300	.....	p 194	N84-14991 *	NASA-CR-174655	.....	p 172	N84-34036 *
NASA-CR-167881	.....	p 164	N84-11580 *	NASA-CR-168306	.....	p 122	N84-14462 *	NASA-CR-174659	.....	p 74	N84-28960 *
NASA-CR-167890-EXEC-SUM	.....	p 167	N84-23021 *	NASA-CR-168308	.....	p 166	N84-20014 *	NASA-CR-174660	.....	p 169	N84-26165 *
NASA-CR-167916	.....	p 165	N84-15679 *	NASA-CR-168309	.....	p 67	N84-14287 *	NASA-CR-174661	.....	p 62	N84-21677 *
NASA-CR-167926	.....	p 24	N84-14148 *	NASA-CR-168310	.....	p 166	N84-20915 *	NASA-CR-174663	.....	p 29	N84-22568 *
NASA-CR-167927	.....	p 25	N84-15153 *	NASA-CR-168317	.....	p 92	N84-16381 *	NASA-CR-174666	.....	p 145	N84-25065 *
NASA-CR-167973	.....	p 33	N84-28789 *	NASA-CR-168318	.....	p 155	N84-19927 *	NASA-CR-174667	.....	p 30	N84-23649 *
NASA-CR-167980	.....	p 22	N84-11170 *	NASA-CR-168319	.....	p 171	N84-29357 *	NASA-CR-174668	.....	p 35	N84-29877 *
NASA-CR-167989	.....	p 66	N84-10268 *	NASA-CR-168320	.....	p 172	N84-31783 *	NASA-CR-174669	.....	p 91	N84-26813 *
NASA-CR-168004	.....	p 60	N84-11228 *	NASA-CR-168321	.....	p 46	N84-20634 *	NASA-CR-174670	.....	p 100	N84-31464 *
NASA-CR-168005	.....	p 34	N84-29875 *	NASA-CR-168322	.....	p 83	N84-20699 *	NASA-CR-174674	.....	p 196	N84-33307 *
NASA-CR-168053	.....	p 105	N84-10450 *	NASA-CR-168323	.....	p 124	N84-18578 *	NASA-CR-174675	.....	p 31	N84-24580 *
NASA-CR-168056	.....	p 140	N84-10581 *	NASA-CR-168324	.....	p 24	N84-15151 *	NASA-CR-174680	.....	p 10	N84-25646 *
NASA-CR-168062	.....	p 96	N84-10402 *	NASA-CR-168326	.....	p 134	N84-18620 *	NASA-CR-174683	.....	p 72	N84-24774 *
NASA-CR-168063	.....	p 96	N84-10403 *	NASA-CR-168327	.....	p 99	N84-20737 *	NASA-CR-174685	.....	p 36	N84-34444 *
NASA-CR-168064	.....	p 96	N84-10404 *	NASA-CR-168328	.....	p 98	N84-16425 *	NASA-CR-174686	.....	p 76	N84-32503 *
NASA-CR-168076	.....	p 106	N84-11385 *	NASA-CR-168329	.....	p 40	N84-16243 *	NASA-CR-174688	.....	p 29	N84-23629 *
NASA-CR-168081	.....	p 89	N84-10332 *	NASA-CR-168330	.....	p 25	N84-15152 *	NASA-CR-174689	.....	p 196	N84-33309 *
NASA-CR-168133	.....	p 46	N84-18321 *	NASA-CR-168331	.....	p 90	N84-17410 *	NASA-CR-174691	.....	p 76	N84-32504 *
NASA-CR-168135	.....	p 172	N84-31784 *	NASA-CR-168332	.....	p 9	N84-17139 *	NASA-CR-174694	.....	p 195	N84-29805 *
NASA-CR-168139	.....	p 21	N84-10054 *	NASA-CR-168333	.....	p 89	N84-17407 *	NASA-CR-174702	.....	p 49	N84-32428 *
NASA-CR-168156	.....	p 48	N84-28901 *	NASA-CR-168335	.....	p 108	N84-18536 *	NASA-CR-174703	.....	p 49	N84-32429 *
NASA-CR-168159	.....	p 164	N84-11581 *	NASA-CR-168336-VOL-1	.....	p 184	N84-24323 *	NASA-CR-174705	.....	p 74	N84-28961 *
NASA-CR-168172	.....	p 46	N84-18322 *	NASA-CR-168336-VOL-2	.....	p 184	N84-24324 *	NASA-CR-174706	.....	p 148	N84-32828 *
NASA-CR-168176	.....	p 23	N84-13193 *	NASA-CR-171032	.....	p 173	N84-25204 *	NASA-CR-174714	.....	p 170	N84-27329 *
NASA-CR-168177	.....	p 194	N84-17073 *	NASA-CR-171147	.....	p 148	N84-33811 *	NASA-CR-174716	.....	p 112	N84-33715 *
NASA-CR-168178	.....	p 193	N84-14071 *	NASA-CR-172217	.....	p 7	N84-10022 *	NASA-CR-174717	.....	p 34	N84-28794 *
NASA-CR-168179	.....	p 89	N84-15283 *	NASA-CR-172791	.....	p 41	N84-17252 *	NASA-CR-174720	.....	p 173	N84-34037 *
NASA-CR-168181	.....	p 169	N84-25162 *	NASA-CR-173214	.....	p 82	N84-16337 *	NASA-CR-174725	.....	p 172	N84-29358 *
NASA-CR-168183	.....	p 165	N84-14587 *	NASA-CR-173247	.....	p 107	N84-16459 *	NASA-CR-174728	.....	p 197	N84-34331 *
NASA-CR-168191-VOL-1	.....	p 153	N84-10613 *	NASA-CR-173249	.....	p 107	N84-16458 *	NASA-CR-174755	.....	p 196	N84-33306 *
NASA-CR-168191-VOL-2	.....	p 153	N84-10614 *	NASA-CR-173266	.....	p 189	N84-16991 *	NASA-CR-174759	.....	p 129	N84-32751 *
NASA-CR-168193-VOL-1	.....	p 45	N84-12226 *	NASA-CR-173267	.....	p 191	N84-17014 *	NASA-CR-174760	.....	p 35	N84-32390 *
NASA-CR-168193-VOL-2	.....	p 45	N84-13218 *	NASA-CR-173273	.....	p 141	N84-16562 *	NASA-CR-174761	.....	p 92	N84-32552 *
NASA-CR-168196	.....	p 106	N84-13443 *	NASA-CR-173279	.....	p 82	N84-17389 *	NASA-CR-174763	.....	p 50	N84-33462 *
NASA-CR-168203	.....	p 166	N84-18757 *	NASA-CR-173322	.....	p 90	N84-18420 *	NASA-CR-174767	.....	p 57	N84-34575 *
NASA-CR-168205	.....	p 194	N84-18117 *	NASA-CR-173343	.....	p 108	N84-19709 *	NASA-CR-174774	.....	p 159	N84-34774 *
NASA-CR-168206	.....	p 44	N84-10180 *	NASA-CR-173355	.....	p 36	N84-19360 *	NASA-CR-175323	.....	p 98	N84-15360 *
NASA-CR-168210	.....	p 87	N84-28995 *	NASA-CR-173360	.....	p 27	N84-18202 *	NASA-CR-175391	.....	p 125	N84-19746 *
NASA-CR-168217	.....	p 83	N84-20695 *	NASA-CR-173377	.....	p 71	N84-20676 *	NASA-CR-175392	.....	p 124	N84-19744 *
NASA-CR-168218	.....	p 68	N84-15247 *	NASA-CR-173393	.....	p 71	N84-21720 *	NASA-CR-175396	.....	p 61	N84-19495 *
NASA-CR-168221	.....	p 93	N84-19606 *	NASA-CR-173394	.....	p 156	N84-21903 *	NASA-CR-175397	.....	p 125	N84-19745 *
NASA-CR-168224	.....	p 60	N84-11229 *	NASA-CR-173412	.....	p 143	N84-21877 *	NASA-CR-175410	.....	p 9	N84-20488 *
NASA-CR-168225	.....	p 152	N84-10612 *	NASA-CR-173417	.....	p 108	N84-22889 *	NASA-CR-175423	.....	p 98	N84-19620 *
NASA-CR-168227	.....	p 89	N84-13332 *	NASA-CR-173456	.....	p 167	N84-22001 *	NASA-CR-175444	.....	p 27	N84-20524 *
NASA-CR-168229	.....	p 163	N84-10661 *	NASA-CR-173473	.....	p 156	N84-21905 *	NASA-CR-3729	.....	p 153	N84-12530 *
NASA-CR-168231	.....	p 98	N84-16423 *	NASA-CR-173500	.....	p 84	N84-22753 *	NASA-CR-3749	.....	p 148	N84-14525 *
NASA-CR-168232	.....	p 98	N84-16424 *	NASA-CR-173503	.....	p 127	N84-23854 *	NASA-CR-3750	.....	p 148	N84-14526 *
NASA-CR-168233	.....	p 81	N84-13310 *	NASA-CR-173511	.....	p 159	N84-27258 *	NASA-CR-3756	.....	p 149	N84-15565 *
NASA-CR-168234-VOL-1	.....	p 185	N84-33148 *	NASA-CR-173514	.....	p 127	N84-25001 *	NASA-CR-3757	.....	p 188	N84-16984 *
NASA-CR-168234-VOL-2	.....	p 186	N84-33149 *	NASA-CR-173515	.....	p 99	N84-24918 *	NASA-CR-3758	.....	p 185	N84-29661 *
NASA-CR-168234-VOL-3	.....	p 186	N84-33150 *	NASA-CR-173532	.....	p 38	N84-23662 *	NASA-CR-3769	.....	p 123	N84-16488 *
NASA-CR-168235	.....	p 141	N84-15554 *	NASA-CR-173534	.....	p 99	N84-23807 *	NASA-CR-3770	.....	p 149	N84-17606 *
NASA-CR-168236	.....	p 97	N84-14378 *	NASA-CR-173548	.....	p 99	N84-24924 *	NASA-CR-3789	.....	p 183	N84-21275 *
NASA-CR-168237	.....	p 97	N84-14377 *	NASA-CR-173550	.....	p 85	N84-24810 *	NASA-CR-3790	.....	p 155	N84-19925 *
NASA-CR-168238	.....	p 97	N84-14378 *	NASA-CR-173552	.....	p 176	N84-25336 *	NASA-CR-3792	.....	p 127	N84-25941 *
NASA-CR-168239	.....	p 164	N84-13673 *	NASA-CR-173554	.....	p 169	N84-25168 *	NASA-CR-3793	.....	p 145	N84-26027 *
NASA-CR-168240	.....	p 107	N84-17477 *	NASA-CR-173555	.....	p 32	N84-24586 *	NASA-CR-3803	.....	p 184	N84-26384 *
NASA-CR-168242	.....	p 91	N84-27909 *	NASA-CR-173557	.....	p 110	N84-24975 *	NASA-CR-3804	.....	p 127	N84-25943 *
NASA-CR-168243-VOL-2	.....	p 60	N84-12265 *	NASA-CR-173560	.....	p 110	N84-24974 *	NASA-CR-3832	.....	p 36	N84-33412 *
NASA-CR-168244	.....	p 111	N84-31514 *	NASA-CR-173622	.....	p 185	N84-27544 *	NASA-CR-3833	.....	p 11	N84-32355 *
NASA-CR-168247	.....	p 12	N84-11152 *	NASA-CR-173778	.....	p 128	N84-29155 *				
NASA-CR-168248	.....	p 37	N84-10109 *	NASA-CR-173820	.....	p 100	N84-30145 *	NASA-RP-1123	.....	p 145	N84-27041 *
NASA-CR-168251	.....	p 81	N84-12312 *	NASA-CR-173821	.....	p 157	N84-29252 *	NASA-RP-1126	.....	p 147	N84-31640 *
NASA-CR-168252	.....	p 124	N84-17530 *	NASA-CR-173830	.....	p 157	N84-31685 *				
NASA-CR-168253	.....	p 109	N84-24973 *	NASA-CR-173868	.....	p 111	N84-32678 *	NASA-TM-81401	.....	p 173	N84-34038 *
NASA-CR-168254	.....	p 97	N84-13398 *	NASA-CR-173884	.....	p 35	N84-32389 *	NASA-TM-81733	.....	p 193	N84-22488 *
NASA-CR-168255	.....	p 196	N84-33304 *	NASA-CR-173888	.....	p 191	N84-33210 *	NASA-TM-82742	.....	p 174	N84-18806 *
NASA-CR-168256	.....	p 196	N84-32306 *	NASA-CR-173907	.....	p 111	N84-32682 *	NASA-TM-83061	.....	p 187	N84-10923 *
NASA-CR-168257	.....	p 196	N84-32307 *	NASA-CR-173916	.....	p 101	N84-32645 *	NASA-TM-83381	.....	p 96	N84-11358 *
NASA-CR-168258	.....	p 22	N84-13186 *	NASA-CR-173981	.....	p 112	N84-34675 *	NASA-TM-83403	.....	p 164	N84-10665 *
NASA-CR-168260	.....	p 87	N84-13265 *	NASA-CR-174503	.....	p 165	N84-15681 *	NASA-TM-83415	.....	p 97	N84-11360 *
NASA-CR-168261	.....	p 46	N84-19472 *	NASA-CR-174504	.....	p 154	N84-15589 *	NASA-TM-83446	.....	p 26	N84-16185 *
NASA-CR-168262	.....	p 106	N84-11388 *	NASA-CR-174533	.....	p 95	N84-10401 *	NASA-TM-83449	.....	p 81	N84-10310 *
NASA-CR-168266	.....	p 45	N84-12227 *	NASA-CR-174534	.....	p 66	N84-10267 *	NASA-TM-83460	.....	p 164	N84-13670 *
NASA-CR-168267-VOL-1	.....	p 132	N84-16529 *	NASA-CR-174602	.....	p 60	N84-1				



NASA-TM-83478	p 153	N84-11512 * #	NASA-TM-83595	p 69	N84-17353 * #	NASA-TM-83707	p 51	N84-25766 * #
NASA-TM-83479	p 70	N84-17355 * #	NASA-TM-83596	p 83	N84-19567 * #	NASA-TM-83708	p 32	N84-25713 * #
NASA-TM-83481	p 178	N84-11831 * #	NASA-TM-83598	p 47	N84-23691 * #	NASA-TM-83709	p 2	N84-25605 * #
NASA-TM-83483	p 183	N84-10664 * #	NASA-TM-83599	p 71	N84-21719 * #	NASA-TM-83710	p 2	N84-25607 * #
NASA-TM-83486	p 68	N84-14288 * #	NASA-TM-83600	p 191	N84-20404 * #	NASA-TM-83712	p 145	N84-27043 * #
NASA-TM-83488	p 123	N84-16492 * #	NASA-TM-83601	p 46	N84-20639 * #	NASA-TM-83713	p 145	N84-27042 * #
NASA-TM-83489	p 45	N84-11206 * #	NASA-TM-83602	p 190	N84-21329 * #	NASA-TM-83714	p 73	N84-26787 * #
NASA-TM-83490	p 24	N84-14145 * #	NASA-TM-83603	p 190	N84-21330 * #	NASA-TM-83715	p 47	N84-25764 * #
NASA-TM-83492	p 67	N84-12287 * #	NASA-TM-83604	p 143	N84-20658 * #	NASA-TM-83716	p 2	N84-25606 * #
NASA-TM-83495	p 154	N84-13610 * #	NASA-TM-83605	p 177	N84-20258 * #	NASA-TM-83717	p 73	N84-27857 * #
NASA-TM-83497	p 166	N84-20016 * #	NASA-TM-83606	p 177	N84-20259 * #	NASA-TM-83718	p 87	N84-28994 * #
NASA-TM-83502	p 182	N84-11883 * #	NASA-TM-83608	p 145	N84-26029 * #	NASA-TM-83719	p 86	N84-27887 * #
NASA-TM-83503	p 182	N84-13922 * #	NASA-TM-83609	p 74	N84-28962 * #	NASA-TM-83721	p 146	N84-28087 * #
NASA-TM-83504	p 166	N84-20017 * #	NASA-TM-83610	p 54	N84-21666 * #	NASA-TM-83722	p 156	N84-29248 * #
NASA-TM-83506	p 68	N84-15249 * #	NASA-TM-83611	p 126	N84-22910 * #	NASA-TM-83723	p 146	N84-29224 * #
NASA-TM-83507	p 154	N84-14541 * #	NASA-TM-83612	p 167	N84-20916 * #	NASA-TM-83724	p 146	N84-28088 * #
NASA-TM-83508	p 22	N84-12166 * #	NASA-TM-83613	p 126	N84-21632 * #	NASA-TM-83725	p 146	N84-29223 * #
NASA-TM-83509	p 154	N84-14542 * #	NASA-TM-83614	p 126	N84-22911 * #	NASA-TM-83726	p 147	N84-30294 * #
NASA-TM-83510	p 175	N84-12730 * #	NASA-TM-83616	p 184	N84-23235 * #	NASA-TM-83727	p 87	N84-30072 * #
NASA-TM-83512	p 81	N84-11295 * #	NASA-TM-83617	p 126	N84-22909 * #	NASA-TM-83728	p 48	N84-27824 * #
NASA-TM-83513	p 131	N84-11456 * #	NASA-TM-83618	p 168	N84-23026 * #	NASA-TM-83729	p 57	N84-31288 * #
NASA-TM-83514	p 191	N84-14932 * #	NASA-TM-83619	p 144	N84-25064 * #	NASA-TM-83730	p 34	N84-28790 * #
NASA-TM-83515	p 183	N84-16946 * #	NASA-TM-83620	p 188	N84-22421 * #	NASA-TM-83731	p 128	N84-30223 * #
NASA-TM-83516	p 96	N84-10405 * #	NASA-TM-83622	p 86	N84-28990 * #	NASA-TM-83732	p 128	N84-29157 * #
NASA-TM-83518	p 97	N84-13399 * #	NASA-TM-83623	p 73	N84-26785 * #	NASA-TM-83733	p 2	N84-32344 * #
NASA-TM-83519	p 8	N84-14120 * #	NASA-TM-83624	p 47	N84-25762 * #	NASA-TM-83734	p 129	N84-30224 * #
NASA-TM-83520	p 183	N84-20320 * #	NASA-TM-83625	p 110	N84-25926 * #	NASA-TM-83735	p 157	N84-30329 * #
NASA-TM-83522	p 98	N84-19640 * #	NASA-TM-83628	p 83	N84-21739 * #	NASA-TM-83736	p 35	N84-29878 * #
NASA-TM-83523	p 141	N84-11500 * #	NASA-TM-83629	p 84	N84-24803 * #	NASA-TM-83737	p 157	N84-31683 * #
NASA-TM-83524	p 141	N84-11498 * #	NASA-TM-83630	p 132	N84-21849 * #	NASA-TM-83738	p 75	N84-31344 * #
NASA-TM-83525	p 182	N84-13924 * #	NASA-TM-83631	p 55	N84-22702 * #	NASA-TM-83739	p 11	N84-32357 * #
NASA-TM-83526	p 123	N84-16493 * #	NASA-TM-83632	p 57	N84-28917 * #	NASA-TM-83740	p 147	N84-30293 * #
NASA-TM-83528	p 67	N84-13264 * #	NASA-TM-83633	p 99	N84-25908 * #	NASA-TM-83741	p 34	N84-29876 * #
NASA-TM-83529	p 81	N84-11296 * #	NASA-TM-83634	p 156	N84-23923 * #	NASA-TM-83743	p 110	N84-31512 * #
NASA-TM-83530	p 41	N84-18310 * #	NASA-TM-83635	p 10	N84-22533 * #	NASA-TM-83744	p 185	N84-32118 * #
NASA-TM-83531	p 97	N84-13400 * #	NASA-TM-83636	p 1	N84-22527 * #	NASA-TM-83745	p 100	N84-31460 * #
NASA-TM-83532	p 165	N84-14586 * #	NASA-TM-83637	p 29	N84-22565 * #	NASA-TM-83746	p 88	N84-34620 * #
NASA-TM-83533	p 67	N84-11254 * #	NASA-TM-83638	p 47	N84-22631 * #	NASA-TM-83749	p 100	N84-30147 * #
NASA-TM-83534	p 8	N84-14121 * #	NASA-TM-83639	p 29	N84-22566 * #	NASA-TM-83751	p 129	N84-31558 * #
NASA-TM-83535	p 68	N84-15246 * #	NASA-TM-83640	p 29	N84-22564 * #	NASA-TM-83753	p 134	N84-30273 * #
NASA-TM-83536	p 141	N84-14519 * #	NASA-TM-83641	p 31	N84-24581 * #	NASA-TM-83755	p 110	N84-31513 * #
NASA-TM-83537	p 123	N84-16494 * #	NASA-TM-83643	p 168	N84-23025 * #	NASA-TM-83756	p 157	N84-31687 * #
NASA-TM-83538	p 23	N84-13188 * #	NASA-TM-83644	p 47	N84-23690 * #	NASA-TM-83757	p 51	N84-31283 * #
NASA-TM-83539	p 155	N84-16589 * #	NASA-TM-83646	p 109	N84-22890 * #	NASA-TM-83758	p 10	N84-31091 * #
NASA-TM-83540	p 193	N84-14081 * #	NASA-TM-83647	p 168	N84-23024 * #	NASA-TM-83759	p 100	N84-30146 * #
NASA-TM-83541	p 24	N84-14146 * #	NASA-TM-83648	p 42	N84-22615 * #	NASA-TM-83760	p 185	N84-32122 * #
NASA-TM-83542	p 1	N84-14111 * #	NASA-TM-83649	p 195	N84-22512 * #	NASA-TM-83761	p 63	N84-33536 * #
NASA-TM-83543	p 173	N84-11594 * #	NASA-TM-83650	p 195	N84-24509 * #	NASA-TM-83762	p 76	N84-32508 * #
NASA-TM-83544	p 26	N84-16186 * #	NASA-TM-83651	p 167	N84-23022 * #	NASA-TM-83764	p 185	N84-34230 * #
NASA-TM-83545	p 176	N84-13812 * #	NASA-TM-83652	p 109	N84-22891 * #	NASA-TM-83765	p 36	N84-33414 * #
NASA-TM-83546	p 169	N84-27327 * #	NASA-TM-83653	p 62	N84-22712 * #	NASA-TM-83766	p 189	N84-32169 * #
NASA-TM-83547	p 154	N84-16587 * #	NASA-TM-83655	p 32	N84-24589 * #	NASA-TM-83768	p 49	N84-32427 * #
NASA-TM-83548	p 122	N84-13494 * #	NASA-TM-83656	p 109	N84-22892 * #	NASA-TM-83769	p 77	N84-33564 * #
NASA-TM-83549	p 154	N84-16588 * #	NASA-TM-83657	p 169	N84-25166 * #	NASA-TM-83770	p 49	N84-31272 * #
NASA-TM-83550	p 176	N84-16812 * #	NASA-TM-83658	p 133	N84-25019 * #	NASA-TM-83772	p 10	N84-31096 * #
NASA-TM-83551	p 68	N84-14289 * #	NASA-TM-83659	p 75	N84-28963 * #	NASA-TM-83773	p 92	N84-33608 * #
NASA-TM-83552	p 38	N84-16234 * #	NASA-TM-83660	p 32	N84-25712 * #	NASA-TM-83774	p 100	N84-31461 * #
NASA-TM-83553	p 1	N84-13140 * #	NASA-TM-83661	p 50	N84-23693 * #	NASA-TM-83775	p 101	N84-32644 * #
NASA-TM-83554	p 24	N84-14147 * #	NASA-TM-83662	p 100	N84-27954 * #	NASA-TM-83777	p 75	N84-31347 * #
NASA-TM-83555	p 9	N84-17143 * #	NASA-TM-83663	p 72	N84-24772 * #	NASA-TM-83778	p 75	N84-31348 * #
NASA-TM-83557	p 123	N84-14463 * #	NASA-TM-83664	p 167	N84-23023 * #	NASA-TM-83779	p 87	N84-32531 * #
NASA-TM-83558	p 23	N84-13190 * #	NASA-TM-83665	p 75	N84-31345 * #	NASA-TM-83780	p 11	N84-32351 * #
NASA-TM-83559	p 179	N84-17982 * #	NASA-TM-83666	p 127	N84-24999 * #	NASA-TM-83781	p 133	N84-32783 * #
NASA-TM-83560	p 69	N84-16311 * #	NASA-TM-83667	p 168	N84-23027 * #	NASA-TM-83782	p 77	N84-34603 * #
NASA-TM-83561	p 26	N84-16184 * #	NASA-TM-83668	p 31	N84-24583 * #	NASA-TM-83785	p 133	N84-32789 * #
NASA-TM-83562	p 9	N84-20490 * #	NASA-TM-83669	p 10	N84-25647 * #	NASA-TM-83786	p 57	N84-33522 * #
NASA-TM-83563	p 70	N84-17354 * #	NASA-TM-83670	p 85	N84-25830 * #	NASA-TM-83788	p 149	N84-32849 * #
NASA-TM-83564	p 14	N84-13173 * #	NASA-TM-83671	p 186	N84-34231 * #	NASA-TM-83789	p 101	N84-33642 * #
NASA-TM-83565	p 92	N84-16380 * #	NASA-TM-83672	p 74	N84-27858 * #	NASA-TM-83792	p 88	N84-34619 * #
NASA-TM-83566	p 69	N84-17351 * #	NASA-TM-83673	p 74	N84-27859 * #	NASA-TM-83794	p 149	N84-34769 * #
NASA-TM-83568	p 37	N84-16229 * #	NASA-TM-83674	p 48	N84-27825 * #	NASA-TM-83795	p 38	N84-32411 * #
NASA-TM-83569	p 14	N84-29870 * #	NASA-TM-83675	p 156	N84-29247 * #	NASA-TM-83799	p 186	N84-35085 * #
NASA-TM-83570	p 142	N84-17591 * #	NASA-TM-83676	p 73	N84-25793 * #	NASA-TM-83802	p 58	N84-34576 * #
NASA-TM-83571	p 8	N84-16142 * #	NASA-TM-83679	p 30	N84-23648 * #	NASA-TM-85487	p 37	N84-15164 * #
NASA-TM-83572	p 69	N84-17352 * #	NASA-TM-83680	p 171	N84-29347 * #	NASA-TM-85492	p 192	N84-16021 * #
NASA-TM-83574	p 85	N84-25831 * #	NASA-TM-83681	p 132	N84-25017 * #	NASA-TM-85493	p 192	N84-16020 * #
NASA-TM-83575	p 9	N84-17142 * #	NASA-TM-83682	p 31	N84-24584 * #	NASA-TM-85527	p 100	N84-25909 * #
NASA-TM-83576	p 8	N84-16141 * #	NASA-TM-83684	p 172	N84-31782 * #	NASA-TM-85594	p 93	N84-22771 * #
NASA-TM-83577	p 155	N84-18683 * #	NASA-TM-83686	p 31	N84-24582 * #	NASA-TM-86861	p 172	N84-30528 * #
NASA-TM-83578	p 142	N84-17592 * #	NASA-TM-83687	p 47	N84-24708 * #	NASA-TM-86862	p 87	N84-32536 * #
NASA-TM-83579	p 28	N84-21548 * #	NASA-TM-83688	p 39	N84-25753 * #	NASA-TM-86873	p 197	N84-34330 * #
NASA-TM-83580	p 70	N84-20672 * #	NASA-TM-83689	p 30	N84-24579 * #			
NASA-TM-83581	p 107	N84-17479 * #	NASA-TM-83690	p 48	N84-26746 * #	NASA-TP-2052	p 34	N84-28795 * #
NASA-TM-83582	p 132	N84-19787 * #	NASA-TM-83691	p 57	N84-28918 * #	NASA-TP-2193	p 178	N84-13885 * #
NASA-TM-83583	p 71	N84-20673 * #	NASA-TM-83692	p 133	N84-28010 * #	NASA-TP-2220	p 142	N84-17590 * #
NASA-TM-83584	p 108	N84-19708 * #	NASA-TM-83694	p 56	N84-25770 * #	NASA-TP-2221	p 178	N84-16843 * #
NASA-TM-83585	p 82	N84-19586 * #	NASA-TM-83695	p 31	N84-24585 * #	NASA-TP-2225	p 124	N84-19741 * #
NASA-TM-83586	p 124	N84-17533 * #	NASA-TM-83696	p 56	N84-27832 * #	NASA-TP-2231	p 22	N84-11171 * #
NASA-TM-83587	p 184	N84-26383 * #	NASA-TM-83697	p 10	N84-24539 * #	NASA-TP-2232	p 126	N84-21828 * #
NASA-TM-83588	p 9	N84-17138 * #	NASA-TM-83699	p 34	N84-28791 * #	NASA-TP-2237	p 183	N84-19049 * #
NASA-TM-83589	p 1	N84-16119 * #	NASA-TM-83700	p 56	N84-26755 * #	NASA-TP-2238	p 107	N84-16461 * #
NASA-TM-83590	p 108	N84-21803 * #	NASA-TM-83701	p 56	N84-27831 * #	NASA-TP-2239	p 54	N84-13224 * #
NASA-TM-83591	p 99	N84-19641 * #	NASA-TM-83702	p 56	N84-26756 * #	NASA-TP-2240	p 40	N84-16247 * #
NASA-TM-83592	p 142	N84-19816 * #	NASA-TM-83703	p 127	N84-25000 * #	NASA-TP-2243	p 155	N84-20878 * #
NASA-TM-83593	p 195	N84-26484 * #	NASA-TM-83704	p 128	N84-25946 * #	NASA-TP-2248	p 106	N84-15394 * #
NASA-TM-83594	p 55	N84-24712 * #	NASA-TM-83706	p 85	N84-26803 * #	NASA-TP-2257	p 141	N84-13577 * #



NASA-TP-2259	p 183	N84-15894 *	#	R84AEB422	p 72	N84-24774 *	#	US-PATENT-CLASS-118-641	p 134	N84-22944 *	#
NASA-TP-2266	p 25	N84-16181 *	#	SAE PAPER 831438	p 13	A84-29452 *	#	US-PATENT-CLASS-156-630	p 132	N84-22930 *	#
NASA-TP-2267	p 82	N84-16334 *	#	SAE PAPER 831439	p 13	A84-29453 *	#	US-PATENT-CLASS-156-644	p 174	N84-23095 *	#
NASA-TP-2268	p 123	N84-17525 *	#	SAE PAPER 831517	p 17	A84-29460 *	#	US-PATENT-CLASS-156-654	p 132	N84-22930 *	#
NASA-TP-2274	p 142	N84-18653 *	#	SAPR-7	p 195	N84-29805 *	#	US-PATENT-CLASS-156-668	p 174	N84-23095 *	#
NASA-TP-2275	p 142	N84-18654 *	#	SAR-2	p 99	N84-23807 *	#	US-PATENT-CLASS-156-905	p 132	N84-22930 *	#
NASA-TP-2278	p 70	N84-18370 *	#	SAR-3	p 165	N84-15681 *	#	US-PATENT-CLASS-204-192C	p 54	N84-22695 *	#
NASA-TP-2279	p 82	N84-18399 *	#	SAR-5	p 140	N84-10581 *	#	US-PATENT-CLASS-204-192E	p 174	N84-23095 *	#
NASA-TP-2280	p 69	N84-17350 *	#	SAR-7	p 146	N84-28089 *	#	US-PATENT-CLASS-204-192R	p 54	N84-22695 *	#
NASA-TP-2285	p 82	N84-18400 *	#	SASR-5	p 35	N84-32389 *	#	US-PATENT-CLASS-204-192SP	p 54	N84-22695 *	#
NASA-TP-2286	p 83	N84-21740 *	#	SM-8	p 154	N84-15589 *	#	US-PATENT-CLASS-204-290	p 170	N84-28205 *	#
NASA-TP-2289	p 71	N84-21716 *	#	SN-1020-A2-F	p 60	N84-11229 *	#	US-PATENT-CLASS-228-165	p 132	N84-22930 *	#
NASA-TP-2290	p 72	N84-21721 *	#	SN-1021-F	p 60	N84-11228 *	#	US-PATENT-CLASS-252-182.1	p 106	N84-14422 *	#
NASA-TP-2294	p 28	N84-21549 *	#	SR83-R-4663-30	p 23	N84-14143 *	#	US-PATENT-CLASS-29-623 5	p 72	N84-22734 *	#
NASA-TP-2296	p 27	N84-20562 *	#	SWRI-6682/2	p 89	N84-13332 *	#	US-PATENT-CLASS-29-623 5	p 170	N84-28205 *	#
NASA-TP-2296	p 27	N84-20562 *	#	SWRI-6948	p 74	N84-28960 *	#	US-PATENT-CLASS-29-825	p 170	N84-28205 *	#
NASA-TP-2297	p 9	N84-20493 *	#	TELEDYNE-CAE-1987	p 29	N84-22568 *	#	US-PATENT-CLASS-313-106	p 179	N84-28565 *	#
NASA-TP-2301	p 50	N84-20643 *	#	TE4322-251-83	p 196	N84-32306 *	#	US-PATENT-CLASS-313-107	p 179	N84-28565 *	#
NASA-TP-2302	p 51	N84-26749 *	#	TI-08-83-42	p 107	N84-16463 *	#	US-PATENT-CLASS-313-351	p 179	N84-28565 *	#
NASA-TP-2303	p 174	N84-31865 *	#	TRW-37243-EXEC-SUM	p 167	N84-23021 *	#	US-PATENT-CLASS-315-3 5	p 106	N84-16452 *	#
NASA-TP-2304	p 30	N84-24578 *	#	TRW-38603-6009-UT-00	p 148	N84-32828 *	#	US-PATENT-CLASS-315-3 6	p 106	N84-16452 *	#
NASA-TP-2309	p 35	N84-32388 *	#	TRW-38884-6001-UT-00	p 37	N84-10109 *	#	US-PATENT-CLASS-315-39 3	p 106	N84-16452 *	#
NASA-TP-2316	p 84	N84-23764 *	#	U-OF-IOWA-84-5	p 173	N84-25204 *	#	US-PATENT-CLASS-315-39 3	p 110	N84-27974 *	#
NASA-TP-2317	p 90	N84-23774 *	#	UDR-TR-83-57	p 152	N84-10612 *	#	US-PATENT-CLASS-315-5 38	p 179	N84-28565 *	#
NASA-TP-2319	p 74	N84-28958 *	#	UILU-ENG-84-2547	p 100	N84-25909 *	#	US-PATENT-CLASS-323-901	p 111	N84-33663 *	#
NASA-TP-2320	p 63	N84-32446 *	#	UILU-ENG-84-2552	p 100	N84-30145 *	#	US-PATENT-CLASS-331-82	p 110	N84-27974 *	#
NASA-TP-2338	p 73	N84-26783 *	#	US-PATENT-APPL-SN-136652	p 30	N84-24577 *	#	US-PATENT-CLASS-333-162	p 106	N84-16452 *	#
NASA-TP-2339	p 76	N84-31349 *	#	US-PATENT-APPL-SN-157150	p 148	N84-33808 *	#	US-PATENT-CLASS-333-162	p 110	N84-27974 *	#
NASA-TP-2342	p 86	N84-28989 *	#	US-PATENT-APPL-SN-229693	p 143	N84-22958 *	#	US-PATENT-CLASS-363-22	p 111	N84-33663 *	#
NASA-TP-2354	p 75	N84-28965 *	#	US-PATENT-APPL-SN-238257	p 35	N84-33410 *	#	US-PATENT-CLASS-363-49	p 111	N84-33663 *	#
NASA-TP-2355	p 146	N84-29226 *	#	US-PATENT-APPL-SN-242795	p 143	N84-22957 *	#	US-PATENT-CLASS-364-558	p 28	N84-22559 *	#
NASA-TP-2360	p 87	N84-31379 *	#	US-PATENT-APPL-SN-245571	p 28	N84-22560 *	#	US-PATENT-CLASS-415-115	p 35	N84-33410 *	#
NASA-TP-2361	p 42	N84-33452 *	#	US-PATENT-APPL-SN-251009	p 106	N84-16452 *	#	US-PATENT-CLASS-415-174	p 143	N84-22957 *	#
NASA-TP-2362	p 88	N84-33590 *	#	US-PATENT-APPL-SN-264378	p 179	N84-28565 *	#	US-PATENT-CLASS-416-224	p 28	N84-22560 *	#
NASA-TP-2367	p 147	N84-32824 *	#	US-PATENT-APPL-SN-272406	p 106	N84-14422 *	#	US-PATENT-CLASS-416-233	p 28	N84-22560 *	#
NASA-TP-2368	p 147	N84-32825 *	#	US-PATENT-APPL-SN-350473	p 28	N84-22559 *	#	US-PATENT-CLASS-416-241R	p 77	N84-33555 *	#
NASA/DOE/20320-56	p 165	N84-14586 *	#	US-PATENT-APPL-SN-350476	p 72	N84-22734 *	#	US-PATENT-CLASS-416-92	p 28	N84-22560 *	#
NASA/DOE/51040-49	p 194	N84-14989 *	#	US-PATENT-APPL-SN-352821	p 170	N84-28205 *	#	US-PATENT-CLASS-416-97R	p 28	N84-22560 *	#
NAUFP-202-2	p 155	N84-19927 *	#	US-PATENT-APPL-SN-358398	p 134	N84-22944 *	#	US-PATENT-CLASS-423-DIG.10	p 54	N84-22695 *	#
OAI-1512-11-83	p 46	N84-19472 *	#	US-PATENT-APPL-SN-364072	p 179	N84-28565 *	#	US-PATENT-CLASS-423-414	p 54	N84-22695 *	#
P-120	p 143	N84-21877 *	#	US-PATENT-APPL-SN-368188	p 111	N84-33663 *	#	US-PATENT-CLASS-423-445	p 54	N84-22695 *	#
PWA-5574-175-VOL-1	p 76	N84-32504 *	#	US-PATENT-APPL-SN-393589	p 60	N84-16276 *	#	US-PATENT-CLASS-423-446	p 54	N84-22695 *	#
PWA-5594-142	p 35	N84-32389 *	#	US-PATENT-APPL-SN-403378	p 77	N84-33555 *	#	US-PATENT-CLASS-423-446	p 54	N84-22695 *	#
PWA-5594-152	p 33	N84-27739 *	#	US-PATENT-APPL-SN-404809	p 86	N84-27885 *	#	US-PATENT-CLASS-427-113	p 170	N84-28205 *	#
PWA-5594-165	p 33	N84-27737 *	#	US-PATENT-APPL-SN-418139	p 56	N84-27829 *	#	US-PATENT-CLASS-427-115	p 72	N84-22734 *	#
PWA-5594-167	p 33	N84-27738 *	#	US-PATENT-APPL-SN-425203	p 132	N84-22930 *	#	US-PATENT-CLASS-427-115	p 170	N84-28205 *	#
PWA-5594-171	p 33	N84-28788 *	#	US-PATENT-APPL-SN-431448	p 143	N84-22957 *	#	US-PATENT-CLASS-427-125	p 72	N84-22734 *	#
PWA-5594-191	p 33	N84-28789 *	#	US-PATENT-APPL-SN-434084	p 110	N84-27974 *	#	US-PATENT-CLASS-427-125	p 170	N84-28205 *	#
PWA-5697-65	p 89	N84-10332 *	#	US-PATENT-APPL-SN-444124	p 174	N84-23095 *	#	US-PATENT-CLASS-427-126 6	p 72	N84-22734 *	#
PWA-5777-29	p 81	N84-12312 *	#	US-PATENT-APPL-SN-458460	p 73	N84-27855 *	#	US-PATENT-CLASS-427-226	p 170	N84-28205 *	#
PWA-5777-30	p 82	N84-16337 *	#	US-PATENT-APPL-SN-458460	p 73	N84-27855 *	#	US-PATENT-CLASS-427-286	p 72	N84-22734 *	#
PWA-5833-37	p 145	N84-25065 *	#	US-PATENT-APPL-SN-495381	p 54	N84-22695 *	#	US-PATENT-CLASS-427-306	p 72	N84-22734 *	#
PWA-5896-21	p 27	N84-19353 *	#	US-PATENT-APPL-SN-537614	p 106	N84-11389 *	#	US-PATENT-CLASS-427-34	p 143	N84-22957 *	#
PWA-5914-21	p 134	N84-32790 *	#	US-PATENT-APPL-SN-537615	p 131	N84-12447 *	#	US-PATENT-CLASS-427-372.2	p 170	N84-28205 *	#
PWA/GPD-FR-17145-VOL-1	p 132	N84-16529 *	#	US-PATENT-APPL-SN-560035	p 54	N84-15203 *	#	US-PATENT-CLASS-427-379	p 170	N84-28205 *	#
PWA/GPD-FR-17826	p 29	N84-23629 *	#	US-PATENT-APPL-SN-561429	p 55	N84-22699 *	#	US-PATENT-CLASS-427-380	p 170	N84-28205 *	#
QR-10	p 164	N84-13672 *	#	US-PATENT-APPL-SN-561431	p 55	N84-22698 *	#	US-PATENT-CLASS-427-399	p 134	N84-22944 *	#
QR-12	p 170	N84-27329 *	#	US-PATENT-APPL-SN-561434	p 55	N84-22701 *	#	US-PATENT-CLASS-427-405	p 73	N84-27855 *	#
QR-7	p 164	N84-11581 *	#	US-PATENT-APPL-SN-561435	p 55	N84-22700 *	#	US-PATENT-CLASS-427-410 2	p 73	N84-27855 *	#
QR-9	p 164	N84-13673 *	#	US-PATENT-APPL-SN-571617	p 54	N84-16266 *	#	US-PATENT-CLASS-427-423	p 143	N84-22957 *	#
REPT-020547-IR-1	p 127	N84-23854 *	#	US-PATENT-APPL-SN-580419	p 126	N84-20782 *	#	US-PATENT-CLASS-427-443	p 170	N84-28205 *	#
REPT-11982	p 109	N84-24973 *	#	US-PATENT-APPL-SN-580573	p 167	N84-20918 *	#	US-PATENT-CLASS-427-53 1	p 134	N84-22944 *	#
REPT-274	p 32	N84-25710 *	#	US-PATENT-APPL-SN-591089	p 54	N84-22696 *	#	US-PATENT-CLASS-427-53 1	p 143	N84-22957 *	#
REPT-38945-6012-UT-00	p 87	N84-28995 *	#	US-PATENT-APPL-SN-596960	p 29	N84-22562 *	#	US-PATENT-CLASS-428-155	p 143	N84-22957 *	#
REPT-41763-6001-UT-00	p 39	N84-23667 *	#	US-PATENT-APPL-SN-602050	p 29	N84-22563 *	#	US-PATENT-CLASS-428-632	p 77	N84-33555 *	#
REPT-83-47	p 7	N84-10022 *	#	US-PATENT-APPL-SN-603374	p 143	N84-22959 *	#	US-PATENT-CLASS-428-678	p 77	N84-33555 *	#
REPT-83-9FS-ATRA-NR1	p 106	N84-11388 *	#	US-PATENT-APPL-SN-608742	p 55	N84-24711 *	#	US-PATENT-CLASS-429-206	p 106	N84-14422 *	#
REPT-83-9F5-DISQR-R1	p 108	N84-18536 *	#	US-PATENT-APPL-SN-625077	p 110	N84-29084 *	#	US-PATENT-CLASS-429-223	p 72	N84-22734 *	#
REPT-84-R-958	p 50	N84-33462 *	#	US-PATENT-APPL-SN-628866	p 86	N84-28988 *	#	US-PATENT-CLASS-429-229	p 106	N84-14422 *	#
REPT-84ASE369SA5	p 195	N84-32305 *	#	US-PATENT-APPL-SN-636463	p 49	N84-32425 *	#	US-PATENT-CLASS-429-234	p 72	N84-22734 *	#
RI/RD84-191	p 148	N84-33811 *	#	US-PATENT-APPL-SN-638541	p 133	N84-32782 *	#	US-PATENT-CLASS-429-244	p 170	N84-28205 *	#
R81-915395-12	p 195	N84-21445 *	#	US-PATENT-APPL-SN-640712	p 88	N84-33595 *	#	US-PATENT-CLASS-431-1	p 60	N84-16276 *	#
R81AEG282	p 36	N84-33417 *	#	US-PATENT-APPL-SN-642310	p 172	N84-32909 *	#	US-PATENT-CLASS-526-262	p 86	N84-27885 *	#
R82AEB491-VOL-1	p 185	N84-33148 *	#	US-PATENT-CLASS-101-395	p 132	N84-22930 *	#	US-PATENT-CLASS-528-322	p 86	N84-27885 *	#
R82AEB491-VOL-2	p 186	N84-33149 *	#	US-PATENT-CLASS-110-186	p 60	N84-16276 *	#	US-PATENT-CLASS-528-342	p 86	N84-27885 *	#
R82AEB491-VOL-3	p 186	N84-33150 *	#	US-PATENT-CLASS-110-262	p 60	N84-16276 *	#	US-PATENT-CLASS-60-303	p 148	N84-33808 *	#
R82AEB494	p 185	N84-29661 *	#	US-PATENT-CLASS-110-263	p 60	N84-16276 *	#	US-PATENT-CLASS-60-39 29	p 35	N84-33410 *	#
R82AEB532	p 22	N84-11170 *	#	US-PATENT-CLASS-110-265	p 60	N84-16276 *	#	US-PATENT-CLASS-60-606	p 148	N84-33808 *	#
R83-900011-F	p 122	N84-14462 *	#	US-PATENT-CLASS-118-50.1	p 134	N84-22944 *	#	US-PATENT-CLASS-60-730	p 143	N84-22958 *	#
R83-915540-26	p 124	N84-17530 *	#	US-PATENT-CLASS-118-624	p 134	N84-22944 *	#	US-PATENT-CLASS-73-757	p 30	N84-24577 *	#
R83-956077-1	p 153	N84-10613 *	#	US-PATENT-CLASS-101-395	p 132	N84-22930 *	#	US-PATENT-CLASS-73-115	p 28	N84-22559 *	#
R83-956077-2	p 153	N84-10614 *	#	US-PATENT-CLASS-110-186	p 60	N84-16276 *	#	US-PATENT-CLASS-73-833	p 56	N84-27829 *	#
R83-956152-10	p 45	N84-12225 *	#	US-PATENT-CLASS-110-262	p 60	N84-16276 *	#	US-PATENT-CLASS-73-856	p 56	N84-27829 *	#
R83AEB358-VOL-1	p 184	N84-24323 *	#	US-PATENT-CLASS-110-263	p 60	N84-16276 *	#	US-PATENT-4,349,424	p 179	N84-28565 *	#
R83AEB358-VOL-2	p 184	N84-24324 *	#	US-PATENT-CLASS-110-265	p 60	N84-16276 *	#	US-PATENT-4,377,371	p 143	N84-22957 *	#
R84-956393-8	p 11	N84-32355 *	#	US-PATENT-CLASS-118-50.1	p 134	N84-22944 *	#	US-PATENT-4,411,597	p 28	N84-22580 *	#
R84AEB012	p 31	N84-24580 *	#	US-PATENT-CLASS-118-624	p 134	N84-22944 *	#	US-PATENT-4,414,816	p 30	N84-24577 *	#
								US-PATENT-4,416,111	p 35	N84-33410 *	#

## REPORT NUMBER INDEX

W-R/D-83-9C1-LK00L-R1

US-PATENT-4,417,175	p 179	N84-28565 * #
US-PATENT-4,418,130	p 106	N84-14422 * #
US-PATENT-4,422,012	p 106	N84-16452 * #
US-PATENT-4,425,854	p 60	N84-16276 * #
US-PATENT-4,428,226	p 28	N84-22559 * #
US-PATENT-4,429,537	p 143	N84-22958 * #
US-PATENT-4,430,360	p 143	N84-22957 * #
US-PATENT-4,432,853	p 174	N84-23095 * #
US-PATENT-4,434,189	p 134	N84-22944 * #
US-PATENT-4,437,923	p 132	N84-22930 * #
US-PATENT-4,437,962	p 54	N84-22695 * #
US-PATENT-4,439,465	p 72	N84-22734 * #
US-PATENT-4,446,199	p 77	N84-33555 * #
US-PATENT-4,449,370	p 148	N84-33808 * #
US-PATENT-4,451,496	p 73	N84-27855 * #
US-PATENT-4,452,088	p 56	N84-27829 * #
US-PATENT-4,454,649	p 170	N84-28205 * #
US-PATENT-4,455,418	p 86	N84-27885 * #
US-PATENT-4,459,562	p 110	N84-27974 * #
US-PATENT-4,464,710	p 111	N84-33663 * #
USAAVSCOM-TR-83-C-16	p 11	N84-32357 * #
USAAVSCOM-TR-84-C-10	p 147	N84-30294 * #
USAAVSCOM-TR-84-C-11	p 147	N84-30293 * #
USAAVSCOM-TR-84-C-13	p 36	N84-33414 * #
USAAVSCOM-TR-84-C-16	p 77	N84-33564 * #
USAAVSCOM-TR-84-C-1	p 10	N84-25647 * #
USAAVSCOM-TR-84-C-1	p 14	N84-29670 * #
USAAVSCOM-TR-84-C-8	p 2	N84-25606 * #
USAAVSCOM-TR-84-C-9	p 146	N84-29223 * #
UTRC-884-915908-29	p 89	N84-17407 * #
UTRC63-6	p 153	N84-12530 * #
UVA/52810/MAE84/101	p 141	N84-16562 * #
UVA/528219/EE84/102	p 36	N84-19360 * #
UVA/528219/EE84103	p 110	N84-24974 * #
W-R/D-83-9C1-LK00L-R1	p 134	N84-18620 * #

1 Report No. NASA TM-87012		2 Government Accession No.		3 Recipient's Catalog No.	
4 Title and Subtitle  Bibliography of Lewis Research Center Technical Publications Announced in 1984				5 Report Date May 1985	
				6 Performing Organization Code None	
7. Author(s)				8. Performing Organization Report No. E-2556	
				10. Work Unit No	
9 Performing Organization Name and Address National Aeronautics and Space Administration Lewis Research Center Cleveland, Ohio 44135				11. Contract or Grant No.	
				13 Type of Report and Period Covered Technical Memorandum	
12. Sponsoring Agency Name and Address National Aeronautics and Space Administration Washington, D.C. 20546				14. Sponsoring Agency Code	
15. Supplementary Notes Compiled by Technical Information Services Division, Lewis Research Center.					
16 Abstract  This compilation of abstracts describes and indexes the technical reporting that resulted from the scientific and engineering work performed and managed by the Lewis Research Center in 1984. All the publications were announced in the 1984 issues of STAR (Scientific and Technical Aerospace Reports) and/or IAA (International Aerospace Abstracts). Included are research reports, journal articles, conference presentations, patents and patent applications, and theses.					
17. Key Words (Suggested by Author(s))  Bibliographies Abstracts Documentation Indexes (Documentation)			18. Distribution Statement  Unclassified - unlimited STAR Category 82		
19. Security Classif. (of this report) Unclassified		20. Security Classif. (of this page) Unclassified		21. No. of pages 327	
				22. Price* A15	

\*For sale by the National Technical Information Service, Springfield, Virginia 22161

National Aeronautics and  
Space Administration

**Lewis Research Center**  
Cleveland, Ohio 44135

Official Business  
Penalty for Private Use \$300

SECOND CLASS MAIL

ADDRESS CORRECTION REQUESTED



Postage and Fees Paid  
National Aeronautics and  
Space Administration  
NASA-451

**NASA**

---